

TRANSITION METAL-CATALYZED ENANTIOSELECTIVE
 α -FUNCTIONALIZATION OF NITROGEN AND OXYGEN-CONTAINING
HETEROCYCLES

Thesis by
Carina I. Jette

In Partial Fulfillment of the Requirements
for the Degree of
Doctor of Philosophy

CALIFORNIA INSTITUTE OF TECHNOLOGY
Pasadena, California

2021

(Defended November 11, 2020)

© 2020

Carina I. Jette
ORCID: 0000-0002-8476-6032

All Rights Reserved

To all my teachers and mentors

ACKNOWLEDGEMENTS

First of all, I would like to thank my mentor, Brian Stoltz, who made this research possible. I benefited a lot from his mentorship strategy, as he gave me the freedom to pursue my own interests, but was always there when I veered a little too off course. For this I will always be thankful, as it allowed me to develop my own chemical intuition. I also have to thank Sarah Reisman for being a second mentor and for always providing additional insight into my research. Thank you to Bob Grubbs and Bil Clemons for being on my committee and for everything I learned in the discussions we had during our meetings. I also have to thank Bruce Lipshutz at UCSB, as without his class or the opportunity to work in his lab, this thesis would have never been written. My labmates in the Lipshutz lab at UCSB were truly inspirational and showed me how much fun research could be.

I also have to thank Scott Virgil for all of the helpful discussions, as well as keeping the catalysis center up and running. He has always been there when I had chemistry problems that I had no idea how to solve, and I will always appreciate that. I also enjoyed learning how to use the robot, and will always remember the fun stories I got to hear while watching him fix the SFC or the LC.

I have to thank all of my project partners, as without them, this work would not have been possible. I would like to thank all my chemistry pen-pals at the Gwangju Institute of Science and Technology in Korea, including Woo-ok Jung, Dongseong Park, and Doohyun Baek, whom I was able to meet in person. Thank you to Jeremy Morgan, who worked on the arylation project with me. Our discussions on reaction mechanisms revived a little of my enthusiasm in catalysis and learning about his reaction optimization strategies helped guide my future endeavors, both in the arylation project as well as in the copper

allylic alkylation project. In addition, I would like to thank Shunya Sakurai, who worked on the Pd-catalyzed α -vinylation project with me.

I am especially thankful for my partners on the copper project, Jaron Tong and Ryan Hadt. Ryan's door was always open for any discussions, both about the copper project and my future career plans. His willingness to take on the copper project and put me in contact with Jaron allowed me to put together exactly the type of paper I had dreamed of publishing. Some of my favorite memories will be of Jaron and I running around Caltech, talking to Mona, Dave, and Scott while trying to figure out which techniques would tell us the most about the catalyst. Jaron has always been very willing to answer my questions, no matter how fundamental they were, which gave me the confidence to pursue a post-doc with a more inorganic emphasis.

I also need to thank Fa Ngamnithiporn. Fa has truly been there with me every step of the way. We took our classes together, were project partners, and got to share a fume hood for (almost) five years. She has always been there to help me laugh about how hard chemistry is sometimes and remind me to take a vacation. I truly admire her work ethic and I know that she will be a great professor one day.

Chris Reimann has been an awesome friend, labmate, and very briefly, project partner. Chris is so passionate about chemistry, particularly synthesis, and I've always had really exciting discussions with him. More importantly, though, he was always there to help me take my mind off chemistry when I needed it most, drink a white claw or two, or discuss the latest drama on our favorite TV show.

I also have to thank the rest of the members of my cohort, Eric Alexy, Sean Feng, and Zainab Al Saihati. Even though it feels like it all went by so fast, if I think about it, we

have all grown and changed so much during these years. I am so glad that you were all there to go through this process with me.

To the older students that have since left the Stoltz lab: thank you. Especially Gerit Pototschnig, Jaika Doerfler, and Eric Welin, who constantly reminded us all that hanging out and being friends with your labmates is one of the most important things. Also, thank you to Shoshana Bachman for being a true friend and an ally when I needed one the most. I am also especially thankful for Nick O'Connor, whose stories made working in the lab after dinner so much more fun. He also taught me how to fix rotovaps, a job that seemed horribly daunting at first, but his patience and kindness while teaching me the tricks made all the difference.

I also need to thank Nick Hafeman, Tyler Fulton, Alexia Kim, Alex Cusumano, Zack Sercel, Joel Munroy, Melinda Chan, Tyler Casselman, and Trevor Lohrey. You guys are awesome labmates and I am happy to see that the Stoltz lab is left in good hands.

To the Supper Club, Stefan, Jess, Lucas, and George, thank you for making my weekends a little bit brighter. I'm sorry that I always fall asleep so early.

I also need to thank Sean Friedowitz, who helped me get through all of my classes at UCSB and is also a truly loyal friend. Even though we live far away from each other now, he has always been there for me, and that has meant a lot over these past 5 years.

To the Linstadts and the Hadleys, thanks for all the dinners, fun trips, and the cards. I look forward to being able to do all of those things with you guys again soon! To Tío Daniel and Tía Evelyn, I am glad we got to have dinners and coffees before you moved. Although you are far away now, I am so happy for you guys and look forward to one day visiting you in Florida.

I also need to thank my sisters, Dani and Akie. Thanks for always being there for me, and inspiring me to be a better person and scientist. We have all come a long way from 6502 Sabado Tarde and I am excited to see where life continues to take us.

To Roscoe, thanks for being my best friend. Even though grad school has been very hard, you have always been there at the end of a long day to cheer me up. We have been on so many awesome adventures already and I can't wait to see where life takes you, me, and Ollie Bungo.

To Paulie and G, thank you for all the awesome camping trips and trips to Oregon. I am glad you both introduced me to rock climbing, and I hope we get to share many more trips in the future. You have both been great role models; thank you for always reminding me that there is more to life than just work.

And lastly, Mamina, thank you for everything. From when I was very young, you have always been there and cheered me on, and during grad school, it was no different. You have always believed in me, even when I did not believe in myself. I love you so much. Thank you for all the lunches, mates, and walks.

ABSTRACT

Research in the Stoltz group is focused on the development of synthetic methods for the preparation of stereochemically rich molecules and the total synthesis of complex natural products. One major theme of our group's methods development is transition-metal catalyzed α -functionalization of carbonyl derivatives, with a particular focus on the development of allylic alkylation protocols. Although the α -functionalization of carbonyl derivatives such as enolates, has been extensively studied, the use of nitrogen and oxygen-containing heterocycles, such as lactams and lactones, remains significantly underdeveloped. These types of nucleophiles are significantly more reactive, and in the case of the γ -butyrolactones and γ -lactams, may be smaller in size. Because of these differences, the conditions that have been developed for the functionalization of carbonyl derivatives such as ketones does not translate well to these nucleophiles. Furthermore, within the context of enantioselective functionalization, the unique characteristics of these nucleophiles necessitates the development of large, bulky ligands that enable the formation of a very well-defined chiral environment around the transition metal catalyst. This thesis mainly describes strategies that have been developed for the enantioselective α -functionalization of nitrogen and oxygen-containing heterocycles, with a particular focus on the γ -lactams and γ -butyrolactones.

PUBLISHED CONTENT AND CONTRIBUTIONS

1. Jette, C. I.; Tong, Z. J.; Hadt, R. G.; Stoltz, B. M. “Copper-Catalyzed Enantioselective Allylic Alkylation with a γ -Butyrolactone-Derived Silyl Ketene Acetal.” *Angew. Chem. Int. Ed.* **2020**, *59*, 2033–2038. DOI: 10.1002/anie.201912618 and *Angew. Chem.* 2020, *132*, 2049–2054. DOI: 10.1002/ange.201912618.

C.I.J. participated in reaction optimization, experimental work, data analysis, and manuscript preparation.

2. Park, D. ‡; Jette, C. I. ‡; Kim, J. ‡; Jung, W.–O.; Lee, Y.; Park, J.; Kang, S.; Han, M. S.; Stoltz, B. M.; Hong, S. “Enantioselective Alkynylation of Trifluoromethyl Ketones Catalyzed by Cation-Binding Salen Nickel Complexes.” *Angew. Chem. Int. Ed.* **2020**, *59*, 775–779. DOI:10.1002/anie.201913057. and *Angew. Chem.* **2020**, *132*, 785–789 DOI: 10.1002/ange.201912057.

C.I.J. participated in reaction optimization, experimental work, data analysis, and manuscript preparation.

3. Jette, C. I.; Geibel, I.; Bachman, S.; Hayashi, M.; Sakurai, S.; Shimizu, H.; Morgan, J. B.; Stoltz, B. M. “Palladium-Catalyzed Construction of Quaternary Stereocenters by Enantioselective Arylation of γ -Lactams with Aryl Chlorides and Bromides.” *Angew. Chem. Int. Ed.* **2019**, *58*, 4297–4301. DOI:10.1002/anie.201814475 and *Angew. Chem.* DOI:10.1002/anie.201814475

C.I.J. participated in reaction optimization, experimental work, data analysis, and manuscript preparation.

4. Ngamnithiporn, A.; Jette, C. I. Bachman, S.; Virgil, S.; Stoltz, B. M. “Nickel-Catalyzed Enantioselective Allylic Alkylation of Lactones and Lactams with Unactivated Allylic Alcohols.” *Chem. Sci.* **2018**, *9*, 2547–2551. DOI:10.1039/C7SC05216B.

C.I.J participated in experimental work, data analysis, and manuscript preparation.

TABLE OF CONTENTS

Dedication	iii
Acknowledgements	iv
Abstract	viii
Published Content and Contributions	ix
Table of Contents	xi
List of Figures	xvi
List of Schemes	xxviii
List of Tables	xxx
List of Abbreviations	xxxiv

CHAPTER 1

1

Enantioselective Alkynylation of Trifluoromethyl Ketones Catalyzed by Cation-Binding Salen Nickel Complexes

1.1	Introduction, Background, and Synthetic Utility	1
1.2	Catalyst Development and Optimization of Reaction Conditions	5
1.3	Aryl Trifluoromethyl Ketone Substrate Scope	7
1.4	Alkynylation of Unsaturated Trifluoromethyl Ketones	9
1.5	Reaction Optimization for Unsaturated Trifluoromethyl Ketones.....	10
1.6	Scope of Enantioselective Alkynylation of Unsaturated Trifluoromethylketones	14
1.7	Preliminary Mechanistic Investigations	15
1.8	Conclusions	17
1.9	Experimental Section	17
1.9.1	Materials and Methods.....	17
1.9.2	Experimental Procedures and Spectroscopic Data	19
1.9.2.1	Synthesis and Spectroscopic Data for Salen-Crown Ether Ligands	19
1.9.2.2	Complexation Procedure and HRMS for Salen-Ni Complexes.....	27
1.9.2.3	Synthesis of Trifluoromethyl Ketones.....	29
1.9.2.4	Procedure and Spectroscopic Data for Alkynylation of Aryl Trifluoromethyl Ketones.....	32

1.9.2.5	Procedure and Spectroscopic Data for Alkynylation of Unsaturated Trifluoromethylketones	41
1.9.3.	UV-Vis Data for Metal Titration	51
1.10	References and Notes	55

APPENDIX 1 **61**

Spectra Relevant to Chapter 1

CHAPTER 2 **109**

Palladium-Catalyzed Enantioselective Arylation of γ -Lactams with Aryl Chlorides and Bromides

2.1	Introduction and Background.....	109
2.2	Overview on α -Arylation	110
2.3	Reaction Optimization with Aryl Chlorides.....	112
2.4	Reaction Optimization with Aryl Bromides	118
2.5	Reaction Scope	119
2.6	Product Transformations	122
2.7	Conclusion	123
2.8	Experimental Section	124
2.8.1	Materials and Methods.....	124
2.8.2	Experimental Procedures and Spectroscopic Data.....	126
2.8.2.1	Synthesis of <i>N</i> -Substituted γ -Lactams.....	126
2.8.2.2	Synthesis of α -Substituted γ -Lactams	128
2.8.2.3	General Procedure for the Pd-Catalyzed α -Arylation of γ -Lactams	135
2.8.2.4	Spectroscopic Data for Products from the Catalytic Reactions	136
2.9	References and Notes	157

APPENDIX 2 **162**

Challenging Substrates in the Palladium-Catalyzed Enantioselective Arylation of γ -Lactams with Aryl Chlorides and Bromides

A2.1	Introduction	162
A2.2	Limitations in the Protecting Group and α -Substituent on the γ -Lactam.....	162
A2.3	Limitations in the Functional Group Tolerance on the Electrophile	164

APPENDIX 3 **167**

Spectra Relevant to Chapter 2

APPENDIX 4 244

X-Ray Crystallography Reports Relevant to Chapter 2

A4.1	General Experimental Information	245
A4.2	X-Ray Crystal Structure Analysis of Arylation Product 32ab	246
A4.3	X-Ray Crystal Structure Analysis of Pd/L10	257
A4.4	References	296

CHAPTER 3 296

Copper-Catalyzed Enantioselective Allylic Alkylation with a γ -Butyrolactone-Derived Silyl Ketene Acetal

3.1	Introduction, Background, and Synthetic Utility	296
3.2	Initial Ligand Screen	300
3.3	Challenges in the Consistency of the Reaction Outcome	302
3.4	Chiral Ligand Identification	313
3.5	Final Reaction Optimization	320
3.6	Reaction Scope	324
3.7	Derivatization of Allyl γ -Butyrolactone Products	326
3.8	Conclusion	327
3.9	Experimental Section	327
3.9.1	Materials and Methods	327
3.9.2	Experimental Procedures and Spectroscopic Data	330
3.9.2.1	Procedures for the Evaluation of Commercially Available Ligands and Synthesized Picolinamide Ligands	330
3.9.2.2	Synthesis of Chiral Picolinamide Ligands	335
3.9.2.3	Synthesis of Allylic Chloride Electrophiles	356
3.9.2.4	Procedure for Cu-Catalyzed Allylic Alkylation Reactions	366
3.9.2.5	Spectroscopic Data for Products from Catalytic Reactions	367
3.9.2.6	Procedures and Spectroscopic Data for the Product Transformations ...	379
3.10	Other Potential Product Transformations	383
3.11	References and Notes	384

APPENDIX 5 388

Challenging Substrates in Cu-Catalyzed Enantioselective Allylic Alkylation with Silyl Ketene Acetals

A5.1	Introduction	388
------	--------------------	-----

A5.2	Limitations in the Allylic Chloride Electrophile	388
A5.3	Limitations in the Nucleophile	393
A5.4	Acyclic Nucleophiles and Bicyclo[2.2.2]octane Backbone	396
A5.5	Cu-Catalyzed Allylic Alkylation with Silyl Enol Ethers	399
A5.6	Conclusion	404
A5.7	References and Notes	40
APPENDIX 6		406
<i>Spectra for Amide Ligands Synthesized and Tested in Chapter 3</i>		
APPENDIX 7		453
<i>Spectra for Substrates and Products Synthesized in Chapter 3</i>		
APPENDIX 8		518
<i>X-Ray Crystallography Reports Relevant to Chapter 3</i>		
A8.1	General Experimental Information	519
A8.2	X-Ray Crystal Structure Analysis of Allylation Product 44b	519
CHAPTER 4		531
<i>Mechanistic Investigations for Copper-Catalyzed Enantioselective Allylic Alkylation with a γ-Butyrolactone-Derived Silyl Ketene Acetal</i>		
4.1	Introduction	531
4.2	Overview on Mechanisms for Copper-Catalyzed Allylic Alkylations	532
4.3	Investigations into a Radical Mechanism.....	536
4.4	Characterization of the Starting Copper/ L73 Complex	537
4.5	Ligand Coordination Geometry: DFT Calculations	541
4.6	Reduction of Copper (II) to Copper (I)	543
4.7	FTIR: Additional Structural Insight for Copper (I)	547
4.8	Importance of Olefin Geometry	552
4.9	Proposed Catalytic Cycle	555
4.10	Conclusion	557
4.11	Experimental Section	558
4.11.1	Materials and Methods.....	558
4.11.2	Experimental Procedures and Spectroscopic Data	561
4.11.2.1	Preparation of L73 • CuCl₂ in THF for UV-vis, EPR, and HRMS	561
4.11.2.2	Spin Quantification Experiment	561

4.11.2.3	Supporting Computational Results	564
4.11.2.4	Synthesis of Allylic Chloride Electrophiles	566
4.11.2.5	Procedure for Cu-Catalyzed Allylic Alkylation Reaction	568
4.11.2.6	Spectroscopic Data for Products from the Catalytic Reactions.....	569
4.12	References and Notes	571

APPENDIX 9 **576**

Spectra Relevant to Chapter 4

APPENDIX 10 **589**

Coordinates for Optimized Geometries Relevant to Chapter 4

A10.1	Coordinates For B3(0HF)LYP Optimized L73^{NNO}•CuCl₂	590
A10.2	Coordinates For B3(0HF)LYP Optimized L73^{NNN}•CuCl₂	592
A10.3	Coordinates For B3(38HF)LYP Optimized L73^{NNO}•CuCl₂	594
A10.4	Coordinates For B3(38HF)LYP Optimized L73^{NNN}•CuCl₂	596
A10.5	Coordinates For L73^{NNO}•Cu^{II}Cl	599
A10.6	Coordinates For L73^{NNN}•Cu^{II}Cl	601
A10.7	Coordinates For L73^{NNO}•Cu^I	603
A10.8	Coordinates For L73^{NNN}•Cu^I	605
A10.9	Coordinates For L73^{NNO}•Cu^ICl	608
A10.10	Coordinates For L73^{NNN}•Cu^ICl	610
A10.11	Coordinates For L73^{NNN}•Cu^I	612
A10.12	Coordinates For L73^{NNN}•Cu^I	614
A10.13	Coordinates For Relaxed L73²⁻	617
A10.14	Coordinates For L73^{NNO}•Cu^ICl₂	619
A10.15	Coordinates For L73^{NNN}•Cu^ICl₂	621

APPENDIX 11 **623**

Palladium-Catalyzed Construction of Quaternary Stereocenters by Enantioselective Vinylation of γ -Lactams and γ -Butyrolactones

A11.1	Introduction and Background.....	623
A11.2	Preliminary Investigations	626
A11.3	Reaction Optimization.....	627
A11.4	Preliminary Results with γ -Butyrolactones and Vinyl Bromides	632
A11.5	Conclusion	633

A11.6	Representative Procedure for Pd-Catalyzed α -Vinylolation of γ -Lactams and γ -Butyrolactones	634
A11.7	References and Notes	635

APPENDIX 12

638

Nickel-Catalyzed Enantioselective Allylic Alkylation of Lactones and Lactams with Unactivated Allylic Alcohols

A12.1	Introduction, Background and Synthetic Utility	638
A12.2	Reaction Optimization	640
A12.3	Scope of the Nucleophile and the Electrophile.....	641
A12.4	Product Transformations	645
A12.5	Conclusion	646
A12.6	References and Notes	647

LIST OF FIGURES

CHAPTER 1

Enantioselective Alkynylation of Trifluoromethyl Ketones Catalyzed by Cation-Binding Salen Nickel Complexes

Figure 1.1.1.	Examples of Bioactive Compounds Containing a Trifluoromethylcarbinol	2
Figure 1.1.2.	Previous Reports of Asymmetric Alkynylation of Trifluoromethyl Ketones	2
Figure 1.1.3.	Chiral Bifunctional Catalysts	4
Figure 1.7.1.	Metal Ion Titration Studies via UV-Vis Absorption.....	15
Figure 1.7.2.	Proposed Reaction Mechanism	17

APPENDIX 1

Spectra Relevant to Chapter 1

Figure A1.1	^1H NMR (300 MHz, CDCl_3) of compound SI2	62
Figure A1.2	Infrared spectrum (Thin Film, NaCl) of compound SI2	63
Figure A1.3	^{13}C NMR (101 MHz, CDCl_3) of compound SI2	63
Figure A1.4	^1H NMR (400 MHz, CDCl_3) of compound 10f	64
Figure A1.5	Infrared spectrum (Thin Film, NaCl) of compound 10f	65
Figure A1.6	^{13}C NMR (101 MHz, CDCl_3) of compound 10f	65
Figure A1.7	^{19}F NMR (282 MHz, CDCl_3) of compound 10f	66

Figure A1.8	^1H NMR (400 MHz, CDCl_3) of compound 11aa	67
Figure A1.9	Infrared spectrum (Thin Film, NaCl) of compound 11aa	68
Figure A1.10	^{13}C NMR (101 MHz, CDCl_3) of compound 11aa	68
Figure A1.11	^{19}F NMR (282 MHz, CDCl_3) of compound 11aa	69
Figure A1.12	^1H NMR (400 MHz, CDCl_3) of compound 11ba	70
Figure A1.13	Infrared spectrum (Thin Film, NaCl) of compound 11ba	71
Figure A1.14	^{13}C NMR (101 MHz, CDCl_3) of compound 11ba	71
Figure A1.15	^{19}F NMR (282 MHz, CDCl_3) of compound 11ba	72
Figure A1.16	^1H NMR (400 MHz, CDCl_3) of compound 11ca	73
Figure A1.17	Infrared spectrum (Thin Film, NaCl) of compound 11ca	74
Figure A1.18	^{13}C NMR (101 MHz, CDCl_3) of compound 11ca	74
Figure A1.19	^{19}F NMR (282 MHz, CDCl_3) of compound 11ca	75
Figure A1.20	^1H NMR (400 MHz, CDCl_3) of compound 11da	76
Figure A1.21	Infrared spectrum (Thin Film, NaCl) of compound 11da	77
Figure A1.22	^{13}C NMR (101 MHz, CDCl_3) of compound 11da	77
Figure A1.23	^{19}F NMR (282 MHz, CDCl_3) of compound 11da	78
Figure A1.24	^1H NMR (400 MHz, CDCl_3) of compound 11ea	79
Figure A1.25	Infrared spectrum (Thin Film, NaCl) of compound 11ea	80
Figure A1.26	^{13}C NMR (101 MHz, CDCl_3) of compound 11ea	80
Figure A1.27	^{19}F NMR (282 MHz, CDCl_3) of compound 11ea	81
Figure A1.28	^1H NMR (400 MHz, CDCl_3) of compound 11fa	82
Figure A1.29	Infrared spectrum (Thin Film, NaCl) of compound 11fa	83
Figure A1.30	^{13}C NMR (101 MHz, CDCl_3) of compound 11fa	83
Figure A1.31	^{19}F NMR (282 MHz, CDCl_3) of compound 11fa	84
Figure A1.32	^1H NMR (400 MHz, CDCl_3) of compound 11ga	85
Figure A1.33	Infrared spectrum (Thin Film, NaCl) of compound 11ga	86
Figure A1.34	^{13}C NMR (101 MHz, CDCl_3) of compound 11ga	86
Figure A1.35	^{19}F NMR (282 MHz, CDCl_3) of compound 11ga	87
Figure A1.36	^1H NMR (400 MHz, CDCl_3) of compound 11ha	88
Figure A1.37	Infrared spectrum (Thin Film, NaCl) of compound 11ha	89
Figure A1.38	^{13}C NMR (101 MHz, CDCl_3) of compound 11ha	89
Figure A1.39	^{19}F NMR (282 MHz, CDCl_3) of compound 11ha	90
Figure A1.40	^1H NMR (400 MHz, CDCl_3) of compound 11ia	91
Figure A1.41	Infrared spectrum (Thin Film, NaCl) of compound 11ia	92
Figure A1.42	^{13}C NMR (101 MHz, CDCl_3) of compound 11ia	92

Figure A1.43	^{19}F NMR (282 MHz, CDCl_3) of compound 11ia	93
Figure A1.44	^1H NMR (400 MHz, CDCl_3) of compound 11ja	94
Figure A1.45	Infrared spectrum (Thin Film, NaCl) of compound 11ja	95
Figure A1.46	^{13}C NMR (101 MHz, CDCl_3) of compound 11ja	95
Figure A1.47	^{19}F NMR (282 MHz, CDCl_3) of compound 11ja	96
Figure A1.48	^1H NMR (400 MHz, CDCl_3) of compound 11ka	97
Figure A1.49	Infrared spectrum (Thin Film, NaCl) of compound 11ka	98
Figure A1.50	^{13}C NMR (101 MHz, CDCl_3) of compound 11ka	98
Figure A1.51	^{19}F NMR (282 MHz, CDCl_3) of compound 11ka	99
Figure A1.52	^1H NMR (400 MHz, CDCl_3) of compound 11la	100
Figure A1.53	Infrared spectrum (Thin Film, NaCl) of compound 11la	101
Figure A1.54	^{13}C NMR (101 MHz, CDCl_3) of compound 11la	101
Figure A1.55	^{19}F NMR (282 MHz, CDCl_3) of compound 11la	102
Figure A1.56	^1H NMR (400 MHz, CDCl_3) of compound 11ma	103
Figure A1.57	Infrared spectrum (Thin Film, NaCl) of compound 11ma	104
Figure A1.58	^{13}C NMR (101 MHz, CDCl_3) of compound 11ma	104
Figure A1.59	^{19}F NMR (282 MHz, CDCl_3) of compound 11ma	105
Figure A1.60	^1H NMR (400 MHz, CDCl_3) of compound 11na	106
Figure A1.61	Infrared spectrum (Thin Film, NaCl) of compound 11na	107
Figure A1.62	^{13}C NMR (101 MHz, CDCl_3) of compound 11na	107
Figure A1.63	^{19}F NMR (282 MHz, CDCl_3) of compound 11na	108

CHAPTER 2

Palladium-Catalyzed Enantioselective Arylation of γ -Lactams with Aryl Chlorides and Bromides

Figure 2.1.1	Pd-Catalyzed Enantioselective Arylation of γ -Lactams	110
Figure 2.2.1	Mechanism for Pd-Catalyzed α -Arylation of Carbonyl Derivatives	111
Figure 2.2.2	α -Arylation of Piperidinones and Oxindoles	112

APPENDIX 3

Spectra Relevant to Chapter 2

Figure A3.1	^1H NMR (400 MHz, CDCl_3) of compound 30e	168
Figure A3.2	Infrared spectrum (Thin Film, NaCl) of compound 30e	169
Figure A3.3	^{13}C NMR (125 MHz, CDCl_3) of compound 30e	169

Figure A3.4	^{19}F NMR (282 MHz, CDCl_3) of compound 30e	170
Figure A3.5	^1H NMR (500 MHz, CDCl_3) of compound 30g	171
Figure A3.6	Infrared spectrum (Thin Film, NaCl) of compound 30g	172
Figure A3.7	^{13}C NMR (100 MHz, CDCl_3) of compound 30g	172
Figure A3.8	^1H NMR (500 MHz, CDCl_3) of compound 30h	173
Figure A3.9	Infrared spectrum (Thin Film, NaCl) of compound 30h	174
Figure A3.10	^{13}C NMR (100 MHz, CDCl_3) of compound 30h	174
Figure A3.11	^1H NMR (300 MHz, CDCl_3) of compound 30j	175
Figure A3.12	Infrared spectrum (Thin Film, NaCl) of compound 30j	176
Figure A3.13	^{13}C NMR (100 MHz, CDCl_3) of compound 30j	176
Figure A3.14	^1H NMR (300 MHz, CDCl_3) of compound 30i	177
Figure A3.15	Infrared spectrum (Thin Film, NaCl) of compound 30i	178
Figure A3.16	^{13}C NMR (100 MHz, CDCl_3) of compound 30i	178
Figure A3.17	^1H NMR (500 MHz, CDCl_3) of compound 30k	179
Figure A3.18	Infrared spectrum (Thin Film, NaCl) of compound 30k	180
Figure A3.19	^{13}C NMR (125 MHz, CDCl_3) of compound 30k	180
Figure A3.20	^1H NMR (400 MHz, CDCl_3) of compound 32aa	181
Figure A3.21	Infrared spectrum (Thin Film, NaCl) of compound 32aa	182
Figure A3.22	^{13}C NMR (125 MHz, CDCl_3) of compound 32aa	182
Figure A3.23	^1H NMR (500 MHz, CDCl_3) of compound 32ba	183
Figure A3.24	Infrared spectrum (Thin Film, NaCl) of compound 32ba	184
Figure A3.25	^{13}C NMR (125 MHz, CDCl_3) of compound 32ba	184
Figure A3.26	^1H NMR (400 MHz, CDCl_3) of compound 32ca	185
Figure A3.27	Infrared spectrum (Thin Film, NaCl) of compound 32ca	186
Figure A3.28	^{13}C NMR (125 MHz, CDCl_3) of compound 32ca	186
Figure A3.29	^1H NMR (400 MHz, CDCl_3) of compound 32da	187
Figure A3.30	Infrared spectrum (Thin Film, NaCl) of compound 32da	188
Figure A3.31	^{13}C NMR (125 MHz, CDCl_3) of compound 32da	188
Figure A3.32	^1H NMR (500 MHz, CDCl_3) of compound 32ea	189
Figure A3.33	Infrared spectrum (Thin Film, NaCl) of compound 32ea	190
Figure A3.34	^{13}C NMR (125 MHz, CDCl_3) of compound 32ea	190
Figure A3.35	^{19}F NMR (282 MHz, CDCl_3) of compound 32ea	191
Figure A3.36	^1H NMR (500 MHz, CDCl_3) of compound 32fa	192
Figure A3.37	Infrared spectrum (Thin Film, NaCl) of compound 32fa	193
Figure A3.38	^{13}C NMR (125 MHz, CDCl_3) of compound 32fa	193

Figure A3.39	^1H NMR (400 MHz, CDCl_3) of compound 32ab	194
Figure A3.40	Infrared spectrum (Thin Film, NaCl) of compound 32ab	195
Figure A3.41	^{13}C NMR (125 MHz, CDCl_3) of compound 32ab	195
Figure A3.42	^1H NMR (400 MHz, CDCl_3) of compound 32ac	196
Figure A3.43	Infrared spectrum (Thin Film, NaCl) of compound 32ac	197
Figure A3.44	^{13}C NMR (100 MHz, CDCl_3) of compound 32ac	197
Figure A3.45	^{19}F NMR (282 MHz, CDCl_3) of compound 32ac	198
Figure A3.46	^1H NMR (400 MHz, CDCl_3) of compound 32ad	199
Figure A3.47	Infrared spectrum (Thin Film, NaCl) of compound 32ad	200
Figure A3.48	^{13}C NMR (100 MHz, CDCl_3) of compound 32ad	200
Figure A3.49	^{19}F NMR (282 MHz, CDCl_3) of compound 32ad	201
Figure A3.50	^1H NMR (400 MHz, CDCl_3) of compound 32ae	202
Figure A3.51	Infrared spectrum (Thin Film, NaCl) of compound 32ae	203
Figure A3.52	^{13}C NMR (100 MHz, CDCl_3) of compound 32ae	203
Figure A3.53	^1H NMR (400 MHz, CDCl_3) of compound 32af	204
Figure A3.54	Infrared spectrum (Thin Film, NaCl) of compound 32af	205
Figure A3.55	^{13}C NMR (100 MHz, CDCl_3) of compound 32af	205
Figure A3.56	^1H NMR (400 MHz, CDCl_3) of compound 32ag	206
Figure A3.57	Infrared spectrum (Thin Film, NaCl) of compound 32ag	207
Figure A3.58	^{13}C NMR (100 MHz, CDCl_3) of compound 32ag	207
Figure A3.59	^1H NMR (400 MHz, CDCl_3) of compound 32ah	208
Figure A3.60	Infrared spectrum (Thin Film, NaCl) of compound 32ah	209
Figure A3.61	^{13}C NMR (100 MHz, CDCl_3) of compound 32ah	209
Figure A3.62	^1H NMR (300 MHz, CDCl_3) of compound 32ai	210
Figure A3.63	Infrared spectrum (Thin Film, NaCl) of compound 32ai	211
Figure A3.64	^{13}C NMR (100 MHz, CDCl_3) of compound 32ai	211
Figure A3.65	^1H NMR (400 MHz, CDCl_3) of compound 32aj	212
Figure A3.66	Infrared spectrum (Thin Film, NaCl) of compound 32aj	213
Figure A3.67	^{13}C NMR (100 MHz, CDCl_3) of compound 32aj	213
Figure A3.68	^{19}F NMR (282 MHz, CDCl_3) of compound 32aj	214
Figure A3.69	^1H NMR (400 MHz, CDCl_3) of compound 32ak	215
Figure A3.70	Infrared spectrum (Thin Film, NaCl) of compound 32ak	216
Figure A3.71	^{13}C NMR (100 MHz, CDCl_3) of compound 32ak	216
Figure A3.72	^1H NMR (400 MHz, CDCl_3) of compound 32al	217
Figure A3.73	Infrared spectrum (Thin Film, NaCl) of compound 32al	218

Figure A3.74	^{13}C NMR (100 MHz, CDCl_3) of compound 32al	218
Figure A3.75	^1H NMR (400 MHz, CDCl_3) of compound 32gb	219
Figure A3.76	Infrared spectrum (Thin Film, NaCl) of compound 32gb	220
Figure A3.77	^{13}C NMR (100 MHz, CDCl_3) of compound 32gb	220
Figure A3.78	^1H NMR (500 MHz, CDCl_3) of compound 32hb	221
Figure A3.79	Infrared spectrum (Thin Film, NaCl) of compound 32hb	222
Figure A3.80	^{13}C NMR (125 MHz, CDCl_3) of compound 32hb	222
Figure A3.81	^1H NMR (500 MHz, CDCl_3) of compound 32ga	223
Figure A3.82	Infrared spectrum (Thin Film, NaCl) of compound 32ga	224
Figure A3.83	^{13}C NMR (125 MHz, CDCl_3) of compound 32ga	224
Figure A3.84	^1H NMR (500 MHz, CDCl_3) of compound 32ha	225
Figure A3.85	Infrared spectrum (Thin Film, NaCl) of compound 32ha	226
Figure A3.86	^{13}C NMR (125 MHz, CDCl_3) of compound 32ha	226
Figure A3.87	^1H NMR (400 MHz, CDCl_3) of compound 32ia	227
Figure A3.88	Infrared spectrum (Thin Film, NaCl) of compound 32ia	228
Figure A3.89	^{13}C NMR (100 MHz, CDCl_3) of compound 32ia	228
Figure A3.90	^1H NMR (400 MHz, CDCl_3) of compound 32ja	229
Figure A3.91	Infrared spectrum (Thin Film, NaCl) of compound 32ja	230
Figure A3.92	^{13}C NMR (100 MHz, CDCl_3) of compound 32ja	230
Figure A3.93	^1H NMR (400 MHz, CDCl_3) of compound 32ka	231
Figure A3.94	Infrared spectrum (Thin Film, NaCl) of compound 32ka	232
Figure A3.95	^{13}C NMR (100 MHz, CDCl_3) of compound 32ka	232
Figure A3.96	^1H NMR (400 MHz, CDCl_3) of compound 32gc	233
Figure A3.97	Infrared spectrum (Thin Film, NaCl) of compound 32gc	234
Figure A3.98	^{13}C NMR (100 MHz, CDCl_3) of compound 32gc	234
Figure A3.99	^{19}F NMR (282 MHz, CDCl_3) of compound 32gc	235
Figure A3.100	^1H NMR (400 MHz, CDCl_3) of compound 32gk	236
Figure A3.101	Infrared spectrum (Thin Film, NaCl) of compound 32gk	237
Figure A3.102	^{13}C NMR (125 MHz, CDCl_3) of compound 32gk	237
Figure A3.103	^1H NMR (400 MHz, CDCl_3) of compound 34	238
Figure A3.104	Infrared spectrum (Thin Film, NaCl) of compound 34	239
Figure A3.105	^{13}C NMR (100 MHz, CDCl_3) of compound 34	239
Figure A3.106	^1H NMR (400 MHz, CDCl_3) of compound 35	240
Figure A3.107	Infrared spectrum (Thin Film, NaCl) of compound 35	241
Figure A3.108	^{13}C NMR (100 MHz, CDCl_3) of compound 35	241

Figure A3.109	^1H NMR (400 MHz, CDCl_3) of compound 36	242
Figure A3.110	Infrared spectrum (Thin Film, NaCl) of compound 36	243
Figure A3.111	^{13}C NMR (100 MHz, CDCl_3) of compound 36	243

APPENDIX 4

X-Ray Crystallography Reports Relevant to Chapter 2

Figure A4.1	X-Ray Coordination of α -Aryl γ -Lactam 32ab	246
Figure A4.2	X-Ray Coordination of Pd/L10	257

CHAPTER 3

Copper-Catalyzed Enantioselective Allylic Alkylation with a γ -Butyrolactone-Derived Silyl Ketene Acetal

Figure 3.1.1	Summary of Previous Work in Allylic Alkylations in the Stoltz Lab.....	297
Figure 3.1.2	Previous Reports of α -Allylation of γ -Butyrolactones	298
Figure 3.3.1	Precedent for Cu/Bis-Picolinamide Complexes and the Use of L38 in Enantioselective Allylic Alkylations	310
Figure 3.3.2	Deprotonation of L38 with <i>n</i> -BuLi (Set-up E)	311

APPENDIX 6

Spectra for Amide Ligands Synthesized and Tested in Chapter 3

Figure A6.1	^1H NMR (500 MHz, CDCl_3) of compound L44	407
Figure A6.2	^1H NMR (500 MHz, CDCl_3) of compound L45	408
Figure A6.3	^{13}C NMR (125 MHz, CDCl_3) of compound L45	409
Figure A6.4	^{19}F NMR (282 MHz, CDCl_3) of compound L45	409
Figure A6.5	^1H NMR (500 MHz, CDCl_3) of compound L47	410
Figure A6.6	^1H NMR (500 MHz, CDCl_3) of compound L50	411
Figure A6.7	^1H NMR (400 MHz, CDCl_3) of compound L54	412
Figure A6.8	Infrared spectrum (Thin Film, NaCl) of compound L54	413
Figure A6.9	^{13}C NMR (100 MHz, CDCl_3) of compound L54	413
Figure A6.10	^1H NMR (400 MHz, CDCl_3) of compound L59	414
Figure A6.11	Infrared spectrum (Thin Film, NaCl) of compound L59	415
Figure A6.12	^{13}C NMR (100 MHz, CDCl_3) of compound L59	415
Figure A6.13	^1H NMR (400 MHz, CDCl_3) of compound L62	416
Figure A6.14	^1H NMR (400 MHz, CDCl_3) of compound L64	417

Figure A6.15	Infrared spectrum (Thin Film, NaCl) of compound L64	418
Figure A6.16	^{13}C NMR (100 MHz, CDCl_3) of compound L64	418
Figure A6.17	^1H NMR (400 MHz, CDCl_3) of compound SI10	419
Figure A6.18	Infrared spectrum (Thin Film, NaCl) of compound SI10	420
Figure A6.19	^{13}C NMR (100 MHz, CDCl_3) of compound SI10	420
Figure A6.20	^1H NMR (400 MHz, CDCl_3) of compound L61	421
Figure A6.21	Infrared spectrum (Thin Film, NaCl) of compound L61	422
Figure A6.22	^{13}C NMR (100 MHz, CDCl_3) of compound L61	422
Figure A6.23	^1H NMR (400 MHz, CDCl_3) of compound L63	423
Figure A6.24	^{13}C NMR (100 MHz, CDCl_3) of compound L63	424
Figure A6.25	^1H NMR (400 MHz, CDCl_3) of compound L67	425
Figure A6.26	Infrared spectrum (Thin Film, NaCl) of compound L67	426
Figure A6.27	^{13}C NMR (100 MHz, CDCl_3) of compound L67	426
Figure A6.28	^1H NMR (400 MHz, CDCl_3) of compound L66	427
Figure A6.29	Infrared spectrum (Thin Film, NaCl) of compound L66	428
Figure A6.30	^{13}C NMR (100 MHz, CDCl_3) of compound L66	428
Figure A6.31	^1H NMR (400 MHz, CDCl_3) of compound L68	429
Figure A6.32	Infrared spectrum (Thin Film, NaCl) of compound L68	430
Figure A6.33	^{13}C NMR (100 MHz, CDCl_3) of compound L68	430
Figure A6.34	^1H NMR (400 MHz, CDCl_3) of compound L69	431
Figure A6.35	Infrared spectrum (Thin Film, NaCl) of compound L69	432
Figure A6.36	^{13}C NMR (100 MHz, CDCl_3) of compound L69	432
Figure A6.37	^1H NMR (400 MHz, CDCl_3) of compound L70	433
Figure A6.38	^1H NMR (400 MHz, CDCl_3) of compound L72	434
Figure A6.39	^{13}C NMR (100 MHz, CDCl_3) of compound L72	435
Figure A6.40	^1H NMR (400 MHz, CDCl_3) of compound SI11	436
Figure A6.41	Infrared spectrum (Thin Film, NaCl) of compound SI11	437
Figure A6.42	^{13}C NMR (100 MHz, CDCl_3) of compound SI11	437
Figure A6.43	^1H NMR (400 MHz, CDCl_3) of compound L73	438
Figure A6.44	Infrared spectrum (Thin Film, NaCl) of compound L73	439
Figure A6.45	^{13}C NMR (100 MHz, CDCl_3) of compound L73	439
Figure A6.46	^1H NMR (400 MHz, CDCl_3) of compound L74	440
Figure A6.47	Infrared spectrum (Thin Film, NaCl) of compound L74	441
Figure A6.48	^{13}C NMR (100 MHz, CDCl_3) of compound L74	441
Figure A6.49	^1H NMR (400 MHz, CDCl_3) of compound L75	442

Figure A6.50	Infrared spectrum (Thin Film, NaCl) of compound L75	443
Figure A6.51	^{13}C NMR (100 MHz, CDCl_3) of compound L75	443
Figure A6.52	^1H NMR (400 MHz, CDCl_3) of compound L76	444
Figure A6.53	Infrared spectrum (Thin Film, NaCl) of compound L76	445
Figure A6.54	^{13}C NMR (100 MHz, CDCl_3) of compound L76	445
Figure A6.55	^1H NMR (400 MHz, CDCl_3) of compound L77	446
Figure A6.56	Infrared spectrum (Thin Film, NaCl) of compound L77	447
Figure A6.57	^{13}C NMR (100 MHz, CDCl_3) of compound L77	447
Figure A6.58	^1H NMR (400 MHz, CDCl_3) of compound L78	448
Figure A6.59	Infrared spectrum (Thin Film, NaCl) of compound L78	449
Figure A6.60	^{13}C NMR (100 MHz, CDCl_3) of compound L78	449
Figure A6.61	^1H NMR (400 MHz, CDCl_3) of compound L79	450
Figure A6.62	Infrared spectrum (Thin Film, NaCl) of compound L79	451
Figure A6.63	^{13}C NMR (100 MHz, CDCl_3) of compound L79	451
Figure A6.64	^{19}F NMR (282 MHz, CDCl_3) of compound L79	452

APPENDIX 7

Spectra for Amide Ligands Synthesized and Tested in Chapter 3

Figure A7.1	^1H NMR (400 MHz, CDCl_3) of compound 43m	454
Figure A7.2	Infrared spectrum (Thin Film, NaCl) of compound 43m	455
Figure A7.3	^{13}C NMR (100 MHz, CDCl_3) of compound 43m	455
Figure A7.4	^1H NMR (500 MHz, CDCl_3) of compound 43e	456
Figure A7.5	Infrared spectrum (Thin Film, NaCl) of compound 43e	457
Figure A7.6	^{13}C NMR (100 MHz, CDCl_3) of compound 43e	457
Figure A7.7	^1H NMR (400 MHz, CDCl_3) of compound 43i	458
Figure A7.8	Infrared spectrum (Thin Film, NaCl) of compound 43i	459
Figure A7.9	^{13}C NMR (100 MHz, CDCl_3) of compound 43i	459
Figure A7.10	^{19}F NMR (282 MHz, CDCl_3) of compound 43i	460
Figure A7.11	^1H NMR (400 MHz, CDCl_3) of compound SI12	461
Figure A7.12	Infrared spectrum (Thin Film, NaCl) of compound SI12	462
Figure A7.13	^{13}C NMR (100 MHz, CDCl_3) of compound SI12	462
Figure A7.14	^1H NMR (400 MHz, CDCl_3) of compound 43n	463
Figure A7.15	Infrared spectrum (Thin Film, NaCl) of compound 43n	464
Figure A7.16	^{13}C NMR (100 MHz, CDCl_3) of compound 43n	464
Figure A7.17	^1H NMR (400 MHz, CDCl_3) of compound SI13	465

Figure A7.18	Infrared spectrum (Thin Film, NaCl) of compound SI13	466
Figure A7.19	^{13}C NMR (100 MHz, CDCl_3) of compound SI13	466
Figure A7.20	^{19}F NMR (282 MHz, CDCl_3) of compound SI13	467
Figure A7.21	^1H NMR (400 MHz, CDCl_3) of compound 43f	468
Figure A7.22	Infrared spectrum (Thin Film, NaCl) of compound 43f	469
Figure A7.23	^{13}C NMR (100 MHz, CDCl_3) of compound 43f	469
Figure A7.24	^{19}F NMR (282 MHz, CDCl_3) of compound 43f	470
Figure A7.25	^1H NMR (400 MHz, CDCl_3) of compound 43o	471
Figure A7.26	Infrared spectrum (Thin Film, NaCl) of compound 43o	472
Figure A7.27	^{13}C NMR (100 MHz, CDCl_3) of compound 43o	472
Figure A7.28	^1H NMR (400 MHz, CDCl_3) of compound 44a	473
Figure A7.29	Infrared spectrum (Thin Film, NaCl) of compound 44a	474
Figure A7.30	^{13}C NMR (100 MHz, CDCl_3) of compound 44a	474
Figure A7.31	^1H NMR (400 MHz, CDCl_3) of compound 44b	475
Figure A7.32	Infrared spectrum (Thin Film, NaCl) of compound 44b	476
Figure A7.33	^{13}C NMR (100 MHz, CDCl_3) of compound 44b	476
Figure A7.34	^1H NMR (400 MHz, CDCl_3) of compound 44c	477
Figure A7.35	Infrared spectrum (Thin Film, NaCl) of compound 44c	478
Figure A7.36	^{13}C NMR (100 MHz, CDCl_3) of compound 44c	478
Figure A7.37	^1H NMR (400 MHz, CDCl_3) of compound 44d	479
Figure A7.38	Infrared spectrum (Thin Film, NaCl) of compound 44d	480
Figure A7.39	^{13}C NMR (100 MHz, CDCl_3) of compound 44d	480
Figure A7.40	^1H NMR (400 MHz, CDCl_3) of compound 44e	481
Figure A7.41	Infrared spectrum (Thin Film, NaCl) of compound 44e	482
Figure A7.42	^{13}C NMR (100 MHz, CDCl_3) of compound 44e	482
Figure A7.43	^1H NMR (400 MHz, CDCl_3) of compound 44f	483
Figure A7.44	Infrared spectrum (Thin Film, NaCl) of compound 44f	484
Figure A7.45	^{13}C NMR (100 MHz, CDCl_3) of compound 44f	484
Figure A7.46	^{19}F NMR (282 MHz, CDCl_3) of compound 44f	485
Figure A7.47	^1H NMR (400 MHz, CDCl_3) of compound 44g	486
Figure A7.48	Infrared spectrum (Thin Film, NaCl) of compound 44g	487
Figure A7.49	^{13}C NMR (100 MHz, CDCl_3) of compound 44g	487
Figure A7.50	^1H NMR (400 MHz, CDCl_3) of compound 44h	488
Figure A7.51	Infrared spectrum (Thin Film, NaCl) of compound 44h	489
Figure A7.52	^{13}C NMR (100 MHz, CDCl_3) of compound 44h	489

Figure A7.53	^1H NMR (400 MHz, CDCl_3) of compound 44i	490
Figure A7.54	Infrared spectrum (Thin Film, NaCl) of compound 44i	491
Figure A7.55	^{13}C NMR (100 MHz, CDCl_3) of compound 44i	491
Figure A7.56	^{19}F NMR (282 MHz, CDCl_3) of compound 44i	492
Figure A7.57	^1H NMR (400 MHz, CDCl_3) of compound 44j	493
Figure A7.58	Infrared spectrum (Thin Film, NaCl) of compound 44j	494
Figure A7.59	^{13}C NMR (100 MHz, CDCl_3) of compound 44j	494
Figure A7.60	^1H NMR (400 MHz, CDCl_3) of compound 44k	495
Figure A7.61	Infrared spectrum (Thin Film, NaCl) of compound 44k	496
Figure A7.62	^{13}C NMR (100 MHz, CDCl_3) of compound 44k	496
Figure A7.63	^1H NMR (400 MHz, CDCl_3) of compound 44l	497
Figure A7.64	Infrared spectrum (Thin Film, NaCl) of compound 44l	498
Figure A7.65	^{13}C NMR (100 MHz, CDCl_3) of compound 44l	498
Figure A7.66	^{19}F NMR (282 MHz, CDCl_3) of compound 44l	499
Figure A7.67	^1H NMR (400 MHz, CDCl_3) of compound 44m	500
Figure A7.68	Infrared spectrum (Thin Film, NaCl) of compound 44m	501
Figure A7.69	^{13}C NMR (100 MHz, CDCl_3) of compound 44m	501
Figure A7.70	^1H NMR (400 MHz, CDCl_3) of compound 44n	502
Figure A7.71	Infrared spectrum (Thin Film, NaCl) of compound 44n	503
Figure A7.72	^{13}C NMR (100 MHz, CDCl_3) of compound 44n	503
Figure A7.73	^1H NMR (400 MHz, CDCl_3) of compound 44o	504
Figure A7.74	Infrared spectrum (Thin Film, NaCl) of compound 44o	505
Figure A7.75	^{13}C NMR (100 MHz, CDCl_3) of compound 44o	505
Figure A7.76	^1H NMR (400 MHz, CDCl_3) of compound 44p	506
Figure A7.77	Infrared spectrum (Thin Film, NaCl) of compound 44p	507
Figure A7.78	^{13}C NMR (100 MHz, CDCl_3) of compound 44p	507
Figure A7.79	^1H NMR (400 MHz, CDCl_3) of compound 42a	508
Figure A7.80	Infrared spectrum (Thin Film, NaCl) of compound 42a	509
Figure A7.81	^{13}C NMR (100 MHz, CDCl_3) of compound 42a	509
Figure A7.82	^1H NMR (400 MHz, CDCl_3) of compound 45	510
Figure A7.83	Infrared spectrum (Thin Film, NaCl) of compound 45	511
Figure A7.84	^{13}C NMR (100 MHz, CDCl_3) of compound 45	511
Figure A7.85	^1H NMR (400 MHz, CDCl_3) of compound 46	512
Figure A7.86	Infrared spectrum (Thin Film, NaCl) of compound 46	513
Figure A7.87	^{13}C NMR (100 MHz, CDCl_3) of compound 46	513

Figure A7.88	^1H NMR (400 MHz, CDCl_3) of compound 47	514
Figure A7.89	Infrared spectrum (Thin Film, NaCl) of compound 47	515
Figure A7.90	^{13}C NMR (100 MHz, CDCl_3) of compound 47	515
Figure A7.91	^1H NMR (400 MHz, CDCl_3) of compound 48	516
Figure A7.92	Infrared spectrum (Thin Film, NaCl) of compound 48	517
Figure A7.93	^{13}C NMR (100 MHz, CDCl_3) of compound 48	517

APPENDIX 8

X-Ray Crystallography Reports Relevant to Chapter 3

Figure A8.1	X-Ray Coordination of α -Allyl γ -Butyrolactone 44b	520
--------------------	--	-----

CHAPTER 4

Mechanistic Investigations for Cu-Catalyzed Enantioselective Allylic Alkylation With a γ -Butyrolactone-Derived Silyl Ketene Acetal

Figure 4.1.1	Final Conditions for Cu-Catalyzed Allylic Alkylations with a γ -Butyrolactone-Derived Silyl Ketene Acetal	532
Figure 4.2.1	Traditional Cu-Catalyzed Allylic Alkylations	533
Figure 4.2.2	Cu-Catalyzed Allylic Alkylations with β -Ketoesters	535
Figure 4.2.3	Outer-Sphere Allylic Alkylation Mechanism	535
Figure 4.4.1	Absorption Spectrum of L73 • CuCl₂	538
Figure 4.6.1	Room Temperature UV-vis and 77 K X-band EPR (inset) Spectroscopic Monitoring of the Reaction of 5 mol % of L73 • CuCl₂ with Silyl Ketene Acetal 41	543
Figure 4.6.2	UV-Vis/NIR: Observation of Intermediate During Reduction	544
Figure 4.7.1	^1H NMR (400 MHz, THF-d_8) Spectrum of L73 • CuCl₂ + 30 equivalents of 41	548
Figure 4.7.2	FTIR Spectrum of L73 • CuCl₂ + 30 equivalents of 41	549
Figure 4.7.3	Pd-Catalyzed Enantioselective Arylation of γ -Butyrolactone Silyl Ketene Acetals	551
Figure 4.11.1	Calibration Curve for Spin Quantification	562
Figure 4.11.2	77 K EPR Spectrum of L73 • CuCl₂ in 2-MeTHF	563
Figure 4.11.3	Hartree-Fock dependence on L73 ^{NO} • CuCl₂ (left) versus L73 ^{NN} • CuCl₂ (right) geometry	563

APPENDIX 9

Spectra Relevant to Chapter 4

Figure A9.1	^{13}C NMR (100 MHz, <i>d</i> -THF) of L73•CuCl₂ +30 equiv 41	577
Figure A9.2	^7Li NMR (155 MHz, <i>d</i> -THF) of L73•CuCl₂	577
Figure A9.3	^7Li NMR (155 MHz, <i>d</i> -THF) of L73•CuCl₂ +30 equiv 41	578
Figure A9.4	^1H NMR (400 MHz, CDCl ₃) of compound 43u	579
Figure A9.5	Infrared spectrum (Thin Film, NaCl) of compound 43u	580
Figure A9.6	^{13}C NMR (100 MHz, CDCl ₃) of compound 43u	580
Figure A9.7	^1H NMR (400 MHz, CDCl ₃) of compound 44r	581
Figure A9.8	Infrared spectrum (Thin Film, NaCl) of compound 44r	582
Figure A9.9	^{13}C NMR (100 MHz, CDCl ₃) of compound 44r	582
Figure A9.10	^1H NMR (400 MHz, CDCl ₃) of compound 44s	583
Figure A9.11	Infrared spectrum (Thin Film, NaCl) of compound 44s	584
Figure A9.12	^{13}C NMR (100 MHz, CDCl ₃) of compound 44s	584
Figure A9.13	^1H NMR (400 MHz, CDCl ₃) of compound 44t	585
Figure A9.14	Infrared spectrum (Thin Film, NaCl) of compound 44t	586
Figure A9.15	^{13}C NMR (100 MHz, CDCl ₃) of compound 44t	586
Figure A9.16	^1H NMR (400 MHz, CDCl ₃) of compound 44u	587
Figure A9.17	Infrared spectrum (Thin Film, NaCl) of compound 44u	588
Figure A9.18	^{13}C NMR (100 MHz, CDCl ₃) of compound 44u	588

APPENDIX 11

Palladium-Catalyzed Construction of Quaternary Stereocenters by Enantioselective Vinylation of γ -Lactams and γ -Butyrolactones

Figure A11.1.1	α -Arylation of Lactams and Previously Reported Methods for the Synthesis of Vinyl γ -Lactams	624
-----------------------	---	-----

LIST OF SCHEMES

CHAPTER 1

Enantioselective Alkynylation of Trifluoromethyl Ketones Catalyzed by Cation-Binding Salen Nickel Complexes

Scheme 1.4.1	Initial Results With Unsaturated Trifluoromethyl Ketones	9
Scheme 1.4.2	Precedent for Alkynylation of Unsaturated Trifluoromethyl Ketones	10

Scheme 1.5.1 Effect of KO ^t -Bu on 10a and 11aa	12
---	----

CHAPTER 2

Palladium-Catalyzed Enantioselective Arylation of γ -Lactams with Aryl Chlorides and Bromides

Scheme 2.6.1 Derivatization of Arylation Products.....	123
---	-----

CHAPTER 3

Copper-Catalyzed Enantioselective Allylic Alkylation with a γ -Butyrolactone-Derived Silyl Ketene Acetal

Scheme 3.7.1 Derivatization of 44a and 44q	326
Scheme 3.11.1 Potential Product Transformations for 44q	383

APPENDIX 5

Challenging Substrates in Cu-Catalyzed Enantioselective Allylic Alkylation With Silyl Ketene Acetals

Scheme A5.3.1 With α -Methyl γ -Butyrolactone-Derived Silyl Ketene Acetal	394
Scheme A5.5.1 Proposed Reaction Mechanism.....	402

CHAPTER 4

Mechanistic Investigations for Cu-Catalyzed Enantioselective Allylic Alkylation With a γ -Butyrolactone-Derived Silyl Ketene Acetal

Scheme 4.3.1 Cu-Catalyzed Allylic Alkylation with TEMPO.....	536
Scheme 4.3.2 Cu-Catalyzed Alkylation with Benzyl Chloride.....	537
Scheme 4.6.1 Possible Reaction Mechanisms for Reduction of L73 •CuCl ₂ by 41	545
Scheme 4.8.1 Importance of Olefin Substitution Pattern.....	554
Scheme 4.9.1 Proposed Reaction Mechanism	556

APPENDIX 12

Nickel-Catalyzed Enantioselective Allylic Alkylation of Lactones and Lactams with Unactivated Allylic Alcohols

638

Scheme A12.1.1 Metal-Catalyzed Enantioselective Allylic Alkylations of α -Acyl Lactone and Lactam Prochiral Nucleophiles	639
Scheme A12.4.1 Product Transformations for 122aa	645
Scheme A12.4.2 Product Transformations for 124aa	646

LIST OF TABLES

CHAPTER 1

Enantioselective Alkynylation of Trifluoromethyl Ketones Catalyzed by Cation-Binding Salen Nickel Complexes

Table 1.2.1 Catalyst Development and Reaction Optimization	6
Table 1.3.1 Scope with Aryl Trifluoromethylketones	7
Table 1.3.2 Scope of the Alkyne in the Alkynylation of Aryl Trifluoromethylketones	8
Table 1.5.1 Replication of Hong and Coworkers' Results	11
Table 1.5.2 Amount of KOt-Bu Base	12
Table 1.5.3 Effect of 4 Å Mol Sieves	13
Table 1.6.1 Scope of Enantioselective Alkynylation of Unsaturated Trifluoromethyl Ketones	14

CHAPTER 2

Palladium-Catalyzed Enantioselective Arylation of γ -Lactams with Aryl Chlorides and Bromides

Table 2.3.1 Preliminary Ligand Screen	113
Table 2.3.2 Pd and Additional Ferrocene Ligand Screening	114
Table 2.3.3 Additional Pd and Solvent Screen	115
Table 2.3.4 Examination of the Base, Substrate Stoichiometry, and Temperature	116
Table 2.4.1 Optimization with Aryl Bromides	118
Table 2.5.1 Scope of the <i>N</i> -Protecting Group	119
Table 2.5.2 Scope of the Aryl Halide	120
Table 2.5.3 Scope of the Lactam	121

APPENDIX 2

Challenging Substrates in the Palladium-Catalyzed Enantioselective Arylation of γ -Lactams with Aryl Chlorides and Bromides

Table A2.2.1	γ -Lactams that Resulted in Low Reactivity	163
Table A2.3.1	Additional Aryl Electrophiles Tested	165

APPENDIX 4

X-Ray Crystallography Reports Relevant to Chapter 2

Table A4.1	Crystal Data and Structure Refinement for 32ab	246
Table A4.2	Atomic Coordinates and Equivalent Isotropic Displacement Parameters for 32ab	248
Table A4.3	Bond Lengths and Angles for 32ab	249
Table A4.4	Anisotropic Displacement Parameters for 32ab	253
Table A4.5	Hydrogen Coordinates and Isotropic Displacement Parameters for 32ab	254
Table A4.6	Torsion Angles for 32ab	255
Table A4.7	Crystal Data and Structure Refinement for Pd/L10	257
Table A4.8	Atomic Coordinates and Equivalent Isotropic Displacement Parameters for Pd/L10	258
Table A4.9	Bond Lengths And Angles for Pd/L10	262
Table A4.10	Anisotropic Displacement Parameters for Pd/L10	285
Table A4.11	Hydrogen Coordinates and Isotropic Displacement Parameters for Pd/L10	289
Table A4.12	Torsion Angles for Pd/L10	292

CHAPTER 3

Copper-Catalyzed Enantioselective Allylic Alkylation with a γ -Butyrolactone-Derived Silyl Ketene Acetal

Table 3.2.1	Preliminary Ligand Screen.....	300
Table 3.3.1	Issues with Irreproducibility	302
Table 3.3.2	Effect of Metal:Ligand Ratio.....	303
Table 3.3.3	Initial Bis-Picolinamide Ligand Screen	304
Table 3.3.4	Cu Source Screen.....	305
Table 3.3.5	Importance of Timing of Addition of CsOAc	307
Table 3.3.6	Equivalents of Silyl Ketene Acetal 41	308
Table 3.3.7	Time Difference Between the Addition of 41 and 43a Using Set-up B	309
Table 3.3.8	Timing of the Addition of 43a with Set-up E	313
Table 3.4.1	Importance of Picolinyl Moieties.....	314
Table 3.4.2	Cu Source Screen with L56	315
Table 3.4.3	Ligand Screen	316

Table 3.4.4	Modification of Benzamide Portion of the Ligand.....	317
Table 3.4.5	ANDEN Backbone	318
Table 3.4.6	Modification of the Picolinamide	319
Table 3.5.1	Solvent Screen	321
Table 3.5.2	Catalyst Loading and Concentration.....	322
Table 3.5.3	Cu Salt Screen.....	323
Table 3.5.4	Base Screen.....	323
Table 3.5.5	Catalytic Base Screen	324
Table 3.6.1	Scope of the Allylic Chloride.....	325

APPENDIX 5

Challenging Substrates in Cu-Catalyzed Enantioselective Allylic Alkylation with Silyl Ketene Acetals

Table A5.2.1	Bulky Allylic Electrophiles.....	389
Table A5.2.2	Electrophiles with Coordinating Heteroatoms.....	390
Table A5.2.3	Internal Allylic Chlorides	391
Table A5.2.4	Electrophiles with Two Reactive Sites	392
Table A5.3.1	Other Silyl Ketene Acetals Tested	393
Table A5.3.2	Unreactive Silyl Ketene Acetals.....	396
Table A5.4.1	Acyclic Silyl Ketene Acetals	397
Table A5.4.2	Additional Nucleophiles Tested with L80	398
Table A5.5.1	Cu-Catalyzed Allylic Alkylation With Silyl Enol Ethers With L73	400
Table A5.5.2	Cu-Catalyzed Allylic Alkylation With Silyl Enol Ethers With L21	285
Table A5.5.3	Cu-Catalyzed Allylic Alkylation With Silyl Enol Ethers and TBAT	289

APPENDIX 8

X-Ray Crystallography Reports Relevant to Chapter 3

Table A8.1	Crystal Data and Structure Refinement for 44b	520
Table A8.2	Atomic Coordinates and Equivalent Isotropic Displacement Parameters for 44b ..	522
Table A8.3	Bond Lengths and Angles for 44b	523
Table A8.4	Anisotropic Displacement Parameters for 44b	528
Table A8.5	Hydrogen Coordinates and Isotropic Displacement Parameters for 44b	529

CHAPTER 4*Mechanistic Investigations for Cu-Catalyzed Enantioselective Allylic Alkylation With a γ -Butyrolactone-Derived Silyl Ketene Acetal*

Table 4.5.1	DFT Calculations on L73 and L73•CuCl₂	541
Table 4.5.2	DFT Calculations on L56 and L56•CuCl₂	542
Table 4.7.1	Energetic Preference for C-Bound Enolate	552
Table 4.11.1	Effects of Levels of Theory on the Optimized Geometry of L73•CuCl₂	565
Table 4.11.2	Effects of Levels of Theory on the Energy Barrier	565

APPENDIX 11*Palladium-Catalyzed Construction of Quaternary Stereocenters by Enantioselective Vinylation of γ -Lactams and γ -Butyrolactones*

Table A11.2.1	Initial Hit and Temperature Screen With 2-Chloropropene.....	625
Table A11.2.2	Vinylation With 2-Bromopropane	626
Table A11.3.1	Temperature Screen with Isocrotyl Chloride.....	627
Table A11.3.2	Effect of the <i>N</i> -Protecting Group	628
Table A11.3.3	Examination of Different Pd(0) Sources	629
Table A11.3.4	Additional Ligand Screen	630
Table A11.3.5	Effect of LiCl on the Reaction Outcome and Solvent Screen	631
Table A11.3.6	Concentration, Temperature, and Reaction Time	632
Table A11.4.1	Preliminary Results With α -Methyl- γ -Butyrolactone	633

APPENDIX 12**638***Nickel-Catalyzed Enantioselective Allylic Alkylation of Lactones and Lactams with Unactivated Allylic Alcohols*

Table A12.2.1	Optimization of Reaction Parameters	641
Table A12.3.1	Nucleophile and Electrophile Scope	642
Table A12.3.2	α -Acyl Lactam Prochiral Nucleophiles.....	643
Table A12.3.3	Linear versus Branched Cinnamyl Alcohol	644

LIST OF ABBREVIATIONS

$[\alpha]_D$	specific rotation at wavelength of sodium D line
$^{\circ}\text{C}$	degrees Celsius
\AA	Ångstrom
aq	aqueous
Ar	aryl
atm	atmosphere
Bn	benzyl
Boc	<i>tert</i> -butoxycarbonyl
bp	boiling point
br	broad
Bz	benzoyl
<i>c</i>	concentration for specific rotation measurements
calc'd	calculated
cat	catalytic
cm^{-1}	wavenumber(s)
cod	1,5-cyclooctadiene
d	doublet
D	deuterium
dba	dibenzylideneacetone
DMAP	4-diethylaminopyridine
DME	1,2-dimethoxyethane

DMF	<i>N,N</i> -dimethylformamide
DMS	dimethylsulfide
<i>ee</i>	enantiomeric excess
EI+	electron impact
equiv	equivalent(s)
ESI	electrospray ionization
Et	ethyl
EtOAc	ethyl acetate
FAB	fast atom bombardment
G	gram(s)
GC	gas chromatography
H	hour(s)
HG-II	Hoveyda-Grubbs catalyst 2 nd generation
HPLC	high-performance liquid chromatography
HRMS	high-resolution mass spectroscopy
Hz	hertz
IPA	isopropanol
IR	infrared (spectroscopy)
<i>J</i>	coupling constant
K	Kelvin(s) (absolute temperature)
kcal	kilocalorie
KHMDS	potassium hexamethyldisilazide
L	liter; ligand

L*	chiral ligand
LDA	lithium diisopropylamide
LiHMDS	lithium hexamethyldisilazide
M	multiplet; milli
<i>m</i>	meta
<i>m/z</i>	mass to charge ratio
Me	methyl
mg	milligram(s)
MHz	megahertz
min	minute(s)
MM	mixed method
mol	mole(s)
MOM	methoxymethyl acetal
mp	melting point
n	nano
NaHMDS	sodium hexamethyldisilazide
<i>n</i> -Bu	butyl
NMR	nuclear magnetic resonance
Nu	nucleophile
<i>o</i>	ortho
<i>p</i>	para
Pd/C	palladium on carbon
Ph	phenyl

pH	hydrogen ion concentration in aqueous solution
PHOX	phosphinooxazoline ligand
pmdba	bis(4-methoxybenzylidene)acetone
ppm	parts per million
Pr	propyl
q	quartet
R	generic for any atom or functional group
RCM	ring-closing metathesis
Ref.	reference
R_f	retention factor
s	singlet
sat.	saturated
SFC	supercritical fluid chromatography
t	triplet
<i>t</i> -Bu	<i>tert</i> -butyl
TBAF	tetrabutylammonium fluoride
TBME	<i>tert</i> -butyl methyl ether
TBS	<i>tert</i> -butyldimethyl silyl
THF	tetrahydrofuran
TIPS	triisopropylsilyl
TLC	thin-layer chromatography
TMS	trimethylsilyl
TOF	time-of-flight

t_R	retention time
UV	ultraviolet
v/v	volume to volume
w/v	weight to volume
λ	wavelength
μ	micro

CHAPTER 1

Enantioselective Alkynylation of Trifluoromethyl Ketones

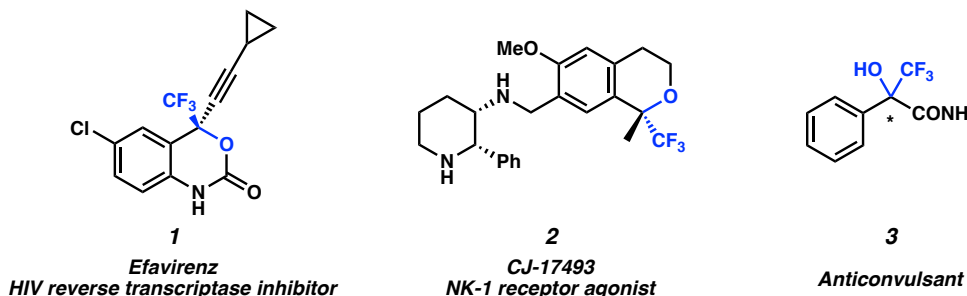
Catalyzed by Cation-Binding Salen Nickel Complexes[†]

1.1 INTRODUCTION, BACKGROUND, AND SYNTHETIC UTILITY

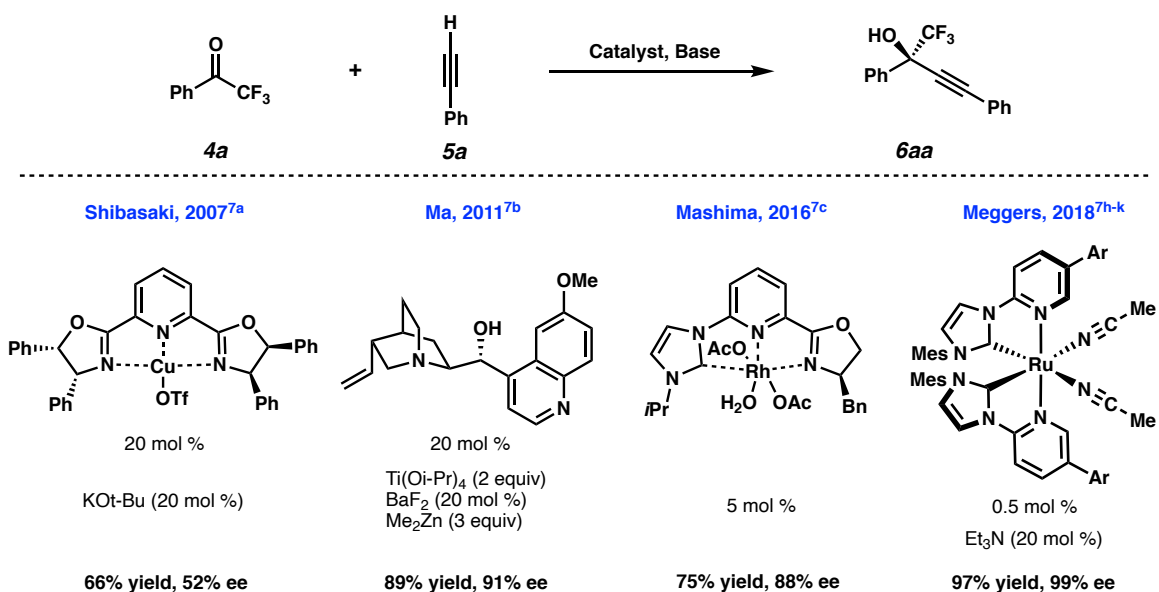
Fluorinated organic compounds have proven to be exceptionally useful in many areas of organic chemistry, including materials, agrochemicals, and pharmaceuticals.¹ In particular, the trifluoromethyl group has emerged as a crucial motif in medicinal chemistry, as its incorporation may have a significant effect on the physicochemical and biological properties of drug targets through alteration of steric, electronic, lipophilic, and metabolic properties. The trifluoromethyl group possesses a van der Waals volume of 39.8 Å³, and is an isostere of the isopropyl group.^{2a} It is also highly electron-withdrawing, affecting the reactivity of adjacent functional groups, and in many cases increasing the molecule's stability. In addition, the fluorine atoms may also participate in hydrogen bonding, which can be useful for the rational design of molecules that bind selectively to their specific target.^{2b}

[†] This research was performed in collaboration with the Hong lab at the Gwangju Institute of Science and Technology in Korea. This research has been published and adapted with permission from Park, D.; Jette, C. I.; Kim, J.; Jung, W. -O.; Lee, Y.; Park, J.; Kang, S.; Han, M. S.; Stoltz, B. M.; Hong, S. *Angew. Chem. Int. Ed.* **2020**, 59, 775–779. Copyright 2020 Wiley-VCH.

Figure 1.1.1. Examples of Bioactive Compounds Containing a Trifluoromethylcarbinol



More specifically, chiral trifluoromethyl substituted tertiary alcohols and related derivatives are structural motifs present in numerous bioactive compounds (Figure 1.1.1, **1–3**). Of particular importance is Efavirenz (**1**), a frequently prescribed HIV reverse transcriptase inhibitor.³ One attractive strategy for the enantioselective synthesis of these motifs is the asymmetric alkynylation of trifluoromethyl ketones. This type of reaction may be catalytic in base, resulting in exceptionally mild reaction conditions, and the newly installed alkyne may be easily converted to

Figure 1.1.2 Previous Reports of Asymmetric Alkynylation of Trifluoromethyl Ketones⁷

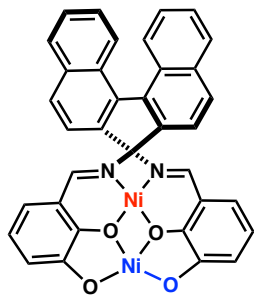
a diverse array of functional groups (Figure 1.1.2). Since Carreira's pioneering report,^{4a} several catalysts have been developed for the enantioselective alkynylation of aldehydes,⁴ imines,⁵ and alkyl ketones.⁶ In contrast, there are fewer reports on the enantioselective alkynylation of trifluoromethyl ketones,^{7,8} as the high reactivity of these electron-deficient electrophiles has led to significant challenges associated with facial selectivity. Although there have been some reports on the enantioselective variant of this transformation, they all suffer from significant drawbacks, such as high temperatures,^{7a} large excesses of expensive reagents,^{7b,d} or the use of precious, second-row transition metals as catalysts.^{7c,h-k}

In an effort to develop a more sustainable method for the enantioselective alkynylation of trifluoromethyl ketones, we turned our attention to the development of a bifunctional catalyst, in which two metals are held in place by the same ligand scaffold. One metal activates the nucleophile (a Brønsted base) and the other activates the electrophile (a Lewis acid).^{9a} These types of bifunctional catalysts typically rely on a Salen-type framework to position both the Lewis Acid and the Brønsted base in the optimal geometry (Figure 1.1.3.A). Previously reported catalysts of this type have been used for Michael additions, as well as Mannich and Aldol reactions. In two of these examples, the Brønsted base is the metal phenoxide incorporated into the framework (Figure 1.1.3. A, **7** and **9**). One characteristic of these catalysts is that they furnish the desired products in very high yields and selectivities,^{9a-h} as the use of a single species to activate and bring together both the nucleophile and electrophile leads to a well-defined environment for the reactive intermediates.^{9a} For this reason, we envisioned that the use of a bifunctional catalyst would enable efficient control over the facial selectivity of the highly reactive trifluoromethyl ketone. The use of the salen ligand framework with a pendant crown ether^{10,11} which can interact with an alkali

metal cation would facilitate this form of cooperative catalysis, as the Lewis acid and Brønsted base could be held in close proximity by a very rigid and specific structure. In addition, the crown ether should increase the reactivity of the base, and impart a larger degree of rigidity to the catalyst (1.1.3.B).

Figure 1.1.3. Chiral Bifunctional Catalysts⁹

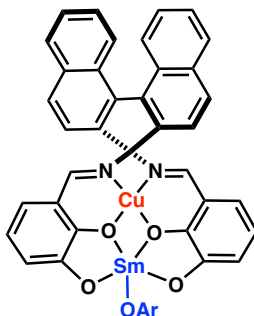
A. Examples of previously reported bifunctional catalysts:



7

Michael additions
to nitro-olefins

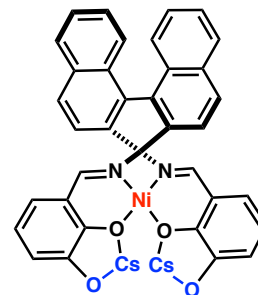
up to 98% yield,
94% de,
99% ee



8

Mannich reactions
with alkyl nitrates

up to 96% yield,
90% de,
98% ee

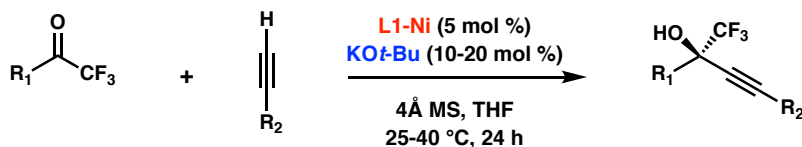


9

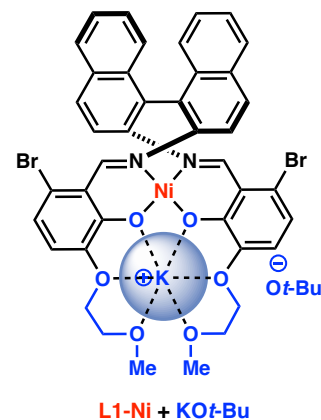
Michael additions
of β -ketoesters

up to 45% yield,
90% ee

B. This research: Ni-catalyzed enantioselective alkynylation via bifunctional catalysis:



R₁ = aryl vinyl
R₂ = aryl, cyclopropyl



Red = Lewis Acid, Blue = Brønsted Base.^{9a-h}

1.2 CATALYST DEVELOPMENT AND OPTIMIZATION OF REACTION CONDITIONS

To assess the efficacy of this type of cooperative catalyst we first synthesized and tested a number of ligand frameworks possessing oligo-ethers of varying length. We were pleased to find that ligand **L2**, with a binaphthyl backbone and methoxyethane side chains, in combination with a Ni Lewis acid and KO*t*-Bu Brønsted base, furnished the desired product in excellent yields and ee (Table 1.2.1, entry 1). Interestingly, we found that although oligo-ether chain length did not have a significant effect on the ee, it did have an effect on the yield. Switching to a ligand possessing methoxy substituents (**L3**), or extending the chain length (**L4**) resulted in less efficient catalysts (entries 2 and 3). It is also important to note that the presence of a coordinating ether moiety was critical for reactivity, as a *tert*-butyl substituent at this position completely shut down the reaction (entry 4, **L5**). In addition, we found Ni^{II} to be the optimal Lewis acid; switching to Co or Zn led to a significant drop in ee, and Pd led to complete loss of reactivity (entries 5-7).

Next, we examined the importance of the counter-ion on the *tert*-butoxide base. The highest enantioselectivity and yield was observed with KO*t*-Bu; both LiO*t*-Bu and NaO*t*-Bu led to a slight reduction in yield and ee (entry 1 vs entries 8 and 9). When the reaction temperature was lowered from 50 °C to 25 °C, the ee was increased to 89% ee (entry 10). Lowering the temperature even further to -10 °C, however, led to the complete loss of reactivity (entry 11). Having investigated all other parameters, we returned to our ligand, focusing on examining the effect of different steric and electronic modifications on the backbone. We found that the binaphthyl backbone was crucial for reactivity: when a ligand possessing a cyclohexyl backbone was used instead, no product was observed (**L6**, entry 12). In agreement with the work of Wang and co-workers¹² we found that the

Table 1.2.1. Catalyst Development and Reaction Optimization^a

$\text{4a} + \text{5a} \xrightarrow[\text{4 Å MS, THF (0.48 M), Temp, 24 h}]{\text{Catalyst (5 mol \%), Base (20 mol \%)}} \text{6aa}$

Entry	Metal	Ligand	Base	Temp (°C)	Yield (%) ^b	% ee ^c
1	Ni	L2	KOt-Bu	50	97	84
2	Ni	L3	KOt-Bu	50	48	82
3	Ni	L4	KOt-Bu	50	86	86
4	Ni	L5	KOt-Bu	50	—	—
<hr/>						
5	Co	L2	KOt-Bu	50	91	49
6	Zn	L2	KOt-Bu	50	64	77
7	Pd	L2	KOt-Bu	50	—	—
<hr/>						
8	Ni	L2	LiOt-Bu	50	86	78
9	Ni	L2	NaOt-Bu	50	83	85
10	Ni	L2	KOt-Bu	25	93	89
11	Ni	L2	KOt-Bu	−10	—	—
<hr/>						
12	Ni	L6	KOt-Bu	50	—	—
13	Ni	L7	KOt-Bu	50	97	88
14	Ni	L1	KOt-Bu	50	95	91
15	Ni	L1	KOt-Bu	25	93	93

L2: R₁ = O-CH₂CH₂O-CH₃
L3: R₁ = O-CH₃
L4: R₁ = O-[CH₂CH₂O]₂-CH₃
L5: R₁ = *t*-Bu

L6

L7: R₂ = Br, R₃ = H
L1: R₂ = H, R₃ = Br

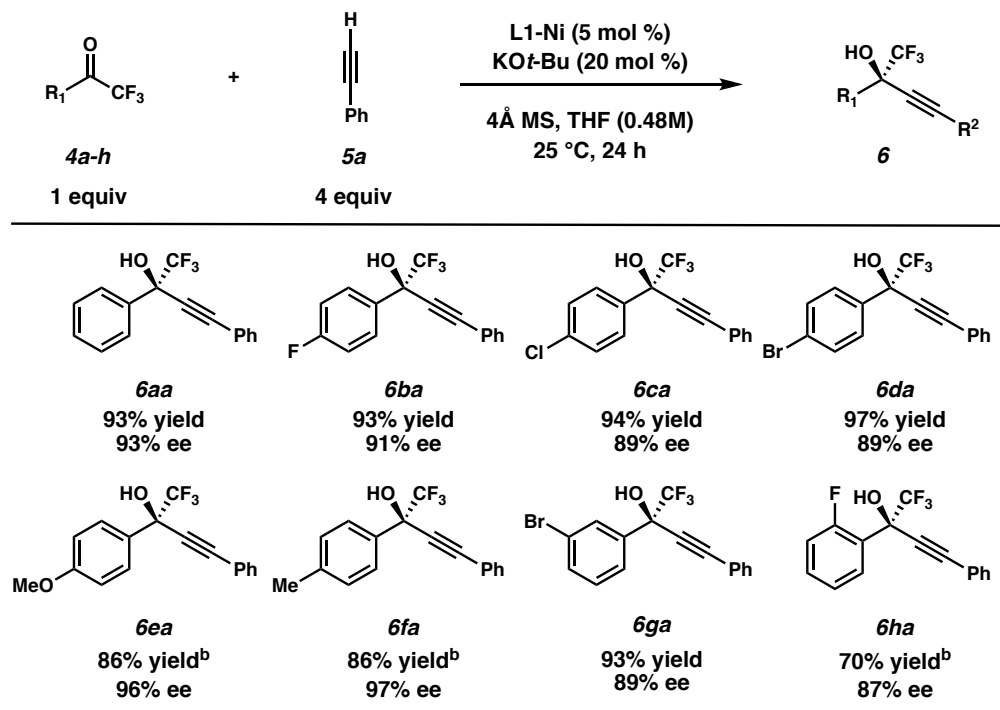
[a] Reactions were performed on a 0.242 mmol scale. [b] Isolated yields. [c] The ee values were determined by HPLC analysis.

introduction of bromide substituents on the salicyl arenes led to a slight improvement in the ee (entries 13 and 14). Using the 6-Bromo-Salen ligand (**L1**), the product was obtained in 93% yield and 93% ee at 25 °C under air (entry 15).

1.3 ARYL TRIFLUOROMETHYL KETONE SUBSTRATE SCOPE

With the optimized reaction conditions in hand, the substrate scope of the asymmetric alkynylation of aryl trifluoromethyl ketones was explored (Table 1.3.1). Electrophiles possessing both electron-donating substituents (**6aa**, **6ea**, **6fa**) and electron-withdrawing substituents (**6ba**, **6ca**, **6da**) at the *para*-position of the arene were well-tolerated, resulting in the desired products in up to a 97% ee and 97% yield. Although substitution at the *meta*-position of the aryl ring was also tolerated (**6ga**), *ortho*-substitution did lead to a

Table 1.3.1. Scope with Aryl Trifluoromethyl Ketones^a

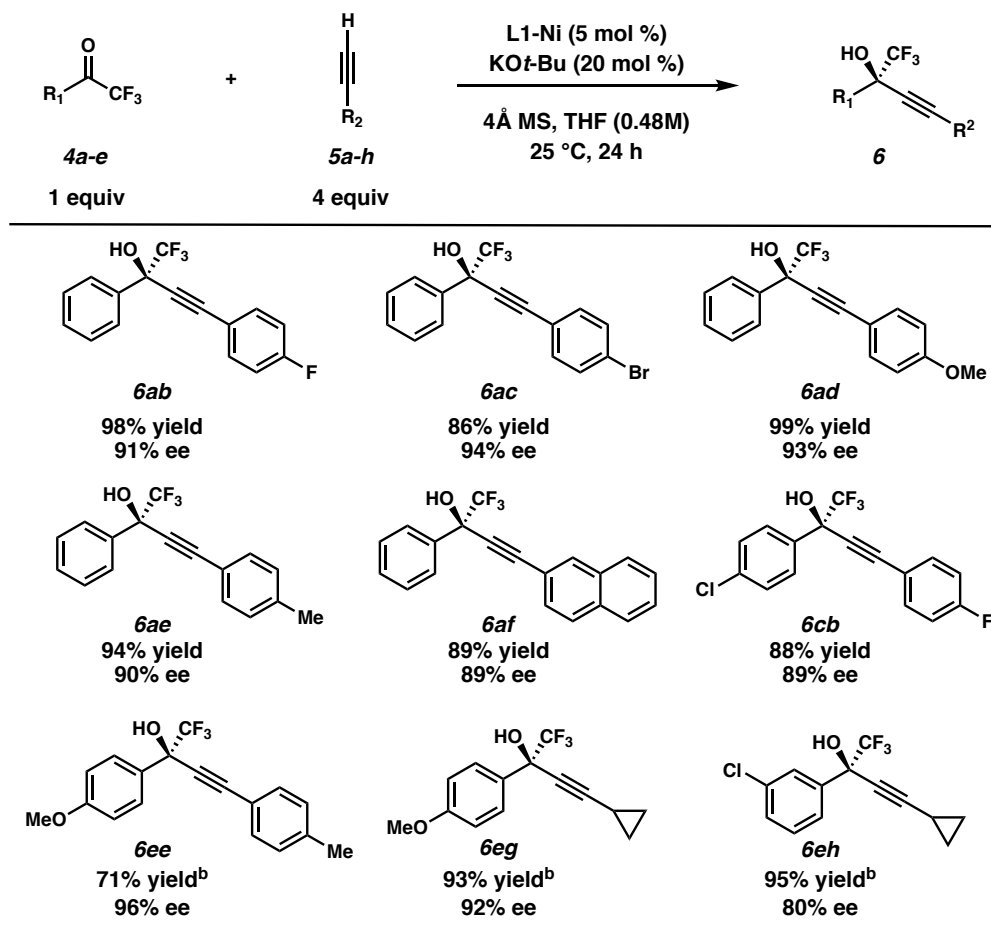


[a] Isolated yields on 0.242 mmol scale. Enantiomeric excess was determined by HPLC analysis. [b] Isolated yield after 48 h.

drop in yield (**6ha**). We noted that generally, the yields for electron-deficient trifluoromethyl ketones were slightly higher than with electron-rich substrates, with the latter requiring extended reaction times. However, we did note that the ee's for electron-rich substrates were consistently higher than their electron-deficient counter-parts.

We found that the nature of the alkyne had a less pronounced effect on the overall outcome of the reaction, and alkynes possessing both electron-withdrawing (**6ab**, **6ac**, **6cb**) and electron-donating substituents (**6ad**, **6ae**, **6ee**) at the *para*-position of the aryl substituent were well-tolerated. Furthermore,

Table 1.3.2. Scope of the Alkyne in the Alkynylation of Aryl Trifluoromethyl Ketones^a

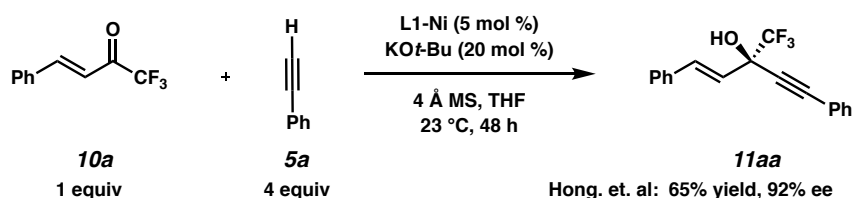


[a] Isolated yields on 0.242 mmol scale. Enantiomeric excess was determined by HPLC analysis. [b] Isolated yield after 48 h.

we were pleased to observe that a bulky naphthyl substituent (**6af**) and a cyclopropyl substituent (**6eg** and **6eh**) also led to product formation in good yields and ee.

1.4 ALKYNYLATION OF UNSATURATED TRIFLUOROMETHYL KETONES

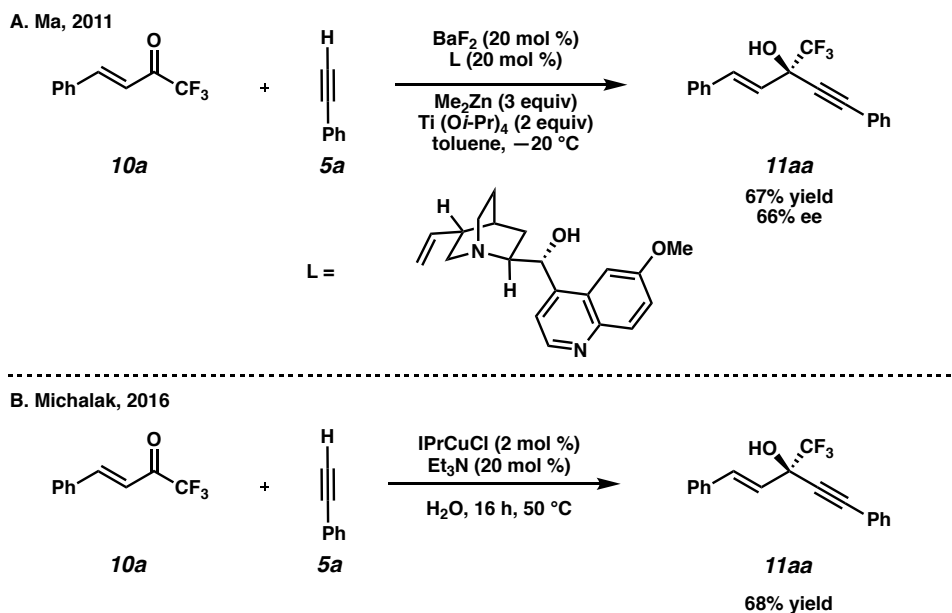
Scheme 1.4.1. Initial Results with Unsaturated Trifluoromethyl Ketones



In addition to the extensive scope with aryl trifluoromethyl ketones, Hong and coworkers found that phenylacetylene **5a** could be added to unsaturated trifluoromethyl ketone **10a** exclusively in a 1,2 fashion to form the vinyl trifluoromethyl carbinol **11aa** in 65% yield and 92 % ee (Scheme 1.4.1).¹³ The products of the alkynylation of these unsaturated ketones are especially useful synthetic intermediates, as they contain three functional handles: an alcohol, an alkene, and an alkyne.

Examination of the literature showed that the synthesis of **11aa** has been reported twice before. In 2011, Ma and coworkers showed that exclusive 1,2 addition of phenylacetylene to unsaturated ketone **10a** could be achieved in 68% yield and 66% ee using a system involving BaF₂, Ti(Oi-Pr)₄, Me₂Zn, and a cinchona-derived ligand (Scheme 1.4.2.A).^{7b} More recently, Michalak reported the formation of the alkenyl trifluoromethyl carbinol with a Cu-NHC catalyst and Et₃N as the base (Scheme 1.4.2.B).^{7k} Although the yields achieved in both of these systems are comparable to that reported by Hong and coworkers, the high ee achieved using the Ni^{II} salen

Scheme 1.4.2. Precedent for Alkynylation of Unsaturated Trifluoromethyl Ketones^{7b,k}



catalyst makes the current system the best to date for the formation of these products.

1.5 REACTION OPTIMIZATION FOR UNSATURATED TRIFLUOROMETHYL KETONES

We initiated our studies by attempting to replicate the results reported by Hong and coworkers.¹³ Unfortunately, with the reported procedure, the product was obtained in no greater than a 20% yield and 88% ee (Table 1.5.1, entries 1 and 2). Analysis of the reported procedure showed that there were a few parameters that could be modified. The first is that a commercially available 1.0 M solution of KO*t*-Bu in THF was being used. By switching to solid KO*t*-Bu, possible errors in titration or fluctuations in concentration would be avoided, and variability in the

amount of base added would be reduced. Gratifyingly, we found that switching to solid KO*t*-Bu resulted in over a 22% boost in yield (entry 3).

Table 1.5.1 Replication of Hong and Coworkers' Results

entry	set-up location	concentration (M)	KO <i>t</i> -Bu source	conversion (%) ^a	yield (%) ^a	ee (%) ^b
1	fume hood	0.5	1.0 M in THF	40	10	–
2 ^c	fume hood	0.5	1.0 M in THF	60	20	88
3	fume hood	0.5	solid KO <i>t</i> -Bu	100	42	88
4	glovebox	0.5	solid KO <i>t</i> -Bu	100	65	88
5	glovebox	0.1	solid KO <i>t</i> -Bu	76	62	88
6 ^d	glovebox	0.1	solid KO <i>t</i> -Bu	100	68	88

[a] Conversions and yields were determined by ¹HNMR with trimethoxybenzene as an internal standard. [b] Enantiomeric excess (% ee) was determined by SFC. [c] With distilled alkyne, new bottle of KO*t*-Bu solution. [d] Pre-mix KO*t*-Bu and Ni-cat.

By switching to a glovebox reaction set-up, we were finally able to replicate the 65% yield reported by Hong and coworkers, although the ee was slightly lower than their reported 92% (entry 4). In order to facilitate reaction screening at very low quantities, the reaction concentration was lowered to 0.1 M (entry 5), with no significant effect on the yield or ee. Finally, pre-stir of the Ni-catalyst with the KO*t*-Bu base resulted in a slight improvement in yield (entry 6).

With these results in hand, two more reaction parameters were examined; the amount of KO*t*-Bu base and mol sieves used in the reaction. In the initial conditions developed by Hong and coworkers, 20 mol % KO*t*-Bu is used (entry 2, Table 1.5.2.). Increasing the amount of base to 40

mol % was detrimental to the reaction (entry 3), while decreasing the amount down to 10 mol %

Table 1.5.2. Amount of *KOt*-Bu Base

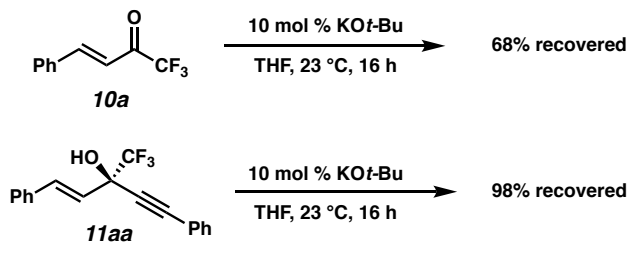
entry	mol % <i>KOt</i> -Bu	conversion (%) ^a	yield (%) ^a	ee (%) ^b
1	10	91	72	90
2	20	100	68	88
3	40	89	13	–

[a] Conversions and yields were determined by ¹HNMR with trimethoxybenzene as an internal standard. [b] Enantiomeric excess (% ee) was determined by SFC.

resulted in a modest boost in yield (entry 1).

To determine if these results were due to basic decomposition of the starting material or the product, both **10a** and **11aa** were stirred for 16 h with 10 mol % *KOt*-Bu (Scheme 1.5.1). The product was fully recovered, but only 68% of the starting material was recovered, suggesting that the low yield with excess base may be due to the decomposition of the starting material **10a**.

Scheme 1.5.1. Effect of *KOt*-Bu on **10a** and **11aa**^a

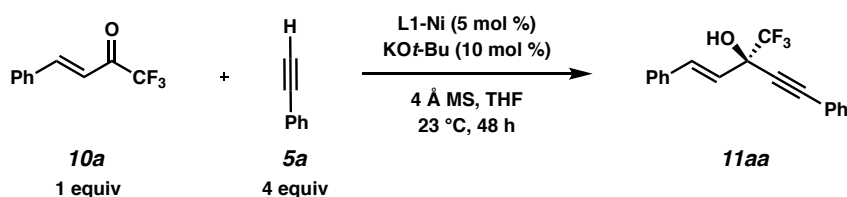


[a] Yields were determined by ¹HNMR with trimethoxybenzene as an internal standard.

Hong and coworkers' original reaction conditions did not involve a moisture-free reaction set-up, and we envisioned that this could be the reason that a large excess of 4 Å molecular sieves

was required. Since we had switched to a glovebox set-up, the last parameter we decided to investigate was the quantity of molecular sieves in the reaction. Entry 2 (Table 1.5.3.) shows the initial amount of molecular sieves used for a 0.05 mmol scale reaction. Increasing the amount of molecular sieves does lead to a slight drop in yield (entry 1). As the amount of molecular sieves is

Table 1.5.3. Effect of 4 Å Mol Sieves



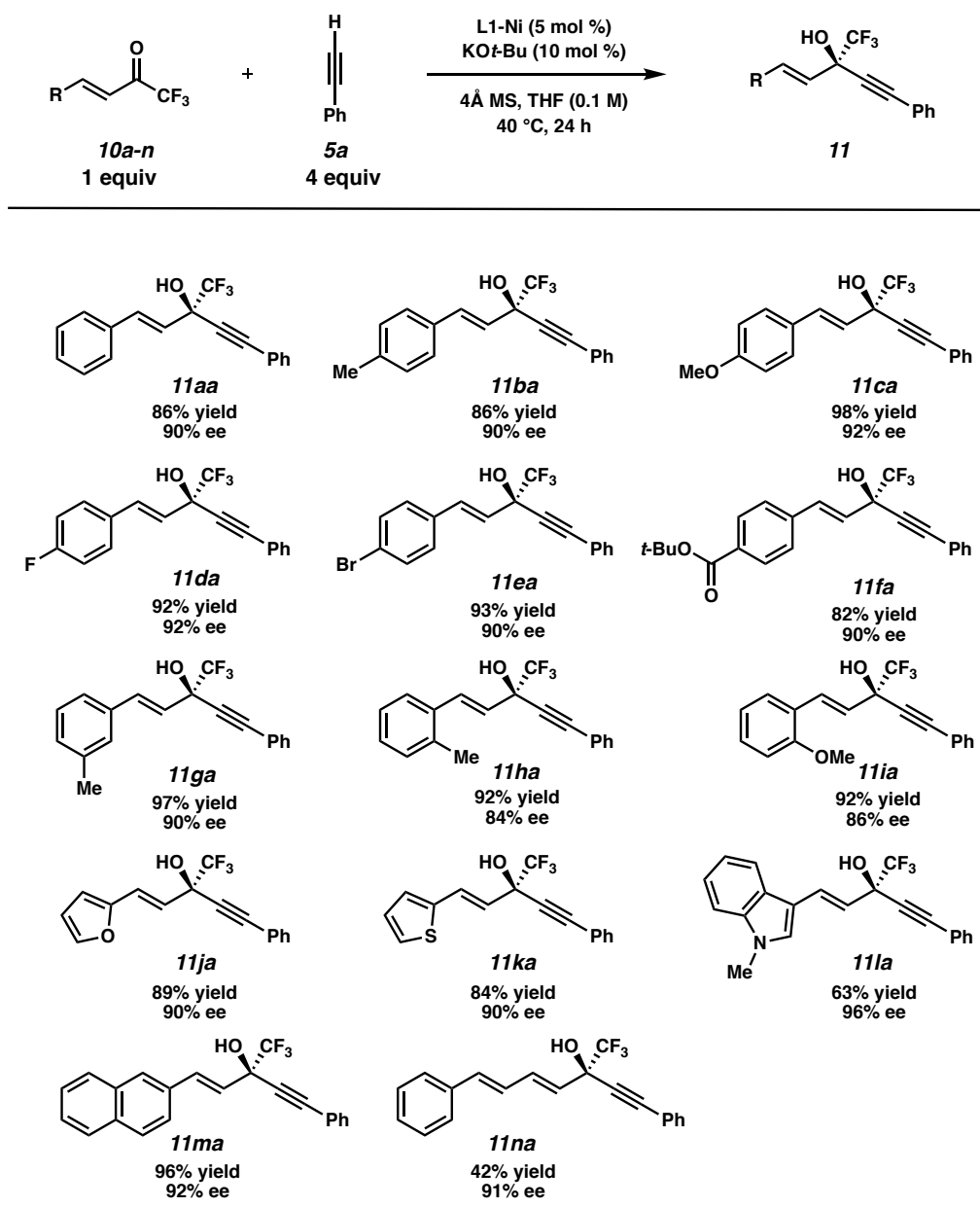
entry	4 Å mol sieves 0.05 mmol scale (mg)	conversion (%) ^a	yield (%) ^a	ee (%) ^b
1	45	66	65	90
2	32	77	75	90
3	24	78	78	88
4	18	82	78	88
5	8	84	81	90
6	5	82	77	90
7	0	0	73	90
8 ^c	8	—	84	88

[a] Yields were determined by ¹H NMR with trimethoxybenzene as an internal standard. [b] Enantiomeric excess (% ee) was determined by SFC. [c] At 40 °C, 24 h.

decreased, the yield increases, up to 81% with 8 mg of mol sieves (entry 5). Decreasing the quantity of molecular sieves even further (entry 6), or excluding them altogether (entry 7) led to no improvements. These results indicate that the molecular sieves are beneficial but not critical for reactivity.

1.6 SCOPE OF ENANTIOSELECTIVE ALKYNYLATION OF UNSATURATED TRIFLUOROMETHYL KETONES

Table 1.6.1 Scope of Enantioselective Alkynylation of Unsaturated Trifluoromethyl Ketones^a

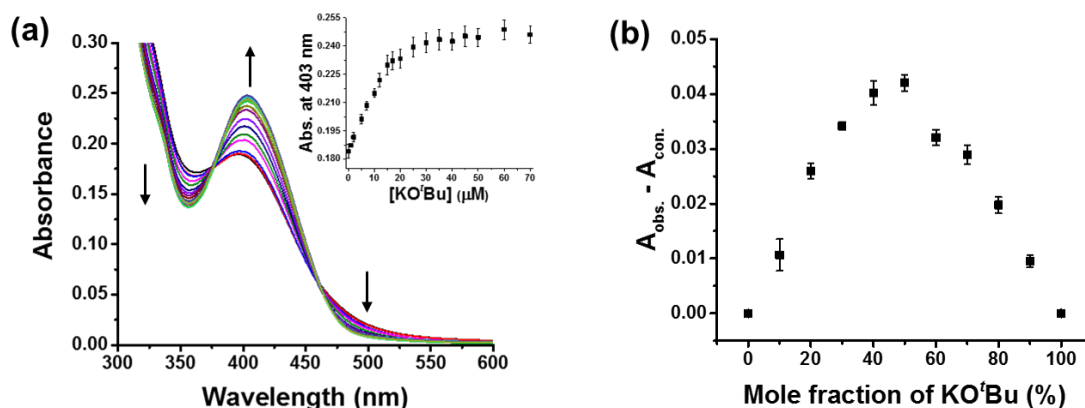


[a] Isolated yields on 0.2 mmol scale. Enantiomeric excess (% ee) was determined by SFC analysis.

We next examined the scope of the enantioselective alkynylation of unsaturated trifluoromethyl ketones. Enones possessing aryl rings with substituents at the *para* (**11ba**, **11ca**, **11da**, **11ea**), *meta* (**11ga**), and even *ortho* (**11ha** and **11ia**) positions were all well-tolerated. We were also pleased to see that a *tert*-butyl ester-containing substrate (**11fa**) and a diene (**11na**) fared well under these mild reaction conditions. Even substrates possessing heteroaromatic substituents such as a furan (**11aj**), thiophene (**11ak**), and indole (**11al**) led to product formation in good yield and excellent ee.

1.7 PRELIMINARY MECHANISTIC INVESTIGATIONS

Figure 1.7.1. Metal Ion Titration Studies via UV-Vis Absorption



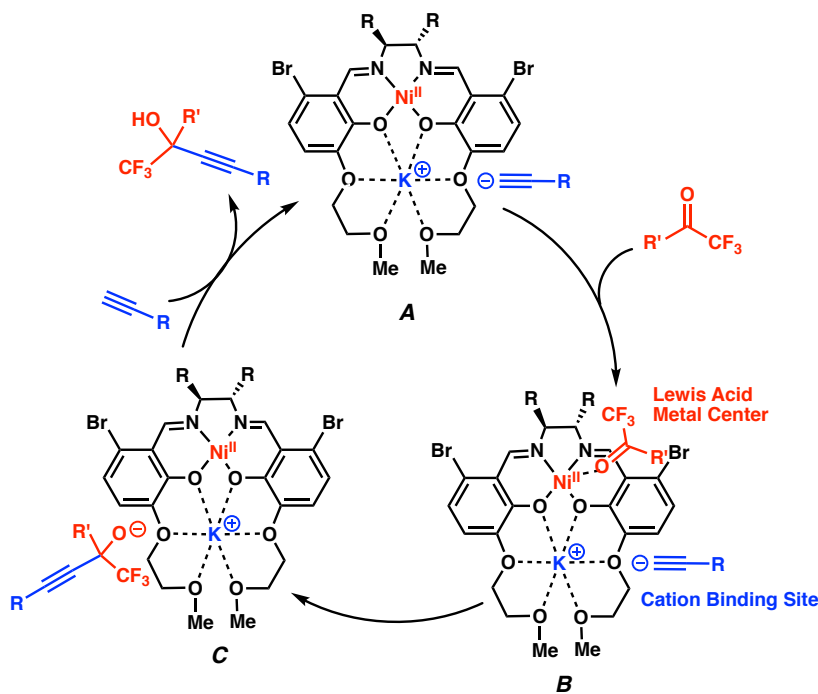
(a) UV-Vis spectra of **L1-Ni** (20 μM) in the presence of varying amounts of KOt-Bu (0 ~ 70 μM) in THF. Inset: Plot of absorbance at 403 nm versus concentration of KOt-Bu . (b) Job plot for binding mode between **L1-Ni** and K^+ ions in THF. A_{obs} : Absorbance of **L1-Ni** at 403 nm with varying amounts of KOt-Bu ; $[\text{L1-Ni}] + [\text{KOt-Bu}] = 40 \mu\text{M}$, $A_{\text{con.}}$: Absorbance of **L1-Ni** (40 to 0 μM) at 403 nm without KOt-Bu .

To investigate the binding behavior between **L1-Ni** and K^+ , we carried out metal ion titration studies, which were monitored by UV-vis absorption spectroscopy.¹⁴ Upon addition of KOt-Bu to a solution of **L1-**

Ni, the UV-vis absorption spectrum exhibited characteristic peaks at 350, 403, and 350 nm with two clear isosbestic points at 376 and 460 nm (Figure 1.7.1.A). The absorbance at 403 nm for **L1-Ni**/ K^+ tended to proportionally increase with KOt -Bu concentration up to 20 μ M, and then reached saturation region. Job plot analysis (Figure 1.7.1.B) was in good agreement with the titration study, clearly confirming that **L1-Ni** binds to K^+ with 1:1 binding stoichiometry. From the titration data based on the 1:1 binding model, the association constant (K_a) for binding of **L1-Ni** and K^+ ions was calculated to be $6.6 \times 10^5 \text{ M}^{-1}$ using non-linear regression analysis by DynaFit.¹⁵

A plausible catalytic cycle for the alkynylation reaction is shown in Figure 1.7.2. The mechanism is expected to begin with the deprotonation of the terminal alkyne to form potassium acetylide **A**. Then, the trifluoromethyl ketone can coordinate to the Ni Lewis acid to form intermediate **B**. Once both the nucleophile and electrophile are bound to the catalyst, they are in close enough proximity for bond

Figure 1.7.2. Proposed Reaction Mechanism



formation to occur. The resulting propargyl alcohol can then bind to the potassium cation (C), and function as the base for the deprotonation of the next molecule of terminal alkyne.

1.8 CONCLUSIONS

We have developed cation-binding salen Ni catalysts for enantioselective alkynylation of aryl and unsaturated trifluoromethyl ketones. Critical to the improvement of the reaction conditions for the alkynylation of the unsaturated trifluoromethyl ketones was the use of a glove box set-up, reduction in quantities of both KO t -Bu and molecular sieves, and slightly elevated temperatures. The cation-binding Ni^{II}/K⁺ heterobimetallic catalyst plays a key role in promoting the alkynylation with substoichiometric base and open to air in select cases,¹⁴ resulting in high enantioselectivity (up to 97% ee) and yield (up to 99%). Additionally, we confirmed a 1:1 binding stoichiometry of the designed catalyst with K⁺ by UV-vis absorption spectroscopy.

1.9 EXPERIMENTAL SECTION

1.9.1 MATERIALS AND METHODS

Unless otherwise stated, all reactions were carried out under air atmosphere. Reaction progress was monitored by thin-layer chromatography (TLC) or Agilent 1290 UHPLC-MS. TLC was performed using E. Merck silica gel 60 F254 precoated glass plates (0.25 mm) and visualized by UV fluorescence quenching, *p*-anisaldehyde, or KMnO₄ staining. Silicycle SiliaFlash® P60 Academic Silica gel (particle size 40–63 nm) or 230-400 Mesh 60 Å Silica Gel (Merck Inc.) was used for flash chromatography. All alkynylation reactions were performed in a 10 ml vial sealed

with a screw cap. At the Gwangju Institute of Science and Technology (GIST), all NMR spectra was recorded on a JEOL spectrometer, operating at 400 MHz or 300 MHz for ^1H NMR and at 100 MHz or 75 MHz for ^{13}C NMR. At the California Institute of Technology (Caltech), ^1H NMR spectra were recorded on Bruker 400 MHz or Varian Mercury 300 MHz spectrometers. ^{13}C NMR spectra were recorded on Bruker 400 MHz spectrometer (101 MHz). ^{19}F NMR spectra were recorded on Varian Mercury 300 MHz spectrometer (282 MHz). Data for ^1H NMR are reported as follows: chemical shift (δ ppm) (multiplicity, coupling constant (Hz), integration). Multiplicities are reported as follows: s = singlet, d = doublet, t = triplet, q = quartet, p = pentet, sept = septuplet, m = multiplet, br s = broad singlet, br d = broad doublet, app = apparent. Data for ^{13}C NMR are reported in terms of chemical shifts (δ ppm). All chemical shifts for ^1H and ^{13}C NMR were referenced to residual signals from CDCl_3 (^1H) 7.26 ppm and (^{13}C) 77.16 ppm. High-resolution mass spectra (HRMS) were recorded on a JEOL JMS-700 MStation mass spectrometer. At the GIST, Infrared (IR) spectra were obtained on a Nicolet iS10 FT-IR spectrometer with an ATR unit and recorded in wave numbers (cm^{-1}). At Caltech, the IR spectra were obtained using Perkin Elmer Spectrum BXII spectrometer or Nicolet 6700 FTIR spectrometer using thin films deposited on NaCl plates and reported in frequency of absorption (cm^{-1}). High-performance liquid chromatography (HPLC) was performed on an Agilent 1260 Infinity Series machine equipped with a variable wavelength detector and Daicel Chiralpak I Series columns (0.46 cm x 25 cm). Analytical SFC was performed with a Mettler SFC supercritical CO_2 analytical chromatography system utilizing Chiralpak (AD-H, AS-H or IC) or Chiralcel (OD-H, OJ-H, or OB-H) columns (4.6 mm x 25 cm) obtained from Daicel Chemical Industries, Ltd. High resolution mass spectra (HRMS) were obtained from Agilent 6200 Series TOF with an Agilent G1978A Multimode source

in electrospray ionization (ESI+), atmospheric pressure chemical ionization (APCI+), or mixed ionization mode (MM: ESI-APCI+), or obtained from the Caltech Mass Spectrometry Laboratory. Specific optical rotations were measured with a Jasco P-2000 polarimeter operating on the sodium D-line (589 nm), using a 100 mm path-length cell and are reported as: $[\alpha]_D^T$ (concentration in 10 mg/1 mL, solvent). Yields refer to the isolated yield of analytically pure material, unless otherwise noted.

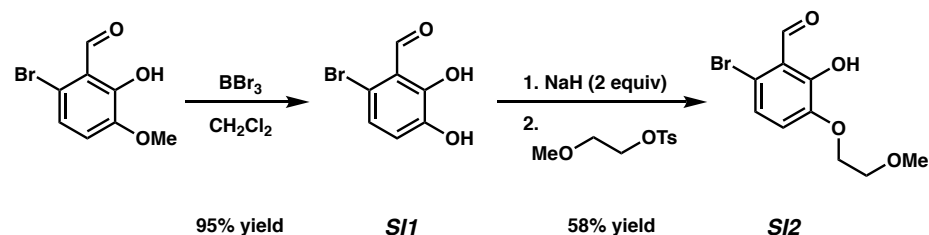
All chemicals were purchased from Aldrich, Acros, TCI, or Alfa-Aesar Chemical Co. and used as received unless otherwise noted. At GIST, anhydrous tetrahydrofuran (THF), diethyl ether (Et₂O), and dichloromethane (CH₂Cl₂) were dried using J.C. Meyer solvent purification system. Hexane was distilled from calcium hydride (CaH₂). At Caltech, solvents were dried by passage through an activated alumina column under argon. Unless specified, all the other chemicals were purchased from Sigma-Aldrich Co., Acros Organics, TCI, Alfa Aesar, and Strem Chemicals Inc. and were used as received without further purification.

1.9.2 EXPERIMENTAL PROCEDURES AND SPECTROSCOPIC DATA

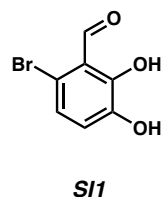
1.9.2.1 Synthesis and Spectroscopic Data for Salen-Crown Ether Ligands

L3 and **L5** are both known compounds, and were synthesized according to previously reported procedures.^{16,17}

General Procedure for Aldehyde Synthesis

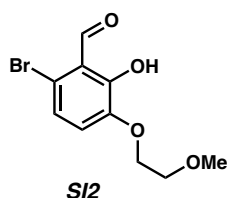


Spectroscopic Data for Ligand Intermediates



6-bromo-2,3-dihydroxybenzaldehyde (SI1): To a flame-dried round bottom flask under argon was added 6-bromo-2-hydroxy-3-methoxybenzaldehyde (5.74 g, 24.8 mmol, 1.0 equiv) and methylene chloride (50 mL). The solution was cooled to $-78\text{ }^\circ\text{C}$ and boron tribromide (7.1 mL, 74.5 mmol, 3.0 equiv) in methylene chloride (68 mL) was added dropwise. The reaction was warmed to room temperature and stirred for 5 h. Upon reaction completion, the crude reaction mixture was poured into ice water and stirred for 1 h. The aqueous layer was extracted with methylene chloride three times. The combined extracts were washed with water and dried with sodium sulfate, and concentrated by rotary evaporator. The crude solid was then rinsed with hexanes to afford 6-bromo-2,3-dihydroxybenzaldehyde (**SI1**) as an orange solid (4.58 g, 21.1

mmol, 85% yield). ^1H NMR (300 MHz, CDCl_3) δ 12.24 – 12.06 (m, 1H), 10.27 (s, 1H), 7.17 – 6.95 (m, 2H), 5.65 (s, 1H). All characterization data match those reported.¹⁸

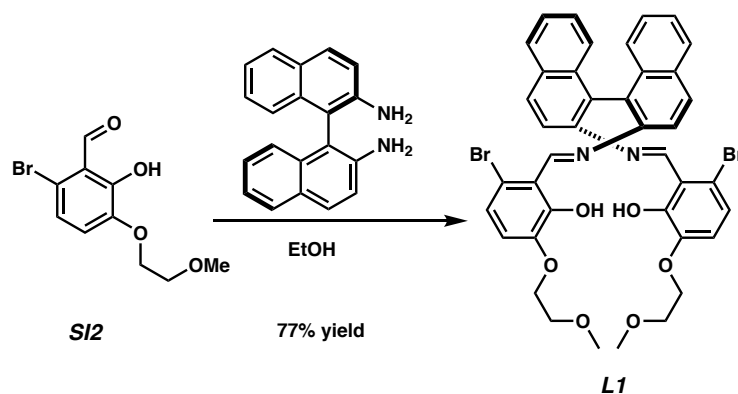


6-bromo-2-hydroxy-3-(2-methoxyethoxy)benzaldehyde (SI2): Sodium hydride (1.17 g, 48.75 mmol, 2.3 equiv) was added to a flame-dried flask under argon. This flask was placed in an ice bath, and a solution of 6-bromo-2,3-dihydroxybenzaldehyde (**SI1**, 4.6 g, 21.2 mmol, 1.0 equiv) in DMSO (42 mL) was added dropwise. The resulting solution was stirred for 3 hours and then 2-methoxyethyl 4-methylbenzenesulfonate¹⁹ (5.37 g, 23.22 mmol, 1.1 equiv) in DMSO (4.2 mL) was added dropwise. The reaction was stirred for 24 hours at room temperature. The reaction was quenched with water and the pH was checked and adjusted to pH = 7. The aqueous layer was extracted with methylene chloride three times and the combined organic extracts were washed with 1M HCl, dried with Na_2SO_4 , and then concentrated. The crude reaction mixture was filtered through a pad of silica and concentrated to afford 6-bromo-2-hydroxy-3-(2-methoxyethoxy)benzaldehyde as a yellow solid (3.38 g, 12.3 mmol, 58% yield); ^1H NMR (300 MHz, CDCl_3) δ 12.25 (s, 1H), 10.29 (s, 1H), 7.07 (d, J = 8.6 Hz, 1H), 6.99 (d, J = 8.6 Hz, 1H), 4.23 – 4.15 (m, 2H), 3.82 – 3.75 (m, 2H), 3.45 (s, 3H); ^{13}C NMR (101 MHz, CDCl_3) δ 198.5, 155.3, 147.8, 123.6, 121.3, 117.6, 71.0, 69.4, 59.4; IR (neat) 2984, 2942, 2933, 2932, 2750, 1686,

1641, 1579, 1467, 1454, 1438, 1388, 1370, 1332, 1317, 1285, 1274, 1250, 1211, 1202, 1127, 1102, 1081, 898, 861, 822, 789, 749, 676; HRMS $C_{10}H_{12}BrO_4$ ($M+H$) $^+$: 274.9913, Found: 274.9921.

The corresponding aldehydes for other ligands tested were synthesized according to the procedure described above.

Synthesis of Salen Crown Ether Ligands: Imine Formation

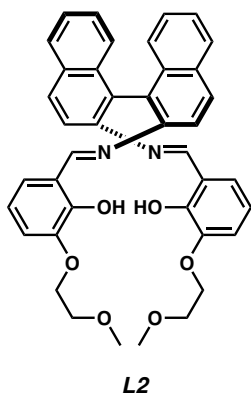


6,6'-((1E,1'E)-(((R)-[1,1'-binaphthalene]-2,2'-

diyl)bis(azanylylidene))bis(methanylylidene))bis(5-bromo-2-(2-

methoxyethoxy)phenol)(L1): 6-bromo-2-hydroxy-3-(2-methoxyethoxy)benzaldehyde (2.38 g, 8.67 mmol, 2.0 equiv) and (R)-(+)-1,1'-Binaphthyl-2,2'-diamine (1.7 g, 4.33 mmol, 1.0 equiv) were combined in EtOH (14 mL). The reaction mixture was heated to 120 °C and stirred for 6 h. Upon completion, the reaction was cooled to room temperature and subsequently filtered. The

filtered solid was washed with EtOH, concentrated under reduced pressure, affording scarlet solids (2.69 g, 3.36 mmol, 77% yield); $[\alpha]_D^{20} = -301.6$ (c 0.652, CH₂Cl₂); ¹H NMR (400 MHz, C₆D₆) δ 13.84 (s, 1H), 9.08 (s, 1H), 7.65 (d, 12 Hz, 1H), 7.56 (d, 8 Hz, 1H), 7.30 (d, 12 Hz, 1H), 7.25 (d, 8 Hz, 1H), 7.03 (t, 8 Hz, 1H), 6.87 (t, 8 Hz, 1H), 6.54 (d, 8 Hz, 1H), 6.12 (d, 8 Hz, 1H), 3.55 (t, 6 Hz, 2H), 3.21 (t, 4 Hz, 2H), 3.01 (s, 3H); ¹³C NMR (75 MHz, C₆D₆) δ 162.8, 155.0, 147.8, 143.6, 133.5, 132.8, 130.3, 129.4, 128.4, 127.2, 126.5, 126.1, 121.7, 118.2, 117.6, 117.0, 116.8, 70.7, 68.8, 58.5; IR (neat) 2925, 2876, 2817, 1600, 1586, 1440, 1338, 1246, 1224.50, 1125, 1085, 871, 814, 790, 752; HRMS (EI) Calcd. for C₄₀H₃₄Br₂N₂O₆: 796.0784, Found: 796.0782.

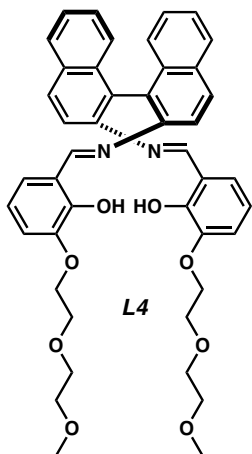


6,6'-((1E,1'E)-(((R)-[1,1'-binaphthalene]-2,2'-

diyl)bis(azanylylidene))bis(methanylylidene))bis(2-(2-methoxyethoxy)phenol)(L2):

2-hydroxy-3-(2-methoxyethoxy)benzaldehyde (365 mg, 1.86 mmol, 2.0 equiv) and (*R*)-(+)-1,1'-binaphthyl-2,2'-diamine (264.5 mg, 0.930 mmol, 1.0 equiv) were combined in EtOH (7 mL). The reaction mixture was stirred at room temperature for 48 h. The suspension was filtered. The filtered solid was washed with EtOH, concentrated under reduced pressure, affording orange solids (556.8 mg, 0.869 mmol, 94% yield); $[\alpha]_D^{20} = -371.3$ (c = 0.6, CH₂Cl₂); ¹H NMR (400 MHz, CDCl₃) δ

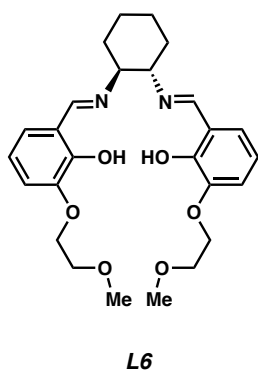
12.33 (s, 2H), 8.05, 8.02 (d, $J = 12$ Hz, 2H), 8.55 (s, 2H), 7.93, 7.91 (d, $J = 8$ Hz, 2H), 7.54, 7.51 (d, $J = 12$ Hz, 2H), 7.40 – 7.44 (t, $J = 8$ Hz, 2H), 7.22 – 7.24 (d, $J = 8$ Hz, 2H), 7.19, 7.17 (d, $J = 8$ Hz, 2H), 6.89, 6.88 (d, $J = 4$ Hz, 2H), 6.80, 6.79 (d, $J = 4$ Hz, 2H), 6.66 – 6.70 (t, $J = 8$ Hz, 2H), 4.03 – 4.06 (m, 4H), 3.65 – 3.68 (t, $J = 6$ Hz, 4H), 3.39 (s, 6H); HRMS (EI) Calcd. for $C_{40}H_{36}N_2O_6$: 640.2573, Found: 640.2573.



6,6'-((1E,1'E)-(((R)-[1,1'-binaphthalene]-2,2'-diyl)bis(azanylylidene))bis(methanylylidene))bis(2-(2-(2-methoxyethoxy)ethoxy)phenol)(L4):

2-hydroxy-3-(2-(2-methoxyethoxy)ethoxy)benzaldehyde (191.3 mg, 0.797 mmol, 2.0 equiv) and (*R*)-(+)-1,1'-binaphthyl-2,2'-diamine (96.4 mg, 0.339 mmol, 1.0 equiv) were combined in EtOH (3 mL). The reaction mixture was stirred at room temperature for 48 h. The suspension was filtered. The filtered solid was washed with EtOH and concentrated under reduced pressure to afford an

orange solid (196.5 mg, 0.2697 mmol, 80% yield); $[\alpha]_{\text{D}}^{20} = -352.1$ (c 0.518, CH_2Cl_2); ^1H NMR (400 MHz, CDCl_3) δ 12.28 (s, 2H), 8.03 (d, $J = 8$ Hz, 2H), 7.92 (d, $J = 8$ Hz, 2H), 7.52 (d, $J = 8$ Hz, 2H), 7.44-7.40 (m, 2H), 7.26-7.22 (m, 2H), 7.18 (d, $J = 8$ Hz, 2H), 6.88 (d, $J = 8$ Hz, 2H), 6.79 (d, $J = 8$ Hz, 2H), 6.70 – 6.66 (m, 2H), 4.09 – 4.06 (m, 4H), 3.79 – 3.76 (m, 4H), 3.67 – 3.65 (m, 4H), 3.53 – 3.51 (m, 4H), 3.37 (s, 6H); ^{13}C NMR (75 MHz, CDCl_3) δ 163.0, 151.7, 147.2, 144.4, 133.3, 132.6, 130.2, 128.4, 127.0, 126.6, 125.8, 124.9, 119.7, 118.2, 118.0, 117.8, 72.0, 70.7, 69.7, 69.1, 59.1; IR (neat) 3269, 3046, 2955, 2362, 1603, 1574, 1506, 1470, 1429, 1389, 1359, 1306, 1261, 1194, 1143, 1087, 969, 856, 815, 744, 700; HRMS (EI) Calcd. for $\text{C}_{44}\text{H}_{44}\text{N}_2\text{O}_8$: 728.3098, Found: 728.3096.

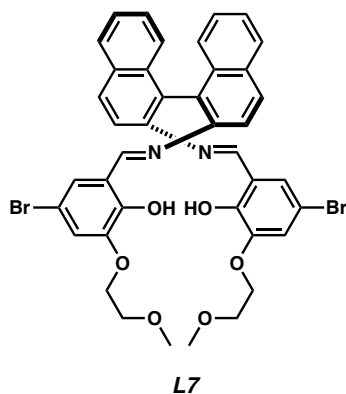


6,6'-((1E,1'E)-(((1R,2R)-cyclohexane-1,2-

diyl)bis(azanylylidene))bis(methanylylidene))bis(2-(2-methoxyethoxy)phenol)(L6):

2-hydroxy-3-(2-methoxyethoxy)benzaldehyde (193 mg, 0.986 mmol, 2.0 equiv) and (1R,2R)-cyclohexane-1,2-diamine (56.3 mg, 0.493 mmol, 1.0 equiv) were combined in EtOH (8 mL). The reaction mixture was stirred at room temperature for 48 h. The solvent was removed under reduced pressure. The residue was purified by column chromatography on silica-gel (*n*-hexane/EtOAc = 2/1, 1/2, 1/4), affording an oil (195 mg, 0.414 mmol, 84% yield): $[\alpha]_{\text{D}}^{20} = +120.0$ (c = 0.5, CH_2Cl_2);

^1H NMR (300 MHz, CDCl_3) δ 13.83 (s, 2H), 8.21 (s, 2H), 6.88 – 6.90 (m, 2H), 6.77 – 6.80 (m, 2H), 6.67 – 6.71 (t, J = 6 Hz, 2H), 4.13 – 4.16 (t, J = 4.5 Hz, 4H), 3.76 – 3.78 (t, J = 3 Hz, 4H), 3.43 (s, 6H), 1.84 – 1.93 (m, 4H), 1.66 – 1.69 (d, J = 9 Hz, 2H), 1.42 – 1.47 (m, 2H) ppm; ^{13}C NMR (75 MHz, CDCl_3) δ 164.8, 152.2, 147.4, 124.0, 118.7, 117.9, 116.6, 72.5, 71.2, 68.6, 59.3, 33.1, 24.1; IR (neat) 3315, 2929, 2856, 1625, 1578, 1477, 1450, 1376, 1338, 1289, 1233, 1022; HRMS (EI) Calcd. for $\text{C}_{26}\text{H}_{34}\text{N}_2\text{O}_6$: 470.2417, Found: 470.2425.



6,6'-((1E,1'E)-(((R)-[1,1'-binaphthalene]-2,2'-

diyl)bis(azanylylidene))bis(methanylylidene))bis(4-bromo-2-(2-

methoxyethoxy)phenol)(L7): 5-bromo-2-hydroxy-3-(2-(2-ethoxyethoxy)ethoxy)benzaldehyde

(80 mg, 0.291 mmol) and (*R*)-(+)-1,1'-Binaphthyl-2,2'-diamine (41.232 mg, 0.145 mmol) were

combined in EtOH (10 mL). The reaction mixture was stirred at room temperature for 48 h. The

suspension was filtered. The filtered solid was washed with EtOH and concentrated under reduced

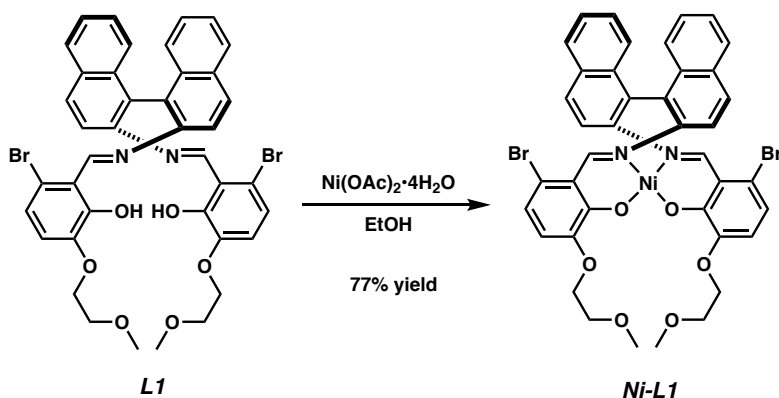
pressure, affording scarlet solids (100 mg, 0.125 mmol, 86% yield); $[\alpha]_{\text{D}}^{20} = -298.5$ (c 0.5,

CH_2Cl_2); ^1H NMR (400 MHz, CDCl_3) δ 12.32 (s, 2H), 8.45 (s, 2H), 8.02 (d, 12 Hz, 2H), 7.91 (d,

8 Hz, 2H), 7.48 (d, 12 Hz, 2H), 7.41 (m, 2H), 7.21 (m, 2H), 7.13 (d, 8 Hz, 2H), 6.96 (d, 4 Hz, 2H), 6.91 (d, 4 Hz, 2H), 4.01 (m, 4H), 3.65 (t, 4H, 4H), .38 (s, 6H); ^{13}C NMR (75 MHz, CDCl_3) δ 161.6, 150.9, 148.2, 143.7, 133.2, 132.8, 130.4, 126.2, 120.4, 120.2, 117.5, 109.5, 77.5, 77.2, 76.9, 70.8, 69.1, 59.2; IR (neat) 2875, 2360, 2342, 1605, 1569, 1450, 1398, 1363, 1332, 1250, 1199, 1125, 1089, 1026, 972, 900, 817, 751; HRMS (EI) Calcd. for $\text{C}_{40}\text{H}_{34}\text{Br}_2\text{N}_2\text{O}_6$: 796.0784, Found: 796.0784.

1.9.2.2 Complexation Procedure (Ni-L Synthesis) and HRMS for Salen-Ni Complexes

Complexation Procedure (Ni-L Synthesis)



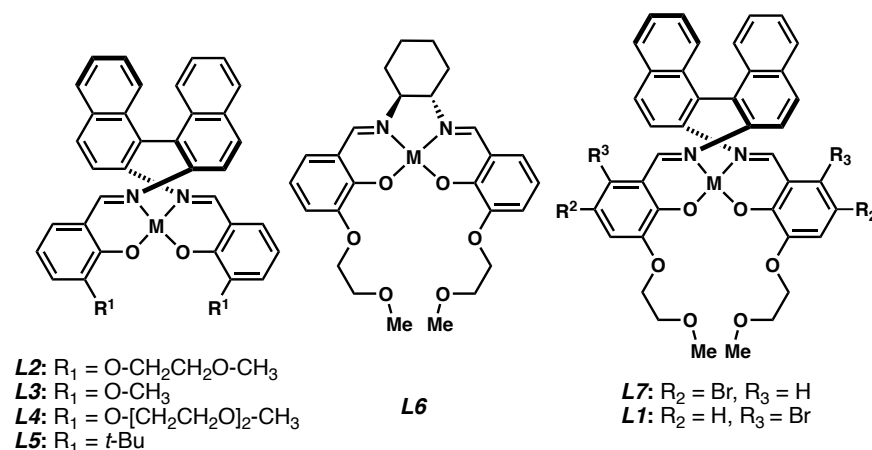
Ni-Salen Complex (Ni-L1): $\text{Ni(OAc)}_2 \cdot 4\text{H}_2\text{O}$ (1.17 g, 4.7 mmol, 1.4 equiv) and **L1** (2.69 g, 3.36 mmol, 1.0 equiv) were combined in EtOH and heated to 100 °C for 12 h. While still hot, the crude mixture was transferred into a 20 mL vial, rinsing with a small amount of additional EtOH. The

vial was placed in the freezer for 12h. The crude mixture was then centrifuged down, and the EtOH was decanted. The mother liquor was then reduced via rotary evaporator, and the crude reaction mixture was allowed to rest in the freezer, and centrifuged a second time. The combined precipitates were washed with hexanes, and dried under vacuum to afford a yellow solid (2.2 g, 2.58 mmol, 77% yield).

All other metal complexes were prepared using this identical procedure.

HRMS for the Catalysts with Nickel

The normal spectral region could not be determined by ^1H NMR, since Ni(II)-salen complexes are paramagnetic. High-resolution mass spectra (HRMS) shows desired Ni(II)-salen complexes bearing one nickel atom. Similar effects for Ni(II)-salen complexes have been reported before.^{20,21}



L2-Ni: HRMS (EI) Calcd. $\text{C}_{40}\text{H}_{34}\text{N}_2\text{NiO}_6$: 696.1770, Found: 696.1769

L3-Ni: HRMS (EI) Calcd. $\text{C}_{36}\text{H}_{26}\text{N}_2\text{NiO}_4$: 608.1246, Found: 608.1243

L4-Ni: HRMS (EI) Calcd. $C_{44}H_{42}N_2NiO_8$: 784.2295, Found: 784.2294

L5-Ni: HRMS (EI) Calcd. $C_{42}H_{38}N_2NiO_2$: 660.2287, Found: 660.2286

L6-Ni: HRMS (EI) Calcd. $C_{26}H_{32}N_2NiO_6$: 526.1614, Found: 526.1614

L7-Ni: HRMS (EI) Calcd. $C_{40}H_{33}Br_2N_2NiO_6$: 853.0059, Found: 853.0068

L1-Ni: HRMS (EI) Calcd. $C_{40}H_{32}Br_2N_2NiO_6$: 851.9980, Found: 851.9981

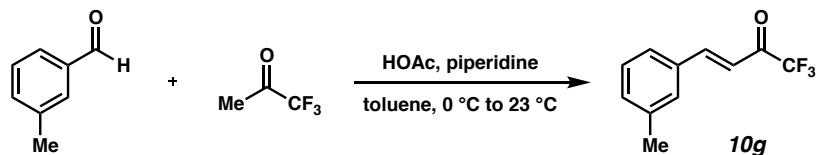
1.9.2.3 Synthesis of Trifluoromethyl Ketones

Aryl trifluoromethylketone **4h** was prepared according to a previously reported procedure.²² All other aryl trifluoromethylketones were purchased from Alfa Aesar, Sigma-Aldrich, or TCI and used without further purification.

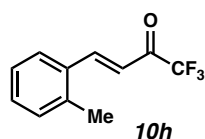
Synthesis of Unsaturated Trifluoromethyl Ketones:

Previously reported methods were used to prepare **10a**²³, **10b**²³, **10c**²⁴, **10d**²³, **10e**²³, **10i**²⁵, **10j**²⁵, **10k**²⁴, and **10n**²⁵.

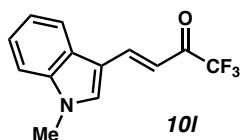
General Procedure for the Synthesis of Unsaturated Trifluoromethyl ketones:



(E)-1,1,1-trifluoro-4-(*m*-tolyl)but-3-en-2-one (10g): 3-methylbenzaldehyde (601 mg, 5.0 mmol, 1.0 equiv), piperidine (493 μL , 5.0 mmol, 1.0 equiv), and acetic acid (429 μL , 7.5 mmol, 1.5 equiv) were all combined in dry toluene (5 mL) in a flame-dried flask under argon. The resultant solution was cooled to 0 °C, and then trifluoroacetone (1.8 mL, 20 mmol, 4 equiv) in toluene (5 mL) was added slowly. The reaction was stirred at 0 °C for 2 hours and then allowed to stir at room temperature for 24 h. The reaction was quenched with saturated ammonium chloride solution and the aqueous layer was extracted three times with ethyl acetate. The combined organic extracts were washed with water, and dried with sodium sulfate. Product **10g** was purified by column chromatography (5% EtOAc in hexanes) to provide a colorless oil (415 mg, 38% yield); ^1H NMR (500 MHz, CDCl_3) δ 7.95 (d, J = 15.9 Hz, 1H), 7.48 – 7.42 (m, 2H), 7.37 – 7.29 (m, 2H), 7.01 (dq, J = 16.0, 1.0 Hz, 1H), 2.41 (t, J = 0.7 Hz, 3H). All characterization data match those reported.²⁶

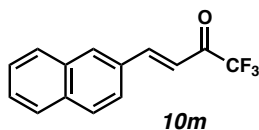


(E)-1,1,1-trifluoro-4-(*o*-tolyl)but-3-en-2-one (10h): Product **10h** was purified by column chromatography (8% EtOAc in hexanes) to provide a colorless oil (107 mg, 50% yield); ^1H NMR (300 MHz, CDCl_3) δ 8.31 (dt, J = 15.9, 0.6 Hz, 1H), 7.74 – 7.64 (m, 1H), 7.38 (td, J = 7.3, 1.4 Hz, 1H), 7.26 (m, 2H), 6.96 (dq, J = 15.8, 0.9 Hz, 1H), 2.50 (s, 3H). All characterization data match those reported.²⁶

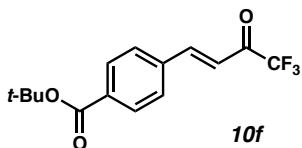


(*E*)-1,1,1-trifluoro-4-(1-methyl-1*H*-indol-3-yl)but-3-en-2-one (10l): Product **10l** was purified by column chromatography (20% EtOAc in hexanes) to provide a yellow oil (192 mg, 15% yield); ^1H NMR (500 MHz, CDCl_3) δ 8.21 (dd, $J = 15.5, 0.7$ Hz, 1H), 7.97 – 7.91 (m, 1H), 7.58 (s, 1H), 7.44 – 7.32 (m, 3H), 6.97 (dt, $J = 15.6, 1.0$ Hz, 1H), 3.88 (s, 3H).

All characterization data match those reported.²⁷



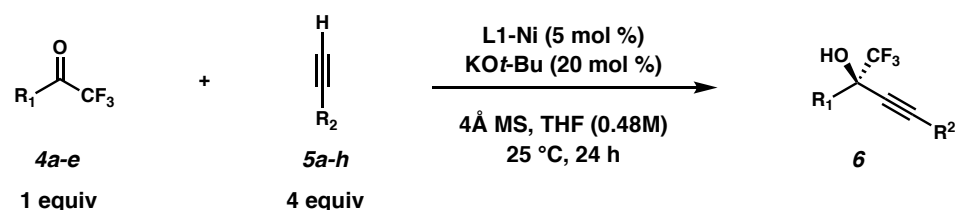
(*E*)-1,1,1-trifluoro-4-(naphthalen-2-yl)but-3-en-2-one (10m): Product **10m** was purified by column chromatography (8% EtOAc in hexanes) to provide a light yellow oil (500 mg, 40% yield); ^1H NMR (500 MHz, CDCl_3) δ 8.19 – 8.05 (m, 2H), 7.95 – 7.86 (m, 3H), 7.75 (dd, $J = 8.6, 1.8$ Hz, 1H), 7.64 – 7.52 (m, 2H), 7.13 (dq, $J = 16.0, 0.9$ Hz, 1H). All characterization data match those reported.²⁸



***tert*-butyl (*E*)-4-(4,4,4-trifluoro-3-oxobut-1-en-1-yl)benzoate (10f):** Product **10f** was prepared using the general procedure and purified by column chromatography (8% EtOAc in hexanes) to

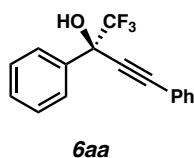
provide a colorless oil (687 mg, 2.3 mmol, 46% yield); ^1H NMR (400 MHz, CDCl_3) δ 8.05 (d, J = 8.1 Hz, 2H), 7.97 (d, J = 16.0 Hz, 1H), 7.68 (d, J = 8.1 Hz, 2H), 7.07 (dt, J = 16.0, 1.0 Hz, 1H), 1.61 (d, J = 0.9 Hz, 9H); ^{13}C NMR (101 MHz, CDCl_3) δ 164.8, 148.8, 136.9, 135.2, 130.3, 129.0, 118.5, 82.0, 28.30; ^{19}F NMR (282 MHz, CDCl_3) δ -77.66; IR (Neat Film, NaCl) 3051, 2995, 1709, 1613, 1568, 1417, 1392, 1368, 1305, 1265, 1189, 1141, 1063, 994, 896, 844, 772, 733, 705, 683 cm^{-1} .

1.9.2.4 Procedure for Enantioselective Alkynylation of Aryl Trifluoromethyl Ketones

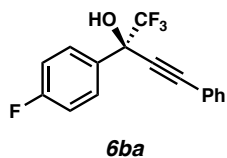


To a stirred solution of catalyst (0.012 mmol, 0.05 equiv) in THF (0.5 mL), alkyne (0.968 mmol, 4 equiv), 4 Å molecular sieve (377 mg), and KOtBu (0.484 mmol, 0.2 equiv) were added at room temperature slowly. After the solution had been stirred at room temperature for 30 min to give a dark yellow mixture, ketone (0.242 mmol, 1.0 equiv) was added dropwise to a solution. After the resulting mixture was stirred at room temperature for 24 h, saturated ammonium chloride (2mL) was added to quench the reaction. The solution was extracted with ethyl acetate (3×15 mL). The combined organic layers were washed with brine, dried over anhydrous magnesium sulfate, and concentrated by rotary evaporation. The residue was purified by flash column chromatography

ethyl acetate/hexane. Enantiomeric excesses were determined by HPLC on chiral stationary phase (Daicel Chiralpak IB or ID column (0.46 cm \times 25 cm)).

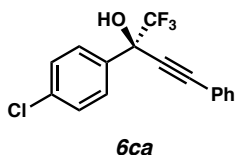


1,1,1-trifluoro-2,4-diphenylbut-3-yn-2-ol (6aa) : Product **6aa** was prepared using the general procedure to provide a pale yellow oil (93% yield, 93% ee); $[\alpha]_D^{24} = +26.8$ ($c = 0.5$, CH_2Cl_2); The enantiomeric excess was determined by chiral HPLC analysis: Daicel Chiralpak IB column; Hexane/*i*-PrOH = 98:2; flow rate 1 mL/min, 254 nm wave length UV; minor $t_R = 11.081$ min, major $t_R = 9.556$ min. All characterization data match those reported.²⁹

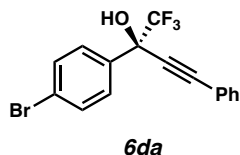


1,1,1-trifluoro-2-(4-fluorophenyl)-4-phenylbut-3-yn-2-ol (6ba):

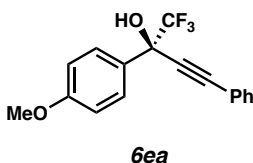
Product **6ba** was prepared using the general procedure to provide a pale yellow oil (93% yield, 90% ee); $[\alpha]_D^{24} = +25.2$ ($c = 0.5$, CH_2Cl_2); The enantiomeric excess was determined by chiral HPLC analysis: Daicel Chiralpak ID column; Hexane/*i*-PrOH = 99:1; flow rate 0.5 mL/min, 254 nm wave length UV; minor $t_R = 11.809$ min, major $t_R = 11.014$ min. All characterization data match those reported.³⁰



2-(4-chlorophenyl)-1,1,1-trifluoro-4-phenylbut-3-yn-2-ol (6ca): Product **6ca** was prepared using the general procedure to provide a pale yellow oil (94% yield, 89% ee); $[\alpha]_{\text{D}}^{24} = +17.8$ ($c = 0.5$, CH_2Cl_2); The enantiomeric excess was determined by chiral HPLC analysis: Daicel Chiralpak ID column; Hexane/*i*-PrOH = 99:1; flow rate 0.5 mL/min, 254 nm wave length UV; minor $t_{\text{R}} = 12.818$ min, major $t_{\text{R}} = 11.254$ min. All characterization data match those reported.²⁹

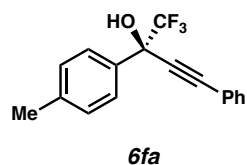


2-(4-bromophenyl)-1,1,1-trifluoro-4-phenylbut-3-yn-2-ol (6da): Product **6da** was prepared using the general procedure to provide a pale yellow oil (97% yield, 89% ee); $[\alpha]_{\text{D}}^{24} = +14.2$ ($c = 0.8$, CH_2Cl_2); The enantiomeric excess was determined by chiral HPLC analysis: Daicel Chiralpak ID column; Hexane/*i*-PrOH = 99:1; flow rate 0.5 mL/min, 254 nm wave length UV; minor $t_{\text{R}} = 14.004$ min, major $t_{\text{R}} = 11.924$ min. All characterization data match those reported.³⁰

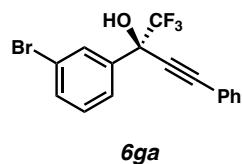


(R)-1,1,1-trifluoro-2-(4-methoxyphenyl)-4-phenylbut-3-yn-2-ol (6ea): Product **6ea** was prepared using the general procedure to provide a pale yellow oil (86% yield, 97% ee); $[\alpha]_{\text{D}}^{24} =$

+22.7 (c = 0.6, CH₂Cl₂); The enantiomeric excess was determined by chiral HPLC analysis: Daicel Chiralpak IB column; Hexane/i-PrOH = 98:2; flow rate 1 mL/min, 254 nm wave length UV; minor t_R = 12.240 min, major t_R = 22.694 min. All characterization data match those reported.²⁹

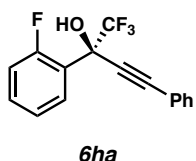


1,1,1-trifluoro-4-phenyl-2-(p-tolyl)but-3-yn-2-ol (6fa): Product **6fa** was prepared using the general procedure to provide a pale yellow oil (86% yield, 97% ee); [α]_D²⁴ = +22.4 (c = 0.6, CH₂Cl₂); The enantiomeric excess was determined by chiral HPLC analysis: Daicel Chiralpak ID column; Hexane/i-PrOH = 99:1; flow rate 1 mL/min, 254 nm wave length UV; minor t_R = 8.663 min, major t_R = 7.225 min. All characterization data match those reported.²⁹

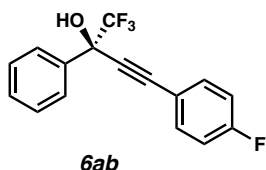


2-(3-bromophenyl)-1,1,1-trifluoro-4-phenylbut-3-yn-2-ol (6ga) : Product **6ga** was prepared using the general procedure to provide a pale yellow oil (92% yield, 85% ee); [α]_D²⁴ = +23.0 (c = 0.7, CH₂Cl₂); ¹H NMR (400 MHz, CDCl₃) δ 7.96 (s, 1H), 7.74 (d, 8 Hz, 1H), 7.53 (m, 3H), 7.35 (m, 3H), 7.29 (t, 8 Hz, 1H), 3.25 (s, 1H); ¹³C NMR (75 MHz, CDCl₃) δ 137.6, 132.8, 132.2, 130.44, 129.9, 128.6, 126.1, 125.2, 122.5, 121.4, 120.7, 88.7, 83.8, 73.1, 72.7; ¹⁹F NMR (282 MHz, CDCl₃) δ -80.08; IR (Neat) 3547, 3066, 2233, 1594, 1570, 1490, 1473, 1444, 1423, 1348, 1246, 1168, 1111, 1074, 1012, 997, 937, 884, 782, 755, 735, 708, 687; HRMS (EI) Calcd. for C₁₆H₁₀BrF₃O:

353.9867, Found: 353.9871. The enantiomeric excess was determined by chiral HPLC analysis: Daicel Chiralpak ID column; Hexane/i-PrOH = 99:1; flow rate 0.5 mL/min, 254 nm wave length UV; minor t_R = 12.137 min, major t_R = 11.398 min.

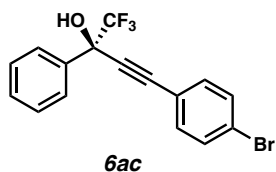


1,1,1-trifluoro-2-(2-fluorophenyl)-4-phenylbut-3-yn-2-ol (6ha): Product **6ha** was prepared using the general procedure to provide a pale yellow oil (70% yield, 87% ee); $[\alpha]_D^{24} = +10.6$ ($c = 0.2$, CH_2Cl_2); ^1H NMR (400 MHz, CDCl_3) δ 7.83 (m, 1H), 7.53 (m, 2H), 7.32 (m, 4H), 7.11 (m, 2H), 3.55 (s, 1H); ^{13}C NMR (75 MHz, CDCl_3) δ 162.4, 158.9, 132.2, 131.8, 131.7, 129.9, 129.6, 128.5, 124.3, 124.2, 121.0, 117.0, 116.7, 88.2, 83.1, 72.4, 71.9; ^{19}F NMR (282 MHz, CDCl_3) δ -80.24, -110.69; IR (neat) 3576, 2927, 2235, 1655, 1613, 1585, 1489, 1453, 1377, 1249, 1228, 1174, 1153, 1120, 1000, 1010, 922, 823, 755, 740, 711, 689; HRMS (EI) Calcd. for $\text{C}_{16}\text{H}_{10}\text{F}_4\text{O}$: 294.0668, Found: 294.0670; The enantiomeric excess was determined by chiral HPLC analysis: Daicel Chiralpak ID column; Hexane/i-PrOH = 99:1; flow rate 1 mL/min, 254 nm wave length UV; minor t_R = 7.523 min, major t_R = 6.467 min.

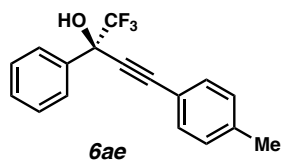


(R)-1,1,1-trifluoro-2-phenyl-4-(p-tolyl)but-3-yn-2-ol (6ab): Product **6ab** was prepared using the general procedure to provide a pale yellow oil (98% yield, 91% ee); $[\alpha]_D^{24} = +18.0$ ($c = 0.2$,

CH₂Cl₂); The enantiomeric excess was determined by chiral HPLC analysis: Daicel Chiralpak IB column; Hexane/i-PrOH = 98:2; flow rate 1 mL/min, 254 nm wave length UV; minor t_R = 12.079 min, major t_R = 8.448 min. All characterization data match those reported.³⁰

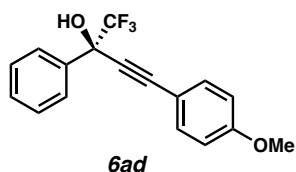


(R)-4-(4-bromophenyl)-1,1,1-trifluoro-2-phenylbut-3-yn-2-ol (6ac): Product **6ac** was prepared using general procedure to provide a pale yellow oil (90% yield, 91% ee); [α]_D²⁴ = +29.9 (c = 0.7, CH₂Cl₂); ¹H NMR (400 MHz, CDCl₃) δ 7.80 (m, 2H), 7.38(m, 7H), 3.19(s, 1H); ¹³C NMR (75 MHz, CDCl₃) δ 135.1, 133.6, 131.9, 129.7, 128.4, 127.2, 125.3, 124.2, 121.5, 119.9, 87.1, 85.6, 73.7, 73.3; ¹⁹F NMR (282 MHz, CDCl₃) δ -80.06; IR (neat) 3566, 2926, 2360, 2234, 1605, 1587, 1452, 1394, 1361, 1248, 1166, 1116, 1098, 1064, 1012, 932, 906, 822, 761, 729, 696, 668; HRMS (EI) Calcd. for C₁₆H₁₀BrF₃O: 353.9867, Found: 353.9868; The enantiomeric excess was determined by chiral HPLC analysis: Daicel Chiralpak IB column; Hexane/i-PrOH = 98:2; flow rate 1 mL/min, 254 nm wave length UV; minor t_R = 13.405 min, major t_R = 9.004 min.

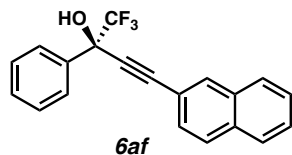


(R)-1,1,1-trifluoro-2-phenyl-4-(p-tolyl)but-3-yn-2-ol (6ae) : Product **6ae** was prepared using general procedure to provide a pale yellow oil (94% yield, 90% ee); [α]_D²⁴ = +26.5 (c = 0.6, CH₂Cl₂); The enantiomeric excess was determined by chiral HPLC analysis: Daicel Chiralpak IB

column; Hexane/i-PrOH = 98:2; flow rate 1 mL/min, 254 nm wave length UV; minor t_R = 10.213 min, major t_R = 7.287 min. All characterization data match those reported.³⁰

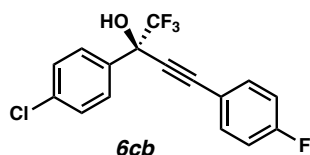


(R)-1,1,1-trifluoro-4-(4-methoxyphenyl)-2-phenylbut-3-yn-2-ol (6ad): Product **6ad** was prepared using general procedure to provide a pale yellow oil (99% yield, 93% ee); $[\alpha]_D^{24} = +26.7$ ($c = 0.2$, CH_2Cl_2); ^1H NMR (300 MHz, CDCl_3) δ 7.81 (m, 2H), 7.41 (m, 5H), 6.86 (m, 2H), 3.83 (s, 3H), 3.12 (s, 1H); ^{13}C NMR (75 MHz, CDCl_3) δ 160.6, 135.6, 133.7, 129.5, 128.3, 127.3, 114.2, 113.0, 88.3, 83.3, 73.7, 73.2, 55.4, 29.7; ^{19}F NMR (282 MHz, CDCl_3) δ -80.19; IR (neat) 3428, 2923, 2230, 1605, 1570, 1510, 1451, 1359, 1294, 1248, 1172, 1108, 1065, 1016, 933, 907, 832, 764, 706; HRMS (EI) Calcd. for $\text{C}_{17}\text{H}_{13}\text{F}_3\text{O}_2$: 306.0868, Found: 306.0869; The enantiomeric excess was determined by chiral HPLC analysis: Daicel Chiralpak IB column; Hexane/i-PrOH = 98:2; flow rate 1 mL/min, 254 nm wave length UV; minor t_R = 17.337 min, major t_R = 12.175 min.

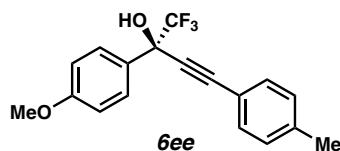


(R)-1,1,1-trifluoro-4-(naphthalen-2-yl)-2-phenylbut-3-yn-2-ol (6af): Product **6af** was prepared using general procedure to provide a pale orange solid (89% yield, 89% ee); $[\alpha]_D^{24} = +2.59$ ($c = 0.6$, CH_2Cl_2); ^1H NMR (300 MHz, CDCl_3) δ 8.09 (s, 1H), 7.81 (m, 5H), 7.47 (m, 6H), 3.23 (s, 1H); ^{13}C NMR (75 MHz, CDCl_3) δ 135.5, 133.5, 132.9, 132.7, 129.7, 128.4, 128.3, 128.2, 128.0,

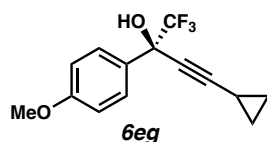
127.9, 127.4, 127.3, 127.0, 125.5, 121.7, 118.3, 88.6, 84.8, 73.8, 73.4, 29.8; ^{19}F NMR (282 MHz, CDCl_3) δ -80.01; IR (neat) 3528, 3061, 2924, 2853, 2360, 2228, 1595, 1501, 1488, 1450, 1360, 1226, 1168, 1097, 1063, 1005, 906, 868, 822, 767, 751, 700, 663; HRMS (EI) Calcd. for $\text{C}_{20}\text{H}_{13}\text{F}_3\text{O}$: 326.0918, Found: 326.0918; The enantiomeric excess was determined by chiral HPLC analysis: Daicel Chiralpak IB column; Hexane/*i*-PrOH = 98:2; flow rate 1 mL/min, 254 nm wave length UV; minor t_R = 16.764 min, major t_R = 11.734 min.



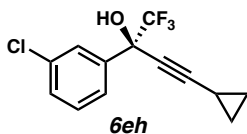
(*R*)-2-(4-chlorophenyl)-1,1,1-trifluoro-4-(4-fluorophenyl)but-3-yn-2-ol (6cb) : Product **6cb** was prepared using general procedure to provide a pale yellow oil (92% yield, 89% ee); $[\alpha]_D^{24}$ = +14.6 (c = 0.7, CH_2Cl_2); ^1H NMR (300 MHz, CDCl_3) δ 7.71 (d, 9 Hz, 2H), 7.49 (m, 2H), 7.40 (m, 2H), 7.03 (m, 2H), 3.10 (s, 1H); ^{13}C NMR (75 MHz, CDCl_3) δ 165.1, 161.7, 135.9, 134.3, 134.2, 133.8, 128.7, 128.6, 125.2, 121.4, 116.9, 116.2, 115.9, 87.4, 83.8, 73.3, 72.8; ^{19}F NMR (282 MHz, CDCl_3) δ -80.27, -108.15; IR (neat) 3453, 2928, 2235, 1706, 1652, 1601, 1507, 1491, 1406, 1359, 1233, 1184, 1121, 1093, 1010, 949, 917, 765, 730, 717, 694; HRMS (EI) Calcd. for $\text{C}_{16}\text{H}_9\text{ClF}_4\text{O}$: 328.0278, Found: 328.0278; The enantiomeric excess was determined by HPLC through chiral HPLC analysis: Daicel Chiralpak IB column; Hexane/*i*-PrOH = 98:2; flow rate 1 mL/min, 254 nm wave length UV; minor t_R = 9.181 min, major t_R = 7.976 min.



(*R*)-1,1,1-trifluoro-2-(4-methoxyphenyl)-4-(p-tolyl)but-3-yn-2-ol (6ee): Product **6ee** was prepared using general procedure to provide a pale yellow oil (92% yield, 96% ee); $[\alpha]_D^{24} = +17.5$ ($c = 0.5$, CH_2Cl_2); The enantiomeric excess was determined by chiral HPLC analysis: Daicel Chiralpak IB column; Hexane/*i*-PrOH = 98:2; flow rate 1 mL/min, 254 nm wave length UV; minor $t_R = 28.064$ min, major $t_R = 9.684$ min. All characterization data match those reported.³⁰

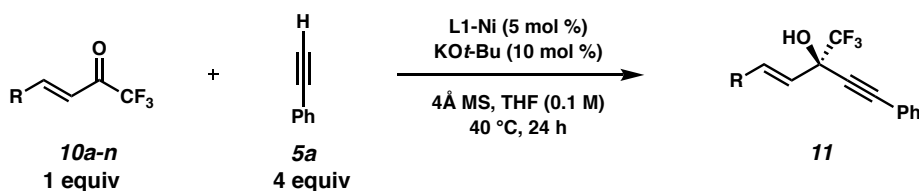


(*R*)-4-cyclopropyl-1,1,1-trifluoro-2-(4-methoxyphenyl)but-3-yn-2-ol (6eg): Product **6eg** was prepared using general procedure to provide a pale yellow solid (93% yield, 96% ee); $[\alpha]_D^{24} = +3.84$ ($c = 0.3$, CH_2Cl_2); ^1H NMR (300 MHz, CDCl_3) δ 7.61 (d, 9 Hz, 2H), 6.89 (m, 2H), 3.82 (s, 3H), 2.93 (s, 1H), 1.26 (m, 1H), 0.76 (m, 4H); ^{13}C NMR (75 MHz, CDCl_3) δ 160.4, 128.6, 127.9, 125.4, 121.6, 113.5, 92.5, 71.3, 55.4, 8.5; ^{19}F NMR (282 MHz, CDCl_3) δ -80.69; IR (neat) 2994, 2931, 2828, 1605, 1573, 1505, 1458, 1431, 1396, 1345, 1249, 1204, 1078, 970, 923, 818, 781, 733, 713, 687; HRMS (EI) Calcd. for $\text{C}_{14}\text{H}_{13}\text{F}_3\text{O}_2$: 270.0868, Found: 270.0868; The enantiomeric excess was determined by HPLC through chiral HPLC analysis: Daicel Chiralpak ID column; Hexane/*i*-PrOH = 99:1; flow rate 1 mL/min, 254 nm wave length UV; minor $t_R = 12.873$ min, major $t_R = 11.879$ min.



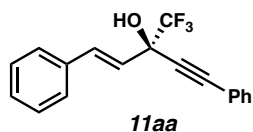
(R)-2-(3-chlorophenyl)-4-cyclopropyl-1,1,1-trifluorobut-3-yn-2-ol (6eh): Product **6eh** was prepared using general procedure to provide a pale yellow oil (95% yield, 80% ee); $[\alpha]_D^{24} = +2.4$ ($c = 0.3$, CH_2Cl_2); ^1H NMR (300 MHz, CDCl_3) δ 7.70 (s, 1H), 7.58 (m, 1H), 7.30 (m, 2H), 2.95 (s, 1H), 1.32 (m, 1H), 0.78 (m, 4H); ^{13}C NMR (75 MHz, CDCl_3) δ 137.7, 134.2, 129.6, 129.4, 127.6, 125.5, 93.2, 72.7, 72.1, 70.6, 29.8, 8.6, 0.6 ^{19}F NMR (282 MHz, CDCl_3) δ -80.46; IR (neat) 3458, 3016, 2441, 1597, 1578, 1475, 1428, 1364, 1261, 1165, 1106, 1076, 1027, 943, 925, 884, 814, 787, 721, 688; HRMS (EI) Calcd. for $\text{C}_{13}\text{H}_{10}\text{ClF}_3\text{O}$: 274.0323, Found: 274.0372; The enantiomeric excess was determined by chiral HPLC analysis: Daicel Chiralpak IB column; Hexane/i-PrOH = 99:1; flow rate 1 mL/min, 254 nm wave length UV; minor $t_R = 9.858$ min, major $t_R = 9.287$ min.

1.9.2.5 PROCEDURE FOR ENANTIOSELECTIVE ALKYNYLATION OF VINYL TRIFLUOROMETHYL KETONES

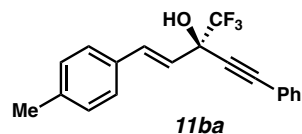


n = number of reactions. All reactions were set up in a N_2 -filled glovebox. To a vial containing **L1-Ni** (8.6n mg, 0.01n mmol, 0.05 equiv) was added KO^tBu (2.24n mg, 0.02 n mmol, 0.1 equiv) in THF (1.6n mL). The resulting solution was stirred until the solids were fully dissolved. To a

new 4 dram vial was added 4 Å MS (32 mg) and phenylacetylene (88 µL, 0.8 mmol, 4.0 equiv). The **L1-Ni** + KO*t*-Bu solution (1.6 mL) was then added to this vial, and the solution was stirred for 30 min. The vinyl trifluoromethyl ketone (0.2 mmol, 1.0 equiv) in THF (0.8 mL) was then added and the reaction was stirred at 40 °C for 24 h. The reaction was then quenched with sat. NH₄Cl solution and the aqueous layer was extracted three times with ethyl acetate. The combined organic extracts were dried with sodium sulfate and concentrated by rotary evaporator. The crude oil was then purified by column chromatography to afford the desired product.

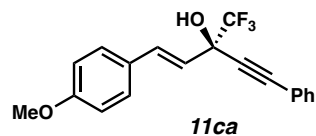


(*R,E*)-1,5-diphenyl-3-(trifluoromethyl)pent-1-en-4-yn-3-ol (11aa). Product **11aa** was purified by column chromatography (8% EtOAc in hexanes) to provide a colorless oil (51.8 mg, 86% yield); 90% ee, $[\alpha]_D^{25} +11.8$ (*c* 1.0, CHCl₃); ¹H NMR (400 MHz, CDCl₃) δ 7.55 (dd, *J* = 8.0, 1.6 Hz, 2H), 7.48 (dd, *J* = 8.3, 1.3 Hz, 2H), 7.45 – 7.27 (m, 6H), 7.21 (d, *J* = 15.8 Hz, 1H), 6.35 (d, *J* = 15.8 Hz, 1H), 2.91 (s, 1H); ¹³C NMR (101 MHz, CDCl₃) δ 135.8, 135.3, 132.2, 129.7, 129.0, 128.9, 128.6, 127.4, 123.6 (d, *J* = 285.3 Hz), 122.4, 121.1, 88.7, 82.7, 72.4 (q, *J* = 32.9 Hz); ¹⁹F NMR (282 MHz, CDCl₃) δ 80.72 IR (Neat Film, NaCl) 3412, 3030, 2924, 1491, 1445, 1249, 1187, 1130, 1056, 966, 753, 690 cm⁻¹; HRMS (MM) *m/z* calc'd for C₁₈H₁₂F₃ [M-OH]⁺: 285.0886 found 285.0883; SFC Conditions: 15% IPA, 2.5 mL/min, Chiralpak OD-H column, λ = 254 nm, *t_R* (min): major = 3.89, minor = 4.43.



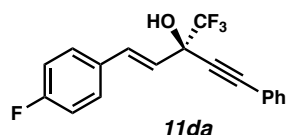
(*R,E*)-5-phenyl-1-(*p*-tolyl)-3-(trifluoromethyl)pent-1-en-4-yn-3-ol (11ba):

Product (**11ba**) was prepared using general procedure and purified by column chromatography (10% EtOAc in hexanes) to provide a colorless oil (62.2 mg, 98% yield); 92% ee, $[\alpha]_D^{25} +8.5$ (*c* 0.99, CHCl₃); ¹H NMR (400 MHz, CDCl₃) δ 7.55 (dd, *J* = 8.0, 1.6 Hz, 2H), 7.46 – 7.32 (m, 5H), 7.23 – 7.15 (m, 3H), 6.31 (d, *J* = 15.8 Hz, 1H), 2.96 (s, 1H), 2.38 (s, 3H); ¹³C NMR (101 MHz, CDCl₃) δ 139.1, 135.7, 132.5, 132.2, 129.63, 129.55, 128.6, 127.3, 123.6 (q, *J* = 285.3 Hz), 121.3, 121.1, 88.7, 82.8, 72.5 (q, *J* = 32.8 Hz); ¹⁹F NMR (282 MHz, CDCl₃) δ –80.72; IR (Neat Film, NaCl) 3412, 2924, 1654, 1515, 1491, 1444, 1361, 1249, 1186, 1131, 1054, 968, 797, 756, 727, 689 cm^{–1}; HRMS (MM) *m/z* calc'd for C₁₉H₁₄F₃ [M–OH]⁺: 299.1042 found 299.1041; SFC Conditions: 6% IPA, 2.5 mL/min, Chiralpak OD-H column, λ = 254 nm, *t_R* (min): major = 14.12, minor = 15.02.



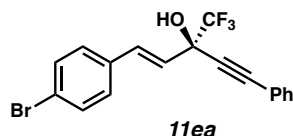
(*R,E*)-1-(4-methoxyphenyl)-5-phenyl-3-(trifluoromethyl)pent-1-en-4-yn-3-ol (11ca): Product (**11ca**) was prepared using general procedure and purified by column chromatography (10% EtOAc in hexanes) to provide a colorless oil (63.9 mg, 98% yield); 92% ee, $[\alpha]_D^{25} +7.7$ (*c* 0.97, CHCl₃); ¹H NMR (400 MHz, CDCl₃) δ 7.58 – 7.50 (m, 2H), 7.46 – 7.32 (m, 5H), 7.15 (d, *J* = 15.8 Hz, 1H), 6.94 – 6.85 (m, 2H), 6.20 (dd, *J* = 15.8, 0.7 Hz, 1H), 3.83 (s, 3H), 2.92 (s, 1H); ¹³C NMR (101 MHz, CDCl₃) δ 160.3, 135.3, 132.2, 129.6, 128.7, 128.6, 128.0, 125.0, 122.2, 121.2, 120.1,

114.3, 88.6, 82.9, 72.5 (q, 32.8 Hz), 55.5; ^{19}F NMR (282 MHz, CDCl_3) δ -80.73; IR (Neat Film, NaCl) 3411, 2936, 2840, 1654, 1608, 1513, 1466, 1444, 1422, 1250, 1176, 1132, 1106, 1059, 967, 850, 824, 803, 757, 728, 690 cm^{-1} ; HRMS (MM) m/z calc'd for $\text{C}_{19}\text{H}_{14}\text{F}_3\text{O}$ $[\text{M}-\text{OH}]^+$: 315.0991 found 315.0993; SFC Conditions: 15% IPA, 2.5 mL/min, Chiralpak OD-H column, λ = 254 nm, t_{R} (min): major = 5.17, minor = 5.42.



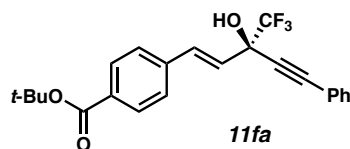
(*R, E*)-1-(4-fluorophenyl)-5-phenyl-3-(trifluoromethyl)pent-1-en-4-yn-3-ol (11da):

Product **11da** was prepared using general procedure and purified by column chromatography (8% EtOAc in hexanes) to provide a colorless oil (61.7 mg, 92% yield); 91% ee, $[\alpha]_{\text{D}}^{25} +12.0$ (c 1.0, CHCl_3); ^1H NMR (400 MHz, CDCl_3) δ 7.54 (dd, J = 8.1, 1.6 Hz, 2H), 7.45 (dd, J = 8.7, 5.3 Hz, 2H), 7.42 – 7.34 (m, 3H), 7.16 (d, J = 15.8 Hz, 1H), 7.06 (t, J = 8.7 Hz, 2H), 6.25 (d, J = 15.8 Hz, 1H), 2.92 (s, 1H); ^{13}C NMR (101 MHz, CDCl_3) δ 164.4, 161.9, 134.6, 132.2, 131.5 (q, J = 3.3 Hz), 129.7, 129.1 (d, J = 8.2 Hz), 128.6, 125.0, 122.2, 121.0, 116.0, 115.8, 88.8, 82.7, 72.3 (q, J = 32.9 Hz); ^{19}F NMR (282 MHz, CDCl_3) δ -80.76, -112.35; IR (Neat Film, NaCl) 3401, 3056, 2927, 1602, 1510, 1492, 1444, 1362, 1234, 1187, 1159, 1130, 1094, 1055, 967, 854, 826, 808, 757, 728, 690 cm^{-1} ; HRMS (MM) m/z calc'd for $\text{C}_{18}\text{H}_{11}\text{F}_4$ $[\text{M}-\text{OH}]^+$: 303.0791 found 303.0794; SFC Conditions: 20% IPA, 2.5 mL/min, Chiralpak AD-H column, λ = 254 nm, t_{R} (min): major = 7.83, minor = 10.52.



(*R*, *E*)-1-(4-bromophenyl)-5-phenyl-3-(trifluoromethyl)pent-1-en-4-yn-3-ol (11ea):

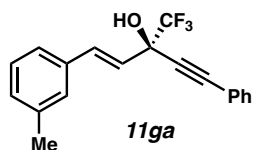
Product **11ea** was prepared using general procedure and purified by column chromatography (15% Et₂O in hexanes) to provide a colorless oil (70.8 mg, 93% yield); 90% ee, $[\alpha]_{\text{D}}^{25} -0.6$ (*c* 0.98, CHCl₃); ¹H NMR (400 MHz, CDCl₃) δ 7.59 – 7.46 (m, 4H), 7.45 – 7.31 (m, 5H), 7.13 (d, *J* = 15.8 Hz, 1H), 6.32 (d, *J* = 15.8 Hz, 1H), 2.93 (s, 1H); ¹³C NMR (101 MHz, CDCl₃) δ 134.5, 134.2, 132.2, 132.0, 129.8, 128.9, 128.6, 123.5 (q, *J* = 285.4 Hz), 123.1, 123.0, 120.9, 88.9, 82.5, 72.3 (q, *J* = 33.0 Hz); ¹⁹F NMR (282 MHz, CDCl₃) δ –80.71; IR (Neat Film, NaCl) 3400, 1489, 1248, 1187, 1130, 1056, 1010, 967, 816, 756, 690 cm^{–1}; HRMS (MM) *m/z* calc'd for C₁₈H₁₁BrF₃O [M–OH]⁺: 362.9991 found 362.9984; SFC Conditions: 8% IPA, 2.5 mL/min, Chiralpak OD-H column, λ = 254 nm, *t_R* (min): major = 12.79, minor = 13.56.



***tert*-butyl(*R*,*E*)-4-(3-hydroxy-5-phenyl-3-(trifluoromethyl)pent-1-en-4-yn-1-yl)benzoate**

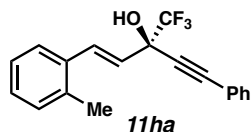
(11fa) Product **11fa** was prepared using general procedure and purified by column chromatography (15% EtOAc in hexanes) to provide a colorless oil (65.9 mg, 82% yield); 89% ee, $[\alpha]_{\text{D}}^{25} -10.4$ (*c* 0.95, CHCl₃); ¹H NMR (400 MHz, CDCl₃) δ 7.97 (d, *J* = 8.4 Hz, 2H), 7.58 – 7.47 (m, 4H), 7.45 – 7.32 (m, 3H), 7.22 (d, *J* = 15.8 Hz, 1H), 6.41 (d, *J* = 15.8 Hz, 1H), 2.95 (s, 1H), 1.60 (s, 9H); ¹³C NMR (101 MHz, CDCl₃) δ 165.7, 139.3, 134.6, 132.2, 132.0, 130.0, 129.7,

128.6, 127.1, 125.0, 124.8, 123.5 (q, $J = 285.5$ Hz), 88.7, 82.6, 81.6, 72.2 (q, $J = 32.9$ Hz), 28.3; ^{19}F NMR (282 MHz, CDCl_3) δ -80.66 IR (Neat Film, NaCl) 3402, 2979, 1711, 1691, 1608, 1478, 1492, 1445, 1394, 1370, 1317, 1299, 1250, 1184, 1127, 1070, 1018, 972, 846, 757, 691, 613 cm^{-1} ; HRMS (MM) m/z calc'd for $\text{C}_{23}\text{H}_{20}\text{F}_3\text{O}_2$ $[\text{M}-\text{OH}]^+$: 385.1410 found 385.1409; SFC Conditions: 10% IPA, 2.5 mL/min, Chiralpak IC column, $\lambda = 210$ nm, t_{R} (min): minor = 3.47, major = 4.28.



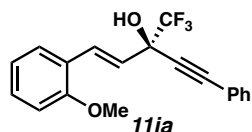
(*R,E*)-5-phenyl-1-(*m*-tolyl)-3-(trifluoromethyl)pent-1-en-4-yn-3-ol (11ga)

Product **11ga** was prepared using general procedure and purified by column chromatography (8% EtOAc in hexanes) to provide a colorless oil (61.2 mg, 97% yield); 90% ee, $[\alpha]_{\text{D}}^{25} +8.5$ (c 0.88, CHCl_3); ^1H NMR (400 MHz, CDCl_3) δ 7.53 (dd, $J = 8.0, 1.6$ Hz, 2H), 7.43 – 7.31 (m, 3H), 7.30 – 7.21 (m, 3H), 7.17 (d, $J = 15.8$ Hz, 1H), 7.13 (d, $J = 6.8$ Hz, 1H), 6.32 (d, $J = 15.8$ Hz, 1H), 2.93 (s, 1H), 2.36 (s, 3H); ^{13}C NMR (101 MHz, CDCl_3) δ 138.5, 135.9, 135.2, 132.2, 129.8, 129.7, 128.8, 128.6, 128.0, 126.1 (q, $J = 229.9$ Hz), 124.6, 122.2, 121.1, 88.7, 82.8, 72.5 (q, $J = 32.8$ Hz), 21.5; ^{19}F NMR (282 MHz, CDCl_3) δ -80.7; IR (Neat Film, NaCl) 3407, 2924, 1490, 1444, 1379, 1252, 1186, 1130, 1055, 1000, 966, 918, 844, 778, 756, 726, 689, 629 cm^{-1} ; HRMS (MM) m/z calc'd for $\text{C}_{19}\text{H}_{14}\text{F}_3$ $[\text{M}-\text{OH}]^+$: 299.1042 found 299.1045; SFC Conditions: 15% IPA, 2.5 mL/min, Chiralpak OD-H column, $\lambda = 254$ nm, t_{R} (min): major = 3.83, minor = 4.20.



(*R,E*)-5-phenyl-1-(*o*-tolyl)-3-(trifluoromethyl)pent-1-en-4-yn-3-ol (11ha)

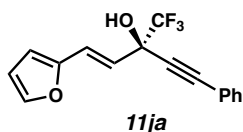
Product **11ha** was prepared using general procedure and purified by column chromatography (8% EtOAc in hexanes) to provide a colorless oil (57.8 mg, 92% yield); 86% ee, $[\alpha]_{\text{D}}^{25} +15.4$ (*c* 0.87, CHCl₃); ¹H NMR (400 MHz, CDCl₃) δ 7.57 – 7.46 (m, 4H), 7.45 – 7.33 (m, 3H), 7.25 – 7.16 (m, 3H), 6.24 (d, *J* = 15.7 Hz, 1H), 2.93 (s, 1H), 2.42 (s, 3H); ¹³C NMR (101 MHz, CDCl₃) δ 136.4, 134.5, 133.8, 132.2, 130.6, 129.7, 128.8, 128.6, 126.4, 126.3, 123.7, 123.6 (q, *J* = 285.3 Hz), 121.1, 88.7, 82.9, 72.6 (q, *J* = 32.8 Hz), 19.9; ¹⁹F NMR (282 MHz, CDCl₃) δ –80.73; IR (Neat Film, NaCl) 3411, 3061, 2926, 1600, 1490, 1462, 1444, 1381, 1261, 1248, 1185, 1133, 1098, 1058, 1000, 967, 817, 753, 690, 628 cm^{–1}; HRMS (MM) *m/z* calc'd for C₁₉H₁₄F₃ [M–OH]⁺: 299.1042 found 299.1043; SFC Conditions: 15% IPA, 2.5 mL/min, Chiralpak OD-H column, λ = 254 nm, *t*_R (min): major = 3.58, minor = 4.33.



(*E*)-1-(2-methoxyphenyl)-5-phenyl-3-(trifluoromethyl)pent-1-en-4-yn-3-ol (11ia):

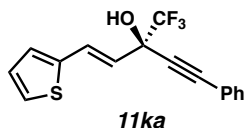
Product **11ia** was prepared using general procedure and purified by column chromatography (12% EtOAc in hexanes) to provide a colorless oil (59.6 mg, 92% yield); 86% ee, $[\alpha]_{\text{D}}^{25} +19.5$ (*c* 0.97, CHCl₃); ¹H NMR (400 MHz, CDCl₃) δ 7.58 – 7.50 (m, 3H), 7.48 (d, *J* = 7.7 Hz, 1H), 7.43 – 7.33 (m, 3H), 7.33 – 7.27 (m, 1H), 6.96 (t, *J* = 7.5 Hz, 1H), 6.91 (d, *J* = 8.3 Hz, 1H), 6.43 (d, *J* = 15.9

Hz, 1H), 3.88 (s, 3H), 2.88 (s, 1H). ^{13}C NMR (101 MHz, CDCl_3) δ 157.5, 132.2, 131.0, 130.1, 129.6, 128.6, 128.1, 123.6 (q, $J = 285.2$ Hz), 124.2, 123.0, 121.3, 120.8, 111.4, 111.2, 88.6, 83.0, 72.8 (q, $J = 32.7$ Hz), 55.7; ^{19}F NMR (282 MHz, CDCl_3) δ -80.66; IR (Neat Film, NaCl) 3429, 2940, 2360, 2237, 1599, 1490, 1465, 1248, 1185, 1136, 1103, 1048, 971, 754, 690 cm^{-1} ; HRMS (MM) m/z calc'd for $\text{C}_{19}\text{H}_{14}\text{F}_3\text{O}$ $[\text{M}-\text{OH}]^+$: 315.09860 found 315.09993; SFC Conditions: 15% IPA, 2.5 mL/min, Chiralpak OD-H column, $\lambda = 254$ nm, t_R (min): major = 4.95, minor = 5.67.

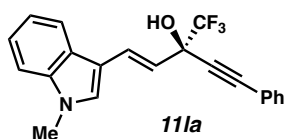


(*R,E*)-1-(4-bromophenyl)-5-phenyl-3-(trifluoromethyl)pent-1-en-4-yn-3-ol (11ja):

Product **11ja** was prepared using general procedure and purified by column chromatography (15% Et_2O in hexanes) to provide a colorless oil (52 mg, 89% yield); 90% ee, $[\alpha]_{\text{D}}^{25} -7.42$ (c 1.0, CHCl_3); ^1H NMR (400 MHz, CDCl_3) δ 7.52 (d, $J = 8.2$ Hz, 2H), 7.45 – 7.32 (m, 4H), 6.99 (d, $J = 15.6$ Hz, 1H), 6.42 (m, 2H), 6.29 (d, $J = 15.6$ Hz, 1H), 2.85 (s, 1H); ^{13}C NMR (101 MHz, CDCl_3) δ 151.1, 143.3, 132.2, 129.7, 128.6, 123.5 (q, $J = 285.3$ Hz), 123.5, 121.0, 120.6, 111.8, 111.2, 88.6, 82.6, 72.2 (q, $J = 33.1$ Hz); ^{19}F NMR (282 MHz, CDCl_3) δ -80.78; IR (Neat Film, NaCl) 3429, 3060, 2926, 1661, 1600, 1564, 1491, 1445, 1400, 1300, 1266, 1249, 1188, 1154, 1127, 1056, 1016, 1000, 960, 928, 884, 844, 804, 757, 742, 728, 690, 673, 654, 612 cm^{-1} ; HRMS (MM) m/z calc'd for $\text{C}_{16}\text{H}_{10}\text{F}_3\text{O}$ $[\text{M}-\text{OH}]^+$: 275.0678 found 275.0668; SFC Conditions: 15% IPA, 2.5 mL/min, Chiralpak OJ-H column, $\lambda = 210$ nm, t_R (min): major = 3.12, minor = 3.86.

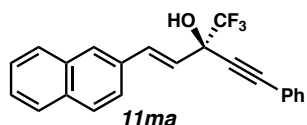


(*R,E*)-5-phenyl-1-(thiophen-2-yl)-3-(trifluoromethyl)pent-1-en-4-yn-3-ol (11ka): Product **11ka** was prepared using general procedure and purified by column chromatography (8% EtOAc in hexanes) to provide a colorless oil (51.8 mg, 84% yield); 90% ee, $[\alpha]_D^{25} +25.8$ (*c* 0.88, CHCl₃); ¹H NMR (400 MHz, CDCl₃) δ 7.54 (dd, *J* = 8.0, 1.5 Hz, 2H), 7.45 – 7.30 (m, 5H), 7.28 (dd, *J* = 4.8, 1.5 Hz, 1H), 7.21 (d, *J* = 15.7 Hz, 1H), 6.20 (d, *J* = 15.7 Hz, 1H), 2.94 (s, 1H); ¹³C NMR (101 MHz, CDCl₃) δ 137.9, 132.2, 129.8, 129.7, 128.6, 126.7, 125.2, 125.0, 122.1, 121.0, 88.7, 82.7, 72.4 (q, *J* = 32.9 Hz); ¹⁹F NMR (282 MHz, CDCl₃) δ –80.78; IR (Neat Film, NaCl) 3406, 2924, 1656, 1491, 1444, 1358, 1308, 1249, 1186, 1126, 1054, 1000, 964, 868, 775, 757, 725, 690, 606 cm^{–1}; HRMS (MM) *m/z* calc'd for C₁₆H₁₀F₃S [M–OH]⁺: 291.045 found 291.045; SFC Conditions: 15% IPA, 2.5 mL/min, Chiralpak OD-H column, λ = 210 nm, *t_R* (min): major = 4.20, minor = 4.50.



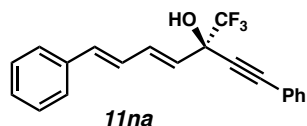
(*R,E*)-1-(1-methyl-1*H*-indol-3-yl)-5-phenyl-3-(trifluoromethyl)pent-1-en-4-yn-3-ol (11la): Product **11la** was prepared using general procedure and purified by column chromatography (30% EtOAc in hexanes) to provide a yellow oil (32.2 mg, 63% yield); 96% ee, $[\alpha]_D^{25} +4.2$ (*c* 0.95 CHCl₃); ¹H NMR (400 MHz, CDCl₃) δ 7.81 (d, *J* = 7.8 Hz, 1H), 7.48 (d, *J* = 8.1 Hz, 2H), 7.30 (dd, *J* = 11.5, 4.2 Hz, 4H), 7.26 – 7.19 (m, 2H), 7.18 – 7.12 (m, 2H), 6.22 (d, *J* = 15.8 Hz, 1H), 3.71 (s, 3H); ¹³C NMR (101 MHz, CDCl₃) δ 137.8, 132.2, 130.3, 129.5, 128.8, 128.6, 126.1, 122.6,

121.4, 120.6, 120.3, 117.6, 111.9, 88.6, 83.3, 73.13 (q, $J = 32.8$ Hz), 33.1, 29.9; ^{19}F NMR (282 MHz, CDCl_3) δ -80.83; IR (Neat Film, NaCl) 3382, 2922, 1651, 1535, 1491, 1444, 1378, 1333, 1255, 1184, 1125, 1060, 960, 787, 758, 741, 691, 645 cm^{-1} ; HRMS (MM) m/z calc'd for $\text{C}_{21}\text{H}_{15}\text{F}_3\text{N}$ $[\text{M}-\text{OH}]^+$: 338.1151 found 338.1151; SFC Conditions: 30% IPA, 2.5 mL/min, Chiralpak AD-H column, $\lambda = 254$ nm, t_R (min): major = 6.29, minor = 7.80.



(*R, E*)-1-(naphthalen-2-yl)-5-phenyl-3-(trifluoromethyl)pent-1-en-4-yn-3-ol (11ma):

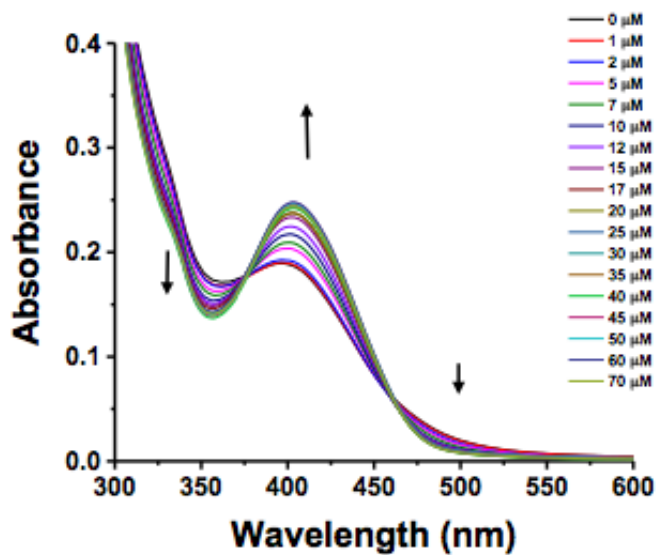
Product **11ma** was prepared using general procedure and purified by column chromatography (10% EtOAc in hexanes) to provide a colorless oil (67.7 mg, 96% yield); 92% ee, $[\alpha]_D^{25} +13.8$ (c 1.0, CHCl_3); ^1H NMR (400 MHz, CDCl_3) δ 7.90 – 7.80 (m, 4H), 7.66 (dd, $J = 8.7, 1.6$ Hz, 1H), 7.58 (d, $J = 6.3$ Hz, 2H), 7.50 (d, $J = 9.4$ Hz, 2H), 7.46 – 7.34 (m, 4H), 6.47 (d, $J = 15.8$ Hz, 1H), 2.98 (s, 1H); ^{13}C NMR (101 MHz, CDCl_3) δ 135.9, 133.7, 133.5, 132.7, 132.2, 129.7, 128.62, 128.60, 128.3, 128.2, 127.9, 126.7, 126.6, 123.2 (q, $J = 110.0$ Hz), 88.8, 82.8, 72.5 (q, $J = 32.9$ Hz); ^{19}F NMR (282 MHz, CDCl_3) δ -80.62; IR (Neat Film, NaCl) 3400, 3057, 1652, 1491, 1444, 1361, 1252, 1186, 1126, 1054, 965, 894, 843, 810 cm^{-1} ; HRMS (MM) m/z calc'd for $\text{C}_{18}\text{H}_{11}\text{BrF}_3\text{O}$ $[\text{M}-\text{OH}]^+$: 335.1042 found 335.1043; SFC Conditions: 8% IPA, 2.5 mL/min, Chiralpak IC column, $\lambda = 210$ nm, t_R (min): major = 6.56, minor = 7.11.



(*R*,4*E*,6*E*)-1,7-diphenyl-3-(trifluoromethyl)hepta-4,6-dien-1-yn-3-ol (11na): Product **11na** was prepared using general procedure and purified by column chromatography (8% EtOAc in hexanes) to provide a colorless oil (28.1 mg, 43% yield); 91% ee, $[\alpha]_D^{25} +11.3$ (*c* 0.67, CHCl₃); ¹H NMR (400 MHz, CDCl₃) δ 7.54 (dd, *J* = 8.0, 1.6 Hz, 2H), 7.47 – 7.26 (m, 8H), 6.99 (dd, *J* = 14.9, 10.4 Hz, 1H), 6.86 (dd, *J* = 15.4, 10.5 Hz, 1H), 6.74 (d, *J* = 15.5 Hz, 1H), 5.95 (d, *J* = 14.9 Hz, 1H), 2.85 (s, 1H); ¹³C NMR (101 MHz, CDCl₃) δ 136.6, 136.5, 135.9, 132.2, 129.7, 128.9, 128.6, 128.4, 126.9, 126.7, 125.6, 123.5 (q, *J* = 285.3 Hz), 121.1, 88.6, 82.7, 72.3 (q, *J* = 33.0 Hz); ¹⁹F NMR (282 MHz, CDCl₃) δ –80.78; IR (Neat Film, NaCl) 3396, 3027, 2922, 2850, 1644, 1491, 1447, 1253, 1186, 1127, 1051, 990, 974, 828, 756, 726, 690 cm^{–1}; HRMS (MM) *m/z* calc'd for C₂₀H₁₄F₃ [M–OH]⁺: 311.1042 found 311.1037; SFC Conditions: 35% IPA, 2.5 mL/min, Chiralpak AD-H column, λ = 254 nm, *t_R* (min): major = 3.3, minor = 4.4.

1.9.3 UV-VIS DATA FOR METAL TITRATION

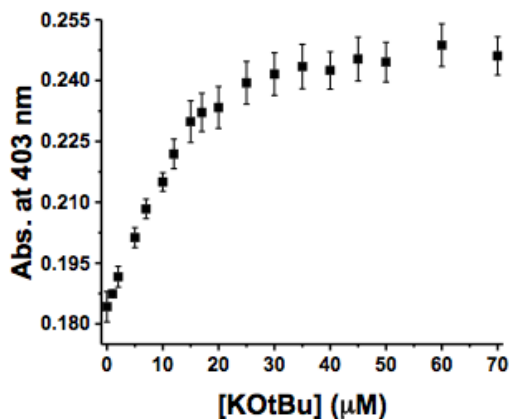
A sample solution containing **L1-Ni** (20 M) and different amounts of KO*t*-Bu (0, 1, 2, 5, 7, 10, 12, 15, 17, 20, 25, 30, 35, 40, 45, 50, 60, and 70 M) prepared in dry THF, respectively. After incubation for 30 min at room temperature, UV-Vis spectra were recorded at 25 °C and each measurement was repeated thrice.



Isobestic point 1. 376 nm 2. 460 nm

Job plot

A solution of **L1-Ni** (40 M) in THF was mixed with solutions of KOtBu in THF (40 M) at varying ratios. After incubation for 30 min at room temperature, UV-Vis spectra were recorded at 25 °C and each measurement was repeated thrice.



Association constant for the binding of L1-Ni and K⁺

The program DynaFit was used for non-linear regression fitting of the titration data based on absorbance changes observed at 403 nm. From the result of Job plot, the fitting of titration data were performed as a 1:1 binding mode. The DynaFit scripts for the binding models used are provided below.

[task]

task = fit

data = equilibria

[mechanism]

$L + M \rightleftharpoons LM$: K1 association

[constants]

K1 = 0.5?

[concentrations]

L = 20

[responses]

L = 0.0092?

LM = 0.0125

[data]

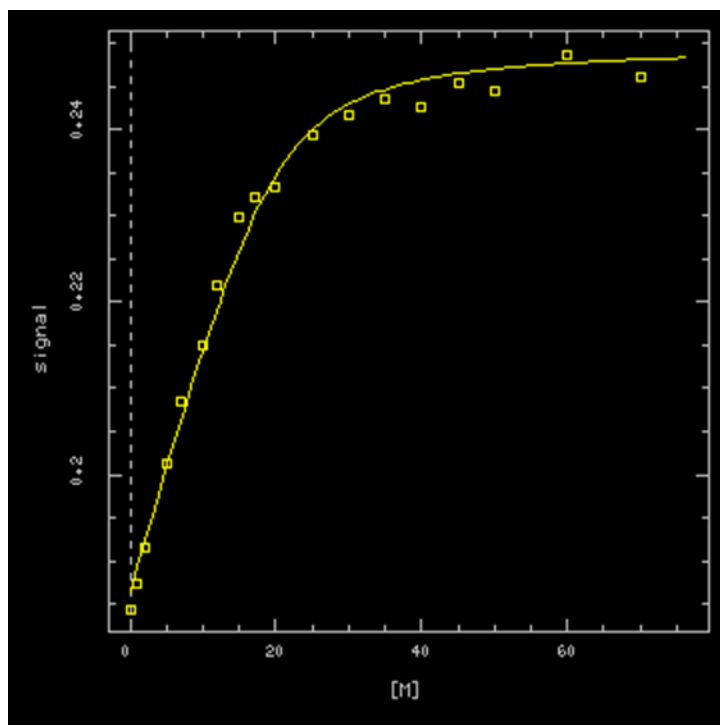
variable M

file C:\Users\skang\Desktop\dynafit4-win/DynaFit4/input/titration.txt

[output]

directory C:\Users\skang\Desktop\dynafit4-win/DynaFit4/output

[end]



The association constant for the binding of **L1-Ni** and K⁺ ion. $K_a = 6.6 \times 10^5 \text{ M}^{-1}$

1.10 NOTES AND REFERENCES

1. Zhou, Y.; Wang, J.; Gu, Z.; Wang, S.; Zhu, W.; Aceña, J. L.; Soloshonok, V. A.; Izawa, K.; Liu, H. *Chem. Rev.* **2016**, *116*, 422–518.
2. (a) Although both CF₃ and *i*Pr groups possess very different van der Waals radii (*i*Pr = 56.2 Å³), their A-values are nearly identical, which is why they are considered isosteric. For more information see: Tredwell, M.; Gouverneur, V. Fluorine in Medicinal Chemistry: Importance of Chirality. *Comprehensive Chirality*, Yamamoto, H.; Carreira, E., Eds.; Elsevier Ltd. 2012; Vol. 1, pp 70–85. (b) (a) Nie, J.; Guo, H.-C.; Cahard, D.; Ma, J. –A. *Chem. Rev.* **2011**, 455–529. (b) Noda, H.; Kumagai, N.; Shibasaki, M. *Asian J. Org. Chem.* **2018**, *7*, 599–612.
3. Vrouenraets, S. M. E.; Wit, F. W. N. M.; Tongeren, J. V.; Lange, J. M. A. **2007**, *8*, 851–871.
4. For examples of enantioselective alkynylation of aldehydes, see: (a) Anand, N. K.; Carreira, E. M. *J. Am. Chem. Soc.* **2001**, *123*, 9687–9688. (b) Li, X.; Lu, G.; Kwok, W. H.; Chan, A. S. C. *J. Am. Chem. Soc.* **2002**, *124*, 12636–12637. (c) Takita, R.; Yakura, K.; Ohshima, T.; Shibasaki, M. *J. Am. Chem. Soc.* **2005**, *127*, 13760–13761. (d) Wolf, C.; Liu, S. *J. Am. Chem. Soc.* **2006**, *128*, 10996–10997. (e) Trost, B. M.; Weiss, A. H. *J. Am. Chem. Soc.* **2006**, *128*, 8–9. (f) Asano, Y.; Hara, K.; Ito, H. *Org. Lett.* **2007**, *9*, 3901–3904. (g) Ito, J.-I.; Asai, R.; Nishiyama, H. *Org. Lett.* **2010**, *12*, 3860–3862. (h) Trost, B. M.; Quintard, A. *Angew. Chem. Int. Ed.* **2012**, *51*, 6704–6708, and *Angew. Chem.* **2012**, *124*, 6808–6812. (i) Trost, B. M.; Burns, A. C.; Bartlett, M. J.; Tautz, T.; Weiss, A. H. *J. Am. Chem. Soc.*

- 2012**, *134*, 1474–1477. (j) Trost, B. M.; Bartlett, M. J.; Weiss, A. H.; von Wangelin, A. J.; Chan, V. S. *Chem.–Eur. J.* **2012**, *18*, 16498–16509. (k) Song, T.; Zheng, L.-S.; Ye, F.; Deng, W.-H.; Wei, Y.-L.; Jiang, K.-Z.; Xu, L.-W. *Adv. Synth. Catal.* **2014**, *356*, 1708–1718.
5. For examples of enantioselective alkynylation of imines, see: (a) Morisaki, K.; Sawa, M.; Nomaguchi, J.-Y.; Morimoto, H.; Takeuchi, Y.; Mashima, K.; Ohshima, T. *Chem. Eur. J.* **2013**, *19*, 8417–8420. (b) de Armas, P.; Tejedor, D.; García-Tellado, F. *Angew. Chem. Int. Ed.* **2010**, *49*, 1013–1016 and *Angew. Chem.* **2010**, *122*, 1029–1032. (c) Morisaki, K.; Sawa, M.; Yonesaki, R.; Morimoto, H.; Mashima, K.; Ohshima, T. *J. Am. Chem. Soc.* **2016**, *138*, 6194–6203. (d) Liu, R.-R.; Zhu, L.; Hu, J.-P.; Lu, C.-J.; Gao, J.-R.; Lan, Y.; Jia, Y.-X. *Chem. Commun.* **2017**, *53*, 5890–5893.
6. For examples of enantioselective alkynylation of ketones see: (a) Cozzi, P.G. *Angew. Chem. Int. Ed.* **2003**, *42*, 2895–2898 and *Angew. Chem.* **2003**, *115*, 3001–3004. (b) Zhou, Y.; Wang, R.; Xu, Z.; Yan, W.; Liu, L.; Kang, Y.; Han, Z. *Org. Lett.* **2004**, *23*, 4147–4149. (b) Lu, G.; Li, X.; Li, Y.-M.; Kwong, F. Y.; Chan, A. S. C. *Adv. Synth. Catal.* **2006**, *348*, 1926–1933. (c) Lu, G.; Li, X.; Jia, X.; Chan, W. L.; Chan, A. S. C. *Angew. Chem. Int. Ed.* **2003**, *42*, 5057–5058 and *Angew. Chem.* **2003**, *115*, 5211–5212. (d) Lu, G.; Li, Y.-M.; Li, X.-S.; Chan, A. S. C. *Coord. Chem. Rev.* **2005**, *249*, 1736–1744. (e) Liu, L.; Wang, R.; Kang, Y.-F.; Chen, C.; Xu, Z.-Q.; Zhou, Y.-F.; Ni, M.; Cai, H.-Q.; Gong, M.-Z. *J. Org. Chem.* **2005**, *70*, 1084–1086. (f) Chen, C.; Hong, L.; Xu, Z. Q.; Liu, L.; Wang, R. *Org. Lett.* **2006**, *8*, 2277–2280.

7. For alkynylation of trifluoromethyl ketones: (a) Motoki, R.; Kanai, M.; Shibasaki, M. *Org. Lett.* **2007**, *9*, 2997–3000. (b) Zhang, G.-W.; Meng, W.; Ma, H.; Nie, J.; Zhang, W.-Q.; Ma, J.-A. *Angew. Chem. Int. Ed.* **2011**, *50*, 3538–3542 and *Angew. Chem.* **2011**, *123*, 3600–3604. (c) Ohshima, T.; Kawabata, T.; Takeuchi, Y.; Kakinuma, T.; Iwasaki, T.; Yonezawa, T.; Murakami, H.; Nishiyama, H.; Mashima, K. *Angew. Chem., Int. Ed.* **2011**, *50*, 6296–6300. (d) Dhayalan, V.; Murakami, R.; Hayashi, M. *Asian J. Chem.* **2013**, *25*, 7505–7508. (e) Cook, A. M.; Wolf, C. *Angew. Chem. Int. Ed.* **2016**, *55*, 2929–2933 and *Angew. Chem.* **2016**, *128*, 2982–2986. (f) Ito, J.-I.; Ubukata, S.; Muraoka, S.; Nishiyama, H. *Chem. Eur. J.* **2016**, *22*, 16801–16804. (g) Zheng, Y.; Harms, K.; Zhang, L.; Meggers, E. *Chem. Eur. J.* **2016**, *22*, 11977–11981. (h) Zheng, Y.; Zhang, L.; Meggers, E. *Org. Process Res. Dev.* **2018**, *22*, 103–107. (i) Chen, S.; Zheng, Y.; Cui, T.; Meggers, E.; Houk, K. N. *J. Am. Chem. Soc.* **2018**, *140*, 5146–5152. (j) Cui, T.; Qin, J.; Harms, K.; Meggers, E. *Eur. J. Inorg. Chem.* **2019**, 195–198. (k) For a racemic example, see: Czerwinski, P.; Molga, E.; Cavallo, L.; Poater, A.; Michalak, M. *Chem. Eur. J.* **2016**, *22*, 8089–8094. For alkenylation and phenylation of trifluoromethyl ketones: (l) Motoki, R.; Tomita, D.; Kanai, M.; Shibasaki, M. *Tetrahedron Lett.* **2006**, *47*, 8083–8086.
8. For alkynylation of trifluoromethyl β -ketoesters: (a) Aikawa, K.; Hioki, Y.; Mikami, K. *Org. Lett.* **2010**, *12*, 5716–5719. (b) Wang, T.; Niu, J.-L.; Liu, S.L.; Huang, J.-J.; Gong, J.-F.; Song, M.-P. *Adv. Synth. Catal.* **2013**, *355*, 927–937.
9. (a) Park, J.; Hong, S. *Chem. Soc. Rev.* **2012**, *41*, 6931–6943. (b) DiMauro, E. F.; Kozlowski, M. C. *Org. Lett.* **2001**, *3*, 1641–1644. (c) Handa, V.; Gnanadesikan, S.; Matsunaga, S.; Shibasaki, M. *J. Am. Chem. Soc.* **2007**, *129*, 4900–4901. (d) Chen, Z.; Morimoto, S.;

- Matsunaga, S.; Shibasaki, M. *J. Am. Chem. Soc.* **2008**, *130*, 2170–2171. (e) Mitsunuma, H.; Matsunaga, S. *Chem. Commun.* **2011**, *47*, 469–471. (f) Shepherd, N. E.; Tanabe, H.; Xu, Y.; Matsunaga, S.; Shibasaki, M. *J. Am. Chem. Soc.* **2010**, *132*, 3666–3667. (g) Yingjie, X.; Matsunaga, S.; Shibasaki, M. *Org. Lett.* **2010**, *12*, 3246–3249. (h) Matsunaga, S.; Shibasaki, M. *Synlett*, **2009**, *10*, 1635–1638. (i) Lang, K.; Park, J.; Hong, S. *Angew. Chem. Int. Ed.* **2012**, *51*, 1620–1624 and *Angew. Chem.* **2012**, *124*, 1652–1656. (j) Park, J.; Lang, K.; Abboud, K. A.; Hong, S. *Chem.–Eur. J.* **2011**, *17*, 2236–2245. (k) Park, J.; Lang, K.; Abboud, K. A.; Hong, S. *J. Am. Chem. Soc.* **2008**, *130*, 16484–16485. (l) Shibasaki, M.; Sasai, H.; Arai, T. *Angew. Chem. Int. Ed.* **1997**, *36*, 1236–1256.
10. For the use of chiral crown-ether type catalysts, see: (a) Cram, D. J.; Sogah, G. D. *J. Chem. Soc., Chem. Commun.* **1981**, 625–628. (b) Brak, K.; Jacobsen, E. N. *Angew. Chem. Int. Ed.* **2013**, *52*, 534–561 and *Angew. Chem.* **2013**, *125*, 558–588. (c) Oliveira, M. T.; Lee, J.–W. *Chem. Cat. Chem.* **2017**, *9*, 377–384. (d) Akiyama, T.; Hara, M.; Fuchibe, K.; Sakamoto, S.; Yamaguchi, K. *Chem. Commun.* **2003**, 1734–1735. (e) Yan, H.; Jang, H. B.; Lee, J.–W.; Kim, H. K.; Lee, S. W.; Yang, J. W.; Song, C. E. *Angew. Chem., Int. Ed.* **2010**, *49*, 8915–8917 and *Angew. Chem.* **2010**, *122*, 9099–9101. (f) Yan, H.; Oh, J. S.; Lee, J.–W.; Song, C. E. *Nat. Commun.* **2012**, *3*, 1212. (g) Park, S. Y.; Lee, J.–W.; Song, C. E. *Nat. Commun.* **2015**, *6*, 7512. (h) Li, L.; Liu, Y.; Peng, Y.; Yu, L.; Wu, X.; Yan, H. *Angew. Chem. Int. Ed.* **2016**, *55*, 331–335 and *Angew. Chem.* **2016**, *128*, 339–343. (i) Liu, Y.; Ao, J.; Paladhi, S.; Song, C. E.; Yan, H. *J. Am. Chem. Soc.* **2016**, *138*, 16486–16492. (j) Vaithiyanathan, V.; Kim, M. J.; Liu, Y.; Yan, H.; Song, C. E. *Chem.–Eur. J.* **2017**, *23*, 1268–1272. (k) Kim, M. J.; Xue, L.; Liu, Y.; Paladhi, S.; Park, S. J.; Yan, H.; Song, C. E.

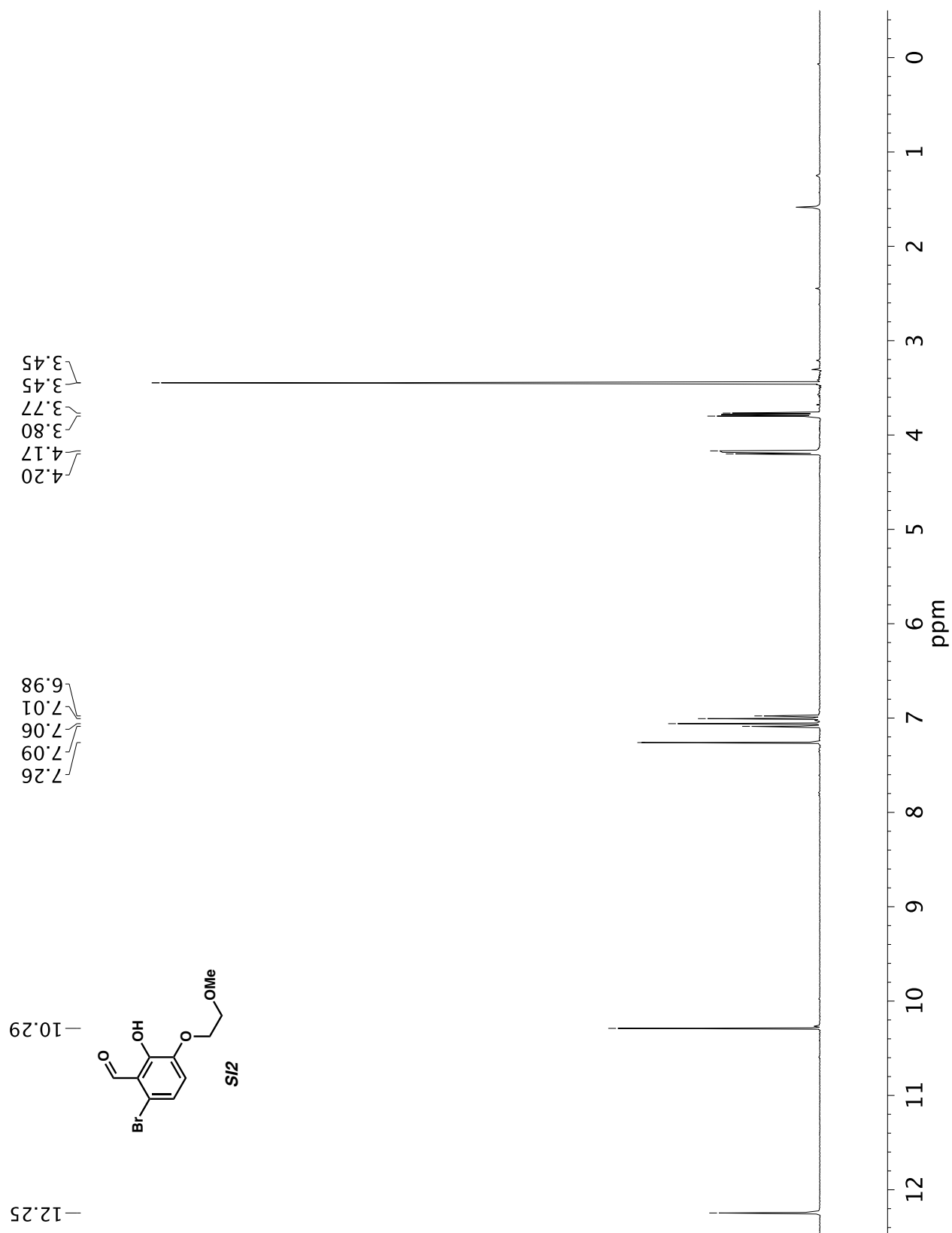
- Adv. Synth. Catal.* **2017**, *359*, 811–823. (l) Yu, L.; Wu, X.; Kim, M. J.; Vaithiyanathan, V.; Liu, Y.; Tan, Y.; Qin, W.; Song, C. E.; Yan, H. *Adv. Synth. Catal.* **2017**, *359*, 1879–1891. (m) Park, S. Y.; Hwang, I.-S.; Lee, H.-J.; Song, C. E. *Nat. Commun.* **2017**, *8*, 14877. (n) Tan, Y.; Luo, S.; Li, D.; Zhang, N.; Jia, S.; Liu, Y.; Qin, W.; Song, C. E.; Yan, H. *J. Am. Chem. Soc.* **2017**, *139*, 6431–6436. (o) Duan, M.; Liu, Y.; Ao, J.; Xue, L.; Luo, S.; Tan, Y.; Qin, W.; Song, C. E.; Yan, H. *Org. Lett.* **2017**, *19*, 2298–2301. (p) Paladhi, S.; Liu, Y.; Kumar, B. S.; Jung, M.-J.; Park, S. Y.; Yan, H.; Song, C. E. *Org. Lett.* **2017**, *19*, 3279–3282. (q) Paladhi, S.; Park, S. Y.; Yang, J. W.; Song, C. E. *Org. Lett.* **2017**, *19*, 5336–5339. (r) Paladhi, S.; Hwang, I.-S.; Yoo, E. J.; Ryu, D. H.; Song, C. E. *Org. Lett.* **2018**, *20*, 2003–2006. (s) Liu, Y.; Liu, S.; Li, D.; Zhang, N.; Peng, L.; Ao, J.; Song, C. E.; Lan, Y.; Yan, H. *J. Am. Chem. Soc.* **2019**, *141*, 1150–1159.
11. For the use of ligands with pendant crown ethers in transition metal-catalysis, see: (a) Sawamura, M.; Nagata, H.; Sakamoto, H.; Ito, Y. *J. Am. Chem. Soc.* **1992**, *114*, 2586–2592. (b) Trost, B. M.; Radinov, R. *J. Am. Chem. Soc.* **1997**, *119*, 5962–5963. (c) Dinuclear Schiff-base catalysts: (d) Matsunaga, S.; Shibasaki, M. *Chem. Commun.*, **2014**, 50, 1044–1057. (e) Chen, Z.; Morimoto, H.; Matsunaga, S.; Shibasaki, M. *J. Am. Chem. Soc.* **2008**, *130*, 2170–2171. (f) Xu, Y.; Lin, L.; Kanai, M.; Matsunaga, S.; Shibasaki, M. *J. Am. Chem. Soc.* **2011**, *133*, 5791–5793.
12. Yang, D.; Wang, L.; Han, F.; Zhao, D.; Zhang, B.; Wang, R. *Angew. Chem. Int. Ed.* **2013**, *52*, 6739–6742 and *Angew. Chem.* **2013**, *125*, 6871–6874.
13. Personal communication
14. Cai, Z.; Xiao, D.; Do, L. H. *J. Am. Chem. Soc.* **2015**, *137*, 15501–15510.

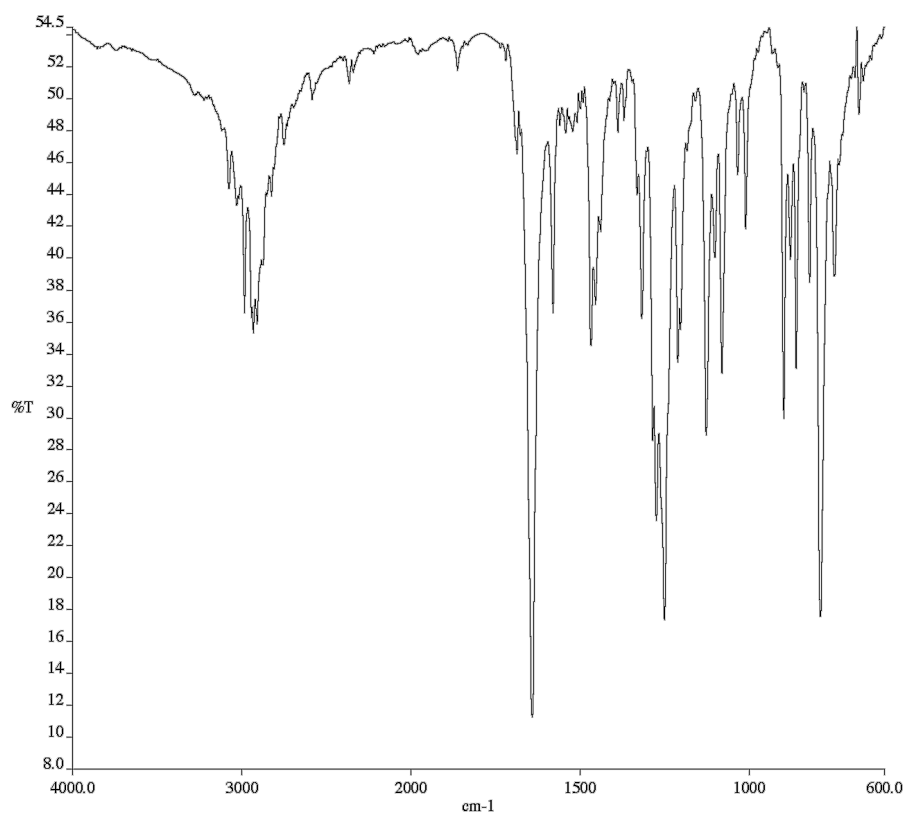
15. See Materials and Methods Section for more details.
16. Bi, W.-Y.; Lü, X.-Q.; Chai, W.-L.; Song, J.-R.; Wong, W.-Y.; Wong, W.-K.; Jones, R. A. *Journal of Molecular Structure* **2008**, *891*, 450-455.
17. Pärssinen, A.; Luhtanen, T.; Pakkanen, T.; Leskelä, M.; Repo, T. *European Journal of Inorganic Chemistry* **2010**, *2010*, 266-274.
18. Moreno, M.; Elgaher, W. A.; Herrmann, J.; Schläger, N.; Hamed, M. M.; Baumann, S.; Müller, R.; Hartmann, R. W.; Kirschning, A. *Synlett*, **2015**, *26*, 1175-1178.
19. Vazquez-Molina, D.; Pope, G. M.; Ezazi, A. A.; Mendoza-Cortes, J. L.; Harper, J. H.; Uribe-Romo, F. J. *Chem. Commun.* **2018**, *54*, 6947-6950.
20. Zhang, H.-C.; Huang, W.-S.; Pu, L. *J. Org. Chem.* **2001**, *66*, 481-487.
21. Mechler, M.; Latendorf, K.; Frey, W.; Peters, R. *Organometallics* **2013**, *32*, 112-130.
22. Kelly, CB.; Mercadante, MA.; Hamlin, TA.; Fletcher, MH. *J. Org. Chem.* **2012**, *77*, 8131-814.
23. Zheng, C.; Li, Y.; Yang, Y.; Wang, H.; Cui, H.; Zhang, J.; Zhao, G. *Adv. Synth. and Catal.* **2009**, *351*, 1685-1691.
24. Ortega, A.; Manzano, R.; Uria, U.; Carrillo, L.; Reyes, E.; Tejero, T.; Merino, P.; Vicario, J. L. *Angew. Chem. Int. Ed.* **2018**, *57*, 8225-8229.
25. Wang, Y.; Han, J.; Chen, J.; Weiguo, C. *Tetrahedron*, **2015**, *71*, 8256-8262.
26. Sasaki, S.; Yamauchi, T.; Higashiyama, K. *Tetrahedron Lett.* **2010**, *51*, 2326-2328.
27. Nenajdenko, V. G.; Krasovsky, A. L.; Lebedev, M. V.; Balenkova, E. S. *Synlett*, **1997**, *12*, 1349-1350.
28. Sanz-Marco, A.; Blay, G.; Muñoz, M. C.; Pedro, J. R. *Chem. Commun.* **2015**, *51*, 8958-8961.
29. Motoki, R.; Kanai, M.; Shibasaki, M. *Org. Lett.* **2007**, *9*, 2997-3000.
30. Zhang, G.-W.; Meng, W.; Ma, H.; Nie, J.; Zhang, W.-Q.; Ma, J.-A. *Angew. Chem. Int. E.* **2011**, *50*, 3538-3542.

APPENDIX 1

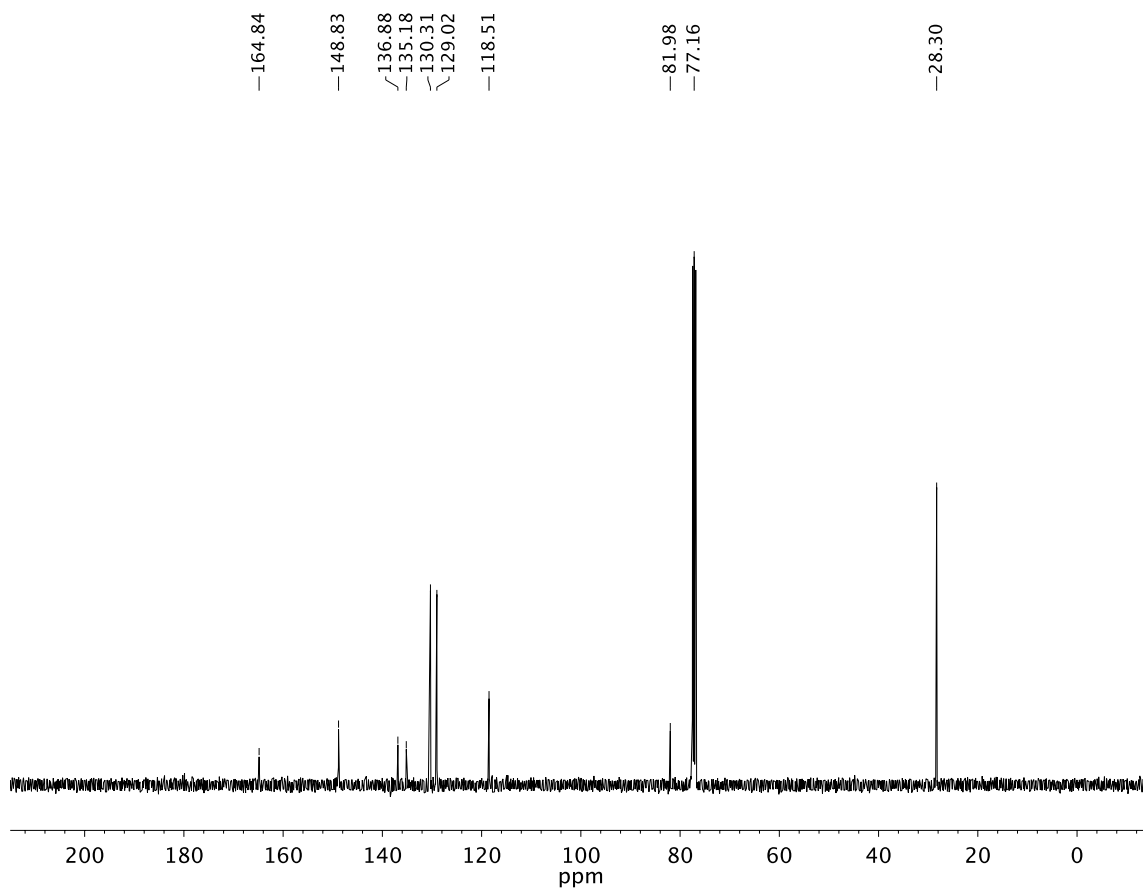
Spectra Relevant to Chapter 1:

*Enantioselective Alkynylation of Trifluoromethyl Ketones Catalyzed by
Cation-Binding Salen Nickel Complexes*

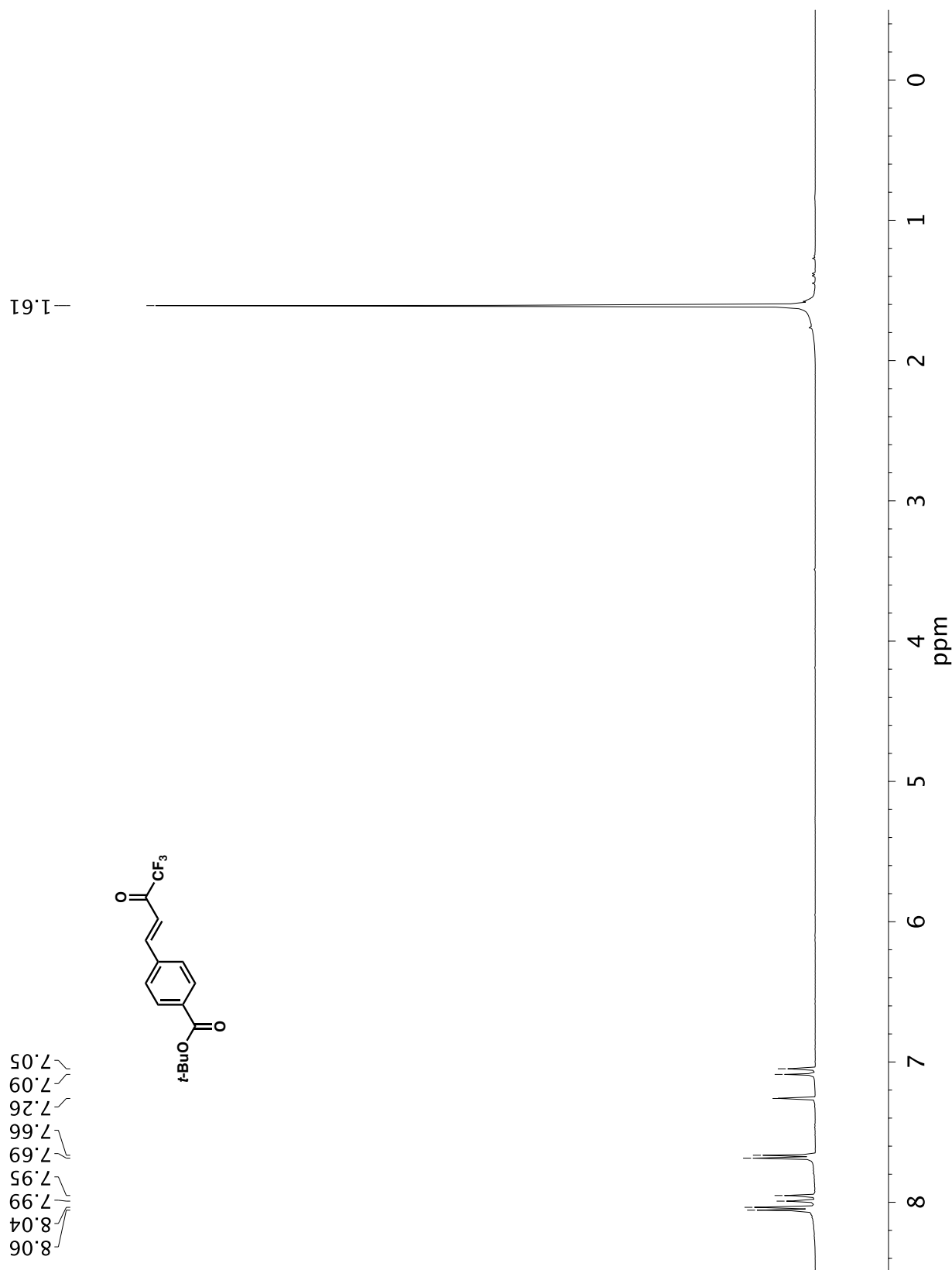
**A1.1** ¹H NMR (300 MHz, CDCl₃) of compound **SI2**.

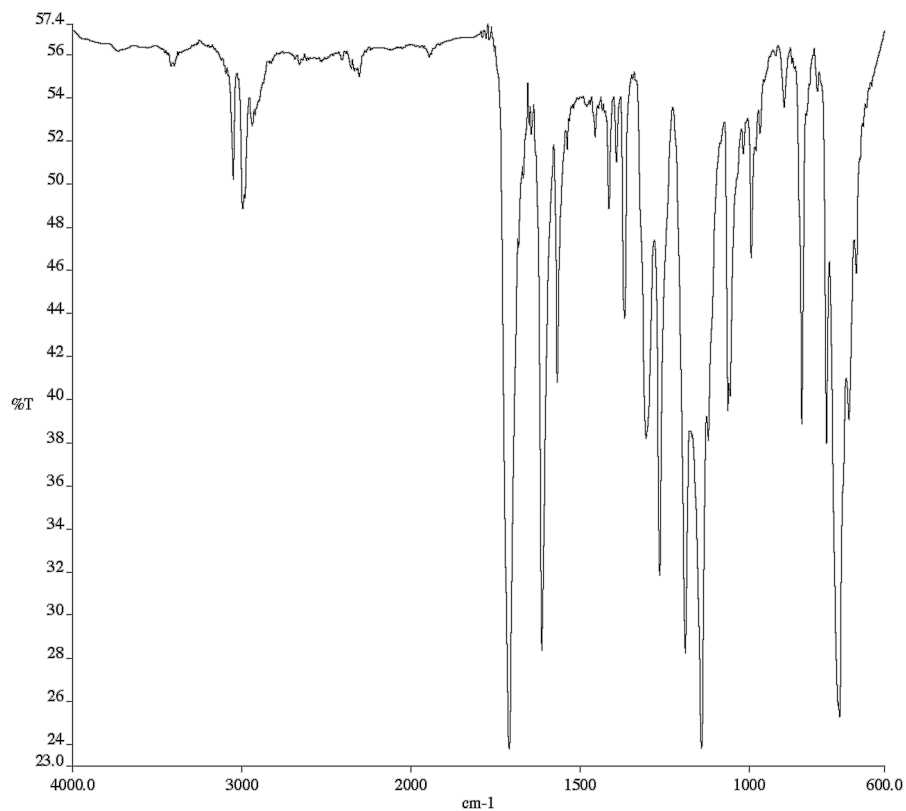


A1.2 Infrared spectrum (Thin Film, NaCl) of compound **SI2**.

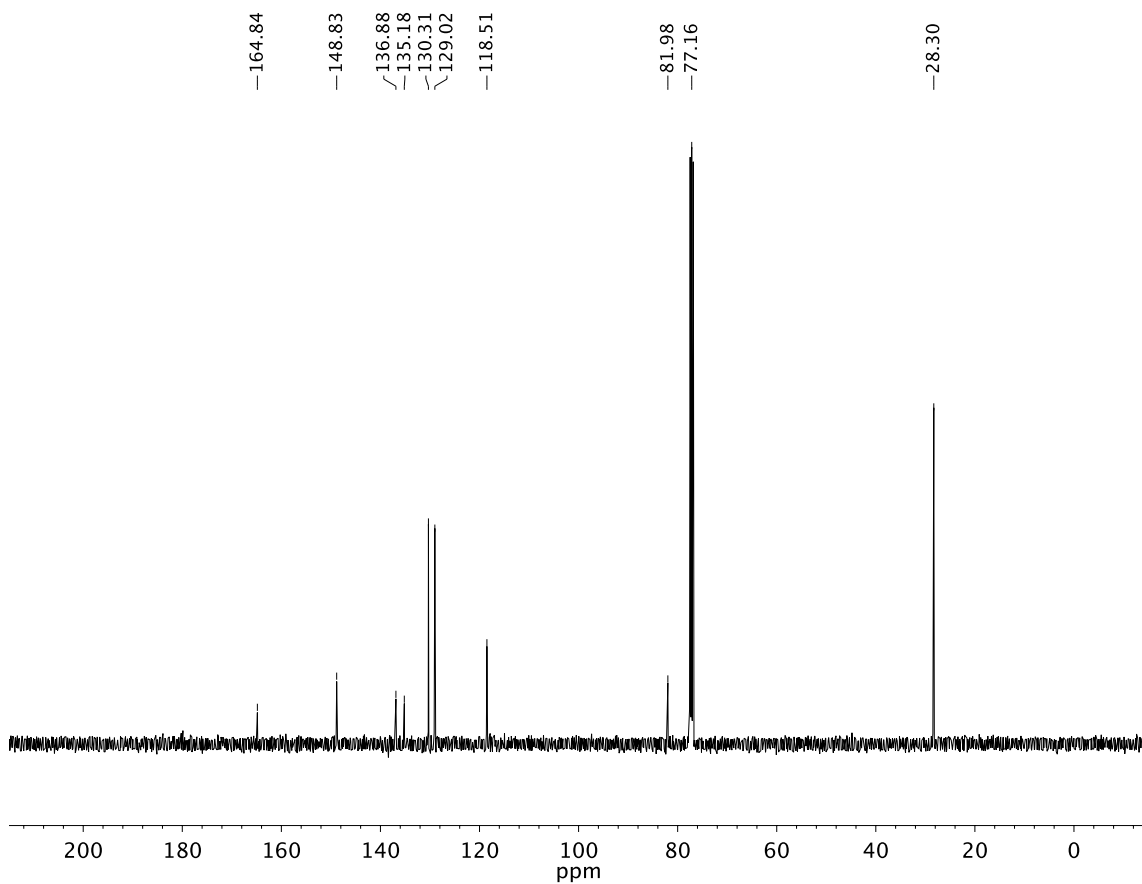


A1.3 ¹³C NMR (101 MHz, CDCl₃) of compound **SI2**.

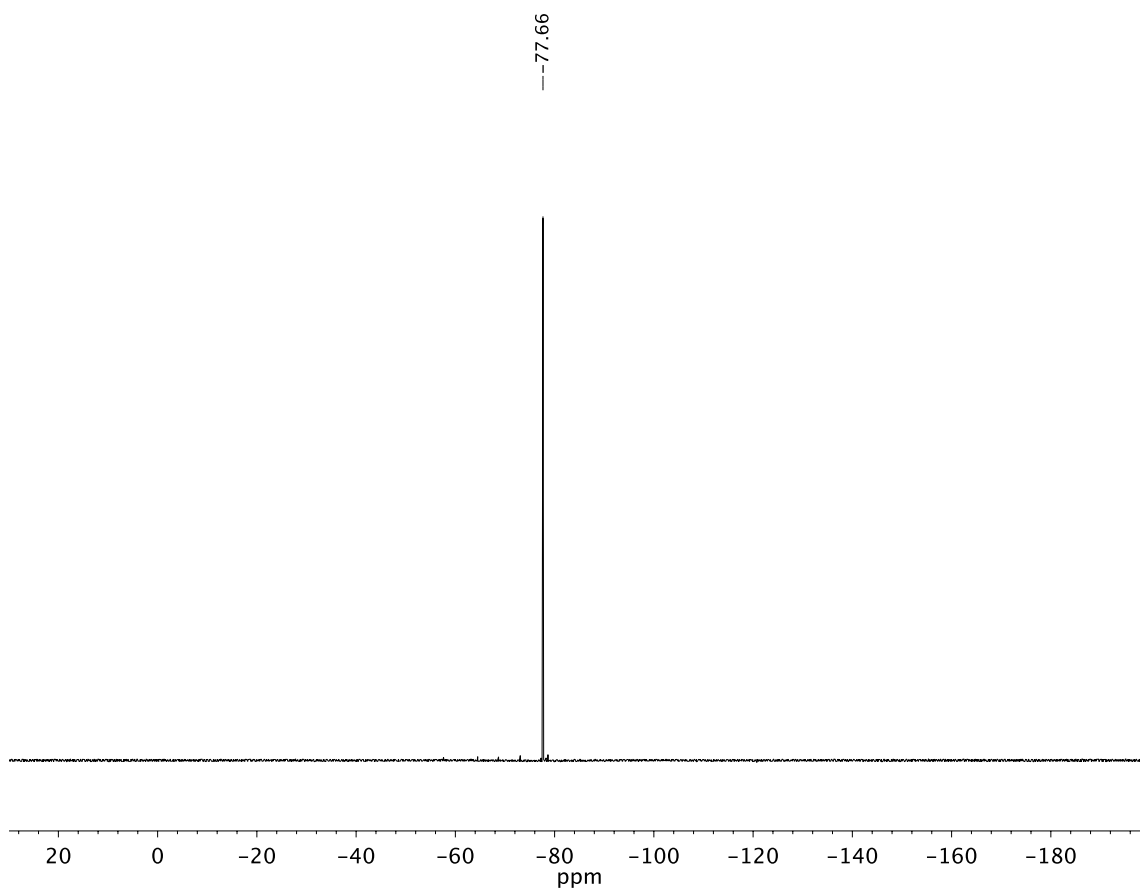




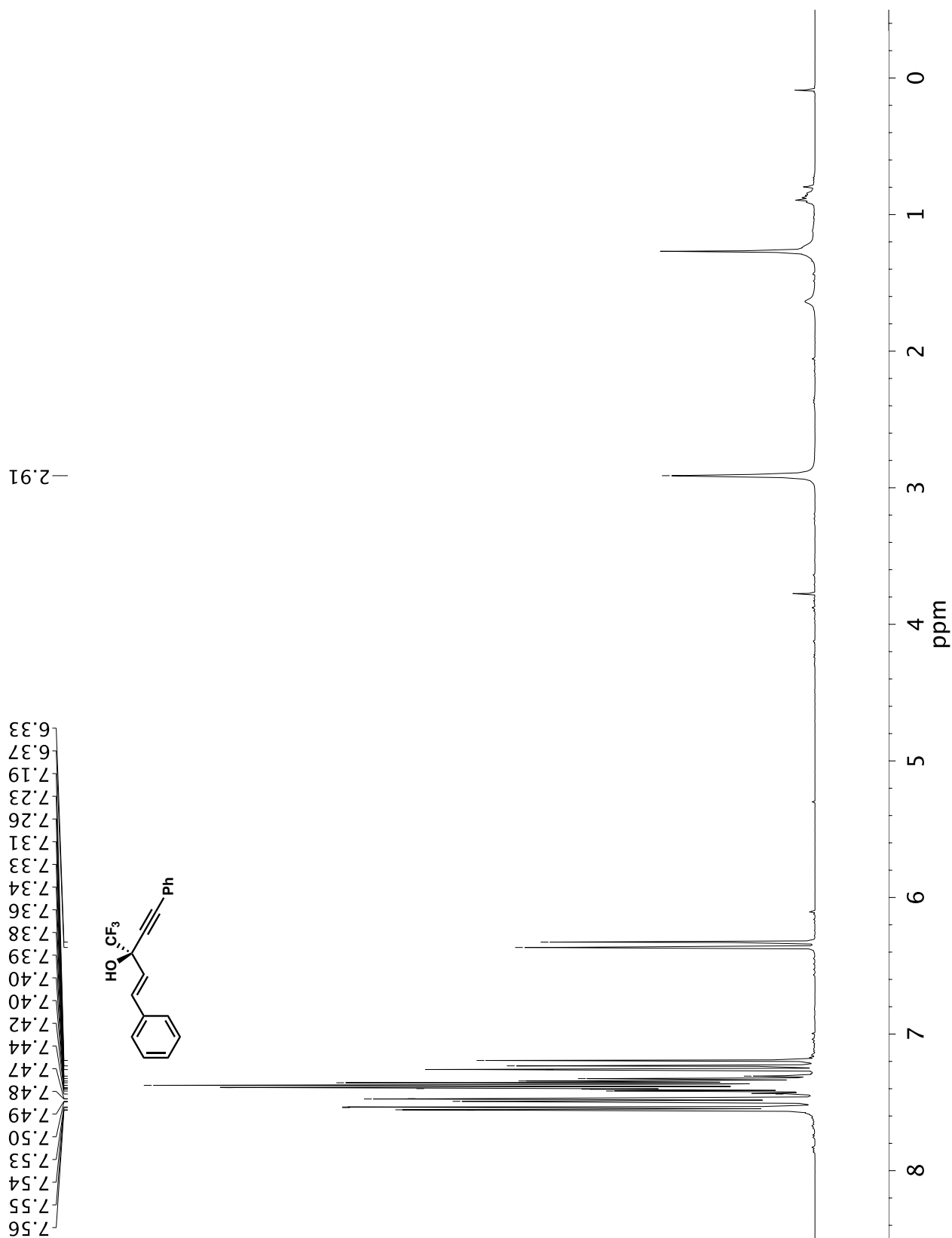
A1.5 Infrared spectrum (Thin Film, NaCl) of compound **10f**.

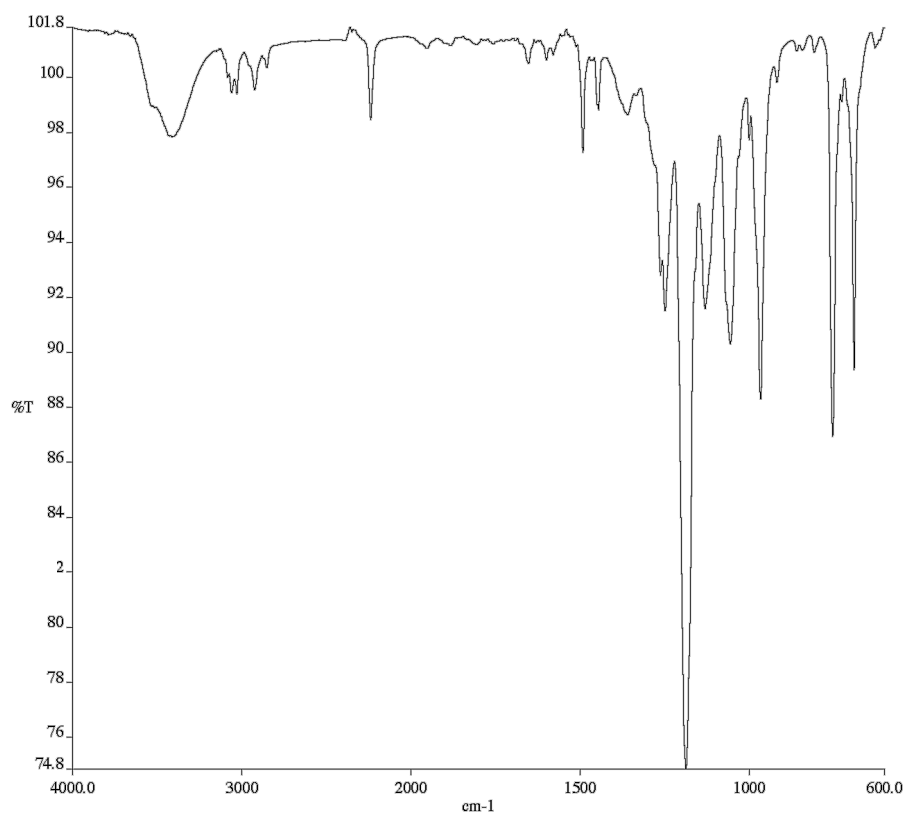


A1.6 ¹³C NMR (101 MHz, CDCl₃) of compound **10f**.

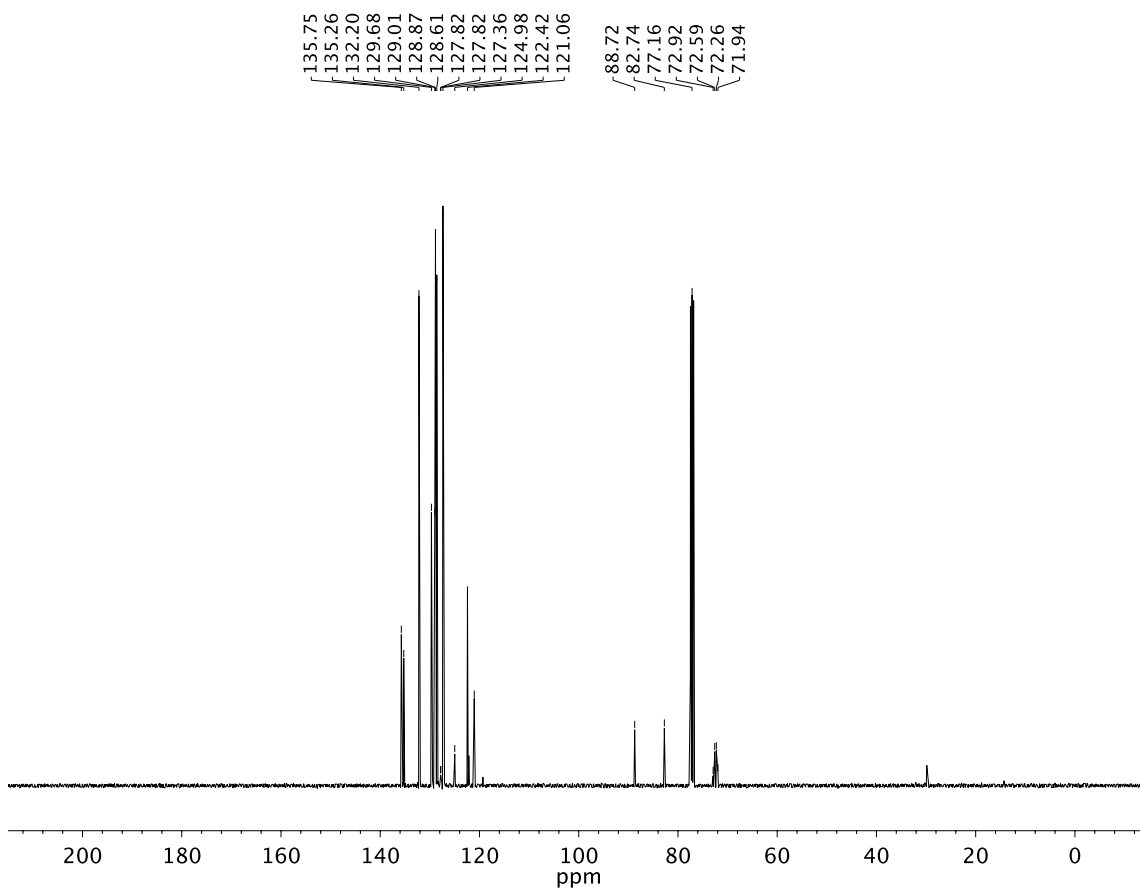


A1.7 ^{19}F NMR (282 MHz, CDCl_3) of compound **10f**.

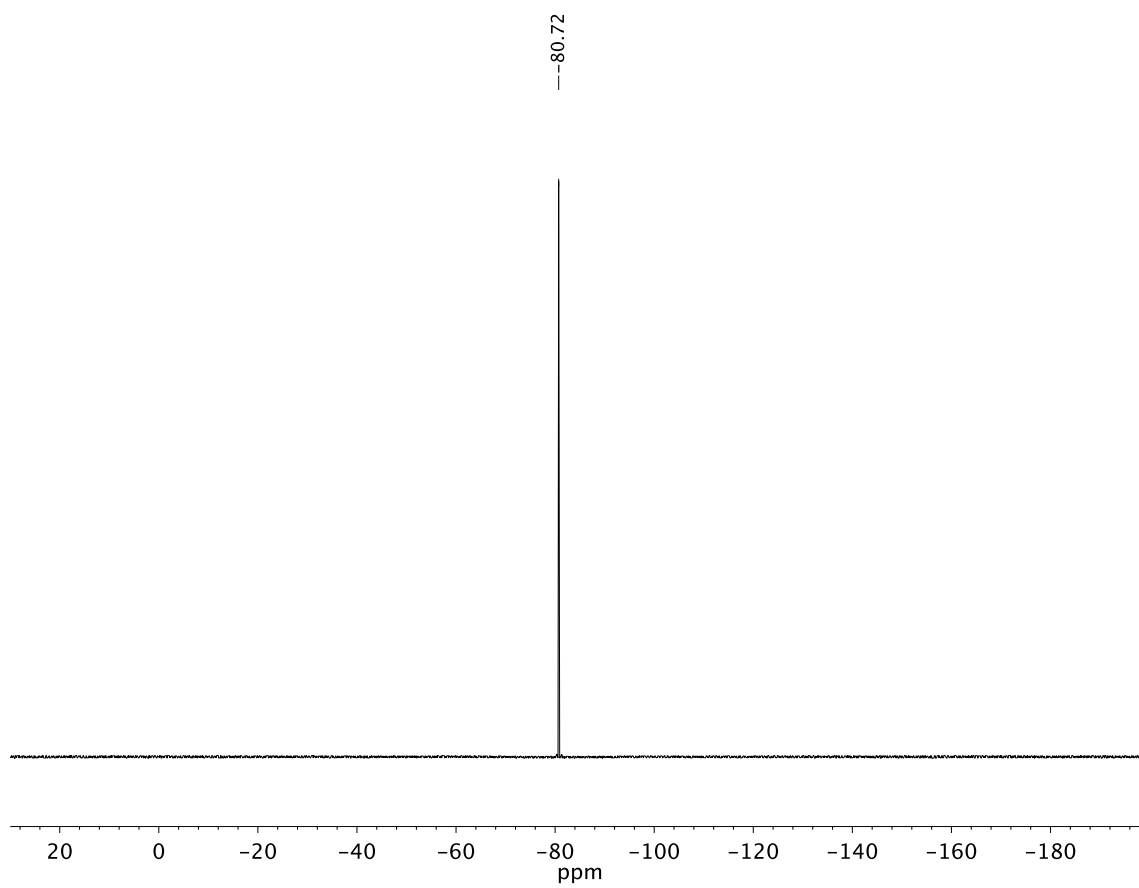




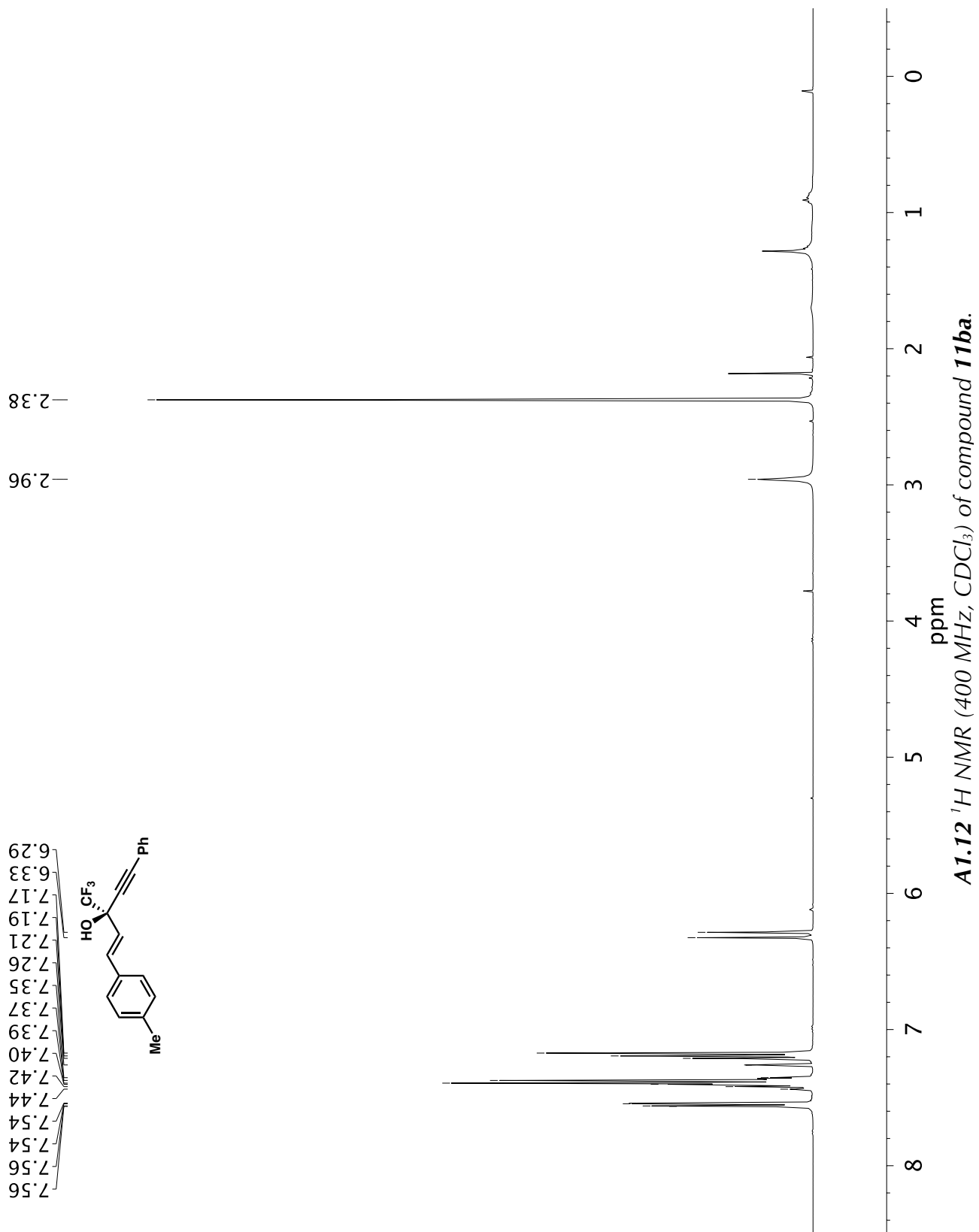
A1.9 Infrared spectrum (Thin Film, NaCl) of compound **11aa**.

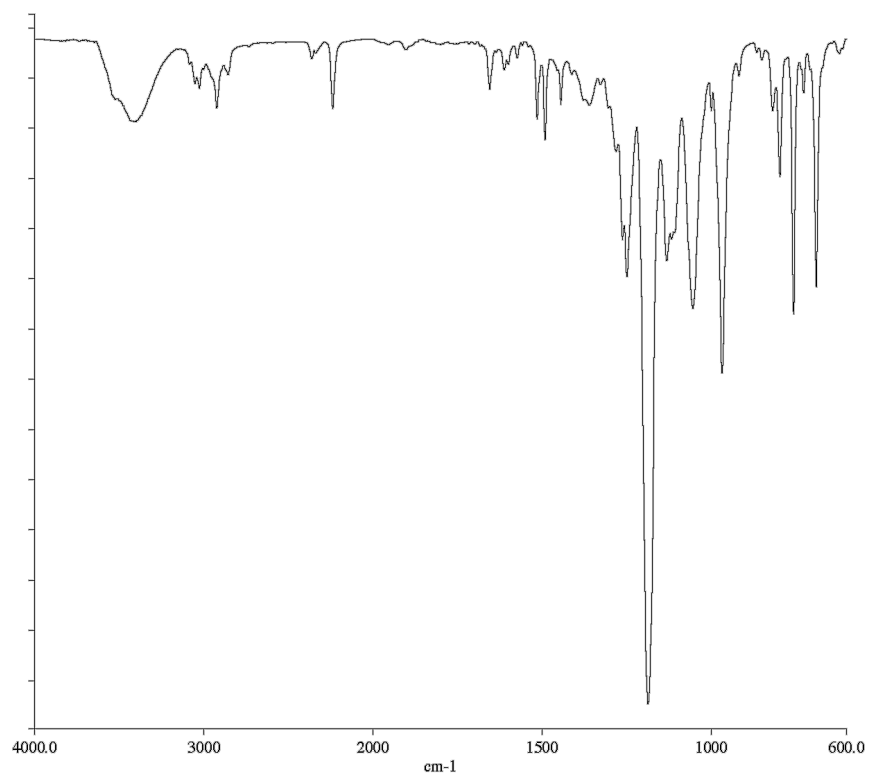


A1.10 ¹³C NMR (101 MHz, CDCl₃) of compound **11aa**.

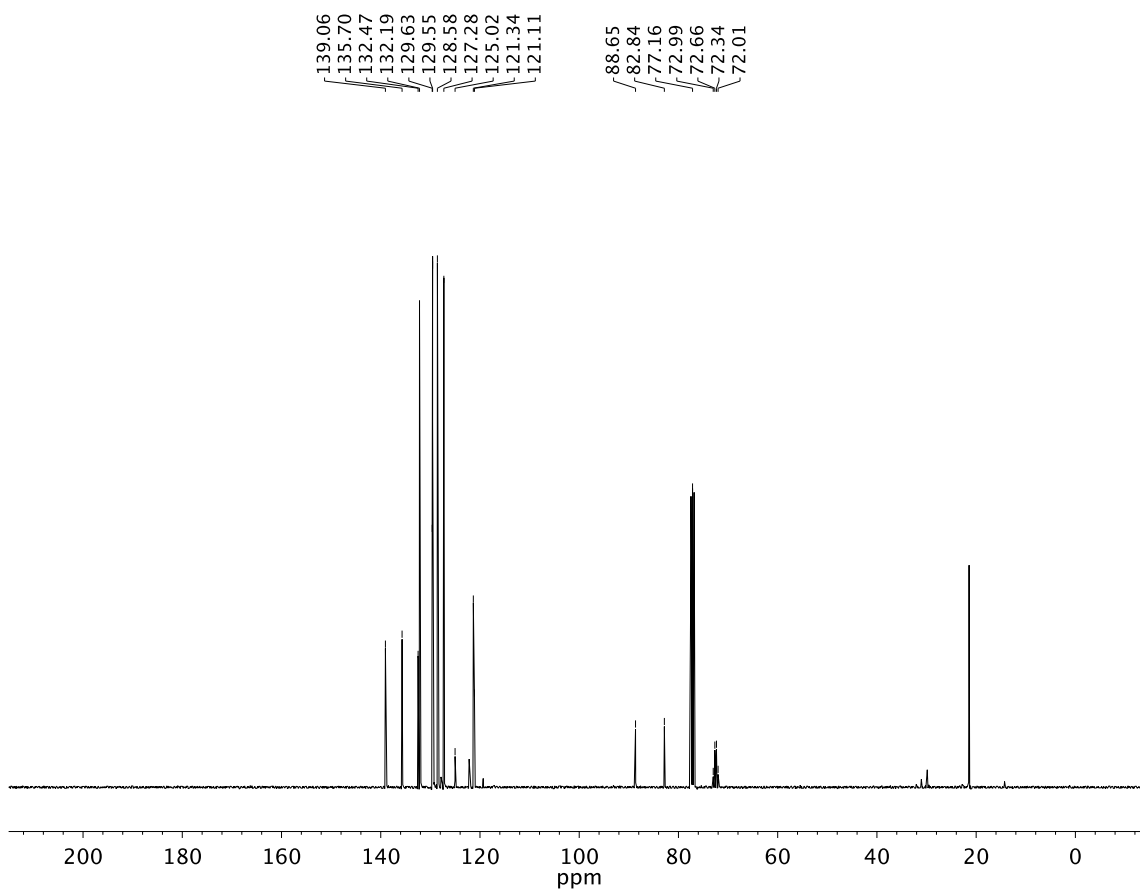


A1.11 ^{19}F NMR (282 MHz, CDCl_3) of compound **11aa**.

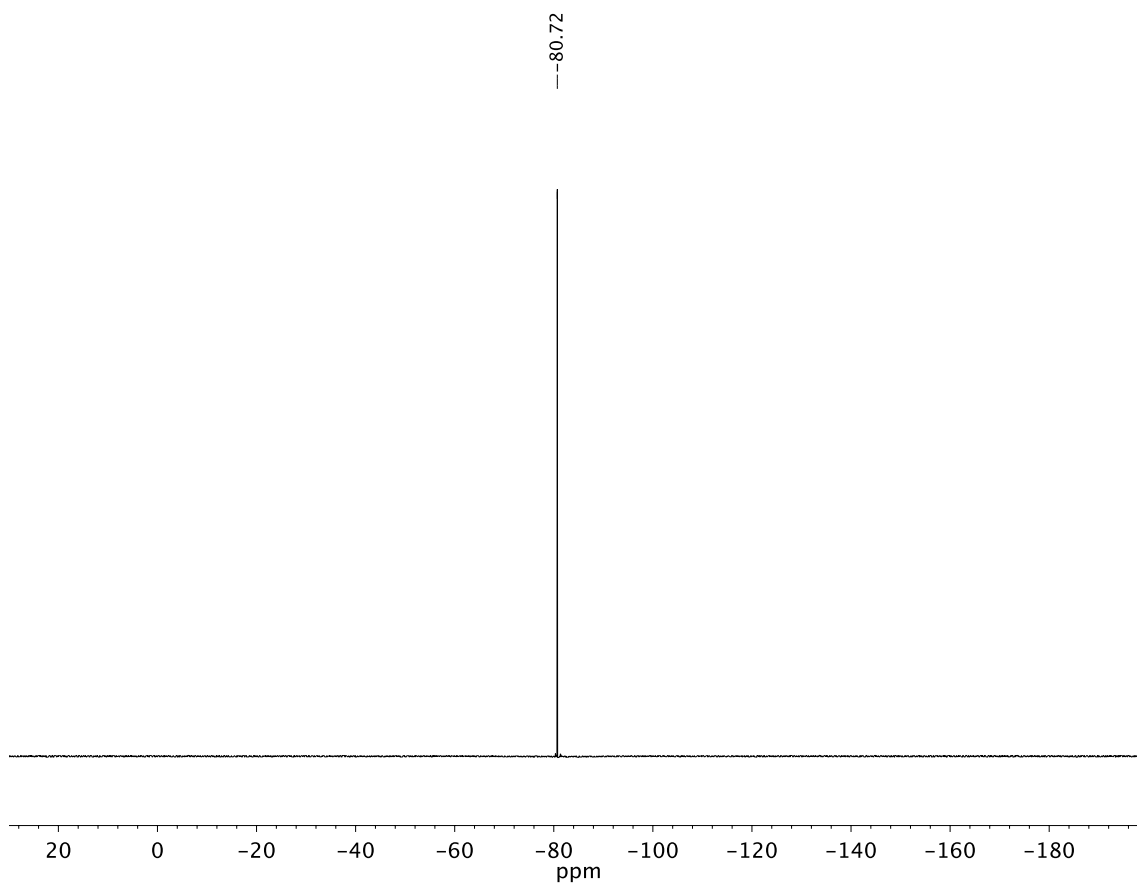




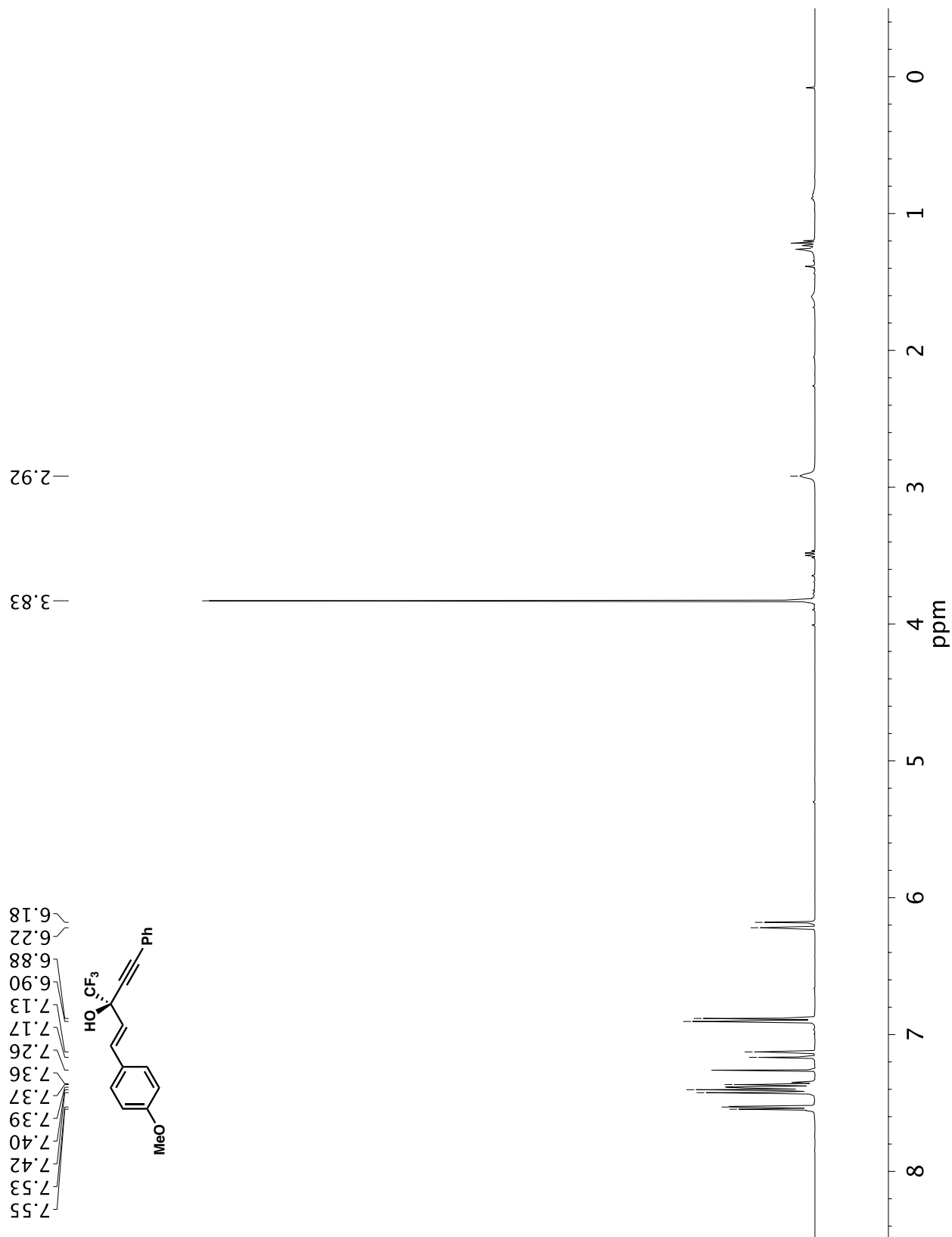
A1.13 Infrared spectrum (Thin Film, NaCl) of compound **11ba**.

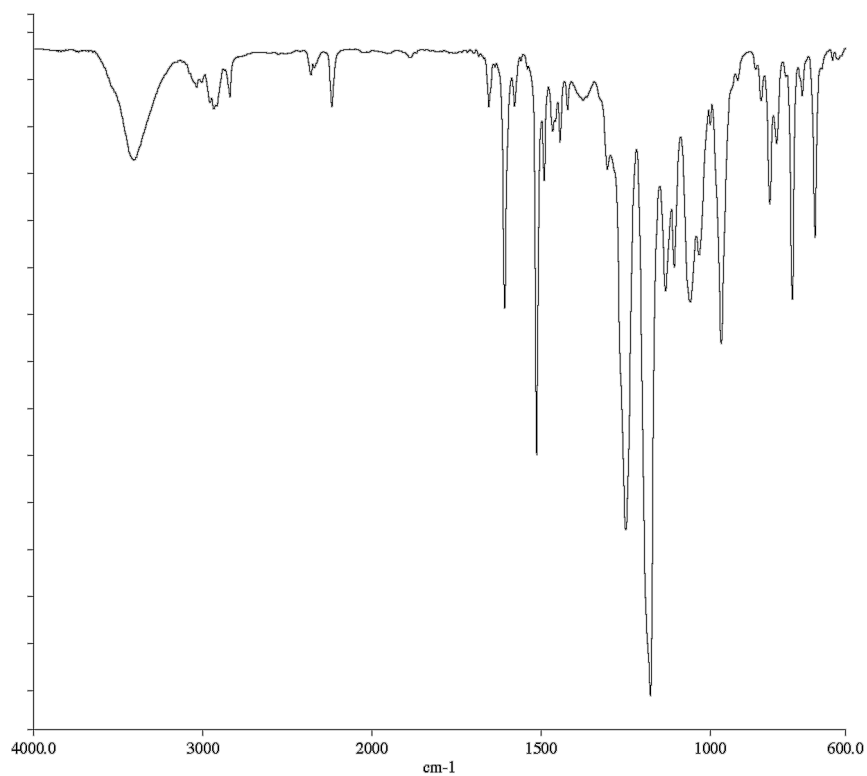


A1.14 ^{13}C NMR (101 MHz, CDCl_3) of compound **11ba**.

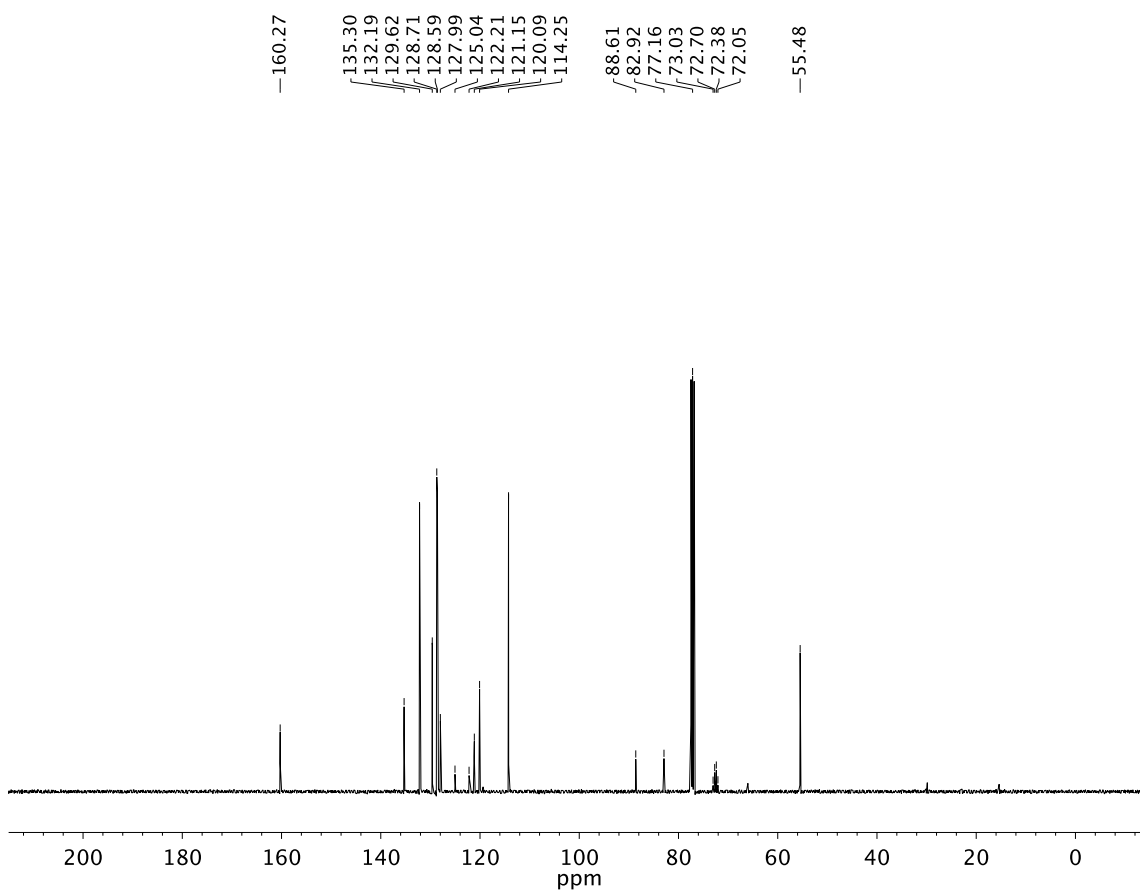


A1.15 ^{19}F NMR (282 MHz, CDCl_3) of compound **11ba**.

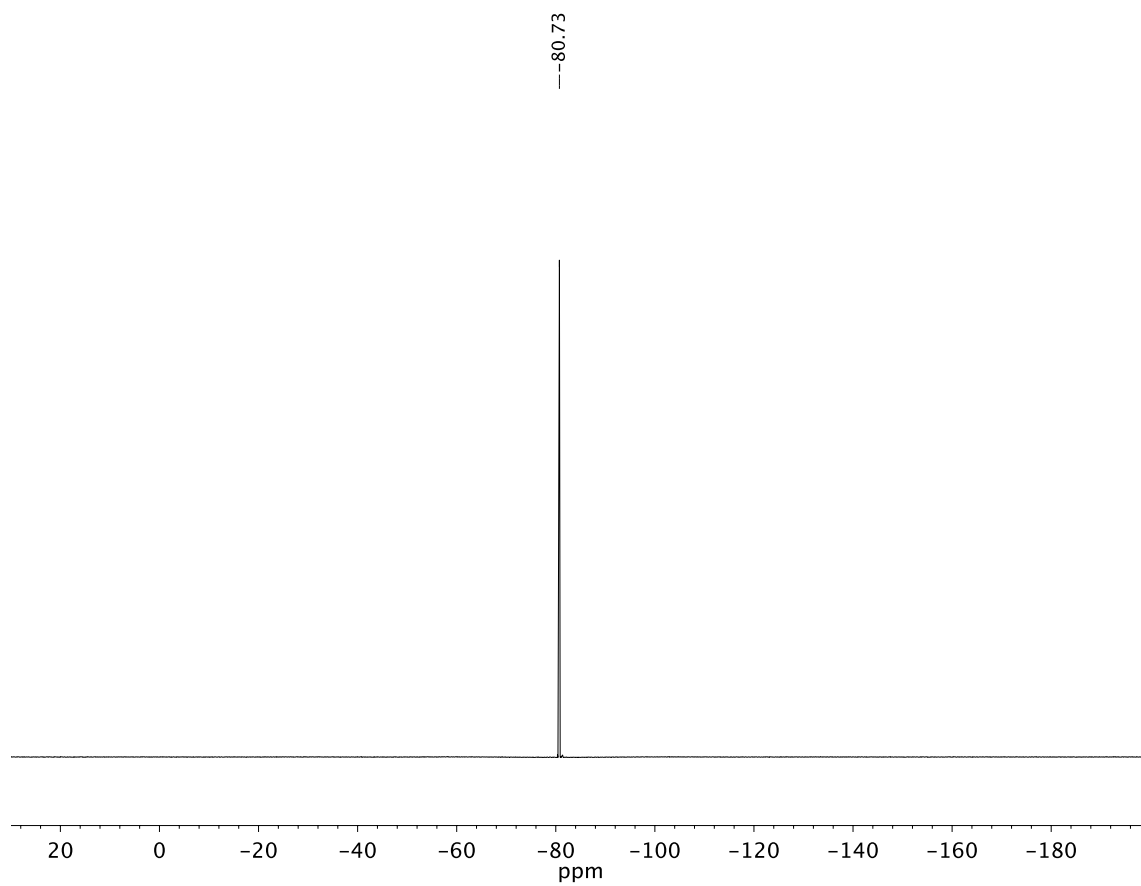
**A1.16** ¹H NMR (400 MHz, CDCl₃) of compound **11ca**.



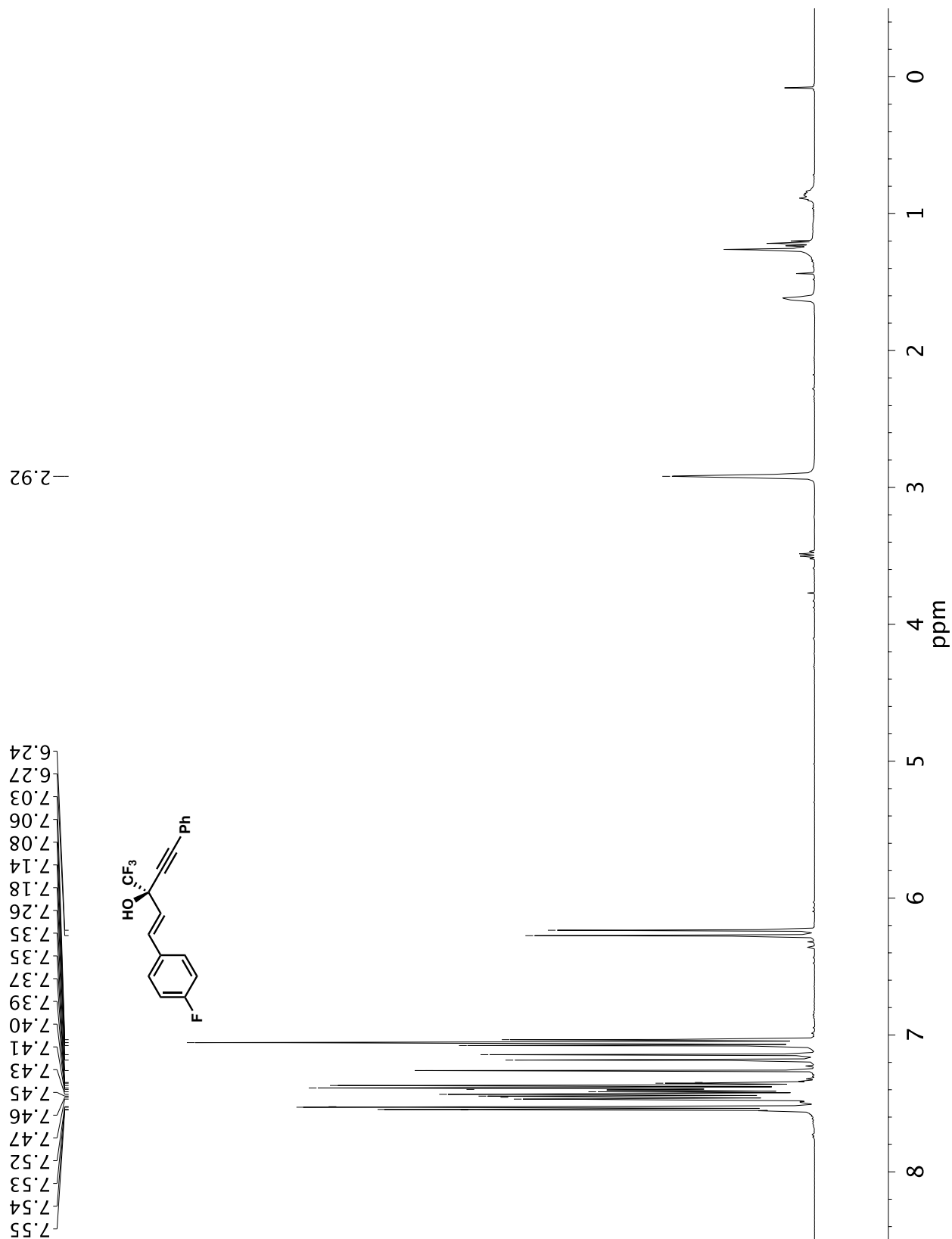
A1.17 Infrared spectrum (Thin Film, NaCl) of compound **11ca**.



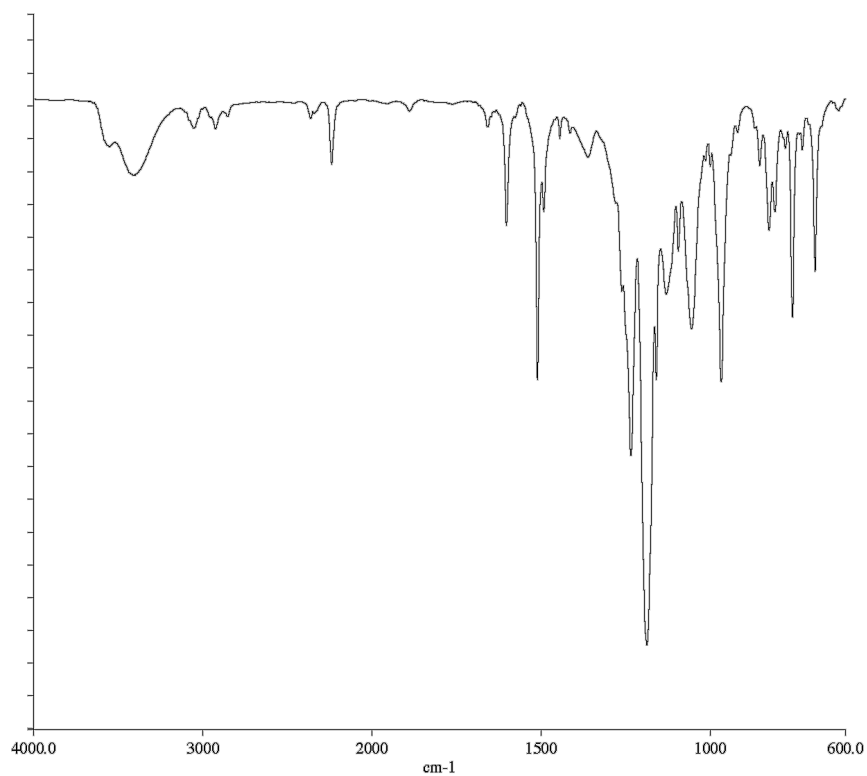
A1.18 ^{13}C NMR (101 MHz, CDCl_3) of compound **11ca**.



A1.19 ^{19}F NMR (282 MHz, CDCl_3) of compound **11ca**.

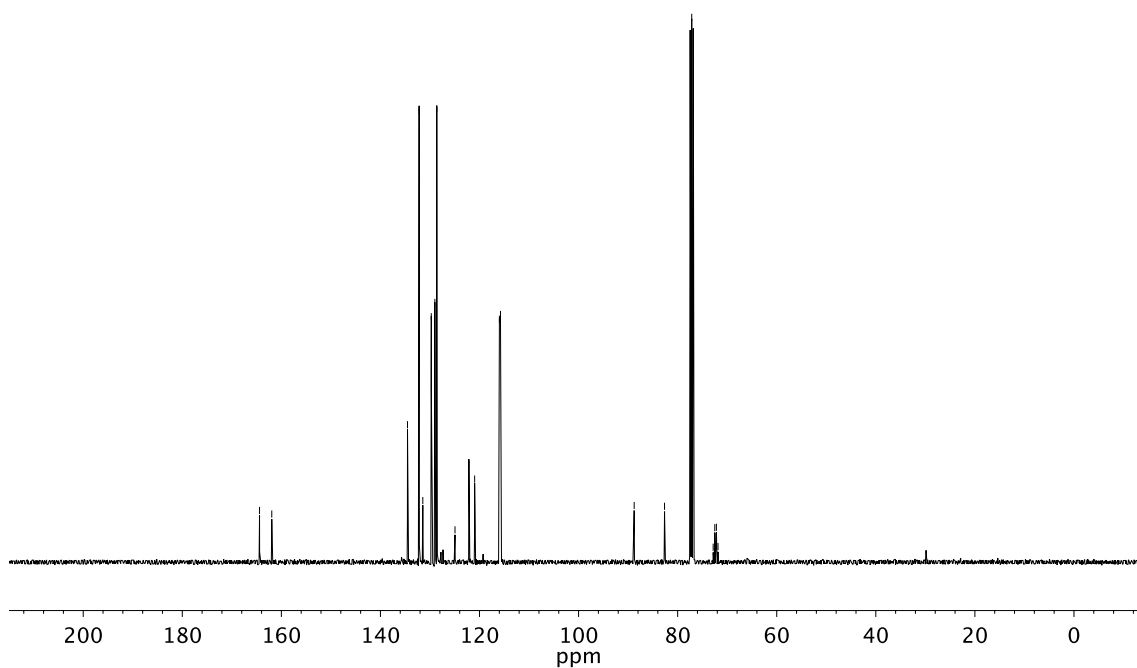


A1.20 ¹H NMR (400 MHz, CDCl₃) of compound **11da**.

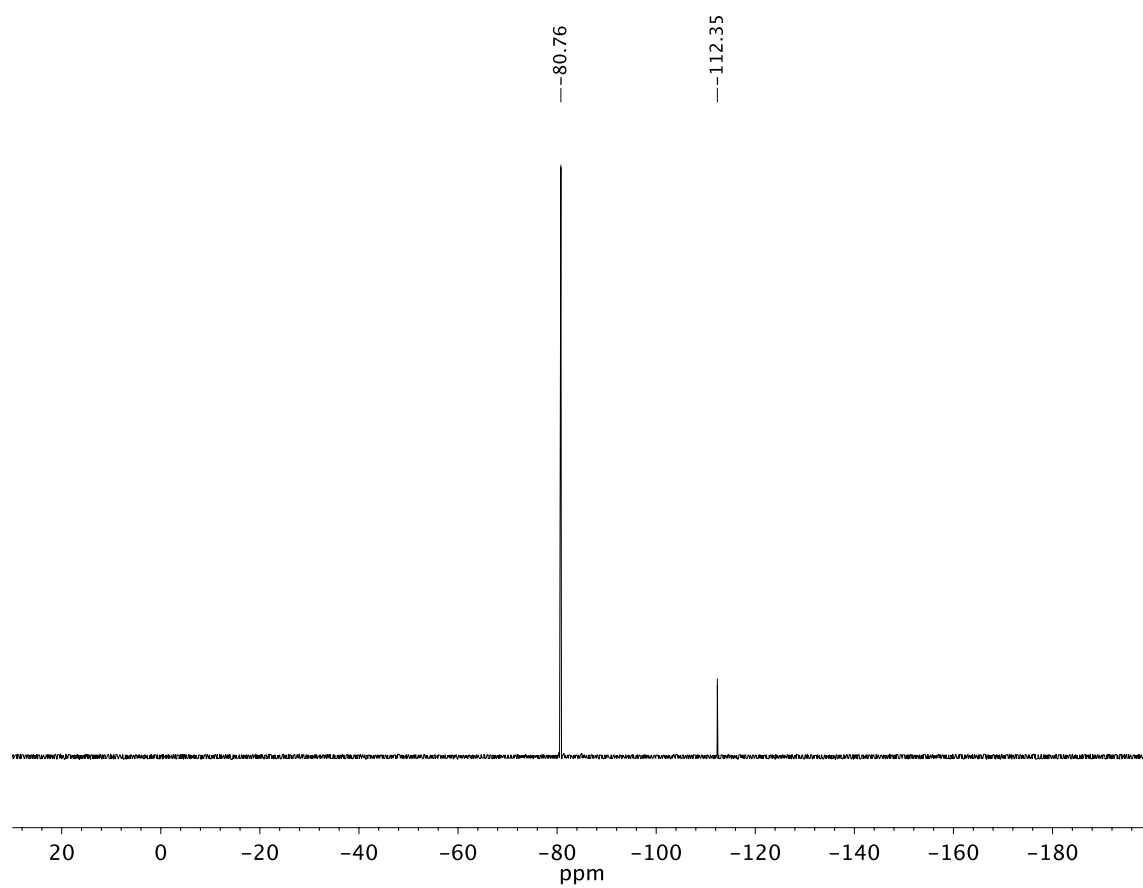


A1.21 Infrared spectrum (Thin Film, NaCl) of compound **11da**.

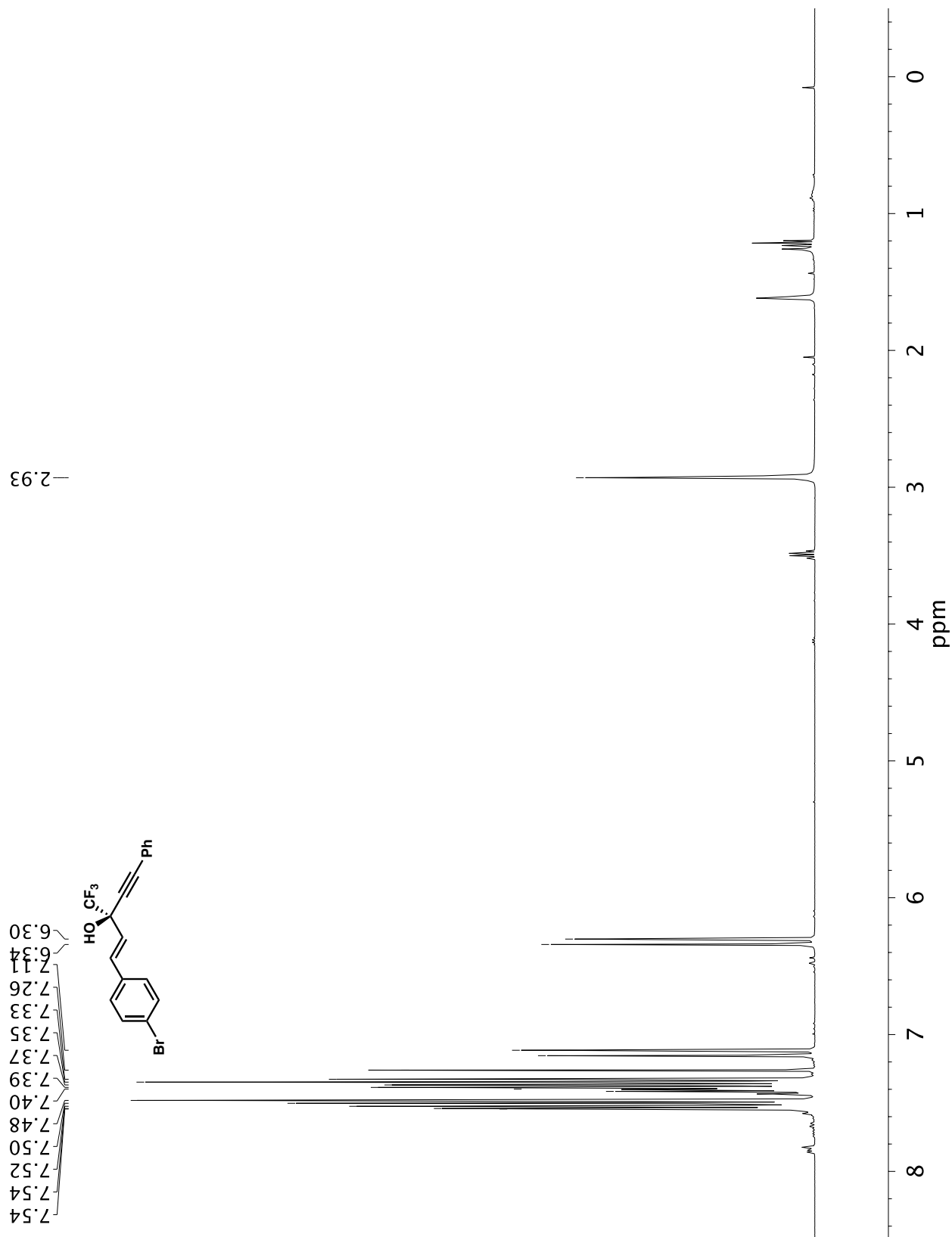
~164.41
~161.94
134.54
132.19
131.45
129.73
129.09
129.01
128.62
124.95
122.17
120.98
115.98
115.77
88.78
82.65
77.16
72.84
72.51
72.18
71.85

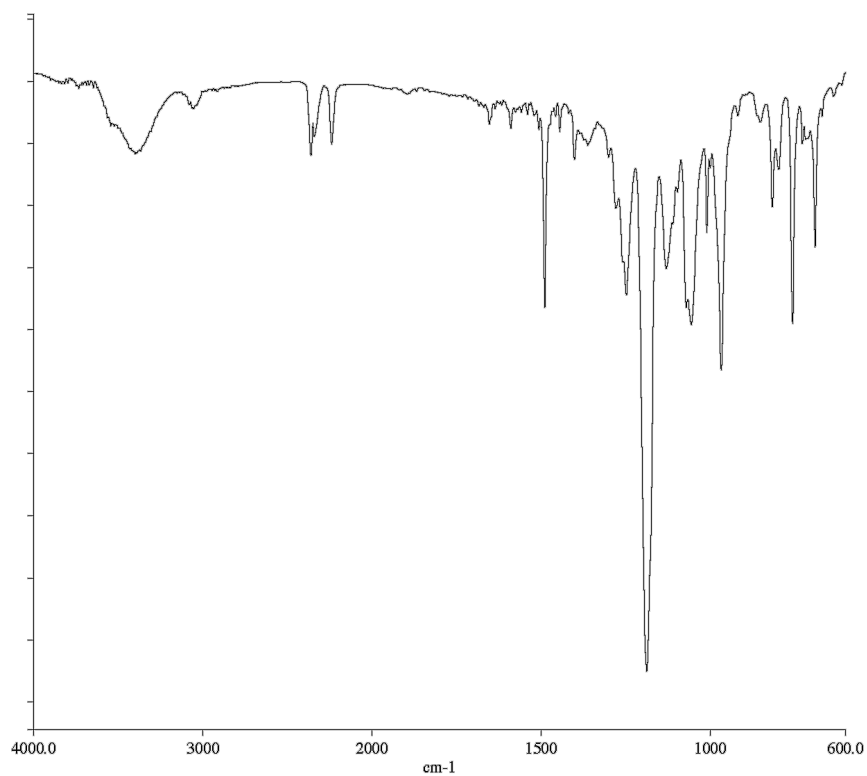


A1.22 ¹³C NMR (101 MHz, CDCl₃) of compound **11da**.

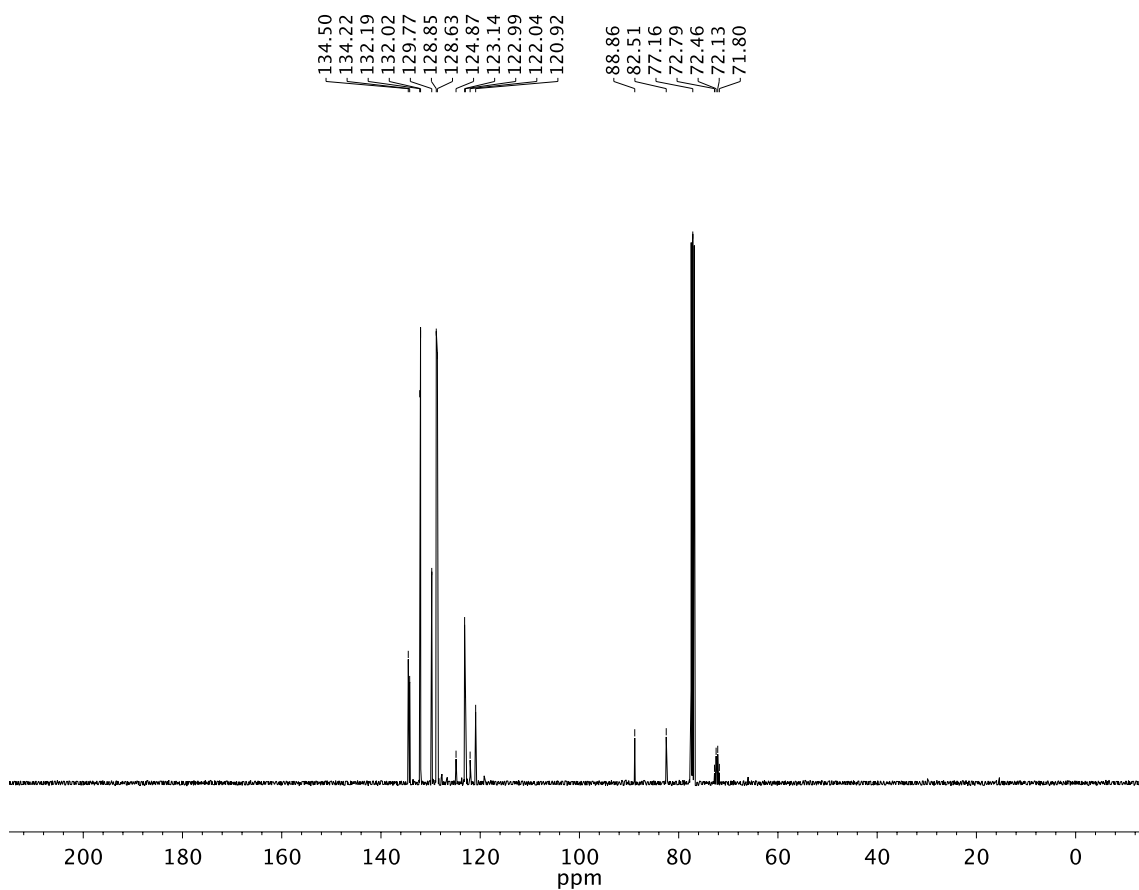


A1.23 ^{19}F NMR (282 MHz, CDCl_3) of compound **11da**.

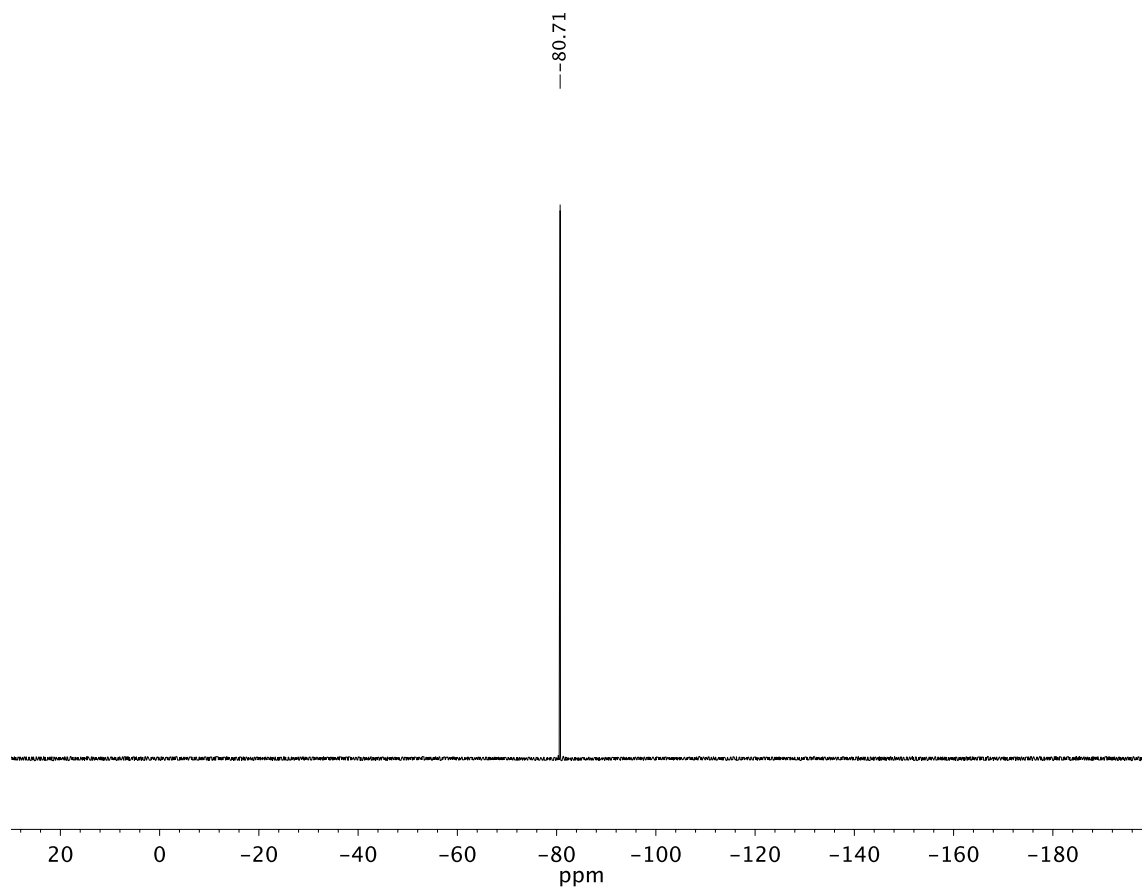
A1.24 ¹H NMR (400 MHz, CDCl₃) of compound **11ea**.



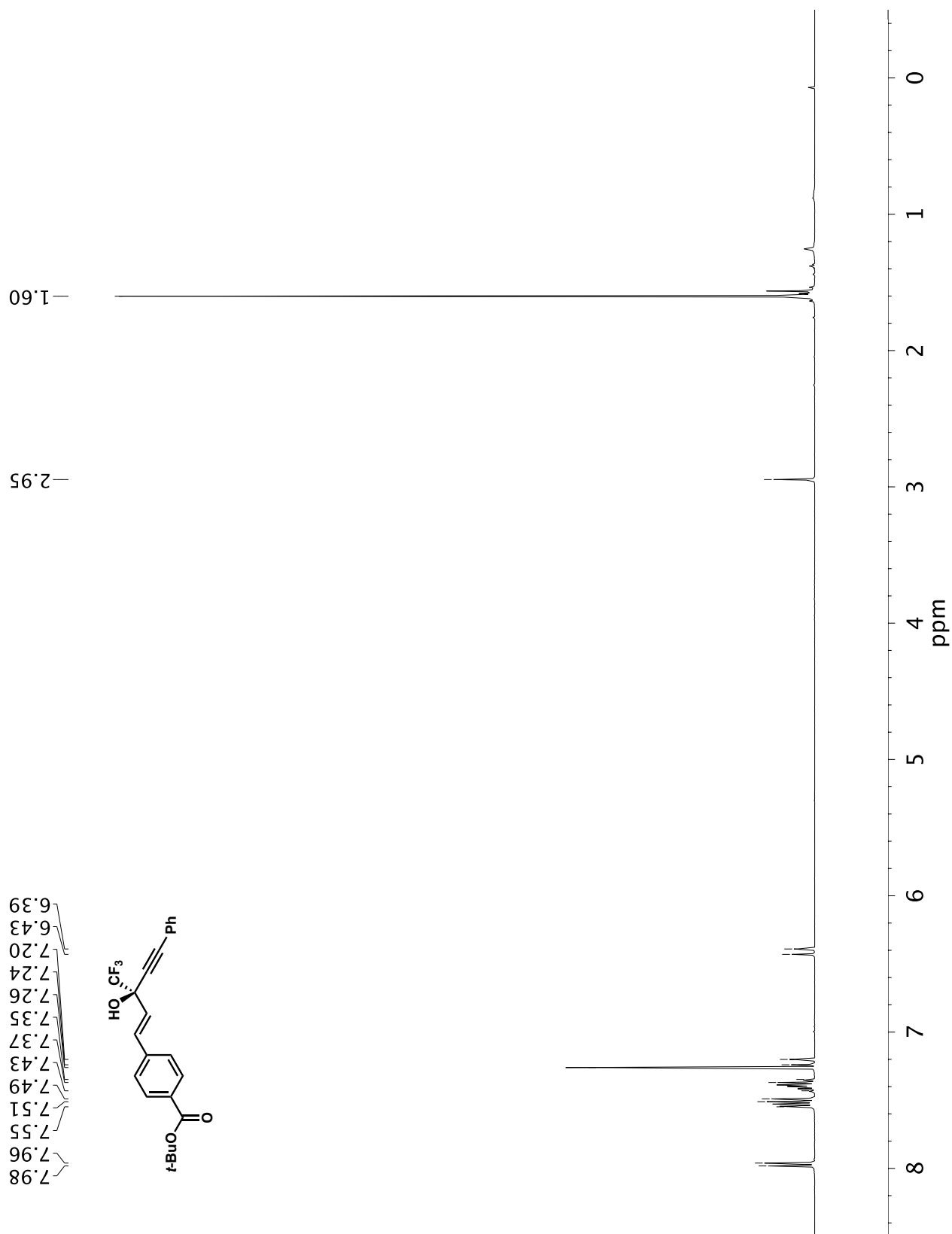
A1.25 Infrared spectrum (Thin Film, NaCl) of compound **11ea**.

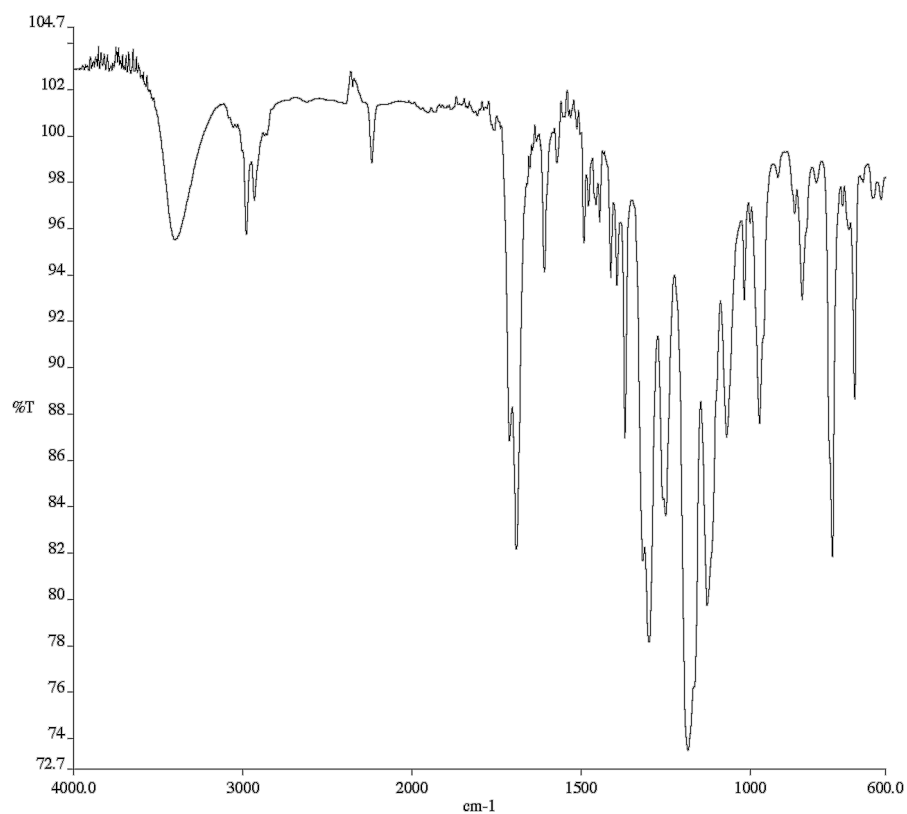


A1.26 ¹³C NMR (101 MHz, CDCl₃) of compound **11ea**.

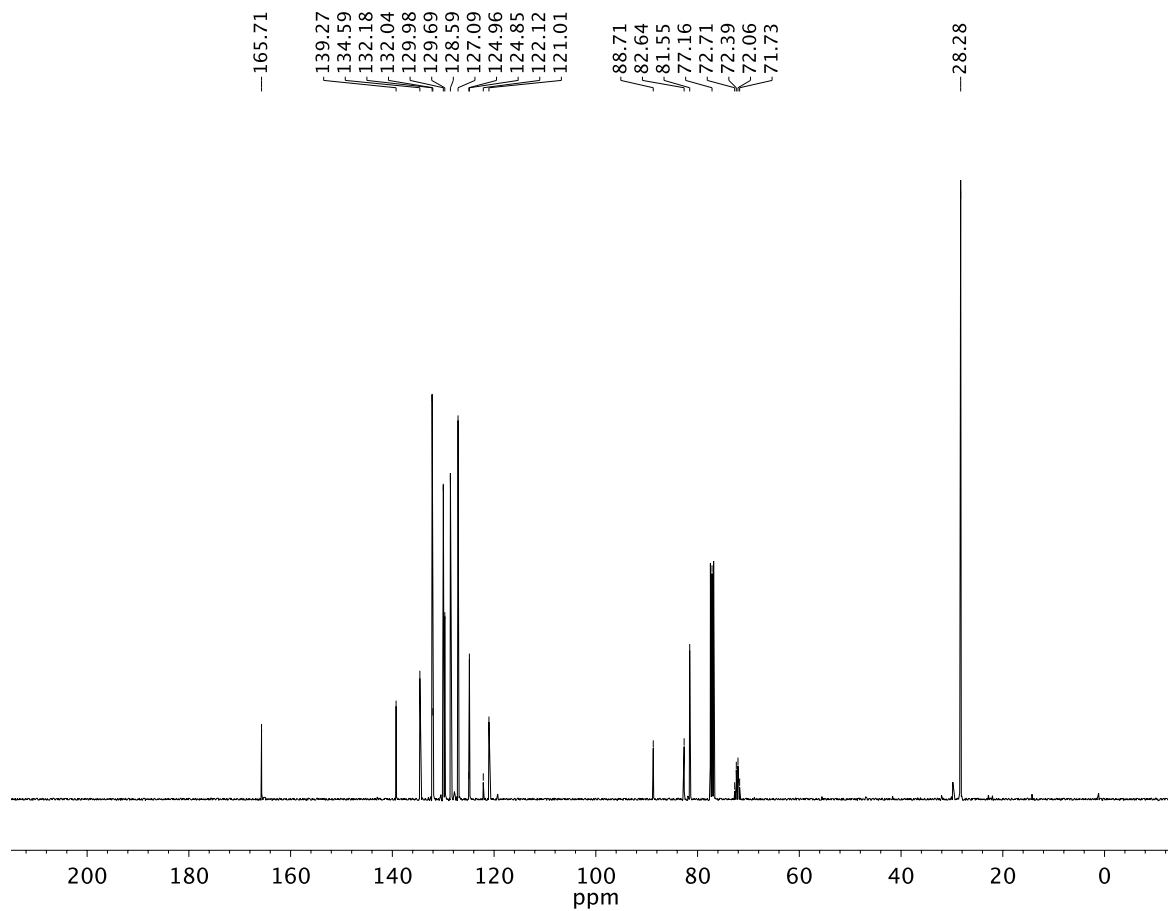


A1.27 ^{19}F NMR (282 MHz, CDCl_3) of compound **11ea**.

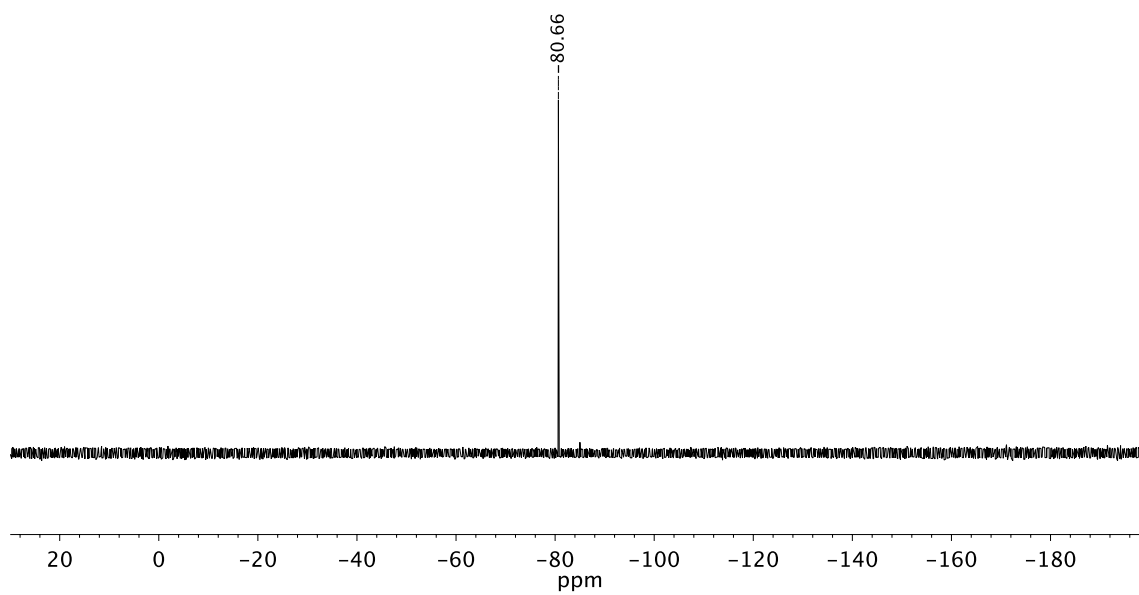




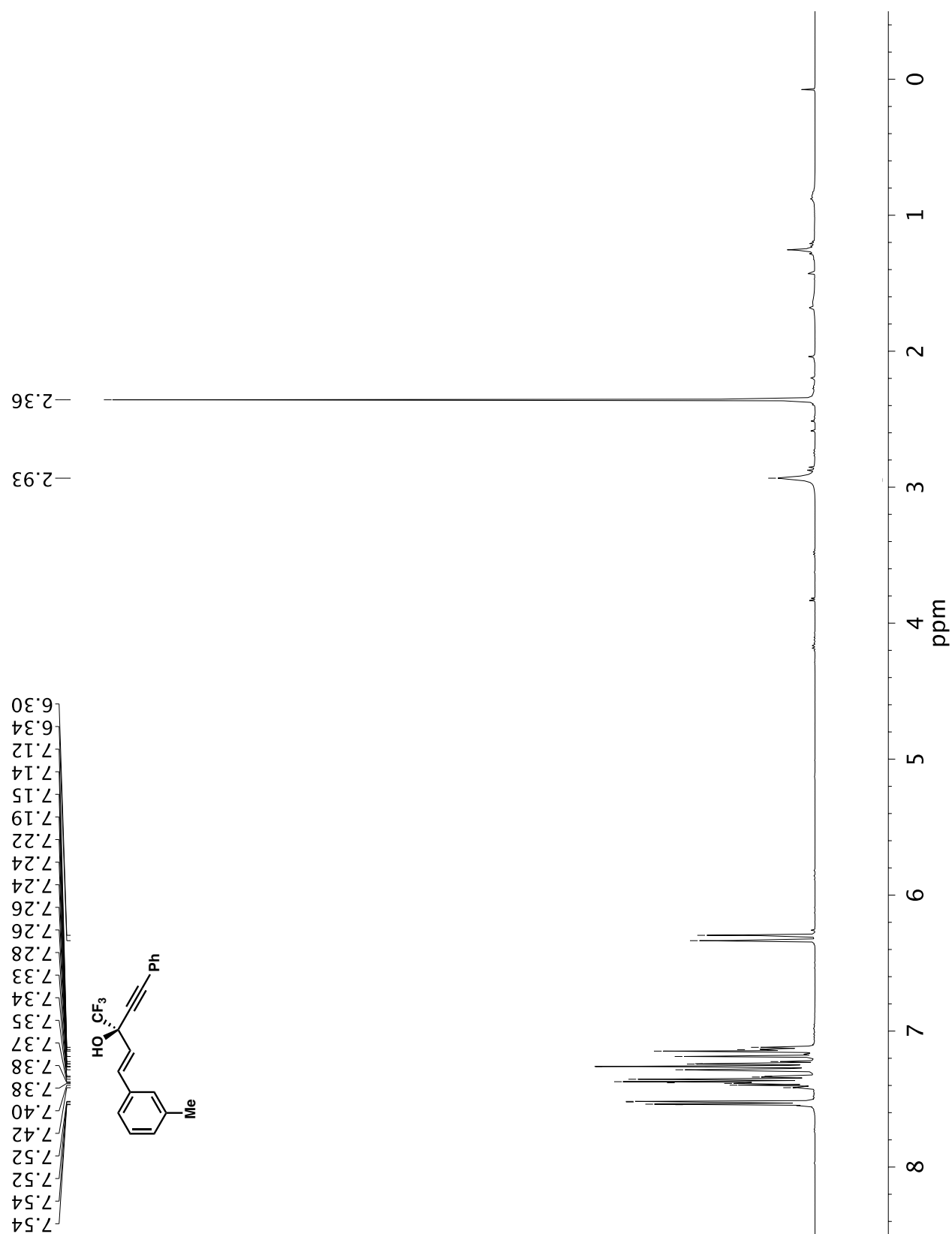
A1.29 Infrared spectrum (Thin Film, NaCl) of compound **11fa**.



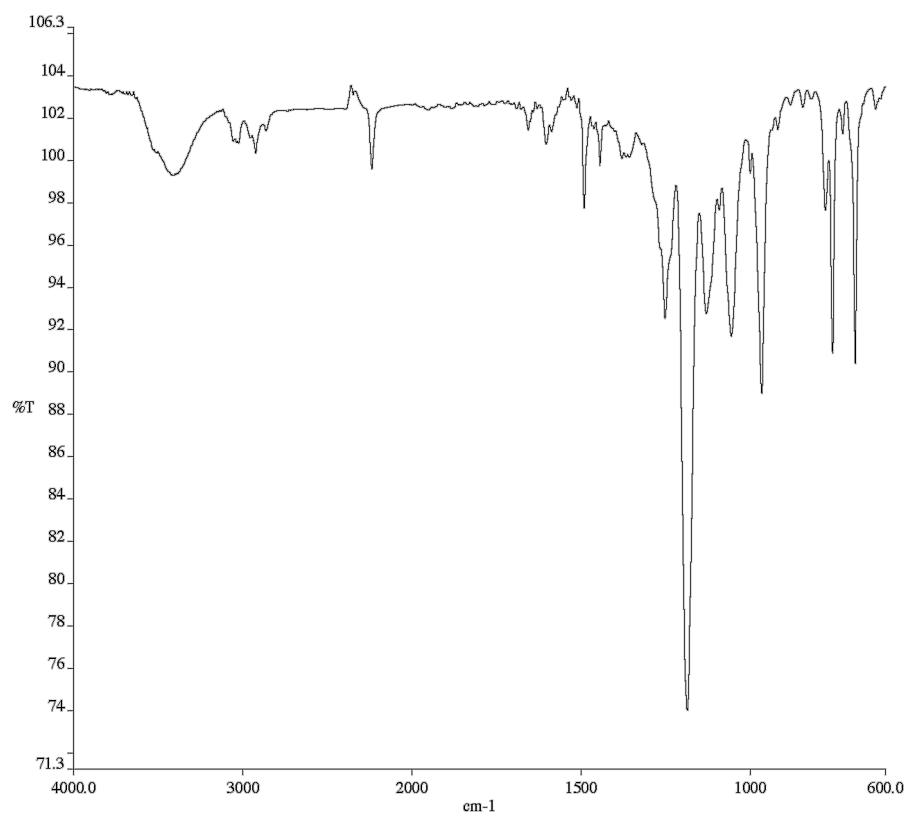
A1.30 ¹³C NMR (101 MHz, CDCl₃) of compound **11fa**.



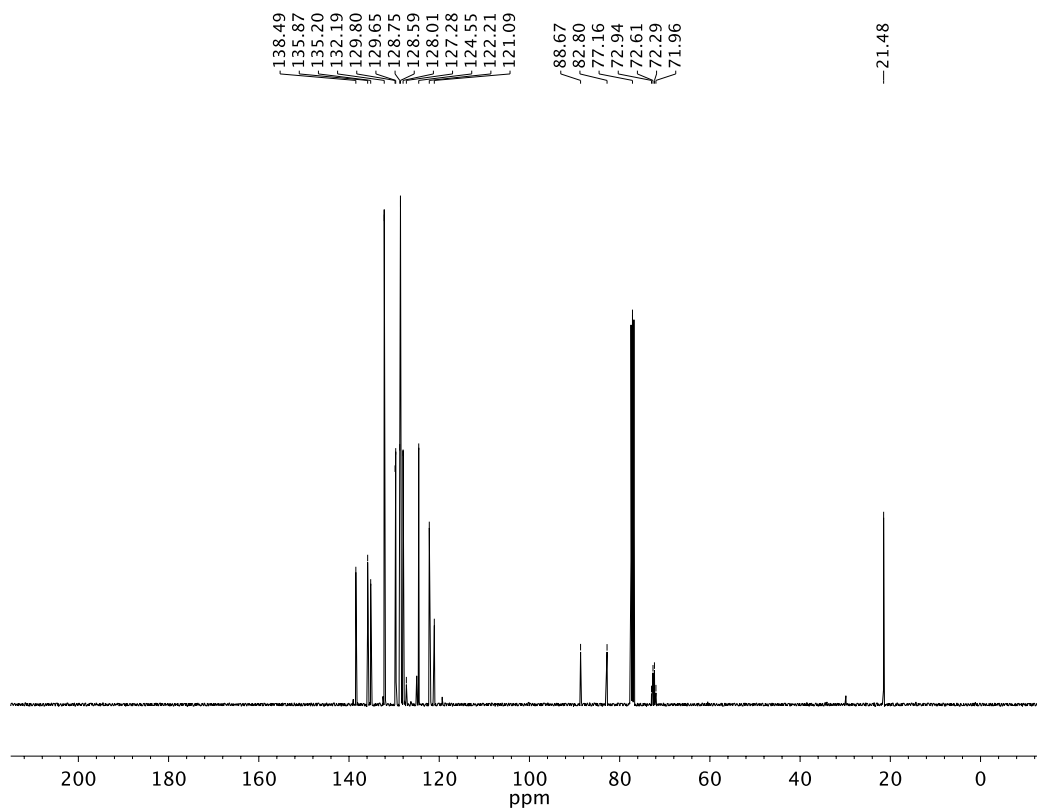
A1.31 ^{19}F NMR (282 MHz, CDCl_3) of compound **11fa**.



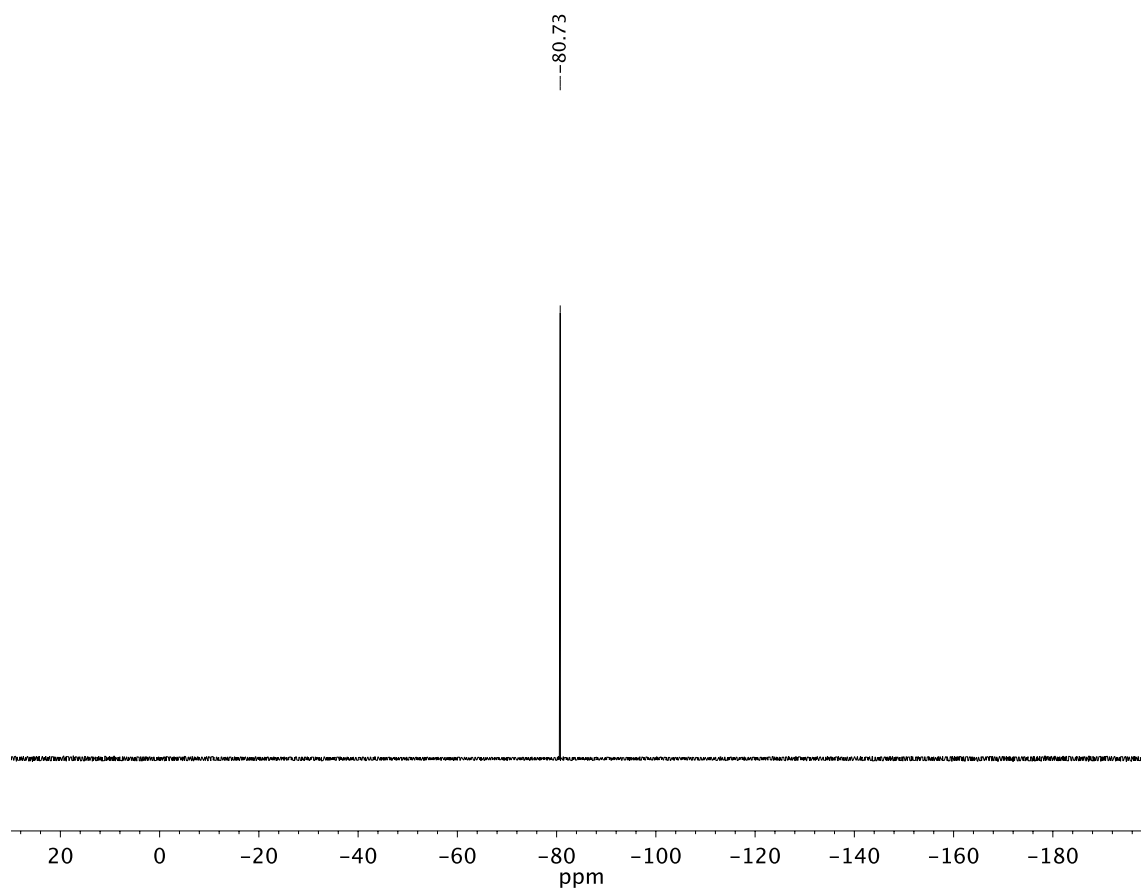
A1.32 ^1H NMR (400 MHz, CDCl_3) of compound **11ga**.



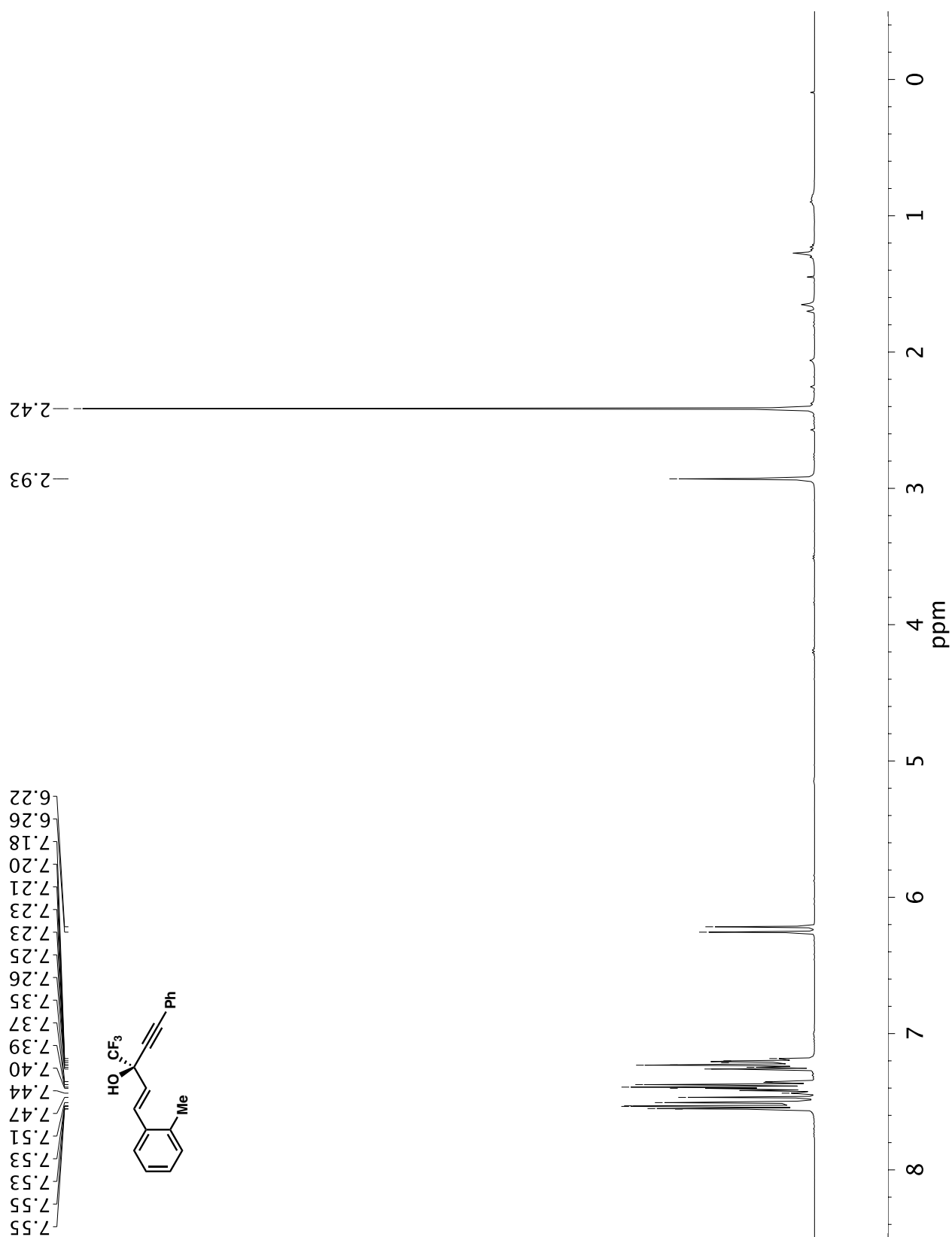
A1.33 Infrared spectrum (Thin Film, NaCl) of compound **11ga**.



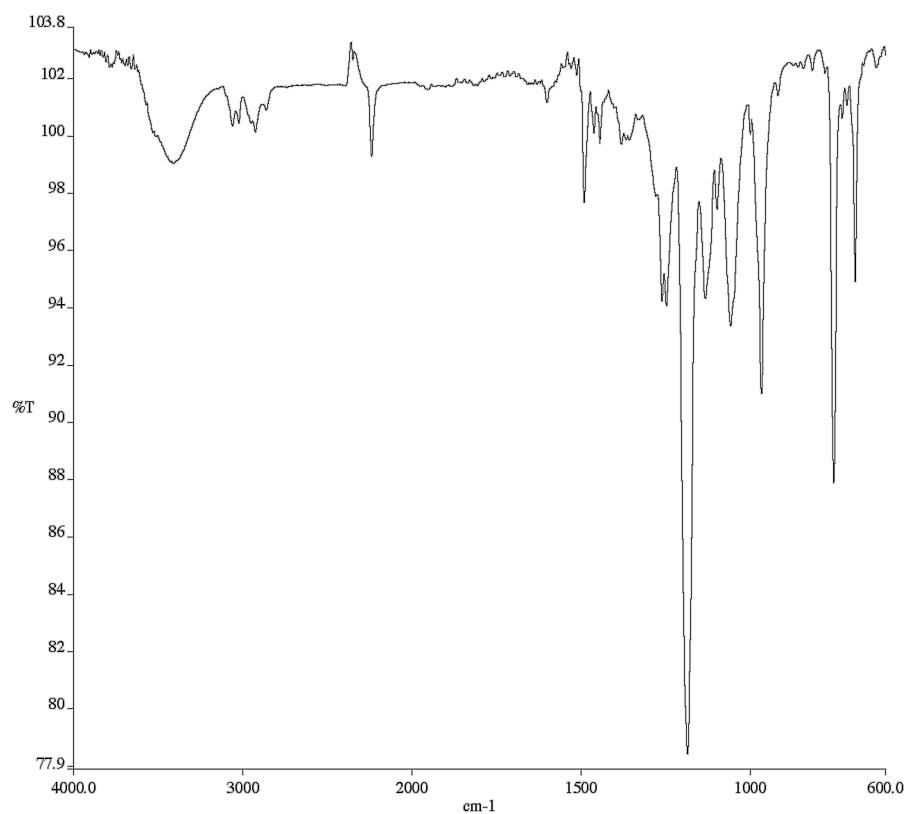
A1.34 ^{13}C NMR (101 MHz, CDCl_3) of compound **11ga**.



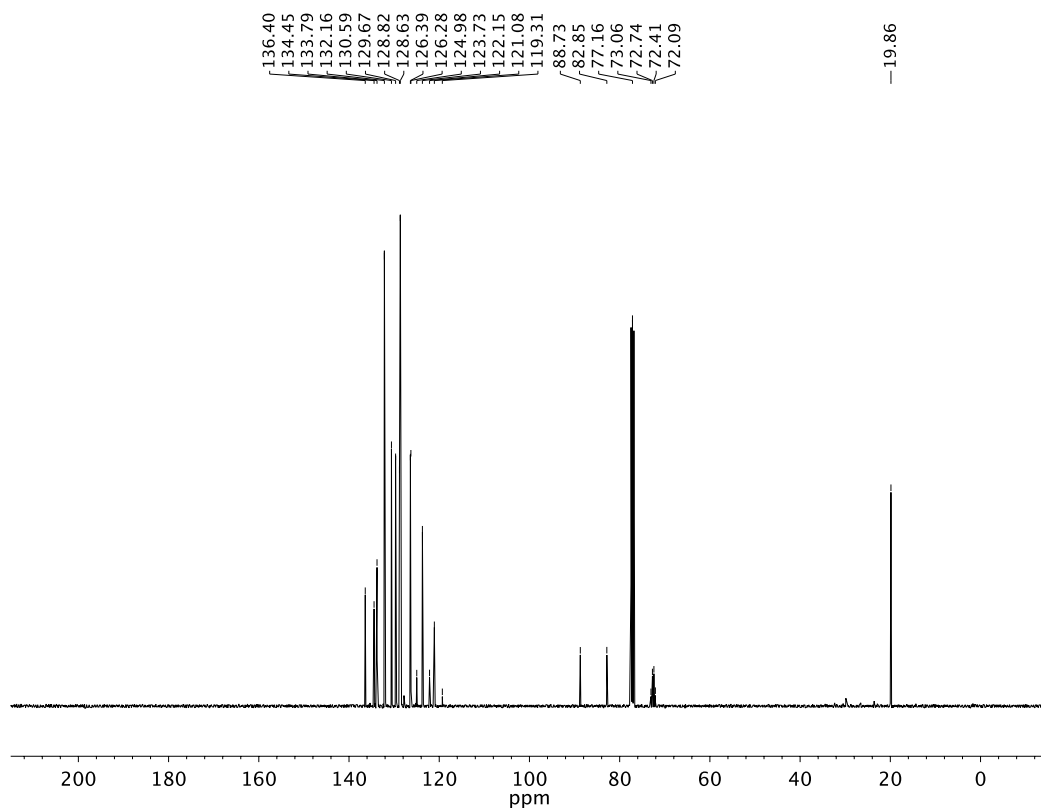
A1.35 ^{19}F NMR (282 MHz, CDCl_3) of compound **11ga**.



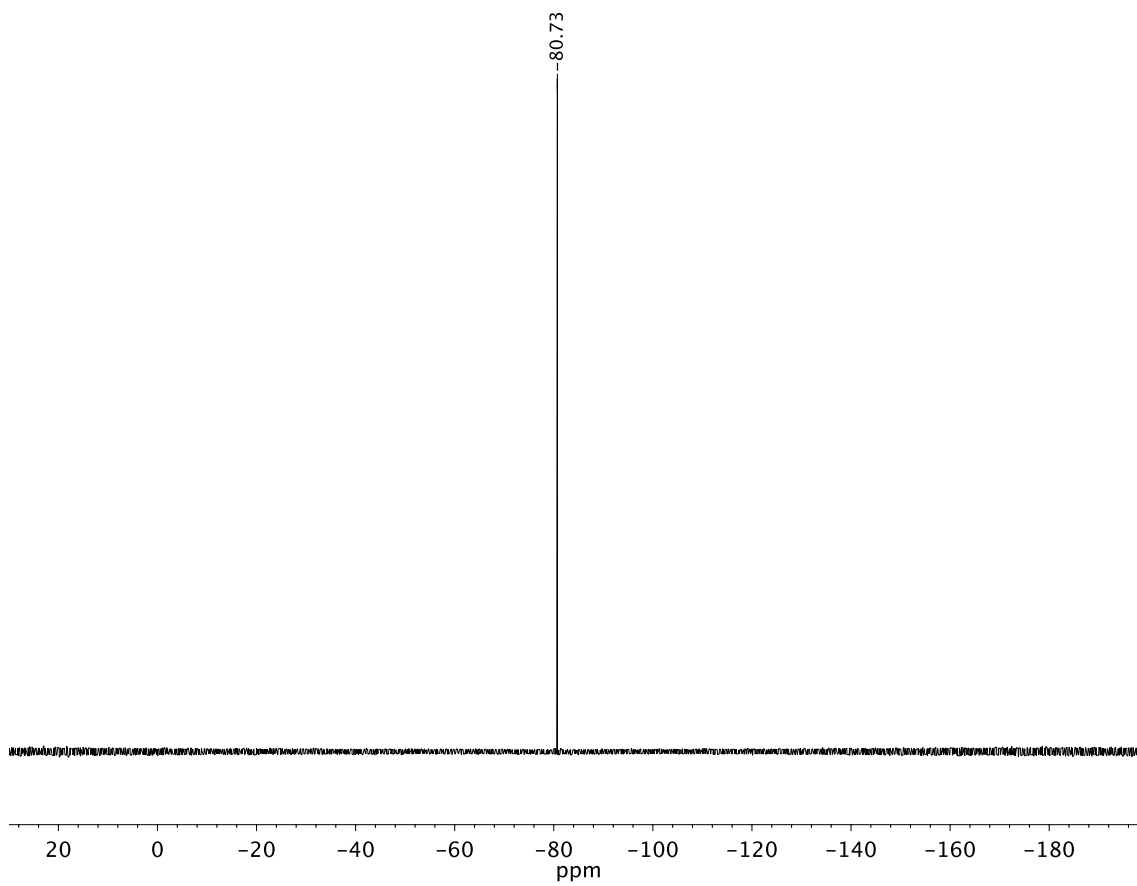
A1.36 ^1H NMR (400 MHz, CDCl_3) of compound **11ha**.



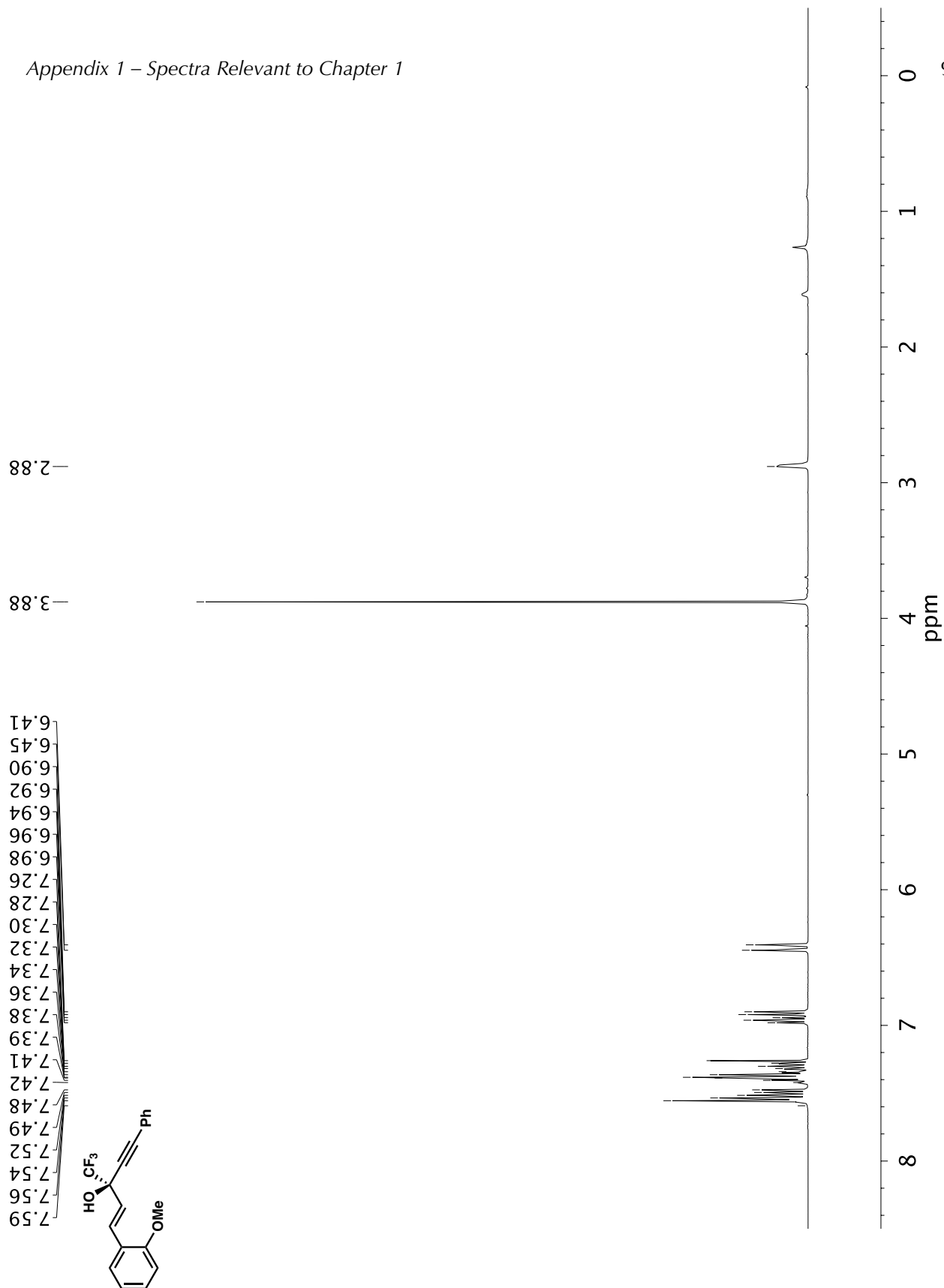
A1.37 Infrared spectrum (Thin Film, NaCl) of compound **11ha**.

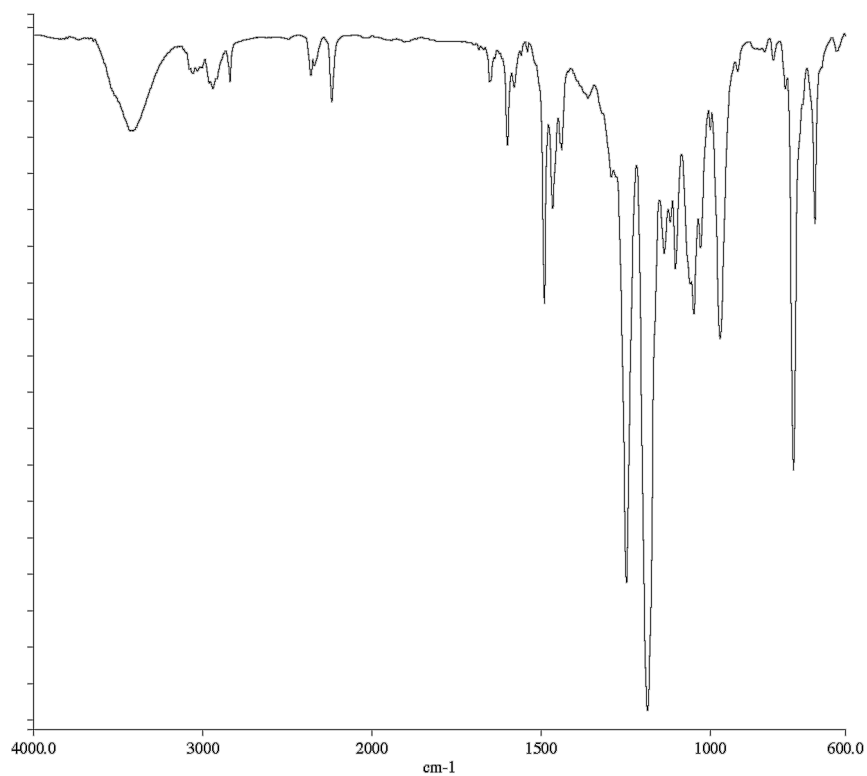


A1.38 ¹³C NMR (101 MHz, CDCl₃) of compound **11ha**.

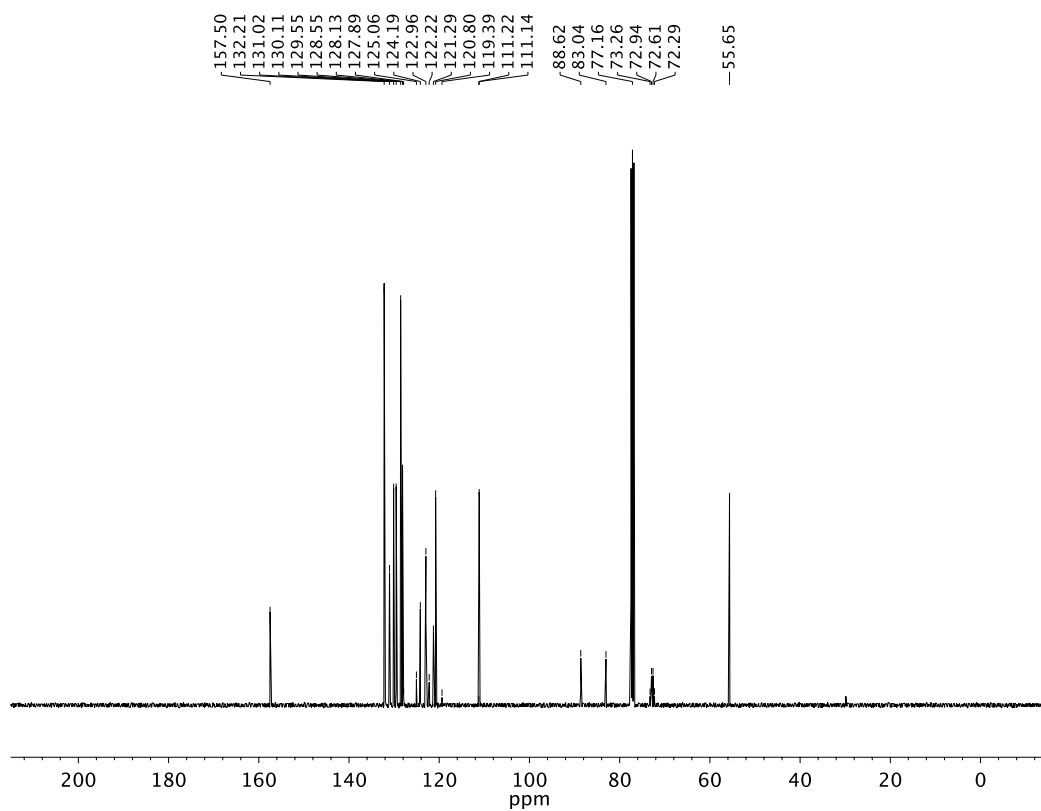


A1.39 ^{19}F NMR (282 MHz, CDCl_3) of compound **11ha**.

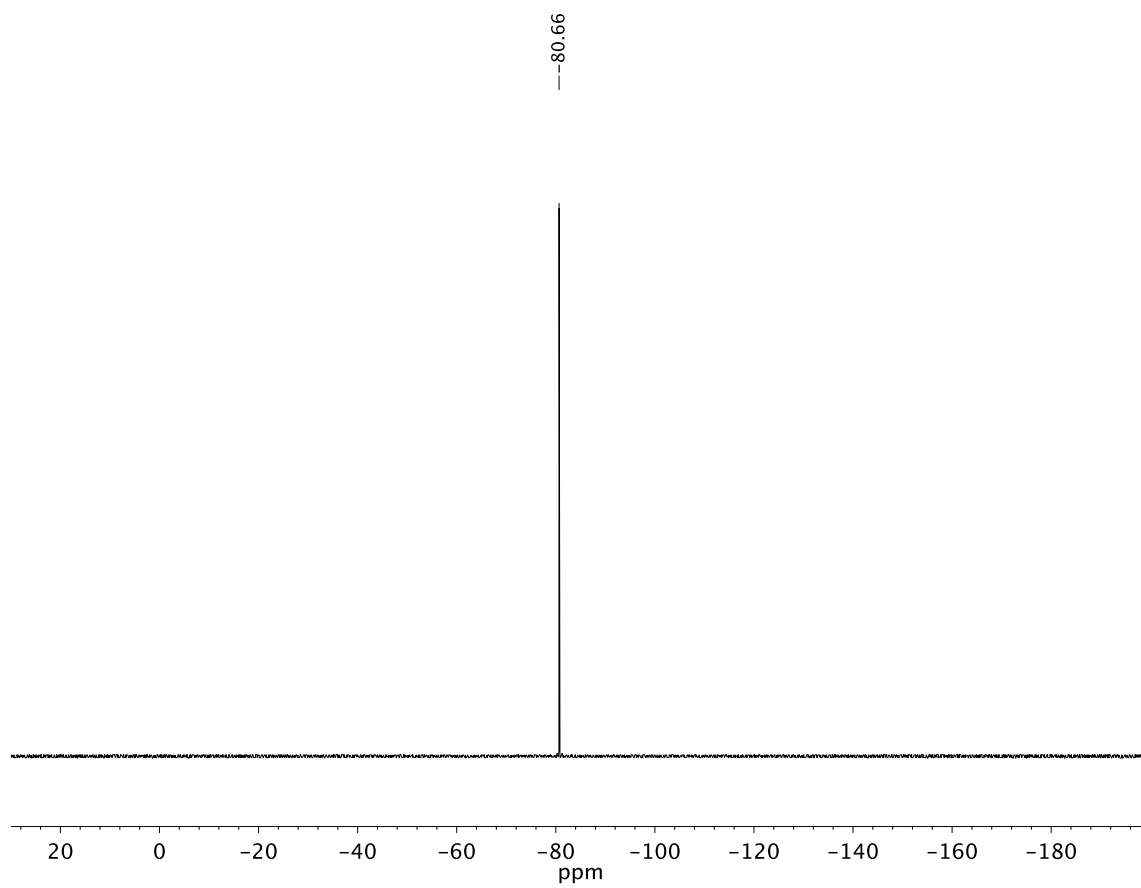




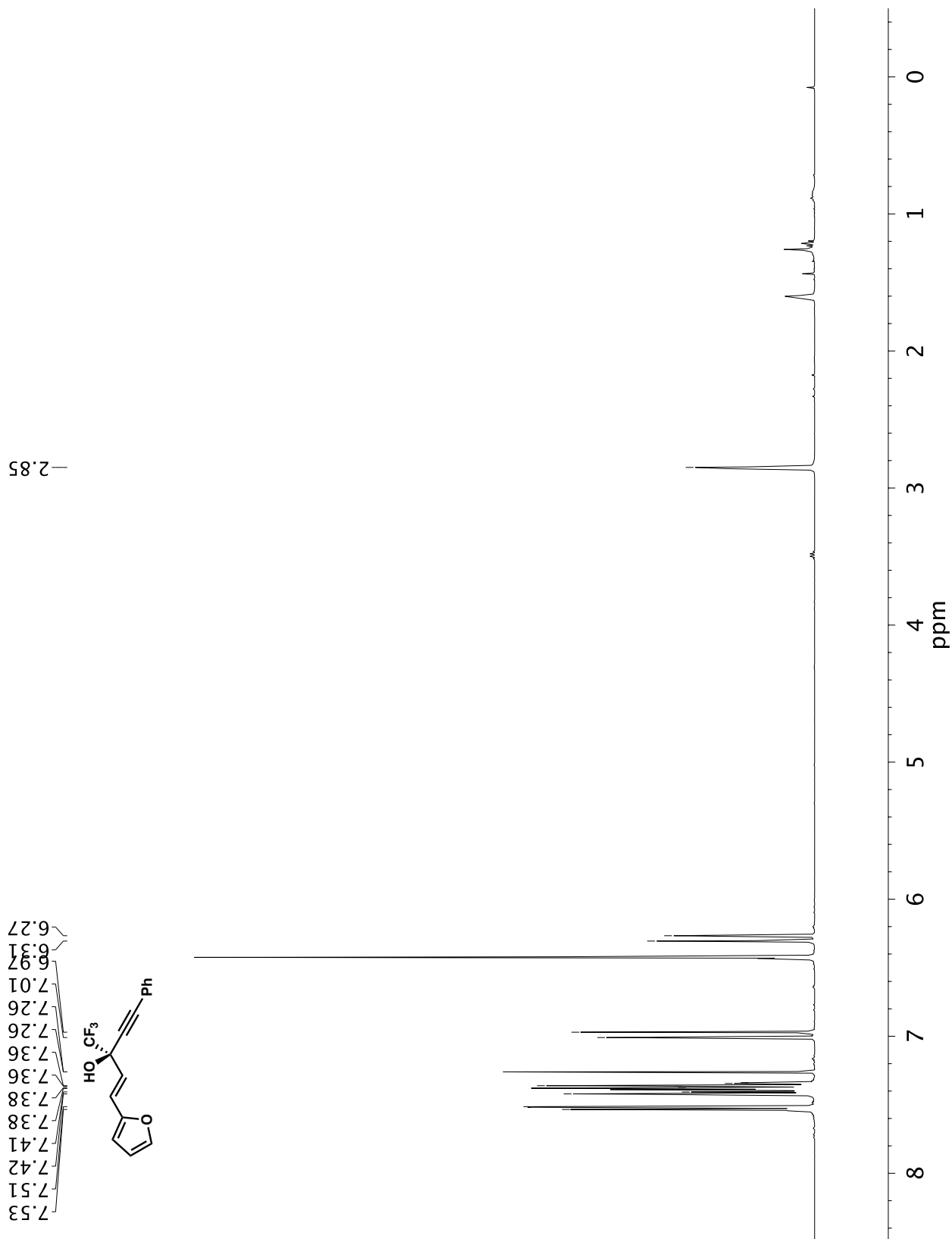
A1.41 Infrared spectrum (Thin Film, NaCl) of compound **11ia**.



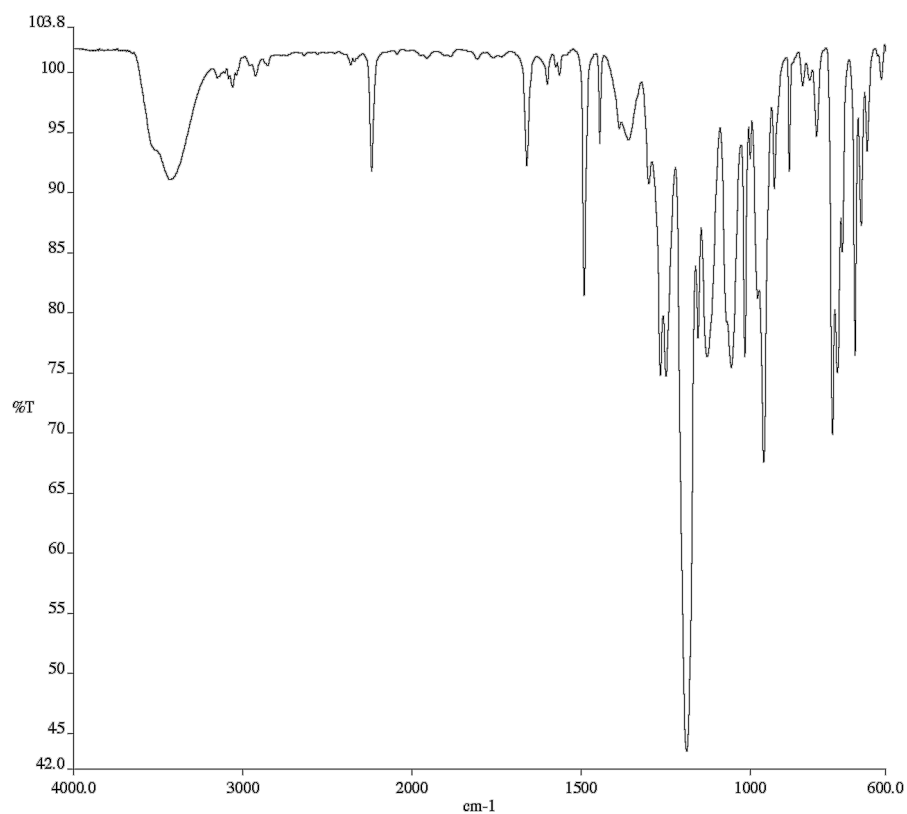
A1.42 ^{13}C NMR (101 MHz, CDCl_3) of compound **11ia**.



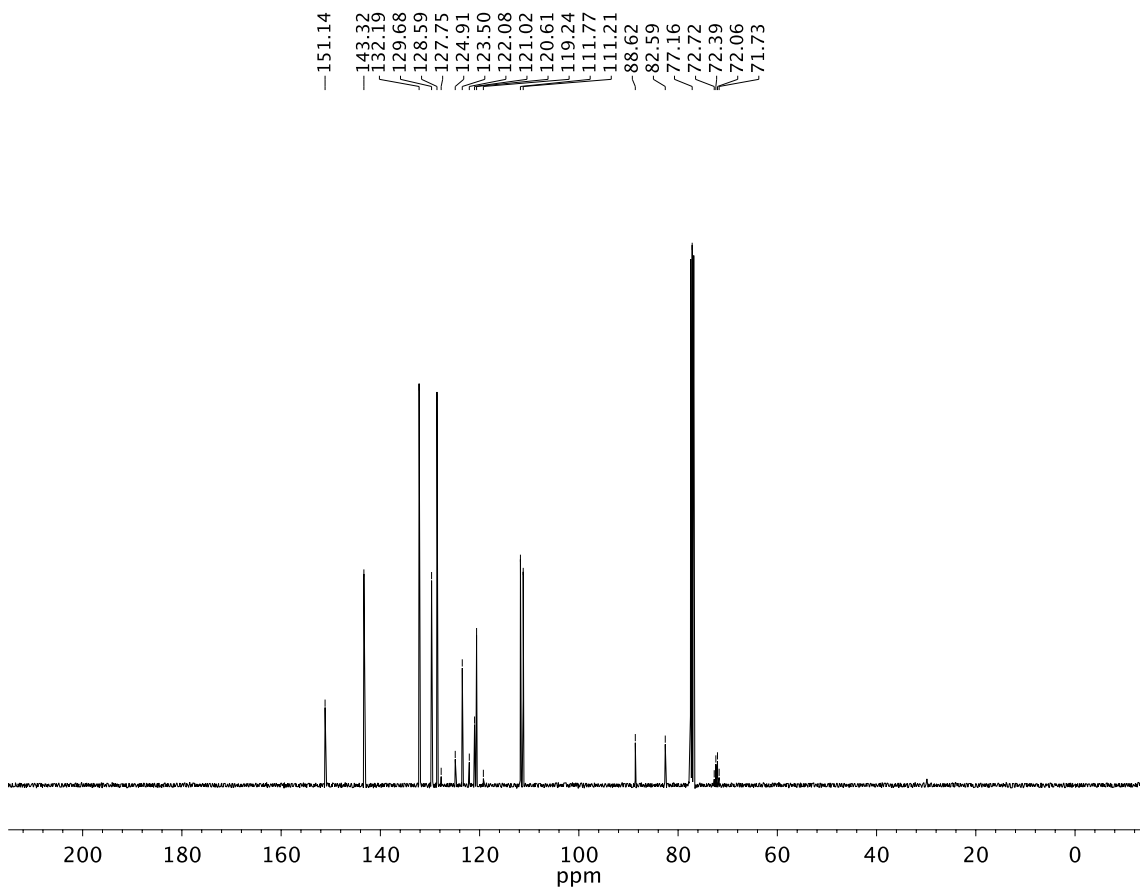
A1.43 ^{19}F NMR (282 MHz, CDCl_3) of compound **11ia**.



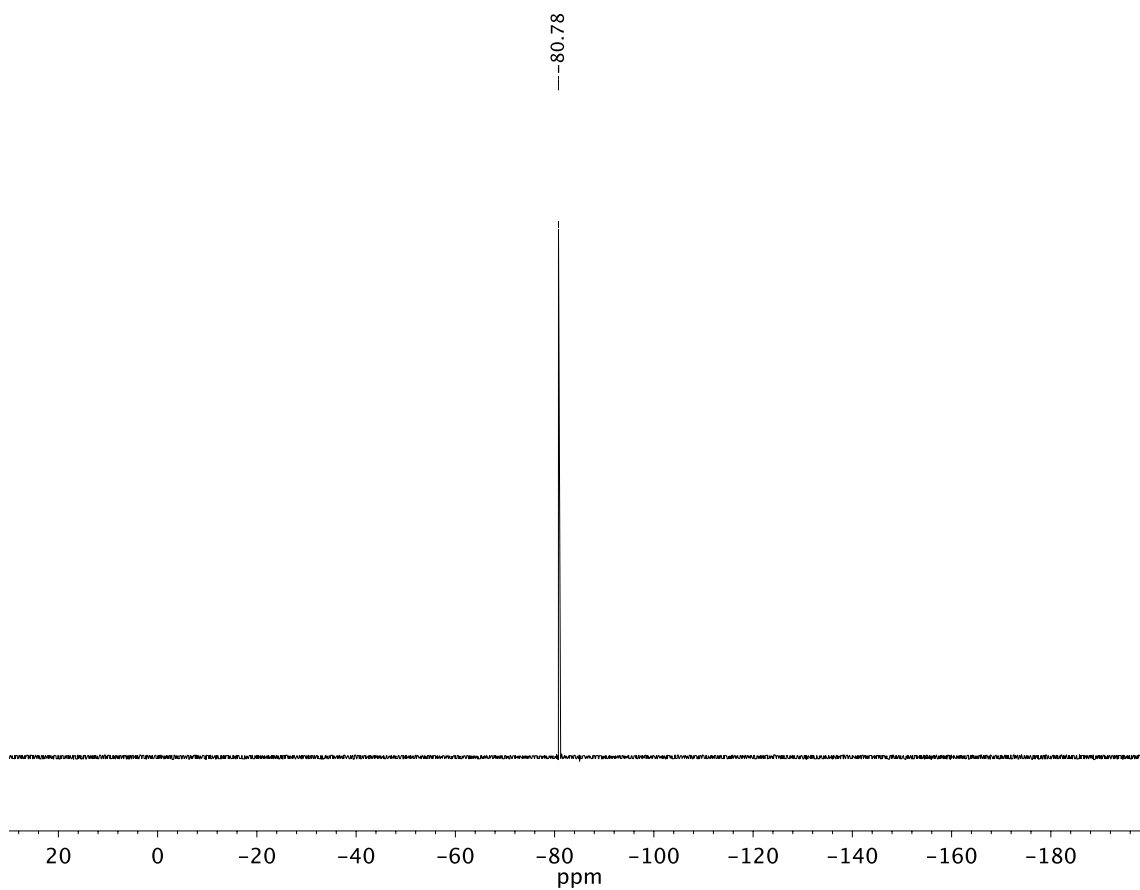
A1.44 ^1H NMR (400 MHz, CDCl_3) of compound **11ia**.



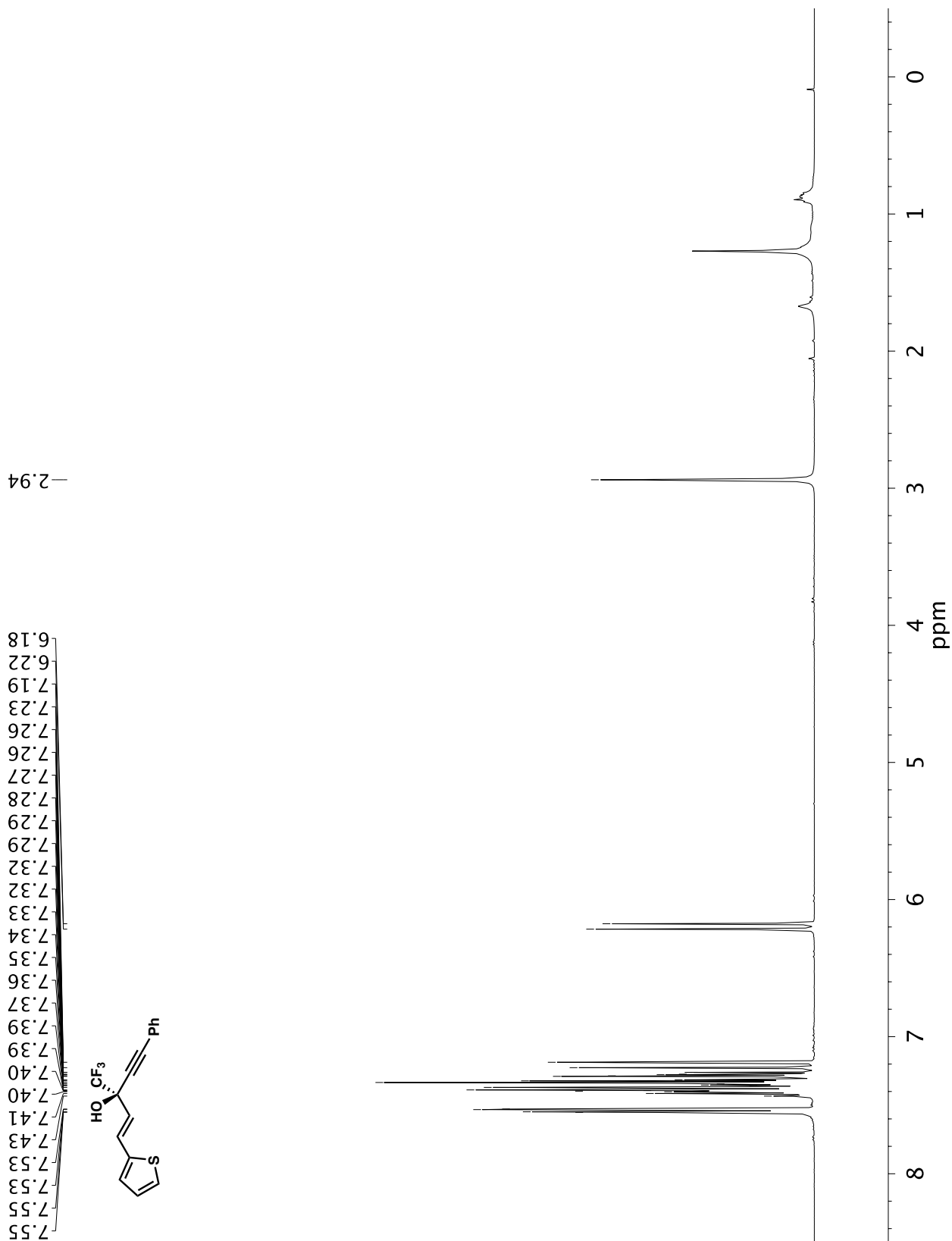
A1.45 Infrared spectrum (Thin Film, NaCl) of compound **11ja**.

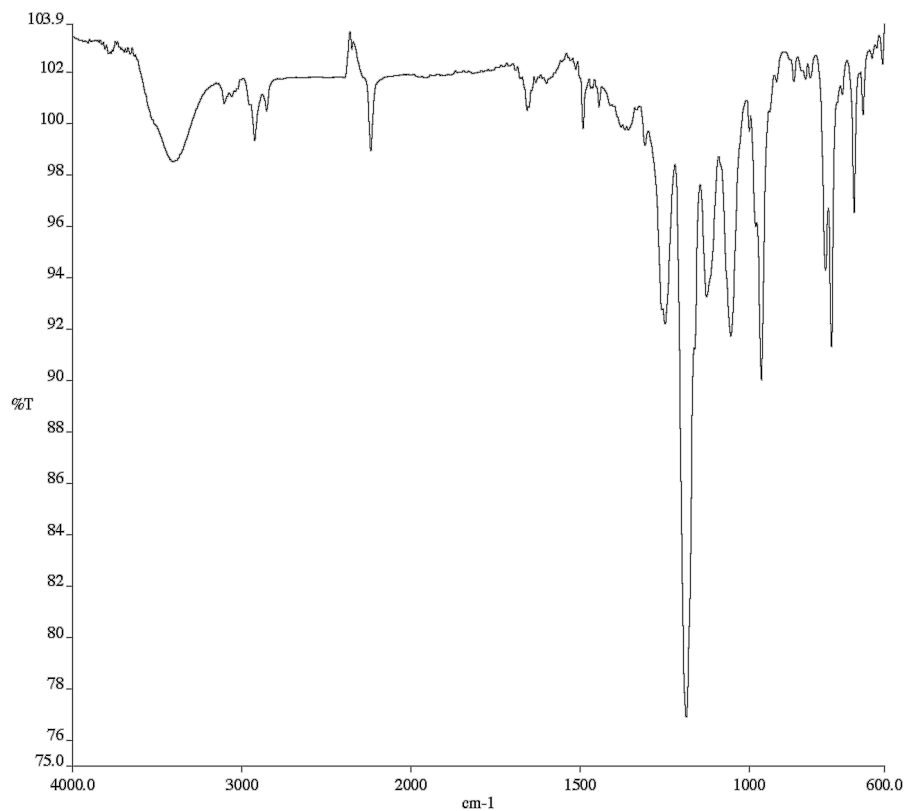


A1.46 ¹³C NMR (101 MHz, CDCl₃) of compound **11ja**.

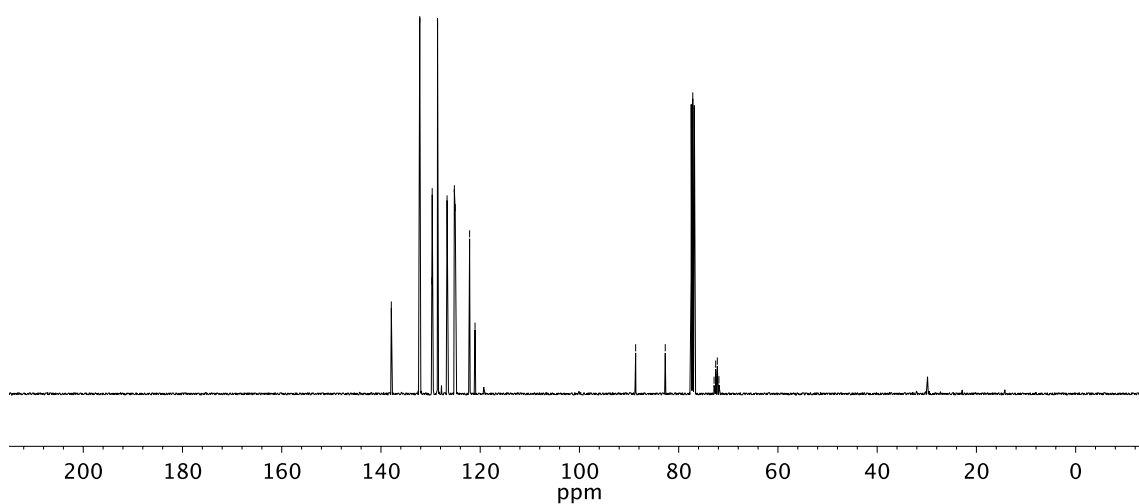


A1.47 ^{19}F NMR (282 MHz, CDCl_3) of compound **11ja**.

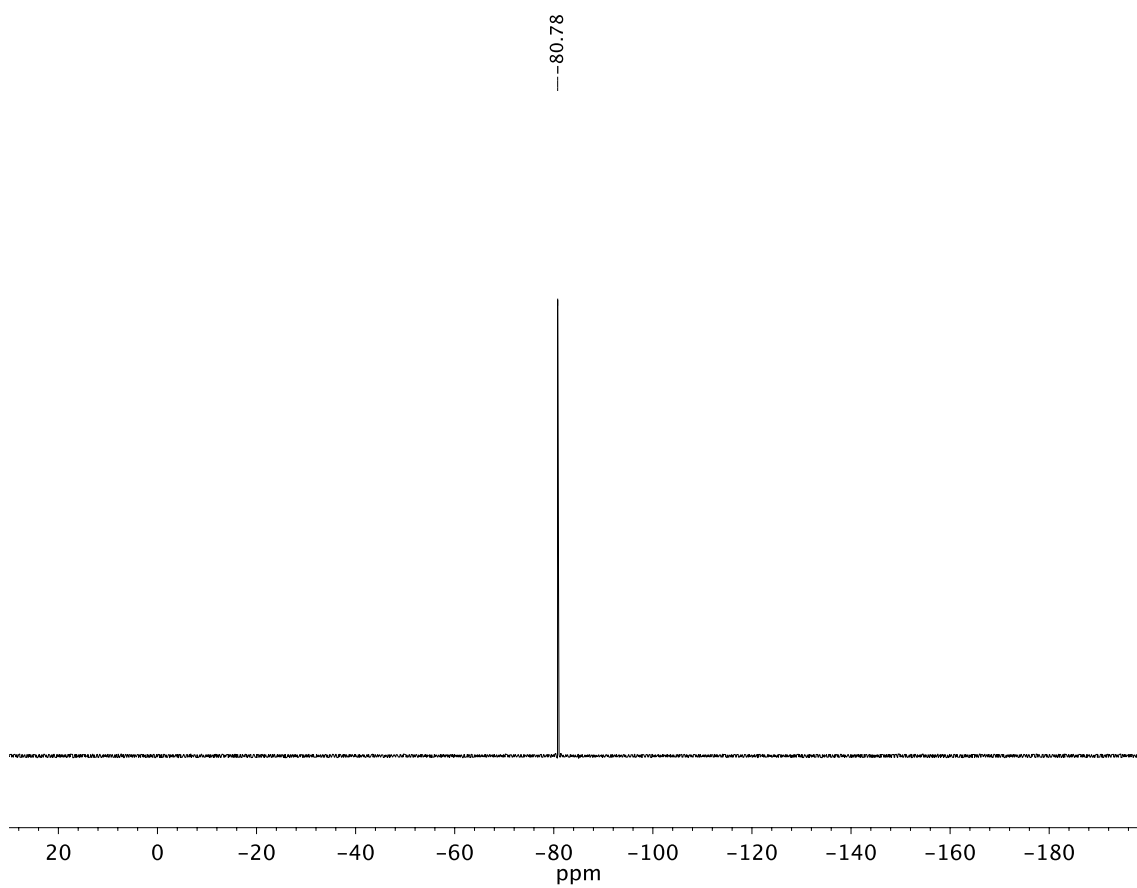




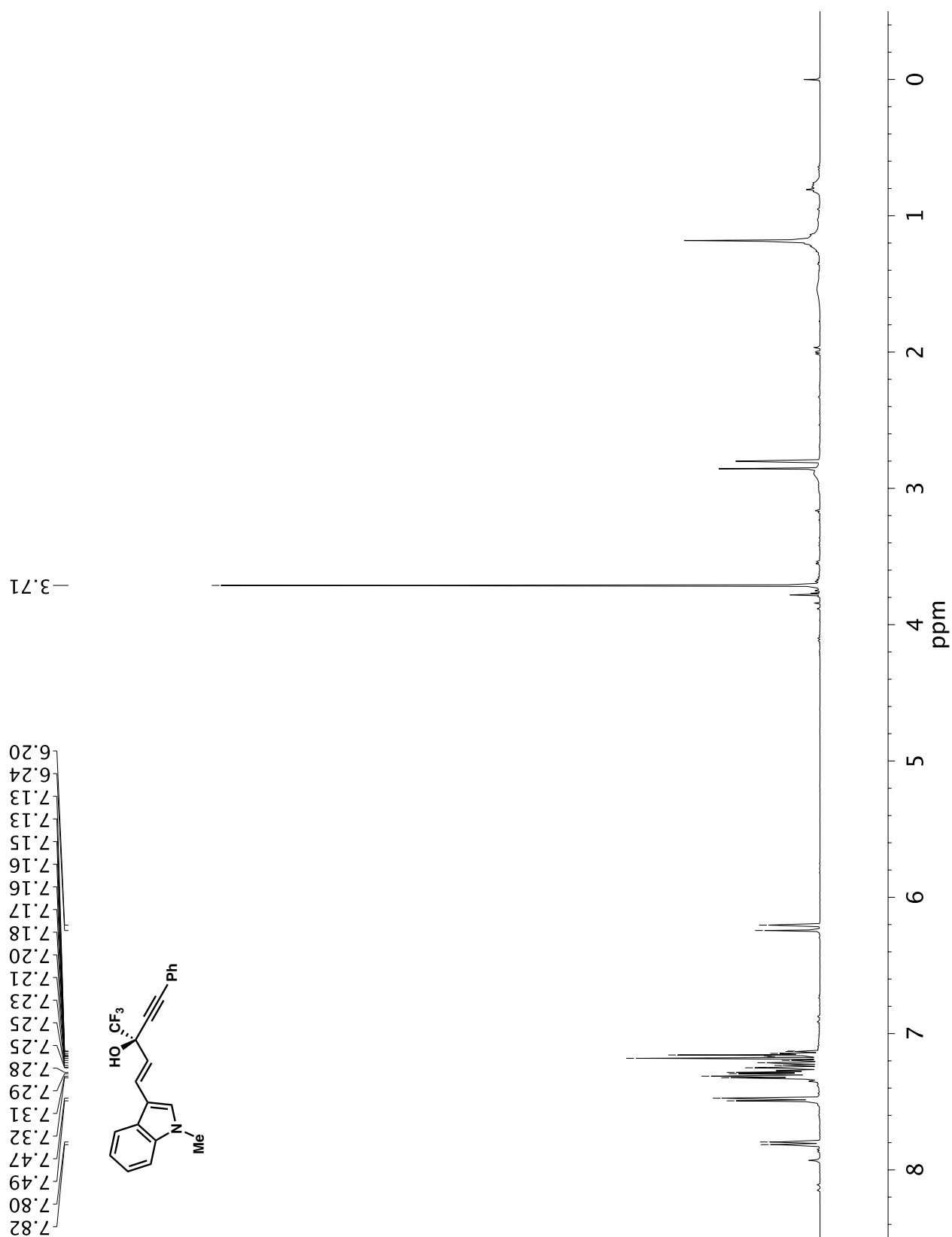
A1.49 Infrared spectrum (Thin Film, NaCl) of compound **11ka**.

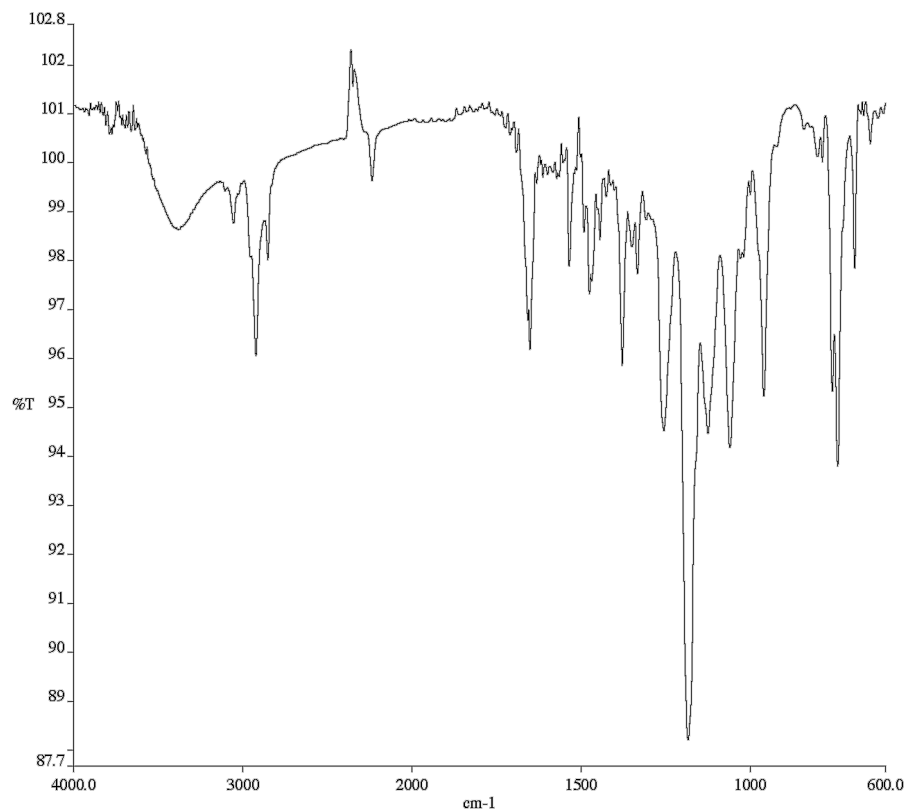


A1.50 ¹³C NMR (101 MHz, CDCl₃) of compound **11ka**.

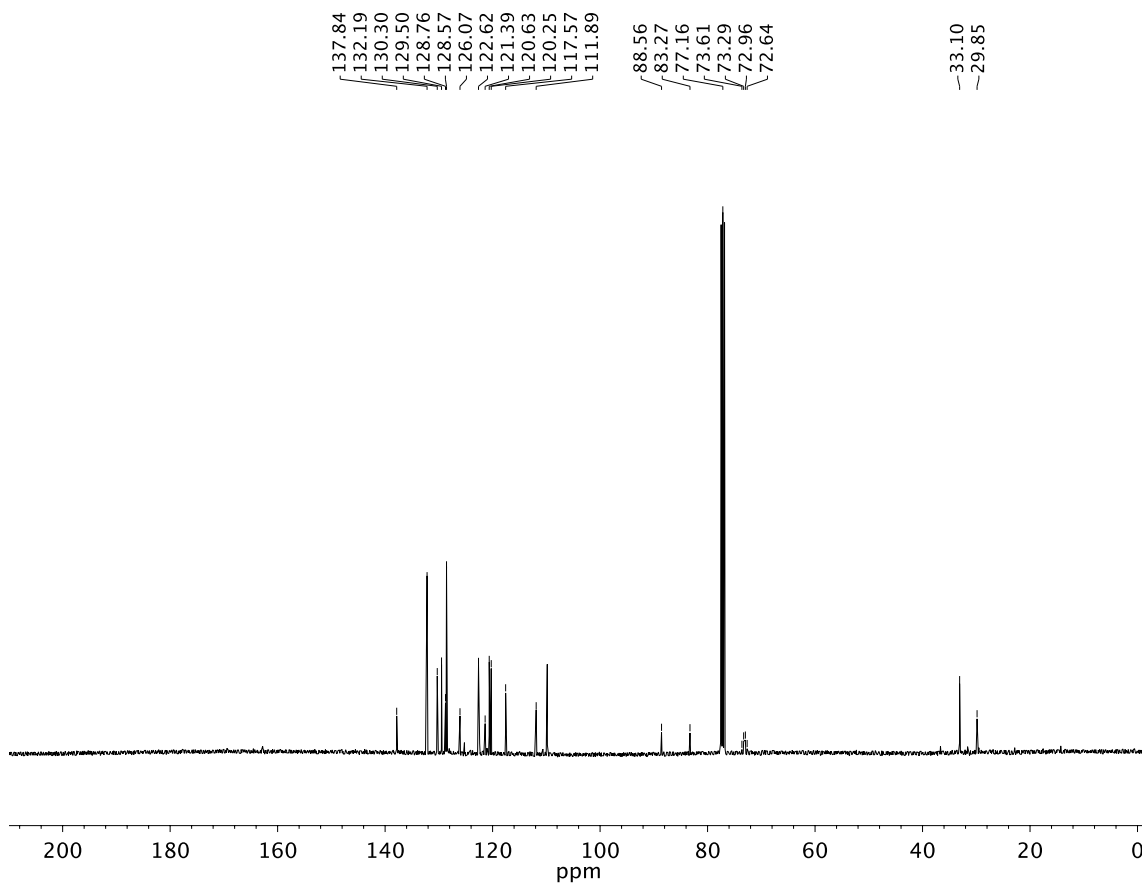


A1.51 ^{19}F NMR (282 MHz, CDCl_3) of compound **11ka**.

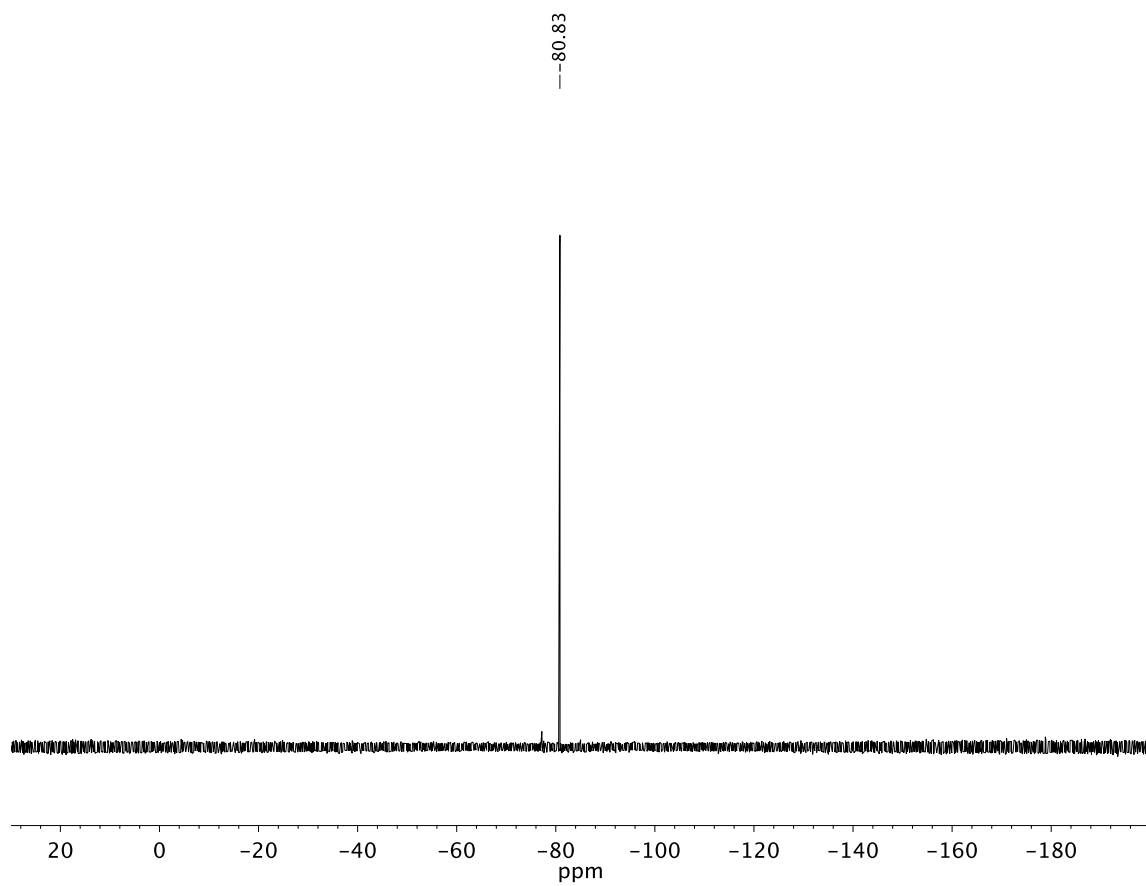




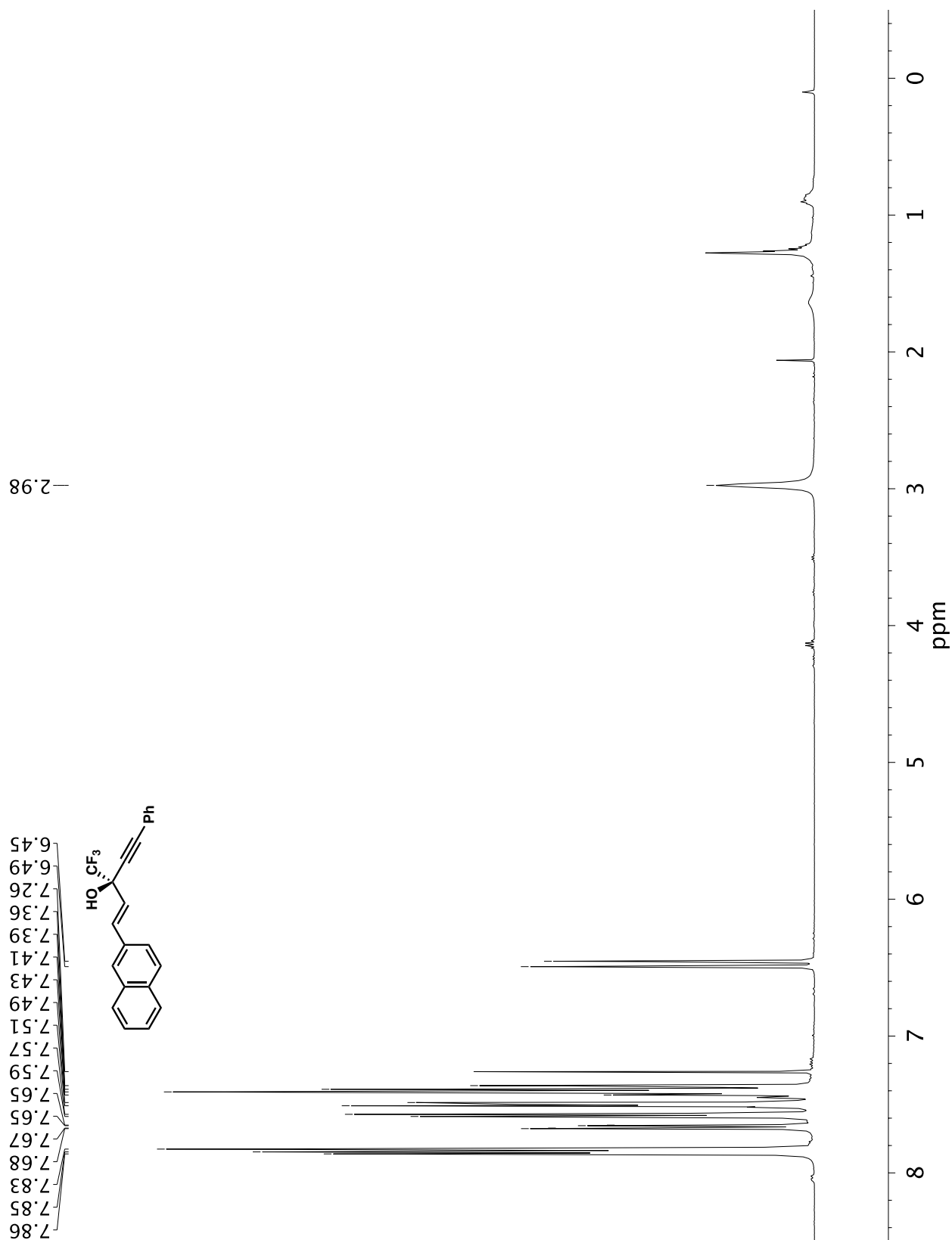
A1.53 Infrared spectrum (Thin Film, NaCl) of compound **11la**.

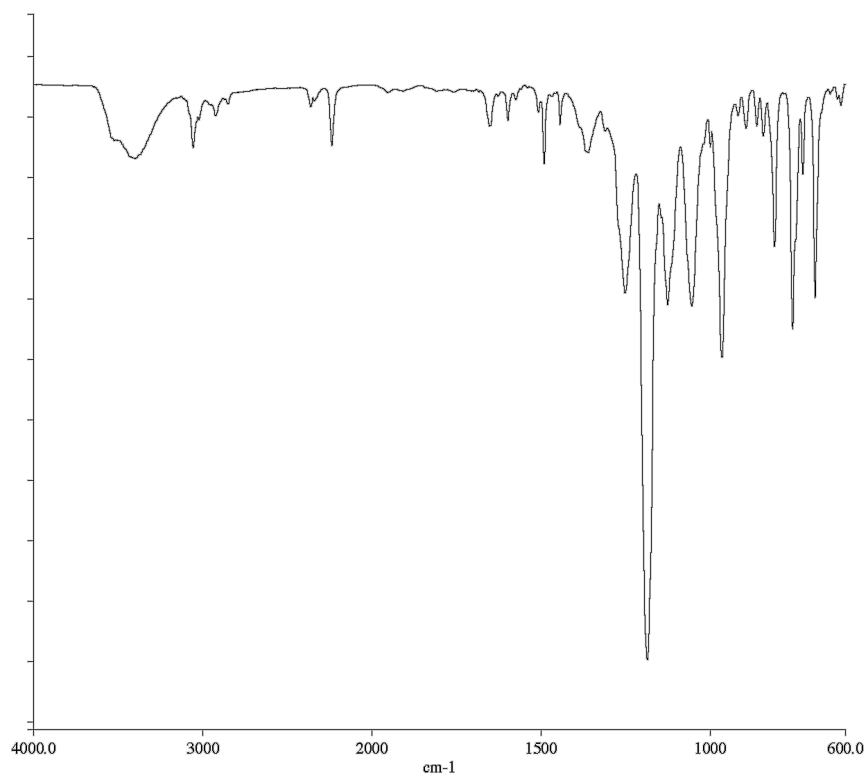


A1.54 ¹³C NMR (101 MHz, CDCl₃) of compound **11la**.

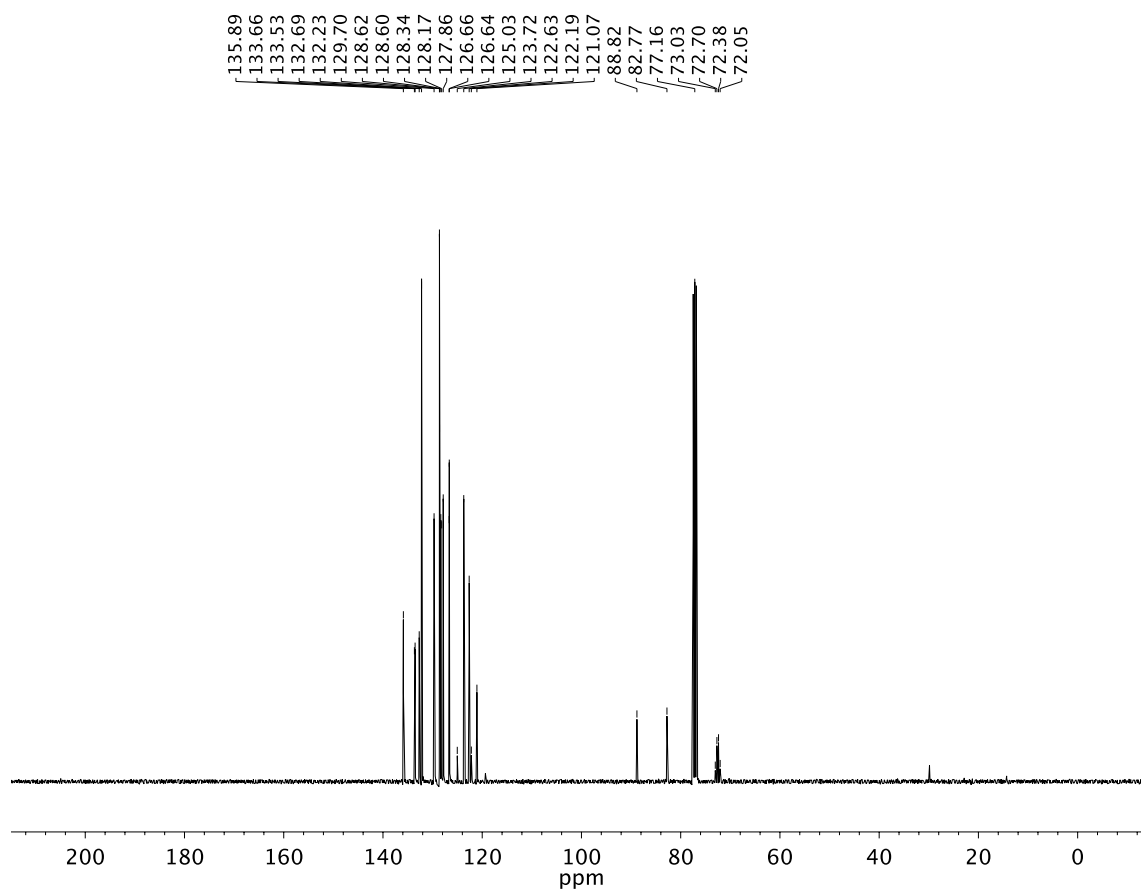


A1.55 ^{19}F NMR (282 MHz, CDCl_3) of compound **11la**.

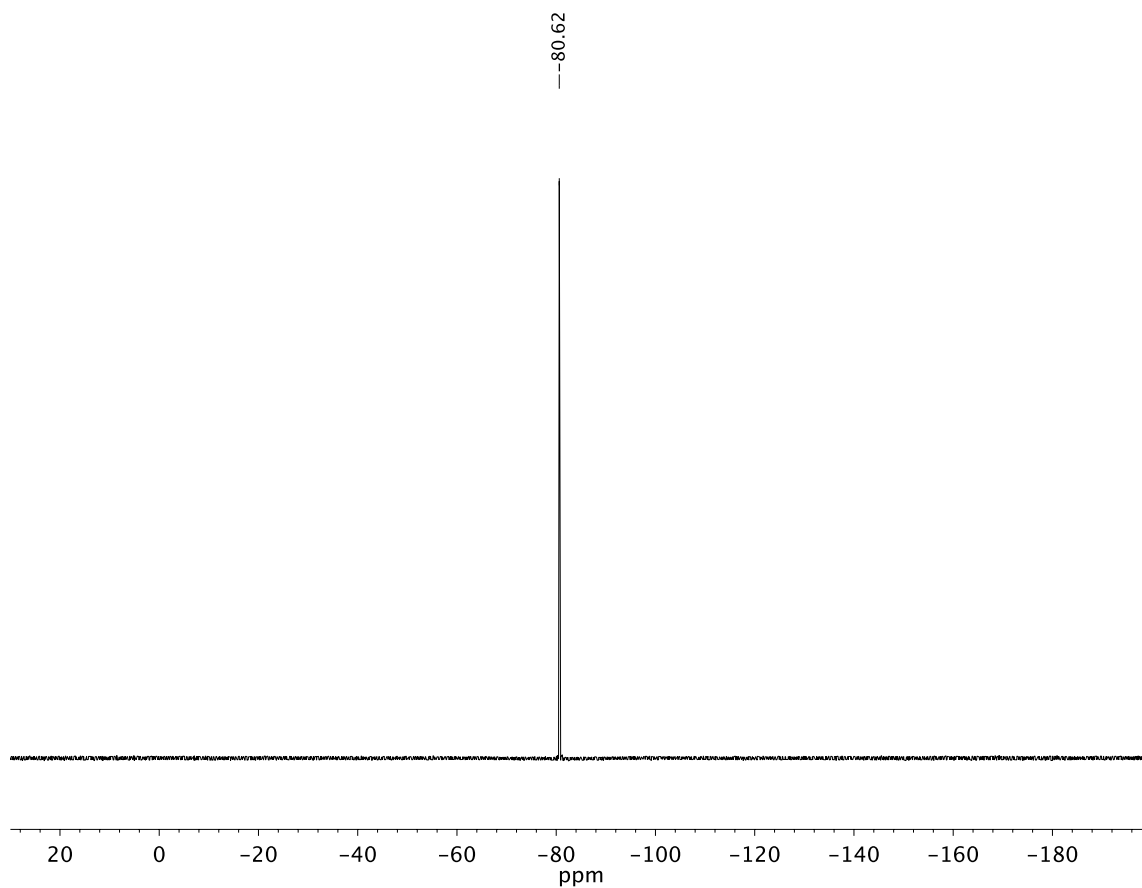
**A1.56** ¹H NMR (400 MHz, CDCl₃) of compound **11ma**.



A1.57 Infrared spectrum (Thin Film, NaCl) of compound **11ma**.

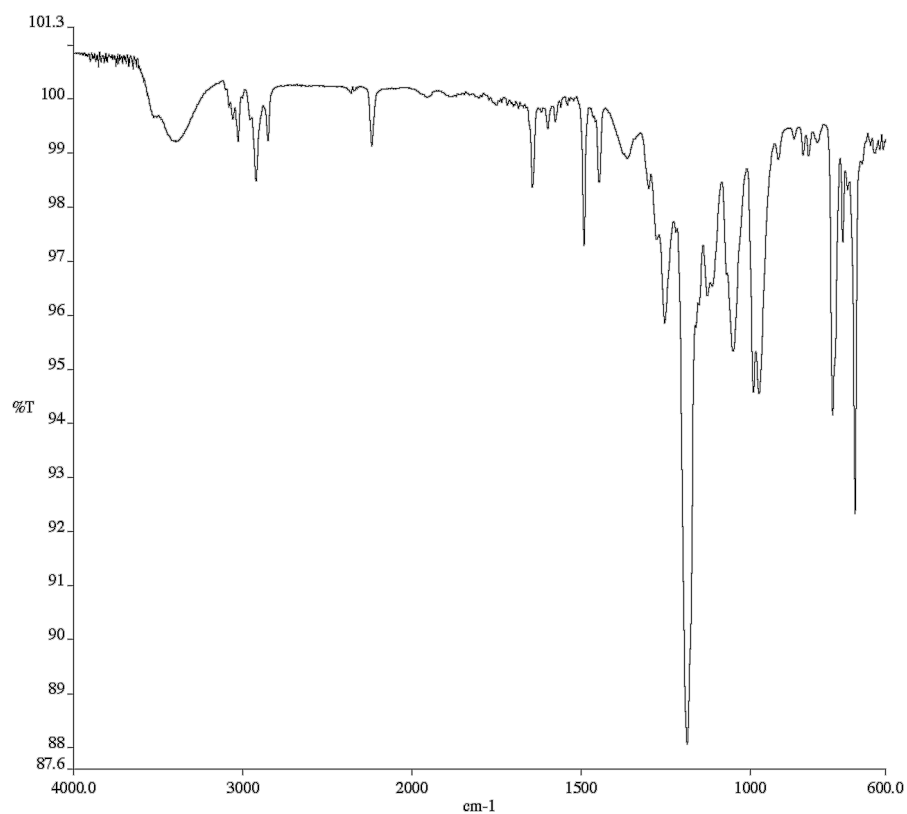


A1.58 ^{13}C NMR (101 MHz, CDCl_3) of compound **11ma**.

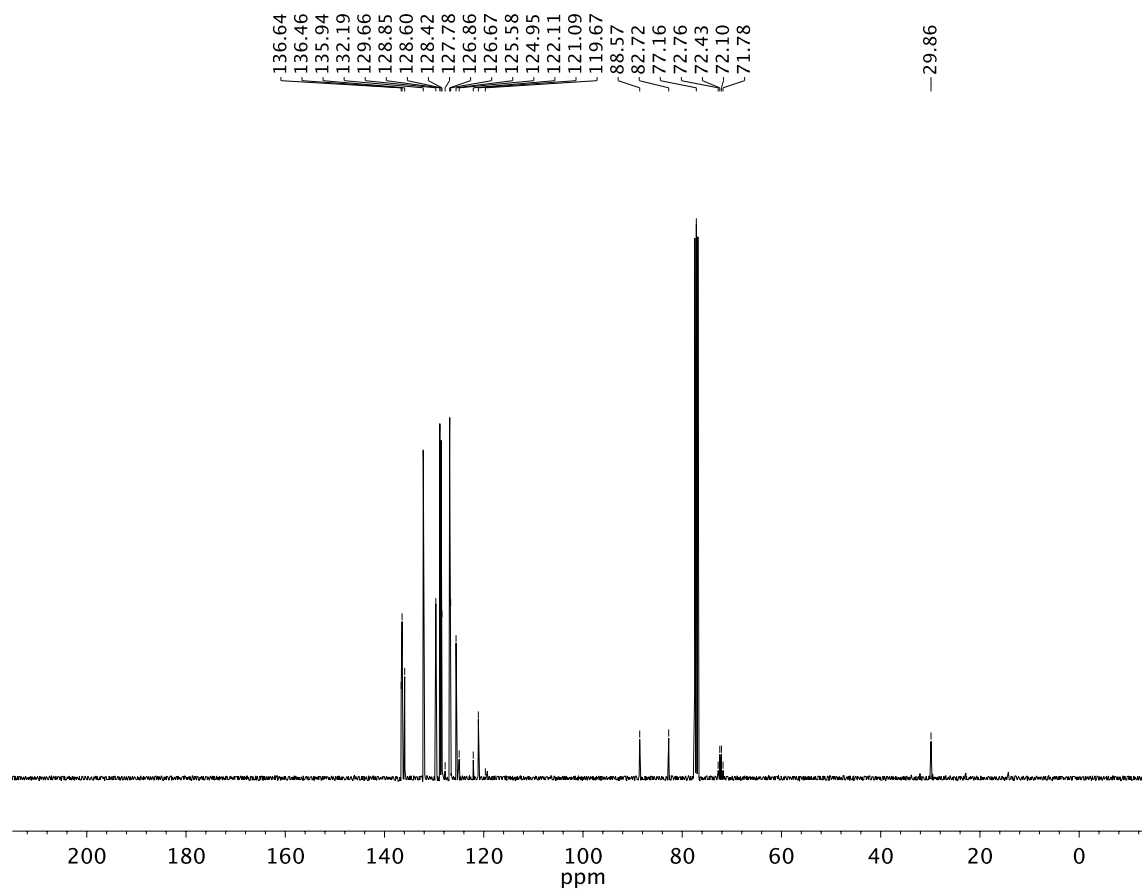


A1.59 ^{19}F NMR (282 MHz, CDCl_3) of compound **11ma**.

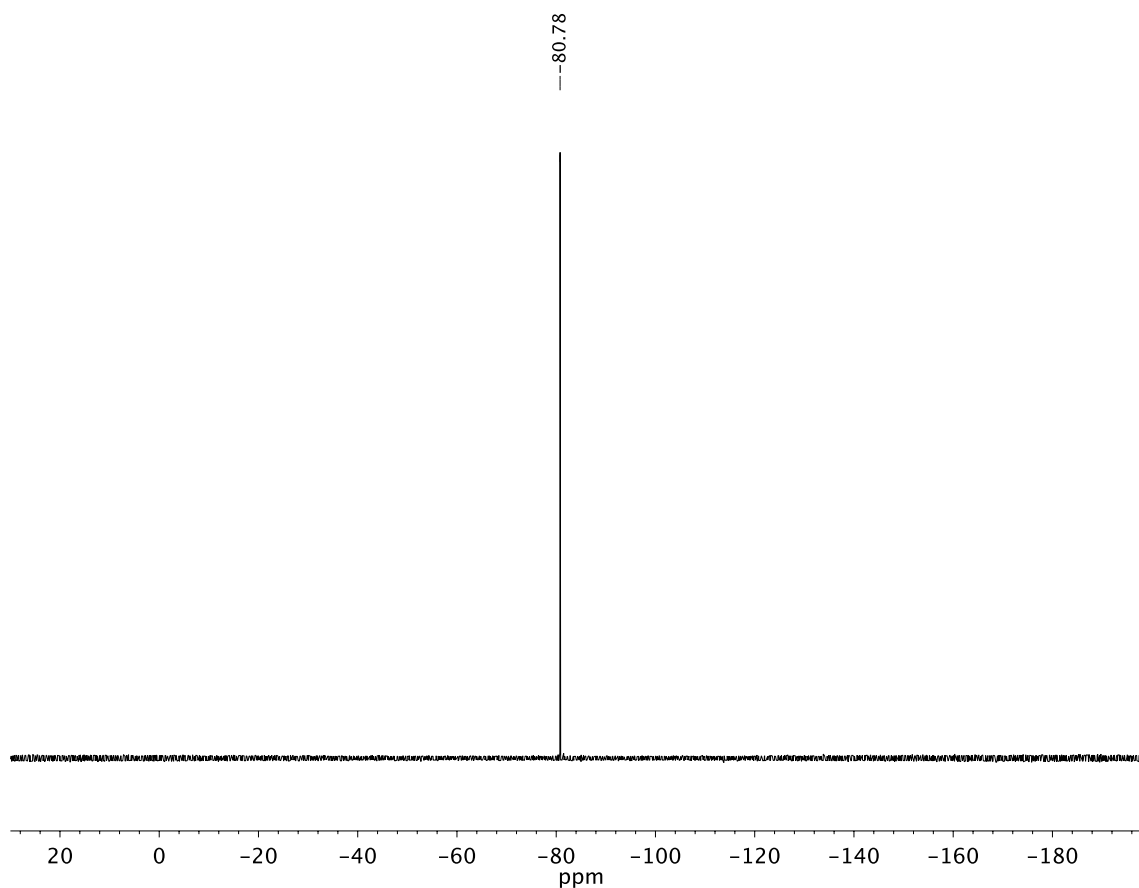




A1.61 Infrared spectrum (Thin Film, NaCl) of compound **11na**.



A1.62 ¹³C NMR (101 MHz, CDCl₃) of compound **11na**.



A1.63 ^{19}F NMR (282 MHz, CDCl_3) of compound **11na**.

The spectra for compounds **L1**, **L2**, **L4**, **L6**, **L7**, **6ga**, **6ha**, **6ac**, **6ad**, **6af**, **6cb**, **6eg**, **6eh** can all be found in: Park, D.; Jette, C. I.; Kim, J.; Jung, W. -O.; Lee, Y.; Park, J.; Kang, S.; Han, M. S.; Stoltz, B. M.; Hong, S. *Angew. Chem. Int. Ed.* **2020**, 59, 775–779.

CHAPTER 2

Palladium-Catalyzed Enantioselective Arylation of γ -Lactams with Aryl Chlorides and Bromides[†]

2.1 INTRODUCTION AND BACKGROUND

Nitrogen heterocycles are ubiquitous structural motifs that can be found across all areas and applications of organic chemistry. A particularly important subgroup of this class are the pyrrolidinones, which along with their saturated counterparts, the pyrrolidines, occur widely in nature,^{1,2} possess a wide range of biological and pharmacological properties,³ and are commonly employed in materials⁴ and catalysis.⁵ For these reasons, the development of stereoselective approaches to functionalized five-membered nitrogen-containing heterocycles is of great interest in the synthesis of small molecules and natural products.

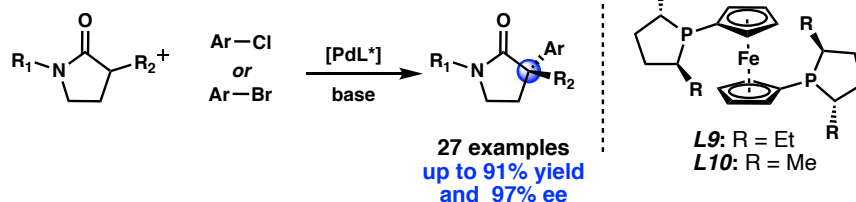
Our group has a long-standing interest in the stereoselective synthesis of five-membered *N*-heterocyclic building blocks, having developed methods for both enantioselective allylic alkylation⁶ and enantioselective α -acylation of γ -lactams.⁷ The α -aryl pyrrolidinone building block is of special interest, as it would enable access to the phenethylbenzylamine structural motif, which is prevalent in a number of biologically active natural products and drug-like molecules

[†] This work was performed in collaboration with Irina Geibel and Shoshana Bachman, both alumni in the Stoltz group, visiting researchers Masaki Hayashi, Hideki Shimizu, and Jeremy B. Morgan, as well as visiting graduate student Shunya Sakurai. This work has been published and adapted with permission from Jette, C. I. Geibel, I.; Bachman, S.; Hayashi, M.; Sakurai, S.; Shimizu, H.; Morgan, J. B.; Stoltz, B. M. *Angew. Chem. Int. Ed.* **2019**, 58, 4297–4301. Copyright 2019 Wiley-VCH.

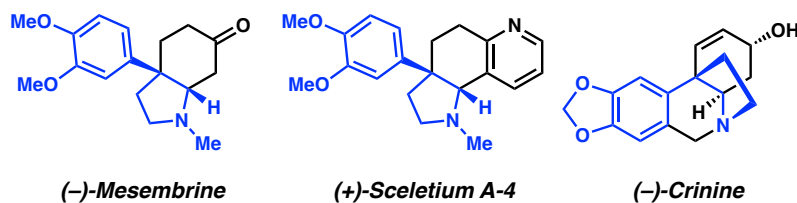
(Figure 2.1.1).⁸ Nevertheless, methods describing the asymmetric α -arylation of substituted pyrrolidinones to produce α -quaternary γ -lactams have remained elusive.

Figure 2.1.1. Pd-Catalyzed Enantioselective Arylation of γ -Lactams⁸

A. This research:



B. Representative benzyphenethylamine-type alkaloids

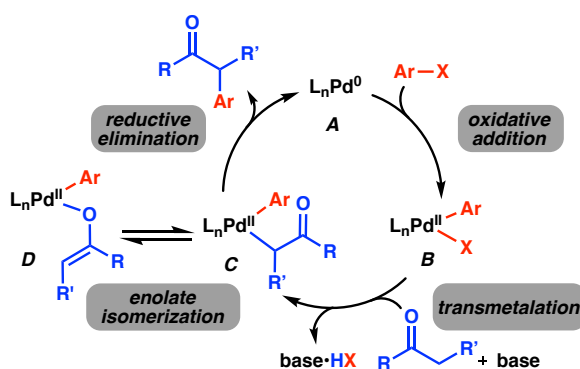


2.2 OVERVIEW ON α -ARYLATION

Over the past 20 years, transition metal-catalyzed α -arylation of carbonyl derivatives has emerged as a powerful method for C–C bond formation as it enables the efficient construction of sp^3 – sp^2 bonds α - to a carbonyl derivative. Although the first report of a transition-metal catalyzed α -arylation dates back to 1973,⁹ it was not until the concomitant reports from Miura¹⁰, Hartwig,¹¹ and Buchwald,¹² in which an enolate formed *in-situ* could be used with a catalytic amount of Pd, that the value of this reaction was truly appreciated. Since then, a number of transition metal catalysts have been developed for this transformation, and although transition metals such as Ni and Cu have been used previously in this transformation, the most developed systems involve the use of a Pd catalyst.

The Pd-catalyzed α -arylation reaction is believed to proceed via a Pd(0)-Pd(II) cycle as outlined in Figure 2.2.1.¹³ Initially, a starting Pd(0) species **A** undergoes oxidative addition into an aryl halide or pseudohalide to afford a Pd(II) aryl species (**B**). This Pd(II) species can then undergo transmetalation to afford either the C-bound (**C**) or the O-bound (**D**) enolate. If the O-bound enolate is generated, a potentially rate-determining isomerization to the C-bound enolate must precede reductive elimination. Finally, reductive elimination results in the desired product and the regeneration of the starting Pd (0) species **A**.

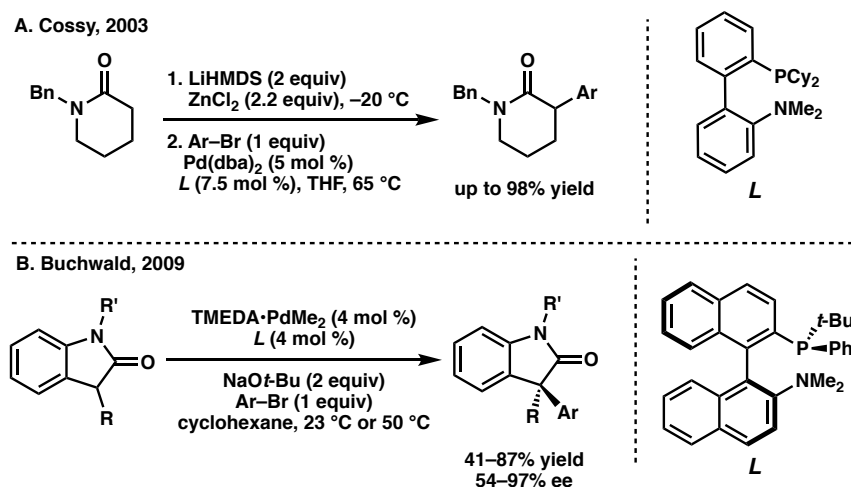
Figure 2.2.1 Mechanism for Pd-Catalyzed α -Arylation of Carbonyl Derivatives¹³



Although the efficiency of the reaction depends on many factors, the nature of the carbonyl compound employed has the greatest impact on the reaction conditions. The acidity of the α -proton and the subsequent reactivity of the enolate generated will dictate which types of bases must be used or whether a less reactive silyl or zinc enolate is required. Furthermore, the steric encumbrance and reactivity of the enolate generated will in turn determine which types of aryl halides, ligands, solvents, and reaction temperatures will be needed to generate the product in synthetically useful quantities. It is for these reasons that reaction conditions tend to be very unique and specific to each new class of nucleophile. Some of the carbonyl derivatives that have already

been used in this chemistry include ketones, amides, esters, aldehydes, nitriles, sulfones, and nitroalkanes.¹³

Figure 2.2.2. α -Arylation of Piperidinones and Oxindoles^{16, 17i}

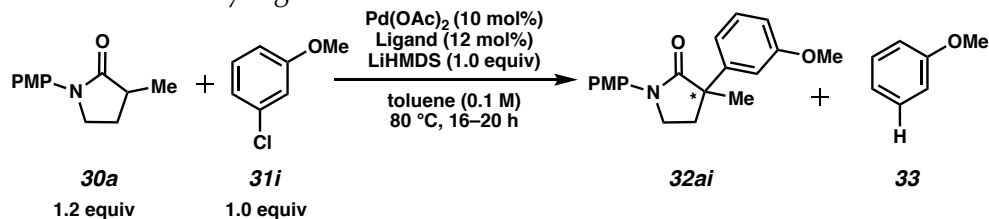


There are a number of subtle challenges that have potentially precluded α -substituted γ -lactams from being successfully implemented in Pd-catalyzed asymmetric α -arylation chemistry. One of the challenges is the necessity for enolization by strong base, which may lead to the generation of unwanted aryne intermediates from the aryl halide^{14,15} in addition to catalyst decomposition. As a result, prior reports are limited to either α -unsubstituted piperidinones, which require pre-formation of a basicity-tempered zinc enolate to generate the desired product (Figure 2.2.2.A),¹⁶ or oxindoles (Figure 2.2.2.B),¹⁷ⁱ which are a special case that do not require high temperatures or strongly basic conditions. Taking these considerations into account, we sought to develop the first method for the direct transition metal-catalyzed enantioselective α -arylation of α -substituted γ -lactams to generate all-carbon quaternary stereocenters.

2.3

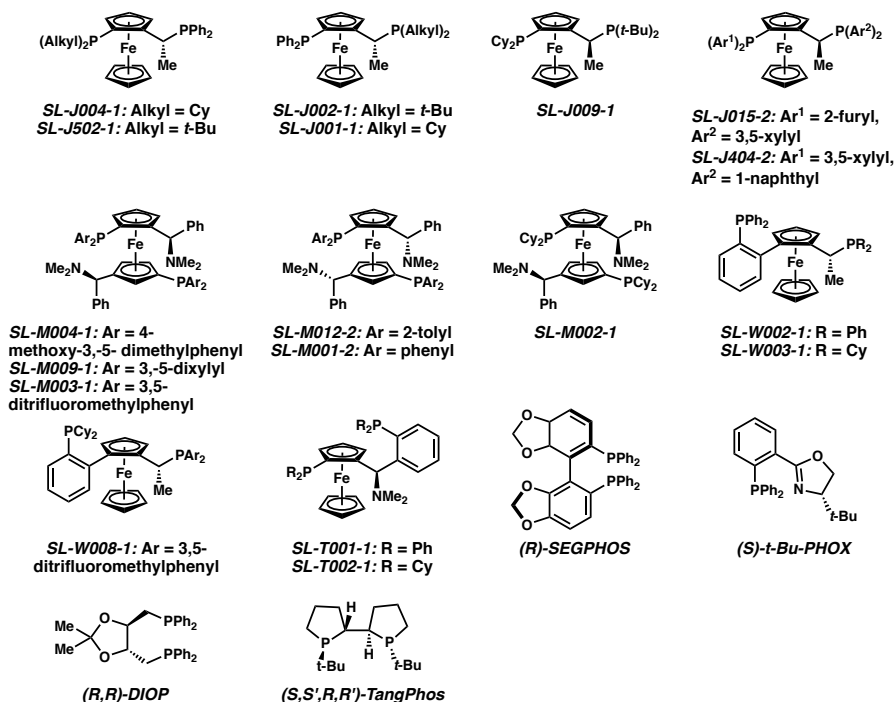
REACTION OPTIMIZATION WITH ARYL CHLORIDES

Table 2.3.1. Preliminary Ligand Screen



Entry	Ligand	Conversion (%) ^a	Yield (%) ^b	33 (%) ^a	ee (%) ^c
1	<i>SL-J004-1</i>	61	27	5	45
2	<i>SL-J502-1</i>	37	< 5	28	–
3	<i>SL-J002-1</i>	88	8	40	–
4	<i>SL-J004-1</i>	62	16	6	18
5	<i>SL-J009-1</i>	41	< 5	25	–
6	<i>SL-J015-1</i>	24	20	5	–10
7	<i>SL-J404-2</i>	66	24	19	–8
8	<i>SL-M004-1</i>	65	47	12	–34
9	<i>SL-M009-1</i>	59	43	12	–48
10	<i>SL-M003-1</i>	14	8	19	–55
11	<i>SL-M012-1</i>	59	< 5	35	–
12	<i>SL-M001-1</i>	35	13	13	54
13	<i>SL-W002-1</i>	4	< 5	4	–
14	<i>SL-W003-1</i>	45	18	13	2
15	<i>SL-W008-1</i>	7	< 5	4	–
16	<i>SL-T001-1</i>	46	21	19	16
17	<i>SL-T002-1</i>	75	38	9	–12
18	<i>(R)</i> -SEGPHOS	< 5	< 5	5	–
19	<i>(S)</i> - <i>t</i> -Bu-Phox	< 5	< 5	< 5	–
20	<i>(R)</i> -Diop	8	7	< 5	–
21	<i>(S,R)</i> -Tangphos	58	6	10	–

Ligands Tested:



[a] Determined by GC using 1,3,5-trimethoxybenzene as an internal standard. [b] Determined by ¹H NMR using 1,3,5-trimethoxybenzene as an internal standard. [c] Determined by SFC, AD column, 40% IPA, 2.5 mL/min method.

In the first round of screening, a number of commercially available ligands were tested in the Pd-catalyzed arylation of *p*-methoxyphenyl-protected lactam **30a** using 3-methoxyphenyl chloride **31i**. With 10 mol% Pd(OAc)₂, 1.0 equiv of LiHMDS, in toluene at 80 °C, over 20 commercially available ligands were tested (Table 2.3.1).

The ferrocene ligands (entries 1–17) generally resulted in the highest levels of reactivity; other aryl and alkyl phosphines such as (R)-Segphos, (S)-*t*-Bu-Phox, (R)-Diop, or (S,R)-Tangphos resulted in very low conversions and negligible amounts of product (entries 18–21). The ferrocene ligand classes examined include Josiphos (entries 1–7), Mandypbos (entries 8–12), Walphos (entries 13–15), and Taniaphos (entries 16 and 17) ligands. The Josiphos ligand class (entries 1–7) generally led to low yields (less than 30% in all cases), and with the exception of ligand J004-

Table 2.3.2. Pd and Additional Ferrocene Ligand Screening

entry	Pd source	ligand	yield(%) ^a	ee(%) ^b
1	Pd(dba) ₂	L8	18	7
2	Pd(dba) ₂	L9	30	95
3	Pd(dba) ₂	L10	< 5	–
4	Pd(dba) ₂	L11	17	< 5
5	Pd(dba) ₂	L12	< 5	–
6 ^c	Pd(dba) ₂	L9	50	90
7	Pd(OAc) ₂	L9	< 5	–
8 ^d	Pd ₂ (dm-dba) ₃	L9	43	90

L8: Ar = 3,5-dixylyl (SL-M009-1)

L9: R = Et
L10: R = Me
L11: R = *i*-Pr

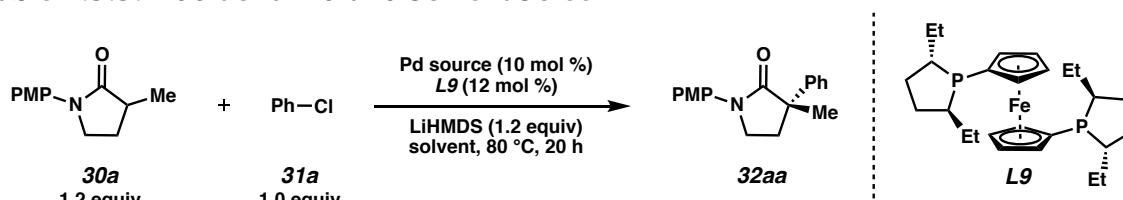
L12

[a] Conditions: 0.1 mmol scale. Yields determined by LC-MS analysis of the crude reaction mixture using 1,3,5-trimethoxybenzene as a standard. [b] Determined by chiral SFC analysis of the isolated product. [c] 1.0 equiv **30a**, 1.5 equiv LiHMDS, 2.0 equiv **31a**. [d] 100% fresh toluene, complete setup in glovebox, run for 36 h. PMP = *p*-methoxyphenyl. dm-dba = 3,5,3',5'-dimethoxydibenzylideneacetone.

1 (entry 1), very low ee's. In a number of cases, a large amount of the dechlorinated product **33** (entries 2, 3, 5, and 7) was observed. Generally, where the yields of the desired product were high, the amount of dechlorinated product **33** was low, and vice versa. These results could be indicating that the slow step in this reaction is not oxidative addition, but could be transmetalation, or O-bound to C-bound enolate isomerization, as a slow reductive elimination is unlikely given the large bite angle of these ligands.¹⁹ The very similar Walphos (entries 13–15) class also led to low yields. The Taniaphos ligands (entries 16, 17) did lead to slightly higher product yields, but the ee's were very low. With the Mandyphos class of ligands, however, the highest yields and ee's were obtained. With M004-1 and M009-1 (entries 8 and 9), the product yields were over 40%, and with M003-1, the product was obtained in 55% ee.

Intrigued by the results obtained with Mandyphos ligand M009-1, we initiated a brief investigation into the Pd source with this ligand (Table 2.3.2). Interestingly, we noted that switching to Pd(dba)₂ led to a significant reduction in reactivity (Table 2.3.2, entry 1 versus Table 2.3.1, entry 9). Upon examination of other ligands in combination with this Pd source, we found that Et-ferrocene (**L9**) led to the formation of **32aa** in very high ee, albeit in only moderate yield.

Table 2.3.3. Additional Pd and Solvent Screen^a

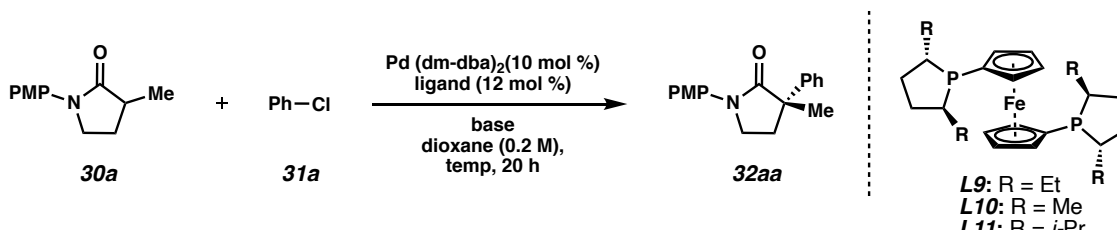
				
entry	Pd source	solvent	yield(%) ^a	ee(%) ^b
1	Pd ₂ (pm-dba) ₃	toluene	45	92
2	Pd ₂ (pm-dba) ₃	benzene	56	91
3	Pd ₂ (pm-dba) ₃	dioxane	62	97
4	Pd ₂ (pm-dba) ₃	DME	50	94
5	Pd ₂ (dba) ₃	dioxane	24	96
6	Pd(dm-dba) ₂	dioxane	59	97
7	Pd ₂ (dba) ₃ ·CHCl ₃	dioxane	15	92
8	Pd(OAc) ₂	dioxane	10	92

[a] 0.1 mmol scale. Yields determined by LC-MS analysis of the crude reaction mixture using 1,3,5-trimethoxybenzene as a standard. [b] Determined by chiral SFC analysis of the isolated product. PMP = *p*-methoxyphenyl. dmdba = 3,5,3',5'-dimethoxydibenzylideneacetone.

It should be noted that these results were unique and specific to this ligand, as other ligands in this class (**L10**, **L11**, and **L12**) resulted in very low conversion. Concerned about consumption of the starting material via formation of the lactam-dba adduct, a product which proved difficult to separate from **32aa**, we chose to examine a few more Pd sources in combination with **L9**. We found that in contrast to what was observed with M009-1, Pd(0) sources resulted in greater reactivity and selectivity with **L9**, and with both Pd₂(dm-dba)₃ (entry 8) and Pd₂(pm-dba)₃ (Table 2.3.3, entry 1), the product was obtained in significantly higher quantities but in similar ee to Pd(dba)₂.

Using Pd₂(pm-dba)₃ as the Pd source, the effect of the solvent on the reaction outcome was tested next. We noted that dioxane led to a significantly better reaction outcome as compared to toluene and benzene (entry 3 versus entries 1 and 2). Interestingly, upon examination of other Pd

Table 2.3.4. Examination of the Base, Substrate Stoichiometry, and Temperature

							
entry	ligand	30a equiv	31a equiv	base (equiv)	temp (°C)	yield(%) ^a	ee(%) ^b
1	L9	1.5	1	LiHMDS (1.5)	100	65	93
2 ^{c,d}	L9	1	2	LiHMDS (1.5)	100	73	95
3	L9	1.2	1	LiOt-Bu (2)	100	0	—
4	L9	1.2	1	NaOt-Bu (2)	100	0	—
5 ^c	L9	1.2	1	KOt-Bu (2)	100	0	—
6	L9	1.3	1	NaHMDS (1.2)	80	28	72
7	L9	1.3	1	KHMDS (1.2)	80	42	8
8	L9	1.3	1	LDA (1.2)	80	31	96
9	L10	1.5	1	LiHMDS (1.5)	100	69	94
10	L11	1.5	1	LiHMDS (1.5)	100	19	< 5
11 ^e	L9	1.5	1	LiHMDS (1.5)	100	65	94

[a] Conditions: 0.1 mmol scale. Yields determined by LC-MS analysis of the crude reaction mixture using 1,3,5-trimethoxybenzene as a standard. [b] Determined by chiral SFC analysis of the isolated product. [c] 14 hour. [d] Isolated yield = 58%. [e] >95% conversion. [f] With 2.5 mol% Pd₂(pm-dba)₃, 7.5 mol % **L9**, 6 h.

sources in dioxane, we noted that Pd(dm-dba)₂ still performed similarly (entry 6) to Pd₂(pm-dba)₃, but other Pd sources did lead to significant drops in reactivity (entries 7 and 8). Having identified two Pd sources that could be used interchangeably under these conditions,¹⁸ as well as the appropriate solvent, we next turned our attention to the nature and equivalents of the base, the nucleophile and electrophile stoichiometry, and the reaction temperature (Table 2.3.4). Increasing the reaction temperature to 100 °C led to a slight boost in yield (entry 1). We noted that inverting the stoichiometry did not lead to significant changes in the reaction outcome (entry 2).

Upon examination of a number of different bases, we found that the hexamethyldisilazide bases proved to be optimal for this transformation. Unsurprisingly, the weaker *t*-butoxide bases led to no product formation even at elevated temperatures (entries 3–5). Notably, employing LDA, a significantly stronger base than the hexamethyldisilazides, did not lead to any significant improvements in reactivity (entry 9). One possible explanation for this could be that LiHMDS, which has a pK_a of 26 in THF,³¹ may not be strong enough to fully deprotonate the γ -lactam, thus limiting the amount of reactive enolate present throughout the course of the reaction. When LDA is used, quantitative enolization is anticipated, which may lead to decomposition of the lactam enolate via other undesirable pathways. Finally, the nature of the cation on the HMDS also had an effect; LiHMDS seemed to be the best base for this reaction, as switching to Na or KHMDS led to significant drops in yield and ee (entries 6 and 7).

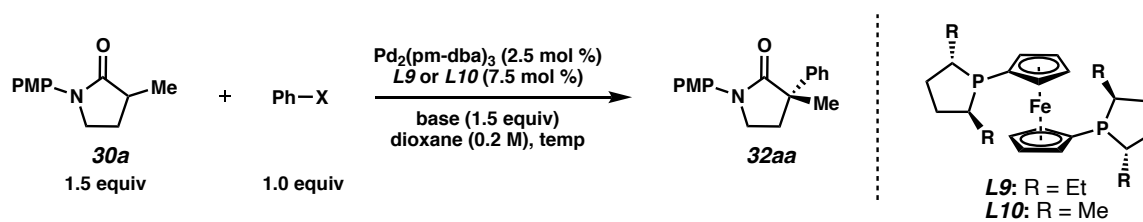
With these slightly modified conditions, we re-tested the remaining ferrocene ligands once again. In contrast to the initial set of conditions (Table 2.3.2, entries 2 and 3), with these new conditions, **L9** and **L10** both led to equally high levels of reactivity and selectivity. The use of the bulkier **L11**, however, still led to both diminished yield and enantioselectivity. We believe there

may be a number of reasons why **L9** and **L10** are optimal ligands for this transformation: these highly electron-rich dialkylphosphine ligands should undergo rapid oxidative addition to the aryl halide, while the large bite angle should encourage facile reductive elimination.¹⁹ Additionally, since alkyl phosphines are less susceptible to P–C cleavage,²⁰ we believe that these ligands might form a Pd/ligand complex that is more stable at high temperatures. Finally, although we found both Pd(dm-dba)₂ and Pd₂(pm-dba)₃ to be equally effective Pd(0) sources at 10 mol% catalyst loading, we did find that Pd₂(pm-dba)₃ led to a more active pre-catalyst, which also allowed us to lower the catalyst loadings and shorten the reaction time (entry 11).²¹

2.4 REACTION OPTIMIZATION WITH ARYL BROMIDES

Although the use of electrophiles such as iodobenzene (entries 1 and 2, Table 2.4.1) and phenyl triflate resulted in no product formation, we were pleased to see that bromobenzene did lead to the α -aryl γ -lactam in moderate yield and selectivity (entry 3). Interestingly, we noted that

Table 2.4.1. Optimization with Aryl Bromides^a

							
entry	Ph–X	base	ligand	temp (°C)	time (h)	yield (%) ^b	ee (%) ^c
1	Ph–I	LiHMDS	L9	100	20	–	–
2	Ph–OTf	LiHMDS	L10	100	20	–	–
3 ^d	Ph–Br	NaHMDS	L9	100	16	64	96
4	Ph–Br	NaHMDS	L10	100	12	86	92
5	Ph–Br	LiHMDS	L10	100	15	31	72
6 ^d	Ph–Br	NaHMDS	L10	80	15	84	92
7 ^e	Ph–Br	NaHMDS	L10	54	15	72	92

[a] Conditions: 0.1 mmol scale. [b] Yield determined by LCMS analysis of the crude reaction mixture using 1,3,5-trimethoxybenzene as a standard. [c] Determined by chiral SFC analysis of the isolated product. [d] Reaction performed at 80 °C. [e] Reaction performed at 54 °C. PMP = *p*-methoxyphenyl. pm-dba = 4,4' – dimethoxydibenzylideneacetone.

L10 was the best ligand when bromobenzene was used, and in contrast to what was observed with chlorobenzene (Table 2.3.4), NaHMDS proved optimal (entries 4 and 5). With this new set of conditions, the reaction proceeds at a lower temperature; the desired product is obtained in 84% yield and 92% ee (entry 6) after 15 h at 80 °C. Moreover, at 54 °C the product is still obtained in good yield and high enantiomeric excess (entry 7).

2.5 REACTION SCOPE

With optimized conditions for aryl chlorides and aryl bromides in hand, the effect of the *N*-protecting group on the reaction was examined (Table 2.5.1). We were pleased to find that a number of different *N*-protecting groups were tolerated in our reaction. Bis-methoxyphenyl lactam **30b** performs just as well as **30a** with Method B, but a slight decrease in yield and

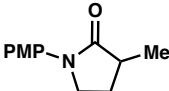
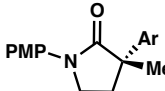
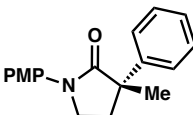
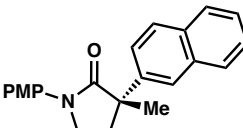
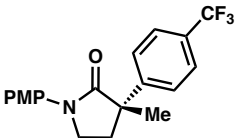
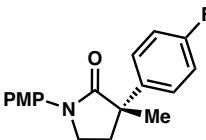
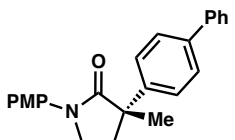
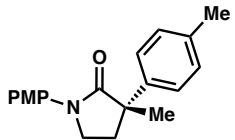
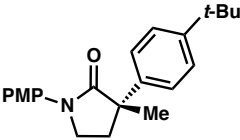
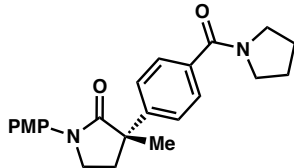
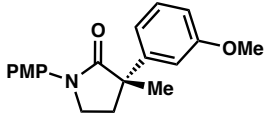
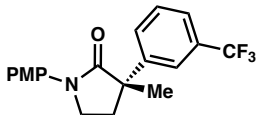
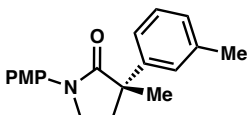
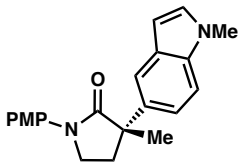
Table 2.5.1. Scope of the *N*-Protecting Group^a

<hr/>		
 32aa	 32ba	 32ca
Method A: 65% yield, 94% ee ^b Method B: 84% yield, 92% ee ^c	Method A: 53% yield, 89% ee Method B: 85% yield, 92% ee	Method A: 33% yield, 79% ee Method B: 47% yield, 90% ee
 32da	 32ea	 32fa
Method A: 58% yield, 90% ee Method B: 91% yield, 93% ee	Method A: 40% yield, 73% ee Method B: 64% yield, 56% ee	Method A: 43% yield, 95% ee Method B: 55% yield, 92% ee

[a] Conditions for each method are as follows: Method A: lactam (1.5 equiv), Ph-Cl (1.0 equiv), Pd₂(pmdba)₃ (2.5 mol%), **L9** (7.5 mol %), LiHMDS (1.5 equiv), dioxane (0.2 M), 100 °C, 20h. Method B: lactam (1.5 equiv), Ph-Br (1.0 equiv), Pd₂(pmdba)₃ (2.5 mol%), **L10** (7.5 mol%), NaHMDS (1.5 equiv), dioxane (0.2 M), 80 °C, 20 h. [b] 6 h. [c] 15 h. pm-dba= 4,4'-dimethoxydibenzylideneacetone.

enantioselectivity is observed when subjected to Method A (**32ba**). Switching to *ortho*-methoxy phenyl substituted **30c** or electron-deficient trifluoromethylphenyl **30e** led to diminished yield and enantioselectivity (**32ca** and **32ea**). Although *N*-phenyl **30d** does not outperform **30a** in Method A, it does exhibit higher reactivity and enantioselectivity when exposed to Method B, furnishing

Table 2.5.2. Scope of the Aryl Halide^a

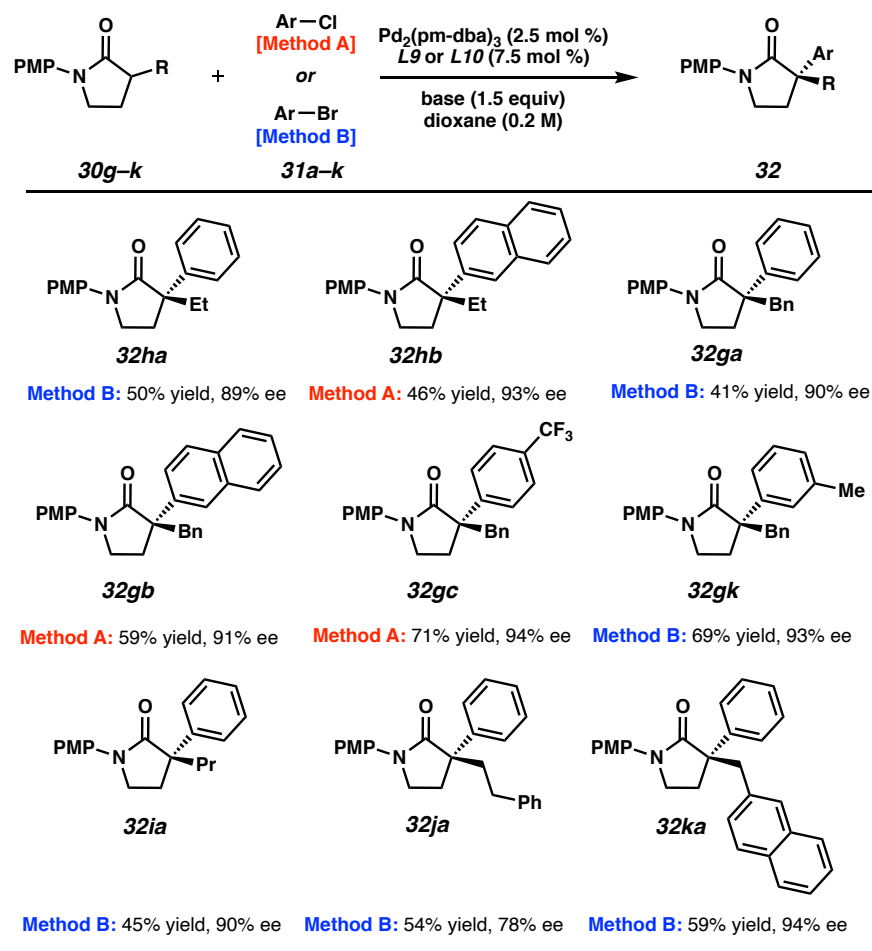
	<p>Ar—Cl [Method A]</p> <p>or</p> <p>Ar—Br [Method B]</p>	<p>$\text{Pd}_2(\text{pm-dba})_3$ (2.5 mol %) L9 or L10 (7.5 mol %)</p> <p>base (1.5 equiv) dioxane (0.2 M)</p>	
30a	31a–l		32
<hr/>			
			
32aa Method A: 65% yield, 94% ee Method B: 83% yield, 92% ee	32ab^b Method A: 83% yield, 95% ee Method B: 75% yield, 93% ee	32ac Method A: 88% yield, 94% ee	
			
32ad Method A: 33% yield, 93% ee	32ae Method A: 78% yield, 97% ee	32af Method A: 49% yield, 91% ee Method B: 57% yield, 95% ee	
			
32ag Method A: 60% yield, 91% ee	32ah Method A: 87% yield, 81% ee	32ai Method A: 69% yield, 86% ee	
			
32aj Method A: 75% yield, 96% ee	32ak Method B: 70% yield, 97% ee	32al Method B: 44% yield, 92% ee	

[a] Conditions for each method are as follows: Method A: **30a** (1.5 equiv), Ar-Cl (1.0 equiv), Pd₂(pmdba)₃ (2.5 mol %), **L9** (7.5 mol %), LiHMDS (1.5 equiv), dioxane (0.2 M), 100 °C, 6 h. Method B: lactam (1.5 equiv), Ar-Br (1.0 equiv), Pd₂(pmdba)₃ (2.5 mol %), **L10** (7.5 mol %), NaHMDS (1.5 equiv), dioxane (0.2 M), 80 °C, 15 h. [b] Absolute configuration determined via single crystal X-ray analysis. PMP = *p*-methoxyphenyl. pm-dba = 4,4' - dimethoxydibenzylideneacetone.

the desired product in 91% yield and 93% ee (**32da**). Benzyl-protected lactam **30f** affords α -quaternary lactam **32fa** in high levels of enantiomeric excess across both methods.

Next, we examined the substrate scope of the enantioselective α -arylation (Table 2.5.2). We found that aryl bromides and aryl chlorides with a variety of substitution patterns are accommodated in the arylation. Aryl halides possessing electron-deficient (see products **32ab**, **32ad**, **32ah**,²² **32ae**) and electron-rich (**32af**, **32ag**) substituents at the *para*-position led to products with excellent enantioselectivities using Method A and B, respectively. Aryl halides possessing

Table 2.5.3. Scope of the Lactam^a



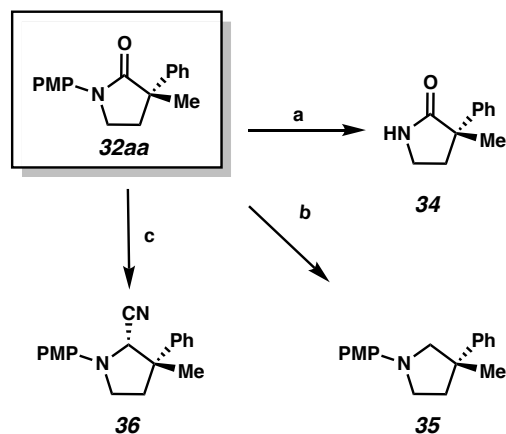
[a] Conditions for each method are as follows: Method A: lactam (1.5 equiv), Ar-Cl (1.0 equiv), Pd₂(pmdba)₃ (2.5 mol %), **L9** (7.5 mol %), LiHMDS (1.5 equiv), dioxane (0.2 M), 100 °C, 20 h. Method B: lactam (1.5 equiv), Ar-Br (1.0 equiv), Pd₂(pmdba)₃ (2.5 mol %), **L10** (7.5 mol %), NaHMDS (1.5 equiv), dioxane (0.2 M), 80 °C, 20 h. PMP = *p*-methoxyphenyl. pm-dba = 4,4'-dimethoxydibenzylideneacetone.

substituents at the *meta*-position are also permissible in both Method A and B, although slightly diminished enantioselectivity is observed when 3-chloroanisole is used as the electrophile (**32ai**). Unfortunately, only trace product is observed when *ortho*-substituted aryl halides are exposed to our reaction conditions.²³ Gratifyingly, an *N*-methyl indole was also tolerated, as we obtained 5-indolyl lactam **32al** in moderate yield and excellent enantioselectivity.

The scope of substitution at the lactam α -carbon was then examined (Table 2.5.3). We found that sterically demanding α -substituents are well tolerated in both methods. Although the yields are slightly diminished, the high levels of enantioselectivity are retained. Examples having ethyl (**32ha**, **32hb**), benzyl (**32ga**, **32gb**), propyl (**32ia**), phenethyl (**32ja**), and 2-naphthylmethyl (**32ka**) substitution all furnish the α -arylated products in good enantioselectivity. α -Benzyl substituted lactam **30g** was also employed in the reaction with a number of different electrophilic coupling partners using both methods. Even with a more hindered substrate, similar patterns of reactivity and selectivity to α -methyl substituted **30a** were observed. When an electron-deficient aryl chloride coupling partner is used in Method A or *m*-bromotoluene is used in Method B with **1g**, the desired product is formed in high enantioselectivity and good yield (**32gc** and **32gd**).

2.6 PRODUCT TRANSFORMATIONS

Recognizing the potential value of these enantioenriched, quaternary center-containing heterocycles to the synthetic and pharmaceutical communities, we sought to utilize this new transformation in the preparation of differentially substituted five-membered heterocycles (Scheme 2.5.1). α -Quaternary lactam **32aa** can be swiftly deprotected with ceric ammonium

Scheme 2.6.1. Derivatization of Arylation Products^a

[a] Conditions: (a) CAN, MeCN/H₂O, 0 °C, 30 min, 73% yield; (b) LAH, Et₂O, 0 °C to 23 °C, 16 h, 93% yield; (c) LiBEt₃H, -78 °C to 23 °C, then AcOH, KCN, 0 °C, 5 h, 43% yield, 93:7 dr.

nitrate (CAN) providing unprotected lactam **34** in 73% yield. Reduction of the lactam carbonyl with lithium aluminum hydride provides the corresponding medicinally valuable pyrrolidine (**35**).²⁴ Partial reduction of the lactam with lithium triethylborohydride and trapping of the resulting iminium ion with potassium cyanide yields chiral aminonitrile **36** in moderate yield but with high diastereoselectivity.

2.7 CONCLUSION

In conclusion, we have developed a protocol for the first transition metal-catalyzed enantioselective α -arylation of γ -lactams. Two related procedures were developed for this transformation, allowing for the use of either aryl chlorides or bromides as electrophiles. We are able to construct α -quaternary stereocenters in good yield and high enantiomeric excess (up to 91% yield and 97% ee). Asymmetry is induced through the use of a chiral, dialkyl bisphosphine ligand that generates a Pd/ligand complex that is stable under strongly basic conditions and elevated temperatures. Critical to the development of these conditions was also the identification

of an appropriate base and electrophile combination. We found that a broad range of substitution is tolerated on either coupling partner. We also demonstrated that these α -quaternary γ -lactams can be efficiently converted to a number of different enantioenriched nitrogen containing heterocyclic building blocks via product derivatizations.

2.8 EXPERIMENTAL SECTION

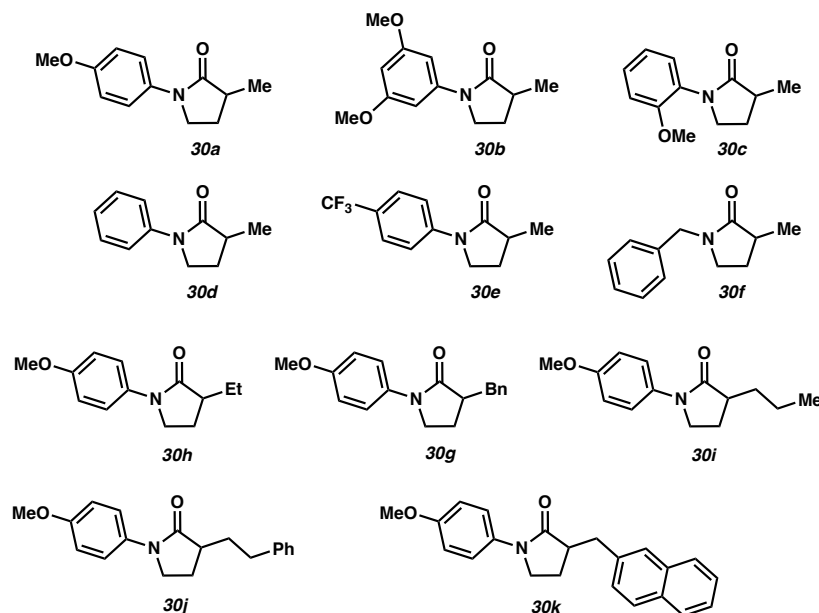
2.8.1 MATERIALS AND METHODS

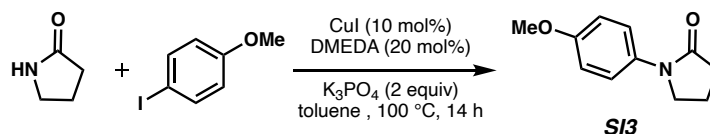
Unless otherwise stated, reactions were performed in flame-dried glassware under an argon or nitrogen atmosphere using dry, deoxygenated solvents. Solvents were dried by passage through an activated alumina column under argon. Reaction progress was monitored by thin-layer chromatography (TLC) or Agilent 1290 UHPLC-MS. TLC was performed using E. Merck silica gel 60 F254 precoated glass plates (0.25 mm) and visualized by UV fluorescence quenching, *p*-anisaldehyde, or KMnO₄ staining. Silicycle SiliaFlash® P60 Academic Silica gel (particle size 40–63 nm) was used for flash chromatography. ¹H NMR spectra were recorded on a Bruker Avance HD 400 MHz or Varian Mercury 300 MHz spectrometers and are reported relative to residual CHCl₃ (δ 7.26 ppm). ¹³C NMR spectra were recorded on a Bruker Avance HD 400 MHz spectrometer (100 MHz) and are reported relative to residual CHCl₃ (δ 77.36 ppm). ¹⁹F NMR spectra were recorded on a Varian Mercury 300 MHz spectrometer (282 MHz). Data for ¹H NMR are reported as follows: chemical shift (δ ppm) (multiplicity, coupling constant (Hz), integration). Multiplicities are reported as follows: s = singlet, d = doublet, t = triplet, q = quartet, p = pentet, sept = septuplet, m = multiplet, br s = broad singlet, br d = broad doublet, app = apparent. Data for ¹³C NMR are reported in terms of chemical shifts (δ ppm). IR spectra were obtained using a

Perkin Elmer Spectrum BXII spectrometer or Nicolet 6700 FTIR spectrometer using thin films deposited on NaCl plates and reported in frequency of absorption (cm^{-1}). Optical rotations were measured with a Jasco P-2000 polarimeter operating on the sodium D-line (589 nm), using a 100 mm path-length cell and are reported as: $[\alpha]_{\text{D}}^{\text{T}}$ (concentration in 10 mg/1 mL, solvent). Analytical SFC was performed with a Mettler SFC supercritical CO_2 analytical chromatography system utilizing Chiralpak (AD-H) or Chiralcel (OD-H) columns (4.6 mm x 25 cm) obtained from Daicel Chemical Industries, Ltd. High resolution mass spectra (HRMS) were obtained from Agilent 6200 Series TOF with an Agilent G1978A Multimode source in electrospray ionization (ESI+), atmospheric pressure chemical ionization (APCI+), or mixed ionization mode (MM: ESI-APCI+). Reagents were purchased from Sigma-Aldrich, Acros Organics, Strem, or Alfa Aesar and used as received unless otherwise stated.

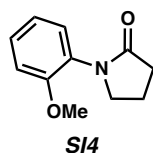
2.8.2 EXPERIMENTAL PROCEDURES

2.8.2.1 *N*-substituted lactams synthesized and tested

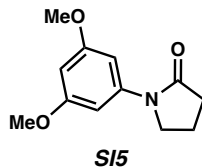


Synthesis of *N*-substituted lactam starting material

1-(4-methoxyphenyl)pyrrolidin-2-one (SI3):²⁵ To a solution of CuI (1.904 g, 10 mmol, 0.1 equiv) in toluene (100 mL, 1.0 M) was added DMEDA (2.15 mL, 20 mmol, 0.2 equiv), 4-iodoanisole (23.4 g, 100 mmol, 1 equiv), 2-pyrrolidinone (9.11 mL, 120 mmol, 1.2 equiv), and anhydrous K₃PO₄ (42.5 g, 200 mmol, 2 equiv). The resultant mixture was heated to 100 °C and allowed to stir for 14 hours. The reaction was cooled, diluted with EtOAc, and filtered through celite. The filtrate was concentrated and recrystallized from 20% EtOAc in hexanes to afford **SI3** as a colorless solid (16.0 g, 83.7 mmol, 84% yield); ¹H NMR (300 MHz, CDCl₃) δ 7.55 – 7.43 (m, 2H), 6.96 – 6.84 (m, 2H), 3.92 – 3.73 (m, 5H), 2.59 (dd, J = 8.5, 7.7 Hz, 2H), 2.25 – 2.07 (m, 2H). All characterization data match those reported.²⁵



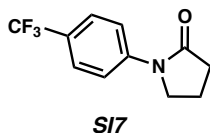
1-(2-methoxyphenyl)pyrrolidin-2-one (SI4):²⁵ Compound **SI4** was prepared from 2-pyrrolidinone using a previously reported procedure; ¹H NMR (300 MHz, CDCl₃) δ 7.26 (m, 2H), 7.04 – 6.90 (m, 2H), 3.84 (s, 3H), 3.76 (t, J = 7.1 Hz, 2H), 2.56 (dd, J = 8.5, 7.7 Hz, 2H), 2.19 (tt, J = 7.7, 6.9 Hz, 2H). All characterization data match those reported.²⁵



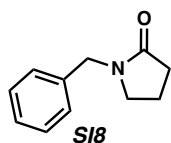
1-(3,5-dimethoxyphenyl)pyrrolidin-2-one (SI5):²⁵ Compound **SI5** was prepared from 2-pyrrolidinone using a previously reported procedure; ¹H NMR (500 MHz, CDCl₃) δ 6.86 (d, J = 2.2 Hz, 2H), 6.27 (t, J = 2.2 Hz, 1H), 3.83 (t, J = 7.0 Hz, 2H), 3.80 (s, 6H), 2.61 (dd, J = 8.5, 7.7 Hz, 2H), 2.15 (tt, J = 7.8, 7.0 Hz, 2H). All characterization data match those reported.²⁵



1-phenylpyrrolidin-2-one (SI6):²⁶ Compound **SI6** was prepared from 2-pyrrolidinone using a previously reported procedure. All characterization data match those reported.²⁶



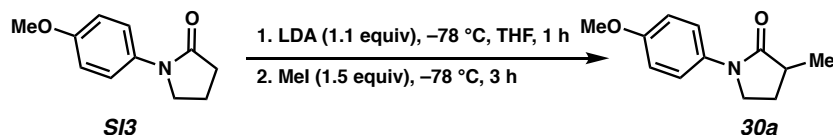
1-(4-(trifluoromethyl)phenyl)pyrrolidin-2-one (SI7): 2-pyrrolidinone (23.5 mmol, 2.0 g), Cs₂CO₃ (1.07 g, 32.9 mmol, 1.4 equiv), Xantphos (460 mg, 0.80 mmol, 3.3 mol%), Pd(OAc)₂ (106 mg, 0.47 mmol, 2.0 mol%), and 4-bromobenzotrifluoride (4.22 mL, 30.6 mmol, 1.3 equiv) in dioxane (70 mL) under inert atmosphere were heated to 100 °C for 24 h. The reaction was then cooled to ambient temperature, filtered through a plug of silica, and concentrated. The filtrate was recrystallized from 20% EtOAc in hexanes to afford **SI7** as a colorless solid (4.52 g, 19.7 mmol, 84% yield); ¹H NMR (500 MHz, CDCl₃) δ 7.79 – 7.74 (m, 2H), 7.64 – 7.59 (m, 2H), 3.90 (t, J = 7.0 Hz, 2H), 2.65 (dd, J = 8.5, 7.8 Hz, 2H), 2.28 – 2.14 (m, 2H). All characterization data match those reported.²⁷



1-benzylpyrrolidin-2-one (SI8): To a flame-dried round-bottom flask under argon was added 2-pyrrolidinone (3.38 g, 39.7 mmol, 1.0 equiv), DMAP (243 mg, 1.39 mmol, 0.05 equiv), dichloromethane (60 mL), and triethylamine (8.30 mL, 60 mmol, 1.5 equiv). The resulting solution was cooled to 0 °C and benzyl chloride (5.54 mL, 47.7 mmol, 1.2 equiv) was added dropwise. The reaction was allowed to warm to ambient temperature and stirred for one hour. The crude reaction mixture was quenched with saturated NH_4Cl solution, extracted three times, then the combined organic layers were washed with saturated NaHCO_3 solution. The organic layer was dried over Na_2SO_4 and concentrated. The filtrate was recrystallized from 25% EtOAc in hexanes to afford **SI8** as a colorless solid (3.64 g, 20.8 mmol, 48% yield); ^1H NMR (300 MHz, CDCl_3) δ 7.26 (m, 5H), 4.45 (s, 2H), 3.26 (dd, $J = 7.5, 6.7$ Hz, 2H), 2.45 (dd, $J = 8.6, 7.6$ Hz, 2H), 2.07 – 1.90 (m, 2H). All characterization data match those reported.²⁸

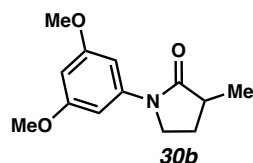
2.8.2.2 Synthesis of α -Substituted γ -Lactams

General Procedure 1: α -alkylation of *N*-substituted lactams with alkyl halides:

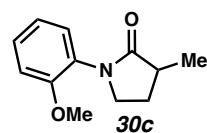


1-(4-methoxyphenyl)-3-methylpyrrolidin-2-one (30a): To a solution of *i*- Pr_2NH (3.45 mL, 24.7 mmol, 1.1 equiv) in THF (22.5 mL) at 0 °C was added a solution *n*-BuLi (2.57 M in hexanes, 9.63 mL, 24.7 mmol, 1.1 equiv) dropwise. The resulting mixture was stirred at 0 °C for 20 min, then cooled to -78 °C. A solution of 1-(4-methoxyphenyl)pyrrolidin-2-one (4.30 g, 22.5 mmol, 1.0 equiv) in THF (60 mL) was added dropwise *via* cannula. The reaction was allowed to stir for 1 h at -78 °C, then a solution of MeI (2.10 mL, 33.75 mmol, 1.5 equiv) in MTBE (17 mL) was added dropwise *via* cannula. The resulting mixture was stirred for 3 h at -78 °C. The reaction was

quenched with a saturated aqueous NH_4Cl solution and allowed to warm to ambient temperature. The aqueous layer was extracted four times with EtOAc, and the resulting organic layers were dried over Na_2SO_4 and concentrated. The resulting crude oil was purified by column chromatography (40% EtOAc in hexanes) to afford **30a** as a colorless solid (4.0 g, 19.5 mmol, 89% yield); ^1H NMR (500 MHz, CDCl_3) δ 7.53 (d, $J = 9.1$ Hz, 2H), 6.90 (d, $J = 9.1$ Hz, 1H), 3.80 (s, 3H), 3.78 – 3.68 (m, 1H), 2.74 – 2.57 (m, 1H), 2.36 (dddd, $J = 12.3, 8.5, 6.7, 3.6$ Hz, 1H), 1.76 (ddt, $J = 12.5, 9.4, 8.6$ Hz, 1H), 1.30 (d, $J = 7.1$ Hz, 3H). All characterization data match those reported.²⁵

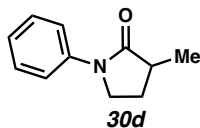


1-(3,5-dimethoxyphenyl)-3-methylpyrrolidin-2-one (30b): Compound **30b** was prepared from **SI5** using a previously reported procedure;¹ ^1H NMR (500 MHz, CDCl_3) δ 6.91 (d, $J = 2.2$ Hz, 2H), 6.26 (t, $J = 2.2$ Hz, 1H), 3.80 (s, 6H), 3.74 (dd, $J = 8.8, 5.0$ Hz, 2H), 2.67 (ddq, $J = 9.7, 8.2, 7.0$ Hz, 1H), 2.35 (ddt, $J = 12.3, 8.4, 5.0$ Hz, 1H), 1.75 (ddt, $J = 12.4, 9.6, 8.8$ Hz, 1H), 1.30 (d, $J = 7.1$ Hz, 3H). All characterization data match those reported.²⁵

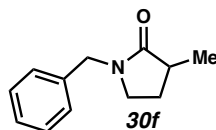


1-(2-methoxyphenyl)-3-methylpyrrolidin-2-one (30c): Compound **30c** was prepared from **SI4** using a previously reported procedure;¹ ^1H NMR (500 MHz, CDCl_3) δ 7.26 (m, 2H), 7.08 – 6.89 (m, 2H), 3.83 (s, 3H), 3.76 – 3.60 (m, 2H), 2.64 (tq, $J = 8.7, 7.1$ Hz, 1H), 2.37 (dddd, $J = 12.2, 8.5,$

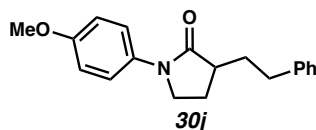
7.3, 3.5 Hz, 1H), 1.81 (dq, $J = 12.4, 8.5$ Hz, 1H), 1.31 (d, $J = 7.2$ Hz, 3H). All characterization data match those reported.²⁵



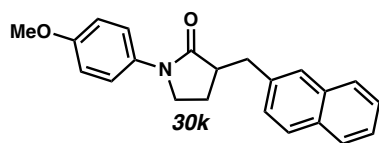
3-methyl-1-phenylpyrrolidin-2-one (30d): Compound **30d** was prepared from **SI6** and iodomethane using General Procedure 1. The filtrate was recrystallized from 25% EtOAc in hexanes to afford **30d** as a colorless solid (3.2 g, 18.3 mmol, 74% yield); ^1H NMR (500 MHz, CDCl_3) δ 7.67 – 7.61 (m, 2H), 7.41 – 7.33 (m, 2H), 7.14 (tt, $J = 7.4, 1.1$ Hz, 1H), 3.85 – 3.72 (m, 2H), 2.68 (ddq, $J = 9.5, 8.5, 7.1$ Hz, 1H), 2.38 (dddd, $J = 12.2, 8.5, 6.6, 3.5$ Hz, 1H), 1.78 (ddt, $J = 12.4, 9.5, 8.6$ Hz, 1H), 1.32 (d, $J = 7.1$ Hz, 3H). All characterization data match those reported.²⁹



1-benzyl-3-methylpyrrolidin-2-one (30f): Compound **30f** was prepared from **SI8** and iodomethane using General Procedure 1. The resulting crude oil was purified by column chromatography (5% MeOH in CH_2Cl_2) to afford **1f** as a yellow oil (4.1 g, 21.7 mmol, 70% yield); ^1H NMR (300 MHz, CDCl_3) δ 7.26 (s, 5H), 4.45 (d, $J = 3.7$ Hz, 2H), 3.23 – 3.09 (m, 2H), 2.52 (ddt, $J = 15.8, 8.7, 7.1$ Hz, 1H), 2.21 (dddd, $J = 12.6, 8.7, 6.0, 4.8$ Hz, 1H), 1.68 – 1.50 (m, 1H), 1.24 (d, $J = 7.1$ Hz, 3H). All characterization data match those reported.³⁰



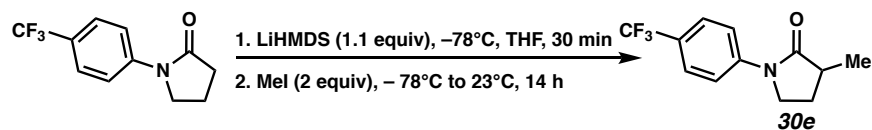
1-(4-methoxyphenyl)-3-phenethylpyrrolidin-2-one (30j): Compound **30j** was prepared from **SI3** and (2-iodoethyl)benzene using General Procedure 1. The resulting crude oil was purified by column chromatography (40% EtOAc in hexanes) to afford **1j** as a colorless solid (487 mg, 1.65 mmol, 33% yield); ^1H NMR (300 MHz, CDCl_3) δ 7.58 – 7.47 (m, 2H), 7.36 – 7.14 (m, 5H), 6.96 – 6.83 (m, 2H), 3.80 (s, 3H), 3.78 – 3.69 (m, 2H), 2.93 – 2.66 (m, 2H), 2.59 (qd, J = 9.1, 4.7 Hz, 1H), 2.40 – 2.24 (m, 2H), 1.91 – 1.68 (m, 2H); ^{13}C NMR (100 MHz, CDCl_3) δ 175.8, 156.8, 141.9, 133.2, 128.8, 126.3, 121.9, 114.3, 55.8, 47.5, 42.8, 33.7, 33.3, 25.4; IR (Neat Film, NaCl) 2930, 2855, 1677, 1518, 1456, 1393, 1318, 1255, 1224, 1181, 1121, 1034, 825, 752, 717, 699 cm^{-1} ; HRMS (MM) m/z calc'd for $\text{C}_{19}\text{H}_{22}\text{NO}_2^+ [\text{M}+\text{H}]^+$: 296.1645, found 296.1646.



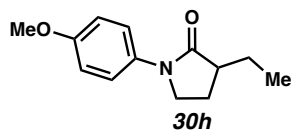
1-(4-methoxyphenyl)-3-(naphthalen-2-ylmethyl)pyrrolidin-2-one (30k): Product **30k** was prepared from **SI3** 2-(bromomethyl)naphthalene using General Procedure 1 and purified by column chromatography (33% EtOAc in hexanes) to provide **30k** as a colorless solid (430 mg, 1.30 mmol, 52% yield); ^1H NMR (500 MHz, CDCl_3) δ 7.80 – 7.83 (m, 1H), 7.77 – 7.80 (m, 2H), 7.68 – 7.69 (m, 1H), 7.48 – 7.51 (m, 2H), 7.42 – 7.47 (m, 2H), 7.39 (dd, J = 8.4, 1.7 Hz, 1H), 6.89 – 6.92 (m, 2H), 3.81 (s, 3H), 3.68 (dt, J = 9.5, 7.8 Hz, 1H), 3.56 (ddd, J = 9.6, 8.7, 3.4 Hz, 1H), 3.47 (dd, J = 13.0, 3.4 Hz, 1H), 2.95 – 3.05 (m, 2H), 2.17 (dddd, J = 12.7, 8.4, 7.5, 3.3 Hz, 1H), 1.91 (dq, J = 12.7, 8.5 Hz, 1H); ^{13}C NMR (125 MHz, CDCl_3) δ 174.9, 156.7, 137.0, 133.7, 132.8, 132.4, 128.3, 127.8, 127.7, 127.6, 127.5, 126.2, 125.6, 121.9, 114.2, 55.6, 47.3, 45.0, 37.4, 24.3; IR (Neat Film, NaCl) 3048, 3014, 2953, 2836, 1677, 1516, 1399, 1328, 1285, 1256, 1180, 1032,

900, 824, 739 cm^{-1} ; HRMS (MM) m/z calc'd for $\text{C}_{22}\text{H}_{22}\text{NO}_2^+$ $[\text{M}+\text{H}]^+$: 332.1645, found 332.1648.

General Procedure 2: α -alkylation of N-substituted lactams with alkyl iodides:

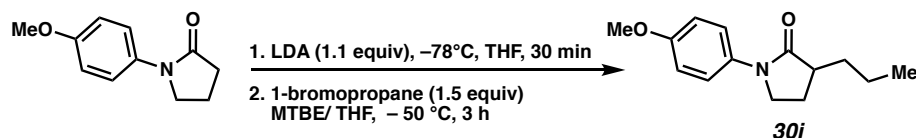


3-methyl-1-(4-(trifluoromethyl)phenyl)pyrrolidin-2-one (30e): To a solution of LiHMDS (1.61 g, 9.60 mmol, 1.1 equiv) in THF (44 mL) at -78°C was added a solution of 1-(4-(trifluoromethyl)phenyl)pyrrolidin-2-one (2.0 g, 8.93 mmol, 1.0 equiv) in THF (4 mL) dropwise. The solution was stirred -78°C for 30 minutes, then iodomethane (1.11 mL, 17.86 mmol, 2 equiv) was added dropwise. The reaction was stirred at -48°C for 30 minutes, then allowed to warm to ambient temperature overnight. The reaction mixture was quenched with a saturated NH_4Cl solution, and extracted with EtOAc three times. The combined organic extracts were washed with saturated NaHCO_3 solution, dried over Na_2SO_4 , and concentrated. The resulting crude oil was purified by column chromatography (10% EtOAc in hexanes) to afford **30e** as a colorless solid (1.30 g, 5.34 mmol, 61% yield); ^1H NMR (500 MHz, CDCl_3) δ 7.82 – 7.77 (m, 2H), 7.64 – 7.59 (m, 2H), 3.85 – 3.77 (m, 2H), 2.71 (ddq, $J = 9.8, 8.5, 7.1$ Hz, 1H), 2.42 (dddd, $J = 12.7, 8.5, 5.7, 4.3$ Hz, 1H), 1.81 (ddt, $J = 12.5, 9.8, 8.7$ Hz, 1H), 1.33 (d, $J = 7.1$ Hz, 3H); ^{13}C NMR (125 MHz, CDCl_3) δ 177.10, 142.53, 125.96 (q, $J = 3.7$ Hz), 118.93, 46.31, 38.38, 26.86, 16.06; ^{19}F NMR (282 MHz, CDCl_3) δ -62.1; (Neat Film, NaCl) 2977, 1697, 1393, 1329, 1221, 1195, 1164, 1113, 1070, 908, 859, 842, 821, 731, 715 cm^{-1} ; HRMS (MM) m/z calc'd for $\text{C}_{12}\text{H}_{13}\text{F}_3\text{NO}^+$ $[\text{M}+\text{H}]^+$: 244.0944, found 244.0947.



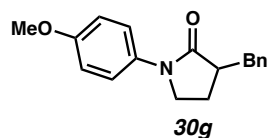
3-ethyl-1-(4-methoxyphenyl)pyrrolidin-2-one (30h): Compound **30h** was prepared from iodoethane using General Procedure 2. The resulting crude oil was purified by column chromatography (20% EtOAc in hexanes) to afford **30h** as a colorless solid (1.18 g, 5.38 mmol, 54% yield); ^1H NMR (500 MHz, CDCl_3) δ 7.55 – 7.49 (m, 2H), 6.93 – 6.80 (m, 2H), 3.80 (s, 3H), 3.78 – 3.71 (m, 2H), 2.54 (qd, J = 8.9, 4.3 Hz, 1H), 2.32 (dddd, J = 12.5, 8.7, 7.1, 3.7 Hz, 1H), 1.98 (dq, J = 13.6, 7.5, 4.3 Hz, 1H), 1.81 (dq, J = 12.5, 8.6 Hz, 1H), 1.58 – 1.47 (m, 1H), 1.02 (t, J = 7.4 Hz, 3H); ^{13}C NMR (125 MHz, CDCl_3) δ 176.0, 156.7, 133.2, 121.8, 114.3, 55.8, 44.9, 24.6, 24.5, 11.8; (Neat Film, NaCl) 3054, 2957, 2935, 2875, 2837, 1682, 1613, 1514, 1486, 1464, 1430, 1398, 1326, 1288, 1252, 1225, 1181, 1121, 1100, 1032, 829, 736, 704, 612 cm^{-1} ; HRMS (MM) m/z calc'd for $\text{C}_{13}\text{H}_{18}\text{NO}_2^+$ $[\text{M}+\text{H}]^+$: 220.1332, found 220.1322.

General Procedure 3: α -alkylation of PMP-pyrrolidinone with alkyl bromides:



1-(4-methoxyphenyl)-3-propylpyrrolidin-2-one (30i): To a solution of $i\text{-Pr}_2\text{NH}$ (0.77 mL, 5.5 mmol, 1.1 equiv) in THF (5.0 mL) at 0 $^\circ\text{C}$ was added a solution $n\text{-BuLi}$ (2.57 M in hexanes, 2.2 mL, 5.5 mmol, 1.1 equiv) dropwise. The resulting mixture was stirred at 0 $^\circ\text{C}$ for 20 min, then cooled to -78 $^\circ\text{C}$. A solution of 1-(4-methoxyphenyl)pyrrolidin-2-one **SI3** (956 mg, 5.0 mmol, 1.0 equiv) in THF (12.5 mL) was added dropwise *via* cannula. The reaction was allowed to stir for 1 h at -78 $^\circ\text{C}$, then a solution of 1-bromopropane (0.68 mL, 7.5 mmol, 1.5 equiv) in MTBE (4 mL) was added dropwise *via* cannula. The resulting mixture was stirred for 3 h at -50 $^\circ\text{C}$. The reaction

was then quenched with saturated NH_4Cl solution and allowed to warm to ambient temperature. The aqueous layer was extracted four times with EtOAc, and the resulting organic layers were dried over Na_2SO_4 and concentrated. The resulting crude oil was purified by column chromatography (40% EtOAc in hexanes) to afford **30i** as a colorless solid (210 mg, 0.90 mmol, 20% yield); ^1H NMR (300 MHz, CDCl_3) δ 7.56 – 7.46 (m, 2H), 6.94 – 6.86 (m, 2H), 3.80 (s, 3H), 3.78 – 3.70 (m, 2H), 2.59 (qd, J = 8.8, 4.1 Hz, 1H), 2.31 (dddd, J = 12.7, 8.7, 6.6, 4.1 Hz, 1H), 1.94 (qd, J = 5.9, 4.9, 3.4 Hz, 1H), 1.79 (dq, J = 12.5, 8.6 Hz, 1H), 1.52 – 1.34 (m, 3H), 0.97 (t, J = 7.1 Hz, 3H); ^{13}C NMR (100 MHz, CDCl_3) δ 176.2, 156.7, 133.3, 121.8, 114.3, 55.8, 47.5, 43.4, 33.8, 25.2, 20.8, 14.4; IR (Neat Film, NaCl) 2955, 2927, 2859, 2837, 1681, 1613, 1517, 1480, 1464, 1398, 1324, 1291, 1252, 1223, 1181, 1123, 1099, 1032, 909, 828, 732, 646, 614 cm^{-1} ; HRMS (MM) m/z calc'd for $\text{C}_{14}\text{H}_{20}\text{NO}_2^+$ $[\text{M}+\text{H}]^+$: 234.1489, found 234.1494.



3-benzyl-1-(4-methoxyphenyl)pyrrolidin-2-one (30g): Compound **30g** was prepared from benzyl bromide using General Procedure 3. The resulting crude oil was purified by column chromatography (20% EtOAc in hexanes) to afford **30g** as a colorless solid (2.25 g, 8.00 mmol, 80% yield); ^1H NMR (500 MHz, CDCl_3) δ 7.55 – 7.44 (m, 2H), 7.33 – 7.28 (m, 2H), 7.26 – 7.21 (m, 3H), 6.95 – 6.86 (m, 2H), 3.81 (s, 3H), 3.68 (dt, J = 9.5, 7.7 Hz, 1H), 3.55 (ddd, J = 9.5, 8.6, 3.5 Hz, 1H), 3.31 (dd, J = 13.6, 4.0 Hz, 1H), 2.96 – 2.88 (m, 1H), 2.80 (dd, J = 13.7, 9.4 Hz, 1H), 2.17 (dddd, J = 12.3, 8.6, 7.5, 3.5 Hz, 1H), 1.86 (dq, J = 12.7, 8.5 Hz, 1H). ^{13}C NMR (125 MHz, CDCl_3) δ 175.1, 156.9, 139.7, 133.1, 129.4, 128.8, 126.7, 122.0, 114.3, 55.8, 47.5, 45.3, 37.4, 24.5; IR (Neat Film, NaCl) 2950, 2924, 2857, 2835, 1674, 1615,

1514, 1494, 1455, 1443, 1396, 1324, 1284, 1256, 1226, 1180, 1125, 1088, 1032, 824, 748, 733, 701, 618 cm^{-1} ; HRMS (MM) m/z calc'd for $\text{C}_{18}\text{H}_{20}\text{NO}_2^+$ $[\text{M}+\text{H}]^+$: 282.1489, found 282.1500.

2.8.2.3 General Procedures for Pd-Catalyzed α -arylation of γ -lactams

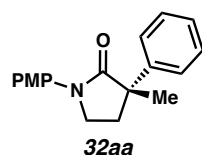
Method A: In a nitrogen-filled glovebox, to an oven-dried 4 mL vial equipped with a stir bar was added 1,1'-Bis[(2*S*,5*S*)-2,5-diethylphospholano]ferrocene **L9** (7.06 mg, 15 μmol , 0.075 equiv), $\text{Pd}_2(\text{pmdba})_3$ (5.5 mg, 5 μmol , 0.025 equiv), and dioxane (0.4 mL). The vial was capped with a PTFE-lined septum cap and stirred at 40 $^\circ\text{C}$. After 20 minutes, the mixture was cooled to ambient temperature and the corresponding aryl chloride **31** (1.0 equiv) was added. A solution of protected-lactam **30** (1.5 equiv) and LiHMDS (50.2 mg, 0.3 mmol, 1.5 equiv) was then added to the resulting mixture, and the reaction was sealed with electrical tape and stirred at 100 $^\circ\text{C}$ for 6 h, unless otherwise noted. The solution was cooled to ambient temperature, quenched with saturated NH_4Cl solution, and extracted with EtOAc five times. The combined organic layers were dried over Na_2SO_4 and concentrated. The crude reaction mixture was purified by silica gel flash chromatography to furnish the product.

Method B: In a nitrogen-filled glovebox, to an oven-dried 4 mL vial equipped with a stir bar was added 1,1'-Bis[(2*S*,5*S*)-2,5-dimethylphospholano]ferrocene **L10** (7.06 mg, 15 μmol , 0.075 equiv), $\text{Pd}_2(\text{pmdba})_3$ (5.5 mg, 5 μmol , 0.025 equiv), and dioxane (0.4 mL). The vial was capped with a PTFE-lined septum cap and stirred at 40 $^\circ\text{C}$. After 20 minutes, the mixture was cooled to ambient temperature and the corresponding aryl bromide **2** (1.0 equiv) was added. A solution of protected-lactam **30** (1.5 equiv) and NaHMDS (55.0 mg, 0.3 mmol, 1.5 equiv) was added to the resulting mixture, and the reaction was sealed with electrical tape and stirred at 80 $^\circ\text{C}$ for 15 h, unless otherwise noted. The solution was cooled to ambient temperature, quenched with saturated NH_4Cl

solution, and extracted with EtOAc five times. The combined organic layers were dried over Na_2SO_4 and concentrated. The crude reaction mixture was purified by silica gel flash chromatography to furnish the product.

2.8.2.4 Spectroscopic Data for Products from Catalytic Reactions

The absolute configuration of **32ab** was determined *via* x-ray crystallographic analysis. The absolute configuration for all other products has been inferred by analogy. See Appendix 4.

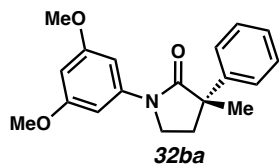


(S)-1-(4-methoxyphenyl)-3-methyl-3-phenylpyrrolidin-2-one (32aa): Product **32aa** was prepared using Method A and purified by column chromatography (25% EtOAc in hexanes) to provide a colorless oil (34.9 mg, 0.124 mmol, 65% yield); 94% *ee*; $[\alpha]_{\text{D}}^{25} -284.5$ (*c* 0.98, CHCl_3); ^1H NMR (400 MHz, CDCl_3) δ 7.56 – 7.42 (m, 2H), 7.40 – 7.30 (m, 2H), 7.32 – 7.12 (m, 3H), 6.91 – 6.79 (m, 2H), 3.73 (s, 3H), 3.64 (qdd, $J = 9.6, 8.0, 5.3$ Hz, 2H), 2.50 (ddd, $J = 12.7, 6.7, 3.9$ Hz, 1H), 2.20 (dt, $J = 12.7, 8.0$ Hz, 1H), 1.56 (s, 3H); ^{13}C NMR (100 MHz, CDCl_3) δ 176.6, 156.9, 143.6, 133.3, 128.9, 127.2, 126.4, 121.8, 114.3, 55.8, 50.3, 45.9, 35.2, 25.8; IR (Neat Film, NaCl) 3057, 2932, 2963, 2874, 1690, 1511, 1429, 1463, 1396, 1321, 1299, 1248, 1181, 1088, 1070, 1032, 881, 829, 768, 699, 634 cm^{-1} ; HRMS (MM) m/z calc'd for $\text{C}_{18}\text{H}_{20}\text{NO}_2^+$ $[\text{M}+\text{H}]^+$: 282.1489, found 282.1490; SFC Conditions: 20% IPA, 2.5 mL/min, Chiralcel OD-H column, $\lambda = 254$ nm, t_{R} (min): minor = 5.69, major = 6.73.

Method B: Product **32aa** was prepared using Method B. The crude product was purified by column chromatography to provide a yellow solid (46.9 mg, 0.167 mmol, 83% yield); 92% *ee*;

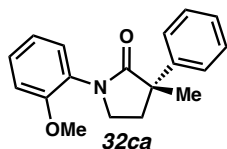
$[\alpha]_{\text{D}}^{25} -284.0$ (c 0.70, CHCl_3); SFC Conditions: 20% IPA, 2.5 mL/min, Chiralcel OD-H column,

$\lambda = 254$ nm, t_{R} (min): minor = 5.70, major = 6.70.



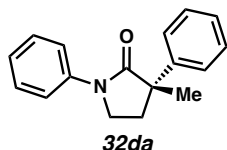
(S)-1-(3,5-dimethoxyphenyl)-3-methyl-3-phenylpyrrolidin-2-one (32ba): Product **32ba** was prepared using general Method A, allowing the reaction to stir for 20 h. The crude product was purified by column chromatography (33% EtOAc in hexanes) to provide a colorless oil (33.1 mg, 0.106 mmol, 53% yield); 89% *ee*; $[\alpha]_{\text{D}}^{25} -123.4$ (c 1.00, CHCl_3); ^1H NMR (500 MHz, CDCl_3) δ 7.41 – 7.43 (m, 2H), 7.32 – 7.36 (m, 2H), 7.25 (ddt, $J = 8.0, 6.6, 1.2$ Hz, 1H), 6.98 (d, $J = 2.2$ Hz, 2H), 6.29 (t, $J = 2.2$ Hz, 1H), 3.80 (s, 6H), 3.75 (ddd, $J = 9.6, 8.1, 3.7$ Hz, 1H), 3.70 (ddd, $J = 9.6, 8.1, 6.9$ Hz, 1H), 2.58 (ddd, $J = 12.7, 6.9, 3.7$ Hz, 1H), 2.26 (dt, $J = 12.7, 8.1$ Hz, 1H), 1.64 (s, 3H); ^{13}C NMR (125 MHz, CDCl_3) δ 177.3, 161.2, 143.2, 141.8, 129.0, 127.2, 126.4, 98.3, 97.0, 55.7, 50.9, 45.7, 34.8, 25.7; IR (Neat Film, NaCl) 3057, 2962, 2934, 2841, 1699, 1598, 1479, 1459, 1447, 1391, 1275, 1249, 1208, 1155, 1067, 835, 701 cm^{-1} ; HRMS (MM) m/z calc'd for $\text{C}_{19}\text{H}_{22}\text{NO}_3^+$ $[\text{M}+\text{H}]^+$: 312.1594, found 312.1594; SFC Conditions: 20% IPA, 2.5 mL/min, Chiralcel OD-H column, $\lambda = 254$ nm, t_{R} (min): minor = 5.29, major = 6.47.

Method B: Product **32ba** was prepared using Method B, allowing the reaction to stir for 20 h. The crude reaction was purified by column chromatography to provide a yellow solid (52.9 mg, 0.170 mmol, 85% yield); 92% *ee*; $[\alpha]_{\text{D}}^{25} -141.0$ (c 1.00, CHCl_3); SFC Conditions: 20% IPA, 2.5 mL/min, Chiralcel OD-H column, $\lambda = 254$ nm, t_{R} (min): minor = 5.31, major = 6.44.



(S)-1-(2-methoxyphenyl)-3-methyl-3-phenylpyrrolidin-2-one (32ca): Product **32ca** was prepared using general Method A, allowing the reaction to stir for 20 h. The crude product was purified by column chromatography (33% EtOAc in hexanes) to provide a colorless oil (18.3 mg, 65 μ mol, 33% yield); 79% *ee*; $[\alpha]_{\text{D}}^{25} - 44.7$ (*c* 1.00, CHCl_3); ^1H NMR (500 MHz, CDCl_3) δ 7.53 – 7.55 (m, 2H), 7.34 – 7.38 (m, 2H), 7.24 – 7.30 (m, 3H), 6.95 – 7.01 (m, 2H), 3.83 (s, 3H), 3.63 – 3.71 (m, 2H), 2.56 (ddd, *J* = 12.6, 6.9, 4.5 Hz, 1H), 2.34 (dt, *J* = 12.5, 7.7 Hz, 1H), 1.66 (s, 3H); ^{13}C NMR (125 MHz, CDCl_3) δ 177.8, 155.3, 144.2, 129.1, 129.0, 128.7, 127.9, 126.9, 126.7, 121.2, 112.4, 55.9, 49.1, 46.9, 36.7, 25.6; IR (Neat Film, NaCl) 3060, 2964, 2927, 1698, 1597, 1504, 1461, 1406, 1304, 1280, 1252, 1122, 1025, 752, 700 cm^{-1} ; HRMS (MM) *m/z* calc'd for $\text{C}_{18}\text{H}_{20}\text{NO}_2^+$ $[\text{M}+\text{H}]^+$: 282.1489, found 282.1492; SFC Conditions: 20% IPA, 2.5 mL/min, Chiralcel OD-H column, λ = 210 nm, t_{R} (min): minor = 4.85, major = 6.04.

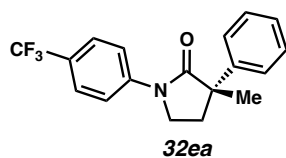
Method B: Product **32ba** was prepared using Method B, allowing the reaction to stir for 20 h. The crude reaction was purified by column chromatography to provide a yellow solid (26.7 mg, 0.1 mmol, 47% yield); 90% *ee*; $[\alpha]_{\text{D}}^{25} - 64.5$ (*c* 0.84, CHCl_3); SFC Conditions: 20% IPA, 2.5 mL/min, Chiralcel OD-H column, λ = 210 nm, t_{R} (min): minor = 4.80, major = 5.83.



(S)-3-methyl-1,3-diphenylpyrrolidin-2-one (32da): Product **32da** was prepared using general Method A, allowing the reaction to stir for 20 h. The crude product was purified by column

chromatography (33% EtOAc in hexanes) to provide a yellow oil (29.3 mg, 0.117 mmol, 58% yield); 90% *ee*; $[\alpha]_{\text{D}}^{25} -87.2$ (*c* 1.00, CHCl_3); ^1H NMR (500 MHz, CDCl_3) δ 7.69 – 7.72 (m, 2H), 7.44 – 7.46 (m, 2H), 7.37 – 7.41 (m, 2H), 7.33 – 7.37 (m, 2H), 7.24 – 7.28 (m, 1H), 7.15 – 7.18 (m, 1H), 3.79 (ddd, *J* = 9.6, 8.0, 3.7 Hz, 1H), 3.74 (ddd, *J* = 9.6, 8.1, 6.9 Hz, 1H), 2.60 (ddd, *J* = 12.6, 6.8, 3.7 Hz, 1H), 2.29 (dt, *J* = 12.7, 8.0 Hz, 1H), 1.65 (s, 3H); ^{13}C NMR (125 MHz, CDCl_3) δ 177.0, 143.4, 139.9, 129.1, 128.9, 127.2, 126.4, 124.8, 120.1, 50.5, 45.5, 35.0, 25.7; IR (Neat Film, NaCl) 3061, 3030, 2967, 2928, 2875, 1710, 1694, 1597, 1494, 1458, 1445, 1393, 1304, 1225, 1091, 1072, 1031, 901, 878, 759, 699 cm^{-1} ; HRMS (MM) *m/z* calc'd for $\text{C}_{17}\text{H}_{18}\text{NO}^+$ $[\text{M}+\text{H}]^+$: 252.1383, found 252.1385; SFC Conditions: 10% IPA, 2.5 mL/min, Chiralcel OD-H column, λ = 254 nm, t_{R} (min): minor = 9.96, major = 10.52.

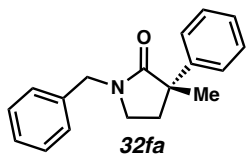
Method B: Product **32da** was prepared using Method B, allowing the reaction to stir for 20 h. The crude reaction mixture was purified by column chromatography to provide a yellow oil (45.8 mg, 0.182 mmol, 91% yield); 93% *ee*; $[\alpha]_{\text{D}}^{25} -82.6$ (*c* 1.00, CHCl_3); SFC Conditions: 10% IPA, 2.5 mL/min, Chiralcel OD-H column, λ = 254 nm, t_{R} (min): minor = 10.51, major = 11.01.



(S)-3-methyl-3-phenyl-1-(4-(trifluoromethyl)phenyl)pyrrolidin-2-one (32ea): Product **32ea** was prepared using general Method A, allowing the reaction to stir for 20 h. The crude product was purified by column chromatography (33% EtOAc in hexanes) to provide a yellow oil (25.3 mg, 79 μmol , 40% yield); 73% *ee*; $[\alpha]_{\text{D}}^{25} -92.0$ (*c* 1.00, CHCl_3); ^1H NMR (500 MHz, CDCl_3) δ 7.83 – 7.87 (m, 2H), 7.61 – 7.65 (m, 2H), 7.41 – 7.43 (m, 2H), 7.33 – 7.37 (m, 2H), 7.25 – 7.28

(m, 1H), 3.81 (ddd, $J = 9.5, 8.0, 3.6$ Hz, 1H), 3.75 (ddd, $J = 9.5, 8.2, 6.9$ Hz, 1H), 2.65 (ddd, $J = 12.8, 6.9, 3.6$ Hz, 1H), 2.31 (dt, $J = 12.8, 8.1$ Hz, 1H), 1.65 (s, 3H); ^{13}C NMR (125 MHz, CDCl_3) δ 177.6, 142.9, 129.1, 127.4, 126.6 – 126.2 (m), 125.5, 123.4, 119.4, 50.7, 45.3, 34.7, 25.8; ^{19}F (282 MHz, CDCl_3) δ –62.1; IR (Neat Film, NaCl) 2925, 1700, 1614, 1520, 1490, 1457, 1387, 1321, 1222, 1163, 1117, 1064, 1012, 839, 765, 698 cm^{-1} ; HRMS (MM) m/z calc'd for $\text{C}_{18}\text{H}_{17}\text{F}_3\text{NO}^+$ $[\text{M}+\text{H}]^+$: 320.1257, found 320.1260; SFC Conditions: 20% IPA, 2.5 mL/min, Chiralcel OD-H column, $\lambda = 254$ nm, t_{R} (min): minor = 3.03, major = 3.23.

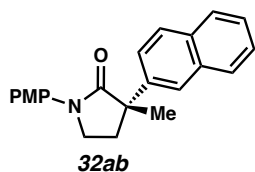
Method B: Product **32ea** was prepared using Method B, allowing the reaction to stir for 20 h. The crude product was purified by column chromatography to provide a yellow oil (40.9 mg, 0.128 mmol, 64% yield); 56% *ee*; $[\alpha]_{\text{D}}^{25} -16.9$ (c 1.00, CHCl_3); SFC Conditions: 20% IPA, 2.5 mL/min, Chiralcel OD-H column, $\lambda = 254$ nm, t_{R} (min): minor = 2.95, major = 3.14.



(S)-1-benzyl-3-methyl-3-phenylpyrrolidin-2-one (32fa): Product **32fa** was prepared using Method A, allowing the reaction to stir for 20 h. The crude product was purified by column chromatography (33% EtOAc in hexanes) to provide a yellow oil (23.0 mg, 87 μmol , 43% yield); 95% *ee*; $[\alpha]_{\text{D}}^{25} -21.4$ (c 1.00, CHCl_3); ^1H NMR (500 MHz, CDCl_3) δ 7.40 – 7.43 (m, 2H), 7.30 – 7.31 (m, 4H), 7.27 – 7.30 (m, 1H), 7.22 – 7.26 (m, 3H), 4.55 (d, $J = 14.7$ Hz, 1H), 4.52 (d, $J = 14.9$ Hz, 1H), 3.15 – 3.22 (m, 2H), 2.41 (ddd, $J = 12.8, 6.7, 5.2$ Hz, 1H), 2.12 (ddd, $J = 12.8, 7.9, 7.1$ Hz, 1H), 1.58 (s, 3H); ^{13}C NMR (125 MHz, CDCl_3) δ 177.7, 144.1, 136.9, 129.0, 128.8, 128.5, 127.9, 127.0, 126.4, 49.1, 47.3, 43.7, 35.7, 25.4; IR (Neat Film, NaCl) 3059, 3028, 2964, 2925,

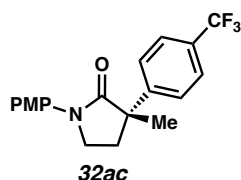
2868, 1686, 1494, 1425, 1269, 1078, 1029, 766, 747, 699 cm^{-1} ; HRMS (MM) m/z calc'd for $\text{C}_{18}\text{H}_{20}\text{NO}^+ [\text{M}+\text{H}]^+$: 266.1539, found 266.1541; SFC Conditions: 20% IPA, 2.5 mL/min, Chiralcel OD-H column, $\lambda = 210$ nm, t_R (min): minor = 6.24, major = 6.48.

Method B: Product **32fa** was prepared using Method B, allowing the reaction to stir for 20 h. The crude product was purified by column chromatography to provide a yellow oil (29.1 mg, 0.110 mmol, 55% yield); 92% *ee*; $[\alpha]_D^{25} -17.7$ (c 1.00, CHCl_3); SFC Conditions: 20% IPA, 2.5 mL/min, Chiralcel OD-H column, $\lambda = 210$ nm, t_R (min): minor = 6.14, major = 6.47.



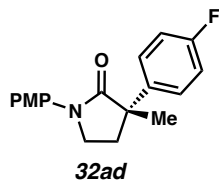
(S)-1-(4-methoxyphenyl)-3-methyl-3-(naphthalen-2-yl)pyrrolidin-2-one (32ab): Product **32ab** was prepared using Method A and purified by column chromatography (25% EtOAc in hexanes) to provide a colorless oil (54.8 mg, 0.165 mmol, 83% yield); 94% *ee*; $[\alpha]_D^{25} -159.0$ (c 0.70, CHCl_3); ^1H NMR (400 MHz, CDCl_3) δ 7.86 – 7.83 (m, 2H), 7.82 – 7.78 (m, 2H), 7.63 – 7.58 (m, 3H), 7.50 – 7.41 (m, 2H), 6.96 – 6.90 (m, 2H), 3.81 (s, 3H), 3.78 – 3.70 (m, 2H), 2.70 (ddd, $J = 12.6, 6.6, 4.0$ Hz, 1H), 2.35 (dt, $J = 12.7, 8.0$ Hz, 1H), 1.73 (s, 3H); ^{13}C NMR (100 MHz, CDCl_3) δ 176.5, 156.9, 140.9, 133.5, 133.2, 132.6, 128.8, 128.4, 127.8, 126.5, 126.2, 125.0, 124.9, 122.0, 114.4, 55.8, 50.6, 46.0, 35.2, 25.8; IR (Neat Film, NaCl) 3054, 2964, 2834, 1689, 1512, 1396, 1290, 1299, 1248, 1182, 1093, 1033, 951, 859, 827, 751, 639 cm^{-1} ; HRMS (MM) m/z calc'd for $\text{C}_{22}\text{H}_{22}\text{NO}_2^+ [\text{M}+\text{H}]^+$: 332.1645, found 332.1649; SFC Conditions: SFC Conditions: 30% IPA, 2.5 mL/min, Chiralcel OD-H column, $\lambda = 254$ nm, t_R (min): minor = 5.71, major = 7.18.

Method B: Product **32ab** was prepared using Method B. The crude product was purified by column chromatography to provide a colorless oil (50 mg, 0.151 mmol, 75% yield); 93% *ee*; $[\alpha]_{\text{D}}^{25} -176.0$ (*c* 0.70, CHCl_3); SFC Conditions: 30% IPA, 2.5 mL/min, Chiralcel OD-H column, $\lambda = 254$ nm, t_{R} (min): minor = 5.69, major = 7.12.

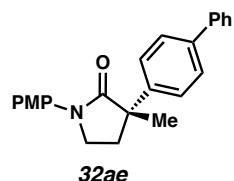


(S)-1-(4-methoxyphenyl)-3-methyl-3-(4-(trifluoromethyl)phenyl)pyrrolidin-2-one (32ac):

Product **32ac** was prepared using Method A and purified by column chromatography (25% EtOAc in hexanes) to provide a colorless oil (61.5 mg, 0.176 mmol, 88% yield); 94% *ee*; $[\alpha]_{\text{D}}^{25} -109.8$ (*c* 0.70, CHCl_3); ^1H NMR (400 MHz, CDCl_3) δ 7.65 – 7.49 (m, 6H), 7.03 – 6.80 (m, 2H), 3.81 (s, 3H), 3.80 (m, 2H), 2.57 (ddd, *J* = 12.8, 7.1, 4.4 Hz, 1H), 2.32 (ddd, *J* = 12.8, 7.9, 7.2 Hz, 1H), 1.65 (s, 3H); ^{13}C NMR (100 MHz, CDCl_3) δ 175.8, 157.1, 147.8, 132.9, 129.5 (q, *J* = 32.5 Hz), 127.0, 125.9 (q, *J* = 3.8 Hz), 122.0, 114.4, 55.8, 50.3, 45.8, 34.9, 25.6; ^{19}F NMR (282 MHz, CDCl_3) δ –62.5; IR (Neat Film, NaCl) 2965, 2935, 1691, 1618, 1513, 1455, 1444, 1398, 1328, 1300, 1250, 1165, 1121, 1078, 1068, 1035, 1016, 829, 708, 618 cm^{-1} ; HRMS (MM) *m/z* calc'd for $\text{C}_{19}\text{H}_{19}\text{F}_3\text{NO}_2^+$ $[\text{M}+\text{H}]^+$: 350.1362, found 350.1367; SFC Conditions: 30% IPA, 2.5 mL/min, Chiralpak AD-H column, $\lambda = 254$ nm, t_{R} (min): minor: 3.80, major = 7.12.

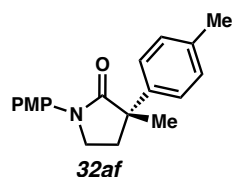


(S)-3-(4-fluorophenyl)-1-(4-methoxyphenyl)-3-methylpyrrolidin-2-one (32ad): Product **32ad** was prepared using Method A and purified by column chromatography (25% EtOAc in hexanes) to provide a colorless oil (19.5 mg, 65 μ mol, 33% yield); 93% *ee*; $[\alpha]_{\text{D}}^{25} -109.9$ (*c* 0.6, CHCl_3); ^1H NMR (400 MHz, CDCl_3) δ 7.64 – 7.50 (m, 2H), 7.47 – 7.34 (m, 2H), 7.07 – 6.96 (m, 2H), 6.96 – 6.87 (m, 2H), 3.81 (s, 3H), 3.85 – 3.63 (m, 2H), 2.59 – 2.48 (m, 1H), 2.28 (dt, *J* = 12.7, 7.8 Hz, 1H), 1.61 (s, 3H); ^{13}C NMR (100 MHz, CDCl_3) δ 176.4, 163.2, 160.8, 157.0, 139.4 (d, *J* = 3.2 Hz), 128.1 (d, *J* = 8.0 Hz), 121.9, 115.7 (d, *J* = 21.2 Hz), 114.4, 55.8, 49.8, 45.8, 35.2, 25.9; ^{19}F NMR (282 MHz, CDCl_3) δ -116.2; IR (Neat Film, NaCl) 2959, 2926, 1689, 1602, 1509, 1463, 1454, 1443, 1397, 1299, 1290, 1248, 1181, 1165, 1085, 1072, 1034, 1015, 830, 750, 621 cm^{-1} ; HRMS (MM) *m/z* calc'd for $\text{C}_{18}\text{H}_{19}\text{FNO}_2^+ [\text{M}+\text{H}]^+$: 300.1394, found 300.1404; SFC Conditions: 30% IPA, 2.5 mL/min, Chiralcel OD-H column, λ = 210 nm, t_{R} (min): minor = 2.78, major = 3.11.



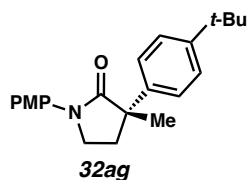
(S)-3-([1,1'-biphenyl]-4-yl)-1-(4-methoxyphenyl)-3-methylpyrrolidin-2-one (32ae): Product **32ae** was prepared using Method A and purified by column chromatography (25% EtOAc in hexanes) to provide a colorless oil (55.4 mg, 0.155 mmol, 78% yield); 97% *ee*; $[\alpha]_{\text{D}}^{25} -129.1$ (*c* 0.94, CHCl_3); ^1H NMR (400 MHz, CDCl_3) δ 7.66 – 7.53 (m, 6H), 7.54 – 7.48 (m, 2H), 7.47 – 7.40 (m, 2H), 7.37 – 7.30 (m, 1H), 6.95 – 6.88 (m, 2H), 3.81 (s, 3H), 3.79 – 3.70 (m, 2H), 2.63 (ddd, *J* = 12.7, 6.5, 4.3 Hz, 1H), 2.31 (d, *J* = 12.7 Hz, 1H), 1.67 (s, 3H); ^{13}C NMR (100 MHz, CDCl_3) δ 176.6, 156.9, 142.7, 141.0, 140.1, 133.2, 129.1, 127.6, 127.4, 126.9, 121.9, 114.4, 55.8, 53.8, 50.1, 45.9, 35.1, 25.7; IR (Neat Film, NaCl) 3028, 2963, 2932, 1689, 1511, 1486, 1396, 1289,

1299, 1248, 1181, 1086, 1034, 1007, 829, 768, 733 cm^{-1} ; HRMS (MM) m/z calc'd for $\text{C}_{24}\text{H}_{24}\text{NO}_2^+$ $[\text{M}+\text{H}]^+$: 358.1802, found 358.1808; SFC Conditions: 30% IPA, 2.5 mL/min, Chiralcel OD-H column, $\lambda = 254$ nm, t_R (min):, minor = 7.40, major = 8.83.

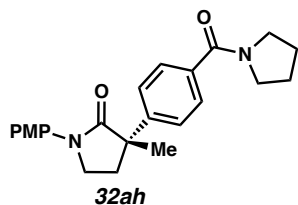


(S)-1-(4-methoxyphenyl)-3-methyl-3-(p-tolyl)pyrrolidin-2-one (32af): Product **32af** was prepared using Method A and purified by column chromatography (25% EtOAc in hexanes) to provide a colorless oil (28.8 mg, 98 μmol , 49% yield); 91% *ee*; $[\alpha]_{\text{D}}^{25} -64.6$ (*c* 0.50, CHCl_3); ^1H NMR (400 MHz, CDCl_3) δ 7.67 – 7.52 (m, 2H), 7.35 – 7.29 (m, 2H), 7.20 – 7.11 (m, 2H), 6.96 – 6.87 (m, 2H), 3.81 (s, 3H), 3.76 – 3.63 (m, 2H), 2.56 (ddd, $J = 12.7, 6.5, 3.9$ Hz, 1H), 2.32 (s, 3H), 2.26 (dt, $J = 12.6, 8.1$ Hz, 1H), 1.61 (s, 3H); ^{13}C NMR (100 MHz, CDCl_3) δ 176.8, 156.8, 140.6, 136.8, 133.3, 129.6, 126.3, 121.8, 114.3, 55.8, 50.0, 45.9, 35.2, 25.8, 21.3; IR (Neat Film, NaCl) 2960, 1689, 1511, 1452, 1395, 1289, 1249, 1182, 1086, 1031, 828, 749 cm^{-1} ; HRMS (MM) m/z calc'd for $\text{C}_{19}\text{H}_{22}\text{NO}_2^+$ $[\text{M}+\text{H}]^+$: 296.1645, found 296.1650; SFC Conditions: 30% IPA, 2.5 mL/min, Chiralcel OD-H column, $\lambda = 254$ nm, t_R (min): minor = 3.29, major = 3.63.

Method B: Product **32af** was prepared using Method B. The crude product was purified by column chromatography to provide a colorless oil (33.6 mg, 0.114 mmol, 57% yield); 95% *ee*; $[\alpha]_{\text{D}}^{25} -125.8$ (*c* 0.70, CHCl_3); SFC Conditions: 30% IPA, 2.5 mL/min, Chiralcel OD-H column, $\lambda = 254$ nm, t_R (min): minor = 3.56, major = 3.93.

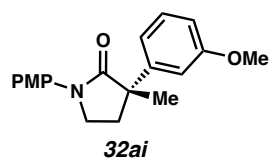


(S)-3-(4-(*tert*-butyl)phenyl)-1-(4-methoxyphenyl)-3-methylpyrrolidin-2-one (32ag): Product **32ag** was prepared using Method A and purified by column chromatography (25% EtOAc in hexanes) to provide a colorless oil (39.9 mg, 0.118 mmol, 60% yield); 91% *ee*; $[\alpha]_{\text{D}}^{25} -121.0$ (*c* 0.93, CHCl_3); ^1H NMR (400 MHz, CDCl_3) δ 7.62 – 7.55 (m, 2H), 7.35 (d, *J* = 0.6 Hz, 4H), 6.97 – 6.84 (m, 2H), 3.80 (s, 3H), 3.73 (ddd, *J* = 8.2, 5.4, 3.1 Hz, 2H), 2.58 (ddd, *J* = 12.6, 6.4, 4.3 Hz, 1H), 2.26 (dt, *J* = 12.7, 7.9 Hz, 1H), 1.62 (s, 3H), 1.30 (s, 9H); ^{13}C NMR (100 MHz, CDCl_3) δ 176.9, 156.8, 149.9, 140.5, 133.4, 126.1, 125.8, 121.8, 114.3, 55.8, 49.9, 45.9, 35.1, 34.7, 31.6, 25.7; IR (Neat Film, NaCl) 2962, 2869, 1693, 1512, 1396, 1363, 1321, 1290, 1299, 1249, 1182, 1121, 1086, 1034, 829, 796, 758, 618 cm^{-1} ; HRMS (MM) *m/z* calc'd for $\text{C}_{22}\text{H}_{28}\text{NO}_2^+$ $[\text{M}+\text{H}]^+$: 338.2115, found 338.2120; SFC Conditions: 30% IPA, 2.5 mL/min, Chiralcel OD-H column, λ = 254 nm, t_{R} (min): major = 3.35, minor = 4.06.



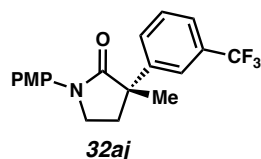
(S)-1-(4-methoxyphenyl)-3-methyl-3-(4-(pyrrolidine-1 carbonyl)phenyl)pyrrolidin-2-one (32ah): Product **32ah** was prepared using Method B and purified by column chromatography (25% EtOAc in hexanes) to provide a colorless oil (65.9 mg, 0.174 mmol, 87% yield); 81% *ee*; $[\alpha]_{\text{D}}^{25} -89.2$ (*c* 0.70, CHCl_3); ^1H NMR (400 MHz, CDCl_3) δ 7.63 – 7.54 (m, 2H), 7.51 – 7.43 (m, 4H), 6.97 – 6.89 (m, 2H), 3.80 (s, 3H), 3.77 – 3.66 (m, 2H), 3.63 (t, *J* = 7.0 Hz, 2H), 3.42 (t, *J* = 6.6 Hz,

2H), 2.54 (ddd, $J = 12.7, 6.9, 3.9$ Hz, 1H), 2.28 (dt, $J = 12.7, 7.9$ Hz, 1H), 2.00 – 1.92 (m, 2H), 1.91 – 1.79 (m, 2H), 1.63 (s, 3H); ^{13}C NMR (100 MHz, CDCl_3) δ 176.3, 169.7, 157.0, 145.4, 136.1, 133.0, 127.7, 126.4, 121.9, 114.4, 55.8, 50.3, 50.0, 46.5, 45.9, 35.1, 26.7, 25.6, 24.8; IR (Neat Film, NaCl) 2968, 2876, 1689, 1623, 1562, 1512, 1426, 1398, 1298, 1249, 1182, 1116, 1085, 1033, 933, 830, 749, 707, 663 cm^{-1} ; HRMS (MM) m/z calc'd for $\text{C}_{23}\text{H}_{27}\text{N}_2\text{O}_3^+$ $[\text{M}+\text{H}]^+$: 379.2016, found 379.2011; SFC Conditions: 30% IPA, 2.5 mL/min, Chiralcel OD-H column, $\lambda = 254$ nm, t_R (min): minor = 9.00, major = 10.34.

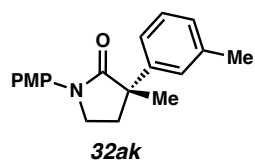


(S)-3-(3-methoxyphenyl)-1-(4-methoxyphenyl)-3-methylpyrrolidin-2-one (32ai):

Product **32ai** was prepared using Method A and purified by column chromatography (25% EtOAc in hexanes) to provide a colorless oil (43.0 mg, 0.138 mmol, 69% yield); 86% *ee*; $[\alpha]_D^{25} -109.9$ (c 0.70, CHCl_3); ^1H NMR (300 MHz, CDCl_3) δ 7.62 – 7.53 (m, 2H), 7.30 – 7.21 (m, 1H), 7.05 – 6.98 (m, 2H), 6.95 – 6.86 (m, 2H), 6.79 (ddd, $J = 8.2, 2.3, 1.1$ Hz, 1H), 3.80 (s, 3H), 3.79 (s, 3H), 3.77 – 3.67 (m, 2H), 2.57 (ddd, $J = 12.7, 6.5, 4.2$ Hz, 1H), 2.26 (dt, $J = 12.7, 8.0$ Hz, 1H), 1.62 (s, 3H); ^{13}C NMR (100 MHz, CDCl_3) δ 176.5, 160.1, 156.9, 145.3, 133.2, 129.9, 121.9, 118.8, 114.4, 112.8, 112.1, 55.8, 55.6, 50.3, 45.9, 35.2, 25.8; IR (Neat Film, NaCl) 3052, 2962, 2935, 2836, 1693, 1682, 1600, 1582, 1513, 1488, 1456, 1464, 1430, 1395, 1320, 1290, 1247, 1181, 1124, 1089, 1036, 932, 914, 882, 829, 792, 751, 701, 667, 637 cm^{-1} ; HRMS (MM) m/z calc'd for $\text{C}_{19}\text{H}_{22}\text{NO}_3^+$ $[\text{M}+\text{H}]^+$: 312.1594, found 312.1590; SFC Conditions: 30% IPA, 4.0 mL/min, Chiralpak AD-H column, $\lambda = 254$ nm, t_R (min): minor = 4.06, major = 5.81.

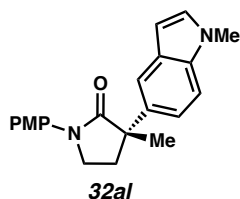
**(S)-1-(4-methoxyphenyl)-3-methyl-3-(3-(trifluoromethyl)phenyl)pyrrolidin-2-one (32aj):**

Product **32aj** was prepared using Method A and purified by column chromatography (20% EtOAc in hexanes) to provide a colorless oil (53.3 mg, 0.153 mmol, 75% yield); 96% *ee*; $[\alpha]_{\text{D}}^{25} -105.7$ (*c* 0.93, CHCl₃); ¹H NMR (400 MHz, CDCl₃) δ 7.74 – 7.70 (m, 1H), 7.67 (dddd, *J* = 7.8, 1.9, 1.3, 0.6 Hz, 1H), 7.61 – 7.40 (m, 4H), 6.97 – 6.89 (m, 2H), 3.81 (s, 4H), 3.75 – 3.69 (m, 1H), 2.58 (ddd, *J* = 12.8, 7.3, 4.7 Hz, 1H), 2.33 (ddd, *J* = 12.9, 7.9, 6.9 Hz, 1H), 1.65 (d, *J* = 1.6 Hz, 3H); ¹³C NMR (100 MHz, CDCl₃) δ 175.9, 157.1, 144.8, 132.9, 131.2 (q, *J* = 32.0 Hz), 130.2, 129.4, 127.0, 126.2 – 125.6 (m), 124.3 – 124.0 (m), 123.2 (q, *J* = 3.8 Hz), 122.0, 114.4, 55.8, 50.1, 45.9, 34.9, 25.7; ¹⁹F NMR (282 MHz, CDCl₃) δ -62.5; IR (Neat Film, NaCl) 2932, 2962, 2838, 1721, 1692, 1681, 1512, 1504, 1493, 1442, 1400, 1329, 1299, 1249, 1163, 1119, 1075, 1034, 829, 802, 702 cm⁻¹; HRMS (MM) *m/z* calc'd for C₁₉H₁₉F₃NO₂⁺ [M+H]⁺: 350.1362, found 350.1359; SFC Conditions: 30% IPA, 2.5 mL/min, Chiralcel OD-H column, λ = 254 nm, *t*_R (min): minor = 2.52, major = 2.97.

**(S)-1-(4-methoxyphenyl)-3-methyl-3-(*m*-tolyl)pyrrolidin-2-one (32ak):**

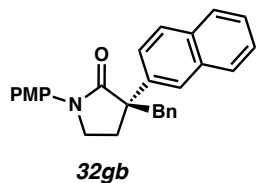
Product **32ak** was prepared using Method B and purified by column chromatography (25% EtOAc in hexanes) to provide a colorless oil (41.4 mg, 0.140 mmol, 70% yield); 97% *ee*; $[\alpha]_{\text{D}}^{25} -209.3$ (*c* 0.79, CHCl₃); ¹H NMR (400 MHz, CDCl₃) δ 7.59 (d, *J* = 9.2 Hz, 2H), 7.31 – 7.18 (m, 3H), 7.06 (t, *J* = 5.5 Hz, 1H), 6.92 (d, *J* = 9.2 Hz, 2H), 3.81 (s, 3H), 3.76 – 3.67 (m, 2H), 2.64 – 2.51 (m, 1H), 2.35 (s, 3H),

2.26 (dt, $J = 12.7, 8.0$ Hz, 1H), 1.62 (s, 3H); ^{13}C NMR (100 MHz, CDCl_3) δ 176.7, 156.8, 143.5, 138.5, 133.3, 128.8, 127.9, 127.2, 123.4, 121.8, 114.3, 55.8, 50.2, 45.9, 35.3, 25.8, 22.0; IR (Neat Film, NaCl) 2962, 2962, 1690, 1606, 1586, 1512, 1488, 1444, 1429, 1396, 1321, 1299, 1249, 1182, 1124, 1086, 1034, 932, 882, 829, 788, 750, 704, 641, 612; HRMS (MM) m/z calc'd for $\text{C}_{19}\text{H}_{22}\text{NO}_2^+$ $[\text{M}+\text{H}]^+$: 296.1645, found 296.1645; SFC Conditions: 30% IPA, 2.5 mL/min, Chiralpak AD-H column, $\lambda = 254$ nm, t_R (min): major = 5.47, minor = 7.72.



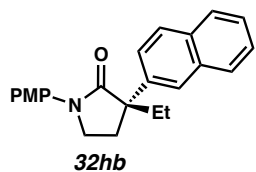
(S)-1-(4-methoxyphenyl)-3-methyl-3-(1-methyl-1H-indol-6-yl)pyrrolidin-2-one (32al):

Product **32al** was prepared using Method B and purified by column chromatography (25% EtOAc in hexanes) to provide a colorless oil (29.2 mg, 87 μmol , 44% yield); 92% *ee*; $[\alpha]_D^{25} -94.5$ (*c* 0.70, CHCl_3); ^1H NMR (400 MHz, CDCl_3) δ 7.67 (dd, $J = 1.9, 0.8$ Hz, 1H), 7.64 – 7.56 (m, 2H), 7.38 – 7.27 (m, 2H), 7.03 (d, $J = 3.1$ Hz, 1H), 6.95 – 6.88 (m, 2H), 6.44 (dd, $J = 3.1, 0.8$ Hz, 1H), 3.81 (s, 3H), 3.77 (s, 3H), 3.71 (dd, $J = 8.3, 4.9$ Hz, 2H), 2.67 (dt, $J = 12.6, 5.0$ Hz, 1H), 2.31 (dt, $J = 12.6, 8.3$ Hz, 1H), 1.69 (s, 3H); ^{13}C NMR (100 MHz, CDCl_3) δ 177.3, 156.7, 135.9, 134.3, 133.5, 129.5, 128.7, 121.8, 120.5, 118.3, 114.3, 109.7, 101.4, 55.8, 50.4, 46.0, 35.8, 33.2, 26.5; IR (Neat Film, NaCl) 2961, 1688, 1614, 1511, 1490, 1394, 1294, 1248, 1181, 1124, 1089, 1034, 884, 827, 798, 730, 654 cm^{-1} ; HRMS (MM) m/z calc'd for $\text{C}_{21}\text{H}_{23}\text{N}_2\text{O}_2^+$ $[\text{M}+\text{H}]^+$: 335.1754, found 335.1752; SFC Conditions: 30% IPA, 2.5 mL/min, Chiralcel OD-H column, $\lambda = 254$ nm, t_R (min): minor = 2.75, major = 5.48.



(S)-3-benzyl-1-(4-methoxyphenyl)-3-(naphthalen-2-yl)pyrrolidin-2-one (32gb):

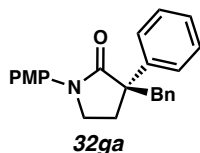
Product **32gb** was prepared using general Method A, allowing the reaction to stir for 20 h. The crude product was purified by column chromatography (33% EtOAc in hexanes) to provide a colorless solid (47.7 mg, 0.117 mmol, 59% yield); 91% *ee*; $[\alpha]_{\text{D}}^{25} -172.6$ (*c* 1.00, CHCl₃); ¹H NMR (500 MHz, CDCl₃) δ 7.96 (d, *J* = 2.0 Hz, 1H), 7.86 (d, *J* = 8.8 Hz, 1H), 7.80 – 7.85 (m, 2H), 7.72 (dd, *J* = 8.7, 2.0 Hz, 1H), 7.46 – 7.49 (m, 2H), 7.41 – 7.45 (m, 2H), 7.21 – 7.23 (m, 3H), 7.15 – 7.17 (m, 2H), 6.87 – 6.90 (m, 2H), 3.79 (s, 3H), 3.51 – 3.56 (m, 2H), 3.24 – 3.29 (m, 2H), 2.60 (ddd, *J* = 12.9, 7.1, 3.7 Hz, 1H), 2.48 (dt, *J* = 13.0, 7.9 Hz, 1H); ¹³C NMR (125 MHz, CDCl₃) δ 175.1, 157.0, 139.4, 137.6, 133.5, 133.0, 132.7, 130.8, 128.6, 128.6, 128.5, 127.7, 127.0, 126.4, 126.3, 125.6, 125.6, 122.3, 114.3, 55.8, 55.2, 46.1, 45.7, 30.2; IR (Neat Film, NaCl) 3058, 2951, 2929, 2836, 1687, 1600, 1512, 1454, 1397, 1321, 1299, 1249, 1181, 1036, 828, 749, 703 cm⁻¹; HRMS (MM) *m/z* calc'd for C₂₈H₂₆NO₂⁺ [M+H]⁺: 408.1958, found 408.1962; SFC Conditions: 30% IPA, 2.5 mL/min, Chiralcel OD-H column, λ = 254 nm, *t_R* (min): major = 8.16, minor = 9.63.



(S)-3-ethyl-1-(4-methoxyphenyl)-3-(naphthalen-2-yl)pyrrolidin-2-one (32hb).

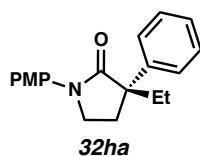
Product **32hb** was prepared using Method A, allowing the reaction to stir for 20 h. The crude product was purified by column chromatography (33% EtOAc in hexanes) to provide a yellow oil (31.3 mg, 91 μ mol,

46% yield); 93% *ee*; $[\alpha]_{\text{D}}^{25} -167.2$ (*c* 1.00, CHCl_3); ^1H NMR (500 MHz, CDCl_3) δ 7.91 – 7.93 (br s, 1H), 7.80 – 7.85 (m, 3H), 7.70 (dd, *J* = 8.5, 1.9 Hz, 1H), 7.54 – 7.57 (m, 2H), 7.44 – 7.49 (m, 2H), 6.88 – 6.92 (m, 2H), 3.80 (s, 3H), 3.74 – 3.77 (m, 2H), 2.74 (ddd, *J* = 12.8, 5.6, 4.0 Hz, 1H), 2.41 (dt, *J* = 12.7, 8.5 Hz, 1H), 2.18 – 2.25 (m, 1H), 2.03 – 2.10 (m, 1H), 0.93 (t, *J* = 7.4 Hz, 3H); ^{13}C NMR (125 MHz, CDCl_3) δ 175.8, 156.8, 138.8, 133.5, 133.2, 132.6, 128.6, 128.4, 127.7, 126.4, 126.2, 125.6 – 125.3 (m), 122.0, 114.3, 55.8, 54.3, 46.1, 32.3, 30.5, 9.5; IR (Neat Film, NaCl) 3055, 2963, 2932, 2877, 1687, 1512, 1464, 1396, 1298, 1249, 1181, 1035, 828, 750 cm^{-1} ; HRMS (MM) *m/z* calc'd for $\text{C}_{23}\text{H}_{24}\text{NO}_2^+$ $[\text{M}+\text{H}]^+$: 346.1802, found 346.1805; SFC Conditions: 30% IPA, 2.5 mL/min, Chiralcel OD-H column, λ = 210 nm, t_{R} (min): minor = 5.01, major = 6.05.

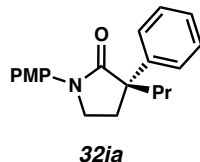


(S)-3-benzyl-1-(4-methoxyphenyl)-3-phenylpyrrolidin-2-one (32ga): Product **32ga** was prepared using Method B, allowing the reaction to stir for 20 h. The crude product was purified by column chromatography (33% EtOAc in hexanes) to provide a colorless oil (29.0 mg, 81 μmol , 41% yield); 90% *ee*; $[\alpha]_{\text{D}}^{25} -90.0$ (*c* 1.00, CHCl_3); ^1H NMR (500 MHz, CDCl_3) δ 7.53 – 7.56 (m, 2H), 7.40 – 7.43 (m, 2H), 7.33 – 7.37 (m, 2H), 7.25 – 7.28 (m, 1H), 7.20 – 7.24 (m, 3H), 7.11 – 7.13 (m, 2H), 6.85 – 6.89 (m, 2H), 3.79 (s, 3H), 3.49 (dt, *J* = 9.4, 7.4 Hz, 1H), 3.44 (d, *J* = 13.4 Hz, 1H), 3.23 (ddd, *J* = 9.3, 8.1, 3.9 Hz, 1H), 3.14 (d, *J* = 13.5 Hz, 1H), 2.48 (ddd, *J* = 12.9, 7.1, 3.9 Hz, 1H), 2.39 (dt, *J* = 13.0, 7.9 Hz, 1H); ^{13}C NMR (125 MHz, CDCl_3) δ 175.2, 156.9, 142.2, 137.7, 133.0, 130.7, 128.8, 128.5, 127.4, 127.1, 127.0, 122.2, 114.3, 55.8, 55.0, 46.0, 45.8, 30.1; IR (Neat Film, NaCl) 3059, 3027, 2925, 1687, 1507, 1455, 1397, 1319, 1298, 1249, 1181, 1034,

828, 701 cm^{-1} ; HRMS (MM) m/z calc'd for $\text{C}_{24}\text{H}_{24}\text{NO}_2^+$ $[\text{M}+\text{H}]^+$: 358.1802, found 358.1805; SFC Conditions: 25% IPA, 2.5 mL/min, Chiralcel OD-H column, $\lambda = 254$ nm, t_R (min): major = 6.45, minor = 7.11.

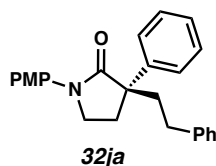


(S)-3-ethyl-1-(4-methoxyphenyl)-3-phenylpyrrolidin-2-one (32ha): Product **32ha** was prepared using Method B, allowing the reaction to stir for 20 h. The crude product was purified by column chromatography (33% EtOAc in hexanes) to provide a light yellow oil (29.5 mg, 0.100 mmol, 50% yield) 89% *ee*; $[\alpha]_D^{25} -77.2$ (c 1.00, CHCl_3); ^1H NMR (500 MHz, CDCl_3) δ 7.52 – 7.56 (m, 2H), 7.43 – 7.52 (m, 2H), 7.31 – 7.36 (m, 2H), 7.22 – 7.27 (m, 1H), 6.87 – 6.91 (m, 2H), 3.79 (s, 3H), 3.65 – 3.75 (m, 2H), 2.60 (ddd, $J = 12.9, 6.5, 3.2$ Hz, 1H), 2.33 (dt, $J = 12.9, 8.5$ Hz, 1H), 2.05 – 2.13 (m, 1H), 1.93 – 2.00 (m, 1H), 0.88 (t, $J = 7.4$ Hz, 3H); ^{13}C NMR (125 MHz, CDCl_3) δ 175.9, 156.8, 141.5, 133.3, 128.8, 127.2, 126.9, 121.9, 114.3, 55.8, 54.1, 46.1, 32.4, 30.5, 9.5; IR (Neat Film, NaCl) 3056, 2962, 2931, 1687, 1512, 1444, 1396, 1322, 1296, 1249, 1181, 1118, 1097, 1034, 829, 764, 700 cm^{-1} ; HRMS (MM) m/z calc'd for $\text{C}_{19}\text{H}_{22}\text{NO}_2^+$ $[\text{M}+\text{H}]^+$: 296.1645, found 296.1638; SFC Conditions: 20% IPA, 2.5 mL/min, Chiralcel OD-H column, $\lambda = 254$ nm, t_R (min): major = 5.32, minor = 6.46.



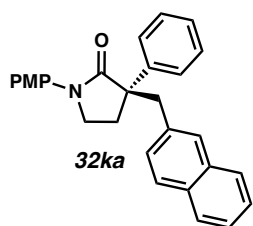
(S)-1-(4-methoxyphenyl)-3-phenyl-3-propylpyrrolidin-2-one (32ia): Product **32ia** was prepared using Method B, allowing the reaction to stir for 20 h. The product was purified by

column chromatography (15% EtOAc in hexanes) to provide a colorless oil (27.6 mg, 89 μ mol, 45% yield); 90% *ee*; $[\alpha]_{\text{D}}^{25} -120.0$ (*c* 0.70, CHCl_3); ^1H NMR (400 MHz, CDCl_3) 7.57 – 7.48 (m, 4H), 7.37 – 7.30 (m, 2H), 7.26 – 7.21 (m, 1H), 6.93 – 6.85 (m, 2H), 3.79 (s, 3H), 3.75 – 3.65 (m, 2H), 2.62 (ddd, *J* = 12.9, 6.3, 3.4 Hz, 1H), 2.33 (dt, *J* = 12.9, 8.5 Hz, 1H), 2.04 (ddd, *J* = 13.7, 11.1, 5.9 Hz, 1H), 1.93 – 1.82 (m, 1H), 1.34 – 1.20 (m, 2H), 0.90 (t, *J* = 7.3 Hz, 3H); ^{13}C NMR (100 MHz, CDCl_3) δ 175.9, 156.8, 141.7, 133.3, 128.8, 127.1, 126.8, 121.8, 114.3, 55.8, 53.7, 46.1, 42.0, 31.0, 18.4, 14.8; IR (Neat Film, NaCl) 2957, 2932, 2872, 1687, 1512, 1463, 1444, 1430, 1396, 1322, 1298, 1249, 1181, 1098, 1034, 883, 829, 964, 731, 700, 638 cm^{-1} ; HRMS (MM) *m/z* calc'd for $\text{C}_{20}\text{H}_{24}\text{NO}_2^+$ $[\text{M}+\text{H}]^+$: 310.1802, found 310.1807; SFC Conditions: 40% IPA, 2.5 mL/min, Chiralpak AD-H column, λ = 210 nm, t_{R} (min): minor = 2.94, major = 3.47.



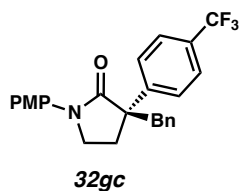
(S)-1-(4-methoxyphenyl)-3-phenethyl-3-phenylpyrrolidin-2-one (32ja): Product **32ja** was prepared using Method B, allowing the reaction to stir for 20 h. The crude product was purified by column chromatography (25% EtOAc in hexanes) to provide a colorless oil (39.9 mg, 0.107 mmol, 54% yield); 78% *ee*; $[\alpha]_{\text{D}}^{25} -95.7$ (*c* 0.70, CHCl_3); ^1H NMR (400 MHz, CDCl_3) δ 7.62 – 7.49 (m, 4H), 7.41 – 7.31 (m, 2H), 7.29 – 7.23 (m, 3H), 7.20 – 7.09 (m, 3H), 6.96 – 6.84 (m, 2H), 3.80 (s, 3H), 3.79 – 3.67 (m, 2H), 2.71 – 2.60 (m, 2H), 2.51 (td, *J* = 12.7, 4.7 Hz, 1H), 2.44 – 2.34 (m, 2H), 2.21 (ddd, *J* = 13.5, 12.2, 4.7 Hz, 1H). ^{13}C NMR (100 MHz, CDCl_3) δ 175.6, 156.9, 142.3, 141.2, 133.2, 129.0, 128.7, 127.4, 126.9, 126.1, 121.9, 114.3, 55.8, 53.7, 46.1, 41.5, 31.4; IR (Neat Film, NaCl) 2961, 1688, 1614, 1511, 1490, 1394, 1294, 1248, 1181, 1124, 1089, 1034, 884, 827, 798,

730, 654 cm^{-1} ; HRMS (MM) m/z calc'd for $\text{C}_{25}\text{H}_{26}\text{NO}_2^+ [\text{M}+\text{H}]^+$: 372.1958, found 372.1961; SFC Conditions: 30% IPA, 2.5 mL/min, Chiralcel OD-H column, $\lambda = 254$ nm, t_R (min): minor = 5.03, major = 5.40.

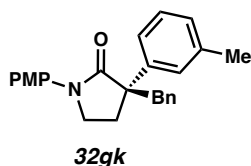


(S)-1-(4-methoxyphenyl)-3-(naphthalen-2-ylmethyl)-3-phenylpyrrolidin-2-one (32ka).

Product **32ka** was prepared using Method B, allowing the reaction to stir for 20 h. The crude product was purified by column chromatography (33% EtOAc in hexanes) to provide a colorless oil (48.0 mg, 0.118 mmol, 59% yield); 94% *ee*; $[\alpha]_D^{25} -128.4$ (c 1.00, CHCl_3); ^1H NMR (500 MHz, CDCl_3) δ 7.77 – 7.81 (m, 1H), 7.72 – 7.75 (m, 1H), 7.68 (d, $J = 8.4$ Hz, 1H), 7.60 (br s, 1H), 7.56 – 7.59 (m, 2H), 7.42 – 7.46 (m, 2H), 7.34 – 7.41 (m, 4H), 7.27 – 7.30 (m, 1H), 7.22 (dd, $J = 8.4$, 1.8 Hz, 1H), 6.84 – 6.87 (m, 2H), 3.79 (s, 3H), 3.62 (d, $J = 13.5$ Hz, 1H), 3.50 (ddd, $J = 9.4$, 8.0, 7.0 Hz, 1H), 3.31 (d, $J = 13.5$ Hz, 1H), 3.24 (ddd, $J = 9.4$, 8.0, 3.6 Hz, 1H), 2.50 (ddd, $J = 12.9$, 7.0, 3.6 Hz, 1H), 2.44 (dt, $J = 12.9$, 8.0 Hz, 1H); ^{13}C NMR (125 MHz, CDCl_3) δ 175.2, 156.9, 142.0, 135.4, 133.6, 133.0, 132.6, 129.4, 129.1, 128.9, 128.0, 127.9, 127.9, 127.4, 127.1, 126.2, 125.9, 122.2, 114.3, 55.8, 55.2, 46.1, 45.9, 30.0; IR (Neat Film, NaCl) 3054, 2952, 2836, 1688, 1511, 1463, 1397, 1321, 1299, 1249, 1181, 1034, 909, 828, 729, 699 cm^{-1} ; HRMS (MM) m/z calc'd for $\text{C}_{28}\text{H}_{26}\text{NO}_2^+ [\text{M}+\text{H}]^+$: 408.1958, found 408.1954; SFC Conditions: 10% IPA, 2.5 mL/min, Chiralcel OD-H column, $\lambda = 254$ nm, t_R (min): minor = 10.69, major = 11.15.

**(S)-3-benzyl-1-(4-methoxyphenyl)-3-(4-(trifluoromethyl)phenyl)pyrrolidin-2-one (32gc).**

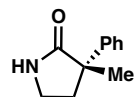
Product **32gc** was prepared using general Method A, allowing the reaction to stir for 20 h. The crude product was purified by column chromatography (25% EtOAc in hexanes) to provide a colorless oil (60.3 mg, 0.142 mmol, 71% yield); 94% *ee*; $[\alpha]_D^{25} -188.3$ (*c* 1.00, CHCl₃); ¹H NMR (500 MHz, CDCl₃) δ 7.69 – 7.72 (m, 2H), 7.59 – 7.63 (m, 2H), 7.37 – 7.41 (m, 2H), 7.22 – 7.25 (m, 3H), 7.11 – 7.13 (m, 2H), 6.87 – 6.90 (m, 2H), 3.80 (s, 3H), 3.49 (t, *J* = 7.2 Hz, 1H), 3.45 (d, *J* = 11.3 Hz, 1H), 3.22 (ddd, *J* = 9.4, 7.2, 5.4 Hz, 1H), 3.13 (d, *J* = 13.4 Hz, 1H), 2.45 – 2.53 (m, 2H); ¹³C NMR (125 MHz, CDCl₃) δ 174.5, 157.1, 146.5, 136.9, 132.6, 130.6, 129.5 (q, *J* = 32.5 Hz), 128.6, 127.5, 127.3, 125.7 (q, *J* = 3.8 Hz), 123.4, 122.3, 114.3, 55.8, 54.9, 45.9, 45.9, 30.0; ¹⁹F NMR (282 MHz, CDCl₃) δ -62.5; IR (Neat Film, NaCl) 3062, 2954, 2926, 2838, 1687, 1616, 1513, 1442, 1400, 1327, 1300, 1251, 1167, 1123, 1072, 1037, 1018, 829, 703 cm⁻¹; HRMS (MM) *m/z* calc'd for C₂₅H₂₃F₃NO₂⁺ [M+H]⁺: 426.1675, found 426.1677; SFC Conditions: 15% IPA, 2.5 mL/min, Chiralpak AD-H column, λ = 254 nm, *t_R* (min): major = 5.17, minor = 5.93.



(S)-3-benzyl-1-(4-methoxyphenyl)-3-(*m*-tolyl)pyrrolidin-2-one (32gd): Product **32gd** was prepared using Method B, allowing the reaction to stir for 20 h. The crude product was purified by column chromatography (33% EtOAc in hexanes) to provide a colorless oil (47.6 mg, 0.128 mmol,

64% yield); 93% *ee*; $[\alpha]_{\text{D}}^{25} -179.0$ (*c* 1.00, CHCl_3); ^1H NMR (500 MHz, CDCl_3) δ 7.41 (d, *J* = 16.1 Hz, 2H), 7.39 (s, 1H), 7.32 (s, 1H), 7.25 (m, 4H), 7.16 (m, 2H), 7.10 (s, 1H), 6.87 (d, *J* = 16.1 Hz, 2H), 3.80 (s, 3H), 3.50 (dt, *J* = 9.3, 7.4 Hz, 1H), 3.45 (d, *J* = 13.4 Hz, 1H), 3.21 (ddd, *J* = 9.2, 8.1, 3.8 Hz, 1H), 3.12 (d, *J* = 13.4 Hz, 1H), 2.47 (ddd, *J* = 12.9, 7.1, 3.8 Hz, 1H), 2.41 (s, 1H), 2.37 (s, 3H); ^{13}C NMR (125 MHz, CDCl_3) δ 175.2, 156.9, 142.2, 138.4, 137.8, 133.1, 130.8, 128.6, 128.4, 128.1, 127.8, 127.0, 124.0, 122.2, 114.3, 55.8, 55.0, 46.0, 45.8, 30.1, 22.0; IR (Neat Film, NaCl) 2923, 1686, 1604, 1584, 1511, 1453, 1299, 1249, 1180, 1119, 1099, 1036, 890, 828, 787, 738, 703, 613 cm^{-1} ; HRMS (MM) *m/z* calc'd for $\text{C}_{25}\text{H}_{26}\text{NO}_2^+$ $[\text{M}+\text{H}]^+$: 372.1958, found 372.1960; SFC Conditions: 15% IPA, 2.5 mL/min, Chiralpak AD-H column, λ = 254 nm, t_{R} (min): major = 8.44, minor = 7.00.

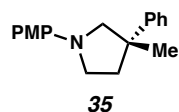
Product Transformations



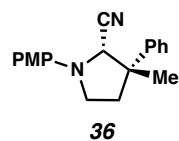
34

(*S*)-3-methyl-3-phenylpyrrolidin-2-one (34): To a solution of **32aa** (30.2 mg, 93% *ee*; 0.107 mmol, 1.0 equiv) in acetonitrile (2.2 mL) at 0 °C was added a solution of ceric ammonium nitrate (88 mg, 0.161 mmol, 1.5 equiv) in de-ionized water (2.2 mL) dropwise. The resulting mixture was stirred for 30 minutes at 0 °C. Upon consumption of the starting material, the reaction was diluted with water and extracted with EtOAc three times. The combined organic extracts were dried over Na_2SO_4 and the product was purified by column chromatography (5% MeOH in CH_2Cl_2) to afford **34** as a yellow solid (13.6 mg, 78 μmol , 73% yield). $[\alpha]_{\text{D}}^{25} -80.8$ (*c* 0.665, CHCl_3); ^1H NMR (400 MHz, CDCl_3) δ 7.47 – 7.39 (m, 2H), 7.39 – 7.30 (m, 2H), 7.26 (s, 1H), 6.88 (d, *J* = 22.5 Hz, 1H), 3.45 – 3.23 (m, 2H), 2.51 (ddd, *J* = 12.3, 7.3, 4.6 Hz, 1H), 2.25 (ddd, *J* = 12.7, 8.0, 6.8 Hz, 1H),

1.56 (s, 3H); ^{13}C NMR (100 MHz, CDCl_3) δ 181.8, 143.7, 128.9, 127.1, 126.4, 48.2, 39.4, 38.3, 24.8, 19.4; IR (Neat Film, NaCl) 3056, 3026, 2960, 2931, 2830, 1619, 1601, 1515, 1488, 1496, 1464, 1445, 1366, 1281, 1240, 1180, 1081, 1042, 967, 811, 764, 700 cm^{-1} ; HRMS (MM) m/z calc'd for $\text{C}_{11}\text{H}_{14}\text{NO}^+$ $[\text{M}+\text{H}]^+$: 176.1070, found 176.1068.

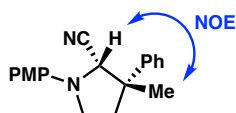


(S)-1-(4-methoxyphenyl)-3-methyl-3-phenylpyrrolidine (35): To a solution of **32aa** (46.3 mg, 93% *ee*, 0.170 mmol, 1.0 equiv) in diethyl ether (1.65 mL) at 0 °C was added LiAlH_4 (31.2 mg, 0.820 mmol, 5 equiv). The reaction was stirred at 0 °C for 5 min, then allowed to warm to ambient temperature. After 15 h, the reaction was quenched with H_2O and extracted with EtOAc seven times. The combined organic layers were dried over Na_2SO_4 and concentrated *in vacuo*. The crude product was purified by column chromatography (10% EtOAc in hexanes) to afford **5** as a light grey solid (41.1 mg, 0.154 mmol, 93% yield); $[\alpha]_{\text{D}}^{25} -85.2$ (*c* 0.70, CHCl_3); ^1H NMR (400 MHz, CDCl_3) δ 7.40 – 7.30 (m, 5H), 7.26 – 7.21 (m, 1H), 6.88 (d, $J = 9.0$ Hz, 2H), 6.56 (d, $J = 8.1$ Hz, 2H), 3.78 (s, 3H), 3.60 – 3.42 (m, 3H), 3.38 (t, $J = 10.5$ Hz, 1H), 2.38 – 2.25 (m, 1H), 2.24 – 2.14 (m, 1H), 1.44 (s, 3H). ^{13}C NMR (100 MHz, CDCl_3) δ 148.4, 143.1, 128.7, 126.5, 126.1, 115.5, 112.3, 60.4, 56.4, 47.6, 46.1, 38.5, 28.6; IR (Neat Film, NaCl) 3056, 3026, 2960, 2931, 2830, 1619, 1601, 1515, 1488, 1496, 1464, 1445, 1366, 1281, 1240, 1180, 1081, 1042, 967, 811, 764, 700 cm^{-1} ; HRMS (MM) m/z calc'd for $\text{C}_{18}\text{H}_{22}\text{NO}^+$ $[\text{M}+\text{H}]^+$: 268.1696, found 268.1702.



(2*S*,3*S*)-1-(4-methoxyphenyl)-3-methyl-3-phenylpyrrolidine-2-carbonitrile (36): To a solution of **32aa** (38.5 mg, 93% *ee*, 0.137 mmol, 1 equiv) in THF (14 mL) was added a solution of LiBEt₃H (1 M in THF, 0.42 mL, 3 equiv) dropwise at $-78\text{ }^{\circ}\text{C}$. The resulting solution was stirred at $-78\text{ }^{\circ}\text{C}$ for 2 hours, then warmed to ambient temperature and allowed to stir for 8 hours. The reaction was cooled to $0\text{ }^{\circ}\text{C}$ and acetic acid (164 μL , 2.9 mmol, 21 equiv) was added dropwise. After 10 min, KCN (171 μL , 4.8 M solution, 0.82 mmol, 6.0 equiv), celite, and Na₂SO₄ were added successively. The reaction was stirred at $0\text{ }^{\circ}\text{C}$ for 5 hours, quenched with anhydrous K₂CO₃, and filtered through celite. The solvent was removed and the crude product was purified by column chromatography (20% EtOAc in hexanes) to afford **6** as a colorless solid (17.5 mg, 60 μmol , 43% yield, 93:7 dr); $[\alpha]_{\text{D}}^{25} -233.7$ (*c* 0.70, CHCl₃); δ ¹H NMR (400 MHz, CD₂Cl₂) δ 7.35 – 7.30 (m, 4H), 7.28 – 7.20 (m, 1H), 6.88 – 6.82 (m, 2H), 6.66 – 6.59 (m, 2H), 4.67 (s, 1H), 3.72 (s, 3H), 3.49 (td, *J* = 8.6, 4.1 Hz, 1H), 3.34 (dt, *J* = 8.8, 7.5 Hz, 1H), 2.51 (dddd, *J* = 12.3, 7.5, 4.2, 0.8 Hz, 1H), 2.31 (ddd, *J* = 13.0, 8.4, 7.6 Hz, 1H), 1.71 (s, 3H); ¹³C NMR (100 MHz, CD₂Cl₂) δ 152.6, 144.5, 139.7, 128.8, 127.1, 125.3, 117.9, 114.9, 113.6, 60.4, 55.7, 49.5, 47.3, 37.0, 25.7; IR (Neat Film, NaCl) 3048, 2929, 2860, 1514, 1456, 146 cm⁻¹; HRMS (MM) *m/z* calc'd for C₁₉H₂₁N₂O⁺ [M+H]⁺: 293.1648, found 293.1642; Please note that the NMR data listed is for the major diastereomer.

Stereochemical Assignment:



2.9 REFERENCES AND NOTES

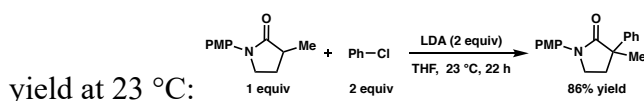
1. (a) Donohoe, T. J.; Bataille, C. J. R.; Churchill, G. W. *Annu. Rep. Prog. Chem., Sect. B* **2006**, *102*, 98–122. (b) Felpin, F. –X.; Lebreton, J. *Eur. J. Org. Chem.* **2003**, *19*, 3693–3712.

2. (a) Long-Wu, Y.; Shu, C.; Gagosz, F. *Org. Biomol. Chem.* **2014**, *12*, 1833–1845. (b) Rivas, F.; Ling, T. *Org. Prep. Proced. Int.* **2016**, *48*, 254–295.
3. (a) Guzikowski, A. P.; Tamiz, A. P.; Acosta-Burrueal, M.; Hong-Bae S.; Cai, S. -X.; Hawkinson, J. E.; Keana, J. F. W.; Kesten, S. R.; Shipp, C. T.; Tran, M.; Whittemore, E. R.; Woodward, R. M.; Wright, J. L.; Zhou, Z. -L. *J. Med. Chem.* **2000**, *43*, 984–994. (b) Lynch, C. L.; Hale, J. J.; Budhu, R. J.; Gentry, A. L.; Mills, S. G.; Chapman, K.T.; MacCoss, M.; Malkowitz, L.; Springer, M. S.; Gould, S. L.; DeMartino, J. A.; Siciliano, S. J.; Cascieri, M. A.; Carella, A.; Carver, G.; Holmes, K.; Schleif, W. A.; Danzeisen, R.; Hazuda, D.; Kessler, J.; Lineberger, J.; Miller, M.; Emini, E. A. *Bioorg. Med. Chem. Lett.* **2002**, *12*, 3001–3004. (c) Hensler, M. E.; Bernstein, G.; Nizet, V.; Nefzi, A. *Bioorg. Med. Chem. Lett.* **2006**, *16*, 5073–5079. (d) Li, X.; Li, J. *Mini-Rev. Med. Chem.* **2010**, *10*, 794–805. (e) Lexa, K. W.; Carlson, H. A. *Proteins* **2011**, *79*, 2282–2290. (f) Whitby, L. R.; Ando, Y.; Setola, V.; Vogt, P. K.; Roth, B. L.; Boger, D. L. *J. Am. Chem. Soc.* **2011**, *133*, 10184–10194. (g) Raghuraman, A.; Ko, E.; Perez, L. M. Ioerger, T. R.; Burgess, K. *J. Am. Chem. Soc.* **2011**, *133*, 12350–12353. (h) Caruano, J.; Muccioli, G.G.; Robiette, R. *Org. Biomol. Chem.*, **2016**, *14*, 10134–10156. (i) Duan, J. J. -W.; Chen, L.; Wasserman, Z. R.; Lu, Z.; Liu, R. -Q.; Covington, M. B.; Qian, M.; Hardman, K. D.; Magolda, R. L.; Newton, R. C.; Christ, D. D.; Wexler, R. R.; Decicco, C. P. *J. Med. Chem.* **2002**, *45*, 4954–4957.
4. M. Teodorescu, M. Bercea, *Polym Plast Technol Eng.* **2015**, *54*, 923–943.
5. (a) Dalko, P. I.; Moisan, L.; *Angew. Chem.* **2001**, *113*, 3840–3864. *Angew. Chem. Int. Ed.* **2001**, *40*, 3726–3748. (b) Dalko, P. I.; Moisan, L.; *Angew. Chem.* **2004**, *116*, 5248–5286 and *Angew. Chem. Int. Ed.* **2004**, *43*, 5138–5175. (c) List, B.; *Synlett* **2001**, *11*, 1675–1686. (d)

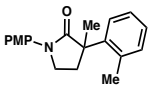
- List, B.; *Tetrahedron* **2002**, *58*, 5573–5590. (e) List, B.; *Acc. Chem. Res.* **2004**, *37*, 548–557.
- (f) Notz, W.; Tanaka, F.; Barbas III, C. F.; *Acc. Chem. Res.* **2004**, *37*, 580–591. (g) Zhang, S.; Wang, W.; Zhou, Q.–L. *Privileged Chiral Ligands and Catalysts*; Ed.; Wiley-VCH: Weinheim, Germany, 2011; pp 409–439. (h) Watson, A. J. B.; MacMillan, D. W. C.; Ojima, I.; *Enantioselective Organocatalysis Involving Iminium, Enamine SOMO and Photoredox Activation*. In *Catalytic Asymmetric Synthesis*, 3rd ed.; Ed.; Wiley & Sons: Hoboken, NJ, 2010; pp 39–57. (i) Caputo, C. A.; Jones, N. D. *Dalton Trans.* **2007**, 4627.
6. D. C. Behenna, Y. Liu, T. Yurino, J. Kim, D. E. White, S. C. Virgil, B. M. Stoltz, *Nat. Chem.* **2012**, *4*, 130–133.
7. M. Hayashi, S. Bachman, S. Hashimoto, C. C. Eichman, B. M. Stoltz, *J. Am. Chem. Soc.* **2016**, *138*, 8997–9000
8. L.–N. Wang, Q. Cui, Z.–X. Yu, *J. Org. Chem.* **2016**, *81*, 10165–10171.
9. (a) Semmelhack, M. F.; Chong, B. P.; Stauffer, R. D.; Rogerson, T. D.; Chong, A.; Jones, L. *J. Am. Chem. Soc.* **1975**, *97*, 2507–2516. (b) Semmelhack, M. F.; Stauffer, R. D.; Rogerson, T. D. *Tetrahedron Lett.* **1973**, *14*, 4519–4522.
10. (a) Satoh, T.; Kawamura, Y.; Miura, M.; Nomura, M.; *Angew. Chem.* **1997**, *109*, 1820–1822; *Angew. Chem. Int. Ed.* **1997**, *36*, 1740–1742. (b) Satoh, T.; Inoh, J.; Kawamura, Y.; Miura, M.; Nomura, M.; *Bull. Chem. Soc. Jpn.* **1998**, *71*, 2239 – 2246. (c) Y. Terao, T. Satoh, M. Miura, M. Nomura, *Bull. Chem. Soc. Jpn.* **1999**, *72*, 2345 – 2350.
11. Palucki, M.; Buchwald, S. L. *J. Am. Chem. Soc.* **1997**, *119*, 11108 – 11109.
12. Hamann, B. C. Hartwig, J. F. *J. Am. Chem. Soc.* **1997**, *119*, 12382 – 12383.
13. Johanssen, C. C. C.; Colacot, T. J. *Angew. Chem. Int. Ed.* **2010**, *49*, 676 – 707.

14. (a) Stewart, J. D.; Fields, S. C.; Kochhar, K. S.; Pinnick, H. W. *J. Org. Chem.* **1987**, *52*, 2110–2113. (b) Shaughnessy, K. H.; Hamann, B. C.; Hartwig, J. F. *J. Org. Chem.* **1998**, *63*, 6546–6553.

15. In the presence of strong base and no transition metal catalyst, the product was formed in good



16. (a) Cossy, J.; de Filippis, A.; Pardo, D. G. *Org. Lett.* **2003**, *5*, 3037–3039. (b) de Filippis, A.; Pardo, D. G.; Cossy, J. *Tetrahedron*, **2004**, *60*, 9757–9767 and *Tetrahedron*, **2004**, *60*, 9757–9767. (c) Cossy, J.; de Filippis, A.; Pardo, D. G. *Synlett*, **2003**, *14*, 2171–2174.
17. (a) Durbin, M. J.; Willis, M. C. *Org. Lett.*, **2008**, *10*, 1413–1415. (b) Altman, R. A.; Hyde, A. M.; Huang, X.; Buchwald, S. L. *J. Am. Chem. Soc.* **2008**, *130*, 9613–9620. (c) Mai, C.-K.; Sammons, M. F.; Sammakia, T. *Org. Lett.* **2010**, *12*, 2306–2309. (d) Koch, E.; Takise, R.; Studer, A.; Yamaguchi, J.; Itami, K. *Chem. Commun.* **2015**, *51*, 855–857. (e) Duan, J.; Kwong, F. Y. A. *J. Org. Chem.* **2017**, *82*, 6468–6473. (f) Panyam, P. K. R.; Ugale, B.; Gandhi, T. *J. Org. Chem.* **2018**, *83*, 7622–7632. (g) Vignesh, A.; Kaminsky, W.; Dharmaraj, N. *Chem. Cat. Chem.* **2017**, *9*, 910–914. (h) Li, P.; Buchwald, S. L. *Angew. Chem.* **2011**, *123*, 6520–6524. *Angew. Chem. Int. Ed.* **2011**, *50*, 6396–6400. For enantioselective examples see: (i) Taylor, A. M.; Altman, R. A.; Buchwald, S. L. *J. Am. Chem. Soc.* **2009**, *131*, 9900–9901. (j) Jin, Y.; Chen, M.; Ge, S.; Hartwig, J. F. *Org. Lett.* **2017**, *19*, 1390–1393. (k) Hamada, T.; Chieffi, A.; Åhman, J.; Buchwald, S. L. *J. Am. Chem. Soc.* **2002**, *124*, 1261–1268. (l) García-Fortanet, J.; Buchwald, S. L. *Angew. Chem. Int. Ed.* **2008**, *47*, 8108–8111 and *Angew. Chem.* **2008**, *120*, 8228–8231. (m) Liao, X.; Weng, Z.; Hartwig, J. F. *J. Am. Chem. Soc.* **2008**, *130*, 195–200.

18. We did note that Pd₂(pm-dba)₃ does lead to a more reactive catalyst. See Table 2.3.5.
19. Marcone, J. E.; Moloy, K. G. *J. Am. Chem. Soc.* **1998**, *120*, 8527–8528.
20. (a) Goodson, F. E.; Wallow, T. I.; Novak, B. M. *J. Am. Chem. Soc.* 1997, *119*, 12441–12453.
(b) Morita, D. K.; Stille, J. K.; Norton, J. R. *J. Am. Chem. Soc.* **1995**, *117*, 8576–8581.
21. We obtained a crystal structure of Pd/L10 complex. See Appendix 4 for details.
22. A control experiment omitting the Pd catalyst revealed a background reaction by which the same product was formed in 80% yield.
23. Using Method A, the corresponding *ortho*-methyl product was obtained in only 14% yield. See Appendix 2 for more details. 
24. Vitaku, E.; Smith, D. T.; Njardarson, J. T. *J. Med. Chem.* **2014**, *57*, 10257–10274.
25. Hayashi, M.; Bachman, S.; Hashimoto, S.; Eichman, C. C.; Stoltz, B. M.; *J. Am. Chem. Soc.* **2016**, *138*, 8997–9000.
26. Garnier, T.; Danel, M.; Magné, V.; Pujol, A.; Bénétteau, V.; Pale, P.; Chassaing, S.; *J. Org. Chem.* **2018**, *83*, 6408–6422.
27. Tan, B. Y.; Teo, Y. *Synlett* **2015**, *26*, 1697-1701.
28. Griffiths, R. J.; Burley, G. A.; Talbot, E. P. A.; *Org. Lett.* **2017**, *19*, 870-873.
29. Buswell, M.; Fleming, I.; Ghosh, U.; Mack, S.; Russell, M.; Clark, B.; *Org. Biomol. Chem.* **2004**, *2*, 3006-3017.
30. Zhou, X.; Zhang, G.; Gao, B.; Huang, H.; *Org. Lett.* **2018**, *20*, 2208-2212
31. Fraser, R. R.; Mansour, T. S. Savard, S. *J. Org. Chem.* **1985**, *50*, 3232–3234.

APPENDIX 2

Challenging Substrates in the Palladium-Catalyzed Enantioselective Arylation of γ -Lactams with Aryl Chlorides and Bromides[†]

A2.1 INTRODUCTION

Although we found that the conditions developed for the Pd-catalyzed α -arylation of γ -lactams were fairly robust and tolerant of a wide range of reactivity, some substrates proved to be very challenging and could not withstand the high temperatures and strongly basic conditions required for efficient and selective product formation. Below are both lactams and aryl halides that resulted in low reactivity, selectivity, or both.

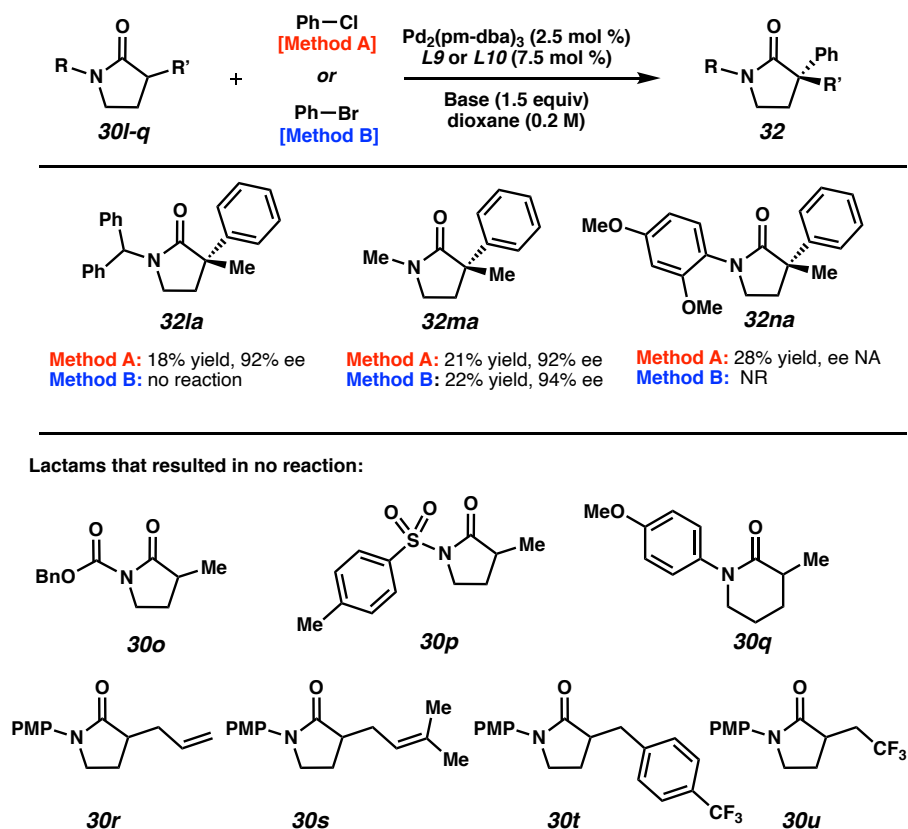
A2.2 LIMITATIONS IN THE PROTECTING GROUP AND α -SUBSTITUENT ON THE γ -LACTAM

Although the optimized conditions for the lactam arylation were highly tolerant of a number of aryl protected lactams, there were a number of limitations. The use of a bulky 2,4-dimethoxyphenyl protecting group led to significantly diminished yields and ee's in Method A,

[†] This work was performed in collaboration with Irina Geibel and Shoshana Bachman, both alumni in the Stoltz group, visiting researchers Masaki Hayashi, Hideki Shimizu, and Jeremy B. Morgan, as well as visiting graduate student Shunya Sakurai. This work has been published and adapted with permission from Jette, C. I. Geibel, I.; Bachman, S.; Hayashi, M.; Sakurai, S.; Shimizu, H.; Morgan, J. B.; Stoltz, B. M. *Angew. Chem. Int. Ed.* **2019**, 58, 4297–4301. Copyright 2019 Wiley-VCH.

and with Method B, no product was observed (**32na**, Table A2.2.1). Switching to lactams possessing alkyl protecting groups other than benzyl resulted in diminished yields in both Method A and B, however, the products were still obtained in excellent ee (**32la** and **32ma**).

Table A2.2.1. γ -Lactams that Resulted in Low Reactivity^a



[a] Conditions for each method are as follows: Method A: lactam (1.5 equiv), Ph-Cl (1.0 equiv), $\text{Pd}_2(\text{pm-dba})_3$ (2.5 mol %), **L9** (7.5 mol %), LiHMDS (1.5 equiv), dioxane (0.2 M), 100 °C, 20h. Method B: lactam (1.5 equiv), Ph-Br (1.0 equiv), $\text{Pd}_2(\text{pm-dba})_3$ (2.5 mol %), **L10** (7.5 mol %), NaHMDS (1.5 equiv), dioxane (0.2 M), 80 °C, 20 h. pmdba= 4,4'-dimethoxydibenzylideneacetone.

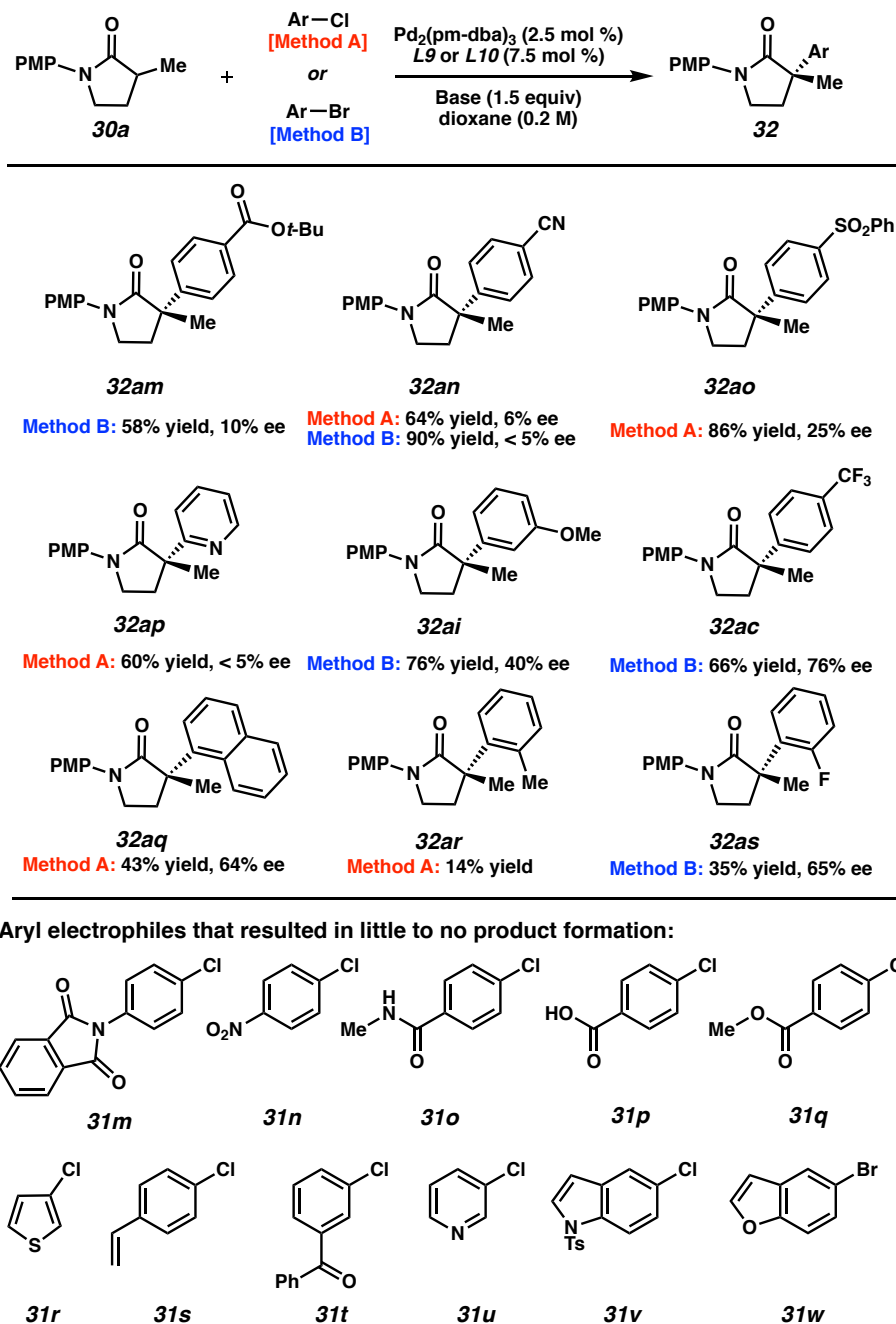
We also found that our reaction conditions were intolerant of *N*-protecting groups such as Cbz (**30o**) and tosyl (**30p**), and were specific to the γ -lactams, as the larger δ -valerolactam nucleophile led to no product formation (**30q**).

As is noted in Chapter 2.4, we found that generally, as we increased the size of the α -substituent on the lactam, significantly lower reactivities were observed. α -Substituents that resulted in no reaction include allyl (**30r**) and isoprenyl (**30s**), as well as electron-deficient benzylic (**30t**) and trifluoroethyl substituents (**30u**).

A2.3 LIMITATIONS IN FUNCTIONAL GROUP TOLERANCE ON THE ELECTROPHILE

A number of additional aryl chlorides and bromides that were not included in Table 2.4.2 were also tested (Table A2.3.1). Electrophiles that resulted in good reactivities but poor enantioselectivities include those with highly electron-withdrawing groups at the *para*-position (**32am**, **32an**, and **32ao**), or 2-chloropyridine (**32ap**), as these may undergo competing S_NAr .

We also observed that Method B works best for electron-neutral substrates: both electron-rich (**32ac**) and electron-poor substrates (**32ai**) resulted in only moderate enantioselectivities. It should be noted, however that these products could both be synthesized in high enantioselectivity with Method A (see Table 2.4.2).

Table A2.3.1. Additional Aryl Electrophiles Tested^a

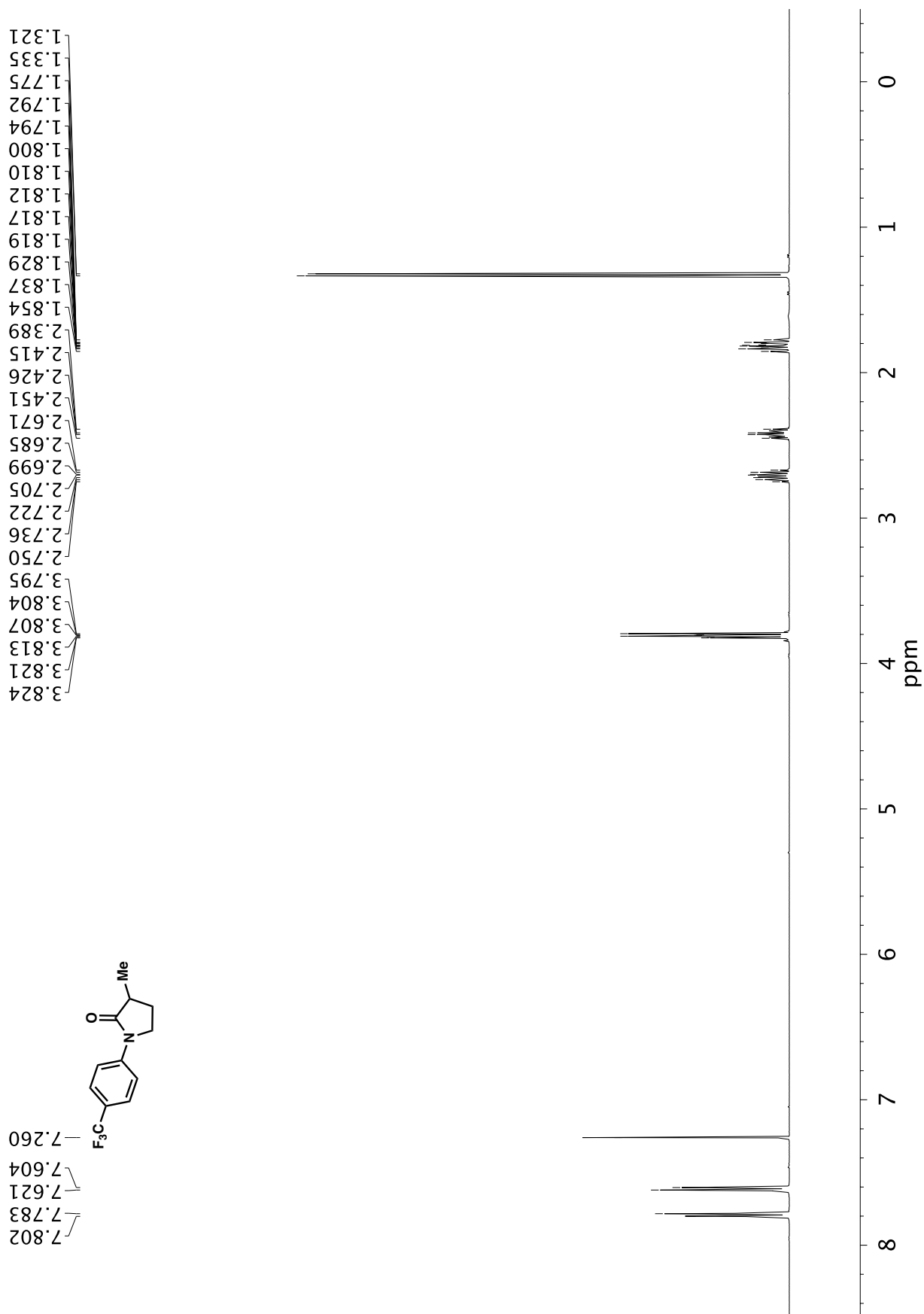
[a] Conditions for each method are as follows: Method A: **1a** (1.5 equiv), Ar-Cl (1.0 equiv), Pd₂(pm-dba)₃ (2.5 mol %), **L9** (7.5 mol %), LiHMDS (1.5 equiv), dioxane (0.2 M), 100 °C, 6 h. Method B: lactam (1.5 equiv), Ar-Br (1.0 equiv), Pd₂(pm-dba)₃ (2.5 mol %), **L10** (7.5 mol %), NaHMDS (1.5 equiv), dioxane (0.2 M), 80 °C, 15 h. [b] Absolute configuration determined via single crystal X-ray analysis. PMP = *p*-methoxyphenyl. pm-dba = 4,4'-dimethoxydibenzylideneacetone

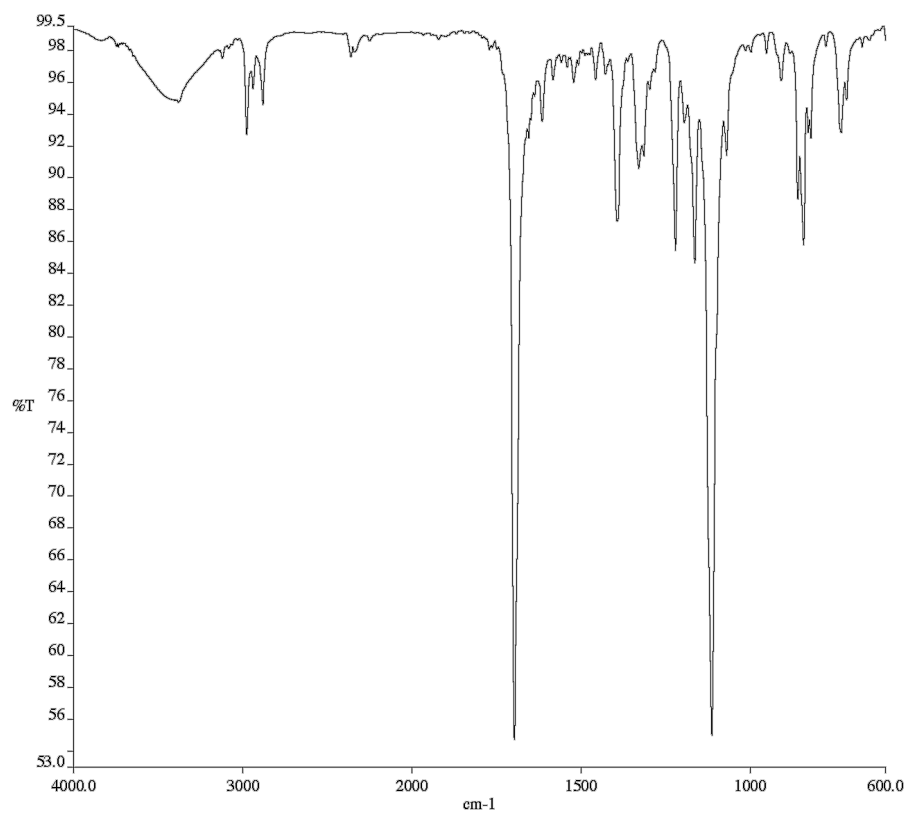
Ortho-substituted electrophiles did not fare well in either of our methods, and the corresponding products were generated in very low yields and only moderate enantioselectivities (**32aq**, **32ar**, and **32as**). In addition, our reaction conditions were intolerant of electrophiles possessing ketone (**31t**), styrene (**31s**), amide-NH (**31o**), methyl ester (**31q**), carboxylic acid (**31p**), nitro (**31n**), or phthalimide (**31m**) functional groups. Although we were able to successfully use a methyl-protected indole electrophile (**32al**, Table 2.4.2), we found that a number of additional heteroaromatic electrophiles such as thiophene (**31r**), pyridine (**31u**), tosyl-protected indole (**31v**), and benzofuran (**31w**) resulted in no product formation.

APPENDIX 3

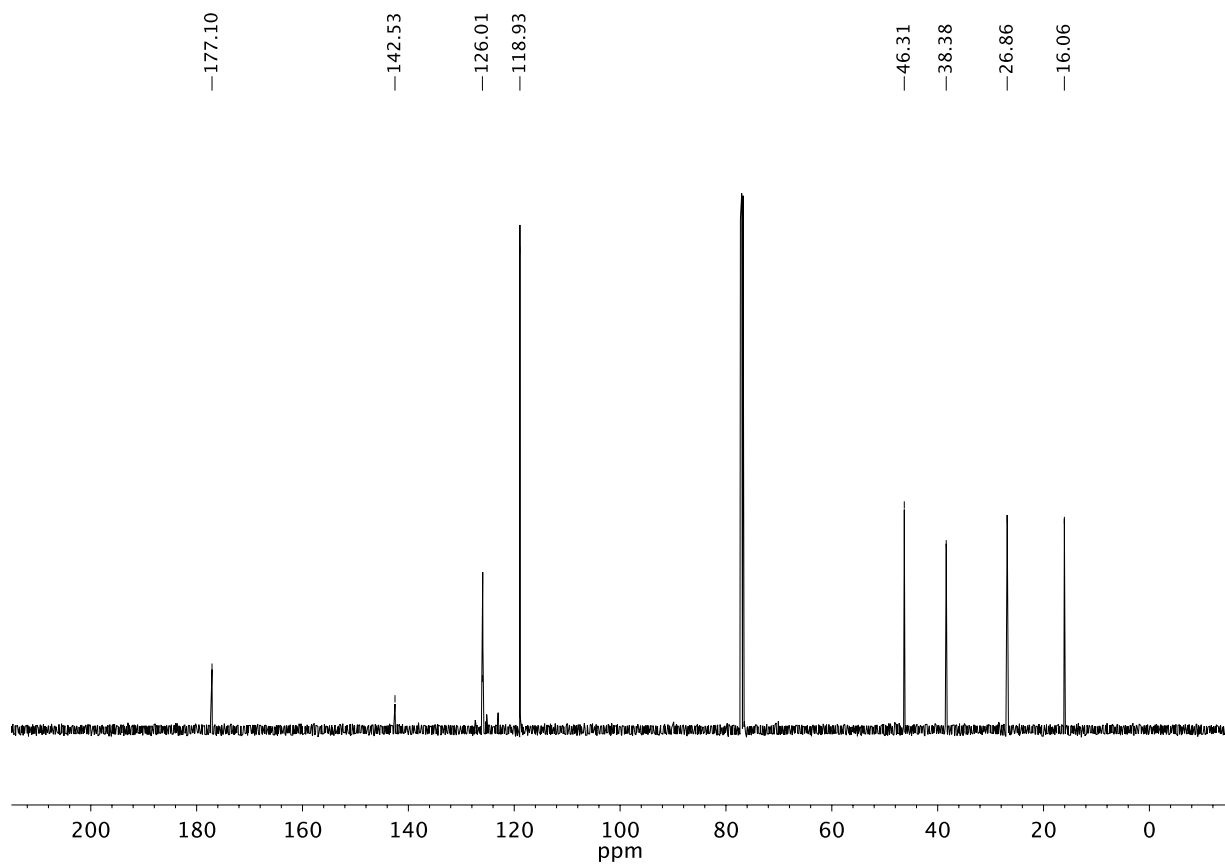
Spectra Relevant to Chapter 2:

*Palladium-Catalyzed Enantioselective Arylation of γ -Lactams with Aryl
Chlorides and Bromides*

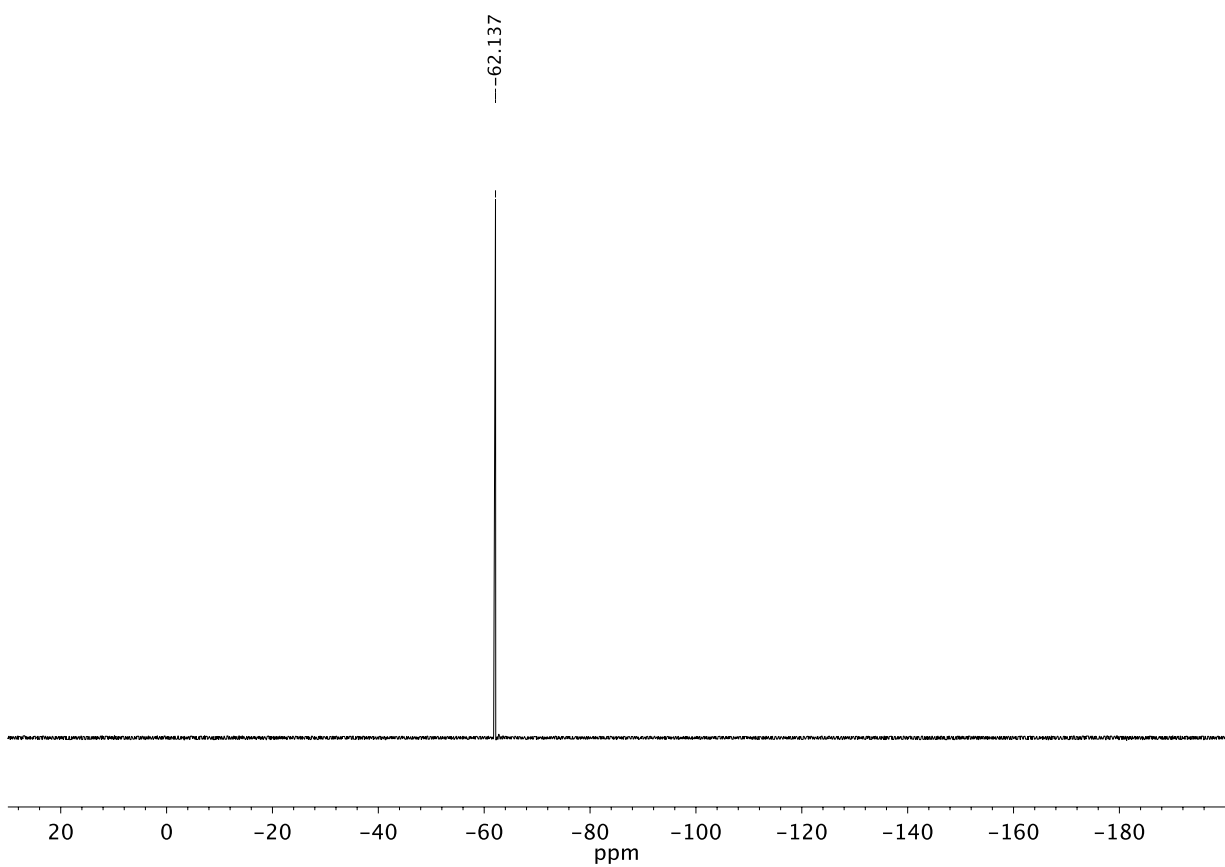




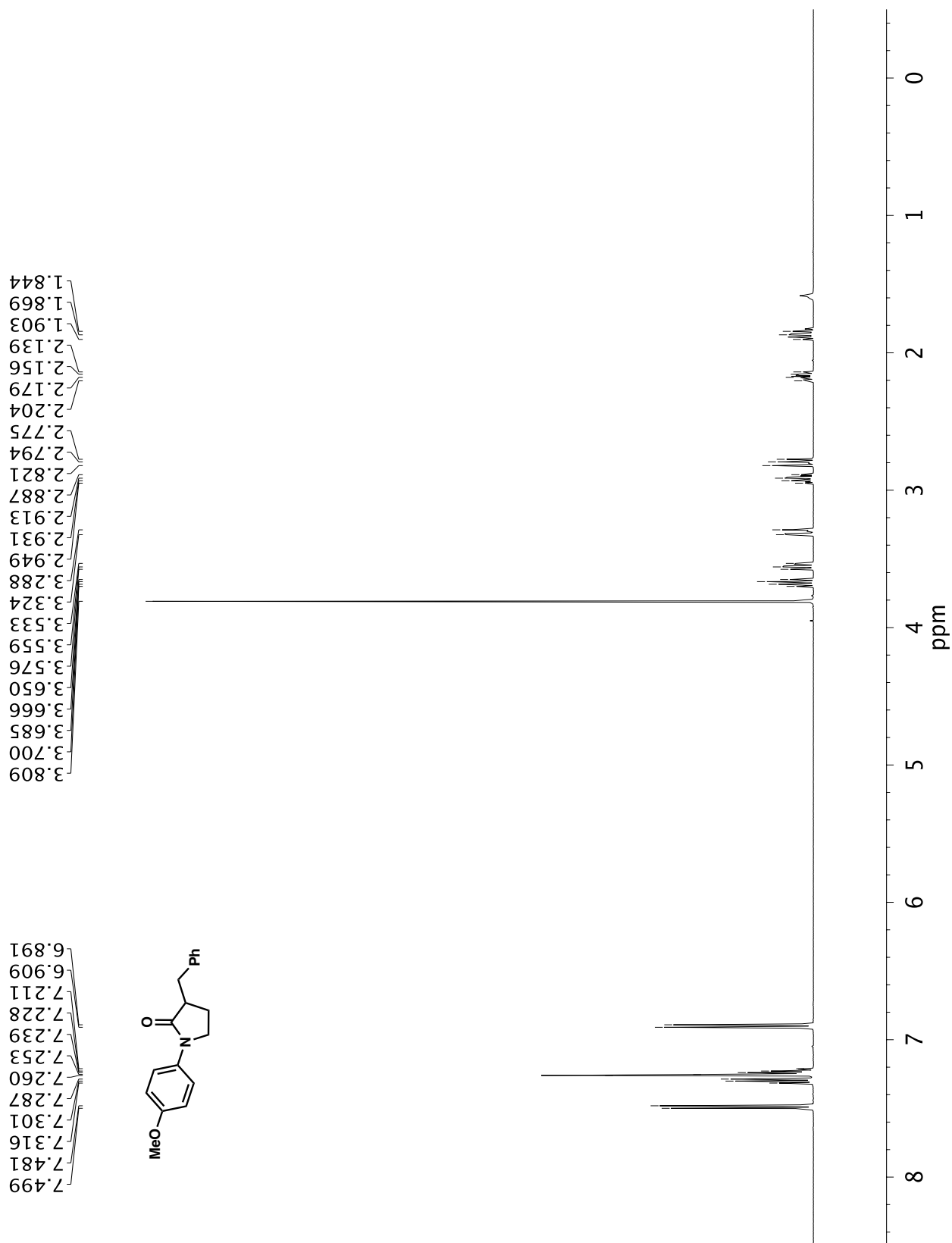
A3.2 Infrared spectrum (Thin Film, NaCl) of compound **30e**.

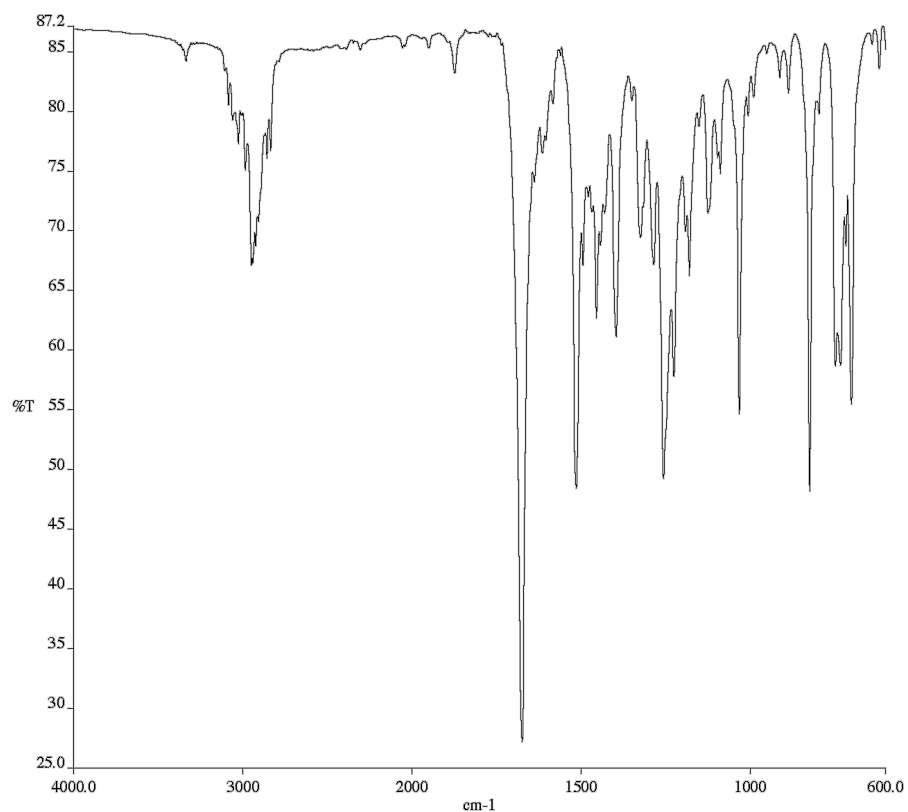


A3.3 ¹³C NMR (125 MHz, CDCl₃) of compound **30e**.

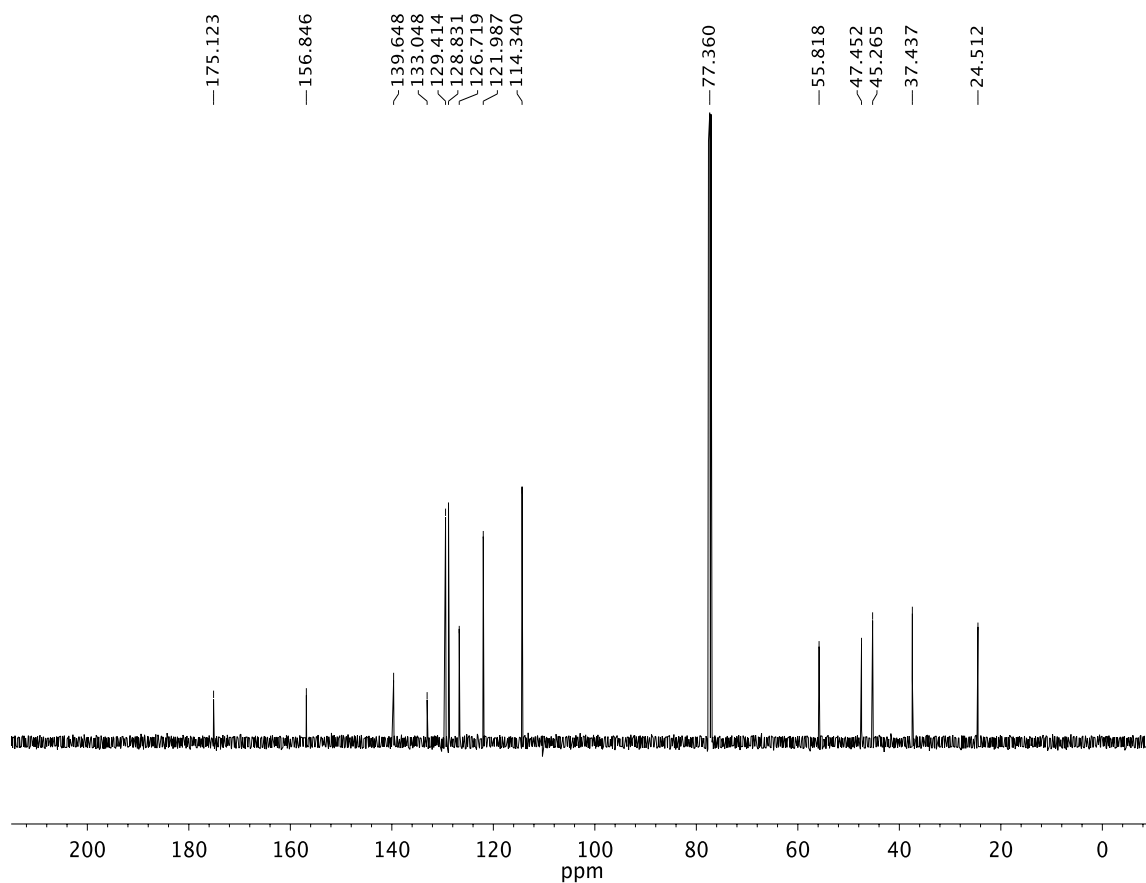


A3.4 ^{19}F NMR (282 MHz, CDCl_3) of compound **30e**.

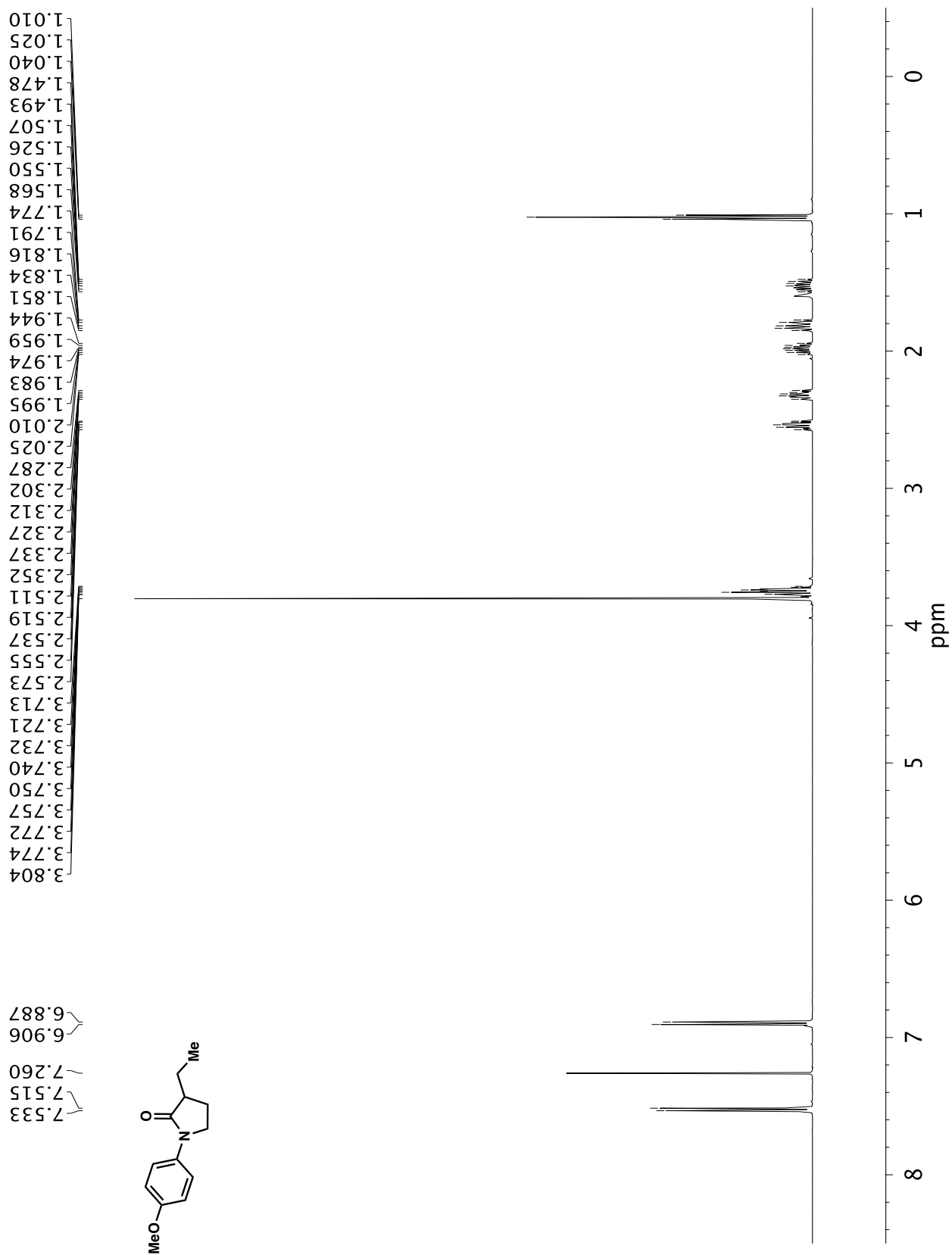
A3.5 ^1H NMR (500 MHz, CDCl_3) of compound **30g**.

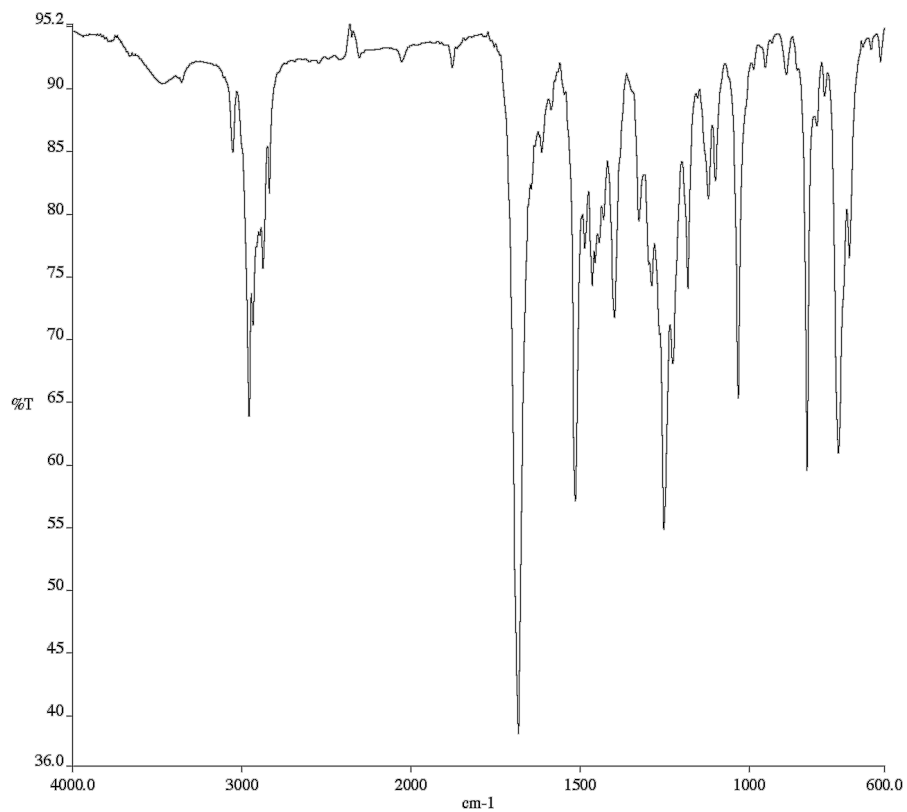


A3.6 Infrared spectrum (Thin Film, NaCl) of compound **30g**.

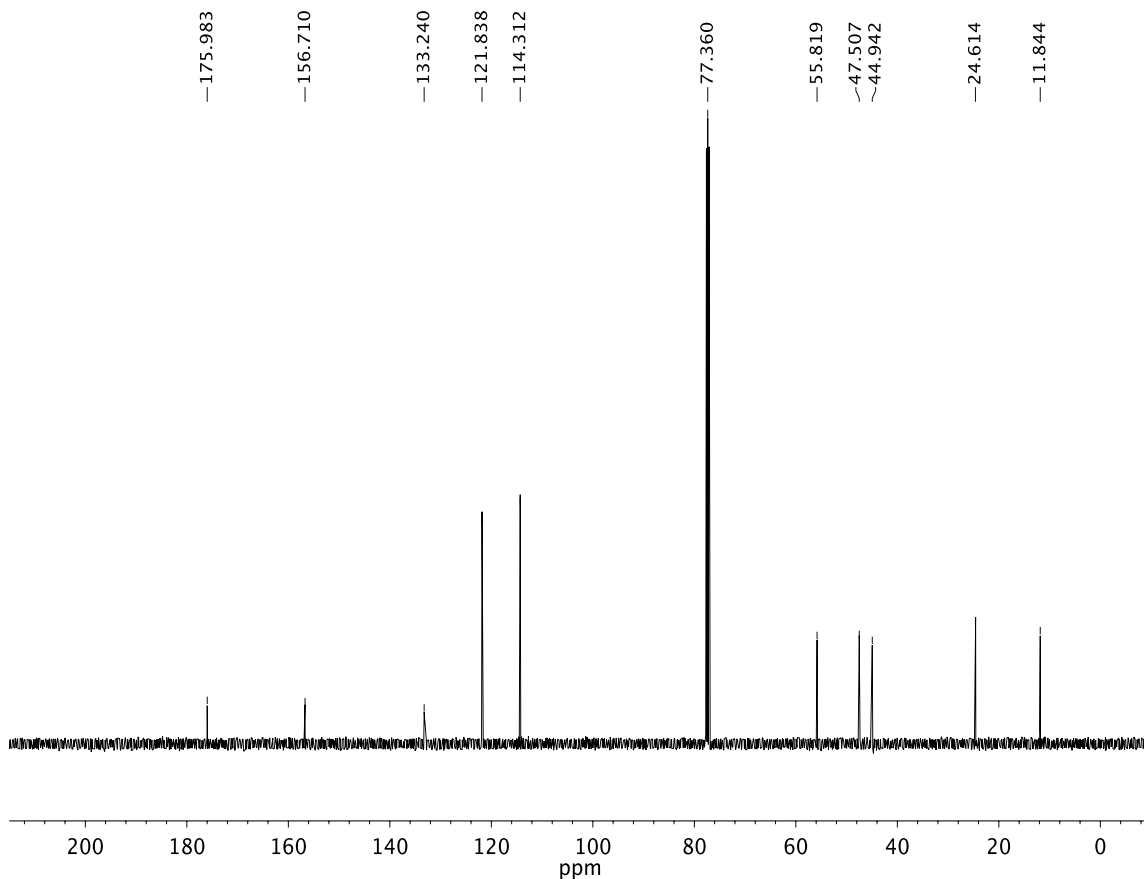


A3.7 ¹³C NMR (125 MHz, CDCl₃) of compound **30g**.

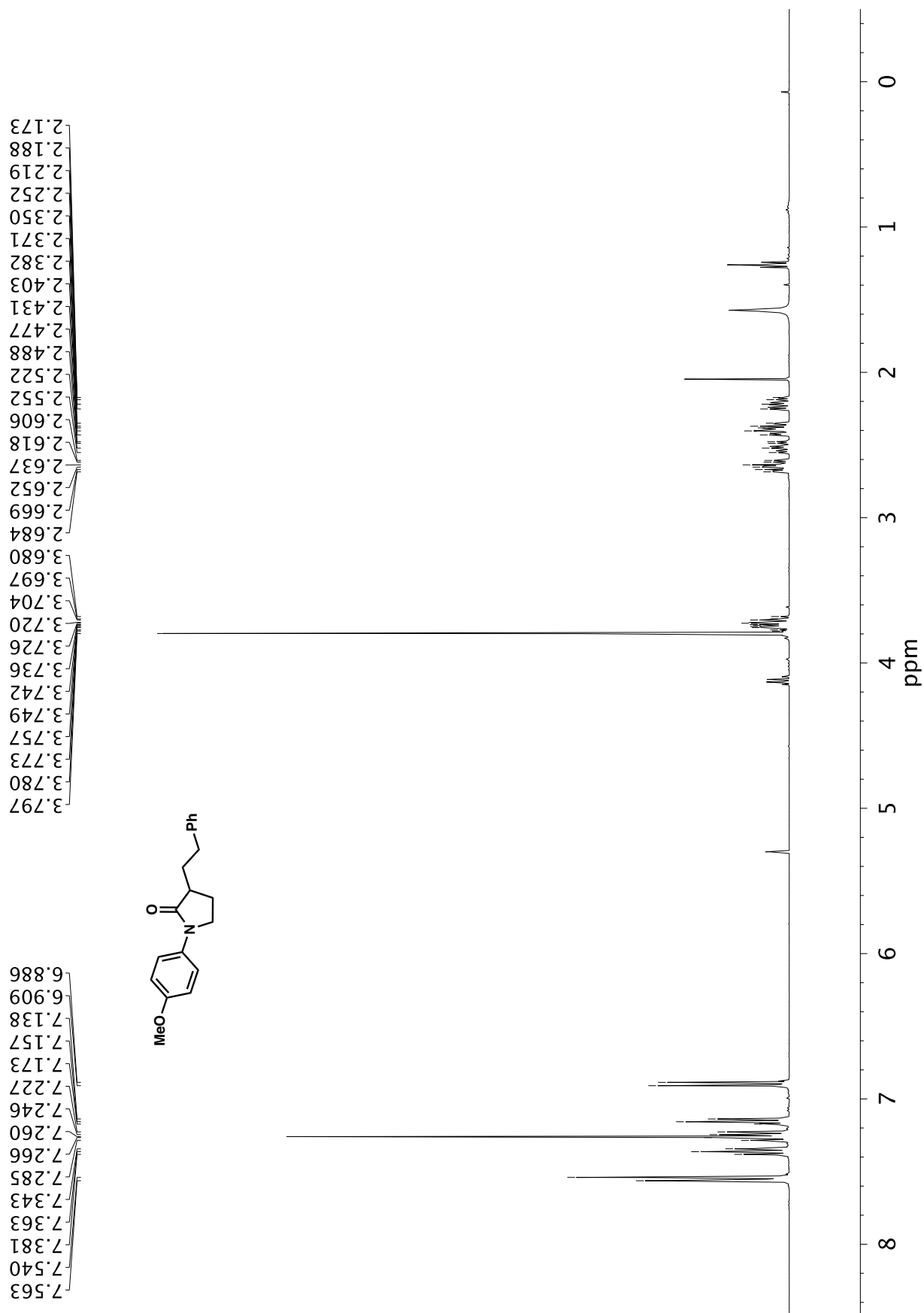




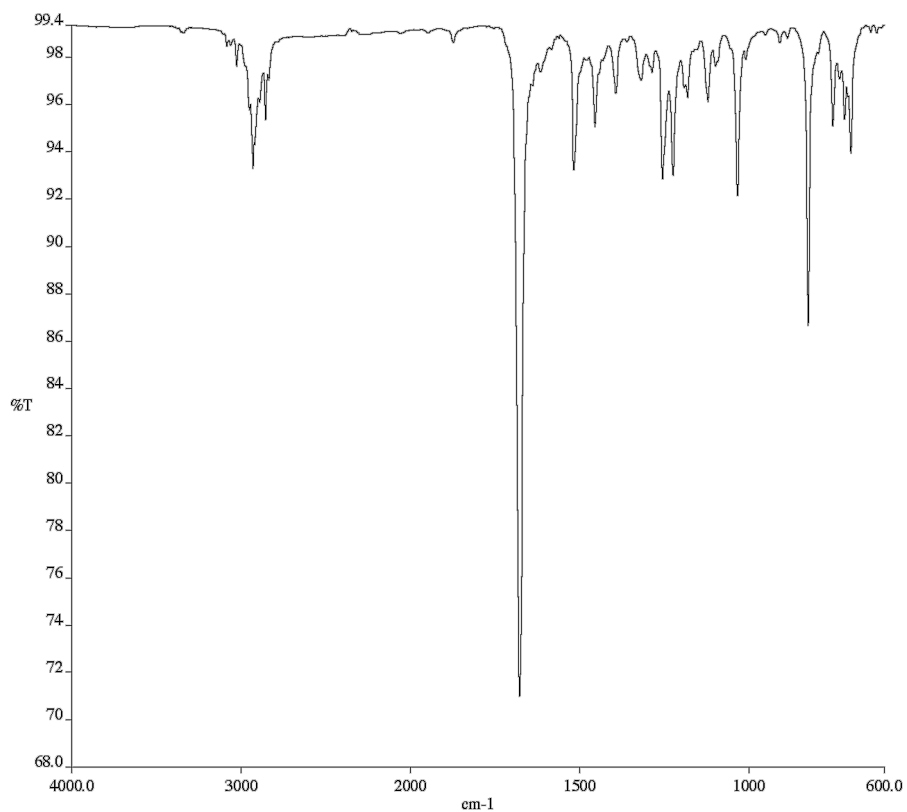
A3.9 Infrared spectrum (Thin Film, NaCl) of compound **30h**.



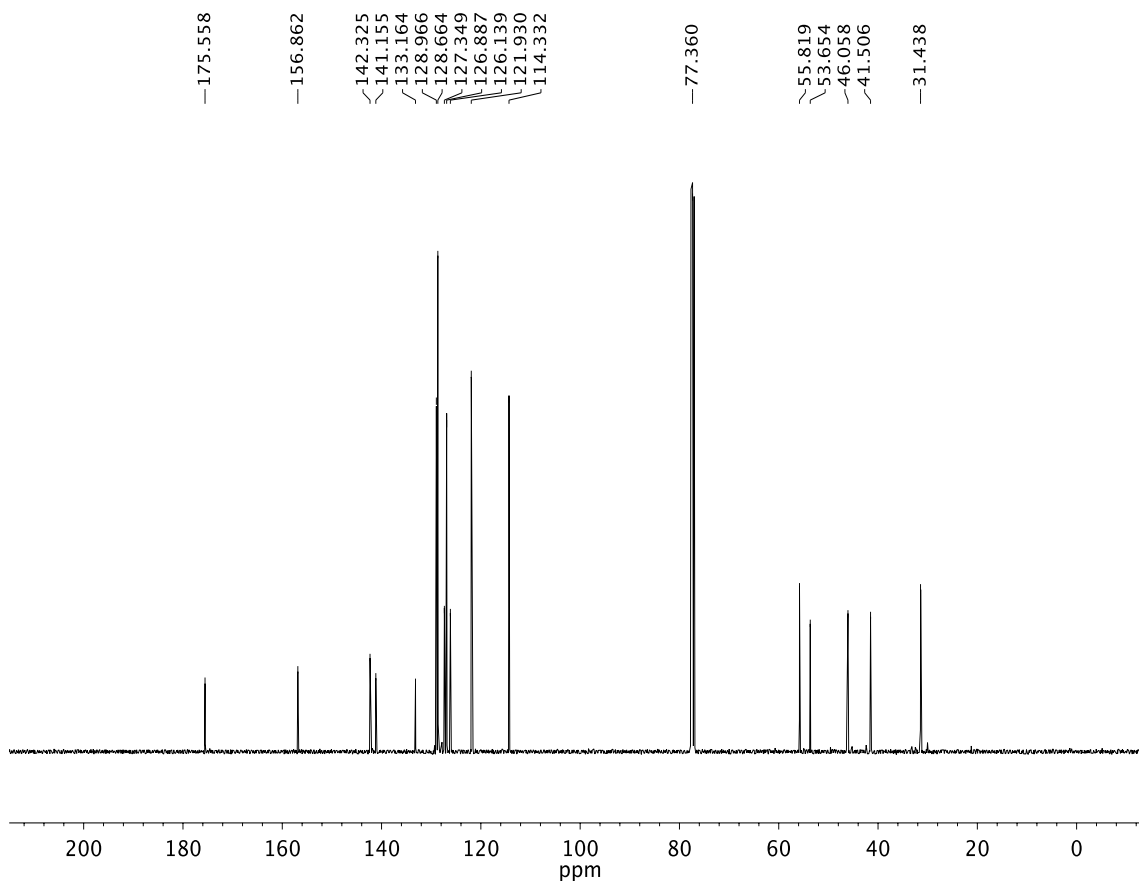
A3.10 ¹³C NMR (125 MHz, CDCl₃) of compound **30h**.



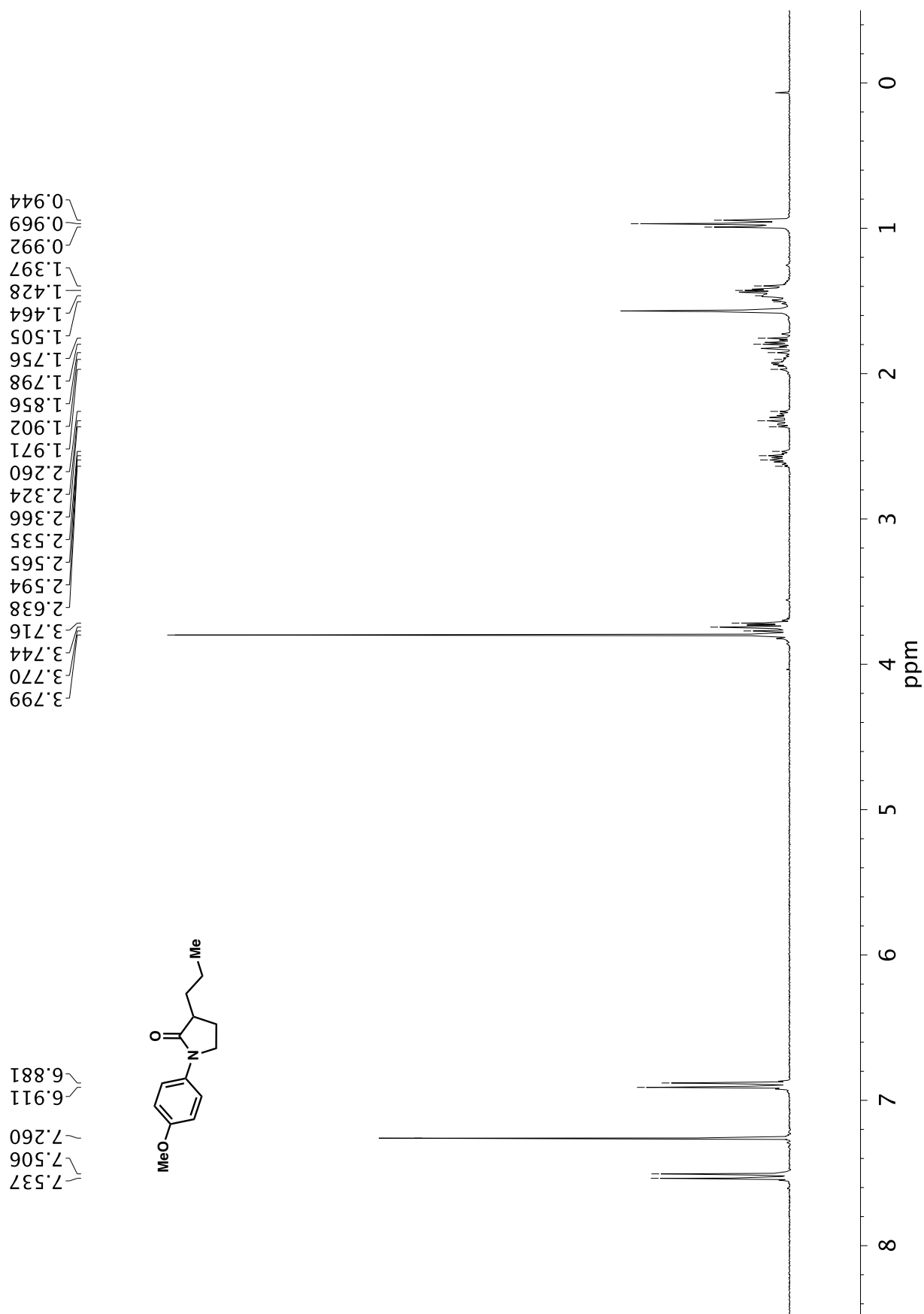
A3.11 ¹H NMR (300 MHz, CDCl₃) of compound **30j**.

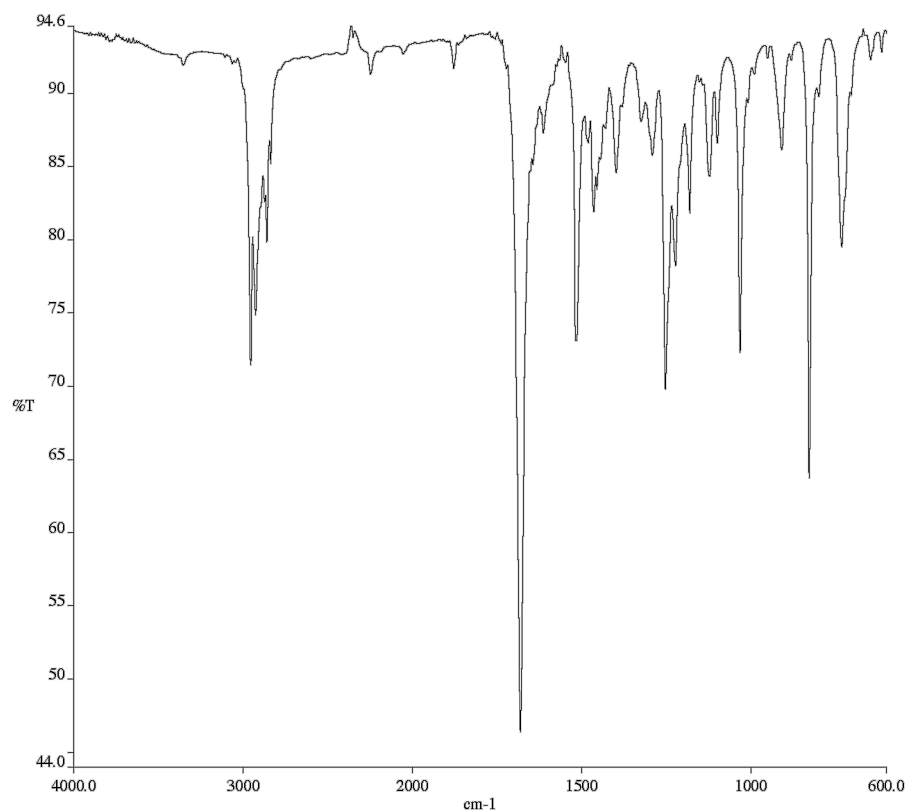


A3.12 Infrared spectrum (Thin Film, NaCl) of compound **30j**.

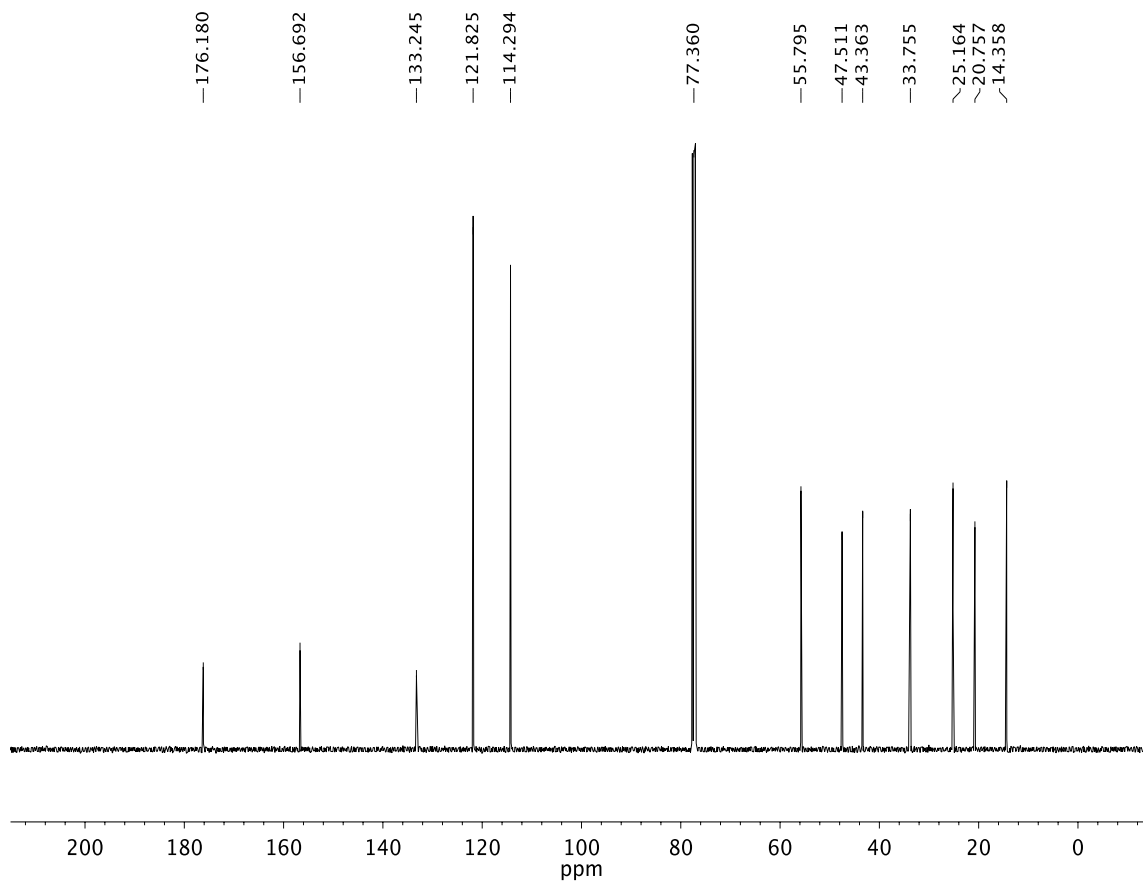


A3.13 ¹³C NMR (100 MHz, CDCl₃) of compound **30j**.

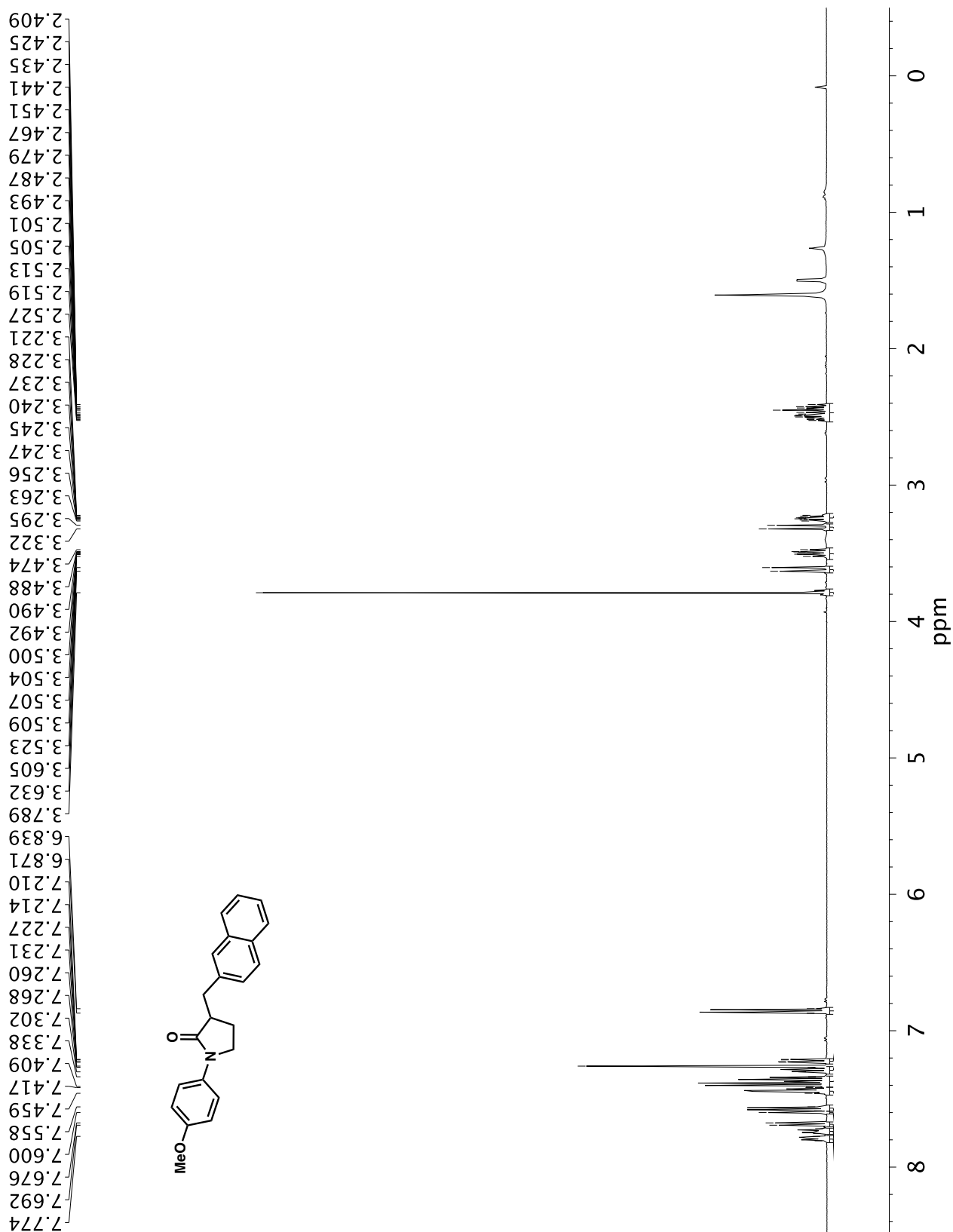
**A3.14** ^1H NMR (300 MHz, CDCl_3) of compound **30i**.

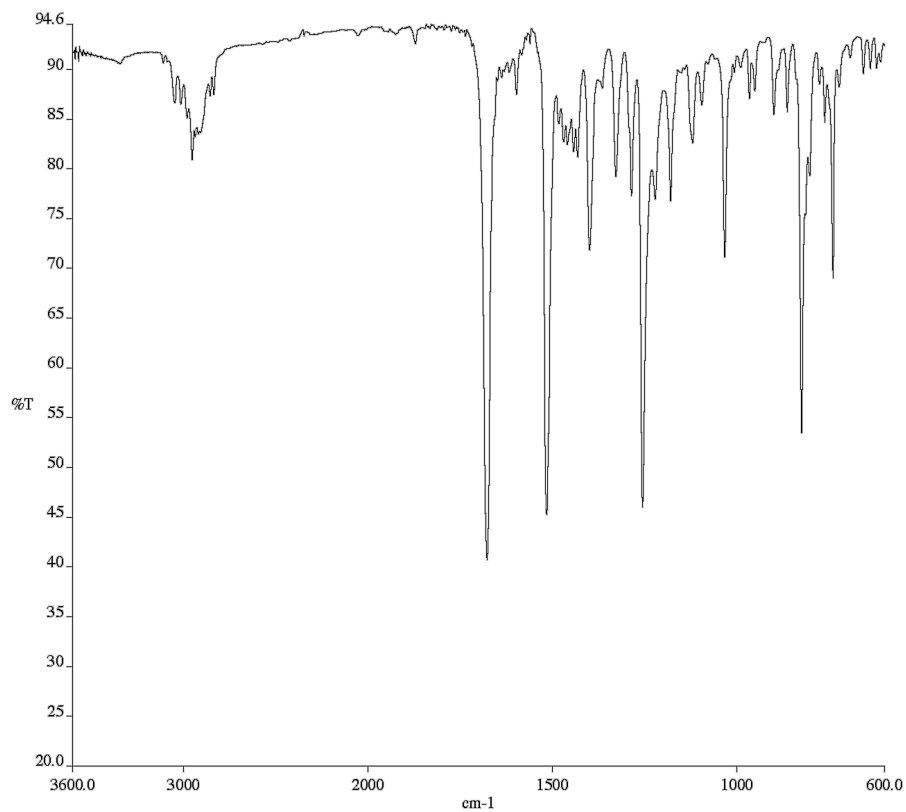


A3.15 Infrared spectrum (Thin Film, NaCl) of compound **30i**.

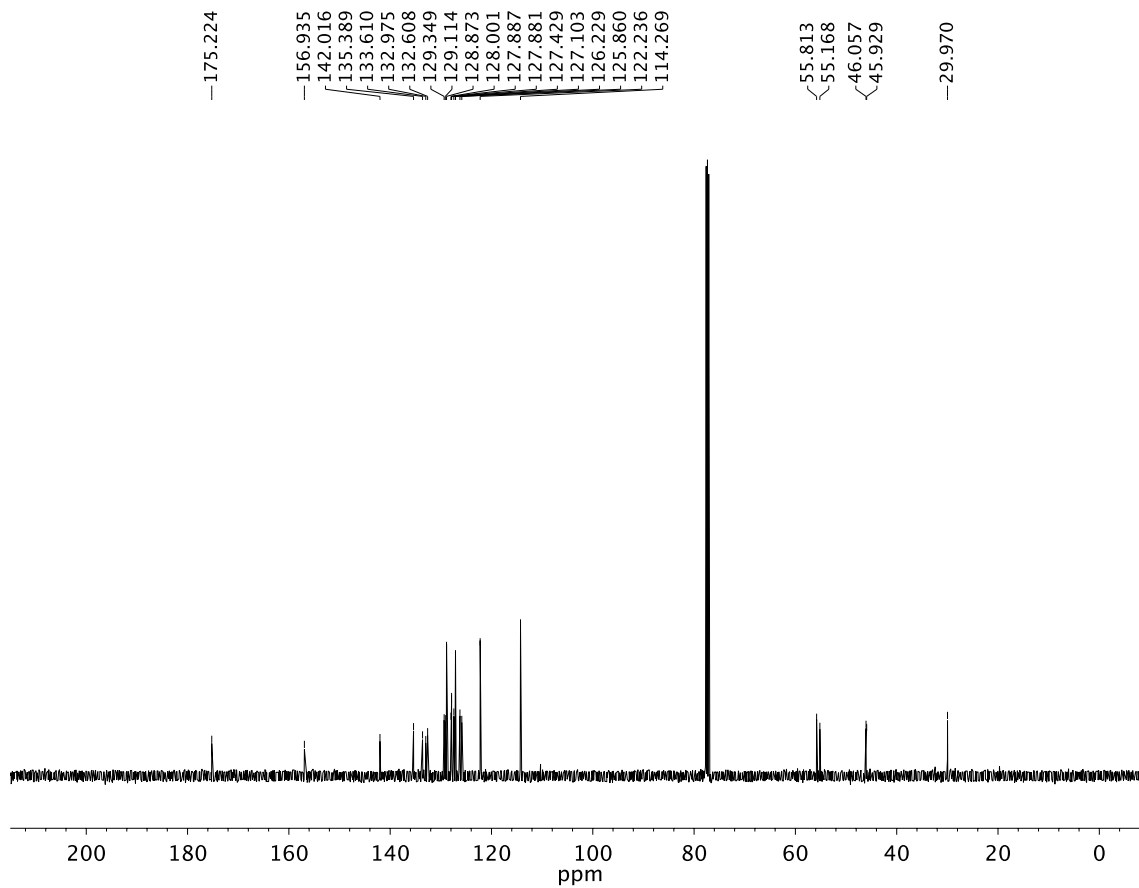


A3.16 ^{13}C NMR (100 MHz, CDCl_3) of compound **30i**.

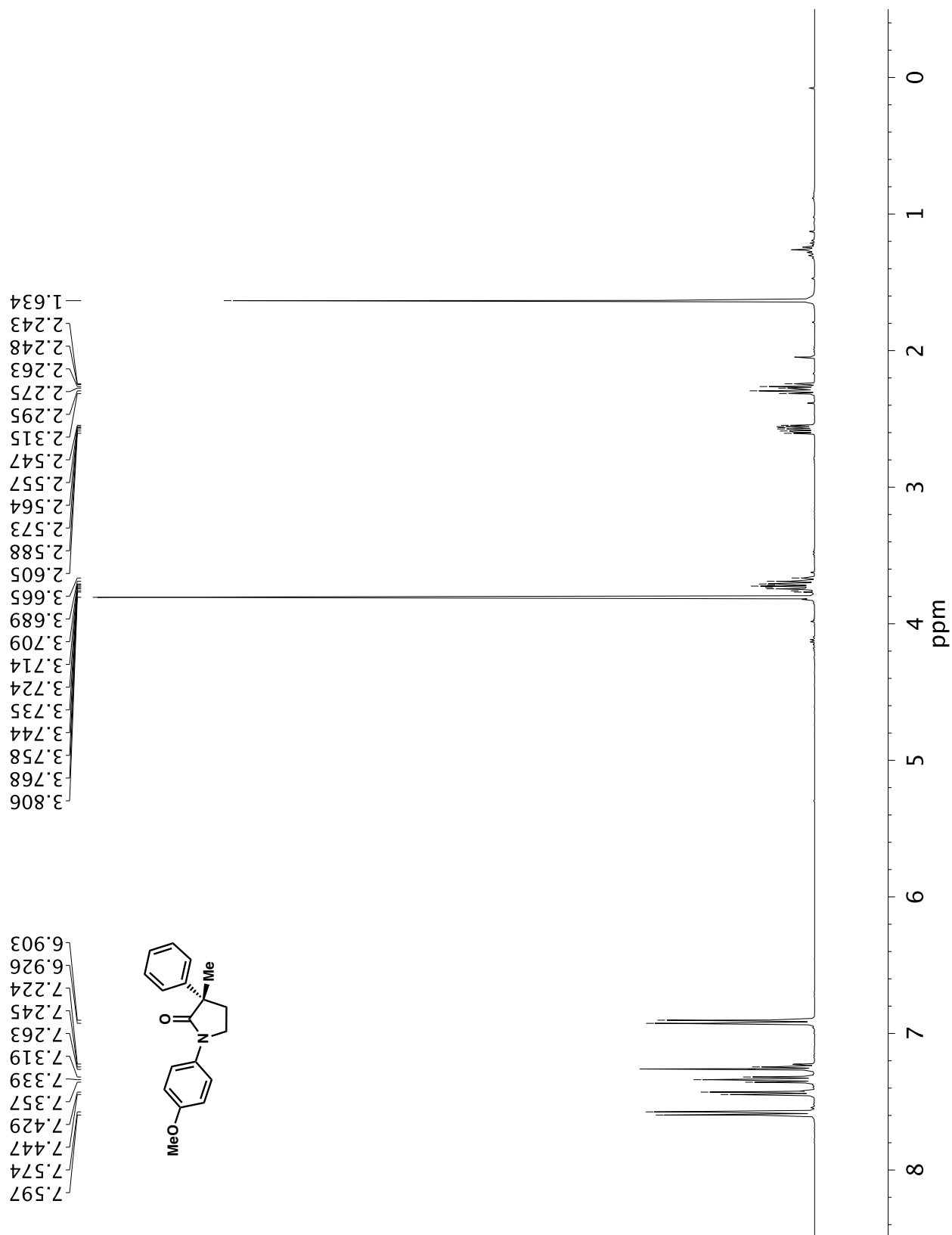
**A3.17** ¹H NMR (500 MHz, CDCl₃) of compound **30k**.

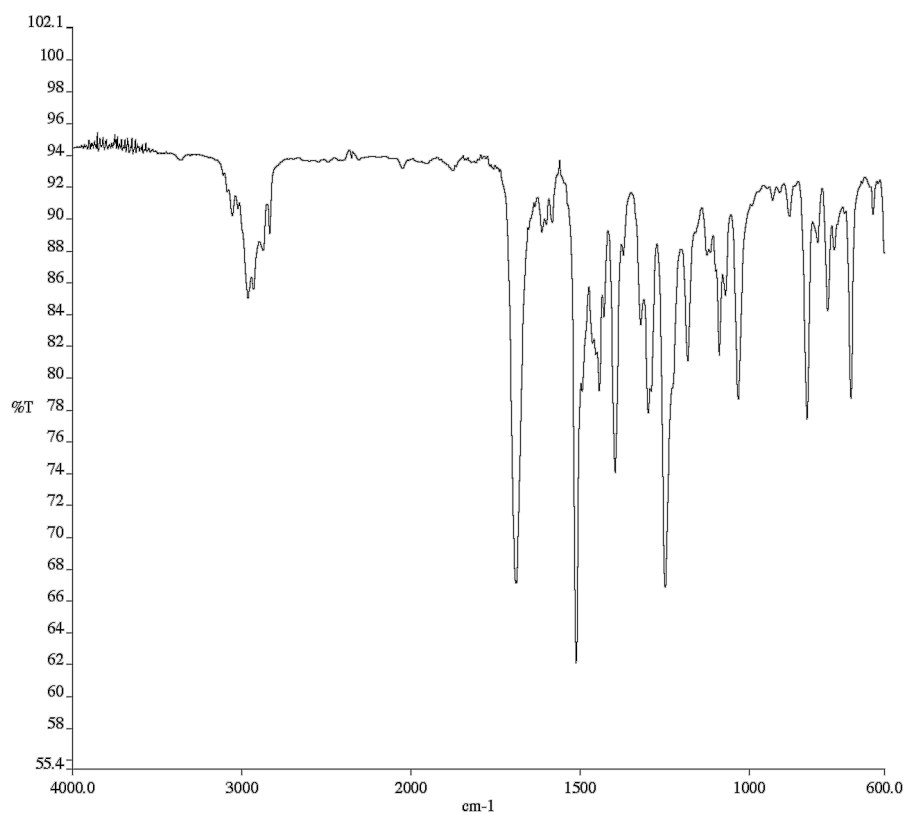


A3.18 Infrared spectrum (Thin Film, NaCl) of compound **30k**.

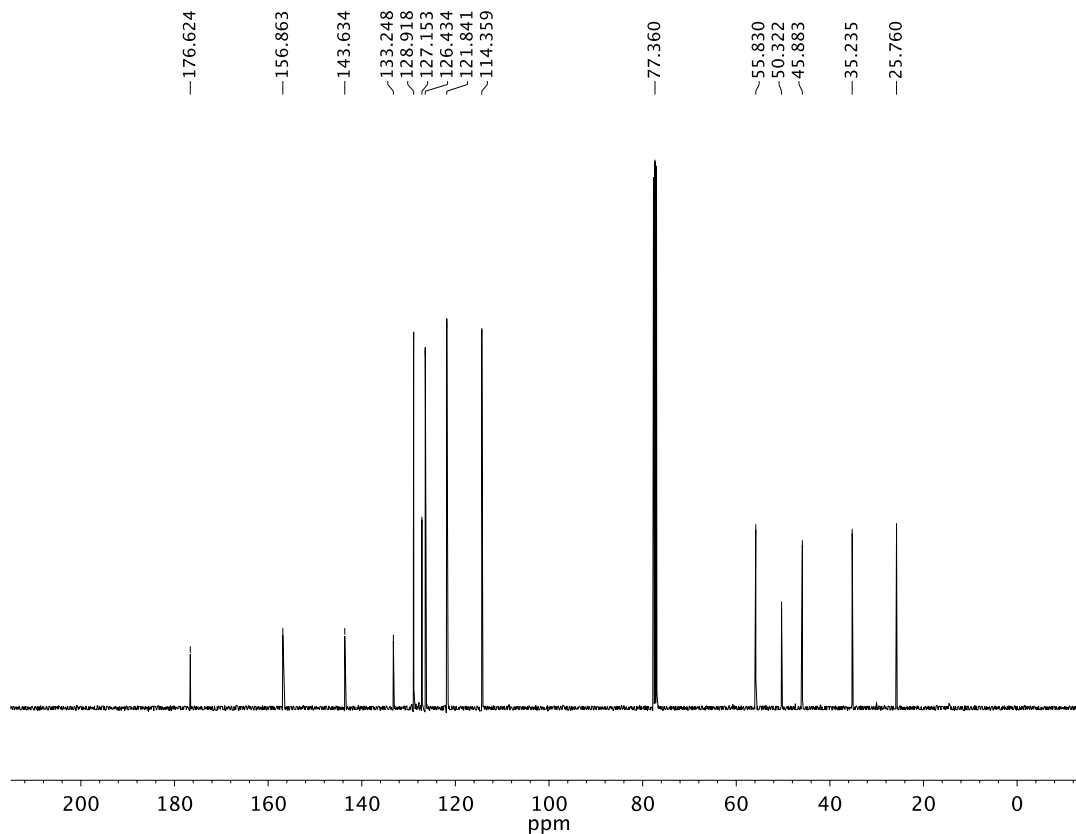


A3.19 ¹³C NMR (125 MHz, CDCl₃) of compound **30k**.

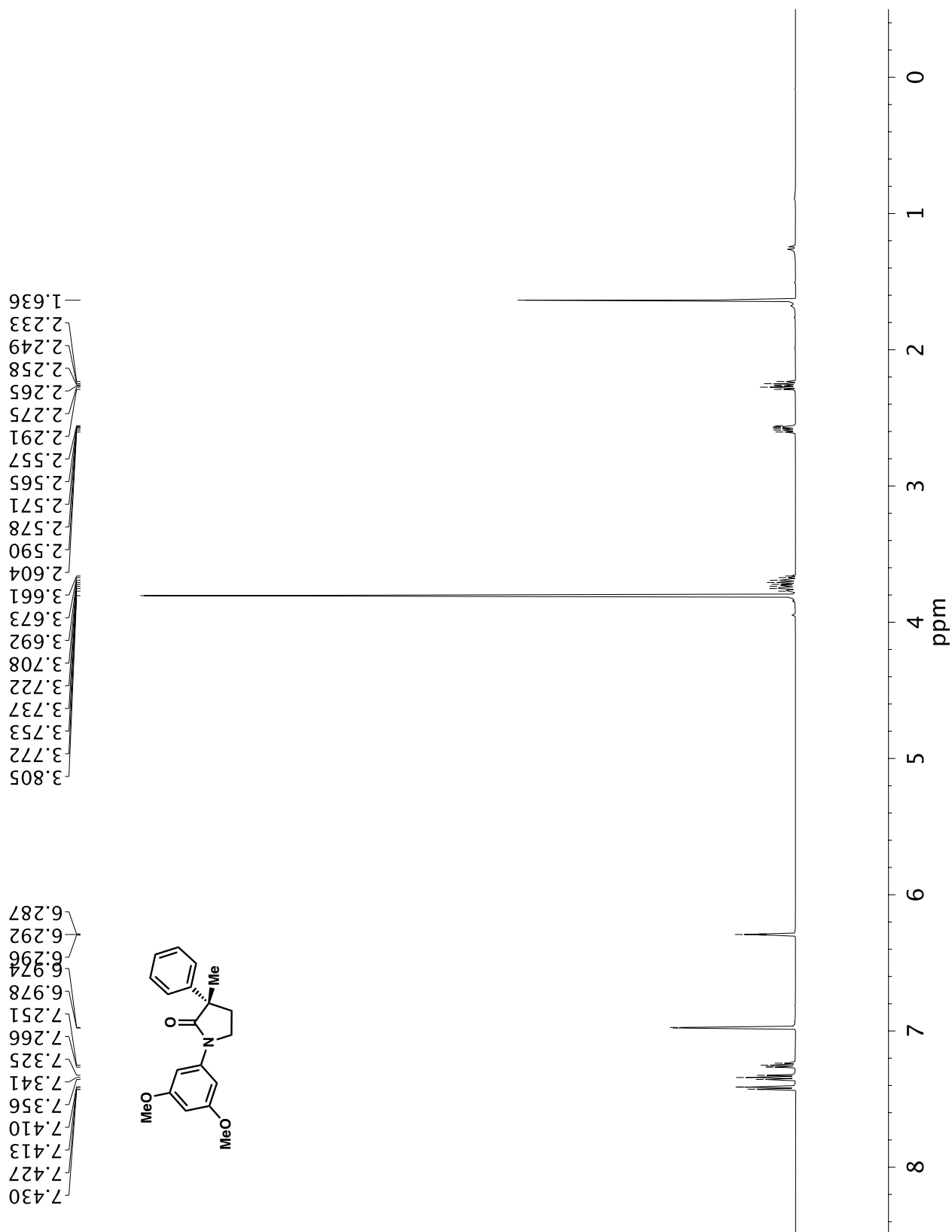
A3.20 ¹H NMR (400 MHz, CDCl₃) of compound 32aa.

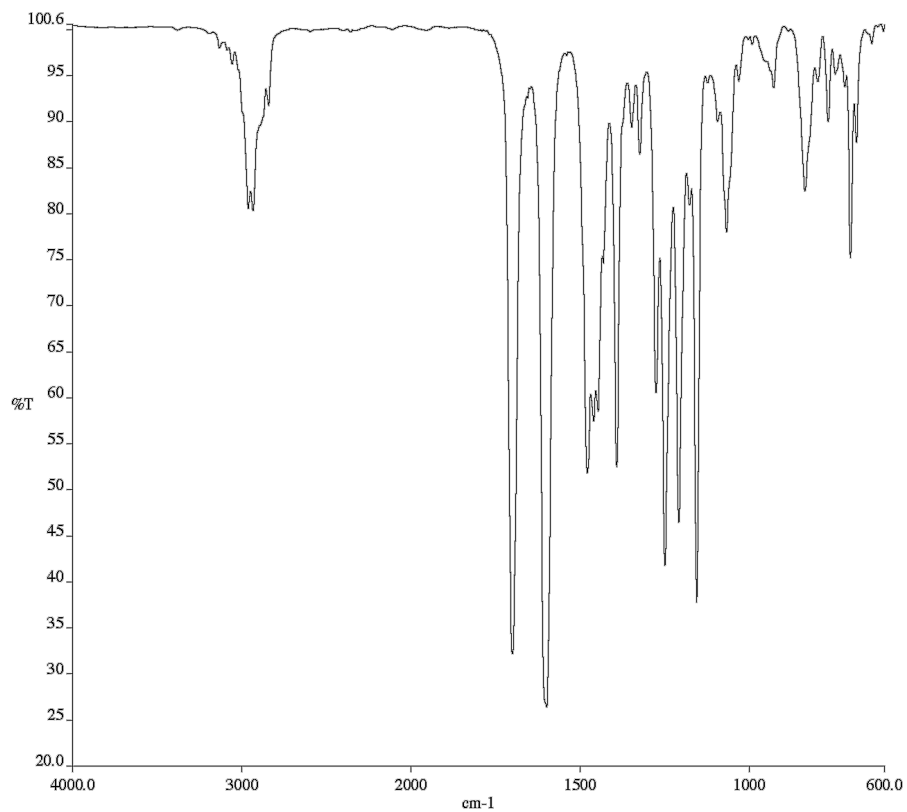


A3.21 Infrared spectrum (Thin Film, NaCl) of compound **32aa**.

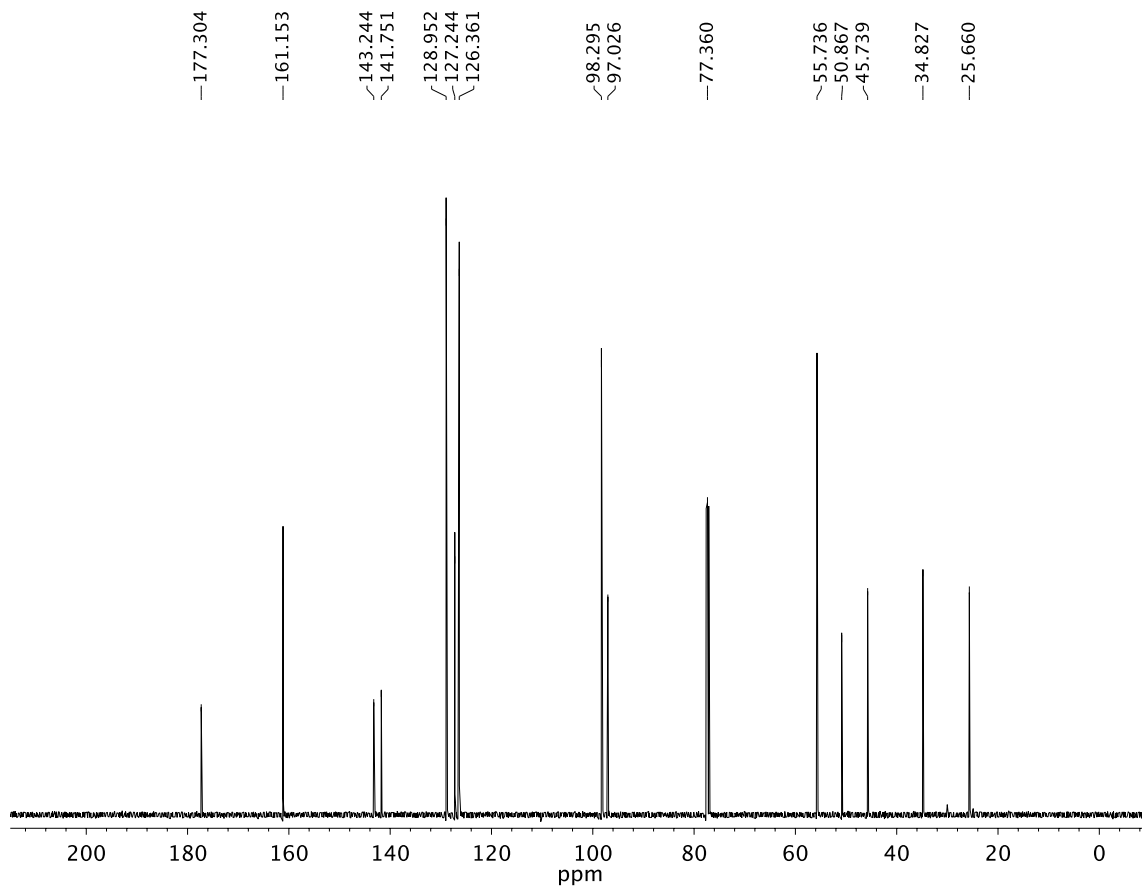


A3.22 ¹³C NMR (125 MHz, CDCl₃) of compound **32aa**.

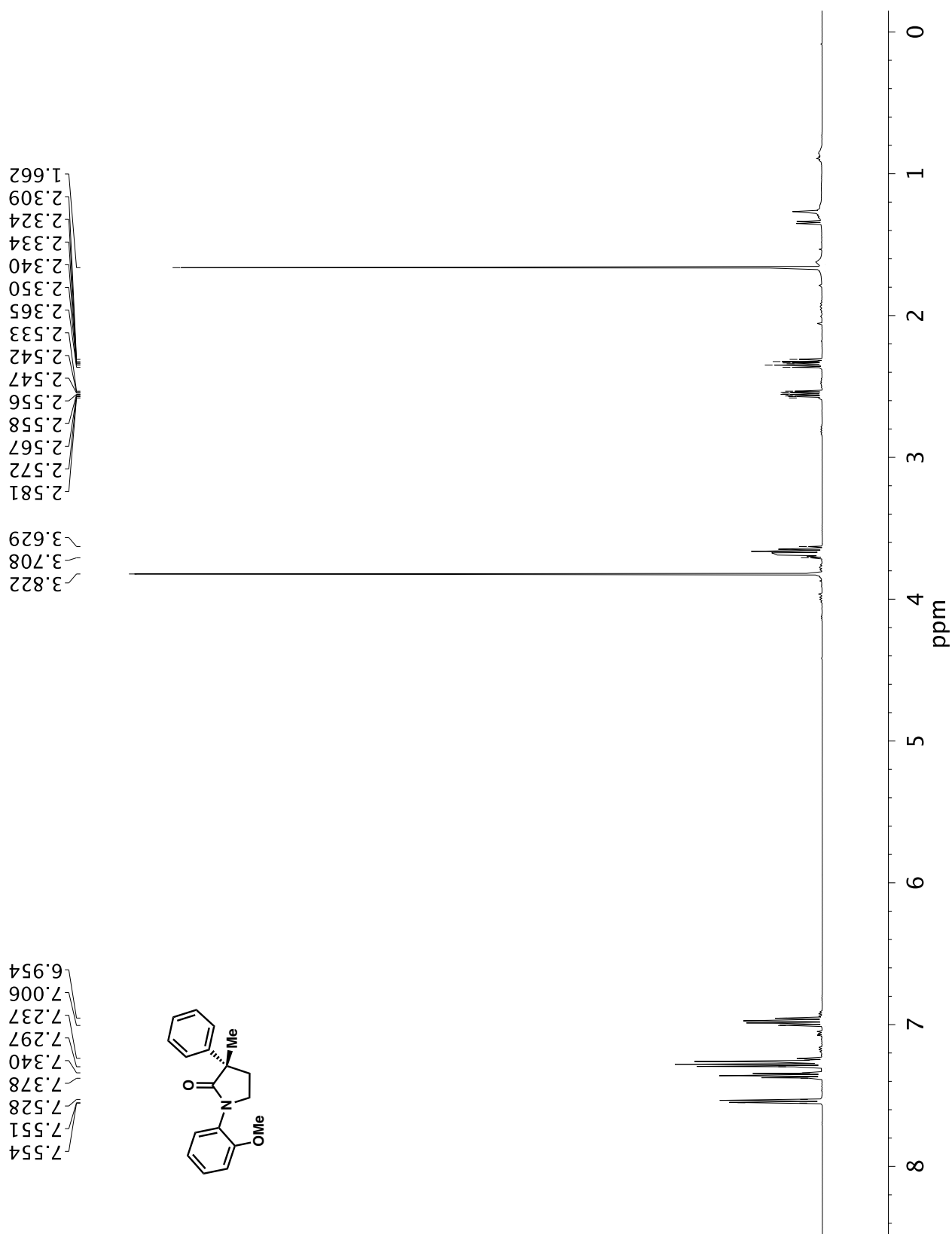


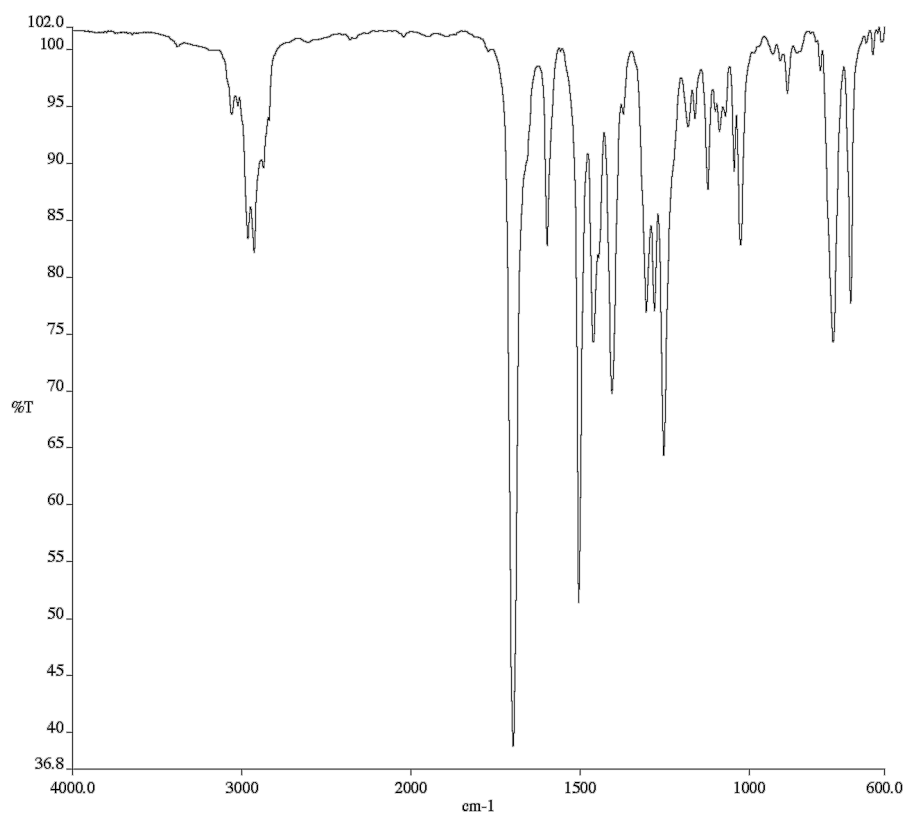


A3.24 Infrared spectrum (Thin Film, NaCl) of compound **32ba**.

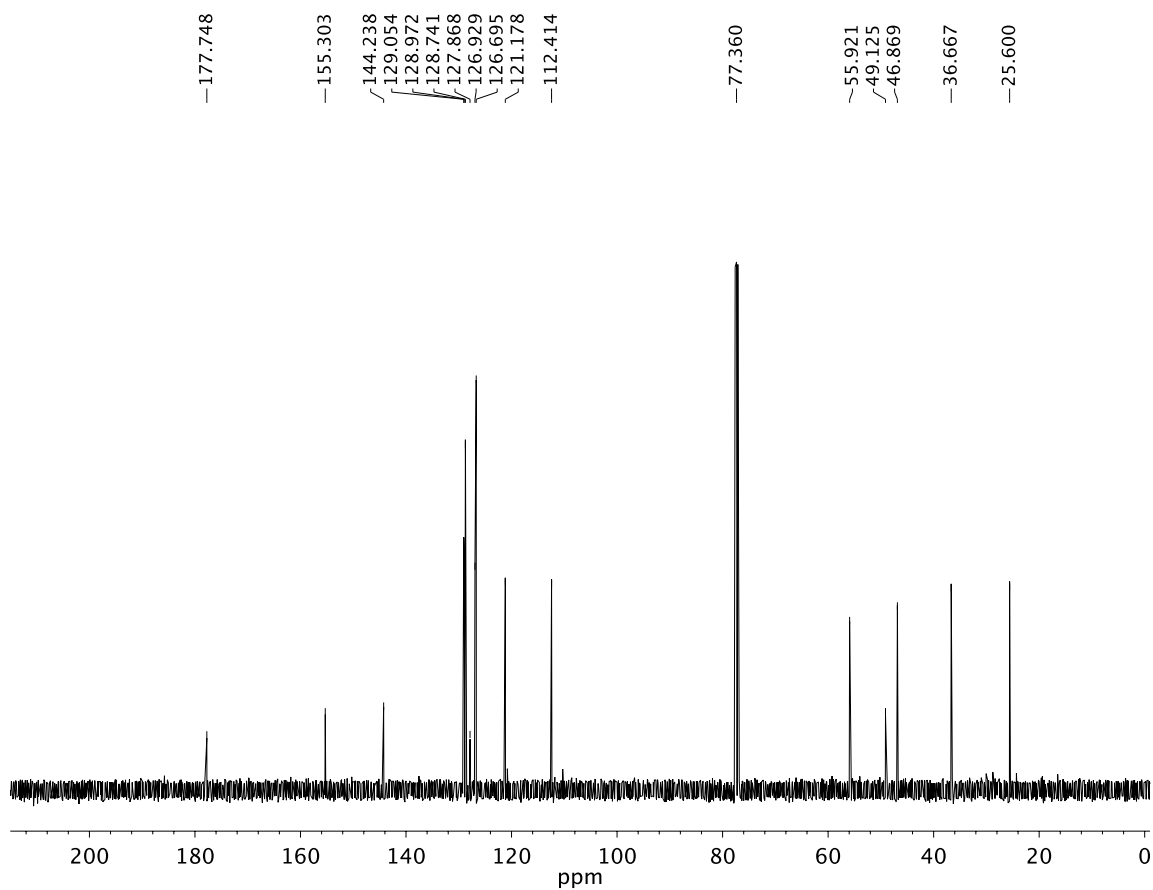


A3.25 ¹³C NMR (125 MHz, CDCl₃) of compound **32ba**.

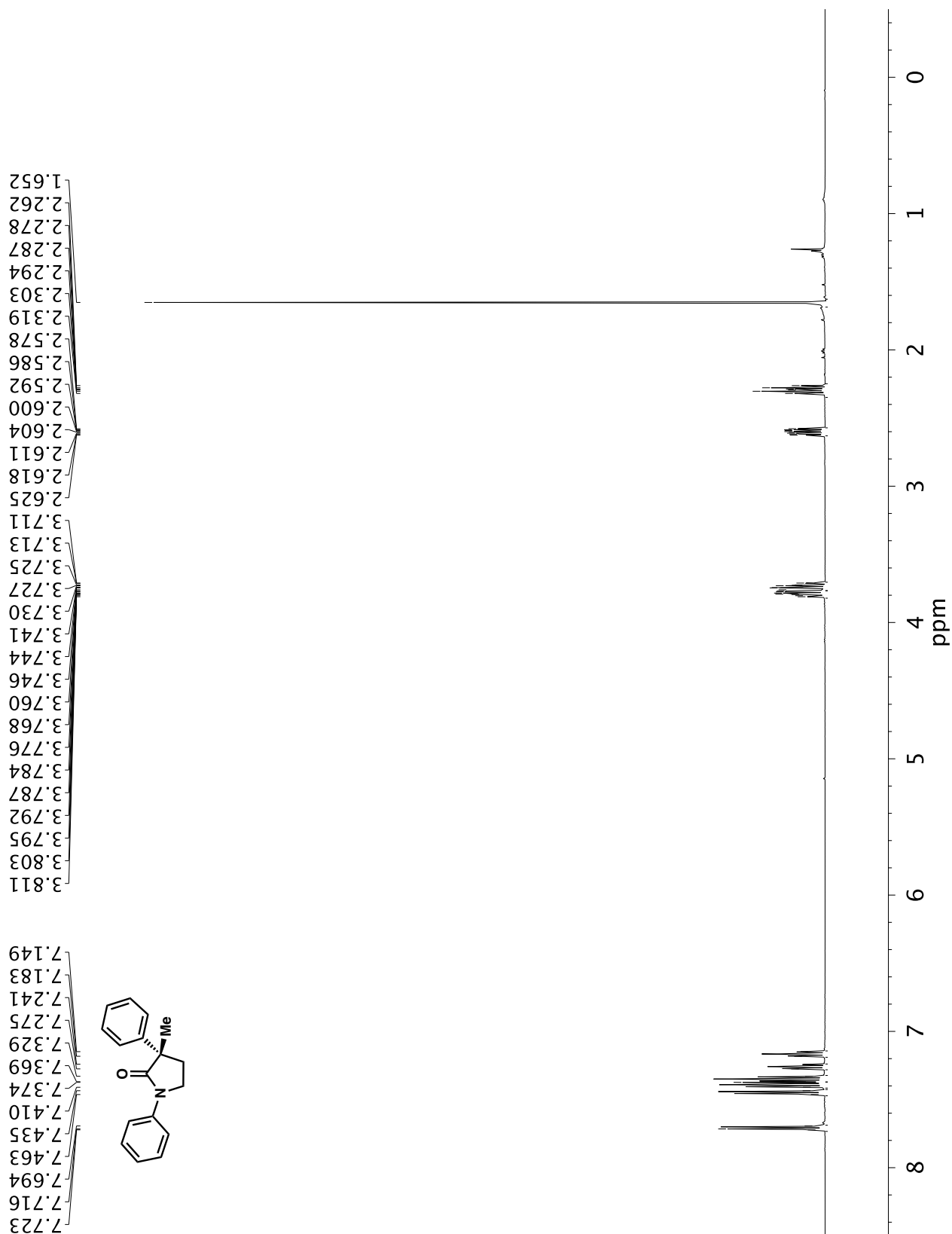


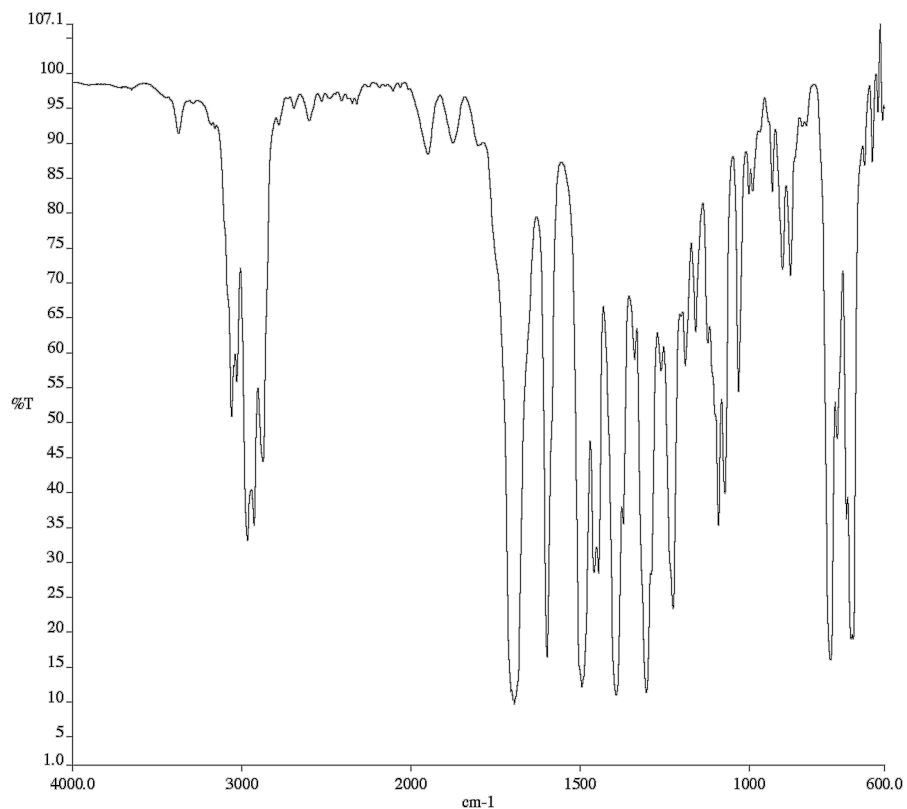


A3.27 Infrared spectrum (Thin Film, NaCl) of compound **32ca**.

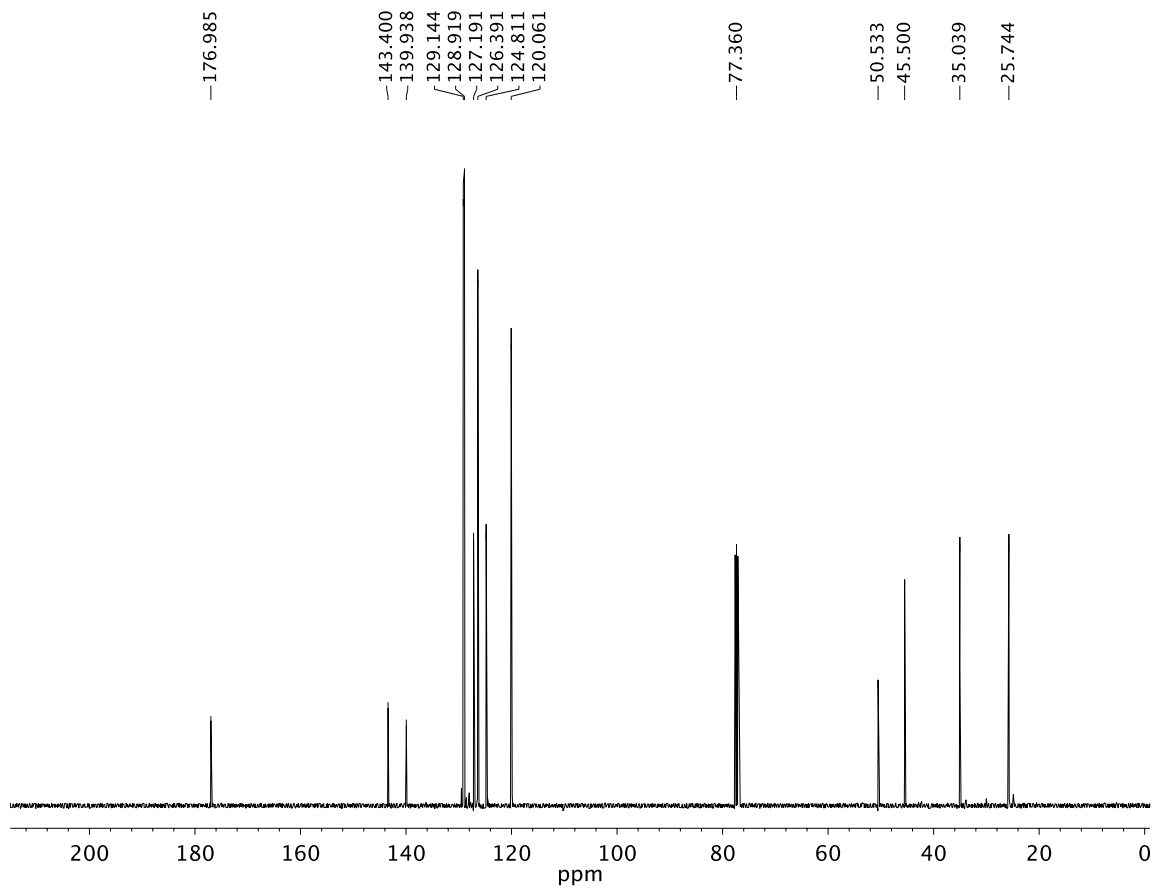


A3.28 ¹³C NMR (125 MHz, CDCl₃) of compound **32ca**.

**A3.29** ¹H NMR (500 MHz, CDCl₃) of compound **32da**.

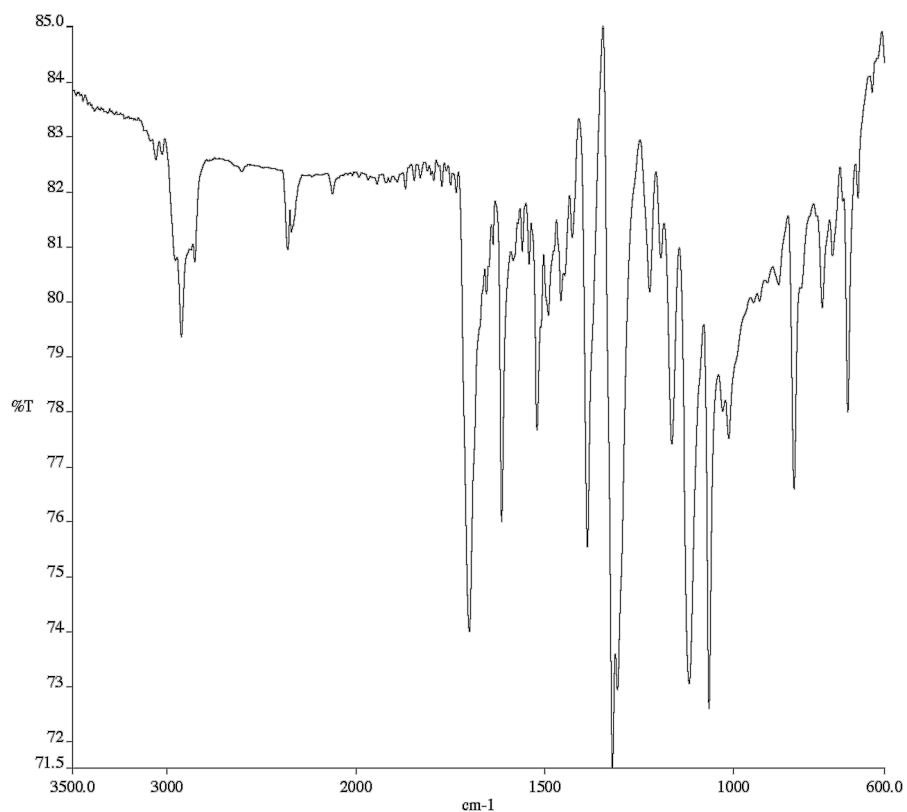


A3.30 Infrared spectrum (Thin Film, NaCl) of compound **32da**.

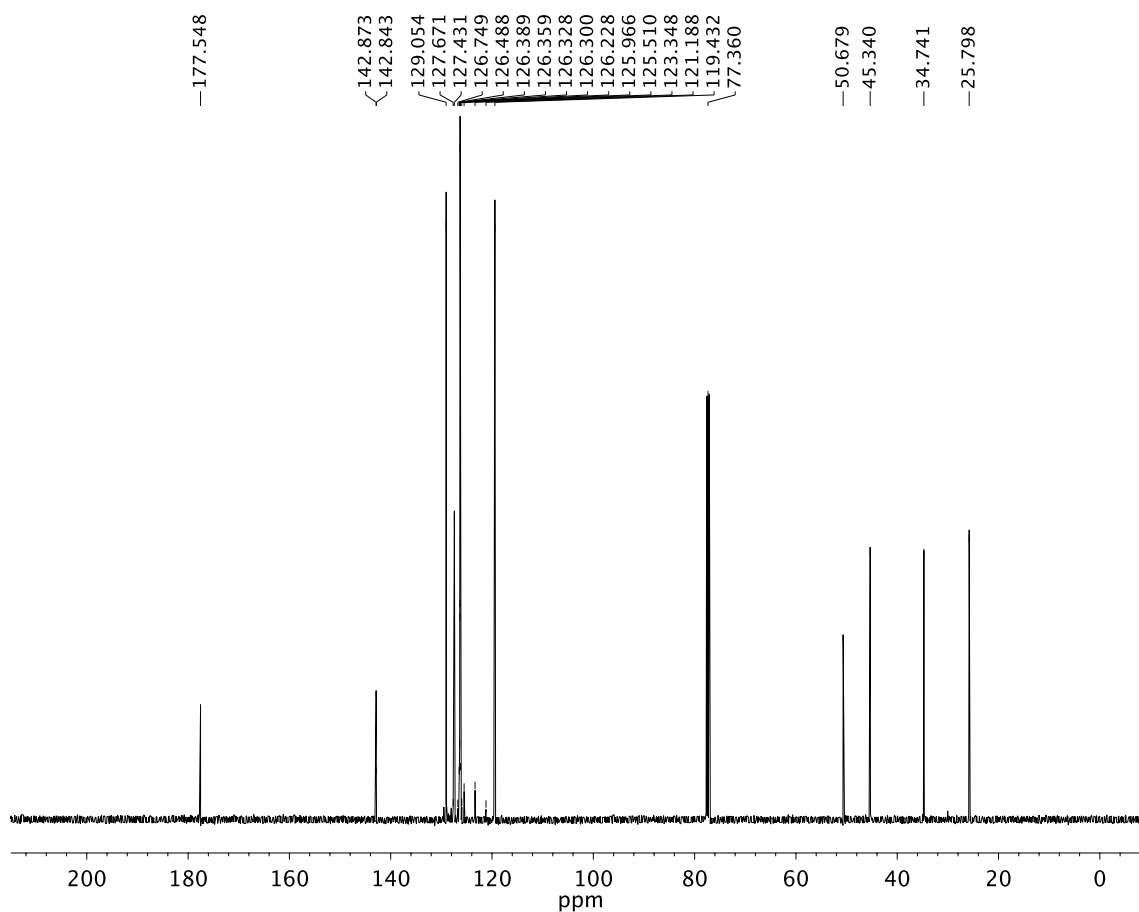


A3.31 ¹³C NMR (125 MHz, CDCl₃) of compound **32da**.

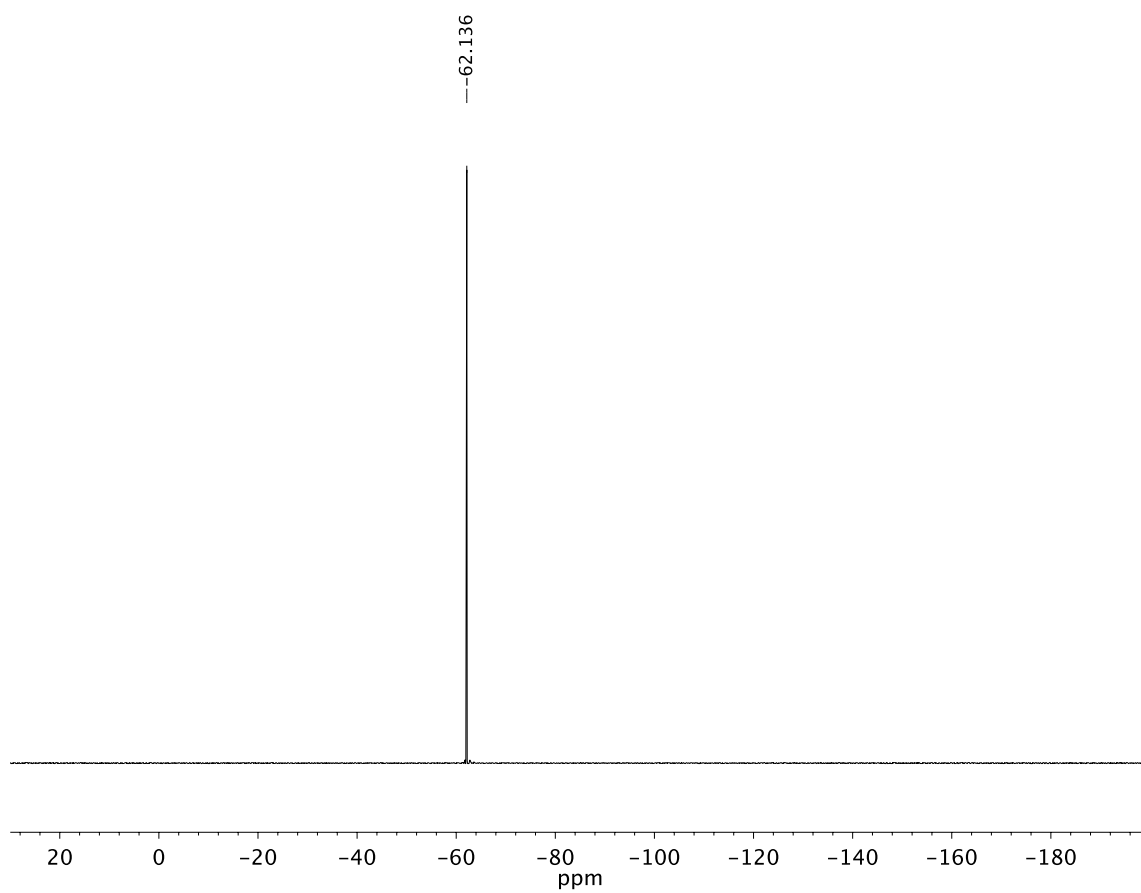




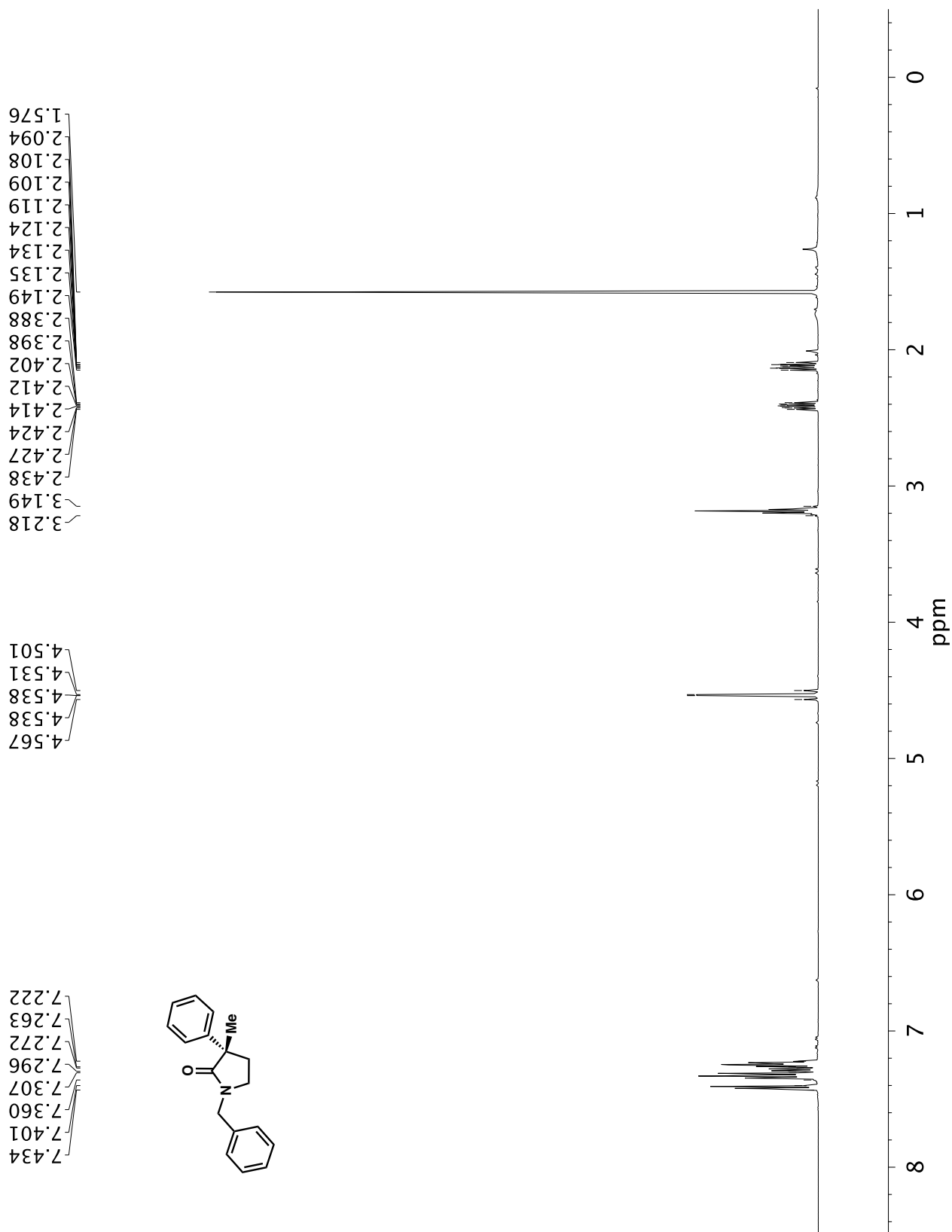
A3.33 Infrared spectrum (Thin Film, NaCl) of compound **32ea**.

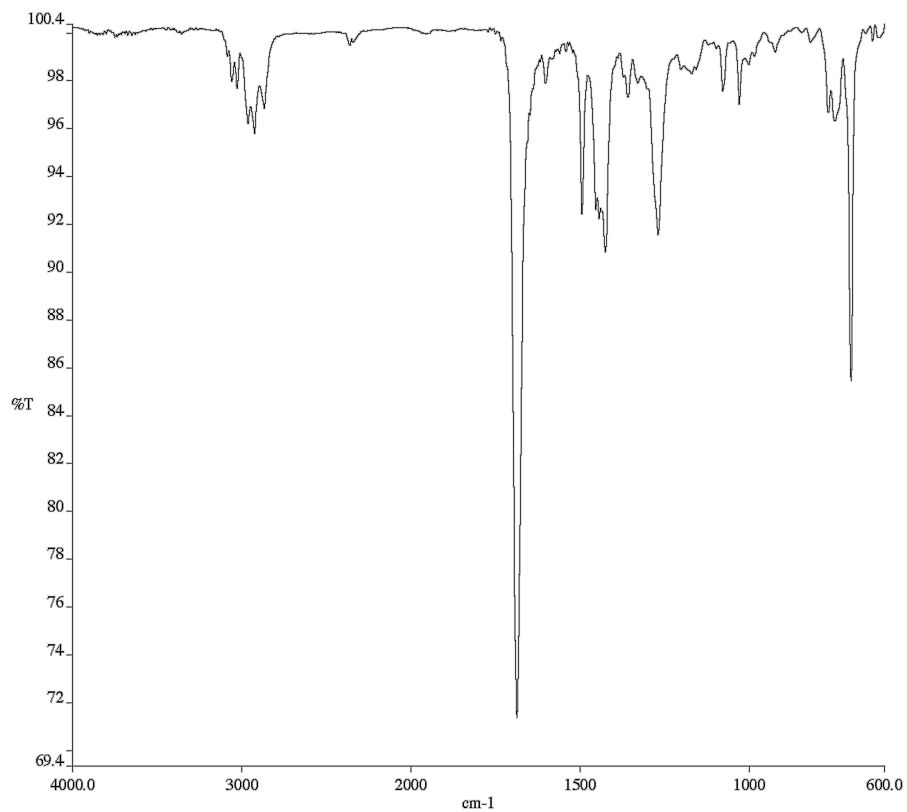


A3.34 ¹³C NMR (125 MHz, CDCl₃) of compound **32ea**.

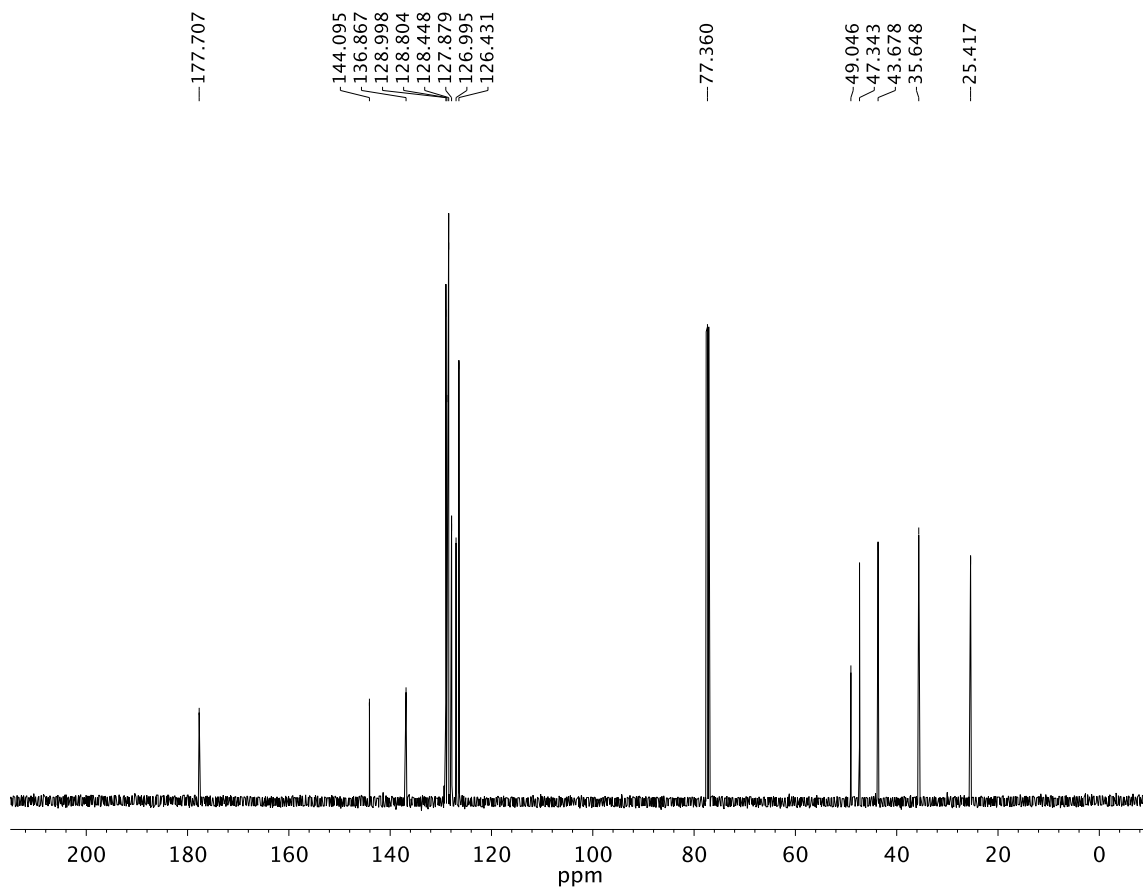


A3.35 ^{19}F NMR (282 MHz, CDCl_3) of compound **32ea**.

**A3.36** ^1H NMR (500 MHz, CDCl_3) of compound **32fa**.

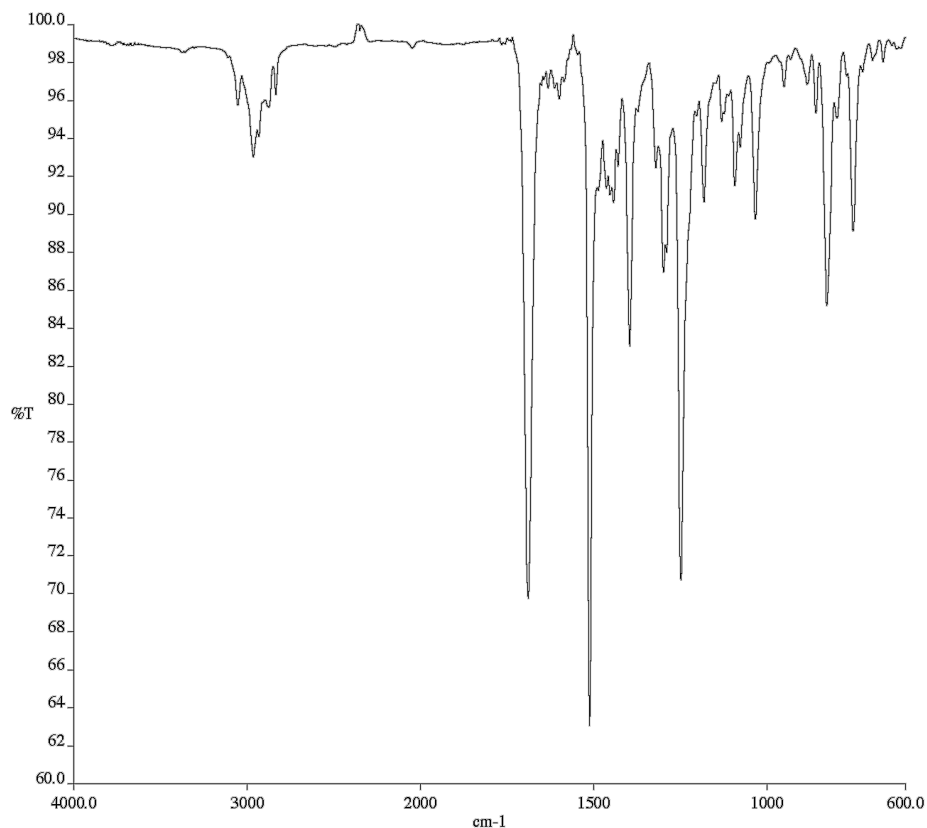


A3.37 Infrared spectrum (Thin Film, NaCl) of compound **32fa**.

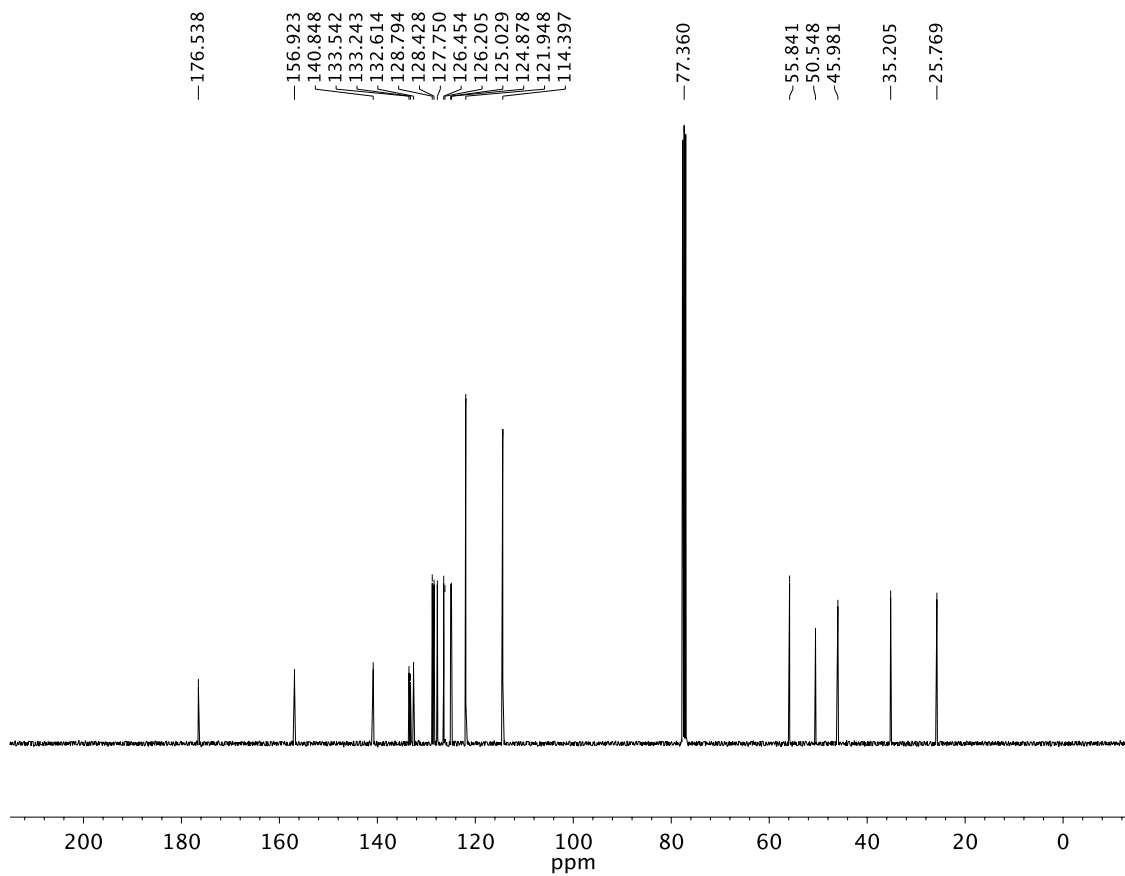


A3.38 ^{13}C NMR (125 MHz, CDCl_3) of compound **32fa**.

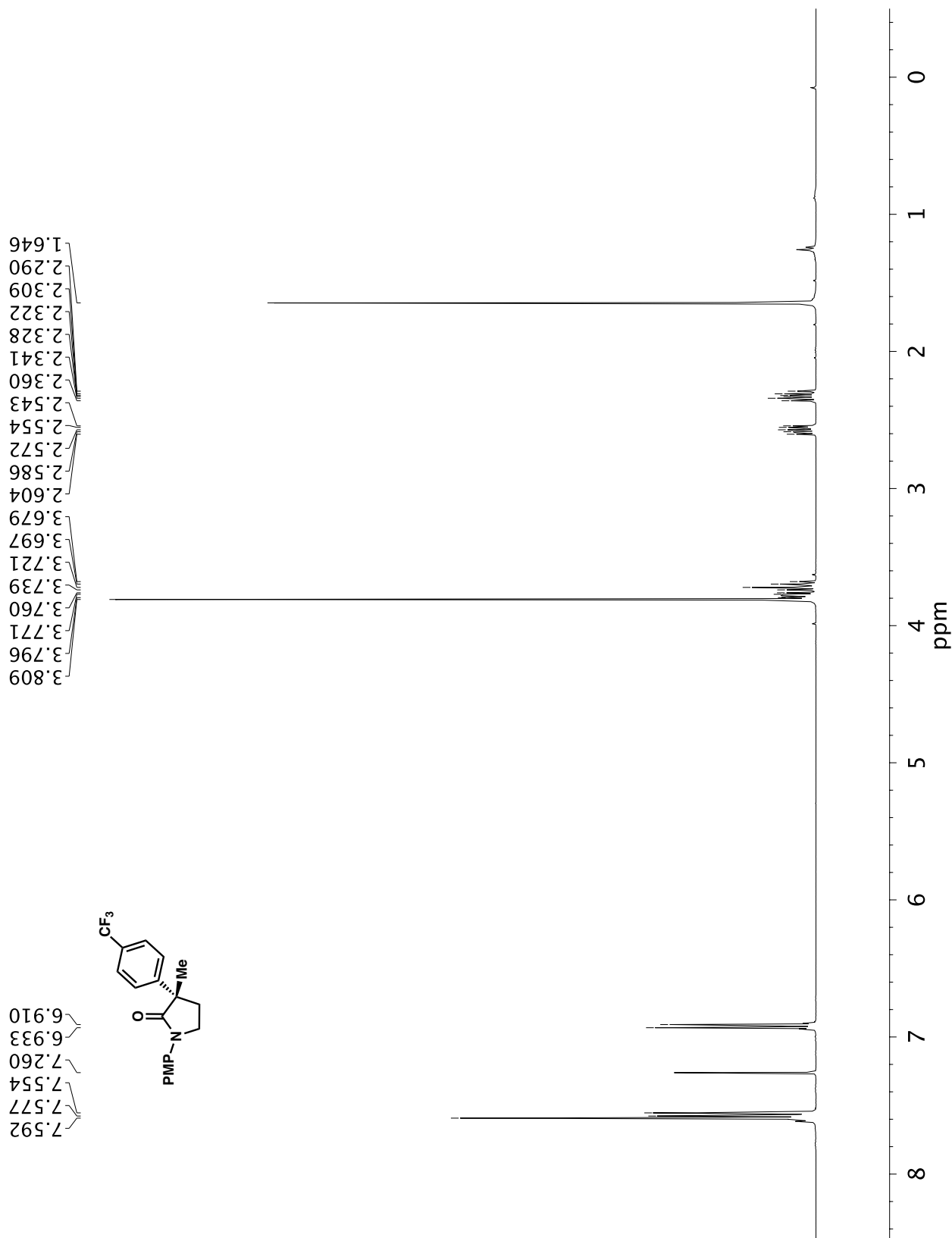


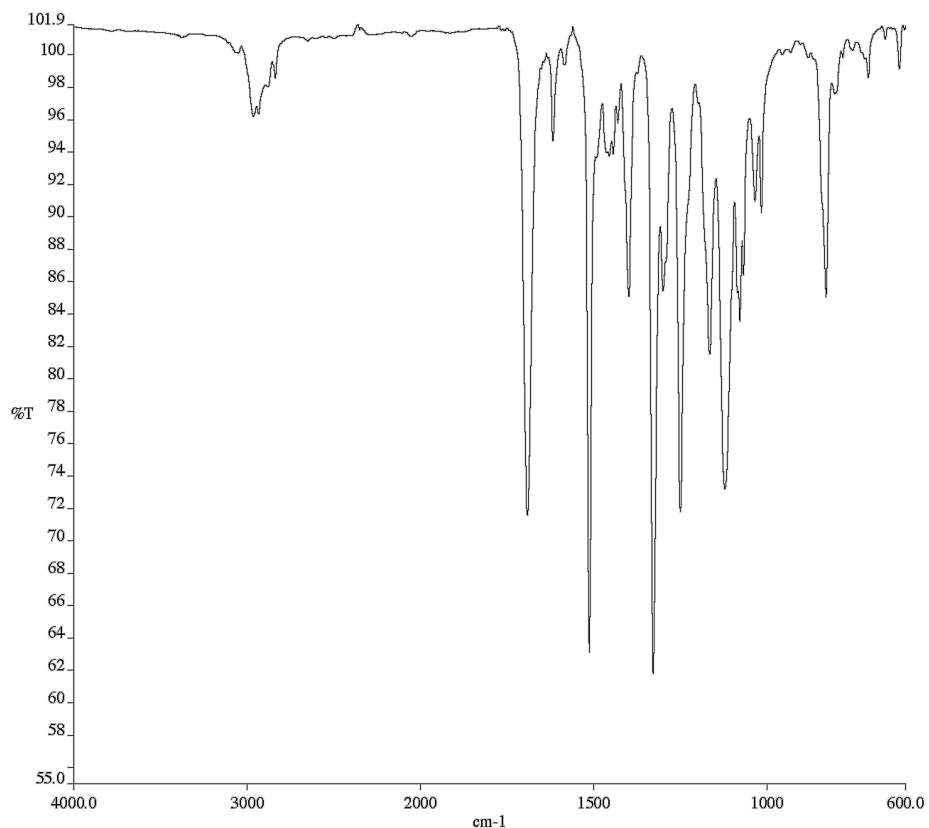


A3.40 Infrared spectrum (Thin Film, NaCl) of compound **32ab**.

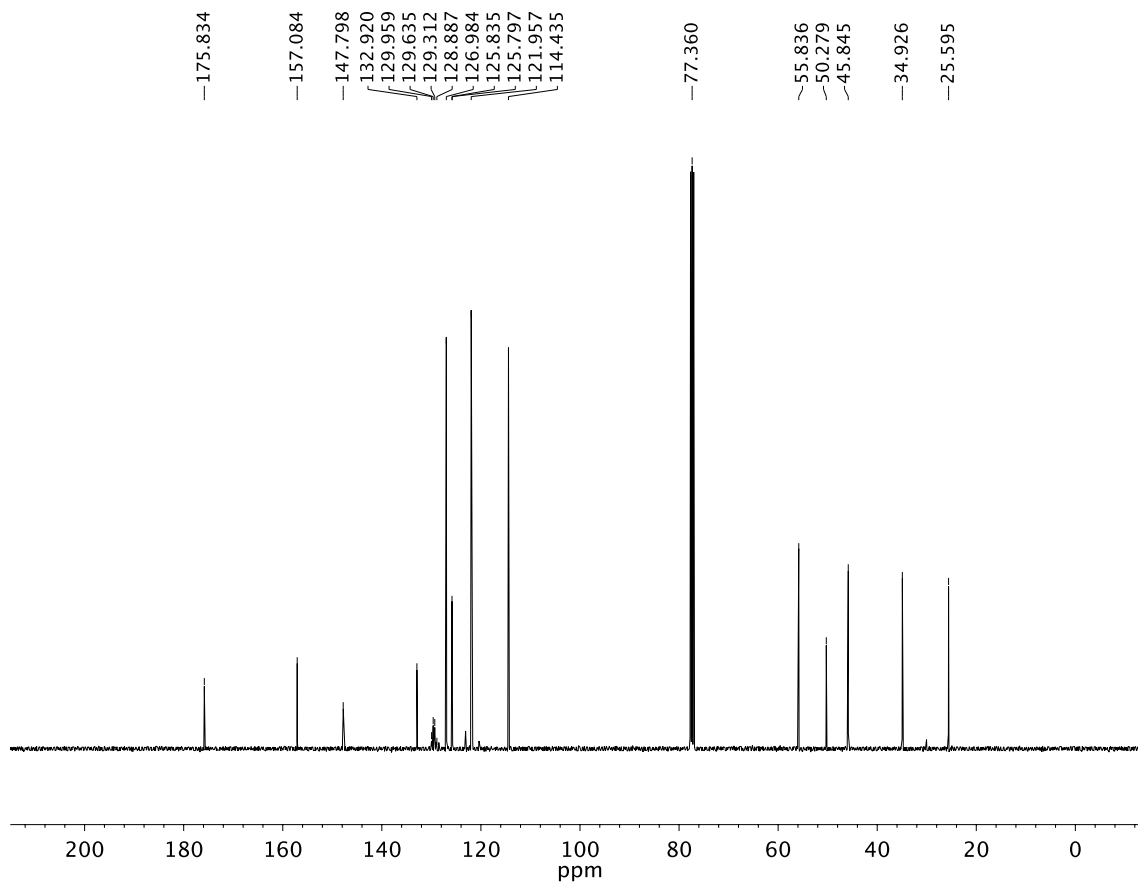


A3.41 ^{13}C NMR (100 MHz, CDCl_3) of compound **32ab**.

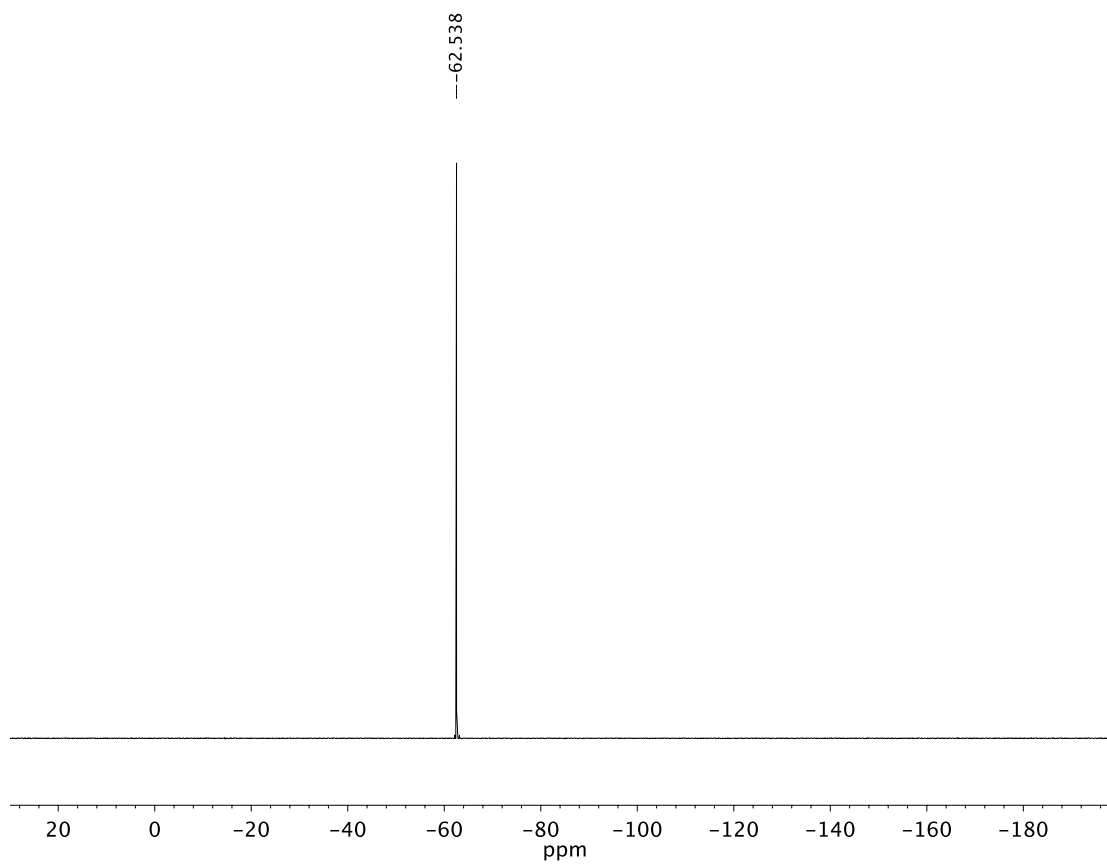
A3.42 ¹H NMR (400 MHz, CDCl₃) of compound **32ac**.



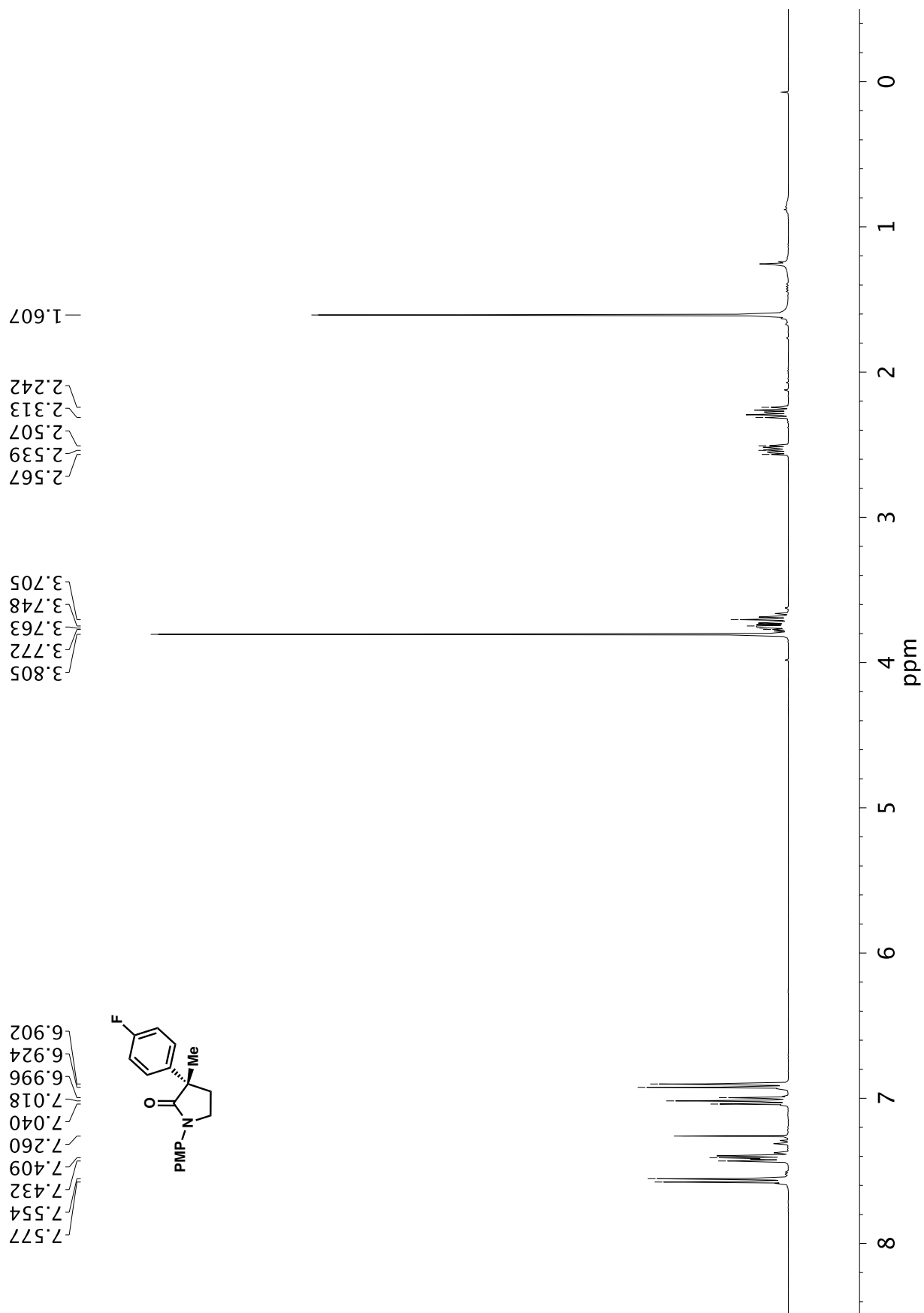
A3.43 Infrared spectrum (Thin Film, NaCl) of compound **32ac**.

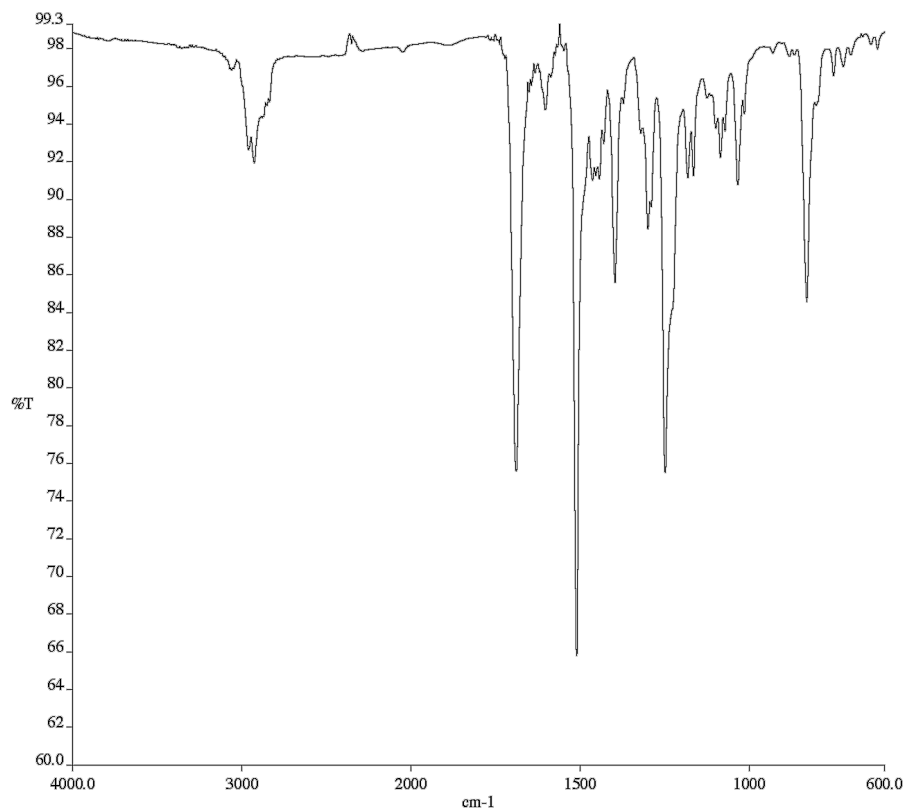


A3.44 ¹³C NMR (100 MHz, CDCl₃) of compound **32ac**.



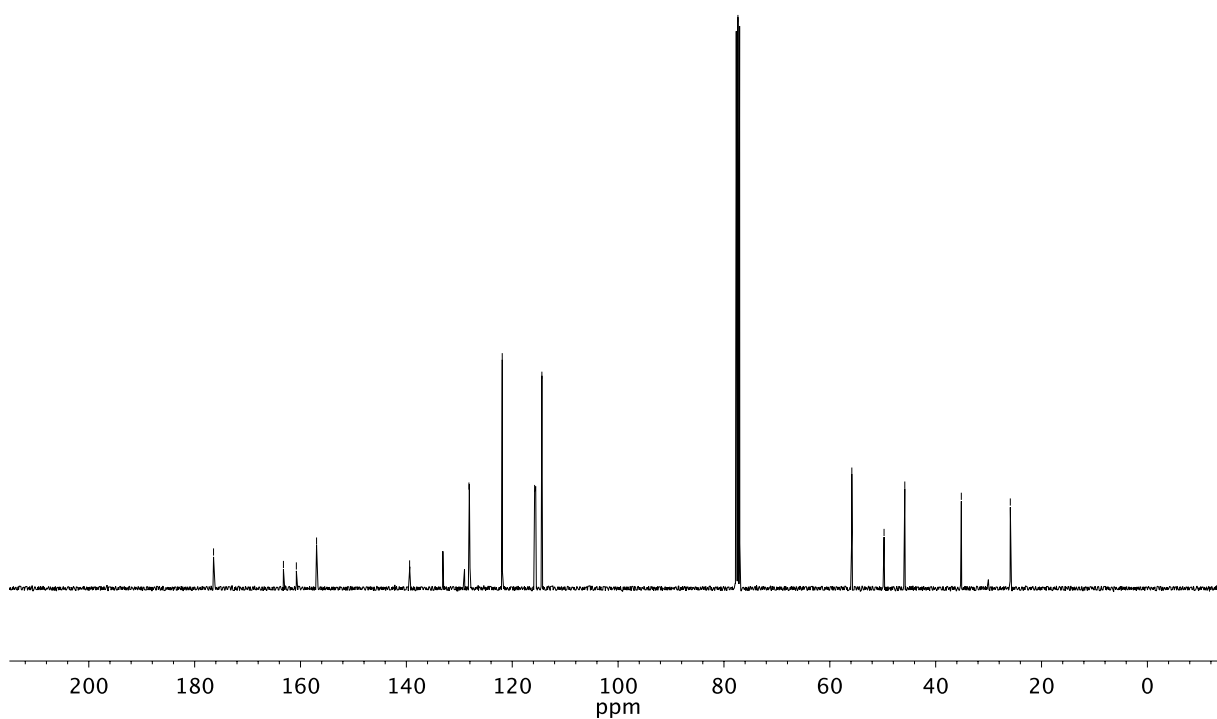
A3.45 ^{19}F NMR (282 MHz, CDCl_3) of compound **32ac**.

**A3.46** ¹H NMR (400 MHz, CDCl₃) of compound **32ad**.

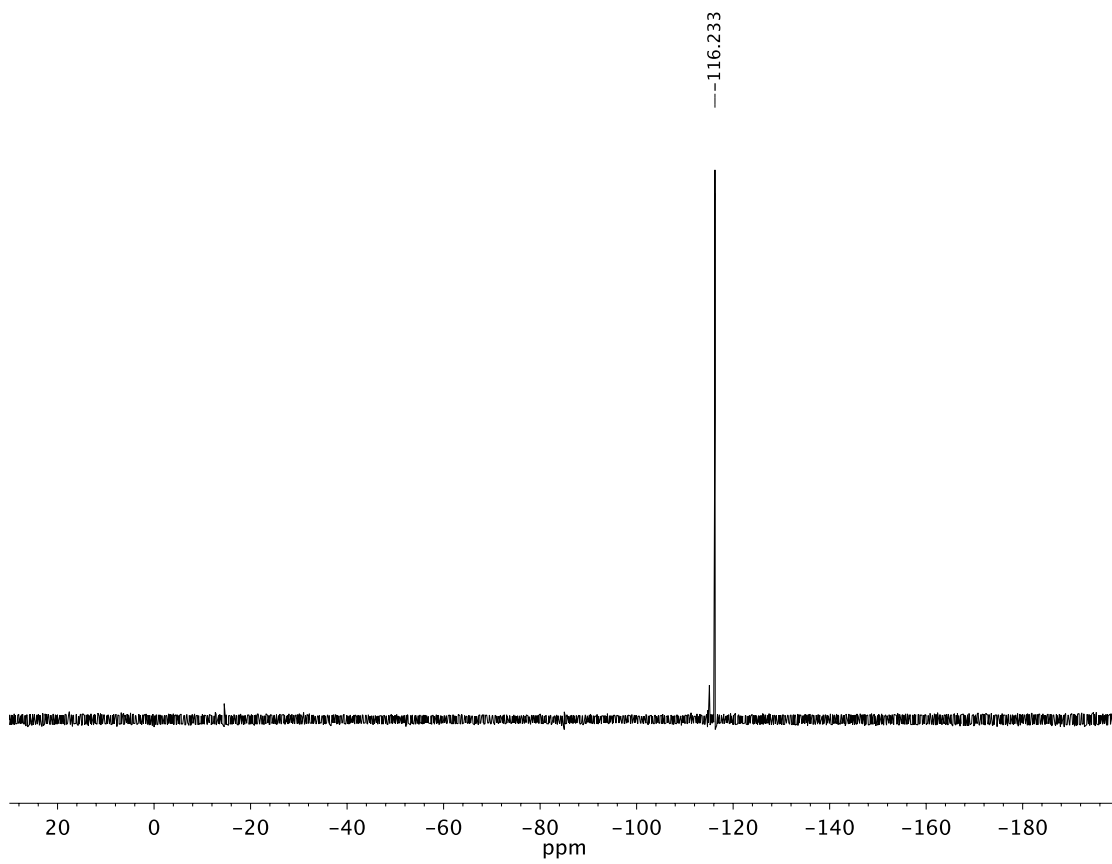


A3.47 Infrared spectrum (Thin Film, NaCl) of compound **32ad**.

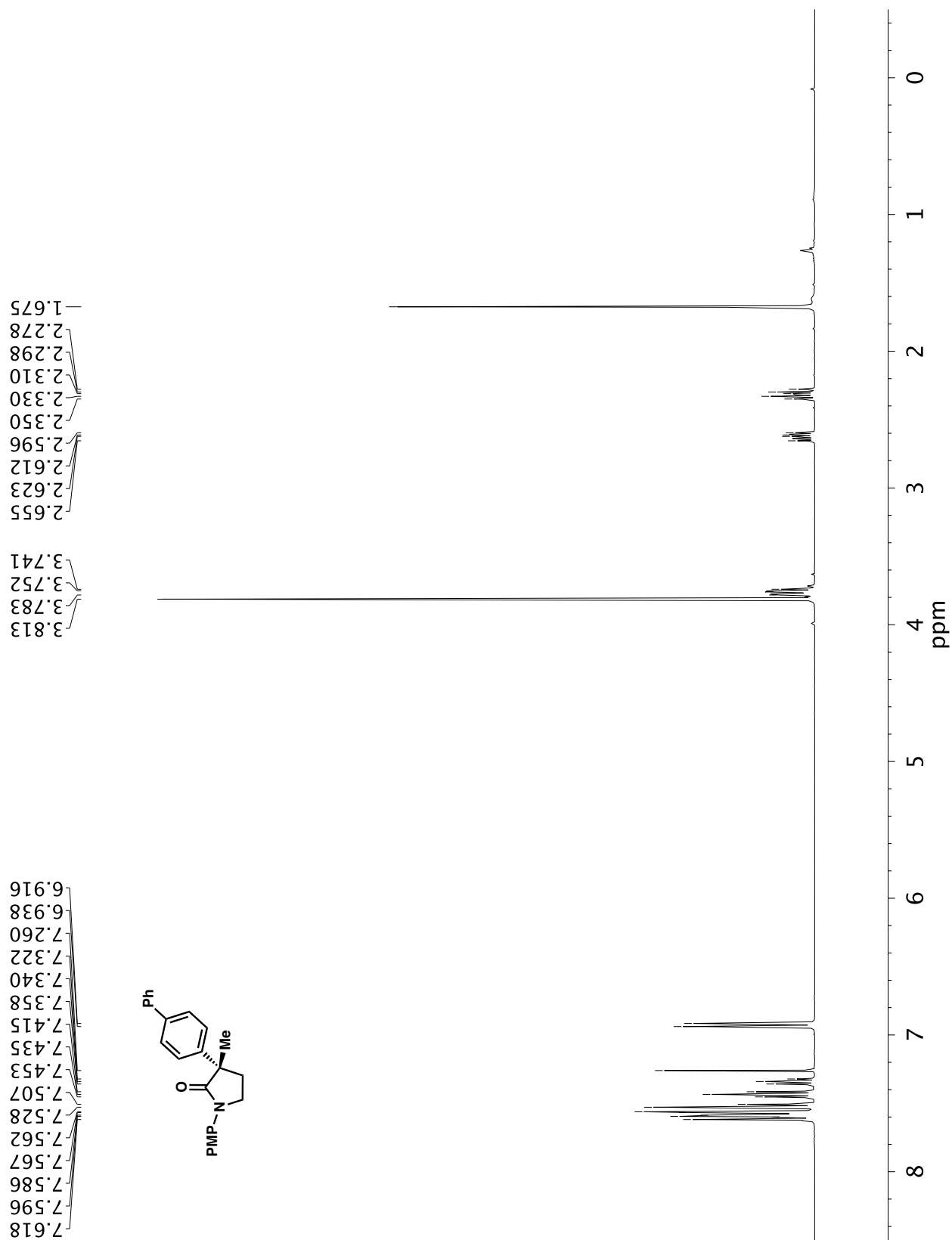
—176.432 ~163.226 ~160.786 ~156.967 —139.389 ~128.181 ~121.890 ~115.772 ~114.400 —77.360 ~55.841 ~49.754 ~45.835 —35.156 —25.900

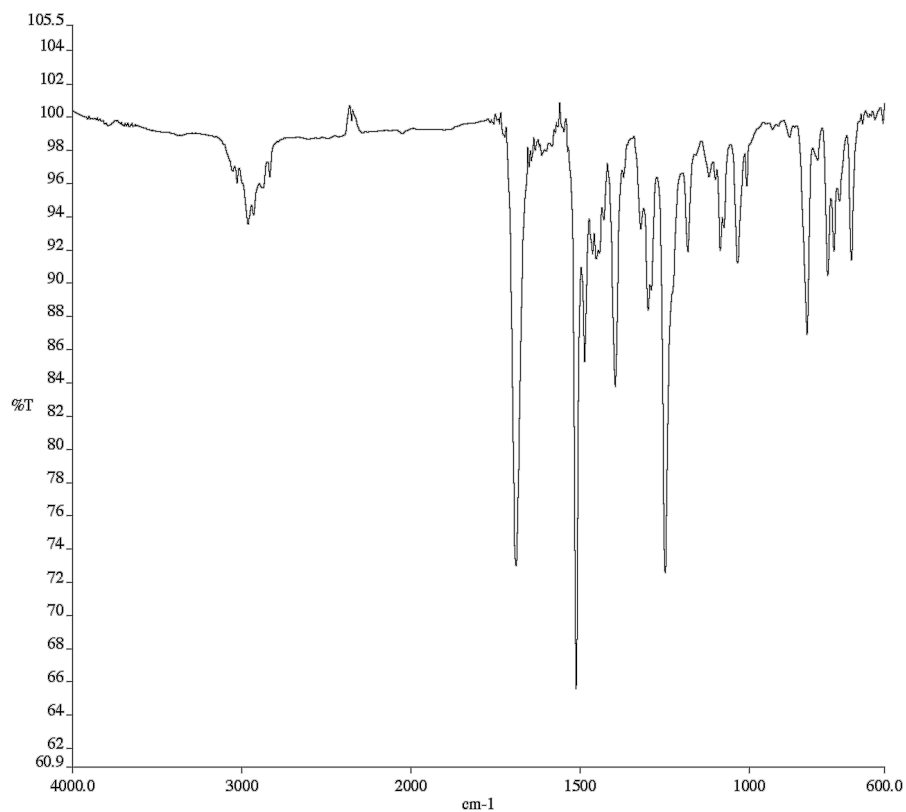


A3.48 ¹³C NMR (100 MHz, CDCl₃) of compound **32ad**.

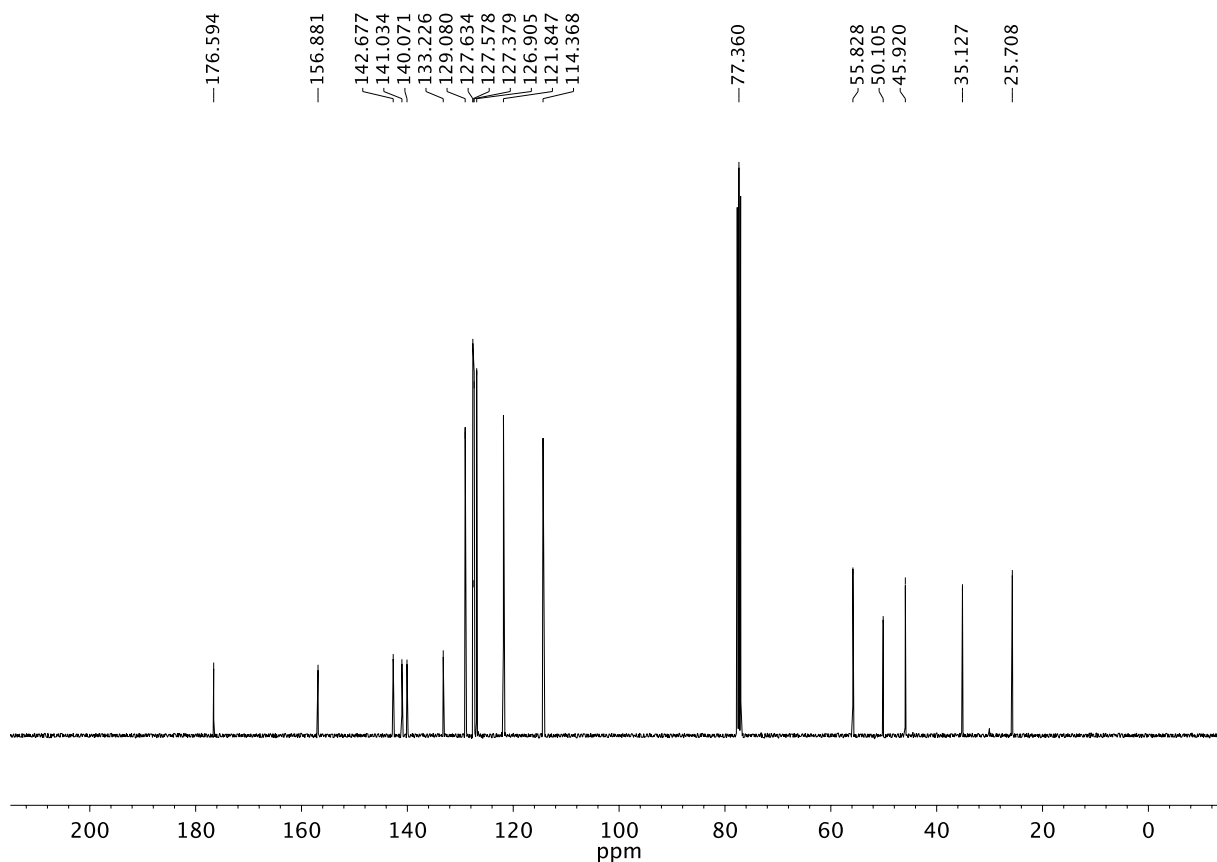


A3.49 ^{19}F NMR (282 MHz, CDCl_3) of compound **32ad**.

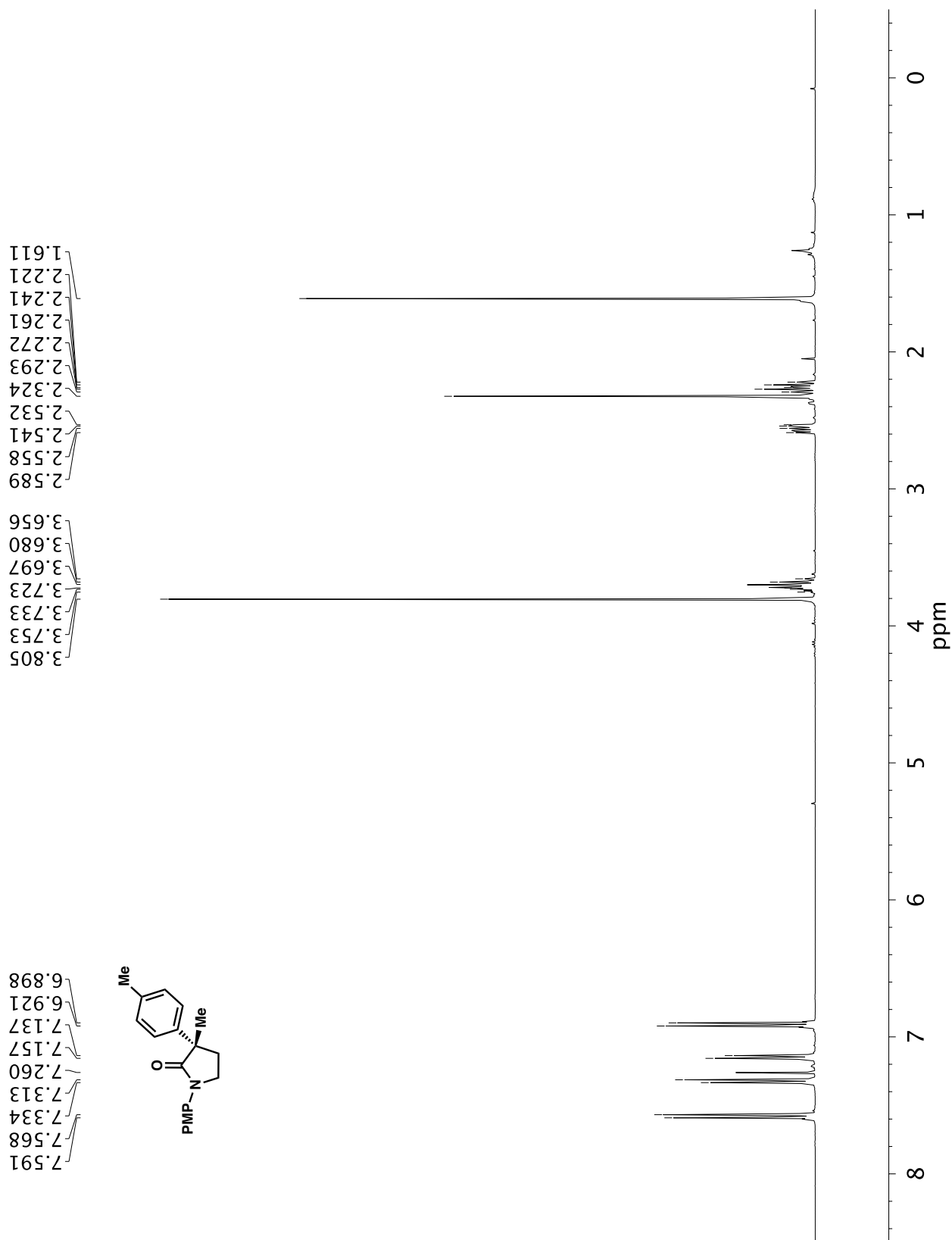
A3.50 ¹H NMR (400 MHz, CDCl₃) of compound 32ae.

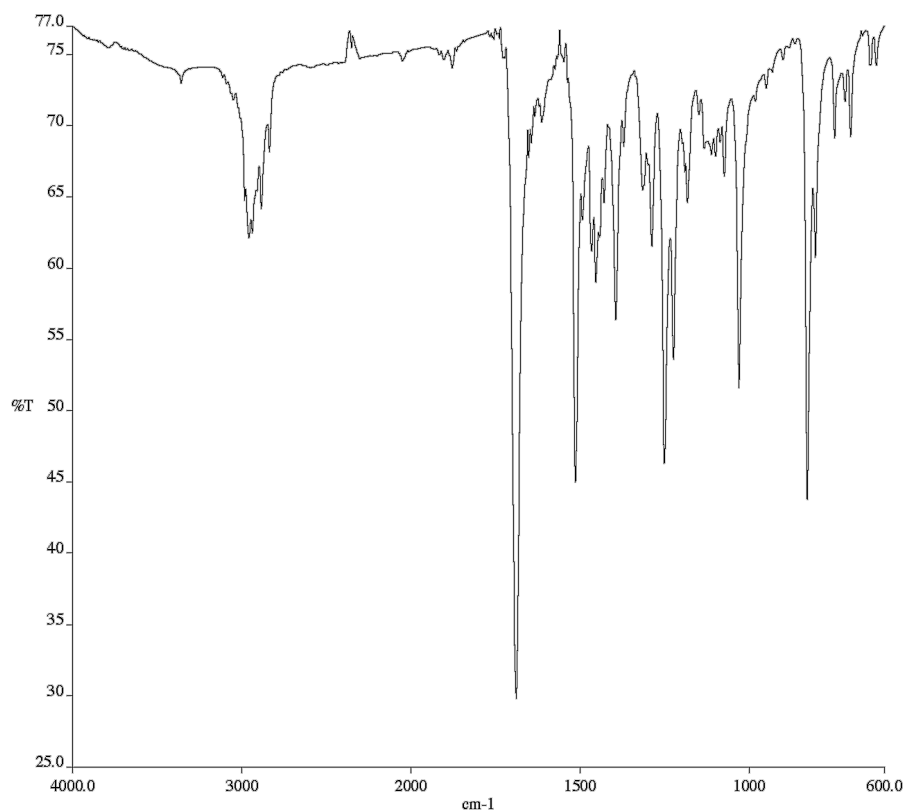


A3.51 Infrared spectrum (Thin Film, NaCl) of compound **32ae**.

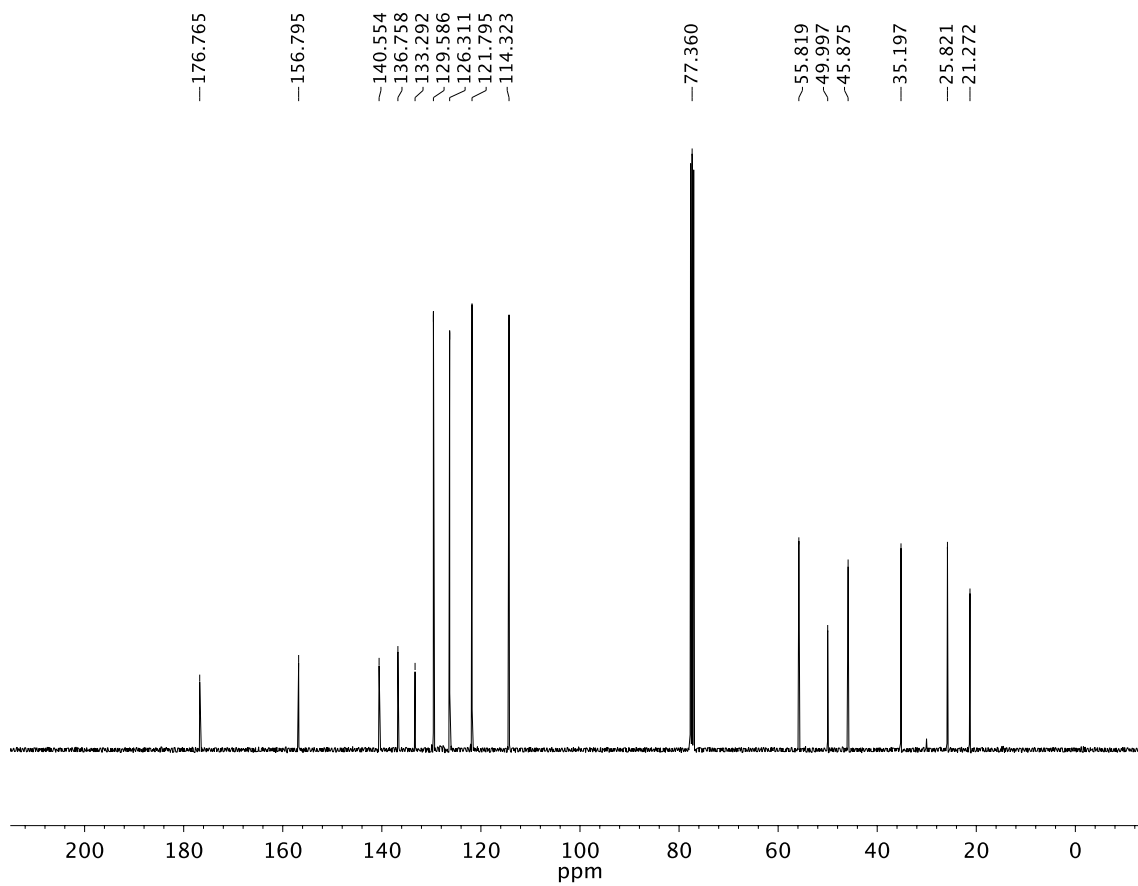


A3.52 ¹³C NMR (126 100 MHz, CDCl₃) of compound **32ae**.

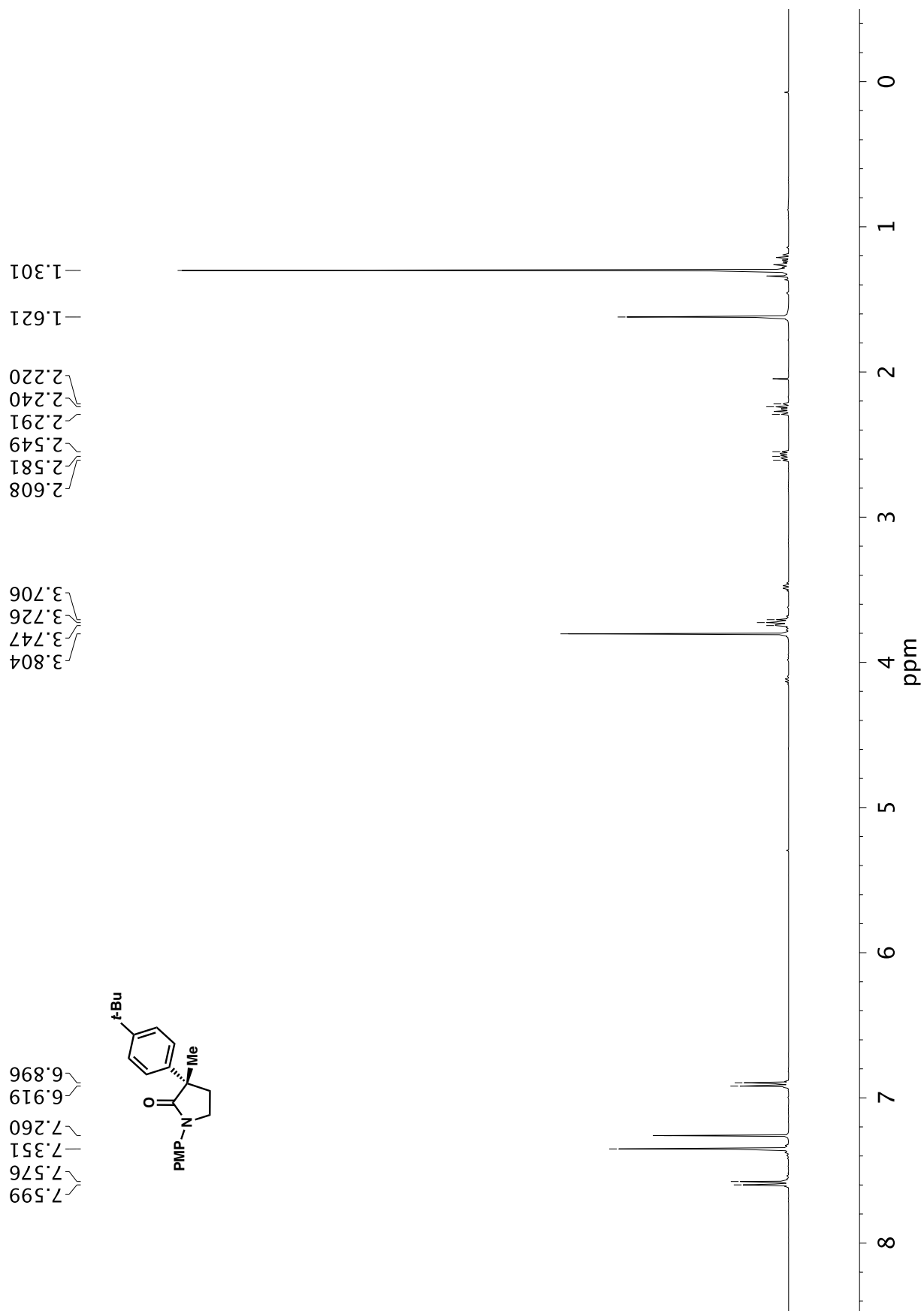
A3.53 ¹H NMR (400 MHz, CDCl₃) of compound **32af**.

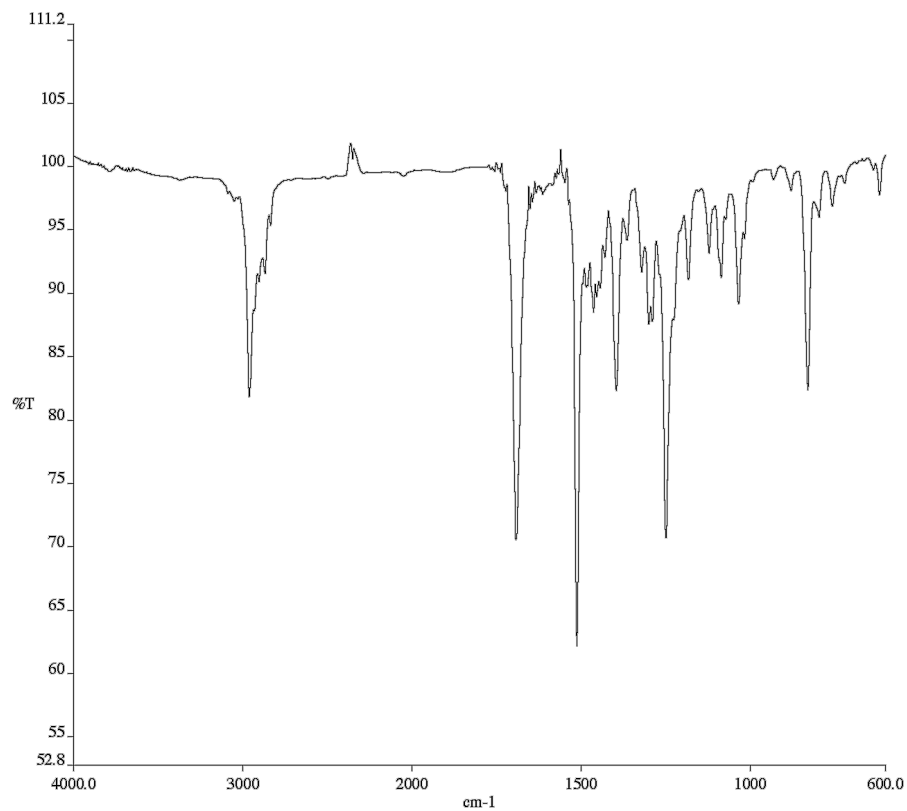


A3.54 Infrared spectrum (Thin Film, NaCl) of compound **32af**.

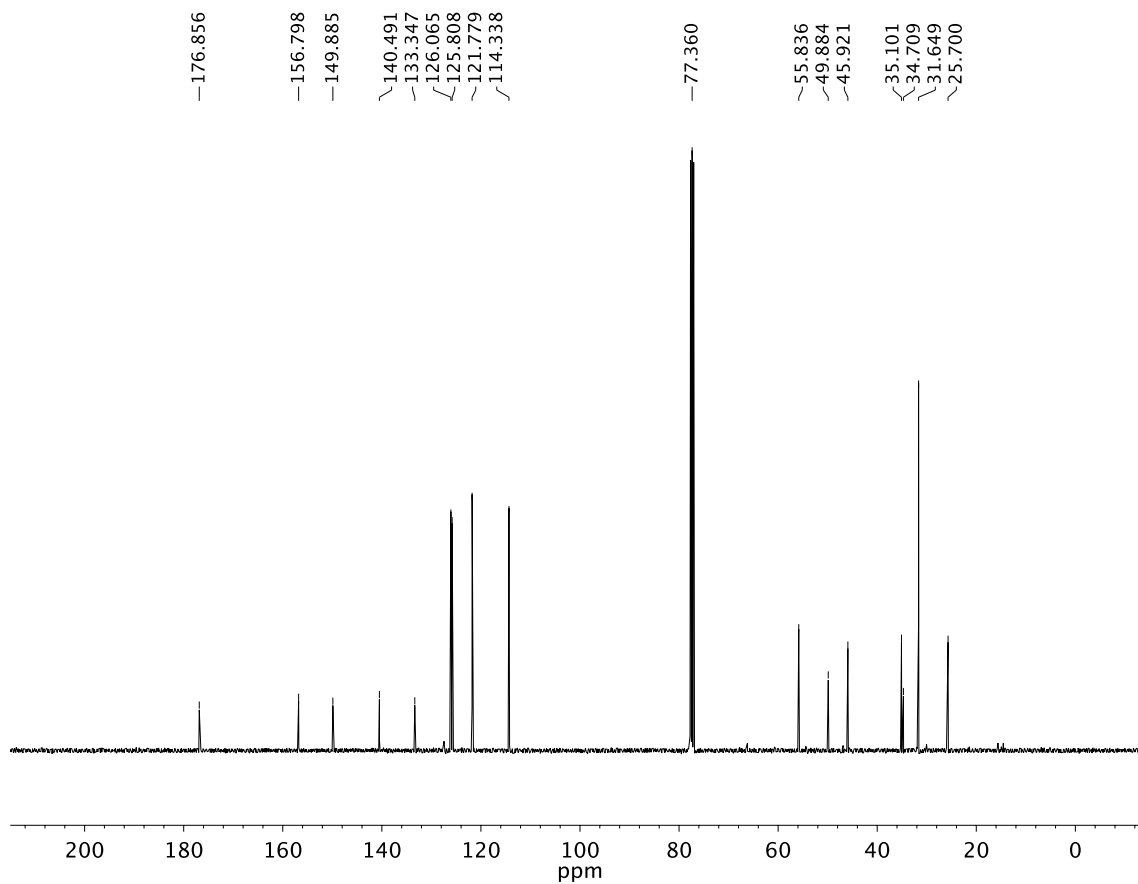


A3.55 ¹³C NMR (100 MHz, CDCl₃) of compound **32af**.

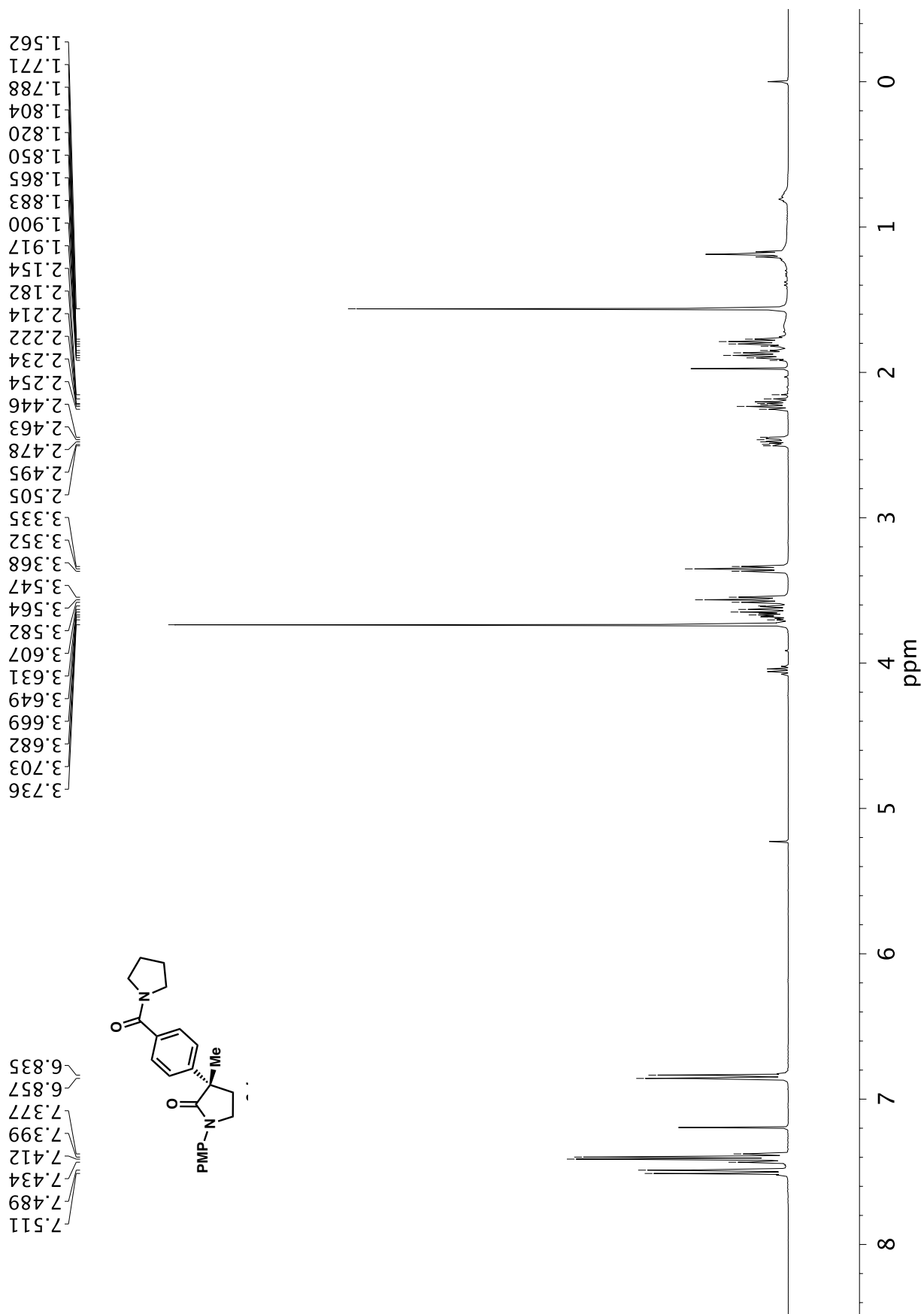
A3.56 ¹H NMR (400 MHz, CDCl₃) of compound 32ag.

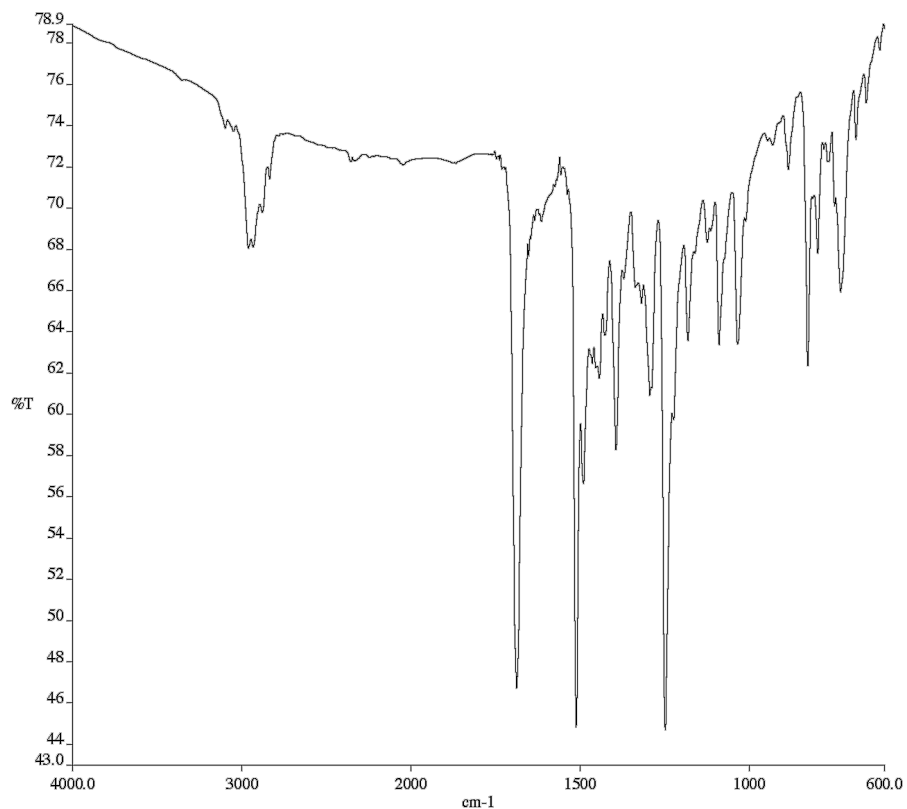


A3.57 Infrared spectrum (Thin Film, NaCl) of compound **32ag**.

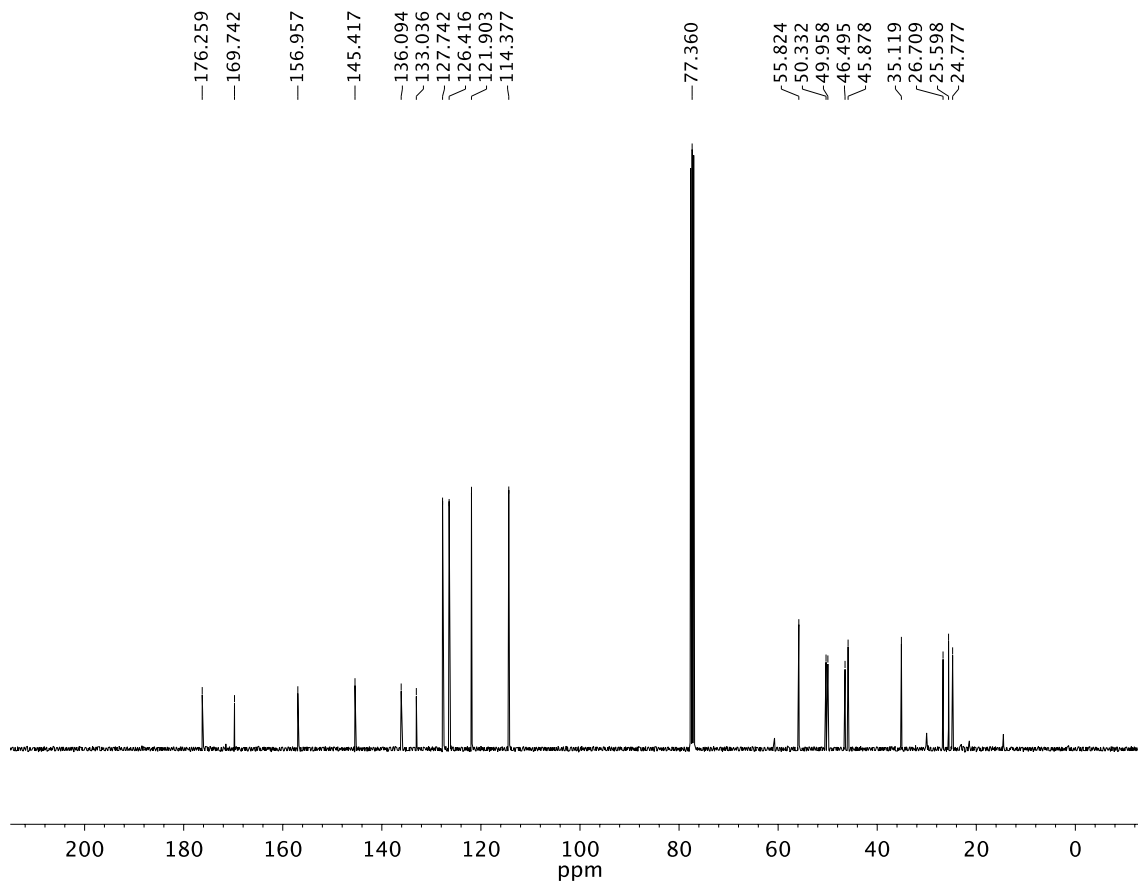


A3.58 ¹³C NMR (100 MHz, CDCl₃) of compound **32ag**.

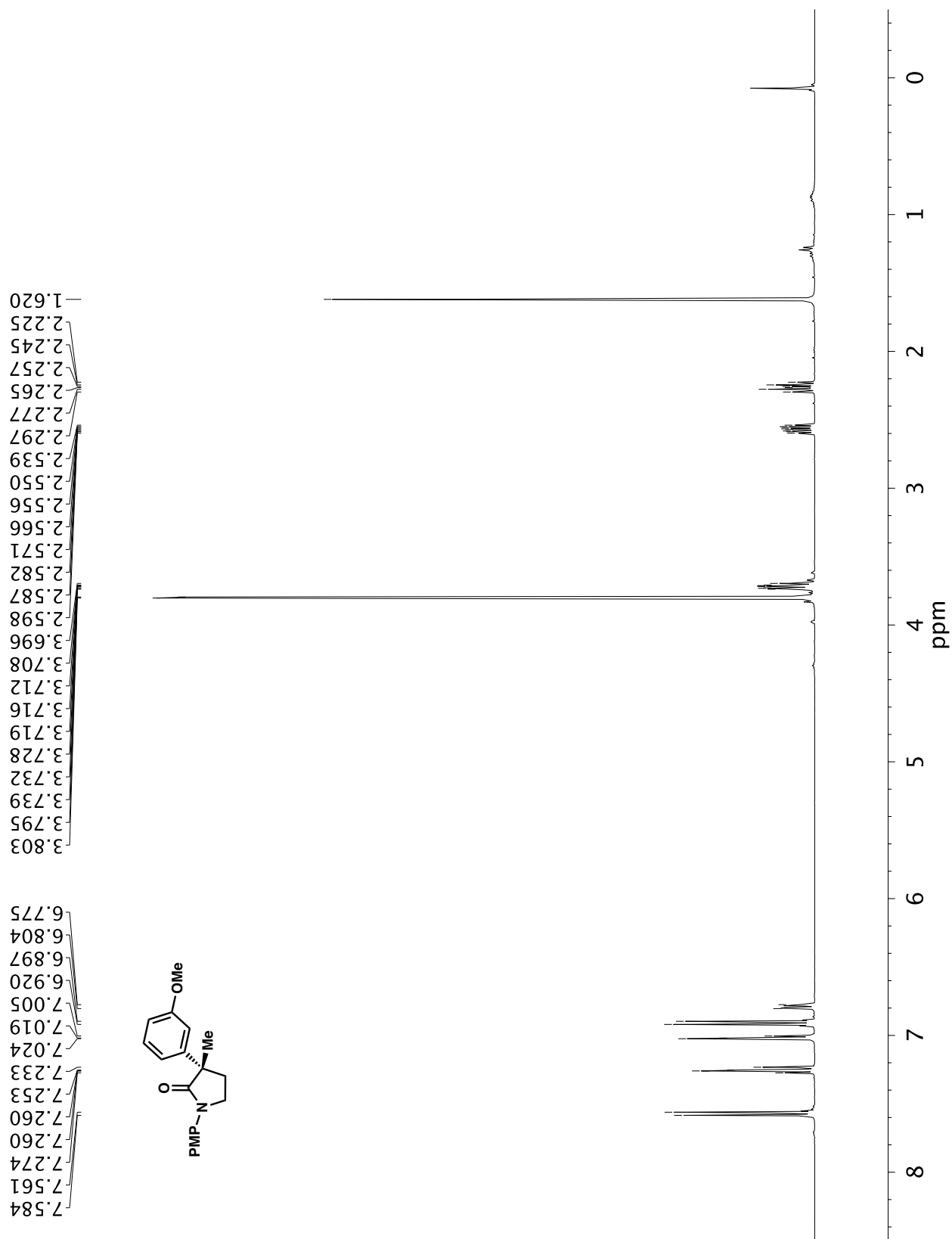


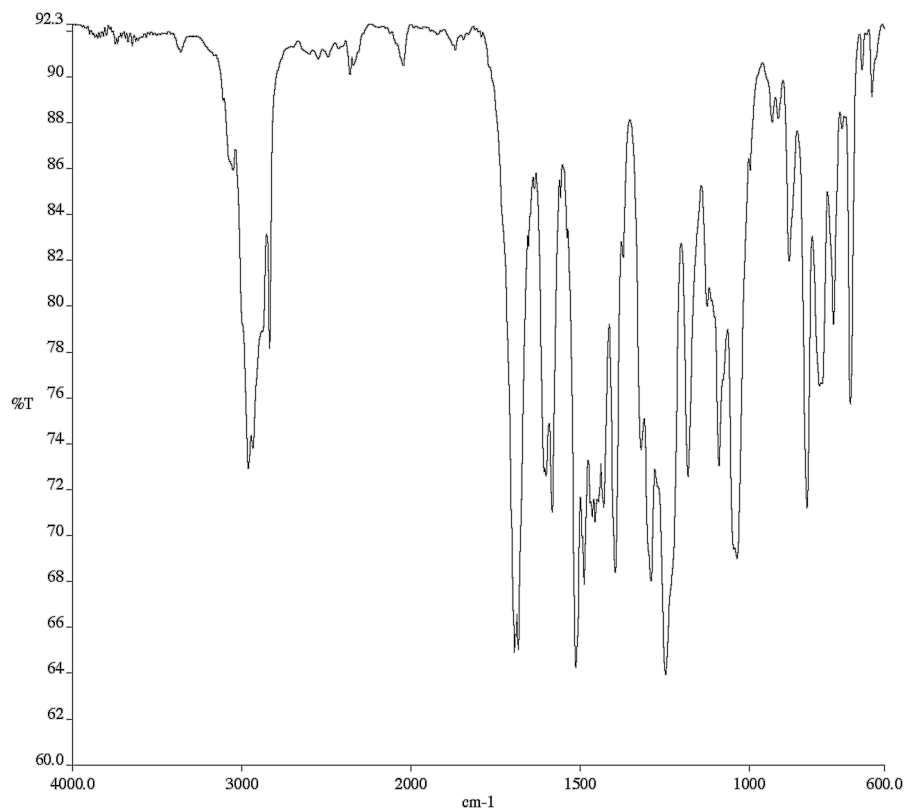


A3.60 Infrared spectrum (Thin Film, NaCl) of compound **32ah**.

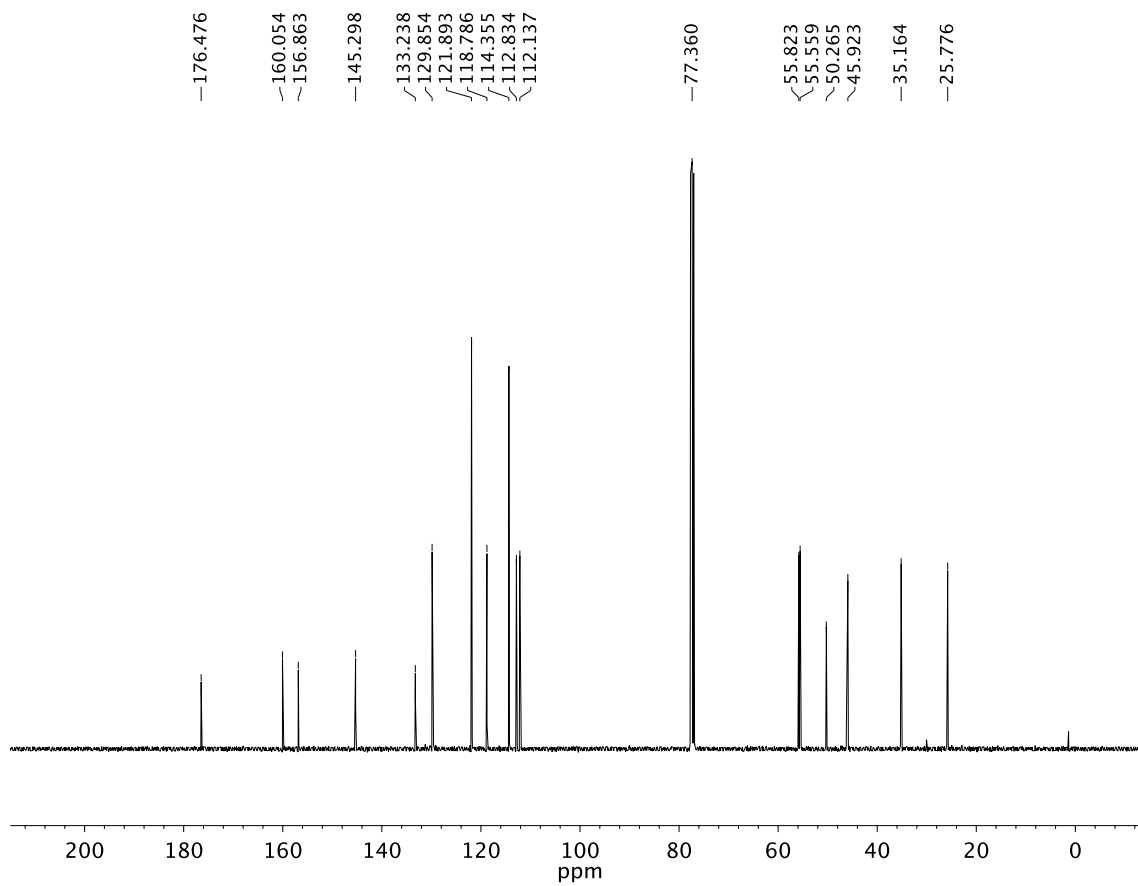


A3.61 ^{13}C NMR (100 MHz, CDCl_3) of compound **32ah**.

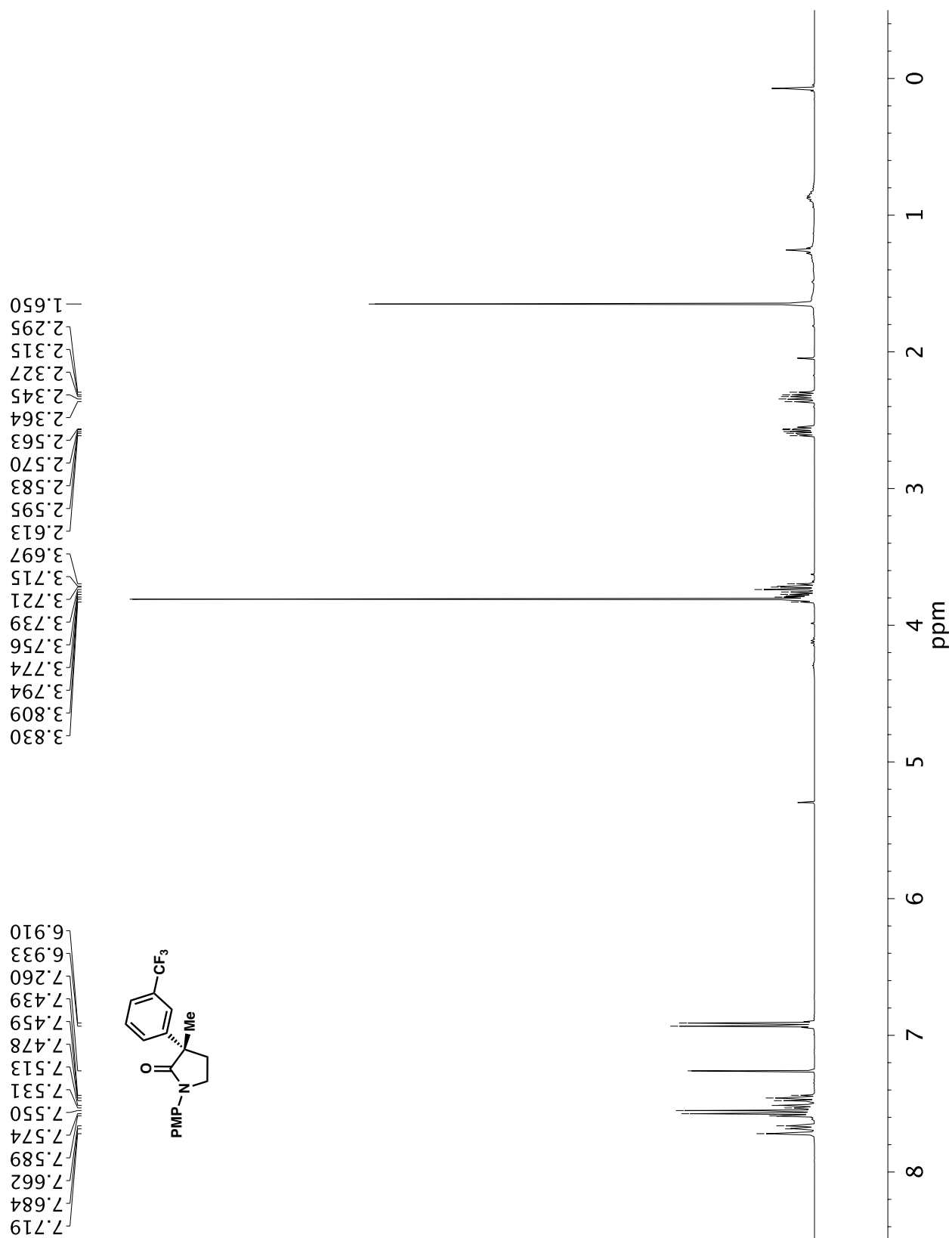
A3.62 ¹H NMR (300 MHz, CDCl₃) of compound **32ai**.

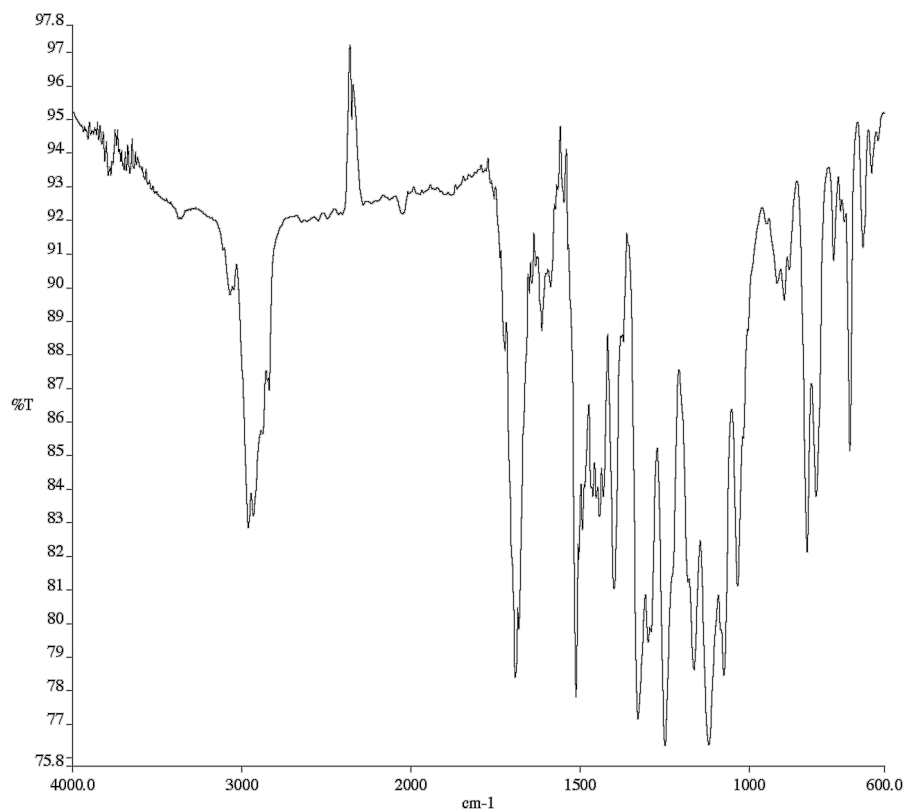


A3.63 Infrared spectrum (Thin Film, NaCl) of compound **32ai**.

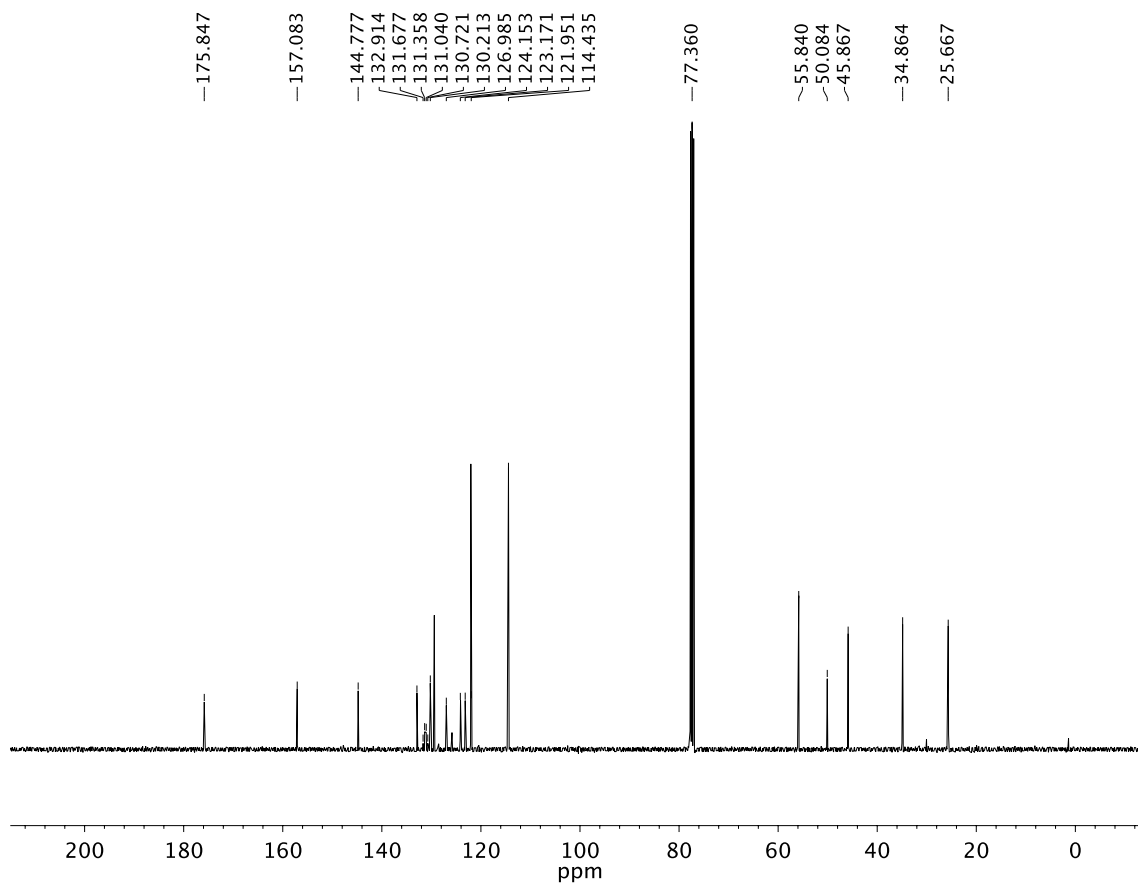


A3.64 ¹³C NMR (100 MHz, CDCl₃) of compound **32ai**.

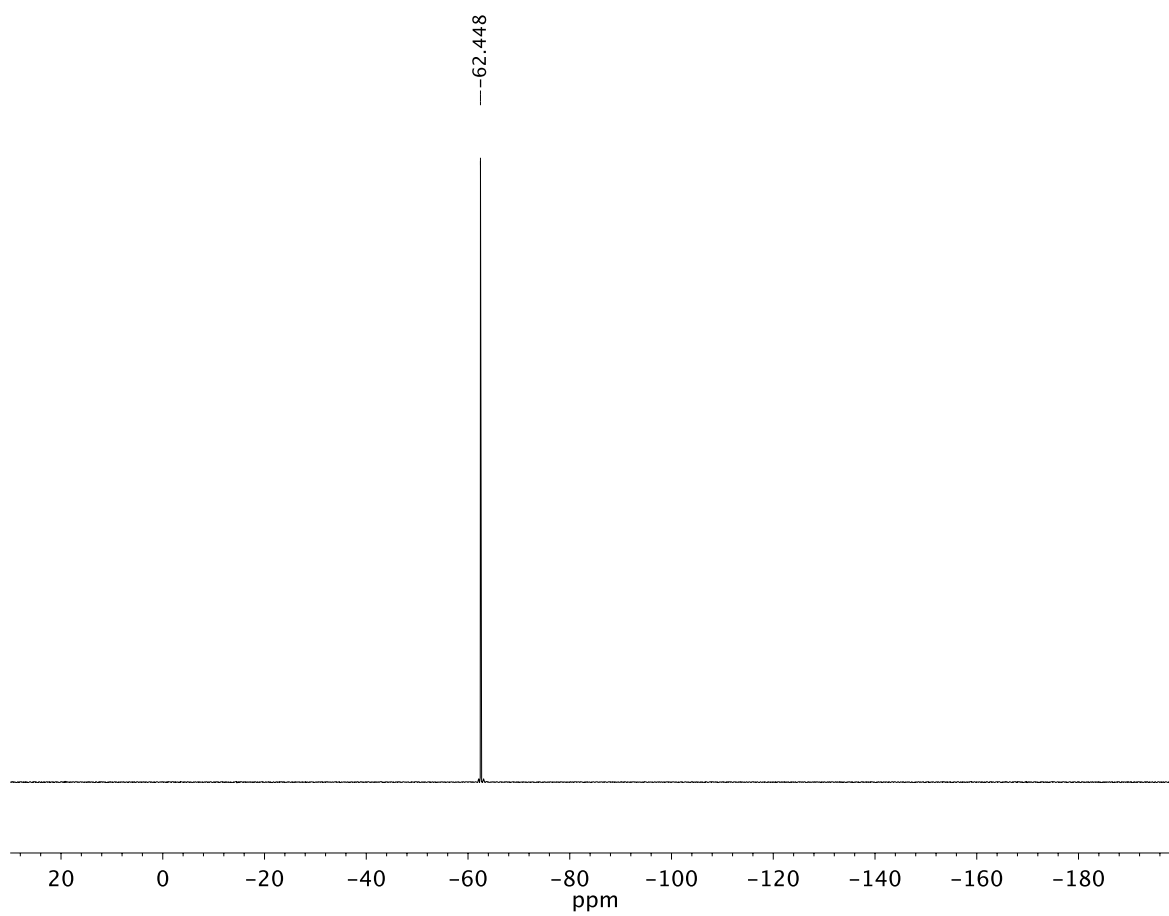




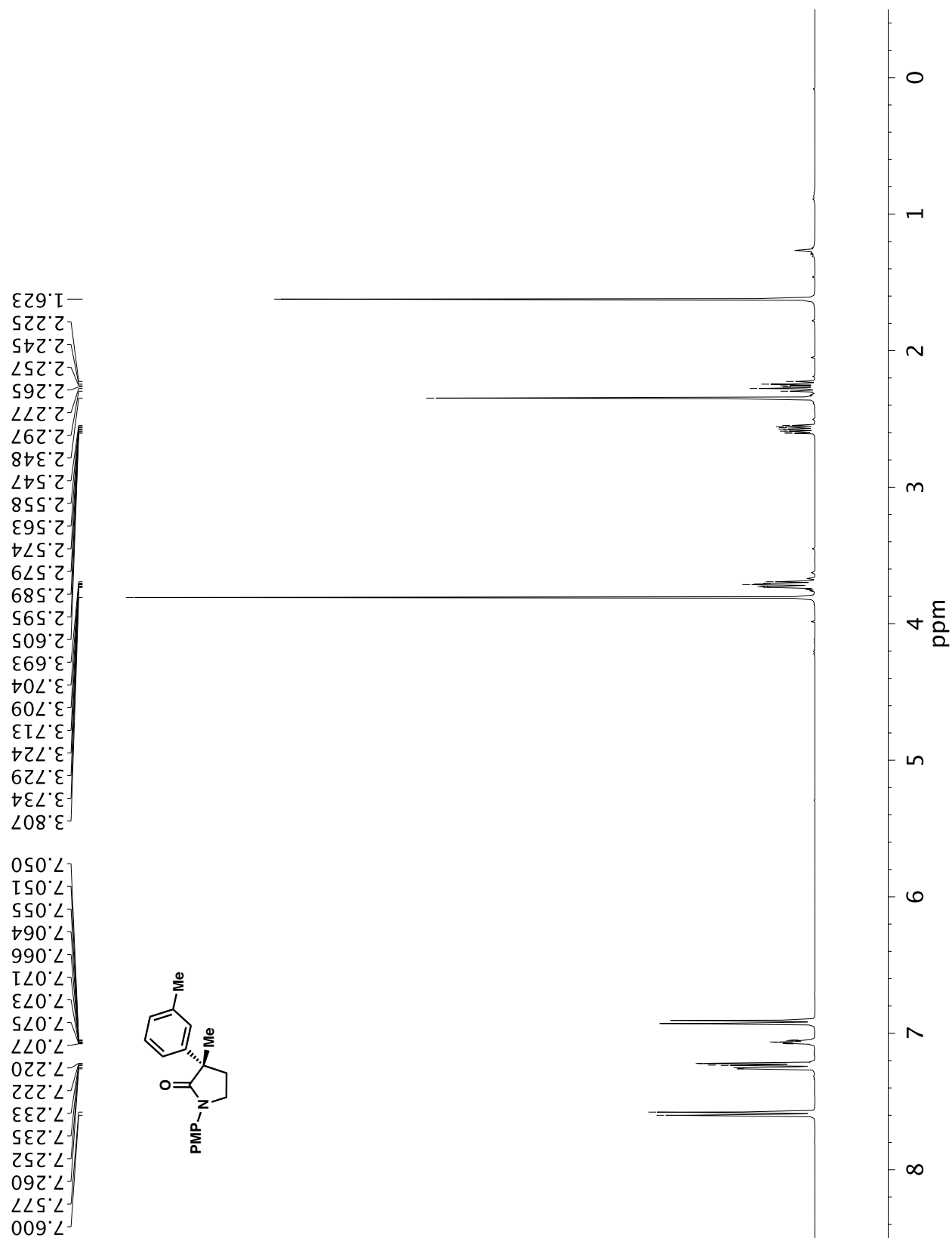
A3.66 Infrared spectrum (Thin Film, NaCl) of compound **32aj**.

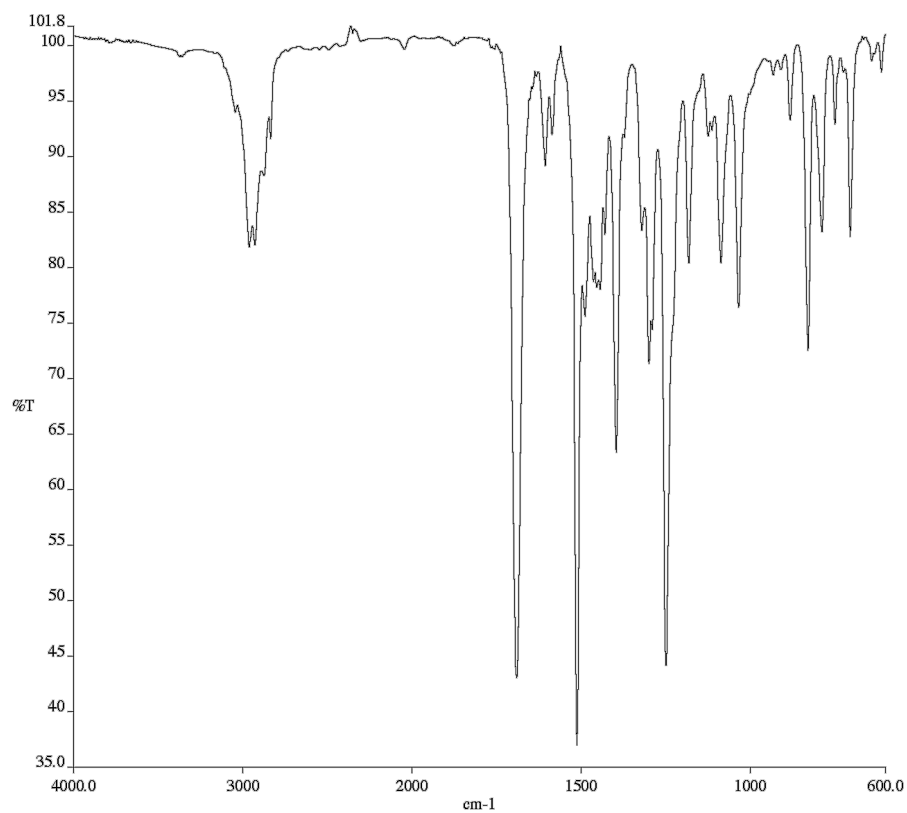


A3.67 ¹³C NMR (100 MHz, CDCl₃) of compound **32aj**.

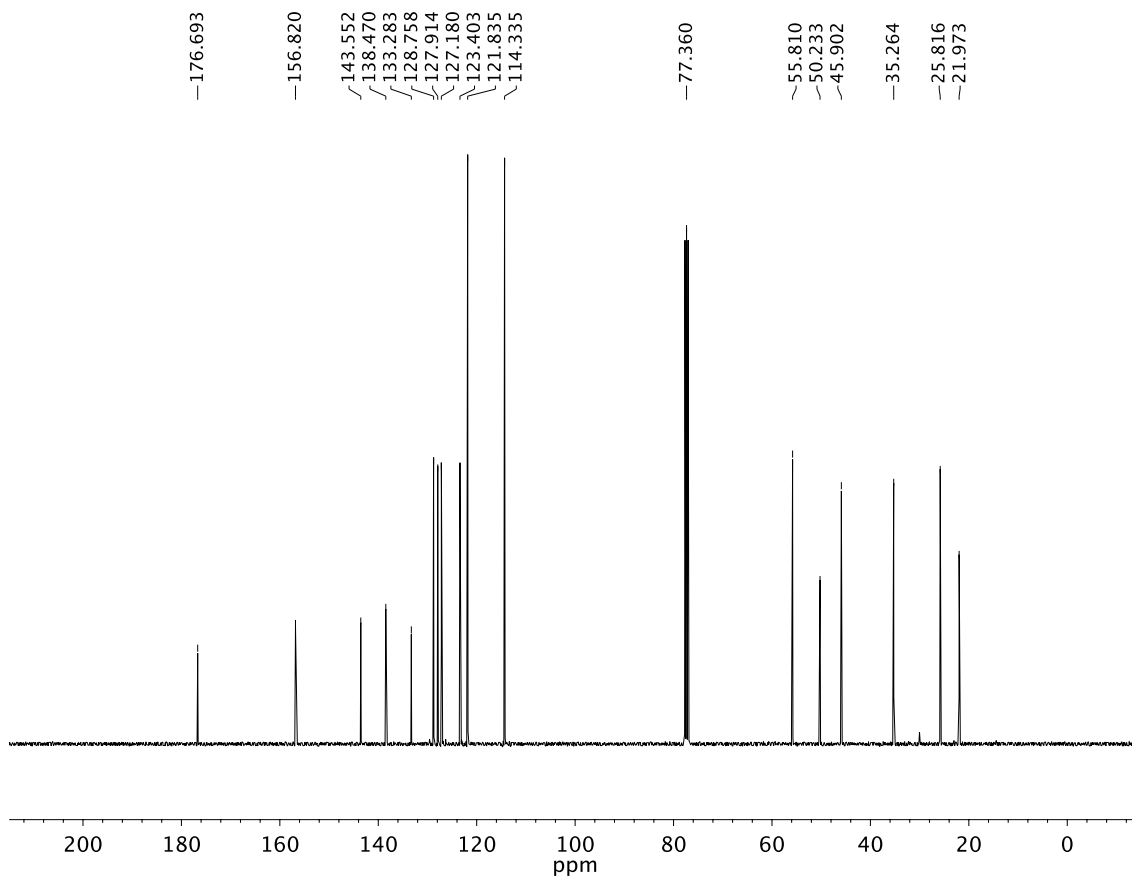


A3.68 ^{19}F NMR (282 MHz, CDCl_3) of compound **32aj**.

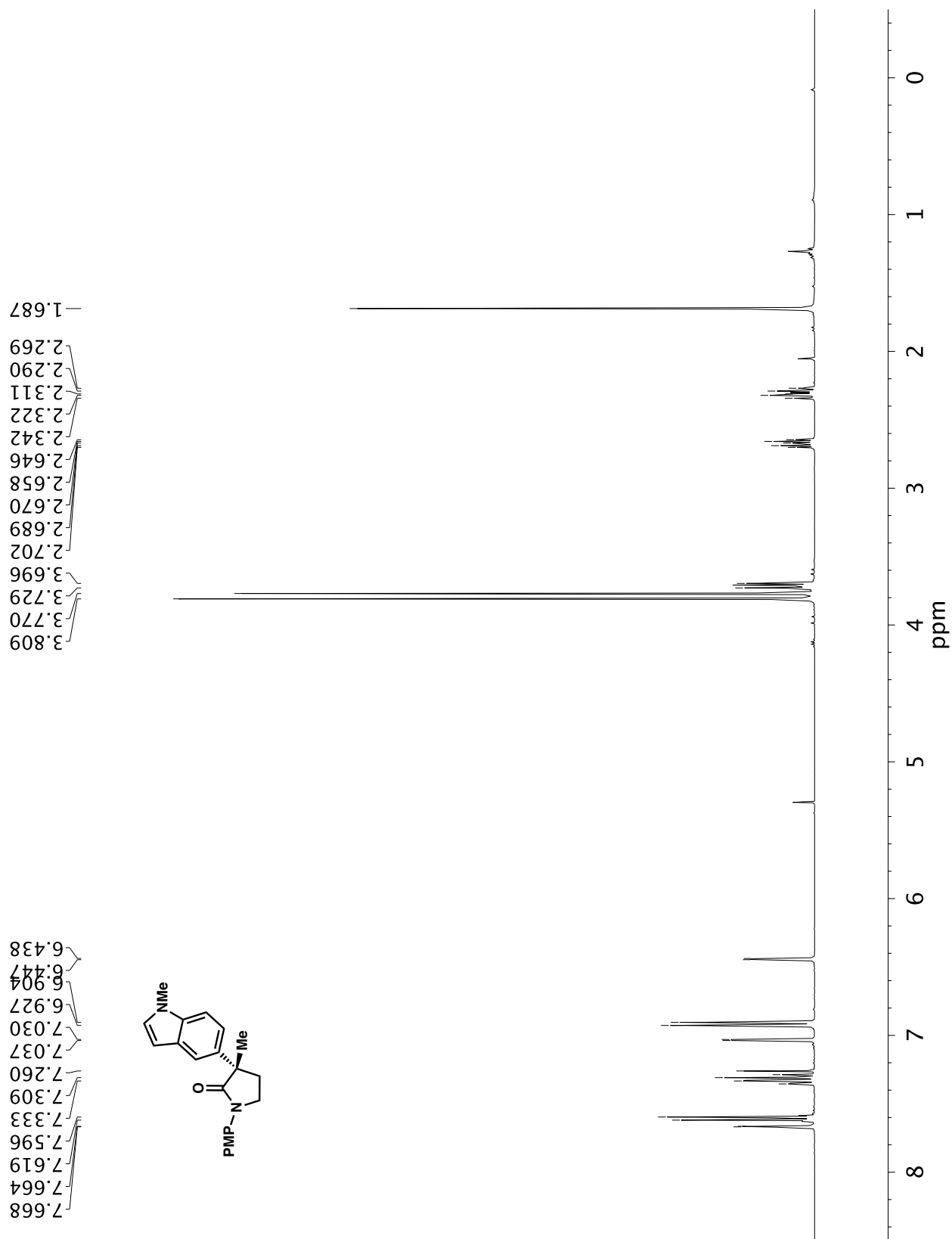
**A3.69** ¹H NMR (400 MHz, CDCl₃) of compound **32ak**.

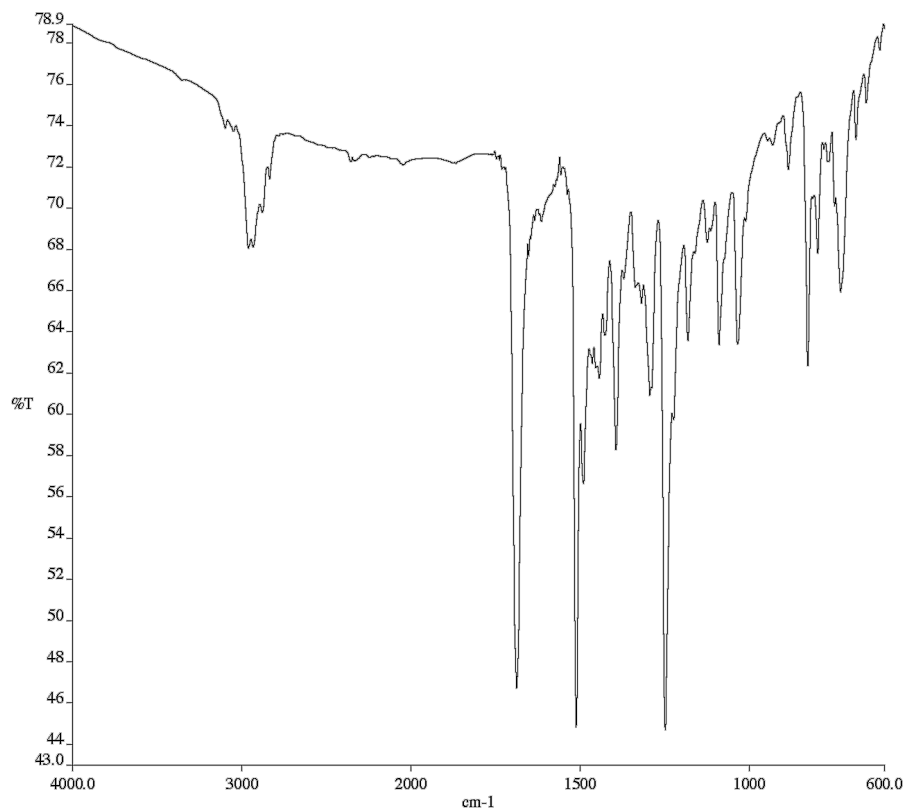


A3.70 Infrared spectrum (Thin Film, NaCl) of compound **32ak**.

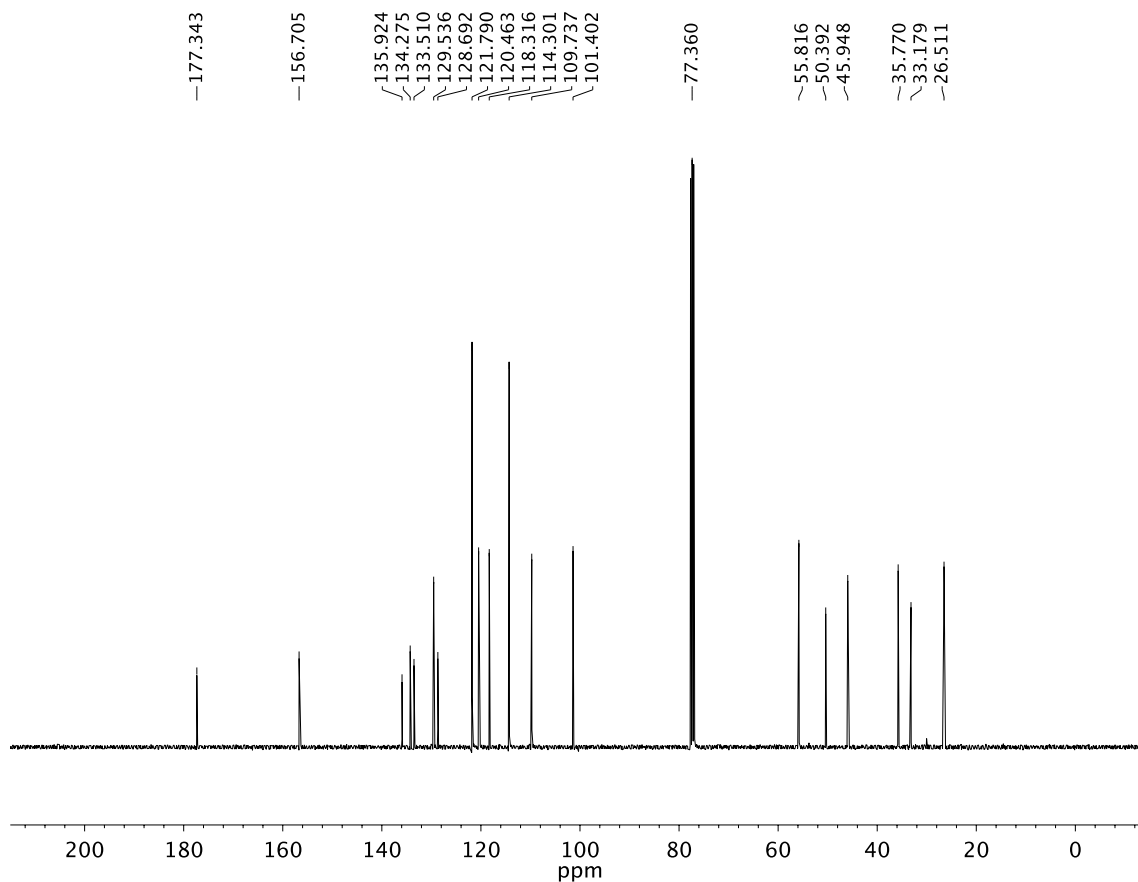


A3.71 ¹³C NMR (100 MHz, CDCl₃) of compound **32ak**.

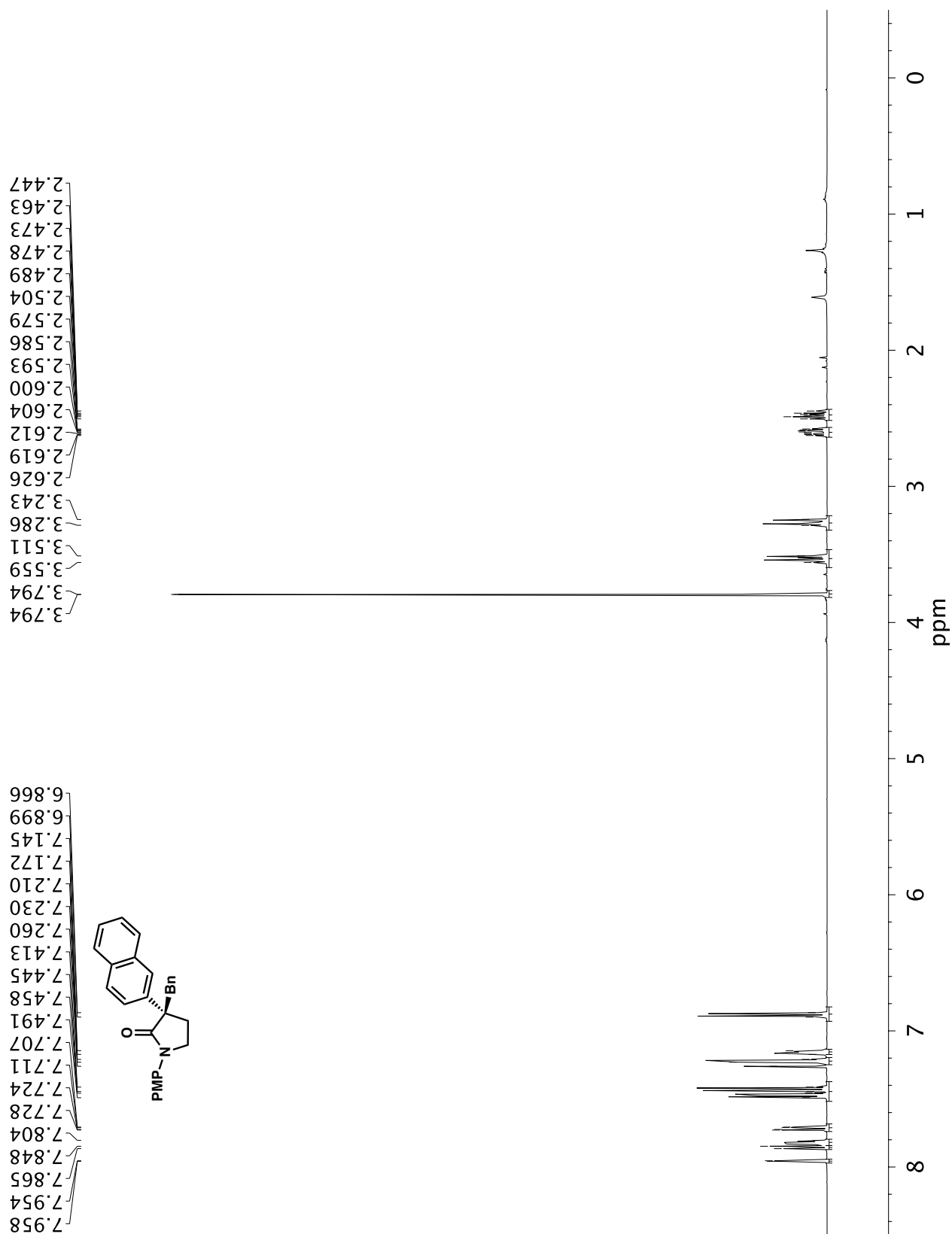


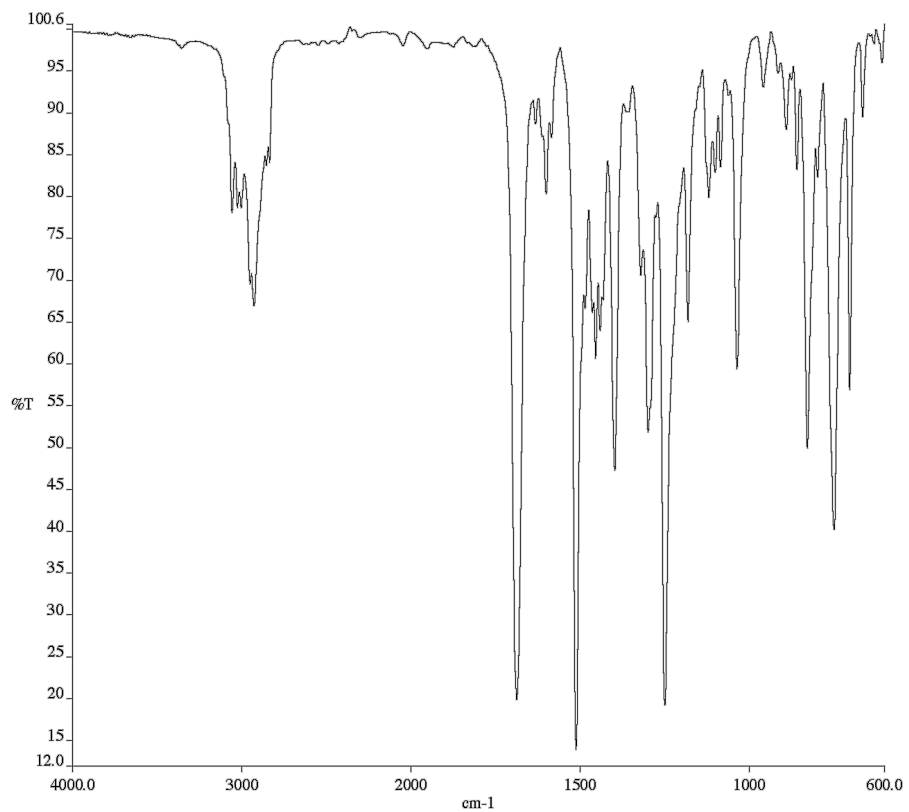


A3.73 Infrared spectrum (Thin Film, NaCl) of compound **32al**.

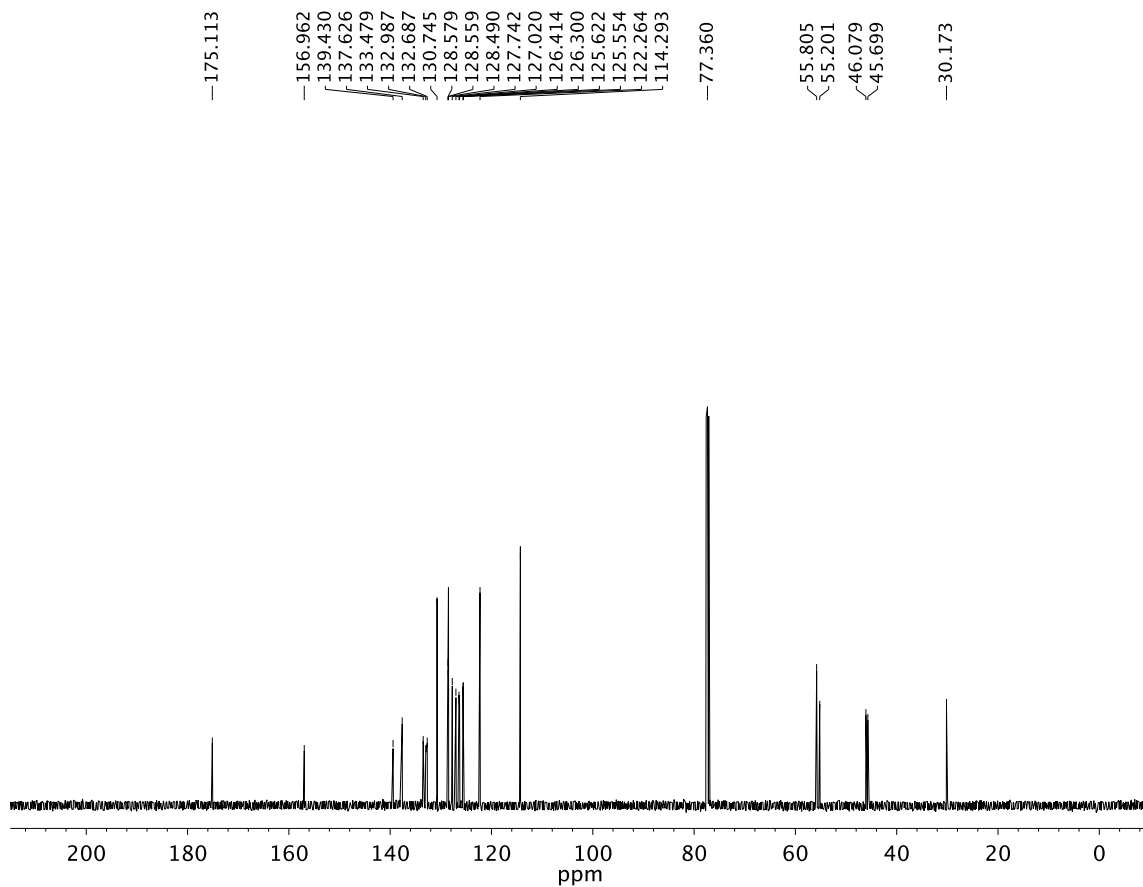


A3.74 ^{13}C NMR (100 MHz, CDCl_3) of compound **32al**.

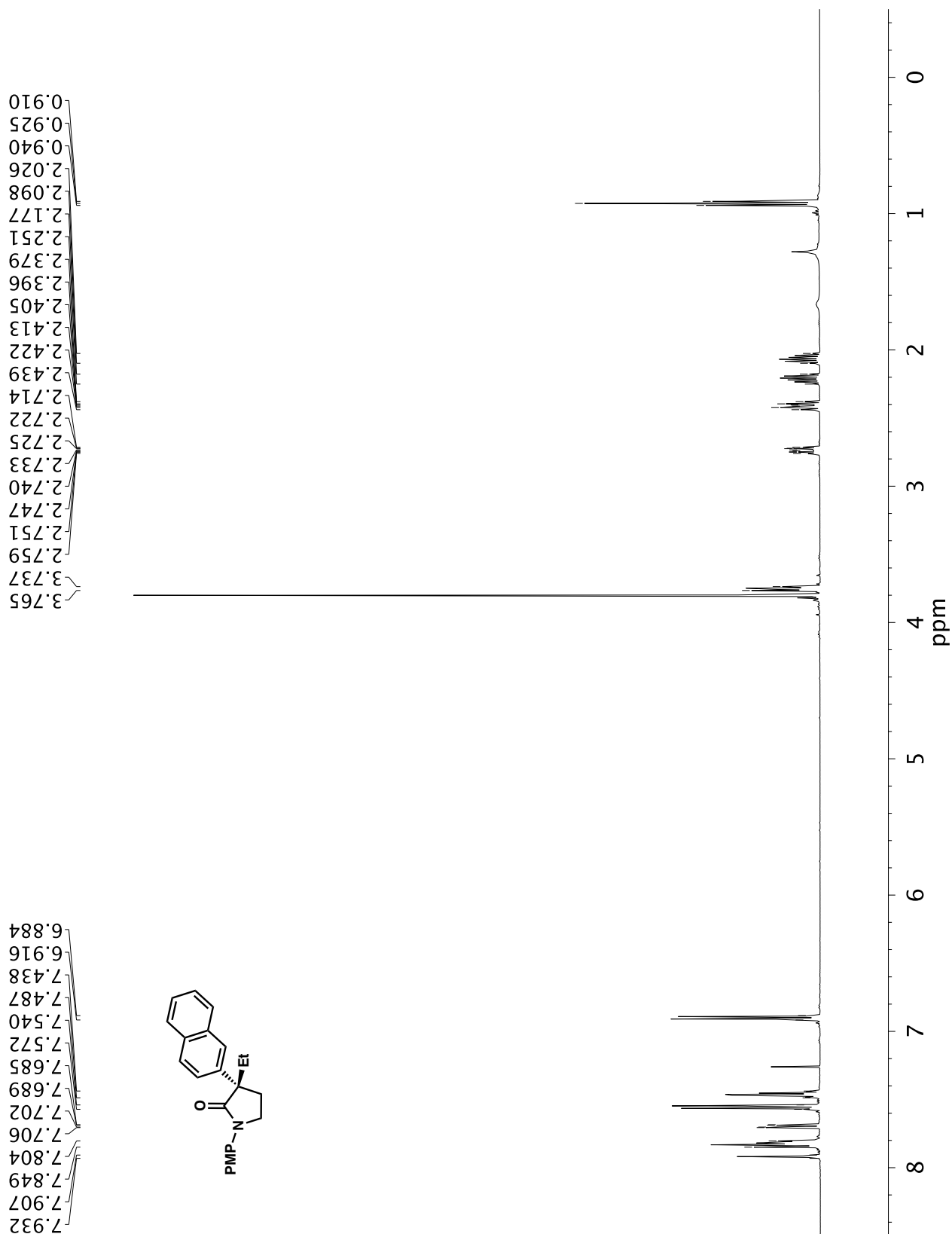
A3.75 ¹H NMR (500 MHz, CDCl₃) of compound 32gb.

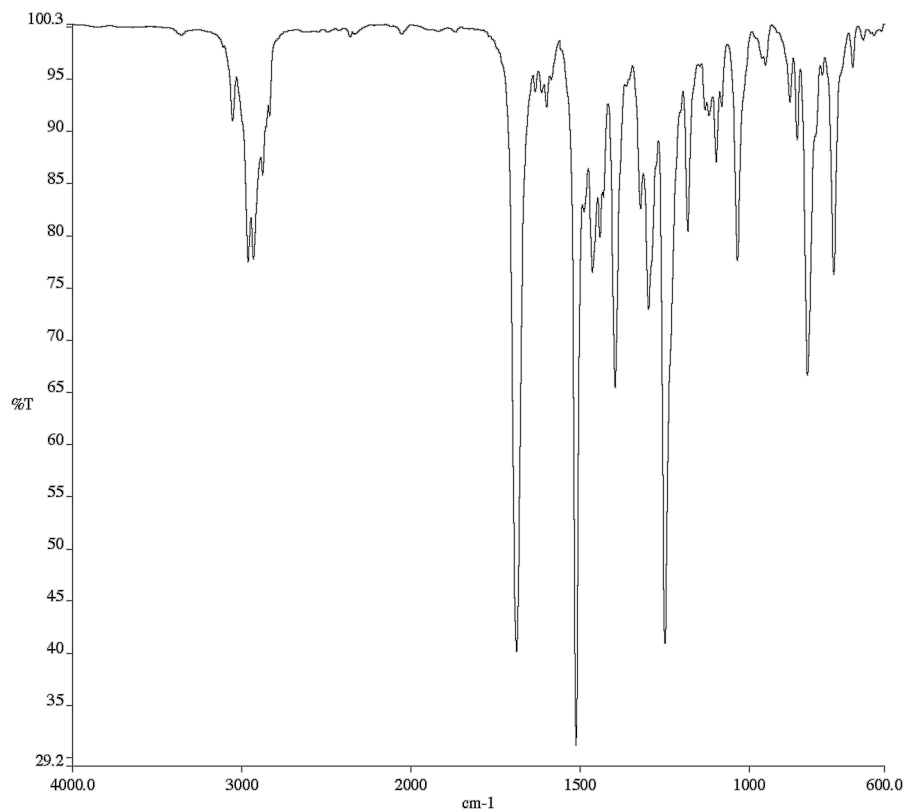


A3.76 Infrared spectrum (Thin Film, NaCl) of compound **32gb**.

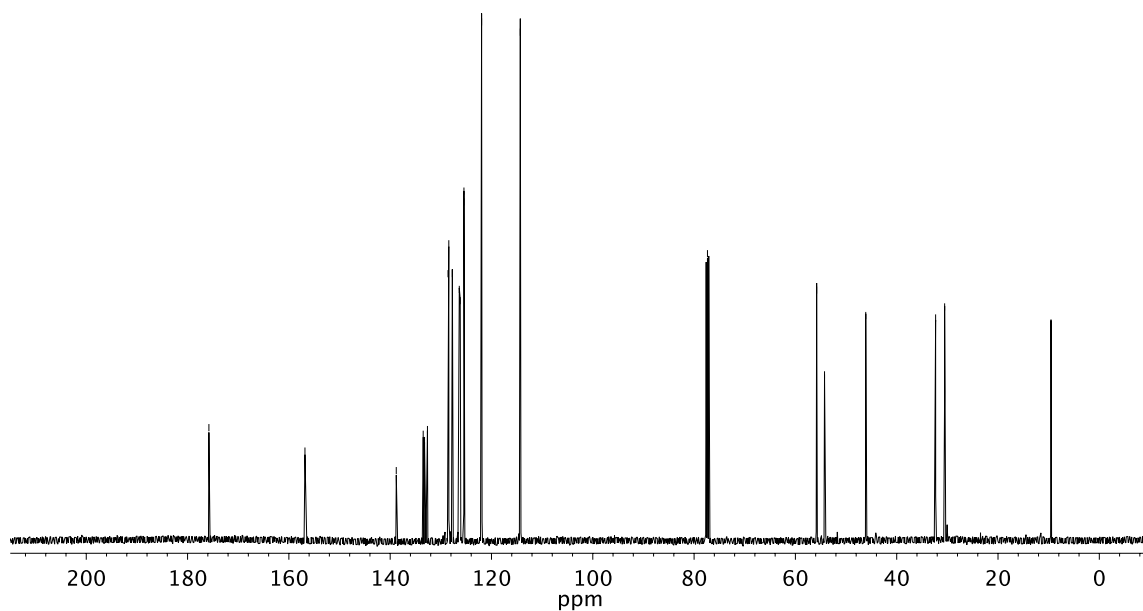


A3.77 ^{13}C NMR (125 MHz, CDCl_3) of compound **32gb**.

**A3.78** ^1H NMR (500 MHz, CDCl_3) of compound **32hb**.

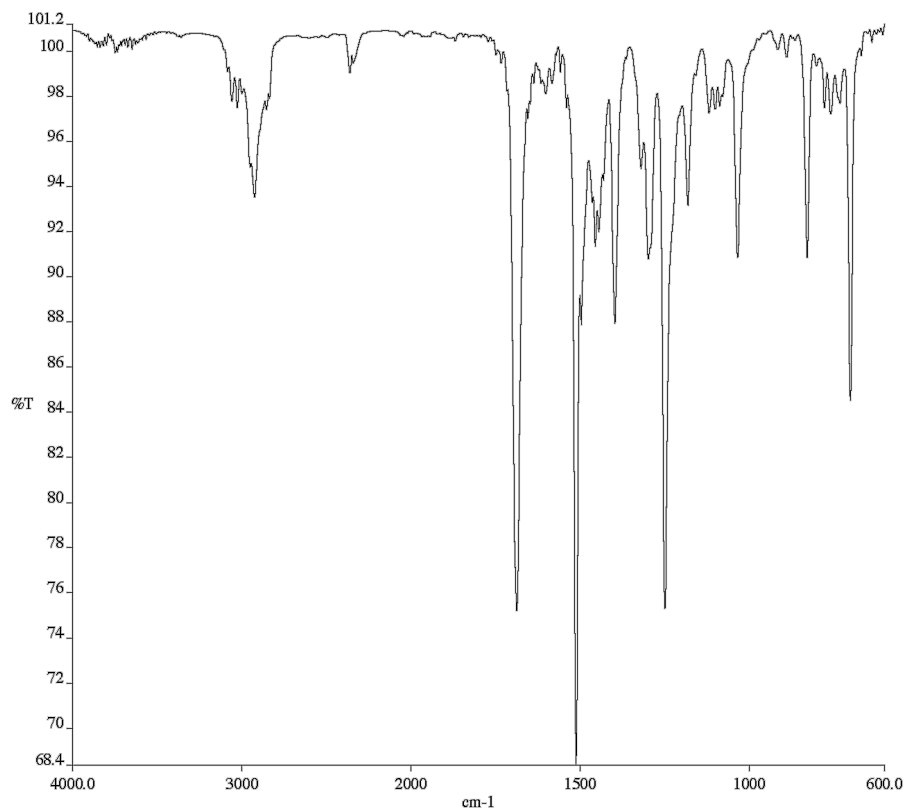


A3.79 Infrared spectrum (Thin Film, NaCl) of compound **32hb**.

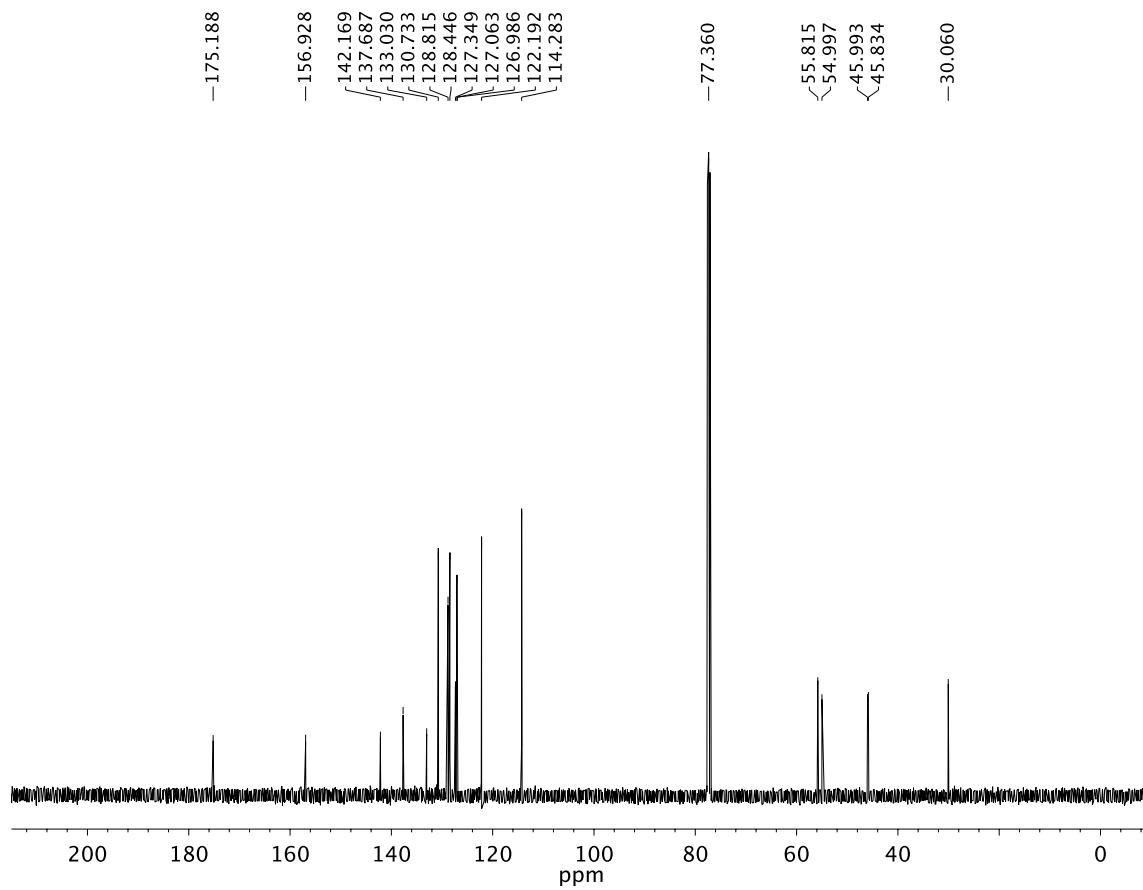


A3.80 ¹³C NMR (125 MHz, CDCl₃) of compound **32hb**.

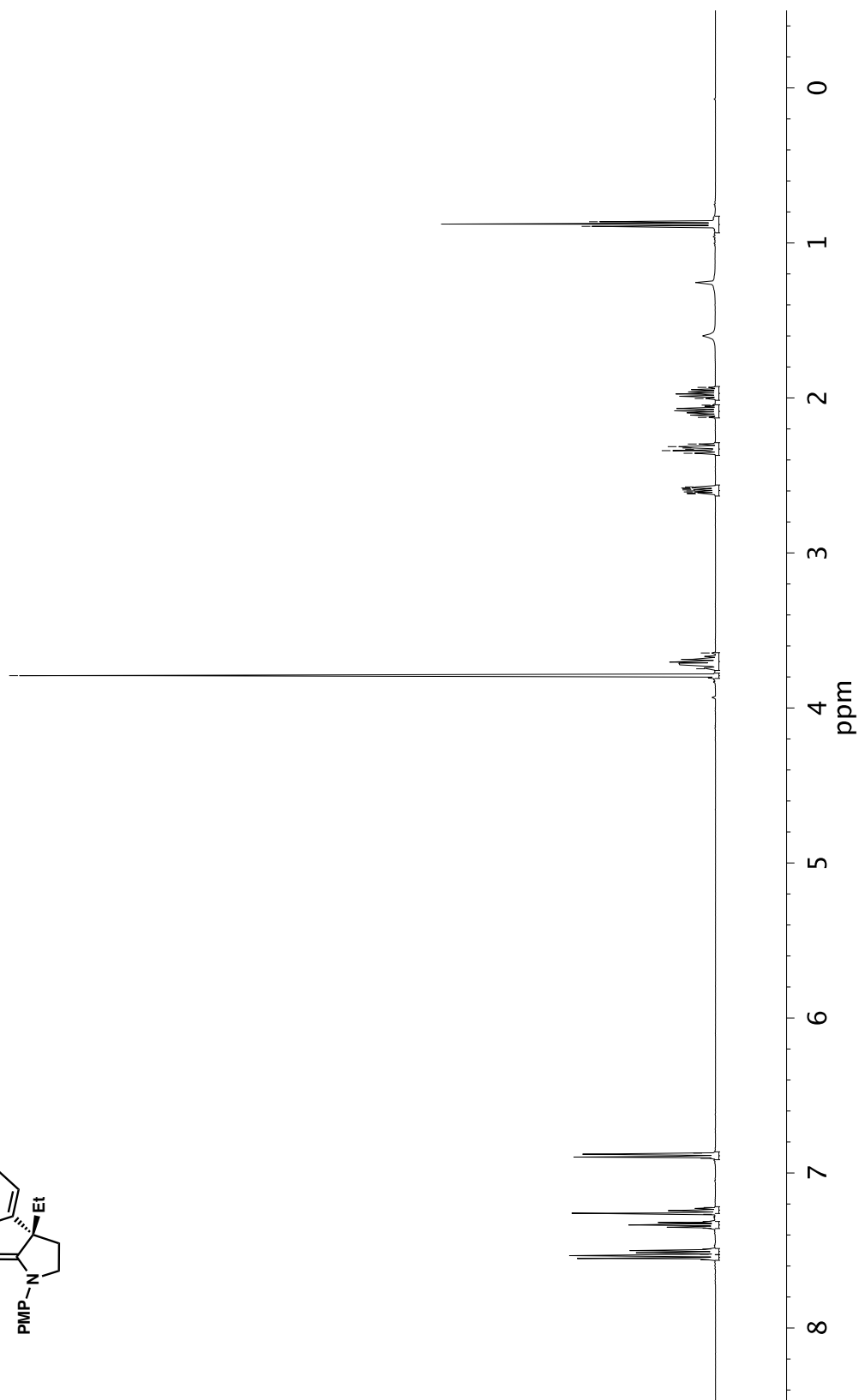
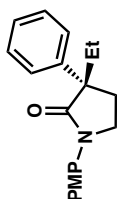
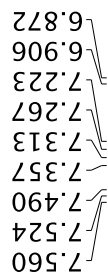




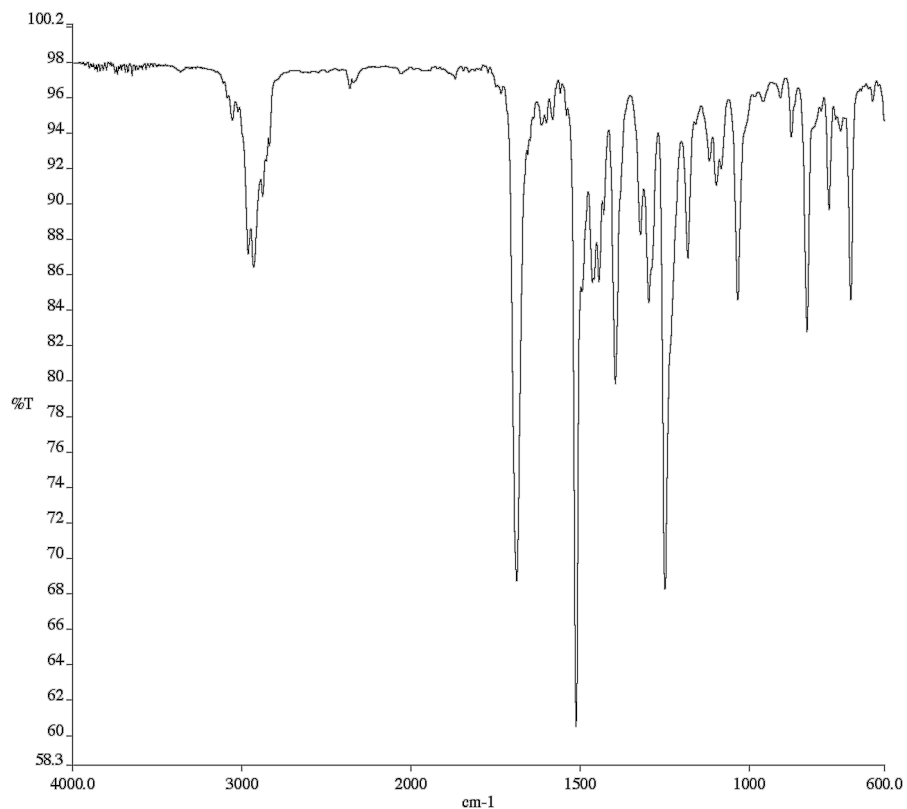
A3.82 Infrared spectrum (Thin Film, NaCl) of compound **32ga**.



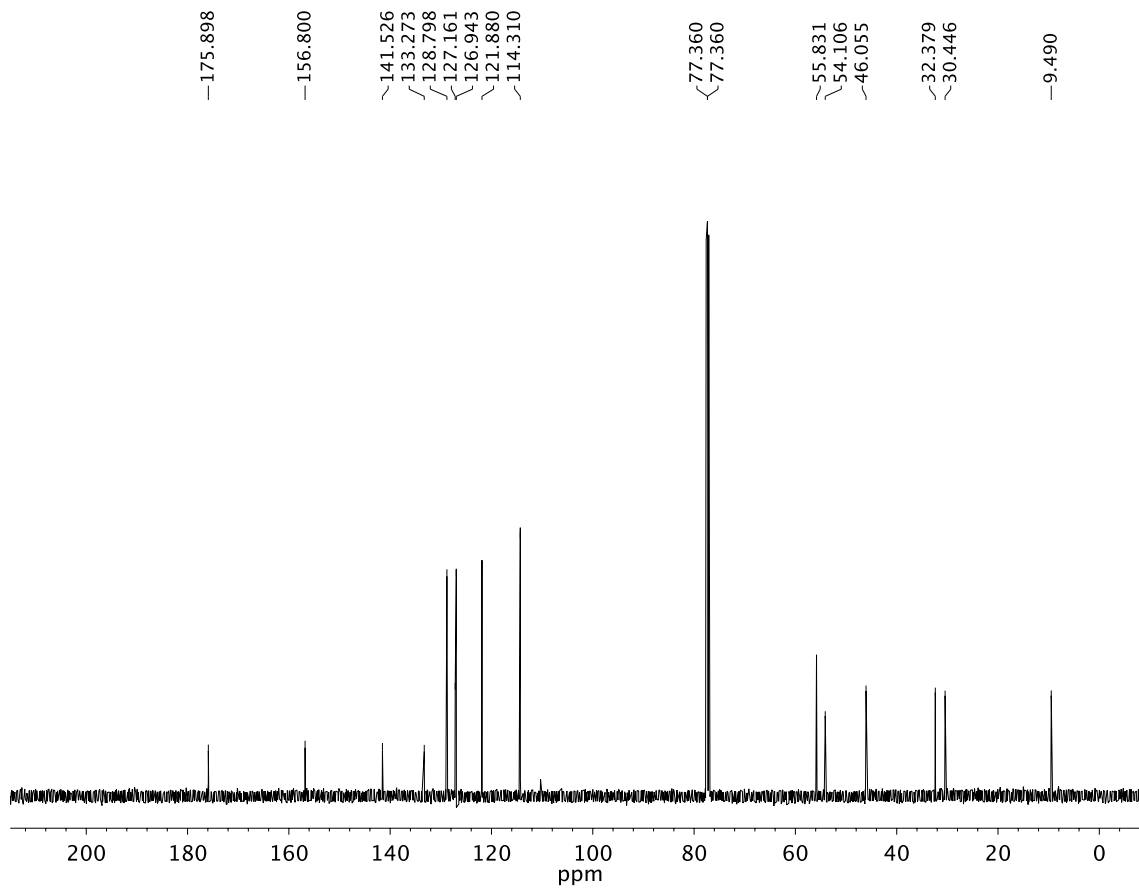
A3.83 ¹³C NMR (125 MHz, CDCl₃) of compound **32ga**.



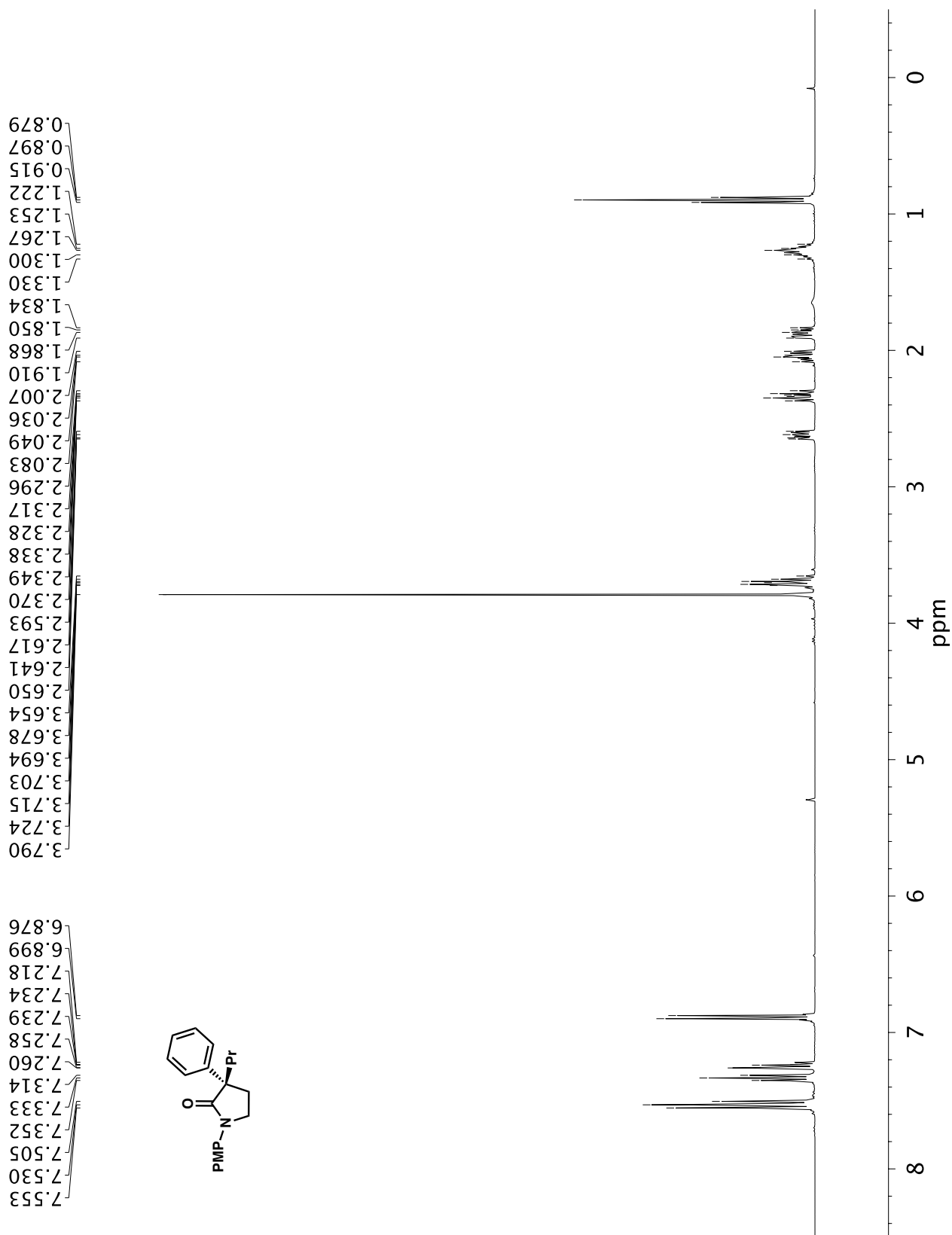
A3.84 ^1H NMR (500 MHz, CDCl_3) of compound **32ha**.

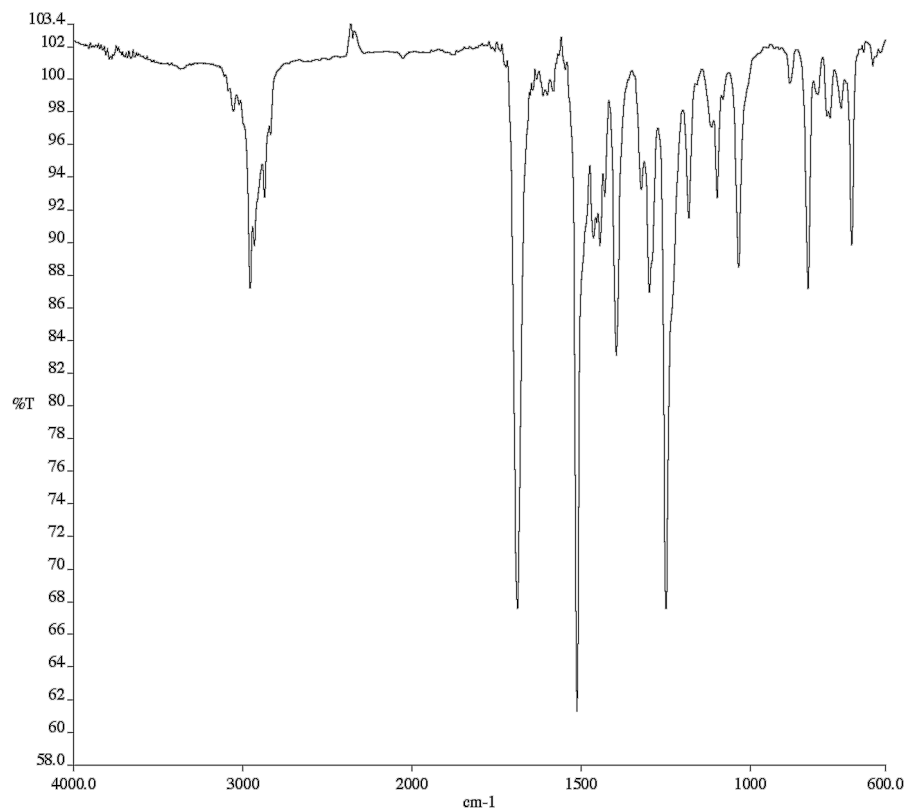


A3.85 Infrared spectrum (Thin Film, NaCl) of compound **32ha**.

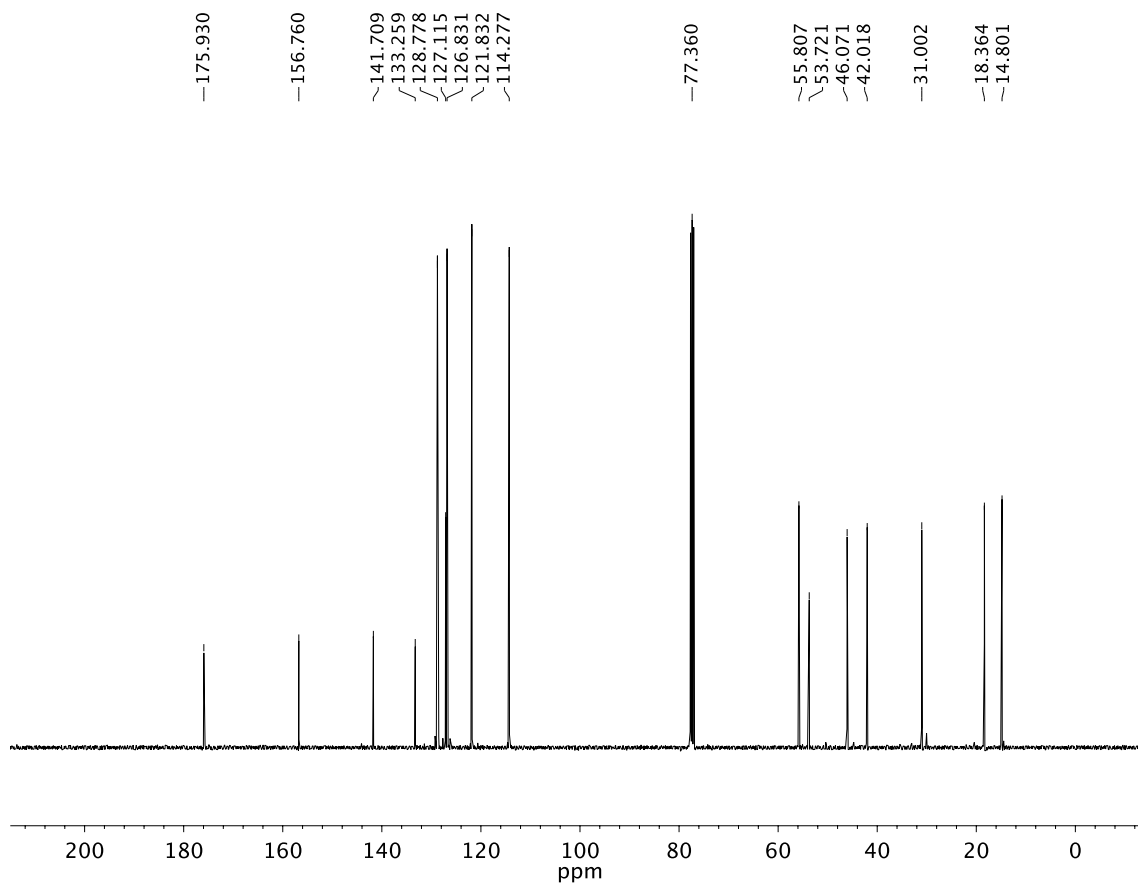


A3.86 ^{13}C NMR (125 MHz, CDCl_3) of compound **32ha**.

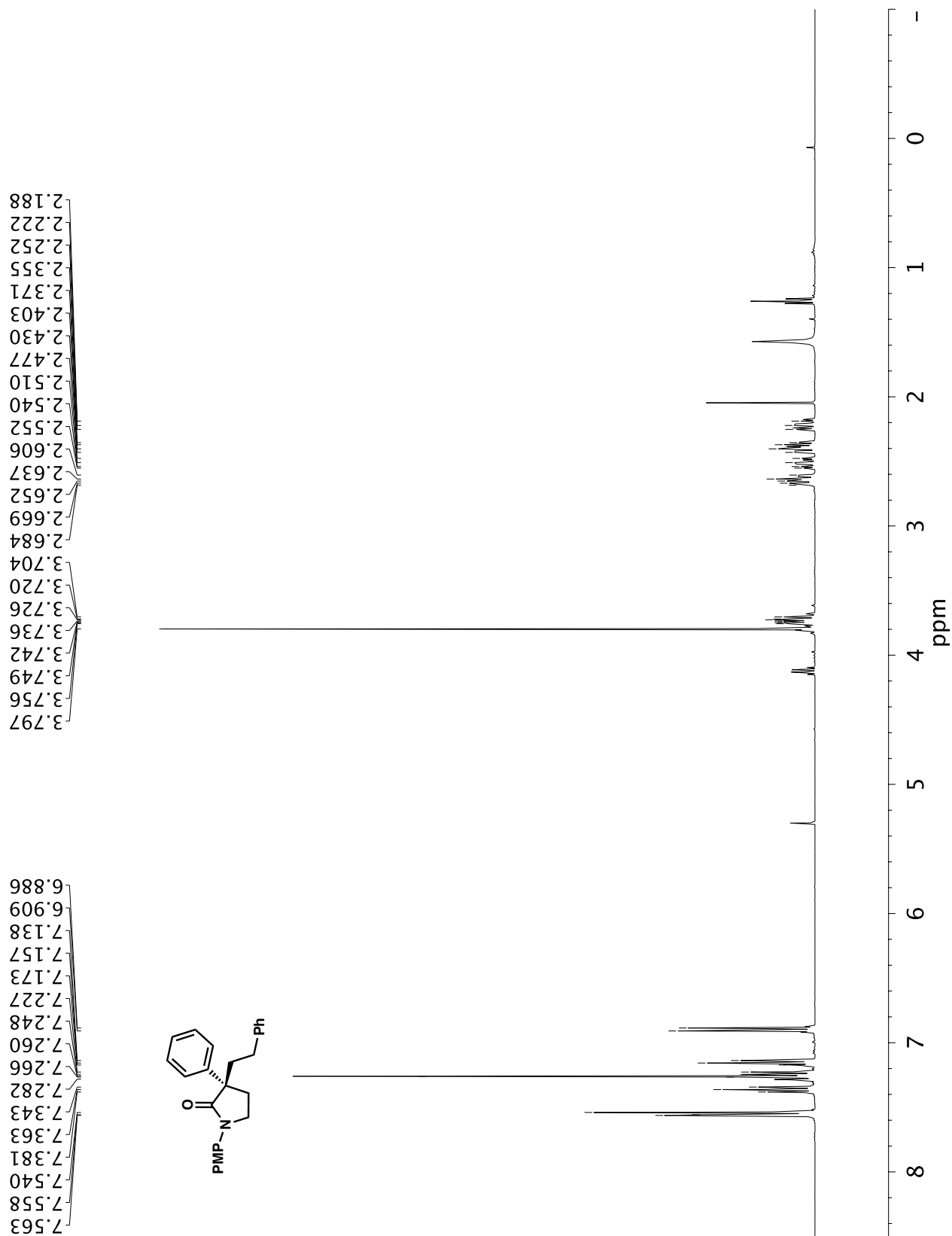
**A3.87** ¹H NMR (400 MHz, CDCl₃) of compound **32ia**.

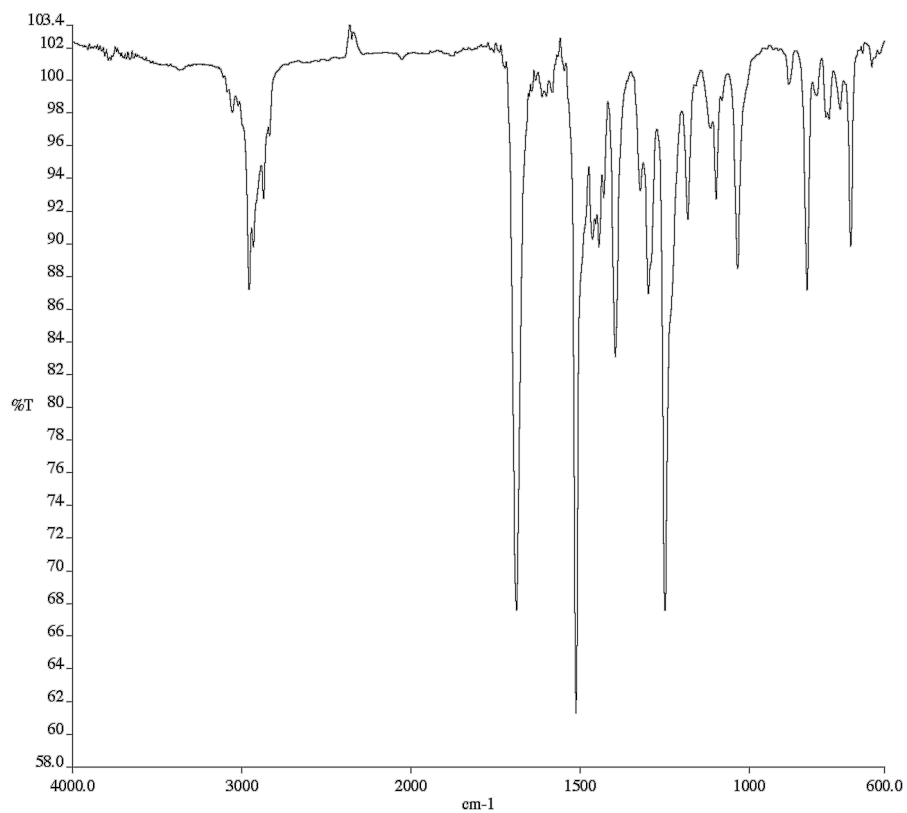


A3.88 Infrared spectrum (Thin Film, NaCl) of compound **32ia**.

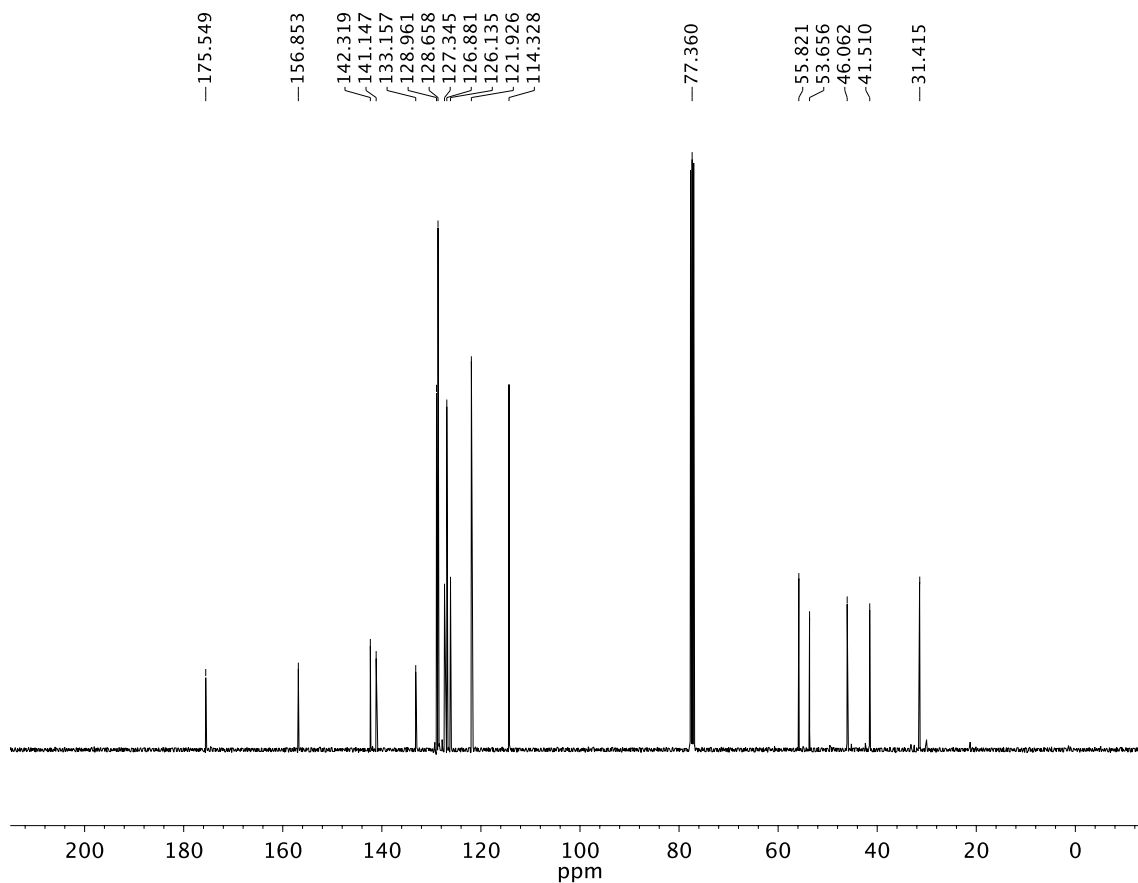


A3.89 ¹³C NMR (100 MHz, CDCl₃) of compound **32ia**.

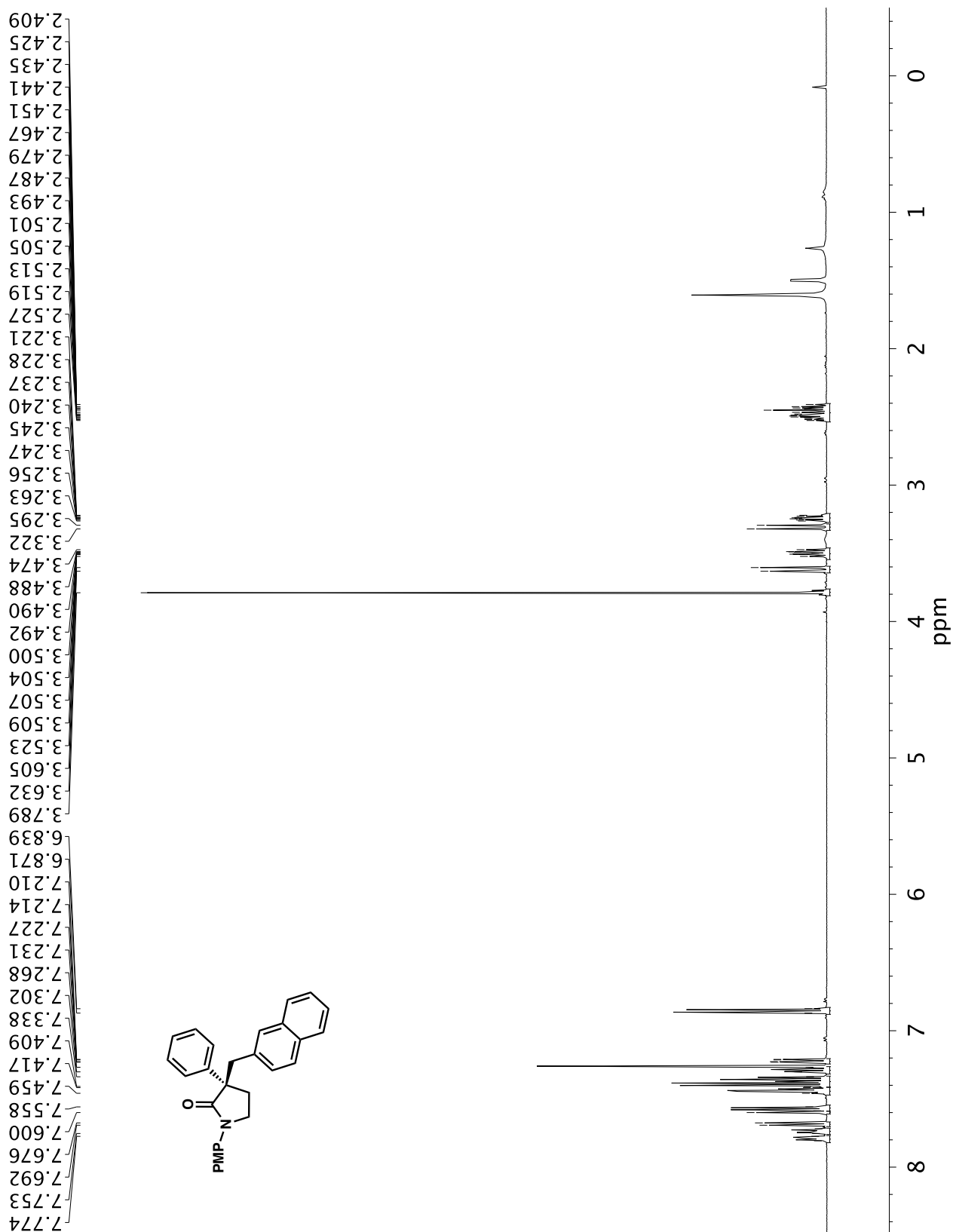
**A3.90** ^1H NMR (400 MHz, CDCl_3) of compound **32ja**.

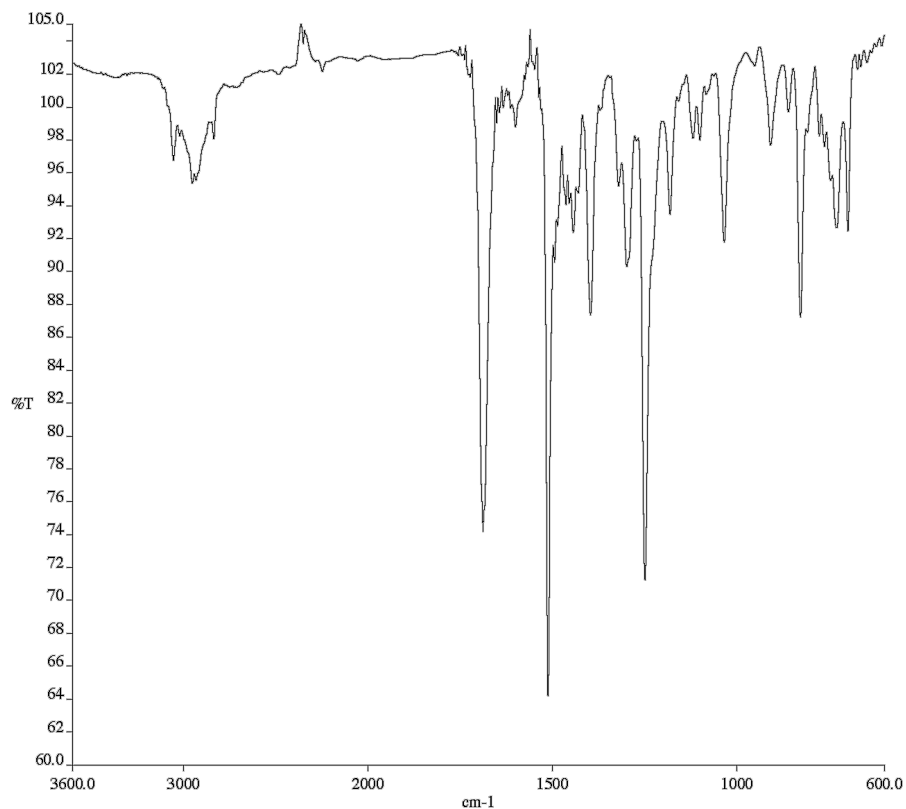


A3.91 Infrared spectrum (Thin Film, NaCl) of compound **32ja**.

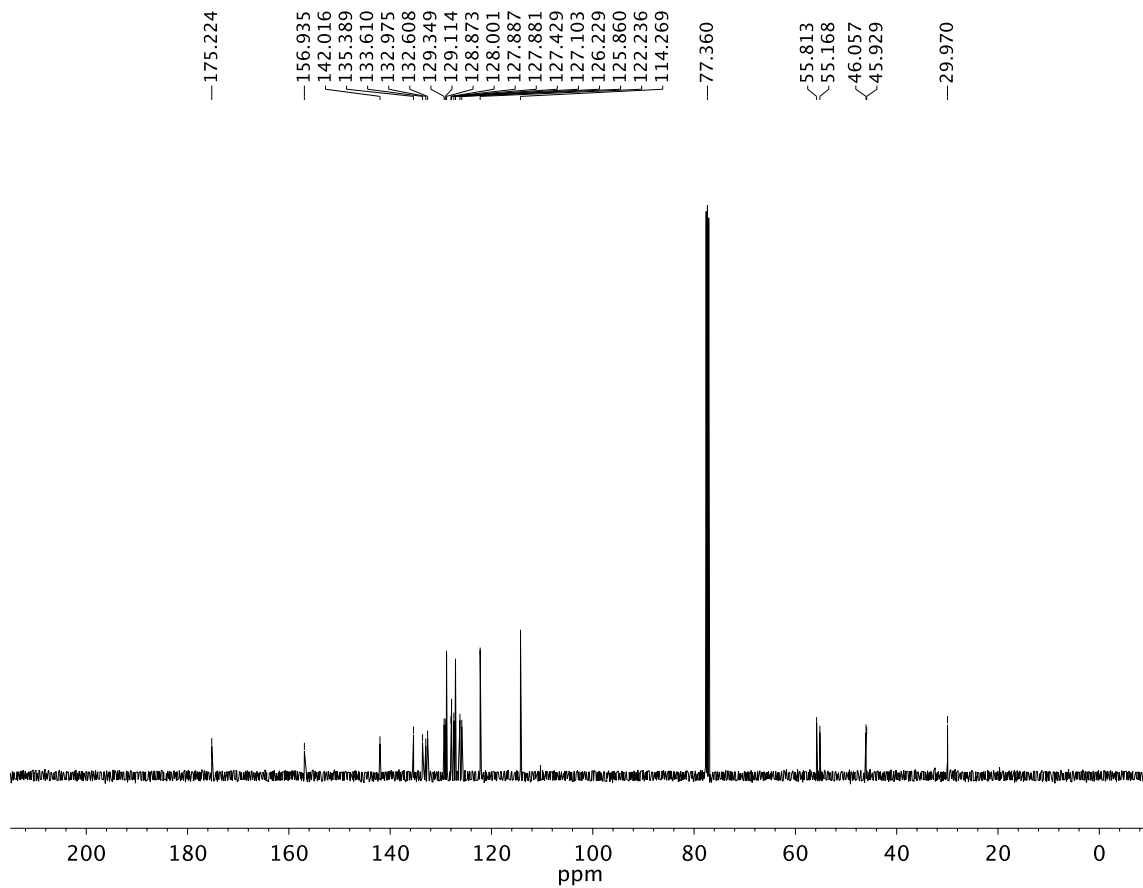


A3.92 ¹³C NMR (100 MHz, CDCl₃) of compound **32ja**.

**A3.93** ^1H NMR (500 MHz, CDCl_3) of compound **32ka**.



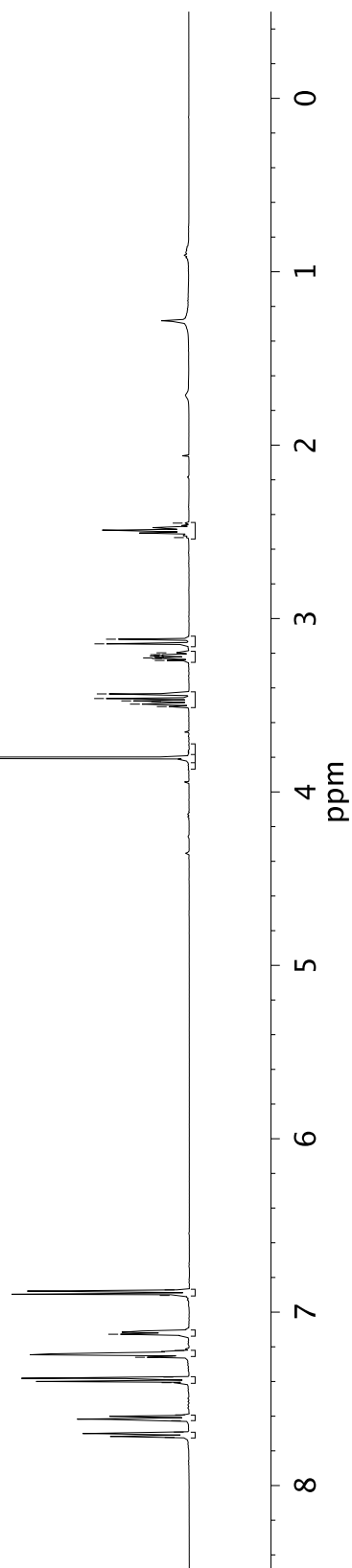
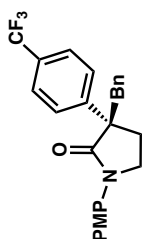
A3.94 Infrared spectrum (Thin Film, NaCl) of compound **32ka**.



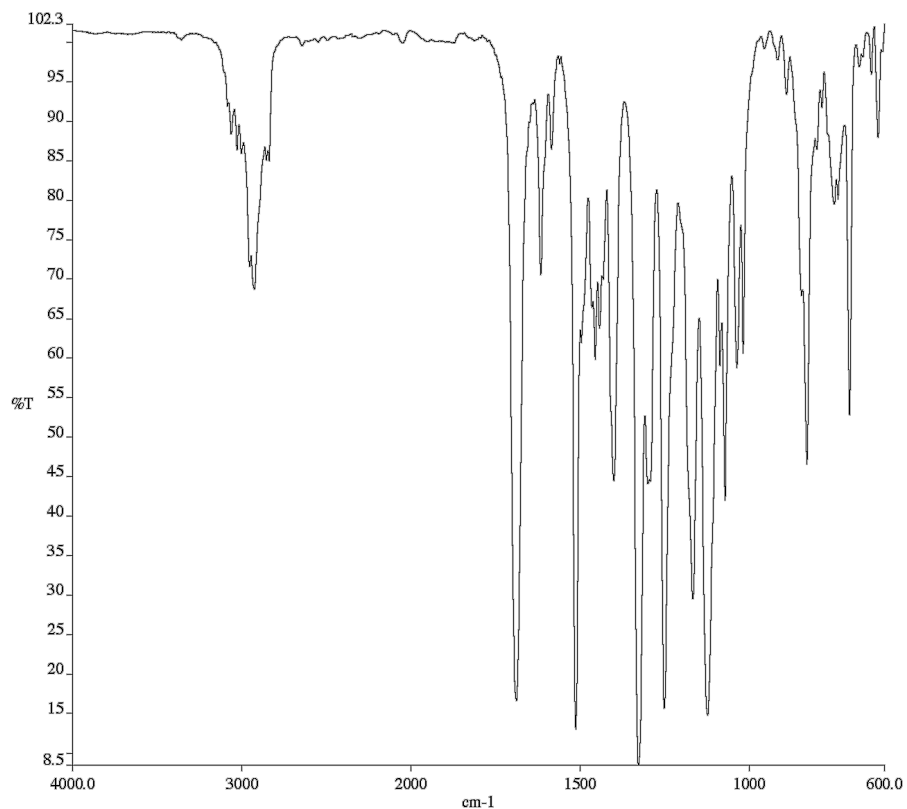
A3.95 ^{13}C NMR (125 MHz, CDCl_3) of compound **32ka**.

7.722
7.692
7.626
7.592
7.407
7.375
7.260
7.253
7.221
7.127
6.904
6.872

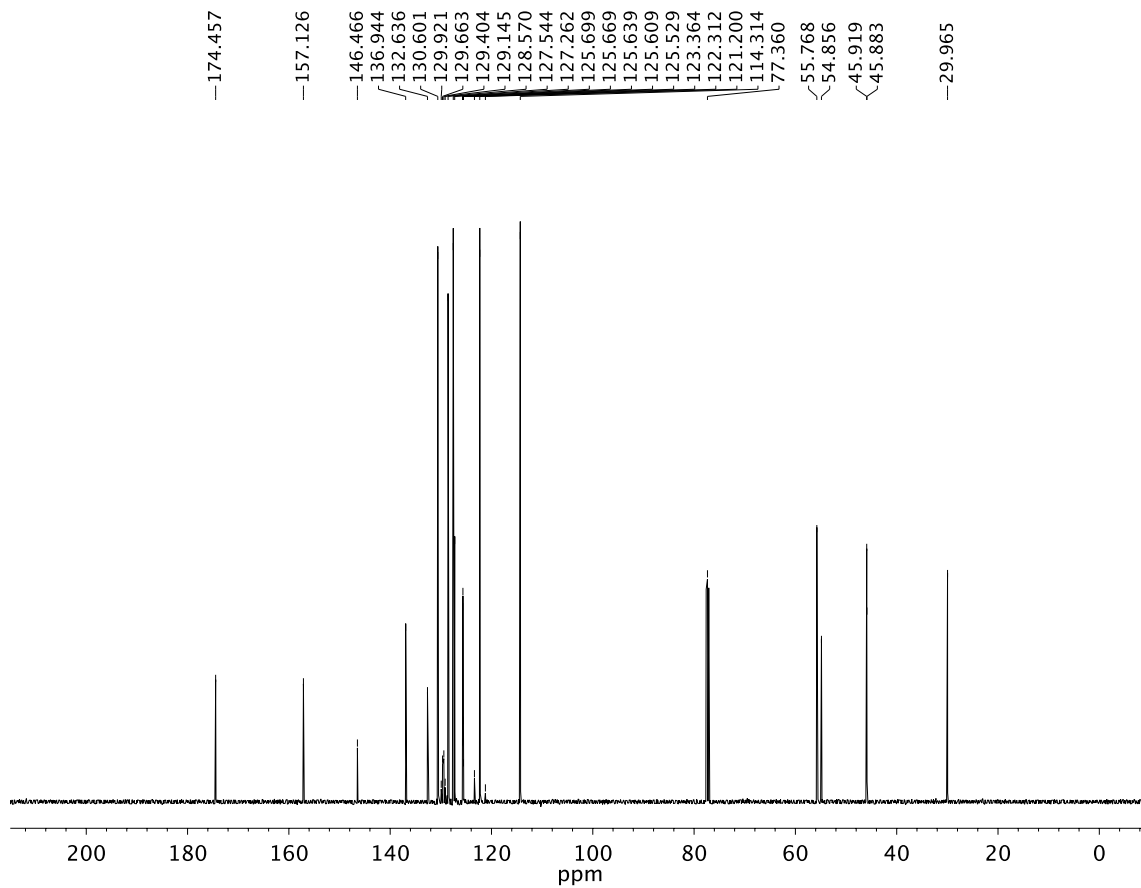
3.801
3.508
3.494
3.479
3.475
3.461
3.435
3.242
3.231
3.227
3.223
3.216
3.212
3.208
3.198
3.146
3.119
2.533
2.450



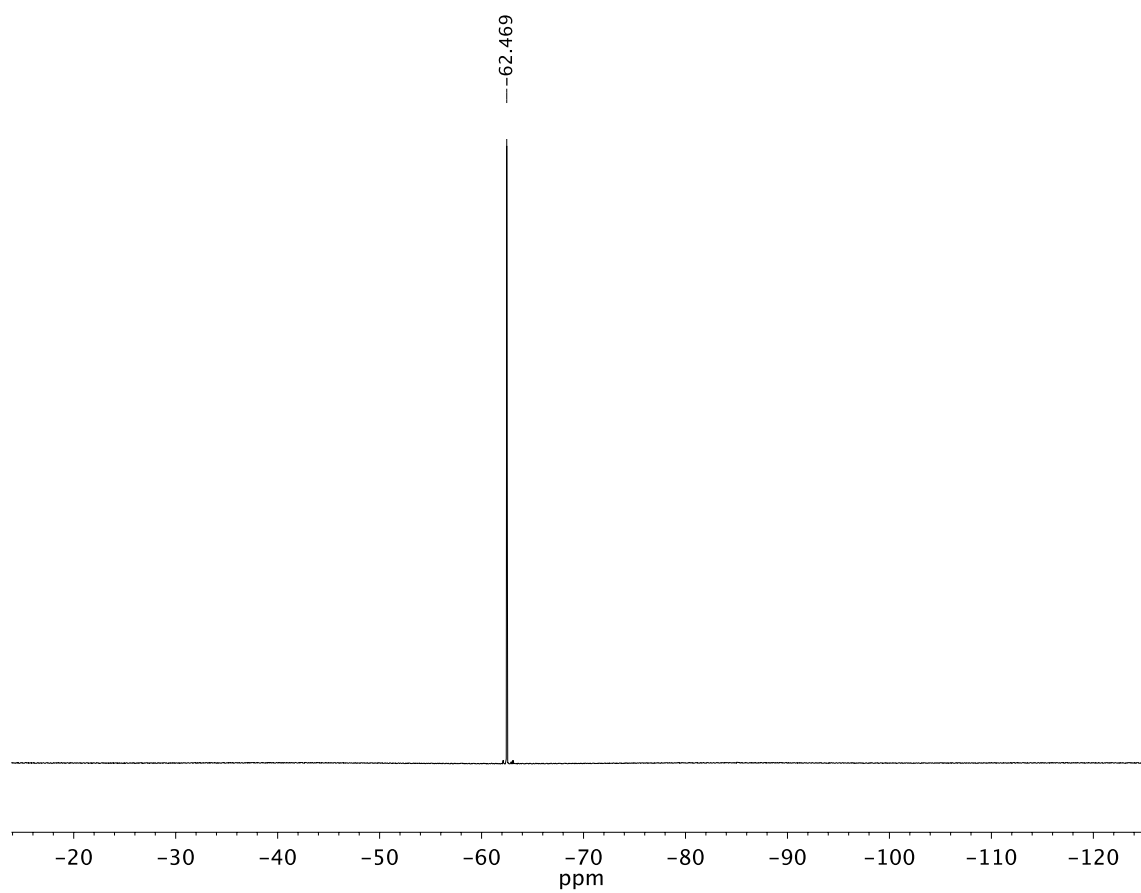
A3.96 ¹H NMR (500 MHz, CDCl₃) of compound 32gc.



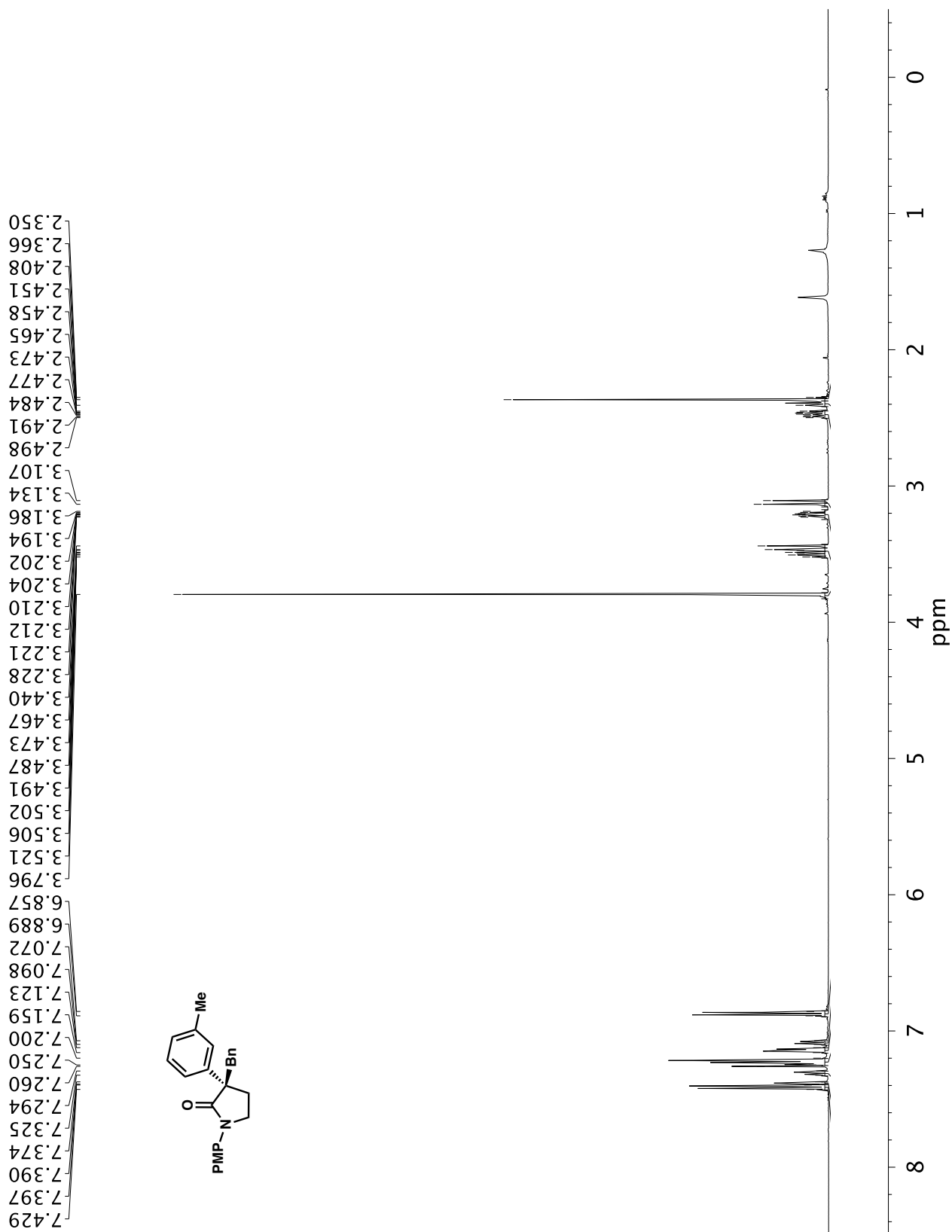
A3.97 Infrared spectrum (Thin Film, NaCl) of compound **32gc**.

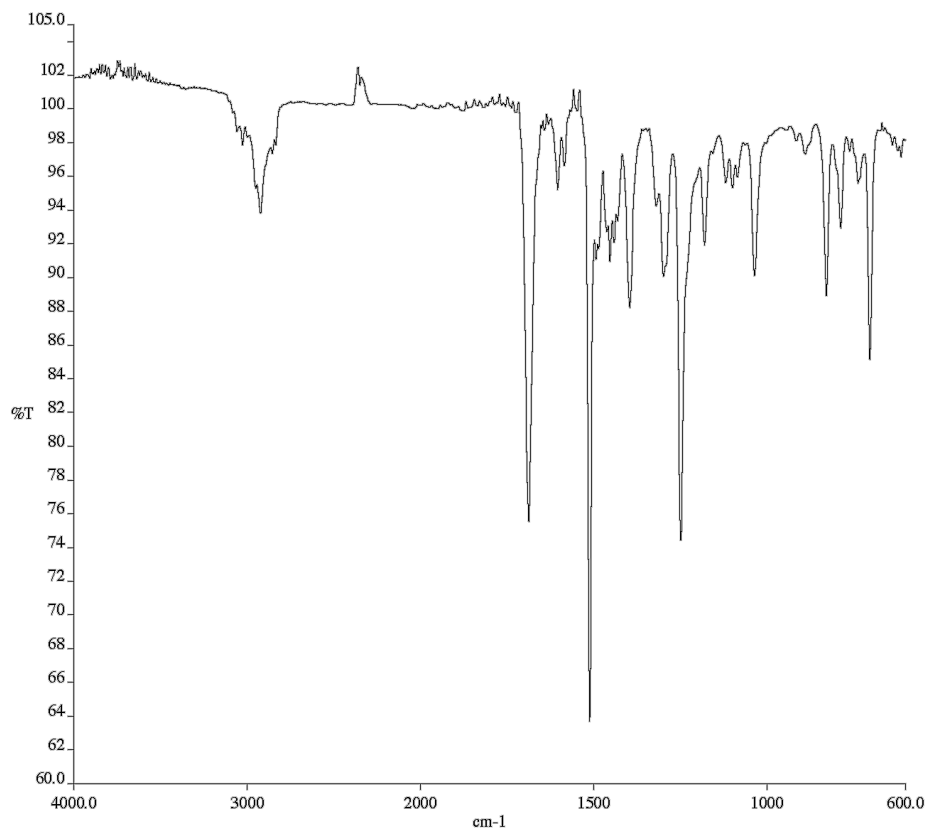


A3.98 ¹³C NMR (125 MHz, CDCl₃) of compound **32gc**.

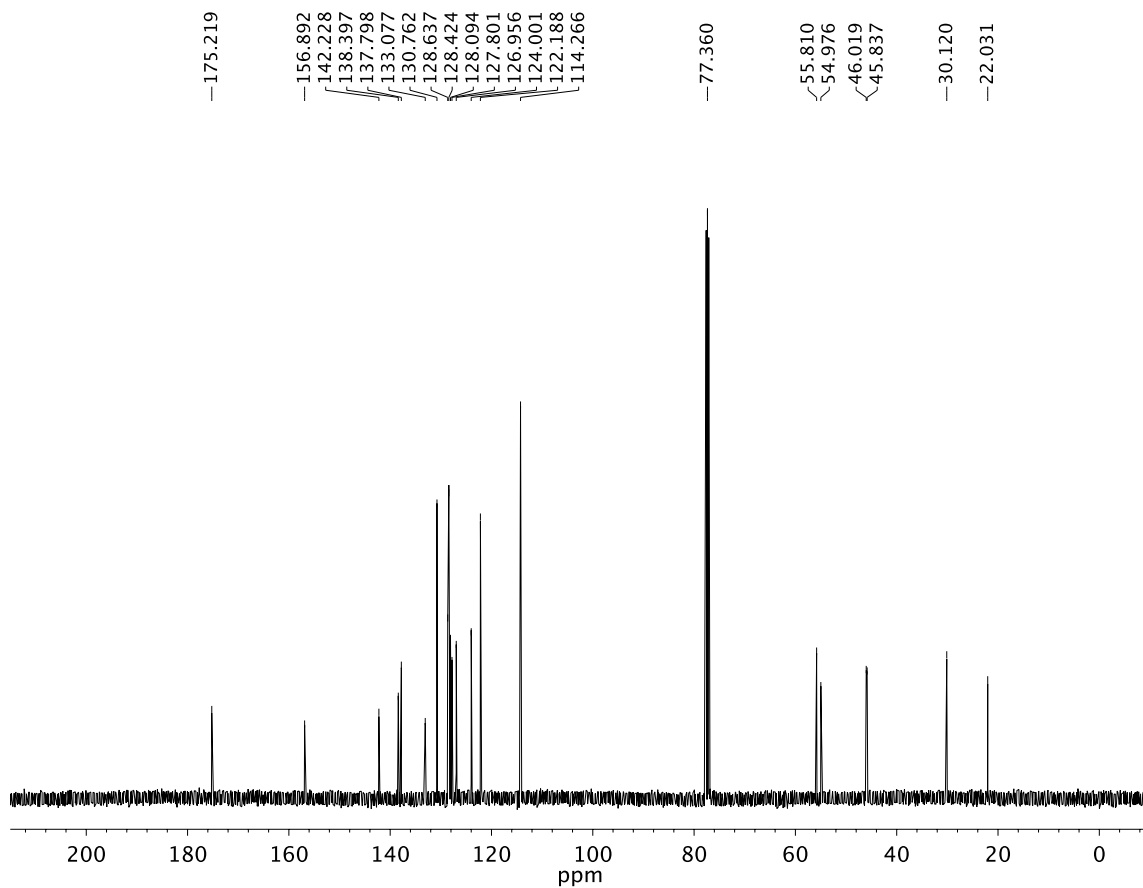


A3.99 ^{19}F NMR (282 MHz, CDCl_3) of compound **32gc**.

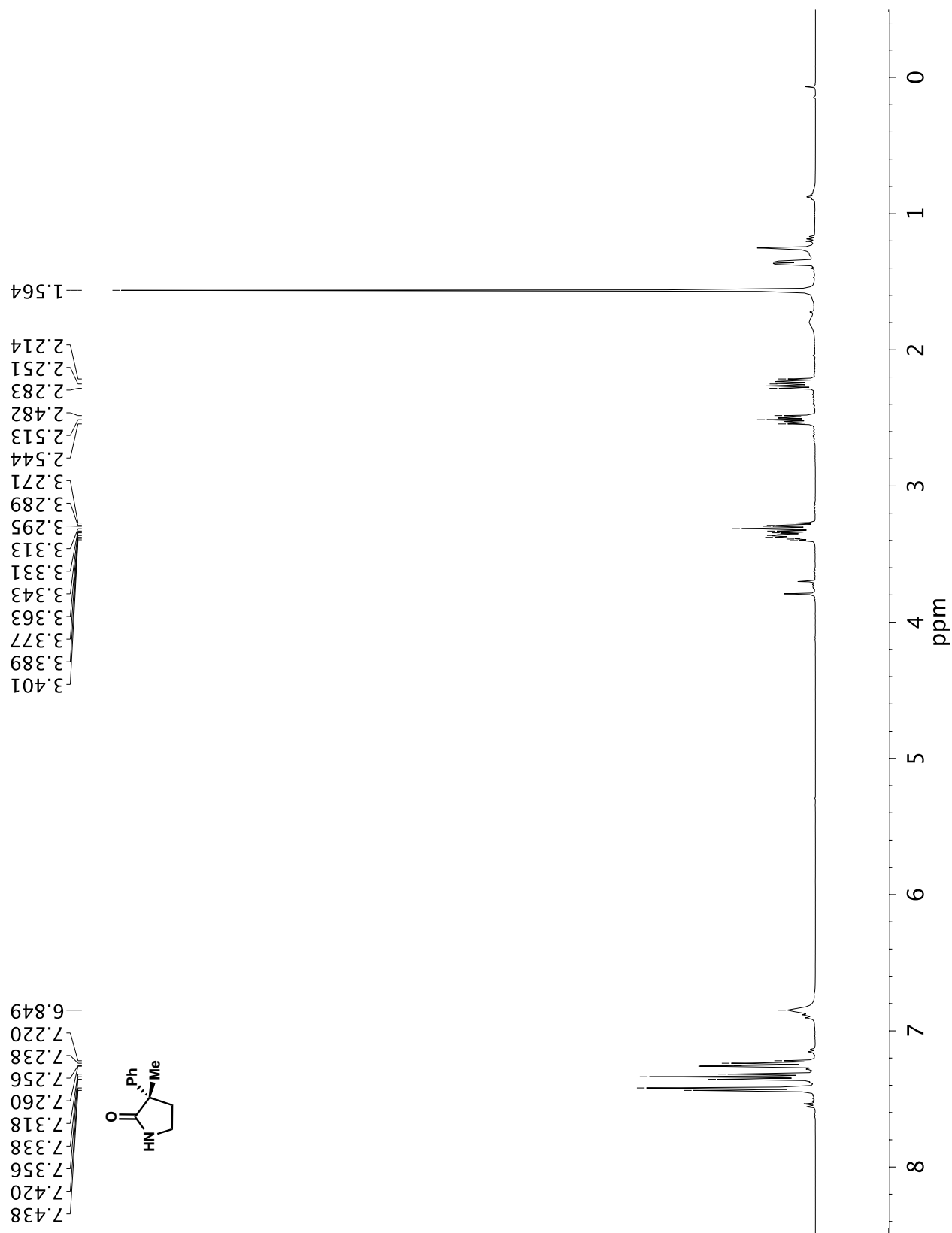
**A3.100** ¹H NMR (400 MHz, CDCl₃) of compound **32gk**.

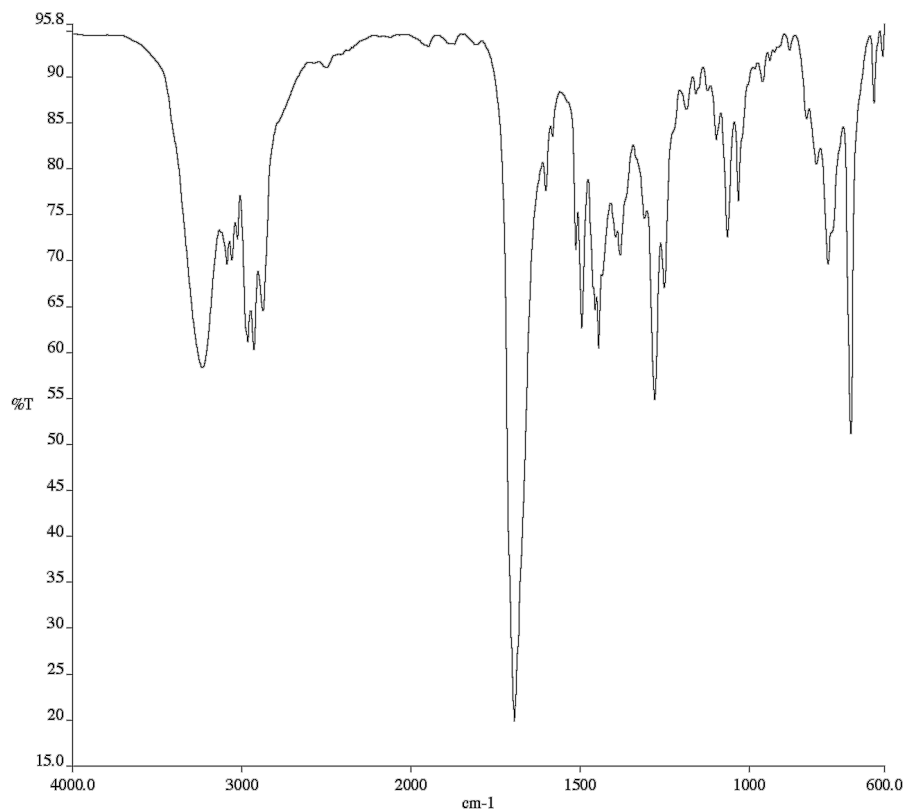


A3.101 Infrared spectrum (Thin Film, NaCl) of compound **32gk**.

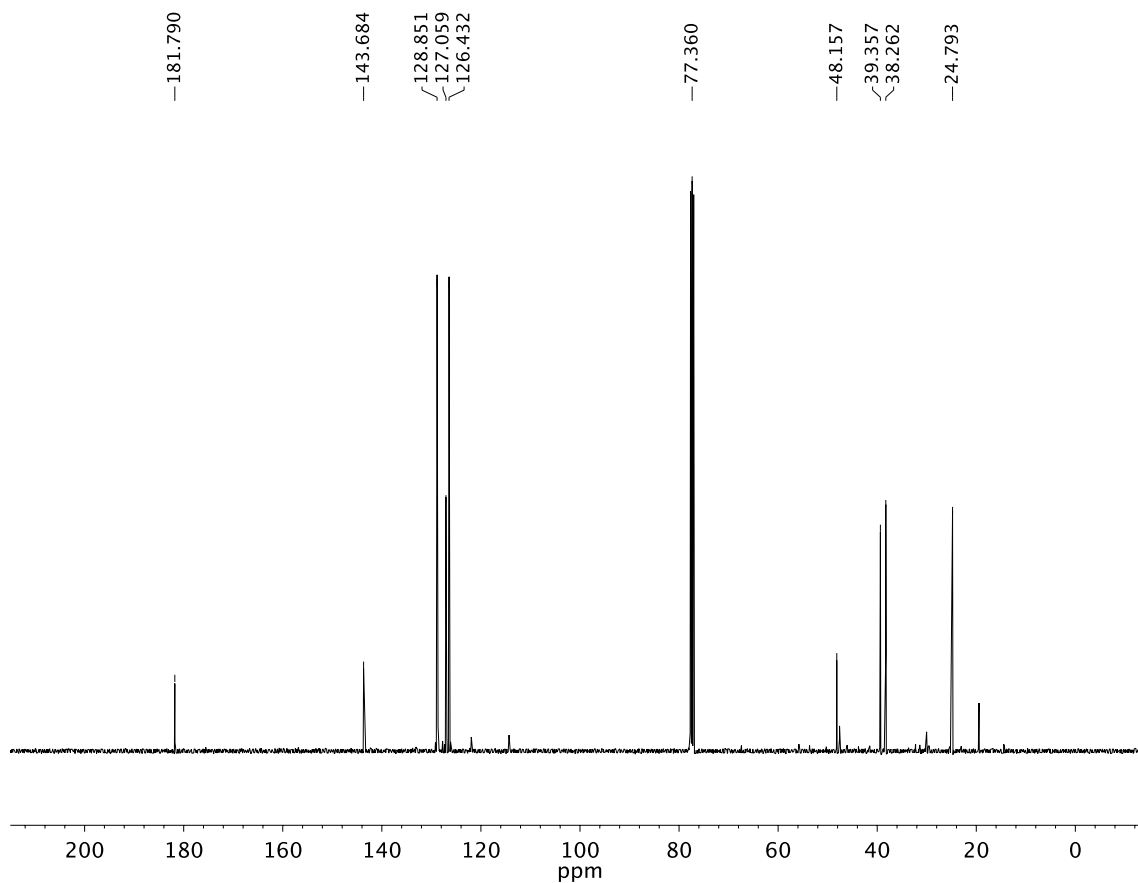


A3.102 ¹³C NMR (125 MHz, CDCl₃) of compound **32gk**.

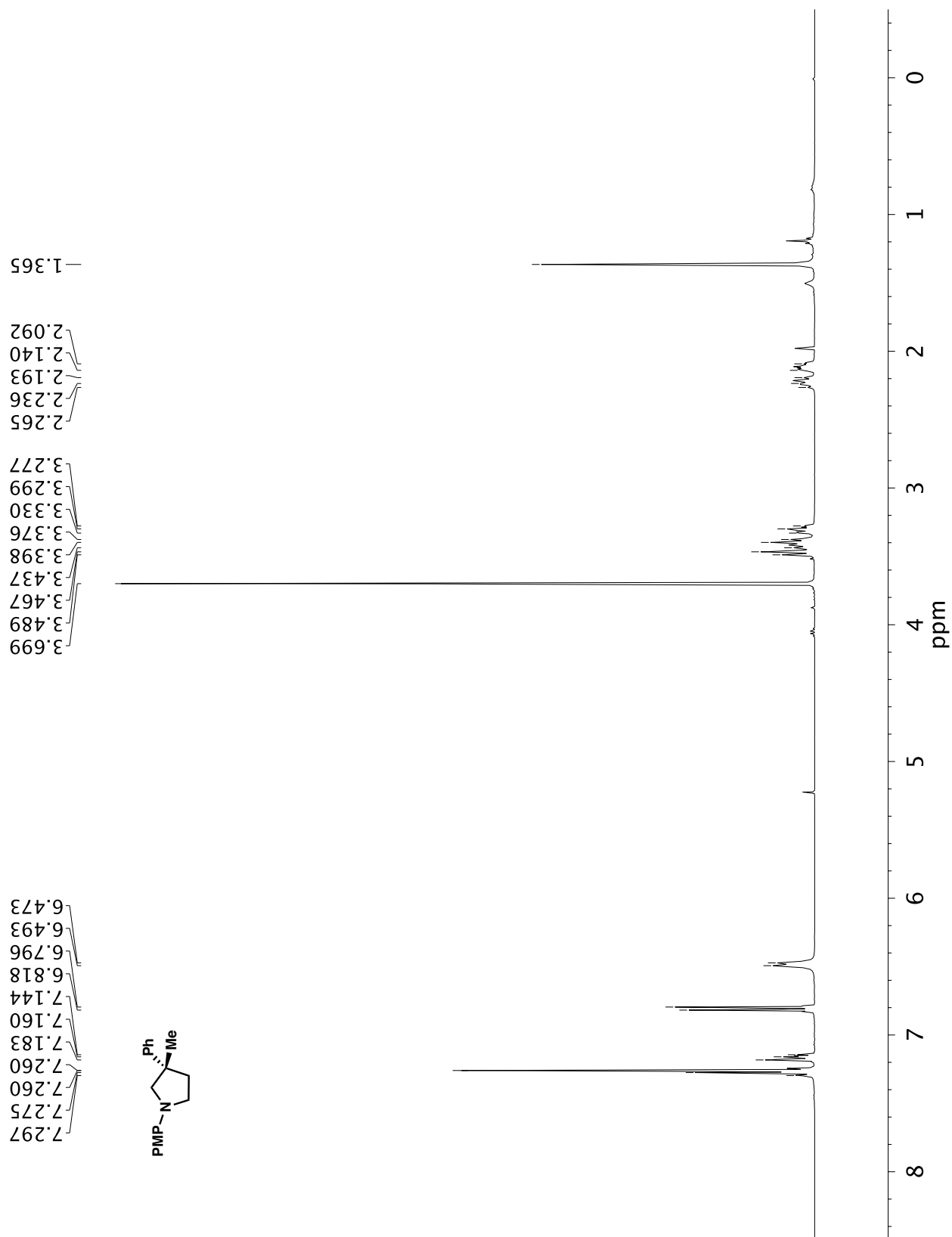
A3.103 ¹H NMR (400 MHz, CDCl₃) of compound 34.

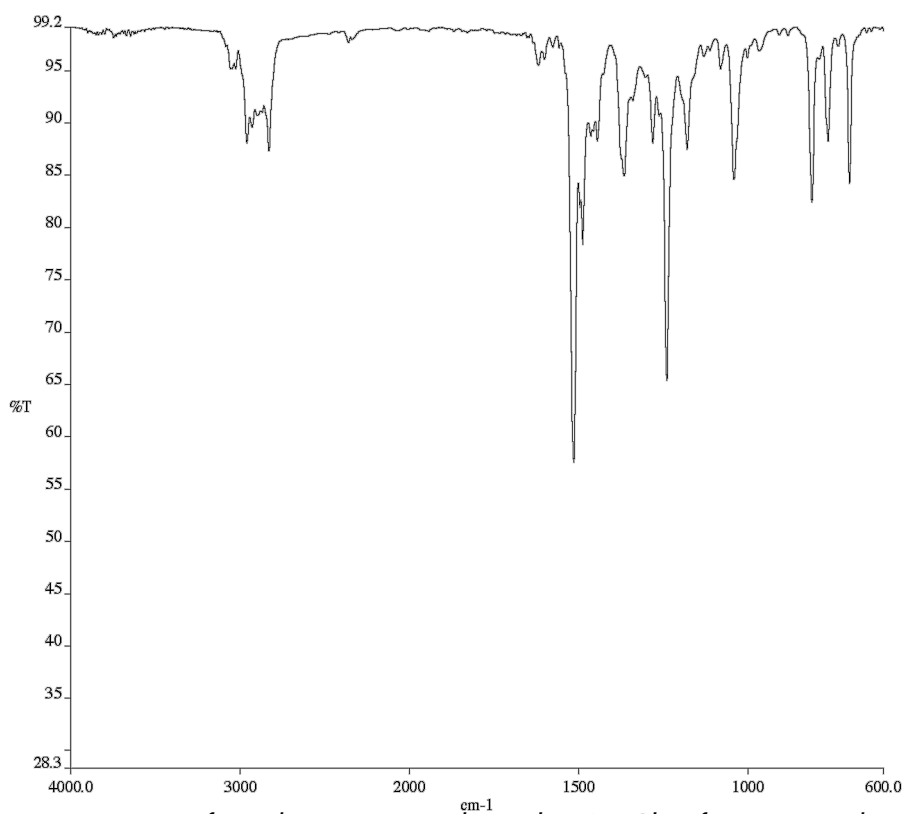


A3.104 Infrared spectrum (Thin Film, NaCl) of compound **34**.

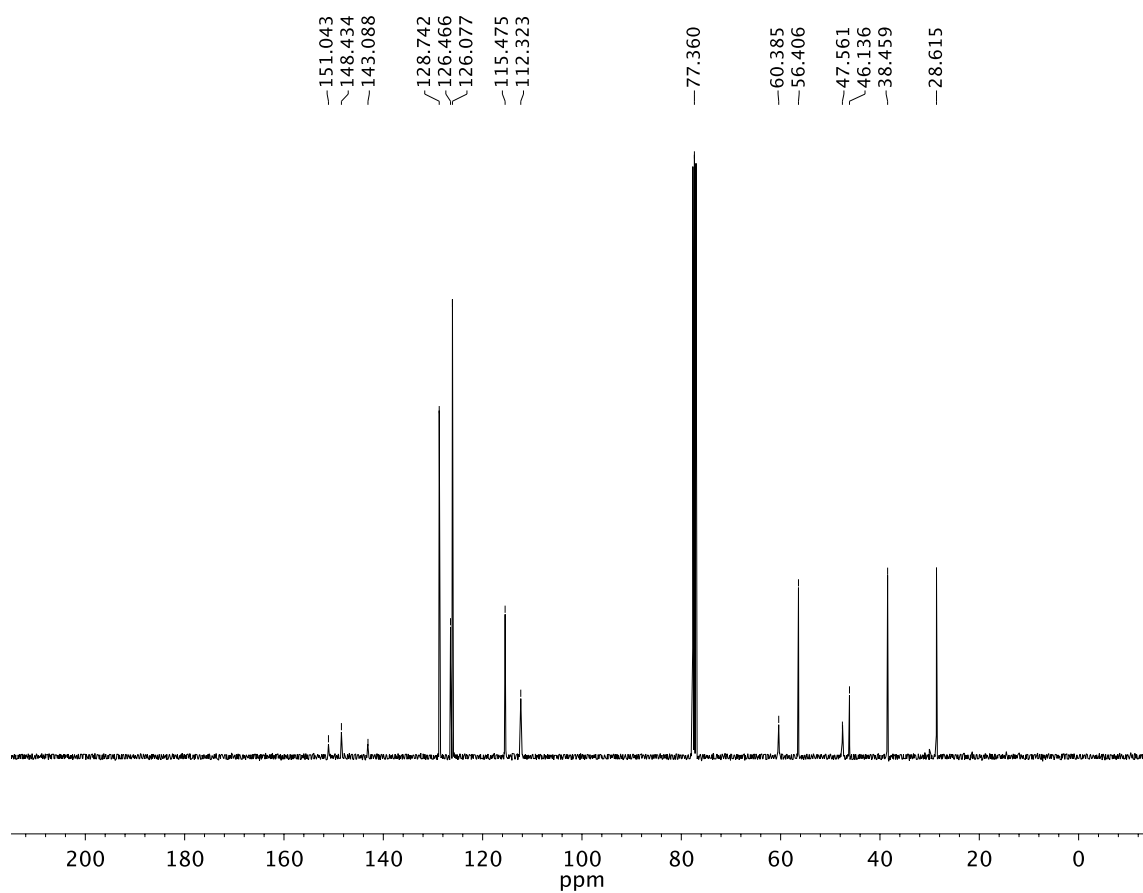


A3.105 ¹³C NMR (100 MHz, CDCl₃) of compound **34**.

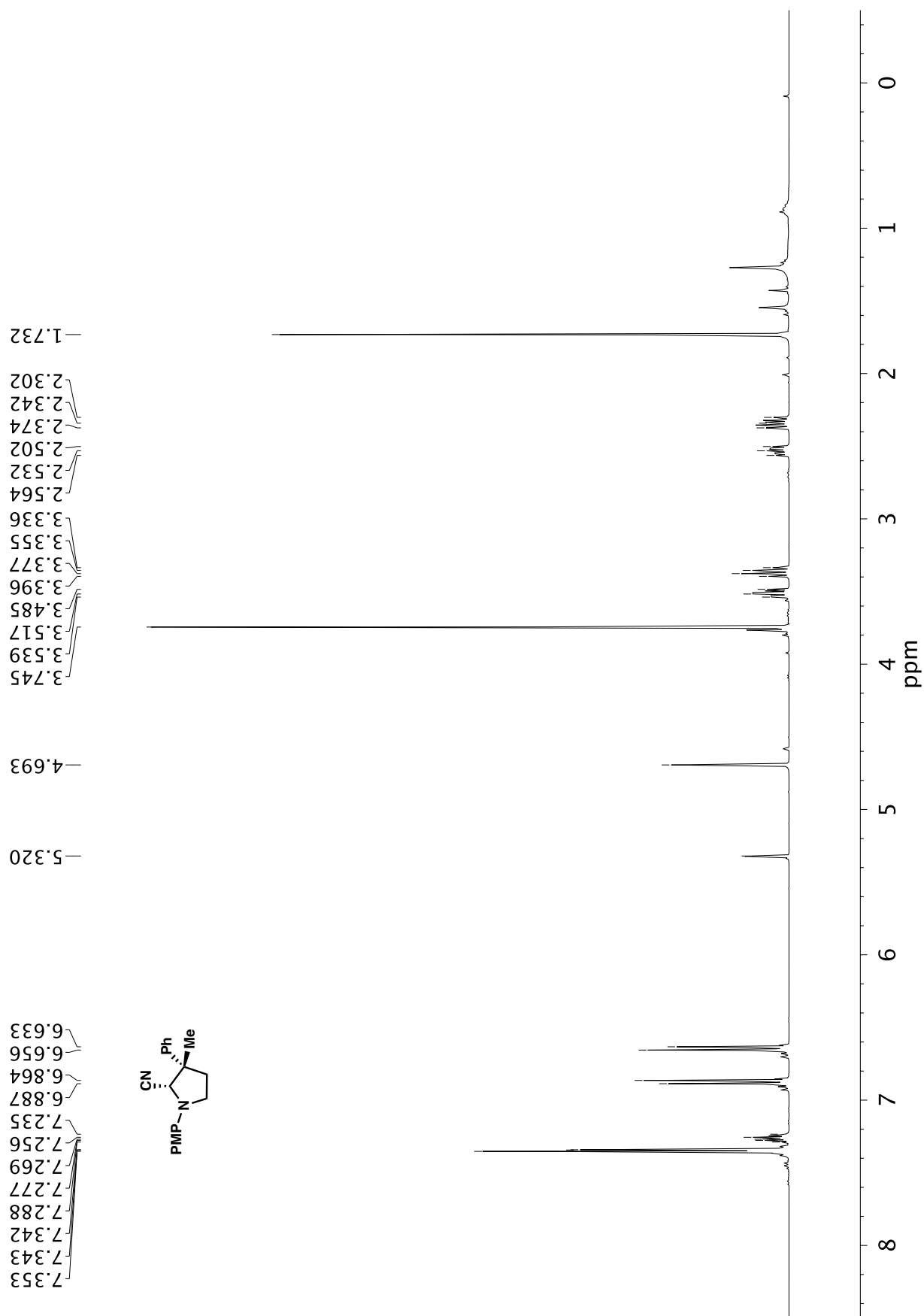
**A3.106** ¹H NMR (400 MHz, CDCl₃) of compound **35**.

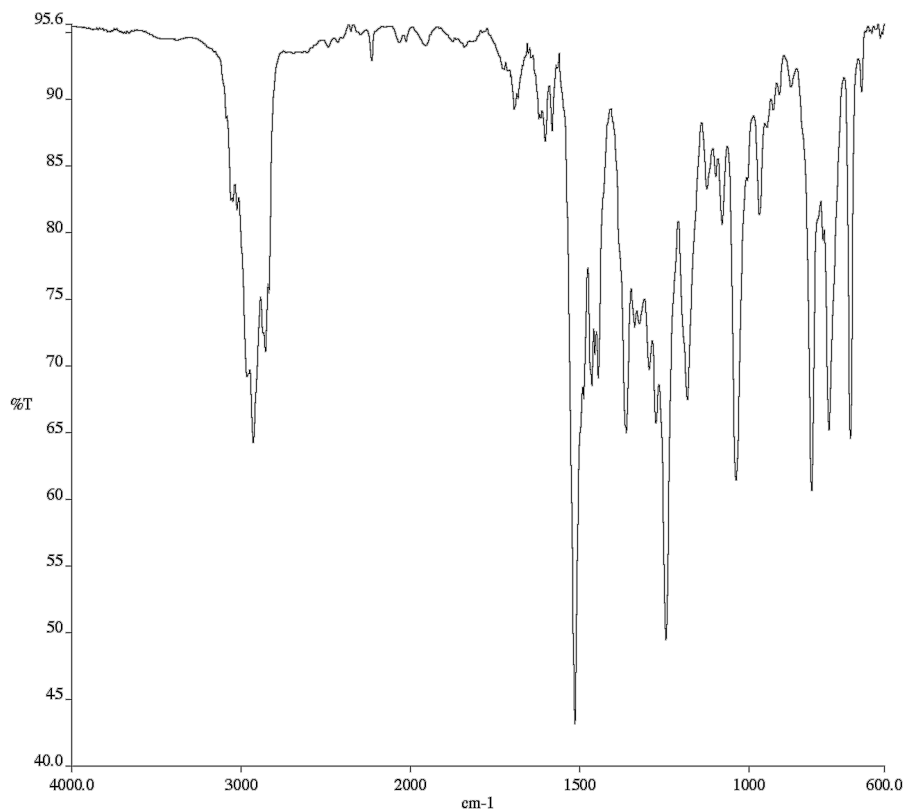


A3.107 Infrared spectrum (Thin Film, NaCl) of compound **35**.



A3.108 ^{13}C NMR (100 MHz, CDCl_3) of compound **35**.

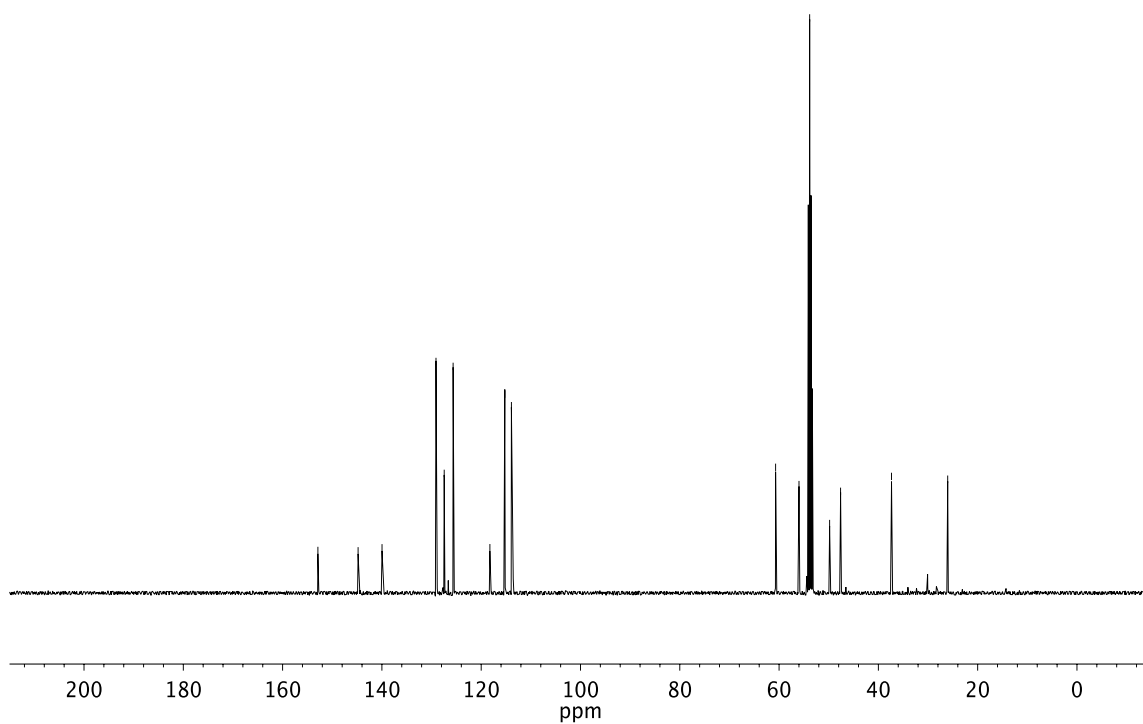
**A3.109** ¹H NMR (400 MHz, CD₂Cl₂) of compound **36**.



A3.110 Infrared spectrum (Thin Film, NaCl) of compound **36**.

—152.890
—144.794
—139.974
—129.105
—127.449
—125.656
—118.247
—115.246
—113.914

—60.698
—55.989
—53.840
—49.819
—47.612
—37.352
—26.035



A3.111 ¹³C NMR (100 MHz, CD₂Cl₂) of compound **36**.

APPENDIX 4

X-Ray Crystallography Reports Relevant to Chapter 2:

Palladium-Catalyzed Enantioselective Arylation of γ -Lactams with Aryl

Chlorides and Bromides

A4.1 GENERAL EXPERIMENTAL

For crystal structure determination of **3ab**: Low-temperature diffraction data (ϕ - and ω -scans) were collected on a Bruker AXS D8 VENTURE KAPPA diffractometer coupled to a PHOTON 100 CMOS detector with Cu K_{α} radiation ($\lambda = 1.54178 \text{ \AA}$) from an I μ S micro-source for the structure of compound P17471. The structure was solved by direct methods using SHELXS¹ and refined against F^2 on all data by full-matrix least squares with SHELXL-2016¹ using established refinement techniques.¹ All non-hydrogen atoms were refined anisotropically. All hydrogen atoms were included into the model at geometrically calculated positions and refined using a riding model. The isotropic displacement parameters of all hydrogen atoms were fixed to 1.2 times the U value of the atoms they are linked to (1.5 times for methyl groups).

For crystal structure determination of **Pd/L10** complex: A crystal was mounted on a polyimide MiTeGen loop with STP Oil Treatment and placed under a nitrogen stream. Low temperature (100K) X-ray data were collected with a Bruker AXS D8 VENTURE KAPPA diffractometer running at 50 kV and 1mA (Mo $K_{\alpha} = 0.71073 \text{ \AA}$; PHOTON II CPAD detector and Helios focusing multilayer mirror optics). All diffractometer manipulations, including data collection, integration, and scaling were carried out using the Bruker APEX3 software. An absorption correction was applied using SADABS. The space group was determined and the structure solved by intrinsic phasing using XT. Refinement was full-matrix least squares on F^2 using XL. All non-hydrogen atoms were refined using anisotropic displacement parameters. Hydrogen atoms were placed in idealized positions and refined using a riding model. The isotropic displacement parameters of all hydrogen atoms were fixed at 1.2 times (1.5 times for methyl groups) the U_{eq} value of the bonded atom.

A4.2 X-RAY CRYSTAL STRUCTURE ANALYSIS OF ARYLATION PRODUCT**32ab**

Product **32ab** was crystallized from EtOAc in hexanes at ambient temperature *via* slow evaporation.

Figure A4.1 X-Ray Coordination of α -Aryl γ -Lactam **32ab**.

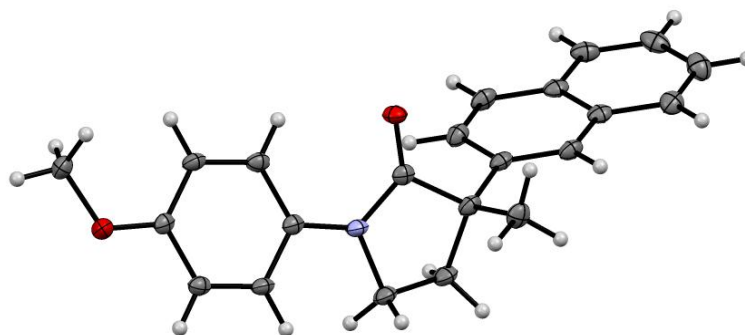


Table A4.1 Crystal Data and Structure Refinement for **32ab**.

Empirical formula	C ₂₂ H ₂₁ N O ₂	
Formula weight	331.40	
Temperature	100(2) K	
Wavelength	1.54178 Å	
Crystal system	Orthorhombic	
Space group	P2 ₁ 2 ₁ 2 ₁	
Unit cell dimensions	a = 6.1796(3) Å	$\alpha = 90^\circ$.
	b = 7.7424(4) Å	$\beta = 90^\circ$.
	c = 34.9981(18) Å	$\gamma = 90^\circ$.
Volume	1674.48(15) Å ³	
Z	4	
Density (calculated)	1.315 Mg/m ³	
Absorption coefficient	0.662 mm ⁻¹	
F(000)	704	
Crystal size	0.500 x 0.200 x 0.050 mm ³	
Theta range for data collection	2.525 to 74.537°.	

Index ranges	-7<= <i>h</i> <=7, -9<= <i>k</i> <=9, -43<= <i>l</i> <=43
Reflections collected	15394
Independent reflections	3423 [R(int) = 0.0559]
Completeness to $\theta = 67.679^\circ$	99.9%
Absorption correction	Semi-empirical from equivalents
Max. and min. transmission	0.7528 and 0.4845
Refinement method	Full-matrix least-squares on F^2
Data / restraints / parameters	3423 / 0 / 228
Goodness-of-fit on F^2	1.142
Final R indices [$I > 2\sigma(I)$]	R1 = 0.0419, wR2 = 0.1076
R indices (all data)	R1 = 0.0434, wR2 = 0.1083
Absolute structure parameter	0.17(9)
Extinction coefficient	n/a
Largest diff. peak and hole	0.215 and -0.302 e. \AA^{-3}

Table A4.2. Atomic Coordinates ($\times 10^4$) and Equivalent Isotropic Displacement Parameters ($\text{\AA}^2 \times 10^3$) for **32ab**. $U(\text{eq})$ is Defined as One Third of the Trace of the Orthogonalized U_{ij} Tensor.

	x	y	z	U(eq)
O(1)	3102(3)	3420(2)	3552(1)	20(1)
C(1)	4333(3)	4646(3)	3530(1)	16(1)
C(2)	6048(3)	5153(3)	3827(1)	18(1)
C(5)	7930(4)	3889(3)	3763(1)	23(1)
C(21)	5192(3)	5139(3)	4235(1)	17(1)
C(22)	6379(3)	4486(3)	4533(1)	19(1)
C(23)	5648(4)	4624(3)	4918(1)	18(1)
C(24)	6887(4)	3964(3)	5226(1)	23(1)
C(25)	6135(4)	4082(3)	5595(1)	27(1)
C(26)	4144(4)	4895(3)	5669(1)	26(1)
C(27)	2910(4)	5554(3)	5378(1)	23(1)
C(28)	3633(4)	5434(3)	4994(1)	19(1)
C(29)	2412(4)	6077(3)	4681(1)	21(1)
C(30)	3175(4)	5943(3)	4316(1)	21(1)
C(3)	6667(4)	6991(3)	3702(1)	22(1)
C(4)	6306(4)	6988(3)	3270(1)	20(1)
N(1)	4552(3)	5731(2)	3219(1)	17(1)
C(11)	3510(3)	5571(3)	2860(1)	17(1)
C(12)	1606(4)	4621(3)	2809(1)	18(1)
C(13)	597(3)	4557(3)	2453(1)	18(1)
C(14)	1476(3)	5434(3)	2142(1)	16(1)
O(2)	637(3)	5431(2)	1780(1)	21(1)
C(17)	-1408(4)	4619(3)	1726(1)	22(1)
C(15)	3386(4)	6368(3)	2190(1)	18(1)
C(16)	4384(4)	6441(3)	2543(1)	18(1)

Table A4.3 Bond lengths [\AA] and angles [$^\circ$] for **32ab**

O(1)-C(1)	1.219(3)
C(1)-N(1)	1.382(3)
C(1)-C(2)	1.535(3)
C(2)-C(21)	1.525(3)
C(2)-C(5)	1.537(3)
C(2)-C(3)	1.537(3)
C(5)-H(5A)	0.9800
C(5)-H(5B)	0.9800
C(5)-H(5C)	0.9800
C(21)-C(22)	1.372(3)
C(21)-C(30)	1.421(3)
C(22)-C(23)	1.423(3)
C(22)-H(22)	0.9500
C(23)-C(24)	1.418(3)
C(23)-C(28)	1.420(3)
C(24)-C(25)	1.375(3)
C(24)-H(24)	0.9500
C(25)-C(26)	1.407(4)
C(25)-H(25)	0.9500
C(26)-C(27)	1.371(4)
C(26)-H(26)	0.9500
C(27)-C(28)	1.418(3)
C(27)-H(27)	0.9500
C(28)-C(29)	1.422(3)
C(29)-C(30)	1.366(3)
C(29)-H(29)	0.9500
C(30)-H(30)	0.9500
C(3)-C(4)	1.527(3)
C(3)-H(3A)	0.9900
C(3)-H(3B)	0.9900
C(4)-N(1)	1.468(3)
C(4)-H(4A)	0.9900
C(4)-H(4B)	0.9900
N(1)-C(11)	1.416(3)

C(11)-C(12)	1.399(3)
C(11)-C(16)	1.406(3)
C(12)-C(13)	1.394(3)
C(12)-H(12)	0.9500
C(13)-C(14)	1.394(3)
C(13)-H(13)	0.9500
C(14)-O(2)	1.366(3)
C(14)-C(15)	1.395(3)
O(2)-C(17)	1.424(3)
C(17)-H(17A)	0.9800
C(17)-H(17B)	0.9800
C(17)-H(17C)	0.9800
C(15)-C(16)	1.382(3)
C(15)-H(15)	0.9500
C(16)-H(16)	0.9500

O(1)-C(1)-N(1)	125.7(2)
O(1)-C(1)-C(2)	126.05(19)
N(1)-C(1)-C(2)	108.06(18)
C(21)-C(2)-C(1)	113.12(17)
C(21)-C(2)-C(5)	113.27(18)
C(1)-C(2)-C(5)	105.12(17)
C(21)-C(2)-C(3)	111.11(17)
C(1)-C(2)-C(3)	102.47(18)
C(5)-C(2)-C(3)	111.11(19)
C(2)-C(5)-H(5A)	109.5
C(2)-C(5)-H(5B)	109.5
H(5A)-C(5)-H(5B)	109.5
C(2)-C(5)-H(5C)	109.5
H(5A)-C(5)-H(5C)	109.5
H(5B)-C(5)-H(5C)	109.5
C(22)-C(21)-C(30)	118.7(2)
C(22)-C(21)-C(2)	121.98(19)
C(30)-C(21)-C(2)	119.13(19)
C(21)-C(22)-C(23)	121.4(2)
C(21)-C(22)-H(22)	119.3

C(23)-C(22)-H(22)	119.3
C(24)-C(23)-C(28)	119.2(2)
C(24)-C(23)-C(22)	121.4(2)
C(28)-C(23)-C(22)	119.4(2)
C(25)-C(24)-C(23)	120.5(2)
C(25)-C(24)-H(24)	119.7
C(23)-C(24)-H(24)	119.7
C(24)-C(25)-C(26)	120.0(2)
C(24)-C(25)-H(25)	120.0
C(26)-C(25)-H(25)	120.0
C(27)-C(26)-C(25)	121.0(2)
C(27)-C(26)-H(26)	119.5
C(25)-C(26)-H(26)	119.5
C(26)-C(27)-C(28)	120.3(2)
C(26)-C(27)-H(27)	119.9
C(28)-C(27)-H(27)	119.9
C(27)-C(28)-C(23)	119.0(2)
C(27)-C(28)-C(29)	122.7(2)
C(23)-C(28)-C(29)	118.3(2)
C(30)-C(29)-C(28)	120.8(2)
C(30)-C(29)-H(29)	119.6
C(28)-C(29)-H(29)	119.6
C(29)-C(30)-C(21)	121.4(2)
C(29)-C(30)-H(30)	119.3
C(21)-C(30)-H(30)	119.3
C(4)-C(3)-C(2)	104.11(17)
C(4)-C(3)-H(3A)	110.9
C(2)-C(3)-H(3A)	110.9
C(4)-C(3)-H(3B)	110.9
C(2)-C(3)-H(3B)	110.9
H(3A)-C(3)-H(3B)	109.0
N(1)-C(4)-C(3)	103.28(17)
N(1)-C(4)-H(4A)	111.1
C(3)-C(4)-H(4A)	111.1
N(1)-C(4)-H(4B)	111.1
C(3)-C(4)-H(4B)	111.1

H(4A)-C(4)-H(4B)	109.1
C(1)-N(1)-C(11)	126.92(18)
C(1)-N(1)-C(4)	112.28(18)
C(11)-N(1)-C(4)	120.13(17)
C(12)-C(11)-C(16)	118.2(2)
C(12)-C(11)-N(1)	122.88(19)
C(16)-C(11)-N(1)	118.90(19)
C(13)-C(12)-C(11)	120.71(19)
C(13)-C(12)-H(12)	119.6
C(11)-C(12)-H(12)	119.6
C(12)-C(13)-C(14)	120.44(19)
C(12)-C(13)-H(13)	119.8
C(14)-C(13)-H(13)	119.8
O(2)-C(14)-C(13)	125.07(19)
O(2)-C(14)-C(15)	115.79(18)
C(13)-C(14)-C(15)	119.1(2)
C(14)-O(2)-C(17)	117.49(17)
O(2)-C(17)-H(17A)	109.5
O(2)-C(17)-H(17B)	109.5
H(17A)-C(17)-H(17B)	109.5
O(2)-C(17)-H(17C)	109.5
H(17A)-C(17)-H(17C)	109.5
H(17B)-C(17)-H(17C)	109.5
C(16)-C(15)-C(14)	120.52(19)
C(16)-C(15)-H(15)	119.7
C(14)-C(15)-H(15)	119.7
C(15)-C(16)-C(11)	121.0(2)
C(15)-C(16)-H(16)	119.5
C(11)-C(16)-H(16)	119.5

Symmetry transformations used to generate equivalent atoms:

Table A4.4 Anisotropic Displacement Parameters ($\text{\AA}^2 \times 10^3$) for **32ab**. The Anisotropic Displacement Factor Exponent Takes the Form: $-2p^2 [h^2 a^{*2} U^{11} + \dots + 2 h k a^* b^* U^{12}]$

	U^{11}	U^{22}	U^{33}	U^{23}	U^{13}	U^{12}
O(1)	20(1)	16(1)	25(1)	2(1)	1(1)	-6(1)
C(1)	14(1)	14(1)	22(1)	-2(1)	3(1)	3(1)
C(2)	12(1)	18(1)	25(1)	-2(1)	0(1)	0(1)
C(5)	16(1)	26(1)	25(1)	-2(1)	3(1)	5(1)
C(21)	14(1)	14(1)	24(1)	-3(1)	1(1)	-3(1)
C(22)	13(1)	17(1)	26(1)	-3(1)	2(1)	0(1)
C(23)	18(1)	12(1)	26(1)	-3(1)	2(1)	-2(1)
C(24)	23(1)	16(1)	30(1)	-2(1)	-2(1)	1(1)
C(25)	35(1)	20(1)	26(1)	0(1)	-3(1)	2(1)
C(26)	37(1)	15(1)	24(1)	-1(1)	6(1)	-2(1)
C(27)	22(1)	16(1)	31(1)	-3(1)	8(1)	-2(1)
C(28)	18(1)	12(1)	27(1)	-2(1)	2(1)	-3(1)
C(29)	13(1)	18(1)	32(1)	-5(1)	3(1)	2(1)
C(30)	17(1)	18(1)	27(1)	-2(1)	-3(1)	1(1)
C(3)	19(1)	20(1)	28(1)	-1(1)	-1(1)	-7(1)
C(4)	16(1)	18(1)	27(1)	0(1)	-1(1)	-6(1)
N(1)	14(1)	14(1)	23(1)	1(1)	2(1)	-4(1)
C(11)	13(1)	12(1)	24(1)	0(1)	2(1)	2(1)
C(12)	14(1)	16(1)	24(1)	1(1)	4(1)	0(1)
C(13)	12(1)	15(1)	26(1)	-1(1)	3(1)	-1(1)
C(14)	12(1)	13(1)	24(1)	-1(1)	1(1)	3(1)
O(2)	16(1)	23(1)	23(1)	4(1)	-2(1)	-2(1)
C(17)	15(1)	25(1)	27(1)	3(1)	-3(1)	-1(1)
C(15)	15(1)	15(1)	26(1)	3(1)	4(1)	1(1)
C(16)	12(1)	14(1)	28(1)	2(1)	3(1)	-2(1)

Table A4.5 Hydrogen coordinates ($\times 10^4$) and Isotropic Displacement Parameters ($\text{\AA}^2 \times 10^{-3}$) for **32ab**.

	x	y	z	U(eq)
H(5A)	9143	4205	3929	34
H(5B)	8393	3943	3495	34
H(5C)	7454	2713	3823	34
H(22)	7718	3929	4482	22
H(24)	8248	3437	5177	27
H(25)	6960	3614	5799	32
H(26)	3646	4989	5925	31
H(27)	1565	6093	5434	27
H(29)	1049	6607	4726	25
H(30)	2340	6397	4111	25
H(3A)	5734	7860	3828	27
H(3B)	8198	7243	3764	27
H(4A)	5871	8146	3178	24
H(4B)	7629	6621	3133	24
H(12)	996	4013	3018	22
H(13)	-700	3912	2422	21
H(17A)	-1264	3373	1768	34
H(17B)	-1909	4827	1464	34
H(17C)	-2457	5097	1907	34
H(15)	4007	6959	1979	22
H(16)	5680	7088	2572	22

Table A4.6 Torsion angles [°] for **32ab**.

O(1)-C(1)-C(2)-C(21)	-46.6(3)
N(1)-C(1)-C(2)-C(21)	138.58(18)
O(1)-C(1)-C(2)-C(5)	77.5(3)
N(1)-C(1)-C(2)-C(5)	-97.33(19)
O(1)-C(1)-C(2)-C(3)	-166.3(2)
N(1)-C(1)-C(2)-C(3)	18.9(2)
C(1)-C(2)-C(21)-C(22)	138.2(2)
C(5)-C(2)-C(21)-C(22)	18.7(3)
C(3)-C(2)-C(21)-C(22)	-107.2(2)
C(1)-C(2)-C(21)-C(30)	-46.7(3)
C(5)-C(2)-C(21)-C(30)	-166.21(19)
C(3)-C(2)-C(21)-C(30)	67.9(2)
C(30)-C(21)-C(22)-C(23)	-1.0(3)
C(2)-C(21)-C(22)-C(23)	174.10(19)
C(21)-C(22)-C(23)-C(24)	-179.3(2)
C(21)-C(22)-C(23)-C(28)	0.9(3)
C(28)-C(23)-C(24)-C(25)	1.0(3)
C(22)-C(23)-C(24)-C(25)	-178.8(2)
C(23)-C(24)-C(25)-C(26)	-1.4(3)
C(24)-C(25)-C(26)-C(27)	1.1(4)
C(25)-C(26)-C(27)-C(28)	-0.4(3)
C(26)-C(27)-C(28)-C(23)	0.0(3)
C(26)-C(27)-C(28)-C(29)	179.3(2)
C(24)-C(23)-C(28)-C(27)	-0.3(3)
C(22)-C(23)-C(28)-C(27)	179.5(2)
C(24)-C(23)-C(28)-C(29)	-179.7(2)
C(22)-C(23)-C(28)-C(29)	0.1(3)
C(27)-C(28)-C(29)-C(30)	179.6(2)
C(23)-C(28)-C(29)-C(30)	-1.0(3)
C(28)-C(29)-C(30)-C(21)	0.9(3)
C(22)-C(21)-C(30)-C(29)	0.1(3)
C(2)-C(21)-C(30)-C(29)	-175.1(2)
C(21)-C(2)-C(3)-C(4)	-150.71(18)
C(1)-C(2)-C(3)-C(4)	-29.6(2)

C(5)-C(2)-C(3)-C(4)	82.2(2)
C(2)-C(3)-C(4)-N(1)	29.8(2)
O(1)-C(1)-N(1)-C(11)	-4.3(3)
C(2)-C(1)-N(1)-C(11)	170.57(18)
O(1)-C(1)-N(1)-C(4)	-174.9(2)
C(2)-C(1)-N(1)-C(4)	0.0(2)
C(3)-C(4)-N(1)-C(1)	-19.0(2)
C(3)-C(4)-N(1)-C(11)	169.66(18)
C(1)-N(1)-C(11)-C(12)	21.1(3)
C(4)-N(1)-C(11)-C(12)	-168.92(19)
C(1)-N(1)-C(11)-C(16)	-160.7(2)
C(4)-N(1)-C(11)-C(16)	9.3(3)
C(16)-C(11)-C(12)-C(13)	-0.7(3)
N(1)-C(11)-C(12)-C(13)	177.52(19)
C(11)-C(12)-C(13)-C(14)	0.3(3)
C(12)-C(13)-C(14)-O(2)	178.80(19)
C(12)-C(13)-C(14)-C(15)	0.4(3)
C(13)-C(14)-O(2)-C(17)	6.8(3)
C(15)-C(14)-O(2)-C(17)	-174.67(18)
O(2)-C(14)-C(15)-C(16)	-179.30(19)
C(13)-C(14)-C(15)-C(16)	-0.7(3)
C(14)-C(15)-C(16)-C(11)	0.4(3)
C(12)-C(11)-C(16)-C(15)	0.3(3)
N(1)-C(11)-C(16)-C(15)	-177.95(19)

Symmetry transformations used to generate equivalent atoms:

Z	2
Density (calculated)	1.456 g/cm ³
Absorption coefficient	0.911 mm ⁻¹
F(000)	940
Crystal size	0.22 x 0.21 x 0.16 mm ³
Theta range for data collection	2.463 to 60.741°.
Index ranges	-27 ≤ h ≤ 27, -31 ≤ k ≤ 31, -35 ≤ l ≤ 35
Reflections collected	761601
Independent reflections	122367 [R(int) = 0.0434]
Completeness to theta = 25.242°	99.8 %
Absorption correction	Semi-empirical from equivalents
Max. and min. transmission	0.9961 and 0.9523
Refinement method	Full-matrix least-squares on F ²
Data / restraints / parameters	122367 / 3 / 985
Goodness-of-fit on F ²	1.027
Final R indices [I>2sigma(I)]	R1 = 0.0322, wR2 = 0.0704
R indices (all data)	R1 = 0.0492, wR2 = 0.0788
Absolute structure parameter [Flack]	0.004(2)
Extinction coefficient	n/a
Largest diff. peak and hole	4.760 and -2.265 e.Å ⁻³

Table A4.8 Atomic coordinates ($\times 10^5$) and equivalent isotropic displacement parameters ($\text{\AA}^2 \times 10^4$) for **Pd/L10**. $U(\text{eq})$ is defined as one third of the trace of the orthogonalized U^{ij} tensor.

	x	y	z	U(eq)
Pd(1)	66302(2)	76561(2)	13310(2)	98(1)
Fe(1)	101781(2)	79532(2)	24779(2)	113(1)
P(1)	77429(2)	92194(2)	18578(2)	107(1)
P(2)	79432(2)	62950(2)	13324(2)	116(1)
O(1)	35675(9)	102732(8)	47613(7)	194(1)
O(2)	47599(9)	54258(7)	-3074(7)	185(1)
O(3)	66651(12)	81266(10)	-47409(8)	245(2)
C(1)	48505(9)	70000(8)	8966(8)	142(1)

C(2)	48417(9)	81293(8)	11766(8)	133(1)
C(3)	44752(8)	86701(8)	21062(7)	129(1)
C(4)	39970(10)	96739(8)	21963(8)	148(1)
C(5)	36668(10)	102337(9)	30659(8)	162(1)
C(6)	38383(10)	97917(9)	38721(8)	150(1)
C(7)	43174(10)	87888(9)	37969(8)	163(1)
C(8)	46244(10)	82352(9)	29252(8)	156(1)
C(9)	30681(14)	112850(11)	48511(11)	233(2)
C(10)	49188(9)	64054(8)	-790(8)	143(1)
C(11)	52127(11)	69958(10)	-8035(9)	156(2)
C(12)	51813(10)	65205(9)	-17361(8)	167(2)
C(13)	55158(10)	69989(9)	-24961(8)	165(2)
C(14)	60938(14)	79891(10)	-23061(9)	221(2)
C(15)	64722(15)	84033(11)	-30348(9)	235(2)
C(16)	62747(12)	78209(10)	-39813(9)	192(2)
C(17)	56621(13)	68470(12)	-41961(9)	217(2)
C(18)	52974(13)	64452(12)	-34600(10)	201(2)
C(19)	72900(20)	91291(14)	-45351(13)	328(3)
C(20)	77475(10)	51844(10)	2496(9)	189(2)
C(21)	84260(14)	53215(14)	-5599(11)	269(3)
C(22)	80131(18)	41884(11)	6354(15)	318(3)
C(23)	74330(20)	43240(11)	15504(16)	345(4)
C(24)	77954(10)	54210(9)	21901(10)	180(2)
C(25)	69277(15)	57873(12)	29127(12)	252(2)
C(26)	84142(10)	98172(9)	9735(8)	159(1)
C(27)	79083(13)	93252(12)	-654(9)	224(2)
C(28)	81897(12)	110239(10)	12363(11)	213(2)
C(29)	79295(11)	113368(9)	22734(10)	195(2)
C(30)	70992(9)	104740(8)	24247(8)	149(1)
C(31)	69132(12)	105680(10)	34682(10)	201(2)
C(32)	89843(8)	91030(7)	27445(7)	125(1)
C(33)	101569(10)	95684(9)	29299(9)	169(2)
C(34)	108213(11)	91287(11)	36489(10)	211(2)
C(35)	100739(14)	83994(13)	39224(10)	209(2)
C(36)	89390(10)	83824(9)	33700(8)	156(1)
C(37)	95133(8)	66319(8)	14991(8)	131(1)

C(38)	104718(9)	63658(8)	21480(9)	158(1)
C(39)	115067(9)	69536(9)	20759(10)	184(2)
C(40)	112081(11)	75730(11)	13823(11)	181(2)
C(41)	99866(9)	73785(9)	10265(8)	151(1)
Pd(1B)	33505(2)	19811(2)	86721(2)	97(1)
Fe(1B)	-1861(2)	16576(2)	75190(2)	115(1)
P(1B)	22117(2)	32635(2)	81434(2)	102(1)
P(2B)	20536(2)	5905(2)	86561(2)	119(1)
O(3B)	32914(10)	54630(9)	147589(7)	216(2)
O(1B)	65209(8)	29095(8)	52638(6)	168(1)
O(2B)	51746(9)	6078(7)	103341(7)	176(1)
C(1B)	51319(9)	15755(8)	91206(8)	135(1)
C(2B)	51356(9)	25618(8)	88273(7)	126(1)
C(3B)	55273(8)	26435(8)	79057(7)	122(1)
C(4B)	59970(9)	36052(8)	78095(7)	139(1)
C(5B)	63509(10)	37319(8)	69447(8)	150(1)
C(6B)	62243(9)	28821(8)	61512(7)	133(1)
C(7B)	57586(10)	19113(8)	62318(7)	146(1)
C(8B)	54175(9)	17930(8)	70964(8)	142(1)
C(9B)	71124(13)	38421(11)	51718(10)	214(2)
C(10B)	50331(9)	14694(8)	100937(7)	132(1)
C(11B)	47387(10)	24269(9)	108040(8)	145(2)
C(12B)	47741(10)	24182(9)	117387(7)	151(1)
C(13B)	44527(9)	32752(9)	124988(7)	146(1)
C(14B)	39291(12)	42022(10)	123235(8)	190(2)
C(15B)	35415(13)	49582(10)	130555(9)	203(2)
C(16B)	36820(10)	48005(9)	139918(8)	167(2)
C(17B)	42476(11)	39065(10)	141926(8)	181(2)
C(18B)	46209(12)	31602(11)	134546(9)	167(2)
C(19B)	26642(16)	63661(13)	145818(12)	274(3)
C(20B)	22290(11)	-705(10)	96843(9)	183(2)
C(21B)	16251(15)	4839(15)	105328(11)	267(3)
C(22B)	18170(18)	-12224(12)	92382(13)	292(3)
C(23B)	23741(17)	-15387(11)	83119(13)	288(3)
C(24B)	21757(10)	-6686(9)	77401(9)	172(2)
C(25B)	31380(15)	-6459(12)	70993(12)	258(2)

C(26B)	15192(9)	42820(8)	90217(8)	143(1)
C(27B)	20266(13)	43219(11)	100653(9)	204(2)
C(28B)	17228(11)	53626(9)	87583(9)	181(2)
C(29B)	19902(10)	51709(8)	77198(9)	165(2)
C(30B)	28477(9)	42602(7)	75925(7)	126(1)
C(31B)	30851(11)	38519(10)	65614(8)	170(2)
C(32B)	9938(8)	26815(7)	72422(7)	121(1)
C(33B)	-1900(9)	30135(9)	70174(9)	161(2)
C(34B)	-8155(10)	21847(10)	63016(9)	187(2)
C(35B)	-348(12)	13412(11)	60707(10)	171(2)
C(36B)	10763(9)	16456(8)	66412(7)	135(1)
C(37B)	4871(9)	8555(8)	85202(8)	134(1)
C(38B)	-5002(9)	2653(8)	79092(9)	157(1)
C(39B)	-15140(10)	9071(10)	79812(10)	184(2)
C(40B)	-11816(12)	18825(11)	86406(11)	187(2)
C(41B)	454(10)	18537(9)	89766(8)	158(1)
O(4)	94593(18)	77923(10)	70024(11)	372(3)
O(5)	92141(13)	56432(10)	60551(11)	329(3)
C(42)	99870(30)	73967(17)	61717(16)	512(7)
C(43)	92730(30)	64705(18)	55379(15)	427(5)
C(44)	86782(15)	60419(12)	68985(14)	280(3)
C(45)	93548(15)	69988(12)	75181(11)	251(2)
O(4B)	8282(12)	21933(9)	33615(11)	297(2)
O(5B)	4502(14)	43546(10)	33786(12)	334(3)
C(42B)	7350(30)	29334(19)	42100(17)	503(7)
C(43B)	-570(30)	38262(18)	40050(20)	561(8)
C(44B)	5650(20)	36016(16)	25116(13)	328(3)
C(45B)	13115(18)	27100(14)	27149(15)	325(3)

Table A4.9 Bond lengths [\AA] and angles [$^\circ$] for **Pd/L10**

Pd(1)-P(1)	2.3154(5)
Pd(1)-P(2)	2.3185(4)
Pd(1)-C(1)	2.1655(11)
Pd(1)-C(2)	2.1351(10)
Fe(1)-C(32)	2.0300(10)
Fe(1)-C(33)	2.0508(11)
Fe(1)-C(34)	2.0606(13)
Fe(1)-C(35)	2.0494(15)
Fe(1)-C(36)	2.0296(12)
Fe(1)-C(37)	2.0370(11)
Fe(1)-C(38)	2.0445(11)
Fe(1)-C(39)	2.0552(12)
Fe(1)-C(40)	2.0616(14)
Fe(1)-C(41)	2.0392(12)
P(1)-C(26)	1.8674(11)
P(1)-C(30)	1.8503(11)
P(1)-C(32)	1.8130(10)
P(2)-C(20)	1.8624(12)
P(2)-C(24)	1.8704(12)
P(2)-C(37)	1.8203(11)
O(1)-C(6)	1.3682(14)
O(1)-C(9)	1.4170(18)
O(2)-C(10)	1.2455(13)
O(3)-C(16)	1.3654(17)
O(3)-C(19)	1.434(2)
C(1)-H(1)	1.0000
C(1)-C(2)	1.4296(15)
C(1)-C(10)	1.4563(16)
C(2)-H(2)	1.0000
C(2)-C(3)	1.4789(15)
C(3)-C(4)	1.3976(14)
C(3)-C(8)	1.4054(15)
C(4)-H(4)	0.9500
C(4)-C(5)	1.3985(15)

C(5)-H(5)	0.9500
C(5)-C(6)	1.3947(16)
C(6)-C(7)	1.3985(16)
C(7)-H(7)	0.9500
C(7)-C(8)	1.3884(16)
C(8)-H(8)	0.9500
C(9)-H(9A)	0.9800
C(9)-H(9B)	0.9800
C(9)-H(9C)	0.9800
C(10)-C(11)	1.4910(17)
C(11)-H(11)	0.9500
C(11)-C(12)	1.3431(17)
C(12)-H(12)	0.9500
C(12)-C(13)	1.4591(17)
C(13)-C(14)	1.3974(17)
C(13)-C(18)	1.4043(17)
C(14)-H(14)	0.9500
C(14)-C(15)	1.3913(19)
C(15)-H(15)	0.9500
C(15)-C(16)	1.3936(18)
C(16)-C(17)	1.395(2)
C(17)-H(17)	0.9500
C(17)-C(18)	1.386(2)
C(18)-H(18)	0.9500
C(19)-H(19A)	0.9800
C(19)-H(19B)	0.9800
C(19)-H(19C)	0.9800
C(20)-H(20)	1.0000
C(20)-C(21)	1.520(2)
C(20)-C(22)	1.529(2)
C(21)-H(21A)	0.9800
C(21)-H(21B)	0.9800
C(21)-H(21C)	0.9800
C(22)-H(22A)	0.9900
C(22)-H(22B)	0.9900
C(22)-C(23)	1.525(3)

C(23)-H(23A)	0.9900
C(23)-H(23B)	0.9900
C(23)-C(24)	1.537(2)
C(24)-H(24)	1.0000
C(24)-C(25)	1.530(2)
C(25)-H(25A)	0.9800
C(25)-H(25B)	0.9800
C(25)-H(25C)	0.9800
C(26)-H(26)	1.0000
C(26)-C(27)	1.5270(18)
C(26)-C(28)	1.5551(18)
C(27)-H(27A)	0.9800
C(27)-H(27B)	0.9800
C(27)-H(27C)	0.9800
C(28)-H(28A)	0.9900
C(28)-H(28B)	0.9900
C(28)-C(29)	1.525(2)
C(29)-H(29A)	0.9900
C(29)-H(29B)	0.9900
C(29)-C(30)	1.5341(16)
C(30)-H(30)	1.0000
C(30)-C(31)	1.5211(18)
C(31)-H(31A)	0.9800
C(31)-H(31B)	0.9800
C(31)-H(31C)	0.9800
C(32)-C(33)	1.4378(15)
C(32)-C(36)	1.4368(15)
C(33)-H(33)	0.9500
C(33)-C(34)	1.4251(17)
C(34)-H(34)	0.9500
C(34)-C(35)	1.423(2)
C(35)-H(35)	0.9500
C(35)-C(36)	1.4299(18)
C(36)-H(36)	0.9500
C(37)-C(38)	1.4397(14)
C(37)-C(41)	1.4392(15)

C(38)-H(38)	0.9500
C(38)-C(39)	1.4332(16)
C(39)-H(39)	0.9500
C(39)-C(40)	1.4217(18)
C(40)-H(40)	0.9500
C(40)-C(41)	1.4269(17)
C(41)-H(41)	0.9500
Pd(1B)-P(1B)	2.3119(4)
Pd(1B)-P(2B)	2.3252(5)
Pd(1B)-C(1B)	2.1589(10)
Pd(1B)-C(2B)	2.1417(11)
Fe(1B)-C(32B)	2.0251(10)
Fe(1B)-C(33B)	2.0400(11)
Fe(1B)-C(34B)	2.0628(12)
Fe(1B)-C(35B)	2.0625(14)
Fe(1B)-C(36B)	2.0340(11)
Fe(1B)-C(37B)	2.0307(11)
Fe(1B)-C(38B)	2.0471(11)
Fe(1B)-C(39B)	2.0568(12)
Fe(1B)-C(40B)	2.0612(14)
Fe(1B)-C(41B)	2.0380(12)
P(1B)-C(26B)	1.8685(11)
P(1B)-C(30B)	1.8486(10)
P(1B)-C(32B)	1.8144(11)
P(2B)-C(20B)	1.8553(11)
P(2B)-C(24B)	1.8756(12)
P(2B)-C(37B)	1.8190(11)
O(3B)-C(16B)	1.3655(15)
O(3B)-C(19B)	1.4269(19)
O(1B)-C(6B)	1.3698(13)
O(1B)-C(9B)	1.4226(16)
O(2B)-C(10B)	1.2439(13)
C(1B)-H(1B)	1.0000
C(1B)-C(2B)	1.4309(14)
C(1B)-C(10B)	1.4545(15)
C(2B)-H(2B)	1.0000

C(2B)-C(3B)	1.4773(14)
C(3B)-C(4B)	1.3970(14)
C(3B)-C(8B)	1.4079(14)
C(4B)-H(4B)	0.9500
C(4B)-C(5B)	1.3986(15)
C(5B)-H(5B)	0.9500
C(5B)-C(6B)	1.3927(15)
C(6B)-C(7B)	1.3983(15)
C(7B)-H(7B)	0.9500
C(7B)-C(8B)	1.3892(15)
C(8B)-H(8B)	0.9500
C(9B)-H(9BA)	0.9800
C(9B)-H(9BB)	0.9800
C(9B)-H(9BC)	0.9800
C(10B)-C(11B)	1.4926(16)
C(11B)-H(11B)	0.9500
C(11B)-C(12B)	1.3423(15)
C(12B)-H(12B)	0.9500
C(12B)-C(13B)	1.4605(16)
C(13B)-C(14B)	1.4005(16)
C(13B)-C(18B)	1.4042(16)
C(14B)-H(14B)	0.9500
C(14B)-C(15B)	1.3898(17)
C(15B)-H(15B)	0.9500
C(15B)-C(16B)	1.3953(16)
C(16B)-C(17B)	1.3947(16)
C(17B)-H(17B)	0.9500
C(17B)-C(18B)	1.3820(18)
C(18B)-H(18B)	0.9500
C(19B)-H(19D)	0.9800
C(19B)-H(19E)	0.9800
C(19B)-H(19F)	0.9800
C(20B)-H(20B)	1.0000
C(20B)-C(21B)	1.521(2)
C(20B)-C(22B)	1.536(2)
C(21B)-H(21D)	0.9800

C(21B)-H(21E)	0.9800
C(21B)-H(21F)	0.9800
C(22B)-H(22C)	0.9900
C(22B)-H(22D)	0.9900
C(22B)-C(23B)	1.526(3)
C(23B)-H(23C)	0.9900
C(23B)-H(23D)	0.9900
C(23B)-C(24B)	1.5359(18)
C(24B)-H(24B)	1.0000
C(24B)-C(25B)	1.527(2)
C(25B)-H(25D)	0.9800
C(25B)-H(25E)	0.9800
C(25B)-H(25F)	0.9800
C(26B)-H(26B)	1.0000
C(26B)-C(27B)	1.5281(17)
C(26B)-C(28B)	1.5529(16)
C(27B)-H(27D)	0.9800
C(27B)-H(27E)	0.9800
C(27B)-H(27F)	0.9800
C(28B)-H(28C)	0.9900
C(28B)-H(28D)	0.9900
C(28B)-C(29B)	1.5299(18)
C(29B)-H(29C)	0.9900
C(29B)-H(29D)	0.9900
C(29B)-C(30B)	1.5307(14)
C(30B)-H(30B)	1.0000
C(30B)-C(31B)	1.5203(15)
C(31B)-H(31D)	0.9800
C(31B)-H(31E)	0.9800
C(31B)-H(31F)	0.9800
C(32B)-C(33B)	1.4403(14)
C(32B)-C(36B)	1.4380(14)
C(33B)-H(33B)	0.9500
C(33B)-C(34B)	1.4303(17)
C(34B)-H(34B)	0.9500
C(34B)-C(35B)	1.4219(19)

C(35B)-H(35B)	0.9500
C(35B)-C(36B)	1.4255(16)
C(36B)-H(36B)	0.9500
C(37B)-C(38B)	1.4418(15)
C(37B)-C(41B)	1.4395(15)
C(38B)-H(38B)	0.9500
C(38B)-C(39B)	1.4295(16)
C(39B)-H(39B)	0.9500
C(39B)-C(40B)	1.421(2)
C(40B)-H(40B)	0.9500
C(40B)-C(41B)	1.4279(18)
C(41B)-H(41B)	0.9500
O(4)-C(42)	1.404(3)
O(4)-C(45)	1.406(2)
O(5)-C(43)	1.438(3)
O(5)-C(44)	1.425(2)
C(42)-H(42A)	0.9900
C(42)-H(42B)	0.9900
C(42)-C(43)	1.504(3)
C(43)-H(43A)	0.9900
C(43)-H(43B)	0.9900
C(44)-H(44A)	0.9900
C(44)-H(44B)	0.9900
C(44)-C(45)	1.504(2)
C(45)-H(45A)	0.9900
C(45)-H(45B)	0.9900
O(4B)-C(42B)	1.392(3)
O(4B)-C(45B)	1.422(3)
O(5B)-C(43B)	1.422(3)
O(5B)-C(44B)	1.425(2)
C(42B)-H(42C)	0.9900
C(42B)-H(42D)	0.9900
C(42B)-C(43B)	1.526(4)
C(43B)-H(43C)	0.9900
C(43B)-H(43D)	0.9900
C(44B)-H(44C)	0.9900

C(44B)-H(44D)	0.9900
C(44B)-C(45B)	1.496(3)
C(45B)-H(45C)	0.9900
C(45B)-H(45D)	0.9900
P(1)-Pd(1)-P(2)	106.356(16)
C(1)-Pd(1)-P(1)	143.96(3)
C(1)-Pd(1)-P(2)	109.62(3)
C(2)-Pd(1)-P(1)	105.15(3)
C(2)-Pd(1)-P(2)	148.17(3)
C(2)-Pd(1)-C(1)	38.82(4)
C(32)-Fe(1)-C(33)	41.26(4)
C(32)-Fe(1)-C(34)	69.15(5)
C(32)-Fe(1)-C(35)	69.43(5)
C(32)-Fe(1)-C(37)	113.61(4)
C(32)-Fe(1)-C(38)	146.99(4)
C(32)-Fe(1)-C(39)	170.14(5)
C(32)-Fe(1)-C(40)	130.66(5)
C(32)-Fe(1)-C(41)	107.12(4)
C(33)-Fe(1)-C(34)	40.56(5)
C(33)-Fe(1)-C(39)	131.72(5)
C(33)-Fe(1)-C(40)	109.28(5)
C(34)-Fe(1)-C(40)	117.11(6)
C(35)-Fe(1)-C(33)	68.49(6)
C(35)-Fe(1)-C(34)	40.50(6)
C(35)-Fe(1)-C(39)	116.52(6)
C(35)-Fe(1)-C(40)	148.76(6)
C(36)-Fe(1)-C(32)	41.46(4)
C(36)-Fe(1)-C(33)	69.02(5)
C(36)-Fe(1)-C(34)	68.72(5)
C(36)-Fe(1)-C(35)	41.04(5)
C(36)-Fe(1)-C(37)	106.30(5)
C(36)-Fe(1)-C(38)	114.76(5)
C(36)-Fe(1)-C(39)	148.06(5)
C(36)-Fe(1)-C(40)	169.65(5)
C(36)-Fe(1)-C(41)	130.02(5)

C(37)-Fe(1)-C(33)	147.48(4)
C(37)-Fe(1)-C(34)	169.64(5)
C(37)-Fe(1)-C(35)	129.96(6)
C(37)-Fe(1)-C(38)	41.31(4)
C(37)-Fe(1)-C(39)	69.34(5)
C(37)-Fe(1)-C(40)	69.33(5)
C(37)-Fe(1)-C(41)	41.35(4)
C(38)-Fe(1)-C(33)	170.61(4)
C(38)-Fe(1)-C(34)	131.43(5)
C(38)-Fe(1)-C(35)	108.24(6)
C(38)-Fe(1)-C(39)	40.92(5)
C(38)-Fe(1)-C(40)	68.62(5)
C(39)-Fe(1)-C(34)	109.74(5)
C(39)-Fe(1)-C(40)	40.41(5)
C(41)-Fe(1)-C(33)	115.94(5)
C(41)-Fe(1)-C(34)	148.68(5)
C(41)-Fe(1)-C(35)	169.49(6)
C(41)-Fe(1)-C(38)	68.89(5)
C(41)-Fe(1)-C(39)	68.43(5)
C(41)-Fe(1)-C(40)	40.72(5)
C(26)-P(1)-Pd(1)	119.76(4)
C(30)-P(1)-Pd(1)	122.07(4)
C(30)-P(1)-C(26)	93.82(5)
C(32)-P(1)-Pd(1)	112.02(3)
C(32)-P(1)-C(26)	103.74(5)
C(32)-P(1)-C(30)	102.26(5)
C(20)-P(2)-Pd(1)	116.06(4)
C(20)-P(2)-C(24)	94.15(6)
C(24)-P(2)-Pd(1)	117.30(4)
C(37)-P(2)-Pd(1)	117.98(3)
C(37)-P(2)-C(20)	103.77(5)
C(37)-P(2)-C(24)	104.19(5)
C(6)-O(1)-C(9)	116.77(10)
C(16)-O(3)-C(19)	116.61(12)
Pd(1)-C(1)-H(1)	116.3
C(2)-C(1)-Pd(1)	69.44(6)

C(2)-C(1)-H(1)	116.3
C(2)-C(1)-C(10)	124.48(10)
C(10)-C(1)-Pd(1)	101.73(7)
C(10)-C(1)-H(1)	116.3
Pd(1)-C(2)-H(2)	114.8
C(1)-C(2)-Pd(1)	71.74(6)
C(1)-C(2)-H(2)	114.8
C(1)-C(2)-C(3)	121.34(10)
C(3)-C(2)-Pd(1)	112.06(7)
C(3)-C(2)-H(2)	114.8
C(4)-C(3)-C(2)	119.37(9)
C(4)-C(3)-C(8)	117.78(9)
C(8)-C(3)-C(2)	122.82(9)
C(3)-C(4)-H(4)	119.1
C(3)-C(4)-C(5)	121.76(10)
C(5)-C(4)-H(4)	119.1
C(4)-C(5)-H(5)	120.3
C(6)-C(5)-C(4)	119.41(10)
C(6)-C(5)-H(5)	120.3
O(1)-C(6)-C(5)	124.49(10)
O(1)-C(6)-C(7)	115.82(10)
C(5)-C(6)-C(7)	119.68(10)
C(6)-C(7)-H(7)	119.9
C(8)-C(7)-C(6)	120.27(10)
C(8)-C(7)-H(7)	119.9
C(3)-C(8)-H(8)	119.5
C(7)-C(8)-C(3)	121.09(10)
C(7)-C(8)-H(8)	119.5
O(1)-C(9)-H(9A)	109.5
O(1)-C(9)-H(9B)	109.5
O(1)-C(9)-H(9C)	109.5
H(9A)-C(9)-H(9B)	109.5
H(9A)-C(9)-H(9C)	109.5
H(9B)-C(9)-H(9C)	109.5
O(2)-C(10)-C(1)	121.48(11)
O(2)-C(10)-C(11)	120.17(10)

C(1)-C(10)-C(11)	118.33(9)
C(10)-C(11)-H(11)	119.1
C(12)-C(11)-C(10)	121.73(11)
C(12)-C(11)-H(11)	119.1
C(11)-C(12)-H(12)	116.7
C(11)-C(12)-C(13)	126.55(11)
C(13)-C(12)-H(12)	116.7
C(14)-C(13)-C(12)	122.56(10)
C(14)-C(13)-C(18)	117.35(12)
C(18)-C(13)-C(12)	120.04(11)
C(13)-C(14)-H(14)	119.1
C(15)-C(14)-C(13)	121.74(11)
C(15)-C(14)-H(14)	119.1
C(14)-C(15)-H(15)	120.2
C(14)-C(15)-C(16)	119.58(12)
C(16)-C(15)-H(15)	120.2
O(3)-C(16)-C(15)	124.30(13)
O(3)-C(16)-C(17)	115.81(11)
C(15)-C(16)-C(17)	119.87(12)
C(16)-C(17)-H(17)	120.2
C(18)-C(17)-C(16)	119.65(11)
C(18)-C(17)-H(17)	120.2
C(13)-C(18)-H(18)	119.1
C(17)-C(18)-C(13)	121.72(13)
C(17)-C(18)-H(18)	119.1
O(3)-C(19)-H(19A)	109.5
O(3)-C(19)-H(19B)	109.5
O(3)-C(19)-H(19C)	109.5
H(19A)-C(19)-H(19B)	109.5
H(19A)-C(19)-H(19C)	109.5
H(19B)-C(19)-H(19C)	109.5
P(2)-C(20)-H(20)	106.9
C(21)-C(20)-P(2)	115.09(10)
C(21)-C(20)-H(20)	106.9
C(21)-C(20)-C(22)	115.47(12)
C(22)-C(20)-P(2)	104.93(10)

C(22)-C(20)-H(20)	106.9
C(20)-C(21)-H(21A)	109.5
C(20)-C(21)-H(21B)	109.5
C(20)-C(21)-H(21C)	109.5
H(21A)-C(21)-H(21B)	109.5
H(21A)-C(21)-H(21C)	109.5
H(21B)-C(21)-H(21C)	109.5
C(20)-C(22)-H(22A)	110.5
C(20)-C(22)-H(22B)	110.5
H(22A)-C(22)-H(22B)	108.7
C(23)-C(22)-C(20)	106.14(12)
C(23)-C(22)-H(22A)	110.5
C(23)-C(22)-H(22B)	110.5
C(22)-C(23)-H(23A)	110.0
C(22)-C(23)-H(23B)	110.0
C(22)-C(23)-C(24)	108.63(12)
H(23A)-C(23)-H(23B)	108.3
C(24)-C(23)-H(23A)	110.0
C(24)-C(23)-H(23B)	110.0
P(2)-C(24)-H(24)	108.3
C(23)-C(24)-P(2)	105.00(11)
C(23)-C(24)-H(24)	108.3
C(25)-C(24)-P(2)	115.23(9)
C(25)-C(24)-C(23)	111.52(12)
C(25)-C(24)-H(24)	108.3
C(24)-C(25)-H(25A)	109.5
C(24)-C(25)-H(25B)	109.5
C(24)-C(25)-H(25C)	109.5
H(25A)-C(25)-H(25B)	109.5
H(25A)-C(25)-H(25C)	109.5
H(25B)-C(25)-H(25C)	109.5
P(1)-C(26)-H(26)	108.8
C(27)-C(26)-P(1)	112.55(8)
C(27)-C(26)-H(26)	108.8
C(27)-C(26)-C(28)	111.36(10)
C(28)-C(26)-P(1)	106.49(8)

C(28)-C(26)-H(26)	108.8
C(26)-C(27)-H(27A)	109.5
C(26)-C(27)-H(27B)	109.5
C(26)-C(27)-H(27C)	109.5
H(27A)-C(27)-H(27B)	109.5
H(27A)-C(27)-H(27C)	109.5
H(27B)-C(27)-H(27C)	109.5
C(26)-C(28)-H(28A)	109.8
C(26)-C(28)-H(28B)	109.8
H(28A)-C(28)-H(28B)	108.2
C(29)-C(28)-C(26)	109.50(9)
C(29)-C(28)-H(28A)	109.8
C(29)-C(28)-H(28B)	109.8
C(28)-C(29)-H(29A)	110.3
C(28)-C(29)-H(29B)	110.3
C(28)-C(29)-C(30)	107.19(10)
H(29A)-C(29)-H(29B)	108.5
C(30)-C(29)-H(29A)	110.3
C(30)-C(29)-H(29B)	110.3
P(1)-C(30)-H(30)	107.9
C(29)-C(30)-P(1)	104.18(8)
C(29)-C(30)-H(30)	107.9
C(31)-C(30)-P(1)	114.89(8)
C(31)-C(30)-C(29)	113.86(10)
C(31)-C(30)-H(30)	107.9
C(30)-C(31)-H(31A)	109.5
C(30)-C(31)-H(31B)	109.5
C(30)-C(31)-H(31C)	109.5
H(31A)-C(31)-H(31B)	109.5
H(31A)-C(31)-H(31C)	109.5
H(31B)-C(31)-H(31C)	109.5
P(1)-C(32)-Fe(1)	121.65(5)
C(33)-C(32)-Fe(1)	70.15(6)
C(33)-C(32)-P(1)	131.41(8)
C(36)-C(32)-Fe(1)	69.26(6)
C(36)-C(32)-P(1)	121.32(8)

C(36)-C(32)-C(33)	107.08(9)
Fe(1)-C(33)-H(33)	127.1
C(32)-C(33)-Fe(1)	68.59(6)
C(32)-C(33)-H(33)	125.8
C(34)-C(33)-Fe(1)	70.09(7)
C(34)-C(33)-C(32)	108.35(10)
C(34)-C(33)-H(33)	125.8
Fe(1)-C(34)-H(34)	127.0
C(33)-C(34)-Fe(1)	69.35(7)
C(33)-C(34)-H(34)	125.9
C(35)-C(34)-Fe(1)	69.33(8)
C(35)-C(34)-C(33)	108.24(11)
C(35)-C(34)-H(34)	125.9
Fe(1)-C(35)-H(35)	126.7
C(34)-C(35)-Fe(1)	70.17(8)
C(34)-C(35)-H(35)	126.0
C(34)-C(35)-C(36)	108.05(11)
C(36)-C(35)-Fe(1)	68.74(7)
C(36)-C(35)-H(35)	126.0
Fe(1)-C(36)-H(36)	126.2
C(32)-C(36)-Fe(1)	69.29(6)
C(32)-C(36)-H(36)	125.9
C(35)-C(36)-Fe(1)	70.23(8)
C(35)-C(36)-C(32)	108.27(11)
C(35)-C(36)-H(36)	125.9
P(2)-C(37)-Fe(1)	120.29(5)
C(38)-C(37)-Fe(1)	69.63(6)
C(38)-C(37)-P(2)	131.10(8)
C(41)-C(37)-Fe(1)	69.41(6)
C(41)-C(37)-P(2)	121.81(7)
C(41)-C(37)-C(38)	106.71(9)
Fe(1)-C(38)-H(38)	126.7
C(37)-C(38)-Fe(1)	69.07(6)
C(37)-C(38)-H(38)	125.9
C(39)-C(38)-Fe(1)	69.94(6)
C(39)-C(38)-C(37)	108.25(9)

C(39)-C(38)-H(38)	125.9
Fe(1)-C(39)-H(39)	126.6
C(38)-C(39)-Fe(1)	69.14(6)
C(38)-C(39)-H(39)	125.8
C(40)-C(39)-Fe(1)	70.04(7)
C(40)-C(39)-C(38)	108.33(10)
C(40)-C(39)-H(39)	125.8
Fe(1)-C(40)-H(40)	127.1
C(39)-C(40)-Fe(1)	69.55(8)
C(39)-C(40)-H(40)	126.1
C(39)-C(40)-C(41)	107.85(10)
C(41)-C(40)-Fe(1)	68.80(7)
C(41)-C(40)-H(40)	126.1
Fe(1)-C(41)-H(41)	126.3
C(37)-C(41)-Fe(1)	69.24(6)
C(37)-C(41)-H(41)	125.6
C(40)-C(41)-Fe(1)	70.48(8)
C(40)-C(41)-C(37)	108.86(10)
C(40)-C(41)-H(41)	125.6
P(1B)-Pd(1B)-P(2B)	106.013(16)
C(1B)-Pd(1B)-P(1B)	144.11(3)
C(1B)-Pd(1B)-P(2B)	109.84(3)
C(2B)-Pd(1B)-P(1B)	105.28(3)
C(2B)-Pd(1B)-P(2B)	148.31(3)
C(2B)-Pd(1B)-C(1B)	38.86(4)
C(32B)-Fe(1B)-C(33B)	41.50(4)
C(32B)-Fe(1B)-C(34B)	69.43(4)
C(32B)-Fe(1B)-C(35B)	69.53(5)
C(32B)-Fe(1B)-C(36B)	41.50(4)
C(32B)-Fe(1B)-C(37B)	113.38(4)
C(32B)-Fe(1B)-C(38B)	148.40(4)
C(32B)-Fe(1B)-C(39B)	167.59(5)
C(32B)-Fe(1B)-C(40B)	128.04(5)
C(32B)-Fe(1B)-C(41B)	105.17(5)
C(33B)-Fe(1B)-C(34B)	40.80(5)
C(33B)-Fe(1B)-C(35B)	68.59(5)

C(33B)-Fe(1B)-C(38B)	169.42(4)
C(33B)-Fe(1B)-C(39B)	130.50(5)
C(33B)-Fe(1B)-C(40B)	108.35(5)
C(35B)-Fe(1B)-C(34B)	40.32(6)
C(36B)-Fe(1B)-C(33B)	68.96(5)
C(36B)-Fe(1B)-C(34B)	68.33(5)
C(36B)-Fe(1B)-C(35B)	40.72(5)
C(36B)-Fe(1B)-C(38B)	116.45(5)
C(36B)-Fe(1B)-C(39B)	150.76(5)
C(36B)-Fe(1B)-C(40B)	166.81(5)
C(36B)-Fe(1B)-C(41B)	127.73(4)
C(37B)-Fe(1B)-C(33B)	148.16(5)
C(37B)-Fe(1B)-C(34B)	168.09(5)
C(37B)-Fe(1B)-C(35B)	128.59(5)
C(37B)-Fe(1B)-C(36B)	105.62(4)
C(37B)-Fe(1B)-C(38B)	41.41(4)
C(37B)-Fe(1B)-C(39B)	69.39(5)
C(37B)-Fe(1B)-C(40B)	69.47(5)
C(37B)-Fe(1B)-C(41B)	41.44(4)
C(38B)-Fe(1B)-C(34B)	130.91(5)
C(38B)-Fe(1B)-C(35B)	109.02(5)
C(38B)-Fe(1B)-C(39B)	40.77(5)
C(38B)-Fe(1B)-C(40B)	68.52(5)
C(39B)-Fe(1B)-C(34B)	110.52(5)
C(39B)-Fe(1B)-C(35B)	118.98(6)
C(39B)-Fe(1B)-C(40B)	40.36(6)
C(40B)-Fe(1B)-C(34B)	118.68(6)
C(40B)-Fe(1B)-C(35B)	151.56(6)
C(41B)-Fe(1B)-C(33B)	115.85(5)
C(41B)-Fe(1B)-C(34B)	150.32(5)
C(41B)-Fe(1B)-C(35B)	167.01(5)
C(41B)-Fe(1B)-C(38B)	68.89(5)
C(41B)-Fe(1B)-C(39B)	68.41(5)
C(41B)-Fe(1B)-C(40B)	40.77(5)
C(26B)-P(1B)-Pd(1B)	120.02(4)
C(30B)-P(1B)-Pd(1B)	121.68(3)

C(30B)-P(1B)-C(26B)	93.33(5)
C(32B)-P(1B)-Pd(1B)	111.64(3)
C(32B)-P(1B)-C(26B)	104.46(5)
C(32B)-P(1B)-C(30B)	102.71(5)
C(20B)-P(2B)-Pd(1B)	118.70(4)
C(20B)-P(2B)-C(24B)	93.85(6)
C(24B)-P(2B)-Pd(1B)	116.94(4)
C(37B)-P(2B)-Pd(1B)	117.00(3)
C(37B)-P(2B)-C(20B)	102.84(5)
C(37B)-P(2B)-C(24B)	104.05(5)
C(16B)-O(3B)-C(19B)	117.40(11)
C(6B)-O(1B)-C(9B)	117.40(10)
Pd(1B)-C(1B)-H(1B)	116.4
C(2B)-C(1B)-Pd(1B)	69.92(6)
C(2B)-C(1B)-H(1B)	116.4
C(2B)-C(1B)-C(10B)	124.51(10)
C(10B)-C(1B)-Pd(1B)	100.47(7)
C(10B)-C(1B)-H(1B)	116.4
Pd(1B)-C(2B)-H(2B)	114.6
C(1B)-C(2B)-Pd(1B)	71.22(6)
C(1B)-C(2B)-H(2B)	114.6
C(1B)-C(2B)-C(3B)	121.43(9)
C(3B)-C(2B)-Pd(1B)	113.17(7)
C(3B)-C(2B)-H(2B)	114.6
C(4B)-C(3B)-C(2B)	119.63(9)
C(4B)-C(3B)-C(8B)	117.68(9)
C(8B)-C(3B)-C(2B)	122.67(9)
C(3B)-C(4B)-H(4B)	119.1
C(3B)-C(4B)-C(5B)	121.86(9)
C(5B)-C(4B)-H(4B)	119.1
C(4B)-C(5B)-H(5B)	120.3
C(6B)-C(5B)-C(4B)	119.44(9)
C(6B)-C(5B)-H(5B)	120.3
O(1B)-C(6B)-C(5B)	125.03(10)
O(1B)-C(6B)-C(7B)	115.30(9)
C(5B)-C(6B)-C(7B)	119.67(9)

C(6B)-C(7B)-H(7B)	119.8
C(8B)-C(7B)-C(6B)	120.36(9)
C(8B)-C(7B)-H(7B)	119.8
C(3B)-C(8B)-H(8B)	119.5
C(7B)-C(8B)-C(3B)	120.98(10)
C(7B)-C(8B)-H(8B)	119.5
O(1B)-C(9B)-H(9BA)	109.5
O(1B)-C(9B)-H(9BB)	109.5
O(1B)-C(9B)-H(9BC)	109.5
H(9BA)-C(9B)-H(9BB)	109.5
H(9BA)-C(9B)-H(9BC)	109.5
H(9BB)-C(9B)-H(9BC)	109.5
O(2B)-C(10B)-C(1B)	121.63(10)
O(2B)-C(10B)-C(11B)	120.28(10)
C(1B)-C(10B)-C(11B)	118.08(9)
C(10B)-C(11B)-H(11B)	119.5
C(12B)-C(11B)-C(10B)	121.08(10)
C(12B)-C(11B)-H(11B)	119.5
C(11B)-C(12B)-H(12B)	116.6
C(11B)-C(12B)-C(13B)	126.80(10)
C(13B)-C(12B)-H(12B)	116.6
C(14B)-C(13B)-C(12B)	123.35(9)
C(14B)-C(13B)-C(18B)	117.27(10)
C(18B)-C(13B)-C(12B)	119.32(10)
C(13B)-C(14B)-H(14B)	119.2
C(15B)-C(14B)-C(13B)	121.64(10)
C(15B)-C(14B)-H(14B)	119.2
C(14B)-C(15B)-H(15B)	120.2
C(14B)-C(15B)-C(16B)	119.60(11)
C(16B)-C(15B)-H(15B)	120.2
O(3B)-C(16B)-C(15B)	124.82(11)
O(3B)-C(16B)-C(17B)	115.32(10)
C(17B)-C(16B)-C(15B)	119.85(11)
C(16B)-C(17B)-H(17B)	120.2
C(18B)-C(17B)-C(16B)	119.68(10)
C(18B)-C(17B)-H(17B)	120.2

C(13B)-C(18B)-H(18B)	119.1
C(17B)-C(18B)-C(13B)	121.85(11)
C(17B)-C(18B)-H(18B)	119.1
O(3B)-C(19B)-H(19D)	109.5
O(3B)-C(19B)-H(19E)	109.5
O(3B)-C(19B)-H(19F)	109.5
H(19D)-C(19B)-H(19E)	109.5
H(19D)-C(19B)-H(19F)	109.5
H(19E)-C(19B)-H(19F)	109.5
P(2B)-C(20B)-H(20B)	107.5
C(21B)-C(20B)-P(2B)	113.94(9)
C(21B)-C(20B)-H(20B)	107.5
C(21B)-C(20B)-C(22B)	115.66(12)
C(22B)-C(20B)-P(2B)	104.30(9)
C(22B)-C(20B)-H(20B)	107.5
C(20B)-C(21B)-H(21D)	109.5
C(20B)-C(21B)-H(21E)	109.5
C(20B)-C(21B)-H(21F)	109.5
H(21D)-C(21B)-H(21E)	109.5
H(21D)-C(21B)-H(21F)	109.5
H(21E)-C(21B)-H(21F)	109.5
C(20B)-C(22B)-H(22C)	110.5
C(20B)-C(22B)-H(22D)	110.5
H(22C)-C(22B)-H(22D)	108.7
C(23B)-C(22B)-C(20B)	105.96(12)
C(23B)-C(22B)-H(22C)	110.5
C(23B)-C(22B)-H(22D)	110.5
C(22B)-C(23B)-H(23C)	109.8
C(22B)-C(23B)-H(23D)	109.8
C(22B)-C(23B)-C(24B)	109.24(12)
H(23C)-C(23B)-H(23D)	108.3
C(24B)-C(23B)-H(23C)	109.8
C(24B)-C(23B)-H(23D)	109.8
P(2B)-C(24B)-H(24B)	108.2
C(23B)-C(24B)-P(2B)	105.69(10)
C(23B)-C(24B)-H(24B)	108.2

C(25B)-C(24B)-P(2B)	114.85(9)
C(25B)-C(24B)-C(23B)	111.55(11)
C(25B)-C(24B)-H(24B)	108.2
C(24B)-C(25B)-H(25D)	109.5
C(24B)-C(25B)-H(25E)	109.5
C(24B)-C(25B)-H(25F)	109.5
H(25D)-C(25B)-H(25E)	109.5
H(25D)-C(25B)-H(25F)	109.5
H(25E)-C(25B)-H(25F)	109.5
P(1B)-C(26B)-H(26B)	108.8
C(27B)-C(26B)-P(1B)	112.91(8)
C(27B)-C(26B)-H(26B)	108.8
C(27B)-C(26B)-C(28B)	110.66(10)
C(28B)-C(26B)-P(1B)	106.62(7)
C(28B)-C(26B)-H(26B)	108.8
C(26B)-C(27B)-H(27D)	109.5
C(26B)-C(27B)-H(27E)	109.5
C(26B)-C(27B)-H(27F)	109.5
H(27D)-C(27B)-H(27E)	109.5
H(27D)-C(27B)-H(27F)	109.5
H(27E)-C(27B)-H(27F)	109.5
C(26B)-C(28B)-H(28C)	109.8
C(26B)-C(28B)-H(28D)	109.8
H(28C)-C(28B)-H(28D)	108.3
C(29B)-C(28B)-C(26B)	109.36(9)
C(29B)-C(28B)-H(28C)	109.8
C(29B)-C(28B)-H(28D)	109.8
C(28B)-C(29B)-H(29C)	110.4
C(28B)-C(29B)-H(29D)	110.4
C(28B)-C(29B)-C(30B)	106.49(9)
H(29C)-C(29B)-H(29D)	108.6
C(30B)-C(29B)-H(29C)	110.4
C(30B)-C(29B)-H(29D)	110.4
P(1B)-C(30B)-H(30B)	107.7
C(29B)-C(30B)-P(1B)	104.37(7)
C(29B)-C(30B)-H(30B)	107.7

C(31B)-C(30B)-P(1B)	114.93(7)
C(31B)-C(30B)-C(29B)	114.09(9)
C(31B)-C(30B)-H(30B)	107.7
C(30B)-C(31B)-H(31D)	109.5
C(30B)-C(31B)-H(31E)	109.5
C(30B)-C(31B)-H(31F)	109.5
H(31D)-C(31B)-H(31E)	109.5
H(31D)-C(31B)-H(31F)	109.5
H(31E)-C(31B)-H(31F)	109.5
P(1B)-C(32B)-Fe(1B)	121.00(5)
C(33B)-C(32B)-Fe(1B)	69.81(6)
C(33B)-C(32B)-P(1B)	132.54(8)
C(36B)-C(32B)-Fe(1B)	69.59(6)
C(36B)-C(32B)-P(1B)	120.70(7)
C(36B)-C(32B)-C(33B)	106.52(9)
Fe(1B)-C(33B)-H(33B)	126.6
C(32B)-C(33B)-Fe(1B)	68.69(6)
C(32B)-C(33B)-H(33B)	125.8
C(34B)-C(33B)-Fe(1B)	70.46(7)
C(34B)-C(33B)-C(32B)	108.40(10)
C(34B)-C(33B)-H(33B)	125.8
Fe(1B)-C(34B)-H(34B)	127.1
C(33B)-C(34B)-Fe(1B)	68.74(6)
C(33B)-C(34B)-H(34B)	125.9
C(35B)-C(34B)-Fe(1B)	69.83(7)
C(35B)-C(34B)-C(33B)	108.28(10)
C(35B)-C(34B)-H(34B)	125.9
Fe(1B)-C(35B)-H(35B)	127.1
C(34B)-C(35B)-Fe(1B)	69.85(8)
C(34B)-C(35B)-H(35B)	126.1
C(34B)-C(35B)-C(36B)	107.81(11)
C(36B)-C(35B)-Fe(1B)	68.56(7)
C(36B)-C(35B)-H(35B)	126.1
Fe(1B)-C(36B)-H(36B)	126.4
C(32B)-C(36B)-Fe(1B)	68.92(6)
C(32B)-C(36B)-H(36B)	125.5

C(35B)-C(36B)-Fe(1B)	70.71(7)
C(35B)-C(36B)-C(32B)	108.99(10)
C(35B)-C(36B)-H(36B)	125.5
P(2B)-C(37B)-Fe(1B)	119.62(5)
C(38B)-C(37B)-Fe(1B)	69.91(6)
C(38B)-C(37B)-P(2B)	131.40(8)
C(41B)-C(37B)-Fe(1B)	69.55(6)
C(41B)-C(37B)-P(2B)	121.55(8)
C(41B)-C(37B)-C(38B)	106.64(9)
Fe(1B)-C(38B)-H(38B)	127.0
C(37B)-C(38B)-Fe(1B)	68.69(6)
C(37B)-C(38B)-H(38B)	125.9
C(39B)-C(38B)-Fe(1B)	69.98(6)
C(39B)-C(38B)-C(37B)	108.26(10)
C(39B)-C(38B)-H(38B)	125.9
Fe(1B)-C(39B)-H(39B)	126.6
C(38B)-C(39B)-Fe(1B)	69.25(6)
C(38B)-C(39B)-H(39B)	125.8
C(40B)-C(39B)-Fe(1B)	69.99(7)
C(40B)-C(39B)-C(38B)	108.48(10)
C(40B)-C(39B)-H(39B)	125.8
Fe(1B)-C(40B)-H(40B)	127.1
C(39B)-C(40B)-Fe(1B)	69.65(7)
C(39B)-C(40B)-H(40B)	126.1
C(39B)-C(40B)-C(41B)	107.81(11)
C(41B)-C(40B)-Fe(1B)	68.74(7)
C(41B)-C(40B)-H(40B)	126.1
Fe(1B)-C(41B)-H(41B)	126.5
C(37B)-C(41B)-Fe(1B)	69.01(6)
C(37B)-C(41B)-H(41B)	125.6
C(40B)-C(41B)-Fe(1B)	70.49(8)
C(40B)-C(41B)-C(37B)	108.80(10)
C(40B)-C(41B)-H(41B)	125.6
C(42)-O(4)-C(45)	110.54(15)
C(44)-O(5)-C(43)	108.75(14)
O(4)-C(42)-H(42A)	109.6

O(4)-C(42)-H(42B)	109.6
O(4)-C(42)-C(43)	110.5(2)
H(42A)-C(42)-H(42B)	108.1
C(43)-C(42)-H(42A)	109.6
C(43)-C(42)-H(42B)	109.6
O(5)-C(43)-C(42)	109.21(19)
O(5)-C(43)-H(43A)	109.8
O(5)-C(43)-H(43B)	109.8
C(42)-C(43)-H(43A)	109.8
C(42)-C(43)-H(43B)	109.8
H(43A)-C(43)-H(43B)	108.3
O(5)-C(44)-H(44A)	109.5
O(5)-C(44)-H(44B)	109.5
O(5)-C(44)-C(45)	110.92(14)
H(44A)-C(44)-H(44B)	108.0
C(45)-C(44)-H(44A)	109.5
C(45)-C(44)-H(44B)	109.5
O(4)-C(45)-C(44)	111.17(14)
O(4)-C(45)-H(45A)	109.4
O(4)-C(45)-H(45B)	109.4
C(44)-C(45)-H(45A)	109.4
C(44)-C(45)-H(45B)	109.4
H(45A)-C(45)-H(45B)	108.0
C(42B)-O(4B)-C(45B)	108.74(14)
C(43B)-O(5B)-C(44B)	108.29(16)
O(4B)-C(42B)-H(42C)	109.6
O(4B)-C(42B)-H(42D)	109.6
O(4B)-C(42B)-C(43B)	110.3(2)
H(42C)-C(42B)-H(42D)	108.1
C(43B)-C(42B)-H(42C)	109.6
C(43B)-C(42B)-H(42D)	109.6
O(5B)-C(43B)-C(42B)	109.5(2)
O(5B)-C(43B)-H(43C)	109.8
O(5B)-C(43B)-H(43D)	109.8
C(42B)-C(43B)-H(43C)	109.8
C(42B)-C(43B)-H(43D)	109.8

H(43C)-C(43B)-H(43D)	108.2
O(5B)-C(44B)-H(44C)	109.5
O(5B)-C(44B)-H(44D)	109.5
O(5B)-C(44B)-C(45B)	110.69(15)
H(44C)-C(44B)-H(44D)	108.1
C(45B)-C(44B)-H(44C)	109.5
C(45B)-C(44B)-H(44D)	109.5
O(4B)-C(45B)-C(44B)	111.24(15)
O(4B)-C(45B)-H(45C)	109.4
O(4B)-C(45B)-H(45D)	109.4
C(44B)-C(45B)-H(45C)	109.4
C(44B)-C(45B)-H(45D)	109.4
H(45C)-C(45B)-H(45D)	108.0

Symmetry transformations used to generate equivalent atoms:

Table A4.10 Anisotropic displacement parameters ($\text{\AA}^2 \times 10^4$) for **Pd/L10**. The anisotropic displacement factor exponent takes the form: $-2p^2 [h^2 a^{*2} U^{11} + \dots + 2 h k a^* b^* U^{12}]$

	U^{11}	U^{22}	U^{33}	U^{23}	U^{13}	U^{12}
Pd(1)	89(1)	90(1)	115(1)	22(1)	17(1)	3(1)
Fe(1)	94(1)	107(1)	142(1)	47(1)	3(1)	0(1)
P(1)	101(1)	91(1)	132(1)	31(1)	16(1)	1(1)
P(2)	105(1)	95(1)	142(1)	17(1)	16(1)	8(1)
O(1)	232(4)	193(3)	158(3)	18(2)	69(3)	17(3)
O(2)	198(3)	130(3)	207(3)	4(2)	16(3)	-28(2)
O(3)	326(5)	258(4)	162(3)	74(3)	30(3)	34(4)
C(1)	117(3)	136(3)	167(4)	22(3)	19(3)	-13(2)
C(2)	114(3)	130(3)	152(3)	26(3)	16(3)	12(2)
C(3)	111(3)	131(3)	150(3)	35(2)	26(2)	17(2)
C(4)	157(3)	144(3)	148(3)	36(3)	25(3)	37(3)
C(5)	176(4)	149(3)	162(3)	31(3)	37(3)	43(3)
C(6)	149(3)	153(3)	151(3)	26(3)	39(3)	3(3)

C(7)	175(4)	166(4)	166(3)	60(3)	43(3)	12(3)
C(8)	165(3)	141(3)	176(4)	54(3)	44(3)	31(3)
C(9)	272(6)	191(5)	228(5)	-3(4)	95(4)	24(4)
C(10)	121(3)	129(3)	167(3)	12(3)	5(2)	-9(2)
C(11)	164(4)	148(4)	147(3)	18(3)	8(3)	2(3)
C(12)	167(4)	157(3)	161(3)	6(3)	11(3)	-17(3)
C(13)	173(4)	161(4)	141(3)	6(3)	-1(3)	-8(3)
C(14)	331(6)	171(4)	143(4)	9(3)	17(4)	-52(4)
C(15)	355(7)	178(4)	162(4)	26(3)	23(4)	-43(4)
C(16)	226(4)	194(4)	149(4)	40(3)	-2(3)	28(3)
C(17)	232(5)	253(5)	138(4)	1(3)	-11(3)	-21(4)
C(18)	206(5)	215(5)	152(4)	-11(4)	-1(4)	-43(4)
C(19)	539(11)	239(6)	257(6)	115(5)	139(7)	40(6)
C(20)	146(3)	162(4)	215(4)	-45(3)	17(3)	14(3)
C(21)	257(6)	302(6)	204(5)	-51(4)	54(4)	20(5)
C(22)	403(8)	123(4)	416(9)	-13(5)	139(7)	37(5)
C(23)	475(10)	114(4)	467(10)	35(5)	194(8)	-45(5)
C(24)	159(4)	150(3)	250(5)	90(3)	24(3)	-3(3)
C(25)	311(6)	218(5)	269(6)	97(4)	115(5)	-15(4)
C(26)	144(3)	174(4)	181(4)	84(3)	28(3)	-5(3)
C(27)	260(5)	266(5)	167(4)	87(4)	36(4)	25(4)
C(28)	224(5)	163(4)	281(5)	125(4)	10(4)	-33(3)
C(29)	191(4)	113(3)	275(5)	49(3)	4(4)	-14(3)
C(30)	139(3)	99(3)	202(4)	25(3)	14(3)	15(2)
C(31)	205(4)	179(4)	205(4)	4(3)	46(3)	30(3)
C(32)	117(3)	111(3)	147(3)	32(2)	7(2)	-2(2)
C(33)	140(3)	125(3)	225(4)	30(3)	-17(3)	-21(3)
C(34)	169(4)	205(4)	221(5)	18(4)	-59(3)	-12(3)
C(35)	238(5)	240(5)	144(4)	58(4)	-22(4)	26(4)
C(36)	168(4)	170(4)	140(3)	54(3)	29(3)	13(3)
C(37)	113(3)	117(3)	164(3)	34(2)	18(2)	13(2)
C(38)	123(3)	130(3)	230(4)	69(3)	1(3)	14(2)
C(39)	109(3)	166(4)	285(5)	74(3)	19(3)	23(3)
C(40)	129(4)	194(4)	243(5)	74(4)	62(3)	3(3)
C(41)	144(3)	165(4)	159(3)	56(3)	39(3)	14(3)
Pd(1B)	89(1)	95(1)	113(1)	34(1)	18(1)	10(1)

Fe(1B)	86(1)	105(1)	157(1)	40(1)	15(1)	5(1)
P(1B)	97(1)	91(1)	124(1)	32(1)	17(1)	11(1)
P(2B)	111(1)	111(1)	146(1)	54(1)	19(1)	3(1)
O(3B)	257(4)	220(4)	150(3)	0(3)	15(3)	52(3)
O(1B)	188(3)	197(3)	128(2)	42(2)	40(2)	-1(2)
O(2B)	204(3)	158(3)	181(3)	77(2)	19(2)	42(2)
C(1B)	123(3)	146(3)	145(3)	45(3)	24(3)	32(2)
C(2B)	115(3)	137(3)	129(3)	32(2)	20(2)	2(2)
C(3B)	106(3)	129(3)	131(3)	28(2)	21(2)	2(2)
C(4B)	149(3)	133(3)	132(3)	17(2)	25(2)	-21(2)
C(5B)	164(3)	143(3)	145(3)	27(3)	33(3)	-24(3)
C(6B)	124(3)	149(3)	129(3)	33(2)	25(2)	9(2)
C(7B)	162(3)	134(3)	137(3)	14(2)	34(3)	7(3)
C(8B)	154(3)	123(3)	151(3)	22(3)	38(3)	-3(3)
C(9B)	226(5)	241(5)	202(4)	90(4)	63(4)	-13(4)
C(10B)	120(3)	142(3)	141(3)	47(2)	12(2)	20(2)
C(11B)	151(3)	161(4)	127(3)	41(3)	16(3)	17(3)
C(12B)	167(3)	162(3)	133(3)	52(3)	22(3)	27(3)
C(13B)	154(3)	163(3)	126(3)	48(3)	16(2)	21(3)
C(14B)	267(5)	176(4)	136(3)	56(3)	21(3)	60(3)
C(15B)	281(5)	178(4)	151(4)	46(3)	15(3)	68(4)
C(16B)	181(4)	172(4)	137(3)	20(3)	6(3)	21(3)
C(17B)	204(4)	218(4)	124(3)	49(3)	9(3)	43(3)
C(18B)	188(4)	191(4)	131(4)	61(3)	13(3)	44(3)
C(19B)	315(7)	227(5)	255(6)	-3(4)	42(5)	89(5)
C(20B)	167(4)	216(4)	198(4)	119(4)	13(3)	-6(3)
C(21B)	276(6)	368(7)	198(5)	130(5)	69(4)	17(5)
C(22B)	394(8)	196(5)	337(7)	156(5)	70(6)	-23(5)
C(23B)	394(8)	147(4)	367(7)	122(5)	104(6)	71(5)
C(24B)	161(4)	126(3)	227(4)	34(3)	30(3)	18(3)
C(25B)	283(6)	187(5)	318(6)	27(4)	141(5)	57(4)
C(26B)	140(3)	134(3)	154(3)	20(2)	37(3)	24(2)
C(27B)	260(5)	204(4)	144(4)	21(3)	40(3)	13(4)
C(28B)	217(4)	113(3)	210(4)	19(3)	45(3)	44(3)
C(29B)	184(4)	119(3)	204(4)	60(3)	28(3)	29(3)
C(30B)	126(3)	107(3)	150(3)	37(2)	25(2)	1(2)

C(31B)	191(4)	176(4)	156(3)	50(3)	49(3)	-4(3)
C(32B)	106(3)	113(3)	148(3)	44(2)	8(2)	8(2)
C(33B)	126(3)	141(3)	227(4)	77(3)	1(3)	21(2)
C(34B)	143(3)	200(4)	221(4)	86(3)	-38(3)	-11(3)
C(35B)	165(4)	182(4)	156(4)	34(3)	-11(3)	-26(3)
C(36B)	129(3)	132(3)	143(3)	29(2)	21(2)	4(2)
C(37B)	120(3)	127(3)	169(3)	54(3)	29(2)	1(2)
C(38B)	124(3)	125(3)	229(4)	54(3)	19(3)	-10(2)
C(39B)	113(3)	173(4)	283(5)	73(3)	46(3)	-4(3)
C(40B)	148(4)	184(4)	247(5)	49(4)	91(3)	31(3)
C(41B)	159(3)	155(4)	171(4)	36(3)	57(3)	15(3)
O(4)	670(10)	150(4)	315(6)	39(4)	158(6)	-10(5)
O(5)	367(6)	179(4)	405(7)	-39(4)	94(5)	-10(4)
C(42)	970(20)	268(8)	317(8)	-2(6)	283(11)	-174(10)
C(43)	691(16)	319(9)	256(7)	7(6)	99(9)	2(9)
C(44)	262(6)	189(5)	392(8)	51(5)	77(5)	-18(4)
C(45)	282(6)	227(5)	242(5)	47(4)	34(4)	-8(4)
O(4B)	300(5)	154(4)	418(7)	63(4)	-24(5)	-24(3)
O(5B)	446(7)	170(4)	428(7)	99(4)	157(6)	71(4)
C(42B)	940(20)	322(9)	310(9)	155(7)	178(11)	7(11)
C(43B)	860(20)	285(8)	670(16)	117(9)	564(16)	157(11)
C(44B)	411(9)	318(7)	255(6)	102(5)	-22(6)	0(6)
C(45B)	335(8)	252(6)	369(8)	-11(6)	115(6)	48(5)

Table A4.11 Hydrogen coordinates ($\times 10^4$) and isotropic displacement parameters ($\text{\AA}^2 \times 10^3$) for **Pd/L10**.

	x	y	z	U(eq)
H(1)	4535	6602	1338	17
H(2)	4622	8493	636	16
H(4)	3893	9984	1652	18
H(5)	3329	10909	3107	19

H(7)	4433	8485	4345	20
H(8)	4940	7551	2882	19
H(9A)	2347	11236	4393	35
H(9B)	3634	11783	4715	35
H(9C)	2878	11535	5507	35
H(11)	5428	7727	-600	19
H(12)	4914	5800	-1919	20
H(14)	6232	8390	-1662	26
H(15)	6863	9079	-2888	28
H(17)	5496	6461	-4844	26
H(18)	4889	5778	-3611	24
H(19A)	7570	9244	-5121	49
H(19B)	7965	9133	-4040	49
H(19C)	6761	9695	-4303	49
H(20)	6891	5138	-12	23
H(21A)	8220	5991	-741	40
H(21B)	8221	4733	-1117	40
H(21C)	9275	5329	-344	40
H(22A)	7683	3550	158	38
H(22B)	8875	4116	779	38
H(23A)	7689	3765	1896	41
H(23B)	6564	4262	1387	41
H(24)	8590	5372	2556	22
H(25A)	7238	6440	3364	38
H(25B)	6823	5236	3268	38
H(25C)	6166	5921	2569	38
H(26)	9284	9712	1055	19
H(27A)	8036	8562	-202	34
H(27B)	8304	9649	-501	34
H(27C)	7061	9449	-160	34
H(28A)	8893	11429	1160	26
H(28B)	7513	11193	799	26
H(29A)	7550	12032	2390	23
H(29B)	8670	11390	2723	23
H(30)	6314	10532	2047	18
H(31A)	6419	9969	3517	30

H(31B)	6523	11231	3697	30
H(31C)	7678	10565	3862	30
H(33)	10440	10081	2625	20
H(34)	11625	9294	3902	25
H(35)	10291	7994	4390	25
H(36)	8270	7966	3410	19
H(38)	10426	5883	2554	19
H(39)	12263	6933	2431	22
H(40)	11729	8034	1190	22
H(41)	9556	7691	555	18
H(1B)	5460	961	8691	16
H(2B)	5342	3196	9364	15
H(4B)	6078	4190	8347	17
H(5B)	6675	4392	6899	18
H(7B)	5675	1330	5692	17
H(8B)	5106	1128	7142	17
H(9BA)	7262	3768	4505	32
H(9BB)	7864	3947	5598	32
H(9BC)	6619	4453	5350	32
H(11B)	4523	3053	10591	17
H(12B)	5036	1789	11925	18
H(14B)	3837	4317	11689	23
H(15B)	3183	5579	12919	24
H(17B)	4376	3811	14834	22
H(18B)	5002	2552	13598	20
H(19D)	1970	6135	14105	41
H(19E)	3179	6821	14337	41
H(19F)	2413	6763	15182	41
H(20B)	3092	-72	9914	22
H(21D)	1936	1214	10758	40
H(21E)	1776	107	11055	40
H(21F)	774	488	10332	40
H(22C)	2081	-1687	9682	35
H(22D)	946	-1278	9098	35
H(23C)	2014	-2218	7922	35
H(23D)	3230	-1635	8466	35

H(24B)	1402	-823	7318	21
H(25D)	2919	-167	6669	39
H(25E)	3227	-1361	6717	39
H(25F)	3886	-395	7501	39
H(26B)	652	4120	8940	17
H(27D)	1933	3622	10206	31
H(27E)	1606	4842	10495	31
H(27F)	2866	4527	10164	31
H(28C)	1010	5790	8830	22
H(28D)	2392	5759	9198	22
H(29C)	2352	5816	7599	20
H(29D)	1257	4979	7265	20
H(30B)	3616	4525	7989	15
H(31D)	3677	3304	6542	25
H(31E)	3379	4438	6316	25
H(31F)	2353	3551	6162	25
H(33B)	-502	3671	7297	19
H(34B)	-1615	2196	6028	22
H(35B)	-220	691	5617	21
H(36B)	1761	1231	6627	16
H(38B)	-480	-431	7525	19
H(39B)	-2281	714	7645	22
H(40B)	-1686	2452	8825	22
H(41B)	496	2403	9427	19
H(42A)	10795	7172	6356	61
H(42B)	10048	7962	5814	61
H(43A)	8467	6694	5345	51
H(43B)	9643	6207	4949	51
H(44A)	8651	5484	7269	34
H(44B)	7858	6234	6713	34
H(45A)	8945	7281	8083	30
H(45B)	10151	6791	7755	30
H(42C)	1528	3229	4508	60
H(42D)	401	2584	4668	60
H(43C)	-850	3533	3704	67
H(43D)	-143	4334	4615	67

H(44C)	927	3953	2068	39
H(44D)	-226	3319	2194	39
H(45C)	1371	2192	2105	39
H(45D)	2117	2988	2996	39

Table A4.12 Torsion angles [°] for **Pd/L10**

Pd(1)-P(1)-C(26)-C(27)	13.50(10)
Pd(1)-P(1)-C(26)-C(28)	135.79(7)
Pd(1)-P(1)-C(30)-C(29)	-157.26(6)
Pd(1)-P(1)-C(30)-C(31)	77.50(9)
Pd(1)-P(1)-C(32)-Fe(1)	54.66(6)
Pd(1)-P(1)-C(32)-C(33)	145.33(9)
Pd(1)-P(1)-C(32)-C(36)	-28.92(10)
Pd(1)-P(2)-C(20)-C(21)	89.36(10)
Pd(1)-P(2)-C(20)-C(22)	-142.60(9)
Pd(1)-P(2)-C(24)-C(23)	114.76(10)
Pd(1)-P(2)-C(24)-C(25)	-8.34(12)
Pd(1)-P(2)-C(37)-Fe(1)	41.00(7)
Pd(1)-P(2)-C(37)-C(38)	129.54(9)
Pd(1)-P(2)-C(37)-C(41)	-42.27(10)
Pd(1)-C(1)-C(2)-C(3)	-105.19(9)
Pd(1)-C(1)-C(10)-O(2)	117.08(10)
Pd(1)-C(1)-C(10)-C(11)	-61.56(10)
Pd(1)-C(2)-C(3)-C(4)	125.75(9)
Pd(1)-C(2)-C(3)-C(8)	-51.89(12)
Fe(1)-C(32)-C(33)-C(34)	-58.97(9)
Fe(1)-C(32)-C(36)-C(35)	59.62(9)
Fe(1)-C(33)-C(34)-C(35)	-58.57(10)
Fe(1)-C(34)-C(35)-C(36)	-58.46(10)
Fe(1)-C(35)-C(36)-C(32)	-59.03(8)
Fe(1)-C(37)-C(38)-C(39)	-59.14(8)
Fe(1)-C(37)-C(41)-C(40)	59.54(9)
Fe(1)-C(38)-C(39)-C(40)	-59.27(9)

Fe(1)-C(39)-C(40)-C(41)	-58.29(9)
Fe(1)-C(40)-C(41)-C(37)	-58.77(8)
P(1)-C(26)-C(28)-C(29)	20.10(12)
P(1)-C(32)-C(33)-Fe(1)	-115.18(9)
P(1)-C(32)-C(33)-C(34)	-174.15(9)
P(1)-C(32)-C(36)-Fe(1)	115.24(8)
P(1)-C(32)-C(36)-C(35)	174.85(9)
P(2)-C(20)-C(22)-C(23)	41.40(16)
P(2)-C(37)-C(38)-Fe(1)	-112.95(9)
P(2)-C(37)-C(38)-C(39)	-172.09(9)
P(2)-C(37)-C(41)-Fe(1)	113.64(8)
P(2)-C(37)-C(41)-C(40)	173.17(9)
O(1)-C(6)-C(7)-C(8)	-179.87(11)
O(2)-C(10)-C(11)-C(12)	7.81(17)
O(3)-C(16)-C(17)-C(18)	176.06(13)
C(1)-C(2)-C(3)-C(4)	-152.82(10)
C(1)-C(2)-C(3)-C(8)	29.53(15)
C(1)-C(10)-C(11)-C(12)	-173.53(11)
C(2)-C(1)-C(10)-O(2)	-169.93(10)
C(2)-C(1)-C(10)-C(11)	11.43(15)
C(2)-C(3)-C(4)-C(5)	-178.16(10)
C(2)-C(3)-C(8)-C(7)	177.07(10)
C(3)-C(4)-C(5)-C(6)	1.28(17)
C(4)-C(3)-C(8)-C(7)	-0.61(16)
C(4)-C(5)-C(6)-O(1)	178.89(11)
C(4)-C(5)-C(6)-C(7)	-1.15(17)
C(5)-C(6)-C(7)-C(8)	0.16(17)
C(6)-C(7)-C(8)-C(3)	0.73(18)
C(8)-C(3)-C(4)-C(5)	-0.40(16)
C(9)-O(1)-C(6)-C(5)	0.68(18)
C(9)-O(1)-C(6)-C(7)	-179.29(11)
C(10)-C(1)-C(2)-Pd(1)	-90.34(10)
C(10)-C(1)-C(2)-C(3)	164.47(9)
C(10)-C(11)-C(12)-C(13)	-176.13(11)
C(11)-C(12)-C(13)-C(14)	10.3(2)
C(11)-C(12)-C(13)-C(18)	-172.00(13)

C(12)-C(13)-C(14)-C(15)	175.87(14)
C(12)-C(13)-C(18)-C(17)	-176.27(13)
C(13)-C(14)-C(15)-C(16)	-0.1(2)
C(14)-C(13)-C(18)-C(17)	1.5(2)
C(14)-C(15)-C(16)-O(3)	-176.27(14)
C(14)-C(15)-C(16)-C(17)	2.4(2)
C(15)-C(16)-C(17)-C(18)	-2.7(2)
C(16)-C(17)-C(18)-C(13)	0.7(2)
C(18)-C(13)-C(14)-C(15)	-1.8(2)
C(19)-O(3)-C(16)-C(15)	-1.7(2)
C(19)-O(3)-C(16)-C(17)	179.58(14)
C(20)-P(2)-C(24)-C(23)	-7.45(11)
C(20)-P(2)-C(24)-C(25)	-130.55(11)
C(20)-P(2)-C(37)-Fe(1)	170.96(6)
C(20)-P(2)-C(37)-C(38)	-100.51(11)
C(20)-P(2)-C(37)-C(41)	87.68(10)
C(20)-C(22)-C(23)-C(24)	-49.7(2)
C(21)-C(20)-C(22)-C(23)	169.22(14)
C(22)-C(23)-C(24)-P(2)	33.22(18)
C(22)-C(23)-C(24)-C(25)	158.68(15)
C(24)-P(2)-C(20)-C(21)	-147.46(11)
C(24)-P(2)-C(20)-C(22)	-19.41(11)
C(24)-P(2)-C(37)-Fe(1)	-91.06(7)
C(24)-P(2)-C(37)-C(38)	-2.53(12)
C(24)-P(2)-C(37)-C(41)	-174.34(9)
C(26)-P(1)-C(30)-C(29)	-28.30(8)
C(26)-P(1)-C(30)-C(31)	-153.54(9)
C(26)-P(1)-C(32)-Fe(1)	-75.89(7)
C(26)-P(1)-C(32)-C(33)	14.78(12)
C(26)-P(1)-C(32)-C(36)	-159.46(9)
C(26)-C(28)-C(29)-C(30)	-42.57(13)
C(27)-C(26)-C(28)-C(29)	143.14(11)
C(28)-C(29)-C(30)-P(1)	44.45(11)
C(28)-C(29)-C(30)-C(31)	170.36(10)
C(30)-P(1)-C(26)-C(27)	-117.12(9)
C(30)-P(1)-C(26)-C(28)	5.17(8)

C(30)-P(1)-C(32)-Fe(1)	-172.97(6)
C(30)-P(1)-C(32)-C(33)	-82.30(11)
C(30)-P(1)-C(32)-C(36)	103.46(9)
C(32)-P(1)-C(26)-C(27)	139.26(9)
C(32)-P(1)-C(26)-C(28)	-98.45(8)
C(32)-P(1)-C(30)-C(29)	76.66(8)
C(32)-P(1)-C(30)-C(31)	-48.58(9)
C(32)-C(33)-C(34)-Fe(1)	58.05(8)
C(32)-C(33)-C(34)-C(35)	-0.52(15)
C(33)-C(32)-C(36)-Fe(1)	-60.25(8)
C(33)-C(32)-C(36)-C(35)	-0.63(13)
C(33)-C(34)-C(35)-Fe(1)	58.59(10)
C(33)-C(34)-C(35)-C(36)	0.12(16)
C(34)-C(35)-C(36)-Fe(1)	59.36(10)
C(34)-C(35)-C(36)-C(32)	0.32(15)
C(36)-C(32)-C(33)-Fe(1)	59.68(7)
C(36)-C(32)-C(33)-C(34)	0.71(13)
C(37)-P(2)-C(20)-C(21)	-41.75(11)
C(37)-P(2)-C(20)-C(22)	86.30(11)
C(37)-P(2)-C(24)-C(23)	-112.78(11)
C(37)-P(2)-C(24)-C(25)	124.11(10)
C(37)-C(38)-C(39)-Fe(1)	58.60(8)
C(37)-C(38)-C(39)-C(40)	-0.66(14)
C(38)-C(37)-C(41)-Fe(1)	-59.93(8)
C(38)-C(37)-C(41)-C(40)	-0.39(13)
C(38)-C(39)-C(40)-Fe(1)	58.71(9)
C(38)-C(39)-C(40)-C(41)	0.42(15)
C(39)-C(40)-C(41)-Fe(1)	58.76(10)
C(39)-C(40)-C(41)-C(37)	-0.01(14)
C(41)-C(37)-C(38)-Fe(1)	59.79(7)
C(41)-C(37)-C(38)-C(39)	0.64(13)
Pd(1B)-P(1B)-C(26B)-C(27B)	13.94(10)
Pd(1B)-P(1B)-C(26B)-C(28B)	135.68(7)
Pd(1B)-P(1B)-C(30B)-C(29B)	-158.20(6)
Pd(1B)-P(1B)-C(30B)-C(31B)	76.08(8)
Pd(1B)-P(1B)-C(32B)-Fe(1B)	56.33(6)

Pd(1B)-P(1B)-C(32B)-C(33B)	146.60(9)
Pd(1B)-P(1B)-C(32B)-C(36B)	-26.98(9)
Pd(1B)-P(2B)-C(20B)-C(21B)	84.54(10)
Pd(1B)-P(2B)-C(20B)-C(22B)	-148.43(9)
Pd(1B)-P(2B)-C(24B)-C(23B)	123.93(9)
Pd(1B)-P(2B)-C(24B)-C(25B)	0.53(11)
Pd(1B)-P(2B)-C(37B)-Fe(1B)	44.77(7)
Pd(1B)-P(2B)-C(37B)-C(38B)	133.30(9)
Pd(1B)-P(2B)-C(37B)-C(41B)	-38.19(10)
Pd(1B)-C(1B)-C(2B)-C(3B)	-106.22(9)
Pd(1B)-C(1B)-C(10B)-O(2B)	115.92(10)
Pd(1B)-C(1B)-C(10B)-C(11B)	-63.29(10)
Pd(1B)-C(2B)-C(3B)-C(4B)	125.76(9)
Pd(1B)-C(2B)-C(3B)-C(8B)	-52.35(11)
Fe(1B)-C(32B)-C(33B)-C(34B)	-59.46(8)
Fe(1B)-C(32B)-C(36B)-C(35B)	59.54(8)
Fe(1B)-C(33B)-C(34B)-C(35B)	-58.79(9)
Fe(1B)-C(34B)-C(35B)-C(36B)	-58.21(9)
Fe(1B)-C(35B)-C(36B)-C(32B)	-58.44(7)
Fe(1B)-C(37B)-C(38B)-C(39B)	-58.96(8)
Fe(1B)-C(37B)-C(41B)-C(40B)	59.44(9)
Fe(1B)-C(38B)-C(39B)-C(40B)	-59.17(9)
Fe(1B)-C(39B)-C(40B)-C(41B)	-58.31(9)
Fe(1B)-C(40B)-C(41B)-C(37B)	-58.53(8)
P(1B)-C(26B)-C(28B)-C(29B)	20.05(11)

A4.3 REFERENCES

1. G. M. Sheldrick, *Acta Cryst.* **1990**, A46, 467.
2. G. M. Sheldrick, *Acta Cryst.* **2015**, C71, 3.
3. P. Müller, *Crystallography Reviews* **2009**, 15, 57.

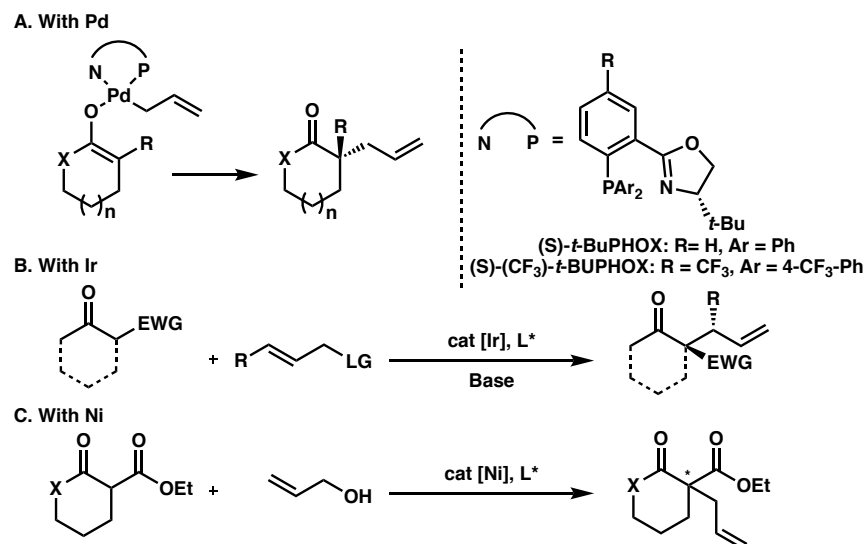
CHAPTER 3

Copper-Catalyzed Enantioselective Allylic Alkylation with a γ -Butyrolactone-Derived Silyl Ketene Acetal[†]

3.1 INTRODUCTION, BACKGROUND, AND SYNTHETIC UTILITY

In the Stoltz lab, transition metal-catalyzed allylic alkylation of enolate-derived nucleophiles has been a subject of intense investigation. The products formed are valuable synthetic intermediates, possessing chirality, as well as carbonyl and alkene functionalities, which can be further derivatized. The most developed system in our group for asymmetric α -alkylation is a Pd-catalyzed decarboxylative allylation of enol-carbonates (Figure 3.1.1.A). Using either (*S*)-*t*-BuPHOX or (*S*)-(CF₃)-*t*-BuPHOX as a supporting ligand for Pd, excellent yields and enantioselectivities have been achieved.¹ In order to expand the scope of allylic alkylations and access motifs currently inaccessible with Pd catalysis, two more systems using Iridium and Nickel

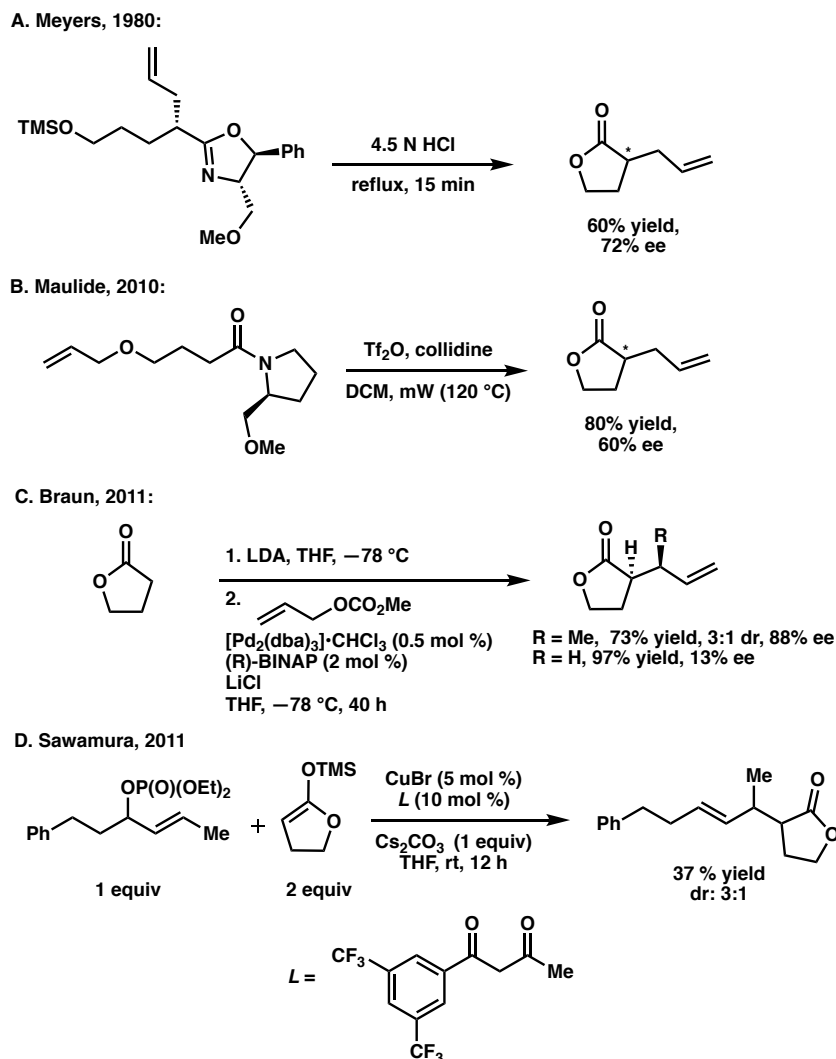
[†] This work was performed in collaboration with the Hadt Lab at Caltech. Additionally, this research has been published and adapted with permission from Jette, C. I.; Tong, Z. J.; Hadt, R. G.; Stoltz B. M. *Angew. Chem. Int. Ed.* **2020**, 59, 2033–2038. Copyright 2020 Wiley-VCH. Alexander Q. Cusumano is thanked for assistance and helpful discussions.

Figure 3.1.1: Summary of Previous Research in Allylic Alkylations in the Stoltz Lab^{1,2,3}

were developed. By exploiting these metals' different modes of action, substrates that reacted poorly under conditions of Pd catalysis could now be successfully employed with a high degree of regio- and stereocontrol. Regarding Iridium, substituted allylic electrophiles were well tolerated, allowing for the formation of products with adjacent chiral centers (Figure 3.1.1.B).² More recently, a Nickel catalyst was shown to be effective for 6-membered lactone derived nucleophiles to form α -quaternary centers with an allylic alcohol as the electrophile (Figure 3.1.1.C).³

One particular class of nucleophiles that had not yet been used successfully with existing methodology are γ -butyrolactone-derived anions. γ -Butyrolactones comprise an important class of compounds predicted to exist in ca. 10% of all natural products. They can be mono-, bi-, and tri-substituted, and can also exist in more complex bicyclic or tri-cyclic frameworks. γ -Butyrolactone-containing natural products are also interesting lead structures for new drugs, as they display a broad biological profile including antibiotic, antihelminthic, antifungal, antitumor, antiviral, anti-inflammatory, and cytostatic properties.⁴

Figure 3.1.2. Previous Reports of α -Allylation of γ -Butyrolactones^{6, 7, 10c, 12}



Despite their prevalence in nature and potential utility as precursor materials, the development of systems for the functionalization of γ -butyrolactones has not reached maturity. More specifically, although there are a number of reports on the α -functionalization of substituted γ -butyrolactones to form chiral quaternary centers, only a limited number of examples have demonstrated the construction of chiral α -tertiary γ -butyrolactones.⁵ Some previously disclosed strategies for the synthesis of α -allyl γ -lactones include chiral auxiliary-directed alkylation and

subsequent cyclization⁶ and a Claisen-type rearrangement.⁷ However, in both cases the α -allyl lactones were obtained in only moderate yield and ee (Figure 3.1.2.A and B). Reports on the construction of these molecules via enantioselective α -functionalization remain limited, as the potential for racemization of the product necessitates the development of exceptionally mild reaction conditions.⁸

One attractive strategy for the synthesis of these molecules is transition metal-catalyzed enantioselective allylic alkylation. Since the seminal report by Tsuji,⁹ transition-metal catalyzed allylic alkylation of enolate-derived nucleophiles continues to be a powerful approach for α -functionalization of carbonyl-containing compounds, as the alkene may be easily converted to a diverse array of functional groups. The use of γ -butyrolactones in this transformation, however, remains underdeveloped.¹⁰ More specifically, there is only one example on the use of this transformation to produce enantioenriched α -tertiary lactones, which requires the pre-formation of the corresponding lithium enolate, and extended reaction times at cryogenic temperatures.^{10c} Although the desired product is obtained in moderate diastereoselectivity and good ee when an electrophile possessing terminal substitution is used, the ee is extremely low when simple allyl carbonate is employed (Figure 3.1.2.C). As part of our ongoing interest in exploring first row transition metals in enantioselective catalysis,^{3,11} we became interested in a system reported by Sawamura, wherein a Cu catalyst was used to obtain the desired α -allyl γ -butyrolactone in a racemic mixture by reaction of silyl ketene acetals with allylic phosphates (Figure 3.1.2.D).¹²

3.2 INITIAL LIGAND SCREEN

Table 3.2.1 Preliminary Ligand Screen^a

<p>A. with Cs₂CO₃:</p>			
<p>L20 No reaction</p>	<p>L21 No reaction</p>	<p>L22 Yield: 77% l:b: 93:7 ee: < 5%</p>	<p>L23 Yield: 73% l:b: 93:7 ee: < 5%</p>
<p>L24 Yield: 51% l:b: 83:17 ee: < 5%</p>	<p>L25 No reaction</p>	<p>L26 No reaction</p>	<p>L27 No reaction</p>
<p>L28 Yield: 32% l:b: 94:6 ee: < 5%</p>	<p>L29 No reaction</p>	<p>L30 Yield: 25% l:b: 90:10 ee: < 5%</p>	<p>L31 No reaction</p>
<p>B. with CsOAc:</p>			
<p>L22 Yield: 44% l:b: 93:7 ee: < 5%</p>	<p>L24 Yield: 35% l:b: 83:17 ee: < 5%</p>	<p>L28 Yield: 79% l:b: 94:6 ee: < 5%</p>	<p>L32 No reaction</p>
<p>L33 No reaction</p>	<p>L34 No reaction</p>	<p>L35 No reaction</p>	<p>L36 Yield: 32% l:b: 83:17 ee: < 5%</p>
<p>L37 No reaction</p>	<p>L38 Yield: 11% l:b: 100:0 ee: 52%</p>	<p>L39 Yield: 55% l:b: 85:15 ee: < 5%</p>	<p>L40 No reaction</p>
<p>L41 No reaction</p>			

[a] Reactions were run on 0.1 mmol scale. Yields and l:b ratios were determined by ¹HNMR using trimethoxybenzene as an internal standard. Enantiomeric excess (ee) was determined by supercritical fluid chromatography. Using Set-up A (See Materials and Methods).

We commenced our studies into the Cu-catalyzed enantioselective allylic alkylation of silyl ketene acetal **41** with allylic phosphate **40a** by initially testing 14 commercially available ligands (Table 3.2.1.A), including N-heterocyclic carbenes (**L20** and **L21**), bis-oxazolines (BOX, **L22**, **L23**, **L25**, **L26**), py-BOX (**L24**), alkyl and aryl bis-phosphines (**L27**, **L31**), and P, N-type ligands (**L28-30**). We generally found that nitrogen ligands such as the gem-dimethyl BOX (**L22**, **L23**) and the pyridyl-BOX (**L24**) ligands resulted in the highest yields. N-heterocyclic carbenes (**L20** and **L21**), which are traditionally used in Cu-catalyzed enantioselective allylic alkylation with hard nucleophiles resulted in no product formation, highlighting the stark difference in reactivity between the present system and traditional Cu-catalyzed enantioselective allylic alkylations. Although we found that bisphosphine ligands (**L27** and **L31**) resulted in no reaction, we did observe product formation with P,N-type ligands such as the Feringa ligand (**L28**) and CF₃-PHOX (**L30**).

It should be noted that this reaction shows a strong preference for the α -product. This preference, although slightly influenced by the ligand (i.e. **L22** versus **L24**) could not be reversed by changing the identity of the ligand employed. Another surprising result was that the enantioselectivity appeared to be independent of the ligand as well; the product was racemic in all cases. This immediately raised concern, as these results indicated that the ligand was having an electronic effect on the reaction, which was reflected by the changes in yield and linear:branched ratios, but there did not seem to be any steric effect, which would be reflected by the ee. One possibility was that the base, Cs₂CO₃ was too strong, causing epimerization of the newly formed stereocenter. Consequently, we re-assessed **L22**, **L24**, and **L28** using CsOAc, a much milder base (Table 3.2.1.B). Unfortunately we found that this did not lead to any significant improvements, as

we still did not observe any ee with these ligands. With this new base, however, we chose to continue testing commercial ligands, with an aim of examining bulkier ligand classes. Unsurprisingly, phosphine-based ferrocene (**L32-35**) and Trost (**L37**) ligands resulted in no product formation. Upon examination of bulkier N-based ligands, however, we found that bis-picolinamide ligand **L38** resulted in 10% yield of product in 53% ee.

3.3 CHALLENGES IN THE CONSISTENCY OF THE REACTION OUTCOME

Having identified an appropriate potential ligand scaffold for this reaction, the steps to follow would include the synthesis of various ligand derivatives in order to identify a ligand that resulted in product formation in very high yield and ee. However, over the course of continued reaction investigation, we noted that when **L38** was employed, the outcome was highly variable. With an identical set-up, we found that the product was obtained in anywhere from trace amounts

Table 3.3.1. Issues with Irreproducibility^a

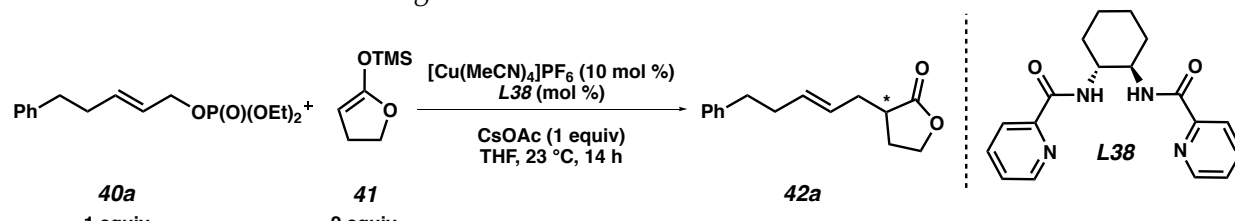
entry	yield (%)	ee (%)
1	11	52
2	42	27
3	90	17
4	< 5	–

[a] Reactions were run on 0.1 mmol scale. Yields and l:b ratios were determined by ¹HNMR using trimethoxybenzene as an internal standard. Enantiomeric excess (ee) was determined by supercritical fluid chromatography. Using Set-up A (See Materials and Methods).

to 90% yield (Table 3.3.1). These large fluctuations in yield were also accompanied by large fluctuations in ee, with the highest ee obtained being 52%.

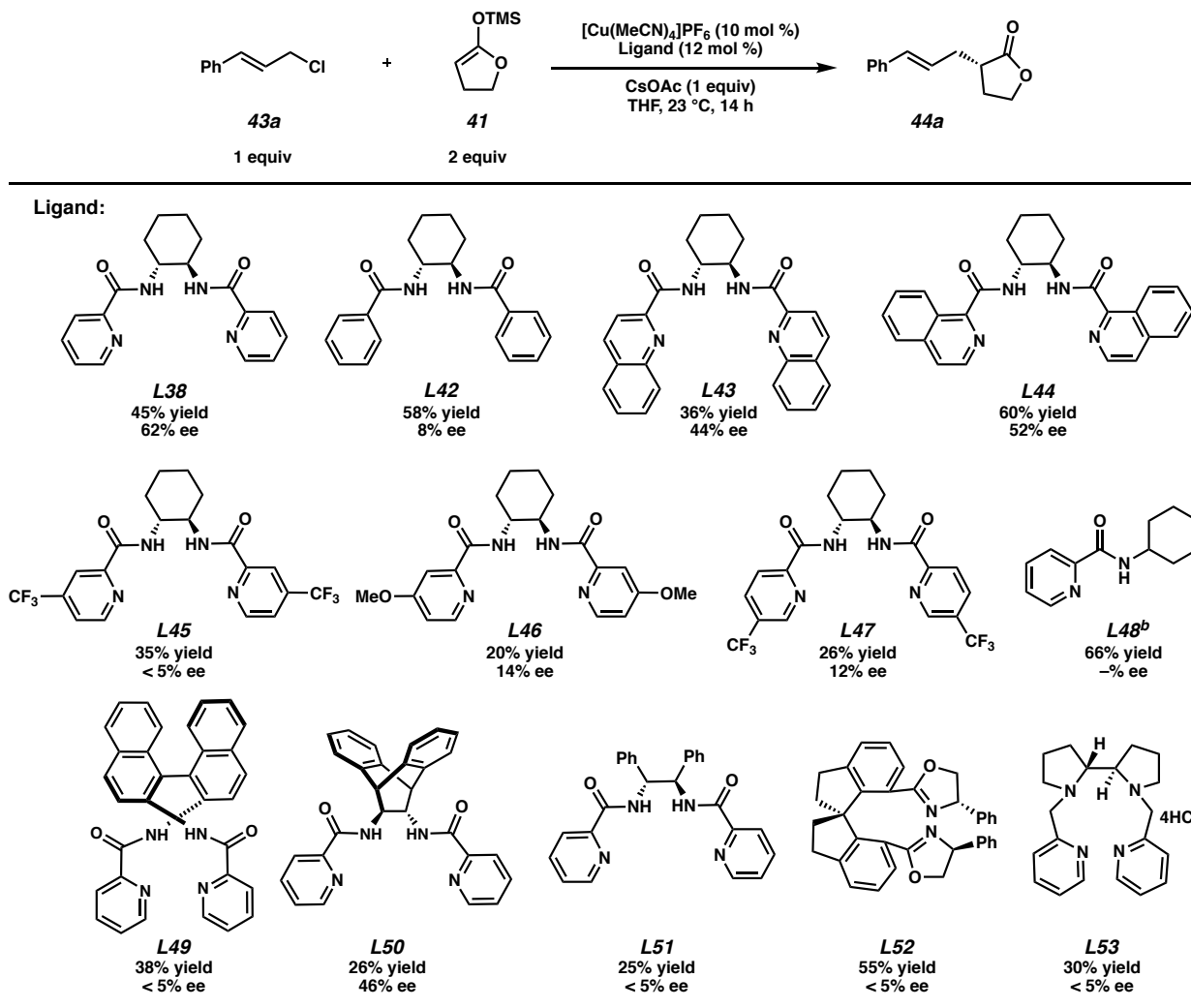
Upon closer examination of these results, we noted that in cases where the yield was low, the ee was high (entry 1), and where the ee was low, the yield was high (entry 3). One possible explanation for these results could be minor fluctuations in the metal:ligand ratio, as we had previously noted that in the absence of ligand, Cu enabled the formation of product in very high yields (Table 3.3.2, entry 1). To probe whether these differences could be attributed to minor fluctuations in the metal:ligand ratio, we examined the reaction outcome with 10 mol% Cu in combination with varying amounts of **L38**. At less than 10 mol% ligand (entries 2-3), we observed moderate yields, and 11-12% ee. As the amount of ligand is increased, a drop in reactivity is observed, however, this is accompanied with an increase in ee, up to 36% (entry 5). We also noted that the use of a 1:2 metal:ligand ratio (entry 7) resulted in a complete shut-down of reactivity.

Table 3.3.2. Effect of Metal:Ligand Ratio^a

				
entry	mol % L38	yield (%)	ee (%)	
1	0	75	0	
2	6	58	12	
3	8	47	11	
4	10	36	23	
5	12	18	36	
6	16	17	–	
7	20	0	–	

[a] Reactions were run on 0.1 mmol scale. Yields were determined by ¹HNMR using trimethoxybenzene as an internal standard. Enantiomeric excess (ee) was determined by supercritical fluid chromatography. Using Set-up **A** (See Materials and Methods).

Table 3.3.3. Initial Bis-Picolinamide Ligand Screen^a



[a] Reactions were run on 0.1 mmol scale. Yields were determined by ^1H NMR using trimethoxybenzene as an internal standard. Enantiomeric excess (ee) was determined by supercritical fluid chromatography. Using Set-up A (See Materials and Methods). [b] with 24 mol % **L48**.

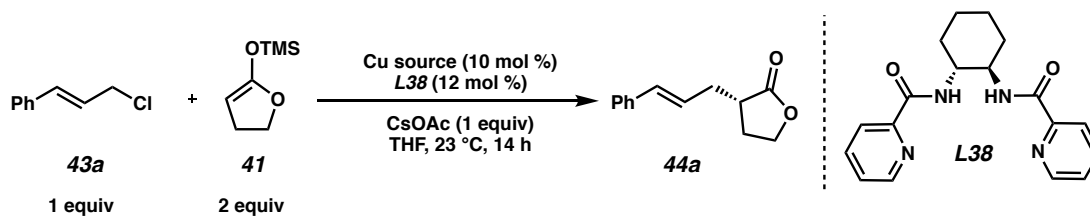
Based on these results, we concluded that the fluctuation in reaction outcome could be attributed to small differences in the metal:ligand ratio, and we reasoned that by using very large stock solutions of both Cu and the ligand, the fluctuations in quantity could be minimized. Another challenge with the present system was due to the low reactivity of hydrocinnamyl phosphate **40a**.

Having observed significantly higher reactivities with cinnamyl chloride **43a** (Table 3.3.3, **L38**), we chose to continue our optimization with this new electrophile.

The next step was to assess which part of **L38** was critical for high reactivity and selectivity, so that the yield and ee's could be improved. To this end, we synthesized and tested a number of different bis-picolinamide ligands with varying sterics and electronics around the bis-picolinamide moiety, as well as ligands with a number of different backbones. Surprisingly, we noted that all changes made to the ligand led to significant drops in reactivity and the selectivity of the reaction, and **L38** remained our best performing ligand. What was most concerning about these results was that we did not observe any trends in selectivity that we could use to inspire and direct the synthesis of the next set of ligands.

One possibility could be that we had not yet identified the appropriate Cu source for our reaction, so before testing additional ligands, we chose to examine the effect of the Cu source on the reaction outcome (Table 3.3.4). As is evident from Table 3.3.4, we found that the yields and

Table 3.3.4. Cu Source Screen^a

			
entry	Cu source	yield (%)	ee (%)
1	[Cu(MeCN) ₄]PF ₆	16	9
2	Cu(OTf) ₂	15	< 5
3	CuBr•SMe ₂	11	–
4	CuCl	64	24
5 ^b	CuBAR _f	9	–
6	CuCl ₂	20	< 5
7	CuOTf•tol	21	< 5
8	Cu(OAc)	31	10
9	[Cu(MeCN) ₄]ClO ₄	22	9
10	[Cu(MeCN) ₄]BF ₄	26	14

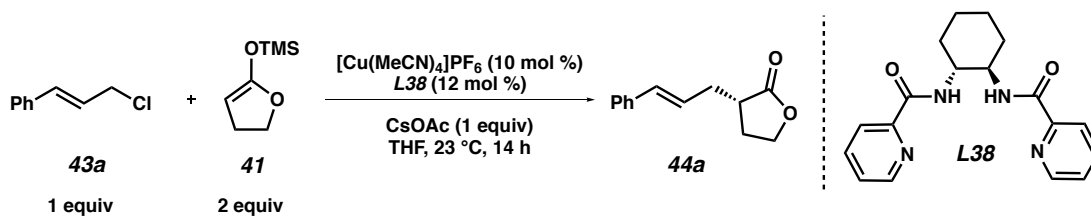
[a] Reactions were run on 0.1 mmol scale. Yields were determined by ¹HNMR using trimethoxybenzene as an internal standard. Enantiomeric excess (ee) was determined by supercritical fluid chromatography. Using Set-up A (See Materials and Methods). b. CuBAR_f was formed by stirring CuCl and NaBAR_f in THF at room temperature for 2 h.¹³

ee's were poor in all cases. We found that these poor results were also observed in our control (entry 1), indicating that the reason for these results could be a small change in the set-up of this screen. It was noted that the pre-stir (Cu source, combined with **L38** and CsOAc in THF), was significantly longer in this case, about 45 min, while in the previous screens, the set-up was typically about 20 min. One particular explanation could be that in this longer pre-stir, salt metathesis was occurring between the different Cu salts and CsOAc. In fact, one salt tested, CuBAr_f (entry 5), was synthesized by a salt metathesis method, combining NaBAr_f and CuCl in THF at room temperature, and allowing the mixture to stir for 2 h.¹³ Given that the Cs⁺ counter-ion is significantly less coordinating than Na⁺, we envisioned that in the case of the CsOAc salt the counter-ion exchange would likely be much more facile and rapid. Notably, CuOAc (entry 8) resulted in very low yields and ee's. Interestingly, Cu salts possessing less coordinating counter-ions (entries 1, 9, and 10) resulted in ee's very close in range to those observed with Cu(OAc).

Taking these observations into account, we next removed the CsOAc from the Cu/**L38** pre-stir (Table 3.3.5). Initially, set-up **A** (entry 1) was being used, resulting in a range of 16-45% yield and 9-62% ee for the product. Upon switching to set-up **B**, which was identical to **A** except that CsOAc was not included in the pre-stir, but was added just prior to the addition of **41**, the product was obtained in 72% yield and 24% ee (entry 2). Switching to set-up **C**, in which **41** was added before the CsOAc, did not lead to any significant improvements in ee, and led to a drop in yield (entry 3). Set-up **D**, in which the CsOAc and **41** were combined in THF and then added to the Cu complex, led to significant drops in both yield and ee (entry 4). To examine the consistency

of set-up **B**, we repeated this same reaction two more times (entries 5 and 6). For the three separate reactions, the yields were within 6% and the ee's within 4% (entries 2, 5, and 6).

Table 3.3.5. Importance of Timing of Addition of CsOAc^a

			
entry	set-up	yield (%)	ee (%)
1 ^b	A	16–45	9–62
2	B	72	24
3	C	57	20
4	D	19	< 5
5	B	70	28
6	B	76	28

Reaction Set-up:

A. Cu, **L38**, and CsOAc was combined in THF, stirred for 20–40 min, then the **41** was added, the reaction was stirred for 10 min, then **43a** was added, and the reaction was allowed to stir overnight.

B. Identical to **A**, but CsOAc was not included in the pre-stir, and was added just prior to the addition of **41**.

C. Identical to **B**, but CsOAc was added after the addition of **41**.

D. Identical to **B**, but **41** and CsOAc were added together.

[a] Reactions were run on 0.1 mmol scale. Yields were determined by ¹HNMR using trimethoxybenzene as an internal standard. Enantiomeric excess (ee) was determined by supercritical fluid chromatography. See Materials and Methods section for details on each reaction set-up. [b] Range is given for 6 different reactions that were set up identically but at different times. See Materials and Methods for description of each set-up.

Concurrent to these experiments, we were also examining other aspects of the reaction that could lead to inconsistent results, such as the amount of silyl ketene acetal **41** added. One particular concern that we had was that because the final product possessed a potentially epimerizable tertiary center, if at any point in the reaction a free lactone enolate was formed, this could deprotonate and racemize the stereocenter. For this reason, we anticipated that using only

the bare minimum amount of silyl ketene acetal **41** and CsOAc could potentially lead to improved and consistent results. Using both set-up **A** and set-up **B**, we examined how altering the equivalents of the silyl ketene acetal would change the reaction outcome (Table 3.4.6). We noted that within both set-up **A** and set-up **B**, lowering or increasing the equivalents of silyl ketene acetal **41** did not result in a significant change in yield (for set up **A**, entries 1-3, for set-up **B**, entries 4-6). However, with set-up **A**, we noted that increasing the equivalents of **41** did have a significant effect on the ee; with 1.5 equiv, the ee is 32% (entry 1), but when 2 equivalents are used, the ee drops significantly to 12 %. In contrast, we found that when set-up **B** is used, the ee is not so significantly affected by the amount of nucleophile added (entries 4-6). Furthermore, besides improving the consistency and reducing the sensitivity of the reaction to equivalents of **41**, the use of set-up **B** also enabled us to lower the amount of silyl ketene acetal used, as the reaction outcome with 1.5 equivalents was identical to when 2 equivalents are used.

Table 3.3.6. Equivalents of Silyl Ketene Acetal **41**^a

43a
1 equiv

41

44a

+

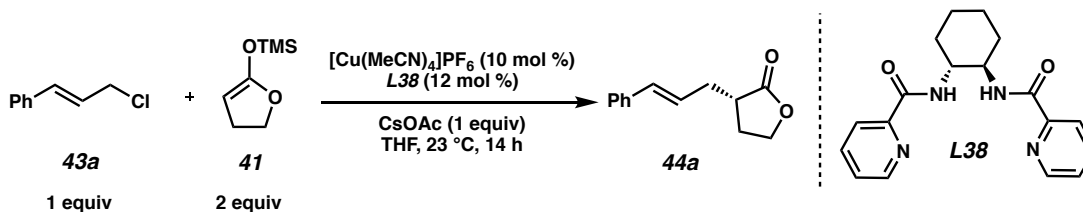
L38

entry	set-up	equiv of 41	yield (%)	ee (%)
1	A	1.5	24	32
2	A	2.0	22	24
3	A	2.5	18	12
4	B	1.5	78	24
5	B	2.0	67	22
6	B	2.5	73	22

[a] Reactions were run on 0.1 mmol scale. Yields were determined by ¹HNMR using trimethoxybenzene as an internal standard. Enantiomeric excess (ee) was determined by supercritical fluid chromatography. Using Set-up **A** and **B** (See Materials and Methods).

Although encouraged by the consistency observed with set-up **B**, the difference between the yield and ee obtained with this set up and our initial hit (45% yield and 65% ee, Table 3.3.3) indicated that we still did not have a full picture of what was occurring in the pre-stir. An additional part of the reaction set-up we chose to investigate was the time difference between the addition of **41** and **43a** (Table 3.3.7). Because we were first adding silyl ketene acetal **41** to all the reactions in the screen, then adding cinnamyl chloride **43a**, the time difference between these two additions was highly dependent on the size of the screen. For small screens this could be around 5 minutes, but for larger screens the time difference between the two additions could be 20 minutes or more. To probe this, we examined the reaction outcome at 0, 5, 15, and 30 minute time differences between the addition of the two substrates. If the two substrates are added together or within 5 minutes of each other, the reaction outcome is very similar, with yields over 70% and over 20% ee (entries 1 and 2. It should be noted that these results were very similar to those obtained in set-up **B** in Table 3.4.5). If **41** is added and the reaction is allowed to stir for 15 min before the addition

Table 3.3.7. Time Difference Between the Addition of **41** and **43a** Using Set-Up **B**^a

				
entry	time difference between addition of 41 and 43a	yield (%)	ee (%)	
1	0 min	79	20	
2	5 min	74	22	
3	15 min	33	30	
4	30 min	23	6	

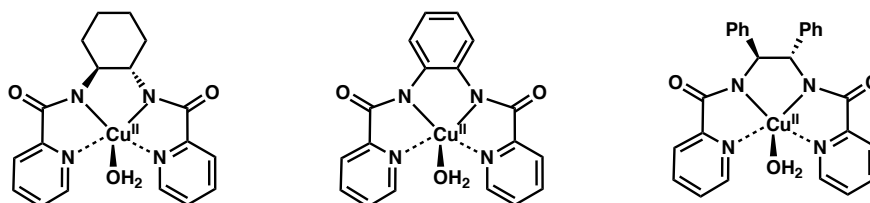
[a] Reactions were run on 0.1 mmol scale. Yields were determined by ¹HNMR using trimethoxybenzene as an internal standard. Enantiomeric excess (ee) was determined by supercritical fluid chromatography. Using Set-up **B** (See Materials and Methods).

of **43a**, the yield drops significantly, down to 33%. However, this is accompanied by a slight boost in ee to 30%. If the reaction is allowed to stir for 30 minutes before the addition of **43a**, the yield and ee both drop significantly (these results look very similar to those obtained in Table 3.3.4, entry 1). These results clearly indicate that the CsOAc and **41** are modifying the catalyst.

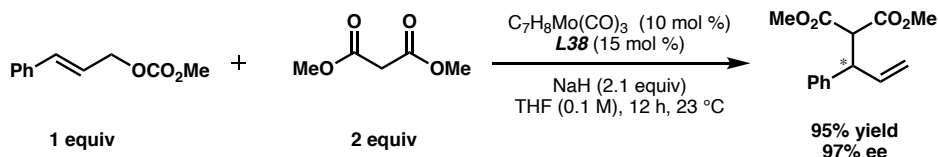
Having identified an additional component to the variability in reaction outcome, we next turned to the literature in order to gain a deeper understanding of what could be occurring. Although at the time the use of Cu/bis-picolinamide complexes in enantioselective catalysis remained unprecedented, there were a handful of reports on the crystal structures of Cu/**L21** and other related Cu/bis-picolinamide complexes by Vagg and coworkers (Figure 3.3.1.A).¹⁴ By combining Cu(OAc)₂ with different bis-picolinamide ligands in hot EtOH, they were able to generate Cu complexes bound to the ligand in a tetradentate fashion, with a water ligand at the apical position. Notably, the amide nitrogens were deprotonated, presumably by the ⁻OAc counterions.

Figure 3.3.1. Precedent for Cu/Bis-Picolinamide Complexes and the Use of **L38** in Enantioselective Allylic Alkylations^{14, 15}

A. Vagg, 1980–1991:



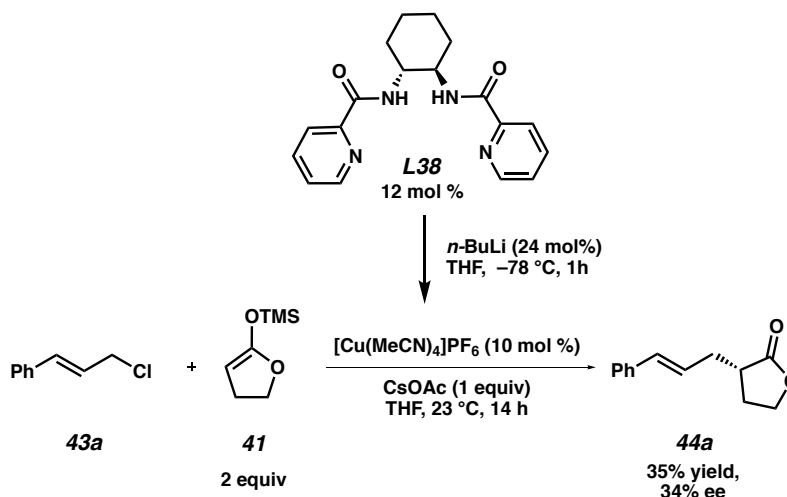
B. Trost, 1998–2002:



The use of **L38** in enantioselective catalysis had also been reported by Trost and coworkers (Figure 3.3.1.B).¹⁵ This ligand, in combination with Mo, proved to be optimal for enantioselective allylic alkylations with β -ketoesters. In agreement with Vagg and coworkers, they also found that the ligand was deprotonated over the course of the reaction, likely by the NaH base that was required to generate the corresponding β -ketoester nucleophile.

Inspired by these two reports, we decided to probe whether or not the ligand in our active Cu complex was deprotonated. The base we chose was *n*-BuLi, as it could be titrated, diluted, and the byproduct *n*-butane does not interact with the substrates or catalyst during the reaction. The ligand was fully deprotonated with 24 mol% *n*-BuLi at $-78\text{ }^{\circ}\text{C}$, and the cold solution of deprotonated ligand was added to a vial containing the Cu salt (Figure 3.3.2), the cold mixture was allowed to warm to room temperature over 45 min, and the rest of the reaction was then set up according to set-up **B**. With these conditions, we obtained the product in 36% yield and 34% ee. Interestingly, these results were very similar to the results obtained in entry 3, Table 3.3.7.

Figure 3.3.2. Deprotonation of **L38** with *n*-BuLi (Set-up **E**)^a



[a] Reactions were run on 0.1 mmol scale. Yields were determined by ^1H NMR using trimethoxybenzene as an internal standard. Enantiomeric excess (ee) was determined by supercritical fluid chromatography. [b] Using Set-up **E** (See Materials and Methods).

To further test if the changes in reaction outcome as a function of the time difference between the two additions could be attributed to the slow deprotonation of the ligand, we chose to set up an identical screen to the one described in Table 3.3.7, but this time with deprotonated ligand (Table 3.3.8). We found that although the reaction outcome was still not fully consistent, the results obtained were now within a smaller range. For the first trial, the results for 0-15 min differences (entries 1-3) between the two additions was only 8% and the ee's were within 3%. We believe that at a 30 min time difference between the two additions (entry 4), significant decomposition of the starting material is occurring, and for this reason the results obtained for this time point were discarded from the analysis. This improved consistency within the screen was extremely important, as it was an indication that some of the disparity in reaction outcome could be attributed to the slow deprotonation of the ligand over the course of the pre-stir.

To determine whether there was improved consistency across different screens, we set up this same set of experiments two more times. We found that the yields for the reaction at a set time point across different screens differed by about 12% in yield, and 20% ee (for entries 1-3). Most importantly, however, we found that for the first time we were able to reproduce our initial hit of 45% yield and 60% ee (entry 2, trial 2). Although this new set-up was not delivering fully consistent results, this last amount of irreproducibility we attributed to the ligand itself; **L38** is highly flexible, and possesses 6 coordinating atoms. For this reason, Cu could likely bind to **L38** in a number of different ways, leading to a distribution of different Cu/**L38** complexes in solution. We hypothesized that even the smallest change in reaction set-up could lead to very significant changes in this distribution, and as a result, in the reaction outcome. Because the maximum ee achieved with **L38** is only 64% (entries 1 and 3, Table 3.4.8), it was clear that we would have to

improve the ee through ligand synthesis and design. For this reason, we chose to move forward with the set-up described in entry 2 of Table 3.4.8, and start synthesizing and testing new ligand derivatives, with a keen eye toward the development of a ligand that would result in a more consistent Cu/ligand complex.

3.4 CHIRAL LIGAND IDENTIFICATION

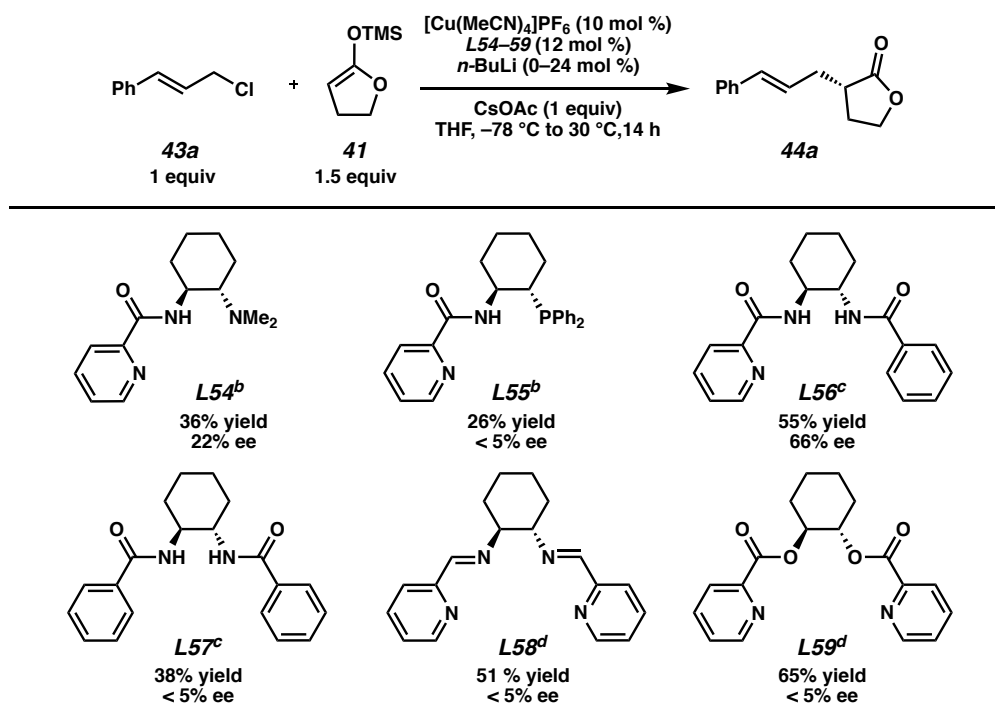
Table 3.3.8. Timing of the Addition of **43a** With Set-Up **E**^a

Reaction scheme showing the synthesis of **44a** from **43a** and **41**. Reagents: $[\text{Cu}(\text{MeCN})_4]\text{PF}_6$ (10 mol %), **L38** (12 mol %), $n\text{-BuLi}$ (24 mol %), CsOAc (1 equiv), THF , $-78\text{ }^\circ\text{C}$ to $30\text{ }^\circ\text{C}$, 14 h. The structure of **L38** is shown as a bis-picolinyl ligand with a cyclohexyl backbone.

entry	time difference between addition of 41 and 43a	yield (%)	ee (%)
		trial: 1 / 2 / 3	trial: 1 / 2 / 3
1	0 min	27 / 38 / 33	42 / 64 / 40
2	5 min	35 / 45 / 37	45 / 60 / 40
3	15 min	35 / 45 / 28	45 / 64 / 50
4	30 min	25 / 24 / 35	16 / 72 / 40

[a] Reactions were run on 0.1 mmol scale. Yields were determined by ¹HNMR using trimethoxybenzene as an internal standard. Enantiomeric excess (ee) was determined by supercritical fluid chromatography. Using Set-up **E** (See Materials and Methods). This same set of experiments was run 3 separate times, the results for each screen is separate by dashes (/).

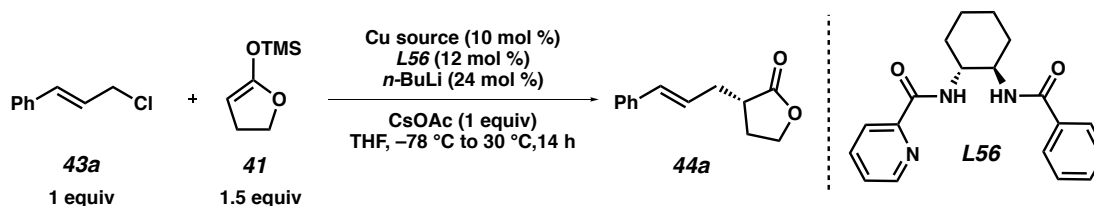
Moving forward, one of the first things we wanted to assess was whether the bis-picolinyl moiety was critical for reactivity and selectivity. To this end, we synthesized a number of different derivatives that retained the cyclohexyl backbone, but varied in their coordinating atoms (Table

Table 3.4.1. Importance of Picolinyl Moieties^a

[a] Reactions were run on 0.1 mmol scale. Yields were determined by ¹HNMR using trimethoxybenzene as an internal standard. Enantiomeric excess (ee) was determined by supercritical fluid chromatography. Using Set-up **E** (See Materials and Methods). [b] With 12 mol% *n*BuLi. [c] With 24 mol% *n*BuLi. [d] No *n*-BuLi added.

3.4.1). When mono-picolinyl ligands possessing an adjacent amine (**L54**) or phosphine (**L55**) group are used, both the yields and ee's are reduced significantly. Interestingly, benzamide ligand **L56** performed just as well, and if not slightly better, than **L38**. The use of bis-benzamide ligand **L57**, Schiff base ligand **L58**, and ester ligand **L59** all resulted in racemic product, indicating that at least one picolinamide moiety is critical for ee.

In order to determine whether ligand **L56** performs better and is more consistent than **L38**, we repeated this reaction a second time, and although the yields are fairly similar, the ee's are still only within 13% of each other (Table 3.4.2, entries 1 and 2). Upon examination of additional Cu sources, we found that with CuCl₂ and **L56**, the product is obtained in a range of 40–48% yield

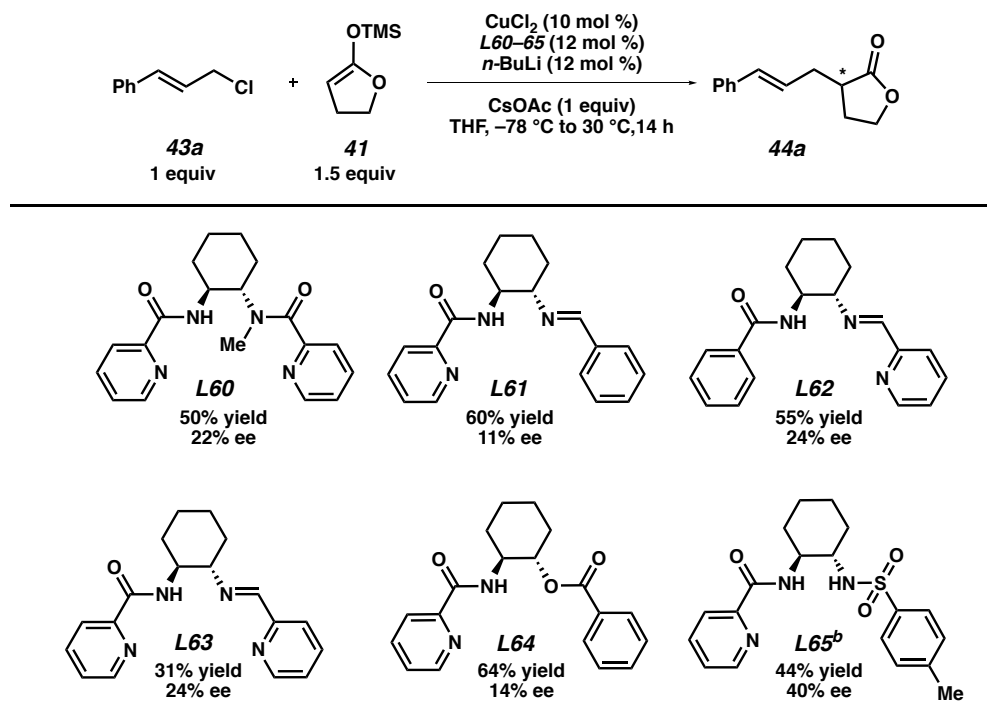
Table 3.4.2. Cu source screen with **L56**^a

entry	Cu source	yield (%)	ee (%)
1	[Cu(MeCN) ₄]PF ₆	55	66
2	[Cu(MeCN) ₄]PF ₆	51	53
3	CuCl	38	36
4	Cu(OTf) ₂	32	20
5	Cu(O <i>t</i> Bu) ₂	47	< 5
6	CuCl ₂	48	62
7	CuCl ₂	45	64
8	CuCl ₂	40	60

[a] Reactions were run on 0.1 mmol scale. Yields were determined by ¹H NMR using trimethoxybenzene as an internal standard. Enantiomeric excess (ee) was determined by supercritical fluid chromatography. Using Set-up E and F (See Materials and Methods).

and 60–64% ee for three reactions (entries 6–8), indicating that with this Cu source and ligand combination, the reaction was finally reproducible.

Having identified the last reaction component that contributed to the irreproducibility, we now turned our attention to the ee. Although **L56** resulted in the highest ee yet, we wanted to ensure that the benzamide moiety was critical for both reactivity and selectivity. To this end, we synthesized a number of ligands possessing slightly modified coordinating groups (Table 3.4.3). We found that with mono-methylated ligand **L60**, we observed a significant drop in ee compared to **L39**. In addition, we tested ligands bearing a mono-imine (**L61**, **L62**, **L63**), an ester moiety (**L64**) and a sulfonamide (**L65**). The anionic benzamide appears to be especially important for stereocontrol, as removing this moiety led to a drastic decrease in ee (**L61**, **L62**, **L63**, **L64**). In comparison, anionic sulfonamide-containing **L65** performed most similarly to **L56**.

Table 3.4.3. Ligand Screen^a

[a] Reactions were run on 0.1 mmol scale. Yields were determined by ^1H NMR using trimethoxybenzene as an internal standard. Enantiomeric excess (ee) was determined by supercritical fluid chromatography. Using Set-up **F** (See Materials and Methods).

Having confirmed that the benzamide functional group was critical for ee, we next turned our attention to how altering the organic substituents on the ligand affected ee. To this end, we synthesized a number of derivatives with varying functional groups on the amide portion of the ligand. Generally, we found that the identity of the organic substituent on the amide did have an effect on the yield, but not as significant an effect on ee. The reaction outcome seemed to be insensitive to the electronics of the functional group at the position *para*- to the amide (**L66** and **L70**, Table 3.4.4), with both electron-donating and withdrawing substituents leading to a similar drop in ee. Alkyl substituents at the *meta*-position led to a significant drop in reactivity, although interestingly, the level of ee was retained with **L68** but not **L69**. In a similar vein, we found that 3-naphthylamide (**L71**) led to a more significant drop in reactivity and selectivity than did the ortho

bridge prevents ring-flipping which is commonly observed in cyclohexyl moieties), and also more bulky. The first time that **L50** was tested was during our initial bis-picolinamide screen (Table 3.3.3). With our initial conditions, with $[\text{Cu}(\text{MeCN})_4]\text{PF}_6$ and **L50**, the product is obtained in 26% yield and 46% ee (entry 1). Upon switching to set-up **F**, the product is now obtained in a 75% yield and 94% ee (entry 2). However, the second time this reaction was performed, the product was obtained in only 55% ee. Having already identified that the bis-picolinyl ligands could be detrimental to the reaction consistency, we rapidly synthesized the mono-picolinyl ligand **L73**. When this ligand is used in set-up **F**, the high yield and ee is restored (entry 4). One of the drawbacks of set-up **F** is that cryogenic temperatures were required for the ligand deprotonation step. Gratifyingly, we found that by switching to LiHMDS, the deprotonation could be carried out in the glovebox at room temperature (entry 5). With this new set-up **G**, we found that the reaction

Table 3.4.5. ANDEN Backbone^a

entry	ligand	set-up	base (mol%)	temp (°C)	yield (%)	ee (%)
1 ^b	L50	A	none	23	26	46
2	L50	F	<i>n</i> -BuLi (24)	−78 to 30	75	94
3	L50	F	<i>n</i> -BuLi (24)	−78 to 30	—	55
4	L73	F	<i>n</i> -BuLi (24)	−78 to 30	90	90
5	L73	G	LiHMDS (26)	23 to 30	94	92
6	L73	G	LiHMDS (26)	23 to 30	92	92

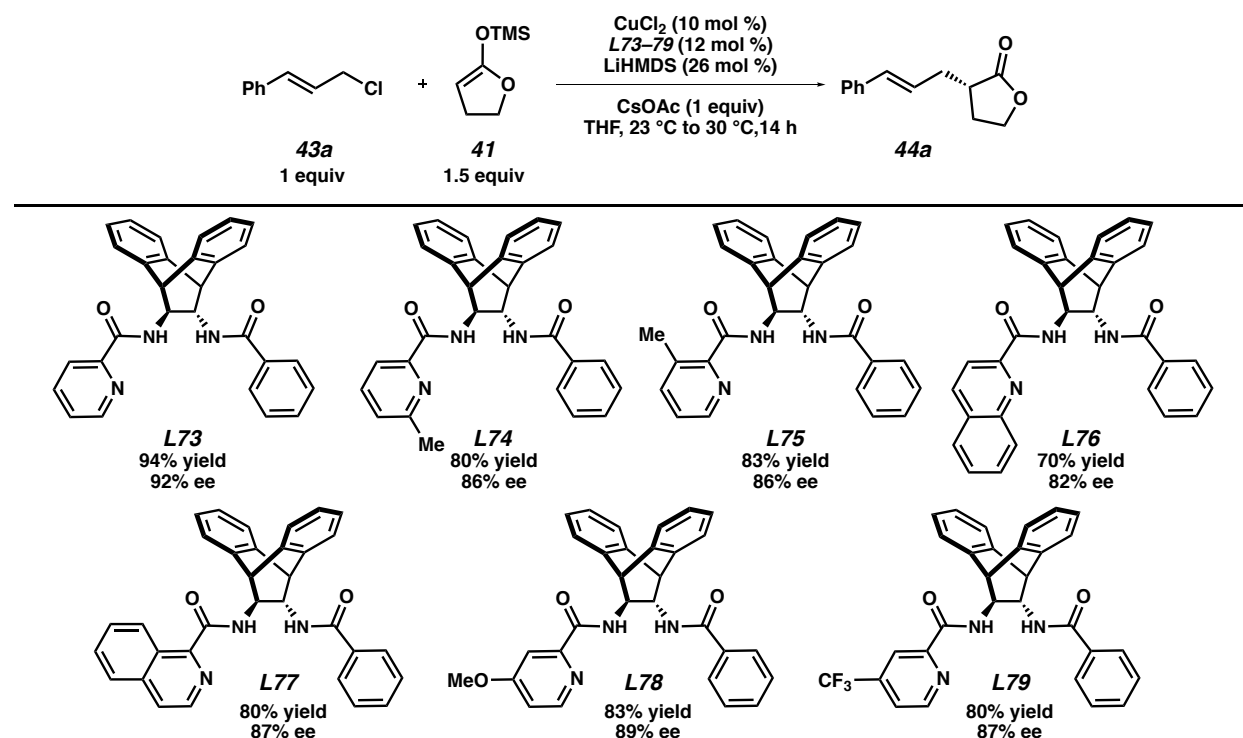
L50	L73

a. Reactions were run on 0.1 mmol scale. Yields were determined by ¹HNMR using trimethoxybenzene as an internal standard. Enantiomeric excess (ee) was determined by supercritical fluid chromatography. See Materials and Methods section for reaction set-up (**A**, **F**, or **G**). b. $[\text{Cu}(\text{MeCN})_4]\text{PF}_6$ was used instead of CuCl_2 .

outcome is consistent, allowing for the formation of the desired product in consistently high yields and ee.

Having identified the appropriate backbone, the final portion of the ligand that we wanted to modify was the pyridine ring. To this end, we synthesized a number of ligand derivatives with varying substitution around the pyridine ring (Table 3.4.6). Incorporating a methyl substituent at the 3- or 6- position of the picolinamide (**L74** and **L75**) both led to slight drops in yield and ee. Interestingly, both **L74** and **L75** seemed to have a very similar effect on the reaction outcome, leading to similar yields and identical ee's. We also tested quinoline (**L76**) and isoquinoline (**L77**) ligand derivatives. In both cases, we noted a drop in yield and ee relative to **L73**, however, it was more pronounced in the case of the quinoline derivative (**L76**). Finally, we found that incorporating electron-donating or withdrawing groups at the 4-position of the pyridine was

Table 3.4.6. Modification of the Picolinamide^a



[a] Reactions were run on 0.1 mmol scale. Yields were determined by ^1H NMR using trimethoxybenzene as an internal standard. Enantiomeric excess (ee) was determined by supercritical fluid chromatography. Using Set-up **G** (See Materials and Methods).

detrimental (**L78** and **L79**). Interestingly, the results for both of these ligands were very similar, indicating that the drop in reactivity and selectivity may be due to sterics rather than electronics.

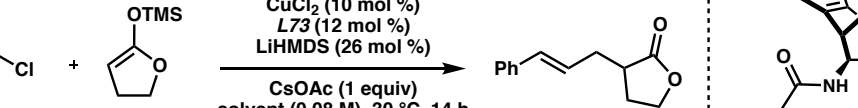
In summary, we identified that the coordinating atoms required for high ee was a picolinyl and a benzamide moiety. We also noted that by far the portion of the ligand that had the greatest effect on the reaction outcome was the backbone. Modifying the substituents at the benzamide or picolinyl moiety had a small effect, and the yields and ee's deviated very minimally from those obtained with the parent ligands **L56** or **L73**. Generally, we found that the substitution around the benzamide had a more significant effect on the yield rather than the ee, and incorporating substitution around the picolinyl moiety led to very slight drops in both yield and ee. Taking these observations into account, it became clear that the optimal ligand for our transformation was **L73**.

3.5 FINAL REACTION OPTIMIZATION

Having finally identified the appropriate ligand for this transformation, we next turned our attention to examining the last few reaction parameters, including solvent, catalyst loading, concentration, Cu source, and the bases used.

We first examined a number of solvents, including both ethereal and non-ethereal solvents (Table 3.5.1). Interestingly, we found that polar solvents were critical for reactivity, as toluene (entry 4) and MTBE (entry 5) led to very low reactivity. We also noted that ethereal solvents such as THF (entry 1) and diethyl ether (entry 3) resulted in the highest ee's, and polar, non-ethereal methylene chloride (entry 2) resulted in a moderate yield, but low ee. These results indicated that THF (entry 1) continued to be the best option.

Table 3.5.1. Solvent Screen^a



Reaction scheme showing the synthesis of **44a** from **43a** and **41** using **CuCl₂** (10 mol %), **L73** (12 mol %), **LiHMDS** (26 mol %), **CsOAc** (1 equiv), solvent (0.08 M), 30 °C, 14 h.

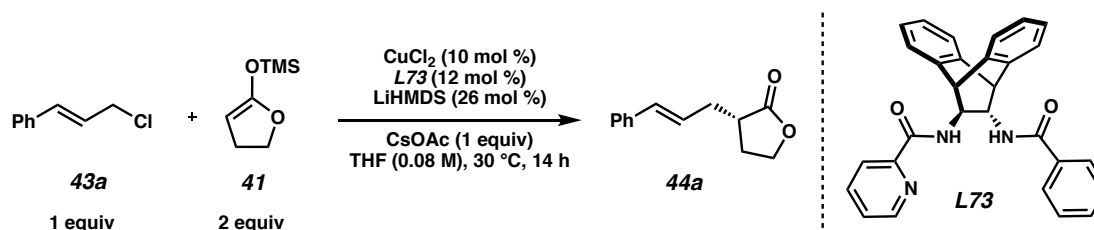
Structure of **L73** is shown on the right.

entry	solvent	conversion (%)	yield (%)	ee (%)
1	THF	100	90	92
2	CH ₂ Cl ₂	66	49	38
3	Et ₂ O	28	20	74
4	toluene	20	7	–
5	MTBE	52	< 5	–

[A] Conditions: Using Set-up **G** (See Materials and Methods). The THF was removed via vacuum, and the resulting solid was re-suspended in the appropriate solvent. Reactions were run on 0.1 mmol scale. Yields were determined by ¹HNMR using trimethoxybenzene as an internal standard. Enantiomeric excess (ee) was determined by supercritical fluid chromatography.

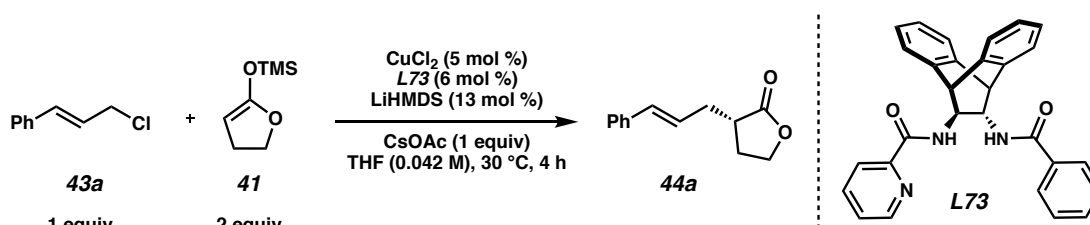
Next, we examined the catalyst loading and concentration (Table 3.5.2). Gratifyingly, we noted that we were able to lower the catalyst loading down to 5 mol% CuCl₂, 6 mol% **L73**, and 13 mol% LiHMDS without observing any drops in reactivity or selectivity (entry 2). However, lowering the catalyst loading even further to 2.5 mol% Cu, 3 mol% **L73**, and 6.5 mol% LiHMDS, was detrimental to the reaction outcome (entry 3). Gratifyingly, we found that the reaction is done in only 6 hours (entry 4), and by lowering the concentration to 0.042 M, the product is obtained in 90% yield and 94% ee (entry 5). The use of anhydrous and oxygen-free conditions were necessary for achieving high reactivity and selectivity, as running the reaction under air led to significant drops in both yield and ee (entry 6).

Table 3.5.2. Catalyst Loading and Concentration^a

				
entry	conditions	yield (%)	ee (%)	
1	no change	94	92	
2	5 mol % CuCl ₂ , 6 mol% L73 , 13 mol % LiHMDS	92	92	
3	2.5 mol % CuCl ₂ , 3 mol% L73 , 6.5 mol% LiHMDS	78	83	
4	5 mol % CuCl ₂ , 6 mol% L73 , 13 mol % LiHMDS, after 6 h	90	92	
5	5 mol % CuCl ₂ , 6 mol% L73 , 13 mol % LiHMDS, after 6 h, 0.042 M	90	94	
6	open to air	32	80	

[a]. Reactions were run on 0.1 mmol scale. Yields were determined by ¹HNMR using trimethoxybenzene as an internal standard. Enantiomeric excess (ee) was determined by supercritical fluid chromatography. Using Set-up **G** (See Materials and Methods).

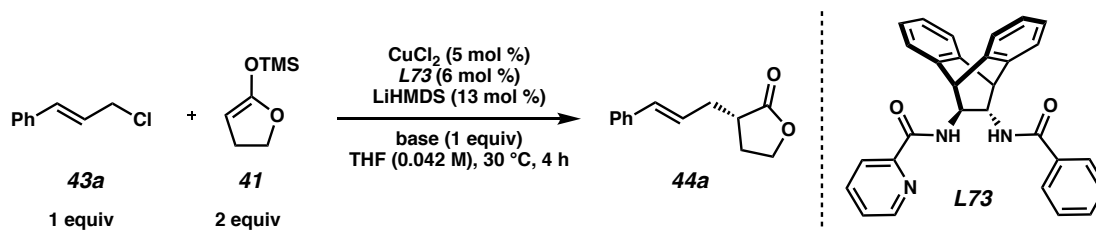
Having identified the appropriate catalyst loading, concentration, and reaction time, we turned our attention to the Cu source, as there were a number of Cu sources that we wanted to re-examine with these final conditions (Table 3.5.3). Interestingly, we found that CuBr₂ (entry 1), Cu(OTf)₂ (entry 2), and Cu(OTf)₂•toluene (entry 5) all led to very similar ee's to those obtained with CuCl₂ (Table 3.5.2, entry 5). Other Cu(I) sources tested, including CuBr (entry 3), CuCN (entry 4), and [Cu(MeCN)₄]PF₆ (entry 6), led to significant drops in reactivity and ee.

Table 3.5.3. Cu Salt Screen^a


entry	Cu source	conversion (%)	yield (%)	ee (%)
1	CuBr ₂	80	73	89
2	Cu(OTf) ₂	94	89	92
3	CuBr	83	79	82
4	CuCN	51	34	45
5	Cu(OTf)·PhMe	65	67	90
6	[Cu(MeCN) ₄]PF ₆	45	42	84

[a]. Reactions were run on 0.1 mmol scale. Yields were determined by ¹HNMR using trimethoxybenzene as an internal standard. Enantiomeric excess (ee) was determined by supercritical fluid chromatography. Using Set-up **G** (See Materials and Methods).

Although a more comprehensive base screen was performed at the outset of this investigation, we chose to re-examine the effect of the base in our final conditions (Table 3.5.4). As in our previous investigations, we found that we do not observe any product when no base is used (entry 1). We also found that the nature of the counter-ion was crucial for reactivity, but not so much for selectivity; with the less soluble LiOAc base, the product is only obtained in 16% yield (entry 2), and with NaOAc (entry 3) or KOAc (entry 4), the product is obtained in moderate

Table 3.5.4. Base Screen^a


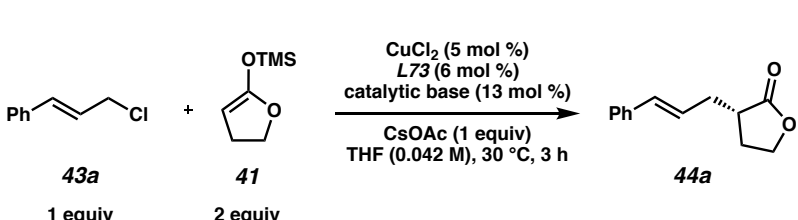
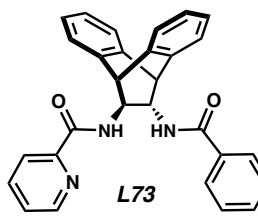
entry	base	conversion (%)	yield (%)	ee (%)
1	None	14	0	–
2	LiOAc	24	16	–
3	NaOAc	66	64	92
4	KOAc	67	66	89
5	CsF	100	30	–
6	Cs ₂ CO ₃	92	0	–

[a]. Reactions were run on 0.1 mmol scale. Yields were determined by ¹HNMR using trimethoxybenzene as an internal standard. Enantiomeric excess (ee) was determined by supercritical fluid chromatography. Using Set-up **G** (See Materials and Methods).

yields, but high ee. Interestingly, with CsF (entry 5), a salt traditionally used to cleave silyl enolates,¹⁷ no product is observed. With Cs₂CO₃, we did not observe any product formation (entry 6).

We also examined the counter-ion on the catalytic base used (Table 3.5.5), and found that with LiHMDS, we still obtain the highest ee's (entry 1). Interestingly, however, we noted that switching to NaHMDS or KHMDS did lead to a significantly faster reaction, and the starting material was fully consumed in under 3 hours (entries 2 and 3).

Table 3.5.5. Catalytic Base Screen^a

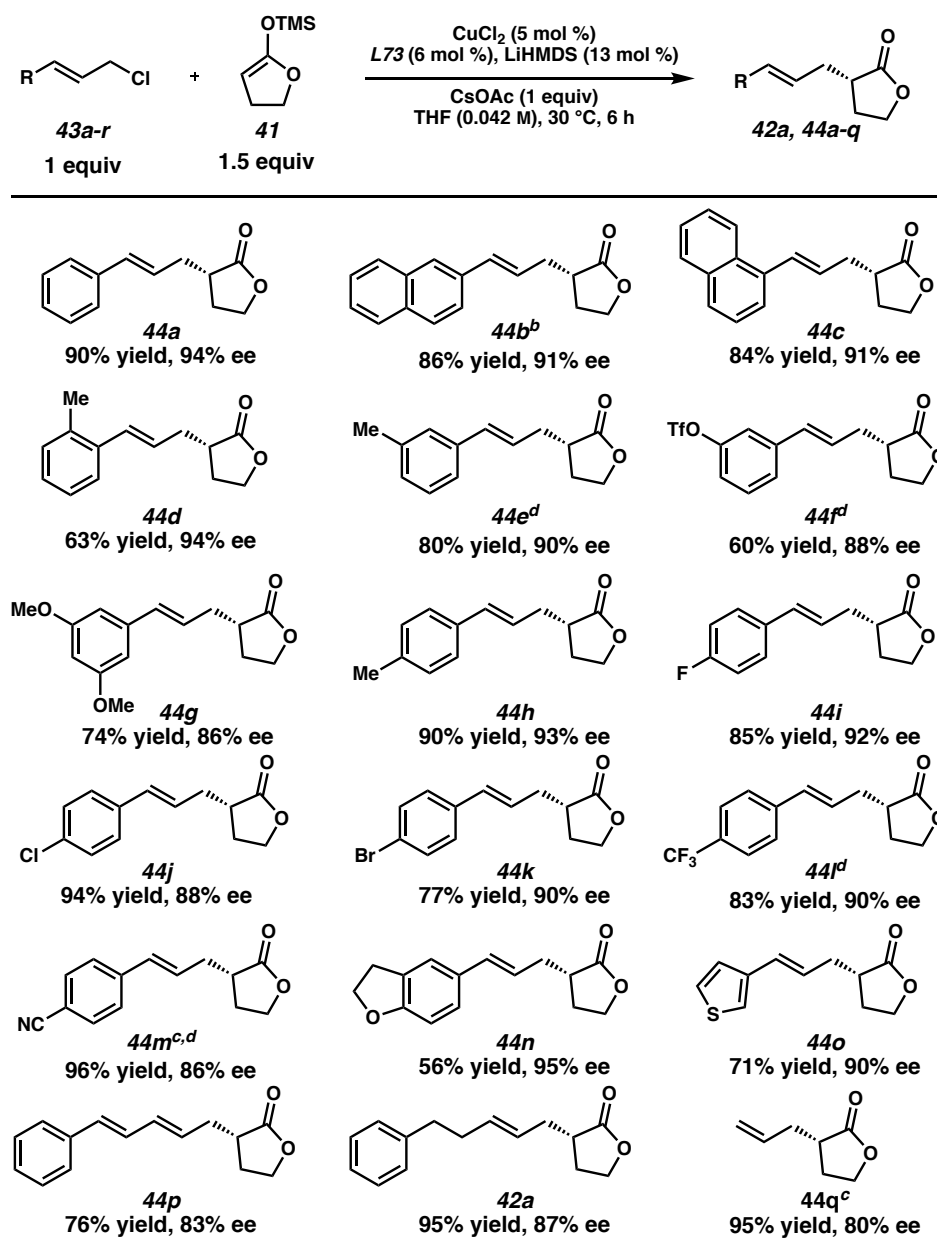
			
entry	catalytic base	yield (%)	ee (%)
1 ^b	LiHMDS	88	94
2	NaHMDS	94	87
3	KHMDS	95	85

[a] Reactions were run on 0.1 mmol scale. Yields were determined by ¹HNMR using trimethoxybenzene as an internal standard. Enantiomeric excess (ee) was determined by supercritical fluid chromatography. Using Set-up **G** (See Materials and Methods). [b] 6 hours instead

3.6 REACTION SCOPE

With optimized conditions in hand, we examined the scope of the electrophile (Table 3.6.1). We were pleased to find that 2-naphthyl **44c** and *ortho*-methylphenyl (**44d**) substituents were well tolerated. *Meta*-phenyl substituted electrophiles (**44b**, **44e**) also fared well, and even a

Table 3.6.1 Scope of the Allylic Chloride^a

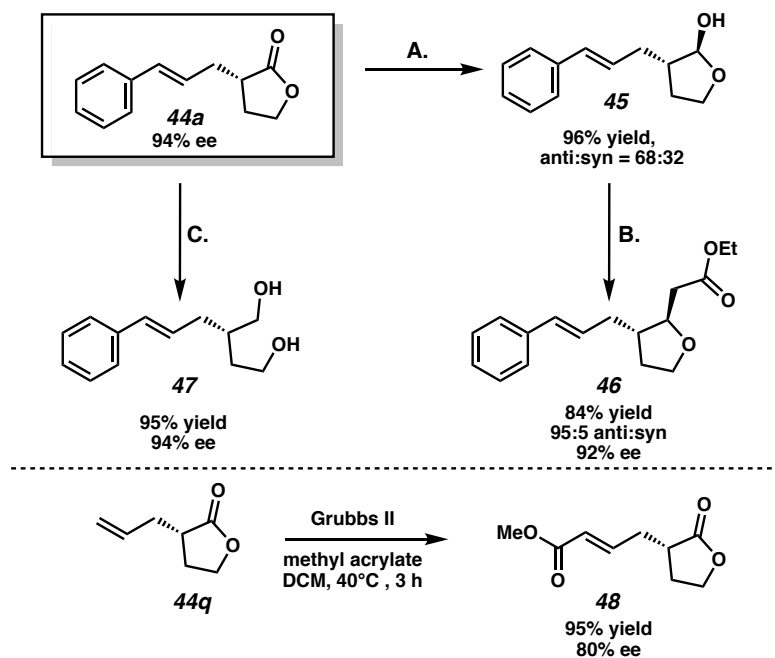


[a] See General Procedure in Materials and Methods section. Isolated yields on 0.2 mmol scale. SFC analysis was used to determine ee. [b] Absolute stereochemistry was determined by X-ray diffraction. [c] With 10 mol % CuCl_2 , 12 mol % **L73**, and 26 mol % LiHMDS. [d] Synthesized from a mixture of linear and branched allylic chlorides (see the Materials and Methods section for more details).

sensitive triflate (**44f**) and a bulky 3,5-dimethoxy phenyl group (**44g**) led to products in high yield and ee. Electrophiles possessing substituents at the *para*-phenyl position such as halogens (**44i**, **44j**, **44k**), a trifluoromethyl (**44l**), and a nitrile (**44m**) were also well-tolerated. Even heterocyclic compounds (**44n** and **44o**), a diene substrate (**44p**), an aliphatic allylic chloride (**42a**) and unsubstituted allyl chloride (**44q**) led to product formation in good yields and ee's.

3.7 DERIVATIZATION OF ALLYL γ -BUTYROLACTONE PRODUCTS

Scheme 3.7.1. Derivatization of **44a** and **44q**



A. DIBAL-H, CH_2Cl_2 , -78°C , 30 min. B. NaH, triethylphosphonoacetate, THF, 0°C to 23°C , 3 h. C. LiAlH_4 , Et_2O , reflux, 3 h.

In order to demonstrate the synthetic utility of these products, we subjected α -allyl γ -butyrolactone **44a** and **44q** to a number of transformations (Scheme 3.7.1). Lactone **44a** was

reduced to the corresponding lactol **45** using DIBAL-H. Lactol **45** was then converted to the unsaturated ester, which spontaneously cyclized to the corresponding tetrahydrofuran **46** in high yield and high diastereoselectivity. Lactone **44a** was also converted to the corresponding chiral diol **47** in good yields using lithium aluminum hydride. We also found that **44q** could be swiftly converted to the corresponding methyl acrylate species **48** via cross metathesis.

3.8 CONCLUSION

In conclusion, we have developed a Cu-catalyzed enantioselective allylic alkylation with a non-stabilized enolate-derived nucleophile. Critical to the development of this reaction was the identification of a set-up that resulted in a consistent reaction outcome and a novel monopicolinamide ligand that led to product formation in high yields (up to 96%) and ee (up to 95%). A number of electrophiles with a broad range of functionality were well-tolerated in this reaction, including aryl, heteroaryl, and aliphatic allylic chlorides. Future work will focus on gaining a deeper understanding of the reaction mechanism and expanding the scope of this reaction to include other enolate derived nucleophiles.

3.9 EXPERIMENTAL SECTION

3.9.1 MATERIALS AND METHODS

Unless otherwise stated, reactions were performed in flame-dried glassware under an argon or nitrogen atmosphere using dry, deoxygenated solvents. Solvents were dried by passage through an activated alumina column under argon. Reaction progress was monitored by thin-layer chromatography (TLC) or Agilent 1290 UHPLC-MS. TLC was performed using E. Merck silica gel 60 F254 precoated glass plates (0.25 mm) and visualized by UV fluorescence quenching, *p*-anisaldehyde, or KMnO_4 staining. ((4,5-dihydrofuran-2-yl)oxy)trimethylsilane (**41**) was synthesized according to a previously reported procedure.¹⁸ Silicycle SiliaFlash® P60 Academic Silica gel (particle size 40–63 nm) was used for flash chromatography. ^1H NMR spectra were recorded on a Bruker Avance HD 400 MHz or Varian Mercury 300 MHz spectrometers and are reported relative to residual CHCl_3 (δ 7.26 ppm). ^{13}C NMR spectra were recorded on a Bruker Avance HD 400 MHz spectrometer (101 MHz) and are reported relative to residual CHCl_3 (δ 77.16 ppm). ^{19}F NMR spectra were recorded on a Varian Mercury 300 MHz spectrometer (282 MHz). Data for ^1H NMR are reported as follows: chemical shift (δ ppm) (multiplicity, coupling constant (Hz), integration). Multiplicities are reported as follows: s = singlet, d = doublet, t = triplet, q = quartet, p = pentet, sept = septuplet, m = multiplet, br s = broad singlet, br d = broad doublet, app = apparent. Data for ^{13}C NMR are reported in terms of chemical shifts (δ ppm). IR spectra were obtained using a Perkin Elmer Spectrum BXII spectrometer or Nicolet 6700 FTIR spectrometer using thin films deposited on NaCl plates and reported in frequency of absorption (cm^{-1}). Optical rotations were measured with a Jasco P-2000 polarimeter operating on the sodium D-line (589 nm), using a 100 mm path-length cell and are reported as: $[\alpha]_{\text{D}}^{\text{T}}$ (concentration in 10 mg/1 mL, solvent). Analytical SFC was performed with a Mettler SFC supercritical CO_2 analytical chromatography system utilizing Chiralpak (AD-H, AS-H or IC) or Chiralcel (OD-H, OJ-H, or

OB-H) columns (4.6 mm x 25 cm) obtained from Daicel Chemical Industries, Ltd. High resolution mass spectra (HRMS) were obtained from Agilent 6200 Series TOF with an Agilent G1978A Multimode source in electrospray ionization (ESI+), atmospheric pressure chemical ionization (APCI+), or mixed ionization mode (MM: ESI-APCI+), or obtained from Caltech Mass Spectrometry Laboratory. X-Band (9.4 GHz) Continuous-wave(CW) EPR spectra were obtained using a Bruker EMX spectrometer with its Bruker Win-EPR software (version 3.0). A vacuum-insulated quartz liquid nitrogen dewar was inserted into the EPR resonator to obtain all spectra at 77 K. For optimal sensitivity, all spectra were collected with 0.5 mW microwave power and averaged over four scans. UV-Vis-NIR spectra were acquired using Varian Cary 500 Scan spectrophotometer with Varian Cary WinUV software (version 4.10 (464)). Samples were loaded into 1 cm Starna Cell borosilicate cuvettes enclosed with screw caps. The spectra were collected from 300 nm to 1650 nm at a 600 nm/min scan rate and corrected for THF background. IR spectra were collected using a Bruker Alpha Platinum ATR spectrometer with OPUS software (version 7.0.129) stored in a glovebox under N₂. An aliquot of sample solution was deposited onto the spectrometer to form a thin film, and the spectra were collected over 32 scans.

Reagents were purchased from Sigma-Aldrich, Acros Organics, Strem, or Alfa Aesar and used as received unless otherwise stated.

List of Abbreviations

ee – enantiomeric excess, SFC – supercritical fluid chromatography, TLC – thin-layer chromatography, IPA – isopropanol, MTBE – methyl *tert*-butyl ether, PE – petroleum ether,

DMAP – 4-dimethylaminopyridine, EtOAc – ethyl acetate, LiHMDS – lithium bis(trimethylsilyl)amide, NaHMDS – sodium bis(trimethylsilyl)amide, KHMDS – potassium bis(trimethylsilyl)amide, THF – tetrahydrofuran, TMEDA – 1,2-tetramethylethylenediamine.

3.9.2 EXPERIMENTAL PROCEDURES AND SPECTROSCOPIC DATA

3.9.2.1 Procedures for the Evaluation of Commercially Available Ligands and Synthesized Picolinamide Ligands

Method A:

n = the number of reactions in the screen. In the glovebox, $[\text{Cu}(\text{MeCN})_4]\text{PF}_6$ (2.33n mg, 0.00625n mmol, 0.1 equiv), THF (0.6n mL), and a stir bar were added to a 4-mL vial A. The solution was stirred until the Cu had fully dissolved. In a separate 4-mL vial B was added the appropriate ligand (0.0075 mmol, 0.12 equiv), and Cs_2CO_3 (20 mg, 0.0625 mmol, 1.0 equiv) or CsOAc (19.2 mg, 0.1 mmol, 1 equiv) and a stir bar. The contents of vial A (0.6 mL) was then added to vial B, and allowed to stir for 20 min. ((4,5-dihydrofuran-2-yl)oxy)trimethylsilane (44 mg, 0.25 mmol, 2.0 equiv) was added to the vial, and the reaction was allowed to stir for 10 min. (*E*)-diethyl (5-phenylpent-2-en-1-yl) phosphate (18.65 mg, 0.0625 mmol, 1.0 equiv) was then added to the reaction, and the reaction was allowed to stir for 14 hours at room temperature. The reaction mixture was filtered through a short silica plug eluting with ethyl acetate (5 mL). The eluate was concentrated by rotary evaporator and dissolved in CD_2Cl_2 to determine ^1H NMR yield with

respect to 1,3,5-trimethoxybenzene. Then, the sample was concentrated and purified by preparative TLC (30% EtOAc/hexanes). The purified product was then dissolved in hexanes for SFC analysis on a Chiralcel AD column (12% IPA/hexanes, 2.5 mL/min).

Method B:

n = the number of reactions in the screen. In the glovebox, $[\text{Cu}(\text{MeCN})_4]\text{PF}_6$ (2.33n mg, 0.00625n mmol, 0.1 equiv), THF (0.6n mL), and a stir bar were added to a 4-mL vial A. The solution was stirred until the Cu had fully dissolved. In a separate 4-mL vial B was added bis-picolinamide **L38** (0.0075 mmol, 0.12 equiv). The contents of vial A (0.6 mL) was then added to vial B, and allowed to stir for 20 min. CsOAc (19.2 mg, 0.1 mmol, 1 equiv) was added, followed immediately by ((4,5-dihydrofuran-2-yl)oxy)trimethylsilane **41** (44 mg, 0.25 mmol, 2.0 equiv) and the reaction was allowed to stir for 10 min. Cinnamyl chloride **43a** (9.53 mg, 0.0625 mmol, 1.0 equiv) was then added to the reaction, and the reaction was allowed to stir for 14 hours at room temperature. The reaction mixture was filtered through a short silica plug eluting with ethyl acetate (5 mL). The eluate was concentrated by rotary evaporator and dissolved in CD_2Cl_2 to determine ^1H NMR yield with respect to 1,3,5-trimethoxybenzene. Then, the sample was concentrated and purified by preparative TLC (30% EtOAc/hexanes). The purified product was then dissolved in hexanes for SFC analysis on a Chiralcel AD column (12% IPA/hexanes, 2.5 mL/min).

Method C:

n = the number of reactions in the screen. In the glovebox, $[\text{Cu}(\text{MeCN})_4]\text{PF}_6$ (2.33n mg, 0.00625n mmol, 0.1 equiv), THF (0.6n mL), and a stir bar were added to a 4-mL vial A. The solution was

stirred until the Cu had fully dissolved. In a separate 4-mL vial B was added bis-picolinamide **L38** (0.0075 mmol, 0.12 equiv). The contents of vial A (0.6 mL) was then added to vial B, and allowed to stir for 20 min. ((4,5-dihydrofuran-2-yl)oxy)trimethylsilane **41** (44 mg, 0.25 mmol, 2.0 equiv) was added, followed immediately by CsOAc (19.2 mg, 0.1 mmol, 1 equiv) and the reaction was allowed to stir for 10 min. Cinnamyl chloride **43a** (9.53 mg, 0.0625 mmol, 1.0 equiv) was then added to the reaction, and the reaction was allowed to stir for 14 hours at room temperature. The reaction mixture was filtered through a short silica plug eluting with ethyl acetate (5 mL). The eluate was concentrated by rotary evaporator and dissolved in CD₂Cl₂ to determine ¹H NMR yield with respect to 1,3,5-trimethoxybenzene. Then, the sample was concentrated and purified by preparative TLC (30% EtOAc/hexanes). The purified product was then dissolved in hexanes for SFC analysis on a Chiralcel AD column (12% IPA/hexanes, 2.5 mL/min).

Method D:

n = the number of reactions in the screen. In the glovebox, [Cu(MeCN)₄]PF₆ (2.33n mg, 0.00625n mmol, 0.1 equiv), THF (0.6n mL), and a stir bar were added to a 4-mL vial A. The solution was stirred until the Cu had fully dissolved. In a separate 4-mL vial B was added bis-picolinamide **L38** (0.0075 mmol, 0.12 equiv). The contents of vial A (0.6 mL) was then added to vial B, and allowed to stir for 20 min. In a separate vial, ((4,5-dihydrofuran-2-yl)oxy)trimethylsilane **41** (44 mg, 0.25 mmol, 2.0 equiv) in THF (XX) was added, followed immediately by CsOAc (19.2 mg, 0.1 mmol, 1 equiv), and THF. The Cu/**L38** solution is then added to this vial, and the reaction is allowed to stir for 10 min. Cinnamyl chloride **43a** (9.53 mg, 0.0625 mmol, 1.0 equiv) was then added to the reaction, and the reaction was allowed to stir for 14 hours at room temperature. The reaction

mixture was filtered through a short silica plug eluting with ethyl acetate (5 mL). The eluate was concentrated by rotary evaporator and dissolved in CD₂Cl₂ to determine ¹H NMR yield with respect to 1,3,5-trimethoxybenzene. Then, the sample was concentrated and purified by preparative TLC (30% EtOAc/hexanes). The purified product was then dissolved in hexanes for SFC analysis on a Chiralcel AD column (12% IPA/hexanes, 2.5 mL/min).

Method E:

To a flame-dried 4 mL vial charged with Ar and a stir bar was added the desired Ligand (0.012n mmol, 0.12 equiv) and THF (0.53n mL). The solution was cooled to –78 °C and *n*-BuLi (174n μ L, 0.024n mmol, 0.138 M in THF, 0.24 equiv) was added dropwise. The reaction was stirred for 1 h at –78 °C. A solution of [Cu(MeCN)₄]PF₆ (3.73n mg, 0.01n mmol, 0.10 equiv) in THF was added, and the reaction was warmed to room temperature and stirred for 1 h. In the glovebox, CsOAc (19.2 mg, 0.1 mmol, 1.0 equiv) was added to a 4 mL vial containing a stir bar. The Cu/L complex in THF was then added (0.8 mL) to the CsOAc followed immediately by the silyl ketene acetal **41** (28 mg, 0.15 mmol, 1.5 equiv) in THF (0.8 mL). The resulting solution was allowed to stir for 5 min and then cinnamyl chloride **43a** (15.3 mg, 0.1 mmol, 1.0 equiv) in THF (0.8 mL) was added, and the reaction was allowed to stir for 14 hours at room temperature. The reaction mixture was filtered through a short silica plug eluting with ethyl acetate (10 mL). The eluate was concentrated by rotary evaporator and dissolved in CD₂Cl₂ to determine ¹H NMR yield with respect to 1,3,5-trimethoxybenzene. Then, the sample was concentrated and purified by preparative TLC (30% EtOAc/hexanes). The purified product was then dissolved in diethyl ether for SFC analysis on a Chiralpak AD column (12% IPA/hexanes, 2.5 mL/min).

Method F:

To a flame-dried 4 mL vial charged with Ar and a stir bar was added the desired Ligand (0.012n mmol, 0.12 equiv) and THF (0.63n mL). The solution was cooled to $-78\text{ }^{\circ}\text{C}$ and *n*-BuLi (174n mL, 0.024n mmol, 0.138M in THF, 0.24 equiv) was added dropwise. The reaction was stirred for 1 h at $-78\text{ }^{\circ}\text{C}$, and then the cold solution was transferred to a flame-dried vial under Ar containing CuCl₂ (1.34n mg, 0.01n mmol, 0.1 equiv). The resulting mixture was then warmed to room temperature. In the glovebox, CsOAc (19.2 mg, 0.1 mmol, 1.0 equiv) was added to a 4 mL vial containing a stir bar. The Cu/L complex in THF made was then added (0.8 mL) to the CsOAc followed immediately by the silyl ketene acetal **41** (28 mg, 0.15 mmol, 1.5 equiv) in THF (0.8 mL). The resulting solution was allowed to stir for 5 min and then cinnamyl chloride **43a** (15.3 mg, 0.1 mmol, 1.0 equiv) in THF (0.8 mL) was added, and the reaction was allowed to stir for 14 hours at room temperature. The reaction mixture was filtered through a short silica plug eluting with ethyl acetate (10 mL). The eluate was concentrated by rotary evaporator and dissolved in CD₂Cl₂ to determine ¹H NMR yield with respect to 1,3,5-trimethoxybenzene. Then, the sample was concentrated and purified by preparative TLC (30% EtOAc/hexanes). The purified product was then dissolved in diethyl ether for SFC analysis on a Chiralpak AD column (12% IPA/hexanes, 2.5 mL/min).

Method G:

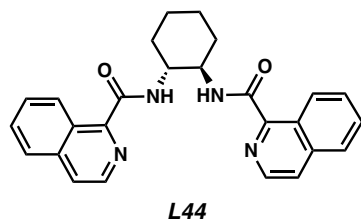
To a 4 mL vial containing CuCl₂ (1.34n mg, 0.01n mmol, 0.1 equiv) in the glovebox was added a solution of the Ligand (0.012n mmol, 0.12 equiv) in THF (0.4n mL), followed by a

solution of LiHMDS (4.35n mg, 0.026n mmol, 0.26 equiv) in THF (0.4n mL). The resulting solution was stirred for 1 h at room temperature. In the glovebox, CsOAc (19.2 mg, 0.1 mmol, 1.0 equiv) was added to a 4 mL vial containing a stir bar. The Cu/L complex in THF was then added (0.8 mL) to the CsOAc followed immediately by the silyl ketene acetal **41** (28 mg, 0.15 mmol, 1.5 equiv) in THF (0.8 mL). The resulting solution was allowed to stir for 5 min and then cinnamyl chloride **43a** (15.3 mg, 0.1 mmol, 1.0 equiv) in THF (0.8 mL) was added, and the reaction was allowed to stir for 14 hours at room temperature. The reaction mixture was filtered through a short silica plug eluting with ethyl acetate (10 mL). The eluate was concentrated by rotary evaporator and dissolved in CD₂Cl₂ to determine ¹H NMR yield with respect to 1,3,5-trimethoxybenzene. Then, the sample was concentrated and purified by preparative TLC (30% EtOAc/hexanes). The purified product was then dissolved in diethyl ether for SFC analysis on a Chiralpak AD column (12% IPA/hexanes, 2.5 mL/min).

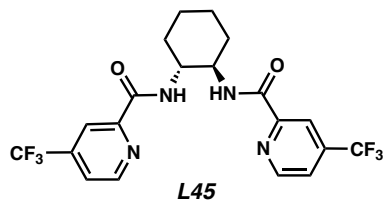
3.9.2.2 Synthesis of Chiral Picolinamide Ligands

Preparation of Known Ligands: Previously reported methods were used to prepare **L43**¹⁹, **L46**²⁰, **L48**²¹, **L49**²², **L51**²², **L55**²³, **L56**²⁴, **L57**²⁵, **L58**²⁶, **L65**²⁷, **L71**²⁴

General Procedure 1: Synthesis of Cyclohexylbispicolinamide Ligands

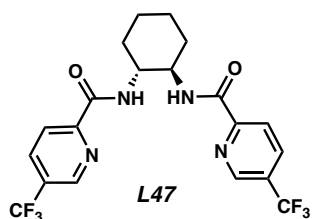


***N,N'*-((1*R*,2*R*)-cyclohexane-1,2-diyl)bis(isoquinoline-1-carboxamide) (L44):** To a solution of isoquinoline-1-carboxylic acid (204.1 mg, 1.18 mmol, 2.5 equiv) in THF (0.87 mL) was added carbonyl diimidazole (183 mg, 1.13 mmol, 2.4 equiv). The resultant mixture was allowed to stir for 1 h at room temperature, or until the solution turned clear. (1*R*,2*R*)-cyclohexane-1,2-diamine (54 mg, 0.47 mmol, 1.0 equiv) was added, and the reaction was allowed to stir overnight. The reaction mixture was diluted with water and stirred for 1 h. The aqueous layer was extracted with methylene chloride three times, and the resulting organic layers were dried over Na₂SO₄ and concentrated. Product **L44** was purified by column chromatography to provide a white solid (120 mg, 0.28 mmol, 60% yield); ¹H NMR (500 MHz, CDCl₃) δ 9.24 (d, *J* = 9.8 Hz, 2H), 8.45 (d, *J* = 5.6 Hz, 2H), 8.38 (d, *J* = 8.1 Hz, 2H), 7.77 – 7.67 (m, 4H), 7.56 (ddd, *J* = 8.2, 6.8, 1.2 Hz, 2H), 7.44 – 7.35 (m, 2H), 4.16 (t, *J* = 8.4 Hz, 2H), 2.33 (d, *J* = 12.0 Hz, 2H), 1.91 (d, *J* = 6.7 Hz, 2H), 1.63 – 1.49 (m, 4H).

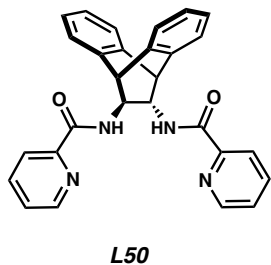


***N,N'*-((1*R*,2*R*)-cyclohexane-1,2-diyl)bis(4-(trifluoromethyl)picolinamide) (L45):** Product **L45** was prepared according to the General Procedure 1 and 4-(trifluoromethyl)picolinic acid. Product **L45** was purified by column chromatography to provide a white solid (147 mg, 0.32 mmol, 60% yield); ¹H NMR (500 MHz, CDCl₃) δ 8.72 (d, *J* = 5.0 Hz, 2H), 8.28 (s, 2H), 8.20 (d, *J* = 8.7 Hz,

2H), 7.58 (d, J = 5.0 Hz, 2H), 4.16 – 3.99 (m, 2H), 2.21 (d, J = 7.4 Hz, 2H), 1.98 – 1.71 (m, 3H), 1.63 – 1.36 (m, 4H); δ ^{13}C NMR (126 MHz, CDCl_3) δ 163.3, 151.2, 149.4, 140.2, 139.9, 139.7, 139.4, 123.7, 121.8, 121.7, 121.5, 118.3, 118.3, 118.3, 118.2, 77.4, 76.9, 53.7, 32.6, 24.9; ^{19}F NMR (282 MHz, CDCl_3) δ –64.90.



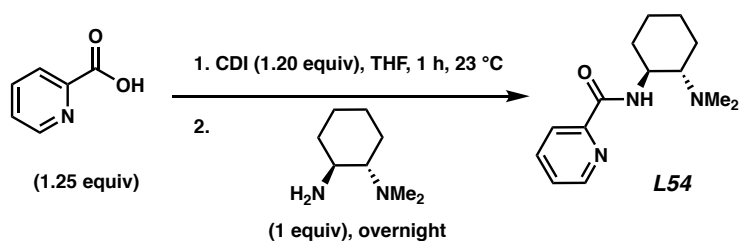
***N,N'*-((1*R*,2*R*)-cyclohexane-1,2-diyl)bis(5-(trifluoromethyl)picolinamide) (L47):** Product **L47** was prepared according to the General Procedure 1 and 4-(trifluoromethyl)picolinic acid. Product **L47** was purified by column chromatography to provide a white solid (276 mg, 0.6 mmol, 60% yield); ^1H NMR (300 MHz, CDCl_3) δ 8.76 (s, 2H), 8.21 (t, J = 8.1 Hz, 4H), 7.99 (dd, J = 8.2, 2.4 Hz, 2H), 4.19 – 3.96 (m, 2H), 2.20 (d, J = 6.9 Hz, 2H), 1.86 (d, J = 6.4 Hz, 2H), 1.48 (d, J = 8.3 Hz, 4H).



***N,N'*-((11*S*,12*S*)-9,10-dihydro-9,10-ethanoanthracene-11,12-diyl)dipicolinamide (L50):**

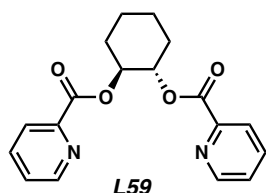
Product **L50** was prepared according to the General Procedure 1 and (11*S*,12*S*)-9,10-dihydro-9,10-ethanoanthracene-11,12-diamine. Product **L50** was purified by column chromatography to

provide a white solid; ^1H NMR (300 MHz, CDCl_3) δ 8.43 (ddd, $J = 4.8, 1.7, 0.9$ Hz, 2H), 8.14 (dt, $J = 7.8, 1.1$ Hz, 2H), 7.91 (d, $J = 8.3$ Hz, 2H), 7.79 (td, $J = 7.7, 1.8$ Hz, 2H), 7.50 – 7.43 (m, 2H), 7.41 – 7.31 (m, 4H), 7.28 – 7.16 (m, 5H), 4.53 (d, $J = 3.0$ Hz, 2H), 4.38 – 4.30 (m, 2H).

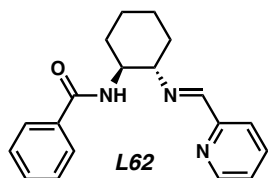


***N*-((1*S*,2*S*)-2-(dimethylamino)cyclohexyl)picolinamide (**L54**):** To a solution of picolinic acid (308 mg, 2.5 mmol, 1.25 equiv) in THF (3.33 mL) was added carbonyl diimidazole (389 mg, 2.5 mmol, 1.2 equiv). The resultant mixture was allowed to stir for 1 h at room temperature, or until the solution turned clear. (1*S*,2*S*)-*N*¹,*N*¹-dimethylcyclohexane-1,2-diamine (285 mg, 2.0 mmol, 1.0 equiv) was added, and the reaction was stirred overnight. The reaction mixture was diluted with water and allowed to stir for 1 h. The aqueous layer was extracted with methylene chloride three times, and the resulting organic layers were dried over Na_2SO_4 and concentrated. Product **L54** was purified by column chromatography to provide a white solid (247 mg, 1.0 mmol, 50% yield); $[\alpha]_{\text{D}}^{25}$ 74.79 (*c* 0.80, CHCl_3); ^1H NMR (400 MHz, CDCl_3) δ 8.56 (ddd, $J = 4.8, 1.8, 0.9$ Hz, 1H), 8.29 (s, 1H), 8.18 (dt, $J = 7.8, 1.1$ Hz, 1H), 7.81 (td, $J = 7.7, 1.8$ Hz, 1H), 7.39 (ddd, $J = 7.5, 4.8, 1.2$ Hz, 1H), 3.80 (tdd, $J = 10.7, 6.6, 4.0$ Hz, 1H), 2.47 (dddd, $J = 11.7, 9.8, 7.3, 3.9$ Hz, 2H), 2.26 (s, 6H), 1.96 – 1.77 (m, 2H), 1.70 (dtd, $J = 13.0, 3.3, 1.8$ Hz, 1H), 1.45 – 1.12 (m, 4H); ^{13}C NMR (101 MHz, CDCl_3) δ 164.3, 150.7, 148.2, 137.3, 125.9, 122.2, 66.6, 51.0, 40.3, 33.0, 25.4, 25.0, 22.2; IR (Neat Film, NaCl) 3376, 2930, 2859, 2824, 2779, 1672, 1590, 1568, 1509, 1464, 1432,

1339, 1270, 1189, 1153, 1084, 1044, 1032, 997, 866, 844, 782, 750, 700, 671, 620 cm^{-1} ; HRMS (MM) m/z calc'd for $\text{C}_{14}\text{H}_{22}\text{N}_3\text{O}$ $[\text{M}+\text{H}]^+$: 248.1757, found 248.1753.

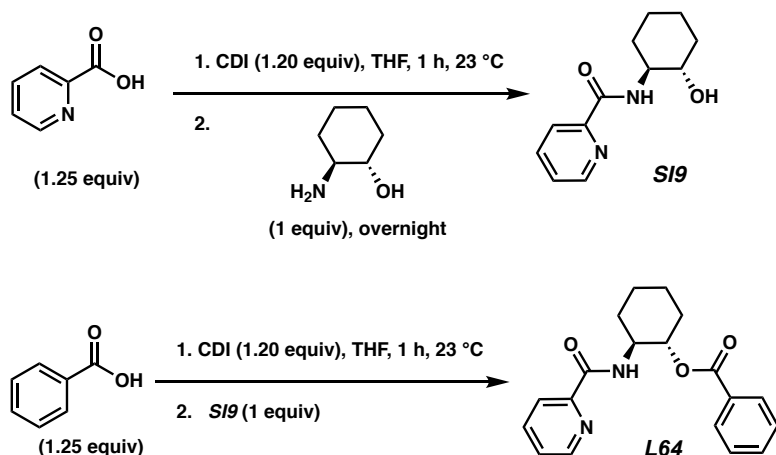


(1S,2S)-cyclohexane-1,2-diyl dipicolinate (L59): To a solution of picolinic acid (345 mg, 2.8 mmol, 2.5 equiv) in THF (1.87 mL) was added carbonyl diimidazole (435 mg, 2.68 mmol, 2.4 equiv). The resultant mixture was allowed to stir for 1 h at room temperature, or until the solution turned clear. (1S,2S)-cyclohexane-1,2-diol (130 mg, 1.12 mmol, 1.0 equiv) was added, and the reaction was allowed to stir overnight. The reaction mixture was diluted with water and stirred for 1 h. The aqueous layer was extracted with methylene chloride three times, and the resulting organic layers were dried over Na_2SO_4 and concentrated. Product **L59** was purified by column chromatography to provide a white solid (189 mg, 0.58 mmol, 52% yield); $[\alpha]_{\text{D}}^{25} -78.88$ (c 0.80, CHCl_3); ^1H NMR (400 MHz, CDCl_3) δ 8.69 (ddd, $J = 4.7, 1.7, 0.9$ Hz, 2H), 8.00 (dt, $J = 7.9, 1.1$ Hz, 2H), 7.74 (td, $J = 7.8, 1.8$ Hz, 2H), 7.38 (ddd, $J = 7.6, 4.7, 1.2$ Hz, 2H), 5.45 – 5.27 (m, 2H), 2.35 – 2.25 (m, 2H), 1.93 – 1.78 (m, 2H), 1.75 – 1.56 (m, 2H), 1.58 – 1.39 (m, 2H); ^{13}C NMR (101 MHz, CDCl_3) δ 164.3, 150.1, 147.9, 137.1, 126.9, 125.2, 75.4, 30.5, 23.8; IR (Neat Film, NaCl) 2940, 2868, 1740, 1716, 1582, 1437, 1325, 1304, 1280, 1224, 1157, 1128, 1087, 1045, 1028, 992, 918, 845, 821, 747, 706, 674, 664, 619 cm^{-1} ; HRMS (MM) m/z calc'd for $\text{C}_{18}\text{H}_{19}\text{N}_2\text{O}_4$ $[\text{M}+\text{H}]^+$: 327.1339, found 327.1346.



***N*-((1*S*,2*S*)-2-(((*E*)-pyridin-2-ylmethylene)amino)cyclohexyl)benzamide (**L62**):** To a solution of *N*-((1*S*,2*S*)-2-aminocyclohexyl)benzamide (109 mg, 0.5 mmol, 1.0 equiv) in MeOH (2.5 mL) at 0°C was added pyridine-2-carboxaldehyde (59 mg, 0.55 mmol, 1.1 equiv) in MeOH (2.5 mL) dropwise. The resulting mixture was warmed to room temperature, and concentrated by rotary evaporator and high-vac to afford **L62**; ¹H NMR (300 MHz, CDCl₃) δ 8.58 (d, *J* = 4.9 Hz, 1H), 8.42 (s, 1H), 8.01 (d, *J* = 7.8 Hz, 1H), 7.69 (t, *J* = 8.6 Hz, 1H), 7.63 – 7.51 (m, 2H), 7.47 – 7.26 (m, 5H), 5.79 (d, *J* = 15.5 Hz, 1H), 4.24 (d, *J* = 9.1 Hz, 1H), 3.33 – 3.17 (m, 1H), 2.23 (s, 1H), 1.87 (d, *J* = 5.2 Hz, 3H), 1.58 – 1.31 (m, 3H).

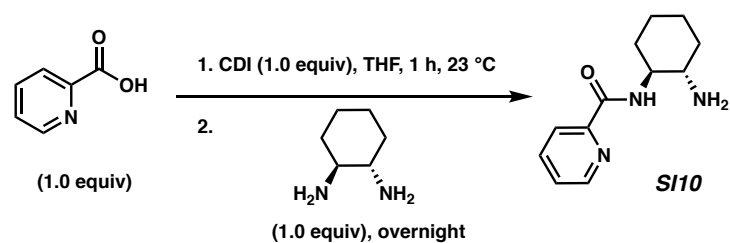
Synthesis of (1*S*,2*S*)-2-(picolinamido)cyclohexyl benzoate (L64**):**



To a solution of picolinic acid (616 mg, 5.0 mmol, 1.1 equiv) in THF (12 mL) was added carbonyl diimidazole (811 mg, 5.0 mmol, 1.1 equiv). The resultant mixture was allowed to stir for 1 h at room temperature, or until the solution turned clear. The solution was then diluted with THF (84 mL) and added slowly to a solution of (1*S*,2*S*)-2-aminocyclohexan-1-ol (576 mg, 5.0 mmol, 1.0 equiv) in THF (100 mL) via a dropping funnel. The reaction was allowed to stir at room temperature overnight. The crude reaction mixture was then concentrated by rotary evaporator and purified by short silica plug (2% MeOH in EtOAc) to afford **SI9** (925 mg, 4.2 mmol, 84% yield).

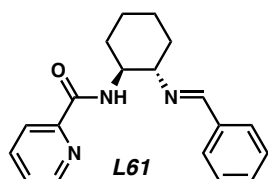
To a solution of benzoic acid (269 mg, 2.2 mmol, 1.1 equiv) in THF (6.1 mL) was added carbonyl diimidazole (357 mg, 2.2 mmol, 1.1 equiv). The resultant mixture was allowed to stir for 1 h at room temperature, or until the solution turned clear. *N*-((1*S*,2*S*)-2-hydroxycyclohexyl)picolinamide (**SI9**, 414 mg, 2.0 mmol, 1.0 equiv) was added, and the reaction was allowed to stir overnight. The reaction mixture was diluted with water and allowed to stir for 1 h. The aqueous layer was extracted with methylene chloride three times, and the resulting organic layers were dried over Na₂SO₄ and concentrated. Product **L64** was purified by column chromatography to provide a white solid (189 mg, 0.59 mmol 30% yield); $[\alpha]_{\text{D}}^{25} - 92.02$ (*c* 0.80, CHCl₃); ¹H NMR (400 MHz, CDCl₃) δ 8.48 (ddd, *J* = 4.8, 1.7, 0.9 Hz, 1H), 8.16 – 8.07 (m, 2H), 8.01 – 7.94 (m, 2H), 7.75 (td, *J* = 7.7, 1.7 Hz, 1H), 7.50 – 7.44 (m, 1H), 7.39 – 7.30 (m, 3H), 5.01 (td, *J* = 10.4, 4.4 Hz, 1H), 4.31 (dddd, *J* = 13.8, 9.6, 7.4, 4.5 Hz, 1H), 2.28 – 2.13 (m, 2H), 1.90 – 1.72 (m, 2H), 1.68 – 1.57 (m, 1H), 1.55 – 1.36 (m, 3H); ¹³C NMR (101 MHz, CDCl₃) δ 166.7, 164.1, 149.8, 148.1, 137.3, 132.9, 130.4, 129.8, 128.3, 126.1, 122.2, 75.7, 52.1, 32.1, 31.2, 24.5, 24.2; IR (Neat Film, NaCl) 3345, 2938, 2860, 1710, 1671, 1568, 1522, 1450, 1319, 1272, 1114,

1027, 997, 749, 713 cm^{-1} ; HRMS (MM) m/z calc'd for $\text{C}_{19}\text{H}_{21}\text{N}_2\text{O}_3$ $[\text{M}+\text{H}]^+$: 325.1547, found 325.1553;

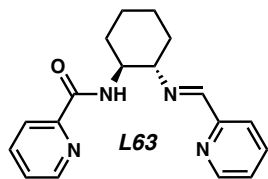


***N*-((1*S*,2*S*)-2-aminocyclohexyl)picolinamide (**SI10**):** To a solution of picolinic acid (1.23 g, 10.0 mmol, 1.0 equiv) in THF (25 mL) was added carbonyl diimidazole (1.62 g, 10.0 mmol, 1.0 equiv). The resultant mixture was stirred for 1 h at room temperature. The reaction was then diluted with THF (170 mL) and added slowly to a solution of (1*S*,2*S*)-cyclohexane-1,2-diamine (1.14 g, 10.0 mmol, 1.0 equiv) in THF (200 mL) via a dropping funnel. The reaction was allowed to stir at room temperature overnight. The crude reaction mixture was then concentrated by rotary evaporator and purified by column chromatography (3:1 ethyl acetate: MeOH to flush out imidazole, then 1% Et_3N to solvent mixture to elute product) to afford **SI10** (1.36 g, 6.2 mmol, 62% yield); $[\alpha]_{\text{D}}^{25}$ 136.06 (c 0.80, CHCl_3); ^1H NMR (400 MHz, CDCl_3) 8.55 (ddd, J = 4.8, 1.7, 0.9 Hz, 1H), 8.20 (dt, J = 7.8, 1.1 Hz, 1H), 7.97 (d, J = 9.4 Hz, 1H), 7.85 (td, J = 7.7, 1.7 Hz, 1H), 7.42 (ddd, J = 7.6, 4.8, 1.2 Hz, 1H), 3.72 (dtd, J = 11.0, 9.6, 4.0 Hz, 1H), 2.60 – 2.52 (m, 1H), 2.04 (ddt, J = 12.7, 9.3, 3.1 Hz, 2H), 1.77 (dq, J = 9.1, 2.5 Hz, 2H), 1.66 (s, 2H), 1.47 – 1.16 (m, 4H); ^{13}C NMR (101 MHz, CDCl_3) δ 164.6, 150.0, 148.1, 137.5, 126.3, 122.5, 56.5, 55.8, 35.3, 32.6,

25.3; IR (Neat Film, NaCl) 3341, 3312, 2929, 2858, 1700, 1590, 1568, 1520, 1448, 1434, 1465, 1326, 1288, 1252, 1147, 1162, 1089, 1027, 997, 923, 906, 853, 821, 753, 692, 680, 620 cm^{-1} ; HRMS (MM) m/z calc'd for $\text{C}_{12}\text{H}_{18}\text{N}_3\text{O}$ $[\text{M}+\text{H}]^+$: 220.1444, found 220.1434.

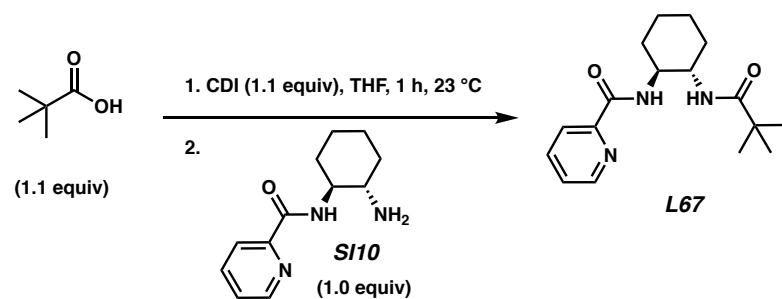


***N*-((1*S*,2*S*)-2-(((*E*)-benzylidene)amino)cyclohexyl)picolinamide (L61):** To a solution of **SI10** (219 mg, 1.0 mmol, 1.0 equiv) in MeOH (5 mL) at 0°C was added benzaldehyde (112 μL , 1.1 mmol, 1.1 equiv) in MeOH (5 mL) dropwise. The resulting mixture was warmed to room temperature, and concentrated by rotary evaporator and high-vac to afford **L61** (257 mg, 0.83 mmol, 83% yield); $[\alpha]_{\text{D}}^{25}$ 128.30 (c 0.80, CHCl_3); ^1H NMR (400 MHz, CDCl_3) δ 8.44 (ddd, J = 4.7, 1.7, 0.9 Hz, 1H), 8.29 (s, 1H), 8.09 (dt, J = 7.8, 1.1 Hz, 1H), 7.92 – 7.83 (m, 1H), 7.73 (td, J = 7.7, 1.7 Hz, 1H), 7.67 – 7.61 (m, 2H), 7.36 – 7.28 (m, 4H), 4.19 (dtd, J = 10.4, 9.1, 4.1 Hz, 1H), 3.27 (td, J = 9.6, 5.0 Hz, 1H), 2.31 – 2.17 (m, 1H), 1.93 – 1.72 (m, 4H), 1.61 – 1.32 (m, 3H); ^{13}C NMR (101 MHz, CDCl_3) δ 163.6, 160.3, 150.2, 147.9, 137.3, 136.4, 130.5, 128.5, 128.3, 126.0, 122.3, 53.2, 33.5, 31.7, 24.9, 24.3; IR (Neat Film, NaCl) 3379, 2932, 2855, 2673, 1643, 1590, 1568, 1519, 1464, 1450, 1434, 1293, 1156, 1042, 998, 752, 695, 680 cm^{-1} ; HRMS (MM) m/z calc'd for $\text{C}_{19}\text{H}_{22}\text{N}_3\text{O}$ $[\text{M}+\text{H}]^+$: 308.1757, found 308.1768.



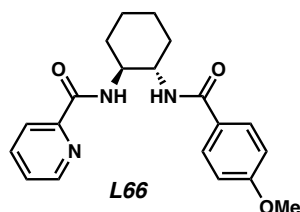
***N*-((1*S*,2*S*)-2-(((*E*)-pyridin-2-ylmethylene)amino)cyclohexyl)picolinamide (L63):** To a solution of **SI10** (219 mg, 1.0 mmol, 1.0 equiv) in MeOH (5 mL) at 0°C was added pyridine-2-carboxaldehyde (112 μ L, 1.1 mmol, 1.1 equiv) in MeOH (5 mL) dropwise. The resulting mixture was warmed to room temperature, and concentrated by rotary evaporator and high-vac to afford **L63** (257 mg, 0.84 mmol, 76% yield); ^1H NMR (400 MHz, CDCl_3) δ 8.49 (d, J = 34.9 Hz, 2H), 8.36 (s, 1H), 8.11 – 8.03 (m, 1H), 7.99 (d, J = 10.4 Hz, 1H), 7.87 (d, J = 10.1 Hz, 1H), 7.78 – 7.70 (m, 1H), 7.70 – 7.59 (m, 1H), 7.36 – 7.29 (m, 1H), 7.26 – 7.18 (m, 1H), 4.36 – 4.19 (m, 1H), 3.42 – 3.21 (m, 1H), 2.23 (d, J = 12.3 Hz, 1H), 1.86 (d, J = 9.3 Hz, 6H), 1.65 – 1.36 (m, 3H); ^{13}C NMR (101 MHz, CDCl_3) δ 164.3, 160.1, 154.4, 151.1, 149.2, 147.1, 137.3, 134.3, 126.8, 124.7, 122.2, 121.3, 69.1, 56.2, 35.2, 29.9, 27.3, 23.4.

General Procedure 2: Synthesis of Cyclohexylpicolinamide Ligands



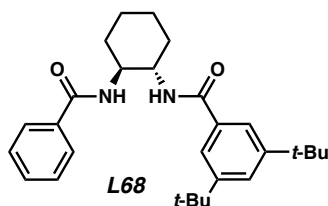
***N*-((1*S*,2*S*)-2-pivalamidocyclohexyl)picolinamide (L67):** To a solution of pivalic acid (56.2 mg, 0.55 mmol, 1.1 equiv) in THF (1.0 mL) was added carbonyl diimidazole (89.2 mg, 0.55 mmol, 1.1 equiv). The resultant mixture was stirred for 1 h at room temperature. *N*-((1*S*,2*S*)-2-aminocyclohexyl)picolinamide (**SI10**, 110 mg, 0.5 mmol, 1.0 equiv) was added, and the reaction

was allowed to stir overnight. The reaction mixture was then diluted with water and allowed to stir for 1 h. The aqueous layer was extracted with methylene chloride three times, and the resulting organic layers were dried over Na₂SO₄ and concentrated. The product was purified by column chromatography to provide a white solid (82.2 mg, 0.27 mmol, 54% yield); [α]_D²⁵ 36.82 (*c* 0.80, CHCl₃); ¹H NMR (400 MHz, CDCl₃) δ 8.54 (ddd, *J* = 4.7, 1.7, 0.9 Hz, 1H), 8.14 (dt, *J* = 7.8, 1.1 Hz, 1H), 8.08 (d, *J* = 9.0 Hz, 1H), 7.82 (td, *J* = 7.7, 1.7 Hz, 1H), 7.41 (ddd, *J* = 7.6, 4.7, 1.2 Hz, 1H), 6.36 (d, *J* = 7.6 Hz, 1H), 3.93 (tdd, *J* = 11.3, 9.0, 4.0 Hz, 1H), 3.73 (tdd, *J* = 11.2, 7.6, 4.0 Hz, 1H), 2.18 – 2.04 (m, 2H), 1.86 – 1.71 (m, 2H), 1.54 – 1.34 (m, 3H), 1.29 – 1.15 (m, 1H), 1.01 (s, 9H); ¹³C NMR (101 MHz, CDCl₃) δ 178.7, 165.2, 149.5, 148.4, 137.4, 126.4, 122.2, 55.0, 52.5, 38.6, 32.7, 32.4, 27.5, 25.2, 24.7; IR (Neat Film, NaCl) 3354, 2935, 2858, 1740, 1715, 1655, 1590, 1570, 1525, 1434, 1398, 1364, 1322, 1289, 1244, 1202, 1129, 1087, 1044, 997, 820, 750, 692, 620 cm⁻¹; HRMS (MM) *m/z* calc'd for C₁₇H₂₆N₃O₂ [M+H]⁺: 304.2020, found 304.2008.



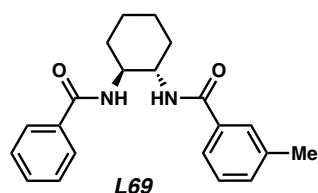
***N*-((1*S*,2*S*)-2-(4-methoxybenzamido)cyclohexyl)picolinamide (L66):** Product **L66** was prepared according to the General Procedure 2 and 4-methoxybenzaldehyde and **SI10**. The product was purified by column chromatography to provide a white solid (106 mg, 0.3 mmol, 60% yield); [α]_D²⁵ 120.32 (*c* 0.80, CHCl₃); ¹H NMR (400 MHz, CDCl₃) δ 8.52 (ddd, *J* = 4.8, 1.7, 0.9 Hz, 1H), 8.20 – 8.06 (m, 2H), 7.79 (td, *J* = 7.7, 1.7 Hz, 1H), 7.76 – 7.70 (m, 2H), 7.39 (ddd, *J* = 7.6, 4.8, 1.2 Hz, 1H), 7.18 (d, *J* = 7.1 Hz, 1H), 6.90 – 6.81 (m, 2H), 4.05 (tdd, *J* = 11.5, 8.8, 4.1 Hz, 1H), 3.89

(tdd, $J = 10.9, 7.1, 4.0$ Hz, 1H), 3.80 (s, 3H), 2.37 (dq, $J = 12.6, 2.3$ Hz, 1H), 2.16 – 2.07 (m, 1H), 1.92 – 1.74 (m, 2H), 1.57 (qd, $J = 12.4, 3.7$ Hz, 1H), 1.44 (ddt, $J = 12.2, 9.9, 3.2$ Hz, 2H), 1.37 – 1.21 (m, 1H); ^{13}C NMR (101 MHz, CDCl_3) δ 166.8, 165.8, 162.0, 149.4, 148.3, 137.5, 128.9, 126.9, 126.5, 122.3, 113.7, 56.5, 55.5, 52.4, 32.7, 32.3, 25.2, 24.6; IR (Neat Film, NaCl) 3316, 2933, 2856, 1656, 1607, 1569, 1507, 1527, 1465, 1330, 1302, 1255, 1178, 1146, 1109, 1092, 1028, 997, 843, 820, 750, 620; HRMS (MM) m/z calc'd for $\text{C}_{20}\text{H}_{24}\text{N}_3\text{O}_3$ $[\text{M}+\text{H}]^+$: 354.1812, found 354.1820.

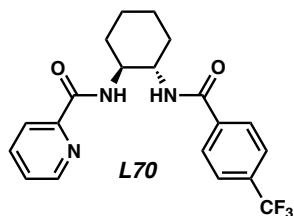


***N*-((1*S*,2*S*)-2-(3,5-di-*tert*-butylbenzamido)cyclohexyl)picolinamide (L68):** Product **L68** was prepared according to General Procedure 2 from **SI10** and 3,5-di-*tert*-butylbenzoic acid. The product was purified by column chromatography to provide a white solid (66.7 mg, 0.15 mmol, 31% yield); $[\alpha]_{\text{D}}^{25}$ 37.12 (c 0.80, CHCl_3); ^1H NMR (400 MHz, CDCl_3) δ 8.53 (ddd, $J = 4.7, 1.7, 0.9$ Hz, 1H), 8.23 – 8.15 (m, 2H), 7.80 (td, $J = 7.7, 1.7$ Hz, 1H), 7.62 (d, $J = 1.8$ Hz, 2H), 7.48 (t, $J = 1.8$ Hz, 1H), 7.39 (ddd, $J = 7.6, 4.8, 1.2$ Hz, 1H), 7.29 (d, $J = 7.1$ Hz, 1H), 4.07 (dddd, $J = 11.7, 10.8, 8.8, 4.0$ Hz, 1H), 3.89 (tdd, $J = 10.9, 7.1, 4.0$ Hz, 1H), 2.42 (ddt, $J = 12.1, 4.9, 2.6$ Hz, 1H), 2.12 (ddp, $J = 12.4, 5.2, 2.6, 2.0$ Hz, 1H), 1.93 – 1.73 (m, 2H), 1.59 (qd, $J = 12.4, 3.7$ Hz, 1H), 1.45 (ddt, $J = 17.1, 11.8, 6.1$ Hz, 2H), 1.32 (s, 19H); ^{13}C NMR (101 MHz, CDCl_3) δ 168.1, 165.6, 151.1, 149.4, 148.3, 137.3, 134.0, 126.5, 125.2, 122.4, 121.5, 56.7, 52.3, 35.1, 32.6, 32.4, 31.5, 25.3, 24.6; IR (Neat Film, NaCl) 3312, 2951, 2862, 1654, 1593, 1569, 1526, 1464, 1434, 1393,

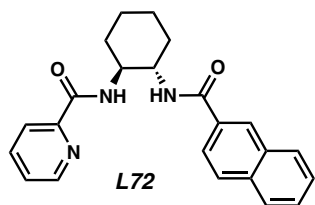
1334, 1264, 1249, 1147, 1097, 998, 888, 820, 750, 706, 612 cm^{-1} ; HRMS (MM) m/z calc'd for $\text{C}_{27}\text{H}_{38}\text{N}_3\text{O}_2$ $[\text{M}+\text{H}]^+$: 436.2959, found 436.2939.



N-((1S,2S)-2-(3-methylbenzamido)cyclohexyl)picolinamide (L69): Product **L69** was prepared according to General Procedure 2 from **SI10** and 3-methylbenzoic acid. The product was purified by column chromatography to provide a white solid (94.2 mg, 76% yield); $[\alpha]_{\text{D}}^{25}$ 75.30 (c 0.80, CHCl_3); ^1H NMR (400 MHz, CDCl_3) δ 8.52 (ddd, $J = 4.8, 1.8, 0.9$ Hz, 1H), 8.18 (d, $J = 8.8$ Hz, 1H), 8.13 (dt, $J = 7.8, 1.1$ Hz, 1H), 7.79 (td, $J = 7.7, 1.7$ Hz, 1H), 7.56 (dp, $J = 1.6, 0.7$ Hz, 1H), 7.55 – 7.50 (m, 1H), 7.39 (ddd, $J = 7.6, 4.8, 1.3$ Hz, 1H), 7.25 – 7.15 (m, 3H), 4.12 – 4.01 (m, 1H), 3.92 (tdd, $J = 11.0, 7.3, 4.0$ Hz, 1H), 2.40 – 2.30 (m, 4H), 2.13 (ddt, $J = 12.8, 4.1, 2.7$ Hz, 1H), 1.92 – 1.76 (m, 2H), 1.64 – 1.49 (m, 1H), 1.48 – 1.40 (m, 2H), 1.39 – 1.23 (m, 1H); ^{13}C NMR (101 MHz, CDCl_3) δ 167.6, 165.7, 149.4, 148.4, 138.2, 137.4, 134.5, 132.0, 128.4, 128.0, 126.5, 124.1, 122.3, 56.3, 52.5, 32.6, 32.3, 25.2, 24.6, 21.5; IR (Neat Film, NaCl) 3304, 3055, 2933, 2857, 1655, 1641, 1606, 1587, 1528, 1485, 1464, 1434, 1328, 1289, 1250, 1216, 1145, 1093, 1043, 998, 936, 816, 746, 688, 665, 620 cm^{-1} ; HRMS (MM) m/z calc'd for $\text{C}_{23}\text{H}_{24}\text{N}_3\text{O}_2$ $[\text{M}+\text{H}]^+$: 338.1863, found 338.1851.

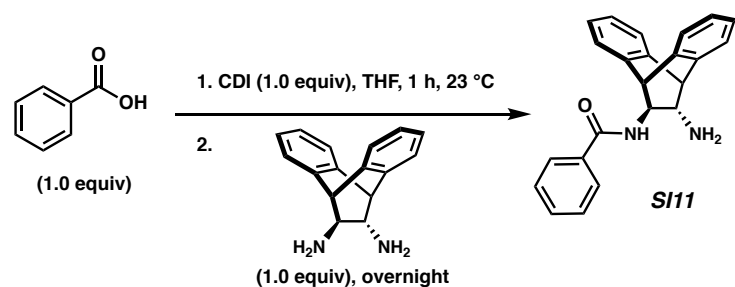


***N*-((1*S*,2*S*)-2-(4-(trifluoromethyl)benzamido)cyclohexyl)picolinamide (L70):** Product **L70** was prepared according to General Procedure 2 from **SI10** and 4-(trifluoromethyl)benzoic acid. The product was purified by column chromatography to provide an off-white solid (117 mg, 0.3 mmol, 60% yield). ^1H NMR (400 MHz, CDCl_3) δ 8.54 (ddd, J = 4.8, 1.7, 0.9 Hz, 1H), 8.22 – 8.11 (m, 2H), 7.89 (d, J = 8.1 Hz, 2H), 7.83 (td, J = 7.7, 1.7 Hz, 1H), 7.64 (d, J = 8.1 Hz, 2H), 7.54 (d, J = 6.5 Hz, 1H), 7.42 (ddd, J = 7.6, 4.8, 1.2 Hz, 1H), 4.17 – 4.00 (m, 1H), 3.95 – 3.81 (m, 1H), 2.41 (d, J = 13.0 Hz, 1H), 2.13 (d, J = 12.8 Hz, 1H), 1.96 – 1.77 (m, 1H), 1.69 – 1.16 (m, 5H).



***N*-((1*S*,2*S*)-2-(2-naphthamido)cyclohexyl)picolinamide (L72):** Product **L72** was prepared according to General Procedure 2 from **SI10** and **2-naphthoic acid**. The product was purified by column chromatography to provide an off-white solid (150 mg, 73% yield); ^1H NMR (400 MHz, CDCl_3) δ 9.24 (dq, J = 8.8, 1.0 Hz, 1H), 8.57 (ddd, J = 4.8, 1.8, 0.9 Hz, 1H), 8.43 (dd, J = 12.3, 7.1 Hz, 2H), 8.17 (d, J = 8.7 Hz, 1H), 8.01 (dt, J = 7.9, 1.1 Hz, 1H), 7.75 (dt, J = 8.4, 1.0 Hz, 1H),

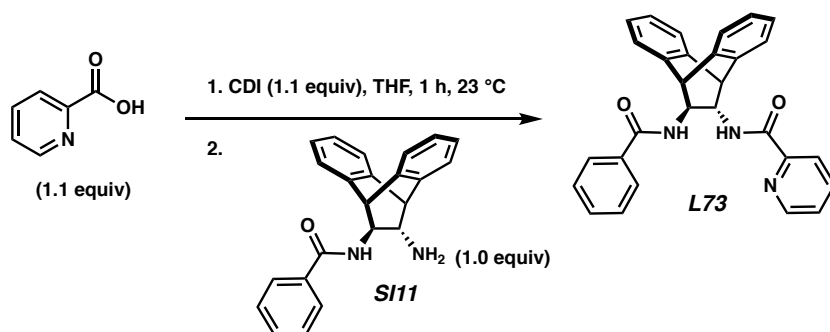
7.73 – 7.65 (m, 2H), 7.60 (ddd, $J = 8.2, 6.8, 1.2$ Hz, 1H), 7.44 (ddd, $J = 8.4, 6.8, 1.3$ Hz, 1H), 7.33 (ddd, $J = 7.6, 4.8, 1.3$ Hz, 1H), 4.16 (tdd, $J = 10.9, 8.6, 3.9$ Hz, 1H), 4.05 (tdd, $J = 10.7, 8.6, 4.1$ Hz, 1H), 2.33 – 2.20 (m, 2H), 1.93 – 1.80 (m, 2H), 1.60 – 1.40 (m, 4H); ^{13}C NMR (101 MHz, CDCl_3) δ 166.7, 164.7, 150.0, 149.0, 148.2, 140.5, 137.3, 137.1, 130.3, 128.2, 127.7, 126.8, 126.8, 126.0, 124.1, 122.2, 54.1, 53.2, 32.8, 32.6, 25.1, 25.0; IR (Neat Film, NaCl) 3310, 3053, 3007, 2934, 1661, 1522, 1381, 1154, 998, 833, 747, 665, cm^{-1} .



***N*-((11*S*,12*S*)-12-amino-9,10-dihydro-9,10-ethanoanthracen-11-yl)benzamide (SI11):** To a solution of benzoic acid (1.04 g, 8.5 mmol) in THF (21 mL) was added carbonyl diimidazole (1.38 g, 8.5 mmol). The resultant mixture was allowed to stir for 1 h at room temperature, or until the solution turned clear. The solution was then diluted with THF (142 mL) and added slowly to a solution of (11*S*,12*S*)-9,10-dihydro-9,10-ethanoanthracene-11,12-diamine (1.14 g, 10.0 mmol) in THF (170 mL) via a dropping funnel. The reaction was allowed to stir at room temperature overnight. The crude reaction mixture was then concentrated by rotary evaporator and purified by column chromatography (9:1 ethyl acetate: MeOH) to afford **SI11** (1.7 g, 5.1 mmol, 60% yield, co-eluted with imidazole, used without further purification); $[\alpha]_{\text{D}}^{25}$ 30.33 (c 0.80, CHCl_3); ^1H NMR (400 MHz, CDCl_3) δ 7.59 – 7.56 (m, 2H), 7.49 – 7.45 (m, 1H), 7.41 – 7.34 (m, 6H), 7.23 – 7.17 (m, 4H), 5.82 (d, $J = 7.7$ Hz, 1H), 4.98 (s, 2H), 4.35 (s, 1H), 4.23 (s, 1H), 3.96 (d, $J = 7.9$ Hz, 1H),

2.97 (s, 1H); ^{13}C NMR (101 MHz, CDCl_3) δ 167.7, 142.4, 140.3, 139.2, 138.7, 134.2, 131.8, 128.8, 127.2, 126.9, 126.7, 126.4, 125.3, 124.9, 124.8, 61.1, 60.2, 52.1, 49.1; IR (Neat Film, NaCl) 3119, 2922, 2838, 2697, 2608, 1960, 1918, 1826, 1638, 1602, 1578, 1542, 1535, 1485, 1466, 1445, 1379, 1326, 1294, 1256, 1228, 1141, 1116, 1095, 1063, 1026, 1000, 931, 866, 826, 751, 720, 664 cm^{-1} ; HRMS (MM) m/z calc'd for $\text{C}_{23}\text{H}_{21}\text{N}_2\text{O}$ $[\text{M}+\text{H}]^+$: 341.1648, found 341.1649.

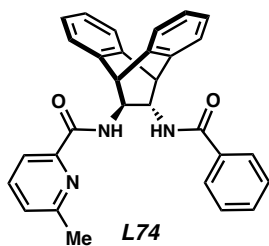
General Procedure 3: Synthesis of ANDEN Picolinyl Ligands.



N-((11*S*,12*S*)-12-benzamido-9,10-dihydro-9,10-ethanoanthracen-11-yl)picolinamide (**L73**):

To a solution of picolinic acid (378 mg, 3.07 mmol) in THF (4.65 mL) was added carbonyl diimidazole (498 mg, 3.07 mmol). The resultant mixture was stirred for 1 h at room temperature. *N*-((11*S*,12*S*)-12-amino-9,10-dihydro-9,10-ethanoanthracen-11-yl)benzamide (**SI11**, 950 mg, 2.79 mmol) was added, and the reaction was allowed to stir overnight. The reaction mixture was then diluted with water and allowed to stir for 1 h. The aqueous layer was extracted with methylene chloride three times, and the resulting organic layers were dried over Na_2SO_4 and concentrated. Product **L73** was purified by column chromatography to provide a white solid (747 mg, 1.68 mmol, 60% yield); $[\alpha]_{\text{D}}^{25}$ 174.63 (c 0.80, CHCl_3); ^1H NMR (400 MHz, CDCl_3) δ 8.43 (ddd, J =

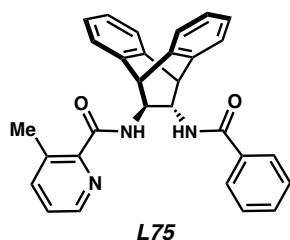
4.8, 1.7, 0.9 Hz, 1H), 8.06 (dt, $J = 7.8, 1.1$ Hz, 1H), 7.92 (d, $J = 8.7$ Hz, 1H), 7.78 (td, $J = 7.7, 1.7$ Hz, 1H), 7.62 – 7.57 (m, 2H), 7.51 – 7.39 (m, 3H), 7.39 – 7.30 (m, 5H), 7.25 – 7.14 (m, 4H), 6.10 (d, $J = 7.7$ Hz, 1H), 4.63 (d, $J = 2.6$ Hz, 1H), 4.49 (d, $J = 2.6$ Hz, 1H), 4.36 – 4.29 (m, 2H); ^{13}C NMR (101 MHz, CDCl_3) δ 167.4, 164.2, 149.3, 148.2, 141.2, 139.2, 138.7, 137.3, 134.3, 131.7, 128.6, 127.11, 127.07, 127.07, 127.01, 126.97, 126.91, 126.4, 126.0, 125.9, 125.1, 124.9, 122.3, 57.8, 56.9, 49.6, 49.4; IR (Neat Film, NaCl) 3360, 3006, 1652, 1569, 1517, 1489, 1465, 1434, 1327, 1293, 1146, 998, 748, 716 cm^{-1} ; HRMS (MM) m/z calc'd for $\text{C}_{29}\text{H}_{24}\text{N}_3\text{O}_2$ $[\text{M}+\text{H}]^+$: 446.1863, found 446.1882.



***N*-((11*S*,12*S*)-12-benzamido-9,10-dihydro-9,10-ethanoanthracen-11-yl)-6-**

methylpicolinamide (L74): Product **L74** was prepared according to General Procedure 3 from **SI11** and 6-methylpicolinic acid. The product was purified by column chromatography to provide a white solid (150 mg, 0.33 mmol, 65% yield); $[\alpha]_{\text{D}}^{25}$ 171.86 (c 0.80, CHCl_3); ^1H NMR (400 MHz, CDCl_3) δ 7.97 (d, $J = 8.6$ Hz, 1H), 7.87 (dt, $J = 7.7, 0.9$ Hz, 1H), 7.66 (t, $J = 7.7$ Hz, 1H), 7.63 – 7.58 (m, 2H), 7.52 – 7.47 (m, 1H), 7.46 – 7.40 (m, 2H), 7.39 – 7.31 (m, 4H), 7.29 – 7.16 (m, 5H), 6.07 (d, $J = 7.4$ Hz, 1H), 4.64 (d, $J = 2.6$ Hz, 1H), 4.48 (d, $J = 2.5$ Hz, 1H), 4.34 – 4.27 (m, 2H),

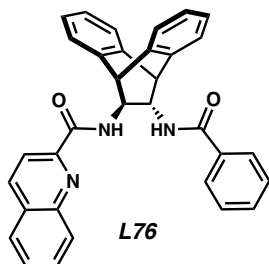
2.45 (s, 3H); ^{13}C NMR (101 MHz, CDCl_3) δ 167.4, 164.3, 157.3, 148.6, 141.2, 139.2, 138.8, 137.5, 134.3, 131.7, 128.6, 127.1, 127.0, 126.9, 126.8, 126.1, 126.0, 125.9, 125.2, 124.9, 119.3, 57.9, 56.7, 49.7, 49.4, 24.3; IR (Neat Film, NaCl) 3328, 3022, 1654, 1595, 1578, 1521, 1489, 1455, 1376, 1312, 1328, 1292, 1258, 1227, 1116, 1084, 1026, 995, 820, 804, 757, 716, 691, 664, 638 cm^{-1} ; HRMS (MM) m/z calc'd for $\text{C}_{30}\text{H}_{26}\text{N}_3\text{O}_2$ $[\text{M}+\text{H}]^+$: 460.2020, found 460.2039.



***N*-((11*S*,12*S*)-12-benzamido-9,10-dihydro-9,10-ethanoanthracen-11-yl)-3-**

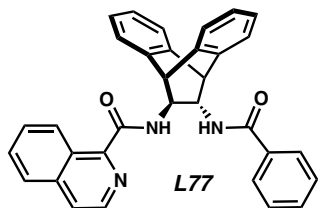
methylpicolinamide (L75): Product **L75** was prepared according to General Procedure 3 from **SI11** and 3-methylpicolinic acid. The product was purified by column chromatography to provide a white solid (148 mg, 0.3 mmol, 64% yield); $[\alpha]_{\text{D}}^{25}$ 165.82 (c 0.80, CHCl_3); ^1H NMR (400 MHz, CDCl_3) δ 8.26 (d, J = 4.5 Hz, 1H), 8.07 (d, J = 8.8 Hz, 1H), 7.64 – 7.58 (m, 2H), 7.53 (ddd, J = 7.8, 1.6, 0.8 Hz, 1H), 7.50 – 7.42 (m, 3H), 7.40 – 7.31 (m, 4H), 7.25 – 7.14 (m, 5H), 5.98 (d, J = 8.0 Hz, 1H), 4.61 (d, J = 2.8 Hz, 1H), 4.50 (d, J = 2.7 Hz, 1H), 4.34 – 4.28 (m, 1H), 4.23 (ddd, J = 8.8, 3.7, 2.8 Hz, 1H), 2.68 (s, 3H); ^{13}C NMR (101 MHz, CDCl_3) δ 167.4, 165.8, 146.6, 145.6, 141.4, 141.1, 140.9, 139.2, 138.9, 135.5, 134.3, 131.7, 128.7, 127.1, 127.0, 126.9, 126.0, 125.0, 124.9, 57.7, 57.0, 53.6, 49.6, 49.5, 20.6; IR (Neat Film, NaCl) 3327, 3046, 2956, 1654, 1602, 1579, 1508, 1466, 1446, 1380, 1308, 1326, 1292, 1222, 1122, 1080, 1026, 1002, 900, 814, 787, 762,

751, 712, 638, 662 cm^{-1} ; HRMS (MM) m/z calc'd for $\text{C}_{30}\text{H}_{26}\text{N}_3\text{O}_2$ $[\text{M}+\text{H}]^+$: 460.2020, found 460.2095.

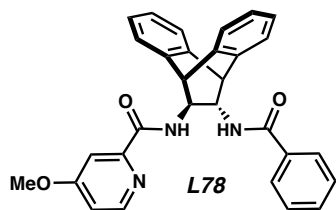


***N*-((11*S*,12*S*)-12-benzamido-9,10-dihydro-9,10-ethanoanthracen-11-yl)quinoline-2-**

carboxamide (L76): Product **L76** was prepared according to General Procedure 3 from **SI11** and quinoline-2-carboxylic acid (174 mg, 0.35 mmol, 70% yield); $[\alpha]_{\text{D}}^{25}$ 221.25 (c 0.80, CHCl_3); ^1H NMR (400 MHz, CDCl_3) δ 8.26 (dd, J = 8.6, 0.8 Hz, 1H), 8.17 (d, J = 8.5 Hz, 1H), 8.15 (s, 1H), 7.98 – 7.92 (m, 1H), 7.87 – 7.81 (m, 1H), 7.73 (ddd, J = 8.4, 6.9, 1.4 Hz, 1H), 7.65 – 7.56 (m, 3H), 7.55 – 7.51 (m, 1H), 7.49 – 7.44 (m, 1H), 7.41 (ddd, J = 7.6, 6.2, 1.8 Hz, 2H), 7.39 – 7.16 (m, 7H), 6.13 (d, J = 7.4 Hz, 1H), 4.67 (d, J = 2.5 Hz, 1H), 4.54 (d, J = 2.5 Hz, 1H), 4.40 (ddt, J = 9.2, 3.5, 1.6 Hz, 2H); ^{13}C NMR (101 MHz, CDCl_3) δ 167.4, 164.3, 149.1, 146.5, 141.1, 139.2, 138.8, 137.5, 134.3, 131.7, 130.2, 130.0, 129.4, 128.6, 128.1, 127.7, 127.2, 127.1, 127.0, 126.02, 125.95, 125.2, 124.9, 118.8, 57.9, 56.9, 49.7, 49.4; IR (Neat Film, NaCl) 3329, 3022, 1654, 1579, 1525, 1499, 1427, 1328, 1211, 1145, 1113, 1026, 904, 844, 794, 750, 715, 674, 638 cm^{-1} ; HRMS (MM) m/z calc'd for $\text{C}_{33}\text{H}_{26}\text{N}_3\text{O}_2$ $[\text{M}+\text{H}]^+$: 496.2020, found 496.2010.

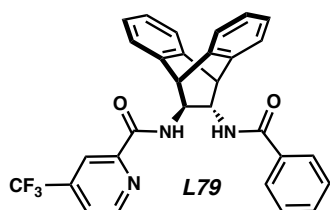


***N*-((11*S*,12*S*)-12-benzamido-9,10-dihydro-9,10-ethanoanthracen-11-yl)isoquinoline-1-carboxamide (L77):** Product L77 was prepared according to General Procedure 3 from SI11 and isoquinoline-1-carboxylic acid (173 mg, 69% yield); $[\alpha]_{\text{D}}^{25}$ 142.51 (c 0.80, CHCl_3); ^1H NMR (400 MHz, CDCl_3) δ 9.52 – 9.48 (m, 1H), 8.34 (d, J = 5.5 Hz, 1H), 8.17 (d, J = 8.5 Hz, 1H), 7.81 (dt, J = 8.4, 0.8 Hz, 1H), 7.74 (dd, J = 5.6, 1.0 Hz, 1H), 7.69 (ddd, J = 8.2, 6.8, 1.4 Hz, 1H), 7.64 (ddt, J = 6.9, 3.7, 1.9 Hz, 3H), 7.49 (dd, J = 7.1, 1.4 Hz, 2H), 7.47 – 7.42 (m, 1H), 7.41 – 7.32 (m, 4H), 7.28 – 7.16 (m, 4H), 6.08 (d, J = 7.7 Hz, 1H), 4.65 (d, J = 2.7 Hz, 1H), 4.58 (d, J = 2.7 Hz, 1H), 4.36 (dddd, J = 12.1, 8.6, 3.6, 2.8 Hz, 2H); ^{13}C NMR (101 MHz, CDCl_3) δ 167.4, 166.0, 147.4, 141.4, 141.1, 140.3, 139.2, 138.9, 137.5, 134.4, 131.7, 130.6, 128.8, 128.7, 127.7, 127.10, 127.07, 127.05, 127.0, 126.9, 126.0, 125.1, 124.9, 124.6, 57.8, 57.2, 49.6, 49.5; IR (Neat Film, NaCl) 3328, 3054, 3022, 2952, 1650, 1602, 1582, 1510, 1489, 1466, 1383, 1325, 1292, 1260, 1222, 1144, 1110, 1024, 878, 834, 812, 800, 756, 715, 637, 619 cm^{-1} ; HRMS (MM) m/z calc'd for $\text{C}_{33}\text{H}_{26}\text{N}_3\text{O}_2$ $[\text{M}+\text{H}]^+$:496.2020, found 496.2014.



***N*-((11*S*,12*S*)-12-benzamido-9,10-dihydro-9,10-ethanoanthracen-11-yl)-4-methoxypicolinamide (L78):** Product L78 was prepared according to General Procedure 3 from

SI11 and 4-methoxypicolinic acid (174 mg, 0.37 mmol, 70% yield); $[\alpha]_{\text{D}}^{25}$ 134.97 (*c* 0.80, CHCl₃); ¹H NMR (400 MHz, CDCl₃) δ 8.22 (dd, *J* = 5.6, 0.5 Hz, 1H), 7.94 (d, *J* = 8.6 Hz, 1H), 7.64 – 7.58 (m, 3H), 7.50 – 7.40 (m, 3H), 7.39 – 7.31 (m, 4H), 7.28 – 7.14 (m, 4H), 6.86 (dd, *J* = 5.7, 2.6 Hz, 1H), 6.12 (d, *J* = 7.6 Hz, 1H), 4.63 (d, *J* = 2.6 Hz, 1H), 4.47 (d, *J* = 2.5 Hz, 1H), 4.31 (dtd, *J* = 10.4, 6.3, 3.1 Hz, 2H), 3.84 (s, 3H); ¹³C NMR (101 MHz, CDCl₃) δ 167.4, 166.9, 164.2, 151.3, 149.4, 141.3, 141.1, 139.2, 138.7, 134.3, 131.7, 128.6, 127.12, 127.09, 127.0, 126.0, 125.1, 124.9, 113.1, 107.6, 57.9, 56.9, 55.6, 49.6, 49.4; IR (Neat Film, NaCl) 3328, 2926, 1654, 1599, 1579, 1566, 1518, 1489, 1308, 1257, 1226, 1138, 1030, 994, 849, 804, 784, 761, 716, 640 cm⁻¹; HRMS (MM) *m/z* calc'd for C₃₀H₂₆N₃O₂⁺ [M+H]: 476.1969, found 476.1950.



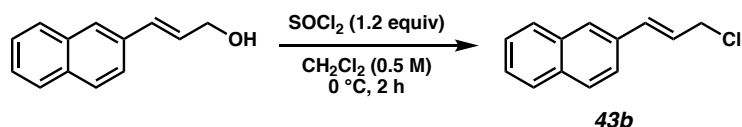
***N*-((11*S*,12*S*)-12-benzamido-9,10-dihydro-9,10-ethanoanthracen-11-yl)-4-**

(trifluoromethyl)picolinamide (L79): Product **L79** was prepared according to General Procedure 3 from **SI11** and 4-(Trifluoromethyl)pyridine-2-carboxylic acid. The product was purified by column chromatography to provide a white solid (107.1 mg, 0.21 mmol, 42% yield); $[\alpha]_{\text{D}}^{25}$ 143.66 (*c* 0.80, CHCl₃); ¹H NMR (400 MHz, CDCl₃) δ 8.62 (dt, *J* = 5.0, 0.8 Hz, 1H), 8.28 (dt, *J* = 1.6, 0.7 Hz, 1H), 7.84 (d, *J* = 8.7 Hz, 1H), 7.62 – 7.56 (m, 3H), 7.51 – 7.40 (m, 3H), 7.38 – 7.30 (m, 4H), 7.29 – 7.15 (m, 4H), 6.13 (d, *J* = 7.9 Hz, 1H), 4.60 (d, *J* = 2.6 Hz, 1H), 4.49 (d, *J* = 2.6 Hz, 1H), 4.39 – 4.32 (m, 2H); ¹³C NMR (101 MHz, CDCl₃) δ 167.4, 162.8, 150.8, 149.3, 141.1, 139.9 (q, *J* = 34.7 Hz), 139.1, 138.6, 134.2, 131.7, 128.6, 127.2 (d, *J* = 8.9 Hz), 125.9 (d, *J* = 10.6 Hz), 125.1

(d, $J = 18.6$ Hz), 124.0, 124.0, 121.9 (d, $J = 3.7$ Hz), 121.2, 121.2, 118.6 – 118.2 (m), 57.7, 57.1, 49.5 (d, $J = 12.8$ Hz); ^{19}F NMR (282 MHz, CDCl_3) δ –64.86; IR (Neat Film, NaCl) 3312, 3069, 1654, 1610, 1580, 1524, 1488, 1411, 1331, 1293, 1265, 1228, 1173, 1141, 1116, 1080, 1026, 857, 842, 797, 752, 720, 699, 665, 639 cm^{-1} ; HRMS (MM) m/z calc'd for $\text{C}_{30}\text{H}_{23}\text{F}_3\text{N}_3\text{O}_2$ $[\text{M}+\text{H}]^+$: 514.1737, found 514.1733.

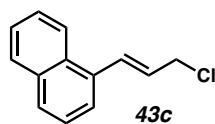
3.9.2.3 Synthesis of Allylic Chloride Electrophiles

General Procedure 4: Synthesis of Aryl-Substituted Allylic Chlorides (**43b-d**, **43g**, **43h**, **43j-m**, **43p**, **43s-u**).

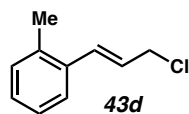


(*E*)-2-(3-chloroprop-1-en-1-yl)naphthalene (43b): (*E*)-3-(naphthalen-2-yl)prop-2-en-1-ol (553 mg, 3.0 mmol, 1.0 equiv) was dissolved in methylene chloride (6 mL, 0.5 M). Then, thionyl chloride (326 μL , 4.5 mmol, 1.2 equiv) was added dropwise. The reaction was allowed to stir for 2 h at 0 °C, then quenched with saturated aqueous NaHCO_3 solution (6 mL) and allowed to warm to room temperature. The aqueous layer was extracted with methylene chloride three times, and the resulting organic layers were dried over Na_2SO_4 and concentrated. The crude oil was then re-

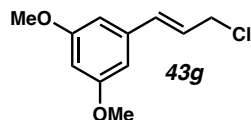
suspended in hexanes (10 mL) and washed with water 4 times. The hexanes layer was then dried with Na₂SO₄ and concentrated to afford the desired allylic chloride **43b** as a white solid (339 mg, 1.68 mmol, 56% yield); ¹H NMR (500 MHz, CDCl₃) δ 7.91 – 7.83 (m, 3H), 7.83 – 7.79 (m, 1H), 7.65 (dd, J = 8.6, 1.7 Hz, 1H), 7.57 – 7.47 (m, 2H), 6.88 (dtd, J = 15.6, 1.2, 0.6 Hz, 1H), 6.51 (dt, J = 15.6, 7.2 Hz, 1H), 4.37 (dd, J = 7.2, 1.2 Hz, 2H); All characterization data match those reported.²⁸



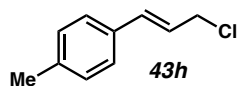
(E)-1-(3-chloroprop-1-en-1-yl)naphthalene (43c): 994 mg, 4.9 mmol, 77% yield; ¹H NMR (300 MHz, CDCl₃) δ 8.19 – 8.02 (m, 1H), 7.96 – 7.77 (m, 2H), 7.62 (dt, J = 7.3, 1.0 Hz, 1H), 7.59 – 7.38 (m, 4H), 6.37 (dtd, J = 15.1, 7.1, 0.8 Hz, 1H), 4.36 (dt, J = 7.1, 1.1 Hz, 2H); All characterization data match those reported.²⁸



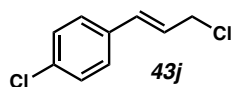
(E)-1-(3-chloroprop-1-en-1-yl)-2-methylbenzene (43d): 274 mg, 1.64 mmol, 55% yield; ¹H NMR (500 MHz, CDCl₃) δ 7.50 – 7.38 (m, 1H), 7.22 – 7.12 (m, 3H), 6.88 (dt, J = 15.5, 1.2 Hz, 1H), 6.22 (dt, J = 15.4, 7.2 Hz, 1H), 4.28 (dd, J = 7.2, 1.2 Hz, 2H), 2.37 (s, 3H); All characterization data match those reported.²⁹



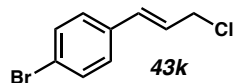
(E)-1-(3-chloroprop-1-en-1-yl)-3,5-dimethoxybenzene (43g): 106 mg, 0.5 mmol, 22% yield; ^1H NMR (500 MHz, CDCl_3) δ 7.02 (dt, $J = 1.5, 0.8$ Hz, 2H), 6.93 (tt, $J = 1.7, 0.8$ Hz, 1H), 6.66 – 6.54 (m, 1H), 6.30 (dt, $J = 15.6, 7.2$ Hz, 1H), 4.24 (dd, $J = 7.3, 1.2$ Hz, 2H), 2.31 (t, $J = 0.7$ Hz, 6H); All characterization data match those reported.³⁰



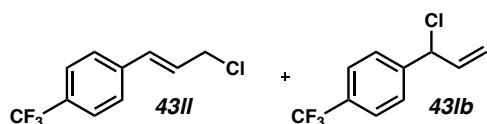
(E)-1-(3-chloroprop-1-en-1-yl)-4-methylbenzene (43h): 442 mg, 2.65 mmol, 88% yield; ^1H NMR (500 MHz, CDCl_3) δ 7.32 – 7.27 (m, 2H), 7.18 – 7.11 (m, 2H), 6.63 (dd, $J = 15.6, 1.1$ Hz, 1H), 6.27 (dt, $J = 15.6, 7.2$ Hz, 1H), 4.25 (dd, $J = 7.3, 1.2$ Hz, 2H), 2.35 (s, 3H); All characterization data match those reported.³²



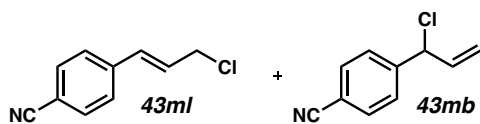
(E)-1-chloro-4-(3-chloroprop-1-en-1-yl)benzene (43j): 609 mg, 3.25 mmol, 81% yield; ^1H NMR (300 MHz, CDCl_3) δ 7.31 (d, $J = 1.1$ Hz, 4H), 6.61 (dt, $J = 15.7, 1.3$ Hz, 1H), 6.30 (dt, $J = 15.6, 7.1$ Hz, 1H), 4.23 (dd, $J = 7.1, 1.2$ Hz, 2H); All characterization data match those reported.²⁸



(E)-1-bromo-4-(3-chloroprop-1-en-1-yl)benzene (43k): 579 mg, 2.5 mmol, 50% yield; ^1H NMR (300 MHz, CDCl_3) δ 7.55 – 7.38 (m, 2H), 7.26 (s, 2H), 6.60 (d, J = 15.7 Hz, 1H), 6.31 (dt, J = 15.6, 7.1 Hz, 1H), 4.23 (dd, J = 7.1, 1.2 Hz, 2H); All characterization data match those reported.²⁸

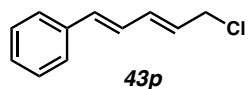


(E)-1-(3-chloroprop-1-en-1-yl)-4-(trifluoromethyl)benzene (43II) and 1-(1-chloroallyl)-4-(trifluoromethyl)benzene (43Ib): 405 mg, 1.8 mmol, 61% yield, **43II:43Ib** = 83:17 (inseparable mixture); **43II:** ^1H NMR (300 MHz, CDCl_3) δ 7.73 – 7.39 (m, 5H), 6.70 (d, J = 15.7 Hz, 1H), 6.41 (dt, J = 15.5, 7.0 Hz, 1H), 4.25 (dd, J = 7.0, 1.3 Hz, 2H). **43Ib:** ^1H NMR (300 MHz, CDCl_3) δ 7.70 – 7.34 (m, 4H), 6.13 (m, 1H), 5.54 – 5.26 (m, 3H); All characterization data match those reported.³³

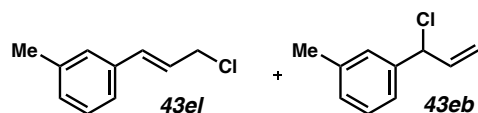


(E)-4-(3-chloroprop-1-en-1-yl)benzonitrile (43mI) and 4-(1-chloroallyl)benzonitrile (43mB): Isolated as an inseparable mixture of constitutional isomers **1mI** and **1mB** (210 mg, 1.18 mmol, 56% yield, **43mI:43mB** = 59:42, **43m** = 86:15, E:Z); ^1H NMR (400 MHz, CDCl_3) **43mI:** δ 7.70 – 7.58 (m, 2H), 7.55 – 7.44 (m, 2H), 6.72 – 6.56 (m, 1H), 6.43 (dt, J = 15.7, 6.9 Hz, 1H), 4.25 (dd, J = 6.9, 1.2 Hz, 2H); **43mB:** δ 7.70 – 7.58 (m, 2H), 7.55 – 7.44 (m, 2H), 6.11 (ddd, J = 17.1, 10.1, 7.2 Hz, 1H), 5.45 (dd, J = 7.1, 1.1 Hz, 1H), 5.35 (dt, J = 16.8, 1.0 Hz, 1H), 5.30 (dt, J = 10.1, 0.9

Hz, 1H); **43ml** and **43mb**: ^{13}C NMR (101 MHz, CDCl_3) δ , 140.5, 136.6, 134.8, 132.6, 132.6, 132.2, 129.3, 128.9, 128.3, 127.3, 118.8, 118.5, 118.3, 112.3, 111.6, 77.2, 57.4, 44.7, 25.2; IR (Neat Film, NaCl) 3042, 2956, 2357, 2227, 1921, 1654, 1606, 1504, 1439, 1412, 1333, 1303, 1250, 1215, 1177, 1156, 1109, 1075, 1017, 969, 936, 834, 811, 760, 722, 688, 672 cm^{-1} ; HRMS (MM) m/z calc'd for $\text{C}_{10}\text{H}_9\text{ClN}$ $[\text{M}+\text{H}]^+$: 178.0418, found 178.0422.

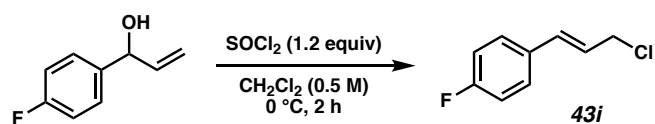


((1E,3E)-5-chloropenta-1,3-dien-1-yl)benzene (43p): 1.32 g, 7.4 mmol, 92% yield; ^1H NMR (300 MHz, CDCl_3) δ 7.26 (m, 5H), 6.78 (dd, $J = 15.6, 10.4$ Hz, 1H), 6.60 (d, $J = 15.7$ Hz, 1H), 6.46 (dd, $J = 14.9, 10.3$ Hz, 1H), 5.92 (dt, $J = 14.8, 7.4$ Hz, 1H), 4.18 (dd, $J = 7.3, 1.1$ Hz, 2H); All characterization data match those reported.³⁴



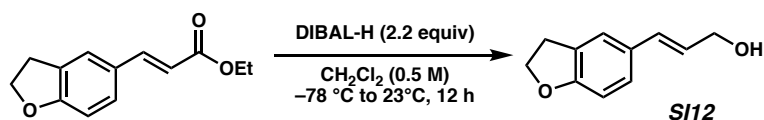
(E)-1-(3-chloroprop-1-en-1-yl)-3-methylbenzene (43el) and 1-(1-chloroallyl)-3-methylbenzene (43eb): 513 mg, 71% yield. To a solution of (E)-3-(*m*-tolyl)prop-2-en-1-ol (640 mg, 4.32 mmol, 1.0 equiv) in anhydrous Et_2O (4.3 mL, 1 M) at 0°C under a nitrogen atmosphere was added thionyl chloride (0.38 mL, 5.2 mmol, 1.2 equiv). Stirring was continued at 0°C for 6 hours. The reaction was then diluted with Et_2O and washed with saturated aqueous NaHCO_3 , followed by brine. The organic layer was dried over anhydrous sodium sulfate, filtered, and solvent was removed in vacuo. The crude was purified by flash column chromatography (5%

EtOAc/hexanes) to yield the title compound colorless oil (513 mg, 3.08 mmol, 71% yield, **43el**:**43eb**= 9:1); ^1H NMR (500 MHz, CDCl_3) **43el**: δ 7.26– 7.20 (m, 3H), 7.11 (d, J = 7.2 Hz, 1H), 6.64 (d, J = 15.4 Hz, 1H), 6.32 (dt, J = 15.4, 7.2 Hz, 1H), 4.26 (d, J = 7.2 Hz, 2H), 2.37 (s, 3H); **43eb**: δ 7.28 (d, J = 7.5 Hz, 1H), 7.26 – 7.20 (m, 3H), 7.14 (d, J = 7.6 Hz, 1H), 6.21 (ddd, J = 17.2, 10.1, 7.2 Hz, 1H), 5.44 (d, J = 7.2 Hz, 1H), 5.36 (d, J = 16.8 Hz, 1H), 5.25 (d, J = 10.1 Hz, 1H), 2.39 (s, 3H); **1el** and **1eb**: ^{13}C NMR (125 MHz, CDCl_3) \square 140.1, 138.6, 138.4, 137.9, 136.0, 134.4, 129.3, 129.2, 128.7, 128.2, 127.5, 124.8, 124.6, 124.0, 116.9, 63.8, 45.7, 21.5; IR (Neat Film, NaCl) 3033, 2952, 2921, 2860, 1651, 1604, 1486, 1439, 1251, 964, 778 cm^{-1} ; HRMS (MM) m/z calc'd for $\text{C}_{10}\text{H}_{12} [\text{M}-\text{Cl}]^+$: 131.0861, found 131.0858.



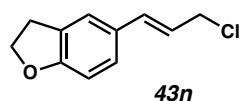
(E)-1-(3-chloroprop-1-en-1-yl)-4-fluorobenzene (43i): 1-(4-fluorophenyl)prop-2-en-1-ol (750 mg, 4.92 mmol, 1.0 equiv) was dissolved in methylene chloride (6 mL, 0.5 M). Then, thionyl chloride (428 μL , 5.9 mmol, 1.2 equiv) was added dropwise. The reaction was allowed to stir for 2 h at $0\text{ }^\circ\text{C}$, then quenched with saturated aqueous NaHCO_3 solution (6 mL) and allowed to warm to room temperature. The aqueous layer was extracted with methylene chloride three times, and the resulting organic layers were dried over Na_2SO_4 and concentrated. The crude oil was then re-suspended in hexanes (10 mL) and washed with water 4 times. The hexanes layer was then dried with Na_2SO_4 and concentrated by rotary evaporator. The crude product was purified by column chromatography (100% hexanes) to afford the desired allylic chloride **43i** as a white solid (420 mg, 2.46 mmol, 50% yield). ^1H NMR (400 MHz, CDCl_3) δ 7.43 – 7.31 (m, 2H), 7.12 – 6.95 (m,

2H), 6.62 (dt, J = 15.6, 1.2 Hz, 1H), 6.24 (dtd, J = 15.6, 7.2, 0.6 Hz, 1H), 4.23 (dd, J = 7.2, 1.2 Hz, 2H); ^{13}C NMR (101 MHz, CDCl_3) δ 164.1, 161.6, 133.1, 132.2, 128.4, 124.8, 115.9, 115.7, 45.5; ^{19}F NMR (282 MHz, CDCl_3) δ -113.30; IR (Neat Film, NaCl) 3043, 2361, 1602, 1508, 1300, 1234, 1158, 966, 814 cm^{-1} ; HRMS (MM) m/z calc'd for $\text{C}_9\text{H}_8\text{ClF} [\text{M}]^+$: 170.0299, found 170.0299

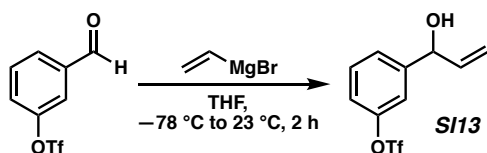


(E)-3-(2,3-dihydrobenzofuran-5-yl)prop-2-en-1-ol (SI4): To a solution of ethyl (E)-3-(2,3-dihydrobenzofuran-5-yl)acrylate (2.40 g, 11.0 mmol, 1.0 equiv) in anhydrous DCM (37 mL, 0.3 M) under nitrogen atmosphere at -78°C was dropwise added neat DIBAL-H (4.37 mL, 24.2 mmol, 2.20 equiv). The reaction was then allowed to warm to room temperature and stirring was continued for 12 hours. Upon completion, the reaction was cooled to 0°C and EtOAc (10 mL) was slowly added. The reaction was then diluted with Et_2O and a saturated aqueous solution of Rochelle's salt (*ca.* 150 mL) was added. Stirring was continued at room temperature for 1 hour. The biphasic mixture was then extracted with EtOAc (3x). The combined organic layers were dried over anhydrous sodium sulfate, filtered, and solvent was removed in vacuo to yield the crude product as a colorless solid (1.66 g, 9.42 mmol, 86% yield). The crude alcohol was isolated in good purity and used directly in the next step. ^1H NMR (400 MHz, CDCl_3) δ 7.27 (s, 1H), 7.13 (dd, J = 8.2, 1.4 Hz, 1H), 6.73 (d, J = 8.2 Hz, 1H), 6.54 (d, J = 15.8 Hz, 1H), 6.20 (dt, J = 15.8, 6.0 Hz, 1H), 4.58 (t, J = 8.7 Hz, 2H), 4.29 (dd, J = 6.0, 1.4 Hz, 2H), 3.20 (t, J = 8.7 Hz, 2H), 1.48 (s, 1H); ^{13}C NMR (100 MHz, CDCl_3) δ 160.1, 131.6, 129.6, 127.6, 127.1, 125.7, 122.9, 109.4,

71.6, 64.2, 29.7; IR (Neat Film, NaCl) 3291, 2914, 2889, 2861, 1610, 1490, 1243, 1218, 1106, 1086, 970; HRMS (MM) m/z calc'd for $C_{11}H_{11}O$ $[M-OH]^+$: 159.0804, found 159.0804.

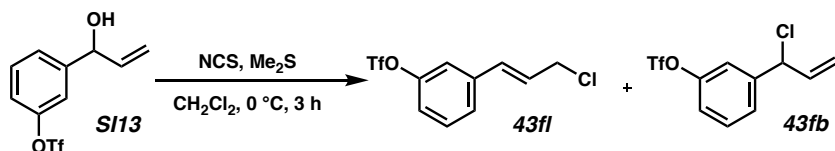


(*E*)-5-(3-chloroprop-1-en-1-yl)-2,3-dihydrobenzofuran (43n): To a solution of (*E*)-3-(2,3-dihydrobenzofuran-5-yl)prop-2-en-1-ol (600 mg, 3.40 mmol, 1.0 equiv) in anhydrous Et_2O (4.3 mL, 1 M) at 0° C under a nitrogen atmosphere was added thionyl chloride (0.30 mL, 4.1 mmol, 1.2 equiv). Stirring was continued at 0° C for 12 hours. The reaction was then diluted with Et_2O and washed with saturated aqueous $NaHCO_3$, followed by brine. The organic layer was dried over anhydrous sodium sulfate, filtered, and solvent was removed in vacuo to yield the crude product as a tan amorphous solid (350 mg, 1.80 mmol, 53% yield). The crude allyl chloride was stored cold under nitrogen and used directly in the next reaction, as it was unstable to silica and neutral alumina (50 mg, 0.26 mmol, 51% yield). 1H NMR (400 MHz, CD_2Cl_2) δ 7.26 (d, J = 1.3 Hz, 1H), 7.10 (d, J = 10.0 Hz, 1H), 6.67 (d, J = 8.2 Hz, 1H), 6.56 (d, J = 15.6 Hz, 1H), 6.19 – 6.07 (m, 1H), 4.53 (t, J = 8.7 Hz, 3H), 4.21 (d, J = 7.4 Hz, 2H), 3.16 (t, J = 8.7 Hz, 2H); ^{13}C NMR (100 MHz, $CDCl_3$) δ 160.5, 134.4, 128.8, 127.7, 127.5, 123.1, 122.1, 109.4, 71.6, 46.2, 29.7; IR (Neat Film, NaCl) 2960, 2894, 1646, 1611, 1492, 1440, 1246, 1102, 982, 808 cm^{-1} ; HRMS (MM) m/z calc'd for $C_{11}H_{12}ClO$ $[M+H]^+$: 195.0571, found 195.0571.



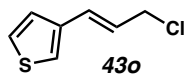
3-(1-hydroxyallyl)phenyl trifluoromethanesulfonate (SI13): To a solution of 3-formylphenyl trifluoromethanesulfonate (635 mg, 2.5 mmol, 1.0 equiv) in THF (6.6 mL, 0.38 M) at -78°C was added vinylmagnesium bromide (2.53 mL, 2.53 mmol, 1M solution in THF) slowly. The reaction was allowed to stir for 4 h at -78°C , then quenched with saturated aqueous NH_4Cl solution (6 mL) and allowed to warm to room temperature. The aqueous layer was extracted with methylene chloride three times, and the resulting organic layers were dried over Na_2SO_4 and concentrated. The crude allylic alcohol was purified by column chromatography to afford a yellow oil (542 mg, 1.92 mmol, 77% yield). ^1H NMR (400 MHz, CDCl_3) δ 7.41 – 7.30 (m, 2H), 7.25 (s, 1H), 7.15 – 7.10 (m, 1H), 6.03 – 5.81 (m, 1H), 5.31 (d, J = 18.3 Hz, 1H), 5.19 (d, J = 11.2 Hz, 2H), 2.00 (d, J = 3.6 Hz, 1H); ^{13}C NMR (101 MHz, CDCl_3) δ 149.9, 145.7, 139.5, 130.4, 126.3, 123.7 – 114.1 (q, J = 320.7 Hz), 120.5, 119.3, 116.7, 114.1, 74.6; ^{19}F NMR (282 MHz, CDCl_3) δ -72.93; IR (Neat Film, NaCl) 3573, 3358, 3087, 2878, 1614, 1583, 1485, 1425, 1249, 1208, 1141, 1035, 990, 960, 912, 841, 96, 775, 753, 696, 657, 666 cm^{-1} ; HRMS (MM) m/z calc'd for $\text{C}_{10}\text{H}_8\text{F}_3\text{O}_3\text{S}$ $[\text{M}-\text{OH}]^+$: 265.0141, found 265.0146.

General Procedure 5: Synthesis of Allylic Chlorides 43f, 43n, and 43o.



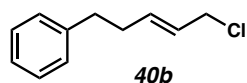
3-(1-chloroallyl)phenyl trifluoromethanesulfonate (43fl) and (E)-3-(3-chloroprop-1-en-1-yl)phenyl trifluoromethanesulfonate (43fb): N-chlorosuccinamide (150 mg, 1.125 mmol, 1.5 equiv) was dissolved in dichloromethane (3.0 mL) and cooled to 0°C . Dimethylsulfide (103 μL ,

1.39 mmol, 1.85 equiv) was added slowly and the resulting suspension was cooled to $-10\text{ }^{\circ}\text{C}$. 3-(1-hydroxyallyl)phenyl trifluoromethanesulfonate (**SI13**, 211mg, 0.75 mmol, 1.0 equiv) in dichloromethane (1.5 mL) was then added slowly. The reaction was warmed to $0\text{ }^{\circ}\text{C}$ and allowed to stir for 3 h. Upon consumption of the starting material, the reaction was quenched with ice-cold water, and extracted with diethyl ether four times. The combined extracts were then rinsed with water and brine, and dried over Na_2SO_4 . The resulting crude oil was purified by column chromatography to afford (*E*)-3-(3-chloroprop-1-en-1-yl)phenyl trifluoromethanesulfonate (**43fl**) 3-(1-chloroallyl)phenyl trifluoromethanesulfonate (**43fb**) and in an inseparable mixture (112 mg, 50% yield, **43fl**:**43fb** = 60:40, **43fl** = 86:14 *E/Z*); ^1H NMR (300 MHz, CDCl_3) **43fl**: δ 7.50–7.12 (m, 4H), 6.12 (ddd, J = 17.0, 10.1, 7.1 Hz, 1H), 5.46 (dt, J = 7.2, 1.1 Hz, 1H), 5.40–5.27 (m, 2H), 4.60 (s, 1H); **43fb**: δ 7.50–7.12 (m, 4H), 6.66 (dt, J = 15.7, 1.2 Hz, 1H), 6.44–6.32 (m, 1H), 4.24 (dd, J = 7.0, 1.2 Hz, 2H); **43fl** and **43fb**: ^{13}C NMR (101 MHz, CDCl_3) δ 150.0, 149.7, 143.0, 138.8, 136.8, 133.7, 132.0, 130.7, 130.6, 128.5, 127.8, 127.5, 126.7, 121.6, 121.4, 120.8, 120.7, 120.4, 119.4, 118.3, 117.3, 61.9, 57.5, 44.8, 44.7, 25.3; ^{19}F NMR (282 MHz, CDCl_3) δ -72.86 (m); IR (Neat Film, NaCl) 2916, 2849, 1611, 1576, 1487, 1422, 1247, 1215, 1140, 1120, 962, 908, 886, 847, 787, 680 cm^{-1} ; HRMS (MM) m/z calc'd for $\text{C}_{10}\text{H}_8\text{ClF}_3\text{SO}_3$ $[\text{M}]^{*+}$: 299.9835, found 299.9846.



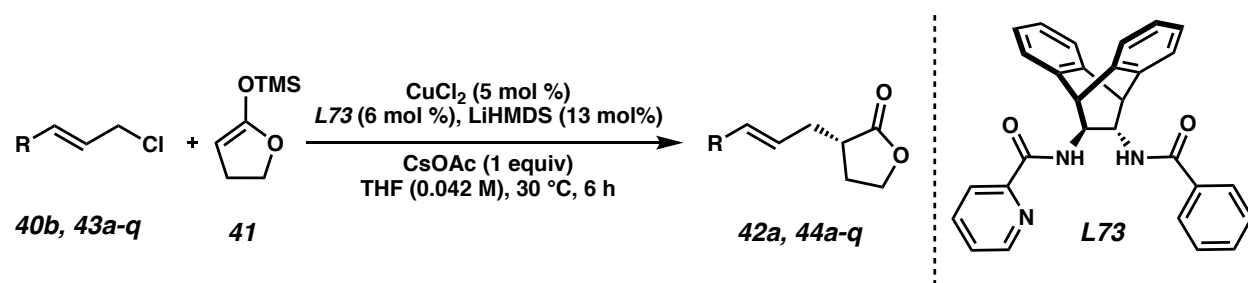
(*E*)-3-(3-chloroprop-1-en-1-yl)thiophene(43o): Synthesized from (*E*)-3-(thiophen-3-yl)prop-2-en-1-ol according to General Procedure 5, and used without further purification (286 mg, 1.84 mmol, 48% yield); ^1H NMR (400 MHz, CDCl_3) δ 7.29 (ddd, J = 5.0, 3.0, 0.6 Hz, 1H), 7.24–7.19 (m, 2H), 6.67 (ddq, J = 15.6, 1.2, 0.6 Hz, 1H), 6.17 (dt, J = 15.5, 7.2 Hz, 1H), 4.22 (dd, J = 7.3,

1.2 Hz, 2H); ^{13}C NMR (101 MHz, CDCl_3) δ 138.7, 128.5, 126.5, 125.1, 124.9, 123.6, 45.7; IR (Neat Film, NaCl) 3736, 3103, 2952, 1650, 1417, 1293, 1247, 1150, 1074, 961, 865, 768 cm^{-1} ; HRMS (MM) m/z calc'd for $\text{C}_7\text{H}_7\text{S} [\text{M}-\text{Cl}]^+$: 123.0268, found 123.0260.



(E)-(5-chloropent-3-en-1-yl)benzene (40b): Compound **40b** was prepared from the corresponding allylic alcohol according to a previously reported procedure.²⁹ ^1H NMR (500 MHz, CDCl_3) δ 7.30 (td, $J = 7.4, 1.4$ Hz, 2H), 7.24 – 7.16 (m, 3H), 5.82 (dtd, $J = 14.5, 6.6, 1.2$ Hz, 1H), 5.66 (dddq, $J = 15.4, 7.1, 6.2, 1.3$ Hz, 1H), 4.04 (dt, $J = 7.1, 1.0$ Hz, 2H), 2.72 (dd, $J = 8.7, 7.0$ Hz, 2H), 2.47 – 2.33 (m, 2H); All characterization data match those reported.²⁹

3.9.2.4 Procedure for Cu-Catalyzed Allylic Alkylation Reactions

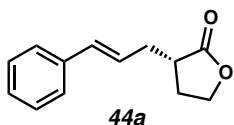


n = number of reactions. To a 4 mL vial containing CuCl_2 (1.34 n mg, 0.01 n mmol, 0.05 equiv) in the glovebox was added a solution of the **L73** (5.2 n mg, 0.012 n mmol, 0.06 equiv) in THF (0.8 n mL), followed by a solution of LiHMDS (4.35 n mg, 0.026 n mmol, 0.13 equiv) in THF (0.8 n mL).

The resulting solution was stirred for 1 h at room temperature. This solution (1.6 mL) was then transferred to a vial containing CsOAc, followed by silyl ketene acetal **41** (47.5 mg, 0.3 mmol, 1.5 equiv) in THF (1.6 mL). The mixture was allowed to stir for 5 min, then allyl chloride (30.4 mg, 0.2 mmol, 1 equiv) in THF (1.6 mL) was added and the reaction was allowed to stir for 6 h at 30 °C. The reaction was then quenched with sat. NH₄Cl solution and a few drops of TMEDA, and the aqueous layer was extracted five times with ethyl acetate. The combined organic extracts were dried with Na₂SO₄, and concentrated by rotary evaporator. The crude oil was then purified by column chromatography to afford the desired product.

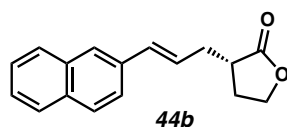
3.9.2.5 Spectroscopic Data for Products from Catalytic Reactions

Please note that the absolute configuration was determined only for compound **44ba** via x-ray crystallographic analysis. The absolute configuration for all other products has been inferred by analogy.

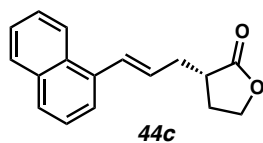


(S)-3-cinnamyldihydrofuran-2(3H)-one (44a): Product **44a** was purified by column chromatography (25% EtOAc in hexanes) to provide a white solid (36.4 mg, 0.18 mmol, 90% yield); 94% *ee*; [α]_D²⁵ 46.62 (*c* 0.80, CHCl₃); ¹H NMR (400 MHz, CDCl₃) δ 7.38 – 7.28 (m, 4H), 7.26 – 7.20 (m, 1H), 6.49 (dt, *J* = 15.7, 1.4 Hz, 1H), 6.29 – 6.08 (m, 1H), 4.35 (td, *J* = 8.8, 3.1 Hz, 1H), 4.22 (td, *J* = 9.2, 6.9 Hz, 1H), 2.82 – 2.67 (m, 2H), 2.53 – 2.34 (m, 2H), 2.15 – 2.00 (m, 1H);

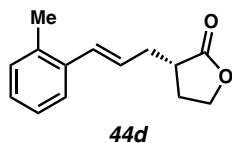
^{13}C NMR (101 MHz, CDCl_3) δ 178.9, 137.0, 133.2, 128.7, 127.6, 126.3, 125.9, 66.8, 39.4, 33.7, 27.9; IR (Neat Film, NaCl) 3057, 3027, 2988, 2936, 2906, 1770, 1480, 1436, 1378, 1314, 1294, 1251, 1208, 1190, 1164, 1074, 1021, 988, 966, 812, 798, 751, 705, 695, 681, 671, 622 cm^{-1} ; HRMS (MM) m/z calc'd for $\text{C}_{13}\text{H}_{15}\text{O}_2$ $[\text{M}+\text{H}]^+$: 203.1067, found 203.1064; SFC Conditions: 15% IPA, 2.5 mL/min, Chiralpak AD-H column, λ = 254 nm, t_R (min): major = 4.70, minor = 5.02.



(*S,E*)-3-(3-(naphthalen-2-yl)allyl)dihydrofuran-2(3*H*)-one (44b): Product **44b** was purified by column chromatography (25% EtOAc in hexanes) to provide a white solid (43.4 mg, 0.17 mmol, 86% yield); 91% *ee*; $[\alpha]_D^{25}$ 32.53 (c 0.80, CHCl_3); ^1H NMR (400 MHz, CDCl_3) δ 7.87 – 7.75 (m, 3H), 7.70 (d, J = 1.7 Hz, 1H), 7.57 (dd, J = 8.6, 1.8 Hz, 1H), 7.51 – 7.39 (m, 2H), 6.65 (dd, J = 15.8, 1.6 Hz, 1H), 6.30 (dt, J = 15.7, 7.1 Hz, 1H), 4.35 (td, J = 8.8, 3.0 Hz, 1H), 4.22 (td, J = 9.3, 6.8 Hz, 1H), 2.90 – 2.68 (m, 2H), 2.62 – 2.28 (m, 2H), 2.08 (dtd, J = 12.7, 9.7, 8.6 Hz, 1H); ^{13}C NMR (101 MHz, CDCl_3) δ 178.9, 134.5, 133.7, 133.2, 133.0, 128.3, 128.0, 127.8, 126.4, 126.3, 126.0, 125.9, 123.5, 66.7, 39.4, 33.8, 28.0; IR (Neat Film, NaCl) 2905, 1767, 1452, 1374, 1154, 1020, 964, 866, 821, 753, 668 cm^{-1} ; HRMS (MM) m/z calc'd for $\text{C}_{17}\text{H}_{17}\text{O}_2$ $[\text{M}+\text{H}]^+$: 253.1223, found 253.1232; SFC Conditions: 35% IPA, 3.5 mL/min, Chiralcel OD-H column, λ = 254 nm, t_R (min): major = 3.63, minor = 3.97.

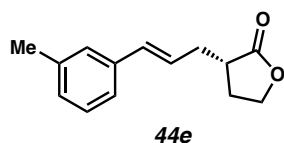


(*S,E*)-3-(3-(naphthalen-1-yl)allyl)dihydrofuran-2(3*H*)-one (44c): Product **44c** was purified by column chromatography (25% EtOAc in hexanes) to provide a colorless solid (42.4 mg, 0.17 mmol, 84% yield); 91% *ee*; $[\alpha]_{\text{D}}^{25}$ 29.405 (*c* 0.80, CHCl₃); ¹H NMR (400 MHz, CDCl₃) δ 8.15 – 8.04 (m, 1H), 7.91 – 7.82 (m, 1H), 7.78 (dt, *J* = 8.1, 1.0 Hz, 1H), 7.59 – 7.39 (m, 4H), 7.22 (s, 1H), 6.19 (dt, *J* = 15.5, 7.2 Hz, 1H), 4.38 (td, *J* = 8.8, 3.1 Hz, 1H), 4.24 (td, *J* = 9.3, 6.9 Hz, 1H), 2.95 – 2.74 (m, 2H), 2.58 (dddd, *J* = 13.9, 8.4, 7.3, 1.4 Hz, 1H), 2.45 (dddd, *J* = 12.7, 8.7, 6.9, 3.1 Hz, 1H), 2.14 (dtd, *J* = 12.7, 9.7, 8.5 Hz, 1H); ¹³C NMR (101 MHz, CDCl₃) δ 178.9, 134.9, 133.7, 131.1, 130.5, 129.3, 128.7, 128.0, 126.2, 125.9, 125.7, 123.9, 123.8, 66.8, 39.5, 34.1, 28.0; IR (Neat Film, NaCl) 3746, 2909, 2358, 1769, 1508, 1374, 1153, 1023, 969, 777 cm⁻¹; HRMS (MM) *m/z* calc'd for C₁₇H₁₇O₂ [M+H]⁺: 253.1223, found 253.1221; SFC Conditions: 25% IPA, 2.5 mL/min, Chiralcel OD-H column, λ = 210 nm, *t_R* (min): major = 10.39, minor = 11.48.

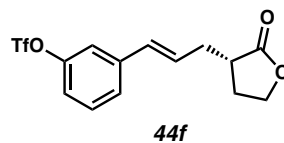


(*S,E*)-3-(3-(*o*-tolyl)allyl)dihydrofuran-2(3*H*)-one (44d): Product **44d** was purified by column chromatography (25% EtOAc in hexanes) to provide a colorless oil (27.2 mg, 0.13 mmol, 63% yield); 94% *ee*; $[\alpha]_{\text{D}}^{25}$ 26.0 (*c* 0.80, CHCl₃); ¹H NMR (400 MHz, CDCl₃) δ 7.26 (s, 2H), 7.11 (s, 2H), 6.45 (d, *J* = 15.7 Hz, 1H), 6.17 – 6.05 (m, 1H), 4.38 – 4.30 (m, 1H), 4.26 – 4.17 (m, 1H), 2.80 – 2.67 (m, 2H), 2.51 – 2.35 (m, 2H), 2.33 (s, 3H), 2.05 (t, *J* = 9.5 Hz, 1H). ¹³C NMR (101 MHz, CDCl₃) δ 131.1, 130.4, 127.5, 127.3, 126.2, 125.7, 66.7, 39.5, 34.0, 27.9, 20.0; IR (Neat Film, NaCl) 2912, 1767, 1597, 1451, 1373, 1200, 1152, 1021, 966, 863, 821, 748 cm⁻¹; HRMS (MM)

m/z calc'd for $C_{14}H_{17}O_2$ $[M+H]^+$: 217.1223, found 217.1221; SFC Conditions: 20% IPA, 2.5 mL/min, Chiralcel OD-H column, λ = 254 nm, t_R (min): major = 5.05, minor = 5.73.

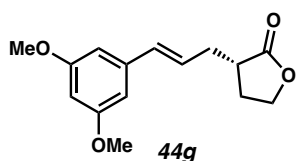


(S,E)-3-(3-(m-tolyl)allyl)dihydrofuran-2(3H)-one (44e): Compound **44e** was purified by column chromatography (30% EtOAc/hexanes) to afford the title compound as a colorless oil (38.3 mg, 0.18 mmol, 88% yield); 90% *ee*; $[\alpha]_D^{23}$ 31.6 (*c* 1.00, $CHCl_3$); 1H NMR (400 MHz, $CDCl_3$) δ 7.22 – 7.14 (m, 3H), 7.05 (d, J = 7.4 Hz, 1H), 6.46 (d, J = 15.7 Hz, 1H), 6.16 (dt, J = 15.8, 7.2 Hz, 1H), 4.34 (td, J = 8.8, 3.1 Hz, 1H), 4.21 (td, J = 9.3, 6.9 Hz, 1H), 2.78 – 2.69 (m, 2H), 2.50 – 2.36 (m, 2H), 2.34 (s, 3H), 2.11 – 2.00 (m, 1H); ^{13}C NMR (100 MHz, $CDCl_3$) δ 179.0, 137.4, 134.3, 133.0, 129.4, 126.2, 124.8, 66.8, 39.5, 33.7, 27.9, 21.3; IR (Neat Film, NaCl) 2911, 1769, 1602, 1486, 1454, 1374, 1152, 1022, 968, 775 cm^{-1} ; HRMS (MM) m/z calc'd for $C_{14}H_{17}O_2$ $[M+H]^+$: 217.1223, found 217.1227; SFC Conditions: 15% IPA, 2.5 mL/min, Chiralcel OD-H column, λ = 254 nm, t_R (min): minor = 6.93, major = 5.48.



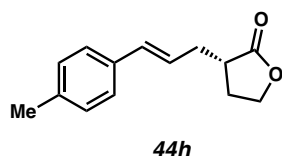
(S,E)-3-(3-(2-oxotetrahydrofuran-3-yl)prop-1-en-1-yl)phenyl trifluoromethanesulfonate (44f): Product **44f** was purified by column chromatography (25% EtOAc in hexanes) to provide a pale yellow oil (41.8 mg, 0.12 mmol, 60% yield); 88% *ee*; $[\alpha]_D^{25}$ 16.88 (*c* 0.80, $CHCl_3$); 1H NMR

(400 MHz, CDCl₃) δ 7.44 – 7.32 (m, 2H), 7.24 – 7.20 (m, 1H), 7.12 (dt, J = 7.2, 2.3 Hz, 1H), 6.48 (dt, J = 15.8, 1.4 Hz, 1H), 6.25 (dt, J = 15.8, 7.1 Hz, 1H), 4.36 (td, J = 8.9, 2.8 Hz, 1H), 4.23 (td, J = 9.4, 6.8 Hz, 1H), 2.85 – 2.68 (m, 2H), 2.54 – 2.35 (m, 2H), 2.12 – 1.97 (m, 1H); ¹³C NMR (101 MHz, CDCl₃) δ 178.6, 150.0, 139.8, 131.2, 130.5, 128.9, 126.2, 120.0, 118.9, 118.8 (q, J = 320.7 Hz), 66.7, 39.2, 33.6, 28.1; ¹⁹F NMR (282 MHz, CDCl₃) δ -72.94; IR (Neat Film, NaCl) 2912, 2356, 1770, 1654, 1609, 1573, 1486, 1421, 1248, 1214, 1141, 1118, 1023, 960, 904, 884, 848, 786, 736, 683, 658, 606 cm⁻¹; HRMS (MM) m/z calc'd for C₁₄H₁₄F₃O₂S [M+H]⁺: 351.0509, found 351.0508; SFC Conditions: 5% IPA, 2.5 mL/min, Chiralcel OJ-H column, λ = 254 nm, t_R (min): minor = 6.9, major = 7.2.

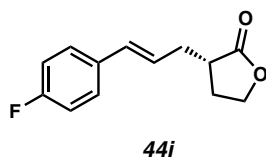


(*S,E*)-3-(3-(3,5-dimethoxyphenyl)allyl)dihydrofuran-2(3*H*)-one (44g): Product **44g** was purified by column chromatography (25% EtOAc in hexanes) to provide a colorless oil (38.8 mg, 0.15 mmol, 74% yield); 80% *ee*; [α]_D²⁵ 30.71 (*c* 0.80, CHCl₃); ¹H NMR (400 MHz, CDCl₃) δ 6.98 (d, J = 1.5 Hz, 2H), 6.92 – 6.85 (m, 1H), 6.49 – 6.38 (m, 1H), 6.14 (dt, J = 15.7, 7.1 Hz, 1H), 4.34 (td, J = 8.8, 3.1 Hz, 1H), 4.21 (td, J = 9.3, 6.9 Hz, 1H), 2.73 (dddd, J = 12.0, 10.4, 6.7, 3.6 Hz, 2H), 2.52 – 2.24 (m, 8H), 2.16 – 2.00 (m, 1H); ¹³C NMR (101 MHz, CDCl₃) δ 179.0, 138.2, 136.9, 133.3, 129.4, 129.3, 125.5, 124.2, 66.7, 39.4, 33.7, 27.9; IR (Neat Film, NaCl) 2914, 1768, 1600, 1438, 1374, 1153, 1022, 970, 844, 692 cm⁻¹; HRMS (MM) m/z calc'd for C₁₅H₁₉O₄ [M+H]⁺:

263.1278, found 263.1268; SFC Conditions: 15% IPA, 2.5 mL/min, Chiralcel OD-H column, λ = 254 nm, t_R (min): major = 5.50, minor = 6.85.

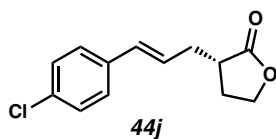


(*S,E*)-3-(3-(*p*-tolyl)allyl)dihydrofuran-2(3*H*)-one (44da): Product **44da** was purified by column chromatography (25% EtOAc in hexanes) to provide a colorless oil (38.9 mg, 0.18 mmol, 90% yield); 93% *ee*; $[\alpha]_D^{25}$ 38.205 (*c* 0.80, CHCl₃); ¹H NMR (400 MHz, CDCl₃) δ 7.26 (d, *J* = 7.9 Hz, 2H), 7.12 (d, *J* = 7.9 Hz, 2H), 6.49 – 6.42 (m, 1H), 6.11 (dt, *J* = 15.7, 7.2 Hz, 1H), 4.34 (td, *J* = 8.8, 3.1 Hz, 1H), 4.21 (td, *J* = 9.2, 6.9 Hz, 1H), 2.82 – 2.66 (m, 2H), 2.52 – 2.30 (m, 5H), 2.05 (dtd, *J* = 12.6, 9.6, 8.5 Hz, 1H); ¹³C NMR (101 MHz, CDCl₃) δ 179.0, 137.4, 134.2, 132.9, 129.4, 126.2, 124.8, 66.7, 39.4, 33.7, 27.9, 21.3; IR (Neat Film, NaCl) 2919, 1770, 1513, 1454, 1373, 1152, 1020, 972, 823, 680 cm⁻¹; HRMS (MM) *m/z* calc'd for C₁₄H₁₇O₂ [M+H]⁺: 217.1223, found 217.1224; SFC Conditions: 10% IPA, 2.5 mL/min, Chiralpak AD-H column, λ = 254 nm, t_R (min): major = 7.90, minor = 8.41.

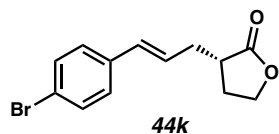


(*S,E*)-3-(3-(4-fluorophenyl)allyl)dihydrofuran-2(3*H*)-one (44i): Product **44i** was purified by column chromatography (25% EtOAc in hexanes) to provide a colorless oil (37.3 mg, 0.17 mmol, 85% yield); 92% *ee*; $[\alpha]_D^{25}$ -30.42 (*c* 0.80, CHCl₃); ¹H NMR (400 MHz, CDCl₃) δ 7.36 – 7.27 (m,

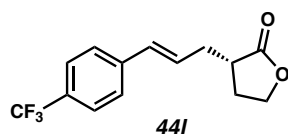
2H), 7.05 – 6.94 (m, 2H), 6.44 (dt, $J = 15.8, 1.4$ Hz, 1H), 6.08 (dt, $J = 15.7, 7.1$ Hz, 1H), 4.35 (td, $J = 8.8, 3.0$ Hz, 1H), 4.22 (td, $J = 9.3, 6.9$ Hz, 1H), 2.79 – 2.66 (m, 2H), 2.51 – 2.33 (m, 2H), 2.05 (dtd, $J = 12.7, 9.6, 8.5$ Hz, 1H); ^{13}C NMR (101 MHz, CDCl_3) δ 178.8, 163.5, 161.1, 133.2 (d, $J = 3.3$ Hz), 131.9, 127.8 (d, $J = 8.0$ Hz), 126.0 – 125.1 (m), 115.6 (d, $J = 21.6$ Hz), 66.7, 39.4, 33.6, 28.0; ^{19}F NMR (282 MHz, CDCl_3) δ -114.71 (tt, $J = 8.5, 5.3$ Hz); IR (Neat Film, NaCl) 3734, 2910, 2358, 1769, 1601, 1508, 1456, 1374, 1226, 1157, 1023, 970, 838 cm^{-1} ; HRMS (MM) m/z calc'd for $\text{C}_{13}\text{H}_{14}\text{FO}_2$ $[\text{M}+\text{H}]^+$: 219.0972, found 219.0974; SFC Conditions: 15% IPA, 2.5 mL/min, Chiralpak OD-H column, $\lambda = 280$ nm, t_{R} (min): major = 5.10, minor = 5.57.



(*S,E*)-3-(3-(4-chlorophenyl)allyl)dihydrofuran-2(3*H*)-one (44j): Product **44j** was purified by column chromatography (25% EtOAc in hexanes) to provide a colorless oil (44.4 mg, 0.19 mmol, 94% yield); 88% *ee*; $[\alpha]_{\text{D}}^{25}$ 32.55 (c 0.80, CHCl_3); ^1H NMR (400 MHz, CDCl_3) δ 7.26 (s, 4H), 6.43 (dt, $J = 15.7, 1.4$ Hz, 1H), 6.14 (dt, $J = 15.8, 7.1$ Hz, 1H), 4.34 (td, $J = 8.8, 3.0$ Hz, 1H), 4.21 (td, $J = 9.3, 6.8$ Hz, 1H), 2.84 – 2.67 (m, 2H), 2.53 – 2.31 (m, 2H), 2.04 (dtd, $J = 12.7, 9.7, 8.5$ Hz, 1H); ^{13}C NMR (101 MHz, CDCl_3) δ 178.8, 135.5, 133.2, 131.9, 128.8, 127.5, 126.7, 66.7, 39.3, 33.6, 28.0; IR (Neat Film, NaCl) 2910, 1770, 1490, 1454, 1405, 1375, 1326, 1154, 1091, 1023, 970, 830 cm^{-1} ; HRMS (MM) m/z calc'd for $\text{C}_{13}\text{H}_{14}\text{ClO}_2$ $[\text{M}+\text{H}]^+$: 237.0667, found 237.0682; SFC Conditions: 20% IPA, 2.5 mL/min, Chiralcel aOD-H column, $\lambda = 254$ nm, t_{R} (min): major = 5.30, minor = 5.90.

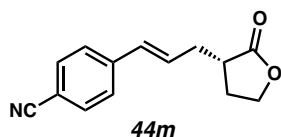


(*S,E*)-3-(3-(4-bromophenyl)allyl)dihydrofuran-2(3*H*)-one (44k): Product **44k** was purified by column chromatography (25% EtOAc in hexanes) to provide a colorless oil (43.5 mg, 0.154 mmol, 77% yield); 90% *ee*; $[\alpha]_{\text{D}}^{25}$ 13.95 (*c* 0.80, CHCl₃); ¹H NMR (400 MHz, CDCl₃) δ 7.45 – 7.38 (m, 2H), 7.24 – 7.17 (m, 2H), 6.42 (dd, *J* = 15.7, 1.5 Hz, 1H), 6.17 (dt, *J* = 15.8, 7.1 Hz, 1H), 4.34 (td, *J* = 8.8, 3.0 Hz, 1H), 4.21 (td, *J* = 9.3, 6.8 Hz, 1H), 2.85 – 2.62 (m, 2H), 2.53 – 2.30 (m, 2H), 2.04 (dtd, *J* = 12.7, 9.7, 8.6 Hz, 1H); ¹³C NMR (101 MHz, CDCl₃) δ 178.7, 135.9, 132.0, 131.8, 127.8, 126.8, 121.3, 66.7, 39.3, 33.6, 28.0; IR (Neat Film, NaCl) 2910, 1769, 1487, 1454, 1401, 1375, 1260, 1156, 1072, 1023, 969, 799, 707 cm⁻¹; HRMS (MM) *m/z* calc'd for C₁₃H₁₄BrO₂ [M+H]⁺: 281.0172, found 281.0175; SFC Conditions: 20% IPA, 2.5 mL/min, Chiralcel OD-H column, λ = 254 nm, *t_R* (min): major = 6.34, major = 7.18.

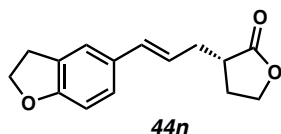


(*S,E*)-3-(3-(4-(trifluoromethyl)phenyl)allyl)dihydrofuran-2(3*H*)-one (44l): Product **44l** was purified by column chromatography (25% EtOAc in hexanes) to provide a colorless oil (44.9 mg, 0.17 mmol, 83% yield); 90% *ee*; $[\alpha]_{\text{D}}^{25}$ 30.89 (*c* 0.80, CHCl₃); ¹H NMR (400 MHz, CDCl₃) δ 7.55 (d, *J* = 8.2 Hz, 2H), 7.44 (d, *J* = 8.1 Hz, 2H), 6.52 (dd, *J* = 15.9, 1.7 Hz, 1H), 6.29 (dt, *J* = 15.8, 7.1 Hz, 1H), 4.36 (td, *J* = 8.8, 2.9 Hz, 1H), 4.22 (td, *J* = 9.4, 6.8 Hz, 1H), 2.84 – 2.68 (m, 2H), 2.56 – 2.34 (m, 2H), 2.05 (dtd, *J* = 12.7, 9.8, 8.5 Hz, 1H); ¹³C NMR (101 MHz, CDCl₃) δ 178.6, 140.4,

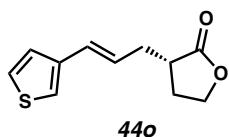
131.8, 129.3 (q, $J = 32.3$ Hz), 126.4, 125.5 (q, $J = 3.8$ Hz), 122.9, 66.7, 39.2, 33.7, 28.0; ^{19}F NMR (282 MHz, CDCl_3) δ -62.50; IR (Neat Film, NaCl) 2914, 1770, 1614, 1414, 1376, 1326, 1157, 1119, 1067, 1018, 970, 834, 682 cm^{-1} ; HRMS (MM) m/z calc'd for $\text{C}_{14}\text{H}_{14}\text{F}_3\text{O}_2$ $[\text{M}+\text{H}]^+$: 271.0940, found 271.0945; SFC Conditions: 10% IPA, 2.5 mL/min, Chiralcel OD-H column, $\lambda = 210$ nm, t_R (min): major = 5.32, minor = 5.86.



(*S,E*)-4-(3-(2-oxotetrahydrofuran-3-yl)prop-1-en-1-yl)benzonitrile (44m): Product **44m** was synthesized according to the General Procedure, but with a doubled catalyst loading (10 mol% CuCl_2 , 12 mol%, **L73**, 26 mol% LiHMDS). The crude product was purified by column chromatography (40% EtOAc in hexanes) to provide a colorless oil (43.6 mg, 0.19 mmol, 96% yield, 98:2 E:Z); 86% *ee*; $[\alpha]_D^{25}$ 48.79 (c 0.80, CHCl_3); ^1H NMR (400 MHz, CDCl_3) δ 7.61 – 7.55 (m, 2H), 7.46 – 7.39 (m, 2H), 6.50 (dd, $J = 15.8, 1.5$ Hz, 1H), 6.33 (dt, $J = 15.8, 7.0$ Hz, 1H), 4.40 – 4.31 (m, 1H), 4.22 (td, $J = 9.4, 6.7$ Hz, 1H), 2.85 – 2.68 (m, 2H), 2.56 – 2.35 (m, 2H), 2.13 – 1.96 (m, 1H); ^{13}C NMR (101 MHz, CDCl_3) δ 178.5, 141.4, 132.5, 131.6, 130.2, 126.8, 119.0, 110.8, 66.7, 39.2, 33.7, 28.1; IR (Neat Film, NaCl) 3432, 2924, 2224, 1766, 1604, 1375, 1156, 1021, 970, 837 cm^{-1} ; HRMS (MM) m/z calc'd for $\text{C}_{14}\text{H}_{14}\text{NO}_2$ $[\text{M}+\text{H}]^+$: 228.1019, found 228.1020; SFC Conditions: 25% IPA, 2.5 mL/min, Chiralcel OD-H column, $\lambda = 280$ nm, t_R (min): major = 4.19, minor = 4.46.

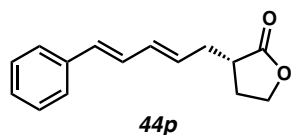


(S,E)-3-(3-(2,3-dihydrobenzofuran-5-yl)allyl)dihydrofuran-2(3H)-one (44n): Compound **44n** was purified by flash column chromatography (40% EtOAc/hexanes) to afford the title compound as a colorless amorphous solid (27.6 mg, 0.11 mmol, 56% yield); 95% *ee*; $[\alpha]_{\text{D}}^{23}$ 35.0 (*c* 1.00, CHCl_3); ^1H NMR (400 MHz, CDCl_3) δ 7.24 (s, 1H), 7.08 (dd, *J* = 8.2, 1.4 Hz, 1H), 6.71 (d, *J* = 8.2 Hz, 1H), 6.41 (d, *J* = 15.7 Hz, 1H), 5.98 (dt, *J* = 15.7, 7.2 Hz, 1H), 4.56 (t, *J* = 8.7 Hz, 2H), 4.33 (td, *J* = 8.8, 3.2 Hz, 1H), 4.21 (td, *J* = 9.2, 6.9 Hz, 1H), 3.19 (t, *J* = 8.6 Hz, 2H), 2.75 – 2.67 (m, 2H), 2.47 – 2.41 (m, 2H), 2.39 – 2.33 (m, 2H), 2.05 (dtd, *J* = 12.9, 9.5, 8.6 Hz, 1H); ^{13}C NMR (100 MHz, CDCl_3) \square 179.0, 159.9, 132.9, 129.9, 127.6, 126.7, 122.9, 122.5, 109.3, 71.5, 66.8, 39.5, 33.7, 29.7, 27.8; IR (Neat Film, NaCl) 2912, 1764, 1608, 1491, 1374, 1244, 1150, 1022, 980 cm^{-1} ; HRMS (MM) *m/z* calc'd for $\text{C}_{15}\text{H}_{17}\text{O}_3$ $[\text{M}+\text{H}]^+$: 245.1172, found 245.1171; SFC Conditions: 20% IPA, 2.5 mL/min, Chiralcel OD-H column, λ = 210 nm, t_{R} (min): minor = 6.93, major = 6.05.

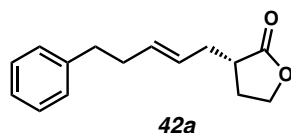


(S,E)-3-(3-(thiophen-3-yl)allyl)dihydrofuran-2(3H)-one (44o): Product **44o** was purified by column chromatography (25% EtOAc in hexanes) to provide a colorless oil (29.6 mg, 0.142 mmol, 71% yield); 90% *ee*; $[\alpha]_{\text{D}}^{25}$ 45.11 (*c* 0.80, CHCl_3); ^1H NMR (400 MHz, CDCl_3) δ 7.26 (s, 1H), 7.18 (dd, *J* = 5.0, 1.4 Hz, 1H), 7.10 (dd, *J* = 3.0, 1.3 Hz, 1H), 6.49 (dd, *J* = 15.8, 1.6 Hz, 1H), 6.09 – 5.91 (m, 1H), 4.43 – 4.28 (m, 1H), 4.25 – 4.16 (m, 1H), 2.77 – 2.63 (m, 2H), 2.49 – 2.32 (m,

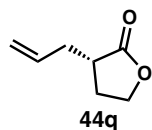
2H), 2.14 – 1.97 (m, 1H); ^{13}C NMR (101 MHz, CDCl_3) δ 178.9, 139.7, 127.4, 126.2, 125.8, 125.0, 121.7, 66.7, 39.4, 33.6, 27.9; IR (Neat Film, NaCl) 3098, 2994, 2909, 1766, 1482, 1454, 1374, 1201, 1183, 1151, 1094, 1022, 967, 862, 832, 772, 696, 673, 616 cm^{-1} ; HRMS (MM) m/z calc'd for $\text{C}_{11}\text{H}_{13}\text{O}_2\text{S}$ $[\text{M}+\text{H}]^+$: 209.0631, found 209.0637; SFC Conditions: 20% IPA, 2.5 mL/min, Chiralcel OD-H column, λ = 254 nm, t_R (min): major = 4.76, major = 5.32.



(S)-3-((2E,4E)-5-phenylpenta-2,4-dien-1-yl)dihydrofuran-2(3H)-one (44p): Product **44p** was purified by column chromatography (25% EtOAc in hexanes) to provide a colorless oil (34.7 mg, 0.152 mmol, 76% yield); 83% *ee*; $[\alpha]_{\text{D}}^{25}$ 34.815 (*c* 0.80, CHCl_3); ^1H NMR (400 MHz, CDCl_3) δ 7.41 – 7.35 (m, 2H), 7.31 (dd, J = 8.5, 6.8 Hz, 2H), 7.25 – 7.19 (m, 1H), 6.75 (ddd, J = 15.7, 10.4, 0.8 Hz, 1H), 6.50 (d, J = 15.7 Hz, 1H), 6.30 (ddq, J = 15.2, 10.4, 1.1 Hz, 1H), 5.85 – 5.69 (m, 1H), 4.35 (td, J = 8.8, 3.1 Hz, 1H), 4.21 (td, J = 9.3, 6.9 Hz, 1H), 2.75 – 2.62 (m, 2H), 2.44 – 2.33 (m, 2H), 2.03 (dtd, J = 12.8, 9.6, 8.5 Hz, 1H); ^{13}C NMR (101 MHz, CDCl_3) δ 178.9, 137.3, 133.7, 131.8, 130.2, 128.7, 128.5, 127.6, 126.4, 66.7, 39.4, 33.5, 28.0; IR (Neat Film, NaCl) 3748, 3671, 3022, 2910, 2358, 1769, 1684, 1652, 1595, 1558, 1540, 1506, 1489, 1448, 1374, 1309, 1157, 1023, 992, 749, 693, 668, 625 cm^{-1} ; HRMS (MM) m/z calc'd for $\text{C}_{15}\text{H}_{17}\text{O}_2$ $[\text{M}+\text{H}]^+$: 229.1223, found 229.1227; SFC Conditions: 20% IPA, 2.5 mL/min, Chiralcel OD-H column, λ = 280 nm, t_R (min): major = 7.08, major = 7.73.

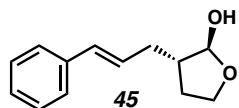


(*S,E*)-3-(5-phenylpent-2-en-1-yl)dihydrofuran-2(3*H*)-one (42a): Product **42a** was purified by column chromatography (25% EtOAc in hexanes) to provide a colorless oil (44.4 mg, 0.19 mmol, 96% yield); 87% *ee*; $[\alpha]_{\text{D}}^{25}$ 20.90 (*c* 0.80, CHCl₃); ¹H NMR (400 MHz, CDCl₃) δ 7.26 (m, 2H), 7.21 – 7.14 (m, 3H), 5.55 (dtt, *J* = 14.8, 6.7, 1.3 Hz, 1H), 5.36 (dtt, *J* = 15.3, 6.9, 1.4 Hz, 1H), 4.24 (td, *J* = 8.8, 3.3 Hz, 1H), 4.15 (td, *J* = 9.1, 6.9 Hz, 1H), 2.68 (dd, *J* = 8.4, 6.9 Hz, 2H), 2.62 – 2.44 (m, 2H), 2.42 – 2.29 (m, 2H), 2.28 – 2.14 (m, 2H), 1.87 (dtd, *J* = 12.8, 9.5, 8.6 Hz, 1H); ¹³C NMR (101 MHz, CDCl₃) δ 179.2, 141.8, 133.1, 128.6, 128.4, 126.6, 125.9, 66.7, 39.3, 35.8, 34.3, 33.2, 27.6; IR (Neat Film, NaCl) 3520, 2918, 1770, 1602, 1496, 1454, 1374, 1297, 1251, 1209, 1171, 1149, 1084, 1024, 972, 906, 843, 748, 701, 666 cm⁻¹; HRMS (MM) *m/z* calc'd for C₁₅H₁₉O₂ [M+H]⁺: 231.1384, found 231.1384; SFC Conditions: 10% IPA, 2.5 mL/min, Chiralpak AD-H column, λ = 210 nm, *t_R* (min): major = 5.84, major = 6.29.



(*S*)-3-allyldihydrofuran-2(3*H*)-one (44r): Product **44r** was synthesized according to the General Procedure, but with a doubled catalyst loading (10 mol% CuCl₂, 12 mol%, **L73**, 26 mol% LiHMDS). The crude product was purified by column chromatography (25% EtOAc in hexanes) to provide a colorless oil (24.2 mg, 96% yield, 80% *ee*); ¹H NMR (300 MHz, CDCl₃) δ 5.78 (ddt, *J* = 16.9, 10.1, 6.9 Hz, 1H), 5.20 – 5.05 (m, 2H), 4.38 – 4.28 (m, 1H), 4.20 (td, *J* = 9.2, 6.9 Hz, 1H), 2.71 – 2.53 (m, 2H), 2.43 – 2.18 (m, 2H), 2.08 – 1.91 (m, 1H). All characterization data match those reported.^{9c} The purified product was converted to the corresponding methyl acrylate species via cross metathesis for SFC analysis (see Product Transformations).

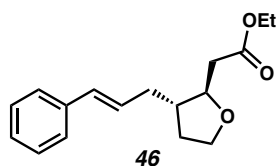
3.9.2.6 Procedures and Spectroscopic Data for Product Transformations



(2*S*,3*S*)-3-cinnamyltetrahydrofuran-2-ol (45): Adapted from a previously reported procedure.³⁵

To a solution of lactone (12.4 mg, 0.061 mmol, 1.0 equiv) in dichloromethane (0.4 mL) at $-78\text{ }^{\circ}\text{C}$ was added diisobutylaluminium hydride (12 μL , 0.067 mmol, 1.1 equiv) in dichloromethane (2.2 mL) dropwise. The reaction was allowed to stir for 30 min at $-78\text{ }^{\circ}\text{C}$. The reaction was quenched slowly with MeOH, and then saturated aqueous potassium tartrate solution was added and the reaction was allowed to warm to room temperature. After 2 h, the layers were separated, and the aqueous layer was extracted 3 times with diethyl ether. The organic layers were combined, washed with brine, dried over sodium sulfate, and concentrated. The crude product was purified by column chromatography to afford product **45** as a white solid (11.9 mg, 0.058 mmol, 95 % yield, 68:32 anti:syn); $[\alpha]_{\text{D}}^{25}$ 4.20 (c 0.75, CHCl_3); **major, anti:** ^1H NMR (400 MHz, CDCl_3) δ 7.31 – 7.20 (m, 4H), 7.17 – 7.11 (m, 1H), 6.39 – 6.33 (m, 1H), 6.15 – 6.07 (m, 1H), 5.19 (d, $J = 1.5\text{ Hz}$, 1H), 4.00 (td, $J = 8.0, 6.6\text{ Hz}$, 1H), 3.91 (td, $J = 8.1, 5.5\text{ Hz}$, 1H), 2.45 (dtd, $J = 14.2, 7.1, 1.4\text{ Hz}$, 1H), 2.34 – 2.18 (m, 3H), 2.18 – 2.06 (m, 1H), 1.65 – 1.55 (m, 1H); ^{13}C NMR (101 MHz, CDCl_3) δ 137.5, 131.8, 128.67, 128.66, 127.3, 126.2, 102.7, 67.1, 46.1, 35.8, 29.7. **minor, syn:** ^1H NMR (400 MHz, CDCl_3) δ 7.31 – 7.20 (m, 4H), 7.17 – 7.11 (m, 1H), 6.43 – 6.38 (m, 1H), 6.24 – 6.16 (m, 1H), 5.30 (d, $J = 4.4\text{ Hz}$, 1H), 4.06 (ddd, $J = 9.3, 8.2, 2.7\text{ Hz}$, 1H), 3.78 (ddd, $J = 9.4, 8.2, 7.3\text{ Hz}$, 1H), 2.45 (dtd, $J = 14.2, 7.1, 1.4\text{ Hz}$, 1H), 2.18 – 2.06 (m, 1H), 1.98 (dtd, $J = 12.0, 7.5, 2.7\text{ Hz}$,

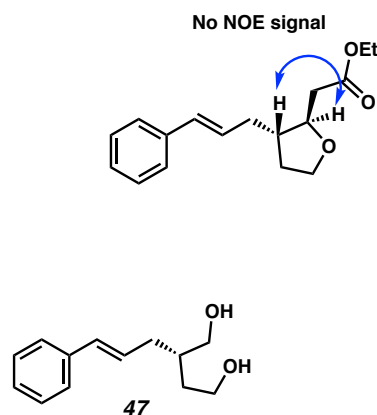
1H), 1.76 (tt, $J = 11.8, 9.2$ Hz, 1H), 1.64 – 1.45 (m, 2H); ^{13}C NMR (101 MHz, CDCl_3) δ 137.7, 131.1, 128.7, 128.1, 127.2, 126.1, 98.4, 67.4, 44.7, 32.2, 28.8. **major, anti** and **minor, syn**: IR (Neat Film, NaCl) 3390, 3024, 2936, 2892, 1598, 1494, 1500, 1266, 1119, 1015, 967, 912, 744, 694 cm^{-1} ; HRMS (MM) m/z calc'd for $\text{C}_{13}\text{H}_{15}\text{O}$ $[\text{M}-\text{OH}]^+$: 187.1117, found 187.1119.



ethyl 2-((2R,3S)-3-cinnamyltetrahydrofuran-2-yl)acetate (46): In a flame-dried round bottom flask under argon was added NaH (3.5 mg, 0.0874 mmol, 1.5 equiv) and THF (0.3 mL). To the resulting suspension was added triethyl phosphonoacetate (17.3 μL , 0.0874 mmol, 1.5 equiv) slowly. After 30 min, the reaction was cooled to $0\text{ }^{\circ}\text{C}$ and lactol **45** (11.9 mg, 0.058 mmol, 1.0 equiv) in THF (0.6 mL) was added slowly. The reaction was allowed to warm to room temperature overnight. The reaction was subsequently quenched with saturated aqueous NaHCO_3 , and extracted with ethyl acetate three times. The organic layers were then combined, dried over Na_2SO_4 , and concentrated. The crude oil was purified by column chromatography to afford product **46** (13.4 mg, 0.049 mmol, 84% yield, 95:5 anti:syn); 93% ee; $[\alpha]_{\text{D}}^{25}$ 18.74 (c 0.75, CHCl_3); ^1H NMR (400 MHz, CDCl_3) δ 7.38 – 7.27 (m, 4H), 7.24 – 7.18 (m, 1H), 6.47 – 6.39 (m, 1H), 6.18 (dt, $J = 15.8, 7.2$ Hz, 1H), 4.15 (q, $J = 7.1$ Hz, 2H), 3.99 (ddd, $J = 7.9, 6.6, 4.8$ Hz, 1H), 3.92 – 3.81 (m, 2H), 2.64 – 2.46 (m, 2H), 2.40 (dddd, $J = 14.1, 7.1, 5.7, 1.4$ Hz, 1H), 2.25 (dddd, $J = 14.0, 8.4, 7.1, 1.4$ Hz, 1H), 2.18 – 1.97 (m, 2H), 1.76 – 1.64 (m, 1H), 1.25 (t, $J = 7.1$ Hz, 3H); ^{13}C NMR (101 MHz, CDCl_3) δ 171.5, 137.5, 131.7, 128.7, 128.2, 127.3, 126.1, 80.3, 67.3, 60.7, 44.4, 40.2,

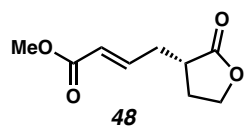
36.3, 32.1, 14.3; IR (Neat Film, NaCl) 3058, 3024, 2978, 2936, 2873, 1736, 1598, 1478, 1495, 1449, 1368, 1302, 1261, 1204, 1158, 1070, 1032, 967, 843, 805, 746, 694, 670, 652 cm^{-1} ; HRMS (MM) m/z calc'd for $\text{C}_{17}\text{H}_{23}\text{O}_3$ $[\text{M}+\text{H}]^+$: 275.1642, found 275.1649. Please note that the NMR data listed is for the major diastereomer. SFC Conditions: 15% IPA, 2.5 mL/min, Chiralcel OJ-H column, $\lambda = 254$ nm, t_R (min): minor= 3.07, major= 3.39.

Stereochemical Assignment:



(S)-2-cinnamylbutane-1,4-diol (47): Product 6 was synthesized according to a slightly modified, previously reported procedure.³⁶ To a suspension of lithium aluminum hydride (3.57 mg, 0.094 mmol, 1.0 equiv) in diethyl ether (0.5 mL) was added a solution of lactone **44a** (19.0 mg, 0.094 mmol, 1.0 equiv) in diethyl ether (0.4 mL), maintaining reflux. Then, the reaction was heated to 40 °C and refluxed for 3 h. The reaction was then quenched by sequentially adding methanol, water, and 2M HCl. Then, brine was added and the aqueous layer was extracted five times with ethyl acetate. The crude diol was then purified by column chromatography to afford the desired product **47** as a clear oil (18.4 mg, 0.089 mmol, 95% yield); 94% ee $[\alpha]_D^{25} -10.61$ (c 0.75, CHCl_3); ^1H NMR (400 MHz, CDCl_3) δ 7.38 – 7.26 (m, 4H), 7.23 – 7.17 (m, 1H), 6.46 – 6.34 (m, 1H), 6.18

(dt, J = 15.8, 7.3 Hz, 1H), 3.78 (ddd, J = 10.8, 6.4, 4.5 Hz, 1H), 3.72 – 3.44 (m, 5H), 2.31 – 2.13 (m, 2H), 1.90 – 1.68 (m, 2H), 1.60 (dtd, J = 14.5, 8.0, 4.4 Hz, 1H); ^{13}C NMR (101 MHz, CDCl_3) δ 137.5, 131.9, 128.6, 127.2, 126.1, 66.0, 61.1, 39.7, 35.6; IR (Neat Film, NaCl) 3322, 3080, 3058, 3024, 2921, 1754, 1598, 1494, 1448, 1053, 967, 742, 694, 661 cm^{-1} ; HRMS (MM) m/z calc'd for $\text{C}_{13}\text{H}_{19}\text{O}_2$ $[\text{M}+\text{H}]^+$: 207.1380, found 207.1383. SFC Conditions: 25% IPA, 2.5 mL/min, Chiralcel OD-H column, λ = 254 nm, t_R (min): minor = 3.64, major = 4.04.

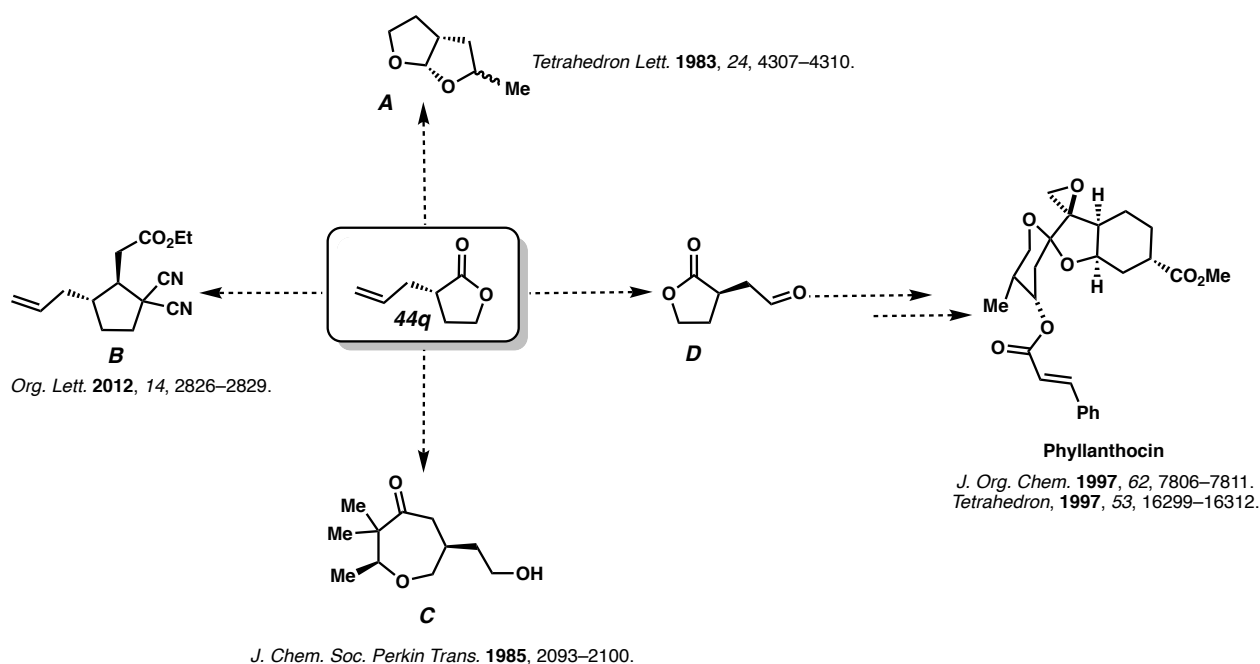


methyl (S,E)-4-(2-oxotetrahydrofuran-3-yl)but-2-enoate (48): Adapted from a previously reported procedure.³⁷ To a solution of lactone **44q** (12.1 mg, 0.096 mmol, 1.0 equiv) and methyl acrylate (86 μL , 0.96 mmol, 1.0 equiv) in dichloromethane (0.7 mL) was added Grubbs II catalyst (4.8 mg, 0.00576 mmol, 6 mol%). The reaction was sealed and heated to 40 $^{\circ}\text{C}$ for 3 h. The crude reaction mixture was filtered with a small pad of SiO_2 , and concentrated. The resulting crude oil was then purified by column chromatography to afford product **48** as a yellow oil (16.8 mg, 0.091 mmol, 95% yield); 80% ee $[\alpha]_{\text{D}}^{25}$ 19.52 (c 0.5, CHCl_3); ^1H NMR (400 MHz, CDCl_3) δ 6.91 (dt, J = 15.4, 7.2 Hz, 1H), 5.93 (dt, J = 15.6, 1.5 Hz, 1H), 4.37 (td, J = 8.9, 2.5 Hz, 1H), 4.28 – 4.17 (m, 1H), 3.74 (s, 3H), 2.85 – 2.66 (m, 2H), 2.46 – 2.34 (m, 2H), 2.06 – 1.91 (m, 1H); ^{13}C NMR (101 MHz, CDCl_3) δ 178.1, 166.5, 144.6, 123.8, 77.2, 66.6, 51.8, 38.5, 32.9, 28.3; IR (Neat Film, NaCl) 2954, 1764, 1719, 1656, 1438, 1376, 1277, 1155, 1022, 988, 702 cm^{-1} ; HRMS (MM) m/z calc'd for $\text{C}_{19}\text{H}_{12}\text{O}_4^+$ $[\text{M}+\text{H}]^+$: 185.0808, found 185.0812. SFC Conditions: 25% IPA, 2.5 mL/min, Chiralpak IC column, λ = 210 nm, t_R (min): major = 9.17, minor = 10.89.

3.10 OTHER POTENTIAL PRODUCT TRANSFORMATIONS

In addition to the product transformations reported above, there are a number of other transformations reported in the literature that lead to very useful products (Scheme 3.11.1).

Scheme 3.11.1. Potential Product Transformations for **44q**



Furthermore, chiral lactols such as **45** can also be converted to acyclic molecules possessing propargylic stereocenters (*Org. Lett.* **2012**, 14, 3648–3651.) or allylic stereocenters (*J. Am. Chem. Soc.* **2017**, 139, 13272–13275.) without loss of enantiomeric excess. In addition, the

high levels of enantiomeric excess can also be retained under mild lactone ring opening reactions. Zhang and coworkers (*ACIE*, **2013**, 5807–5812.) reported a ring opening with a Weinreb amide and subsequent addition of ethylmagnesium bromide to form α -chiral ketones with full retention of enantiomeric excess. Koert and coworkers also demonstrate that an α -chiral γ -butyrolactone can undergo ring opening of the lactone with HBr without loss of stereochemistry: *Chem. Eur. J.* **2013**, *19*, 7423–7436. For an example with HCl, see: *Helv. Chem. Acta*, **1979**, *62*, 474–480.

3.11 REFERENCES

1. Behenna, D. C.; Mohr, J. T.; Sherden, N. H.; Marinescu, S. C.; Harned, A. M.; Tani, K.; Seto, M.; Ma, S.; Novák, Z.; Krout, M. R.; McFadden, R. M.; Roizen, J. L.; Enquist Jr. J. A.; White, D. E.; Levine, S. R.; Petrova, K. V.; Iwashita, A.; Virgil, S. C.; Stoltz, B. M. *Chem. Eur. J.* **2011**, *17*, 14199.
2. Liu, Y.; Han, S.-J.; Liu, W. -B.; Stoltz, B. M. *Acc. Chem. Res.* **2015**, *48*, 740–751. (b)
3. Ngamnithiporn, A.; Jette, C.; Bachman, S.; Virgil, S.; Stoltz, B. M. *Chem. Sci.* **2018**, *9*, 2547–2551.
4. Seitz, M.; Reiser, O. *Curr. Opin. Chem. Biol.* **2005**, *9*, 285-292.
5. Mao, B.; Fañanás-Mastral, M.; Feringa, B. L. *Chem. Rev.* **2017**, *117*, 10502–10566.
6. Meyers, A. I.; Yamamoto, Y.; Mihelich, E. D.; Bell, R. A. *J. Org. Chem.* **1980**, *45*, 2792–2796.
7. Madelaine, C.; Valerio, V.; Maulide, N. *Angew. Chem. Int. Ed.* **2010**, *49*, 1583–1586, *Angew. Chem.* **2010**, *122*, 1628–1631. Huang, Z.; Chen, Z.; Lim, L. H.; Quang, G. C. P.;

- Hirao, H.; Zhou, J. *Angew. Chem. Int. Ed.* **2013**, *52*, 5807–5812, *Angew. Chem.* **2013**, *125*, 5919–5924.
8. Tsuji, J.; Takahashi, H.; Morikawa, M. *Tetrahedron Lett.*, **1965**, *6*, 4387–4388.
9. (a) James, J.; Guiry, P. J. *ACS Catal.* **2017**, *7*, 1397–1402. (b) Nascimento de Oliveira, M.; Fournier, J.; Arseniyadis, S.; Cossy, J. A. *Org. Lett.* **2017**, *19*, 14–17. (c) Meletis, P.; Patil, M.; Thiel, W.; Frank, W.; Braun, M. *Chem. Eur. J.* **2011**, *17*, 11243–11249. (d) Jiang, X.; Hartwig, J. F. *Angew. Chem. Int. Ed.* **2017**, *56*, 8887–8891. *Angew. Chem.* **2017**, *129*, 9013–9017.
10. Hayashi, M.; Bachman, S.; Hashimoto, S.; Eichman, C. C.; Stoltz, B. M. *J. Am. Chem. Soc.* **2016**, *138*, 8997–9000. (c) Han, S.-J.; Doi, R.; Stoltz, B. M. *Angew. Chem. Int. Ed.* **2016**, *55*, 7437–7440, *Angew. Chem.* **2016**, *128*, 7563–7566.
11. Li, D.; Ohmiya, H.; Sawamura, M. *J. Am. Chem. Soc.* **2011**, *133*, 5672–5675.
12. Zhang, Y. -Z.; Zhu, S. -F.; Wang, L.-X. Zhou, Q. -L. *Angew. Chem. Int. Ed.* **2008**, *47*, 8496–8498.
13. (a) Mulqi, M.; Stephens, F. S.; Vagg, R. S. *Inorg. Chim. Acta*, **1981**, *51*, 9–14. (b) Mulqi, M.; Stephens, F. S.; Vagg, R. S. *Inorg. Chim. Acta*, **1981**, *52*, 177–182. (c) Fan, X.; Zhang, X.; Li, C.; Gu, Z. *ACS Catal.* **2019**, *9*, 2286–2291. For an example of Cu/mono-picolinyl complexes in catalysis: (d) Carlo Sambiagio. Investigations on the use of Amidic Ligands in Copper-Catalyzed Arylation Reactions, Ph.D. Dissertation, University of Leeds, Leeds, West Yorkshire, England, 2015. A report on the use of Cu/L21 in catalysis was published one year after these experiments were conducted: (d) Fan, X.; Zhang, X.; Li, C.; Gu, Z. *ACS Catal.* **2019**, *9*, 2286–2291.

14. (a) Trost, B. M.; Hachiya, I. *J. Am. Chem. Soc.* **1998**, *120*, 1104–1105. (b) Krska, S.; Hughes, D. L.; Reamer, R. A.; Mathre, D. J.; Sun, Y.; Trost, B. M. *J. Am. Chem. Soc.* **2002**, *124*, 12656–12657.
15. Trost, B. M.; Van Vranken, D. L. *Chem. Rev.* **1996**, *96*, 395–422.
16. Chae, J.; Yun, J.; Buchwald, S. L. *Org. Lett.* 2004, *6*, 4809–4812.
17. Oisaki, K.; Suto, Y.; Kanai, M.; Shibasaki, M.; *J. Am. Chem. Soc.* **2003**, *125*, 5644–5645.
18. Krska, S. W.; Hughes, D. L.; Reamer, R. A.; Mathre, D. J.; Sun, Y.; Trost, B. M. *J. Am. Chem. Soc.* **2002**, *124*, 43, 12656–12657.
19. Sprague, D. J.; Nugent, B. M.; Yoder, R. A.; Vara, B. A.; Johnston, J. N. *Org. Lett.* **2015**, *17*, 880–883.
20. Belda, O.; Kaiser, N. –F.; Bremberg, U.; Larhed, M.; Hallberg, A.; Moberg, C. *J. Org. Chem.* **2000**, *65*, 5868–5870.
21. Jiang, Y. –J.; Zhang, G. –P.; Huang, J. –Q.; Chen, D.; Ding, C. –H.; Hou, X. –L. *Org. Lett.* **2017**, *19*, 4880–4883.
22. Genoni, A.; Benaglia, M.; Puglisi, A.; Rossi, S. *Synthesis*, **2011**, *12*, 1926–1929.
23. Rexiti, R.; Lu, J.; Wang, G.; Sha, F.; Wu, X. –Y. *Tetrahedron: Asymmetry* **2016**, *27*, 923–929.
24. Trost, B. M.; Yong, Z.; *Chem. Eur. J.* **2011**, *17*, 2916–2922.
25. Guangyou, Z.; Yuqing, L.; Zhaohui, W.; Nohira, H.; Hirose, T. *Tetrahedron: Asymmetry* **2003**, *14*, 3297–3300.
26. Ouali, A.; Taillefer, M.; Spindler, J. –F.; Jutand, A. *Organometallics*, **2007**, *26*, 65–74.

27. Chen, H. –Y.; Hu, Z. –Y.; Tang, C. –P.; Quinn, T. J.; Feng, Y.; Yao, S.; Ye, Y.; *Tetrahedron Letters*, **2013**, *54*, 4250–4253.
28. Bouziane, A.; H  lou, M.; Carboni, B.; Carreaux, F.; Demerseman, B.; Bruneau, C.; Renaud, J.–L. *Chem. Eur. J.* **2008**, *14*, 5630–5637.
29. Fuchter, M. J.; Levy, J.–N. *Org. Lett.* **2008**, *10*, 4919–4922.
30. Trost, B. M.; Rao, M.; Dieskau, A. P. *J. Am. Chem. Soc.* **2013**, *135*, 18697–18704.
31. Falciola, C. A.; Tissot-Crosset, K.; Reyneri, H.; Alexakis, A. *Adv. Synth. Catal.* **2008**, *350*, 1090–1100.
32. L  lsberg, W.; Ye, S.; Schmalz, H.–G. *Adv. Synth. Catal.* **2010**, *352*, 2023–2031.
33. Le, H.; Kyne, R. E.; Brozek, L. A.; Morken, J. P. *Org. Lett.* **2013**, *15*, 1432–1435.
34. Cormier, M.; Ahmad, M.; Maddaluno, J.; de Paolis, M.; *Organometallics*, **2017**, *36*, 4920–4927.
35. Lacharity, J. J.; Fournier, J.; Lu, P.; Mailyan, A. K.; Herrmann, A. T. Zakarian, A. *J. Am. Chem. Soc.* **2017**, *139*, 132721–13275.
36. Koci  nski, P.; Jarowicki, K.; Marczak, S.; *Synthesis*, **1991**, 1191–1200.
37. Starkov, P.; Moore, J. T.; Duquette, D. C.; Stoltz, B. M.; Marek, I. *J. Am. Chem. Soc.* **2017**, *139*, 9615–9620.

APPENDIX 5

Challenging Substrates in Cu-Catalyzed Enantioselective Allylic Alkylation with Silyl Ketene Acetals[†]

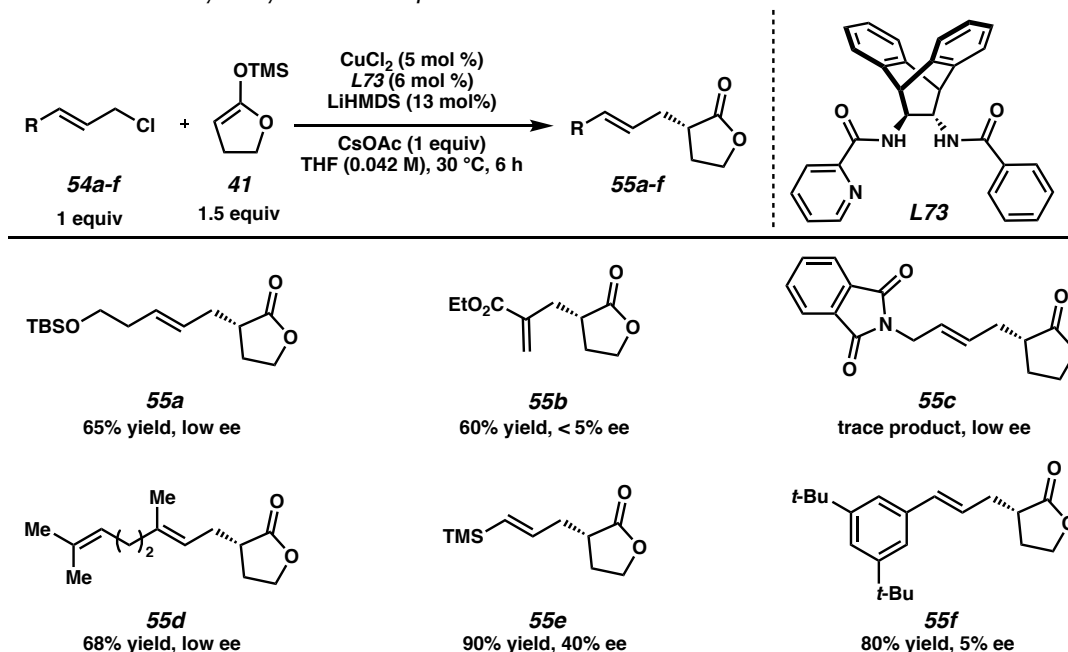
A5.1 INTRODUCTION

Although we found that our developed conditions for the Cu-catalyzed enantioselective allylic alkylation of a γ -butyrolactone-derived silyl ketene acetal were fairly robust and tolerant of a wide range of reactivity on the electrophile component, some substrates proved to be very challenging. Below are allylic electrophiles that resulted in poor reactivity, selectivity, or both. In addition, we examined additional nucleophiles in order to understand why the optimized system is limited to γ -butyrolactones.

A5.2 LIMITATIONS IN THE ALLYLIC CHLORIDE ELECTROPHILE

[†] This work was performed in collaboration with the Hadt Lab at Caltech. Additionally, this research has been published and adapted with permission from Jette, C. I.; Tong, Z. J.; Hadt, R. G.; Stoltz B. M. *Angew. Chem. Int. Ed.* **2020**, 59, 2033–2038. Copyright 2020 Wiley-VCH. Alexander Q. Cusumano is thanked for assistance and helpful discussions.

Table A5.2.1. Bulky Allylic Electrophiles^a



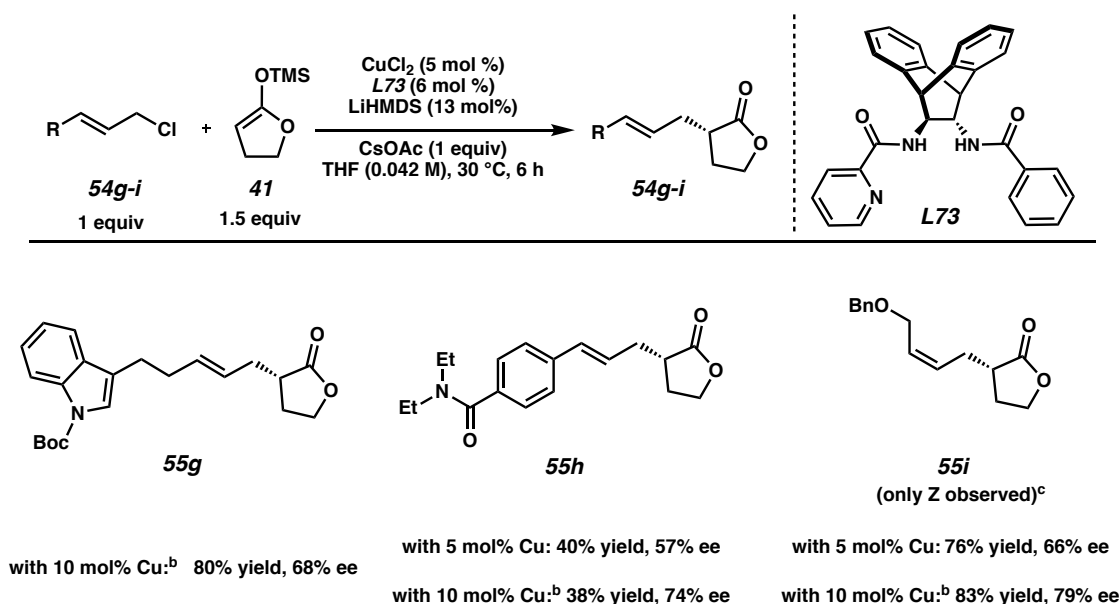
[a] Isolated yields on 0.2 mmol scale. SFC analysis was used to determine ee. See Chapter 3 for reaction set-up.

Although we were able to tolerate a wide range of functionality on the electrophile, a number of limitations were noted. The use of electrophiles possessing a large degree of steric bulk at the α -position resulted in the formation of products in moderate yields and low ee. This type of behavior was noted with α - α -disubstituted electrophiles, such as **43s** discussed in Chapter 4 (Scheme 4.7.1), as well as α -monosubstituted electrophiles possessing very bulky substituents. Electrophiles possessing substituents such as a pendant silyl ether (**55a**, Table A5.2.1), an alkyl silane (**55e**), and 3,5-di-tert-butylphenyl (**55f**) resulted in moderate to high yields, but racemic product. In addition, we found that with a geraniol derivative (**55d**) we observed similar behavior to **43s**. In the case of an electrophile possessing a pendant ethyl ester (**55b**), we also observed low ee. Because we previously noted that substitution at the β -position does not seem to have a significant effect on the overall reaction outcome (Chapter 4, Scheme

4.7.1), the low ee could likely be attributed to a competitive 1,4-addition pathway, rather than sterics. Finally, in the case of the allylic electrophile possessing a phthalamide (**55c**), we obtained the product in both low yield and low ee.

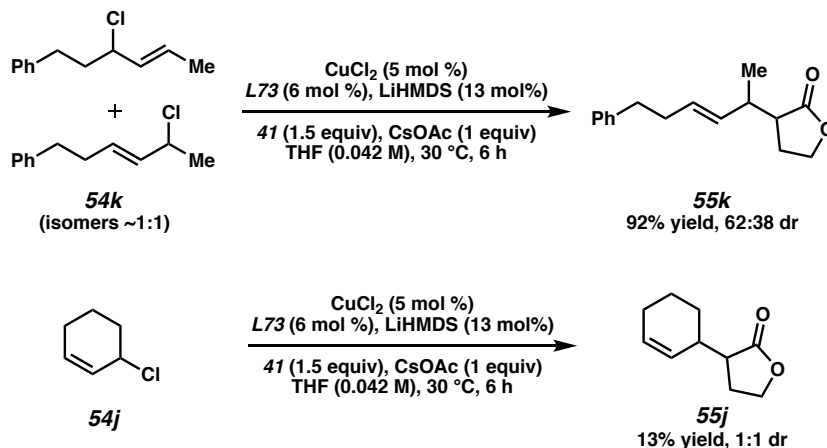
Allylic electrophiles possessing functionality that can competitively bind to the Cu catalyst, such as an indole, amide, or ether generally resulted in lower reactivity and ee's (Table A5.2.2, **55g-i**). We did note, however, that in a handful of cases the ee and yield could be improved by doubling the catalyst loading (**55g** and **55i**). Interestingly, in the case of **55h**, although we did see a significant improvement in the ee when the catalyst loading was doubled, the yield remained constant. It should be noted that this strategy was also implemented to improve the results for the *p*-nitrile substrate (**44m**) in Table 3.7.1, Chapter 3.

Table A5.2.2. Electrophiles with Coordinating Heteroatoms^a



[a] Isolated yields on 0.2 mmol scale. See Chapter 3 for reaction set-up. SFC analysis was used to determine ee. [b] With 10 mol% CuCl₂, 12 mol% **L73**, 26 mol% LiHMDS. [c] Synthesized from the corresponding Z-allylic chloride.

Table A5.2.3. Internal Allylic Chlorides^a

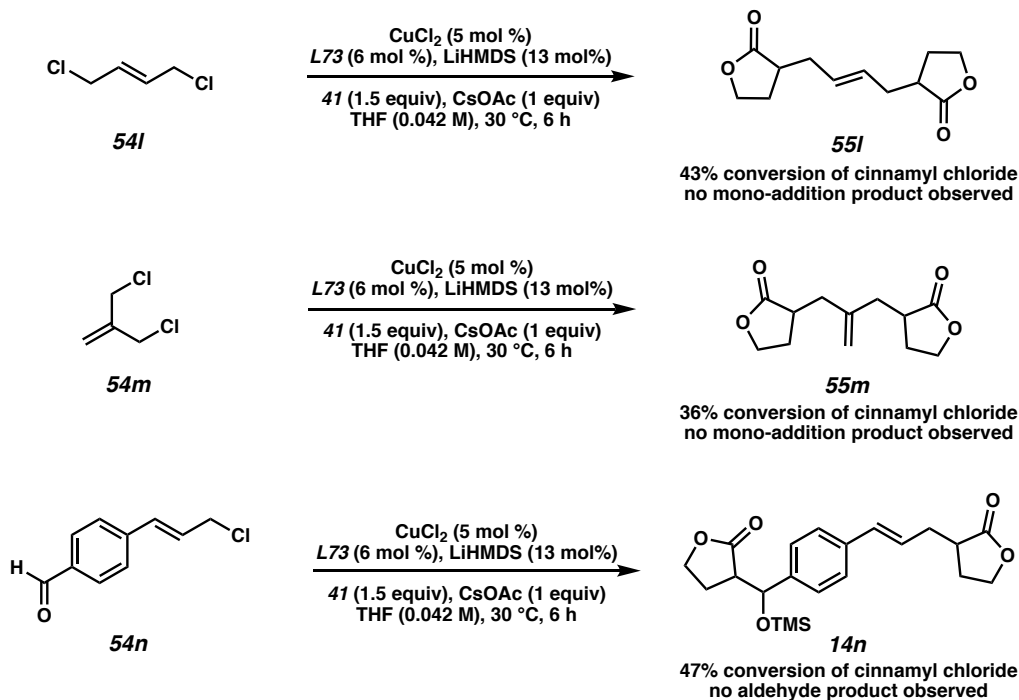


[a] Isolated yields on 0.2 mmol scale. See Chapter 3 for reaction set-up. SFC analysis was used to determine ee.

We also tested allylic electrophiles possessing internal chlorides (Table A5.2.3). Although the yields were high, the products were obtained in approximately a 1:1 mixture of diastereomers (**55k** and **55j**). In their initial disclosure, Sawamura and coworkers reported that this reaction was not stereoablative, and when a chiral electrophile is used, chiral product is formed.¹ These results are in agreement with their observations.

We also examined electrophiles possessing two reactive chlorides (**54l** and **54m**, Table A5.2.4). We noted that in these cases, only the bis-addition product was isolated and no mono-addition products were observed. We also tested a cinnamyl electrophile possessing a sensitive aldehyde group at the *para*-position on the aryl ring, and found that the γ -butyrolactone nucleophile added to both the allylic chloride and the aldehyde (**55n**). Interestingly, we noted that the silyl group was transferred to the newly formed alcohol on the product.

Table A5.2.4. Electrophiles with Two Reactive Sites^a



[a] Isolated yields on 0.2 mmol scale. See Chapter 3 for reaction set-up.

A5.3 LIMITATIONS IN THE NUCLEOPHILE

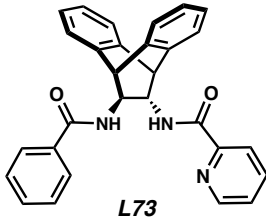
In addition to the γ -butyrolactone-derived silyl ketene acetal, a number of different silyl enolates were also tested in our final conditions. We have noted that our conditions are specific to this nucleophile, and poor reactivity and selectivity has been observed with other silyl enolates under a number of conditions.

Table A5.3.1. Other Silyl Ketene Acetals Tested^a

$\text{Ph}-\text{CH}=\text{CH}-\text{CH}_2-\text{X} + \text{Nu} \xrightarrow[\text{CsOAc (1 equiv), THF, temp, 14 h}]{\text{CuCl}_2 (10 \text{ mol } \%), \text{L73 (12 mol } \%), \text{LiHMDS (26 mol } \%)}$

1 equiv 1.5 equiv

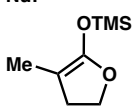
$\text{Ph}-\text{CH}=\text{CH}-\text{CH}_2-\text{Nu}$



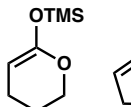
L73

entry	Nu	temp (°C)	X	yield (linear)	yield (branched)	ee (linear)
1	56	30	Cl	13	7	–
2	56	70	Cl	22	10	5
3	56	30	Br	27	29	10
4	57	30	Cl	9	0	–
5	57	70	Cl	22	0	–
6	57	30	Br	0	0	–
7	58	30	Cl	27	0	–
8	59	30	Cl	8	0	–
9	60	30	Cl	0	0	–
10	60	30	Br	16	14	–
11	61	30	Cl	0	0	–
12	61	30	Br	14	18	–

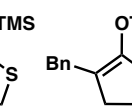
Nu:



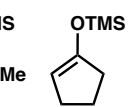
56



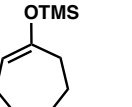
57




58



59



60



61

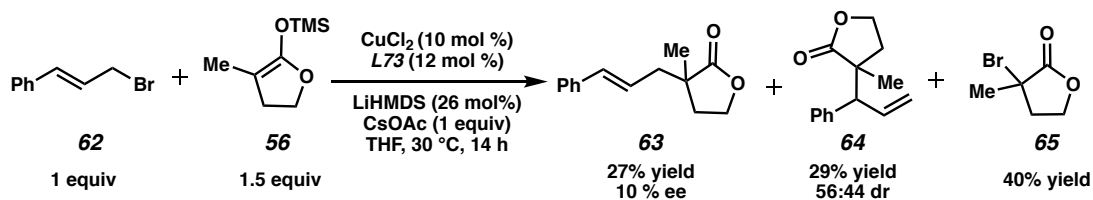
[a]. Reactions were run on 0.1 mmol scale. Yields and l:b ratios were determined by ¹HNMR using trimethoxybenzene as an internal standard. Enantiomeric excess (ee) was determined by supercritical fluid chromatography. See Chapter 3 for reaction Set-up.

Our first investigations into other silyl ketene acetals included an α-methyl γ-butyrolactone (**56**), δ-valerolactone (**57**), and thiolactone (**58**) derived silyl ketene acetals, a silyl ketene aminal (**59**), and two ketone derived silyl enolates of differing ring sizes (**60** and **61**). Unfortunately, with our final set of conditions, we obtained very small quantities of the desired products (entries 1, 4, 8, 9, and 11), with the best-performing nucleophile being thiolactone **58** (entry 7).

At elevated temperatures, the yields for the product derived from the α -methyl γ -butyrolactone **56** and δ -valerolactone **57** improved slightly (entries 2 and 3). In the case of the δ -valerolactone, the linear product continued to be the major isomer. However, when α -methyl γ -butyrolactone is used as the nucleophile, the corresponding product is obtained as a mixture of linear and branched isomers, and the ee of the linear product is low (entry 2).

We found that by switching to the more reactive cinnamyl bromide, we were able to obtain the desired product in low to moderate yields with **56** (entry 3), **60** (entry 9), and **61** (entry 10). Interestingly, with these nucleophiles, the products were obtained in roughly a 1:1 mixture of linear and branched isomers. Upon closer examination of the results obtained with α -methyl γ -butyrolactone **56**, we did note that the ee of the linear product **63** was still low and the branched product **64** was obtained in 56:44 dr (Scheme A5.3.1). We also obtained 40% yield of the α -bromo lactone **65**, which may be an indication that a radical pathway is operative under these conditions.

Scheme A5.3.1. With α -Methyl γ -Butyrolactone-Derived Silyl Ketene Acetal^a



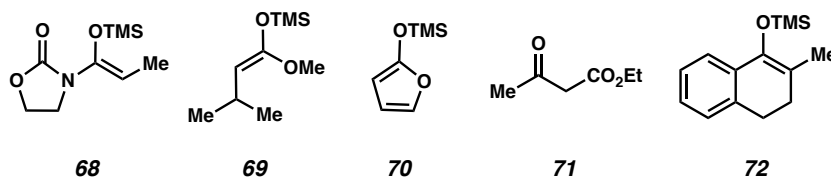
[a] Reactions were run on 0.1 mmol scale. Yields and l:b ratios were determined by ^1H NMR using trimethoxybenzene as an internal standard. Products were isolated by Prep TLC. Enantiomeric excess (ee) was determined by supercritical fluid chromatography. See Chapter 3 for reaction set-up.

There were also a number of nucleophiles that did not result in any product, regardless of the conditions employed (**68-72**, Table A5.3.3.A). It should be noted that with methyl-3-methylbutanoate-derived silyl ketene acetal **69**, the characteristic color change from green to yellow at the start of the reaction did not occur, and the reaction mixture remained green over the course of the entire reaction. With silyl furan **70**, a color change from green to red was noted instead. In both of these cases, perhaps the lack of product formation could be attributed to the inability of these silyl ketene acetals to coordinate and successively reduce the Cu catalyst to the corresponding starting Cu(I) complex (See Chapter 4).

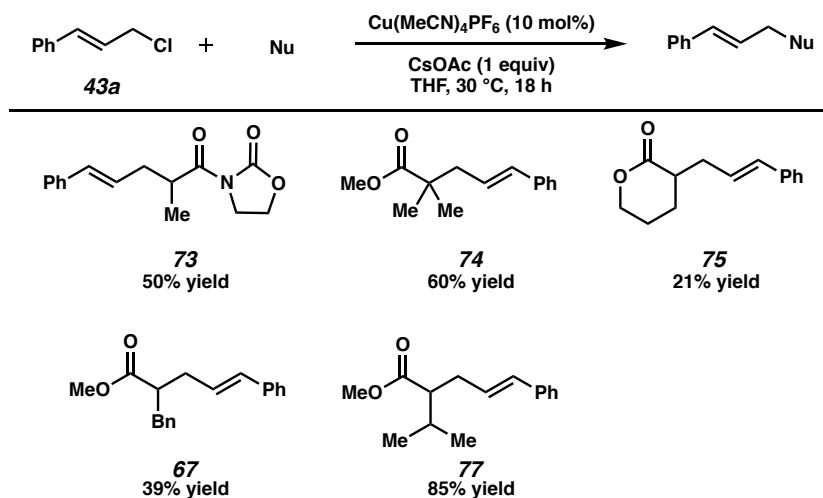
Generally, one possible explanation for the lack of reactivity being observed with all nucleophiles may be due to the large steric bulk of **L73**, which may prevent coordination and subsequent allylic alkylation with larger nucleophiles. Interestingly, in the absence of ligand, some of these nucleophiles allowed for the formation of product in moderate to good yields (Table A5.3.4.B). The one exception to this is methyl 3-phenylpropanoate-derived silyl ketene acetal (**67**), which allows for the formation of the corresponding product in very similar yield to what was observed in the presence of ligand (see Scheme A5.4.1).

Table A5.3.2. Unreactive Silyl Ketene Acetals^a

A. Silyl Ketene Acetals that Resulted in No Product Formation:



B. Without Ligand:



[a] Reactions were run on 0.1 mmol scale. Yields and l:b ratios were determined by ¹HNMR using trimethoxybenzene as an internal standard. See Chapter 3 for reaction set-up.

A5.4 ACYCLIC NUCLEOPHILES AND BICYCLO[2.2.2]OCTANE BACKBONE

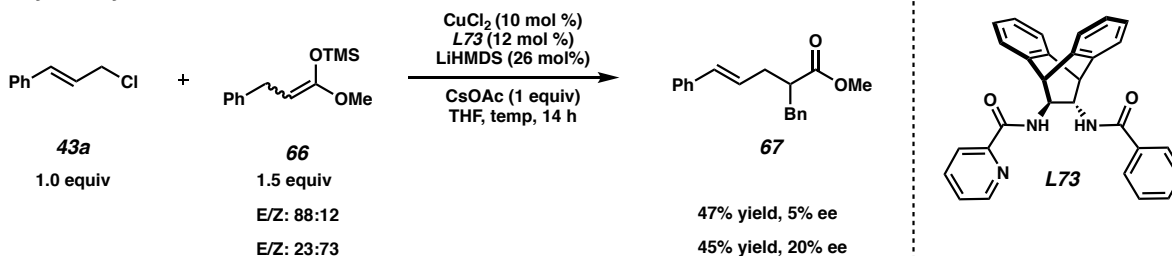
In addition to examining cyclic nucleophiles, we also examined acyclic silyl ketene acetals in our reaction. Gratifyingly, we found that with methyl 3-phenylpropanoate-derived silyl ketene acetal, the corresponding product was obtained in over 40% yield with either the primarily *E* or *Z* nucleophile (**66**, Scheme A5.4.1.A). We did find that the silyl ketene acetal geometry did have an

effect on the ee; with the *E* nucleophile the product obtained is racemic, however, with the *Z* nucleophile, the product is obtained in 20% ee.

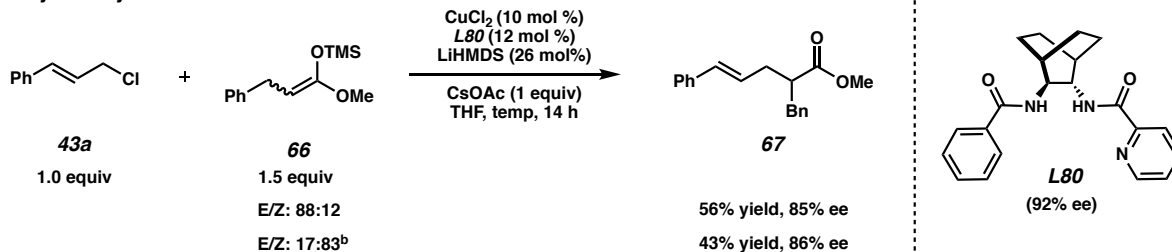
The low level of reactivity we were observing with ligand **L73** with nucleophiles other than the very small and highly reactive γ -butyrolactone-derived silyl ketene acetal **41** prompted us to investigate ligands with alternate backbones. When mono-picolinyl ligands possessing backbones such as diphenylethylene and cyclohexyl were used, no product was observed with **66**. With **L80**, which possesses a bicyclo[2.2.2]octane backbone, the desired acyclic α -benzyl product **67** is obtained in 56% yield and 85% ee. Although this backbone is significantly less bulky than **L73**, the large bite angle between the two amides is still retained, which we believe may be

Scheme A5.4.1. Acyclic Silyl Ketene Acetals^a

A. Acyclic Silyl Ketene Acetals with **L73**



B. Acyclic Silyl Ketene Acetals with **L80**

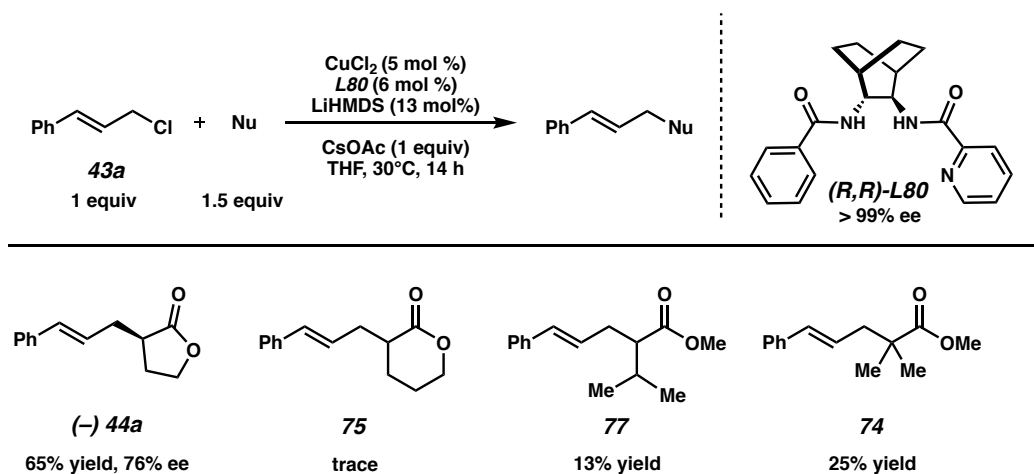


[a] Reactions were run on 0.1 mmol scale. E/Z ratios of **66** were determined by ^1H NMR analysis. Yields and l:b ratios were determined by ^1H NMR using trimethoxybenzene as an internal standard. Enantiomeric excess (ee) was determined by supercritical fluid chromatography. See Chapter 3 for reaction set-up. [b] The primarily *Z* silyl ketene acetal that was used in this experiment was used in slight excess (1.8 equiv), as it was isolated with a large amount of both the α -silyl product and recovered starting material. The purity of the reagent was determined to be close to 50% based on ^1H NMR analysis.

critical for reactivity. In addition, although in the case of **L73**, the E/Z ratio of the silyl ketene acetal does appear to influence the ee of the product, when **L80** is used, nearly identical results are obtained with either the E or Z silyl ketene acetal.

Intrigued by the success of **L80** with **66**, we evaluated additional nucleophiles in combination with this ligand (Scheme A5.4.2). With the γ -butyrolactone-derived silyl ketene acetal, the corresponding product was formed in 65% yield and 76% ee, indicating that the bulkier ANDEN backbone is important for the high yields and ee's in our original conditions ((-)-**44a**). With a δ -valerolactone-derived nucleophile and an α -isopropyl derived nucleophile, very small amounts of desired product were formed (**75** and **77**). Interestingly, with the α,α -dimethyl-derived acyclic nucleophile, the desired product is formed in 25%.

Table A5.4.2. Additional Nucleophiles Tested with **L80**^a

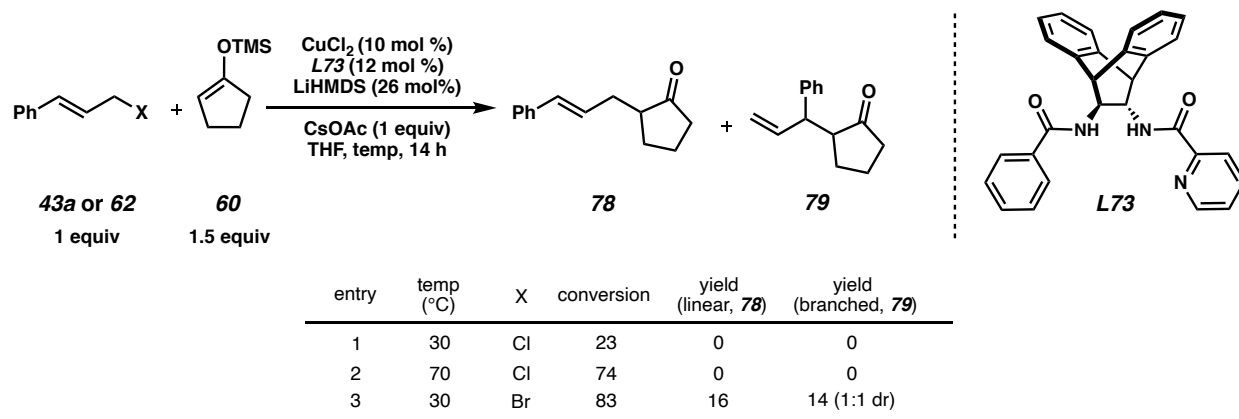


[a] Reactions were run on 0.1 mmol scale. Yields and l:b ratios were determined by ^1H NMR using trimethoxybenzene as an internal standard. Enantiomeric excess (ee) was determined by supercritical fluid chromatography. See Chapter 3 for reaction set-up.

A5.5 COPPER-CATALYZED ALLYLIC ALKYLATION WITH SILYL ENOL ETHERS

Given the large difference in pK_a between a lactone and a ketone, we were curious to see if we could observe Cu-catalyzed allylic alkylations with silyl enol ethers, either under our conditions or under slightly modified conditions. Given that the cyclopentanone-derived silyl enol ether **60** was most similar in size to γ -butyrolactone **41**, we believed that the difference in reactivity between these two nucleophiles could largely be attributed to electronics. As was described in A5.2.1, although we did not observe any product when **60** was exposed to our final set of reaction conditions at 30 °C or at 70 °C (entries 1 and 2, Table A5.5.1), we did note that with a more reactive cinnamyl bromide nucleophile, a small amount of both the linear and branched product isomers is observed (entry 3). Using these results as our starting point, we aimed to understand why these nucleophiles were unreactive and how the reaction conditions needed to be modified in order for α -allyl ketone products to be observed.

Table A5.5.1. Cu-Catalyzed Allylic Alkylation with Silyl Enol Ethers with **L73**^a

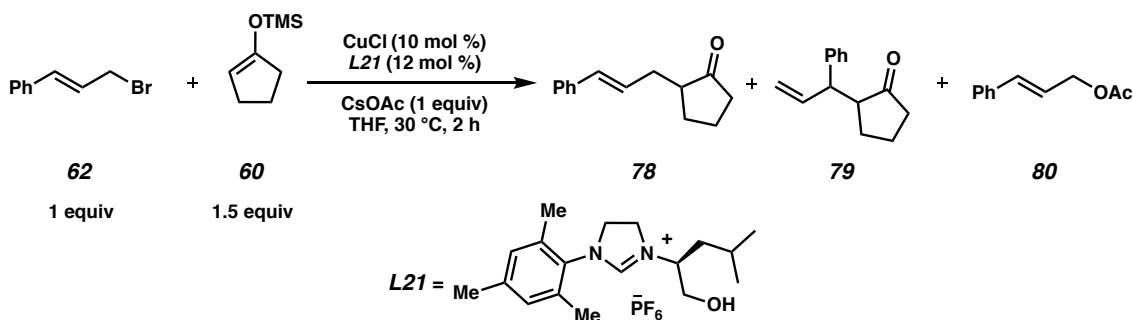


[a] Reactions were run on 0.1 mmol scale. Yields and l:b ratios were determined by ¹HNMR using trimethoxybenzene as an internal standard. See Chapter 3 for reaction set-up.

One of the first things that we chose to assess was whether or not we had identified the appropriate ligand for this transformation. One particular difference that we noted between the reactivity profiles of the silyl ketene acetals and the silyl enol ethers was that in the case of silyl enol ether **60**, no product is observed when Cu is used in the absence of ligand. Consequently, we believed that a different set of chelating atoms may be required on the ligand in order to observe product formation. To this end, we tested 16 commercially available ligands in the Cu catalyzed allylic alkylation using silyl enol ethers. Interestingly, the only ligand to result in product formation was SIMES-leucinol (**L21**, Table A5.5.2), a ligand that led to an unreactive Cu catalyst in our allylic alkylation with the γ -butyrolactone-derived silyl ketene acetal. However, the product was formed in only 13% yield, which was less than what we had observed with cinnamyl bromides in our initial conditions (Table A5.5.2, entry 1). Given that little to no reactivity was being observed with a large variety of ligands, we concluded that the low level of reactivity was not due to an

unfavorable coordination environment around the Cu, but could be due to another aspect of the reaction. To gain a deeper understanding of what was occurring, we ran a number of controls with **L21** as the ligand.

Table A5.5.2. Cu-Catalyzed Allylic Alkylation with Silyl Enol Ethers with **L21**^a

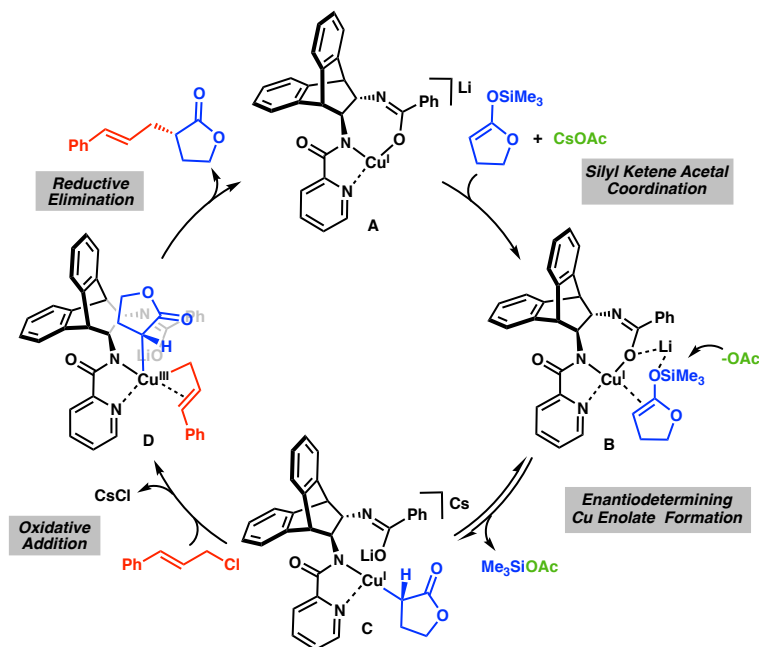


entry	conditions	yield (linear, 78)	yield (branched, 79)	yield (80)
1	no changes	13	0	2
2	no Cu	0	0	0
3	no 60	–	–	23 ^b
4	no Cu, no 60	–	–	0

[a] Reactions were run on 0.1 mmol scale. Yields and l:b ratios were determined by ¹HNMR using trimethoxybenzene as an internal standard. See Chapter 3 for reaction set-up. [b] **79** was obtained as a 73:27 mixture of linear and branched isomers.

Gratifyingly, we noted that in the absence of Cu, no allylic alkylation product was being formed, indicating that the small amount of product being observed with both **L73** and **L21** was formed via a Cu-mediated reaction (entry 2). Interestingly, when silyl enol ether **60** is omitted from the transformation, cinnamyl acetate (**80**) is obtained in a 23% yield after only 2 h (entry 3). To determine whether or not this was Cu-mediated, we ran an additional control, this time omitting both **60** and the Cu catalyst, and found that no cinnamyl acetate product is formed, indicating that the formation of **80** is Cu-mediated.

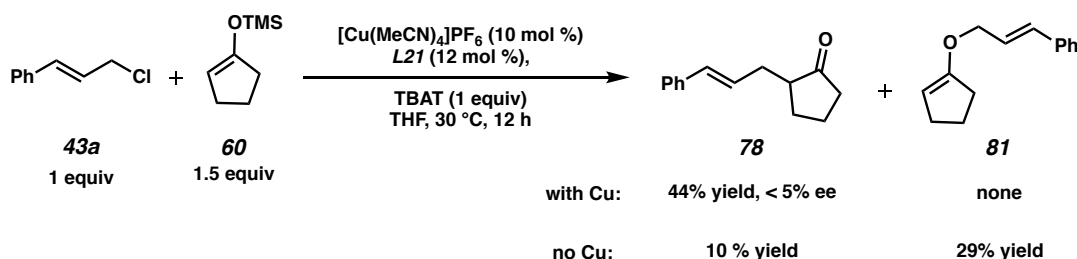
Scheme A5.5.1. Proposed Reaction Mechanism



The observation of a Cu-catalyzed cinnamyl acetate formation was not only intriguing, but also offered some insight into the reaction. We currently believe that the Cu-catalyzed allylic alkylation of a γ -butyrolactone-derived silyl ketene acetal proceeds via an inner-sphere pathway, involving an initial enantiodetermining transmetalation of the silyl ketene acetal **41** to form a Cu(I) enolate (**C**), followed by oxidative addition into the allylic electrophile (**D**), and a fast reductive elimination to form the desired product (Scheme A5.5.1, see Chapter 4 for more details). Taking this mechanistic hypothesis into account, we initially envisioned that when silyl enol ethers are used, the oxidative addition step could be more challenging, as the Cu(I) enolate generated would be less electron-rich than its corresponding lactone counterpart, and consequently, much less prone to undergo oxidative addition. The Cu-mediated formation of cinnamyl acetate could be an indication that the difference in electronics between the two Cu(I) enolates may not be the reason

no α -allyl ketone is formed, as product formation is observed under identical conditions with an even less electron-rich nucleophile, CsOAc.² It is interesting to note that in the presence of **60** (entry 1), the cinnamyl acetate yield is only 2%, indicating that **60** could be slowing down the rate of cinnamyl acetate formation via competitive binding to the Cu catalyst. One possible explanation for this behavior could be that the silyl enol ethers are binding to Cu, but that CsOAc is not a strong enough base to generate the required Cu enolate. For this reason, we tested a number of different bases in this transformation. Gratifyingly, we found that with TBAT, the desired product is obtained in 44% yield, albeit in < 5% ee. We also noted that in the absence of Cu, **60** still reacts with **43a**, but in this case, the O-alkylation product is the major species (Scheme A5.5.3).

Scheme A5.5.3. Cu-Catalyzed Allylic Alkylation with Silyl Enol Ethers and TBAT^a



[a] Reactions were run on 0.1 mmol scale. Yields and linear:branched ratios were determined by ¹HNMR using trimethoxybenzene as an internal standard. See Materials and Methods section for reaction set-up.

A5.6 CONCLUSION

In conclusion, we have observed a number of limitations in both the electrophile and nucleophile in our enantioselective Cu-catalyzed allylic alkylation. With regards to the electrophile, we noted that allylic chlorides possessing either α,α -disubstitution or very bulky α -substituents result in very low ee's, although the yields are generally moderate. In addition, we

noted that electrophiles possessing functional groups that can coordinate to the Cu catalyst result in both lower yields and ee, although the results can be slightly improved by doubling the catalyst loading. Internal allylic chlorides react favorably, but the resulting products were obtained in low diastereoselectivity. Furthermore, if two reactive sites are present on the allylic chloride, di-substitution products are favored, and no mono-substitution is observed.

With respect to the nucleophile, we found that our current conditions are specific to the γ -butyrolactone-derived silyl ketene acetal. Other nucleophiles, including larger cyclic or acyclic silyl ketene acetals, silyl ketene amins, silyl thioketene acetals, and silyl enol ethers result in very low formation of the corresponding products. Strategies such as increasing the temperature or switching to the more reactive cinnamyl bromides led to only slight improvements in the yield, and the ee's are low in all cases. One possible explanation for the lack of reactivity observed with other silyl ketene acetals is that **L73** may be too bulky, preventing the coordination of larger nucleophiles. To this end, we synthesized and tested a ligand possessing a bicyclo[2.2.2]octane backbone (**L80**) and found that this ligand enables the accommodation of larger nucleophiles. Promising reactivity was obtained with larger, acyclic nucleophiles using this backbone.

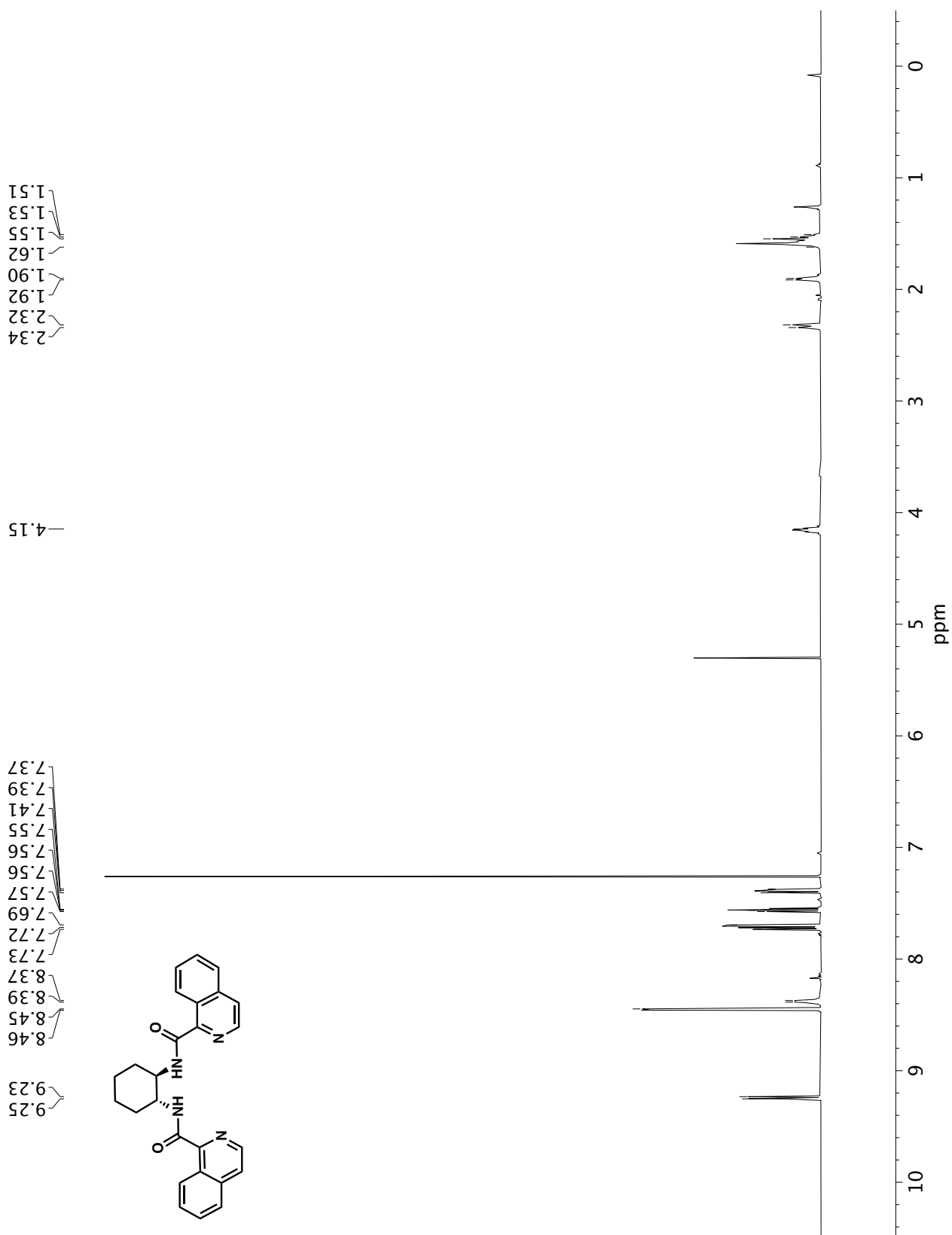
Finally, we also investigated the reaction of a cyclopentanone-derived silyl enol ether (**60**). With this nucleophile, we found that both **L73** and SIMES-leucinol (**L21**) lead to product formation, albeit in low yields. We found that one possible explanation for the lack of reactivity observed with silyl enol ethers may be attributed to the CsOAc base used, as it may not be reactive enough to cleave the silyl enol ether. Switching to a more reactive base, TBAT, led to higher yields of the desired product.

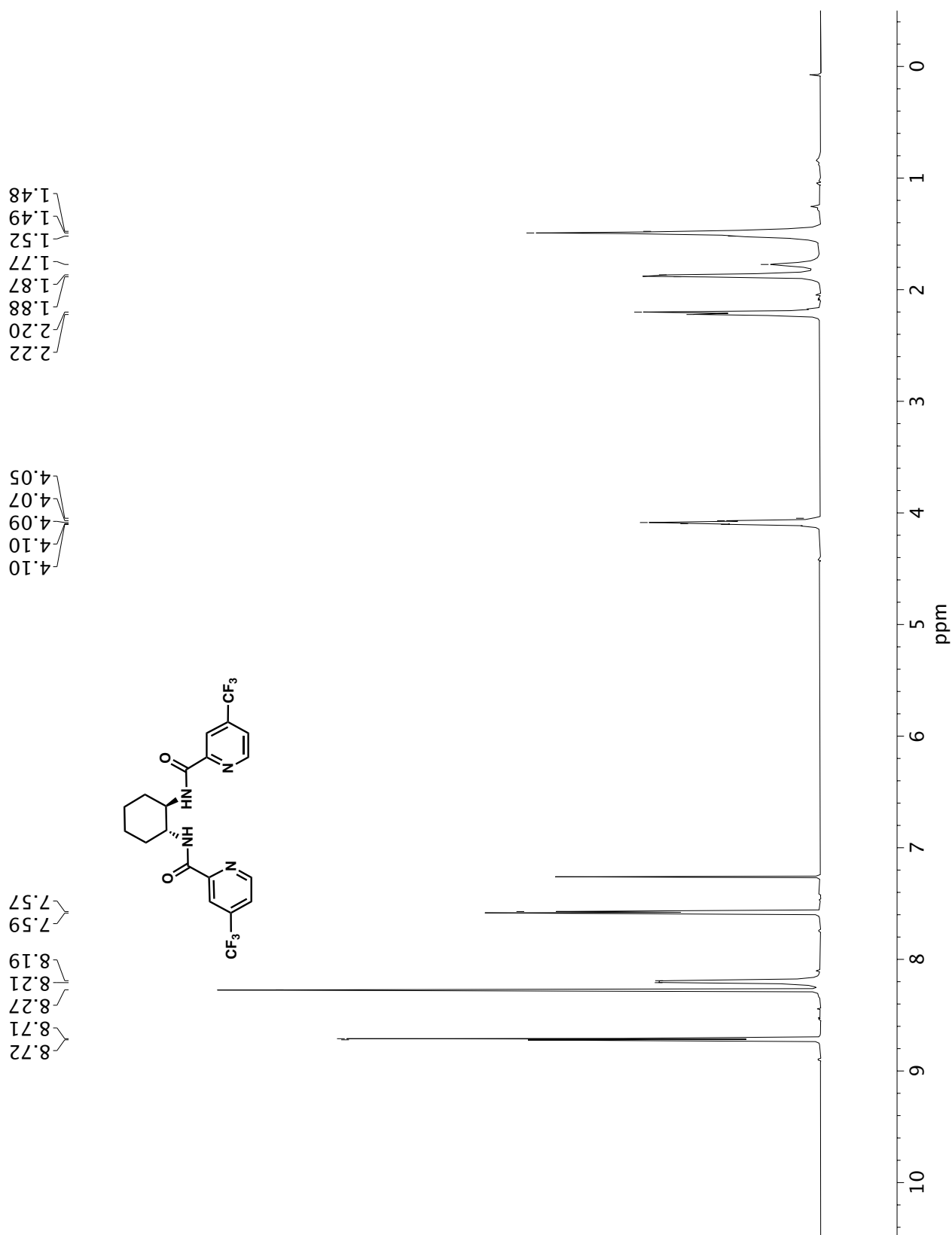
A5.7 REFERENCES AND NOTES

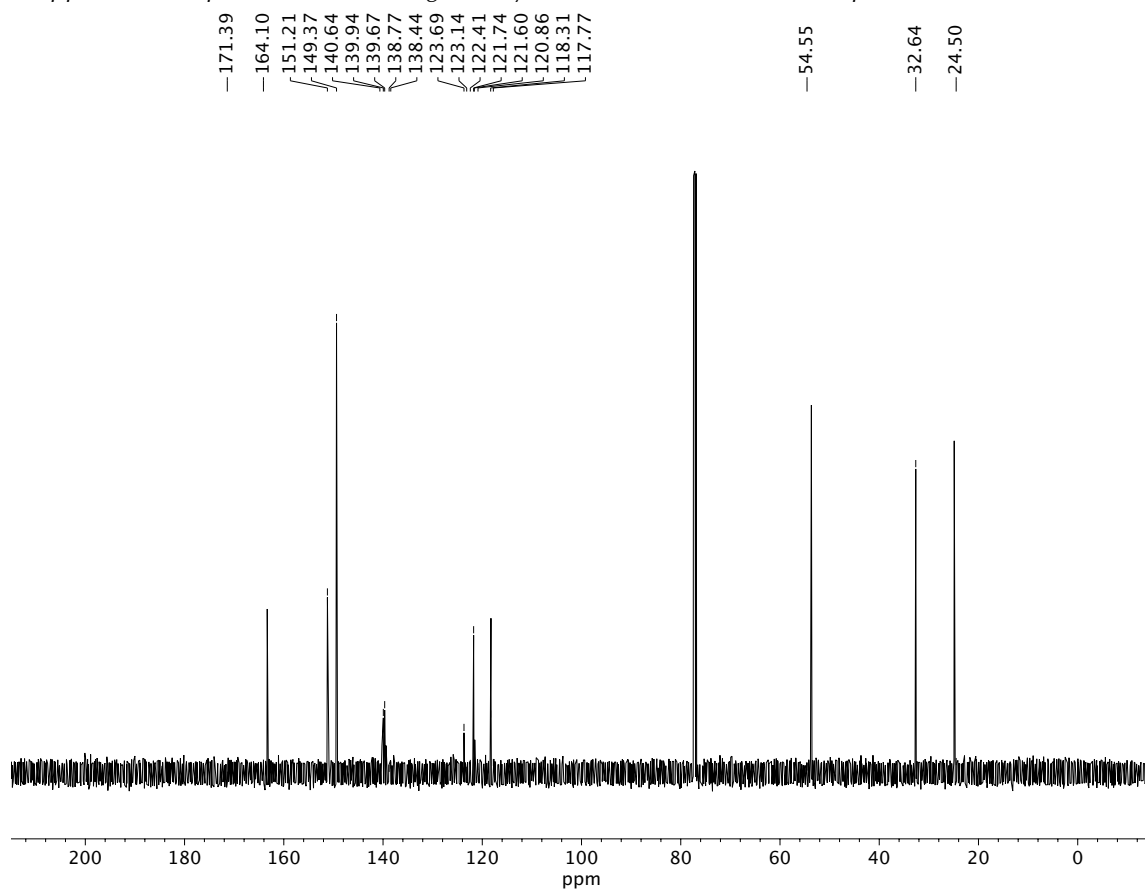
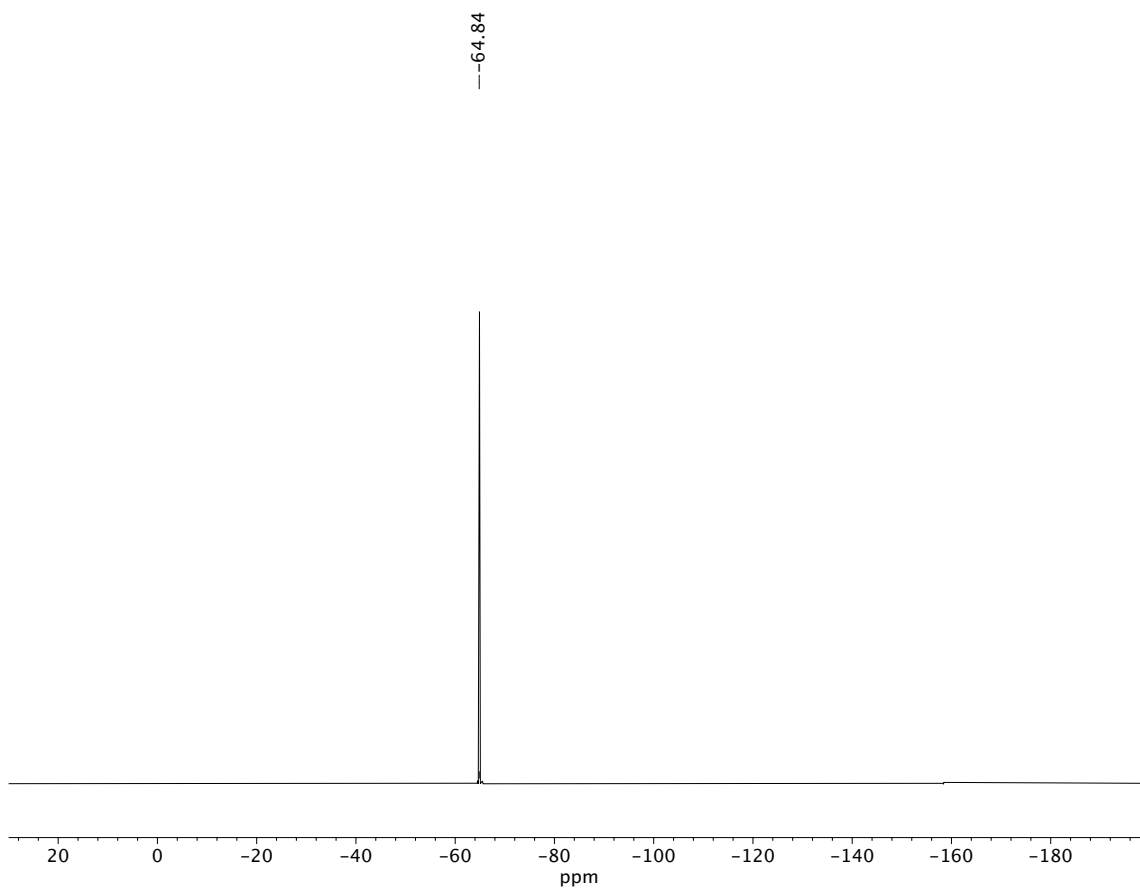
1. Li, D.; Ohmiya, H.; Sawamura, M. *J. Am. Chem. Soc.* **2011**, *133*, 5672-5675.
2. This statement holds true if we assume that the Cu-mediated cinnamyl acetate formation also proceeds via a similar, inner-sphere allylic substitution pathway.

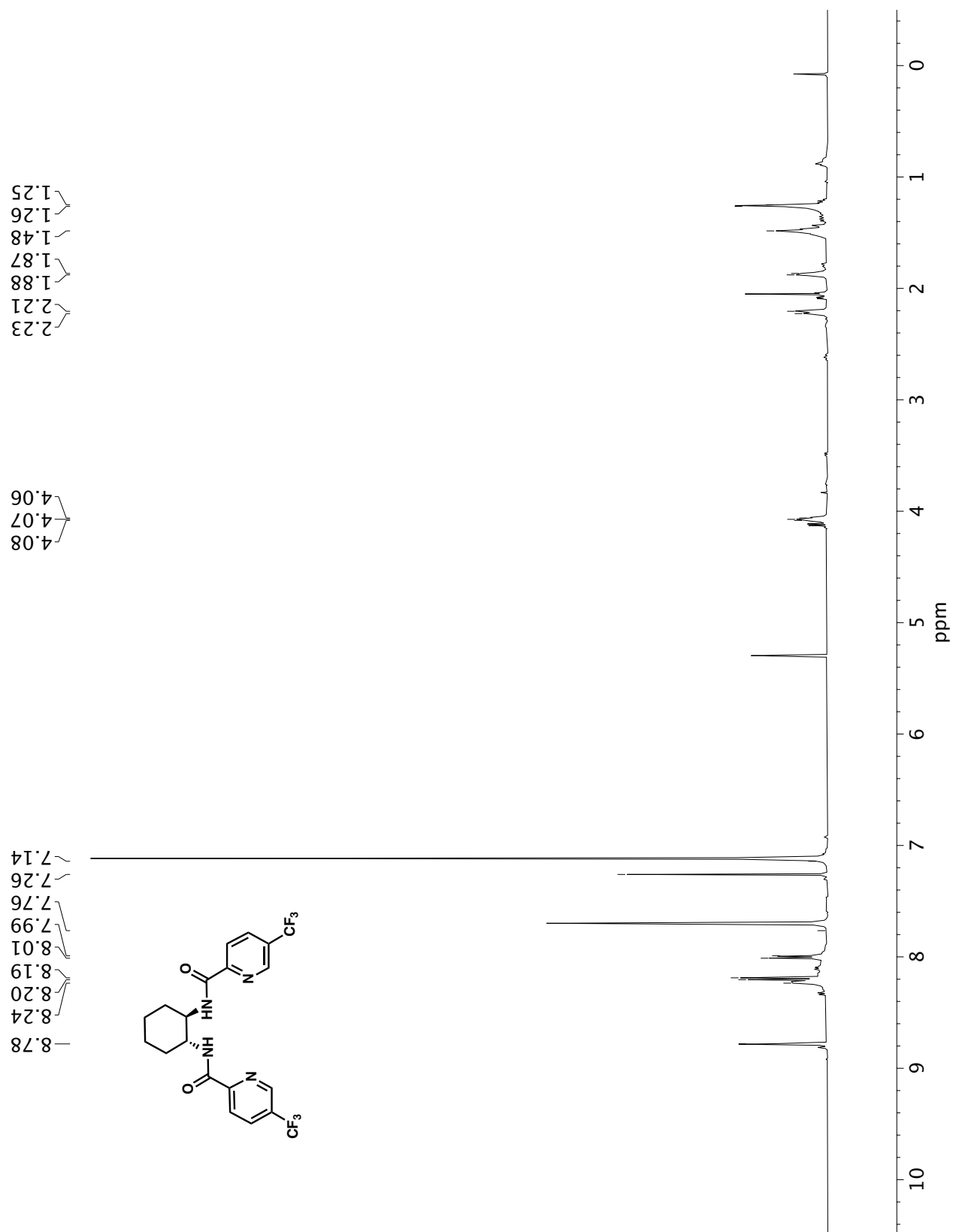
APPENDIX 6

Spectra for Amide Ligands Synthesized and Tested in Chapter 3



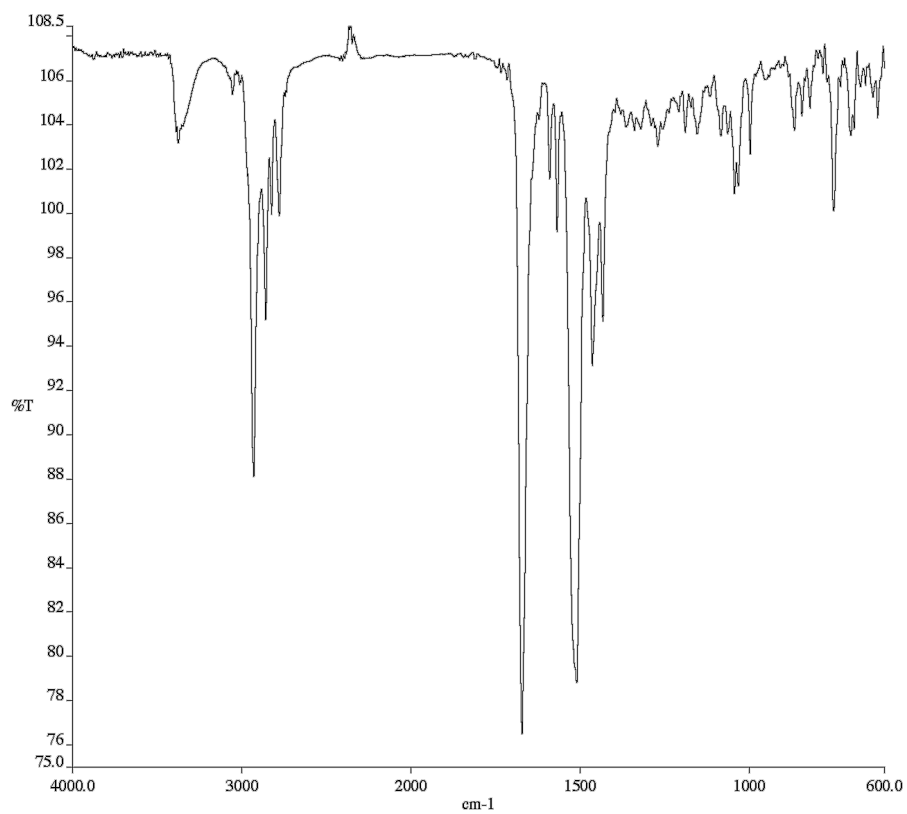
**A6.2** ^1H NMR (500 MHz, CDCl_3) of compound **L45**

**A6.3** ^{13}C NMR (125 MHz, CDCl_3) of compound **L45****A6.4** ^{19}F NMR (282 MHz, CDCl_3) of compound **L45**

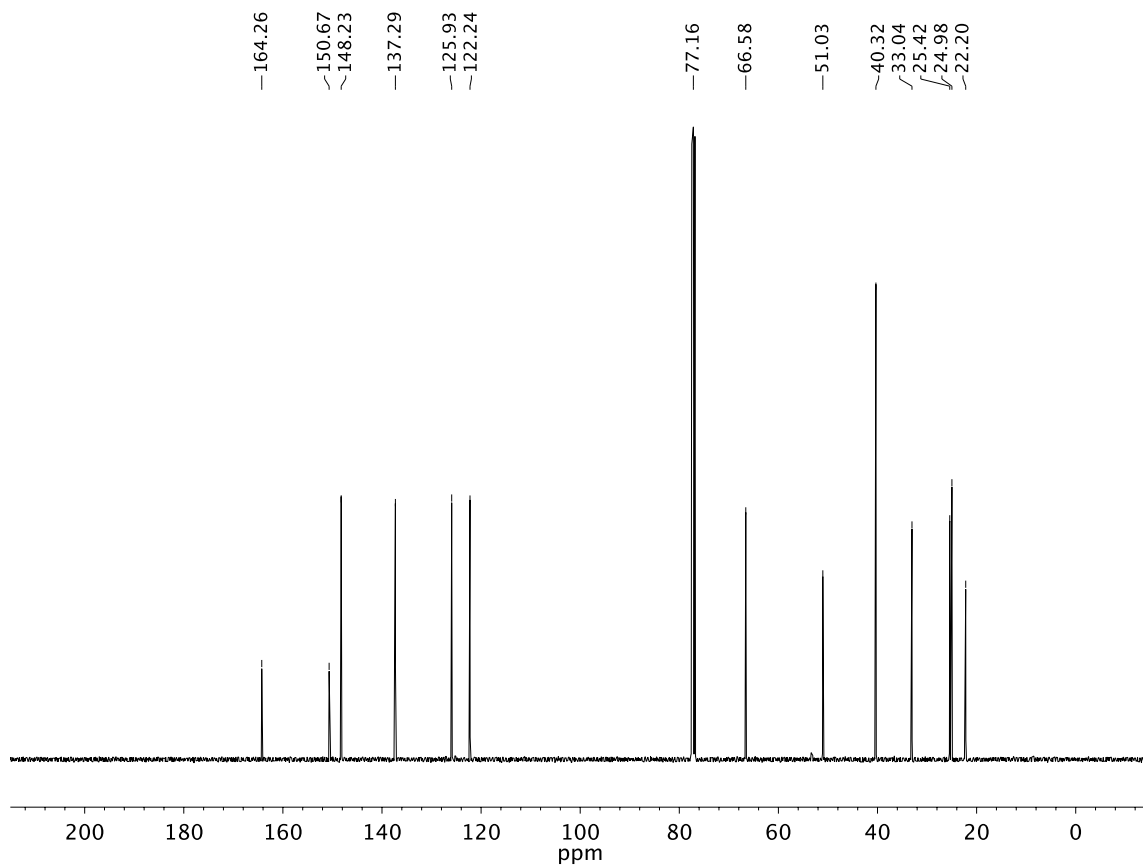




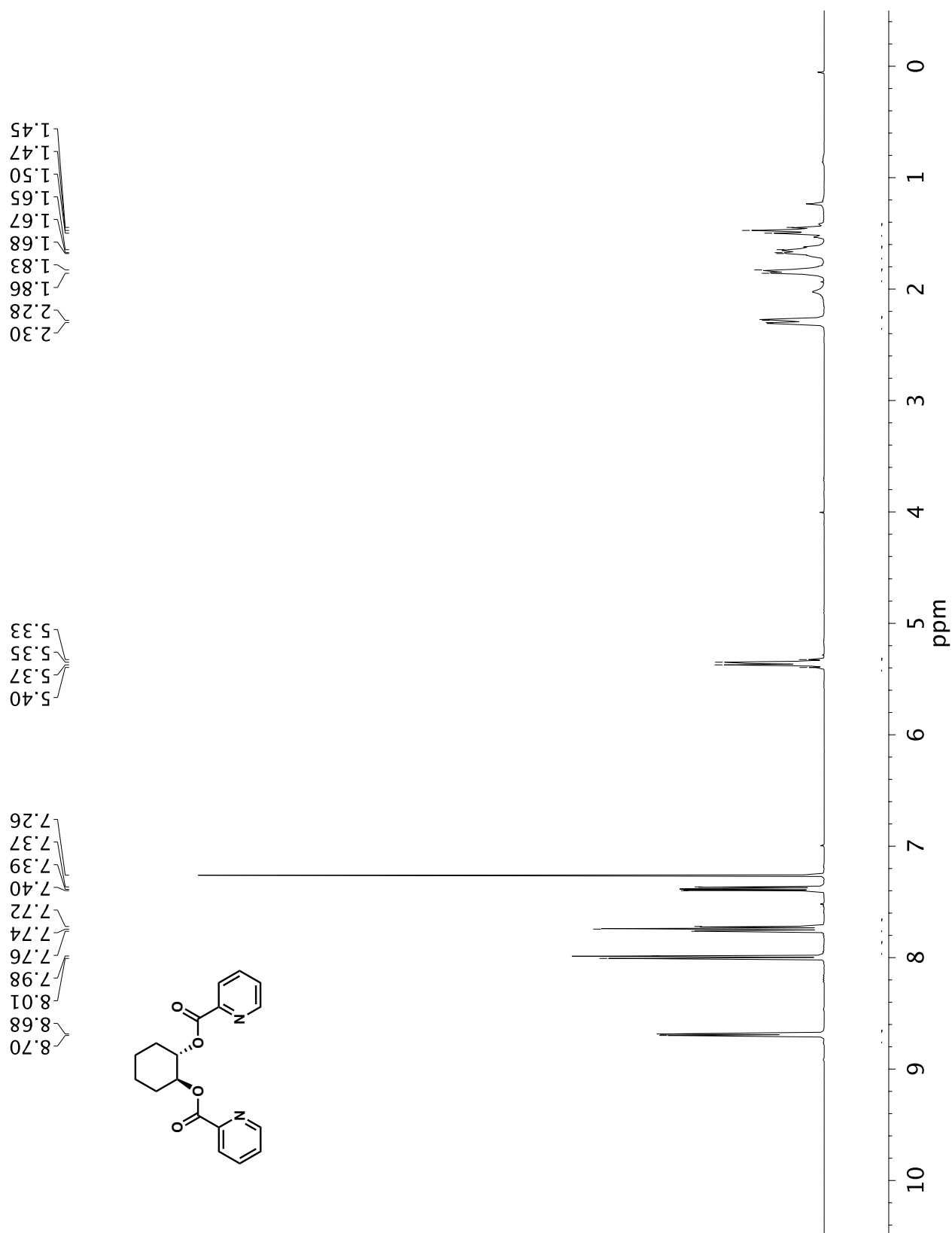


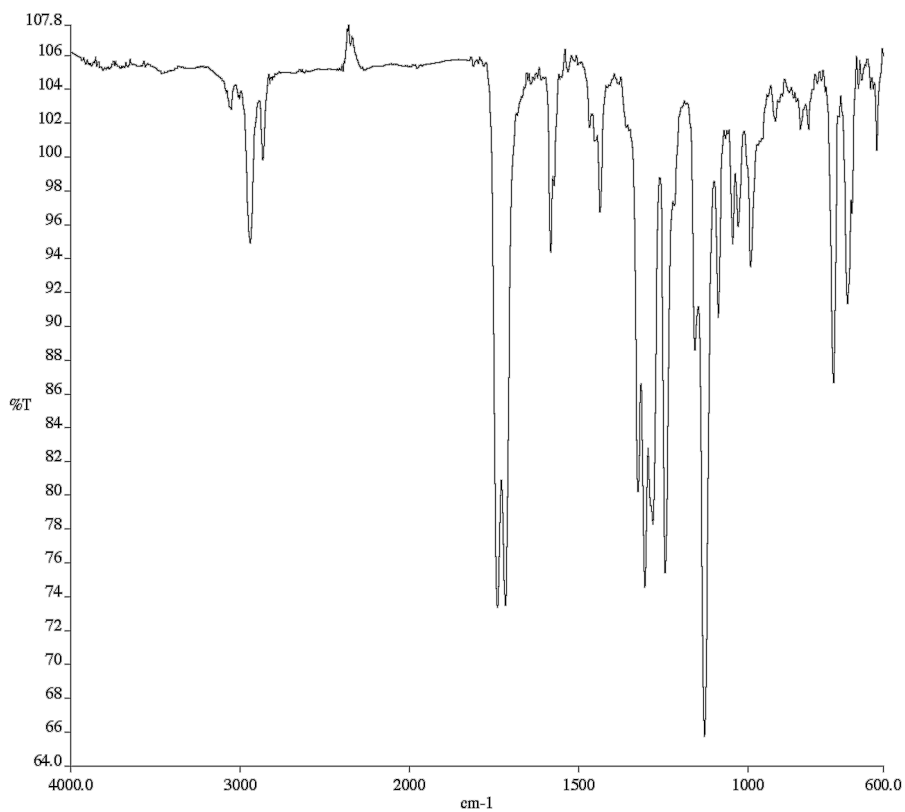
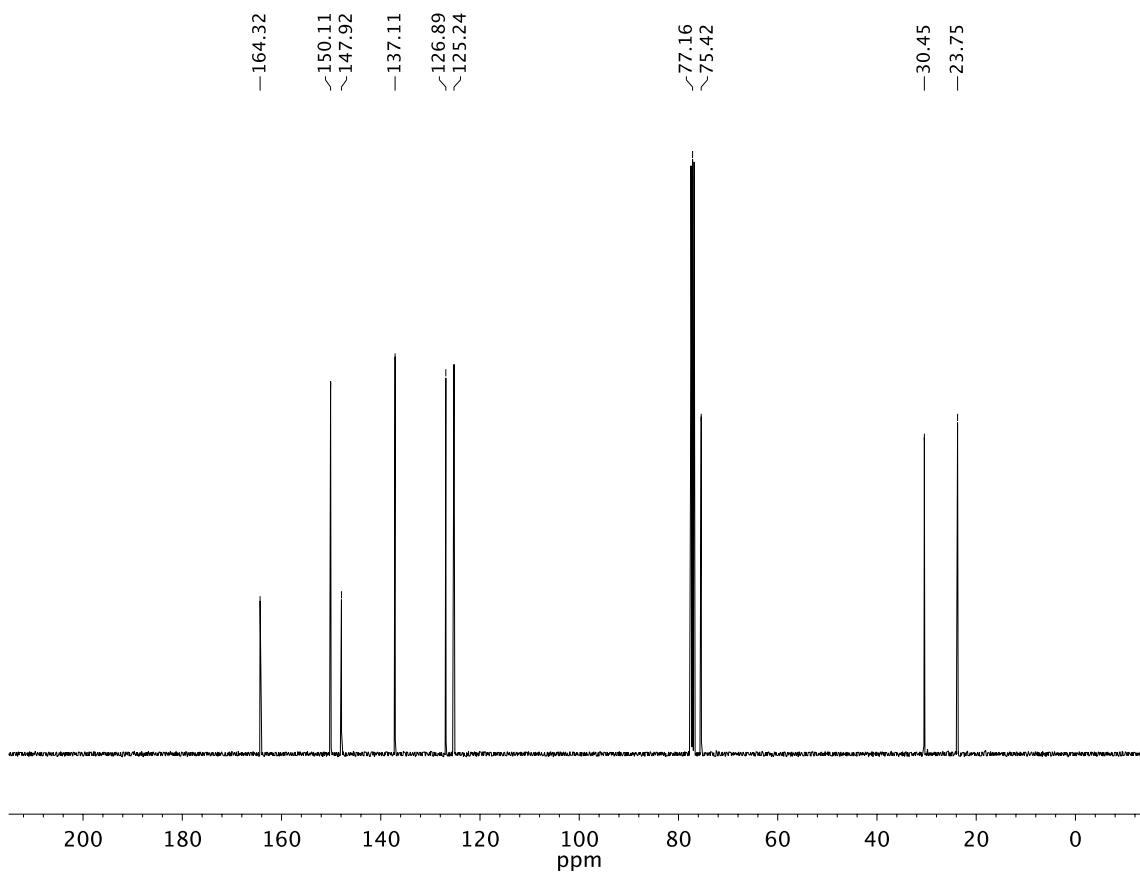


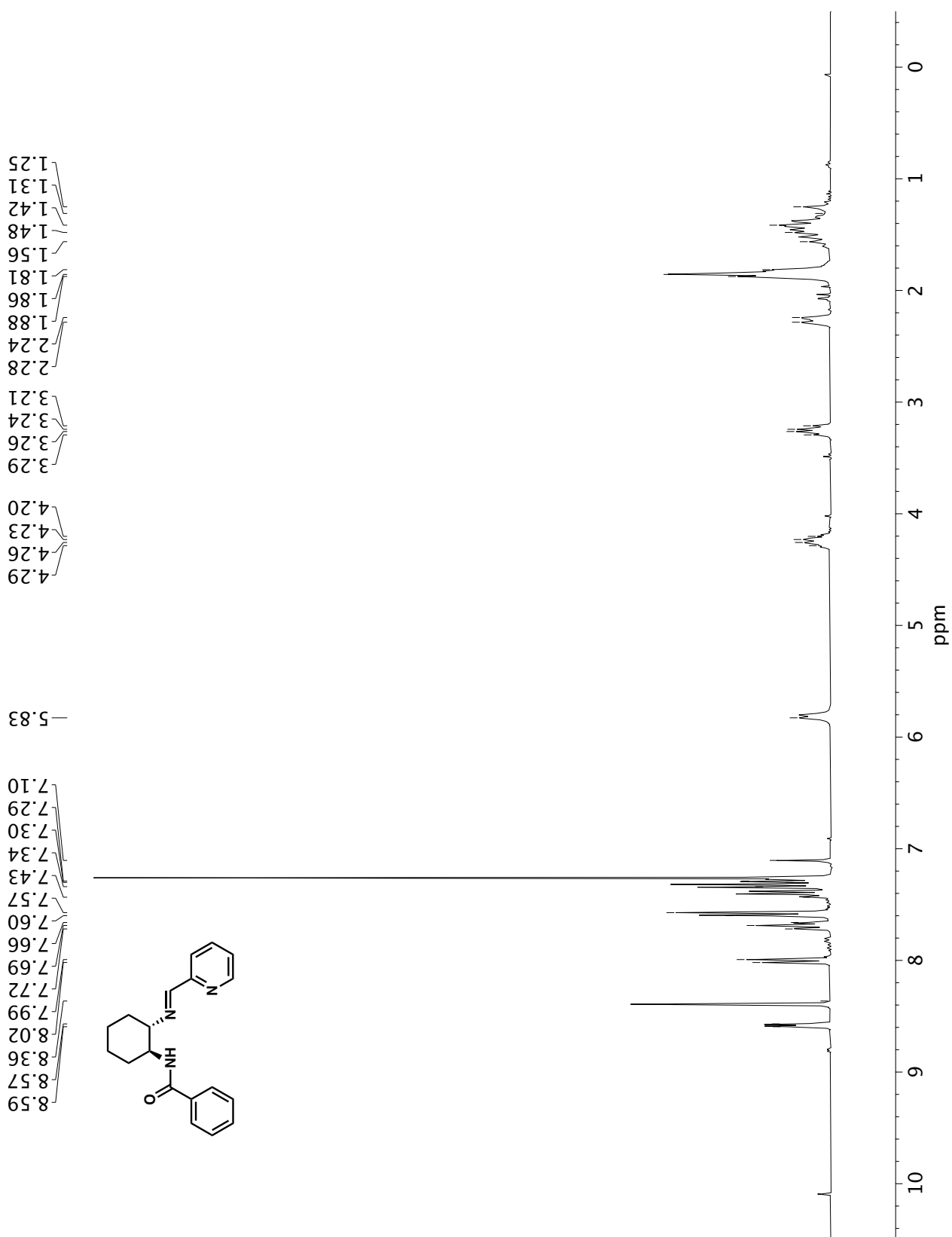
A6.8 Infrared spectrum (Thin Film, NaCl) of compound **L54**

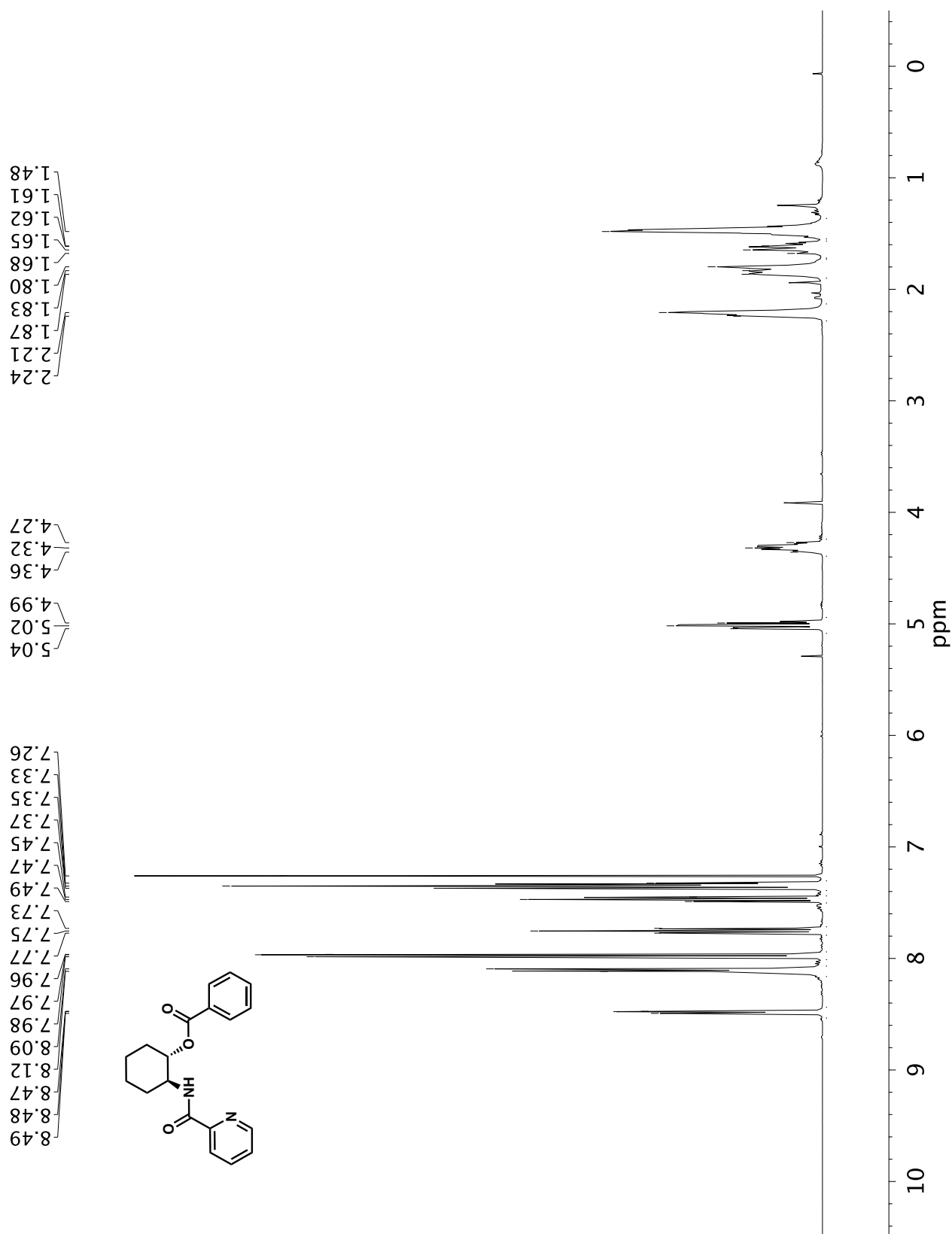


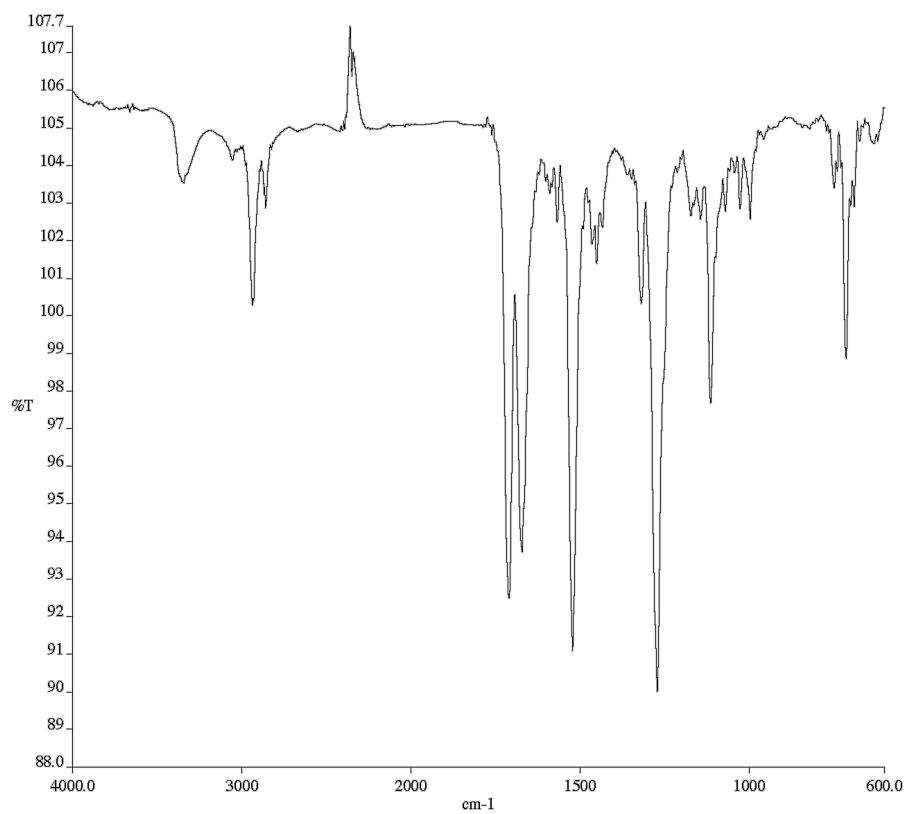
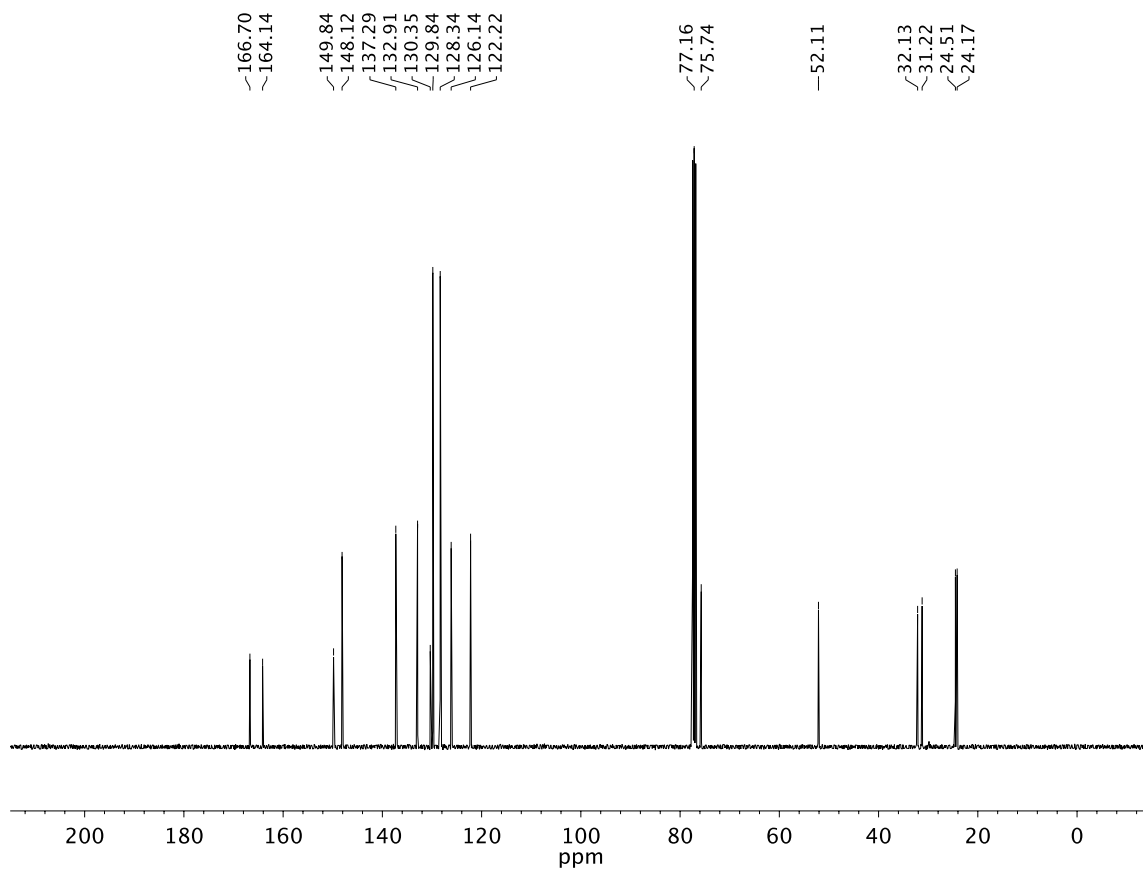
A6.9 ¹³C NMR (100 MHz, CDCl₃) of compound **L54**

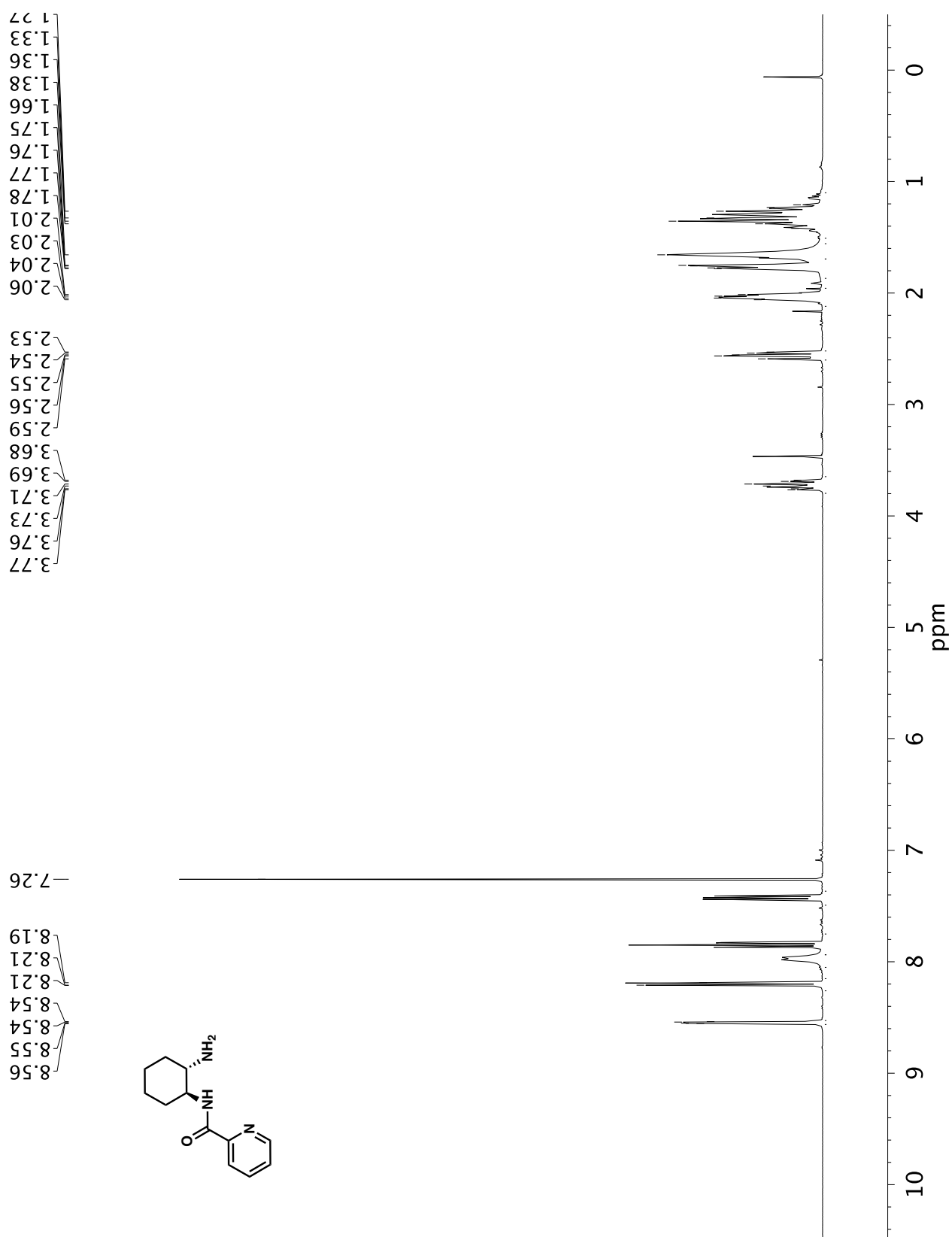


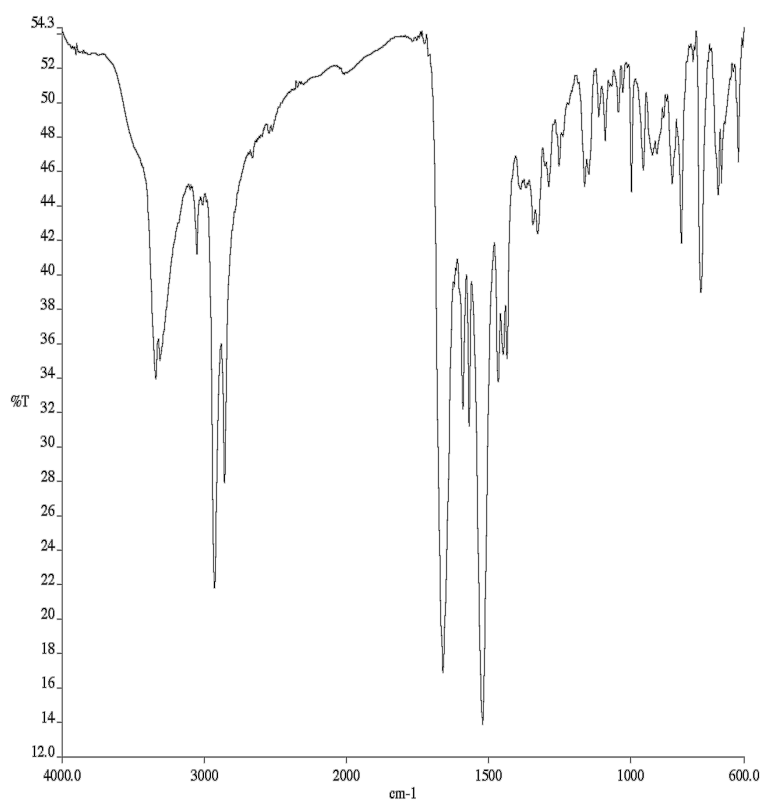
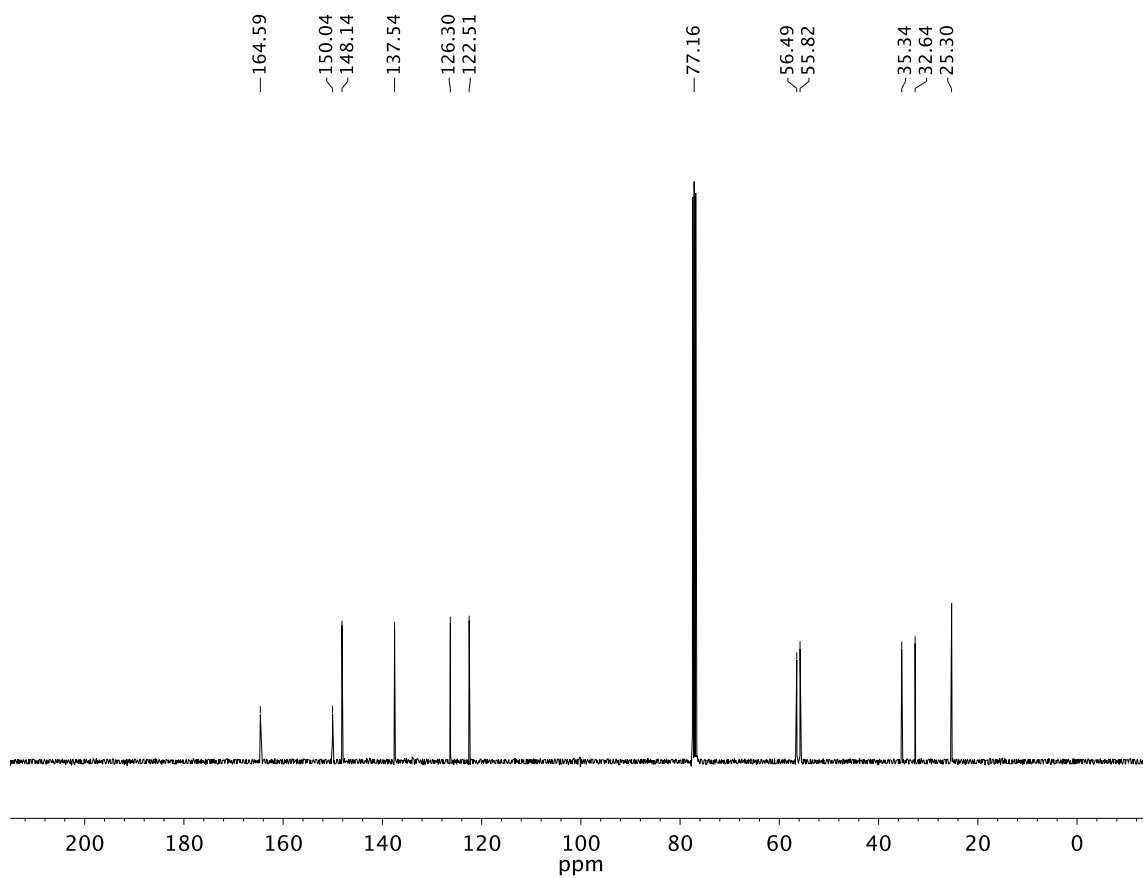
**A6.11** Infrared spectrum (Thin Film, NaCl) of compound **L59****A6.12** ¹³C NMR (100 MHz, CDCl₃) of compound **L59**

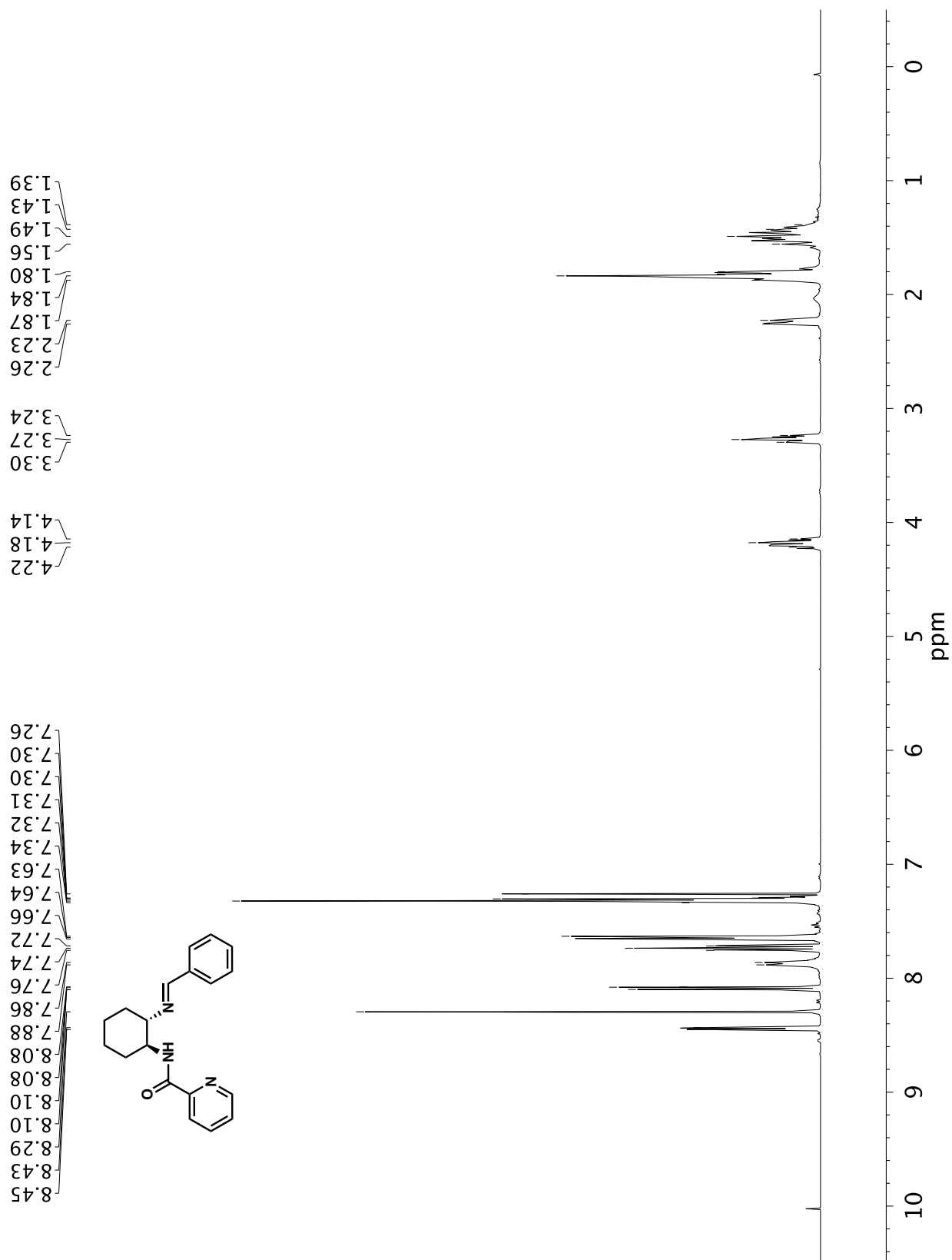
**A6.13** ¹H NMR (400 MHz, CDCl₃) of compound **L62**

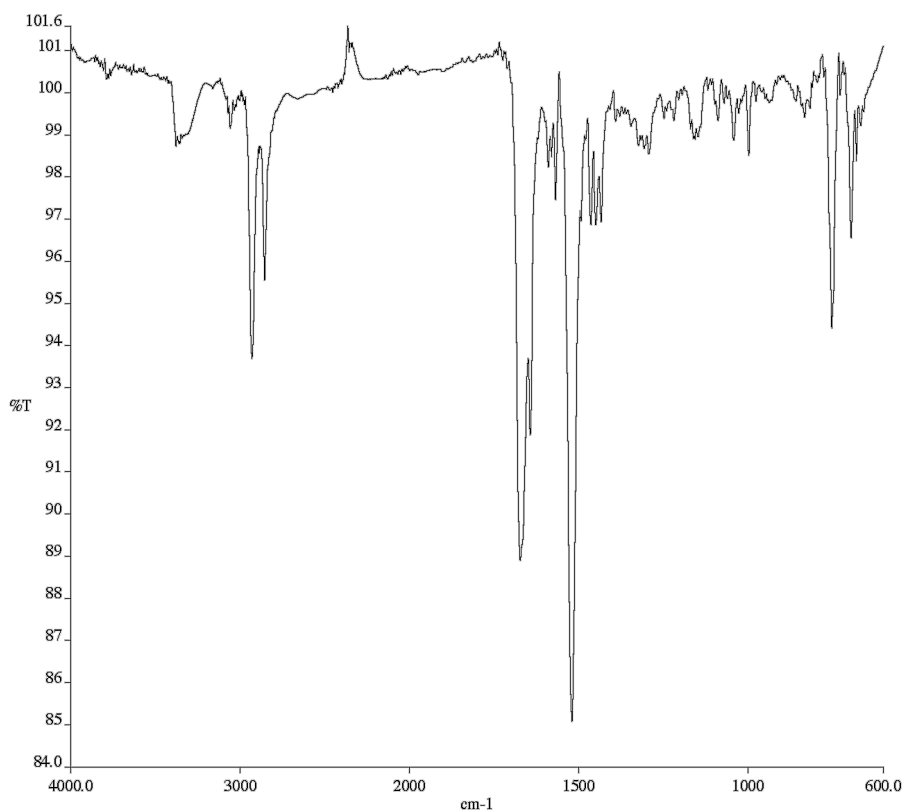
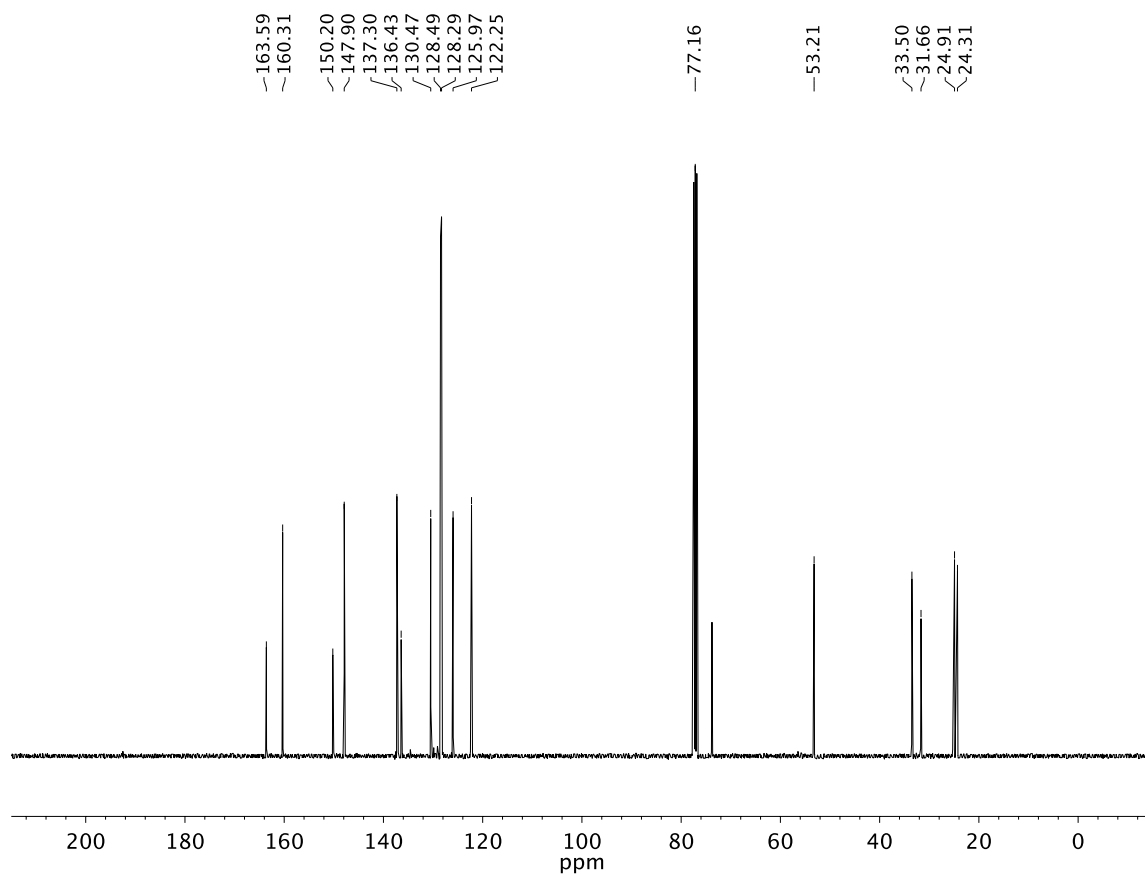


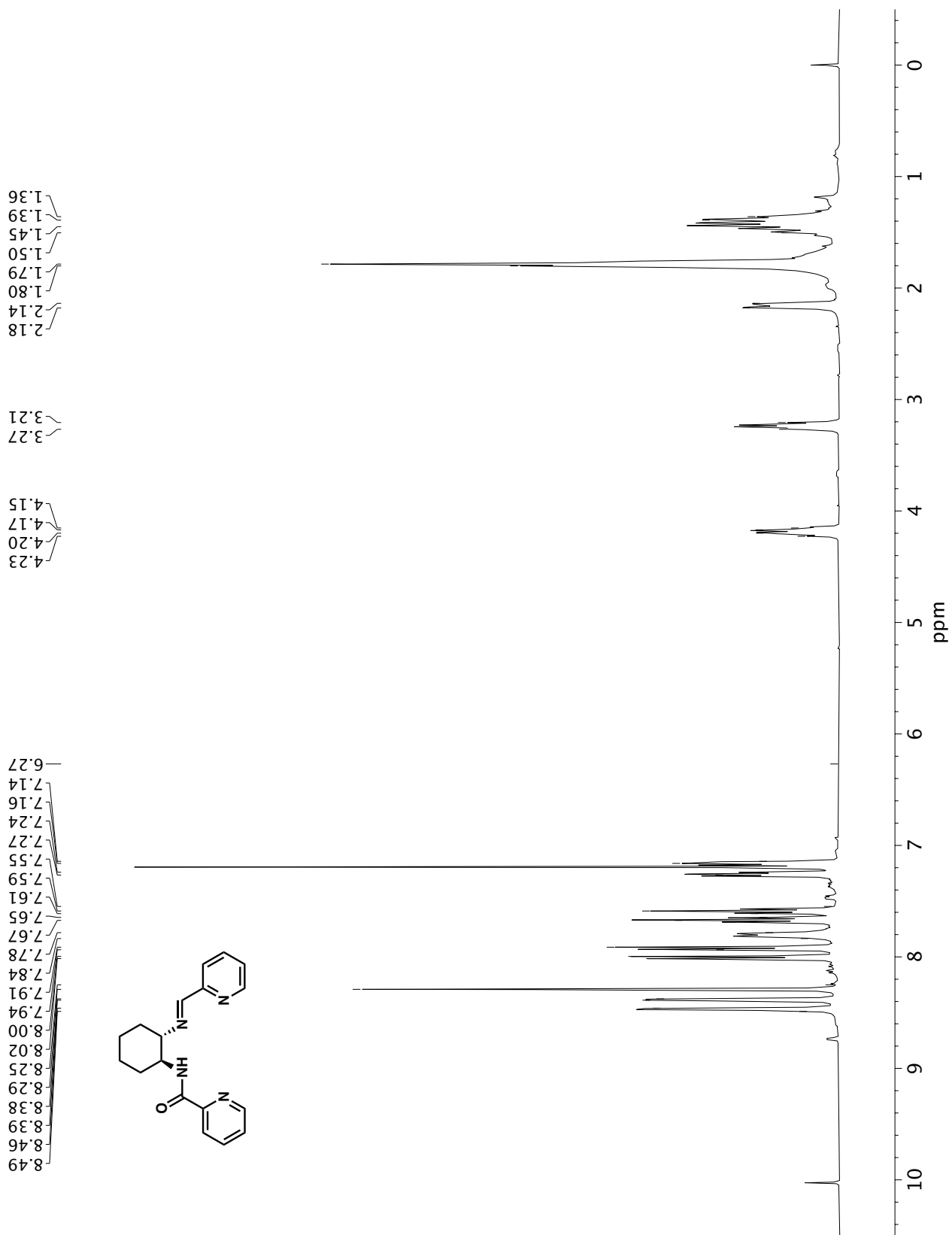
**A6.15** Infrared spectrum (Thin Film, NaCl) of compound **L64****A6.16** ¹³C NMR (100 MHz, CDCl₃) of compound **L64**

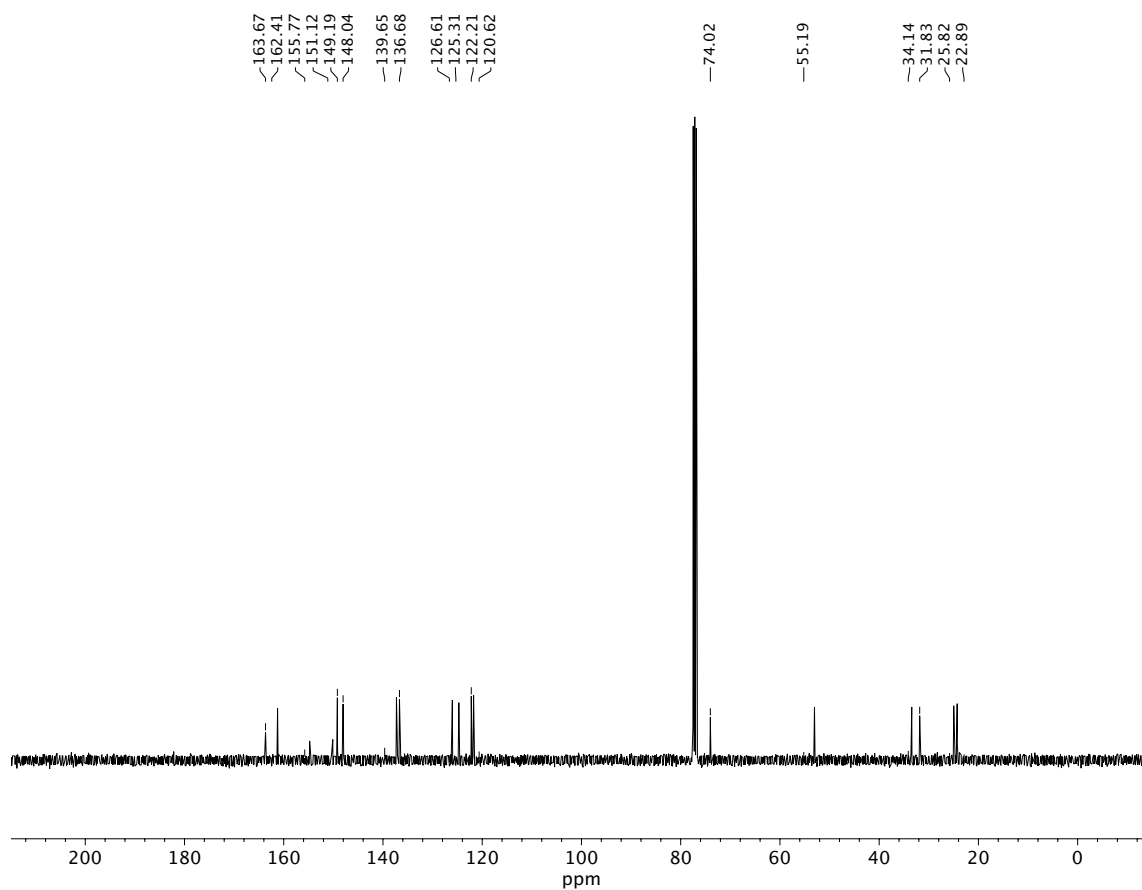
**A6.17** ¹H NMR (400 MHz, CDCl₃) of compound **SI10**

**A6.18** Infrared spectrum (Thin Film, NaCl) of compound **SI10****A6.19** ¹³C NMR (100 MHz, CDCl₃) of compound **SI10**

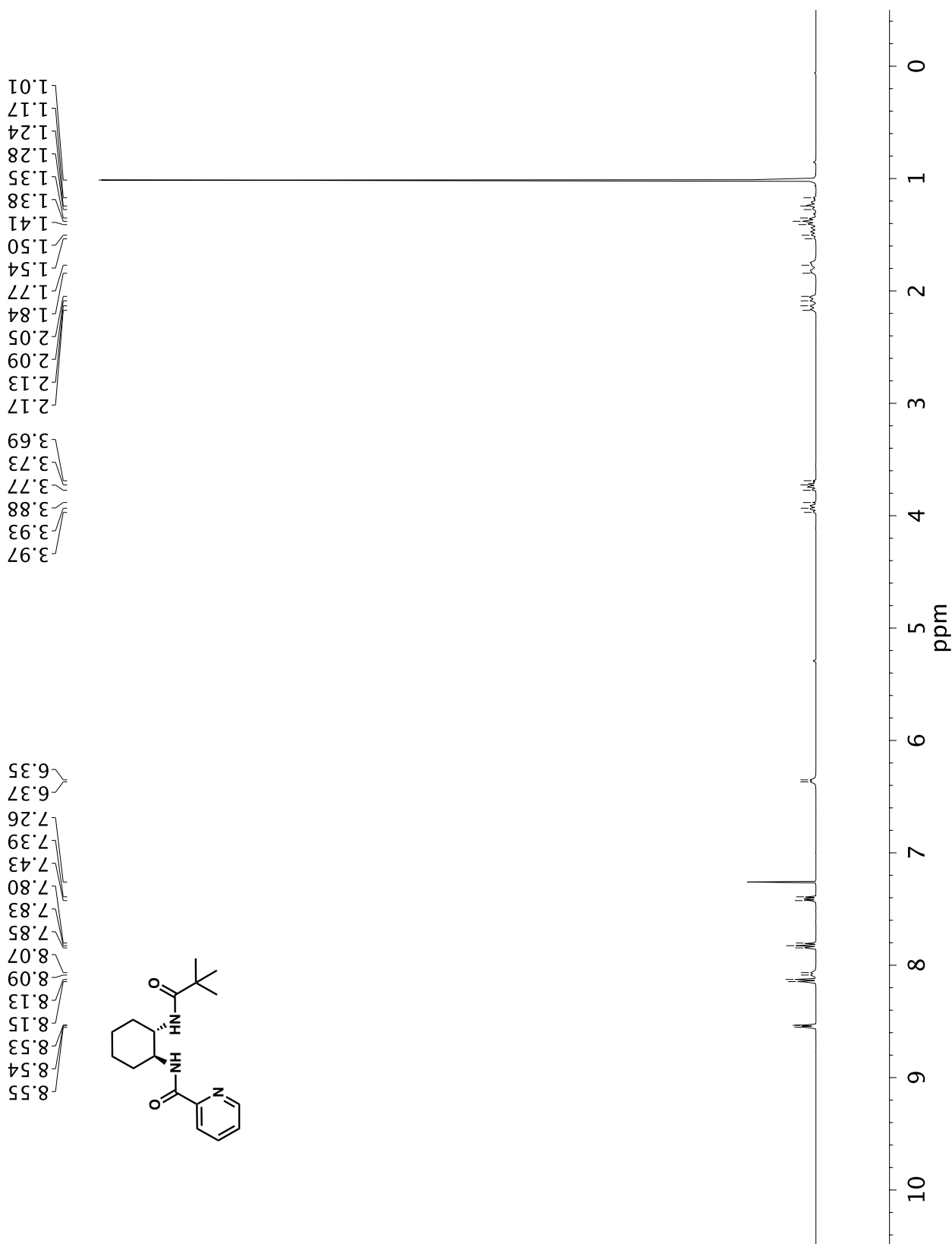


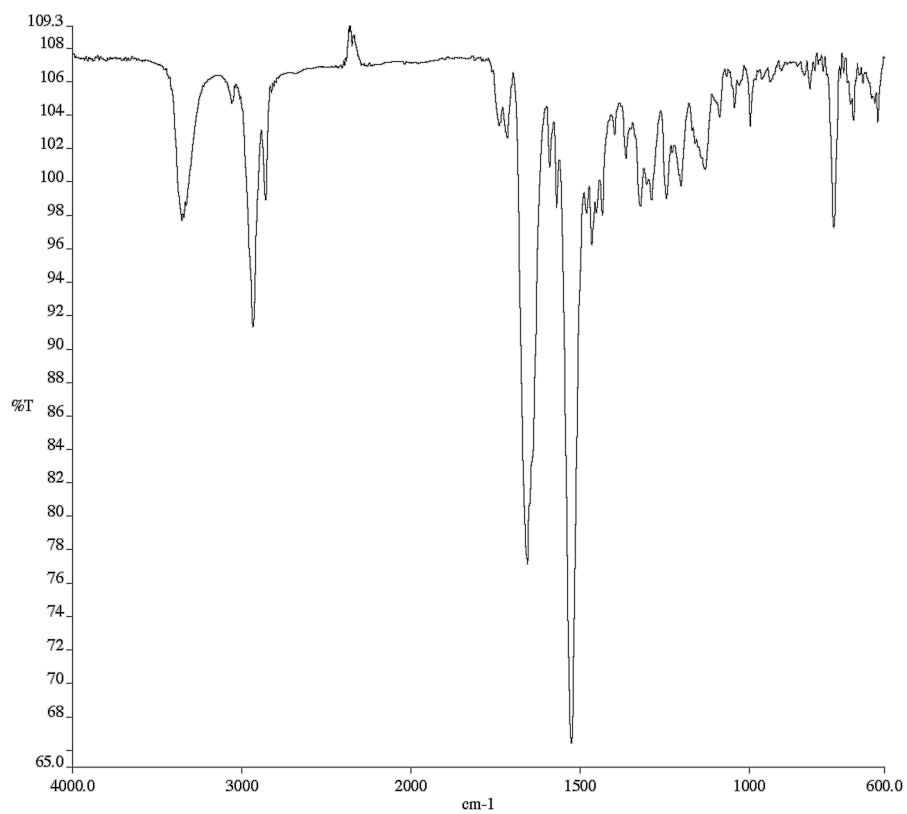
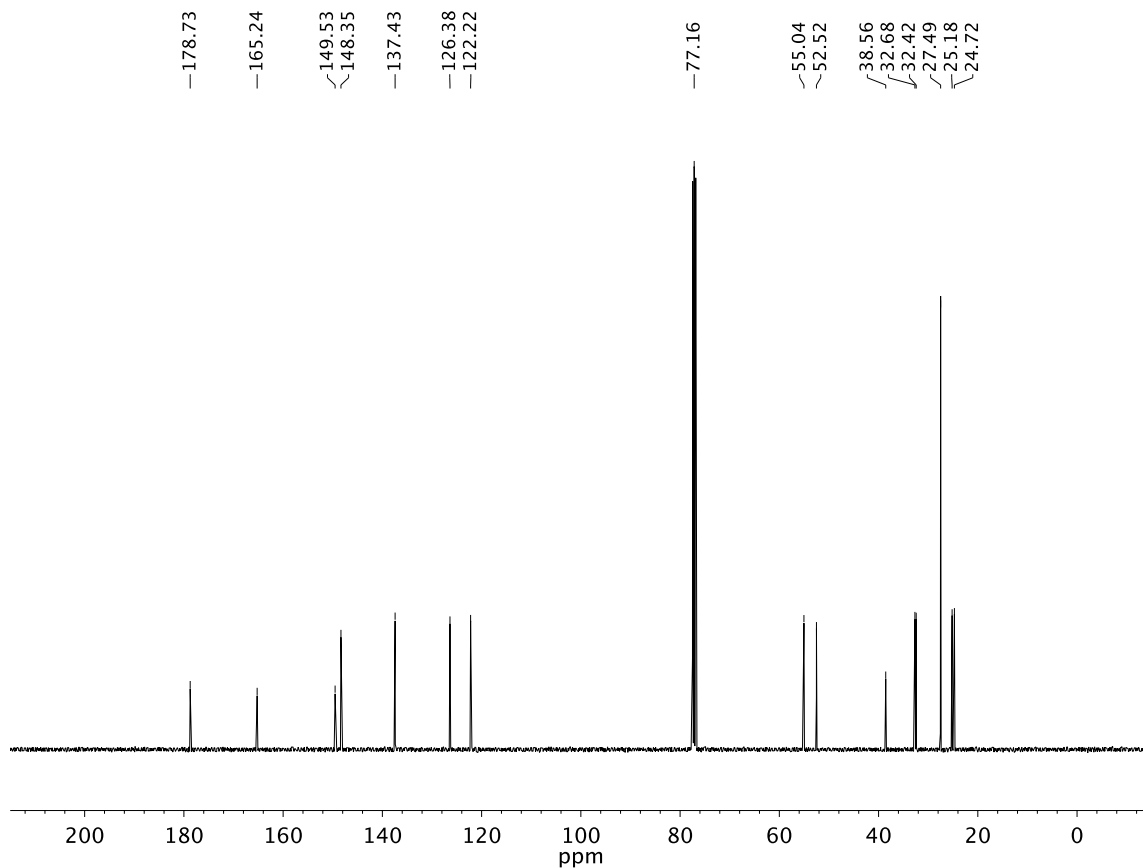
**A6.21** Infrared spectrum (Thin Film, NaCl) of compound **L61****A6.22** ¹³C NMR (100 MHz, CDCl₃) of compound **L61**

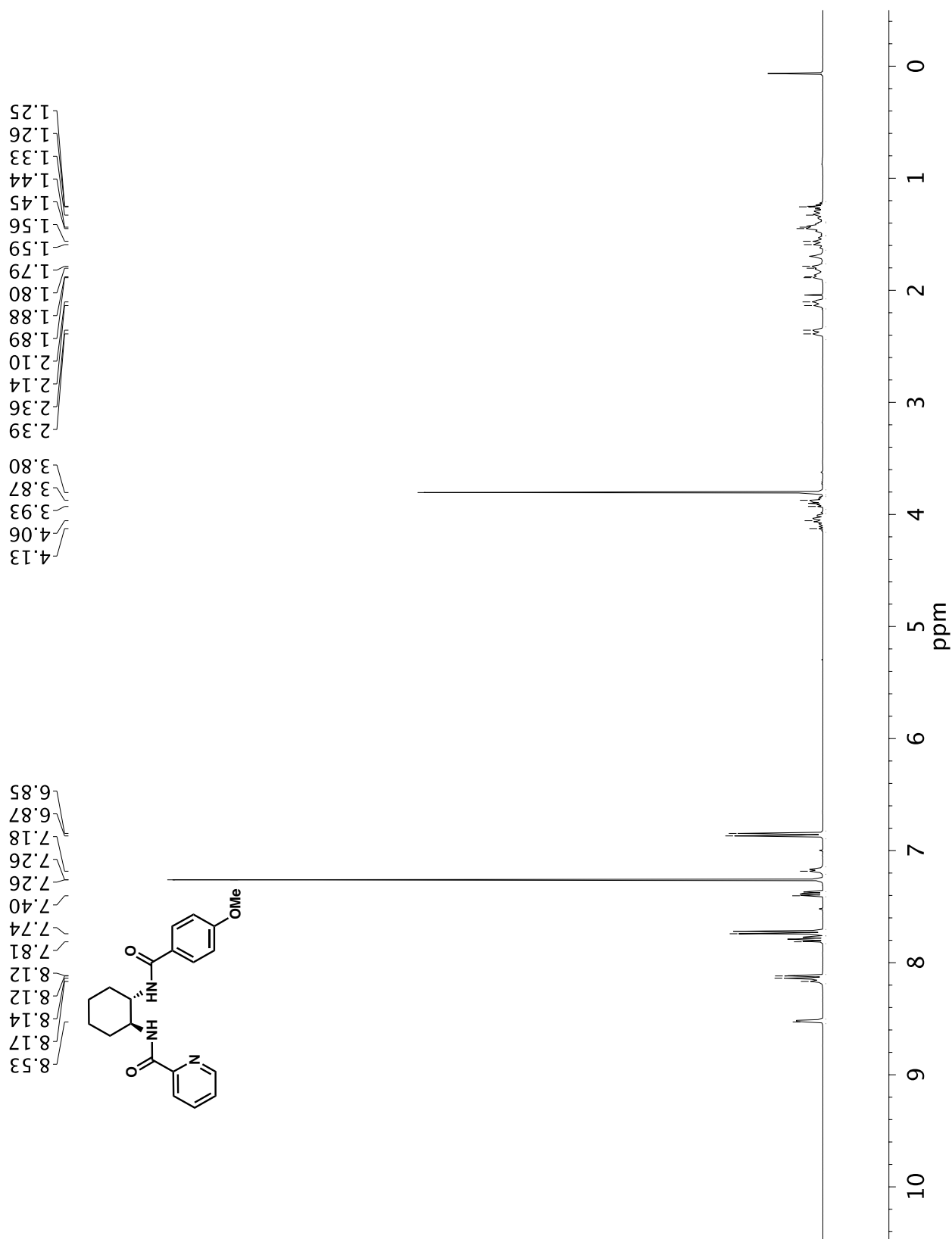


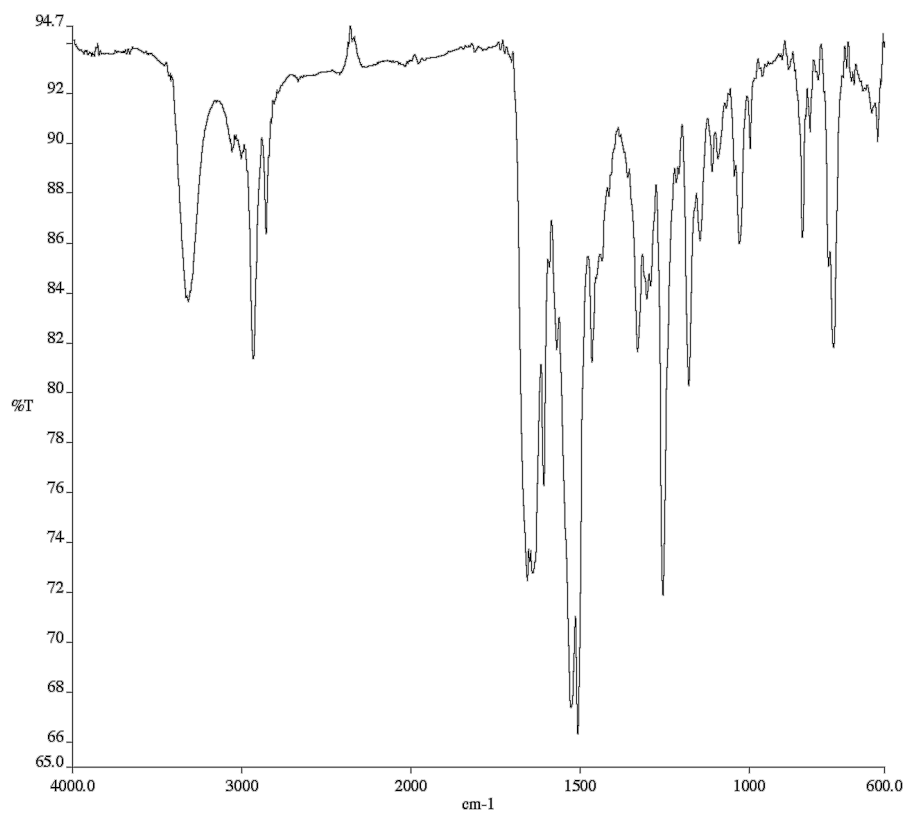


A6.24 ^{13}C NMR (100 MHz, CDCl_3) of compound **L63**

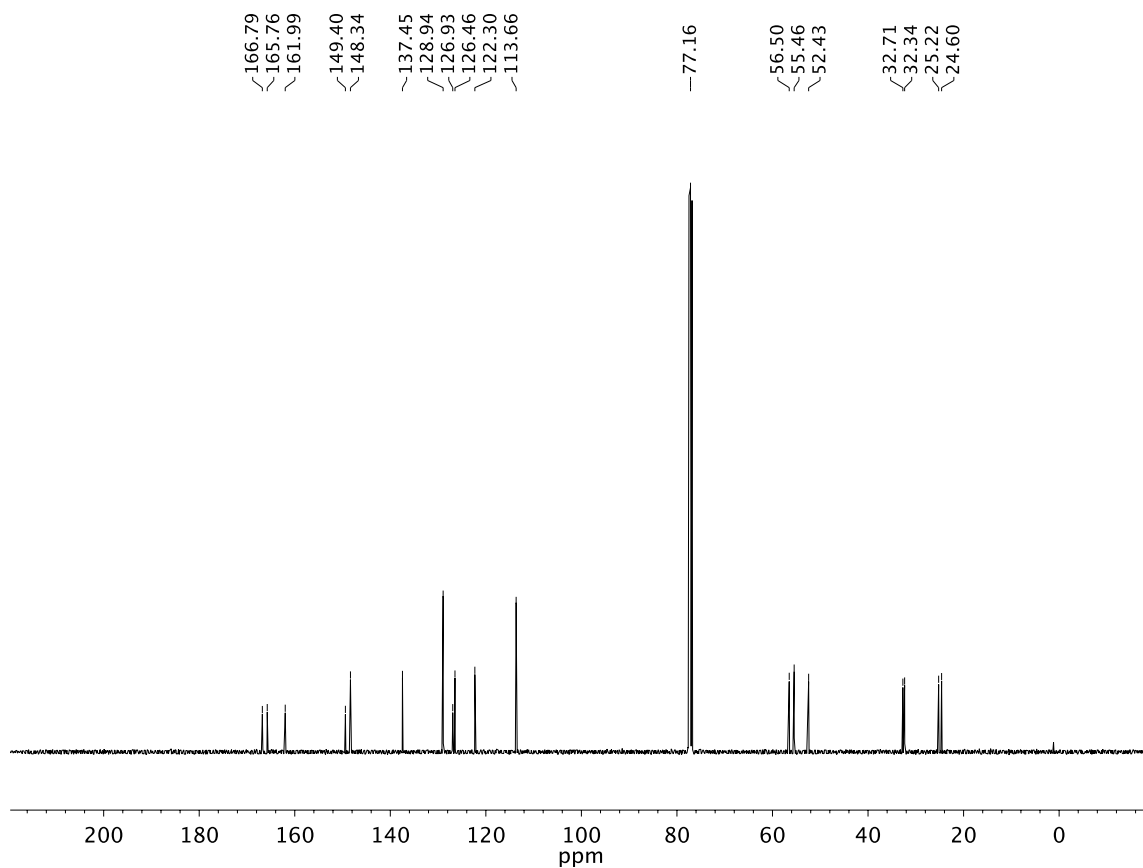
A6.25 ¹H NMR (400 MHz, CDCl₃) of compound L67

**A6.26** Infrared spectrum (Thin Film, NaCl) of compound **L67****A6.27** ¹³C NMR (100 MHz, CDCl₃) of compound **L67**

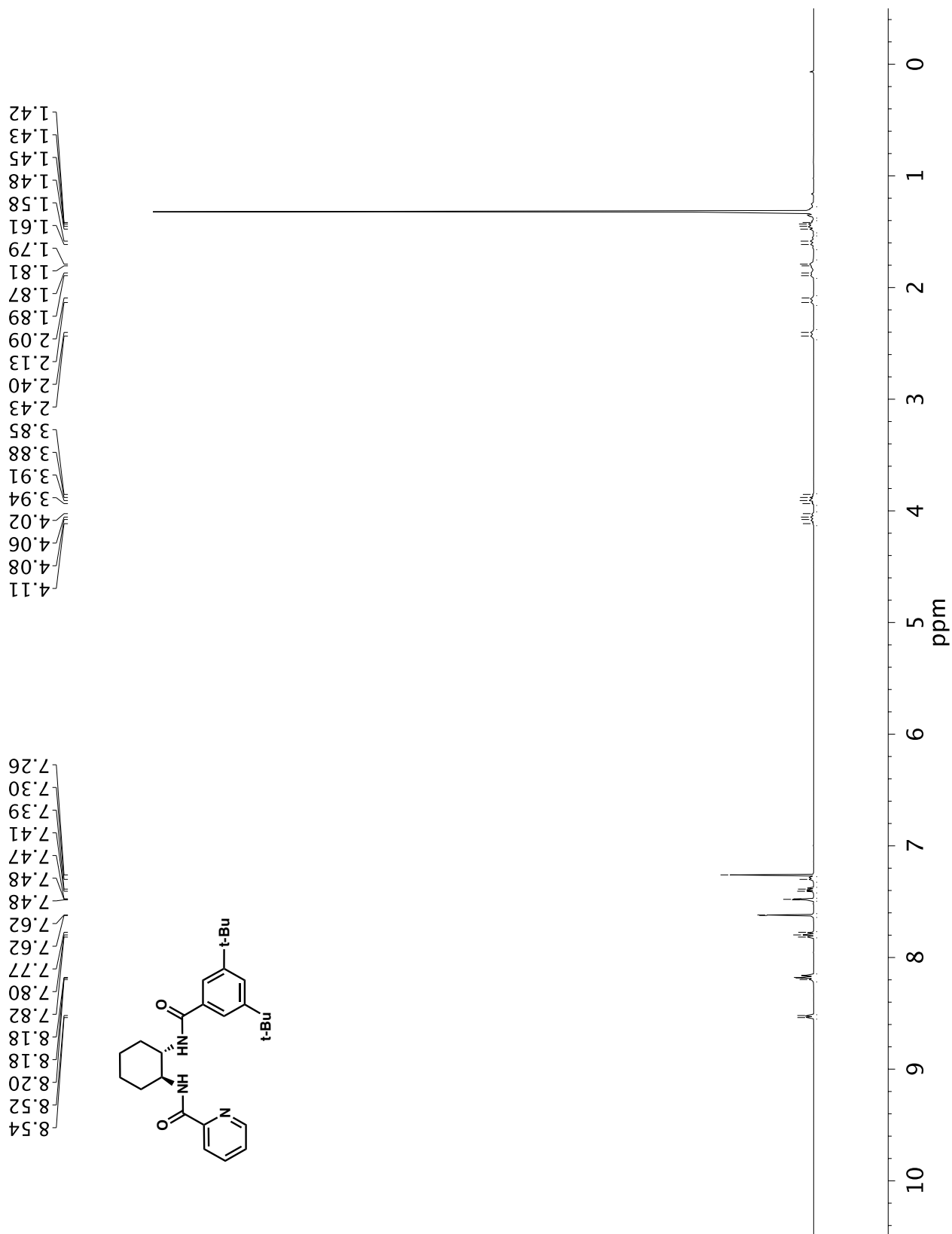


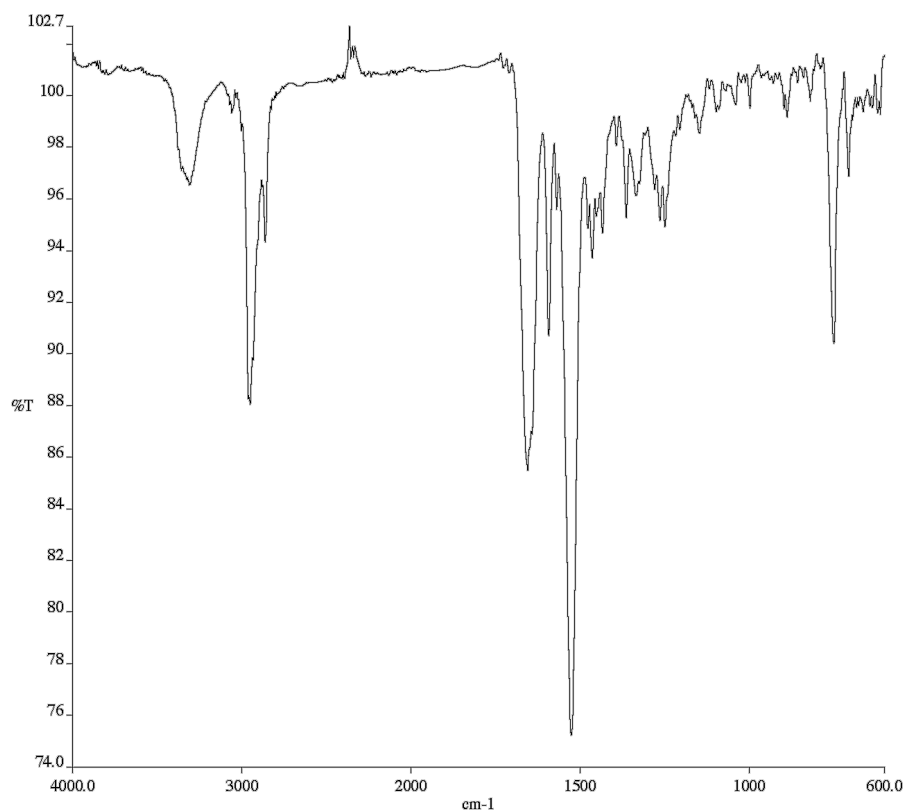


A6.29 Infrared spectrum (Thin Film, NaCl) of compound **L66**

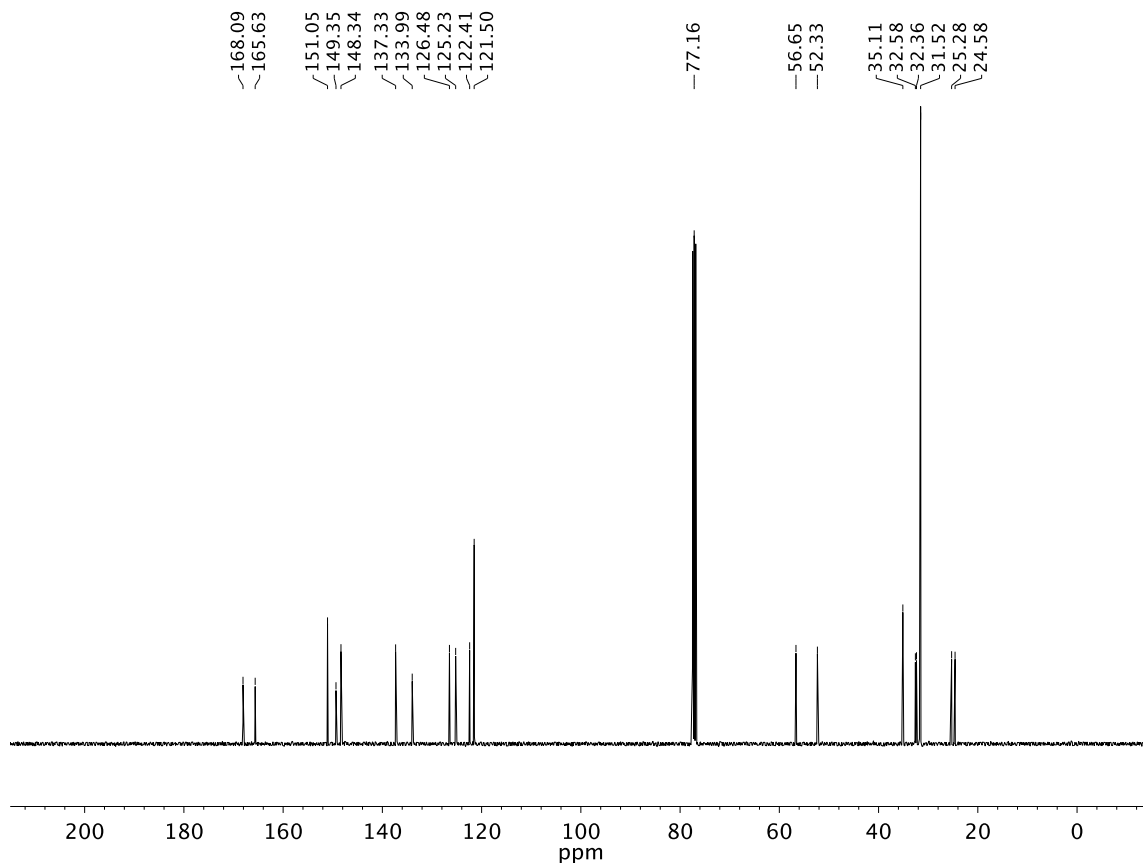


A6.30 ^{13}C NMR (100 MHz, CDCl_3) of compound **L66**

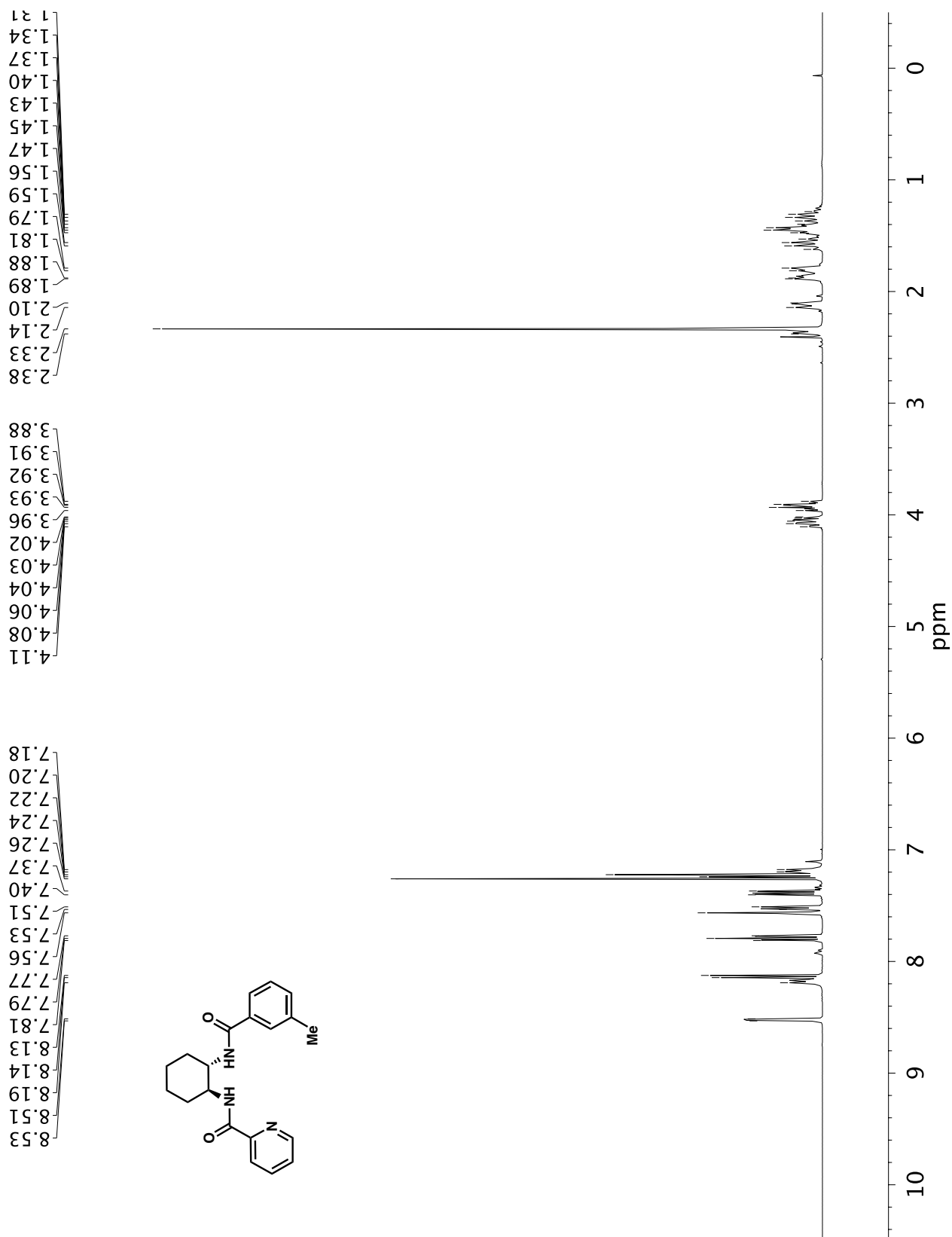


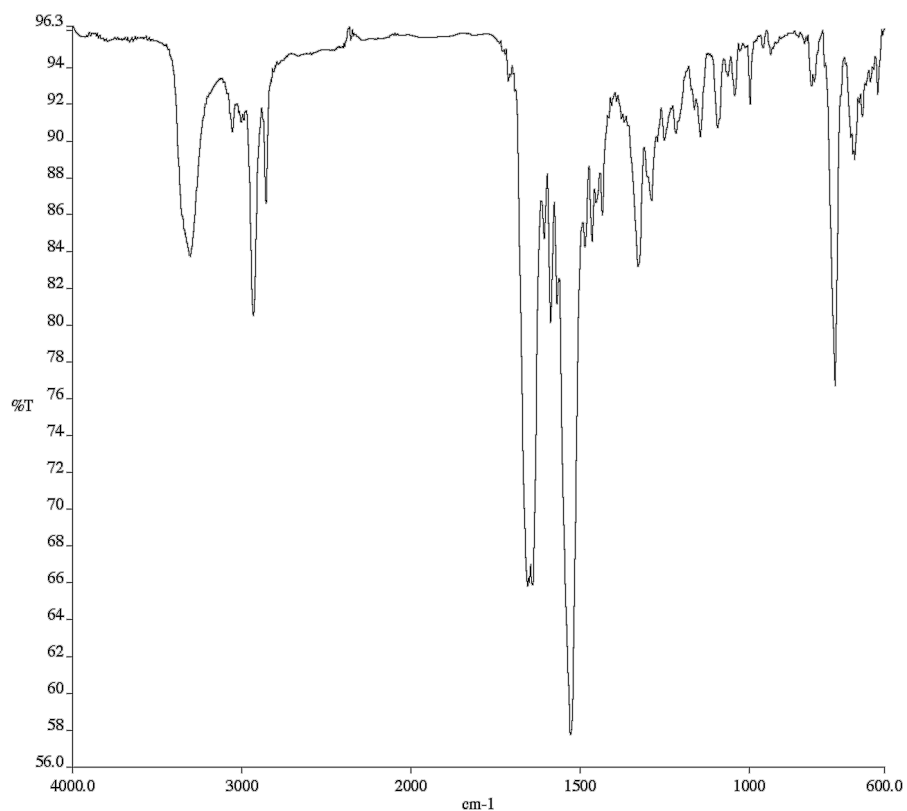
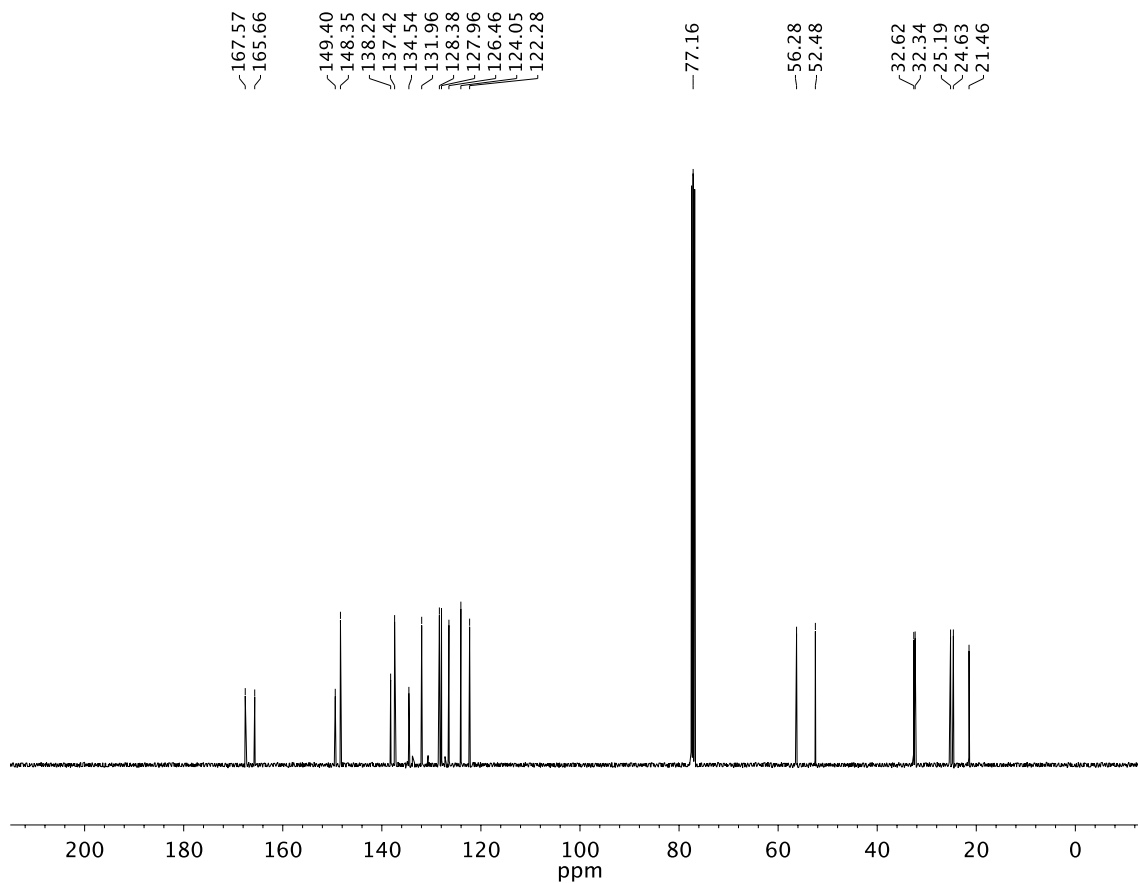


A6.32 Infrared spectrum (Thin Film, NaCl) of compound **L68**

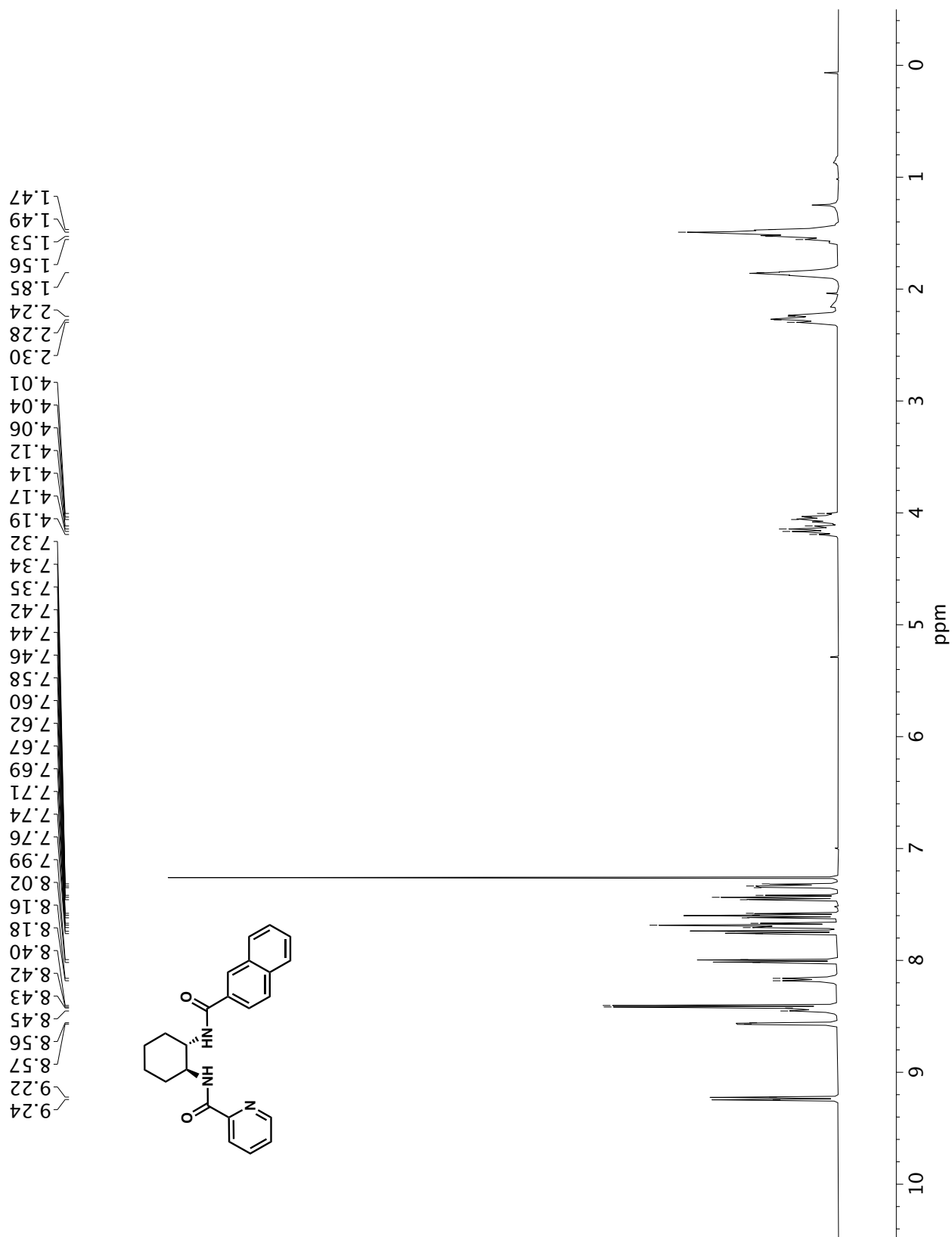


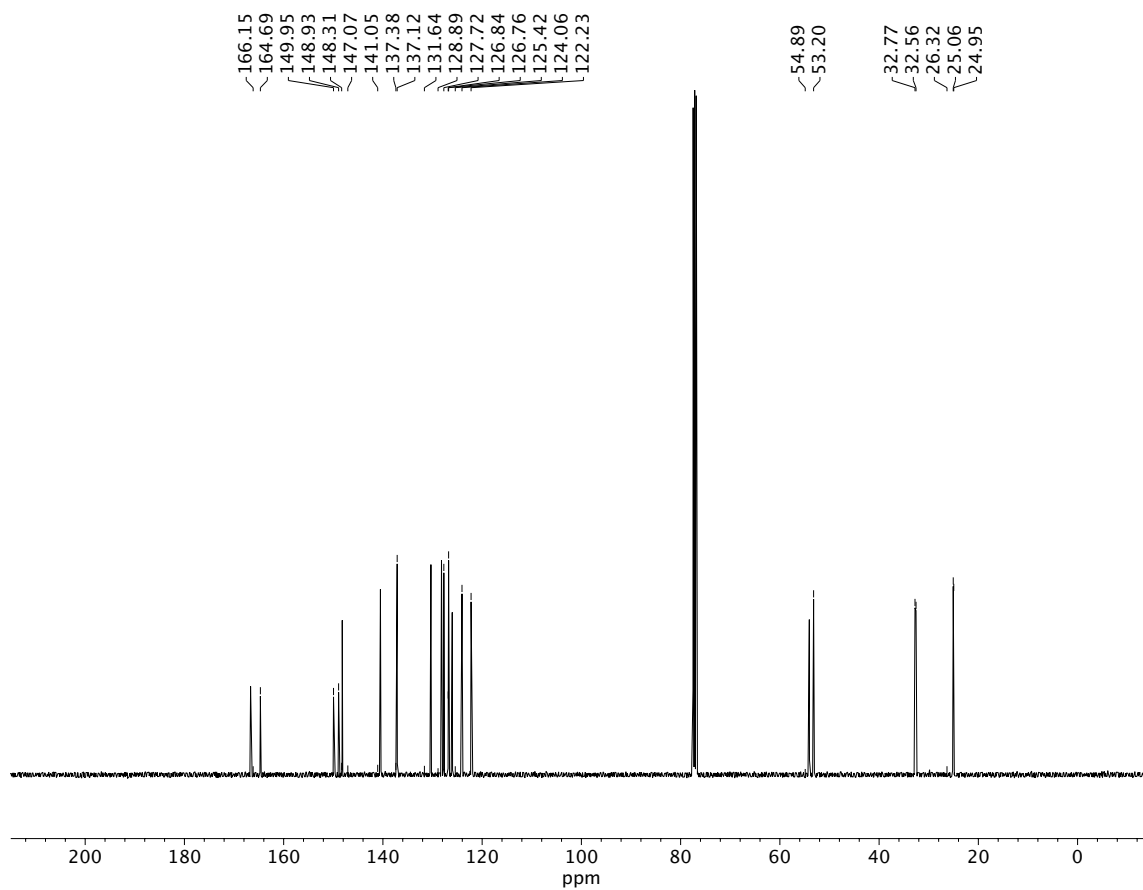
A6.33 ¹³C NMR (100 MHz, CDCl₃) of compound **L68**

**A6.34** ¹H NMR (400 MHz, CDCl₃) of compound **L69**

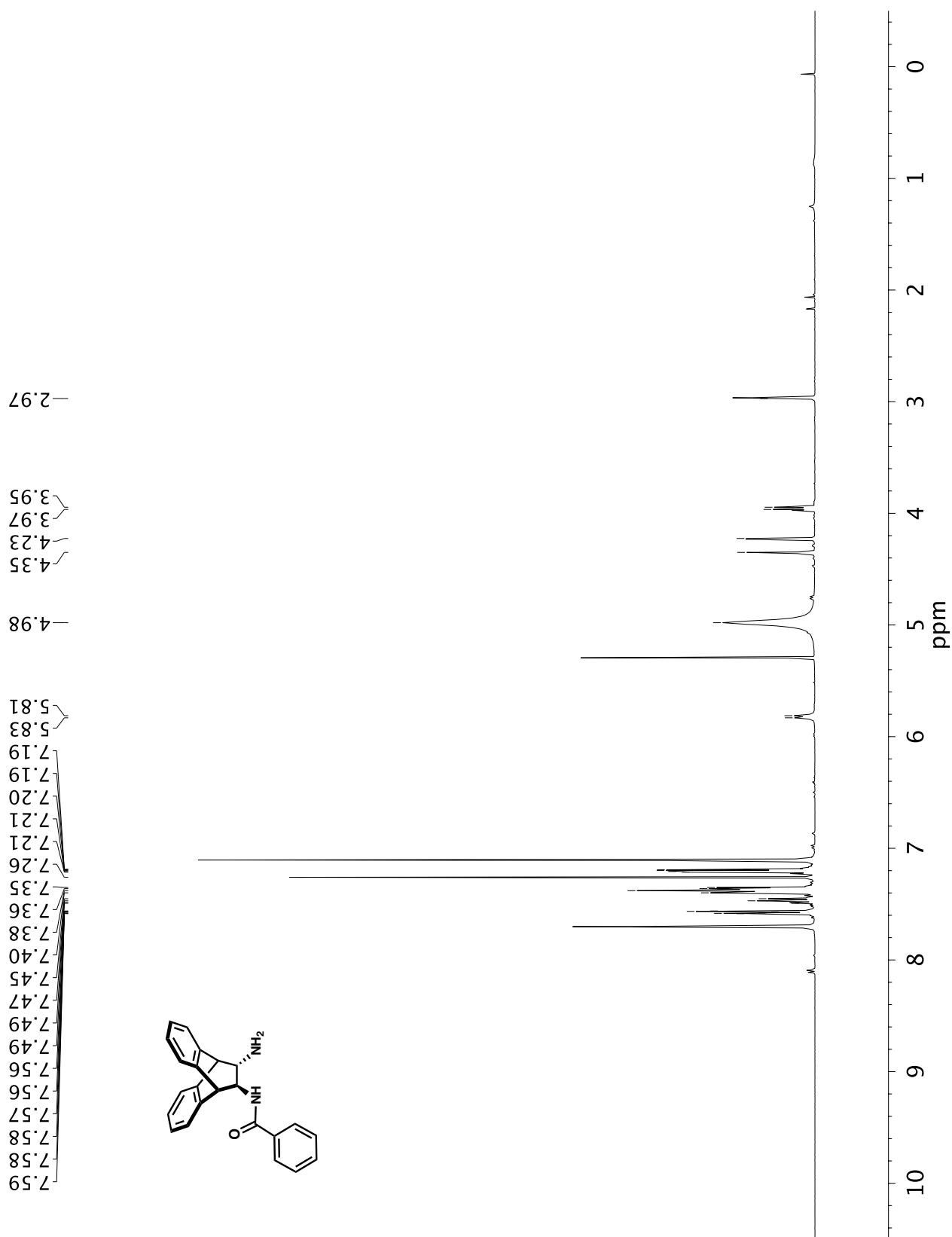
**A6.35** Infrared spectrum (Thin Film, NaCl) of compound **L69****A6.36** ^{13}C NMR (100 MHz, CDCl_3) of compound **L69**

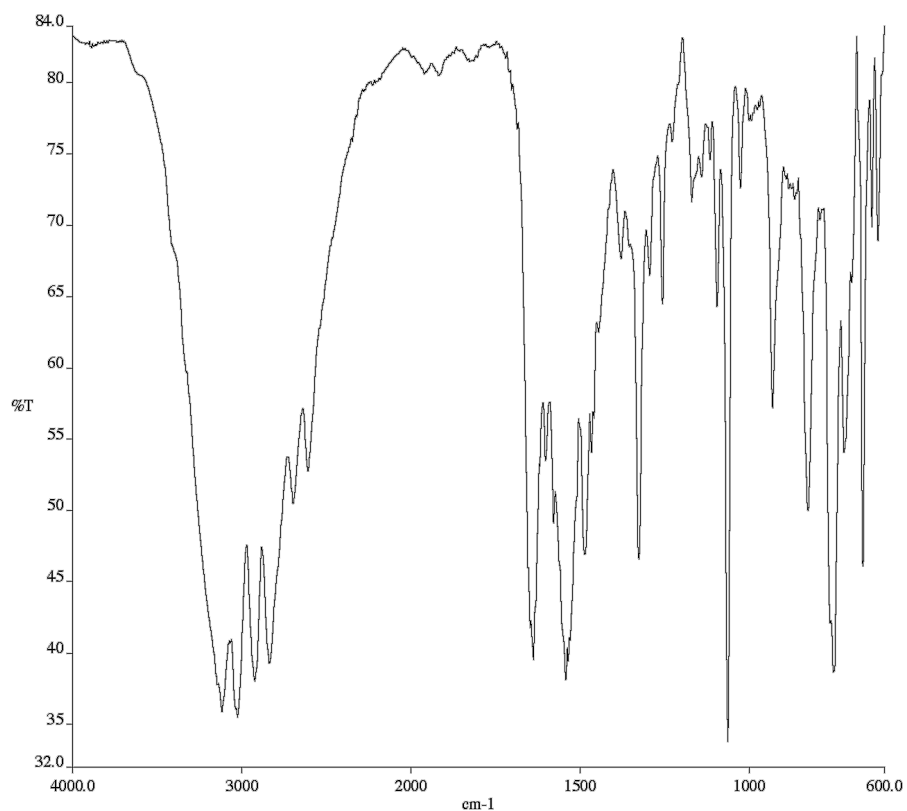


**A6.38** ¹H NMR (400 MHz, CDCl₃) of compound **L72**

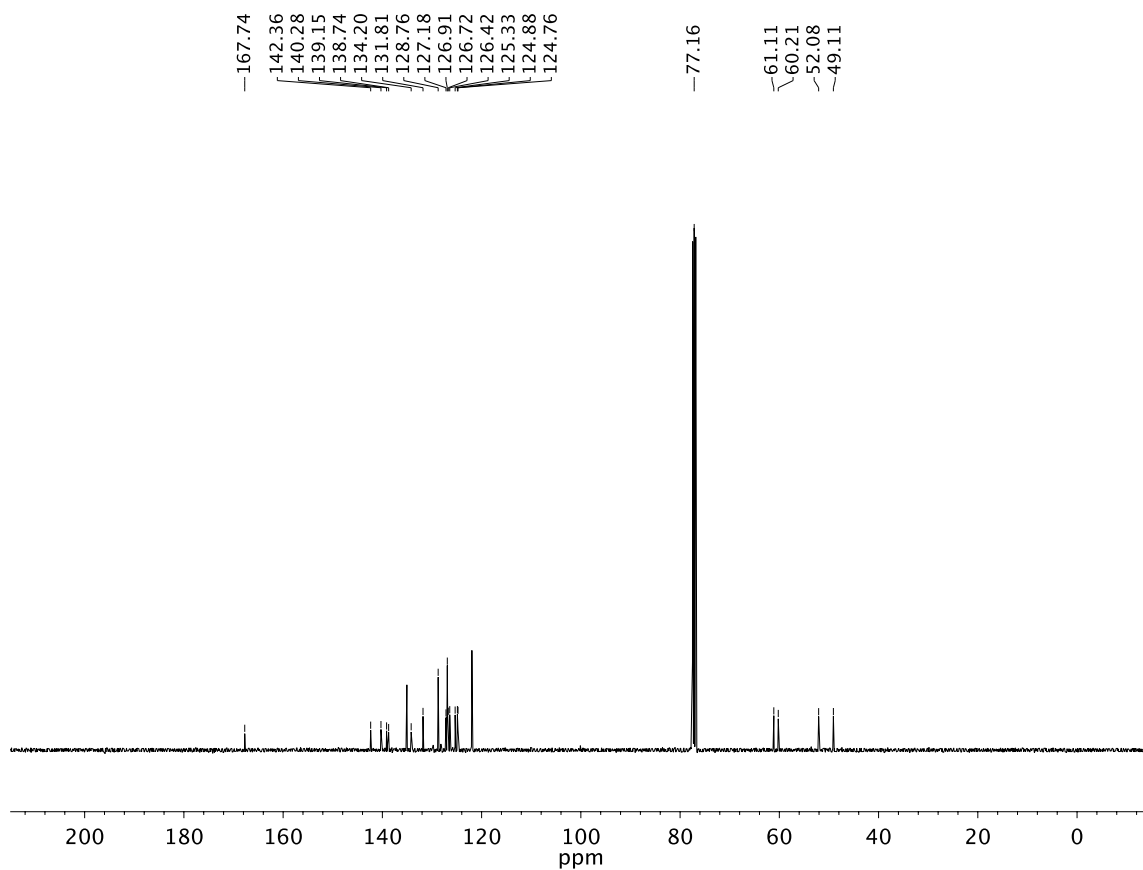


A6.39 ¹³C NMR (100 MHz, CDCl₃) of compound **L72**

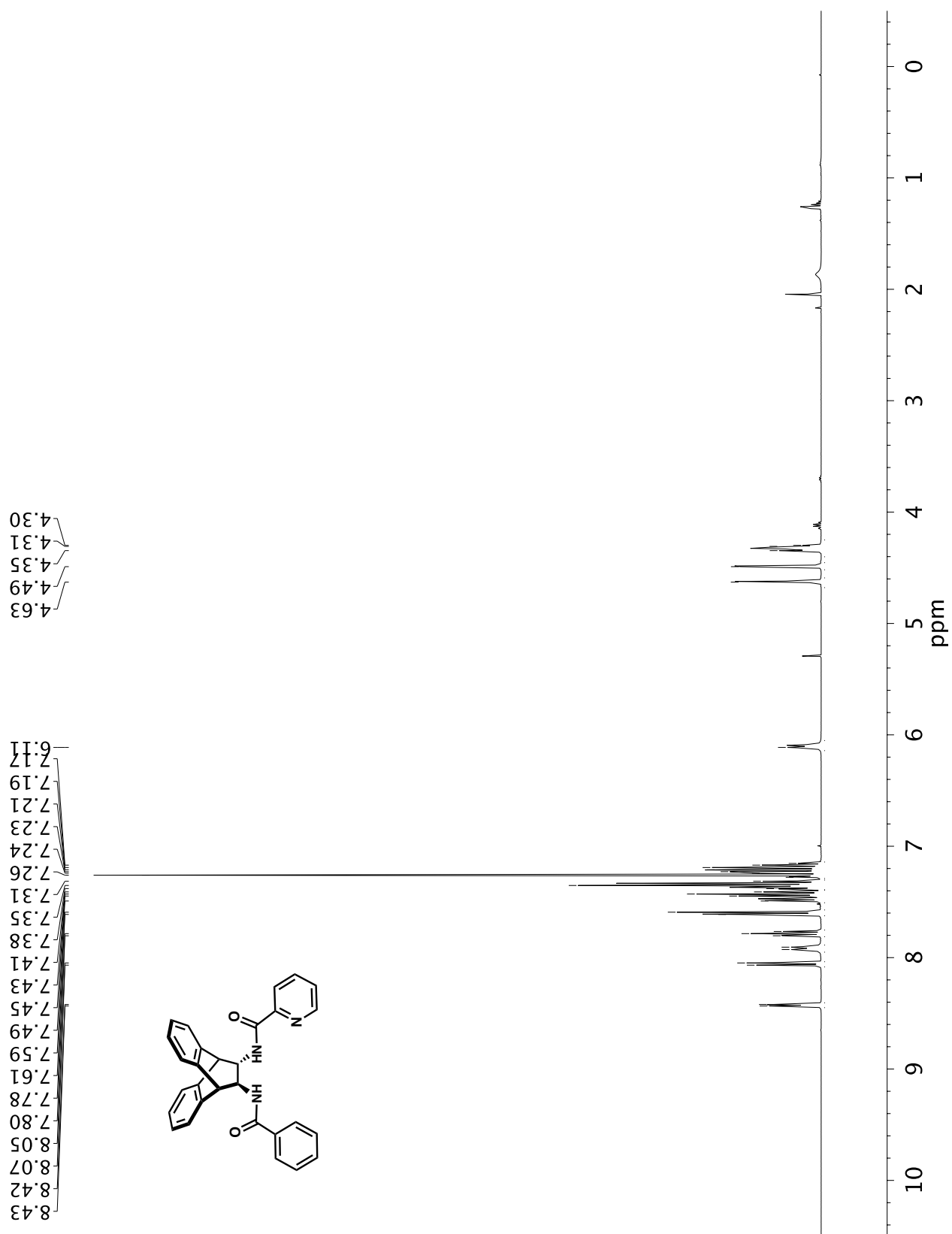
**A6.40** ^1H NMR (300 MHz, CDCl_3) of compound **SI11**

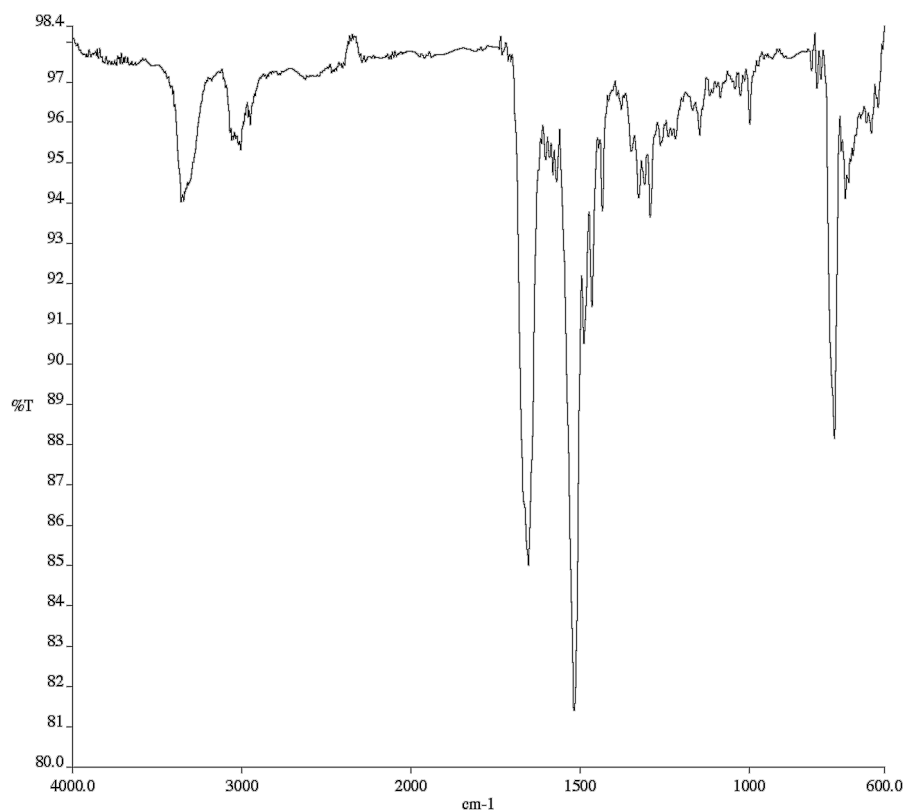


A6.41 Infrared spectrum (Thin Film, NaCl) of compound **SI11**

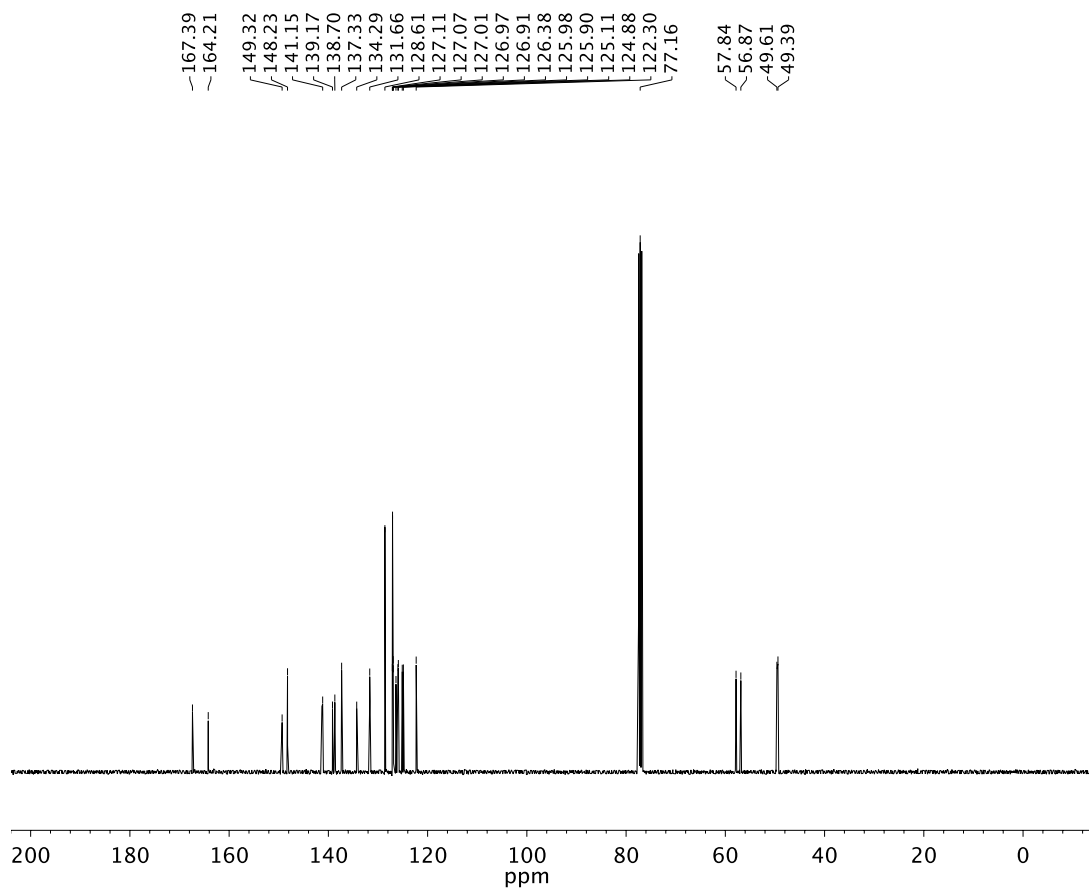


A6.42 ¹³C NMR (100 MHz, CDCl₃) of compound **SI11**

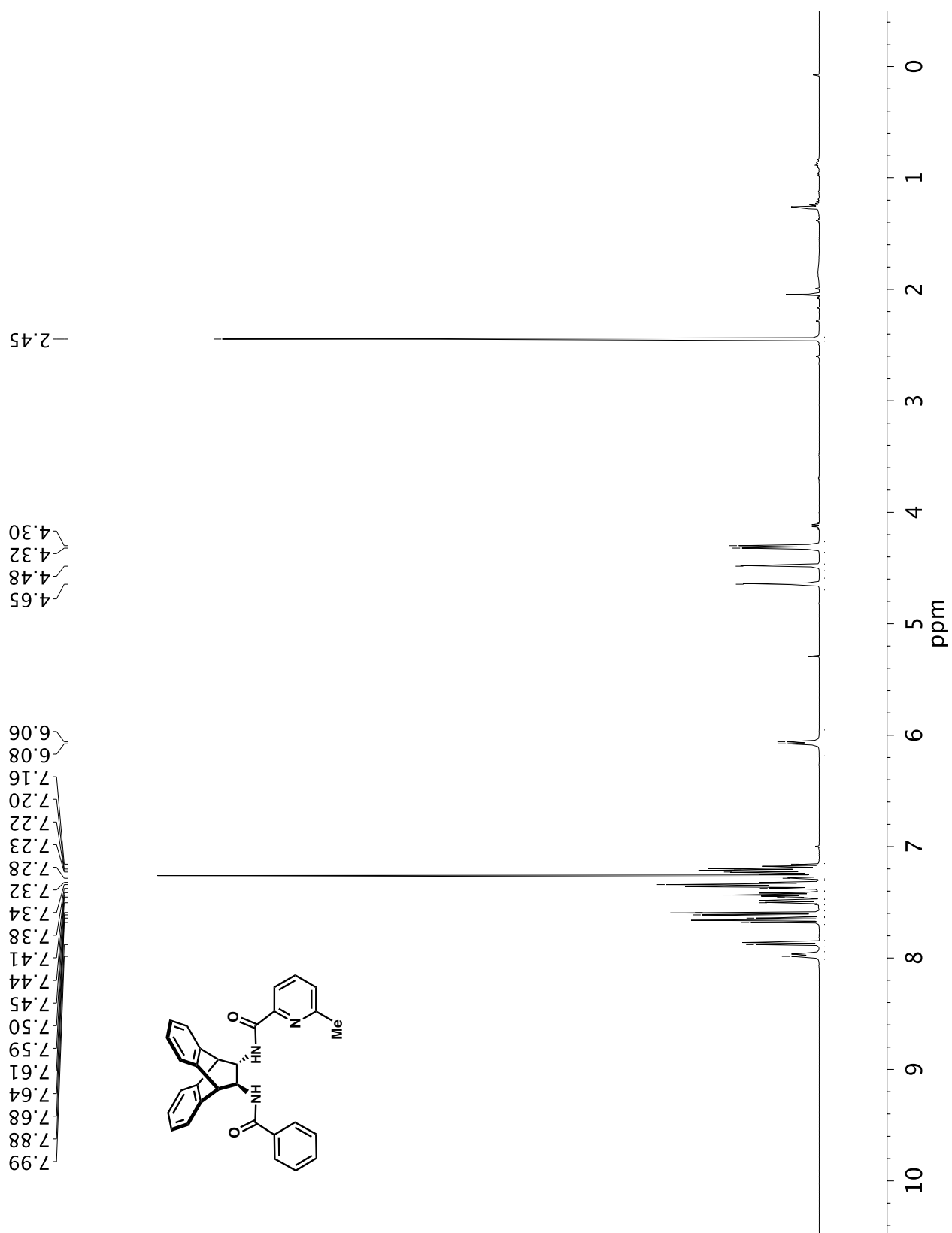
**A6.43** ^1H NMR (400 MHz, CDCl_3) of compound **L73**

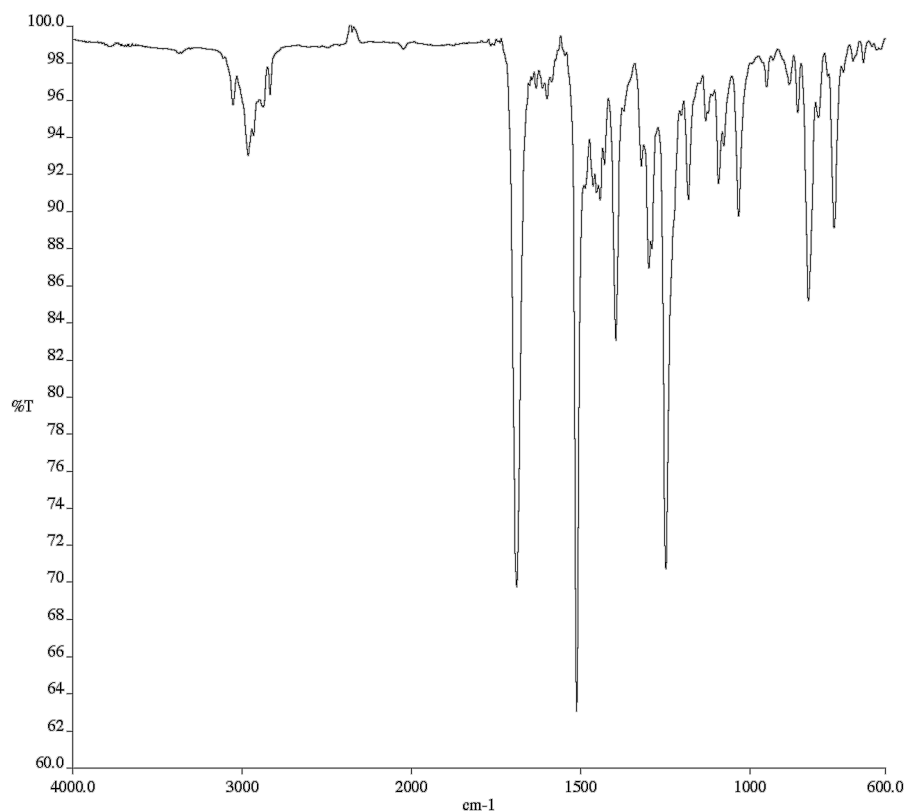
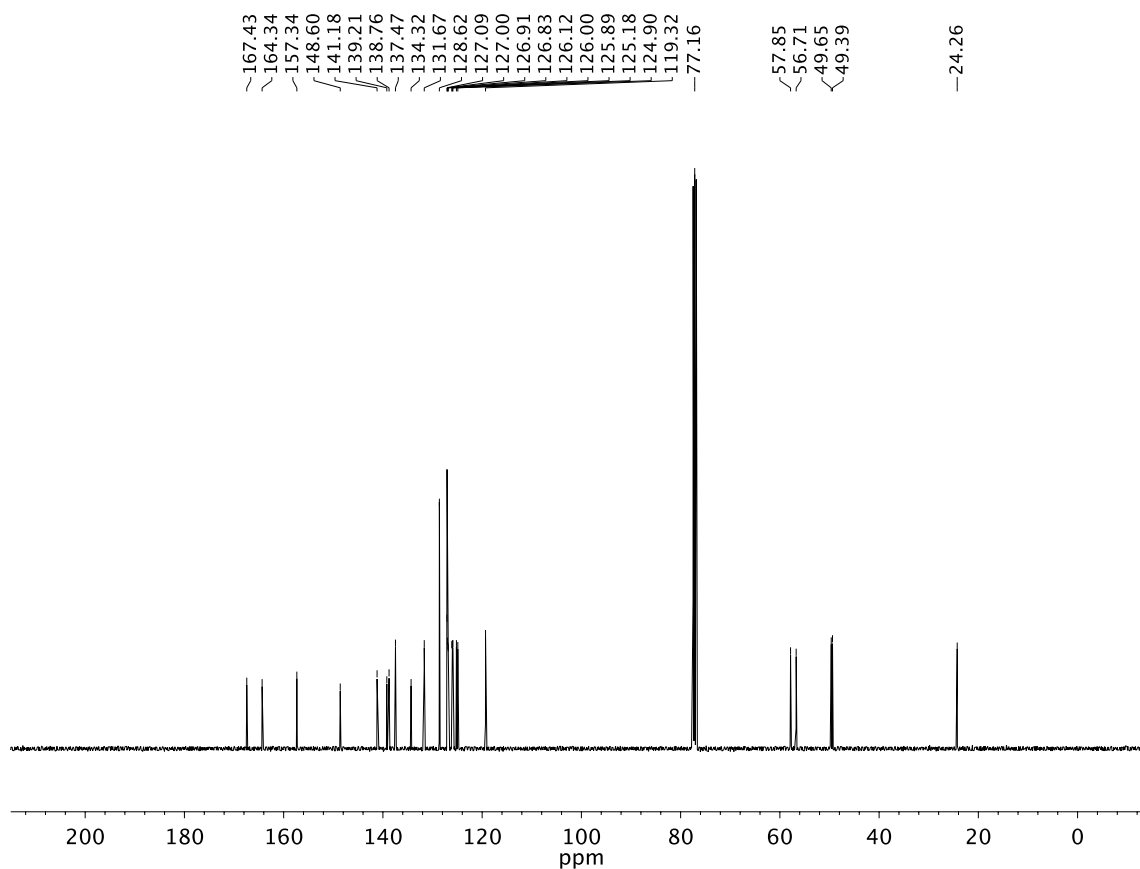


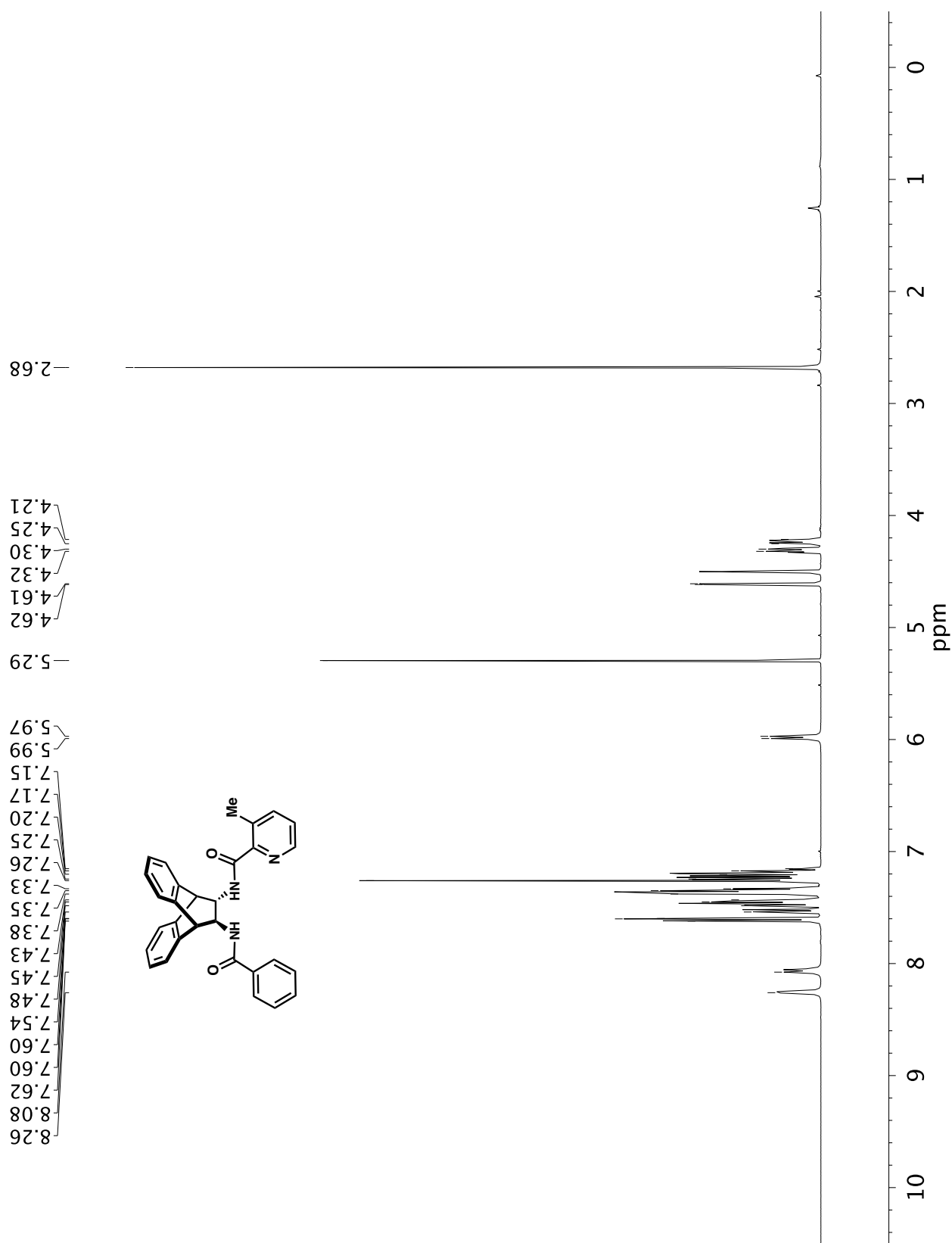
A6.44 Infrared spectrum (Thin Film, NaCl) of compound **L73**

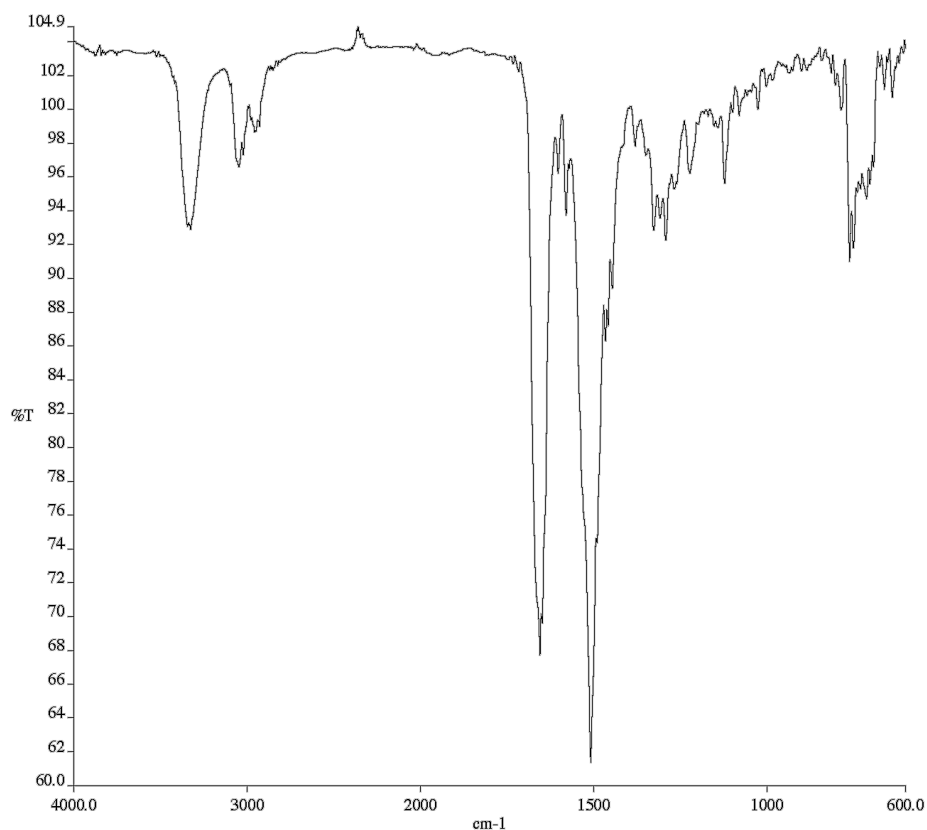


A6.45 ^{13}C NMR (100 MHz, CDCl_3) of compound **L73**

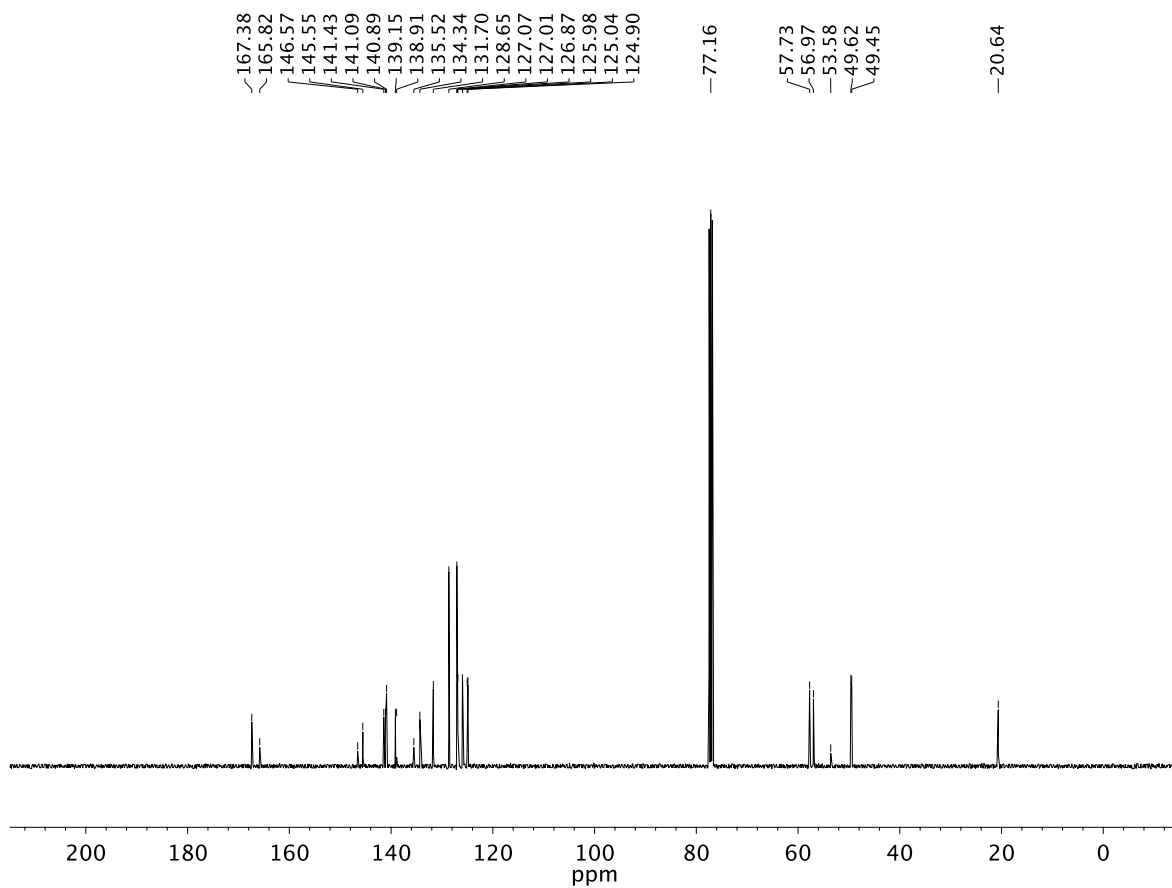


**A6.47** Infrared spectrum (Thin Film, NaCl) of compound **L74****A6.48** ¹³C NMR (100 MHz, CDCl₃) of compound **L74**

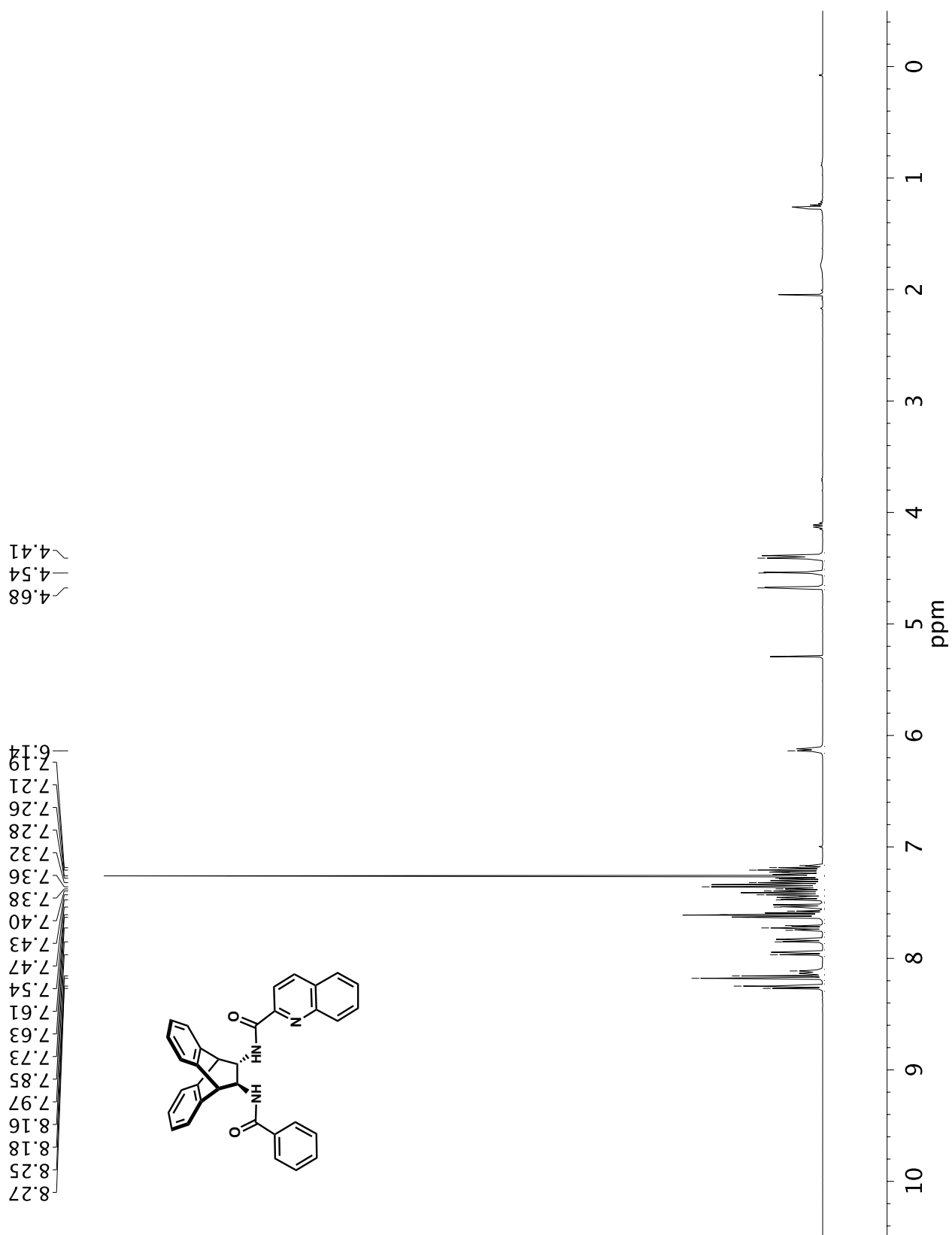
**A6.49** ¹H NMR (400 MHz, CDCl₃) of compound **L75**

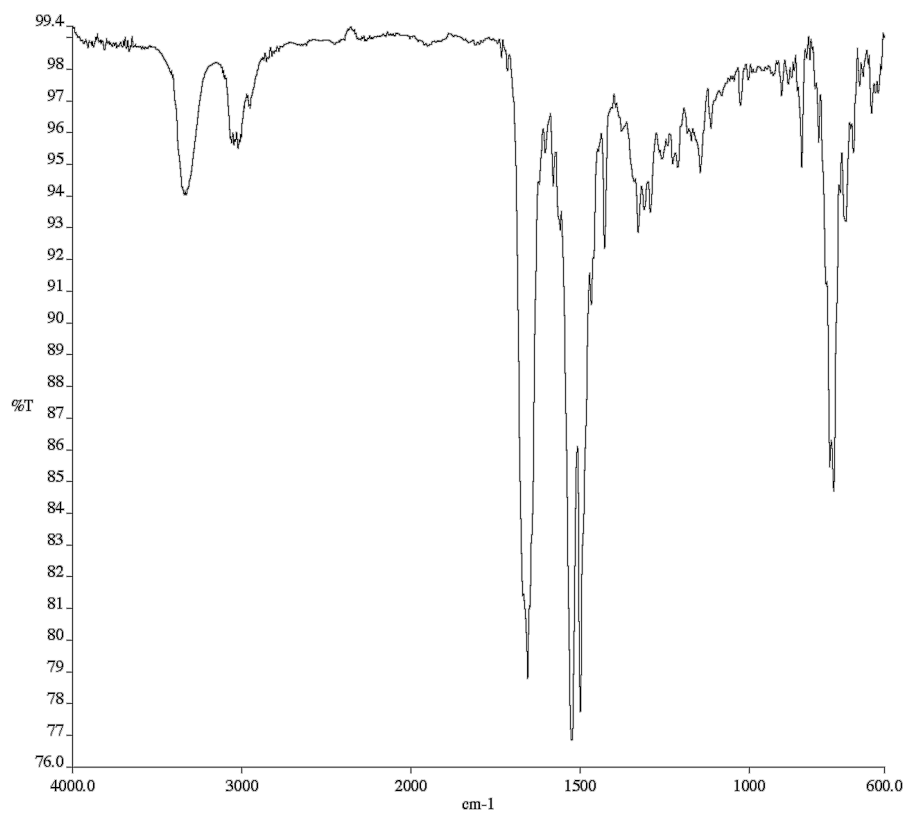
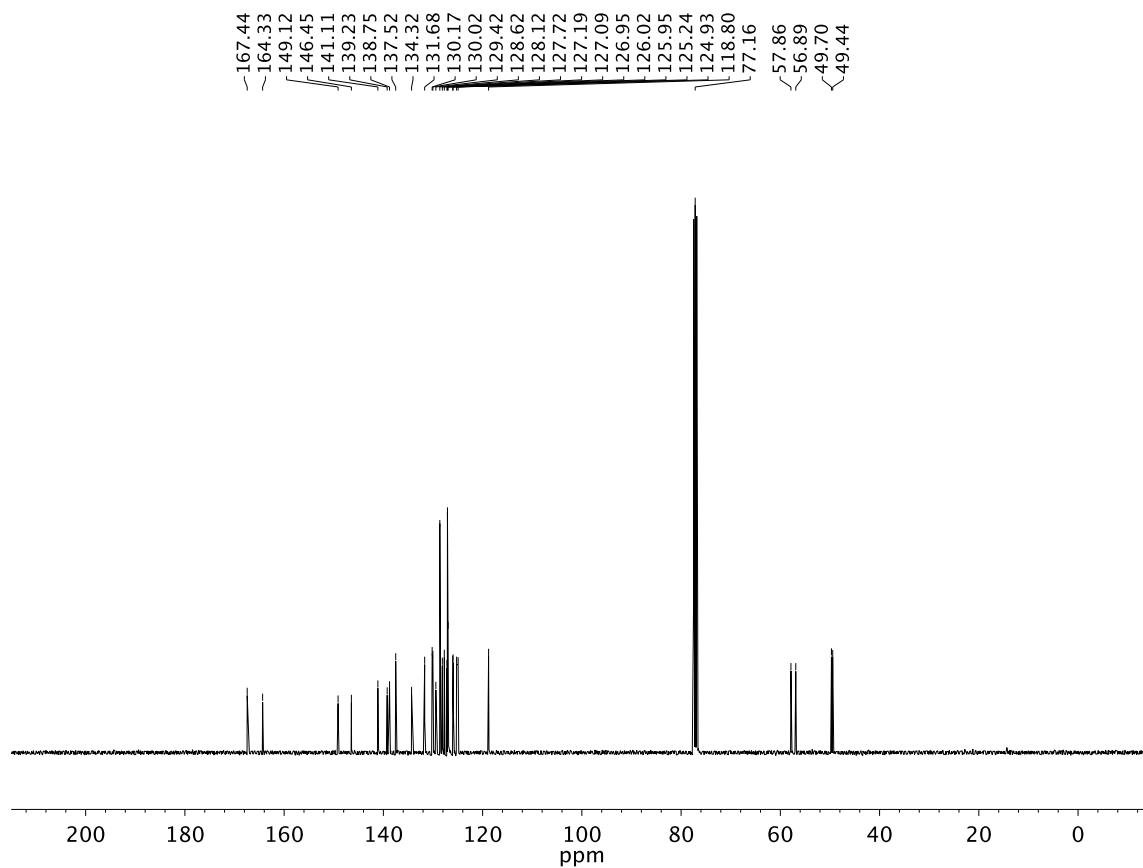


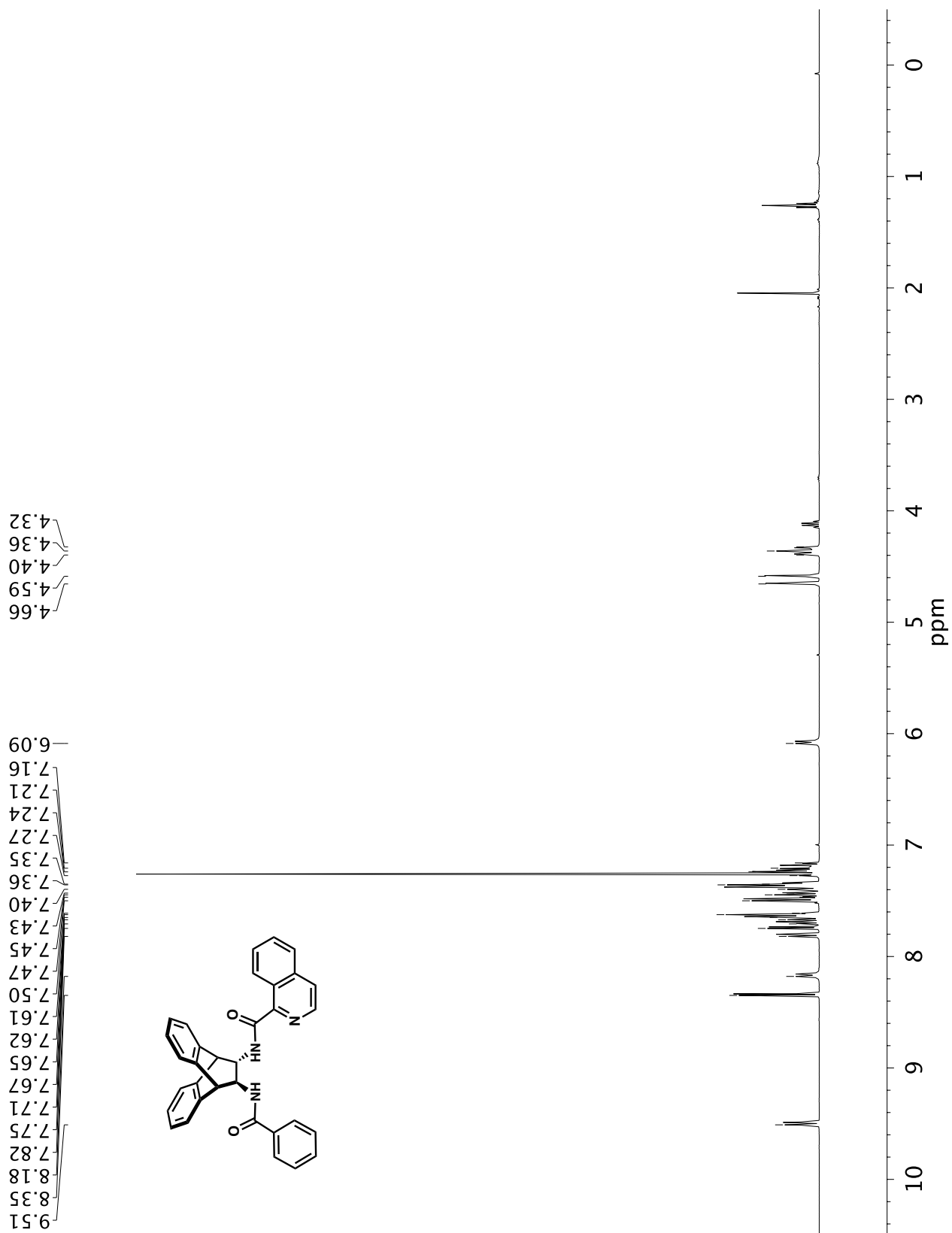
A6.50 Infrared spectrum (Thin Film, NaCl) of compound **L75**

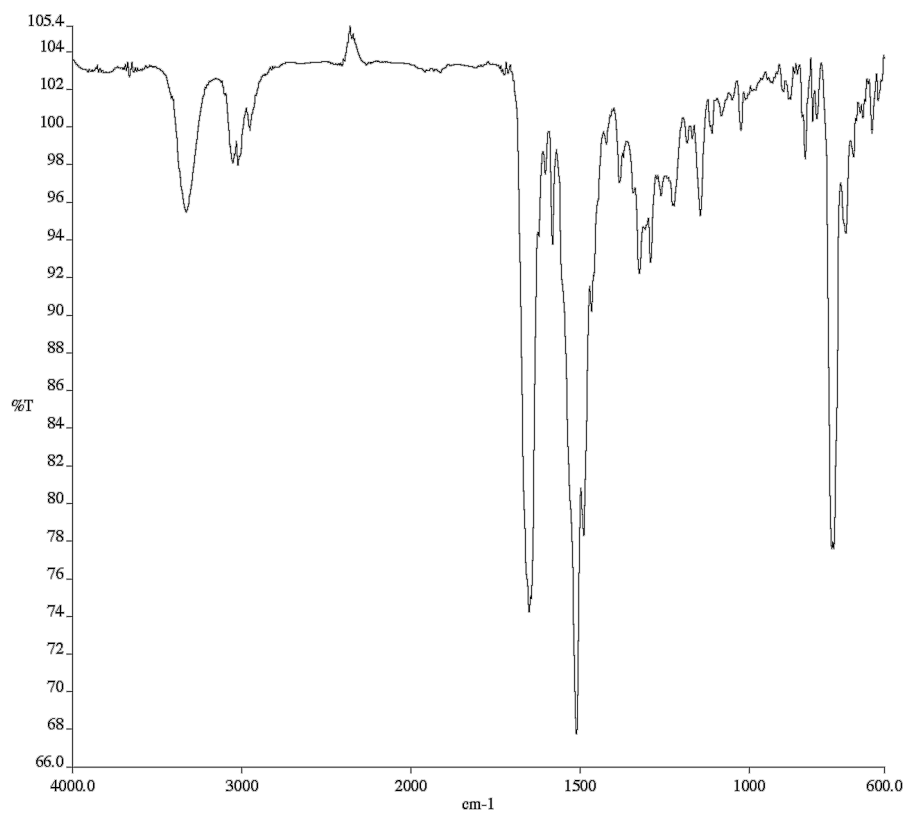


A6.51 ¹³C NMR (100 MHz, CDCl₃) of compound **L75**

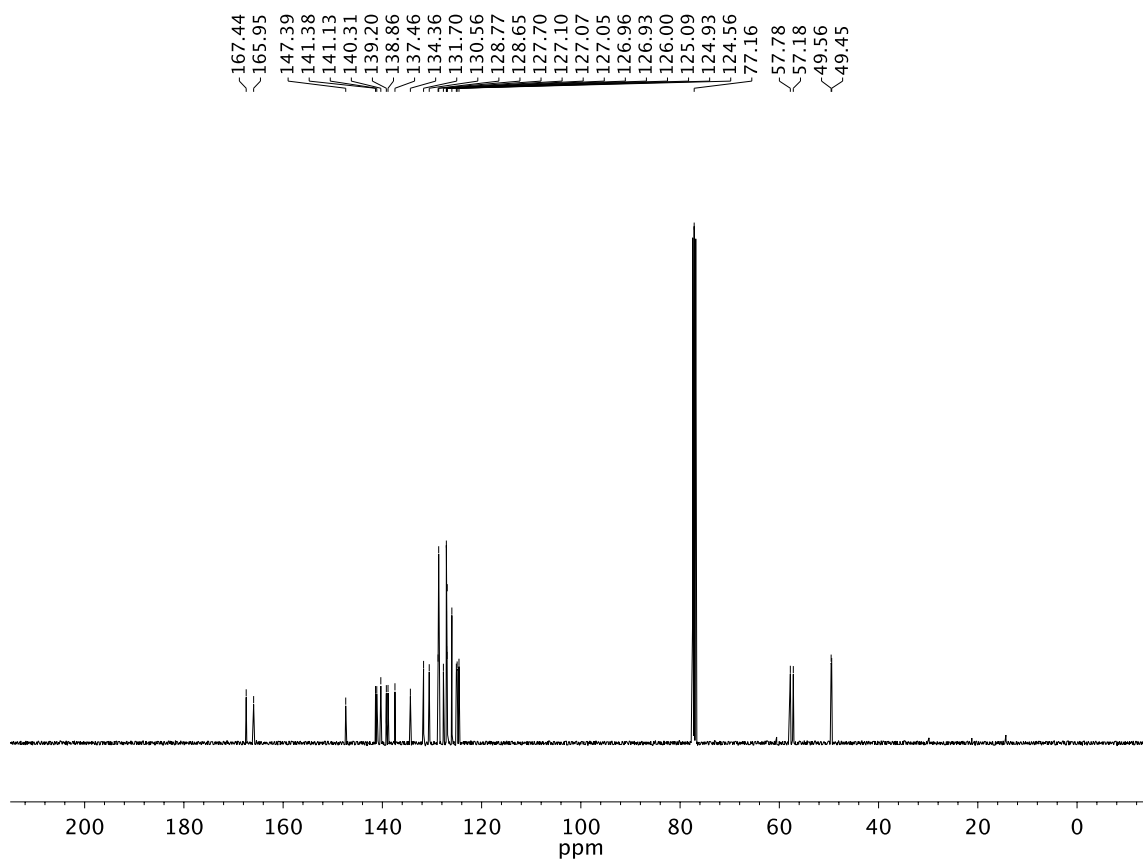
**A6.52** ¹H NMR (400 MHz, CDCl₃) of compound **L76**

**A6.53** Infrared spectrum (Thin Film, NaCl) of compound **L76****A6.54** ¹³C NMR (100 MHz, CDCl₃) of compound **L76**

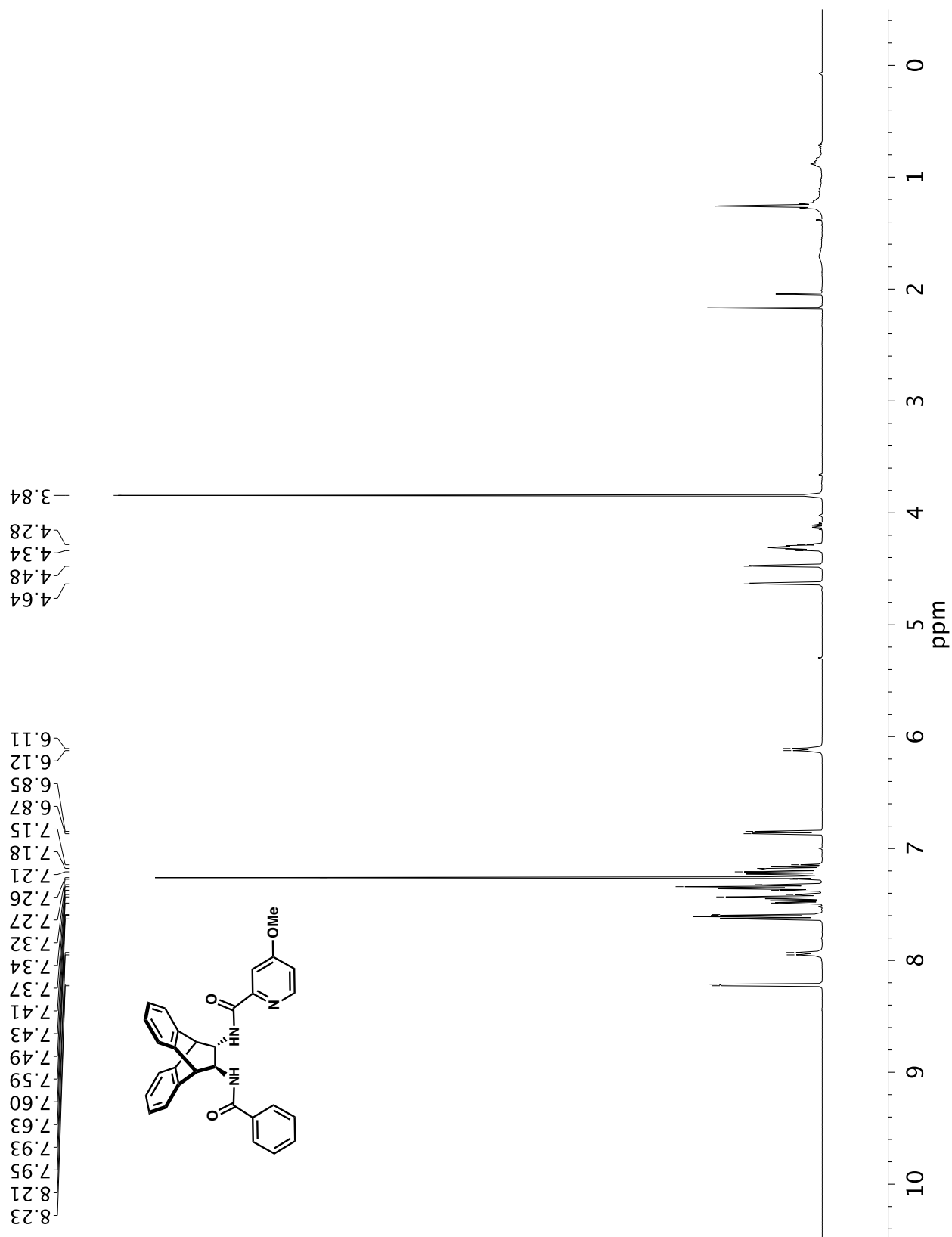
**A6.55** ^1H NMR (400 MHz, CDCl_3) of compound **L77**

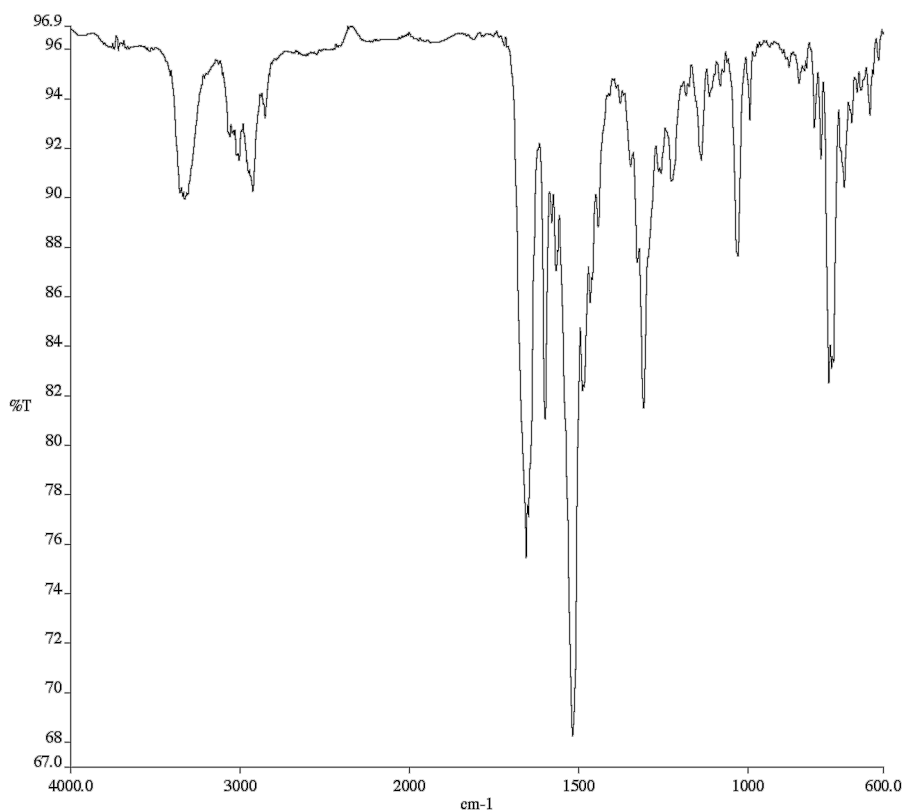
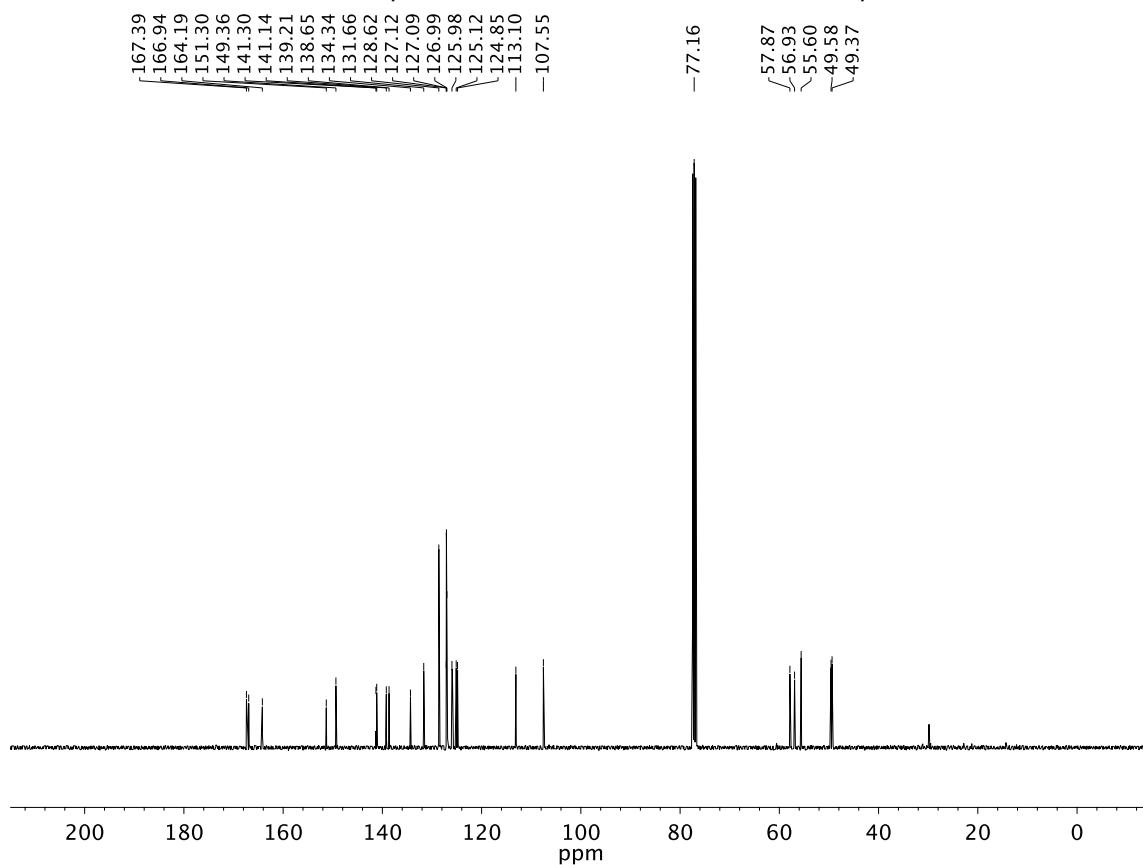


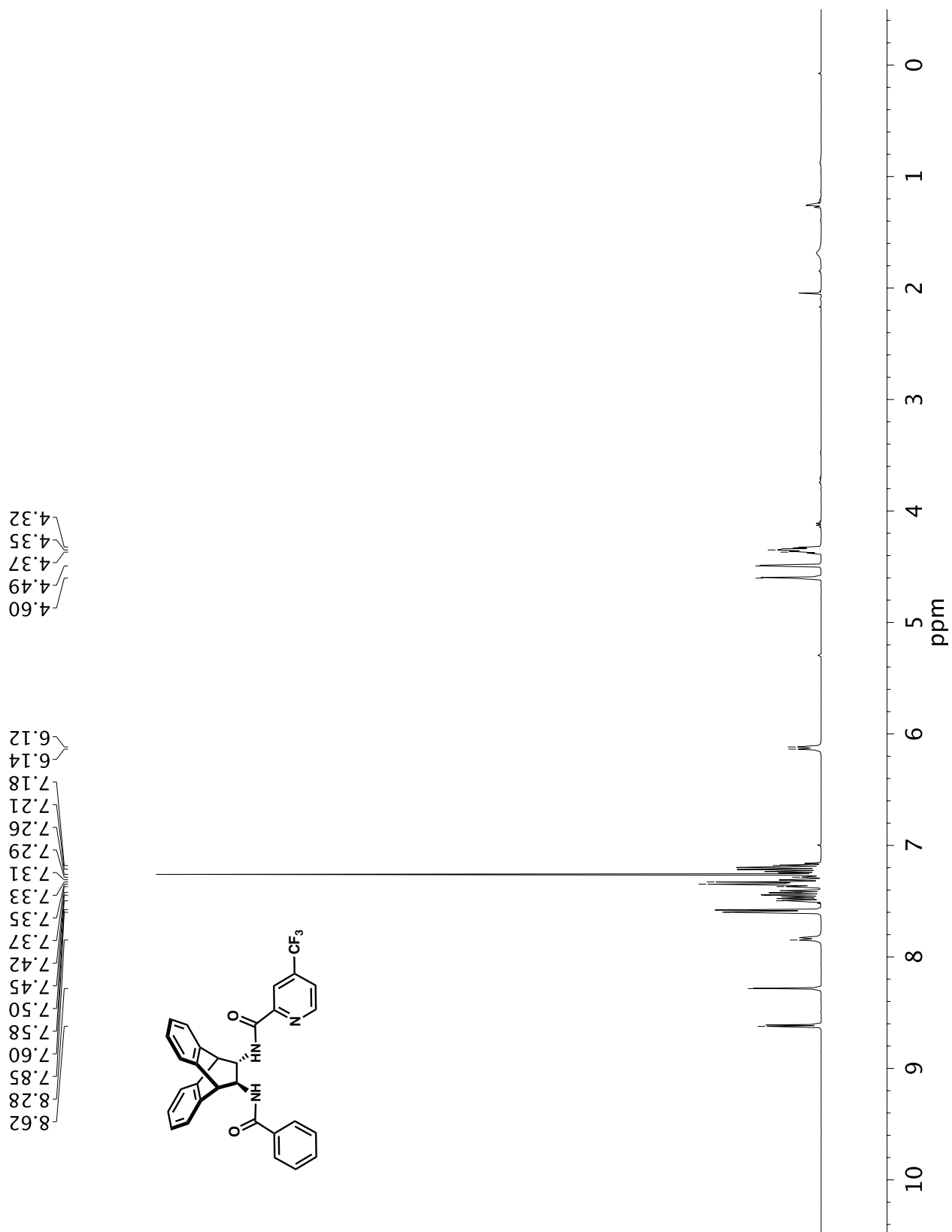
A6.56 Infrared spectrum (Thin Film, NaCl) of compound **L77**

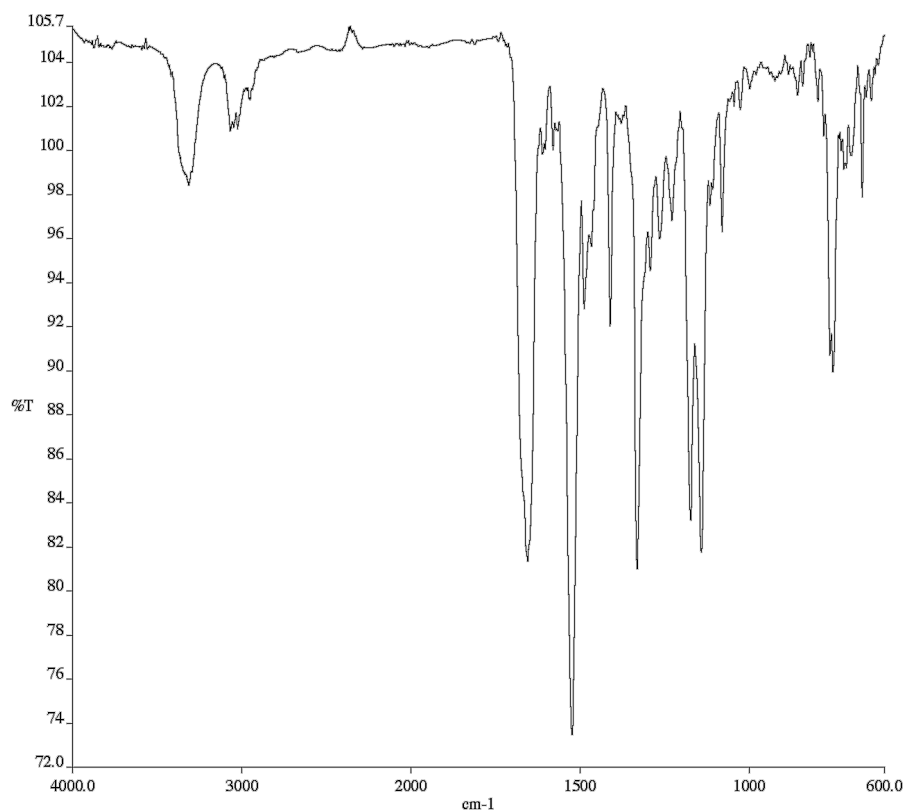
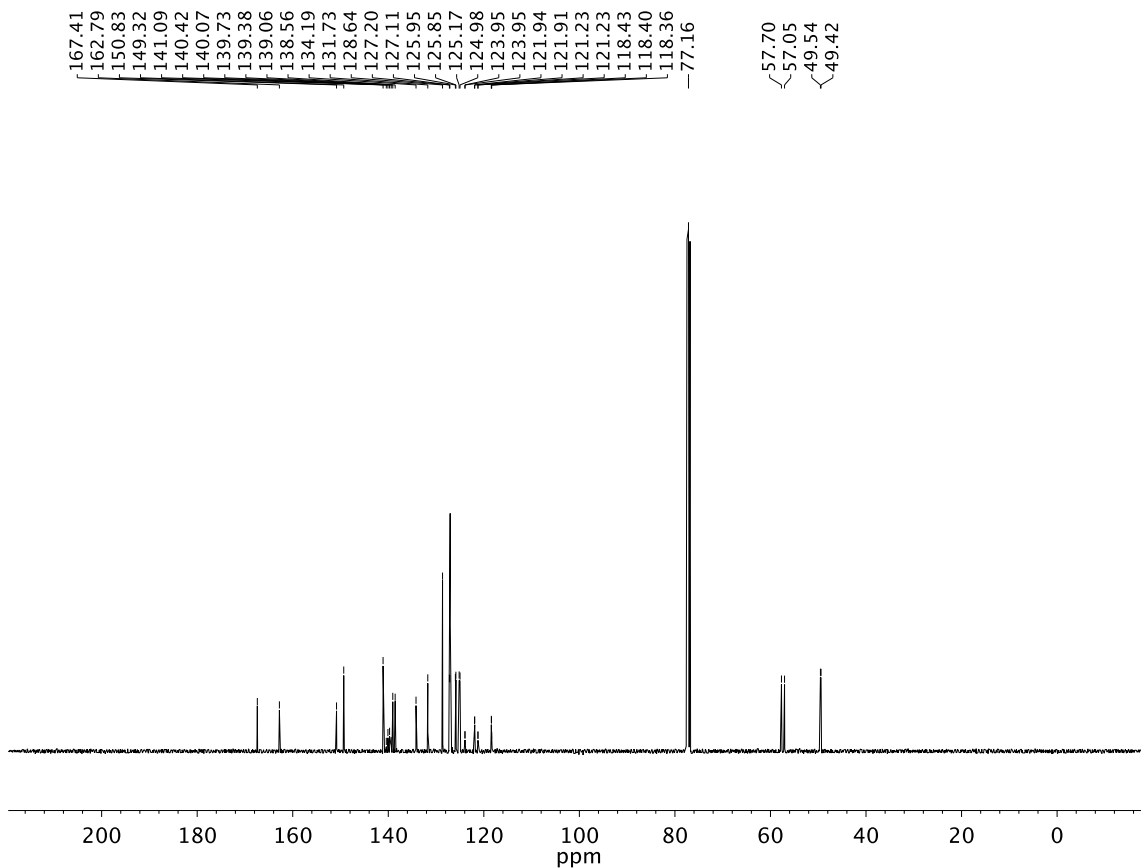


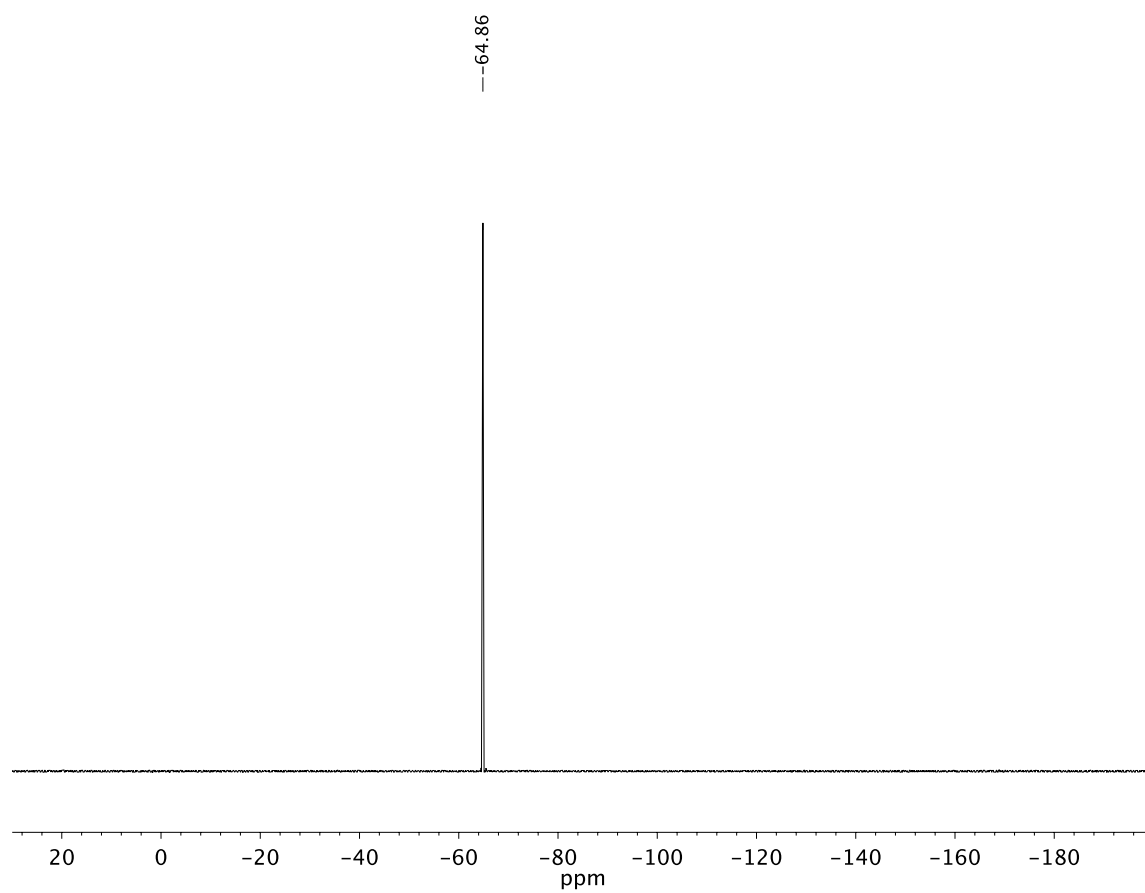
A6.57 ^{13}C NMR (100 MHz, CDCl_3) of compound **L77**

**A6.58** ¹H NMR (400 MHz, CDCl₃) of compound **L78**

**A6.59** Infrared spectrum (Thin Film, NaCl) of compound **L78****A6.60** ¹³C NMR (100 MHz, CDCl₃) of compound **L78**

**A6.61** ¹H NMR (400 MHz, CDCl₃) of compound **L79**

**A6.62** Infrared spectrum (Thin Film, NaCl) of compound **L79****A6.63** ^{13}C NMR (100 MHz, CDCl_3) of compound **L79**



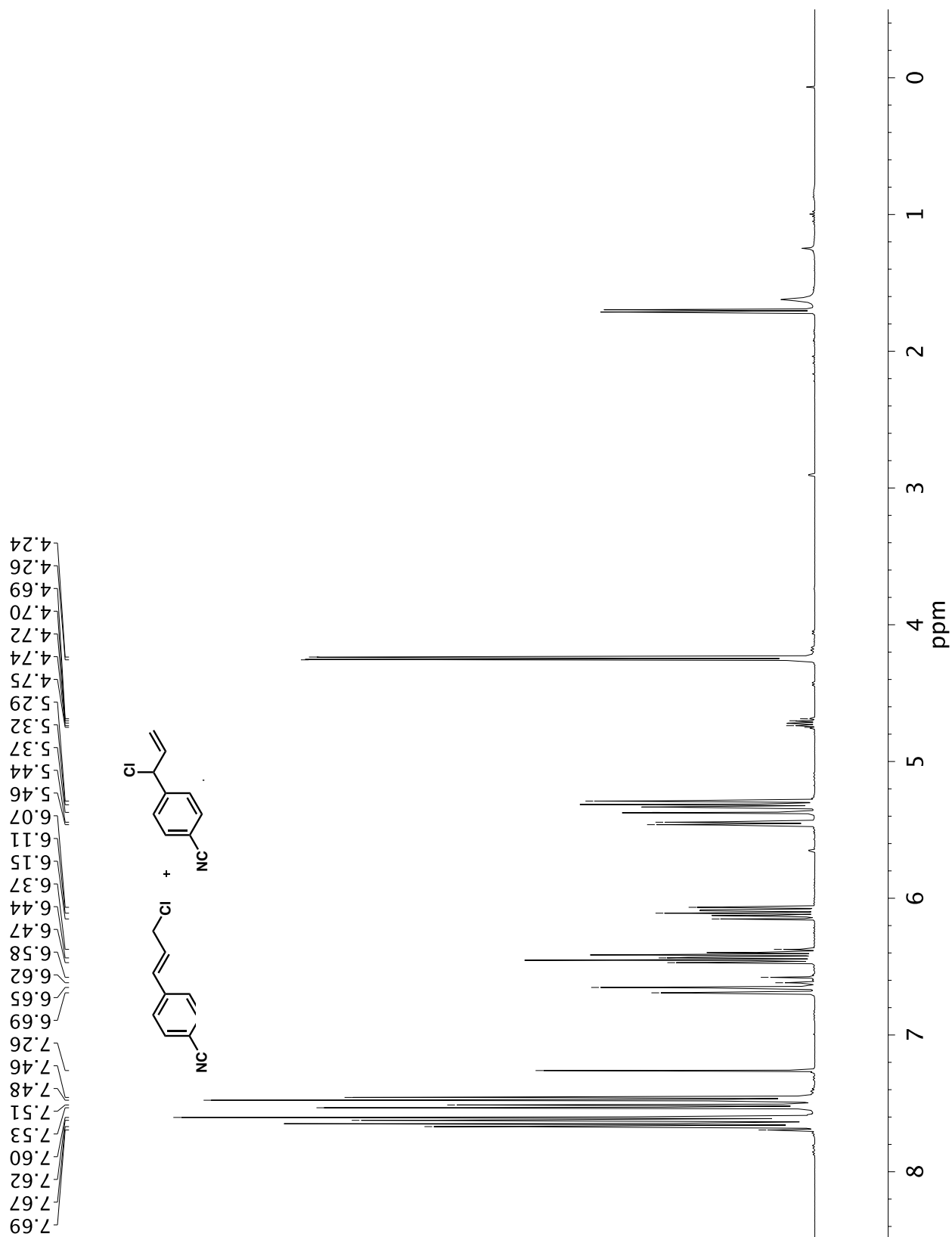
A6.64 ^{19}F NMR (282 MHz, CDCl_3) of compound **L79**

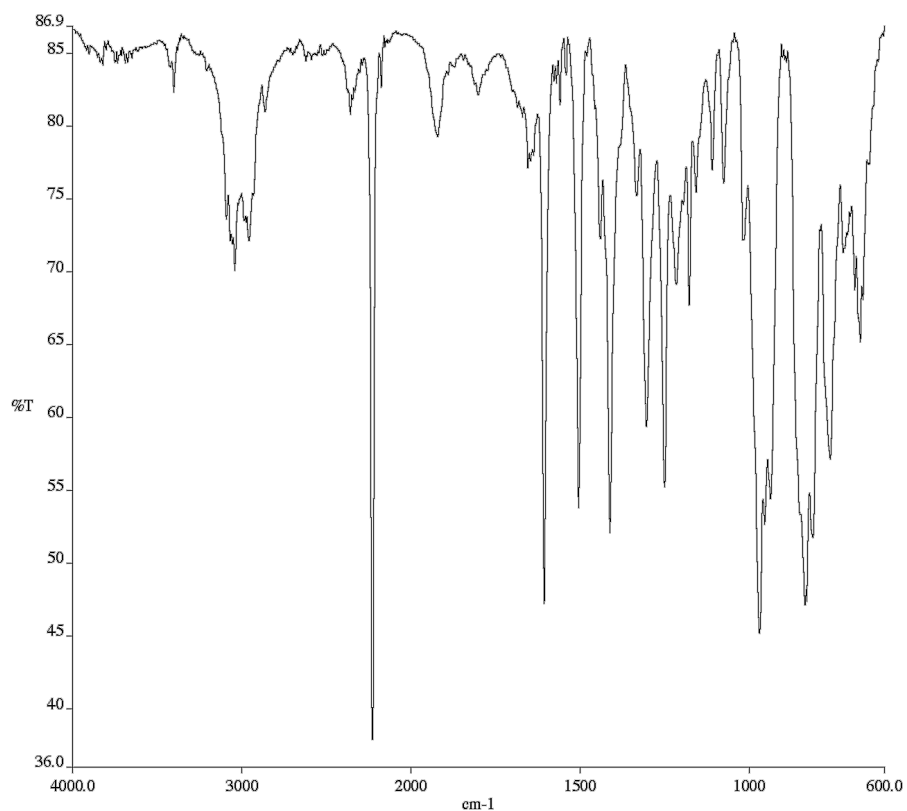
APPENDIX 7

Spectra for Substrates and Products Synthesized in Chapter 3:

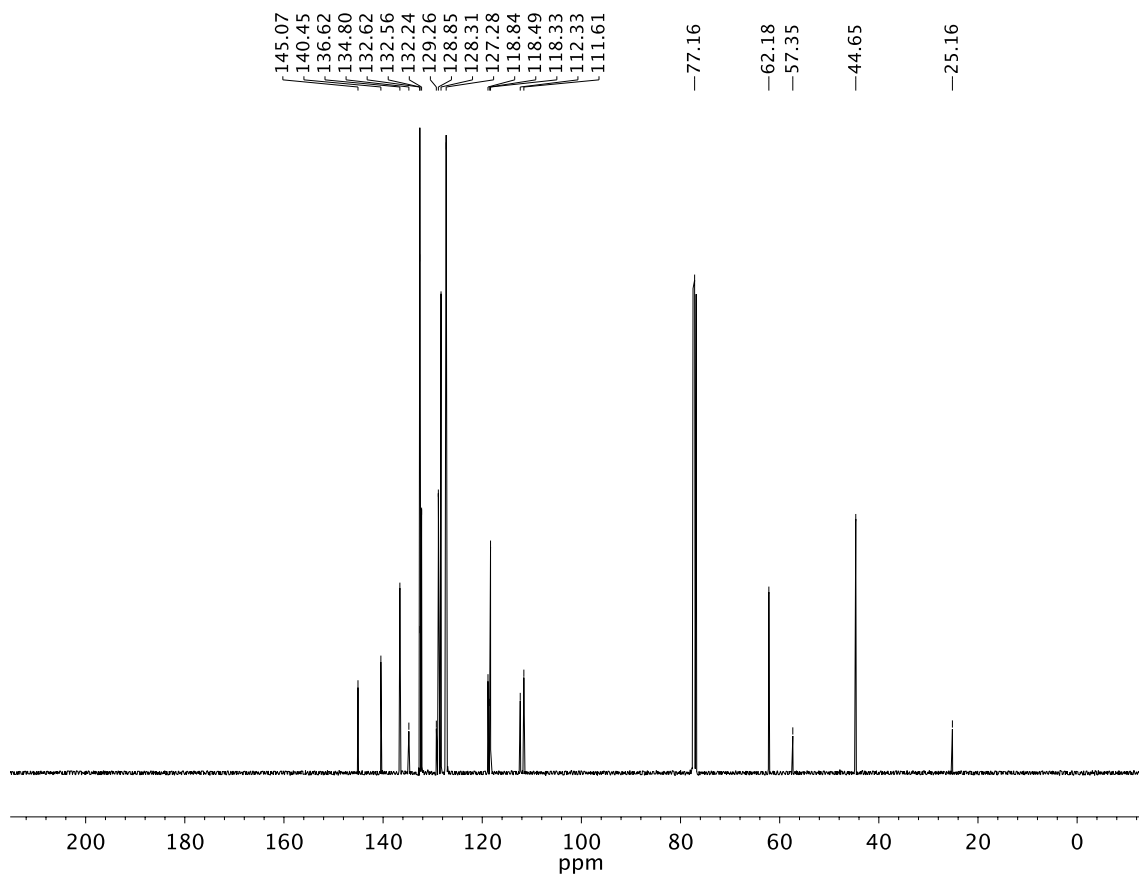
Copper-Catalyzed Enantioselective Allylic Alkylation with a

γ -Butyrolactone-Derived Silyl Ketene Acetal

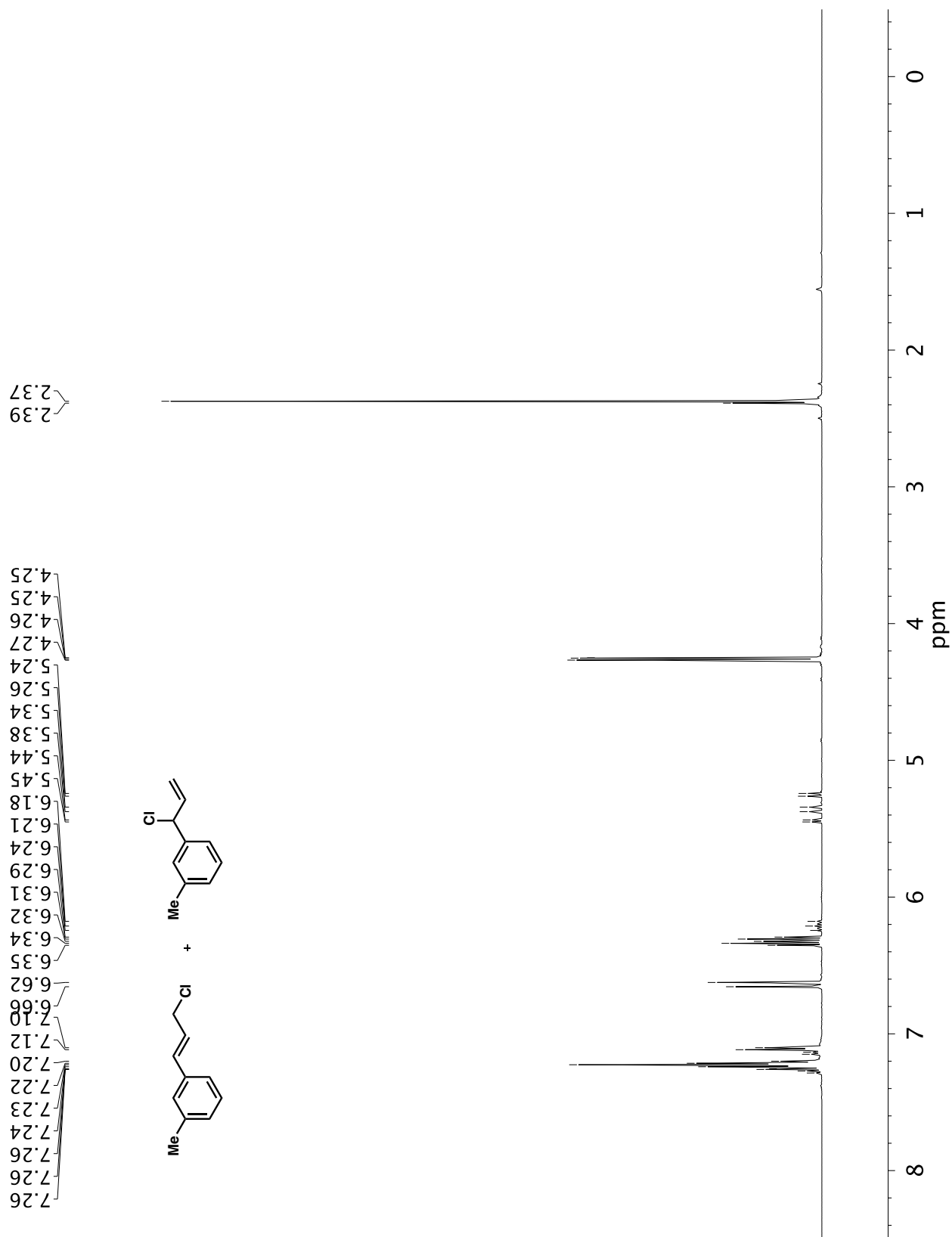
**A7.1** ¹H NMR (400 MHz, CDCl₃) of compound **43m**



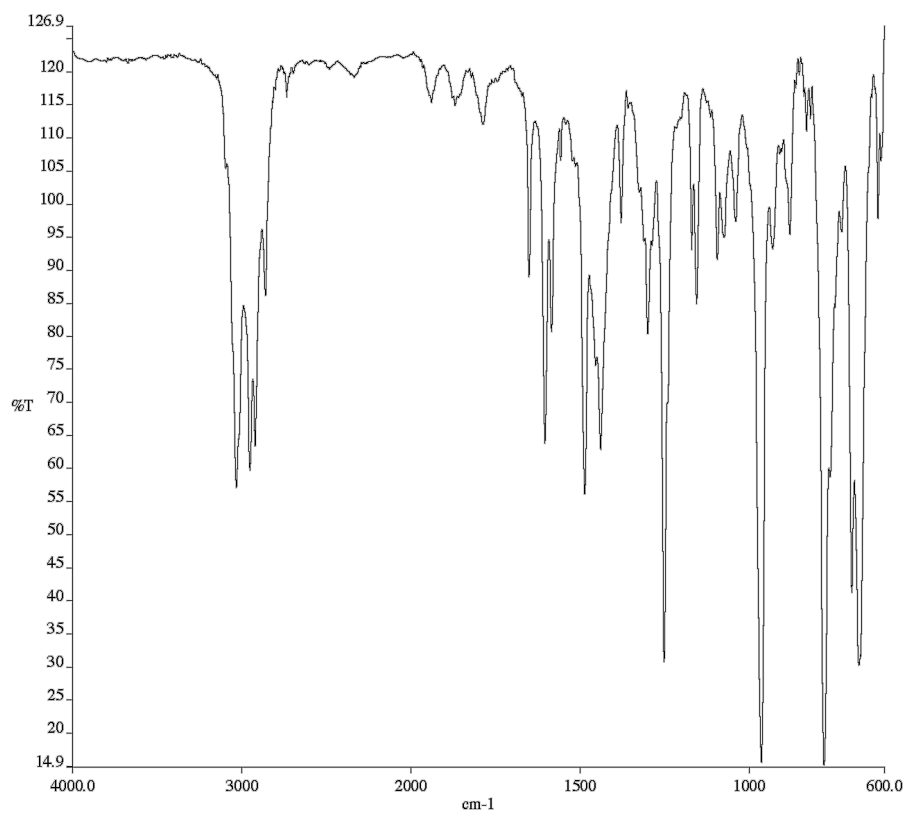
A7.2 Infrared spectrum (Thin Film, NaCl) of compound **43m**



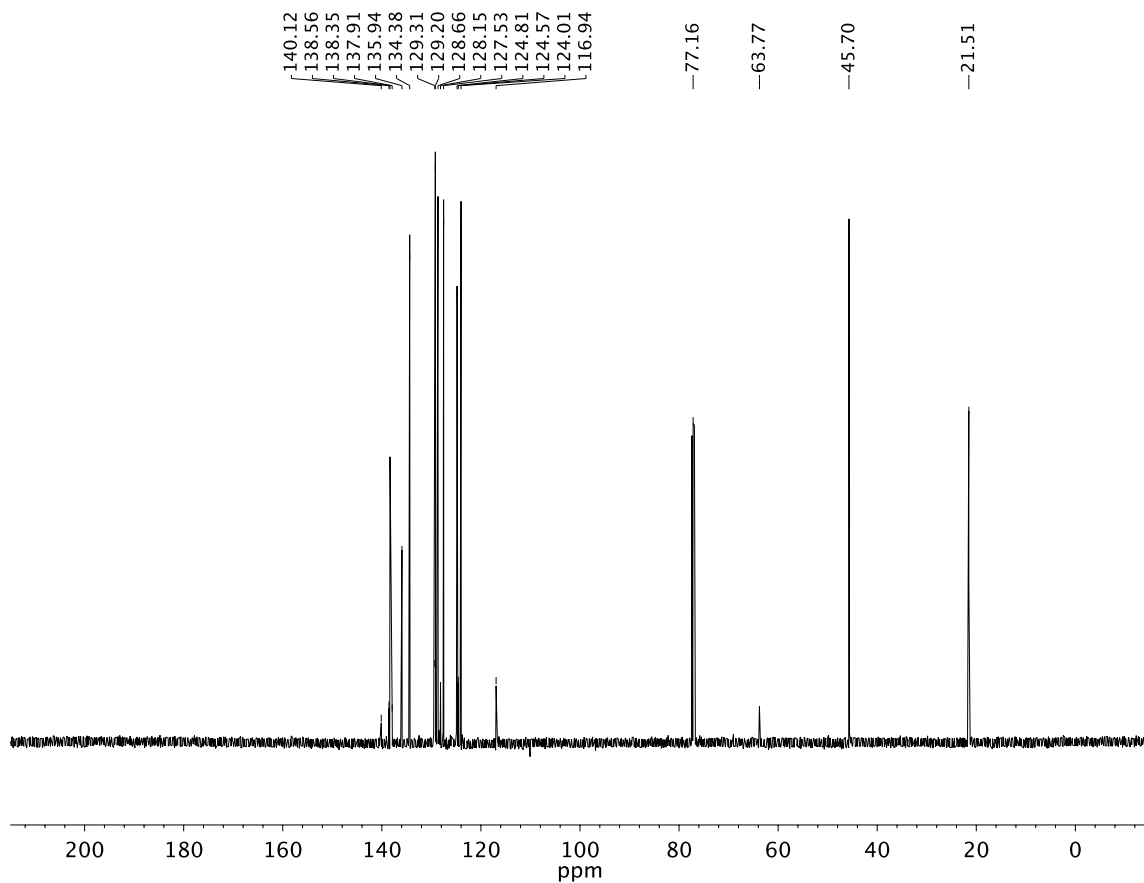
A7.3 ^{13}C NMR (100 MHz, CDCl_3) of compound **43m**



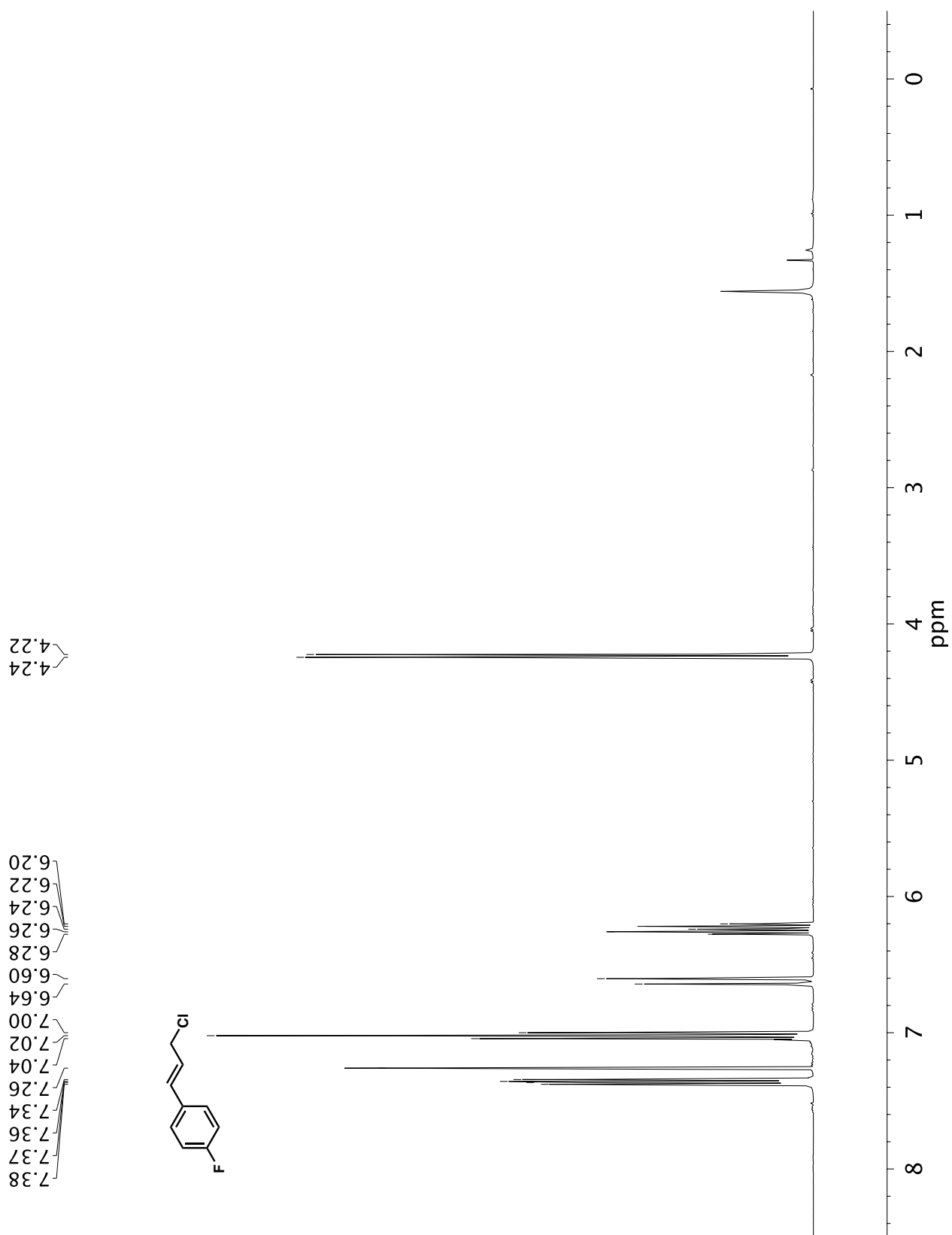
A7.4 ^1H NMR (500 MHz, CDCl_3) of compound **43e**

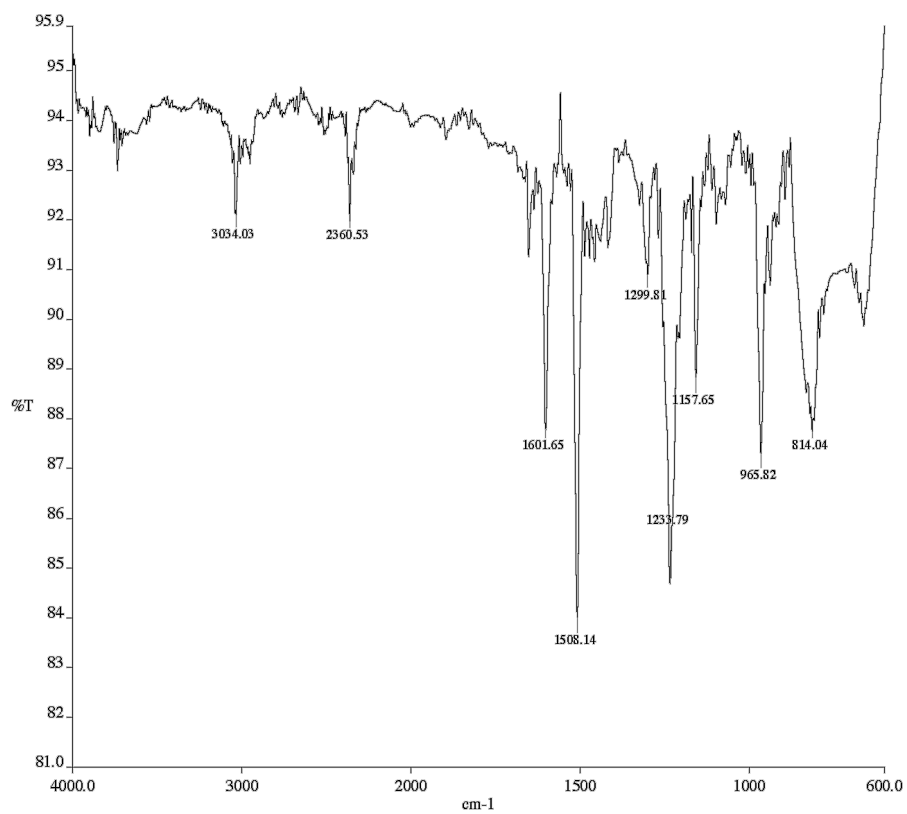


A7.5 Infrared spectrum (Thin Film, NaCl) of compound **43e**

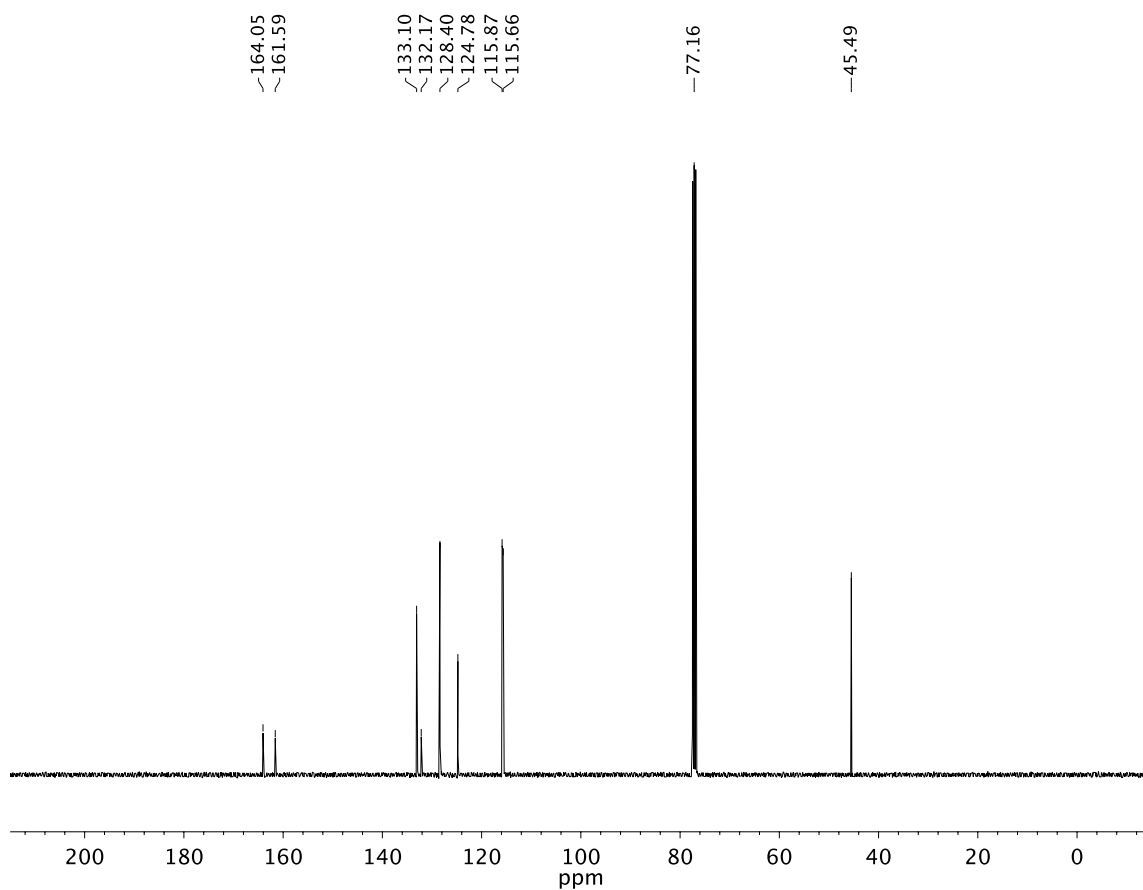


A7.6 ^{13}C NMR (125 MHz, CDCl_3) of compound **43e**

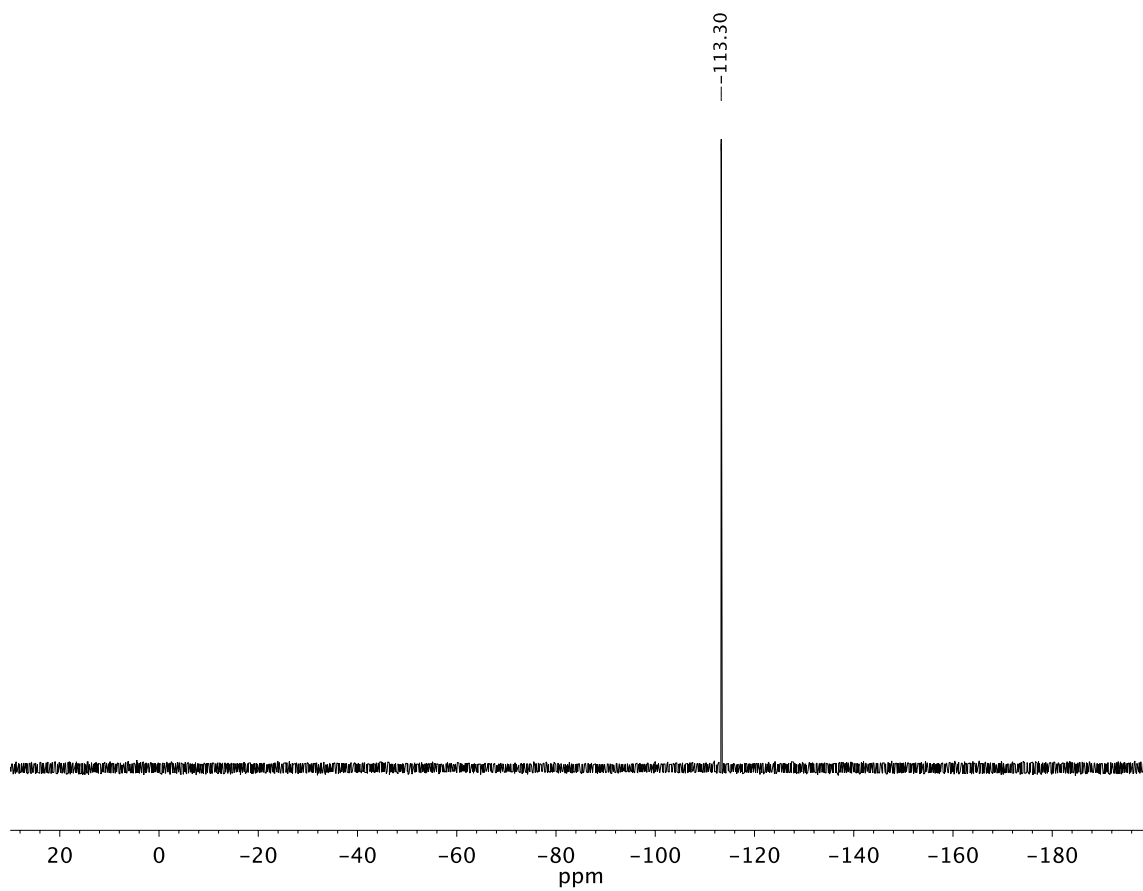




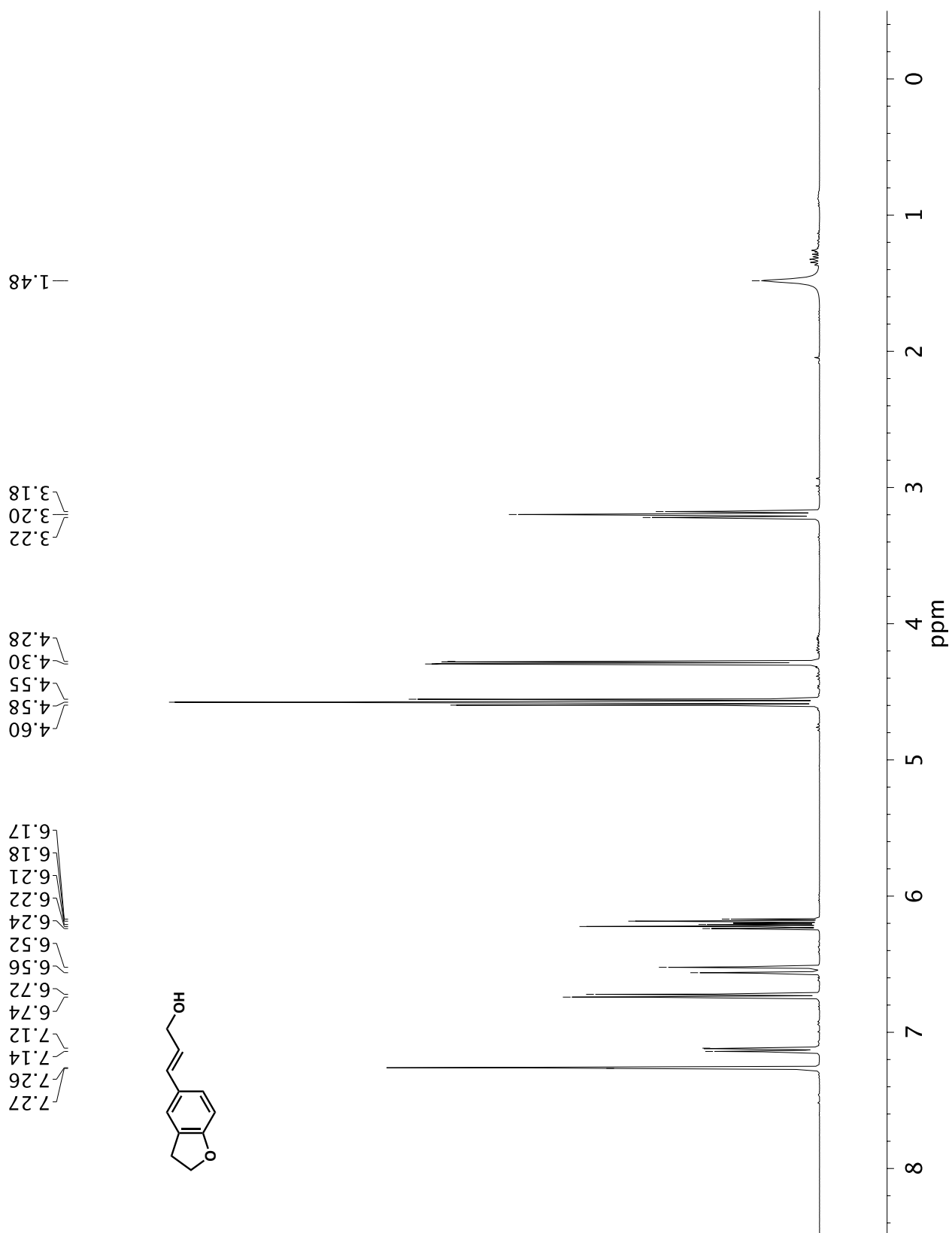
A7.8 Infrared spectrum (Thin Film, NaCl) of compound **43i**

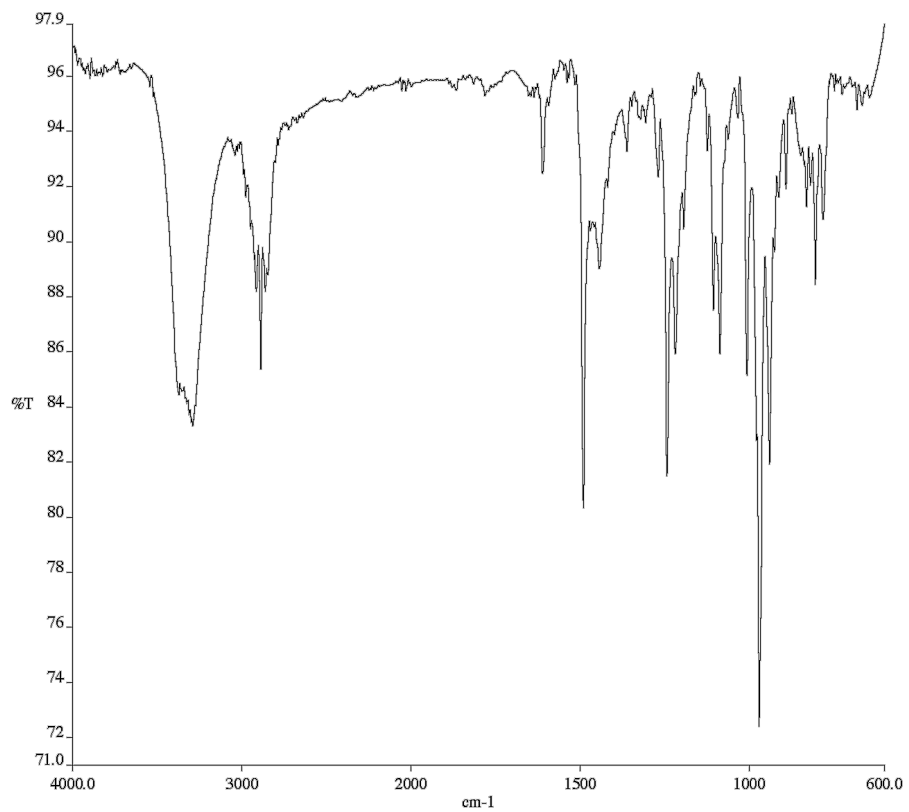


A7.9 ^{13}C NMR (100 MHz, CDCl_3) of compound **43i**

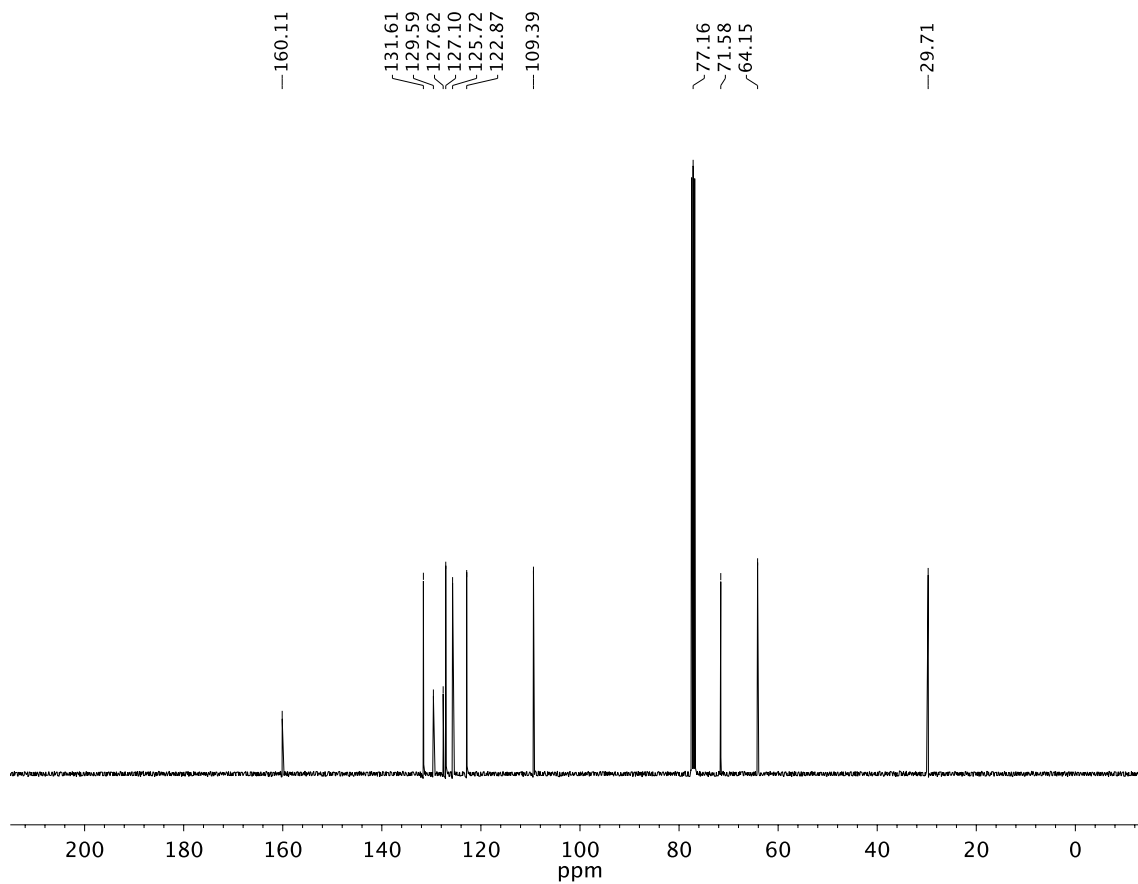


A7.10 ^{19}F NMR (282 MHz, CDCl_3) of compound **43i**

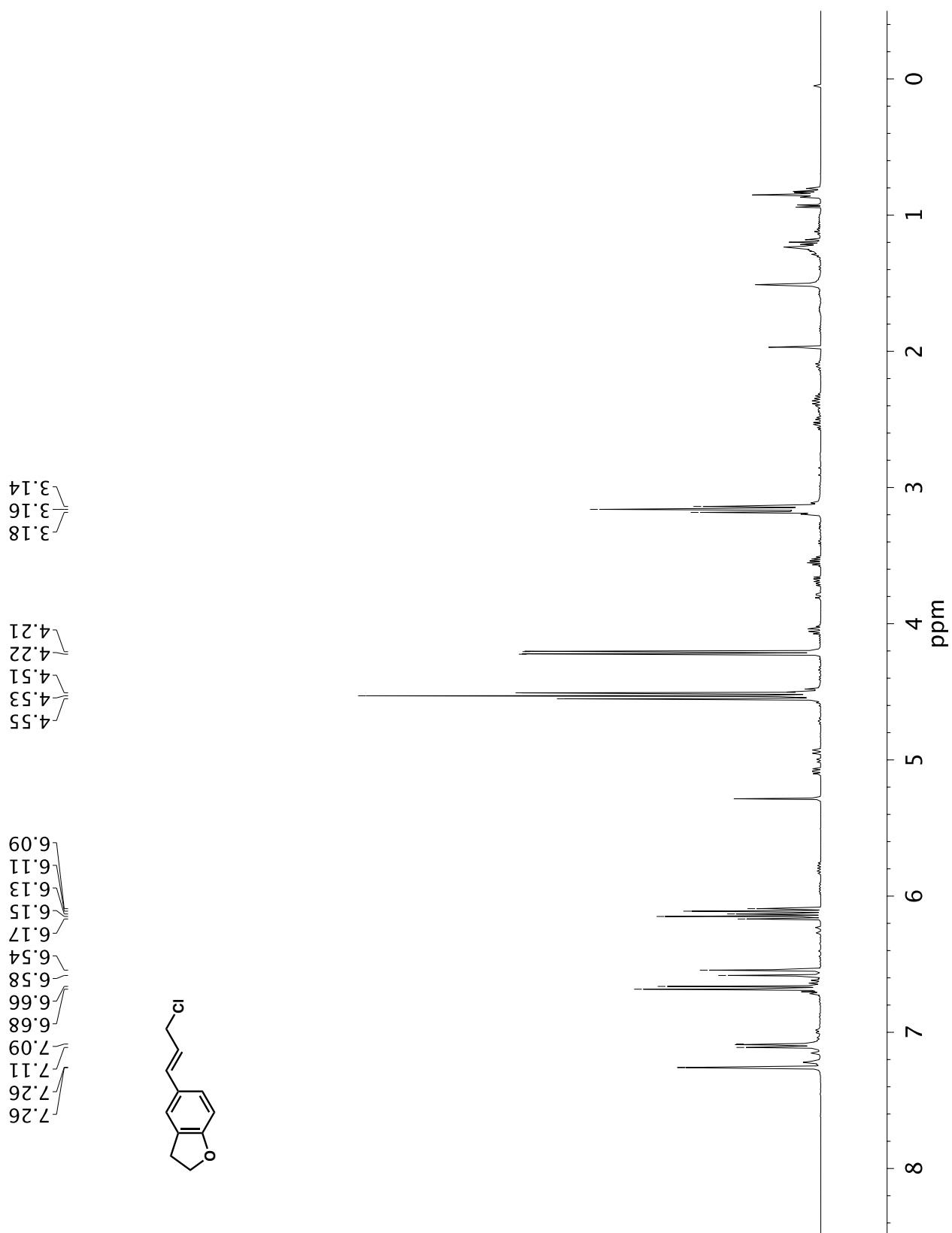


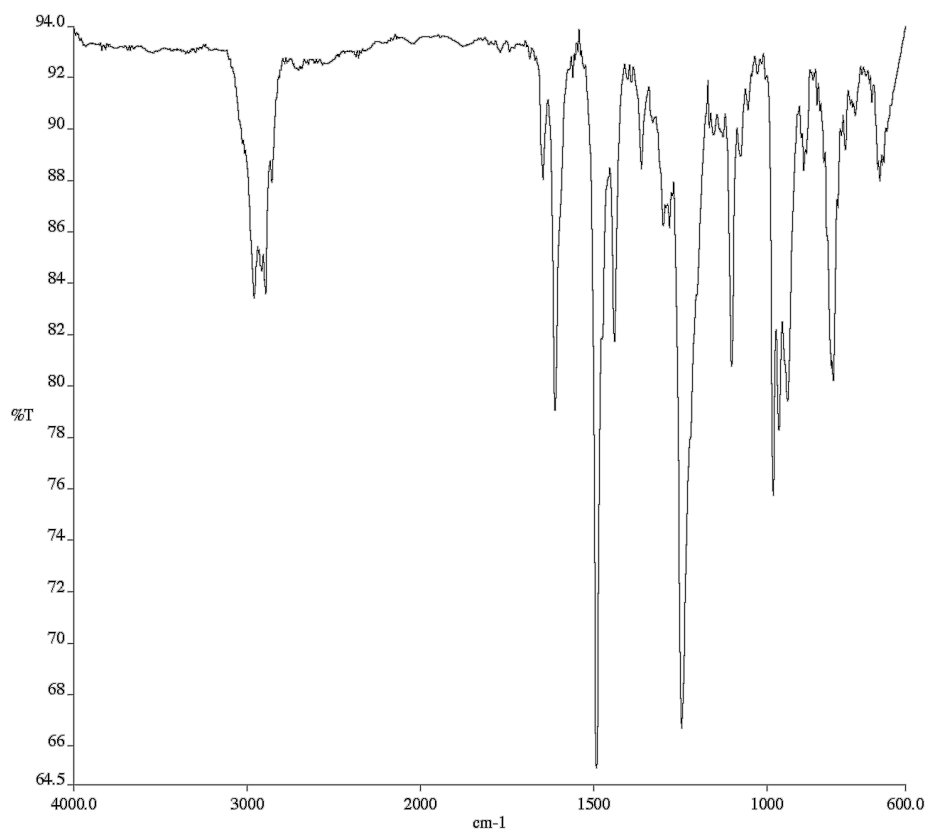


A7.12 Infrared spectrum (Thin Film, NaCl) of compound **SI12**

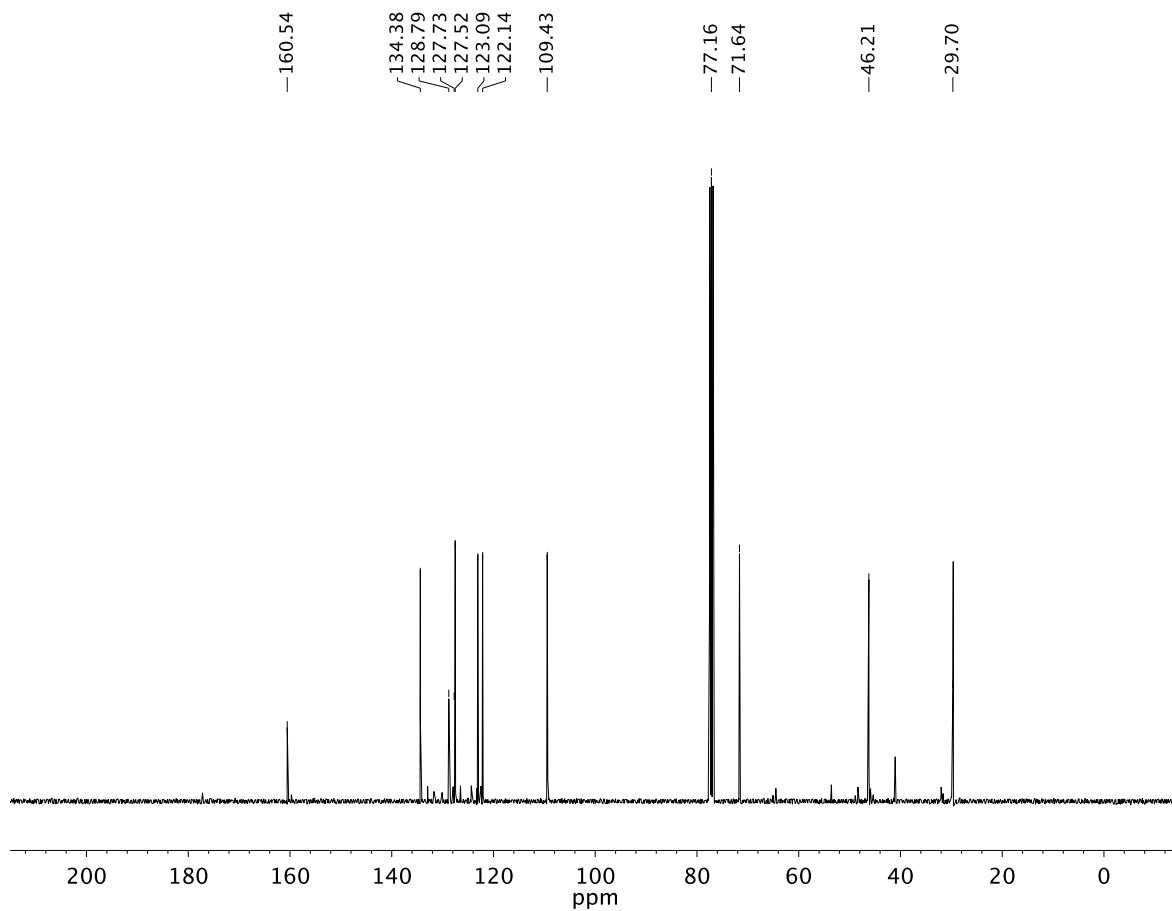


A7.13 ¹³C NMR (100 MHz, CDCl₃) of compound **SI12**

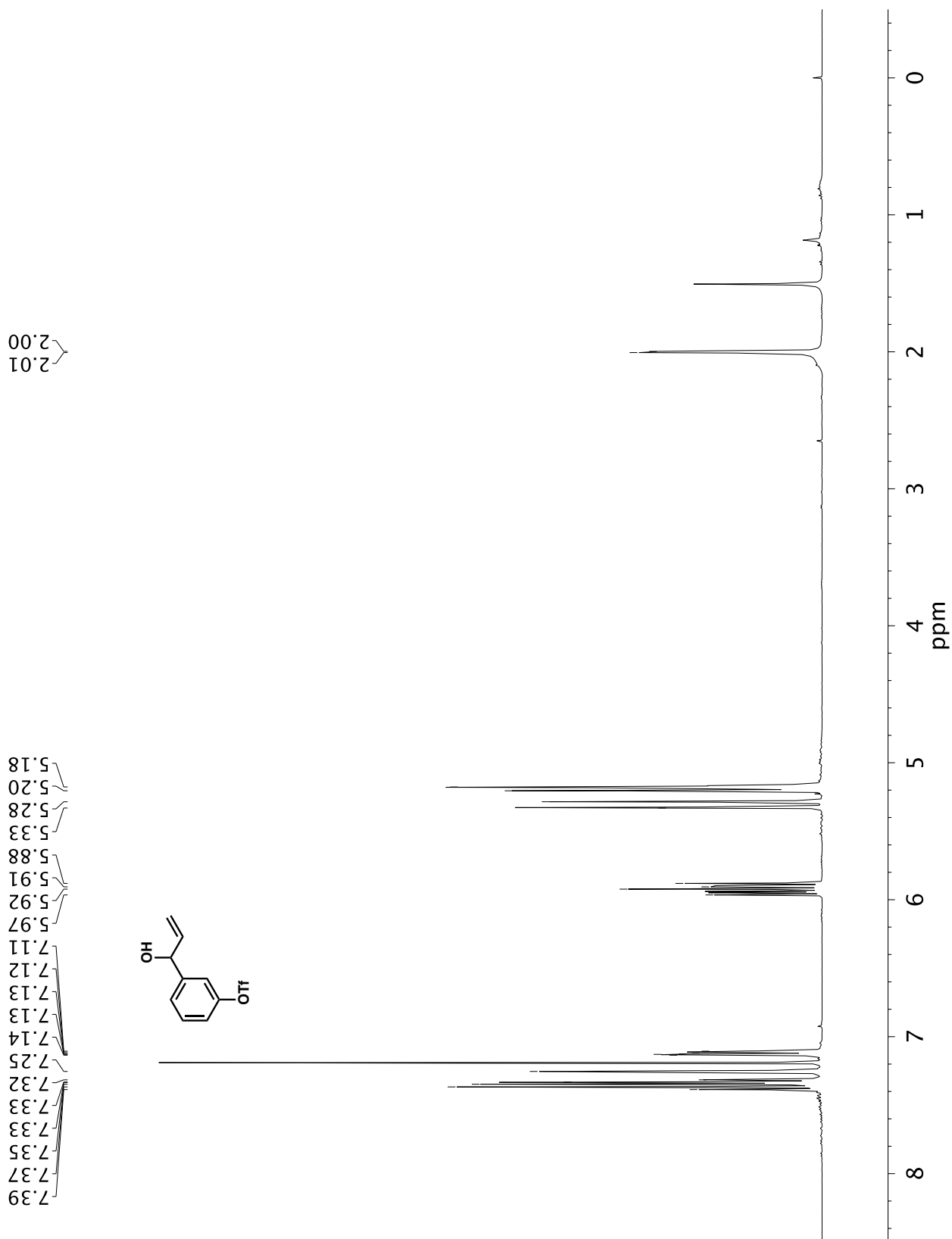


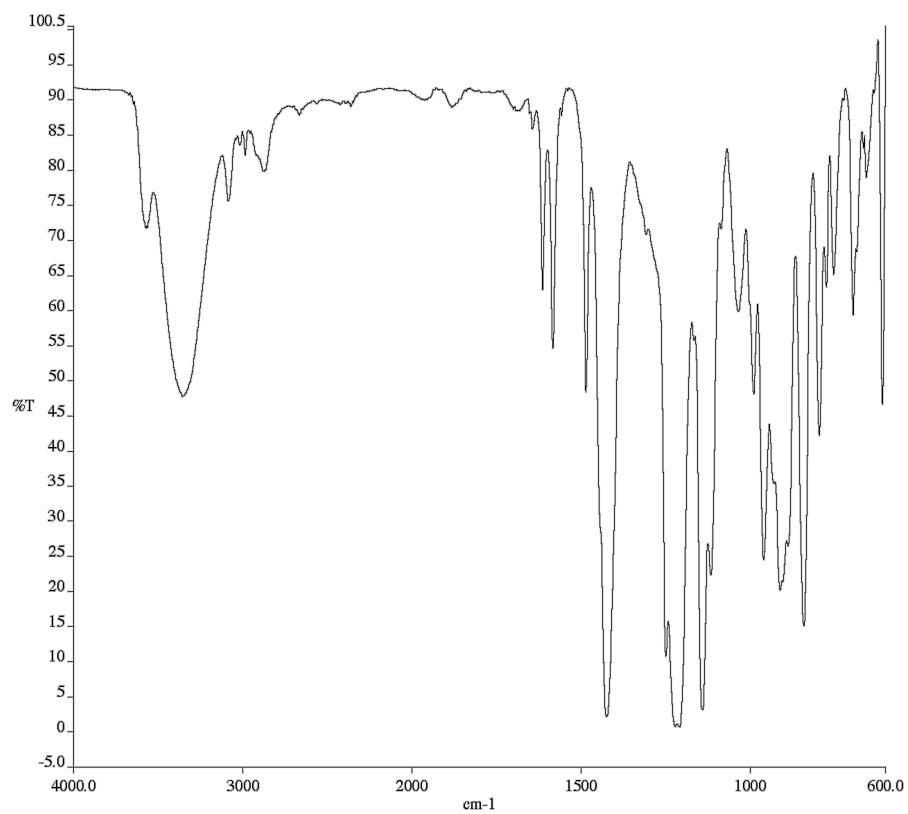


A7.15 Infrared spectrum (Thin Film, NaCl) of compound **43n**

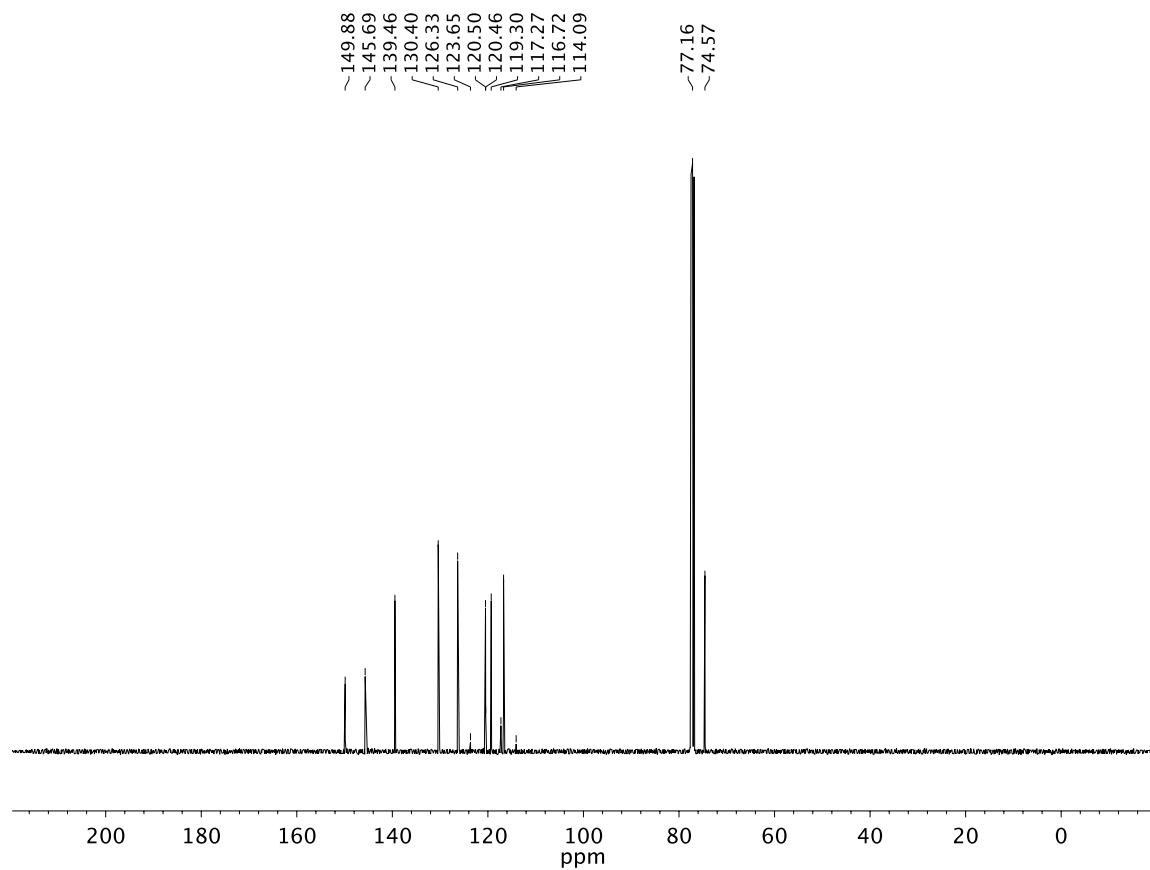


A7.16 ¹³C NMR (100 MHz, CDCl₃) of compound **43n**

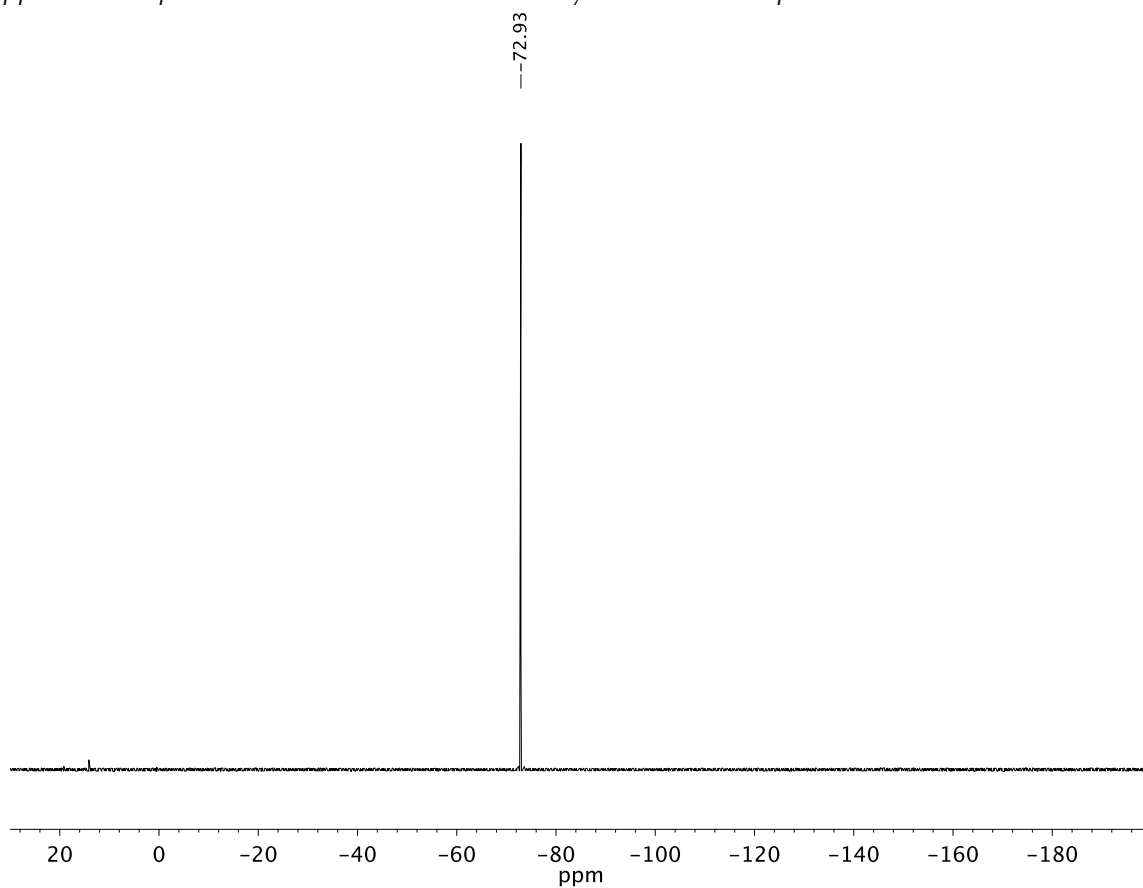
A7.17 ¹H NMR (400 MHz, CDCl₃) of compound **SI13**



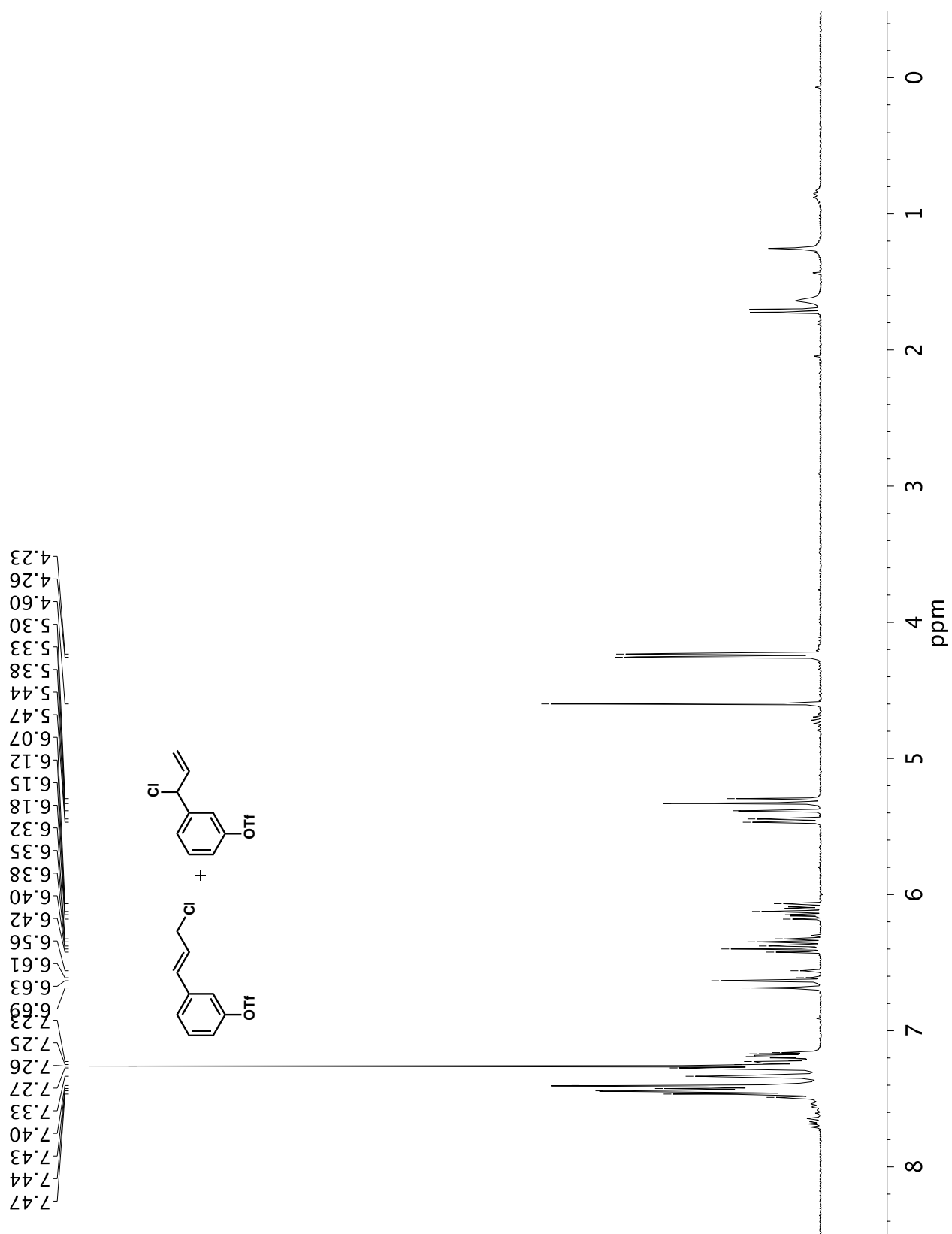
A7.18 Infrared spectrum (Thin Film, NaCl) of compound **SI13**

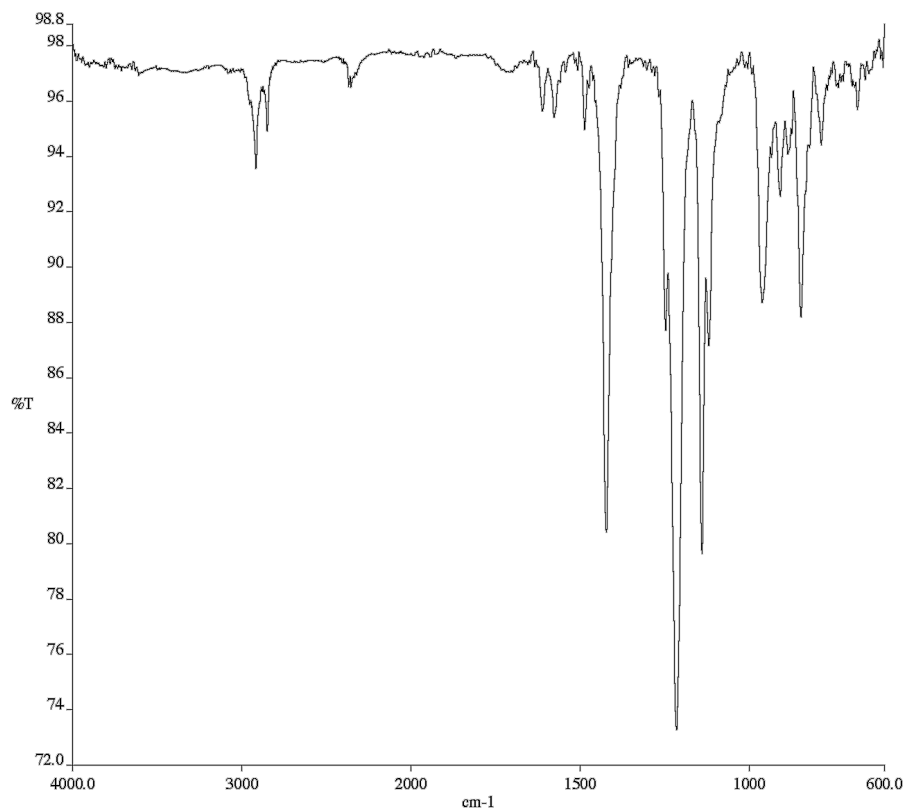


A7.19 ¹³C NMR (100 MHz, CDCl₃) of compound **SI13**

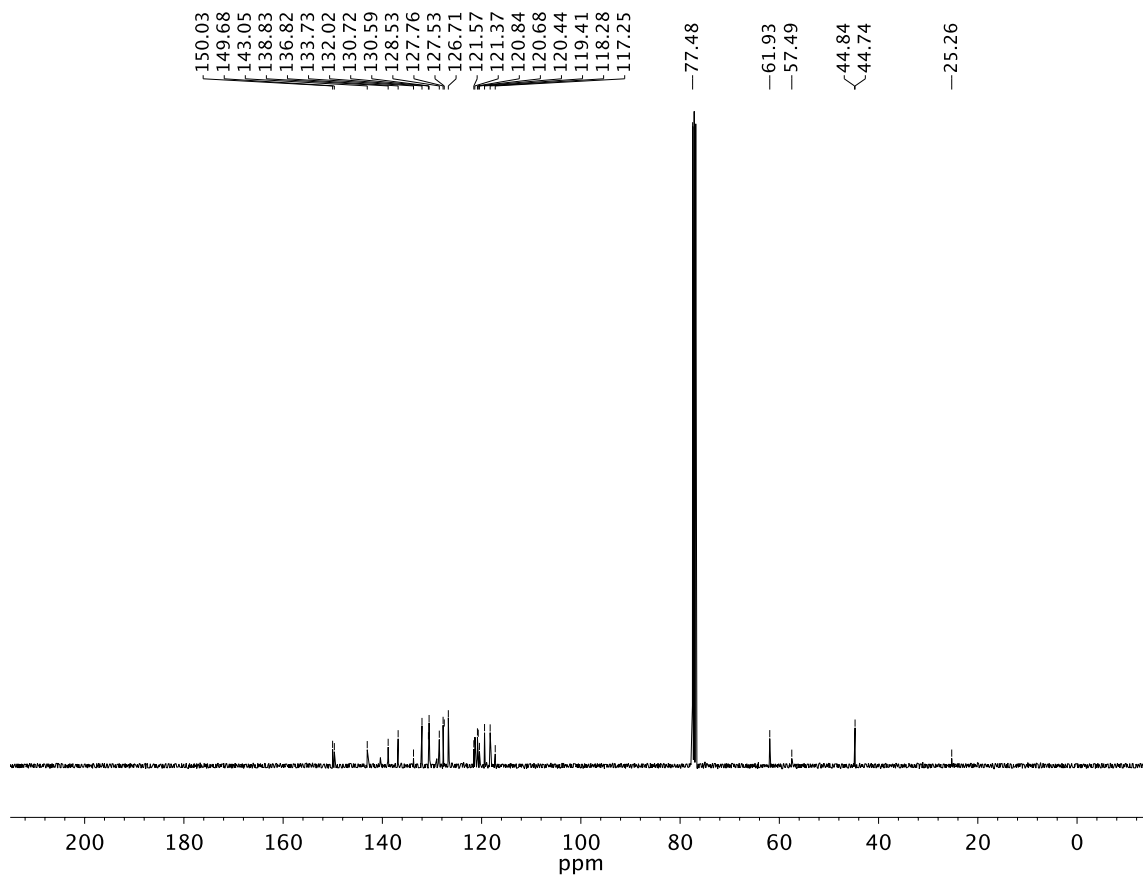


A7.20 ^{19}F NMR (282 MHz, CDCl_3) of compound **SI13**

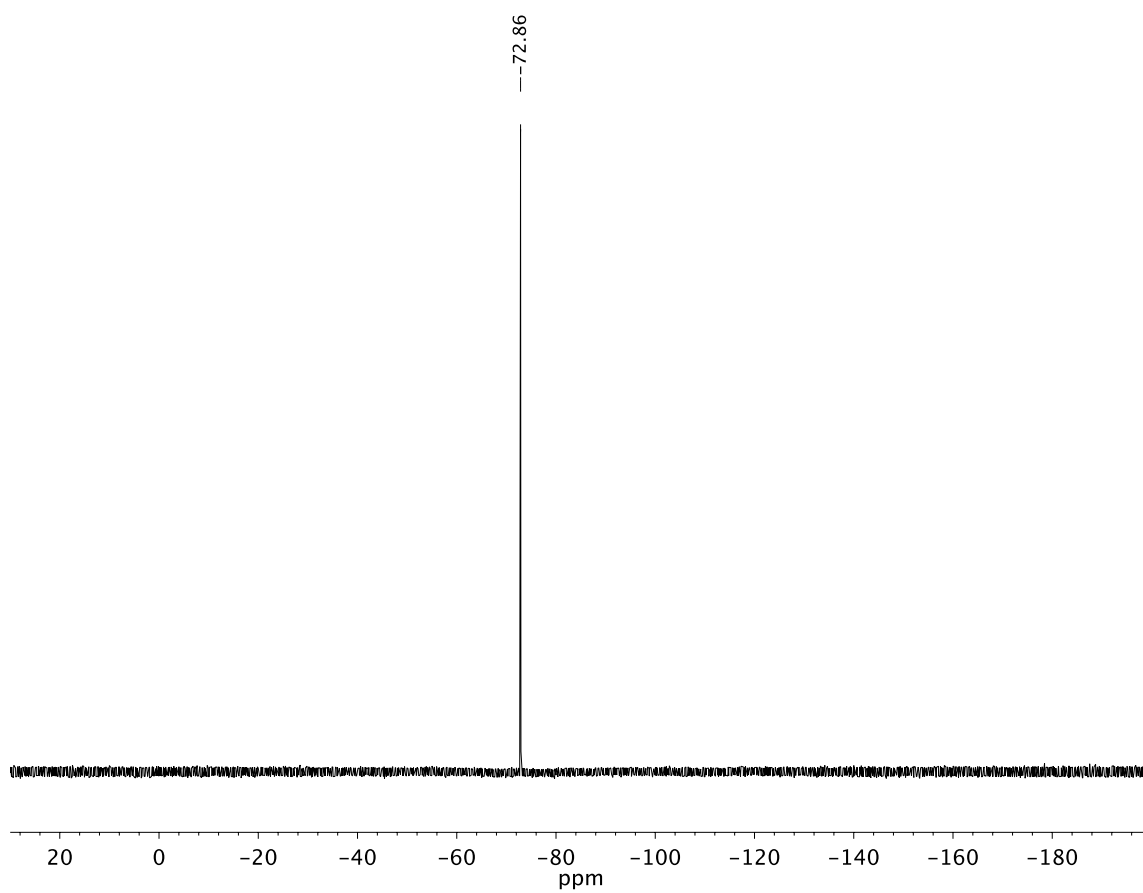
A7.21 ¹H NMR (400 MHz, CDCl₃) of compound **43f**



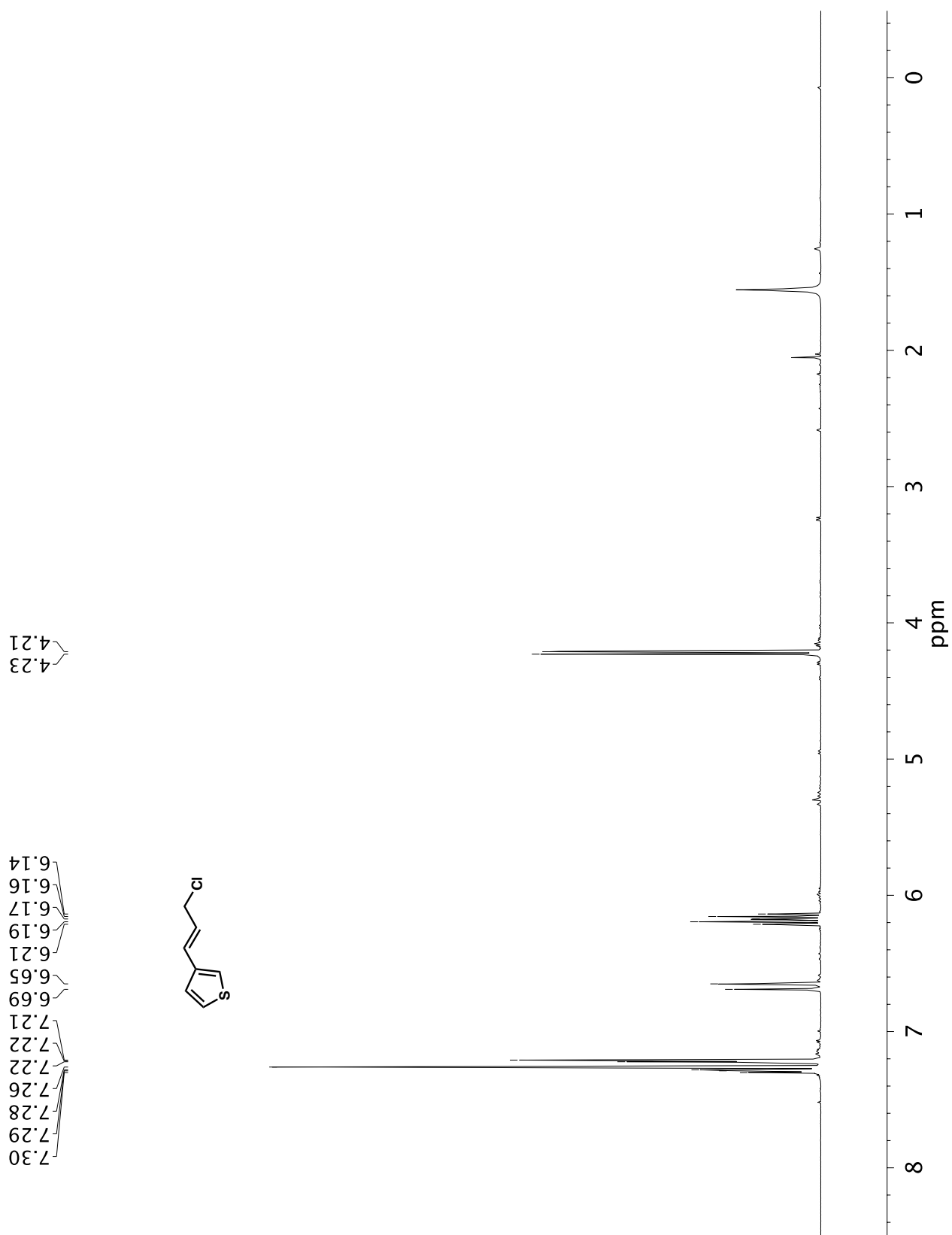
A7.22 Infrared spectrum (Thin Film, NaCl) of compound **43f**

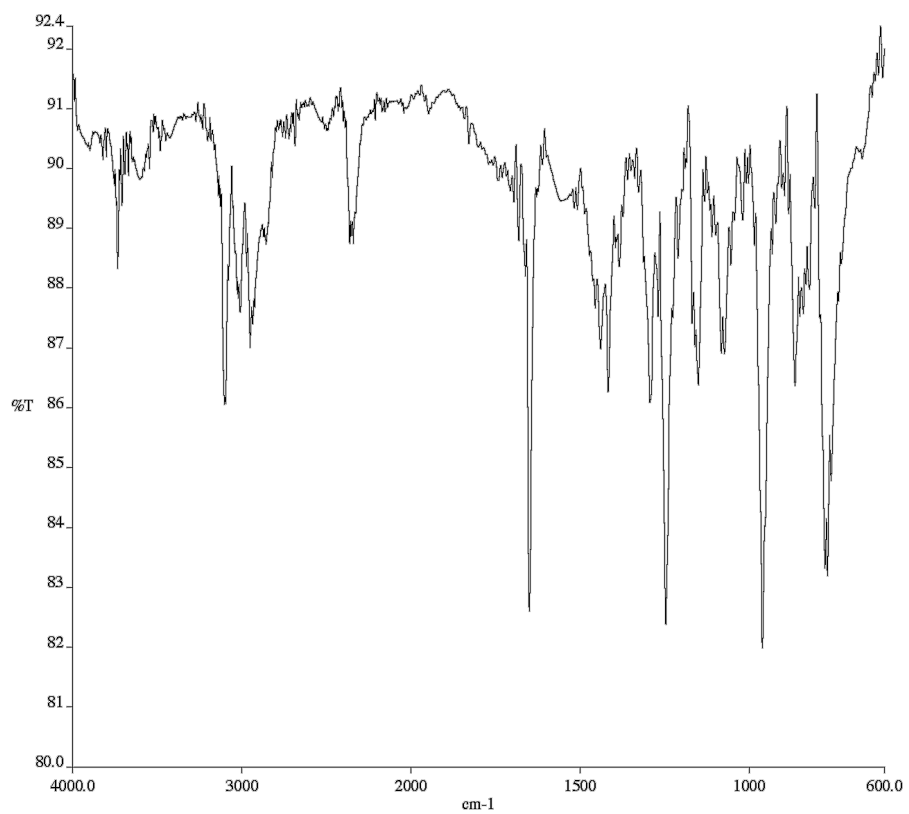


A7.23 ¹³C NMR (100 MHz, CDCl₃) of compound **43f**

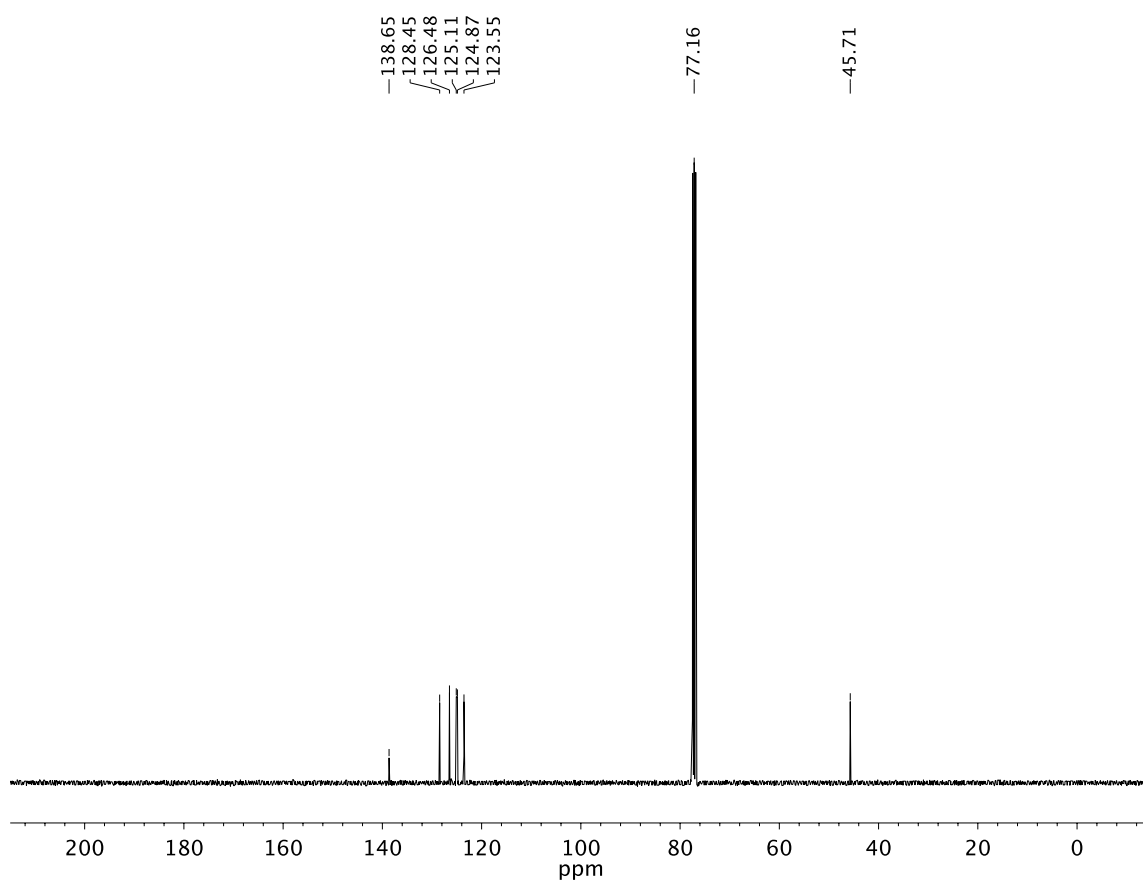


A7.24 ^{19}F NMR (282 MHz, CDCl_3) of compound **43f**

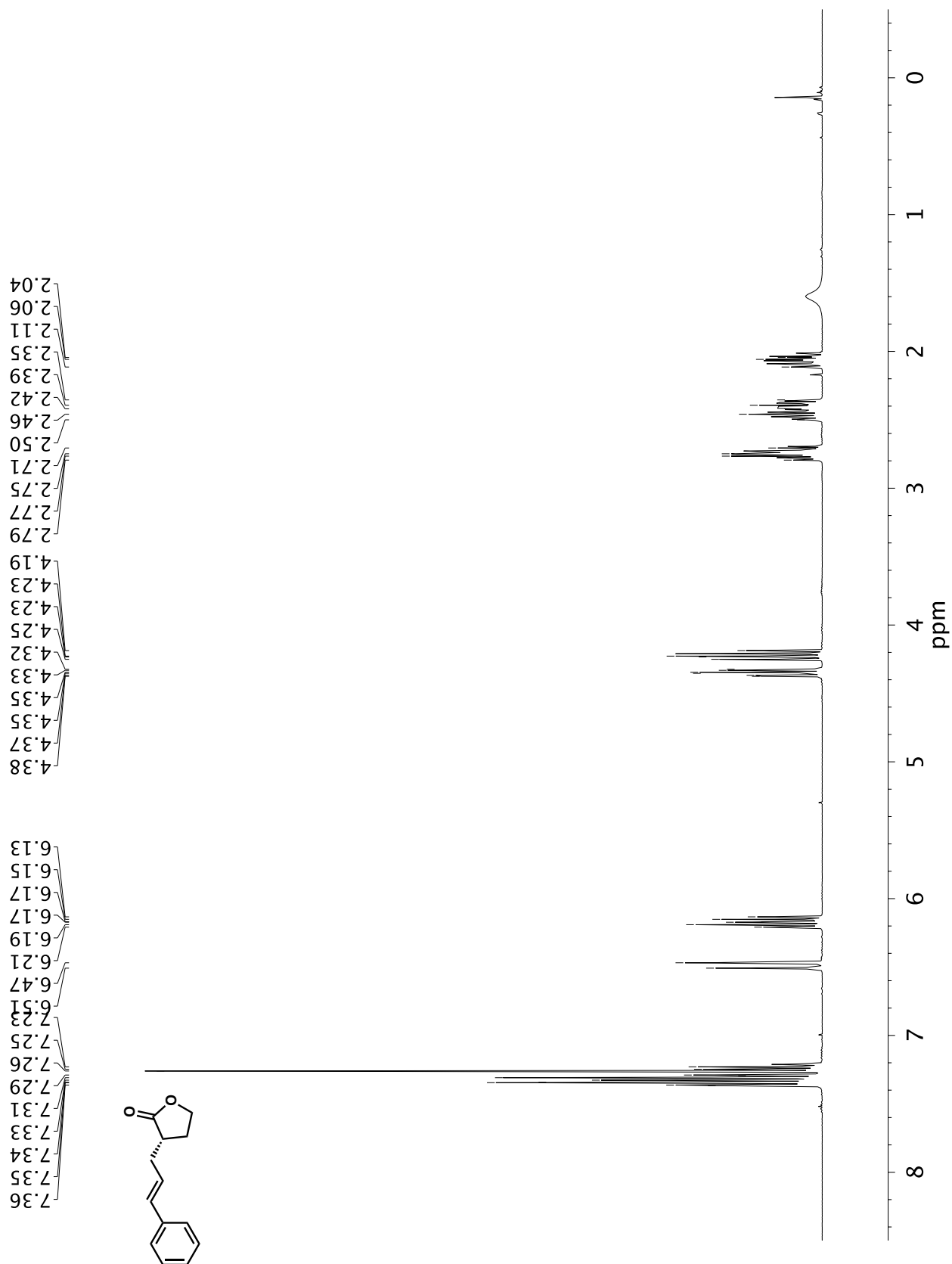
**A7.25** ^1H NMR (400 MHz, CDCl_3) of compound **430**

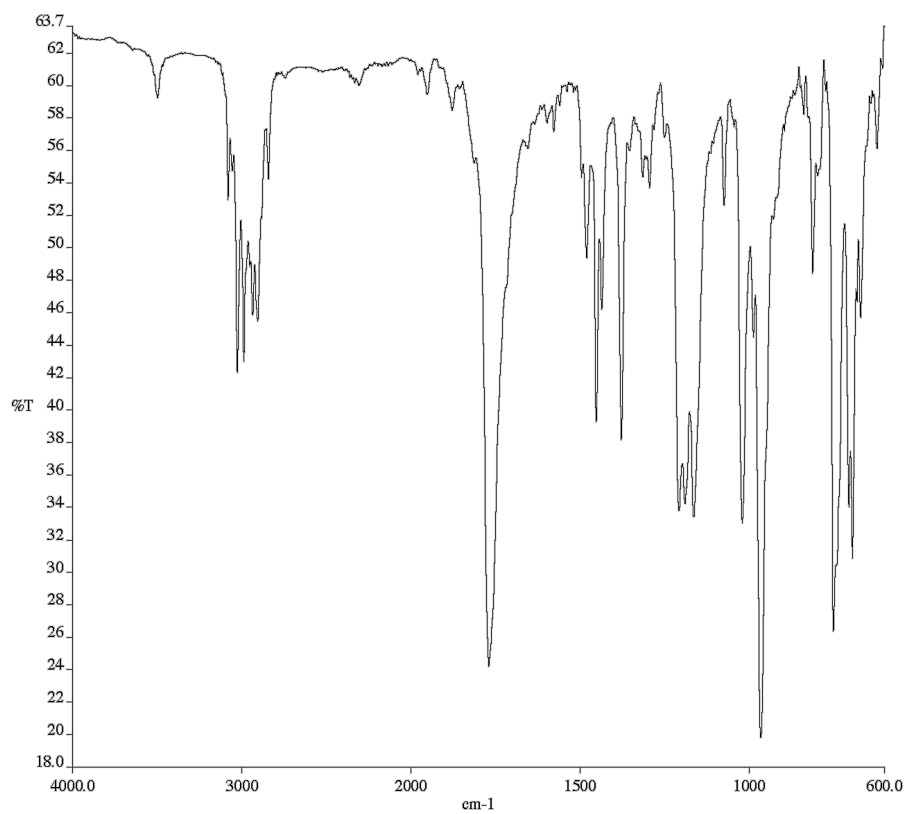


A7.26 Infrared spectrum (Thin Film, NaCl) of compound **43o**

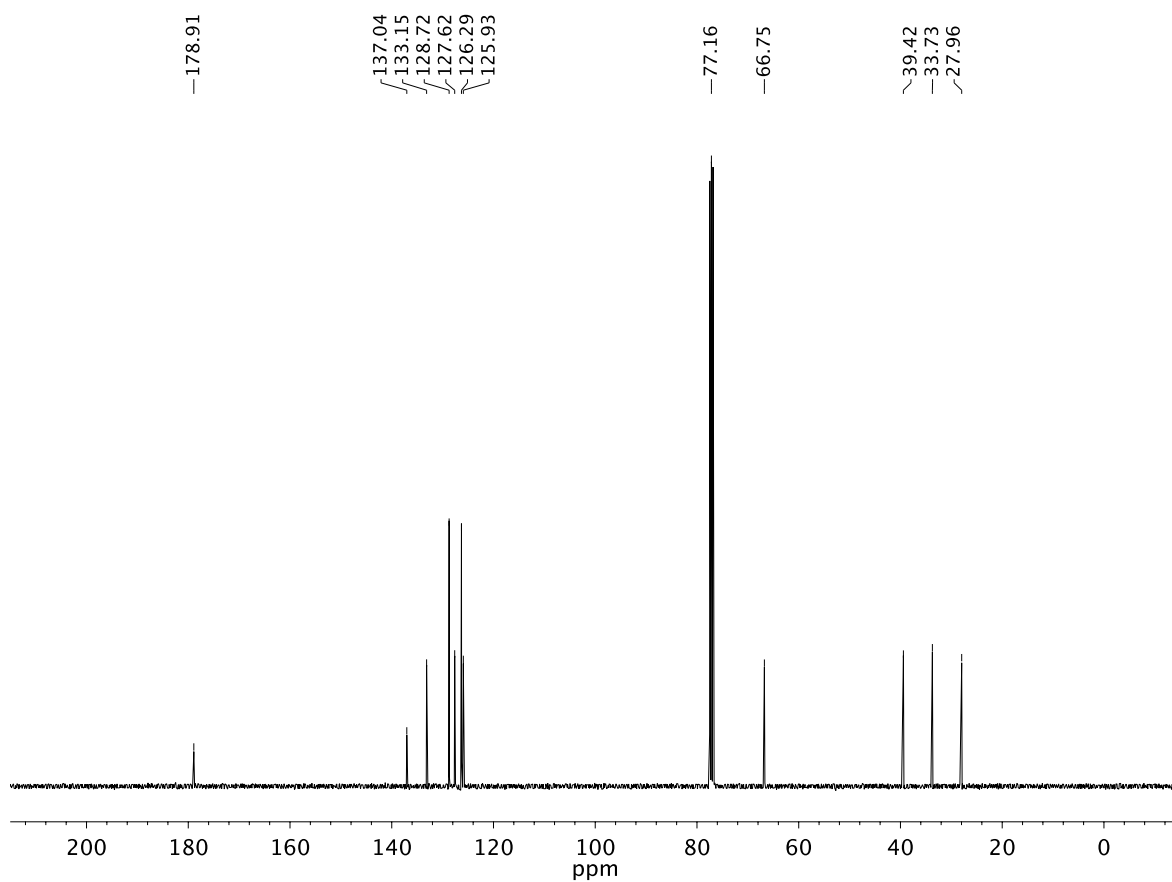


A7.27 ¹³C NMR (100 MHz, CDCl₃) of compound **43o**

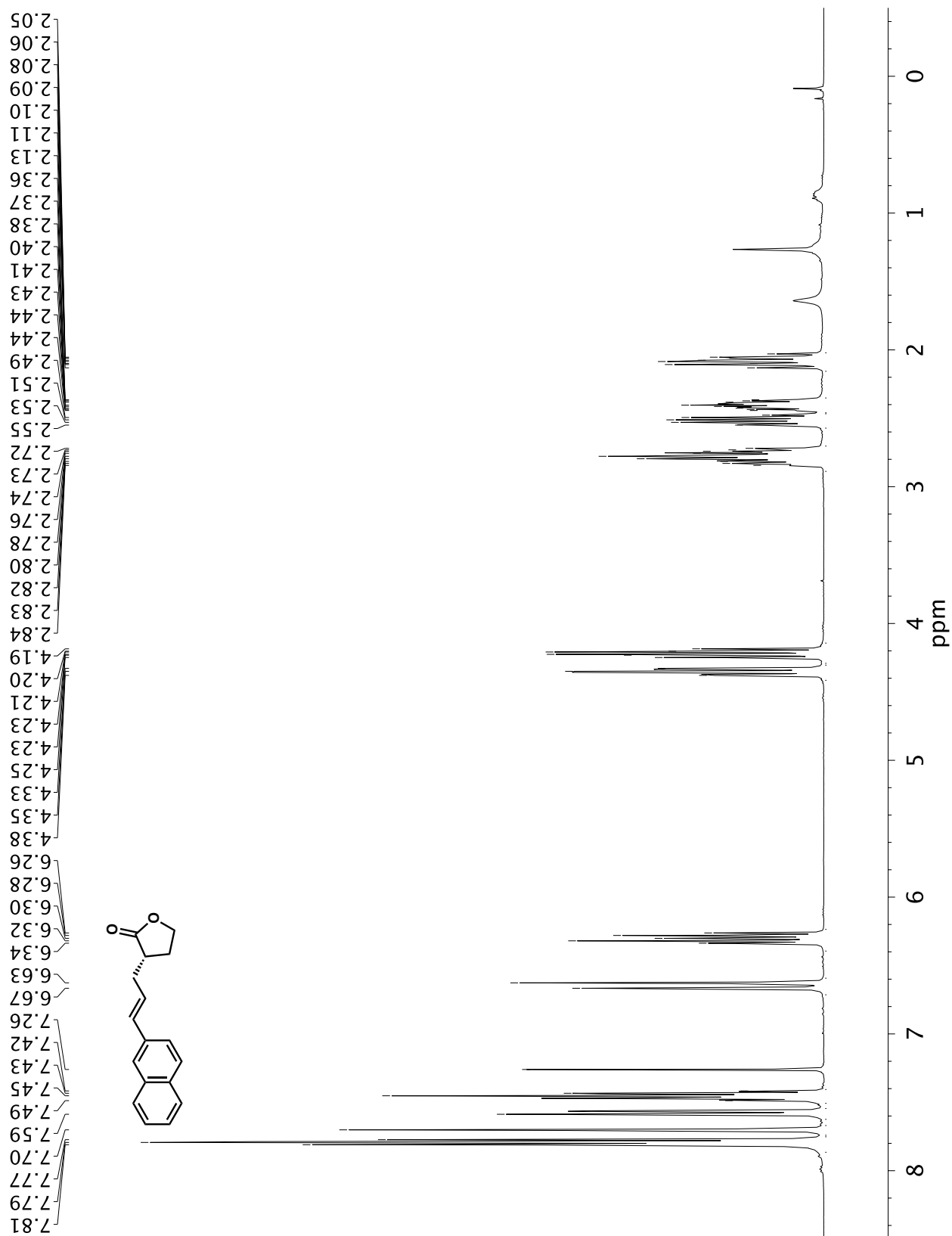
A7.28 ¹H NMR (400 MHz, CDCl₃) of compound **44a**

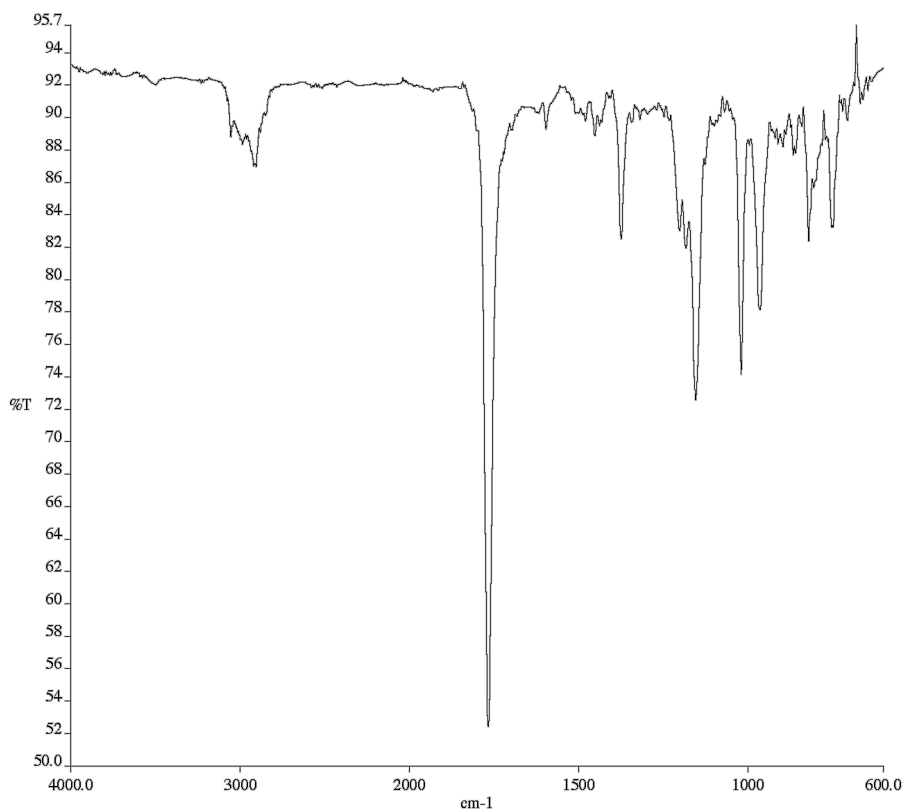


A7.29 Infrared spectrum (Thin Film, NaCl) of compound **44a**

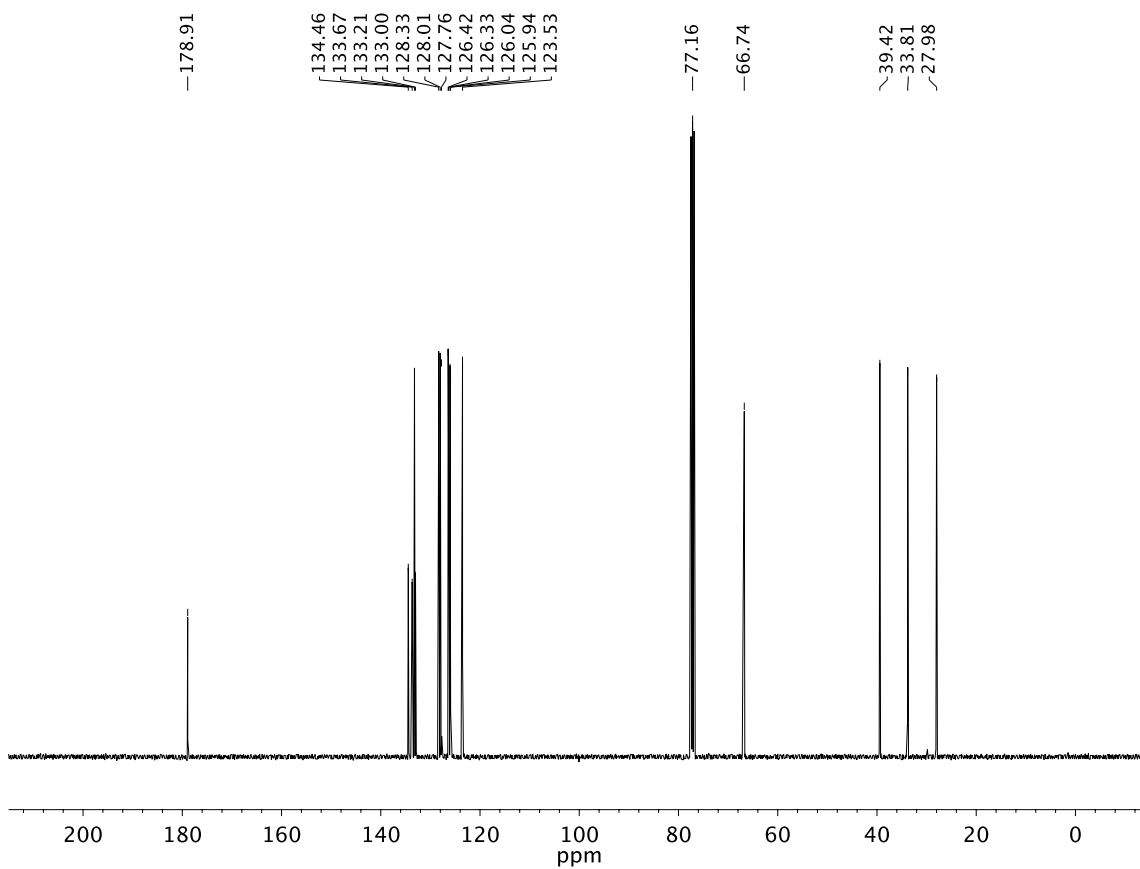


A7.30 ¹³C NMR (100 MHz, CDCl₃) of compound **44a**

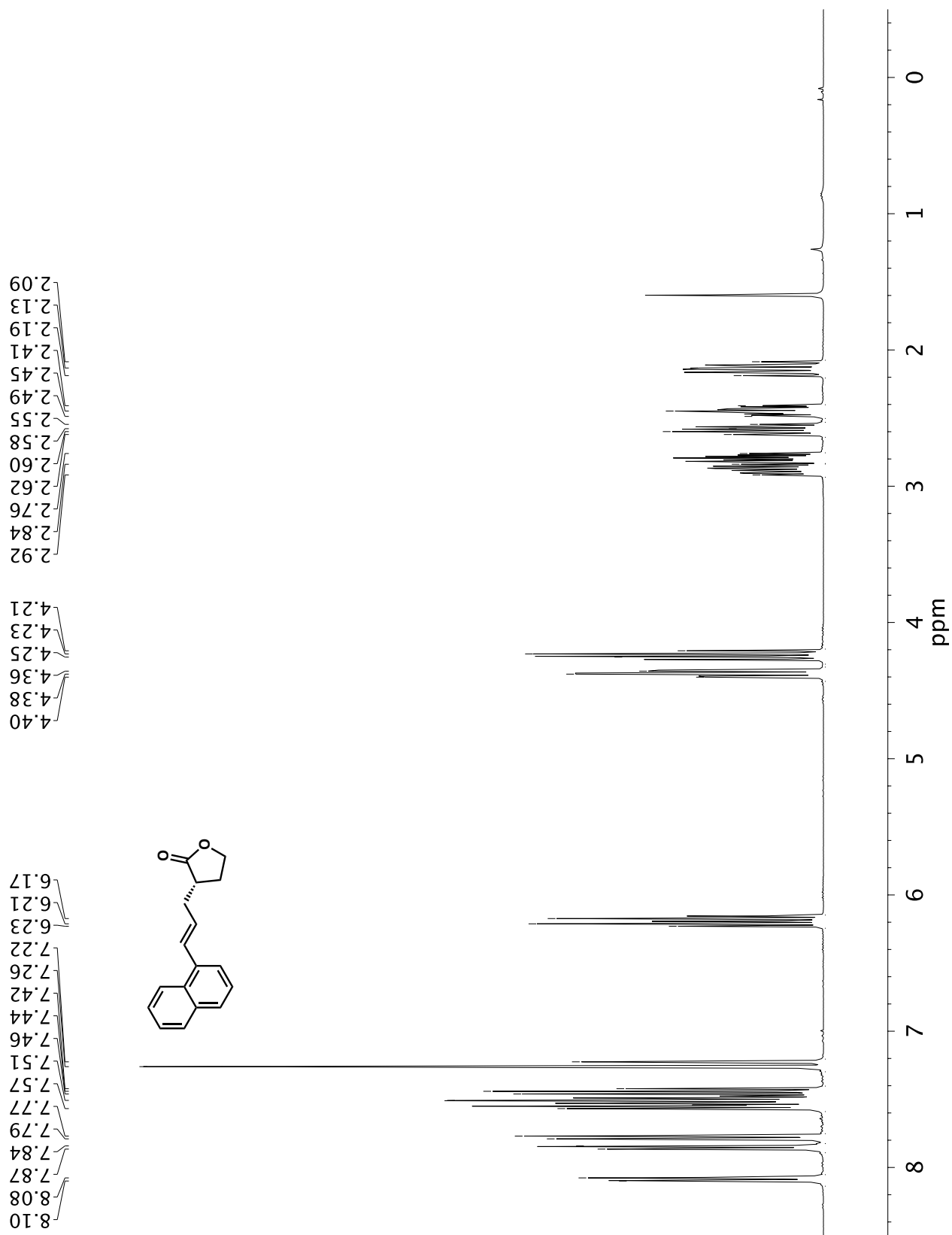
**A7.31** ¹H NMR (400 MHz, CDCl₃) of compound **44b**

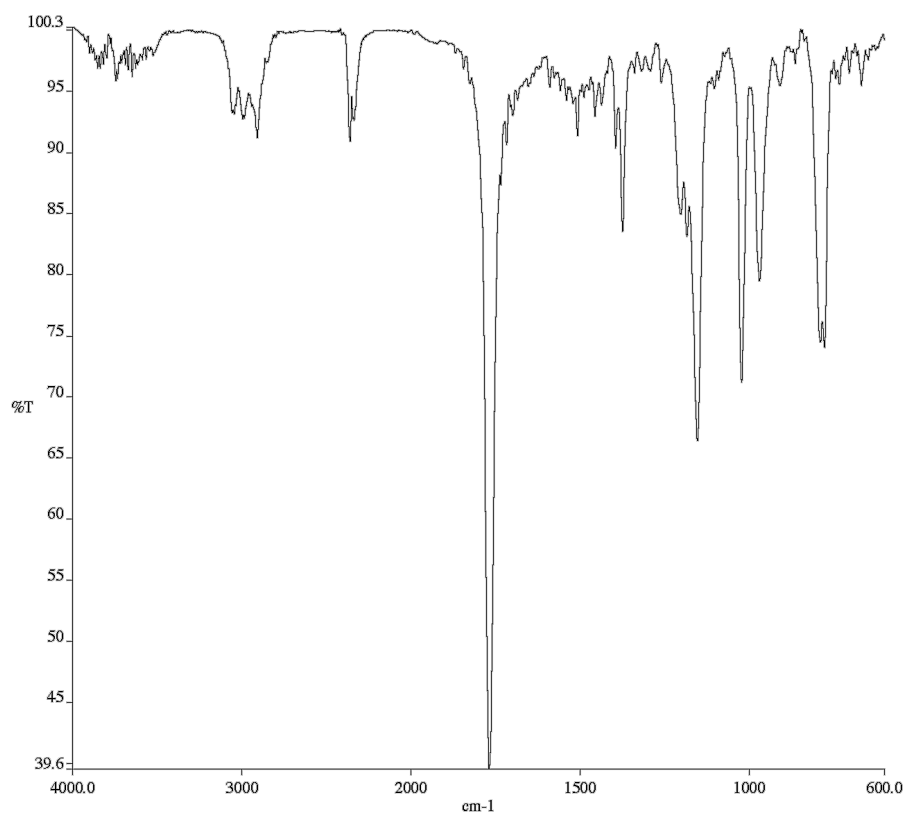


A7.32 Infrared spectrum (Thin Film, NaCl) of compound **44b**

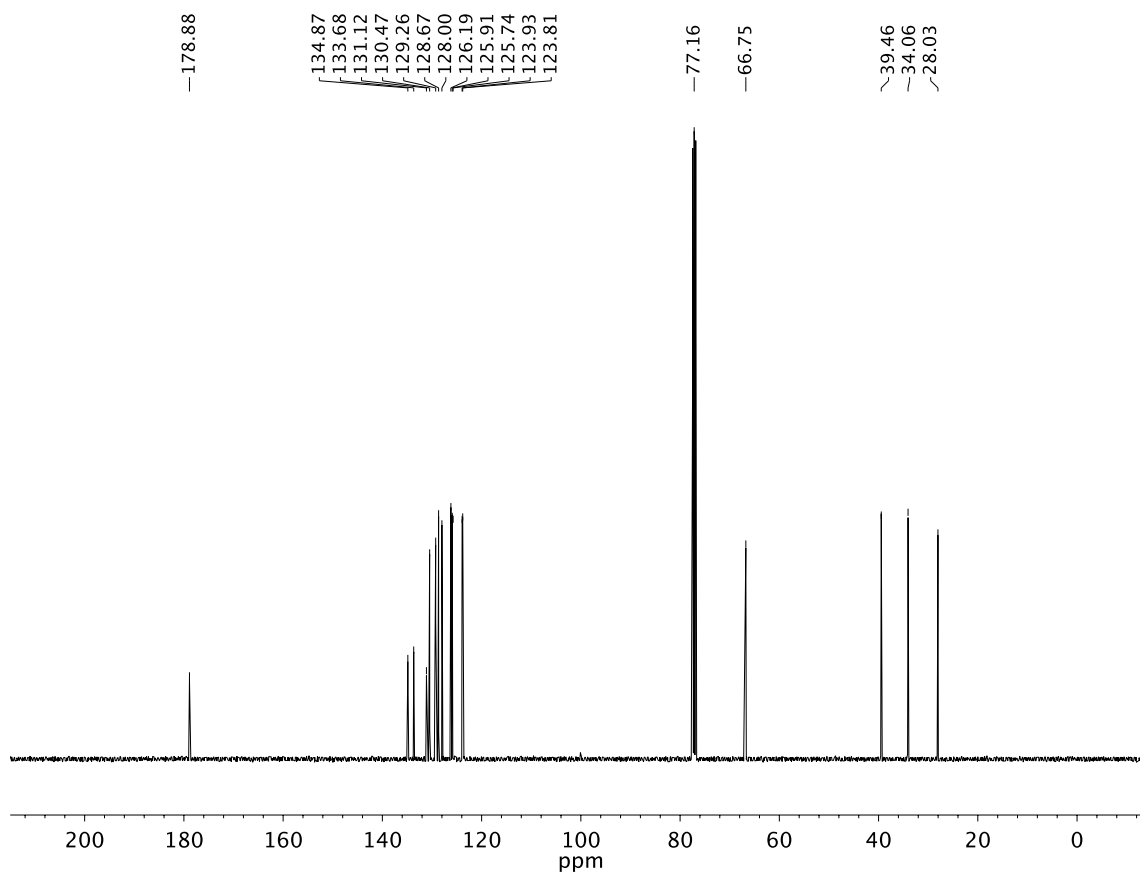


A7.33 ¹³C NMR (1005 MHz, CDCl₃) of compound **44b**

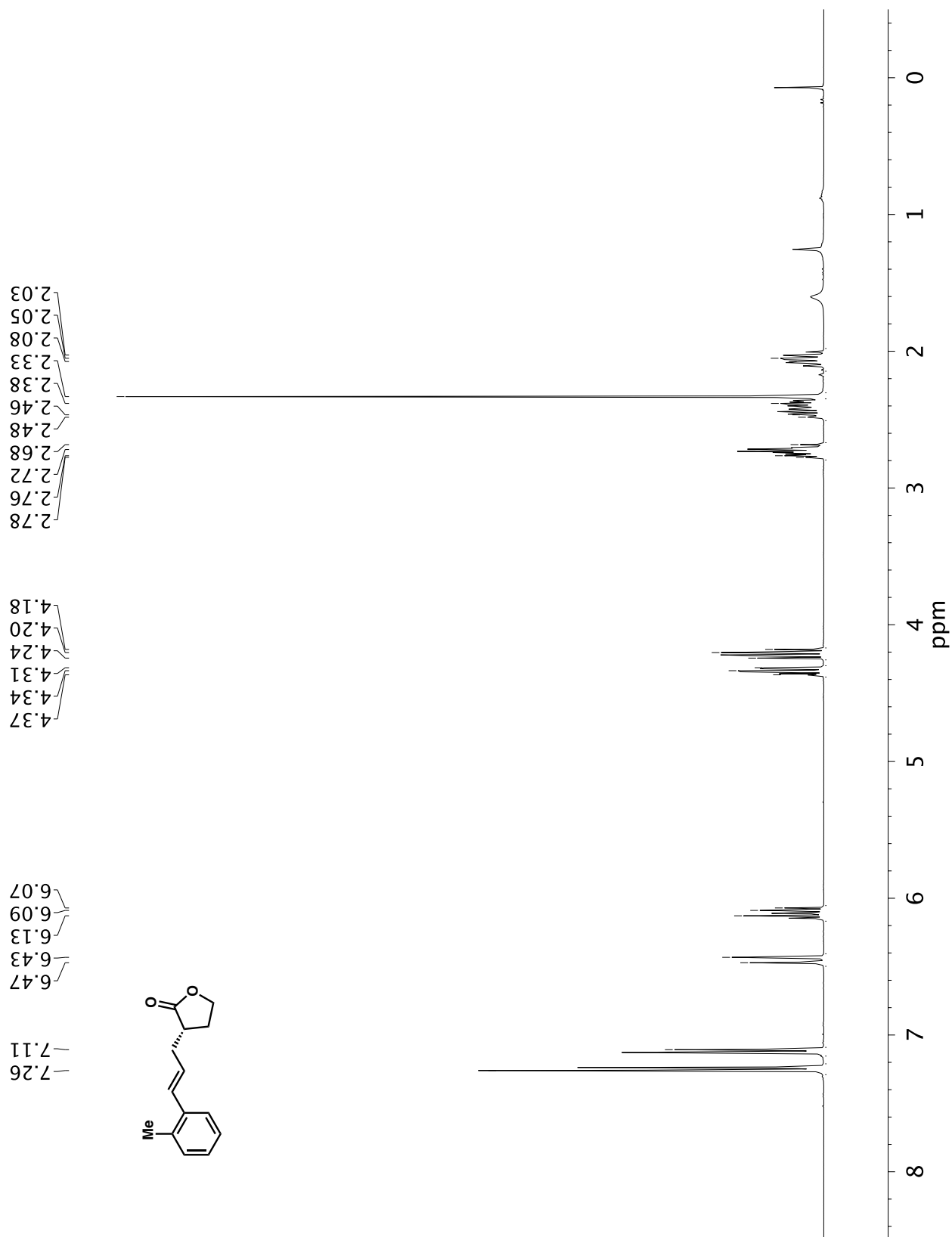
A7.34 ^1H NMR (400 MHz, CDCl_3) of compound **44c**

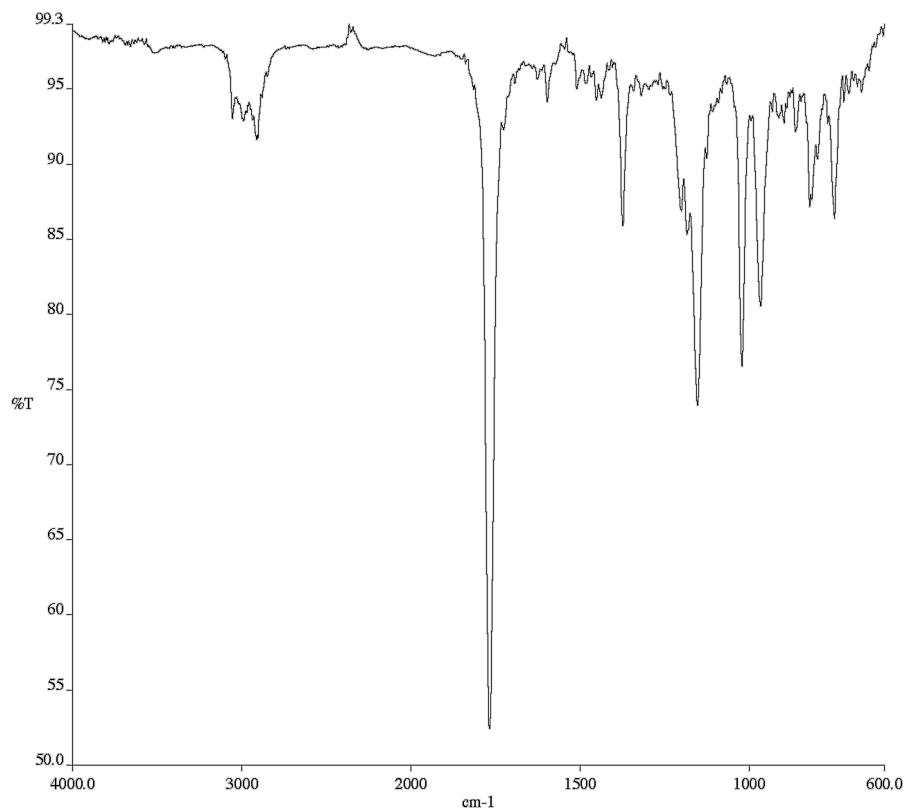


A7.35 Infrared spectrum (Thin Film, NaCl) of compound **44c**

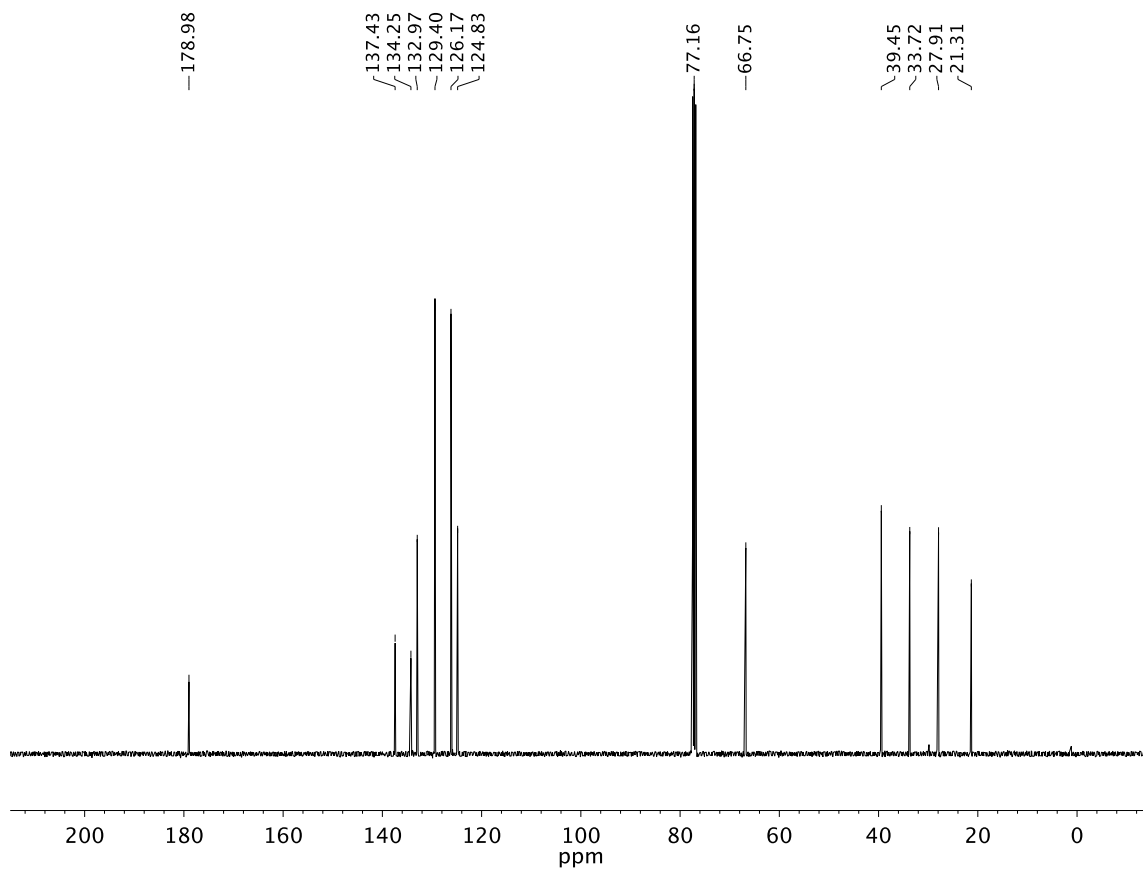


A7.36 ¹³C NMR (100 MHz, CDCl₃) of compound **44c**

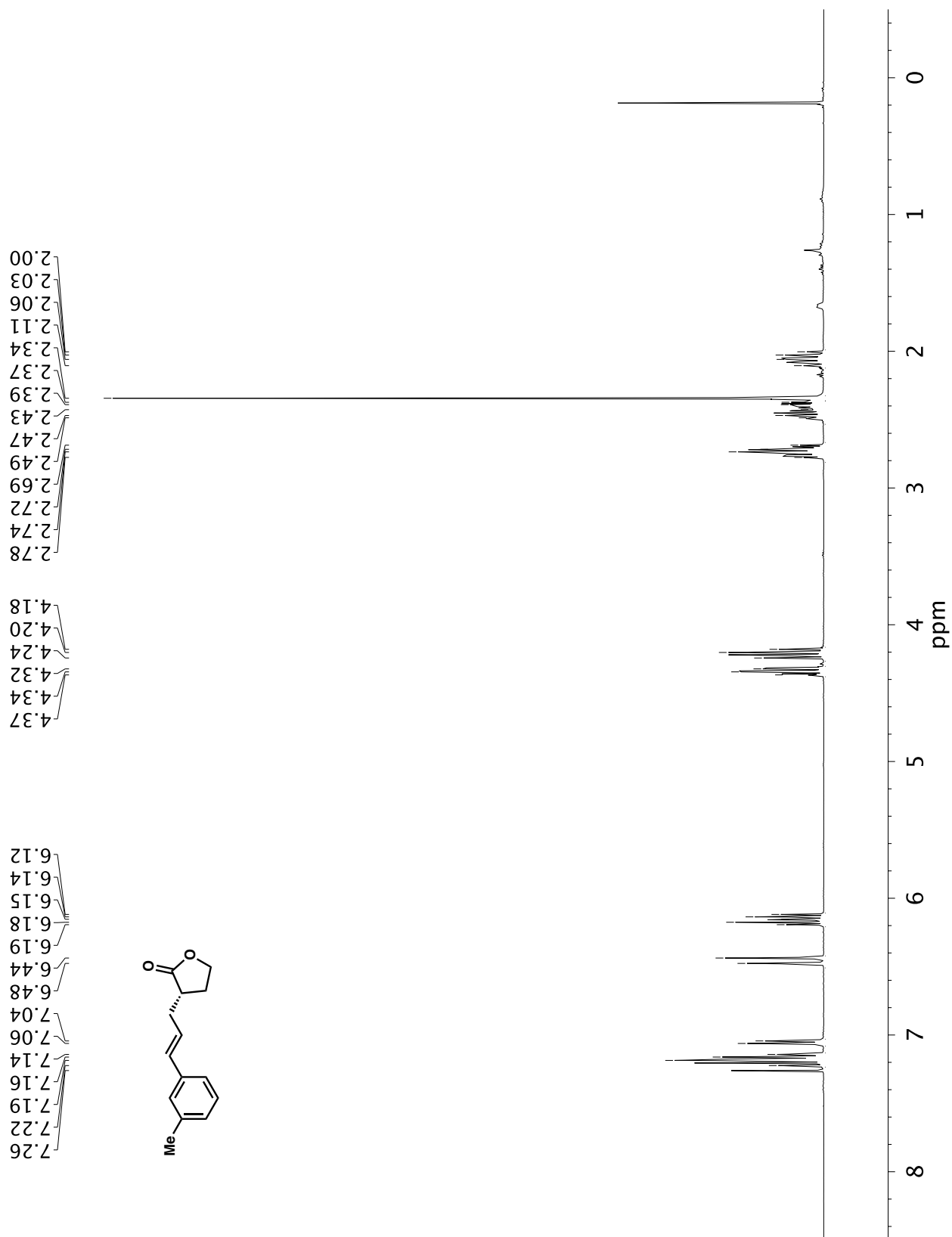
A7.37 ¹H NMR (400 MHz, CDCl₃) of compound **44d**

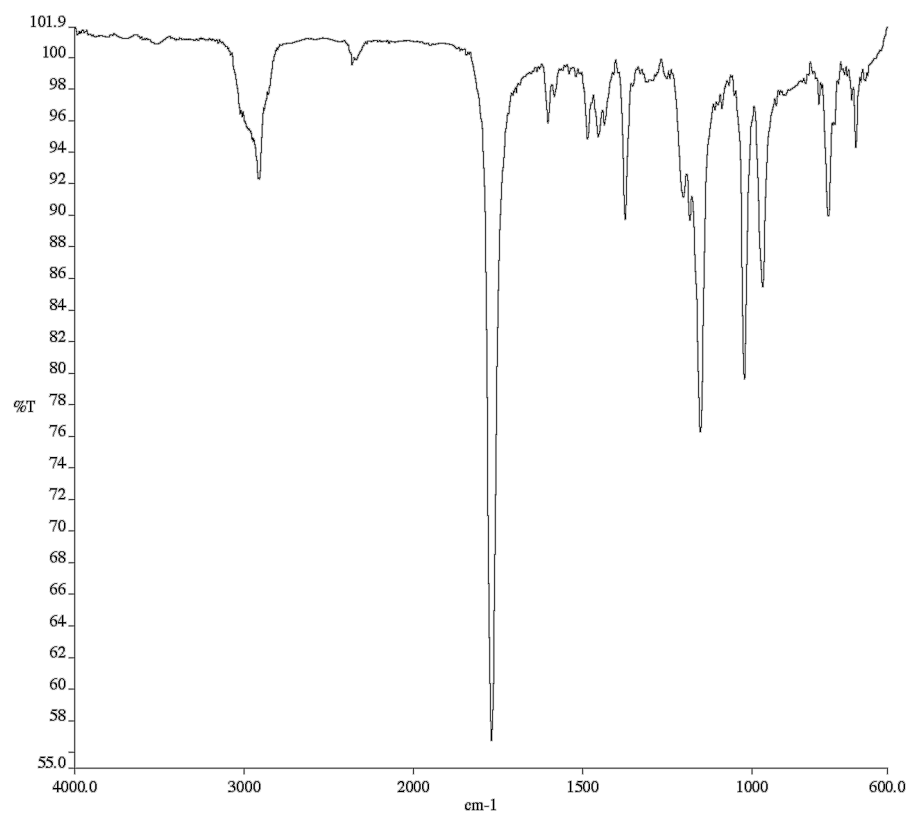
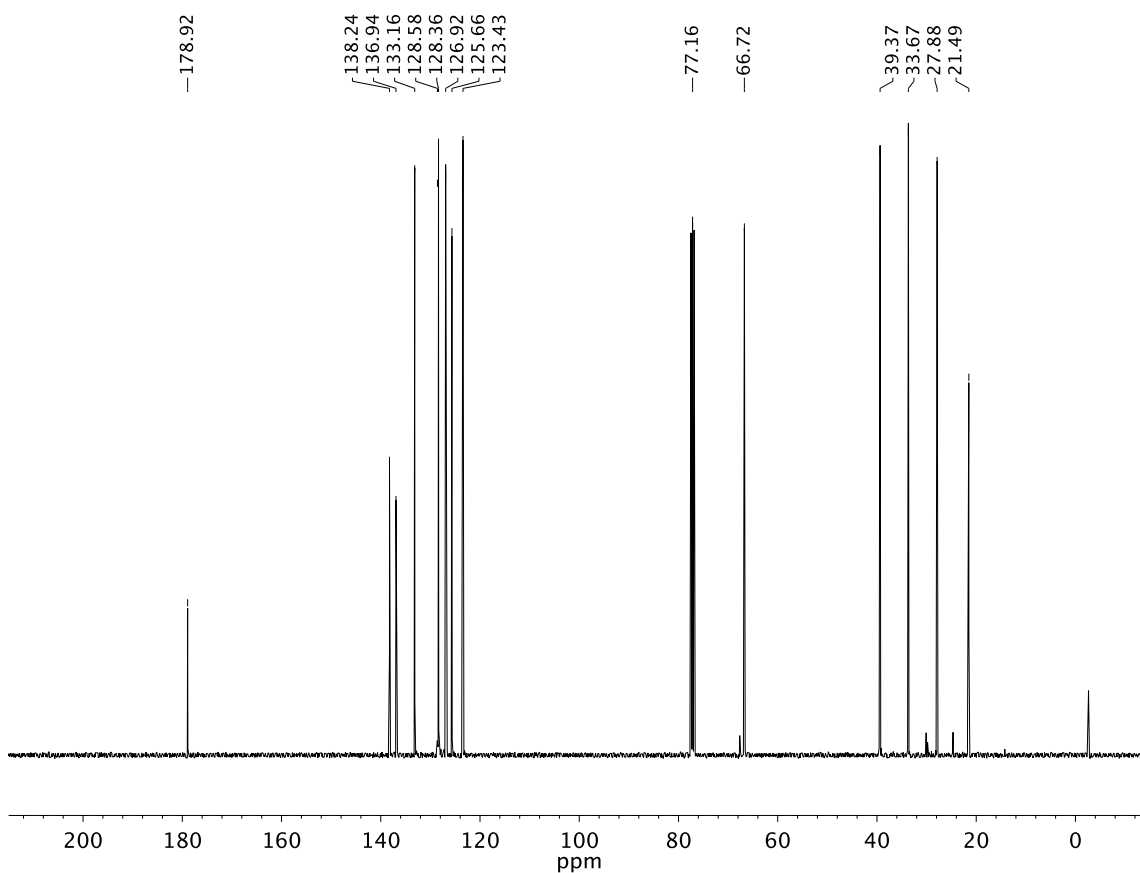


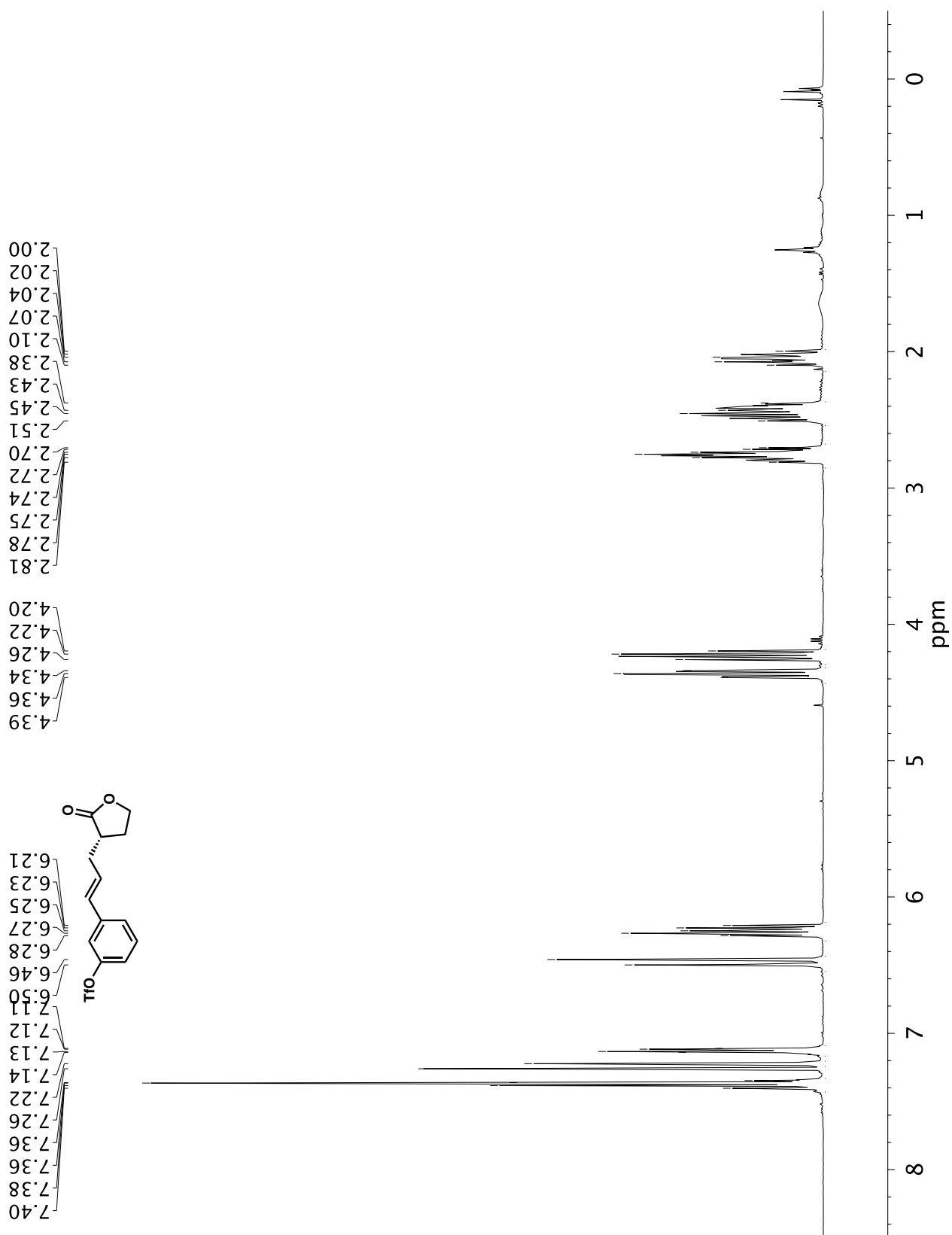
A7.38 Infrared spectrum (Thin Film, NaCl) of compound **44d**

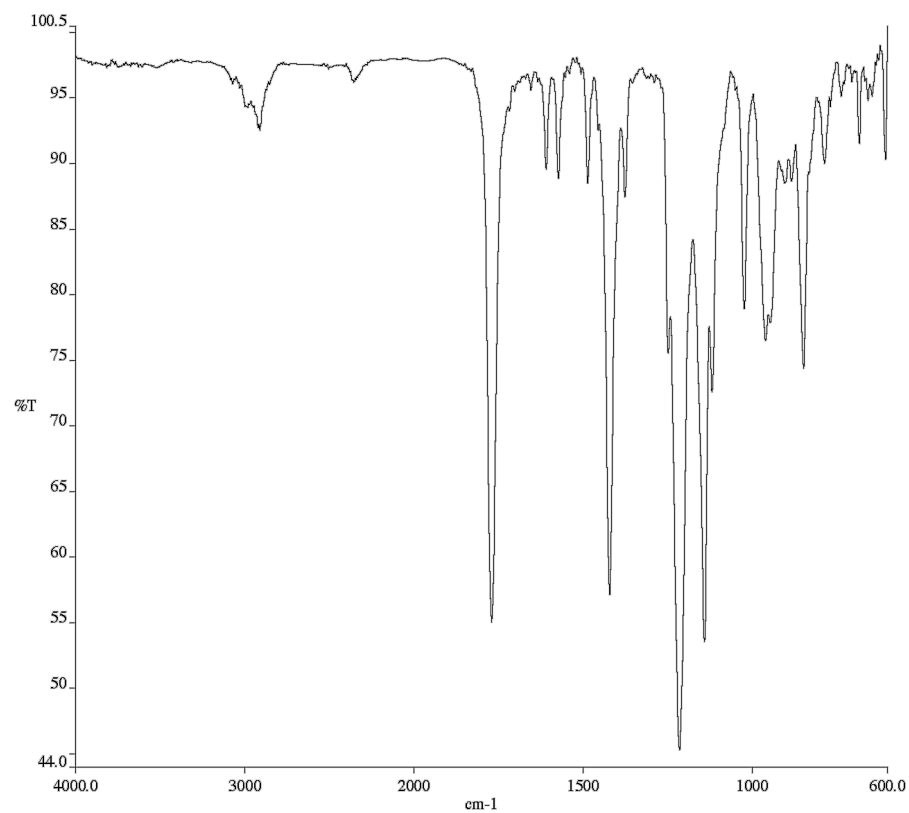


A7.39 ^{13}C NMR (100 MHz, CDCl_3) of compound **44d**

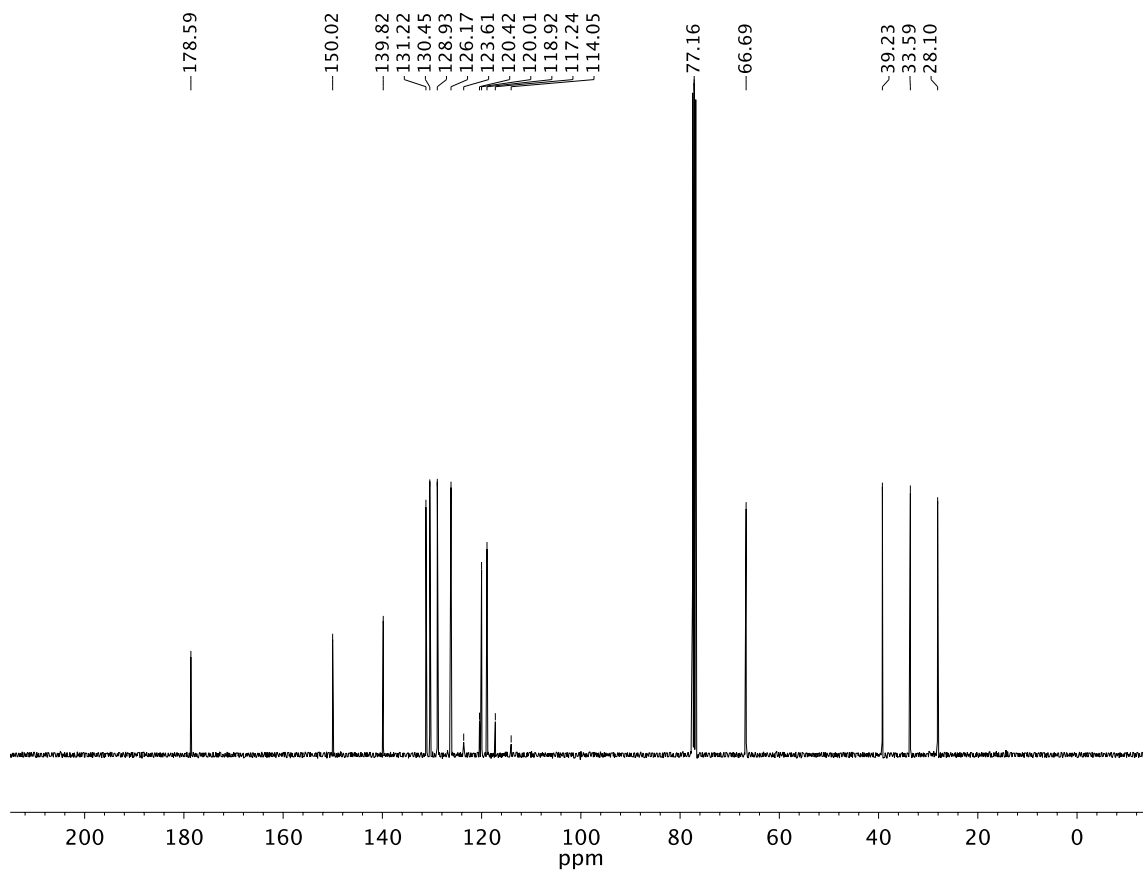
**A7.40** ¹H NMR (400 MHz, CDCl₃) of compound **44e**

**A7.41** Infrared spectrum (Thin Film, NaCl) of compound **44e****A7.42** ¹³C NMR (100 MHz, CDCl₃) of compound **44e**

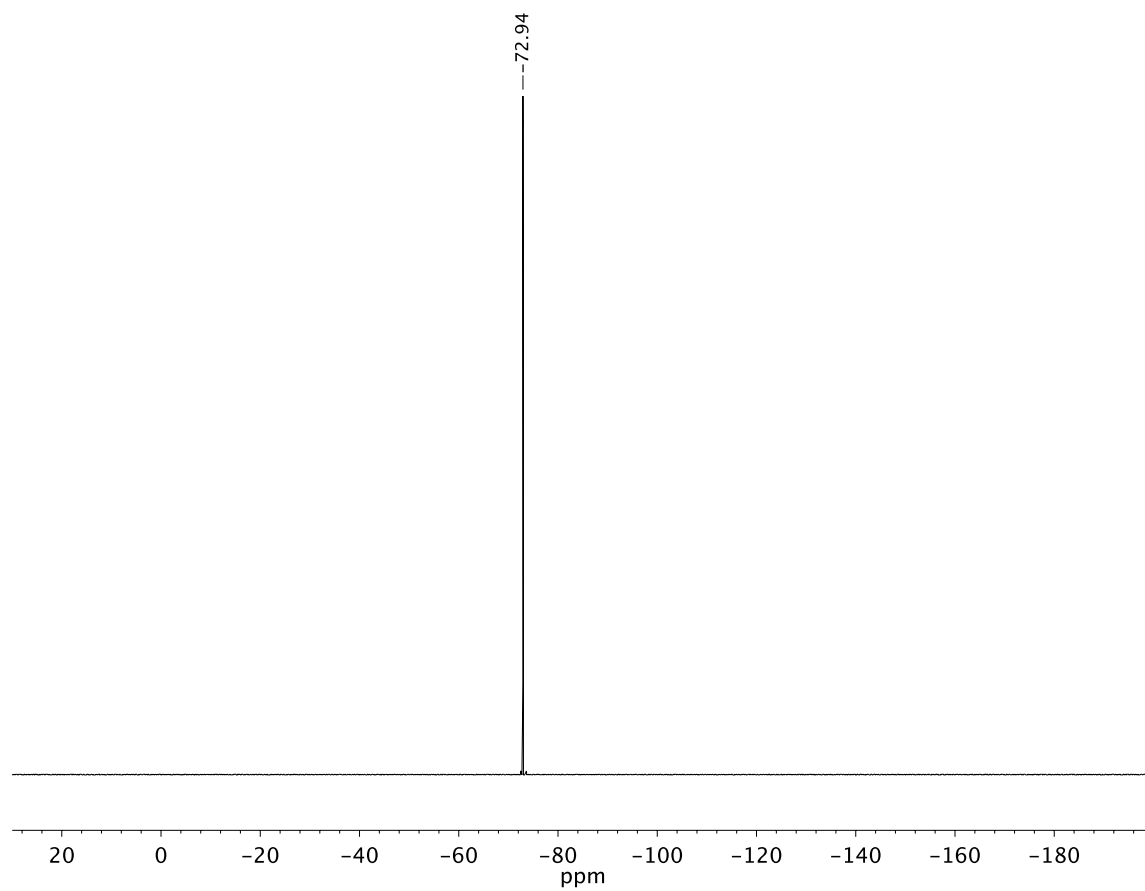
**A7.43** ¹H NMR (400 MHz, CDCl₃) of compound **44f**



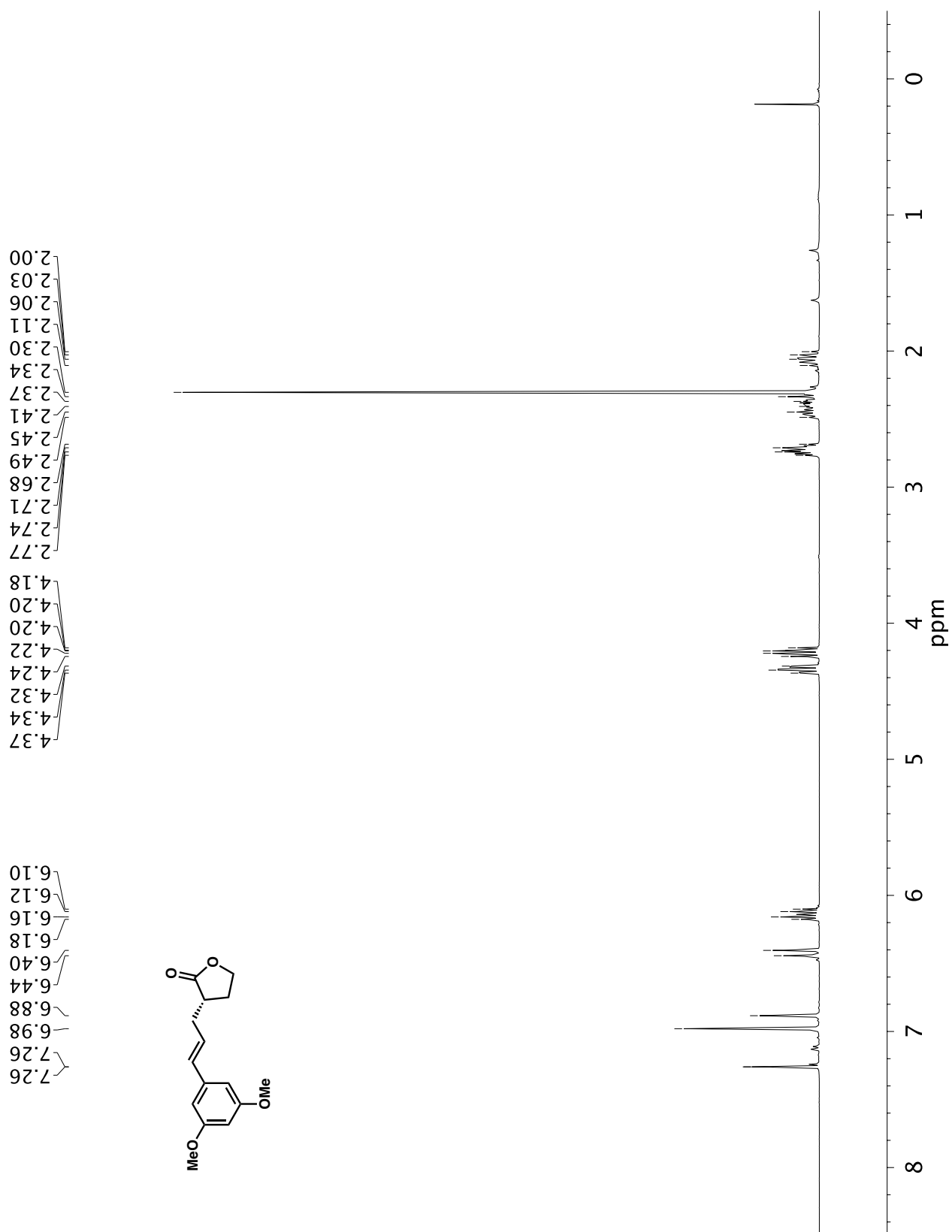
A7.44 Infrared spectrum (Thin Film, NaCl) of compound **44f**

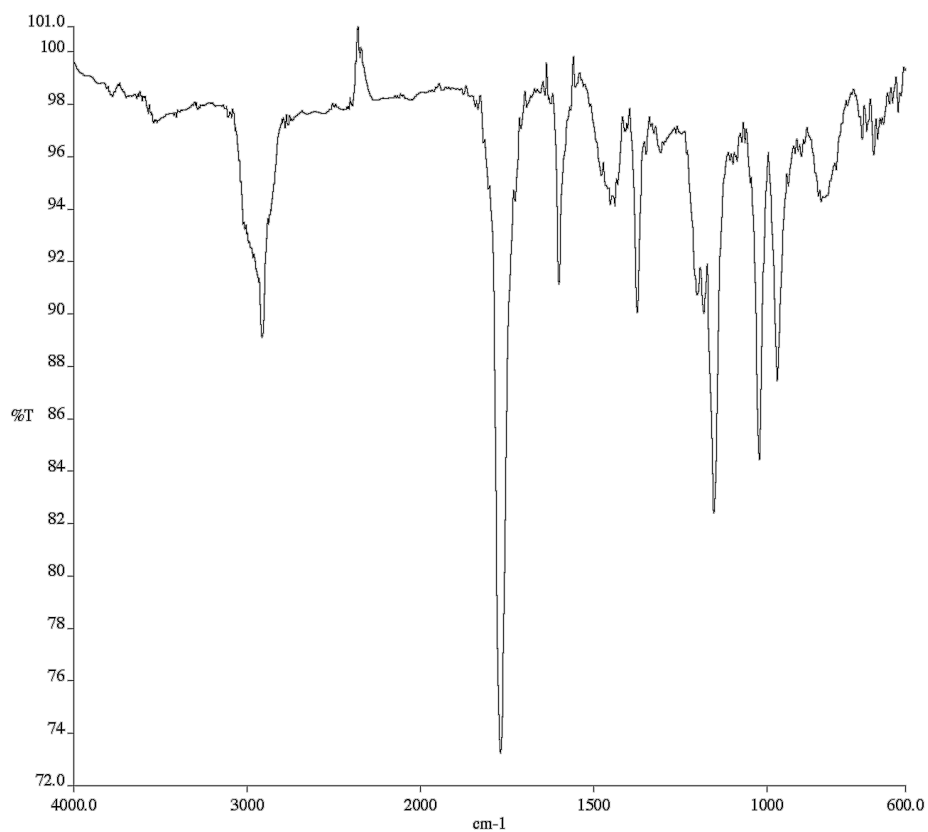


A7.45 ¹³C NMR (100 MHz, CDCl₃) of compound **44f**

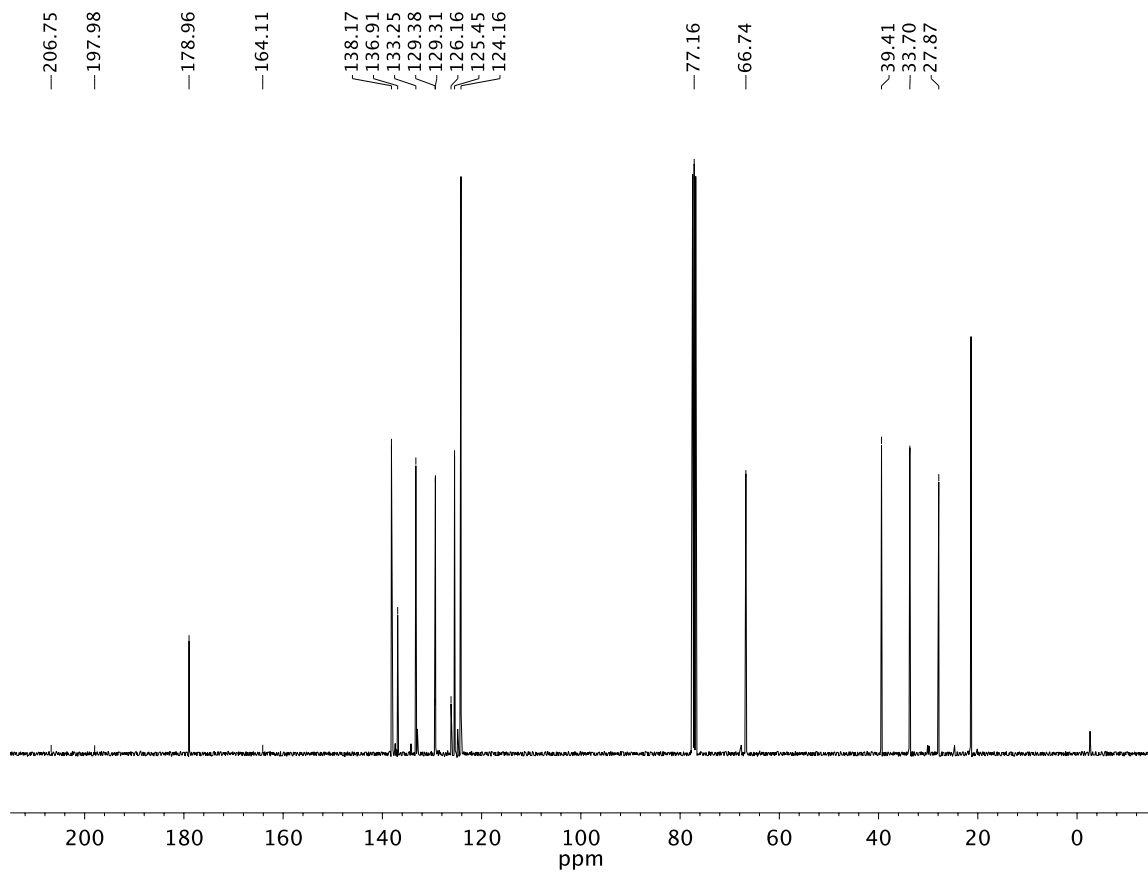


A7.46 ^{19}F NMR (282 MHz, CDCl_3) of compound **44f**

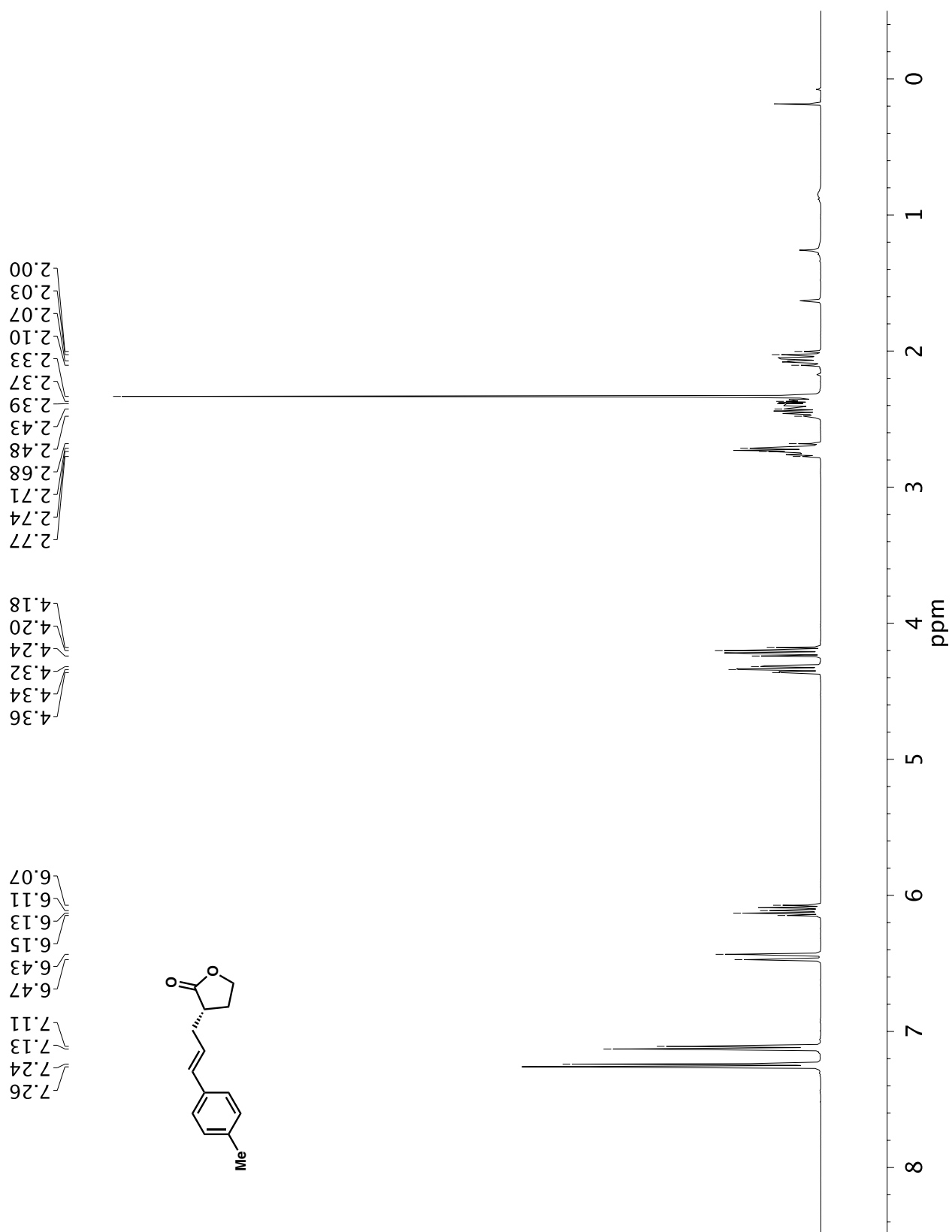
A7.47 ^1H NMR (400 MHz, CDCl_3) of compound **44g**

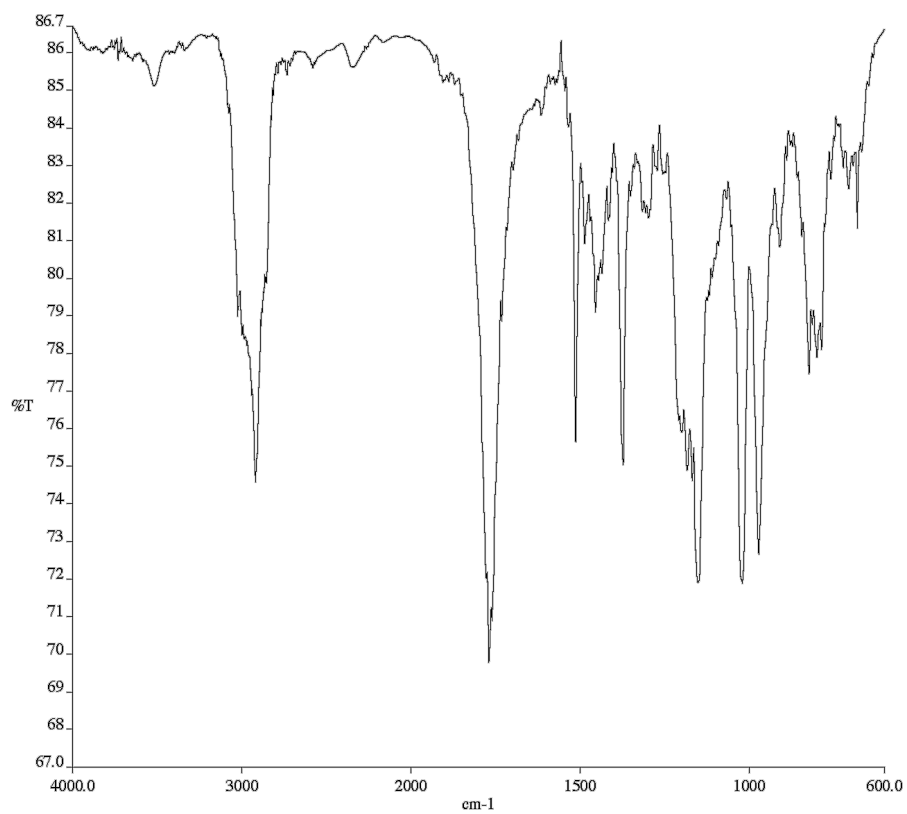


A7.48 Infrared spectrum (Thin Film, NaCl) of compound **44g**

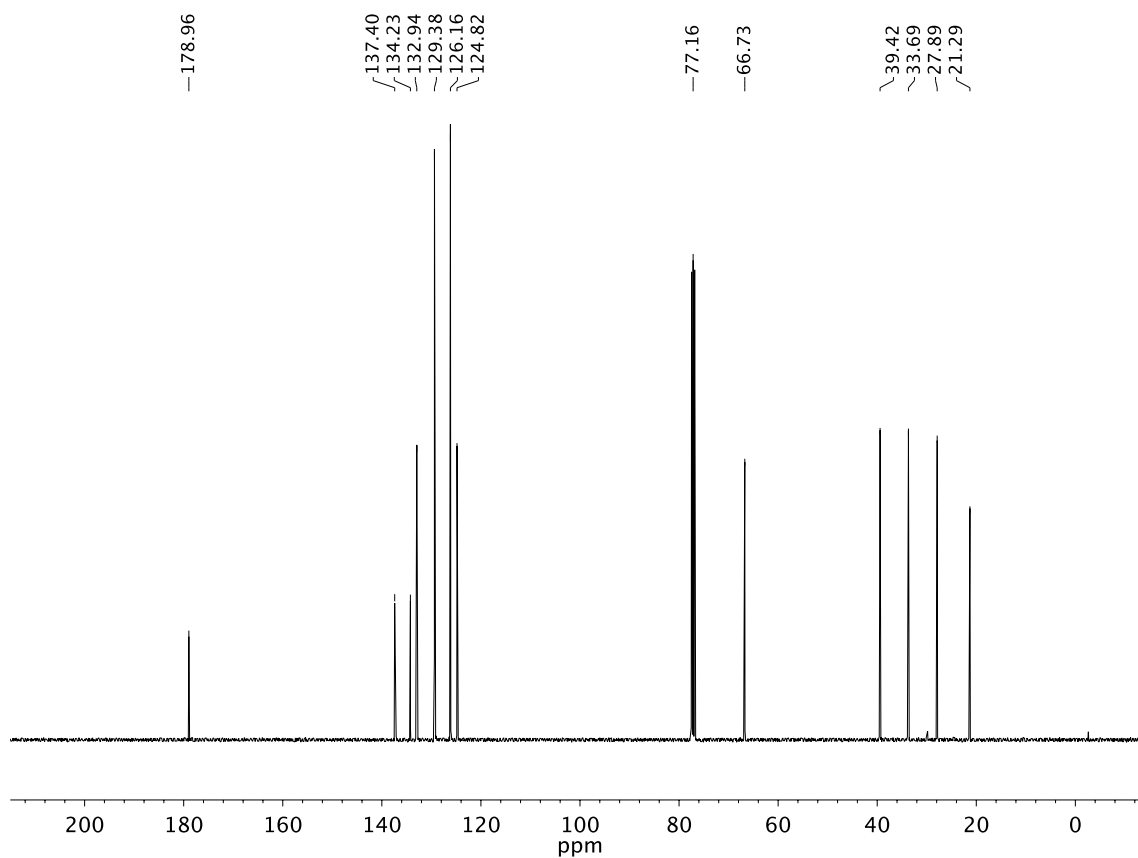


A7.49 ¹³C NMR (100 MHz, CDCl₃) of compound **44g**

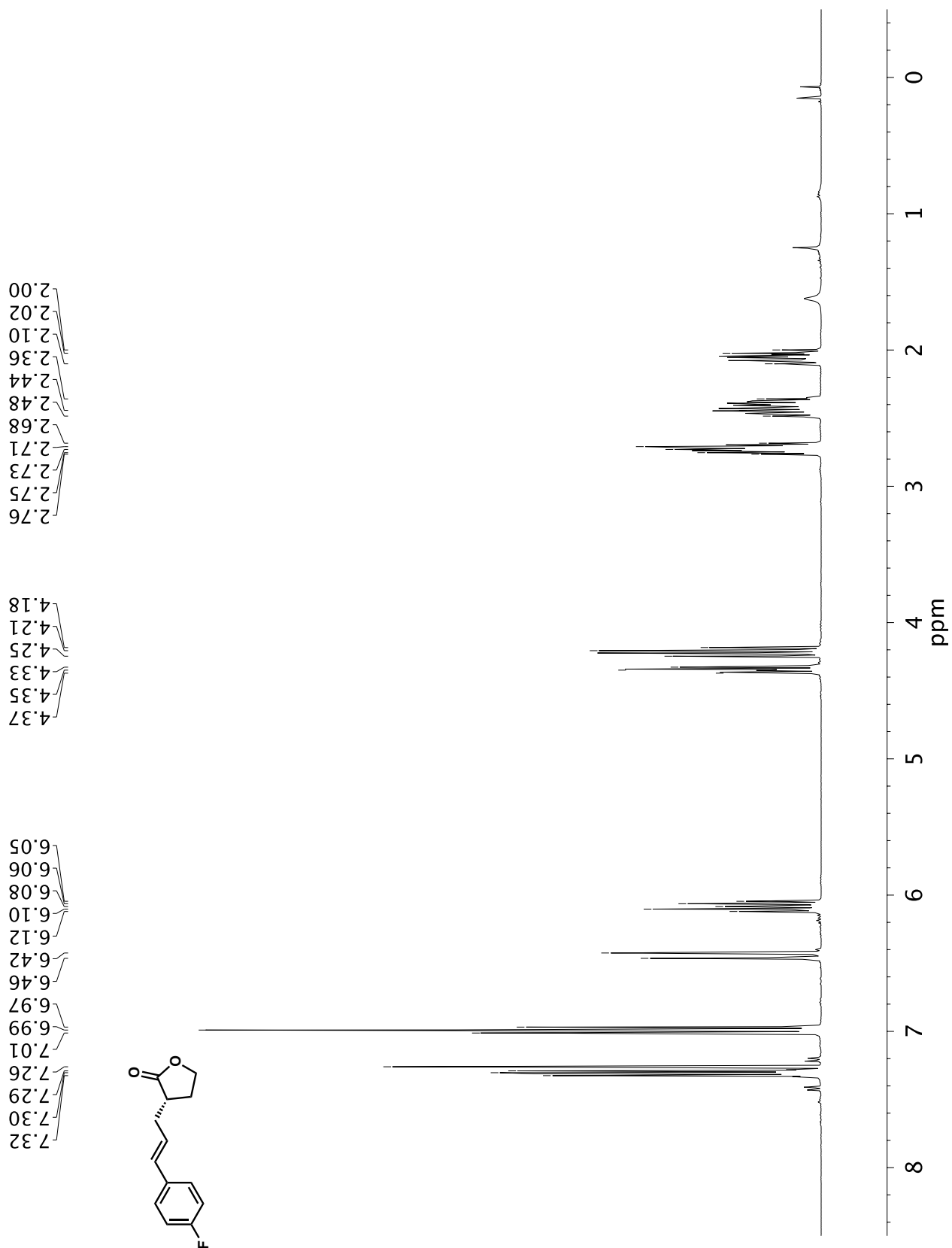
**A7.50** ¹H NMR (400 MHz, CDCl₃) of compound **44h**

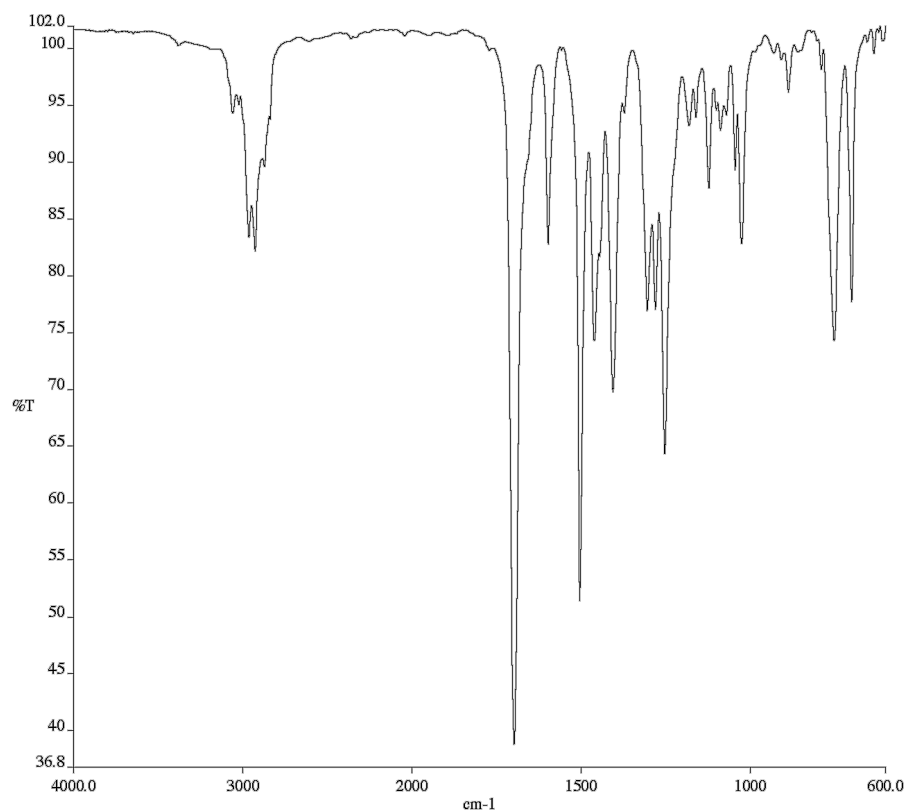


A7.51 Infrared spectrum (Thin Film, NaCl) of compound **44h**

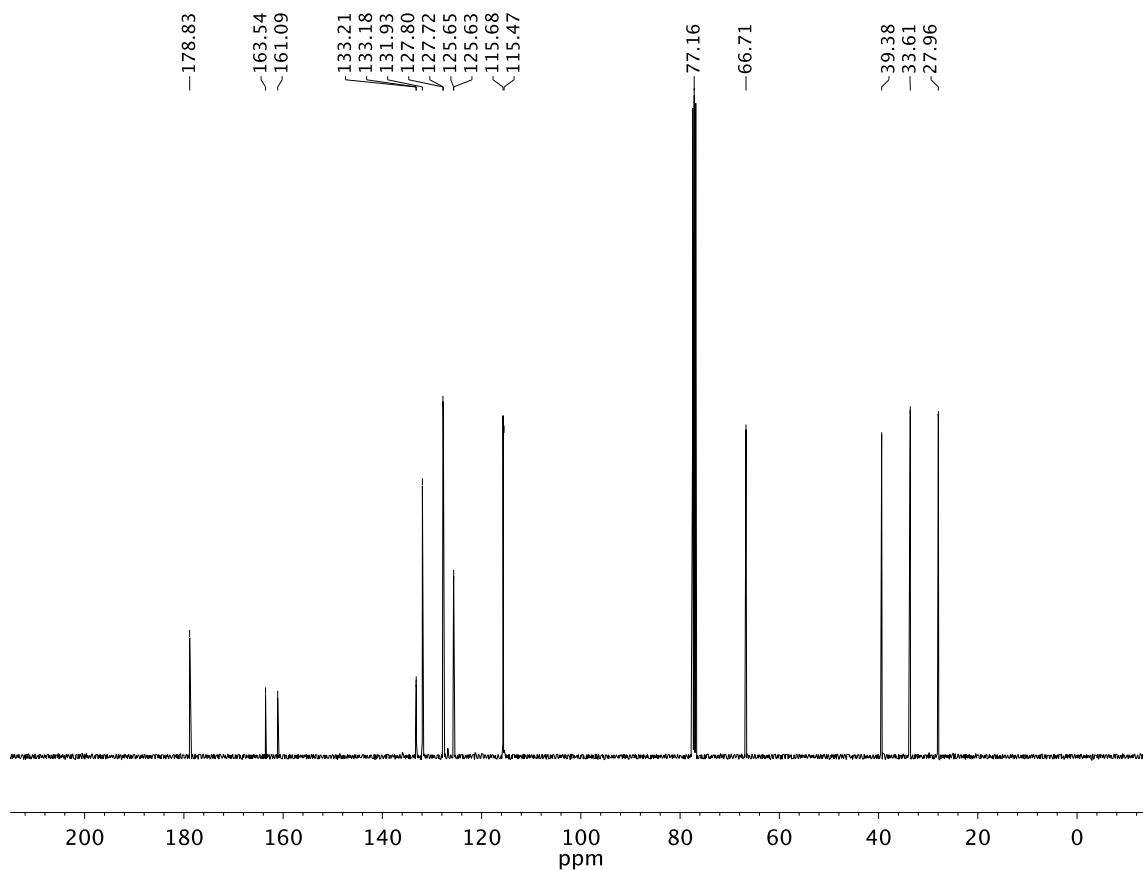


A7.52 ^{13}C NMR (100 MHz, CDCl_3) of compound **44h**

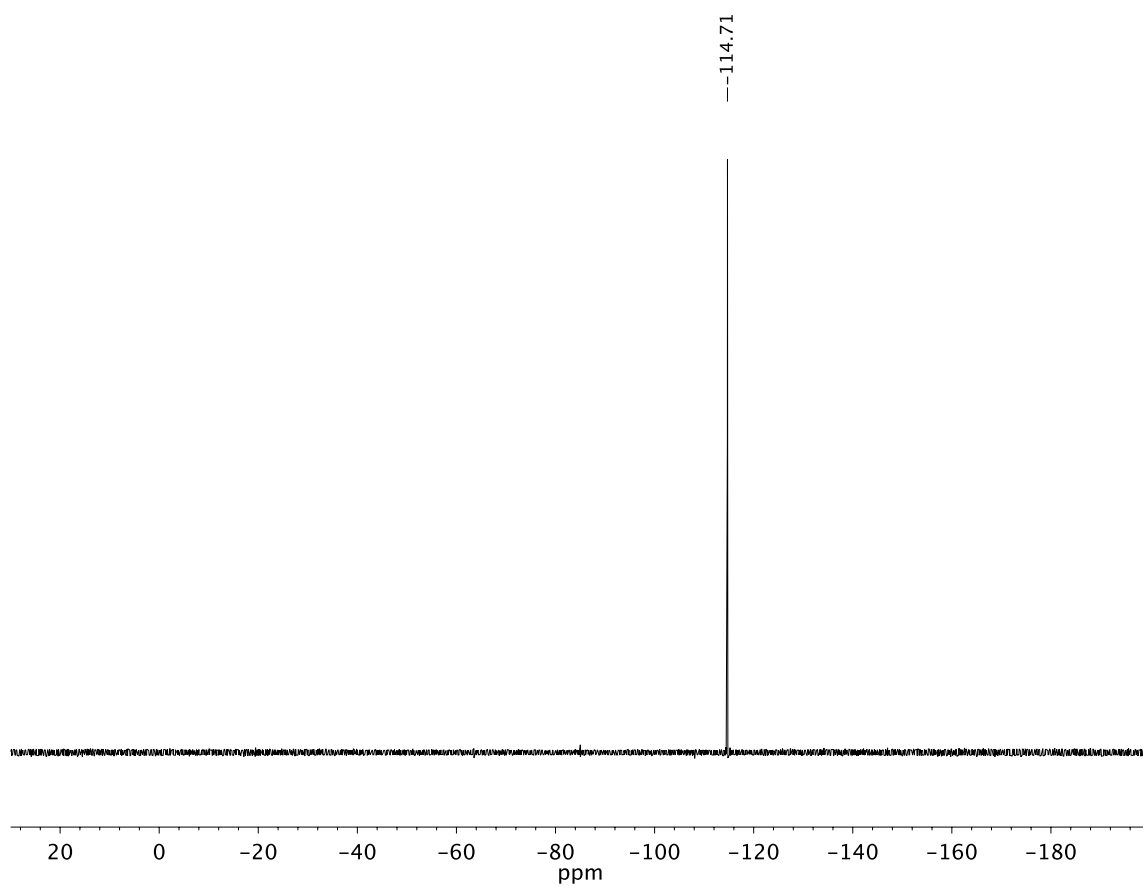




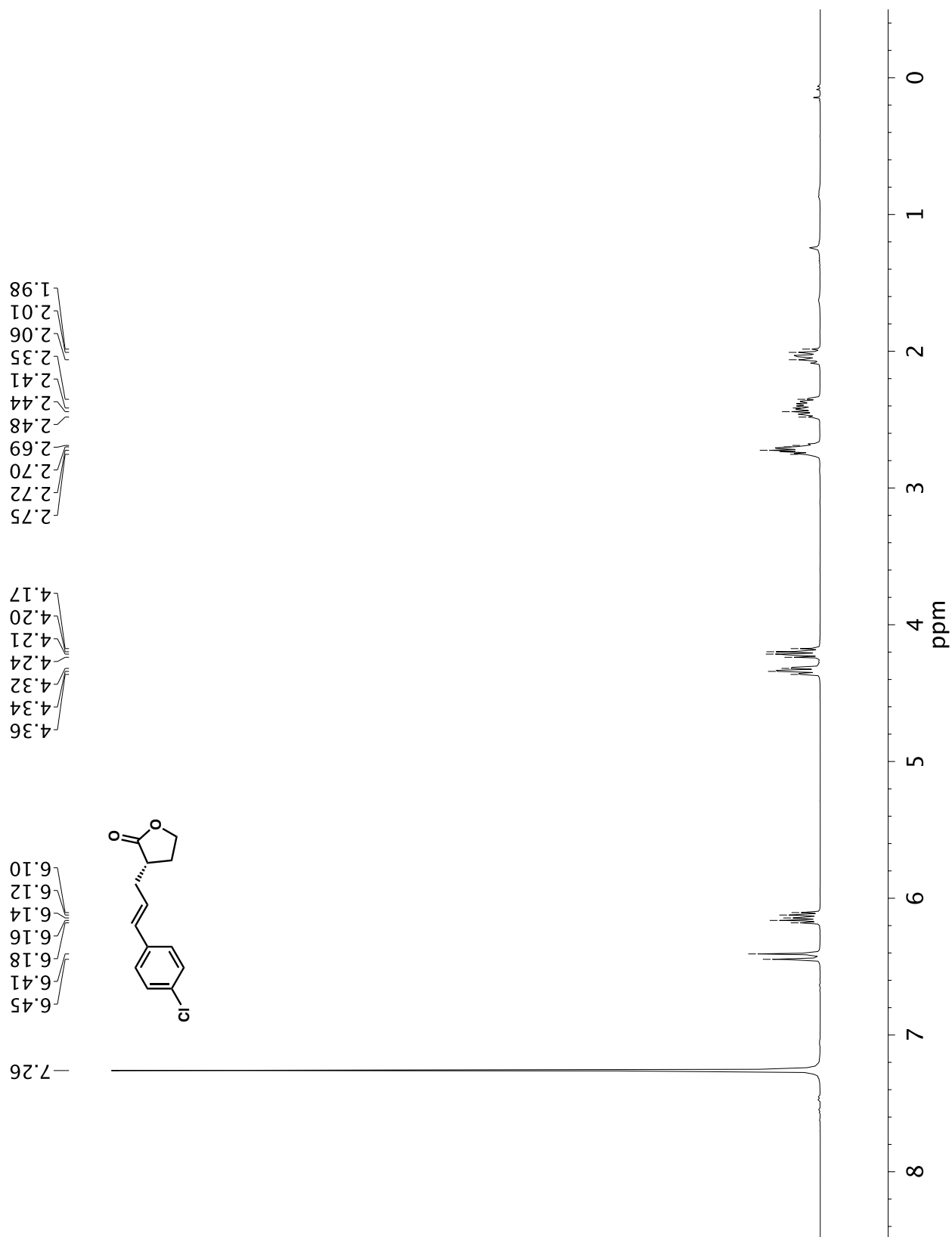
A7.54 Infrared spectrum (Thin Film, NaCl) of compound **44i**

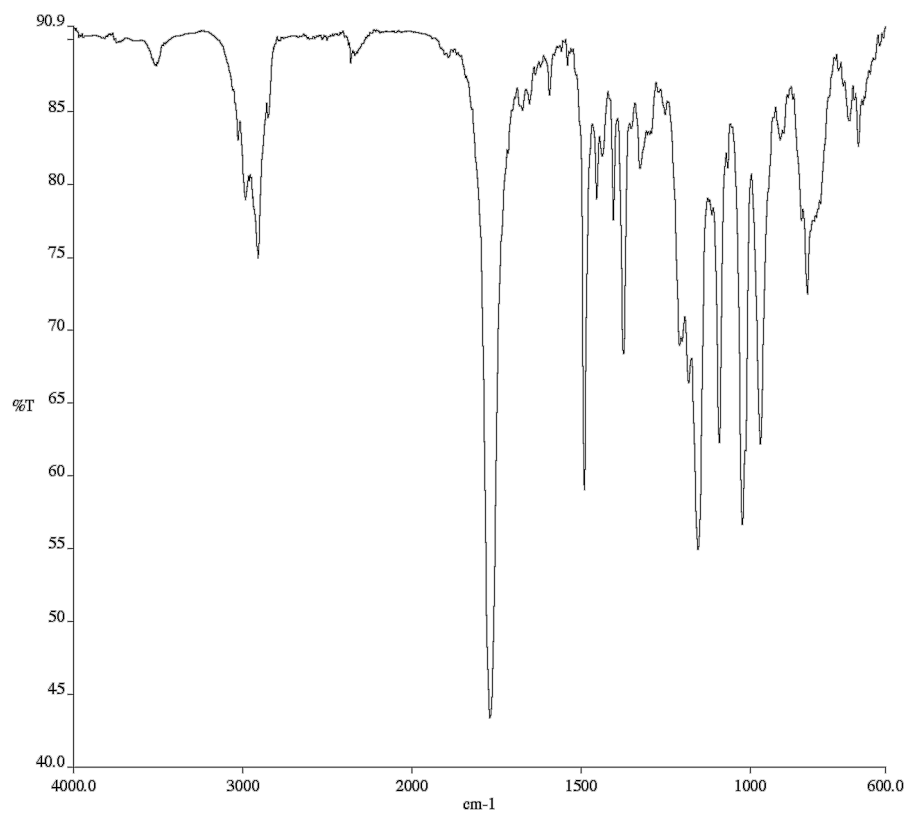


A7.55 ^{13}C NMR (100 MHz, CDCl_3) of compound **44i**

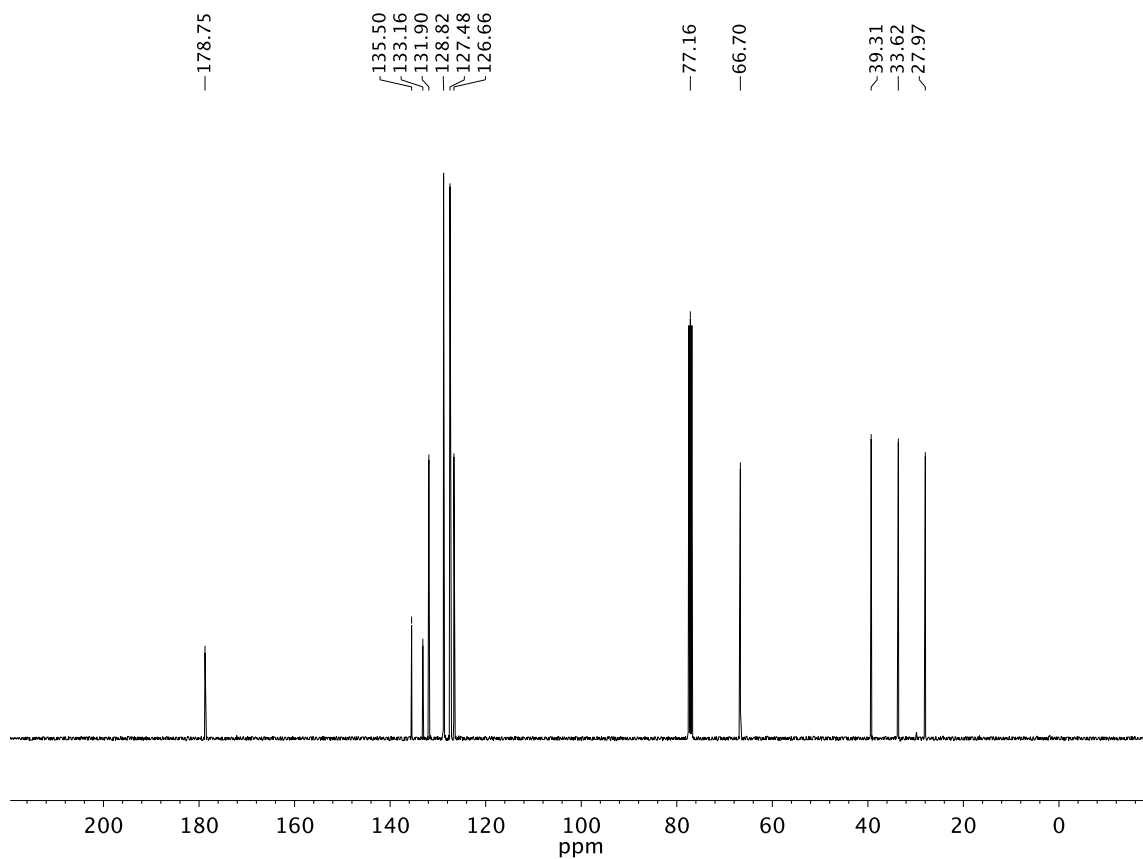


A7.56 ^{19}F NMR (282 MHz, CDCl_3) of compound **44i**

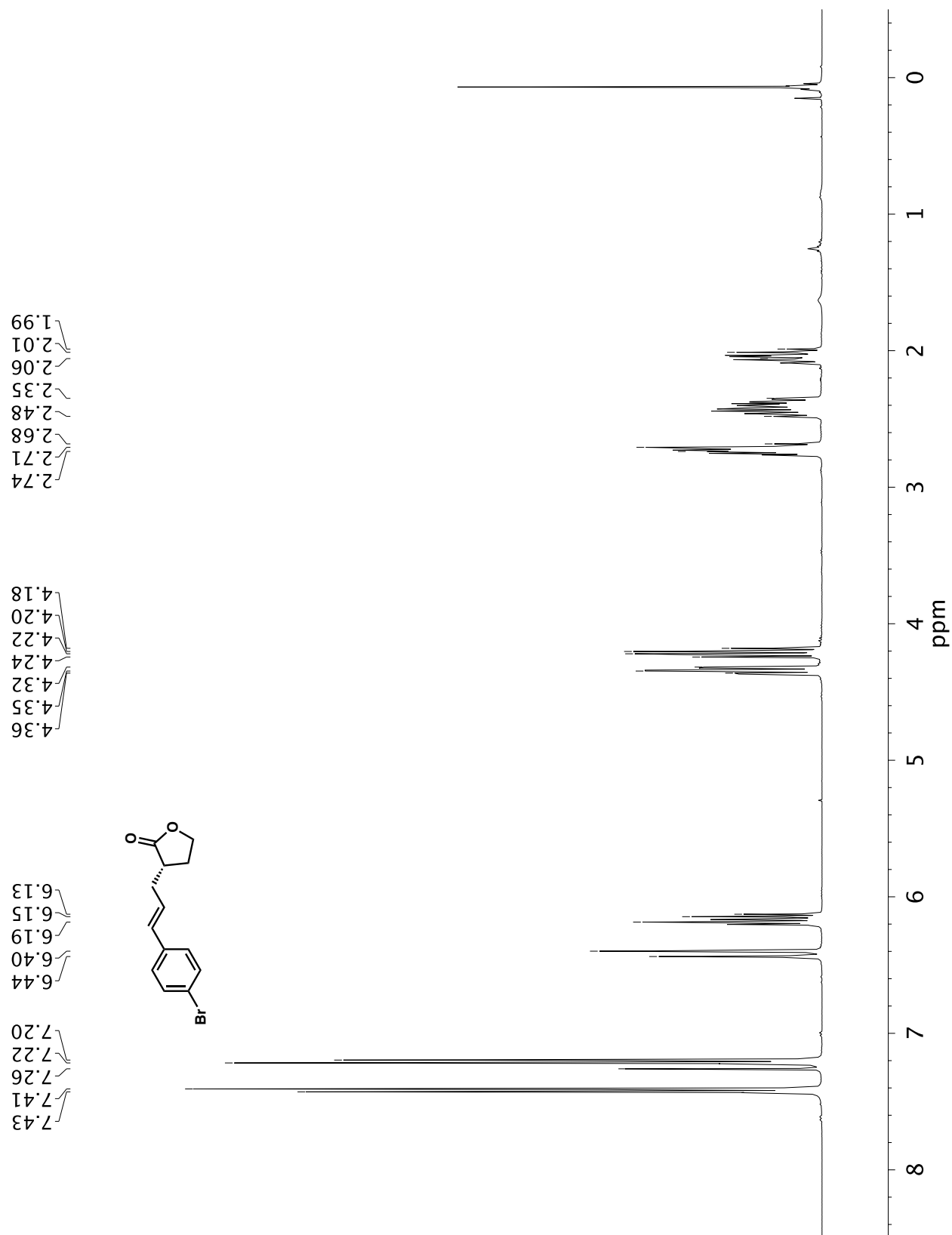
A7.57 ¹H NMR (400 MHz, CDCl₃) of compound **44j**

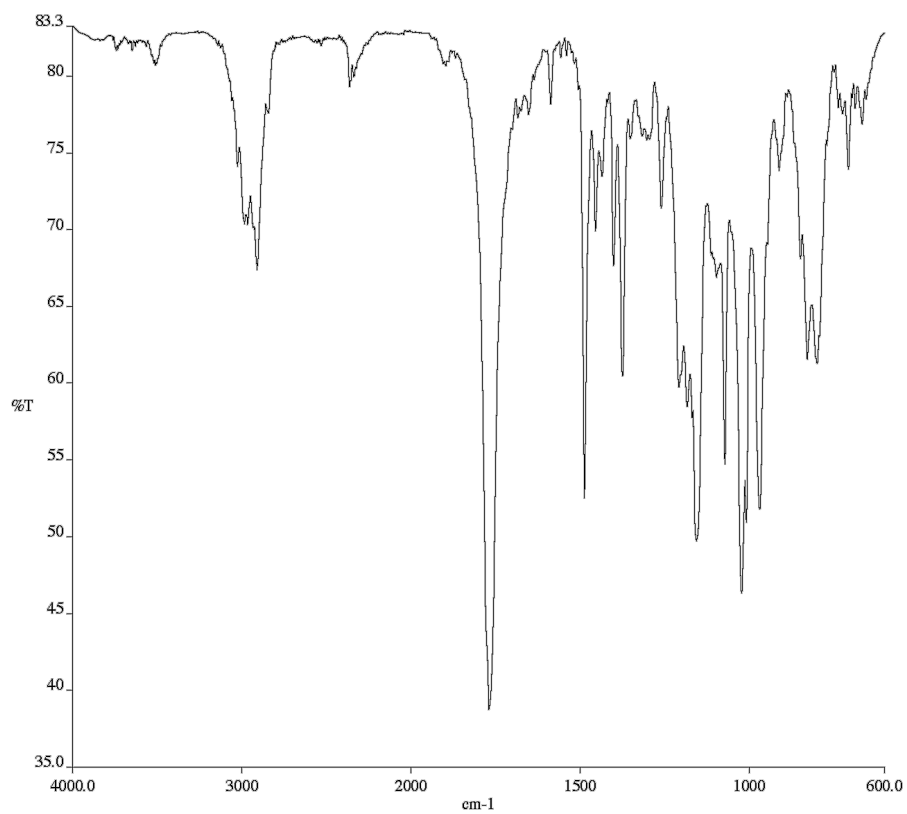


A7.58 Infrared spectrum (Thin Film, NaCl) of compound **44j**

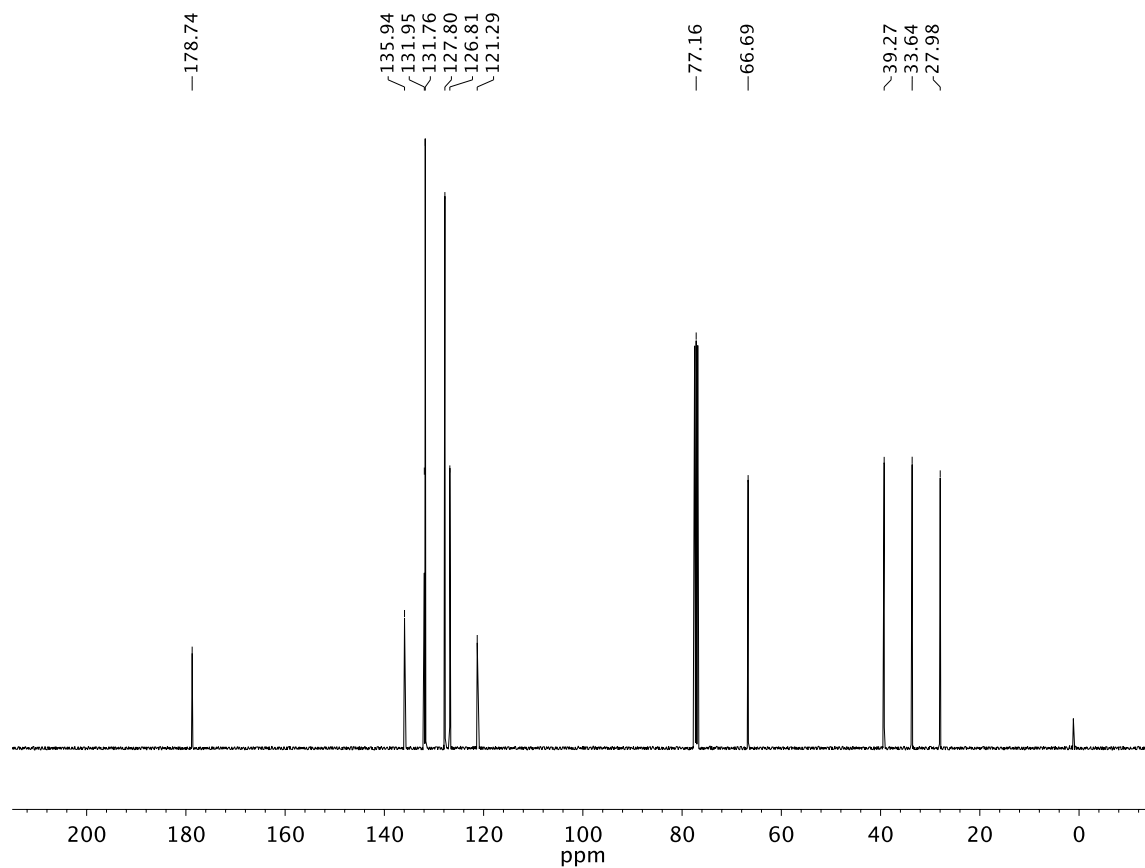


A7.59 ¹³C NMR (100 MHz, CDCl₃) of compound **44j**

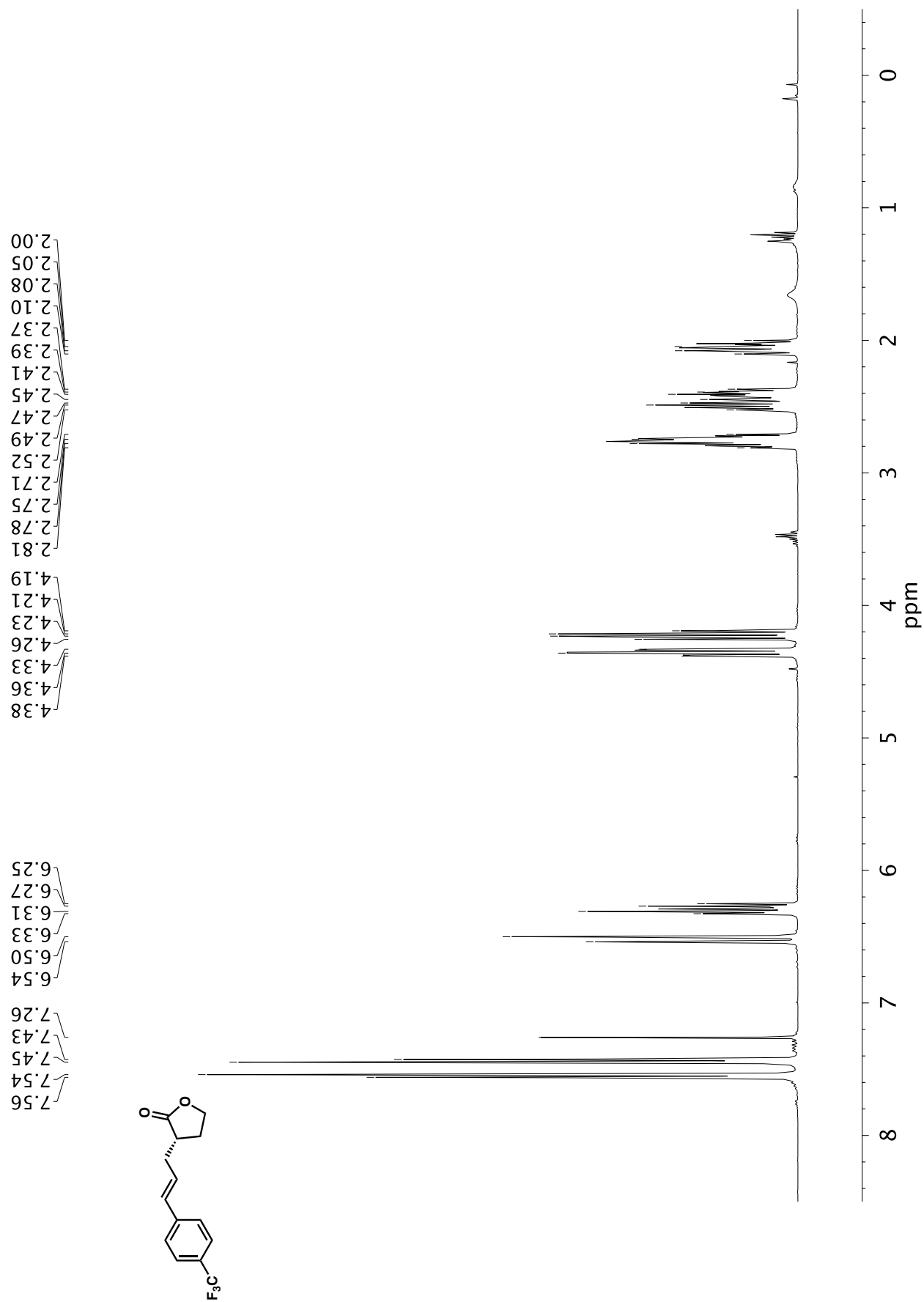
**A7.60** ¹H NMR (400 MHz, CDCl₃) of compound **44k**

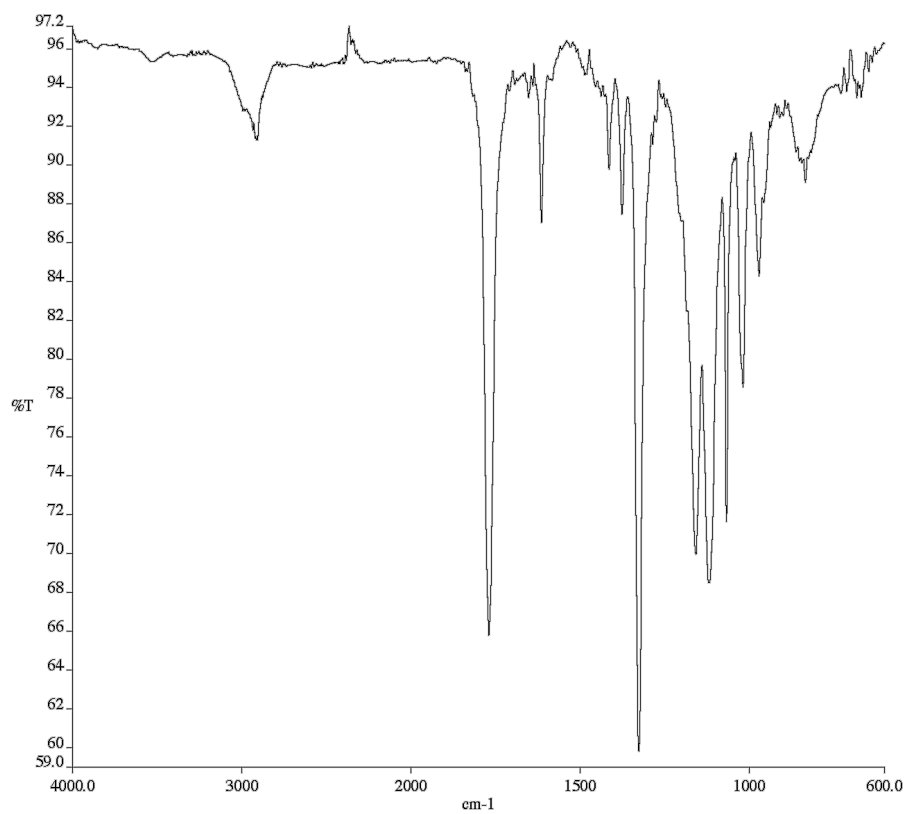
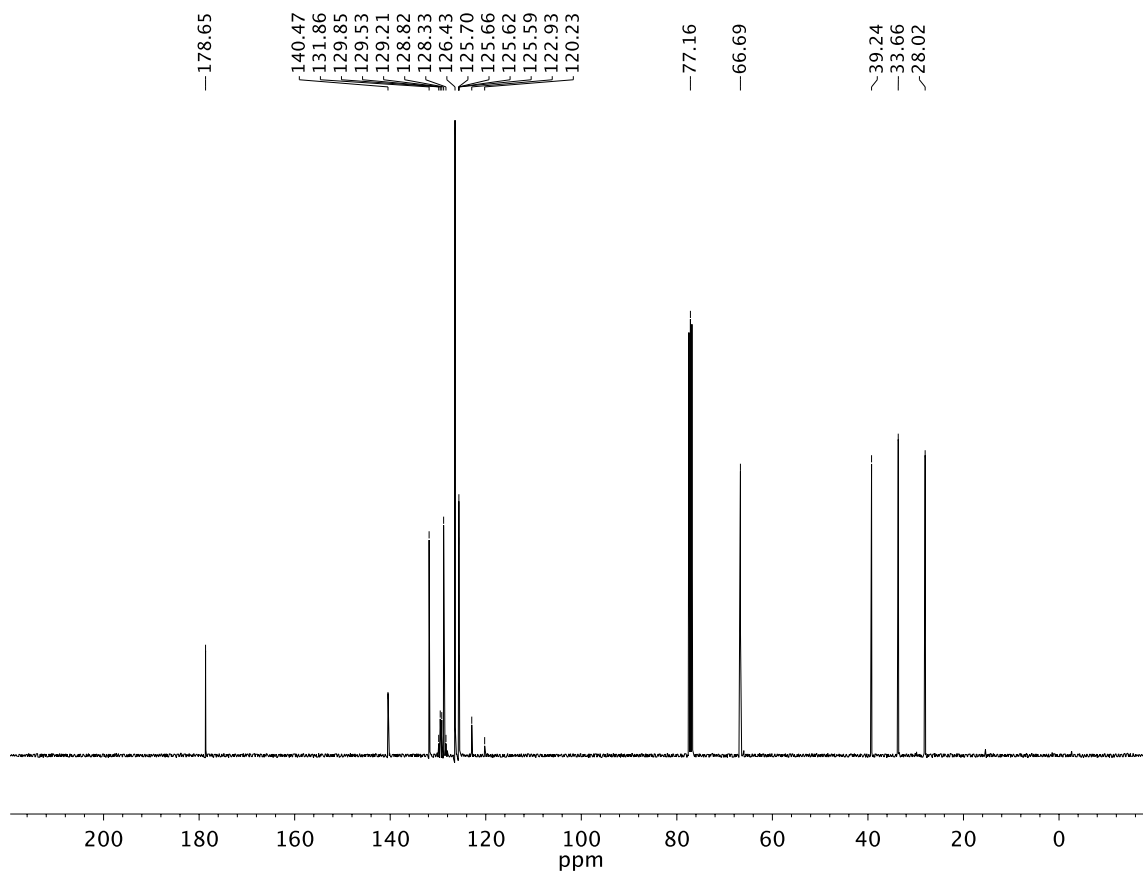


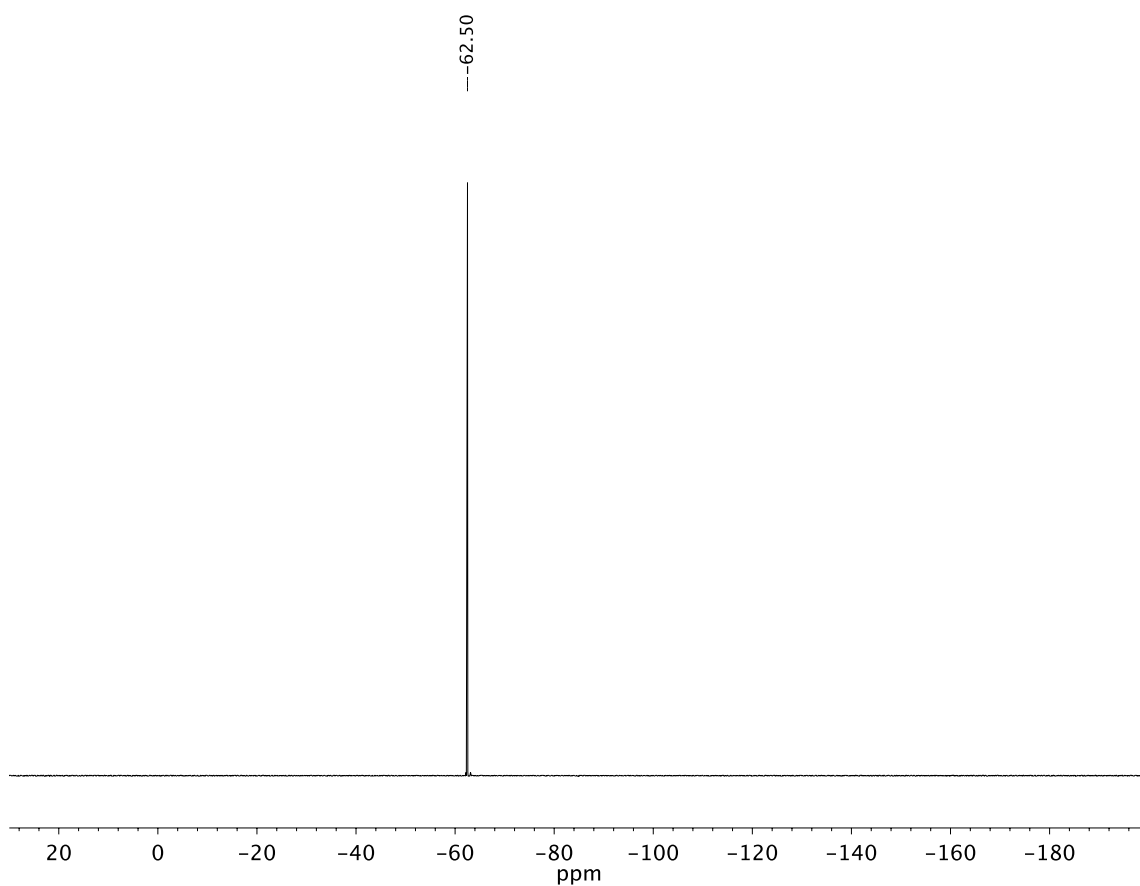
A7.61 Infrared spectrum (Thin Film, NaCl) of compound **44k**



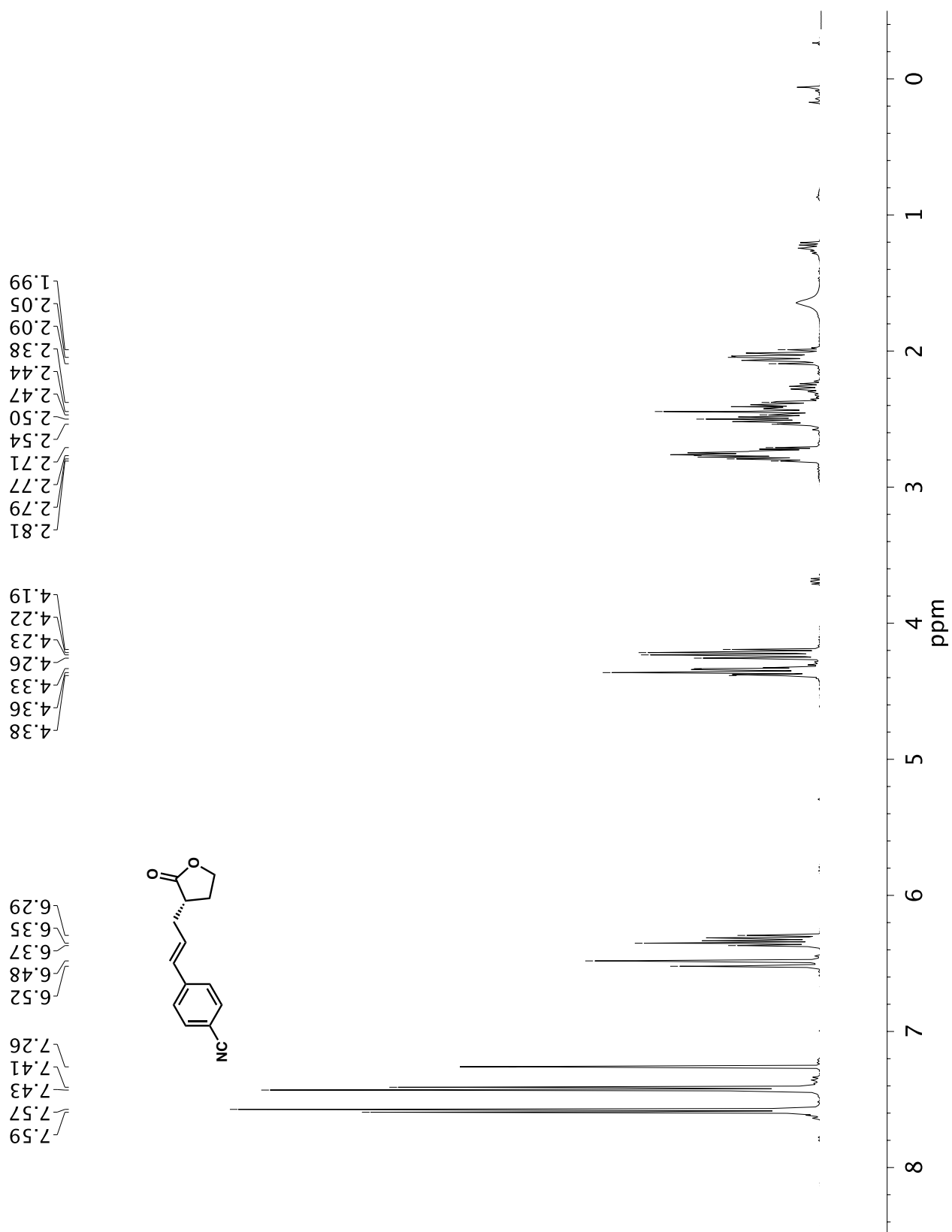
A7.62 ¹³C NMR (100 MHz, CDCl₃) of compound **44k**

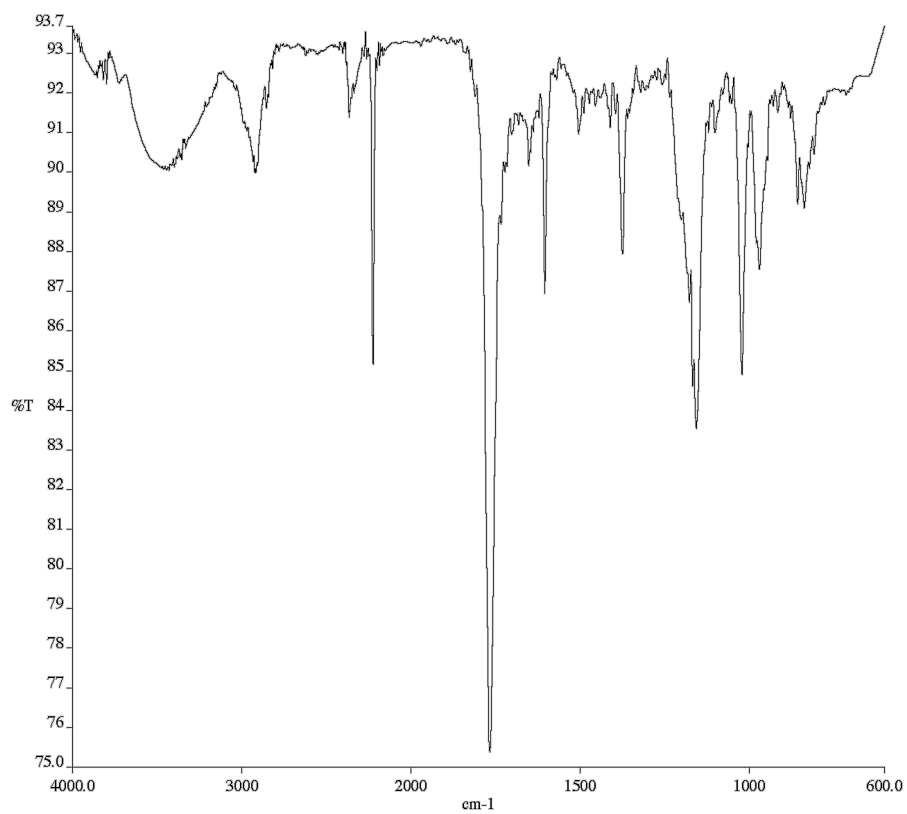
**A7.63** ¹H NMR (400 MHz, CDCl₃) of compound **44I**

**A7.64** Infrared spectrum (Thin Film, NaCl) of compound **44I****A7.65** ¹³C NMR (100 MHz, CDCl₃) of compound **44I**

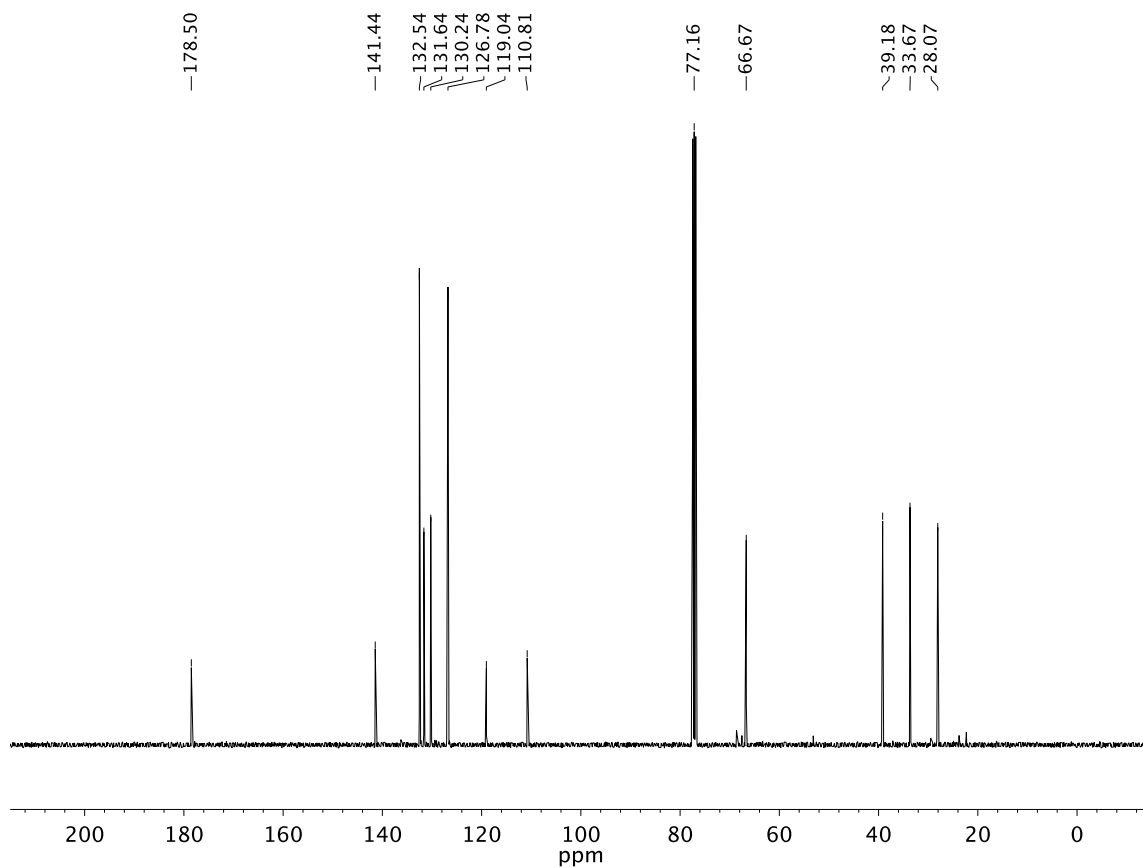


A7.66 ^{19}F NMR (282 MHz, CDCl_3) of compound **44I**

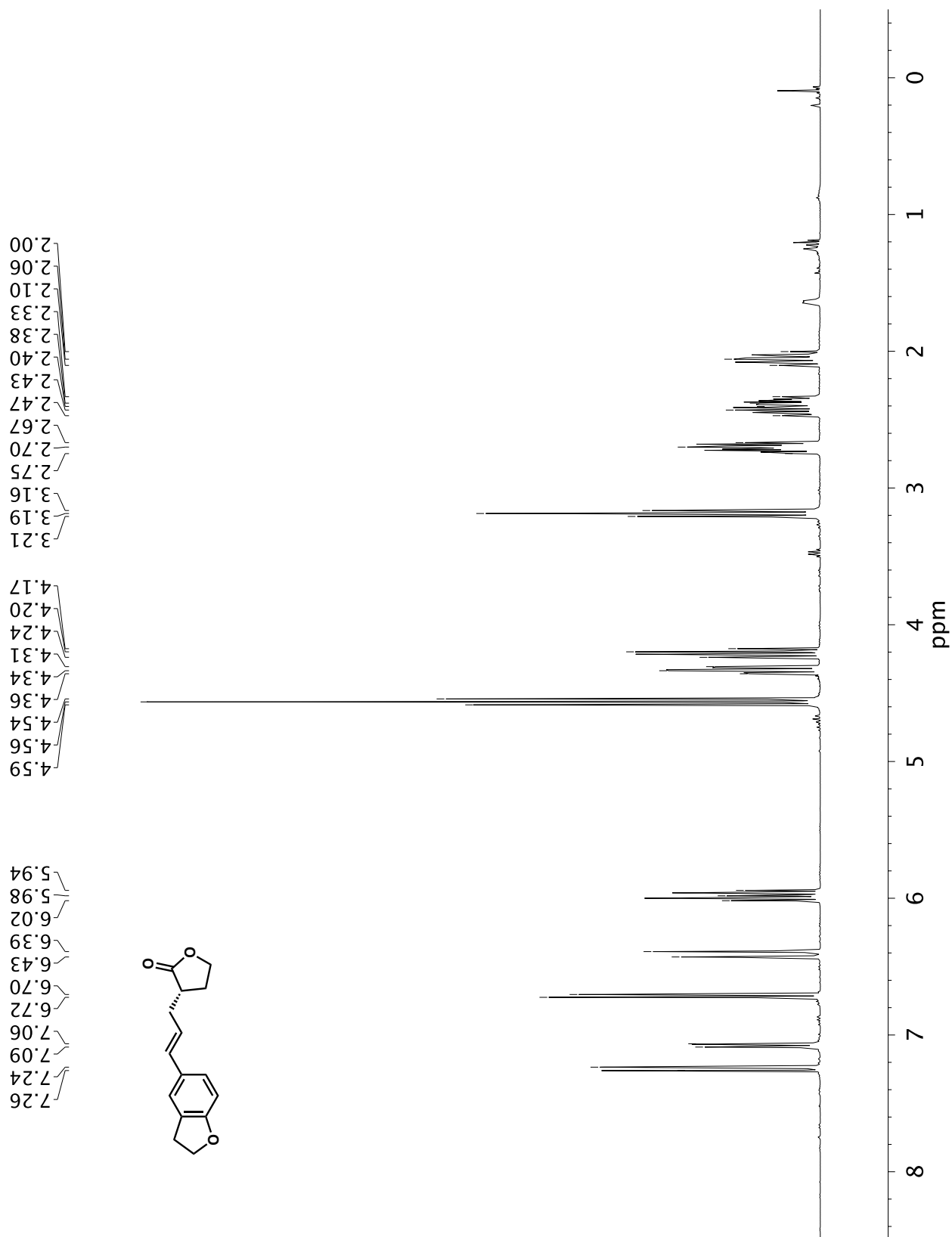
**A7.67** ^1H NMR (400 MHz, CDCl_3) of compound **44m**

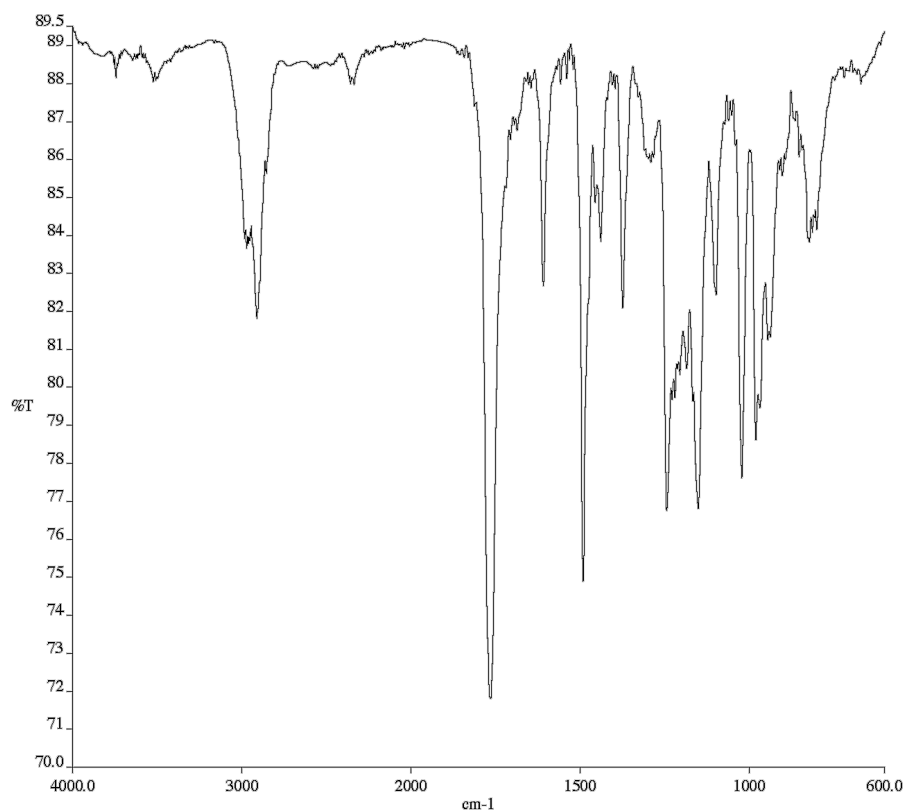


A7.68 Infrared spectrum (Thin Film, NaCl) of compound **44m**

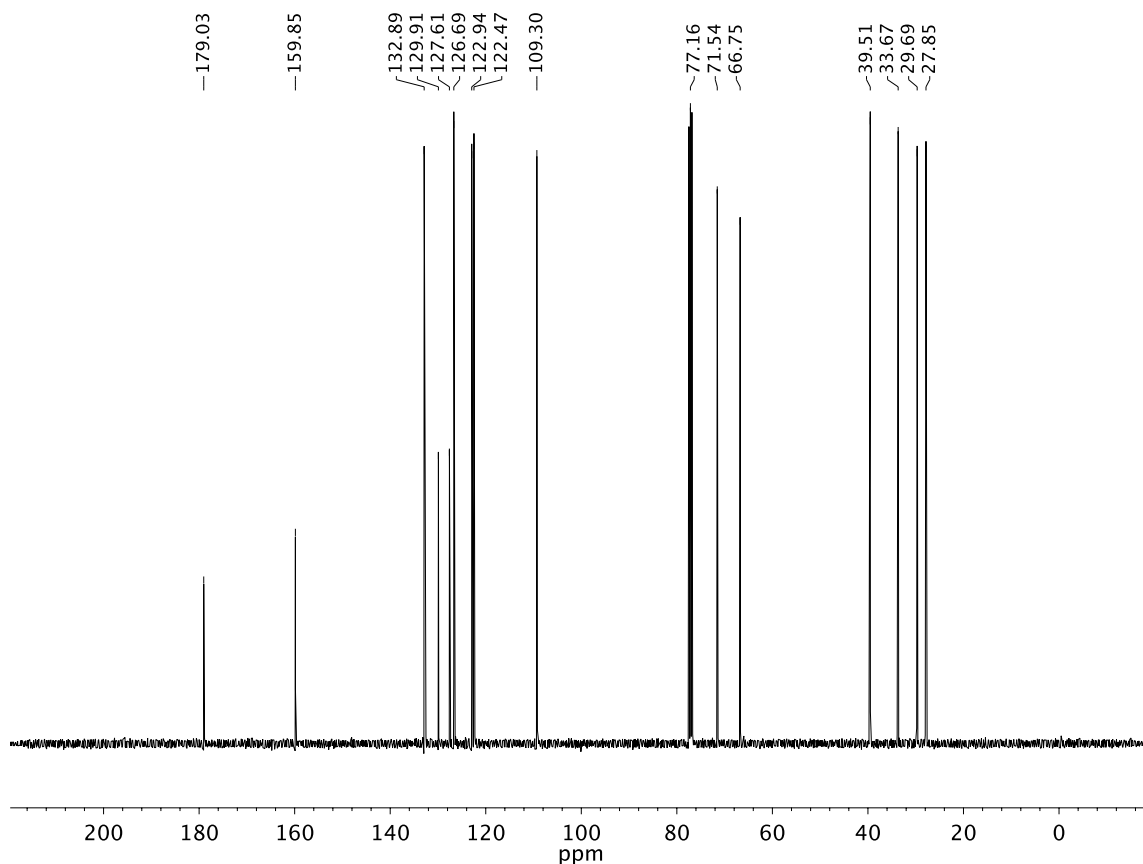


A7.69 ^{13}C NMR (100 MHz, CDCl_3) of compound **44m**

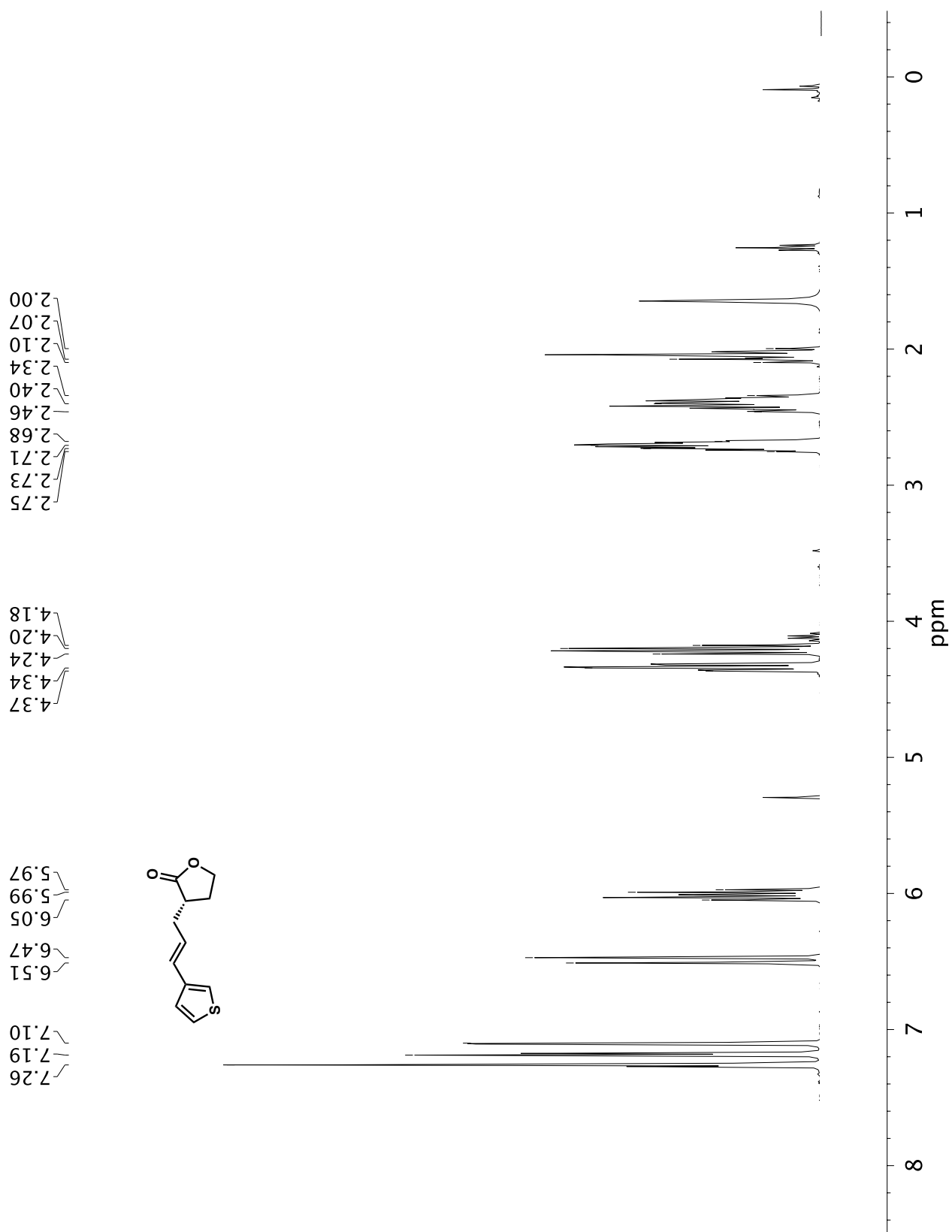
**A7.70** ¹H NMR (400 MHz, CDCl₃) of compound **44n**

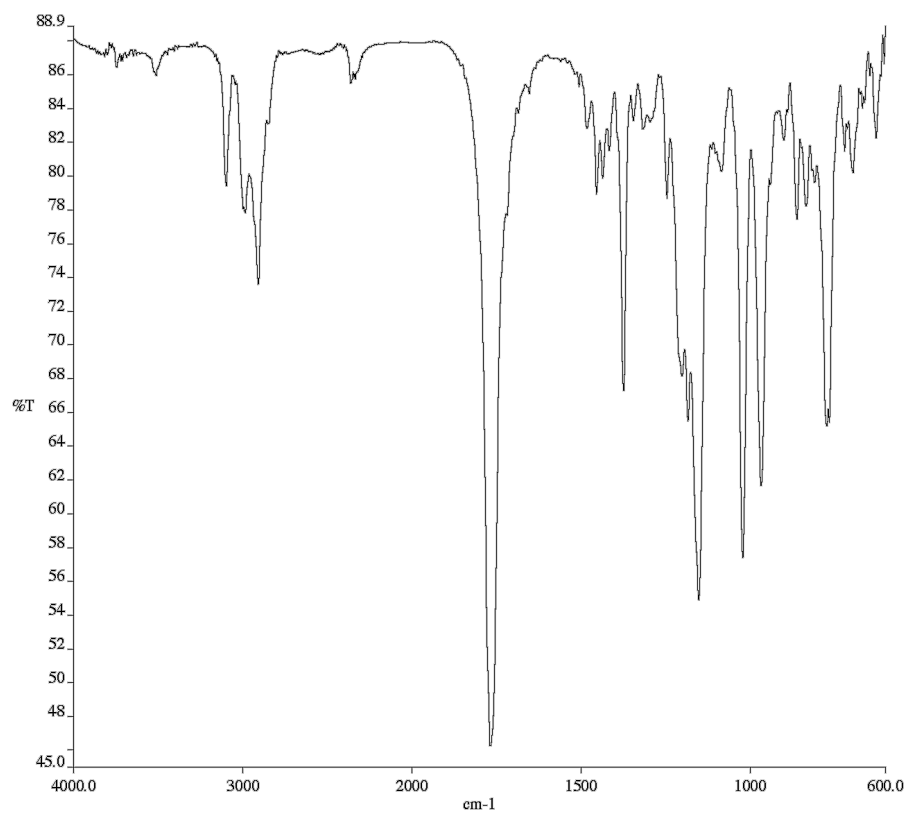


A7.71 Infrared spectrum (Thin Film, NaCl) of compound **44n**

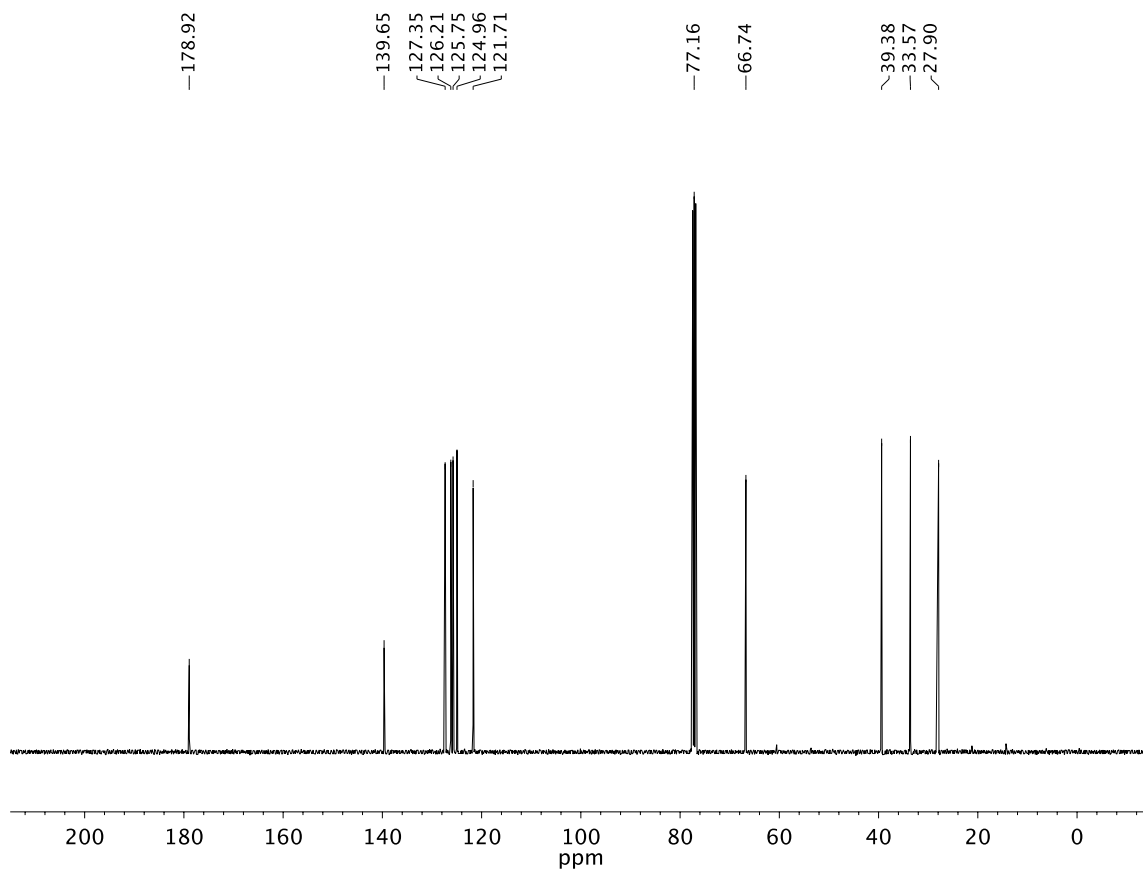


A7.72 ^{13}C NMR (100 MHz, CDCl_3) of compound **44n**

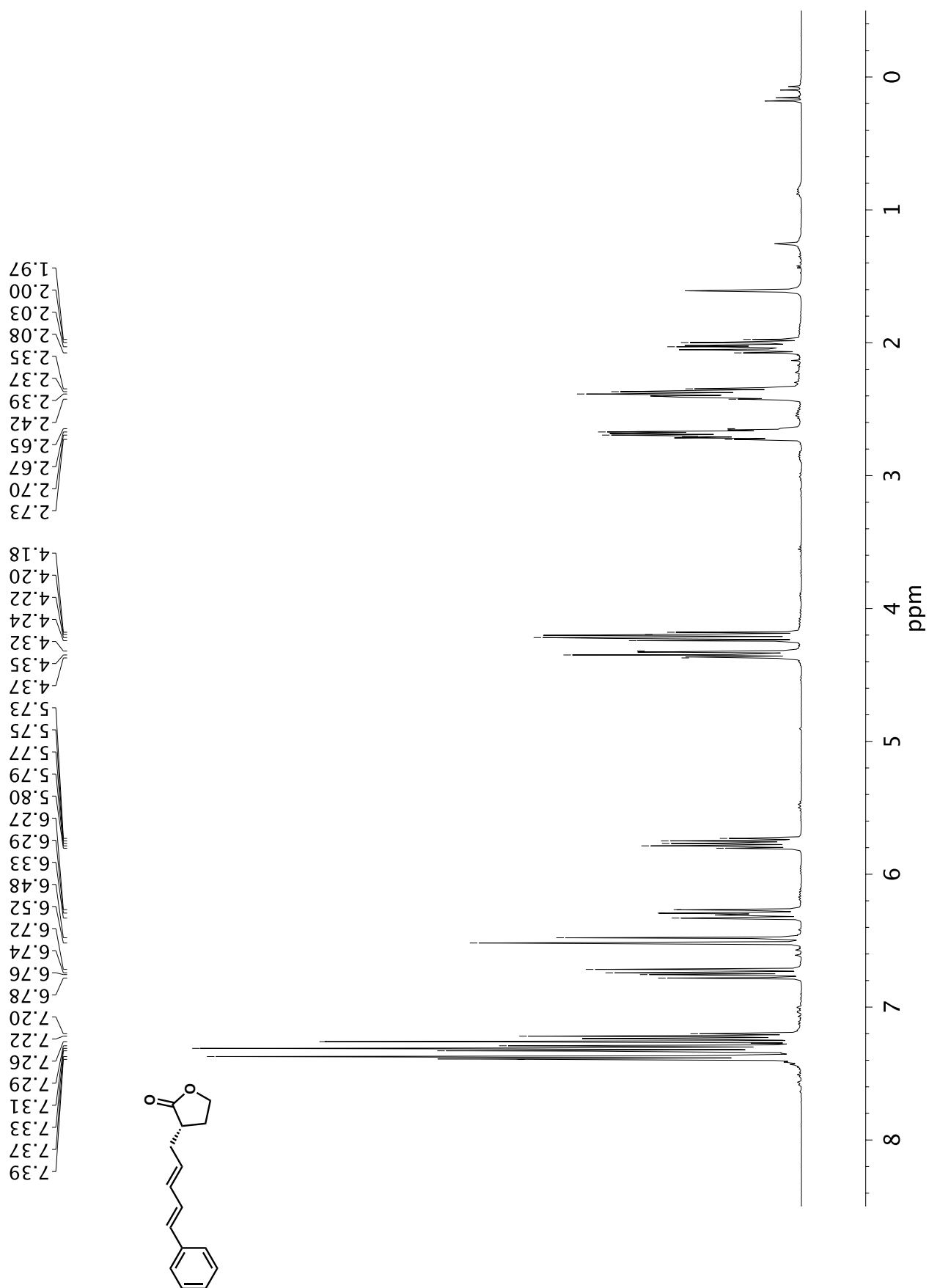




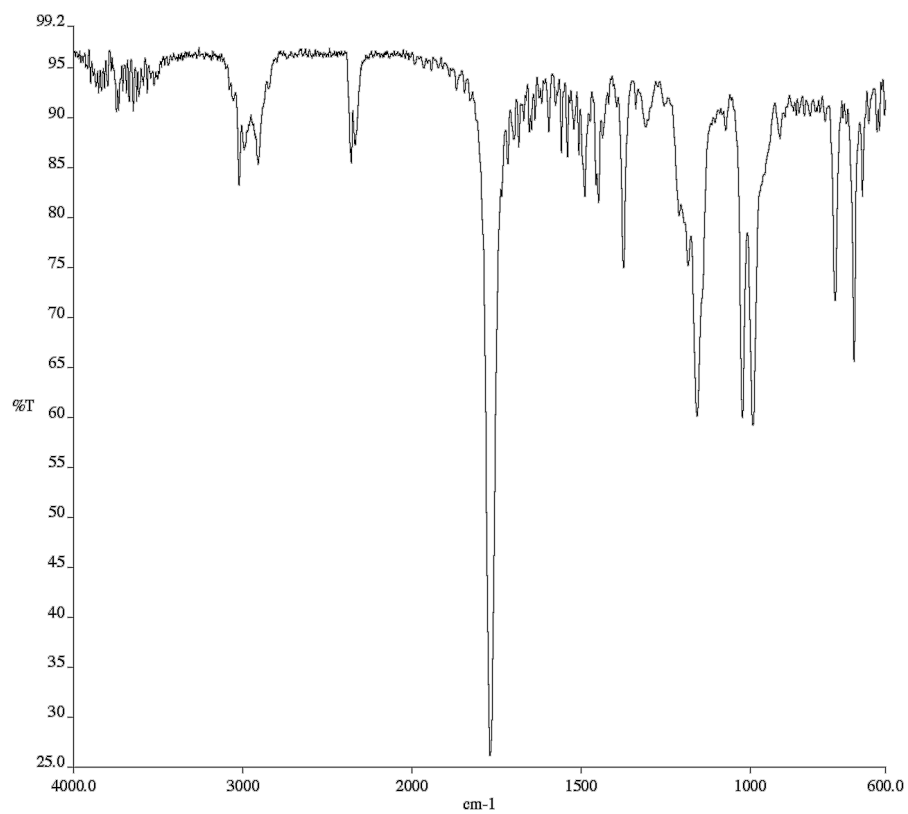
A7.74 Infrared spectrum (Thin Film, NaCl) of compound **44o**



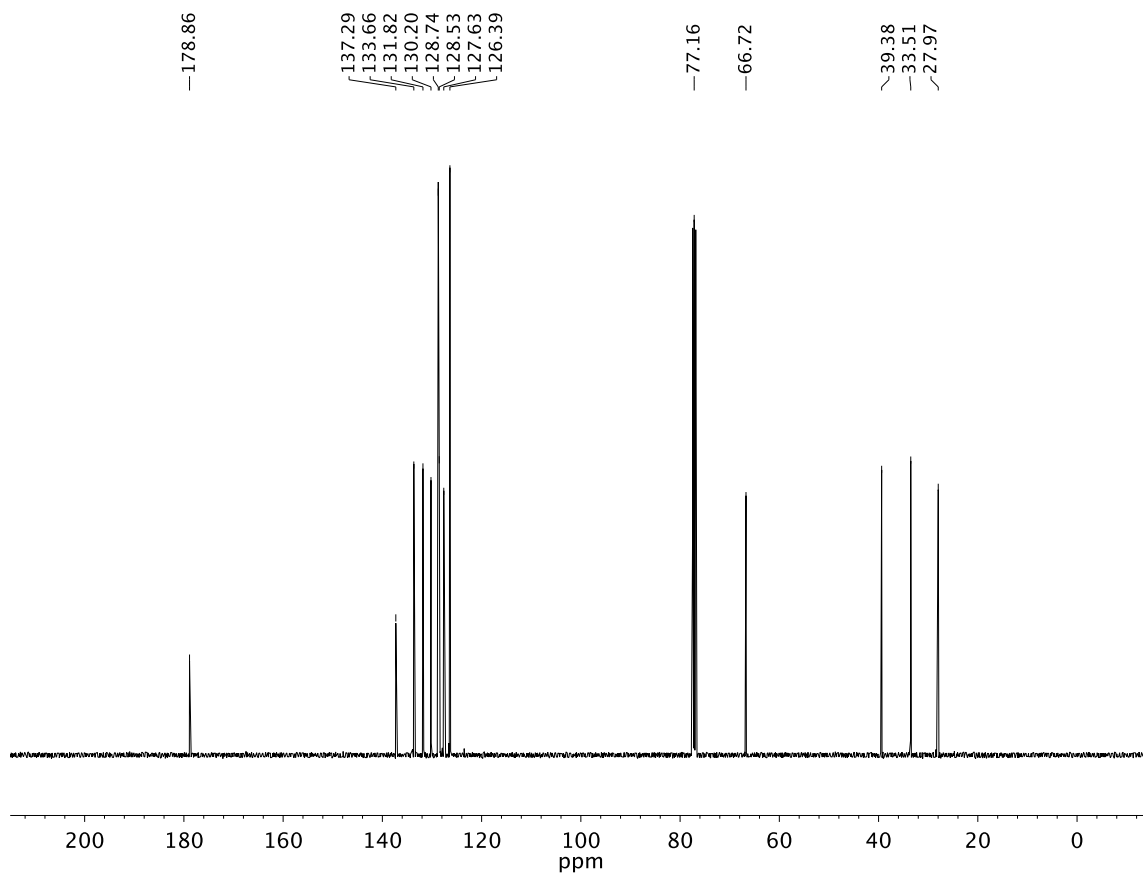
A7.75 ¹³C NMR (100 MHz, CDCl₃) of compound **44o**



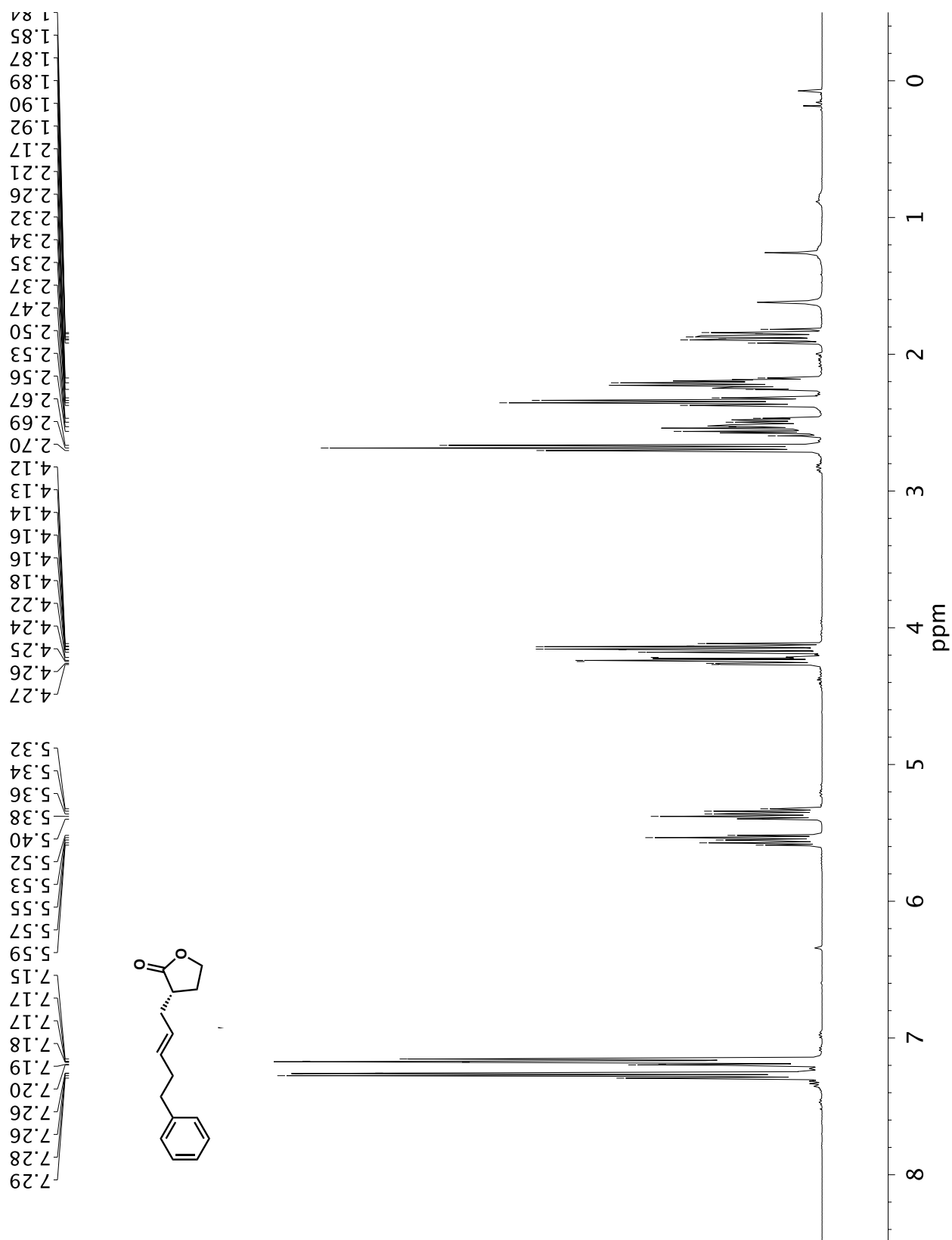
A7.76 ^1H NMR (400 MHz, CDCl_3) of compound **44p**

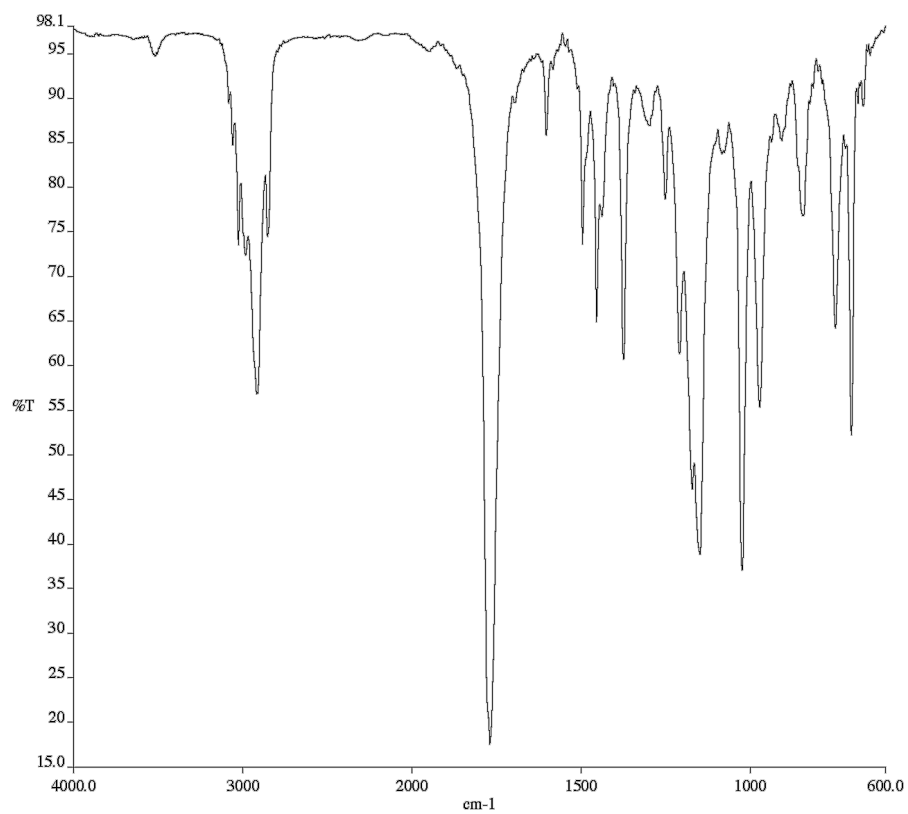


A7.77 Infrared spectrum (Thin Film, NaCl) of compound **44p**

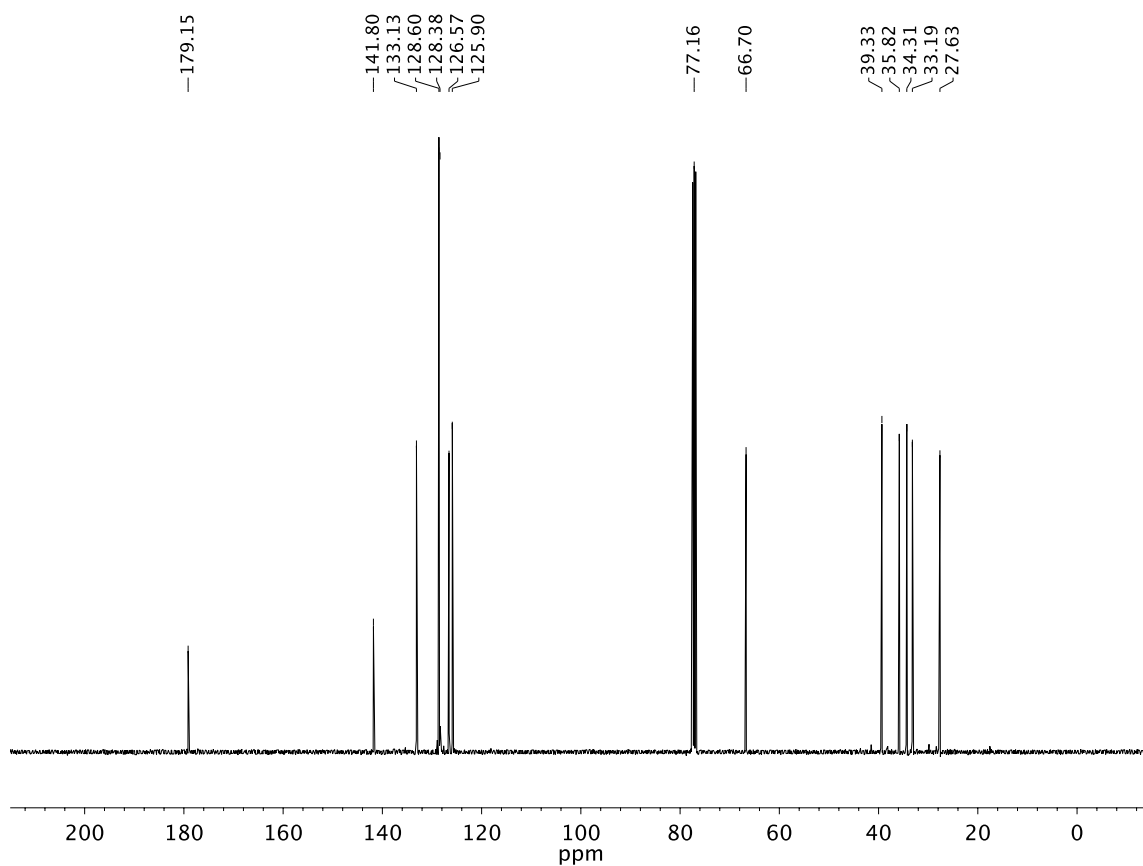


A7.78 ^{13}C NMR (100 MHz, CDCl_3) of compound **44p**

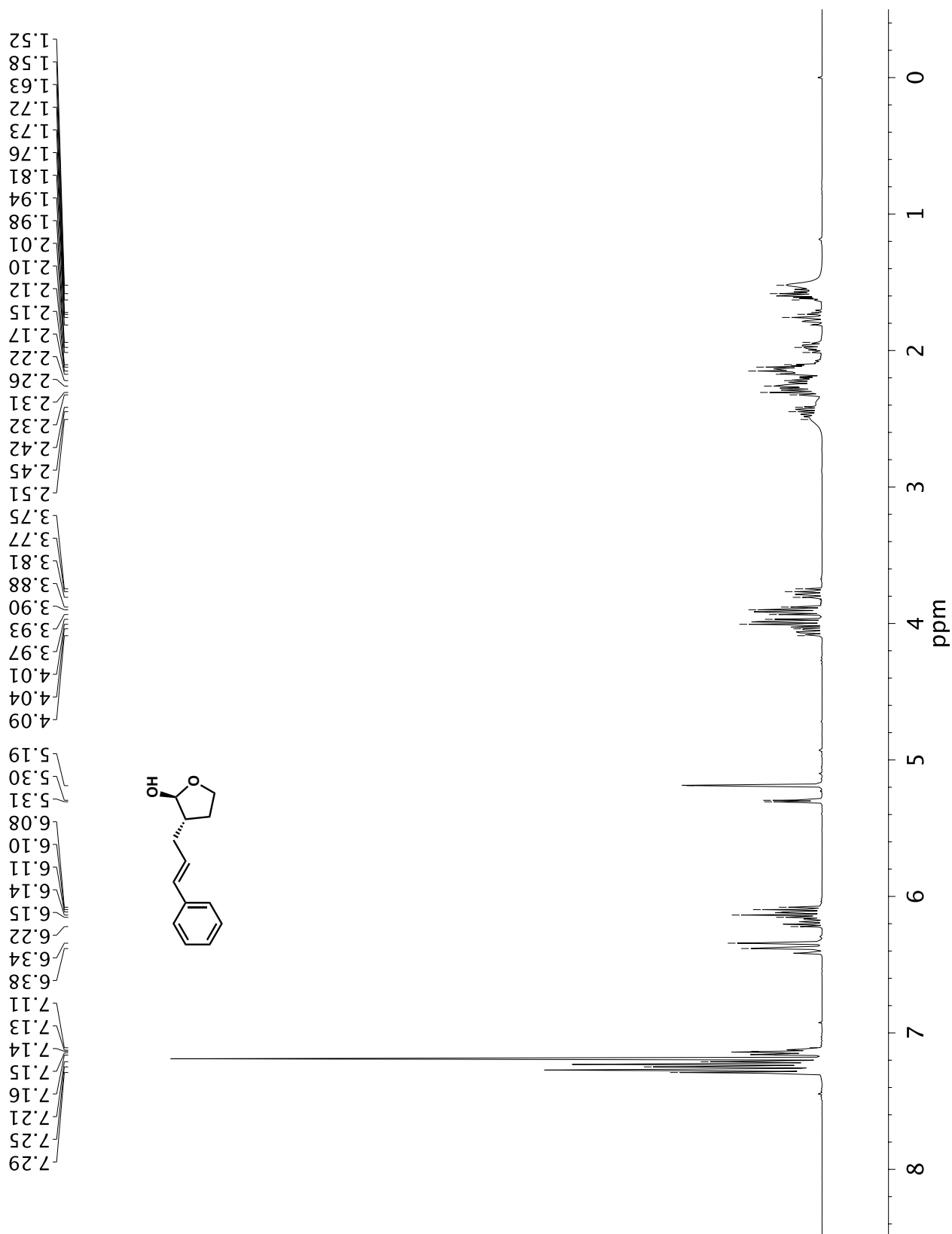
A7.79 ¹H NMR (400 MHz, CDCl₃) of compound **42a**



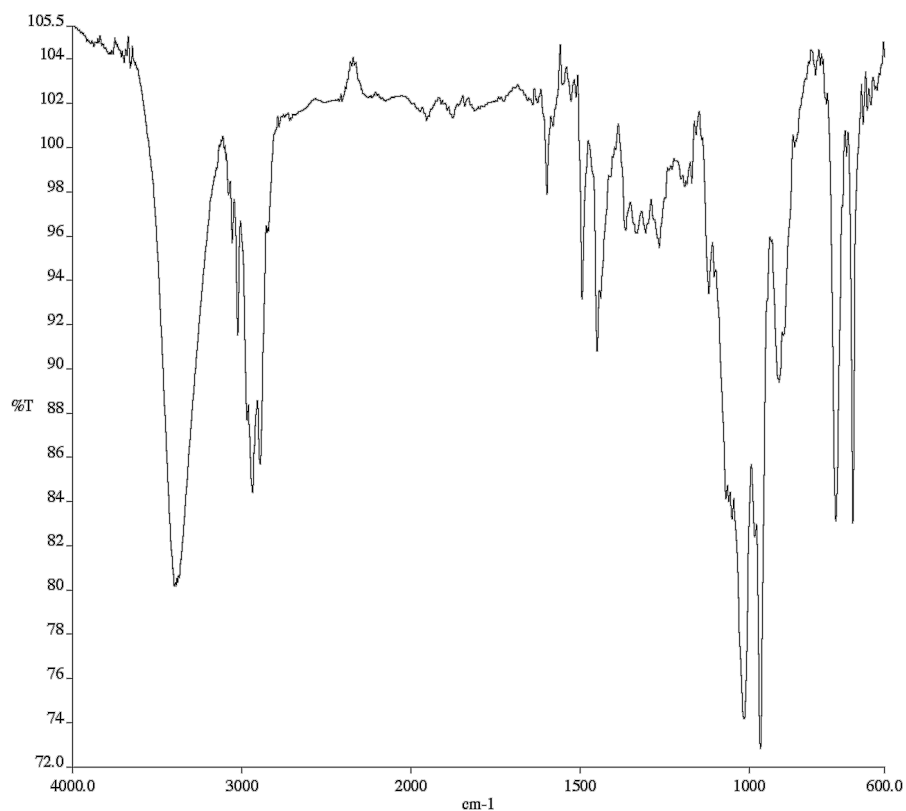
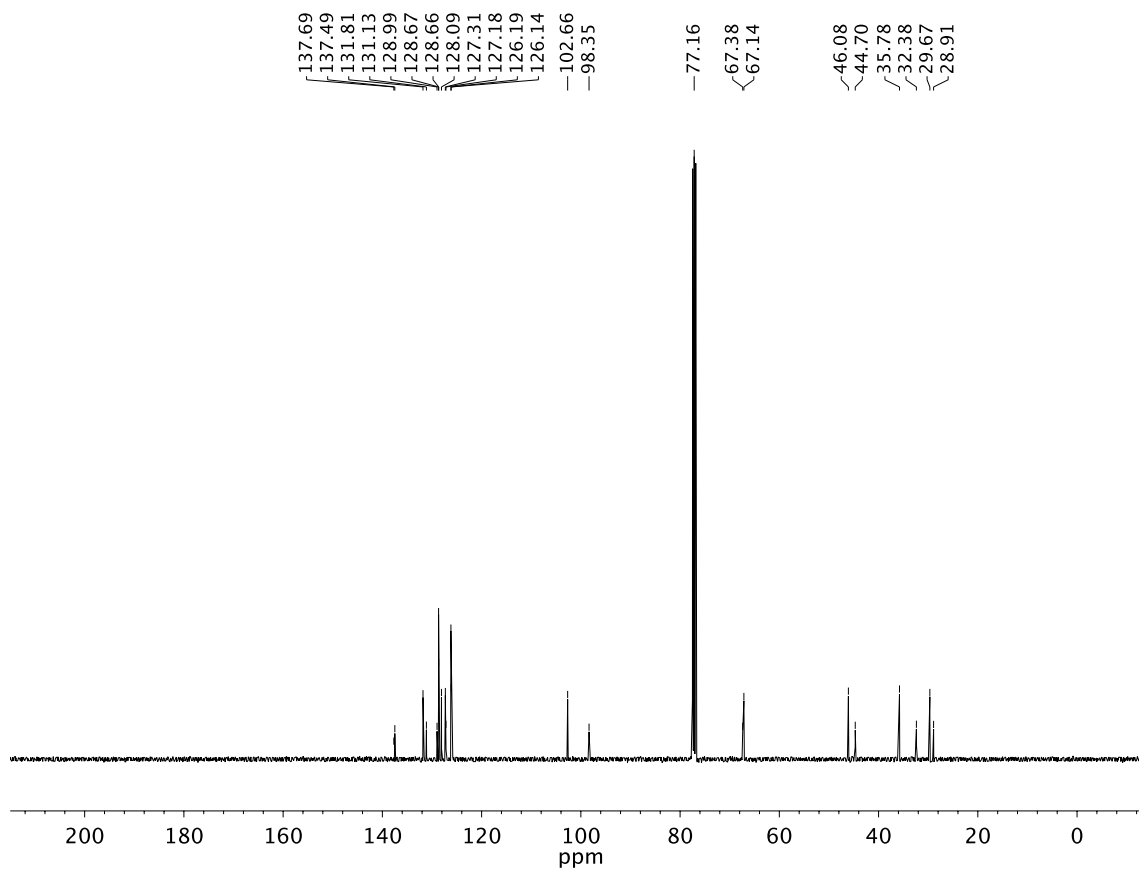
A7.80 Infrared spectrum (Thin Film, NaCl) of compound **42a**

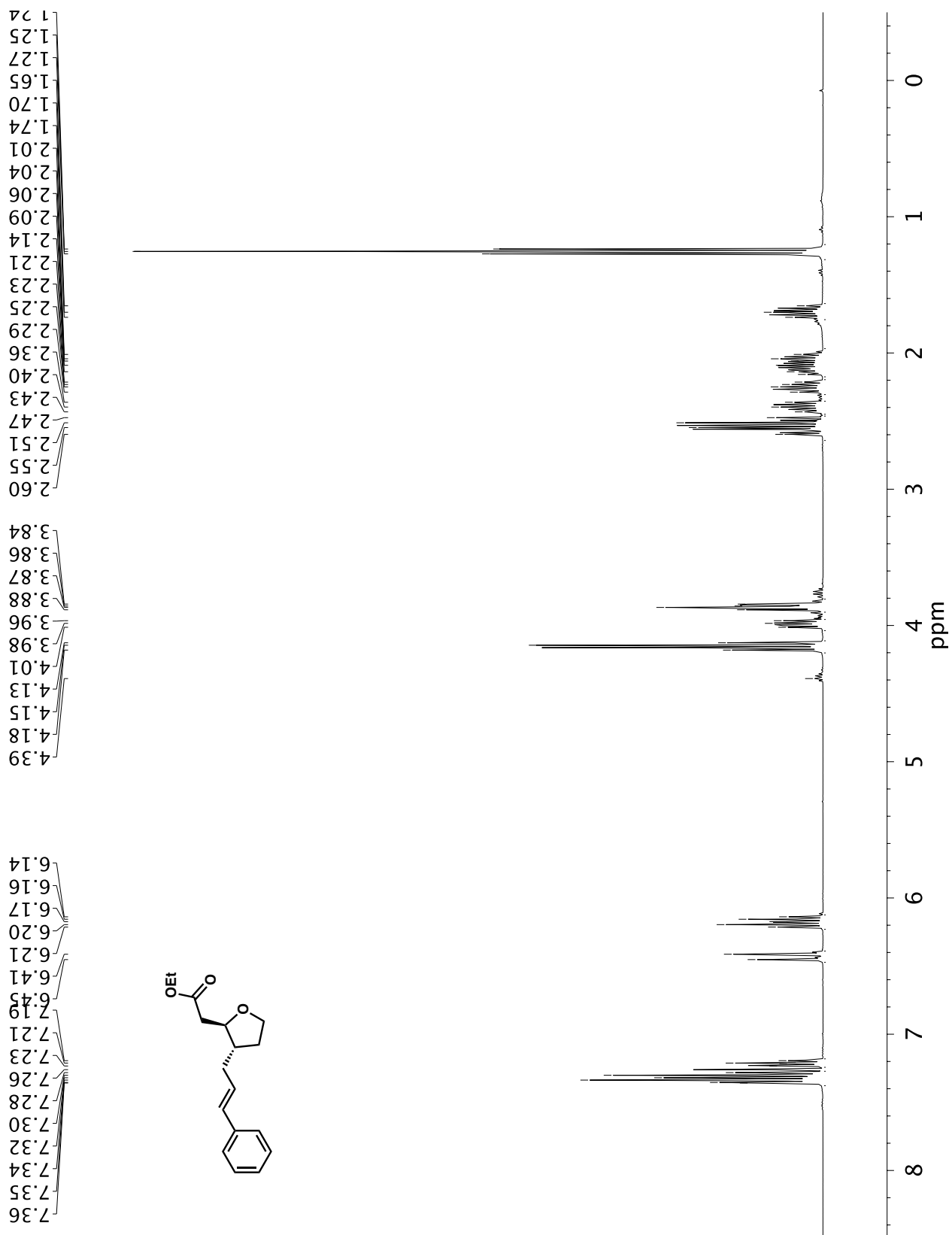


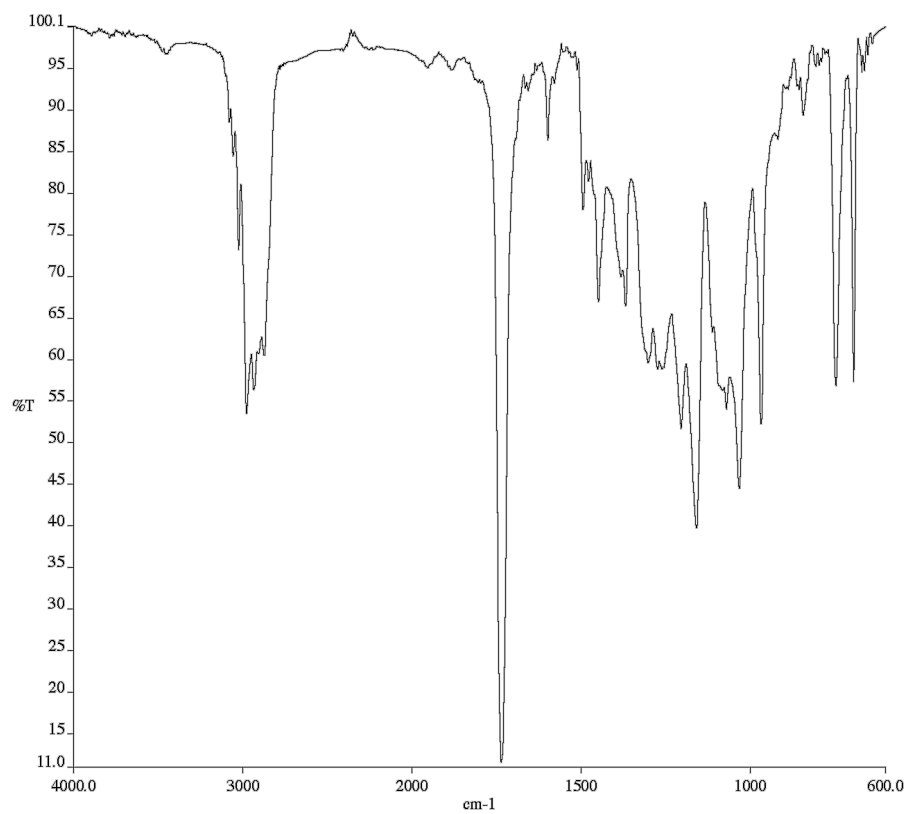
A7.81 ¹³C NMR (100 MHz, CDCl₃) of compound **42a**



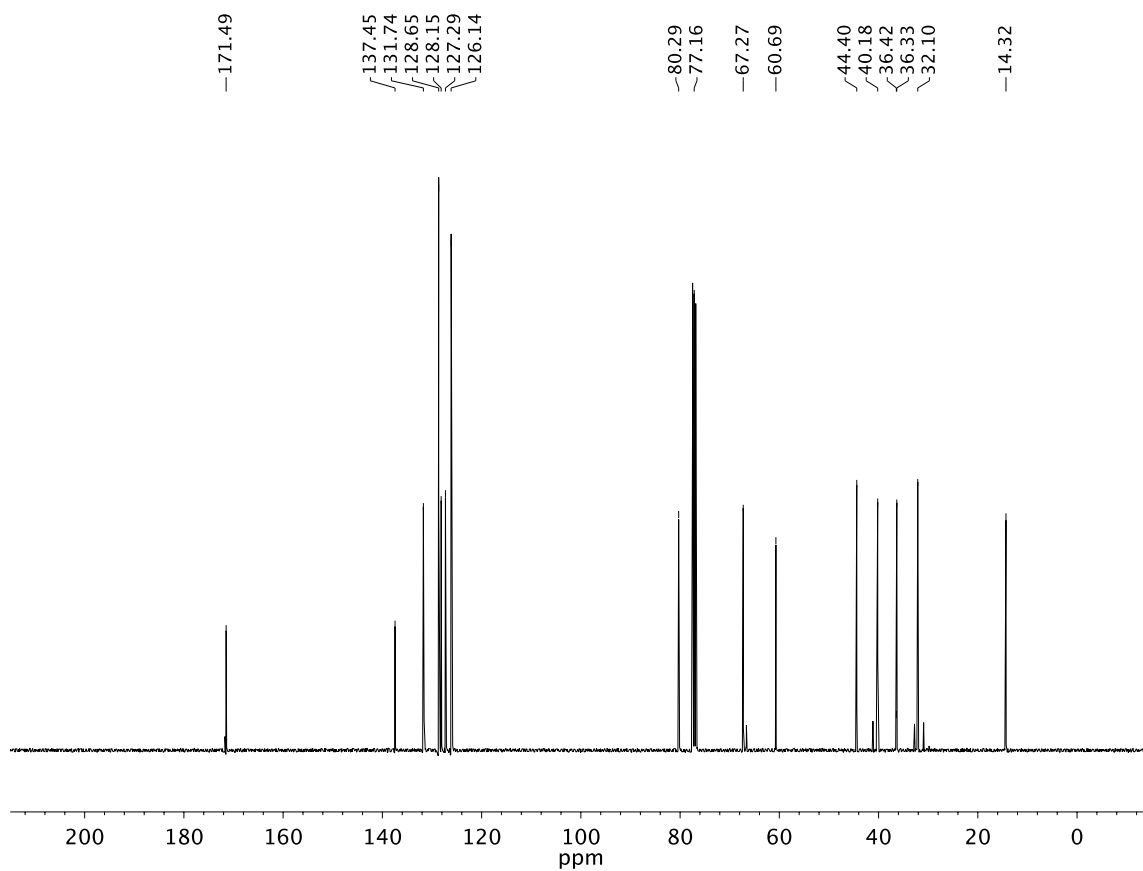
A7.82 ^1H NMR (400 MHz, CDCl_3) of compound **45**

**A7.83** Infrared spectrum (Thin Film, NaCl) of compound 45**A7.84** ¹³C NMR (100 MHz, CDCl₃) of compound 45

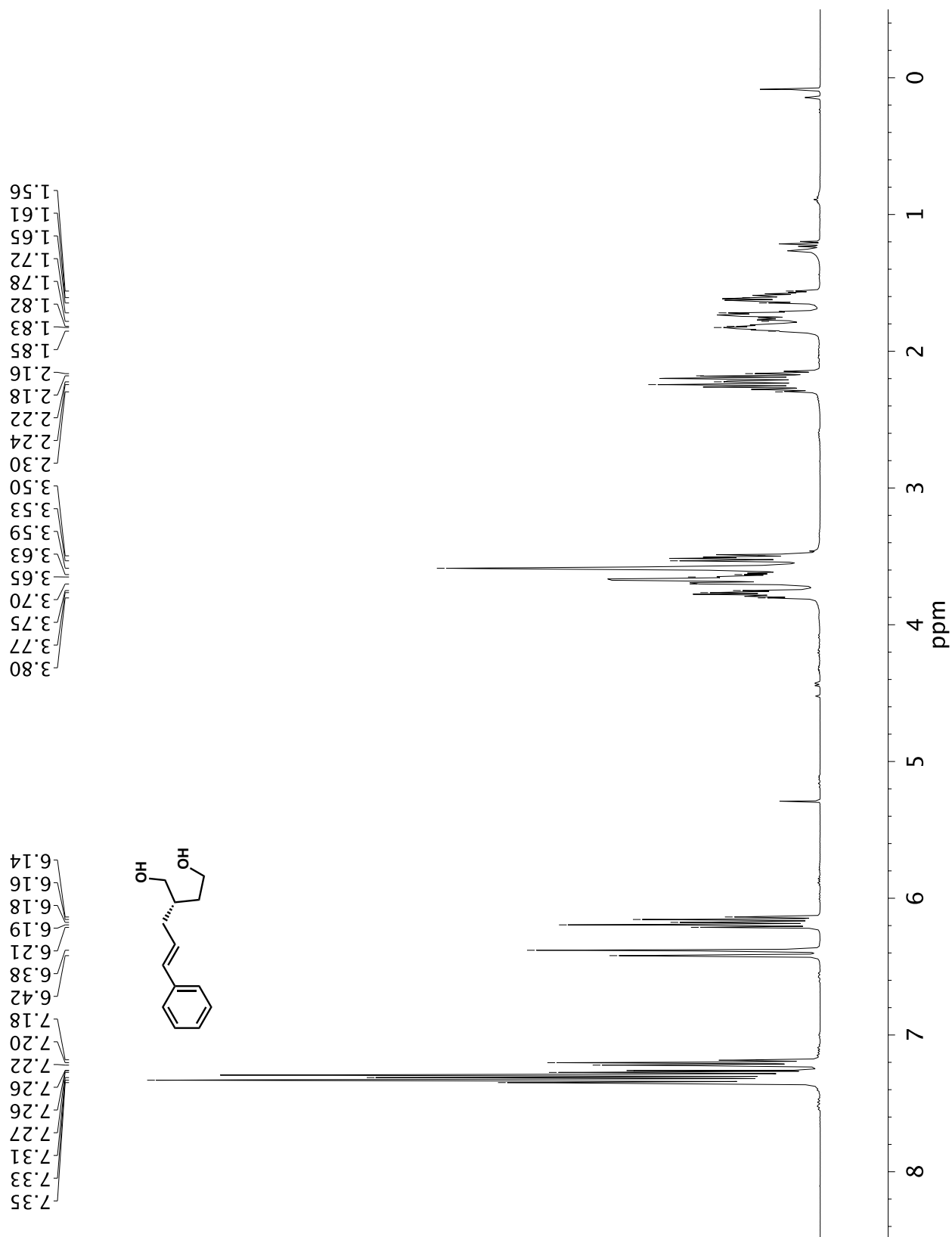


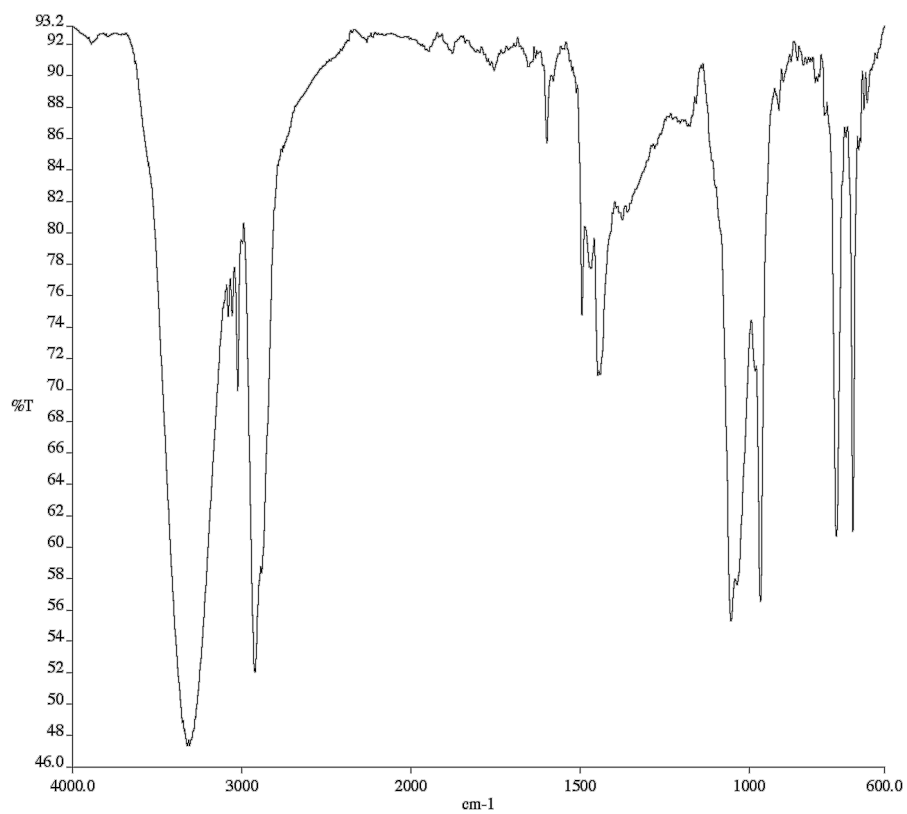
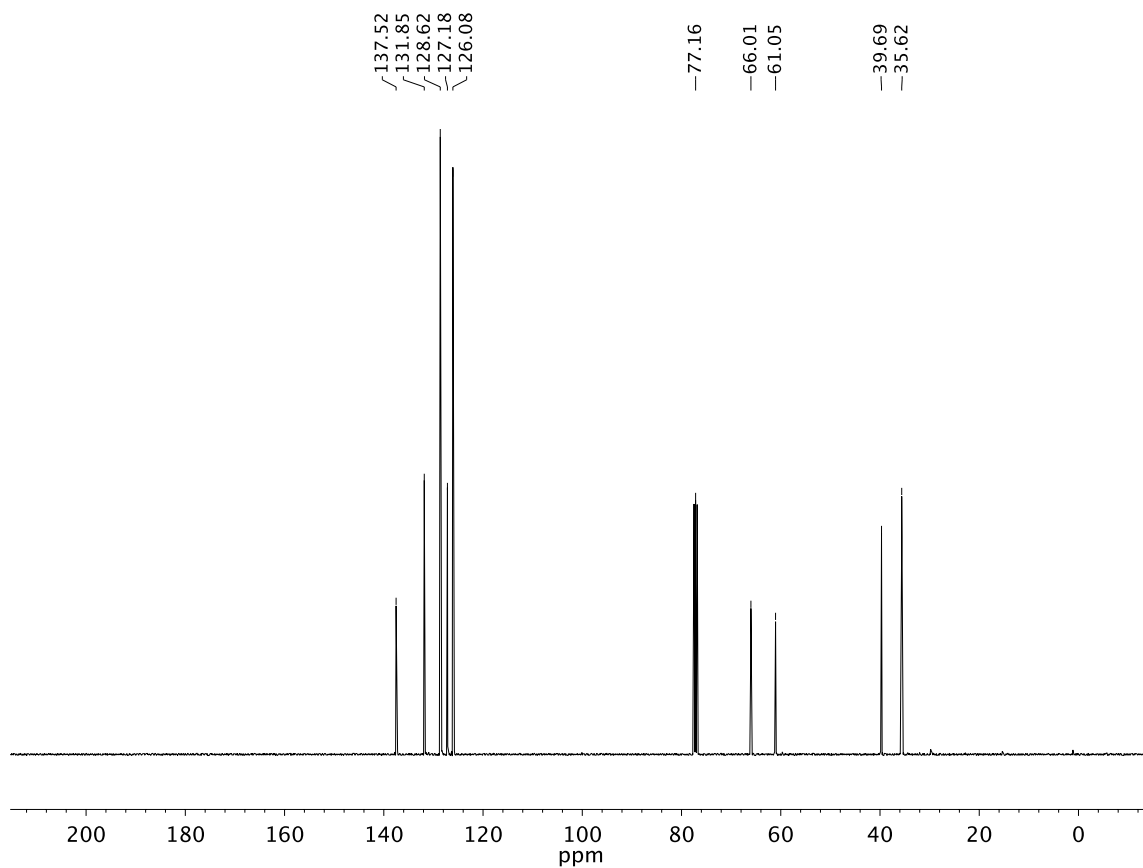


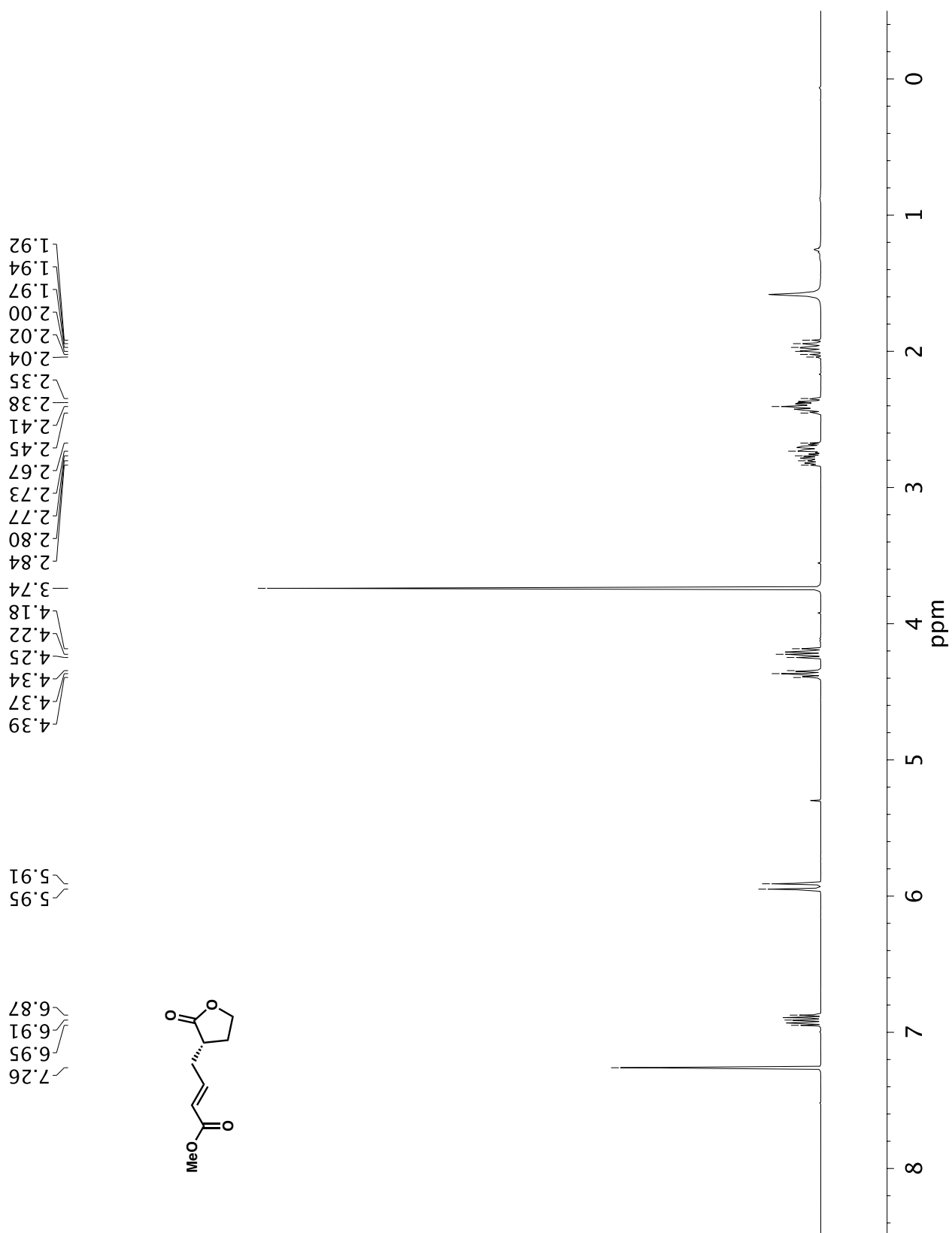
A7.86 Infrared spectrum (Thin Film, NaCl) of compound **46**

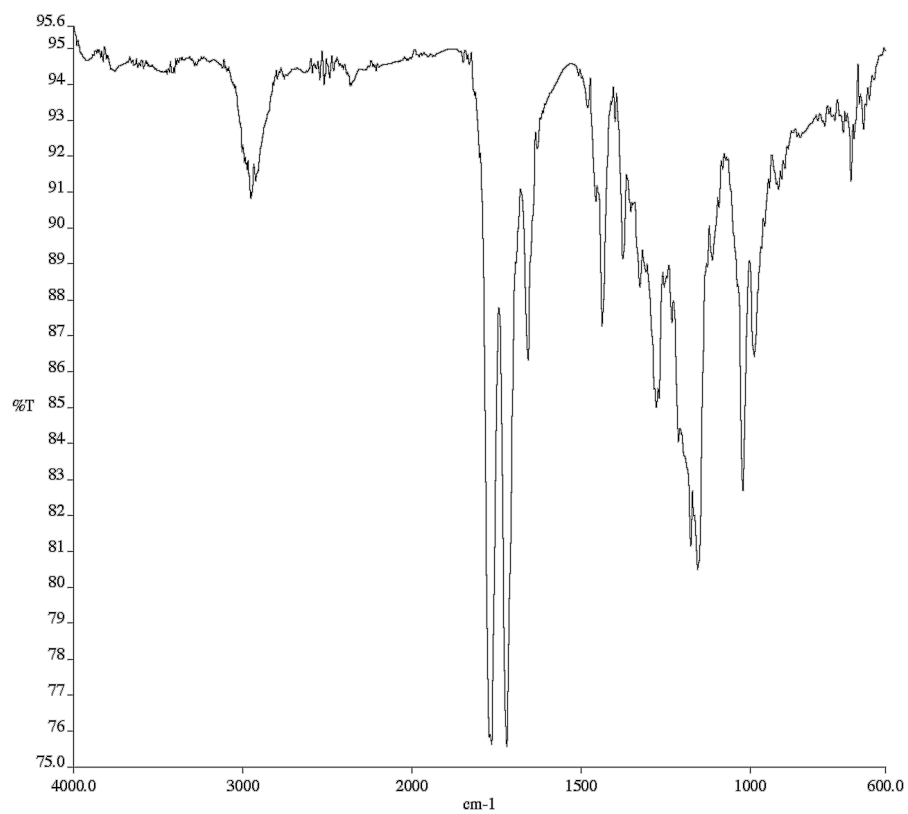


A7.87 ^{13}C NMR (100 MHz, CDCl_3) of compound **46**

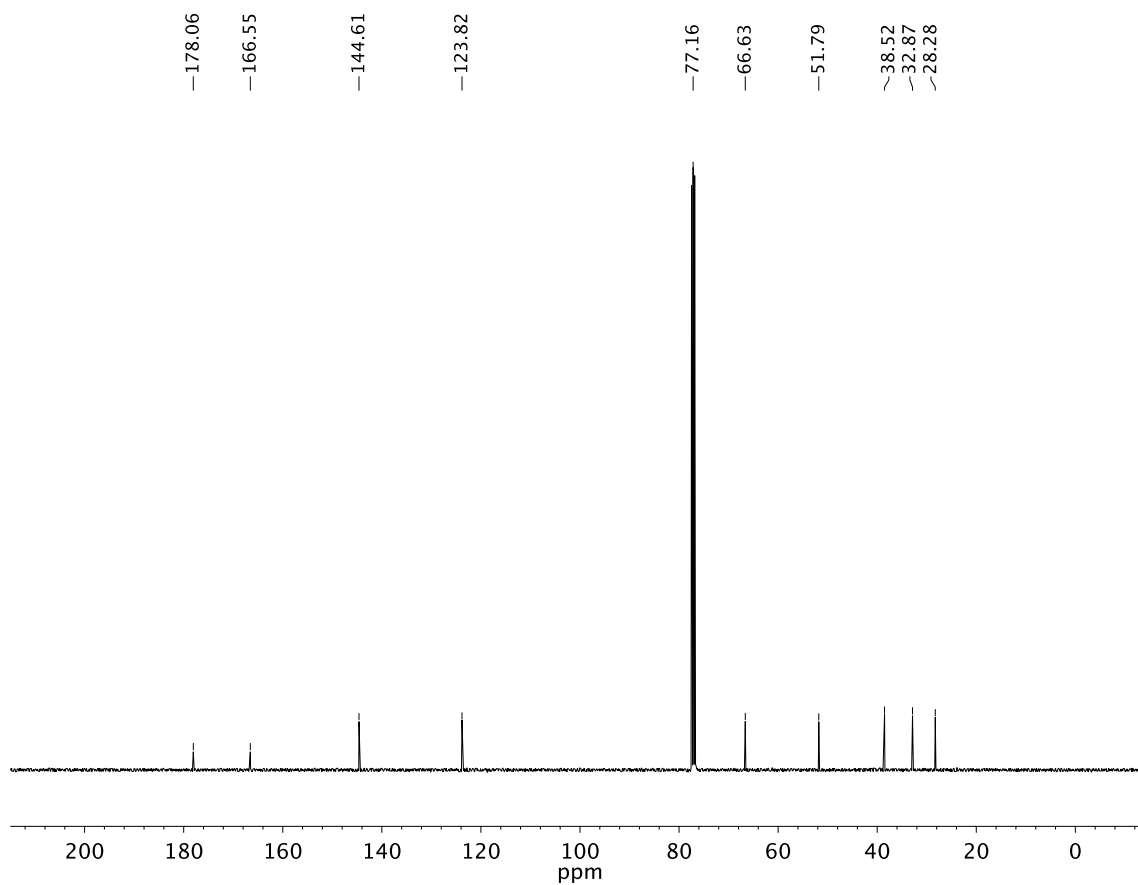
A7.88 ¹H NMR (400 MHz, CDCl₃) of compound 47

**A7.89** Infrared spectrum (Thin Film, NaCl) of compound **47****A7.90** ¹³C NMR (100 MHz, CDCl₃) of compound **47**

**A7.91** ¹H NMR (400 MHz, CDCl₃) of compound **48**



A7.92 Infrared spectrum (Thin Film, NaCl) of compound **48**



A7.93 ¹³C NMR (100 MHz, CDCl₃) of compound **48**

APPENDIX 8

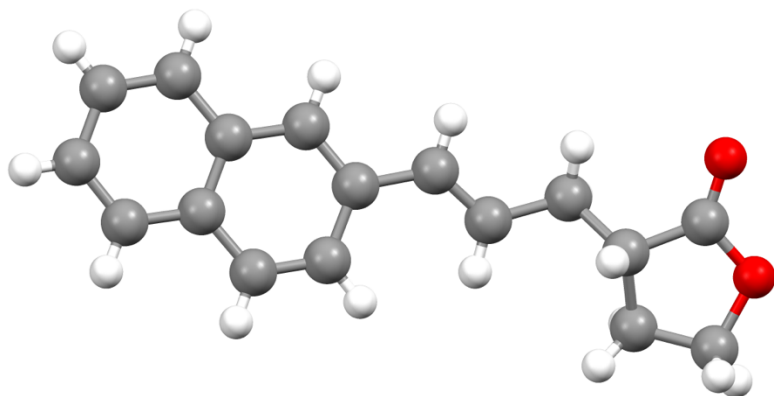
X-Ray Crystallography Reports Relevant to Chapter 3:

*Cu-Catalyzed Enantioselective Allylic Alkylation
with a γ -Butyrolactone-Derived Silyl Ketene Acetal*

A8.1 GENERAL EXPERIMENTAL

For crystal structure determination of **44b** A crystal was mounted on a polyimide MiTeGen loop with STP Oil Treatment and placed under a nitrogen stream. Low temperature (200K; there were crystal issues at lower temperatures) X-ray data were collected with a Bruker AXS D8 VENTURE KAPPA diffractometer running at 50 kV and 1mA (Cu K_{α} = 1.54178 Å; PHOTON II CPAD detector and Helios focusing multilayer mirror optics). All diffractometer manipulations, including data collection, integration, and scaling were carried out using the Bruker APEX3 software. An absorption correction was applied using TWINABS. The space group was determined and the structure solved by intrinsic phasing using XT. Refinement was full-matrix least squares on F^2 using XL. All non-hydrogen atoms were refined using anisotropic displacement parameters. Hydrogen atoms were placed in idealized positions and refined using a riding model. The water molecule was refined as a rigid body. The isotropic displacement parameters of all hydrogen atoms were fixed at 1.2 times (1.5 times for methyl groups) the U_{eq} value of the bonded atom.

A8.2 X-RAY CRYSTAL STRUCTURE ANALYSIS OF ALLYLATION PRODUCT **44b**

Figure A8.1 X-Ray Coordination of α -Allyl γ -Butyrolactone **44b**.**Table A8.1** Crystal Data and Structure Refinement for **44b**.

Empirical formula	C ₁₇ H ₁₆ O ₂	
Formula weight	252.30	
Temperature	100 K	
Wavelength	1.54178 Å	
Crystal system	Monoclinic	
Space group	P 1 2 ₁ 1	
Unit cell dimensions	a = 6.9377(5) Å	a = 90°
	b = 7.1431(5) Å	b = 98.260(5)°
	c = 13.2770(10) Å	g = 90°
Volume	651.14(8) Å ³	
Z	2	

Density (calculated)	1.287 g/cm ³
Absorption coefficient	0.659 mm ⁻¹
F(000)	268
Crystal size	0.32 x 0.17 x 0.05 mm ³
Theta range for data collection	3.364 to 80.143°.
Index ranges	-8 ≤ h ≤ 8, -9 ≤ k ≤ 9, -16 ≤ l ≤ 16
Reflections collected	2467
Independent reflections	2467 [R(int) = ?]
Completeness to theta = 67.679°	97.1 %
Absorption correction	Semi-empirical from equivalents
Refinement method	Full-matrix least-squares on F ²
Data / restraints / parameters	2467 / 1 / 173
Goodness-of-fit on F ²	1.115
Final R indices [I>2sigma(I)]	R1 = 0.0339, wR2 = 0.0996
R indices (all data)	R1 = 0.0349, wR2 = 0.1006
Absolute structure parameter [Flack]	-0.13(13)
Extinction coefficient	n/a
Largest diff. peak and hole	0.163 and -0.178 e.Å ⁻³

Table A8.2. Atomic Coordinates ($\times 10^5$) and Equivalent Isotropic Displacement Parameters ($\text{\AA}^2 \times 10^4$) for **44b**. $U(\text{eq})$ is Defined as One Third of the Trace of the Orthogonalized U^{ij} Tensor.

	x	y	z	U(eq)
O(1)	-94170(30)	-49190(30)	-37017(12)	254(4)
O(2)	-113080(30)	-46280(30)	-51927(13)	277(5)
C(1)	-27370(40)	-55580(30)	-77985(18)	207(5)
C(2)	-13460(40)	-59970(40)	-83901(18)	206(5)
C(3)	-16470(40)	-56390(30)	-94593(18)	200(5)
C(4)	-2330(50)	-60820(40)	-100900(20)	242(6)
C(5)	-5780(50)	-57100(40)	-111190(20)	274(6)
C(6)	-23470(50)	-48680(40)	-115498(17)	280(6)
C(7)	-37520(40)	-44350(40)	-109595(18)	245(6)
C(8)	-34350(40)	-48180(40)	-98950(17)	211(5)
C(9)	-48730(40)	-44210(40)	-92670(17)	206(5)
C(10)	-45640(40)	-47770(40)	-82329(17)	207(5)
C(11)	-61220(40)	-43810(40)	-76283(19)	220(5)
C(12)	-59920(40)	-43400(40)	-66160(20)	235(6)
C(13)	-76880(40)	-38650(40)	-60750(20)	255(6)
C(14)	-78040(40)	-50900(40)	-51425(18)	219(5)
C(15)	-63020(40)	-47120(50)	-42066(19)	296(6)

C(16)	-73710(50)	-53270(40)	-33449(19)	308(7)
C(17)	-97060(40)	-48510(40)	-47252(18)	216(5)

Table A8.3 Bond lengths [\AA] and angles [$^\circ$] for **44b**

O(1)-C(16)	1.459(3)
O(1)-C(17)	1.346(3)
O(2)-C(17)	1.203(3)
C(1)-H(1)	0.9500
C(1)-C(2)	1.366(4)
C(1)-C(10)	1.428(4)
C(2)-H(2)	0.9500
C(2)-C(3)	1.428(3)
C(3)-C(4)	1.415(4)
C(3)-C(8)	1.418(4)
C(4)-H(4)	0.9500
C(4)-C(5)	1.378(4)
C(5)-H(5)	0.9500
C(5)-C(6)	1.412(5)

C(6)-H(6)	0.9500
C(6)-C(7)	1.371(4)
C(7)-H(7)	0.9500
C(7)-C(8)	1.425(3)
C(8)-C(9)	1.418(4)
C(9)-H(9)	0.9500
C(9)-C(10)	1.383(3)
C(10)-C(11)	1.463(4)
C(11)-H(11)	0.9500
C(11)-C(12)	1.334(4)
C(12)-H(12)	0.9500
C(12)-C(13)	1.503(4)
C(13)-H(13A)	0.9900
C(13)-H(13B)	0.9900
C(13)-C(14)	1.527(4)
C(14)-H(14)	1.0000
C(14)-C(15)	1.527(3)
C(14)-C(17)	1.512(4)
C(15)-H(15A)	0.9900
C(15)-H(15B)	0.9900
C(15)-C(16)	1.515(4)
C(16)-H(16A)	0.9900

C(16)-H(16B)	0.9900
--------------	--------

C(17)-O(1)-C(16)	109.4(2)
------------------	----------

C(2)-C(1)-H(1)	119.4
----------------	-------

C(2)-C(1)-C(10)	121.1(2)
-----------------	----------

C(10)-C(1)-H(1)	119.4
-----------------	-------

C(1)-C(2)-H(2)	119.5
----------------	-------

C(1)-C(2)-C(3)	121.1(2)
----------------	----------

C(3)-C(2)-H(2)	119.5
----------------	-------

C(4)-C(3)-C(2)	122.3(3)
----------------	----------

C(4)-C(3)-C(8)	119.4(2)
----------------	----------

C(8)-C(3)-C(2)	118.3(2)
----------------	----------

C(3)-C(4)-H(4)	119.8
----------------	-------

C(5)-C(4)-C(3)	120.5(3)
----------------	----------

C(5)-C(4)-H(4)	119.8
----------------	-------

C(4)-C(5)-H(5)	120.0
----------------	-------

C(4)-C(5)-C(6)	120.1(3)
----------------	----------

C(6)-C(5)-H(5)	120.0
----------------	-------

C(5)-C(6)-H(6)	119.6
----------------	-------

C(7)-C(6)-C(5)	120.8(2)
----------------	----------

C(7)-C(6)-H(6)	119.6
----------------	-------

C(6)-C(7)-H(7)	119.9
----------------	-------

C(6)-C(7)-C(8)	120.1(3)
C(8)-C(7)-H(7)	119.9
C(3)-C(8)-C(7)	119.0(2)
C(9)-C(8)-C(3)	119.4(2)
C(9)-C(8)-C(7)	121.5(2)
C(8)-C(9)-H(9)	119.1
C(10)-C(9)-C(8)	121.7(3)
C(10)-C(9)-H(9)	119.1
C(1)-C(10)-C(11)	122.4(2)
C(9)-C(10)-C(1)	118.3(2)
C(9)-C(10)-C(11)	119.2(3)
C(10)-C(11)-H(11)	116.3
C(12)-C(11)-C(10)	127.5(3)
C(12)-C(11)-H(11)	116.3
C(11)-C(12)-H(12)	118.6
C(11)-C(12)-C(13)	122.9(3)
C(13)-C(12)-H(12)	118.6
C(12)-C(13)-H(13A)	108.9
C(12)-C(13)-H(13B)	108.9
C(12)-C(13)-C(14)	113.3(2)
H(13A)-C(13)-H(13B)	107.7
C(14)-C(13)-H(13A)	108.9

C(14)-C(13)-H(13B)	108.9
C(13)-C(14)-H(14)	108.4
C(15)-C(14)-C(13)	116.7(3)
C(15)-C(14)-H(14)	108.4
C(17)-C(14)-C(13)	112.5(2)
C(17)-C(14)-H(14)	108.4
C(17)-C(14)-C(15)	102.19(19)
C(14)-C(15)-H(15A)	111.3
C(14)-C(15)-H(15B)	111.3
H(15A)-C(15)-H(15B)	109.2
C(16)-C(15)-C(14)	102.3(2)
C(16)-C(15)-H(15A)	111.3
C(16)-C(15)-H(15B)	111.3
O(1)-C(16)-C(15)	104.8(2)
O(1)-C(16)-H(16A)	110.8
O(1)-C(16)-H(16B)	110.8
C(15)-C(16)-H(16A)	110.8
C(15)-C(16)-H(16B)	110.8
H(16A)-C(16)-H(16B)	108.9
O(1)-C(17)-C(14)	110.8(2)
O(2)-C(17)-O(1)	121.2(2)
O(2)-C(17)-C(14)	128.0(2)

Symmetry transformations used to generate equivalent atoms:

Table A8.4 Anisotropic Displacement Parameters ($\text{\AA}^2 \times 10^4$) for **44b**. The Anisotropic Displacement Factor Exponent Takes the Form: $-2p^2 [h^2 a^{*2} U^{11} + \dots + 2 h k a^* b^* U^{12}]$

	U ¹¹	U ²²	U ³³	U ²³	U ¹³	U ¹²
<hr/>						
O(1)	237(10)	304(10)	222(7)	-1(7)	39(7)	23(10)
O(2)	185(9)	358(12)	291(8)	41(8)	43(7)	-7(9)
C(1)	218(14)	191(12)	202(9)	1(9)	-1(10)	-17(11)
C(2)	193(13)	173(11)	240(10)	12(9)	-9(9)	10(11)
C(3)	229(13)	149(11)	220(10)	-11(9)	27(10)	-30(11)
C(4)	271(15)	187(11)	273(11)	-19(9)	56(11)	1(13)
C(5)	354(17)	215(13)	270(11)	-49(10)	101(11)	-33(13)
C(6)	407(17)	224(12)	207(10)	-11(10)	33(10)	-57(15)
C(7)	302(15)	186(12)	229(10)	10(9)	-28(10)	-25(12)
C(8)	257(14)	146(10)	221(10)	-9(9)	10(10)	-37(12)
C(9)	192(11)	151(11)	259(11)	14(9)	-21(10)	7(10)
C(10)	206(12)	166(11)	247(10)	-1(10)	29(10)	-30(13)
C(11)	167(12)	195(12)	297(11)	39(9)	25(9)	6(11)

C(12)	187(13)	232(13)	296(11)	27(10)	66(10)	13(12)
C(13)	207(12)	264(14)	305(12)	25(10)	71(11)	18(12)
C(14)	161(13)	227(12)	276(11)	-4(10)	50(10)	18(12)
C(15)	200(13)	356(16)	318(11)	4(13)	-11(10)	18(13)
C(16)	293(16)	357(16)	254(11)	12(10)	-30(11)	67(13)
C(17)	234(13)	191(11)	225(10)	2(10)	41(9)	-32(14)

Table A8.5 Hydrogen coordinates ($\times 10^4$) and isotropic displacement parameters ($\text{\AA}^2 \times 10^{-3}$) for **44b**.

	x	y	z	U(eq)
H(1)	-2486	-5777	-7086	25
H(2)	-158	-6549	-8085	25
H(4)	964	-6640	-9803	29
H(5)	375	-6021	-11538	33
H(6)	-2566	-4599	-12258	34
H(7)	-4940	-3878	-11261	29
H(9)	-6080	-3897	-9565	25
H(11)	-7369	-4124	-7999	26
H(12)	-4775	-4622	-6220	28

H(13A)	-8909	-4007	-6556	31
H(13B)	-7583	-2538	-5859	31
H(14)	-7687	-6429	-5344	26
H(15A)	-5105	-5459	-4223	36
H(15B)	-5956	-3368	-4150	36
H(16A)	-7178	-6681	-3207	37
H(16B)	-6908	-4620	-2715	37

CHAPTER 4

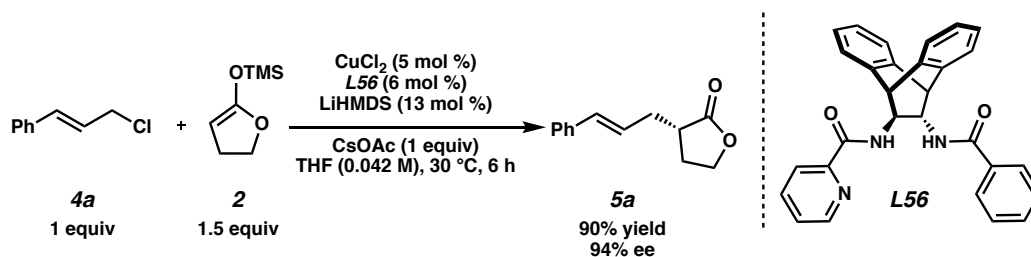
Mechanistic Investigations for Cu-Catalyzed Enantioselective Allylic Alkylation with a γ -Butyrolactone-Derived Silyl Ketene Acetal[†]

4.1 INTRODUCTION

Having developed a ligand and final set of conditions that enabled the Cu-catalyzed enantioselective allylic alkylation with a γ -butyrolactone silyl ketene acetal (Figure 4.1.1), our next goal was to gain a deeper understanding of the reaction mechanism, with an aim of elucidating how the ligand is imparting chirality on the substrate. Furthermore, because of the significant challenges we faced with nucleophiles other than the γ -butyrolactone silyl ketene acetal (see Appendix 5), we hoped that this deeper understanding of the mechanism would enable us to expand the scope of the nucleophile as well.

[†] This work was performed in collaboration with the Hadt Lab at Caltech. Additionally, this research has been published and adapted with permission from Jette, C. I.; Tong, Z. J.; Hadt, R. G.; Stoltz B. M. *Angew. Chem. Int. Ed.* **2020**, 59, 2033–2038. Copyright 2020 Wiley-VCH.

Figure 4.1.1. Final Conditions for Cu-Catalyzed Allylic Alkylations with a γ -Butyrolactone Silyl Ketene Acetal



4.2 OVERVIEW ON MECHANISMS FOR CU-CATALYZED ALLYLIC ALKYLATIONS

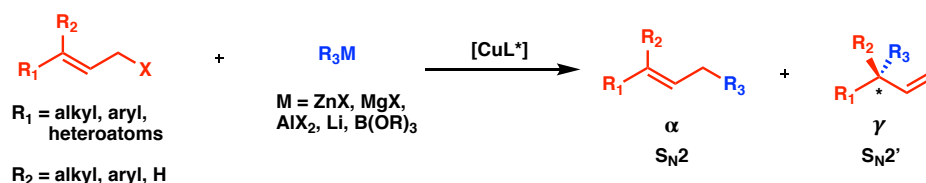
Although Cu as a catalyst in allylic substitutions with softer, enolate-derived nucleophiles ($\text{pK}_a < 30$) remains underexplored, the use of Cu with hard, organometallic nucleophiles ($\text{pK}_a > 40$), such as organomagnesium, dialkylzinc, trialkylaluminum, organolithium, and organoboron reagents is well precedented.¹ This transformation was first reported by Corey and coworkers in 1967², and has been extensively developed over the course of 50 years. Traditionally these reactions are optimized for the branched $\text{S}_{\text{N}}2'$ products, allowing for the opportunity to set a new chiral center on the allyl products (γ , $\text{S}_{\text{N}}2'$, Figure 4.2.1.A). Chiral ligands traditionally used include phosphoramidites, ferrocene ligands, amino acid-derived ligands, and N-heterocyclic carbenes.³

Initially, a ligated Cu (I) species (**A**) will undergo transmetalation, generating an organocuprate species (**B**). This organocuprate can then coordinate to the allylic electrophile,

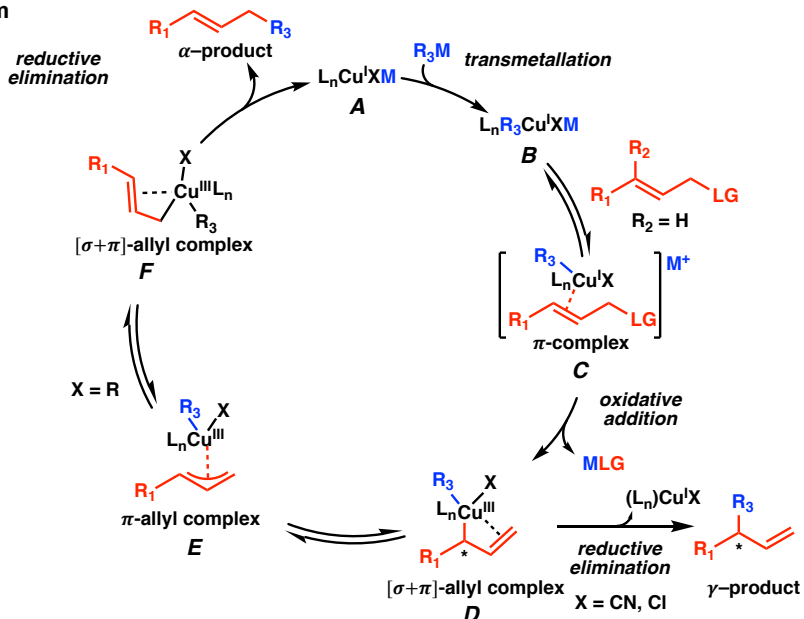
forming π -allyl complex **C**. Upon oxidative addition, it is believed that the branched σ -allyl species **D** forms first, which can either undergo reductive elimination to form the γ -product, or isomerize to π -allyl complex **E**. π -Allyl complex **E** is believed to be in equilibrium with both σ -allyl complex **F** and branched σ -allyl species **D**, and if **D** is formed, reductive elimination from the σ -allyl complex **F** is possible, allowing for formation of the linear, S_N2 product.

Figure 4.2.1 Traditional Cu-Catalyzed Allylic Alkylations^{1,3,4}

A. Traditional Cu-Catalyzed Enantioselective Allylic Alkylation



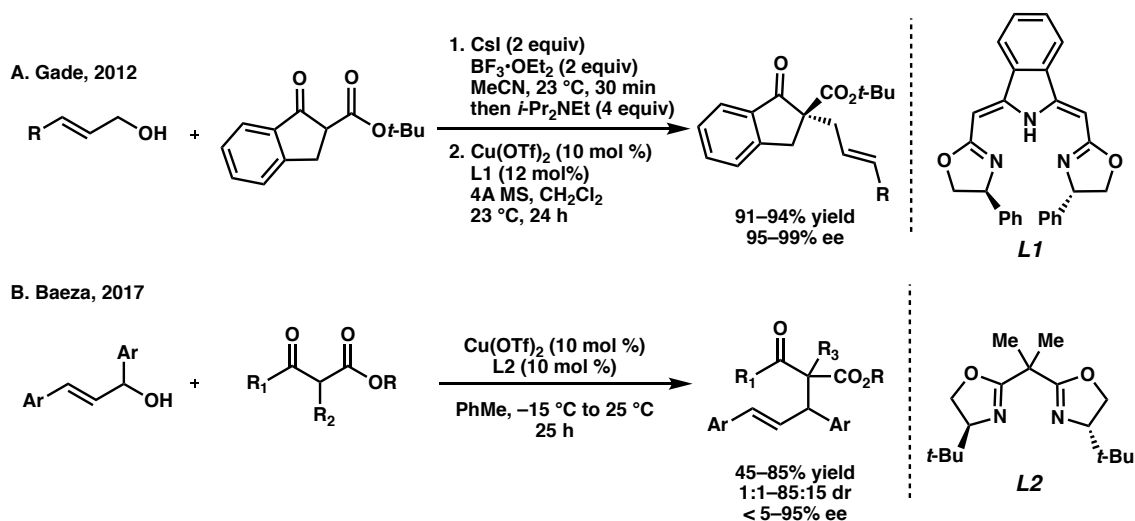
B. Mechanism



Although a number of different strategies have been implemented in order to access either product preferentially, the oldest and most studied method involves the modification of the **X**

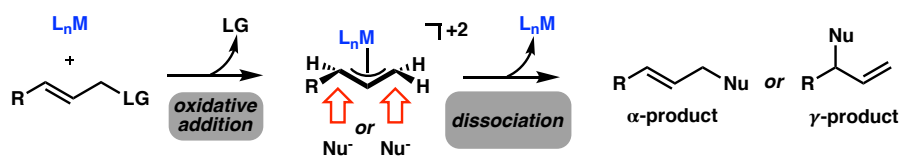
group, a non-transferrable ligand on Cu. If **X** is electron deficient, such as CN or Cl, fast reductive elimination to the γ -product is believed to be favored.³ If the **X** group is more electron-rich, such as an alkyl or alkoxy group, isomerization to the π -allyl species **E** is favored. Consequently, a mixture of both the γ and α products is formed. Under these conditions, other parameters such as the solvent, leaving group, and temperature can be modified in order to favor the formation of the α -product.^{1,3,4} An alternative theory based on DFT calculations states that when X=CN, there is an orbital dissymmetry in the HOMO of the cuprate which favors formation of a $[\sigma+\pi]$ allyl complex with **R**₃ proximal to the benzylic position of the allyl group, allowing for reductive elimination at this position. When X = alkyl, the symmetrical HOMO of the cuprate allows for either formation of the linear or branched product.⁴ Despite the significant effort made toward understanding the role these non-transferrable ligands play in this transformation, modern reports now rely on the influence of sterics and the presence of chelating groups on the auxiliary ligand (**L**_n) to control the site selectivity.⁵

Because the use of Cu in allylic alkylations with softer, enolate derived nucleophiles ($pK_a < 30$) remains underdeveloped, one of the challenges associated with the development of this transformation is that the mechanism was not well understood. Although the inner sphere allylic alkylation with Cu is well precedented (Figure 4.2.1.B), a number of different reaction pathways could logically be expected for the present reaction. One possibility is that Cu could be functioning as a Lewis Acid for the activation of enolate-type nucleophiles, a pathway that has been implicated twice before in the enantioselective allylic alkylation of β -ketoester nucleophiles (Figure 4.2.2).^{6,7} Although in both the present case and in these reports the reaction is hypothesized to proceed

Figure 4.2.2. Cu-Catalyzed Allylic Alkylation with β -Ketoesters^{5,6}

through an enolate nucleophile, β -ketoesters significantly differ both sterically and electronically from γ -butyrolactones, and for this reason, it was unclear whether both types of species would undergo alkylation via a similar pathway.⁸

Outer-sphere allylic alkylation pathways, in which Cu exclusively activates the electrophile could also be operative (Figure 4.2.3). This mechanism is more common when softer nucleophiles are used in combination with metals such as Ir and Pd.¹ In an outer sphere mechanism, the metal will oxidatively insert into the allylic electrophile to form a metal π -allyl species, which then can undergo nucleophilic attack to form the desired product and regenerate the transition metal catalyst.⁹

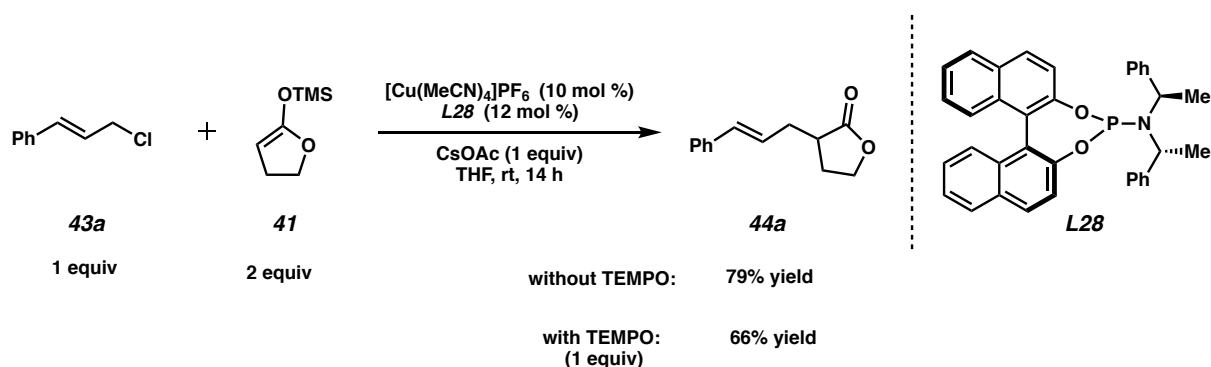
Figure 4.2.3. Outer-Sphere Allylic Alkylation Mechanism⁹

4.3 INVESTIGATIONS INTO A RADICAL MECHANISM

One of the first possible mechanisms we explored was the radical mechanism. Given that carbon-centered radicals can be generated from the corresponding silyl ketene acetals by an oxidative process involving Cu(II),¹⁰ a radical mechanism for alkylation of the γ -butyrolactone-derived silyl ketene acetal seemed plausible. For this reason, a couple of experiments were carried out in order to determine if a radical mechanism was operative.

Early on in the investigation, we performed a reaction in the presence of TEMPO. We found that the yield was comparable to what was observed without TEMPO, and no TEMPO-substrate adducts were observed by ¹H NMR or GC-MS (Scheme 4.3.1).

Scheme 4.3.1. Cu-Catalyzed Allylic Alkylation with TEMPO



Another possibility could be that the reaction proceeds through an allylic radical intermediate. If this is the case, a benzylic radical should be just as viable an intermediate as an allylic radical, as determined by their bond dissociation energies (Scheme 4.3.2.A).¹¹ However, no reaction occurred when benzyl chloride was used as the electrophile instead of cinnamyl

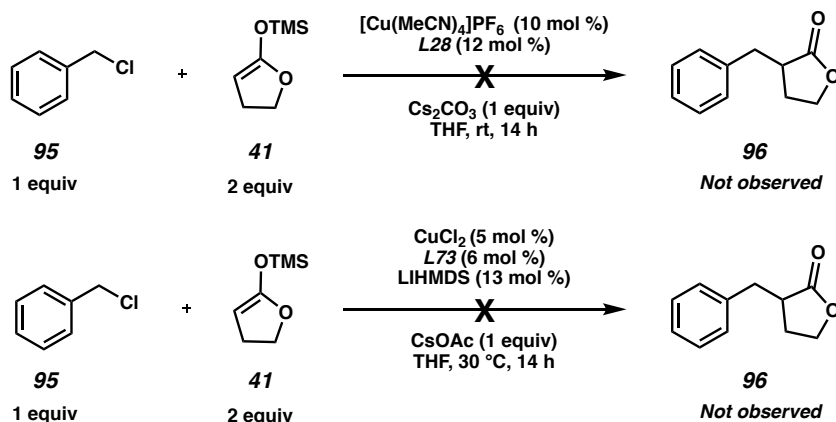
chloride in either our starting or final conditions (Figure 4.3.2.B). Furthermore, this experiment also served to demonstrate that the alkene was a crucial component of the electrophile, and it was not simply the activated nature of the allylic leaving group that was leading to product formation via a mechanism involving a Cu Lewis Acid activation of the nucleophile.

Scheme 4.3.2. Cu-Catalyzed Alkylation with Benzyl Chloride¹¹

A. Bond Dissociation Energies (BDE) for Benzylic and Allylic Hydrogens



B. Cu-Catalyzed Alkylation with Benzyl Chloride



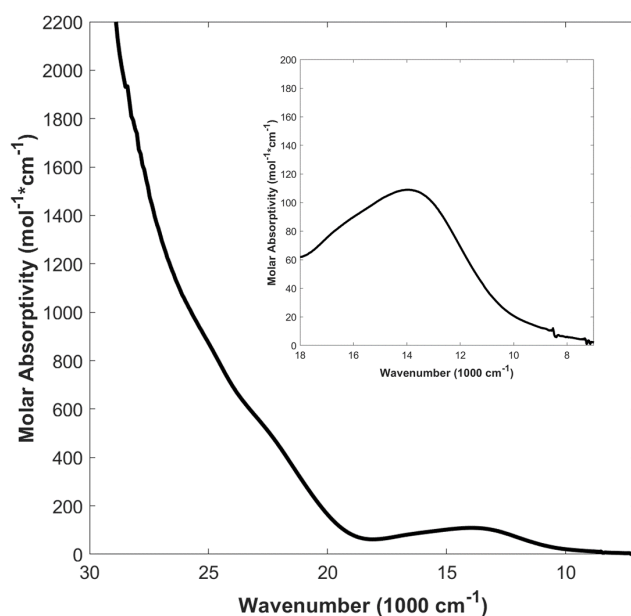
4.4 CHARACTERIZATION OF THE STARTING COPPER/L73 COMPLEX

With preliminary evidence suggesting that both a radical mechanism and a Lewis acid mechanism were unlikely, we next turned our attention to the characterization of the starting Cu complex, with a goal of understanding how the Cu complex was activating either the electrophile

(outer-sphere mechanism) or the nucleophile and electrophile (inner sphere mechanism), and how enantioinduction may be occurring.

Given the novelty of the Cu/**L73** complex, we chose to examine it using continuous wave (CW) X-band electron paramagnetic resonance (EPR), UV-vis spectroscopies, and density functional theory (DFT) calculations. Although the single x-ray diffraction crystal structure of a planar Cu^{II} complex with a tetradentate, deprotonated **L38** has been reported,¹² it was unclear how exclusion of one of the pyridine moieties and the presence of a large, bulky backbone would affect the binding mode of the ligand. For this reason, we aimed to determine whether our best performing ligand **L73** coordinates through the two amide nitrogens, or if it adopts an alternative binding mode through the benzamide oxygen, similarly to the previously disclosed Mo/**L38** complex.¹³

Figure 4.4.1. Absorption Spectrum of **L73**•CuCl₂



One challenge with Cu in catalysis is its propensity to form higher order aggregates.¹⁴ Consequently, we wanted to ensure that the observed catalytic activity could be attributed to a monomeric Cu complex prior to performing any DFT calculations. Given the thermal instability of the Cu(II) catalyst (which also prevented structural determination by techniques such as X-ray crystallography), we chose EPR and electronic absorption spectroscopies for the quantification of monomeric Cu(II) species in the reaction.

Three batches of **L73•CuCl₂** were prepared independently and diluted to 2.1 mM in Cu, which is the concentration of Cu in the final reaction conditions (See Materials and Methods). An aliquot of the sample was loaded into a 4.0 mm standard quartz Norell EPR tube and immediately immersed in liquid nitrogen to avoid sample decomposition (rapid freezing also ameliorates the adverse effect from the non-glassiness of THF, as we found that preparing the complex in the glassy 2-MeTHF solvent led to a yellow solution with a different EPR spectrum. See Figure S2). 2 mL of the same solution of each sample was then loaded into a 1 cm borosilicate cuvette to obtain its absorption spectrum. All three samples afforded a green solution with low intensity d-d transitions ranging from 560 to 1400 nm, (Figure 4.3.1), albeit small variations exist. As a result, we estimate a 5% error associated with the concentrations of the analyte (± 0.1 mM).

The three **L73•CuCl₂** samples show a double integrated intensity of 3.00×10^5 , 2.87×10^5 , and 2.68×10^5 . This resulted in an averaged concentration of 1.81 mM with a standard deviation of 0.1 mM. Moreover, combining various sources of error with standard error of regression, standard error of the slope, and standard error of the intercept resulted in a 6 % error associated with the calibration method described herein. Adding calibration error and the standard deviation in

quadrature, we report the average concentration of monomeric, divalent copper in **L73**•CuCl₂ to be 1.81 (\pm 0.14) mM.

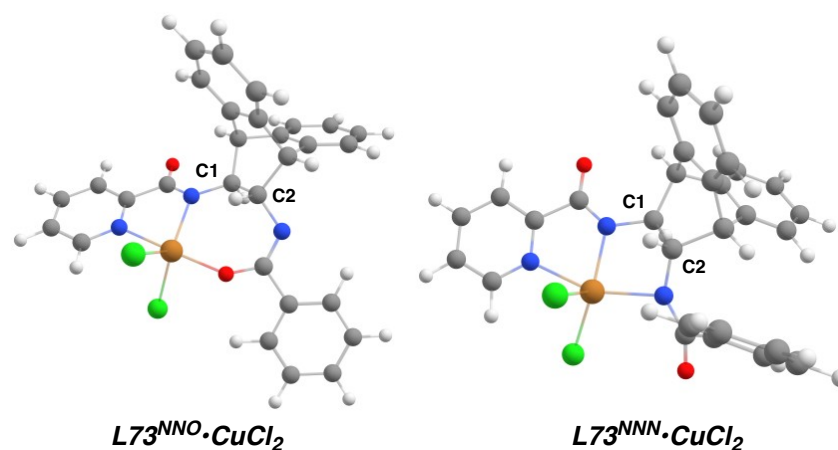
These three different batches of **L73**•CuCl₂ were further diluted down with acetonitrile for ESI-MS. In negative ion mode, we found 577.0364 m/z, which was consistent with the calculated m/z for C₂₉H₂₂Cl₂CuN₃O₂ [M+H]⁻ = 577.0385. We also found that the isotope patterns observed were consistent with the ionization of the fully deprotonated [**L73**•CuCl₂]²⁻ species. It was interesting to note that the Cl⁻ ions remained bound to Cu after coordination of the ligand, indicating that they may be playing a role in the generation of a consistent complex (see Chapter 3, Table 3.5.2).

With some preliminary characterization data in hand, our next focus was to determine whether the **L73** was bound to Cu via the benzamide nitrogen or the benzamide oxygen. Because we were limited to a non-glassy solvent for EPR, it was impossible to determine the fine coupling structure, and thus we were not able to establish the binding mode using this technique. We also attempted to use FTIR, but the Cu-O and Cu-N bonds cannot be directly observed through IR, and although the carbonyl peaks and the bending modes could be used to obtain structural information, the two amides on the ligand have overlapping peaks in the FTIR spectrum (see Figure 4.7.2).

4.5 LIGAND COORDINATION GEOMETRY: DFT CALCULATIONS

Given the challenges we faced with a large variety of experimental techniques, we turned to DFT calculations in order to determine the binding mode of the ligand. We found that DFT calculations indicate that **L73** preferentially binds to Cu in a tridentate fashion, via N_{pyridine}, N_{picolinamide}, and O_{benzamide} atoms (**L73^{NNO}•CuCl₂**, Table 4.5.1, entry 1). Regardless of the level of theory employed, the alternative tridentate binding mode via the benzamide nitrogen (**L73^{NNN}•CuCl₂**) is disfavored by 14–23 kcal/mol (entry 2 and Tables 4.11.1 and 4.11.2). This large

Table 4.5.1. DFT Calculations on **L73** and **L73•CuCl₂**^a




entry	ligand binding mode	E _{gas phase} (kcal/mol)	E _{solvent corrected} (kcal/mol) ^c	t ₄ ' C1	t ₄ ' C2
with CuCl ₂					
1	L73^{NNO}•CuCl₂	0	0	0.93	0.95
2	L73^{NNN}•CuCl₂	22.5	19.5	0.86	0.85
without CuCl ₂ ^b					
3	relaxed L73²⁻	0	0	0.96	0.97
4	L73^{NNO}	18.7	13.6	0.93	0.95
5	L73^{NNN}	39.5	30.0	0.86	0.85

[a] Obtained using B3LYP density functional with 38% Hartree-Fock exchange. [b] Ligand coordination geometry was obtained by removing CuCl₂ from the optimized geometry of the corresponding complex.

energy difference renders the thermal population of the O-bound enolate unlikely; for this reason, we postulate that only one conformer of the pre-catalyst accounts for the observed asymmetric catalytic activity. To further probe the origin for this binding preference, we performed single-point calculations on **L73** in the absence of CuCl_2 (entries 3-5). Interestingly, we found that the energy gap between the two conformations **L73**^{NNO} and **L73**^{NNN} is still retained (entries 4 and 5), implying that ligand sterics affect the binding preference and tune the metal coordination geometry. As demonstrated by the geometry index τ_4' ,¹⁵ the two sp^3 ring carbons **C1** and **C2** exhibit a stronger deviation from the ideal tetrahedral geometry ($\tau_4' = 1$) in **L73**^{NNN} relative to **L73**^{NNO}.

In order to gain a better understanding for why **L73** performed better than **L56**, we performed an identical analysis on **L56**• CuCl_2 (Table 4.5.2). We found that with **L56**, the NNO

Table 4.5.2. DFT Calculations on **L56** and **L56**• CuCl_2 ^a



entry	ligand binding mode	$E_{\text{gas phase}}$ (kcal/mol)	$E_{\text{solvent corrected}}$ (kcal/mol)	τ_4' C1	τ_4' C2
with CuCl_2					
1	L56 ^{NNO} • CuCl_2	0	0	0.95	0.97
2	L56 ^{NNN} • CuCl_2	12.9	7.6	0.94	0.94
without CuCl_2 ^b					
3	relaxed L56 ²⁻	0	0	0.97	0.97
4	L56 ^{NNO}	20.9	12.7	0.97	0.95
5	L56 ^{NNN}	35.8	24.6	0.94	0.93

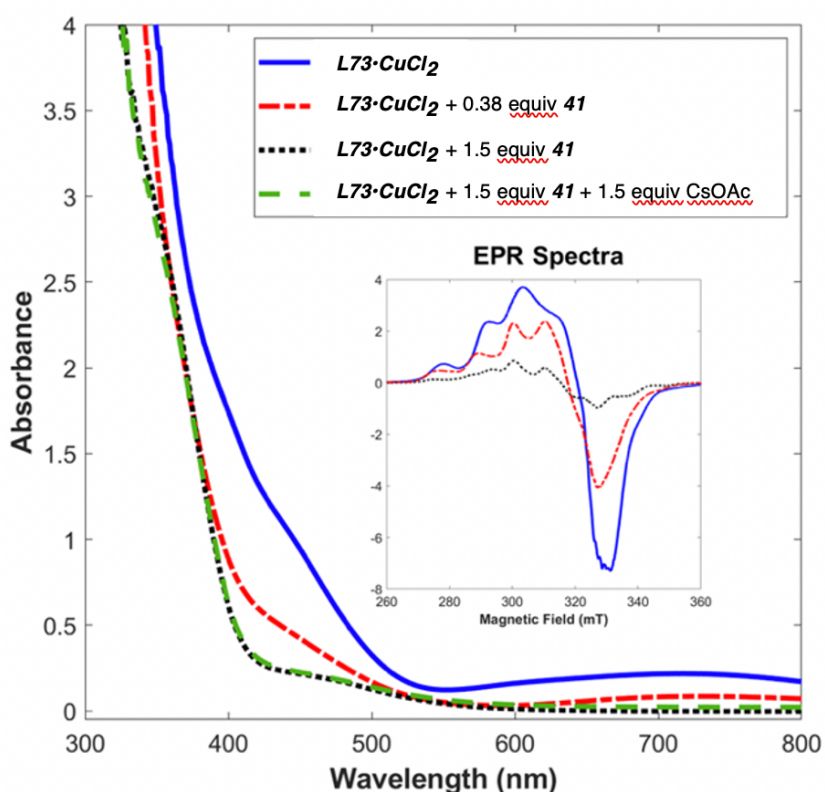
[a] Obtained using B3LYP density functional with 38% Hartree-Fock exchange. [b] Ligand coordination geometry was obtained by removing CuCl_2 from the optimized geometry of the corresponding complex.

binding conformation is still preferred. Even though with **L56** the energy difference between the two conformations is reduced, this energy difference is still too large for the population of both binding modes.

4.6 REDUCTION OF COPPER(II) TO COPPER(I)

Throughout our reaction screening, we consistently noted that both Cu(I) and Cu(II) sources could be used, regardless of the reaction conditions employed. Because our reaction conditions were somewhat reducing, we hypothesized that when a Cu(II) source is used, a reduction to Cu(I) could be occurring at the start of the reaction. In the final conditions, a color change from green to

Figure 4.6.1. Room Temperature UV-vis and 77 K X-band EPR (inset) Spectroscopic Monitoring of the Reaction of 5 mol % of **L73**•CuCl₂ with Silyl Ketene Acetal **41**

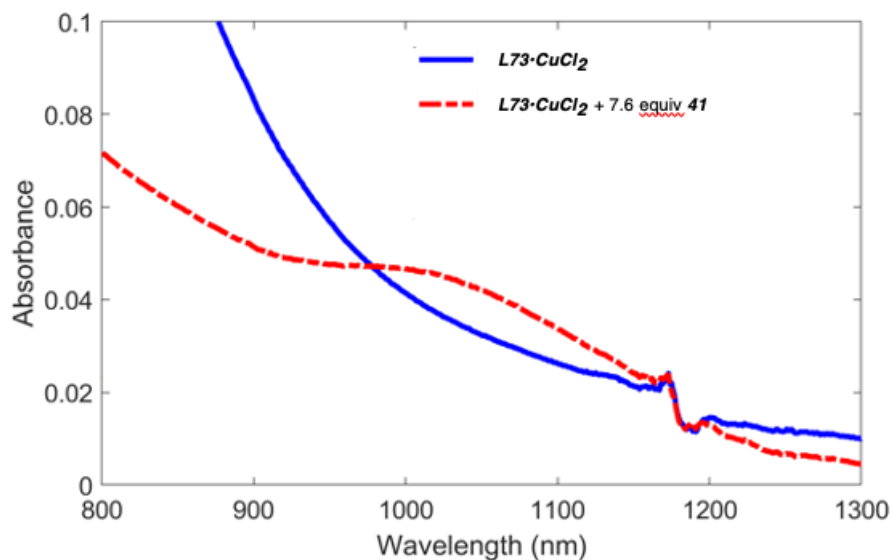


yellow does occur within 5 minutes of the addition of silyl ketene acetal **41** and CsOAc to **L73•CuCl₂**, indicating that a significant change at Cu is occurring.

In order to confirm the occurrence of an oxidation state change, we monitored the change at Cu upon addition of silyl ketene acetal **41** and CsOAc using UV-vis and EPR. In agreement with the above observations, we noted that the characteristic d-d transitions and 77 K X-band EPR signal of the starting **L73•CuCl₂** complex disappear at the start of the reaction, signifying the Cu^{II} precatalyst is reduced to a Cu^I complex (Figure 4.6.1).

Interestingly, we noted that the reduction occurs even in the absence of CsOAc, indicating the silyl ketene acetal **41** is the reductant.¹⁵ Using EPR we quantified the amount of monomeric, divalent Cu after the addition of 1.5 equiv of **41** to 5 mol% **L73•CuCl₂**, and found that the concentration of Cu(II) remaining in solution was 0.29 (+/- 0.02) mM, only 16% of the total amount of Cu(II) present at the start of the reaction (see Section 4.3). It should be noted that this reduction occurs only in the presence of a large excess of silyl ketene acetal **41** relative to Cu. In

Figure 4.6.2. UV-Vis-NIR: Observation of Intermediate During Reduction

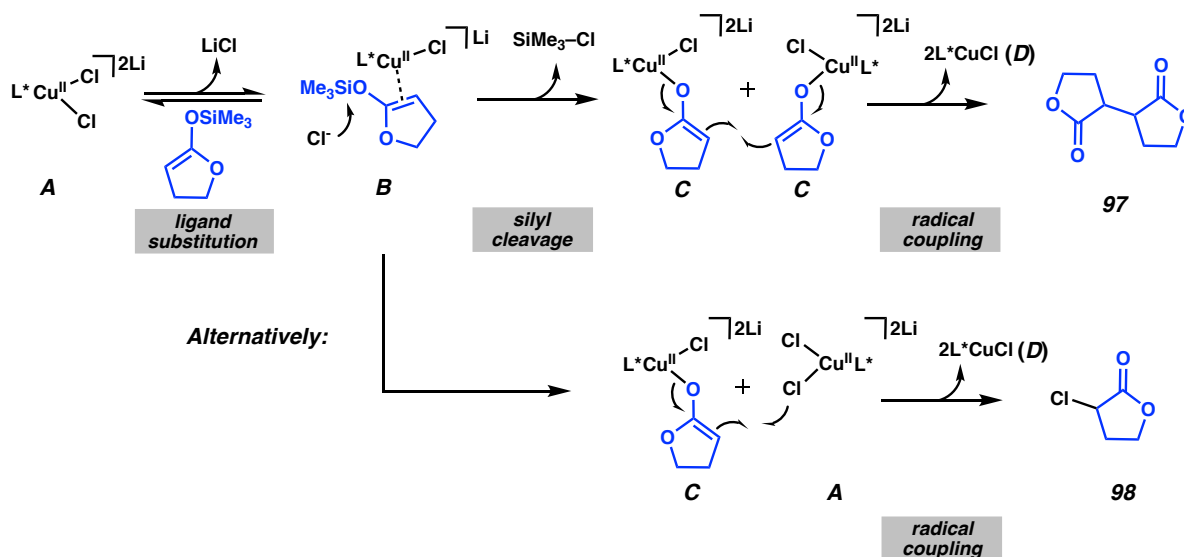


addition, with less than 30 equivalents of **41** relative to Cu, incomplete consumption of the Cu(II) is observed.

From the UV-Vis monitoring of the initial reduction, we were also able to detect a new on pathway reaction intermediate. The addition of 7.6 equivalents of **41** (relative to **L73**•CuCl₂) resulted in both a decrease in Cu(II) signals and a change in the EPR spectrum and the d-d transitions in the 600-800 nm region (Figure 4.6.2). The further characterization of this intermediate will be reported in a follow up study.

For insight into the mechanism for the reduction of the starting Cu(II) complex, we turned to the literature. There are a number of reports on the radical coupling of enolates using CuCl₂ as the oxidant, which led us to postulate a similar mechanism for the reduction of CuCl₂ by **41** (Scheme 4.6.1).¹⁶ Although to our knowledge, no reports on the use of silyl enolates in this type

*Scheme 4.6.1. Possible Reaction Mechanisms for Reduction of **L73**•CuCl₂ by **41***



of transformation exist in the literature, we envision that a chloride assisted cleavage of the silyl enolate could lead to an intermediate (**C**, Scheme 4.5.1) that is commonly postulated in related reports.

Initially, ligand substitution by the electron-rich olefin of the silyl ketene acetal may lead to complex **B**. The displaced chloride anion can then attack the silyl group, allowing for the formation of a Cu enolate **C**. This Cu enolate can then react with an additional Cu enolate to afford the lactone dimer **97** and 2 equivalents of the corresponding Cu(I) salt **D**. Another likely mechanism also involves a bimolecular pathway, but rather than reacting with a second equivalent of **C**, the Cu enolate could also react with **A** to form the α -chlorolactone.¹⁷ Given the low molecular weight of both **97** and **98**, we have not isolated either at this time, and for this reason, neither mechanism can be ruled out.

Having confirmed that a reduction is occurring at the start of the reaction, another question that had to be answered was whether or not the binding mode of the ligand is retained after the reduction. To this end, we performed DFT calculations on a number of possible intermediates. We found that, although the energy differences between the two binding modes may change slightly, the NNO binding mode is still preferred for a number of different Cu complexes.

Table 4.6.1. Steric Preference for **L73**^{NNO} Coordination Across Different Possible Intermediates

Entry	Complex	E _{NNO} (Hartree)	E _{NNN} (Hartree)	ΔE (Hartree)	ΔE (kcal/mol)
without solvent correction					
1	L73 •Cu ^{II} Cl ₂	-3997.8647	-3997.8289	0.0358	22.5
2	L73 •Cu ^{II} Cl	-3537.3202	-3537.2842	0.0360	22.7
3	L73 •Cu ^{II}	-3076.6231	-3076.6029	0.0202	12.7
4	L73 •Cu ^I Cl ₂ ^a	n.a.	n.a.	n.a.	n.a.
5	L73 •Cu ^I Cl	-3537.2750	n.a. ^b	n.a.	n.a.
6	L73 •Cu ^I	-3076.7185	3076.681	0.0375	23.6
with solvent correction					
7	L73 •Cu ^{II} Cl ₂	-3998.0902	-3998.0591	0.0311	19.5
8	L73 •Cu ^{II} Cl	-3537.3972	-3537.3682	0.0290	18.3
9	L73 •Cu ^{II}	-3076.6523	-3076.6288	0.0235	14.8
10	L73 •Cu ^I Cl ₂ ^a	n.a.	n.a.	n.a.	n.a.
11	L73 •Cu ^I Cl	-3537.4968	n.a. ^b	n.a.	n.a.
12	L73 •Cu ^I	-3076.7939	-3076.7650	0.0289	18.2

[a] This structure failed to converge; dissociation of the chloride was energetically favorable during the optimization cycles. [b] The benzamide moiety dissociated in the optimized structure, resulting in a T-shaped Cu complex with a bidentate **L73** ligand.

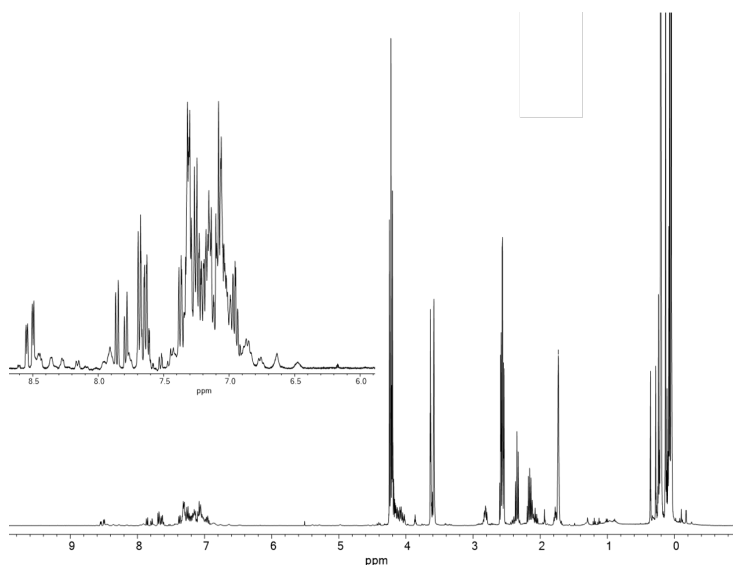
4.7 FTIR: ADDITIONAL STRUCTURAL INSIGHT FOR COPPER(I)

Having identified that the starting Cu(II) complex is reduced to a Cu(I) complex at the start of the reaction, our next goal was to identify whether a Cu(I) enolate was being formed, as this would be a direct indication of whether an inner-sphere or outer-sphere alkylation pathway is operative.

It should be noted that while NMR was not useful for the characterization of the Cu(II) precatalyst, we tried to use ¹H NMR, ¹³C NMR, ⁷Li NMR, and FTIR to gain structural insight on the Cu(I) catalyst. However, the ¹H NMR was extremely messy, as 30 equivalents of the silyl ketene acetal **41** relative to Cu are required to fully reduce the catalyst (Figure 4.7.1). As a

consequence, the alkyl region of the spectrum is congested by the very large silyl ketene acetal peaks. In the aryl region of the ^1H NMR, we observed a large amount of broadened resonances with full width at half-maximum (FWHM) of around 10 Hz, which is indicative of dynamic behavior. As a result, no conclusions could be drawn about the binding mode from the ^1H NMR alone. Given this dynamic movement, we believed that even if we had been able to access our Cu(I) active catalyst cleanly using an alternative method, it would be nearly impossible to discern the binding mode, or any other structural features of the complex from the ^1H NMR data.

Figure 4.7.1: ^1H NMR (400 MHz, THF-d_8) Spectrum of **L73**• CuCl_2 + 30 equivalents of **41**



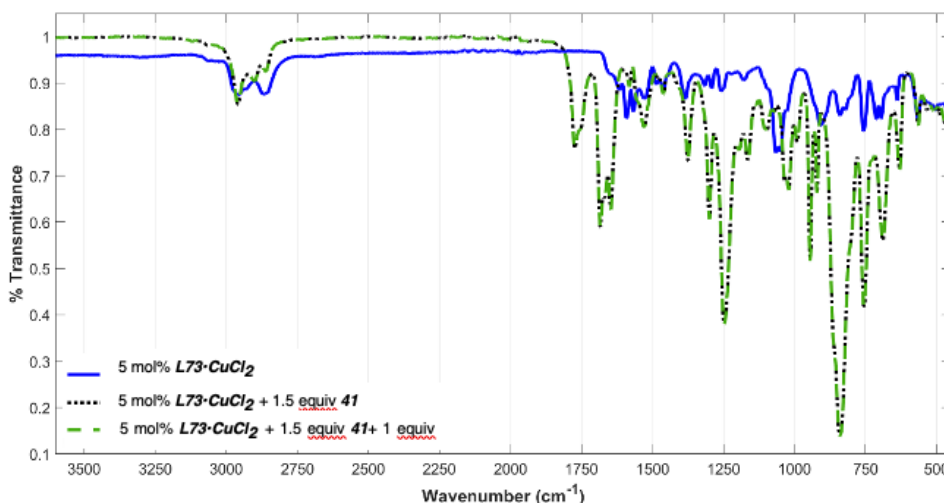
In addition to ^1H NMR, we also collected a ^{13}C NMR spectrum of the Cu(I) form of the complex. Unfortunately, not all ^{13}C signals were cleanly resolved, particularly the sp^2 carbonyl carbons, and the alpha carbons of interest (See A9.1). In the ^7Li NMR spectrum, we did observe that the addition of silyl ketene acetal to the Cu(II) pre-catalyst resulted in a change of less than

0.5 ppm in the lithium spectrum, however, no further structural elucidations could be made (See A9.2 and A9.3).

From the FTIR we were able to gain some insight into the structural changes that were occurring upon exposure of the starting Cu(II) complex to **41**. Compared to that of the free ligand, the pyridine ring bending mode shifted from 748 to 756 cm^{-1} , indicating the coordination of pyridine to copper center (See A6.32 for IR of free **L73**).¹⁸ For **L73**•CuCl₂ (Figure 4.7.2, blue trace), we consistently noted high transmittance. Upon addition of silyl ketene acetal **41**, we observed the reappearance of amide bands at 1683, 1669, and 1646 cm^{-1} . The pyridine remained bound to the copper center as the ring bending mode occurred at 755 cm^{-1} . Interestingly, we observed an intense ring C-H bend from the phenyl moiety. These results suggest that the benzamide moiety may have dissociated upon addition of silyl ketene acetal **41**.

A carbonyl band was also observed at 1774 cm^{-1} , which could be attributed to a Cu(I) enolate, as it is 4 cm^{-1} away from where the γ -butyrolactone carbonyl stretch is observed.

Figure 4.7.2: FTIR Spectrum of **L73**•CuCl₂ + 30 equivalents of **41**



γ -Butyrolactone-Derived Silyl Ketene Acetal

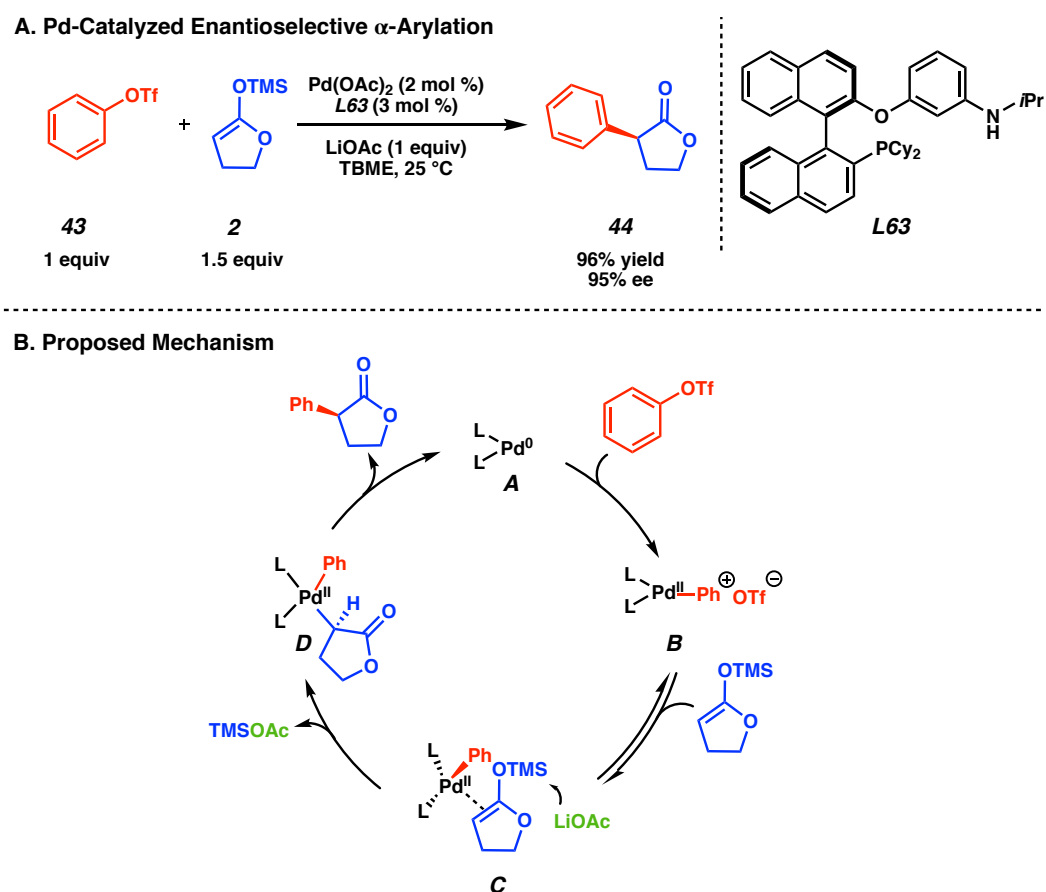
However, although a large excess of silyl ketene acetal is added to the starting precatalyst in order to reduce it down to Cu(I), we observe no peaks that correspond with the silyl ketene acetal or free γ -butyrolactone. One likely explanation is that because these experiments were performed on a dry sample, perhaps the γ -butyrolactone and silyl ketene acetal evaporated prior to spectrum acquisition.

Although we do not have any conclusive data that indicates that a Cu(I) enolate is being formed or that it is the species that undergoes oxidative addition into the cinnamyl chloride, we do have some evidence that indicates this may be likely. The first is that controls run in the absence of Cu result in little to no product formation. Even when cinnamyl bromide is used, only a small amount of product is observed. We believe that this may be an indication that CsOAc is not a strong enough base to cleave the silyl ketene acetal without the assistance of the Cu catalyst. Furthermore, when the analogous lithium or zinc enolates are used as nucleophiles, or when other salts that are designed to cleave silyl enolates such as TBAT and CsF are used, no product is observed, indicating that a free enolate may not be the reactive species.

In addition, the present conditions for silyl ketene acetal cleavage are similar to those developed by Zhou and coworkers for the Pd-catalyzed enantioselective α -arylation (Figure 4.7.3.A). On the basis of DFT calculations, they propose a mechanism for their transformation that involves a reductive elimination step from an aryl Pd(II) enolate (**D**, Figure 4.7.3.B).¹⁹ Furthermore, in their DFT calculations, they found that a C-bound Pd enolate was consistently favored over an O-bound Pd enolate by 15 kcal/mol (we observe similar results, see Figure 4.7.4). After modeling a number of different transmetallation mechanisms, they found that the only one

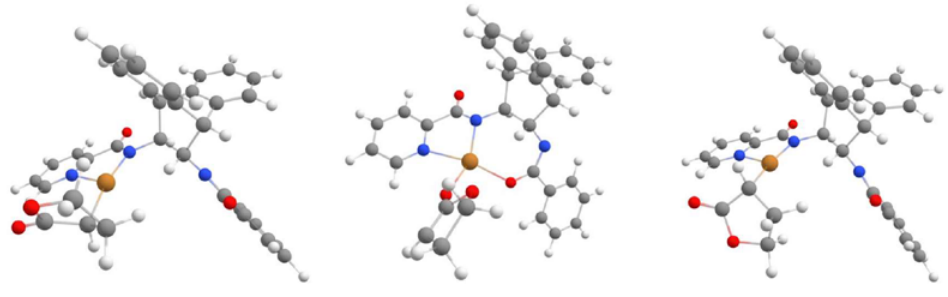
that allows for exclusive formation of a C-bound enolate involves external acetate cleavage of a silyl ketene acetal bound to Pd through the electron-rich olefin (C, Scheme 4.7.3.B). Although Zhou and coworkers have no experimental evidence to confirm that silyl enolates bind to transition metal complexes in this manner, in our own control reactions run during the investigation of silyl enol ether nucleophiles (see Section A5.4), we did observe some reactivity that could be explained by coordination of a silyl enolate to the Cu catalyst.

Figure 4.7.3. Pd-Catalyzed Enantioselective α -Arylation of γ -Butyrolactone Silyl Ketene Acetals¹⁸



Having concluded that the formation of a Cu(I) enolate is likely, we performed DFT calculations in order to establish which enolate geometry is preferred. In agreement with Zhou and coworkers, we found that a C-bound Cu enolate is significantly favored over an O-bound enolate. Interestingly, we noted that the two C-bound enolate enantiomers are very close in energy, with the disfavored (*R*)-enantiomer slightly lower in energy than the desired (*S*)-enantiomer (Table 4.7.4).²⁰

Table 4.7.1. Energetic Preference for C-bound Enolate



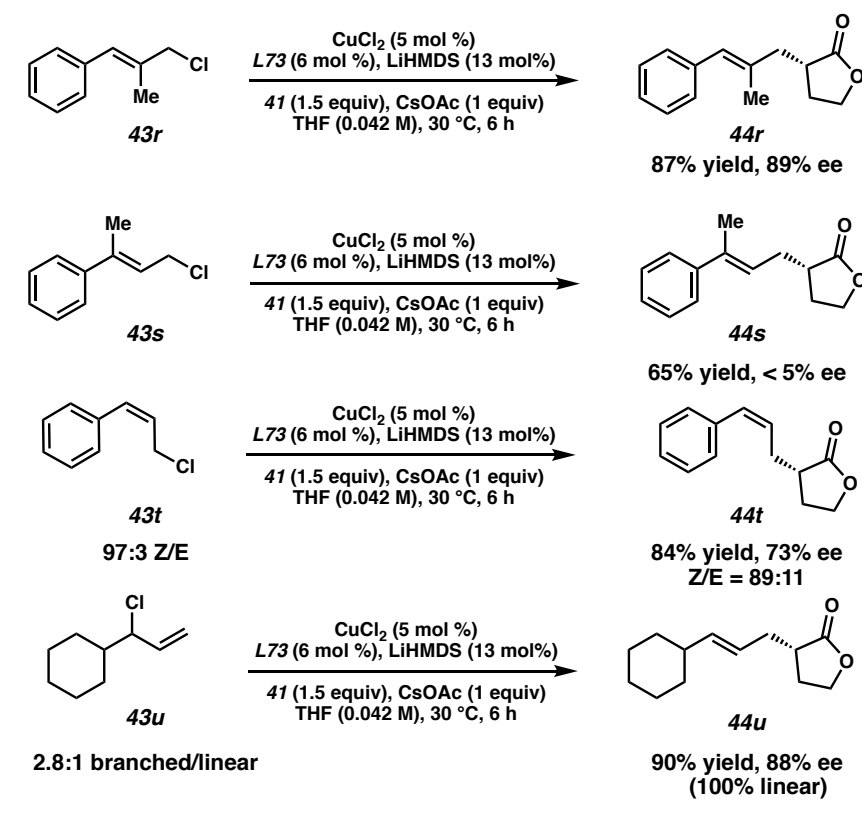
Geometry	E _{gas phase} (kcal/mol)	E _{solvent corrected} (kcal/mol)	G _{gas phase} (kcal/mol) ^a	G _{solvent corrected} (kcal/mol) ^b
<i>R</i>	0.0	0.0	0.0	0
<i>S</i>	0.4	0.3	1.9	1.7
<i>O</i>	16.6	13.5	13.8	10.7

4.8 IMPORTANCE OF OLEFIN GEOMETRY

Another equally important question we hoped to answer is to what extent the Cu is interacting with the electrophile. One unique characteristic of our reaction was that the product was consistently formed in high linear:branched ratios.²¹ From our investigation, it appears that this is regardless of the Cu source, ligand, leaving group, solvent, and base used. This high

linear:branched selectivity, which is uncommon in traditional Cu-catalyzed allylic alkylations, could be explained in a number of ways: the first is that the reaction is going through a pathway that involves direct S_N2 with a Cu(I) enolate, which we deemed unlikely from our experiments with benzyl chloride, but could not yet rule out. The second explanation is that this high selectivity for the linear product is a consequence of the nucleophile used. The γ -butyrolactone silyl ketene acetal significantly differs both in size and electronics from nucleophiles used in traditional Cu-catalyzed allylic alkylations, which are typically unbranched organometallic nucleophiles. If the reaction is going through an inner-sphere mode of attack, perhaps the large size of this nucleophile could be consistently preventing the formation of the branched products, or may alter the geometry of the HOMO on Cu in such a way that consistently favors formation of the linear product.²² Finally, another possibility is that by chance we did not test any ligands that could afford the branched product in high yields. One of the more common ways to direct the site selectivity is through the presence of chelating groups on the ligands. These modifications have been extensively made on NHC's ligands, but unfortunately those ligands resulted in no product formation in the present conditions.

Because the product distribution did not resemble that of traditional Cu-catalyzed allylic alkylations, we hoped to further probe to what extent Cu interacts with the electrophile, as this would be a good indication of whether an inner-sphere mechanism was operative, or an alternate

Scheme 4.8.1 Importance of Olefin Substitution Pattern^a

[a] See General Procedure in 4.11. Isolated yields on 0.2 mmol scale. SFC analysis was used to determine ee.

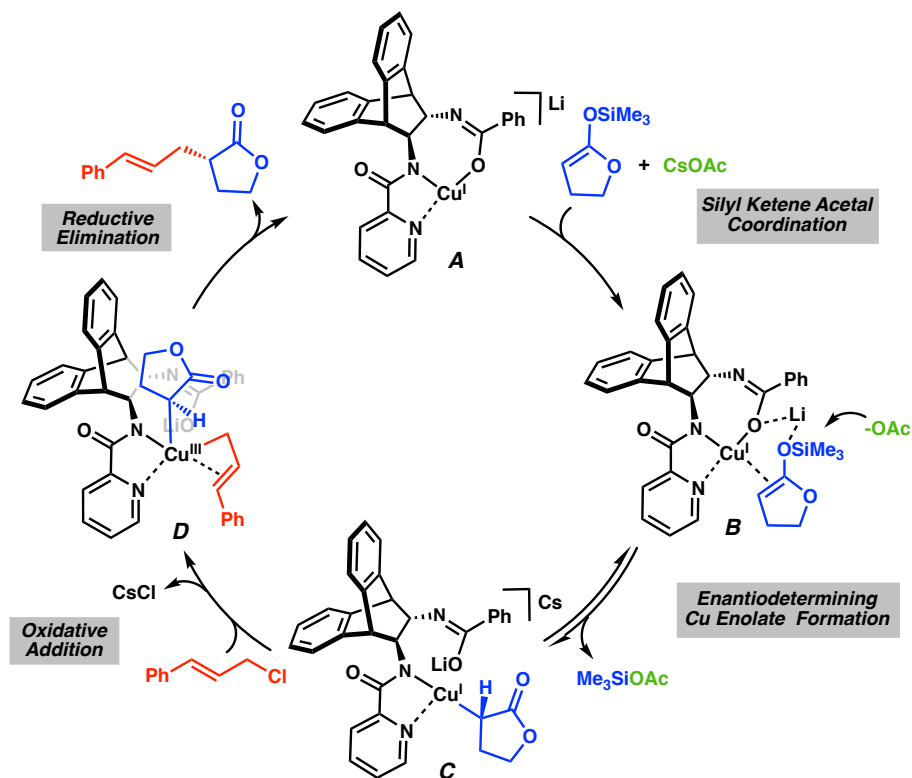
mechanism needed to be considered. To this end, we took a closer look at the effect of the electrophile olefin geometry on the reaction outcome. Interestingly, we found that although trisubstituted olefin **43r** (Scheme 4.8.1) led to the desired product **44r** in good selectivity and yield, the product formed from α,α -substituted olefin **43s** was obtained in significantly lower yield and ee. Intrigued by this result, we exposed Z-olefin substrate **43t** to our reaction conditions. Interestingly, we obtained the corresponding Z-olefin product **44t** in good yield, but in only moderate ee. Furthermore, we also noted that even when a mixture of linear and branched electrophiles is used, only the linear product is obtained (**44u**). Taking these results into account,

and also considering that other electrophiles such as benzyl or phenethyl chloride result in no product formation, we believe that S_N2 of a Cu enolate is an unlikely pathway, and the reaction may be proceeding through a $Cu^{III}[\sigma+\pi]$ allyl species.^{4,5a}

4.9 PROPOSED CATALYTIC CYCLE

Taking all this mechanistic insight into account, we propose that the reaction follows an inner sphere Cu^I - Cu^{III} catalytic cycle as shown in Scheme 4.9.1. We believe that the catalytic cycle commences with coordination of the electron-rich olefin of the silyl ketene acetal to Cu^I bis-amidate complex **A**, forming **B**. The Si-O bond is then cleaved via outer sphere attack by the acetate anion^{2d} to afford the desired C-bound Cu enolate **C**. We envision that this could be the enantiodetermining step, during which the lithium counter-ion may assist through electrostatic interactions, preventing rotation of the silyl ketene acetal. Dissociation of the benzamide then allows for the coordination and subsequent oxidative addition of the allyl chloride, generating $Cu^{III}[\sigma+\pi]$ species **D**.²³ The sterically encumbered Cu^{III} species can then undergo reductive elimination to generate the desired α -allyl γ -butyrolactone and the starting Cu^I species **A**.

Scheme 4.9.1 Proposed Reaction Mechanism



4.10 CONCLUSION

We have performed a preliminary investigation into the reaction mechanism, with the goal of being able to expand this reaction protocol to other silyl enolate nucleophiles. Although the use of experimental techniques for the determination of the binding mode of the ligand proved unsuccessful, from DFT calculations we were able to identify that the NNO binding mode of the ligand was significantly preferred, and this preference seemed to be a consequence of the ligand itself. Furthermore, using UV-vis and EPR spectroscopic techniques, we were able to show that the starting Cu(II) complex was reduced to Cu(I) over the course of the pre-stir, and that the

reducing agent is the silyl ketene acetal **41**. On the basis of these experiments and further examples of similar reactivity in the literature, we proposed a bimolecular, radical mechanism for the reduction of the Cu catalyst. Although we do not have conclusive evidence that suggests that a Cu(I) enolate may be the reactive species, on the basis of some results we obtained during reaction screening, as well as FTIR data, and due to the similarity between our conditions and the Pd-catalyzed α -arylation conditions reported by Zhou,¹⁹ we conclude that a Cu enolate is likely to be the active species. Finally, upon examination of the effect of the electrophile olefin geometry on the reaction outcome, we noted that a Cu^{III}[$\sigma+\pi$] species that has been implicated in previous Cu-catalyzed allylic alkylation reports is a likely intermediate. For these reasons, we have proposed an inner-sphere pathway for bond formation. Future work will focus on the elucidation of the final intermediate prior to C-C bond formation (**D** in Scheme 4.9.1), as this should allow for additional insight into how the ligand sterics and electronics influence the reactivity and selectivity of the Cu catalyst, and also contribute to the ongoing debate in the literature about the viability of d⁸ Cu^{III} species.²⁴

One very interesting aspect of the reaction mechanism is that previously reported Cu-catalyzed allylic alkylations set the stereocenter on the electrophile, not the nucleophile. To our knowledge, this is the first time that a prochiral nucleophile is used in a Cu-catalyzed allylic alkylation involving an inner-sphere type pathway. We believe that this difference is also reflected in the ligand screen (See Chapter 3), as ligands typically used for this type of transformation did not lead to selective product formation. As a consequence, a novel ligand scaffold with a new backbone was required to enable the formation of the desired product in high yield and ee. We

are currently using this mechanistic insight to help us design the next generation of ligands with the aim of accommodating bulkier silyl ketene acetals (See Section A5.4).

4.11 EXPERIMENTAL SECTION

4.11.1 MATERIALS AND METHODS

Unless otherwise stated, reactions were performed in flame-dried glassware under an argon or nitrogen atmosphere using dry, deoxygenated solvents. Solvents were dried by passage through an activated alumina column under argon. Reaction progress was monitored by thin-layer chromatography (TLC) or Agilent 1290 UHPLC-MS. TLC was performed using E. Merck silica gel 60 F254 precoated glass plates (0.25 mm) and visualized by UV fluorescence quenching, *p*-anisaldehyde, or KMnO₄ staining. ((4,5-dihydrofuran-2-yl)oxy)trimethylsilane (**41**) was synthesized according to a previously reported procedure.²⁵ **L73** was synthesized according to the procedure in Chapter 3. Silicycle SiliaFlash® P60 Academic Silica gel (particle size 40–63 nm) was used for flash chromatography. ¹H NMR spectra were recorded on a Bruker Avance HD 400 MHz or Varian Mercury 300 MHz spectrometers and are reported relative to residual CHCl₃ (δ 7.26 ppm). ¹³C NMR spectra were recorded on a Bruker Avance HD 400 MHz spectrometer (101 MHz) and are reported relative to residual CHCl₃ (δ 77.16 ppm) or THF (δ 68.03). ¹⁹F NMR spectra were recorded on a Varian Mercury 300 MHz spectrometer (282 MHz). Data for ¹H NMR are reported as follows: chemical shift (δ ppm) (multiplicity, coupling constant (Hz), integration). Multiplicities are reported as follows: s = singlet, d = doublet, t = triplet, q = quartet, p = pentet, sept = septuplet, m = multiplet, br s = broad singlet, br d = broad doublet, app = apparent. Data

for ^{13}C NMR are reported in terms of chemical shifts (δ ppm). IR spectra were obtained using a Perkin Elmer Spectrum BXII spectrometer or Nicolet 6700 FTIR spectrometer using thin films deposited on NaCl plates and reported in frequency of absorption (cm^{-1}). Optical rotations were measured with a Jasco P-2000 polarimeter operating on the sodium D-line (589 nm), using a 100 mm path-length cell and are reported as: $[\alpha]_{\text{D}}^{\text{T}}$ (concentration in 10 mg/1 mL, solvent). Analytical SFC was performed with a Mettler SFC supercritical CO_2 analytical chromatography system utilizing Chiralpak (AD-H, AS-H or IC) or Chiralcel (OD-H, OJ-H, or OB-H) columns (4.6 mm x 25 cm) obtained from Daicel Chemical Industries, Ltd.. High resolution mass spectra (HRMS) were obtained from Agilent 6200 Series TOF with an Agilent G1978A Multimode source in electrospray ionization (ESI+), atmospheric pressure chemical ionization (APCI+), or mixed ionization mode (MM: ESI-APCI+), or obtained from Caltech mass spectrometry laboratory. X-Band (9.4 GHz) Continuous-wave(CW) EPR spectra were obtained using a Bruker EMX spectrometer with its Bruker Win-EPR software (version 3.0). A vacuum-insulated quartz liquid nitrogen dewar was inserted into the EPR resonator to obtain all spectra at 77 K. For optimal sensitivity, all spectra were collected with 0.5 mW microwave power and averaged over four scans. UV-Vis-NIR spectra were acquired using Varian Cary 500 Scan spectrophotometer with Varian Cary WinUV software(version 4.10(464)). Samples were loaded into 1 cm Starna Cell borosilicate cuvettes enclosed with screw caps. The spectra were collected from 300 nm to 1650 nm at a 600 nm/min scan rate and corrected for THF background. IR spectra were collected using a Bruker Alpha Platinum ATR spectrometer with OPUS software (version 7.0.129) stored in a glovebox under N_2 . An aliquot of sample solution was deposited onto the spectrometer to form a thin film, and the spectra were collected over 32 scans

All calculations were performed using the ORCA 4.1.2 package.²⁶ Unless otherwise specified, the spectroscopically calibrated Becke3-Lee-Yang-Parr density functional with 38% exact Hartree-Fock exchange (B3(38HF)LYP) was employed, similar to that reported by Solomon and coworkers.²⁷ All atoms were described with the def2-TZVP basis set. Calculations were performed with the finest available grid (Grid7) and the chain of sphere approximation (RIJCOSX) for two-electron integrals on the corresponding finest auxiliary integration grid (GRIDX9) for the RI/J auxiliary basis set. Gas-phase geometries were optimized with tight convergence criteria ($\Delta E \leq 1 \times 10^{-8}$ Hartree). Frequency calculations were used to confirm optimized structures represented local minima on the potential energy surfaces. To approximate solvent effects, single point energy calculations were performed on gas-phase optimized geometries using a conductor-like polarizable continuum model for THF. In all cases, counter ions were excluded from calculations.

Reagents were purchased from Sigma-Aldrich, Acros Organics, Strem, or Alfa Aesar and used as received unless otherwise stated.

List of Abbreviations

ee – enantiomeric excess, SFC – supercritical fluid chromatography, TLC – thin-layer chromatography, IPA – isopropanol, MTBE – methyl *tert*-butyl ether, PE – petroleum ether, DMAP – 4-dimethylaminopyridine, EtOAc – ethyl acetate, LiHMDS – lithium bis(trimethylsilyl)amide, NaHMDS – sodium bis(trimethylsilyl)amide, KHMDS – potassium bis(trimethylsilyl)amide, THF – tetrahydrofuran, TMEDA – 1,2-tetramethylethylenediamine.

4.11.2 EXPERIMENTAL PROCEDURES AND SPECTROSCOPIC DATA

4.11.2.1 Preparation of L73•CuCl₂ in THF for UV-vis, EPR, and HRMS

To a 4 mL vial containing CuCl₂ (1.34n mg, 0.01n mmol, 0.1 equiv) in the glovebox was added a solution of the **L73** (0.012n mmol, 0.12 equiv) in THF (0.4n mL), followed by a solution of LiHMDS (4.35n mg, 0.026n mmol, 0.26 equiv) in THF (0.4n mL). The resulting solution was stirred for 1 h at room temperature. The Cu/L73 solution was then diluted to the appropriate concentration (2.1 mM), or was added to a vial containing silyl ketene acetal **41** (28 mg, 0.15 mmol, 1.5 equiv) in THF (0.8 mL), and then diluted to 2.1 mM and allowed to stir for 10 min or until a color change has been observed. For the experiments containing both CsOAc and **41**, the Cu/L complex solution was added to a vial containing CsOAc (19.2 mg, 0.1 mmol, 1.0 equiv), followed immediately by the silyl ketene acetal **41** (28 mg, 0.15 mmol, 1.5 equiv) in THF (0.8 mL), and the resulting solution was diluted down to 2.1 mM. For ESI-MS (negative ion mode), the resulting solutions were diluted down even further in acetonitrile. HRMS (MM) m/z calc'd for C₂₉H₂₂Cl₂CuN₃O₂ [M+H]⁺ = 577.0385, found 577.0364.

4.11.2.2 Spin Quantification Experiment

50.0(2) mg of CuSO₄•5H₂O (0.2 mmol) was added to a 20 mL scintillation vial and dissolved in ca. 3 mL of 20% glycerol 80% water mixture. The solution was then transferred to a 10 mL volumetric flask and diluted accordingly to afford a 20 mM stock solution; calibration standards were then prepared from the stock solution. Briefly, the 1 mM and the 2 mM calibration

γ -Butyrolactone-Derived Silyl Ketene Acetal

standard were prepared directly from the stock solution. The remaining standards were prepared by diluting the 1 mM or 2 mM solution once more using volumetric pipettes and volumetric flasks of varying sizes. The error associated with concentration is estimated to be $\leq 2\%$. Given its relatively small size compared to other sources of error, we have excluded this random error from further consideration and have assumed the concentration to be absolute.

77K X-band EPR spectra were then obtained on a variety of samples with variable Cu^{II} concentrations at 0.5 mW microwave power. A linear baseline correction was performed on the resulting EPR spectra to give a zero baseline. Double integration was performed from 260 to 340 mT. The end point of integration was chosen to minimize any higher-order baseline contribution; we found this results in a 2% definition error to the double integrated intensity of the analyte. Moreover, we collected multiple spectra for a selected number of samples by first removing the sample dewar from the EPR resonator and then collecting a new set of spectra. We estimate

Figure 4.11.1. Calibration Curve for Spin Quantification

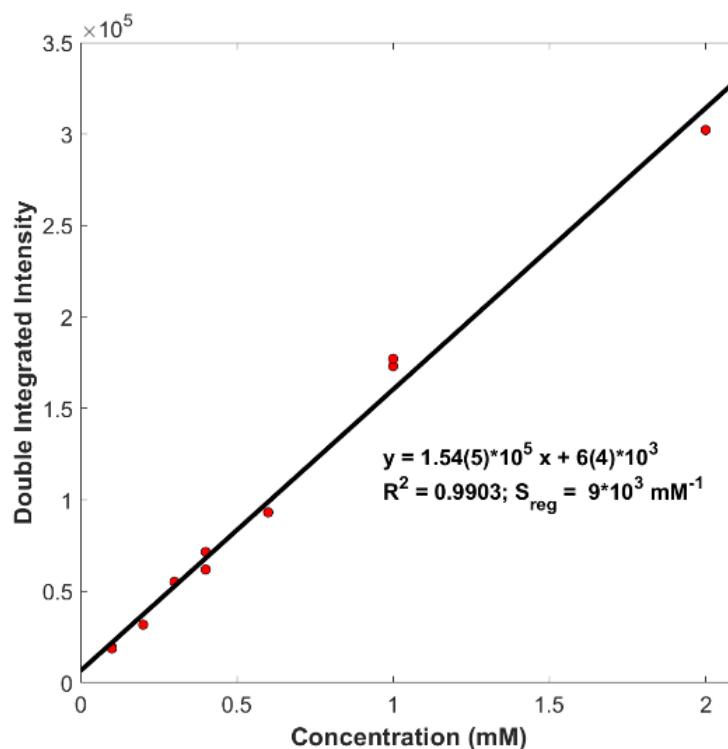
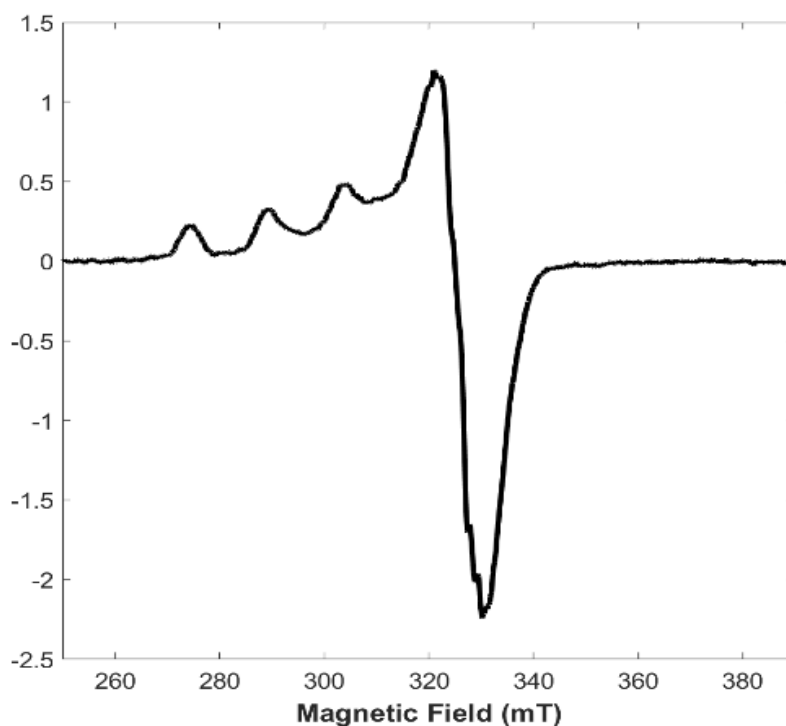


Figure 4.11.2. 77 K EPR Spectrum of **L73**•CuCl₂ in 2-MeTHF



instrument variations and the operator errors contribute 3000 to the total integrated intensity. The calibration curve and relevant statistics have been reported in Figure 4.11.1.

An aliquot of the sample was loaded into a 4.0 mm standard quartz Norell EPR tube and immediately immersed in liquid nitrogen to avoid sample decomposition. Rapid freezing also ameliorates the adverse effect from the non-glassiness of THF, as we found preparing the complex in the glassy 2-MeTHF solvent led to a yellow solution with a different EPR spectrum (Figure 4.10.2). 2 mL of the same solution of each sample was then loaded into a 1 cm borosilicate cuvette to obtain its absorption spectrum. All three samples gave optical spectra similar to that reported herein (Figure S4) and the manuscript, albeit small variations exist. As a result, we estimate a 5% error associated with the concentrations of the analyte (± 0.1 mM). Three **L73**•CuCl₂ samples give

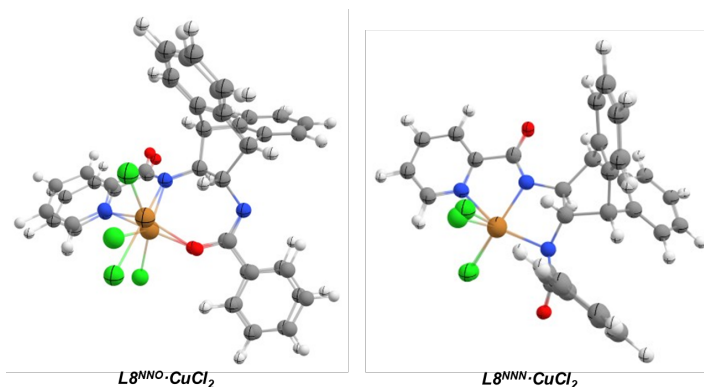
γ -Butyrolactone-Derived Silyl Ketene Acetal

double integrated intensity of $3.00 \cdot 10^5$, $2.87 \cdot 10^5$, and $2.68 \cdot 10^5$. The averaged concentration was 1.81 mM with a standard deviation of 0.1 mM.

4.11.2.3 Supporting Computational Results

To understand how variations in the optimized geometry affected single point energy calculations, we re-optimized the B3(38HF)LYP-optimized geometry (**Geometry B**) with the B3(0HF)LYP density functional (Figure 4.11.3). The resulting structures (**Geometry A**) show increased deviation from a trigonal bipyramidal geometry ($\tau_5 = 1$) towards square pyramidal geometry ($\tau_5 = 0$, Table 4.11.1).

Figure 4.11.3. Hartree-Fock dependence on $L73^{NNO} \cdot CuCl_2$ (left) versus $L73^{NNN} \cdot CuCl_2$ (right) geometry^a



[a] Geometry A (grid): B3(0HF)LYP optimized geometry; Geometry B (filled): B3(38HF)LYP optimized geometry

γ -Butyrolactone-Derived Silyl Ketene Acetal

Using the two optimized structures, we examined the Hartree-Fock dependence on the energy difference between **L73**^{NNO}•CuCl₂ and **L73**^{NNN}•CuCl₂ ($\Delta E \equiv E_{\text{NNN}} - E_{\text{NNO}}$, Table 4.11.2). Despite **L73**^{NNO}•CuCl₂ exhibiting a modest structural variation between different functionals, the energy difference between NNO vs. NNN coordination between the different geometries remains relatively small (entries 1 and 6, or entries 2 and 8). Additionally, within the same geometry, increasing the amount of Hartree-Fock exchange increases the energy gap between NNO/NNN coordination (entries 1 and 2; entries 3-5, or entries 5-8); this observation is maintained for calculations with solvent correction (entries 9-11, or entries 11-14). Solvent correction also

Table 4.11.1. Effects of Levels of Theory on the Optimized Geometry of **L73**•CuCl₂

L73 ^{NNO} •CuCl ₂	Geometry A	Geometry B	L73 ^{NNN} •CuCl ₂	Geometry A	Geometry B
bond lengths (Å)			bond lengths (Å)		
Cu-N1	2.16	2.07	Cu-N1	2.10	2.20
Cu-N2	2.06	2.16	Cu-N2	2.03	2.05
Cu-O	2.10	1.95	Cu-O	2.17	2.15
Cu-Cl1	2.39	2.48	Cu-Cl1	2.62	2.62
Cu-Cl2	2.37	2.54	Cu-Cl2	2.31	2.36
bond angles (°)			bond angles (°)		
N1-Cu-N2	78	77	N1-Cu-N2	77	75
N1-Cu-O	125	174	N1-Cu-N3	160	158
N1-Cu-Cl1	108	89	N1-Cu-Cl1	88	87
N1-Cu-Cl2	90	86	N1-Cu-Cl2	92	89
N2-Cu-O	90	99	N2-Cu-N3	83	83
N2-Cu-Cl1	96	122	N2-Cu-Cl1	99	103
N2-Cu-Cl2	165	120	N2-Cu-Cl2	151	143
O-Cu-Cl1	127	97	N3-Cu-Cl1	96	98
O-Cu-Cl2	89	92	N3-Cu-Cl2	105	108
Cl1-Cu-Cl2	97	114	Cl1-Cu-Cl2	108	109
τ_s	0.64	0.86	τ_s	0.15	0.24

Table 4.11.2. Effects of Levels of Theory on the Energy Barrier

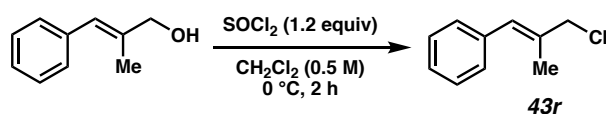
entry	density functional	geometry	solvent correction	E _{NNO} (Hartree)	E _{NNN} (Hartree)	ΔE (Hartree)	ΔE (kcal/mol)
1	B3(0HF)LYP	Geometry A	none	-3987.8133	-3987.7866	0.0267	16.8
2	B3(38HF)LYP	Geometry A	none	-3997.8498	-3997.8189	0.0309	19.4
3	BP86	Geometry B	none	-3994.4699	-3994.4422	0.0277	17.4
4	TPSSh	Geometry B	none	-3994.2266	-3994.1974	0.0292	18.3
5	B3LYP	Geometry B	none	-3993.0735	-3993.0411	0.0324	20.3
6	B3(0HF)LYP	Geometry B	none	-3987.8063	-3987.7774	0.0289	18.1
7	B3(10HF)LYP	Geometry B	none	-3990.4324	-3990.4018	0.0306	19.2
8	B3(38HF)LYP	Geometry B	none	-3997.8647	-3997.8289	0.0358	22.5
9	BP86	Geometry B	CPCM	-3994.6932	-3994.6685	0.0247	15.5
10	TPSSh	Geometry B	CPCM	-3994.4522	-3994.4265	0.0257	16.1
11	B3LYP	Geometry B	CPCM	-3993.2977	-3993.2728	0.0249	15.6
12	B3(0HF)LYP	Geometry B	CPCM	-3988.0281	-3988.0059	0.0222	13.9
13	B3(10HF)LYP	Geometry B	CPCM	-3990.6555	-3990.6321	0.0234	14.7
14	B3(38HF)LYP	Geometry B	CPCM	-3998.0902	-3998.0591	0.0311	19.5

γ -Butyrolactone-Derived Silyl Ketene Acetal

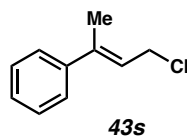
reduces the energy separation between the two coordination modes. As discussed in the manuscript, similar energy differences between **L73**^{NNO} and **L73**^{NNN} are observed upon removal of Cu^{II}Cl₂, suggesting electronic differences between Cu-O and Cu-N bonding do not play a major role in determining the ligand binding and are likely secondary to steric contributions. Indeed, by comparing both electronic energy and Gibbs free energy, we found steric contributions enforce **L73**^{NNO} coordination mode for a series of possible copper intermediates (Table S3).

4.11.2.4 Synthesis of Allylic Chloride Electrophiles

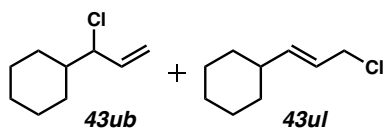
General Procedure: Synthesis of Allylic Chlorides (**43r**, **43s**, **43u**).



(E)-(3-chloro-2-methylprop-1-en-1-yl)benzene (43r): (*E*)-2-methyl-3-phenylprop-2-en-1-ol (1.03 g, 6.98 mmol, 1.0 equiv) was dissolved in methylene chloride (14 mL, 0.5 M). Then, thionyl chloride (610 μ L, 8.4 mmol, 1.2 equiv) was added dropwise. The reaction was allowed to stir for 2 h at 0 °C, then quenched with saturated aqueous NaHCO₃ solution (6 mL) and allowed to warm to room temperature. The aqueous layer was extracted with methylene chloride three times, and the resulting organic layers were dried over Na₂SO₄ and concentrated. The crude oil was then re-suspended in hexanes (10 mL) and washed with water 4 times. The hexanes layer was then dried with Na₂SO₄ and concentrated to afford the desired allylic chloride **43r** as a white solid (1.14 g, 6.84 mmol, 98% yield); ¹H NMR (300 MHz, CDCl₃) δ 7.26 (s, 6H), 6.56 (s, 1H), 4.16 (t, *J* = 2.0 Hz, 2H), 1.96 (q, *J* = 2.2, 1.8 Hz, 3H); All characterization data match those reported.²⁸

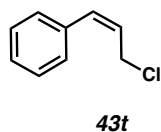


(E)-(4-chlorobut-2-en-2-yl)benzene (1t): 883 mg, 5.29 mmol, 76% yield; ^1H NMR (300 MHz, CDCl_3) δ 7.45 – 7.26 (m, 6H), 6.00 (tq, $J = 8.0, 1.4$ Hz, 1H), 4.29 (d, $J = 8.0$ Hz, 2H), 2.15 (d, $J = 1.5$ Hz, 3H); All characterization data match those reported.²⁸



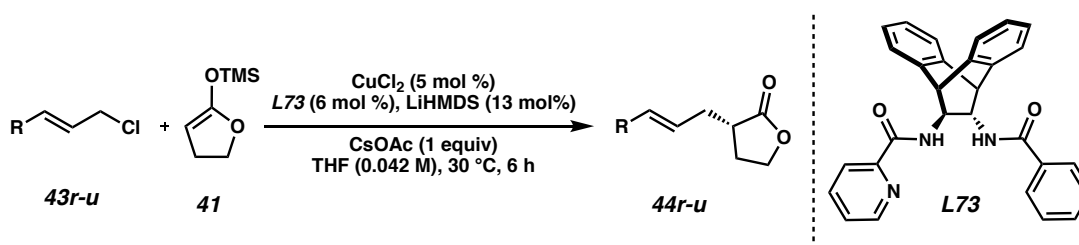
(E)-(3-chloroprop-1-en-1-yl)cyclohexane(43ul) and (1-chloroallyl)cyclohexane (43ub):

Isolated as an inseparable mixture of constitutional isomers **43ul** and **43ub** (623 mg, 3.9 mmol, 78% yield, **43ul**:**43ub** = 1:2.8); ^1H NMR (400 MHz, CDCl_3) **43ul**: 5.71 (ddt, $J = 15.3, 6.5, 1.0$ Hz, 1H), 5.55 (dtd, $J = 15.3, 7.0, 1.3$ Hz, 1H), 4.03 (dt, $J = 7.0, 0.8$ Hz, 2H), 1.93 (m, 1H), 1.83 – 1.56 (m, 5H), 1.33 – 0.95 (m, 5H); **43ub**: δ 5.88 (ddd, $J = 16.9, 10.1, 8.9$ Hz, 1H), 5.31 – 5.09 (m, 2H), 4.17 (dd, $J = 8.9, 6.4$ Hz, 1H), 1.93 (ddt, $J = 12.8, 3.6, 1.8$ Hz, 1H), 1.83 – 1.56 (m, 5H), 1.33 – 0.95 (m, 5H); **43ul** and **43ub**: ^{13}C NMR (101 MHz, CDCl_3) δ 141.9, 137.5, 123.6, 117.2, 69.4, 46.0, 44.5, 40.3, 32.6, 29.8, 29.6, 26.4, 26.2, 26.14, 26.07, 26.05; δ IR (Neat Film, NaCl) 3084, 2926, 2853, 1641, 1450, 1419, 1300, 1249, 1197, 987, 968, 926, 891, 780, 756, 688 cm^{-1} ; HRMS (MM) m/z calc'd for $\text{C}_9\text{H}_{15}\text{Cl}$ $[\text{M}]^{+*}$: 158.0862, found 158.0859.



γ -Butyrolactone-Derived Silyl Ketene Acetal

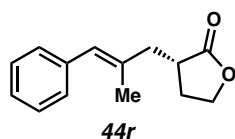
(Z)-(3-chloroprop-1-en-1-yl)benzene (43t): Compound **43t** was prepared from the corresponding allylic alcohol according to a previously reported procedure (Z:E=97:3). ^1H NMR (300 MHz, CDCl_3) δ 7.44 – 7.35 (m, 2H), 7.34 – 7.27 (m, 3H), 6.67 (d, J = 11.4 Hz, 1H), 5.98 – 5.85 (m, 1H), 4.32 – 4.25 (m, 2H); All characterization data match those reported.²⁹

4.11.2.5 Procedure for Cu-Catalyzed Allylic Alkylation Reaction

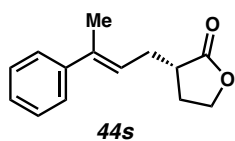
n = number of reactions. To a 4 mL vial containing CuCl_2 (1.34n mg, 0.01n mmol, 0.05 equiv) in the glovebox was added a solution of the **L73** (5.2n mg, 0.012n mmol, 0.06 equiv) in THF (0.8n mL), followed by a solution of LiHMDS (4.35n mg, 0.026n mmol, 0.13 equiv) in THF (0.8n mL). The resulting solution was stirred for 1 h at room temperature. This solution (1.6 mL) was then transferred to a vial containing CsOAc, followed by silyl ketene acetal **41** (47.5 mg, 0.3 mmol, 1.5 equiv) in THF (1.6 mL). The mixture was allowed to stir for 5 min, then allyl chloride (30.4 mg, 0.2 mmol, 1 equiv) in THF (1.6 mL) was added and the reaction was allowed to stir for 6 h at 30 °C. The reaction was then quenched with sat. NH_4Cl solution and a few drops of TMEDA, and the aqueous layer was extracted five times with ethyl acetate. The combined organic extracts were dried with Na_2SO_4 , and concentrated by rotary evaporator. The crude oil was then purified by column chromatography to afford the desired product.

4.11.2.6 Spectroscopic Data for Products from Catalytic Reactions

Please note that the absolute configuration was determined only for compound **44b** via x-ray crystallographic analysis (See Appendix 8). The absolute configuration for all other products has been inferred by analogy.

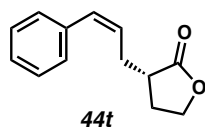


(S,E)-3-(2-methyl-3-phenylallyl)dihydrofuran-2(3H)-one (44r): Product **44r** was purified by column chromatography (25% EtOAc in hexanes) to provide a colorless oil (37.6 mg, 0.17 mmol, 87% yield); 89% *ee*; $[\alpha]_D^{25}$ 57.81 (*c* 0.80, CHCl₃); ¹H NMR (400 MHz, CDCl₃) δ 7.37 – 7.30 (m, 2H), 7.26 – 7.17 (m, 3H), 6.34 (s, 1H), 4.38 (td, *J* = 8.8, 3.2 Hz, 1H), 4.24 (td, *J* = 9.2, 6.9 Hz, 1H), 2.91 – 2.74 (m, 2H), 2.38 (dddd, *J* = 12.8, 8.5, 6.9, 3.3 Hz, 1H), 2.32 – 2.20 (m, 1H), 2.13 – 1.96 (m, 1H), 1.89 (d, *J* = 1.3 Hz, 3H); ¹³C NMR (101 MHz, CDCl₃) δ 179.4, 179.10, 137.8, 135.4, 128.9, 128.3, 127.6, 126.5, 66.7, 41.5, 38.1, 28.4, 17.6; IR (Neat Film, NaCl) 2912, 1768, 1490, 1442, 1373, 1205, 1178, 1149, 1022, 958, 920, 746, 700, 668 cm⁻¹; HRMS (MM) *m/z* calc'd for C₁₄H₁₇O₂ [M+H]⁺: 217.1223, found 217.1224; SFC Conditions: 20% IPA, 2.5 mL/min, Chiralcel OD-H column, λ = 254 nm, *t_R* (min): minor = 4.57, major = 5.37.



γ -Butyrolactone-Derived Silyl Ketene Acetal

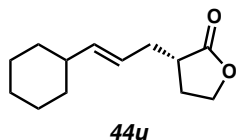
(E)-3-(3-phenylbut-2-en-1-yl)dihydrofuran-2(3H)-one (44s): Product **44s** was purified by column chromatography (20% EtOAc in hexanes) to provide a colorless oil (28.1 mg, 0.13 mmol, 65% yield, 20:1 E:Z); 5% *ee*; ^1H NMR (400 MHz, CDCl_3) δ 7.41 – 7.28 (m, 4H), 7.26 (m, 1H), 5.73 (tq, J = 7.5, 1.5 Hz, 1H), 4.36 (td, J = 8.8, 3.0 Hz, 1H), 4.21 (td, J = 9.3, 6.8 Hz, 1H), 2.83 – 2.65 (m, 2H), 2.52 – 2.33 (m, 2H), 2.13 – 1.95 (m, 4H); ^{13}C NMR (101 MHz, CDCl_3) δ 179.1, 143.5, 138.0, 128.4, 127.2, 125.8, 123.6, 66.7, 39.6, 29.3, 28.2, 16.3; IR (Neat Film, NaCl) 2922, 2855, 1760, 1597, 1494, 1456, 1374, 1311, 1203, 1182, 1149, 1068, 1022, 960, 760, 696, 676, 666; HRMS (MM) m/z calc'd for $\text{C}_{15}\text{H}_{17}\text{O}_2$ $[\text{M}+\text{H}]^+$: 217.1223, found 217.1223; SFC Conditions: 10% IPA, 2.5 mL/min, Chiralpak AD-H column, λ = 254 nm, t_{R} (min): minor = 5.09, major = 5.54.



(S,Z)-3-(3-phenylallyl)dihydrofuran-2(3H)-one (44t): Product **44t** was purified by column chromatography (25% EtOAc in hexanes) to provide a colorless oil (34.0 mg, 0.17 mmol, 84% yield); 73% *ee*; $[\alpha]_{\text{D}}^{25}$ 53.19 (c 0.80, CHCl_3); **Z isomer** (for E isomer, see data for **3a**): ^1H NMR (400 MHz, CDCl_3) δ 7.38 – 7.29 (m, 2H), 7.26 (m, 3H), 6.59 (dt, J = 11.7, 1.9 Hz, 1H), 5.64 (dt, J = 11.5, 7.2 Hz, 1H), 4.31 (td, J = 8.8, 3.0 Hz, 1H), 4.19 (td, J = 9.3, 6.8 Hz, 1H), 2.90 (dddd, J = 15.0, 6.8, 4.5, 1.9 Hz, 1H), 2.68 (dtd, J = 9.9, 8.7, 4.4 Hz, 1H), 2.57 (dddd, J = 14.9, 9.0, 7.3, 1.7 Hz, 1H), 2.37 (dddd, J = 12.8, 8.7, 6.8, 2.9 Hz, 1H), 1.94 (dtd, J = 12.8, 9.8, 8.5 Hz, 1H); ^{13}C NMR (101 MHz, CDCl_3) δ 178.9, 137.0, 131.9, 128.8, 128.5, 128.1, 127.1, 66.7, 39.6, 29.0, 28.2; IR (Neat Film, NaCl) 3016, 2912, 1766, 1598, 1494, 1448, 1374, 1308, 1208, 1150, 1074, 1023, 967, 768, 702 cm^{-1} ; HRMS (MM) m/z calc'd for $\text{C}_{13}\text{H}_{15}\text{O}_2$ $[\text{M}+\text{H}]^+$: 203.1067, found 203.1062; SFC

γ -Butyrolactone-Derived Silyl Ketene Acetal

Conditions: 15% IPA, 2.5 mL/min, Chiralpak AD-H column, λ = 254 nm, t_R (min): major = 3.06, minor = 3.43.



(*S,E*)-3-(3-cyclohexylallyl)dihydrofuran-2(3*H*)-one (44u): Product **44u** was purified by column chromatography (25% EtOAc in hexanes) to provide a colorless oil (37.3 mg, 0.18 mmol, 90% yield); 87% *ee*; $[\alpha]_D^{25}$ 16.32 (*c* 0.60, CHCl₃); ¹H NMR (400 MHz, CDCl₃) δ 5.48 (dd, *J* = 15.4, 6.7 Hz, 1H), 5.37 – 5.26 (m, 1H), 4.30 (td, *J* = 8.8, 3.5 Hz, 1H), 4.19 (td, *J* = 9.1, 7.0 Hz, 1H), 2.59 (qd, *J* = 9.0, 4.4 Hz, 1H), 2.50 (ddd, *J* = 14.2, 6.8, 4.5 Hz, 1H), 2.32 (dddd, *J* = 12.5, 8.9, 7.0, 3.5 Hz, 1H), 2.20 (dt, *J* = 14.8, 7.8 Hz, 1H), 2.05 – 1.86 (m, 2H), 1.67 (dddt, *J* = 19.5, 15.5, 8.6, 4.0 Hz, 5H), 1.31 – 0.96 (m, 5H); ¹³C NMR (101 MHz, CDCl₃) δ , 179.2, 140.3, 123.0, 66.8, 40.8, 39.4, 33.4, 33.2, 27.7, 26.3, 26.1; IR (Neat Film, NaCl) 2923, 2850, 1773, 1483, 1448, 1375, 1300, 1258, 1202, 1180, 1157, 1024, 971, 894, 706, 663 cm⁻¹; HRMS (MM) *m/z* calc'd for C₁₃H₂₁O₂ [M+H]⁺: 209.1536, found 209.1537; SFC Conditions: 10% IPA, 2.5 mL/min, Chiralpak AD-H column, λ = 210 nm, t_R (min): major = 3.32, minor = 3.53.

4.12 REFERENCES AND NOTES

1. Hartwig, J. F. *Organotransition Metal Chemistry: From Bonding to Catalysts*; University Science Books: Mill Valley, CA 2010.
2. Corey, E. J.; Posner, G. H. *J. Am. Chem. Soc.* **1967**, 89, 3911–3912.

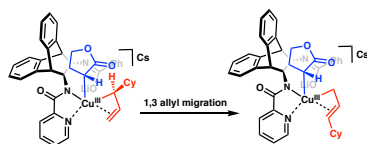
γ-Butyrolactone-Derived Silyl Ketene Acetal

3. For select reviews see: (a) Falciola, C. A.; Alexakis, A. *Eur. J. Org. Chem.* **2008**, 3765–3780.
(b) Alexakis, A.; Bäckvall, J. E.; Krause, N.; Pàmies, O.; Diéguez, M. *Chem. Rev.* **2008**, *108*, 2796–2823. (c) Harutyunyan, S. R.; den Hartog, T.; Geurts, K.; Minnaard, A. J.; Feringa, B. L. *Chem. Rev.* **2008**, *108*, 2824–2852.
4. (a) Yamanaka, M.; Kato, S.; Nakamura, E. *J. Am. Chem. Soc.* **2004**, *126*, 6287–6293. (b) Yoshikai, N.; Zhang, S.-L.; Nakamura, E. *J. Am. Chem. Soc.* **2008**, *130*, 12862–12863. (c) Yoshikai, N.; Nakamura, E. *Chem. Rev.* **2012**, *112*, 2339–2372.
5. For examples see: (a) Harada, A.; Makida, Y.; Sato, T.; Ohmiya, H.; Sawamura, M. *J. Am. Chem. Soc.* **2014**, *136*, 13932–13939. (b) Shi, Y.; Jung, B.; Torker, S.; Hoveyda, A. H. *J. Am. Chem. Soc.* **2015**, *137*, 8948–8964.
6. Trillo, P.; Baeza, A. *Adv. Synth. Catal.* **2017**, *359*, 1735–1741
7. Deng, Q.-H.; Wadehohl, H.; Gade, L. H. *J. Am. Chem. Soc.* **2012**, *134*, 2946–2949
8. The use of first row transition metals in allylation is mainly limited to 1,3-dicarbonyls: (a) Alexakis, A.; Begouin, J. M.; Crawley, M. L.; Guiry, P. J.; Kammerer-Pentier, C.; Kleimark, J.; Klein, J. E. M. N.; Langlois, J. -B.; Liron, F.; Liu, W. -B.; Milhau, L.; Moberg, C.; Norrby, P. -O.; Plietker, B.; Poli, G.; Prestat, G.; Trost, B. M. Weickmann, D.; Xia, J.-B.; You, S. – L. *Transition Metal Catalyzed Enantioselective Allylic Substitution in Organic Synthesis*; Kazmeier, U., Eds.; Springer, New York, 2012, vol. 38, pp1-341. To our knowledge, there is only one report with Ni: (b) Wang, J.; Wang, P.; Wang, L.; Li, D.; Wang, K.; Wang, Y.; Zhu, H.; Yang, D.; Wang, R. *Org. Lett.* **2017**, *19*, 4826–4829.
9. Trost, B. M.; Van Vranken, D. L. *Chem. Rev.* **1996**, *96*, 395–422.
10. Iqbal, J.; Bhatia, B.; Nayyar, N. K. *Chem. Rev.* **1994**, *94*, 519–564.
11. Van Hoomissen, D. J.; Vyas, S. *J. Org. Chem.* **2017**, *82*, 5731–5742.

12. Mulqi, M.; Stephens, F. S.; Vagg, R. S. *Inorg. Chim. Acta*, **1981**, *51*, 9–14. (b) Mulqi, M.; Stephens, F. S.; Vagg, R. S. *Inorg. Chim. Acta*, **1981**, *52*, 177–182. (c) Fan, X.; Zhang, X.; Li, C.; Gu, Z. *ACS Catal.* **2019**, *9*, 2286–2291. (d) Carlo Sambiagio. Investigations on the use of Amidic Ligands in Copper-Catalyzed Arylation Reactions, Ph.D. Dissertation, University of Leeds, Leeds, West Yorkshire, England, 2015.
13. (a) Trost, B. M.; Dogra, K.; Hachiya, I.; Emura, T.; Hughes, D. L.; Krska, S.; Reamer, R. A.; Palucki, M.; Yasuda, N.; Reider, P. *Angew. Chem. Int. Ed.* **2002**, *41*, 1929–1932, *Angew. Chem.* **2002**, *114*, 2009–2012
14. (a) Ouali, A.; Taillefer, M.; Spindler, J. –F. Jutand, A. *Organomet.* **2007**, *26*, 65–74. (b) Giri, R.; Brusoe, A. Troshin, K.; Wang, J. Y. Font, M. Hartwig, J. F. *J. Am. Chem. Soc.* **2018**, *140*, 793–806. (c) Yoshikai, N.; Nakamura, E. *Chem. Rev.* **2012**, *112*, 2339–2372.
15. Okuniewski, A.; Rosiak, D.; Chojnacki, J.; Becker, B. *Polyhedron.* **2015**, *90*, 47–57
16. (a) Ito, Y.; Konoike, T.; Saegusa, T. *J. Am. Chem. Soc.* **1975**, *97*, 2912–2914. (b) Rathke, M.; Lindert, A. *J. Am. Chem. Soc.* **1971**, *93*, 4605–4606. In addition, an outer-sphere electron transfer mechanism could also be plausible.
17. (a) Evans, R. W.; Zbieg, J. R.; Zhu, S.; Li, W.; MacMillan, D. W. C. *J. Am. Chem. Soc.* **2013**, *135*, 16074–16077. (b) Kochi, J. K. *J. Am. Chem. Soc.* **1955**, *77*, 5724–5728. (e) Kosower, E. M.; Cole, W. J.; Wu, G. –S, Cardy, D. E.; Meisters, G. *J. Org. Chem.* **1963**, *28*, 630–633. (c) Kosower, E. M.; Wu, G. –S. *J. Org. Chem.* **1963**, *28*, 633–638.
18. Bowmaker, G. A.; Di Nicola, C.; Pettinari, C.; Skelton, B. W.; Somers, N.; White, A. H. *Dalton Trans.*, **2011**, *40*, 5102–5115.
19. Huang, Z.; Chen, Z.; Lim, L. H.; Quang, G. C. P.; Hirao, H.; Zhou, J. *Angew. Chem. Int. Ed.* **2013**, *52*, 5807–5812, *Angew. Chem.* **2013**, *125*, 5919–5924.

γ -Butyrolactone-Derived Silyl Ketene Acetal

20. Although this result may be counter-intuitive, there are examples that show that the enantiomer that is higher in energy is the favored one, as it is the least stable and may have smaller energetic barriers to cross in order for product formation to occur (see ref. 1).
21. Although we observed a large amount of the branched product when the α -methyl γ -butyrolactone silyl ketene acetal is used, we believe that product formation with this nucleophile is occurring via a different pathway (See Scheme A5.3.2).
22. We envision that if an outer-sphere mode of attack were likely, the reaction outcome could be more sensitive to the size and geometry of the external ligand, and we would have observed a larger distribution of linear:branched ratios in our initial ligand screen.
23. We believe that oxidative addition to **1v** generates a sterically congested $\text{Cu}^{\text{III}}[\sigma+\pi]$ allyl species which undergoes a 1,3 allyl migration (see ref. 4,5a).



24. DiMucci, M. I.; Lukens, J. T.; Chatterjee, s.; CArsch, K. M.; Titus, C. J.; Lee, S. J.; Nordlund, D.; Betley, T. A.; MacMillan, S. N.; Lancaster, K. M. *J. Am. Chem. Soc.* **2019**, *141*, 18508–18520.
25. Oisaki, K.; Suto, Y.; Kanai, M.; Shibasaki, M.; *J. Am. Chem. Soc.* **2003**, *125*, 5644–5645.
26. (a) Neese, F. The ORCA program system. *WIREs. Comput. Mol. Sc.* **2012**, *2*, 73-78 (b) Neese, F. Software update: the ORCA program system, version 4.0. *WIREs. Comput. Mol. Sc.* **2017**, *8*, e1327.

γ-Butyrolactone-Derived Silyl Ketene Acetal

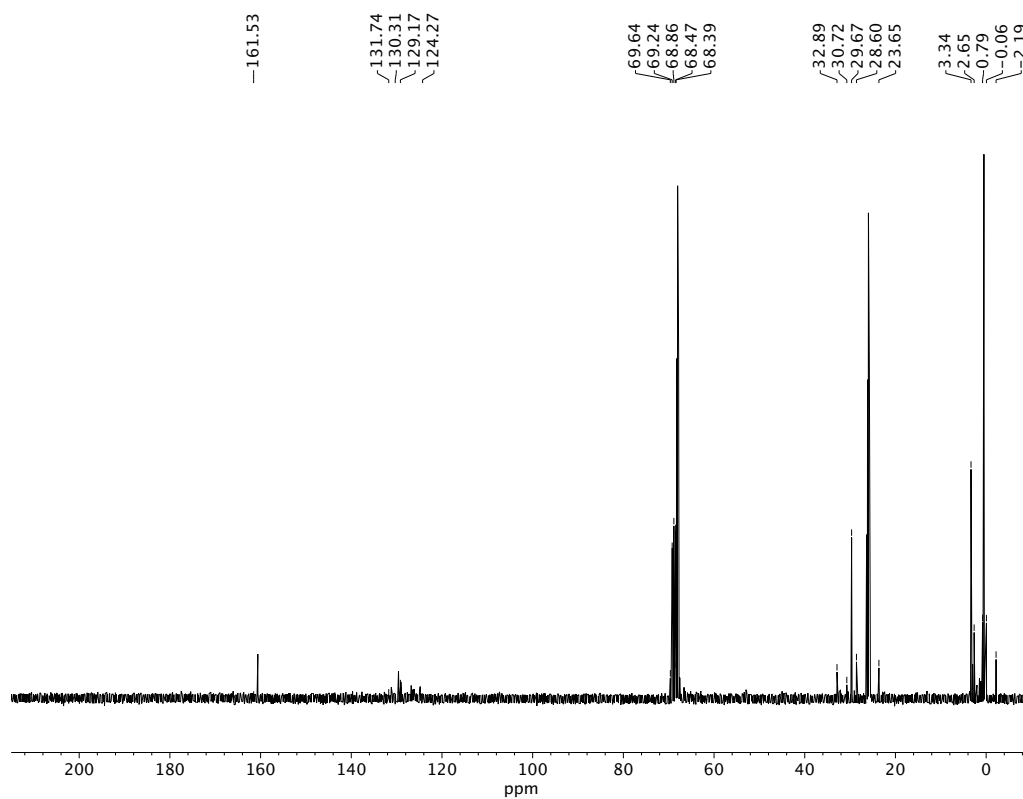
27. (a) Solomon, E. I.; Szilagyi, R. K.; DeBeer George, S.; Basumallick, L. *Chem. Rev.* **2004**, *104*, 419–458. (b) Szilagyi, R. K.; Metz, M.; Solomon, E. I. *J. Phys. Chem. A.* **2002**, *106*, 2994–3007.
28. Falciola, C. A.; Tissot-Crosset, K.; Reyneri, H.; Alexakis, A. *Adv. Synth. Catal.* **2008**, *350*, 1090–1100.
29. Delvos, L. B.; Vyas, D. J.; Oestreich, M. *Angew. Chem. Int. Ed.* **2013**, *52*, 4650–4653.

APPENDIX 9

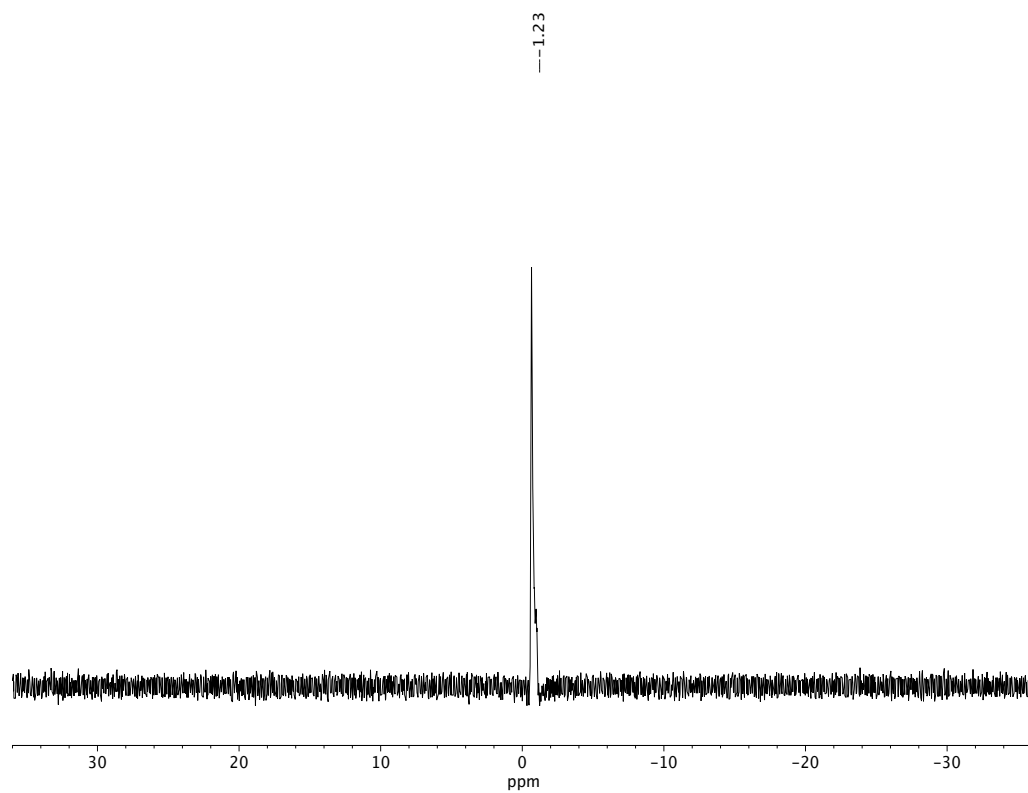
Spectra Relevant to Chapter 4:

Mechanistic Investigations for Cu-Catalyzed Enantioselective Allylic

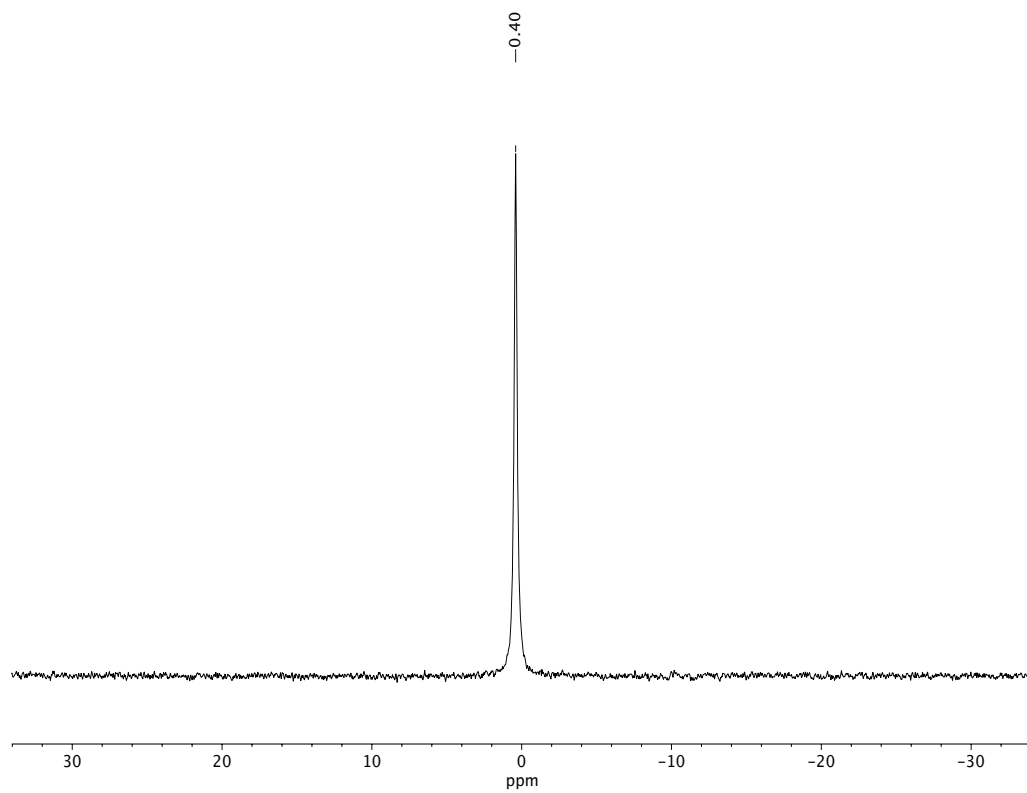
Alkylation with a γ -Butyrolactone-Derived Silyl Ketene Acetal



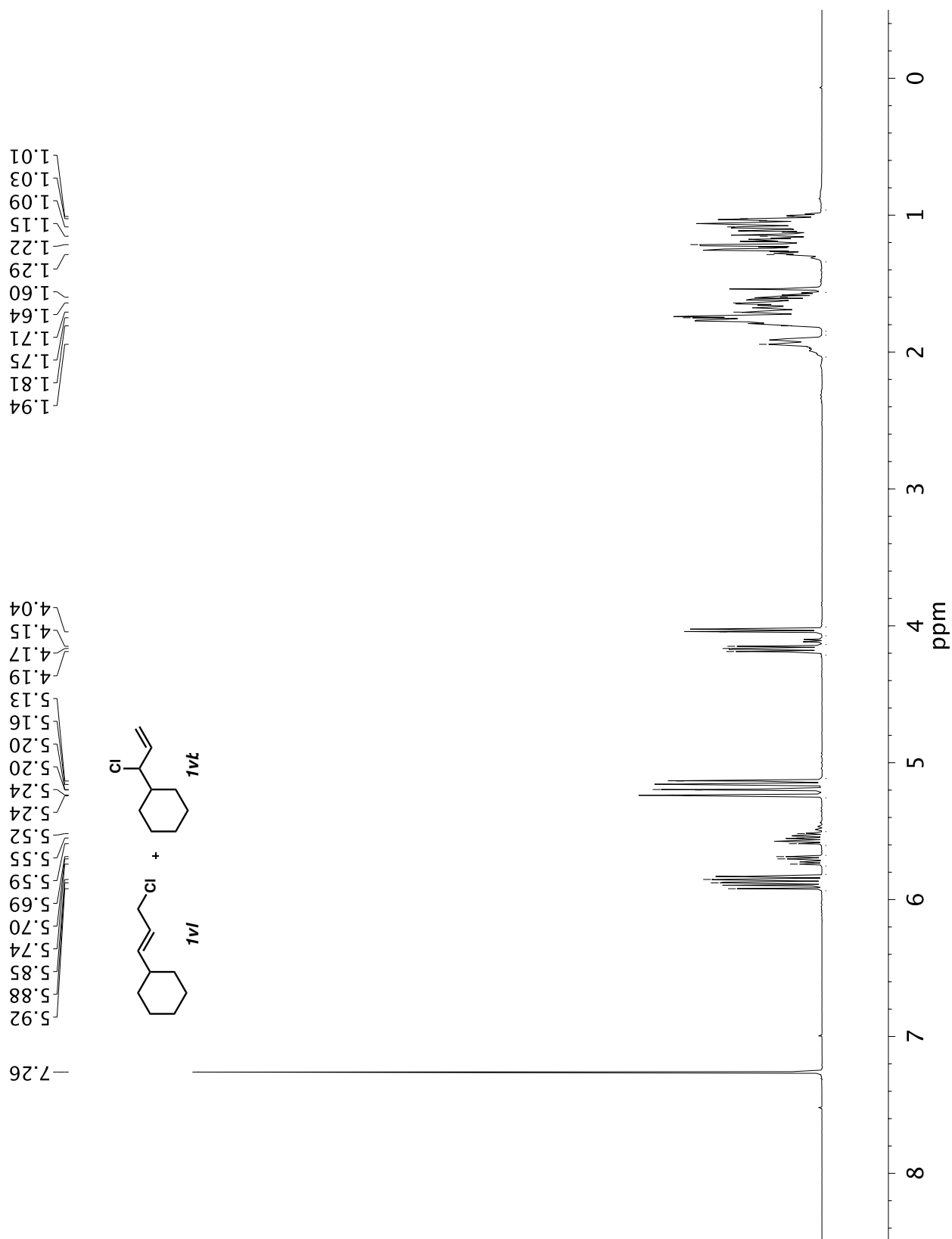
A9.1 ^{13}C NMR (101 MHz, *d*-THF) of **L73**•**CuCl₂** +30 equiv **41**

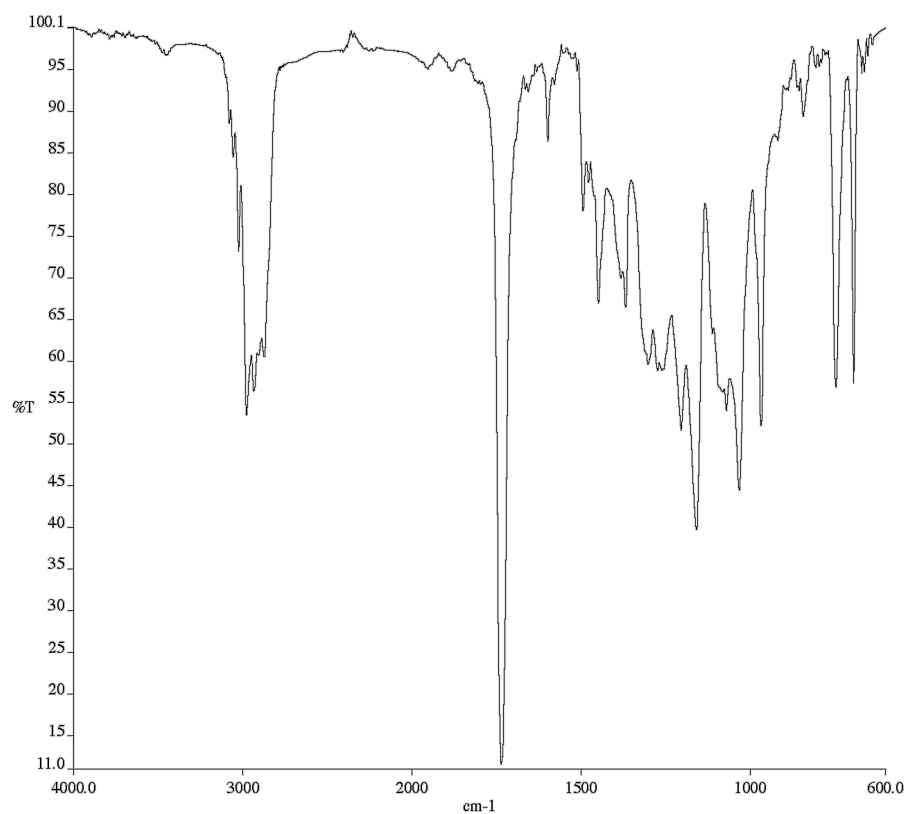


A9.2 ^7Li NMR (155 MHz, *d*-THF) of **L73**•**CuCl₂**

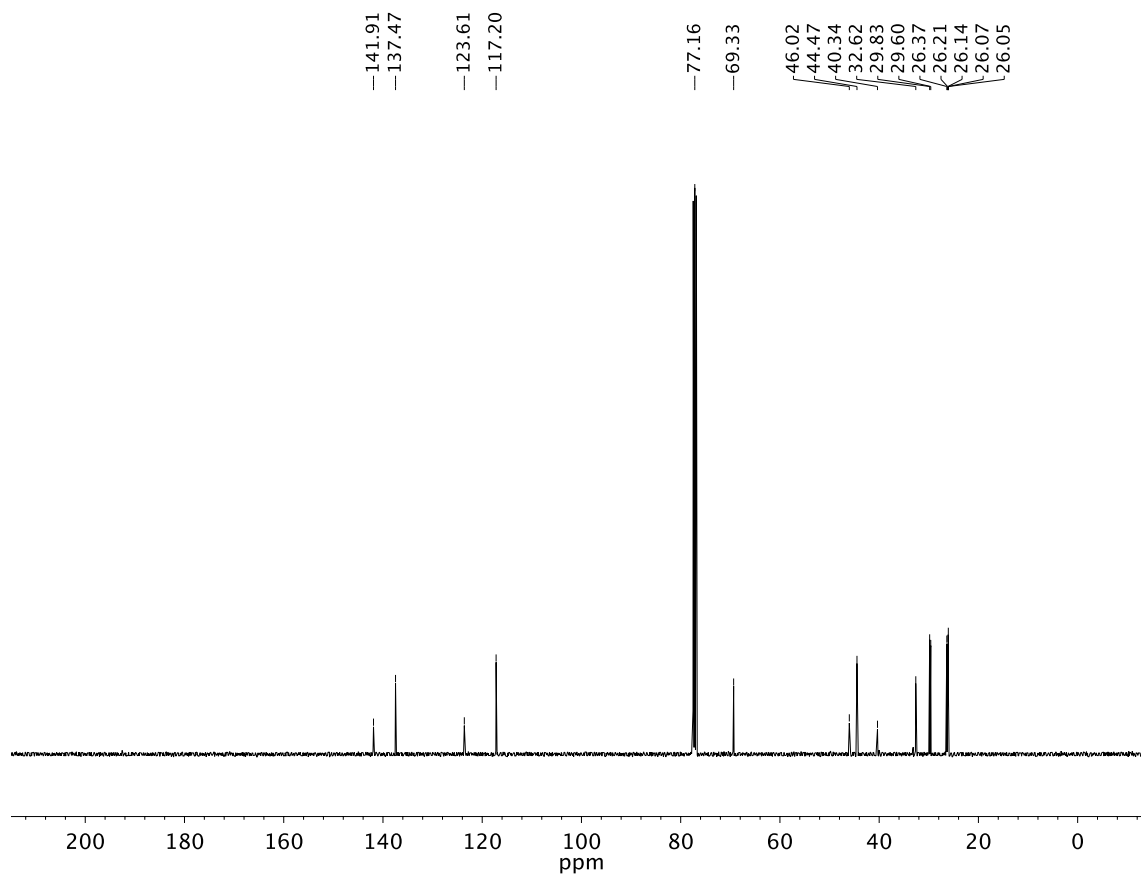


A9.3 ^7Li NMR (155 MHz, *d*-THF) of **L73**• CuCl_2 + 30 equiv **41**

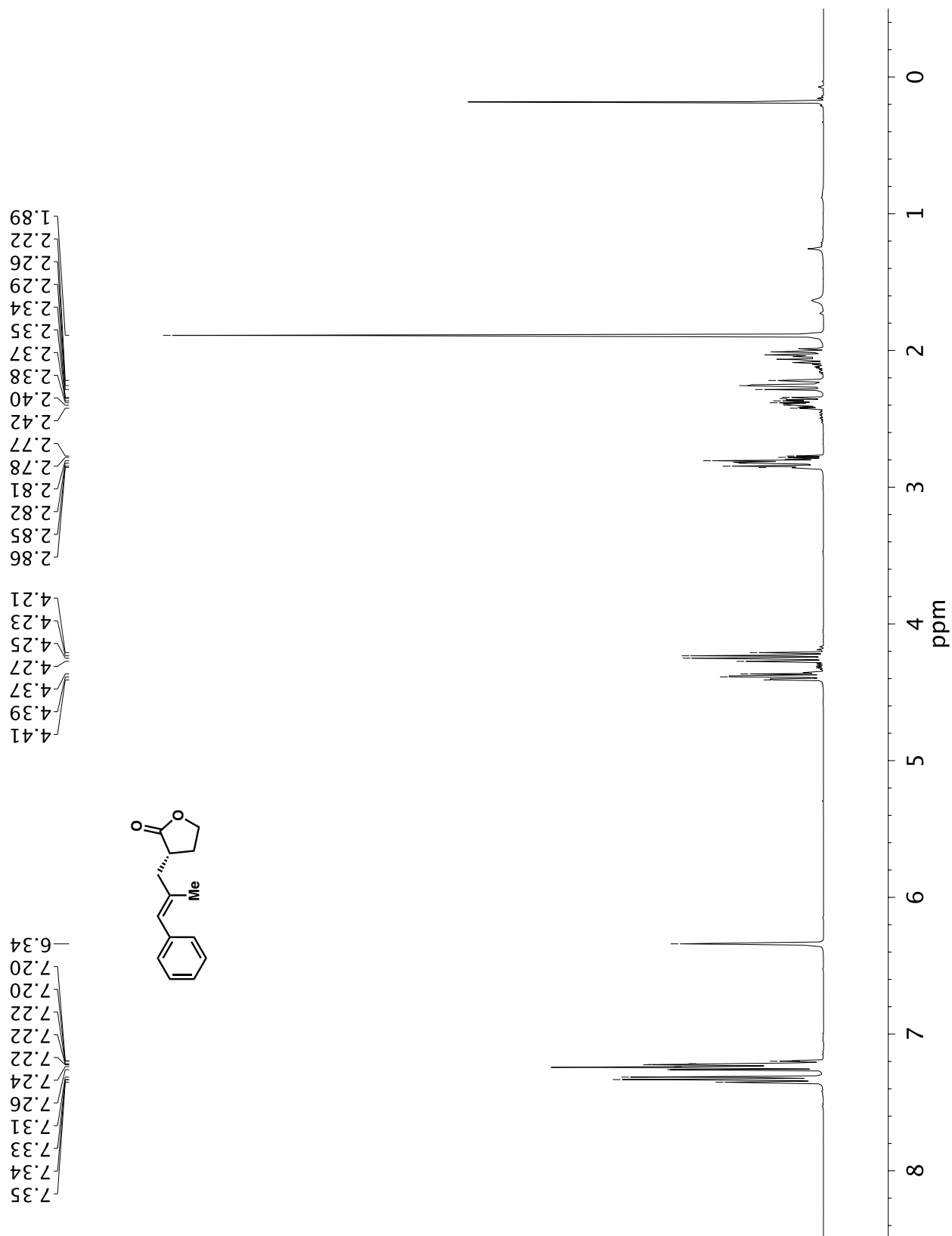


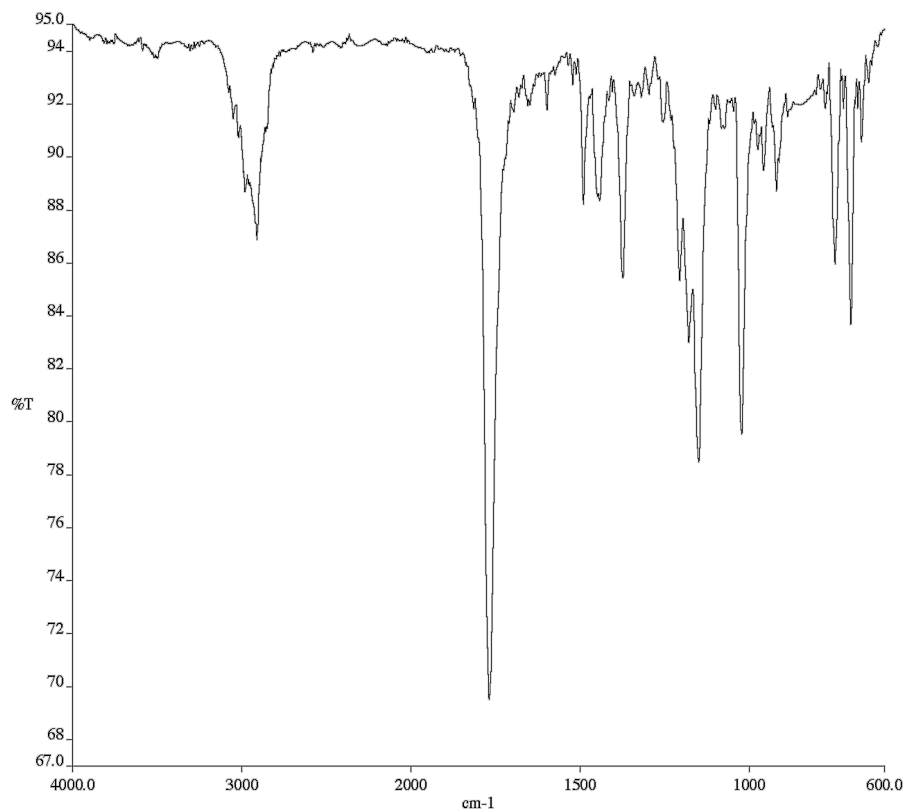


A9.5 Infrared spectrum (Thin Film, NaCl) of compound **43u**

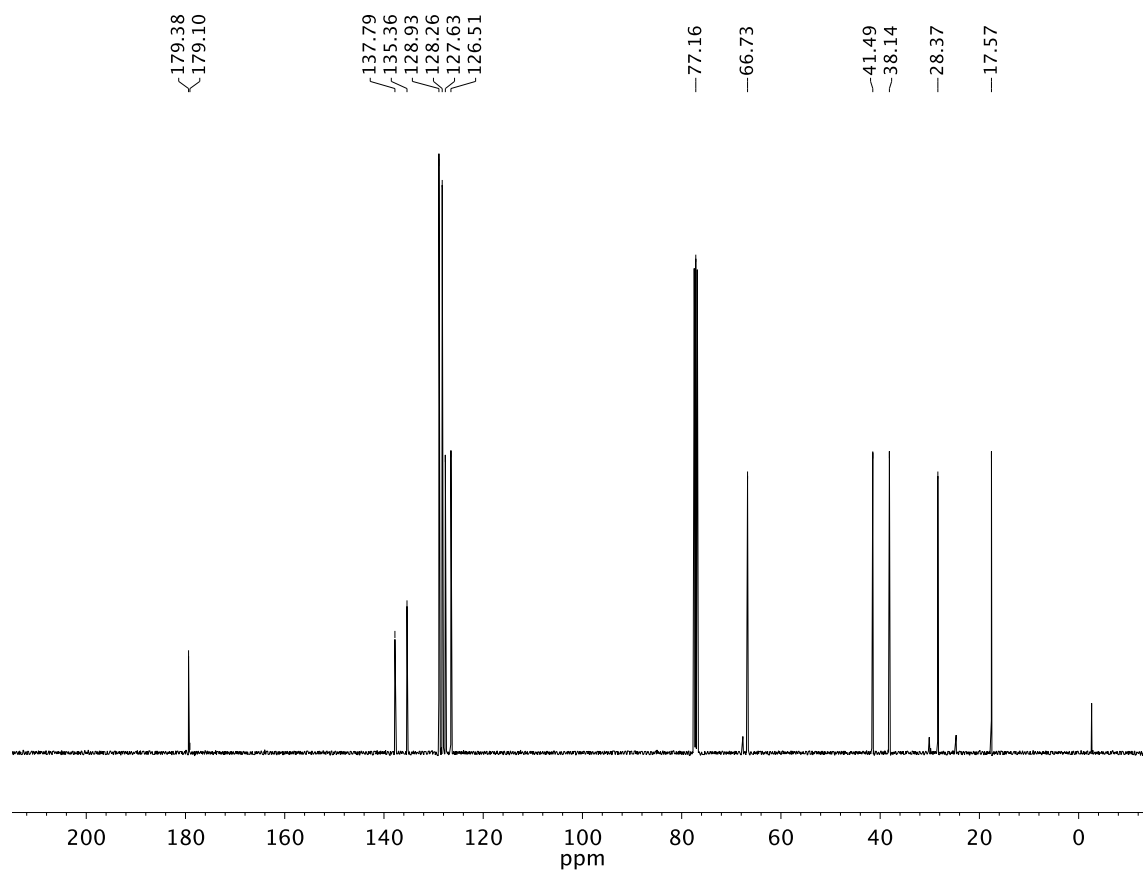


A9.6 ^{13}C NMR (101 MHz, CDCl_3) of compound **43u**

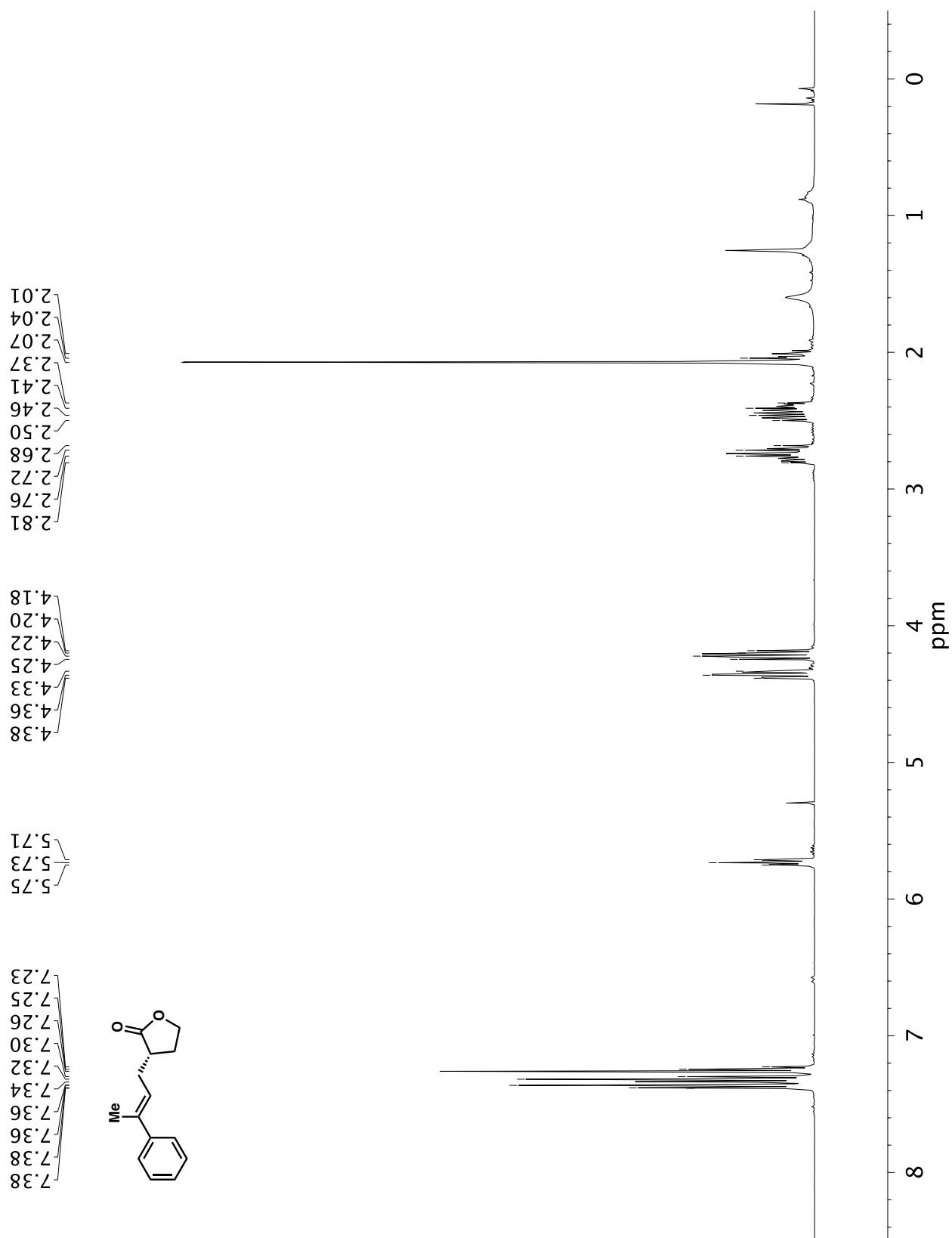
A9.7 ¹H NMR (400 MHz, CDCl₃) of compound **44r**

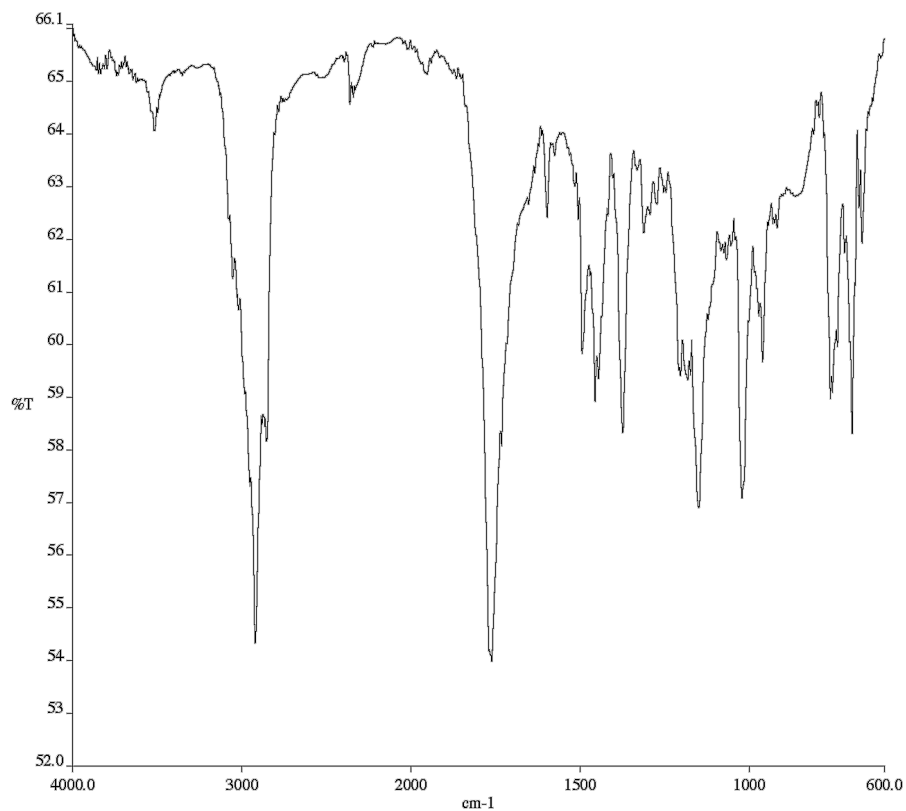
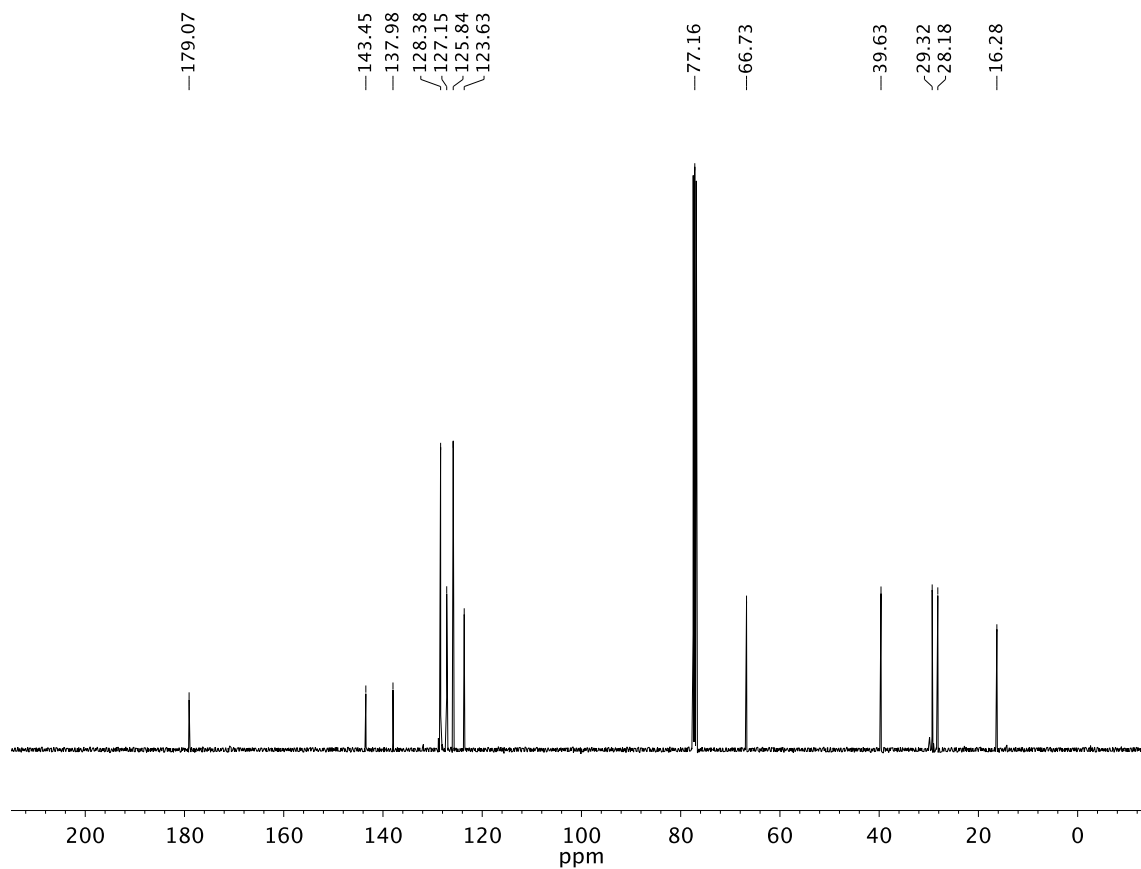


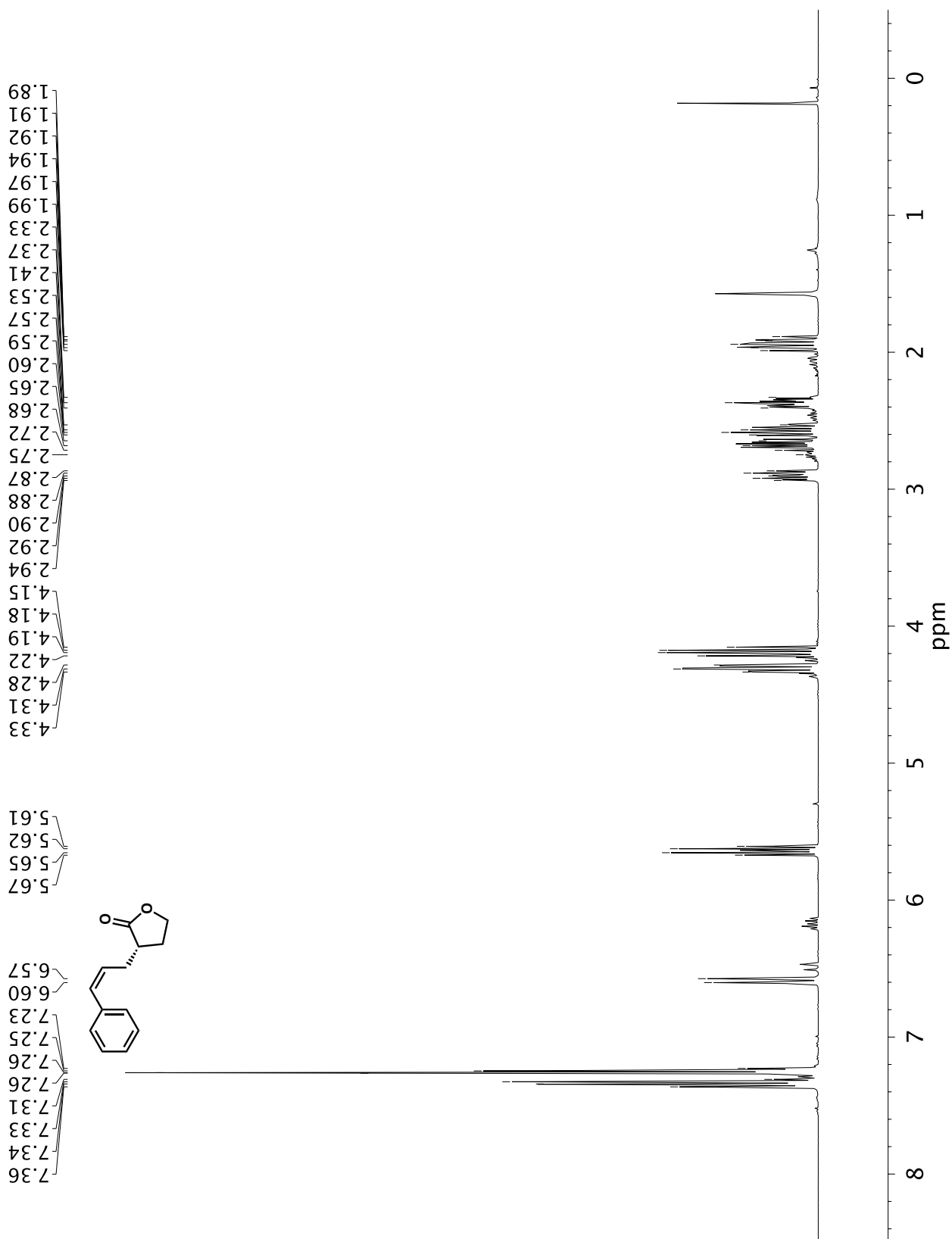
A9.8 Infrared spectrum (Thin Film, NaCl) of compound **44r**

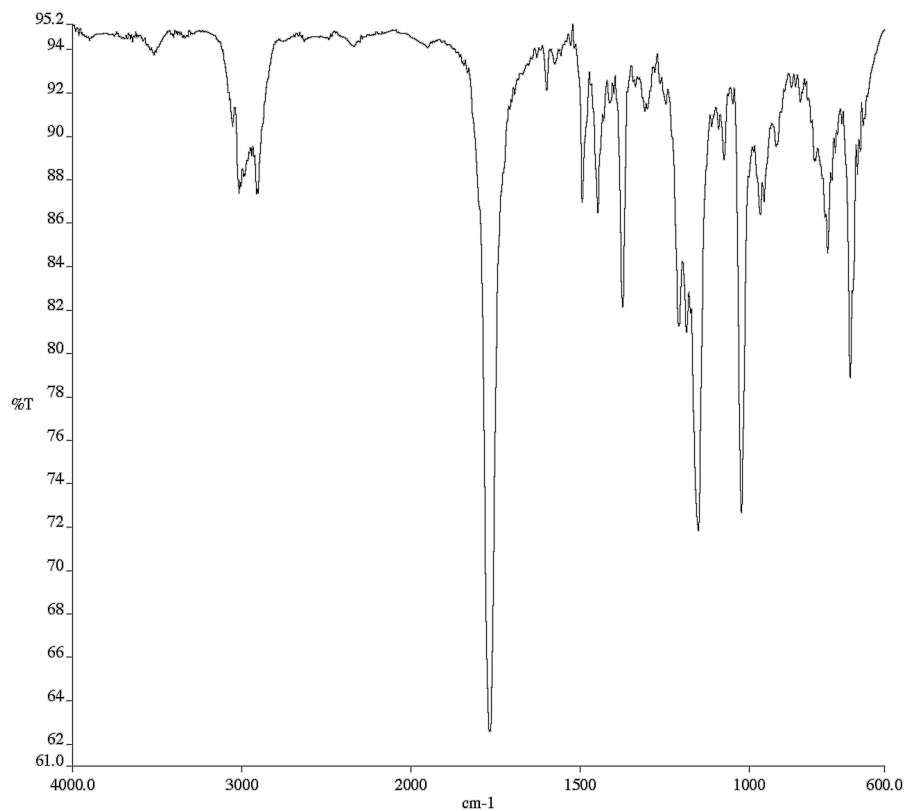


A9.9 ¹³C NMR (101 MHz, CDCl₃) of compound **44r**

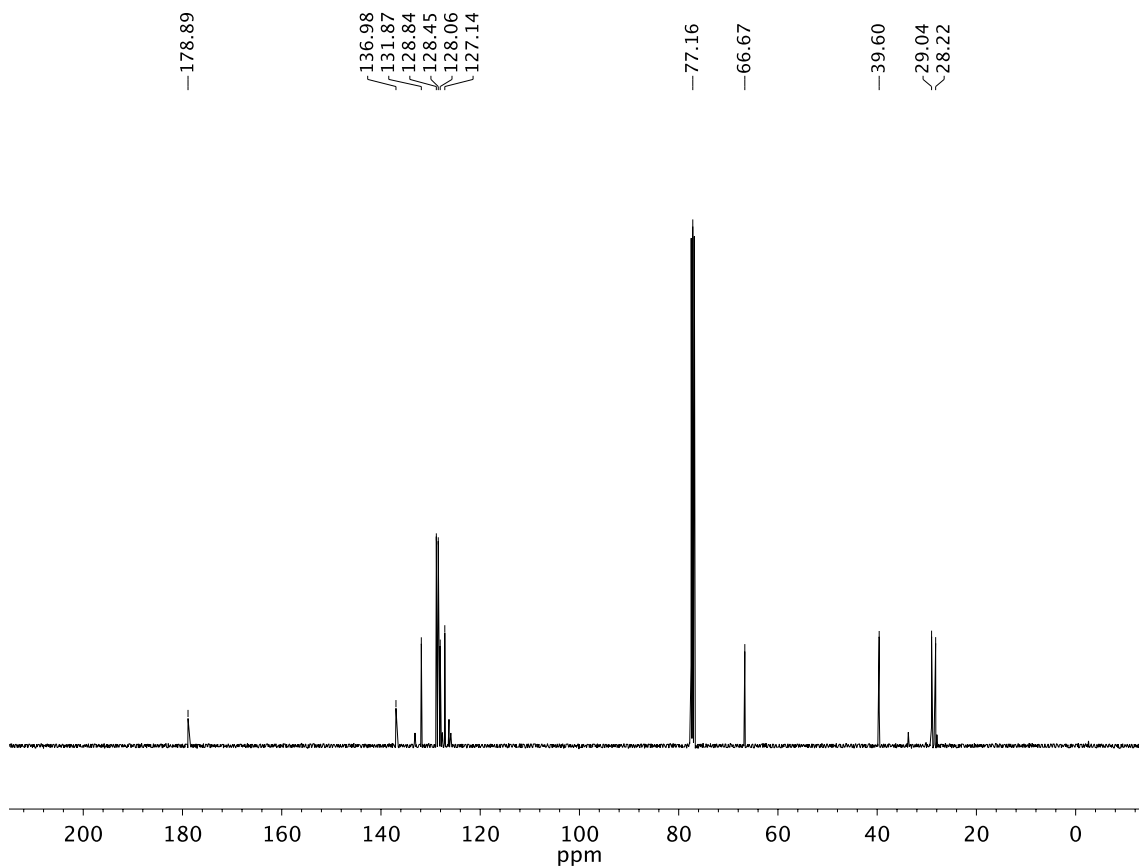
**A9.10** ¹H NMR (400 MHz, CDCl₃) of compound **44s**

**A9.11** Infrared spectrum (Thin Film, NaCl) of compound **44s****A9.12** ¹³C NMR (101 MHz, CDCl₃) of compound **44s**

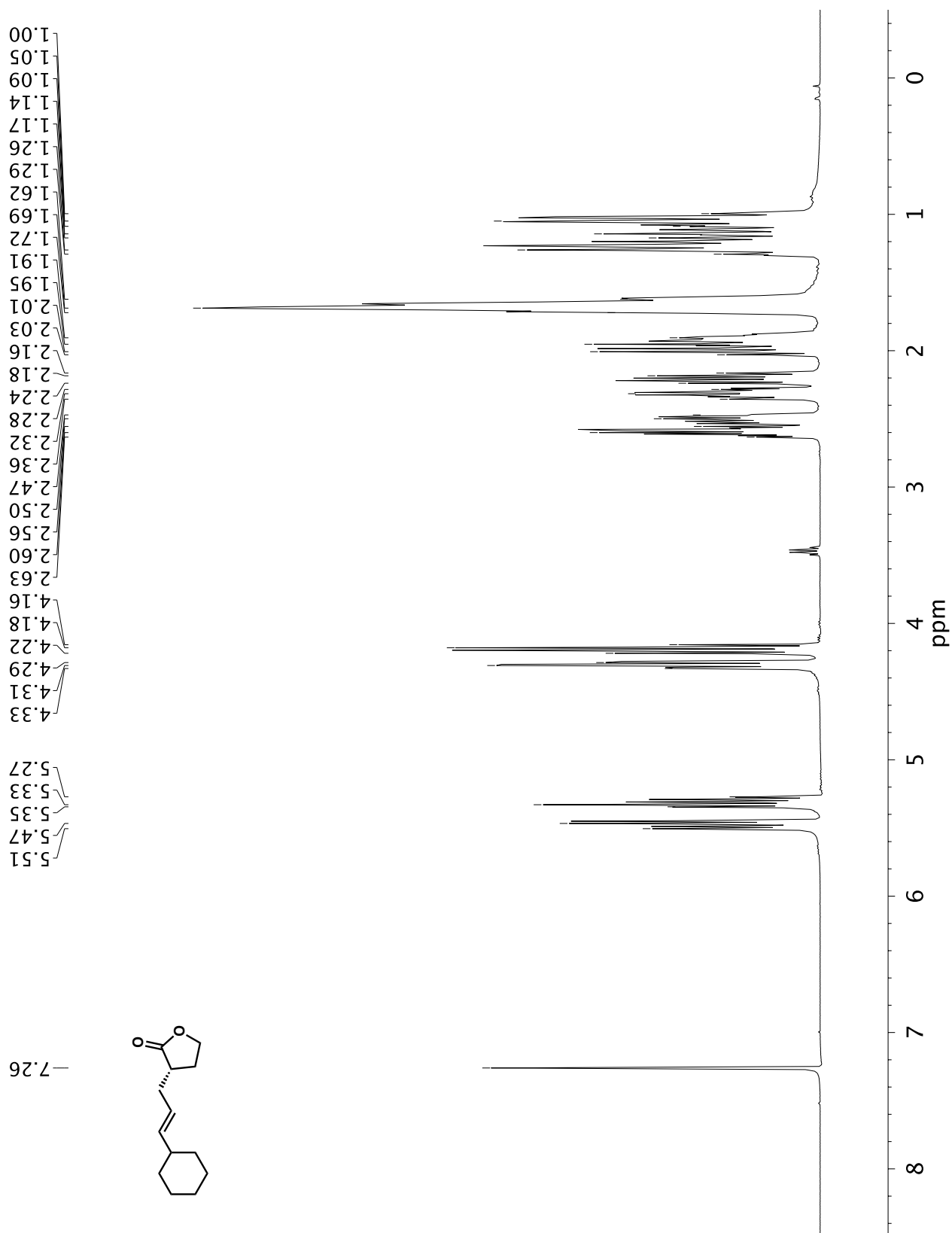
**A9.13** ¹H NMR (400 MHz, CDCl₃) of compound **44t**

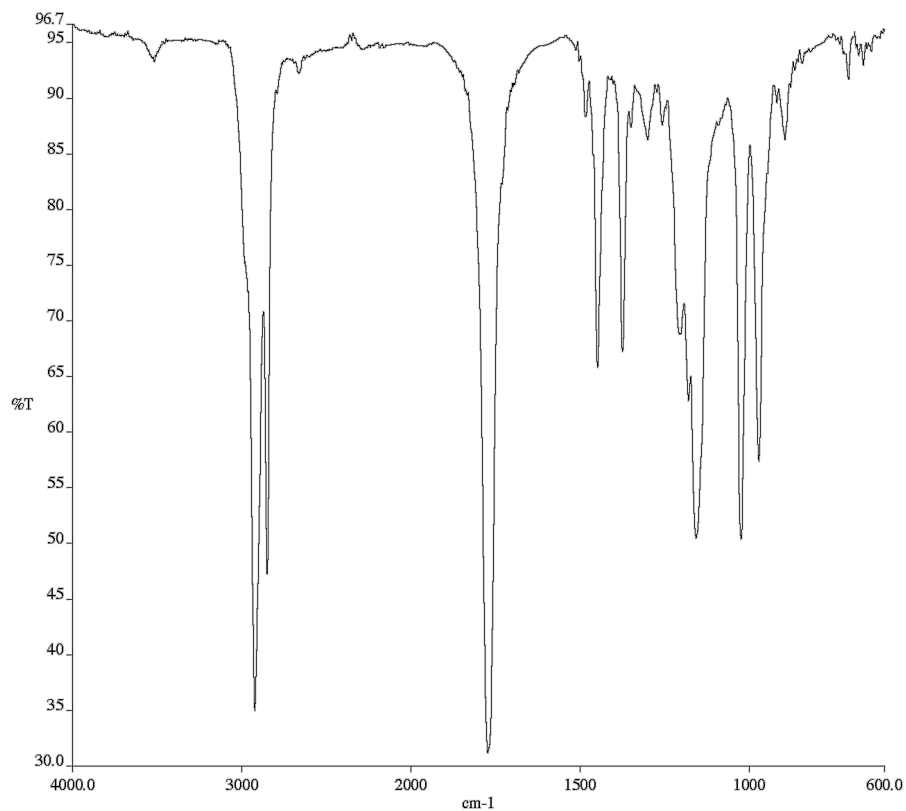
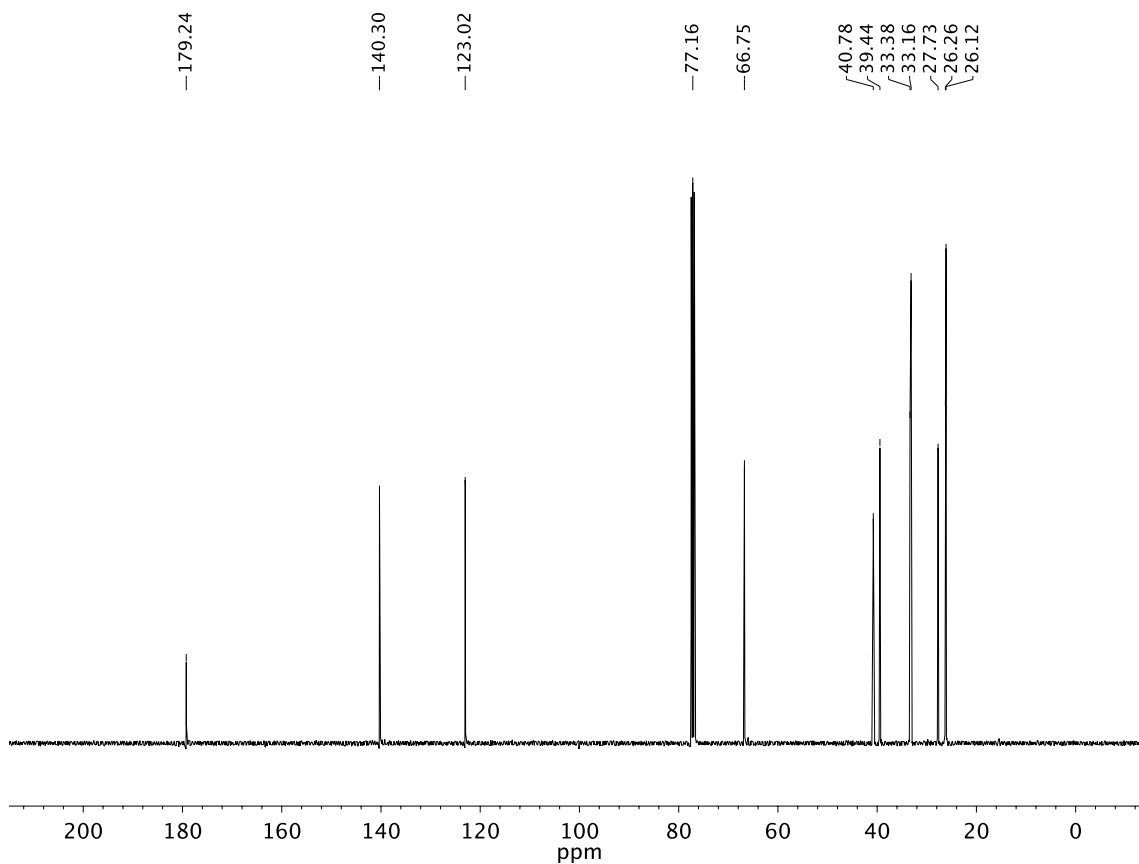


A9.14 Infrared spectrum (Thin Film, NaCl) of compound **44t**



A9.15 ¹³C NMR (101 MHz, CDCl₃) of compound **44t**

**A9.16** ¹H NMR (400 MHz, CDCl₃) of compound **44u**

**A9.17** Infrared spectrum (Thin Film, NaCl) of compound **44u****A9.18** ¹³C NMR (101 MHz, CDCl₃) of compound **44u**

APPENDIX 10

Coordinates for Optimized Geometries Relevant to Chapter 4:

Mechanistic Investigations for Cu-Catalyzed Enantioselective Allylic Alkylation

with a γ -Butyrolactone-Derived Silyl Ketene Acetal

A10.1 COORDINATES FOR B3(0HF)LYP OPTIMIZED L73^{NNO}•CuCl₂

C	5.84649546244608	3.80009699351144	0.35677478540613
C	5.20628526966995	3.54427414304280	-0.85151136053620
H	4.43843795031227	2.76843330873990	-0.90835413876220
C	5.57245233271477	4.26132049922000	-1.99597840840474
H	5.08426380468348	4.04912827253866	-2.95002940226531
C	6.58444927880399	5.21979523225337	-1.92845268989370
H	6.88761810191443	5.75689867271473	-2.83024296532060
C	7.23429840965186	5.47277190941920	-0.71554445088301
H	8.04419813809433	6.20414098150249	-0.66273787952742
C	6.86219041994545	4.77025442858758	0.42717089475257
C	5.30496521823870	4.16228481163829	2.70241434681085
C	4.20464883302810	4.21555948924984	3.55410647567852
H	3.45746943449329	3.41864977965394	3.52367912547705
C	4.06813515504421	5.28043398840012	4.45448458800090
H	3.20513152189289	5.32041239151633	5.12396366085001
C	5.04030065361813	6.28168666930179	4.50798361184927
H	4.93656590251965	7.10682345399245	5.21717236619432
C	6.15553774358018	6.22433546221199	3.66163260937201
H	6.93145199137887	6.99208727144098	3.71326637429685
C	6.28537861380839	5.17385945461384	2.75570481662866
C	5.61451361883679	3.09732596931170	1.67624322562103
H	4.83689219573620	2.32362262990335	1.62166420560046
C	7.44128734641475	4.93417225745630	1.81153173151597
H	8.21660734850250	5.70542260472605	1.87895308012207
C	6.99020539493881	2.42161896893882	2.05109037797509

C	8.04681470655706	3.54298665525527	2.30301787644251
N	9.34198340358532	3.20559310556420	1.74624823044713
N	6.81198664777545	1.53718192569435	3.18054367626867
H	7.31744573425189	1.87555501800638	1.14618124200731
H	8.15806025707222	3.65619677241761	3.39720925522048
C	10.35608981540664	4.04107966120902	1.98321306435662
O	10.32879068814233	5.15956749600066	2.57251240964311
C	11.67870186598739	3.53497846343068	1.46931752768328
C	12.81219652818755	4.35577804506283	1.45892617339345
C	12.88123982953077	1.75127822478929	0.59599020617176
C	14.01311177792603	3.83665616689550	0.98446690292745
H	12.70289569921495	5.37436890327597	1.83253919876009
C	14.05101744738914	2.50967213035211	0.54380980371241
H	12.81813121858895	0.70170982238844	0.28734594617472
H	14.91375003066435	4.45627132189672	0.95763838319354
H	14.97379228418060	2.06315202979394	0.16745155915373
N	11.72791642775386	2.25967329706688	1.04816085785147
C	7.76953333849433	0.65613759361462	3.36999766425075
O	8.85789374960608	0.46005013518106	2.71217330596226
C	7.56202451529443	-0.29073674850832	4.53447474624347
C	6.49076757713324	-0.14352330098897	5.42867366583204
C	8.46271336951653	-1.34796709344498	4.73296718314431
C	6.32332472641905	-1.02850528256569	6.49414479241306
H	5.80337216894331	0.68535771923953	5.25350485451498
C	8.29242956768574	-2.23803661039940	5.79595166187977
H	9.28675271813469	-1.44242311159463	4.02310413232512
C	7.22426313412840	-2.08342462544594	6.68408353157662

H	5.48512663311003	-0.89645921870251	7.18457801423826
H	9.00045801111915	-3.06021158385933	5.93278558227576
H	7.09364084620980	-2.77780189712960	7.51863447158090
Cu	9.78120858103308	1.32888903607831	1.03240081285816
Cl	8.81554460742632	1.66004498732765	-1.12698476570414
Cl	10.77685195326325	-0.77597868178764	0.56658305264232

A10.2 COORDINATES FOR B3(0HF)LYP OPTIMIZED B3(0HF)LYP L73^{NNN}•CuCl₂

C	-2.86181484528682	-3.58940008954456	1.95054375745875
C	-3.31349561668561	-3.69892806317600	3.26250890510869
H	-4.13201981424364	-3.06402295850537	3.60957023087454
C	-2.69166078877141	-4.59997873554681	4.13703540534236
H	-3.03977202382283	-4.68112858726659	5.16951055772232
C	-1.61450006587853	-5.37333267302338	3.70063026890984
H	-1.11918665003785	-6.05923485469390	4.39211883046056
C	-1.15401417694491	-5.25930197698310	2.38244463344789
H	-0.29497713299160	-5.84023114359128	2.03926924108307
C	-1.78033160369459	-4.37729609827755	1.50634650947363
C	-3.75173736489797	-3.46521827440768	-0.30282559372406
C	-4.97750369229859	-3.45829869736675	-0.96435677423204
H	-5.75890544455049	-2.76349384916088	-0.64721581442237
C	-5.20152493383831	-4.33602636614491	-2.03381041432141
H	-6.16297769083989	-4.32618806709272	-2.55283331174731
C	-4.19794824599778	-5.21690234943456	-2.44008383027092
H	-4.37365180775356	-5.89846280196543	-3.27601398450806
C	-2.95831455020654	-5.21994771719559	-1.78496612231822

H	-2.16174467701921	-5.89328943504955	-2.11177768958318
C	-2.73457961553729	-4.35083735592329	-0.72127916470769
C	-3.37331706245782	-2.62165160380954	0.89614157692924
H	-4.20993714530172	-2.01936063426353	1.26309702517890
C	-1.43861634905272	-4.16617112198962	0.04697374420373
H	-0.61530612865887	-4.80049980067353	-0.29977462931757
C	-2.06870834057739	-1.74653729845357	0.60823164693850
C	-1.12654857996390	-2.64169144200025	-0.23329153273700
N	0.17807677174764	-2.07369500144812	-0.07939931260257
N	-2.09369454295182	-0.46650754392405	-0.09469085132616
H	-1.58270398413108	-1.62011890928101	1.59414633634100
H	-1.42476319348728	-2.47473829499704	-1.28631421994704
C	1.35017636433688	-2.68913092021165	-0.13436395652539
O	1.62217792878584	-3.91633192589262	-0.26140901416013
C	2.46882463684969	-1.67935675525097	-0.01466482661331
C	3.80702569585218	-2.06782406847755	0.08881457473474
C	3.04753423417500	0.57234335209120	0.08034955842634
C	4.78601910284615	-1.08485112427463	0.20200902682291
H	4.02479659050468	-3.13652980921024	0.07731692490857
C	4.40177120154489	0.25960948036649	0.19958080239680
H	2.65834052547137	1.59364133141025	0.04256709356220
H	5.84049892387173	-1.35945818433587	0.29304536329919
H	5.13794677710420	1.06064536626853	0.28872484545744
N	2.11506484582269	-0.38003878037524	-0.02380140843529
C	-3.02514947327033	0.48548434128828	0.13683851027035
O	-3.21524042877017	1.48258008233778	-0.58726858437059
C	-3.93226547087433	0.42024079169482	1.36293991576418

C	-5.32290435103615	0.52628181281700	1.21086131984595
C	-3.39013801733346	0.38169637034138	2.65723336046604
C	-6.16566520360415	0.54758700487333	2.32232049749550
C	-4.23537416878162	0.43692714636742	3.76952438980982
H	-2.29879871680153	0.32988609081922	2.78194031834153
C	-5.62265894532815	0.50431892619841	3.61216165872487
H	-7.24940273261483	0.60899672948706	2.18616275181731
H	-3.79882607853386	0.42200923800630	4.77175867899157
H	-6.27834421558201	0.53067053223428	4.48680812861745
Cu	0.03617643535316	-0.05242231160071	-0.01913595566441
Cl	0.18202321645312	0.27002263103041	2.57231415549656
Cl	0.29325881017386	2.02731557064579	-0.99523340875897
H	-5.72956104448254	0.60579524254171	0.20004752957136

A10.3 COORDINATES FOR B3(38HF)LYP OPTIMIZED L73^{NNO}•CuCl₂

C	5.996110782131	3.901206403957	0.452079601878
C	5.423486805078	3.679827078564	-0.786061411137
H	4.667520217538	2.920436572539	-0.904396692789
C	5.839428879551	4.428986077828	-1.882956965284
H	5.399476923526	4.253036574871	-2.851016388804
C	6.831735664453	5.384431642849	-1.735752036232
H	7.163768223835	5.951501965469	-2.590124163908
C	7.414576303946	5.602299341489	-0.490743626918
H	8.200673516229	6.330040744673	-0.376741521911
C	6.993777917947	4.867261840308	0.602015616610
C	5.332116417736	4.195442603273	2.771842483688

C	4.189952214415	4.228420058479	3.549276556945
H	3.452856064764	3.447771617348	3.456712372216
C	4.003114019401	5.262696013321	4.461957736775
H	3.114280724597	5.286917391230	5.071525355996
C	4.963659331499	6.252329528748	4.597542301981
H	4.821097874227	7.048346639473	5.310476614833
C	6.118926140900	6.214766956788	3.821485434612
H	6.875332932452	6.974013361780	3.935563307494
C	6.300724842810	5.192942761987	2.907440975164
C	5.701703622593	3.161820372109	1.736566102369
H	4.938984917382	2.402224595939	1.617074970074
C	7.504965252742	4.987214850609	2.017555170105
H	8.243515277002	5.763153761470	2.130243426082
C	7.051091178732	2.487207621378	2.159542821071
C	8.108184864734	3.596027330405	2.468159587946
N	9.388220838187	3.236459144108	1.885942503798
N	6.821977544490	1.589070334148	3.263889240509
H	7.405838448457	1.949687548234	1.284158346282
H	8.208910724937	3.659528248118	3.549920834187
C	10.361555359048	4.121037817158	1.850408640231
O	10.399565897214	5.302062669248	2.245415300616
C	11.608868581047	3.583798199216	1.172962636089
C	12.662071242279	4.426011550783	0.835823368586
C	12.700918451362	1.759832401351	0.284878185249
C	13.758218129810	3.891235217255	0.188377419153
H	12.584116608080	5.465348971456	1.092656241391
C	13.780532506528	2.533894554776	-0.098888455296

H	12.647574982173	0.703386050431	0.099431046553
H	14.587726990705	4.521367067434	-0.090838439002
H	14.616384137745	2.079333196417	-0.601273669208
N	11.651231278595	2.285805536168	0.900400206884
C	7.627405417897	0.581479742613	3.340901878820
O	8.605258220891	0.274703870437	2.579248858236
C	7.379616572659	-0.398956292953	4.463387474823
C	6.188345145551	-0.405767353400	5.184974754904
C	8.369197171738	-1.322048044660	4.791669699835
C	5.982790318877	-1.321928298980	6.204409970181
H	5.438004240614	0.320923913183	4.931620045610
C	8.166026280491	-2.233333149044	5.818485765358
H	9.293690860245	-1.295770003667	4.242240757041
C	6.972684656387	-2.242128143675	6.525988503078
H	5.052373773028	-1.317837679978	6.750566413328
H	8.945645435044	-2.935109870487	6.066962597461
H	6.815759858662	-2.953772317392	7.321352582794
Cu	10.066149178894	1.192064170598	1.672139645038
Cl	9.898255811504	-0.030829863250	-0.484324121440
Cl	11.773634426644	0.232647107470	3.284474140053

A10.4 COORDINATES FOR B3(38HF)LYP OPTIMIZED L73^{NNN}•CuCl₂

C	5.945807246296	3.107202192485	1.502335399784
C	5.047563103218	2.379285222991	0.746343080120
H	4.570427748968	1.509381540430	1.165978116224

C	4.782768893749	2.760492505325	-0.566855568440
H	4.086869742328	2.189559730583	-1.159765933959
C	5.427200654394	3.855577495917	-1.117654468486
H	5.233426104196	4.137075308720	-2.139949337469
C	6.336557647805	4.587245397077	-0.357878209749
H	6.854912142272	5.428320936185	-0.787303785004
C	6.589595534335	4.219687578302	0.949683852854
C	6.131121302581	4.048341019032	3.724889537997
C	5.400164393550	4.130523241191	4.894877378511
H	4.996481378647	3.236411831315	5.340407106897
C	5.191444046219	5.368653903605	5.498534273740
H	4.623686673517	5.430533231572	6.412629514348
C	5.716271662029	6.516700127011	4.929825554562
H	5.556653039856	7.473481866126	5.400121563219
C	6.462717046995	6.436264224317	3.755789016043
H	6.889172175177	7.325900480823	3.321613355388
C	6.667487660645	5.209672483760	3.155039839766
C	6.399315341173	2.796223001674	2.917976233572
H	5.886576934930	1.938280165358	3.320996928774
C	7.505536128462	4.928401115723	1.922440944151
H	7.964320073348	5.810445406169	1.504147969042
C	7.954403720473	2.549268354511	2.717750668989
C	8.585918378494	3.940571494812	2.491939698213
N	9.839124011004	3.694359168249	1.839109493965
N	8.807338169448	1.905572387920	3.705421189512
H	8.024697362767	2.020819248718	1.769417397151
H	8.820775248370	4.324926197443	3.483186188373

C	10.503389077773	4.531301676875	1.086118307732
O	10.198189428818	5.659984750505	0.656210430818
C	11.861068479588	3.961185481642	0.711618004369
C	12.675513079510	4.584082690324	-0.225750385992
C	13.412394622472	2.298779074916	1.057406317120
C	13.898658859848	4.013502710789	-0.523691904981
H	12.324679512827	5.488339757776	-0.686782941406
C	14.278308649264	2.848471185087	0.126380041060
H	13.646137485181	1.408922428976	1.614059182886
H	14.550361235383	4.468644478482	-1.252684116163
H	15.221910040494	2.373013912293	-0.078326749282
N	12.240182639866	2.848804009728	1.332770866814
C	8.440267134508	0.839528182969	4.427295430888
O	9.018245504531	0.445770563139	5.437324187872
C	7.248873356043	-0.027316676101	4.019906417854
C	6.262057443613	-0.328586452190	4.955173371299
C	7.192197665405	-0.629234895493	2.765958784198
C	5.213160011470	-1.176432268797	4.636283690487
C	6.155472554838	-1.500582048909	2.456242301259
H	7.973801751575	-0.434211589525	2.048418465465
C	5.156086357629	-1.768394043887	3.380474480416
H	4.447866698088	-1.386497338331	5.367167713507
H	6.133377765647	-1.970328285775	1.486261451803
H	4.347359112124	-2.437036387966	3.131266526377
Cu	10.699039502479	2.038456173134	2.682684332339
Cl	10.285273616349	0.175760174498	0.885400531079
Cl	12.394853006098	1.330995784988	4.155710819502

H 6.336071843333 0.102080093511 5.939177444591

A10.5 COORDINATES FOR L73^{NO}•Cu^{II}Cl

C	-2.29864477597556	-3.58731153675347	1.77943236012319
C	-2.82269583769079	-3.37374726294824	3.03998455660984
H	-3.82701029132694	-2.99987819926119	3.15365994361713
C	-2.04382217012108	-3.63643097880283	4.16309273863349
H	-2.44938709680332	-3.47113707563367	5.14708218916788
C	-0.74692298206639	-4.10027993433679	4.01747265080046
H	-0.14471943208168	-4.29563690410795	4.88889274827863
C	-0.21644932181507	-4.30882108586799	2.74781533841623
H	0.79471489534926	-4.66283531029266	2.63394162469672
C	-0.99152935467057	-4.05639183543934	1.63151164098629
C	-2.92616304079229	-4.59253312440871	-0.34787032253630
C	-3.99252998395378	-5.24887761103317	-0.93220535133589
H	-4.98690011244504	-4.84233849291993	-0.85200224855454
C	-3.77399110614694	-6.43152970026845	-1.63192819871353
H	-4.60366358941286	-6.94577359969880	-2.08758384224271
C	-2.49249588495234	-6.94476882736923	-1.75022120629525
H	-2.32665399997289	-7.85839849088098	-2.29624914443834
C	-1.41639760879049	-6.27895395106108	-1.17106628532963
H	-0.41716709085784	-6.66816822521432	-1.27472182824629
C	-1.63499603747155	-5.10971688084549	-0.46705376849506
C	-2.97568433355135	-3.31376200277411	0.45453102760618
H	-3.98244513790593	-2.93275597138695	0.56820717352760
C	-0.58203704396480	-4.24267793578932	0.18890515346645

H	0.41133384563383	-4.64878477147106	0.08119199247920
C	-2.08213664190885	-2.23680469153504	-0.24391464833591
C	-0.69289486801510	-2.86368139642553	-0.56354513184782
N	0.36692221042153	-1.91060487263126	-0.27209249000565
N	-2.74488671788774	-1.68898054010092	-1.39664796206734
H	-1.92507385203720	-1.46753634974589	0.51266858341727
H	-0.67044085044108	-3.10180276561733	-1.62326886176089
C	1.61955311932614	-2.25366741023266	-0.53235408887348
O	2.06711077336694	-3.31925298554036	-0.96323800365650
C	2.60760856798099	-1.14397787826392	-0.22228376371913
C	3.97615308261379	-1.35609408712208	-0.28371544611937
C	2.90837451973131	1.05351522885967	0.41418631597412
C	4.82331858165214	-0.30769085546144	0.02477240521091
H	4.33110696729582	-2.32767490524341	-0.57037334143926
C	4.28461501589137	0.91909299177955	0.38289724643908
H	2.41814557422152	1.97082534856068	0.68889633040352
H	5.89124760642107	-0.44269173167419	-0.01149432966664
H	4.91174677501937	1.75596858370341	0.63248208332725
N	2.10277170126038	0.04132210337837	0.11467101328793
C	-2.37582879730922	-0.52053814375877	-1.78782641323640
O	-1.46101898064543	0.24497554741815	-1.29610585003924
C	-3.11450898600925	0.06644339211880	-2.96387258960770
C	-4.02929985388284	-0.69122830042472	-3.69234886863277
C	-2.89323795160488	1.38779504640400	-3.33956362463047
C	-4.70476365630797	-0.14058928061053	-4.76836571349237
H	-4.19563938467940	-1.71056298780792	-3.39723873440266
C	-3.57487013768014	1.94217056885130	-4.41367458322156

H	-2.18860338374280	1.96971076043692	-2.77500200180587
C	-4.48177831719301	1.18070328920468	-5.13378625825837
H	-5.40618613494452	-0.74153548567637	-5.32354383684020
H	-3.39621849738451	2.96901671045815	-4.68697043539714
H	-5.00942180853932	1.60952082777139	-5.96974728801084
Cu	0.00545942313146	0.03655931315095	-0.03965192972256
Cl	-0.28504383133412	1.95596010134205	1.17118492250833

A10.6 COORDINATES FOR OPTIMIZED L73^{NNN}•Cu^{II}Cl

C	-2.67185294410575	-3.74581222287031	2.27453108077461
C	-3.06931575738793	-4.00680042709489	3.57075494299466
H	-3.85283283661694	-3.42301690421306	4.02475060338536
C	-2.44696427070843	-5.02422576005257	4.29087815398733
H	-2.75709711908311	-5.23194717409296	5.30120386403083
C	-1.42813430987645	-5.76236113702235	3.71373496104396
H	-0.94449163867816	-6.54376649568084	4.27550935977981
C	-1.02642601628321	-5.49888791856164	2.40634789512476
H	-0.23330135470357	-6.07244219795091	1.95630174673321
C	-1.64935923084263	-4.49834593975350	1.68629527124923
C	-3.67620047050665	-3.32978927002081	0.11029168476090
C	-4.93438904848705	-3.22853467283452	-0.45162681167076
H	-5.66770831297295	-2.57033422044106	-0.01772958358513
C	-5.24879805049901	-3.97862314473308	-1.58212535973805
H	-6.22918838658975	-3.89903972405887	-2.02092519099521
C	-4.30597925933208	-4.82308220599138	-2.14256666248858

H	-4.55227533313058	-5.40063297156872	-3.01777090162448
C	-3.03510616038500	-4.92350226480484	-1.58163903098343
H	-2.29517931073666	-5.56889437375397	-2.02497590232605
C	-2.72405800242955	-4.18318233648698	-0.45871876215824
C	-3.19733433828898	-2.63765330556285	1.37296965781113
H	-3.98105212788972	-2.07504395579334	1.85200522688830
C	-1.37881342875729	-4.12312322347919	0.24477697211078
H	-0.62792313081405	-4.74000932181240	-0.22437534130799
C	-1.88435689353236	-1.79458326295217	1.12280910524273
C	-1.03118645221682	-2.60090085502976	0.11739951231122
N	0.30838694415626	-2.08461968010786	0.25108598639121
N	-1.78029546455593	-0.41340313864540	0.67150373471262
H	-1.36075712172097	-1.85292610834637	2.07517741854809
H	-1.37890988953541	-2.31732238050960	-0.87382880519817
C	1.36228541049567	-2.59636894857824	-0.35229231815807
O	1.50853957696851	-3.68260724759085	-0.91832485949395
C	2.53962646111336	-1.63387775496380	-0.30910533605580
C	3.81354985730786	-2.03008832926891	-0.68427614359350
C	3.26036113364100	0.51485504577369	0.11645395624669
C	4.83704758674355	-1.10073859128611	-0.64404672622021
H	3.96189719260342	-3.04571688746704	-0.99932859282961
C	4.55970985896924	0.19511287882489	-0.23732534069413
H	2.97425539484856	1.49598298558185	0.45250357309007
H	5.83823789261706	-1.38071008537193	-0.92593362169702
H	5.32816923871985	0.94588790427340	-0.19266721377797
N	2.28240123289376	-0.38212605980402	0.07595832739248
C	-2.71847730778715	0.51898098152497	0.50689799815197

O	-2.56871367798798	1.51898702453799	-0.19044973788906
C	-4.03443593177107	0.44742844671305	1.26041577357980
C	-5.24136554653843	0.55181179946546	0.57772811326328
C	-4.05237383008002	0.41938367955050	2.65065822638565
C	-6.44299044229318	0.58749772257501	1.26718321993916
C	-5.25219109321234	0.48092815102599	3.34480420258158
H	-3.12023946706383	0.36316250169373	3.18617000573214
C	-6.45308284645493	0.55366168059024	2.65513333200770
H	-7.37120452041003	0.65398758736066	0.72400953807077
H	-5.24837804999414	0.47341100328718	4.42210527636135
H	-7.38594719995050	0.59301863852258	3.19223464585292
Cu	0.21651555259459	-0.12009121619230	0.61690785022554
Cl	0.57798473507685	1.85486886433973	1.68666971388371
H	-5.22714264053895	0.61480449310846	-0.49617888216012

A10.7 COORDINATES FOR B3(38HF)LYP OPTIMIZED L73^{NNO}•Cu^{II}

C	-2.20003181308295	-3.58141656281122	1.72980578537622
C	-2.67251170659025	-3.32934361995174	3.00377026270975
H	-3.65591359556593	-2.91314199726360	3.14714153117363
C	-1.87098971763960	-3.62252535064683	4.10300206477360
H	-2.23843218764835	-3.43739157413717	5.09778572469613
C	-0.60472885349447	-4.15426671431079	3.92095403156063
H	0.01014429537774	-4.38120756723473	4.77502647253295
C	-0.12555478797295	-4.40083663195002	2.63802094037041
H	0.85921862355543	-4.81268939171241	2.49498406884499

C	-0.92463819970519	-4.11743024259730	1.54629262543712
C	-2.94843043643592	-4.57526577975780	-0.37245965740370
C	-4.06470273752915	-5.18299709654796	-0.91404887189210
H	-5.03702631259909	-4.73460921049958	-0.79845355355437
C	-3.92333181310996	-6.37800899044153	-1.61145150210578
H	-4.79034393207008	-6.85805299664567	-2.03173251753519
C	-2.67177324850753	-6.95136003451505	-1.76889581398402
H	-2.56837538446065	-7.87653817592666	-2.30931737160675
C	-1.54664585676470	-6.33459504332720	-1.23180905092176
H	-0.57266114891930	-6.77667149151174	-1.35935545109566
C	-1.68930246370151	-5.15184006919893	-0.53090993496102
C	-2.90990145117784	-3.29237928857963	0.42404050890372
H	-3.89223274381092	-2.86194530566553	0.56900861377191
C	-0.57288230085670	-4.34005592152370	0.09276203433866
H	0.39279395308010	-4.80035695194838	-0.03644132355909
C	-1.99116872518845	-2.26654016195671	-0.31114534129391
C	-0.63105525125306	-2.96525398377875	-0.66173371988612
N	0.45743031916393	-2.03320732958847	-0.39268444586219
N	-2.65985303741974	-1.70343671898111	-1.45599565401705
H	-1.77193108833925	-1.49552044742968	0.42502180056979
H	-0.63676619703201	-3.19458136098921	-1.72334536542498
C	1.73964875486623	-2.37516859188164	-0.30482491546319
O	2.26931544120965	-3.47421997074102	-0.37510151615855
C	2.63921675571763	-1.16737232385632	-0.06047826351092
C	3.98549359402577	-1.32291769224592	0.21520771533571
C	2.82458726791228	1.13839920818660	0.07415845626445
C	4.75829236692057	-0.19740682099372	0.43401954533157

H	4.38533721484551	-2.31849452626147	0.24810355662654
C	4.17026196068306	1.05707520385749	0.36420599559831
H	2.32462731462718	2.08817264814794	0.00175098668223
H	5.80691102448398	-0.29282059461052	0.65509180478838
H	4.73792988943775	1.95444641929036	0.52676516329813
N	2.08197747370914	0.04895001015435	-0.12963616758980
C	-2.38026237370951	-0.51969701087638	-1.83089173672265
O	-1.45887734719449	0.27194819262574	-1.29910429532263
C	-3.14223687384816	0.08706140518041	-2.96493622302119
C	-4.10197125440388	-0.65855221916302	-3.64773822626402
C	-2.90811808646545	1.40123975467590	-3.35825987913847
C	-4.80645494248210	-0.10082703218331	-4.69919236048530
H	-4.27923478681439	-1.67272432397950	-3.34256440711676
C	-3.61883922526160	1.96110733073748	-4.40929938514995
H	-2.17228141772684	1.98245601859803	-2.83508662686981
C	-4.56854236773557	1.21205950384504	-5.08402657095423
H	-5.54198295941802	-0.68935272415562	-5.22020137225018
H	-3.42922109092542	2.98029966851652	-4.69969007390780
H	-5.11895823834202	1.64476885602404	-5.90174351264737
Cu	0.17604730958700	-0.14376904246234	-0.62959785630831

A10.8 COORDINATES FOR L73^{NNN}•Cu^{II}

C	-2.90318100304892	-4.04187347603220	2.19279641678500
C	-3.43224597195278	-4.21500019194389	3.45547496775815
H	-4.33047239074837	-3.69585626757540	3.74635026585597

C	-2.80050152735493	-5.07225340945572	4.35371756449165
H	-3.21387802184112	-5.21561855231104	5.33712409383720
C	-1.64459487311139	-5.73714474850710	3.98487905118704
H	-1.15773145023167	-6.39620176274622	4.68274479983594
C	-1.11101586726088	-5.56349403496826	2.71018792596241
H	-0.21492486551599	-6.08700092463947	2.42261744005074
C	-1.73976663101980	-4.72237149031189	1.81376322258851
C	-3.66783794025881	-3.96824659412816	-0.10932323330323
C	-4.85066999411354	-4.05839146980725	-0.81560233252799
H	-5.69268093792478	-3.44268697291398	-0.54638598721093
C	-4.95294883793043	-4.95566383313711	-1.87561062147900
H	-5.87494413320613	-5.03078410799399	-2.42577521292581
C	-3.87499669398461	-5.75218373650055	-2.21956779631602
H	-3.95906603840380	-6.44660912599990	-3.03764224164616
C	-2.67773412637193	-5.65736455624890	-1.51402774648951
H	-1.83532892866394	-6.26826261087565	-1.79137604796745
C	-2.57726148631347	-4.77116309201715	-0.46135775574593
C	-3.41731083907104	-3.10064990339184	1.11016042281603
H	-4.30212046811460	-2.56017773124244	1.41502948388522
C	-1.33511692554216	-4.48224757634928	0.37126910851063
H	-0.47650928065942	-5.06131454805896	0.06678262997375
C	-2.16838673712002	-2.16765167506992	0.91485047812034
C	-1.13548443761153	-2.95786258611577	0.08145676006216
N	0.11995411109486	-2.23676257039328	0.21655665056979
N	-2.17161671907831	-0.84510807693456	0.30499775616023
H	-1.74230760277207	-2.05447263764764	1.90822936158648
H	-1.43469032156489	-2.83867945125013	-0.95722037027923

C	1.30645248003891	-2.61868450782261	-0.22937550736211
O	1.72481266768451	-3.72826392233376	-0.52904493366089
C	2.24389625581416	-1.41375432032406	-0.36970737814576
C	3.60280590063494	-1.58662884526604	-0.56153422258532
C	2.46830251578818	0.88739894169005	-0.50034493605655
C	4.40784362560222	-0.47182062664978	-0.71226648727216
H	3.98923080997298	-2.58783529342751	-0.59284793896670
C	3.83374457711137	0.78951945906383	-0.68142874387569
H	1.97303513488029	1.84229239152896	-0.47701023952611
H	5.46862260681872	-0.58239008953801	-0.85547390655256
H	4.42438410191922	1.67936605971361	-0.79856615456059
N	1.69588131192471	-0.18648062121858	-0.34647240344066
C	-2.46551583024016	0.37461579828894	0.71092455436005
O	-1.64509702377751	1.26904750227492	0.32015253843435
C	-3.63949027180550	0.80332462945583	1.51922278543182
C	-4.24460638875893	2.02169045903534	1.21638377685715
C	-4.12070145052607	0.05395995676199	2.58754968631844
C	-5.33248012092667	2.46313910631366	1.94820962829467
C	-5.19359008117886	0.51114862682058	3.33656885915325
H	-3.64610175919175	-0.86991844350673	2.85876148343815
C	-5.80839268776599	1.70969518715661	3.01187870375128
H	-5.80297358826453	3.39752926907079	1.69617701802922
H	-5.54643989461316	-0.06796325241184	4.17204157937704
H	-6.64799805141629	2.05833567634167	3.58782336868797
Cu	-0.31170000498584	-0.35176161313300	-0.03318021507640
H	-3.85339977604248	2.61130699768284	0.40774012180214

A10.9 COORDINATES FOR L73^{NNO}•Cu^ICl

C	-2.28511132202420	3.73106744047687	-2.57793739170622
C	-2.39692691199541	3.66956531834250	-3.95412848911881
H	-3.24045965866246	3.17254451525446	-4.40571339663531
C	-1.40898721629852	4.23588797086717	-4.75494130483988
H	-1.49100725985927	4.18172274331999	-5.82837663154526
C	-0.31180894655980	4.84954839097590	-4.17322248951257
H	0.46103117168344	5.27208352875719	-4.79463299835095
C	-0.19516284237603	4.90578496221842	-2.78728505753373
H	0.66652382536033	5.36718290382750	-2.33373700537810
C	-1.18072705865316	4.35409621774475	-1.98997316704677
C	-3.64181048810671	4.25668757882339	-0.63363748124919
C	-4.92884619416002	4.64443446107470	-0.31192066909744
H	-5.76966693672577	4.11839391695666	-0.73355170857326
C	-5.13525635856397	5.70053981303235	0.57183479645403
H	-6.13946180915865	5.99967616047978	0.82643029490338
C	-4.05269867748719	6.35618381183642	1.13635467082542
H	-4.21394358381062	7.16697410881638	1.82871961929167
C	-2.75528380363397	5.96148103241855	0.82020028897557
H	-1.91079228883584	6.45426827078866	1.27347160847765
C	-2.54947094691458	4.92097937610948	-0.06716610830456
C	-3.23185645117395	3.13865241610797	-1.56168527552451
H	-4.08230398263132	2.64656539081825	-2.01729226841549
C	-1.21941910157753	4.33904710162747	-0.48211065865156
H	-0.38322307078077	4.84857203936841	-0.02799636658566

C	-2.39370870058853	2.08821872551069	-0.74641813212193
C	-1.25945112942135	2.83767818776711	0.01872406193722
N	0.01500638741678	2.15065459183480	-0.08090034336732
N	-3.27681420874644	1.32783691980640	0.10086755185853
H	-1.91027542744034	1.45109961033817	-1.48582206058455
H	-1.55328518483392	2.89618175828730	1.06339200362918
C	0.95392335767021	2.58855299680780	0.72636464783328
O	0.93395899351823	3.57120729499236	1.50449865728361
C	2.25115138398183	1.79396718571410	0.69061630121334
C	3.42404954900810	2.35948179761651	1.19388496325031
C	3.36438276901313	-0.13171730250597	0.12405218221461
C	4.59574584885197	1.63047914461443	1.14054027045911
H	3.37457880233114	3.34742162456042	1.61168644211115
C	4.57448939446976	0.35523835994555	0.59030640829246
H	3.28078382634560	-1.10503614531384	-0.33291432186937
H	5.51682508050836	2.04839035382704	1.51620780394193
H	5.46674700972483	-0.24455596503711	0.52253403092397
N	2.24025391919386	0.56636459832514	0.18551794967972
C	-2.89965438935129	0.10702992770664	0.36895968012663
O	-1.86032909766683	-0.51206883511571	0.02163431313980
C	-3.88911486631854	-0.68208902430769	1.22013658562349
C	-5.04574157311707	-0.11013407031261	1.74807891120075
C	-3.63828064635801	-2.02527801700893	1.48725876501040
C	-5.92441037403382	-0.858595555559479	2.51626235739870
H	-5.22975544939440	0.92817094607774	1.54057159359127
C	-4.51826705324332	-2.77937030975318	2.25169333677175
H	-2.74011544158371	-2.45206456926334	1.07822263013634

C	-5.66682038853332	-2.20031734969847	2.77177835993231
H	-6.81234921532667	-0.39590496061548	2.91885286465497
H	-4.30593203390408	-3.81966999387641	2.44360443499005
H	-6.35070177591196	-2.78320671101246	3.36880078122371
Cu	0.15965166358524	0.21642433159637	-0.97694695047009
Cl	0.98588480910045	-1.29740452595581	-2.55736746487380

A10.10 COORDINATES FOR OPTIMIZED L73^{NNN}•Cu^ICl

C	-2.89027943273917	-3.65764678352983	1.86190462355790
C	-3.27799145774849	-3.79508533198864	3.18229823475140
H	-4.18892765309442	-3.33391757112034	3.52722822055543
C	-2.47922933921401	-4.51290739052547	4.06731572347038
H	-2.77566837429579	-4.61014886407740	5.09896586236411
C	-1.29386290465066	-5.08112637001851	3.63074741711613
H	-0.66809950980957	-5.62135632777768	4.32240954914178
C	-0.89612628217139	-4.93316689910695	2.30510643008433
H	0.03652196405351	-5.35616916874674	1.96884037372430
C	-1.69097200752835	-4.22545802379161	1.42308754192795
C	-3.81022994367113	-3.83763329000184	-0.37885132925086
C	-4.99902928356614	-4.13285956396533	-1.01925791707625
H	-5.91200969855846	-3.65487059521556	-0.70537109975801
C	-5.00898163291902	-5.02880964726112	-2.08416723669392
H	-5.93583381105901	-5.25312413734126	-2.58733670427332
C	-3.82906712296715	-5.61709318072916	-2.51102589133925
H	-3.83750389662130	-6.30220927411718	-3.34368262503297

C	-2.62868375229376	-5.31105125883293	-1.87561282341467
H	-1.70470917277514	-5.74726456355136	-2.21912653798744
C	-2.62099725731705	-4.42976441581986	-0.81062234060020
C	-3.61185708091566	-2.89388339286628	0.78047801500128
H	-4.54183101686132	-2.46375684996518	1.12852882632215
C	-1.41308490146772	-3.96032160785722	-0.03628412132904
H	-0.49848736153647	-4.41963188369138	-0.38422830753224
C	-2.63581868694982	-1.72947842923079	0.30408612608387
C	-1.34219897894930	-2.39970077274101	-0.25663709032529
N	-0.09460776849807	-1.84535694560422	0.27225071593212
N	-3.24618054035965	-0.90693751227617	-0.70247647194598
H	-2.36150731329199	-1.20618482306832	1.21824228043870
H	-1.36165049698173	-2.24684781703526	-1.32715678262604
C	0.95515494757272	-2.06133282952991	-0.50095010669386
O	1.01148991021516	-2.70111273589372	-1.56807031228103
C	2.27609101672677	-1.45164069034885	-0.03806577092779
C	3.39993616919129	-1.55894733184259	-0.85890534632165
C	3.48243905794942	-0.30062999858052	1.54149810766304
C	4.59175172552359	-1.00228643659773	-0.43857192786997
H	3.29648376656803	-2.07281685289083	-1.79536544590811
C	4.64389635975096	-0.35669229489746	0.78985332017502
H	3.45367230949712	0.18522951235672	2.50444874215599
H	5.47219298006359	-1.06826029927680	-1.05793358217433
H	5.55363709267580	0.08975021709485	1.15419207052752
N	2.34033124073953	-0.83179571972908	1.13285904999391
C	-4.03969376216117	0.09568561176922	-0.42166943647970
O	-4.66125077508372	0.77815621611317	-1.26881390648136

C	-4.32477978188978	0.54931625757369	1.01615222449665
C	-5.64284735665062	0.53466072663341	1.47582660641364
C	-3.34796307349947	1.05601382518796	1.86835494687795
C	-5.96918496128681	0.98782207033849	2.74342785091478
C	-3.66819670620413	1.51942779827209	3.13813199129166
H	-2.32230035133471	1.08391454719673	1.54646263703077
C	-4.97983929504762	1.48435425494733	3.58446425606429
H	-6.99553593821708	0.95773863527934	3.07680179545669
H	-2.88079243365650	1.87759776263851	3.77943421089528
H	-5.22842341816728	1.83215998899678	4.57454334160896
Cu	0.13942063367543	-0.92049698419207	2.03744876013629
Cl	0.25952373276251	0.08526378649440	4.03135416966742
H	-6.41316952095481	0.18132332874144	0.81138889848157

A10.11 COORDINATES FOR OPTIMIZED L73^{NNO}•Cu^I

C	-2.26607830177772	3.84840594541677	-2.51485661046162
C	-2.35205781243868	3.77737367032772	-3.89245368058958
H	-3.16580365084757	3.24482179143088	-4.35743927888943
C	-1.38021203258064	4.39160823379520	-4.67756412355062
H	-1.44681000296832	4.34015970097817	-5.75166342357540
C	-0.32617337505139	5.06285475590569	-4.07969657086398
H	0.42803400581208	5.53207527104171	-4.68944294251359
C	-0.23587257876524	5.12995228593644	-2.69230663346010
H	0.58834896324131	5.64310773149735	-2.22560605543039
C	-1.20572248530227	4.52947860672319	-1.91148172155414

C	-3.68091073040540	4.29309588898663	-0.58435777470112
C	-4.99284712777604	4.60585405260877	-0.28370168613419
H	-5.79683446376194	4.03672048001798	-0.72021023158543
C	-5.27047122295612	5.65062621111583	0.59282130640122
H	-6.29277697263455	5.89526378309787	0.82902799480762
C	-4.23560851288812	6.37018792114708	1.16809115644150
H	-4.45328777718457	7.17548387183302	1.84990113366513
C	-2.91354145351555	6.05120896371530	0.87200449559254
H	-2.10698099735127	6.60097713072602	1.32833313514942
C	-2.63743225585573	5.01952760656335	-0.00595586106725
C	-3.19728963456280	3.20367888432414	-1.51221406466061
H	-4.01212219548290	2.66852646577478	-1.98375751929999
C	-1.26754121740357	4.51634986531738	-0.40238827657162
H	-0.46600209460068	5.07418616947586	0.05764624026166
C	-2.30041911825567	2.20360602870315	-0.70417328808121
C	-1.23242543768345	3.02278213725117	0.09445617918861
N	0.04022974983659	2.34760549116649	-0.00726197661616
N	-3.12197020020294	1.34345598913872	0.11114655201166
H	-1.75235914247502	1.63163591052737	-1.44879713389807
H	-1.54446531272270	3.05227777366298	1.13683401322458
C	1.11809359878266	2.81716523192603	0.56340325437011
O	1.33880662777686	3.88624888477986	1.15922931277800
C	2.29582952822734	1.84163422447313	0.44744082857580
C	3.58328406048176	2.28273521302633	0.73376585089207
C	3.08570843499959	-0.27738258591983	0.00457186225753
C	4.64248234669974	1.40374266856188	0.63054743459315
H	3.70422466693801	3.30619642717129	1.03414899225863

C	4.39315394301642	0.09166455890008	0.25559529931168
H	2.84247619421291	-1.28812695787111	-0.27530316677604
H	5.64728659000912	1.73025702188774	0.84088658041859
H	5.18486100411556	-0.63089110587110	0.16624604778192
N	2.06222525216131	0.56976329430659	0.09491174681475
C	-2.79190302280291	0.10656241240133	0.26427112424038
O	-1.75470917442183	-0.53404229036675	-0.16543830676096
C	-3.77068589427325	-0.74239704346286	1.04663017742525
C	-4.92337851112514	-0.19695462211894	1.60965526410857
C	-3.52927991845903	-2.10210054851298	1.22029102021348
C	-5.80722351112708	-0.98896337186852	2.32325014992627
H	-5.10336987405111	0.85354944365655	1.47629211212505
C	-4.41660151748437	-2.89874916330598	1.93068945899396
H	-2.63788279175477	-2.51872836832637	0.78950683064733
C	-5.55949843413810	-2.34613742420694	2.48652335685437
H	-6.69122562807580	-0.54802276682174	2.75424585232823
H	-4.21265846673506	-3.95021323666061	2.05200525238463
H	-6.24802818782155	-2.96214805315068	3.04130775846618
Cu	0.02558085140960	0.25081057916660	-0.18507209546837

A10.12 COORDINATES FOR OPTIMIZED L73^{NNN}•Cu^I

C	-2.90781129124592	-3.68046865675812	2.13164834635104
C	-3.46035747886549	-3.82065378319546	3.38984152479710
H	-4.27745436770137	-3.18815854855292	3.69462714512012
C	-2.94985087797712	-4.77635431742260	4.26541256348064

H	-3.38141027011127	-4.88916859673130	5.24608626475853
C	-1.88718271262363	-5.57582522469807	3.87980291619148
H	-1.49039839919948	-6.30989656857782	4.56124261548890
C	-1.32982625116660	-5.43476800885337	2.61144811426673
H	-0.50264613123690	-6.05638808194214	2.31085060144345
C	-1.84070588466859	-4.49472782702951	1.73686569660659
C	-3.62631387091864	-3.43629787997717	-0.17193905515669
C	-4.79552260478670	-3.35342687986923	-0.90377195027406
H	-5.56363751274495	-2.65449244304425	-0.61693963154380
C	-4.97700358320674	-4.17489637845732	-2.01355959189677
H	-5.88815317801540	-4.11058089052533	-2.58461685225351
C	-3.98832493733641	-5.07033753415306	-2.38490531219769
H	-4.12970406139996	-5.70238114862981	-3.24579905701514
C	-2.80588653768993	-5.15120968815544	-1.65352534211520
H	-2.02750420447906	-5.83301311067909	-1.95315690561643
C	-2.62851631577805	-4.34129599935583	-0.54908949140439
C	-3.29501325645231	-2.65334646886807	1.08142256983360
H	-4.12447084248195	-2.04688873137428	1.40600722094273
C	-1.38967270098707	-4.24064621559159	0.31770897504466
H	-0.59479146686010	-4.89690781516964	-0.00621144266850
C	-1.95371407971483	-1.82710957778720	0.91605120623941
C	-0.97195483384726	-2.73600791447806	0.12600287452467
N	0.36195944831228	-2.28574355522053	0.41584244325957
N	-1.89407443279824	-0.49498034100695	0.31203484701908
H	-1.54716107908181	-1.76324214929581	1.92346562280588
H	-1.16030606218252	-2.54403857936095	-0.92956458229663
C	1.36407780174846	-2.63751474885840	-0.34690762686901

O	1.53840160926782	-3.60217243784438	-1.10945226856254
C	2.47815693927773	-1.58459803152473	-0.31865720008314
C	3.81536017185770	-1.94177274375556	-0.44468708212917
C	3.04494803615624	0.65242577966787	-0.30517768723389
C	4.78385163386447	-0.95928812732132	-0.46415229144450
H	4.05532762476149	-2.98497944611403	-0.53309425981839
C	4.39375112772911	0.37099922389786	-0.39307014220096
H	2.69401822844662	1.66957514012908	-0.27208312200388
H	5.82652302714565	-1.21902459896298	-0.54060853851793
H	5.11169272791813	1.17139319063058	-0.41632018437782
N	2.10748555917640	-0.29438288993679	-0.26031436273015
C	-2.69938534261749	0.53290964760177	0.54081627432254
O	-2.54787429567852	1.64877670388144	0.02462768426344
C	-3.88363870891324	0.45147874366222	1.48884965059238
C	-5.17238068873012	0.66827855644842	1.00893602975712
C	-3.70460995718364	0.28538872333586	2.85770078614459
C	-6.25705324149071	0.68531391095161	1.87011196431455
C	-4.78673272079972	0.32465593510361	3.72604441478805
H	-2.71414431579864	0.12571355352052	3.24753035146751
C	-6.06897331945761	0.51560378304089	3.23562744782018
H	-7.24907500265285	0.84062753581404	1.47899902234991
H	-4.62669551863065	0.20225096264092	4.78448593509709
H	-6.91068593675811	0.53681644206987	3.90731135536042
Cu	0.05382852343182	-0.14354025469507	-0.01337905713486
H	-5.31361006582430	0.83208917237764	-0.04513933590688

A10.13 COORDINATES FOR Relaxed L73²⁻

C	-1.50980226084915	-3.62116911105623	2.72615860314258
C	-1.68340799356656	-3.35860169562684	4.07323134827566
H	-2.59483981702770	-2.89582078173036	4.41589570582876
C	-0.67460272951149	-3.67842775539011	4.97826380108572
H	-0.80887890248065	-3.47176667409105	6.02843777746346
C	0.50615731833735	-4.24796831889832	4.52847145142283
H	1.29320272857669	-4.48162267860238	5.22792426735532
C	0.68669722033739	-4.50121342513615	3.17134393436695
H	1.61434478656440	-4.91963513040380	2.81674460300411
C	-0.31759423511593	-4.19425697240955	2.27206048157501
C	-2.70156566335182	-4.58789816231023	0.84738635268309
C	-3.91766838169115	-5.17282443811878	0.54584575846410
H	-4.83244588091537	-4.70326056560895	0.86848478893298
C	-3.95820982278705	-6.35366684773445	-0.19122442266858
H	-4.90795562694109	-6.80556946444191	-0.43014987186307
C	-2.78148982925926	-6.93835136380692	-0.63216536929142
H	-2.81433403966444	-7.84727986952626	-1.21215658252973
C	-1.55577679165536	-6.34613404076767	-0.33785773842845
H	-0.63938107398957	-6.78643853051787	-0.69659752740514
C	-1.51383810284546	-5.17956003763884	0.40443987255748
C	-2.47781918369340	-3.30887238560186	1.61442782916270
H	-3.39401883773722	-2.85918950452032	1.96935068259883
C	-0.28538345053009	-4.38980303622759	0.77679664141039
H	0.62898944866872	-4.84780259174546	0.42676330454808
C	-1.73914522626712	-2.28860317440128	0.64874203888385

C	-0.44890857328055	-2.96687850633627	0.09548401043282
N	0.72920556642948	-2.15321921208103	0.29823579186393
N	-2.61190882184876	-1.84170064435282	-0.41271153494271
H	-1.43091139768558	-1.45903658966913	1.27942782633752
H	-0.60922271938651	-3.16705888891441	-0.96086661376087
C	1.75959584368178	-2.46914083420471	-0.42755916220803
O	1.92057331092540	-3.39500780489706	-1.27345384596586
C	2.97079546861827	-1.54876963249551	-0.26513410139782
C	3.86403878420004	-1.45870114093756	-1.34356549190996
C	4.27070786604539	-0.10161446457716	0.94302848545016
C	4.96893118827598	-0.63980154186559	-1.25597108824262
H	3.65092338169721	-2.05001610006941	-2.21395593853973
C	5.19008931231989	0.06455297620416	-0.07864517959414
H	4.41027948854706	0.41788458259362	1.88207479459363
H	5.65275565563666	-0.55037331279288	-2.08629436119444
H	6.04202779533599	0.71281006179979	0.04598876149418
N	3.19357471421462	-0.87111089682644	0.86235775416589
C	-3.56813982398621	-1.02036339169791	-0.07138394523836
O	-3.88291616298300	-0.56480491561861	1.06007486553971
C	-4.43227795829112	-0.56017595905553	-1.24635941704756
C	-4.20528533029771	-0.98435972663075	-2.55558137309629
C	-5.48918755058185	0.31696887307395	-1.01666631786900
C	-5.00829167357217	-0.54539041526907	-3.59691360457047
H	-3.38646937086661	-1.66017318741823	-2.72330818578493
C	-6.29587989103031	0.76037098089488	-2.05670395926556
H	-5.65164591230094	0.63674086353243	-0.00258438488795
C	-6.06052465872253	0.33105903039748	-3.35482759008372

H	-4.81384611131610	-0.88559736658161	-4.60243093631265
H	-7.10852515135652	1.44178532949650	-1.85442854067287
H	-6.68425261702601	0.67323531461210	-4.16612444786781

A10.14 COORDINATES FOR OPTIMIZED L73^{NNO}•Cu^ICl₂

C	-1.88649399072427	-4.53976587870486	2.72782702458312
C	-0.48502919218565	-4.96273143383004	2.29651665997950
C	-2.60957767751661	-3.83892335299510	1.58055982065353
H	-3.58686011847290	-3.48675161120067	1.90305806781028
C	0.28976427158957	-3.77235621100259	1.73538735644610
H	1.26968359034699	-4.08962189454434	1.39906726459391
C	-1.84233868045315	-2.64064507693845	0.99367500047383
C	-0.42922470969714	-3.07470977893471	0.55858215990898
N	0.38526453982909	-1.95020106834930	0.10681484430566
N	-2.65520472354931	-2.11624193856780	-0.08479163398959
H	-1.71582830179127	-1.89204001542938	1.77830956690188
H	-0.53451455147409	-3.79687133952208	-0.25273293351979
C	1.51524845379303	-2.26617867092129	-0.49021403928215
O	1.93239589309772	-3.37945538892417	-0.86185988470177
C	2.45570217672732	-1.08760735333184	-0.65005818896021
C	3.73530007896181	-1.25254046842614	-1.16927483846763
C	2.84654520408443	1.14245305295259	-0.22293690936261
C	4.58521739725218	-0.16464431524358	-1.19375216366386
H	4.01813164360290	-2.22644198901454	-1.52131203435920
C	4.14105189590896	1.05483861916263	-0.70169472022958

H	2.42627709034077	2.05689723007802	0.15012019239676
H	5.58531039457651	-0.26229344136905	-1.58609690994936
H	4.77492842567471	1.92433018057947	-0.69857243628480
N	2.03970466333009	0.09065491166226	-0.20401763430390
C	-2.63949209190348	-0.84368653704707	-0.27413716383796
O	-1.92762930555714	0.04377885271604	0.32629898886650
C	-3.62396557968075	-0.30519946887745	-1.28944853028947
C	-4.66017203078304	-1.09359718917730	-1.78784907790013
C	-3.51437470703289	1.01109161178586	-1.72939339011029
C	-5.57120124940920	-0.57933678354885	-2.69656113473524
H	-4.72813359538719	-2.11105213764763	-1.44794437447946
C	-4.42406966182256	1.52388305977081	-2.64482815089316
H	-2.69487219185000	1.60709594915265	-1.36959751293908
C	-5.45847652661991	0.73680000423998	-3.12857076686367
H	-6.36918996640720	-1.20323485507527	-3.06893287170665
H	-4.31490741111953	2.54130716570057	-2.98448676374390
H	-6.16488115798038	1.13909367321711	-3.83820252523004
Cu	0.01909162342559	0.13210409542787	0.29598271739894
Cl	0.53003247806746	1.12867232642933	2.53340096521830
Cl	-0.02448529228963	2.04531022952820	-1.48380698797233
H	-2.79105969100433	-4.54963642477851	0.77417492347649
H	-1.80747696782295	-3.86155059313215	3.57779979579056
H	-2.46355384808443	-5.40171293652907	3.06841272461078
H	0.05822973811298	-5.40233740540651	3.13442247193106
H	-0.56184481854012	-5.73958788732545	1.53407610626102
H	0.43746562043702	-3.03186067960819	2.51976273816863

A10.15 **COORDINATES FOR L73^{NNN}•Cu^ICl₂**

C	-3.76732416474454	-3.71903771504974	0.26022618571144
C	-2.61658187688120	-4.60644859180410	-0.21469754664906
C	-3.60694782979964	-2.26678821888084	-0.20264441539727
H	-3.68277482667684	-2.20866762798681	-1.28895220465478
C	-1.25178465110627	-3.99904447860014	0.11835164743162
H	-0.45521570109036	-4.59890565448462	-0.30195208161755
C	-2.24629530223693	-1.68543165988688	0.22370912199325
C	-1.15022211164922	-2.56431298082626	-0.42163233272824
N	0.12440223323475	-1.92014578193149	-0.21116236530148
N	-2.00785683649429	-0.29943004248951	-0.17598668695174
H	-2.14736952632392	-1.81768815136154	1.30398632767587
H	-1.35072310877546	-2.59844951674723	-1.49810335255874
C	1.25843510044054	-2.45977826095302	-0.58182027903736
O	1.49655260402214	-3.55353998939383	-1.12906104098198
C	2.43565505057576	-1.55751825805794	-0.25857075520056
C	3.74568142010302	-2.00890648370203	-0.36671023945065
C	3.13638402600041	0.51626879222276	0.44952541240640
C	4.77312179065858	-1.14665601501045	-0.03423661219095
H	3.91210916797015	-3.01476357909475	-0.70409995785489
C	4.46800484807159	0.14010710363604	0.38526213113985
H	2.82148223420132	1.50254831046559	0.74113575364067
H	5.80011290818702	-1.47022894561147	-0.09977294786994
H	5.23938764713039	0.84061850816170	0.65512144005093
N	2.15802636391888	-0.31856077442172	0.13407174997778
C	-2.93457666107770	0.65516082596400	0.03051920320034

O	-3.05064817024354	1.67270765378880	-0.64519364060163
C	-3.91311500159120	0.56516838045517	1.20506844334957
C	-5.25526814690576	0.88225535682735	1.00759587024009
C	-3.47209468875868	0.29096002472273	2.49647125204633
C	-6.15091949888211	0.88833498947134	2.06444857576535
C	-4.36595059422270	0.32208866027987	3.56034788757997
H	-2.42833930157959	0.08359970908513	2.67648919329414
C	-5.70678210522904	0.60731598007666	3.35111906140889
H	-7.18958757288823	1.12373624523693	1.89010999598464
H	-4.00294410746271	0.12442947695904	4.55588016078229
H	-6.39750745430310	0.62123993196946	4.17977189907866
Cu	0.00288195582255	0.04525948537972	0.20110302065726
Cl	0.14067032411241	-0.22517690517628	2.97018365237010
Cl	0.38576165541683	2.33076864844883	-0.18709649686925
H	-5.58112081369467	1.13616600092855	0.01343965998913
H	-2.68994898598036	-4.73757389770071	-1.29547683260359
H	-4.72164391333099	-4.11899551253384	-0.08651717263661
H	-1.10631027618951	-3.97387418479918	1.19735172142107
H	-2.70362062989036	-5.60241578674092	0.22224302342695
H	-4.42149746723664	-1.67783298496365	0.19921720503885
H	-3.80357728962073	-3.73597501287071	1.34936787149486

APPENDIX 11

Palladium-Catalyzed Enantioselective Vinylation of γ -Lactams and γ -Butyrolactones[†]

A11.1 INTRODUCTION AND BACKGROUND

Nitrogen heterocycles are ubiquitous structural motifs that can be found across all areas and applications of organic chemistry. A particularly important subgroup of these compounds are the pyrrolidinones along with their saturated counterparts the pyrrolidines, with both occurring widely in nature,^{1,2} possessing a wide range of biological and pharmacological properties,³ and finding use in functional materials⁴ and catalysis.⁵ For these reasons, the development of enantioselective approaches to functionalized five-membered nitrogen-containing heterocycles is a topic of great interest for the synthesis of natural products and other small molecules.

Our group has a long-standing interest in the stereoselective synthesis of five-membered N-heterocyclic building blocks, having developed methods for both enantioselective allylic alkylation,⁶ enantioselective α -acylation,⁷ and more recently, α -arylation of γ -lactams.⁸ In our α -

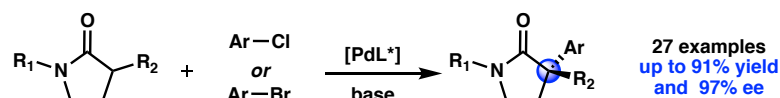
[†] This research was performed in collaboration with visiting graduate student Shunya Sakurai. This research has been published and adapted with permission from Jette, C. I. Geibel, I.; Bachman, S.; Hayashi, M.; Sakurai, S.; Shimizu, H.; Morgan, J. B.; Stoltz, B. M. *Angew. Chem. Int. Ed.* **2019**, 58, 4297–4301. Copyright 2019 Wiley-VCH.

arylation protocol, α -quaternary γ -lactams can be smoothly afforded from the corresponding aryl bromides or chlorides in the presence of a Pd catalyst (Figure A11.1.1.A). Given the importance of β - γ -unsaturated carbonyls in bioactive compounds,⁹ as well as the diversity of methods in the literature for alkene functionalization, we envisioned that the extension of our α -arylation method to also include vinyl electrophiles would be of great synthetic value.

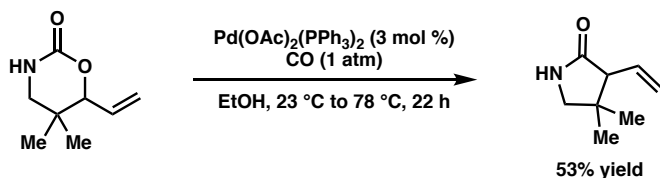
Although there are numerous reports on the α -vinylation of carbonyl derivatives such as ketones, esters, and nitriles,¹⁰ there are few reports on the synthesis of vinyl γ -lactams, and to our knowledge, no reports on the enantioselective variant. One strategy for the synthesis of these

Figure A11.1.1. α -Arylation of Lactams and Previously Reported Methods for the Synthesis of Vinyl γ -Lactams^{8,11,12}

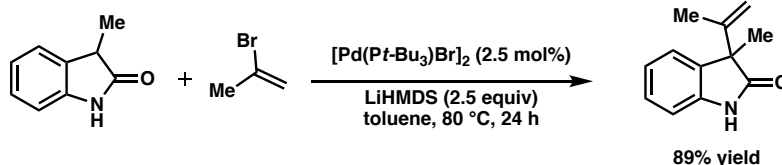
A. Pd-catalyzed enantioselective α -arylation of lactams



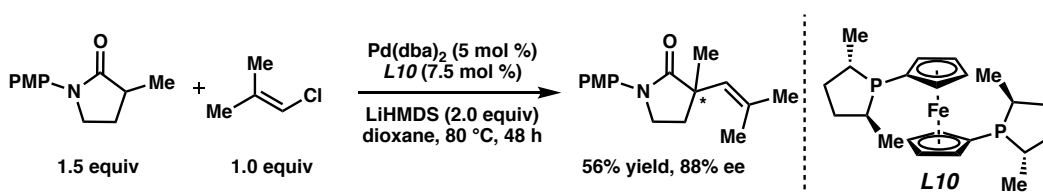
B. Tamaru: α -vinyl lactams via Pd-catalyzed decarboxylative carbonylation



C. Faul: direct α -vinylation of oxindoles

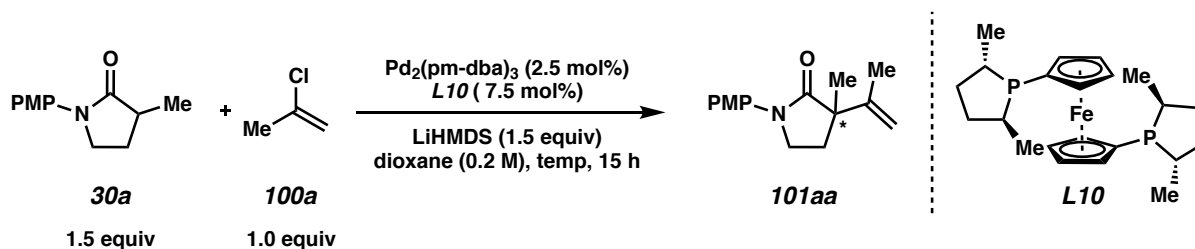


D. This research: Pd-catalyzed enantioselective direct α -vinylation of lactams



compounds is the Pd-catalyzed decarboxylative carbonylation approach, which converts cyclic carbamates to the corresponding unsubstituted α -vinyl lactams (Figure A11.1.1.B).¹¹ To our knowledge, there is only one report of a direct α -vinylation approach of a cyclic amide, however the scope of this reaction is limited to oxindoles (Figure A11.1.1.C).¹² Given the large pK_a difference between γ -lactams and oxindoles, it is unsurprising that these scaffolds should exhibit significant differences in their reactivity profiles. One critical challenge in the development of enantioselective α -vinylation of γ -lactams is that as a result of their enolates' high reactivity, direct α -vinylation (*via* addition/elimination) may occur in the absence of a Pd catalyst. Uncatalyzed direct vinylation may be detrimental to the selectivity of the reaction, resulting in significant challenges associated with retention of olefin geometry and generation of enantioenriched product. In order to circumvent these challenges, a Pd-catalyst that generates the desired α -vinyl product significantly faster than the unwanted background reaction will have to be identified. Herein, we

Table A11.2.1 Initial Hit and Temperature Screen with 2-Chloropropene^a



entry	temp (°C)	yield (%) ^b	% ee ^c
1	80	23	82
2	60	37	88
3	50	42	86
4	40	8	—
5	23	0	—

[a] Conditions: See Section A11.6, 0.1 mmol scale. [b] Yields determined by ¹HNMR analysis of the crude reaction mixture using 1,3,5-trimethoxybenzene as a standard. [c] Determined by chiral SFC analysis of the isolated product. PMP = *p*-methoxyphenyl. pm-dba = 4,4'-dimethoxydibenzylideneacetone.

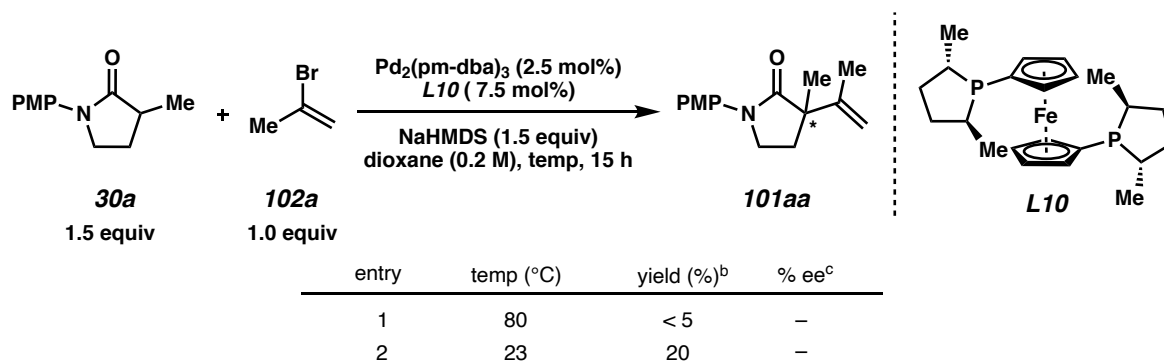
report our progress toward the development of an enantioselective α -vinylation of γ -lactams (Figure A11.1.1.D).

A11.2 PRELIMINARY INVESTIGATIONS

We first exposed 2-chloropropene (**100a**) to PMP-lactam **30a** using our optimized conditions for the enantioselective α -arylation (Table A11.2.1). At 80 °C, we obtained the product in 23% yield and 82% ee (entry 1). Interestingly, we noted that although in the arylation conditions higher temperatures are required for efficient product formation, in this case the yields increase slightly at lower temperatures. At 50 °C, we obtained the product in 47% yield and a slightly higher 86% ee (entry 3). As the temperature is lowered even further, however, a drop in yield is observed, and at 23 °C, no product is formed (entries 4 and 5).

Using our previously developed conditions for the α -arylation of γ -lactams using aryl bromides, we examined the analogous 2-bromopropene in our reaction conditions. At 80 °C, we found that only a trace amount of product was formed (entry 1, Table A11.2.2). When the reaction

Table A11.2.2. Vinylation With 2-Bromopropene^a



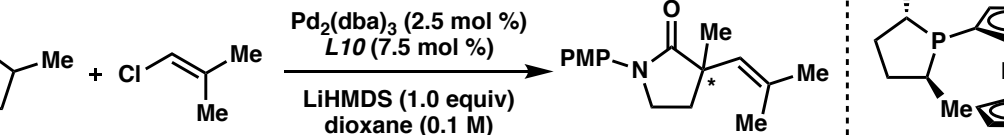
[a] Conditions: See Section A11.6, 0.1 mmol scale. [b] Yields determined by ¹HNMR analysis of the crude reaction mixture using 1,3,5-trimethoxybenzene as a standard. [c] Determined by chiral SFC analysis of the isolated product. PMP = *p*-methoxyphenyl. pm-dba = 4,4'-dimethoxydibenzylideneacetone.

temperature is lowered to 23 °C, the desired product is formed in 20% yield. Given the greater amount of reactivity observed with 2-chloropropene, we chose to move ahead with these conditions.

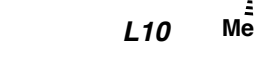
A11.3 REACTION OPTIMIZATION

During the course of optimization we noted that an alternative Pd source, $\text{Pd}_2(\text{dba})_3$ resulted in higher enantioselectivity, and that the lactam nucleophile could be used as the limiting reagent without leading to a significant change in reaction outcome (Table A11.3.1). Given that the vinyl chloride is the least precious of the two coupling partners, we chose to switch to conditions in which the electrophile is used in excess. We also noted that the boiling point of 2-chloropropene is 30 °C, which we believed could be affecting the reaction consistency, as this was leading to significant challenges in the accurate weighing of this reagent. For this reason, we switched the electrophile to isocrotyl chloride which we found to be significantly less reactive, and only a small

Table A11.3.1. Temperature Screen with Isocrotyl Chloride^a



Reaction scheme showing the vinylation of lactam **30a** (1.0 equiv) with isocrotyl chloride **100b** (1.5 equiv) to form product **101ab**. The reaction conditions are $\text{Pd}_2(\text{dba})_3$ (2.5 mol %), **L10** (7.5 mol %), LiHMDS (1.0 equiv), dioxane (0.1 M), temp, time.



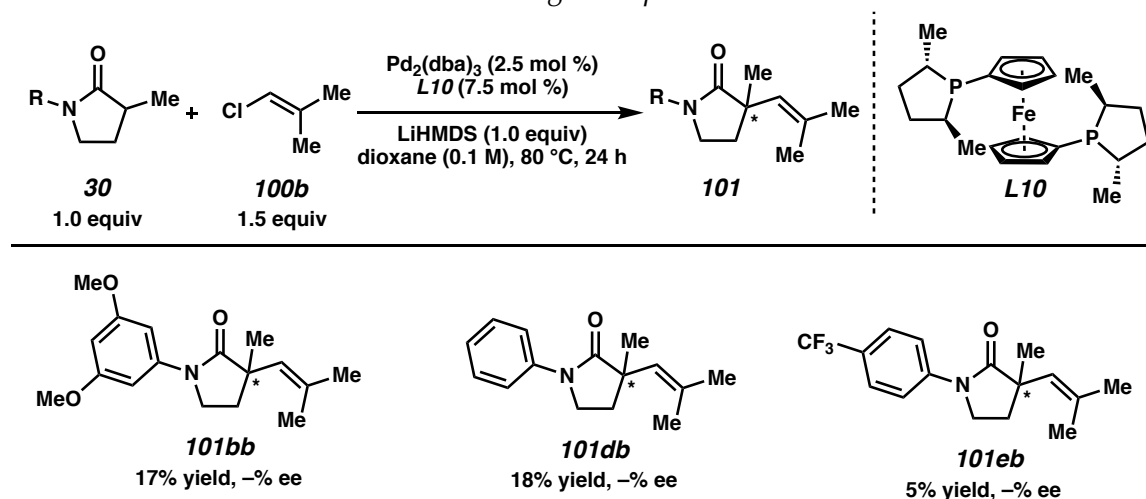
Chemical structure of the chiral ferrocenyl phosphine ligand **L10**, which is a ferrocene derivative with two phosphine groups and methyl substituents.

entry	temp (°C)	time (h)	yield (%) ^b	% ee ^c
1	50	15	<5	—
2	60	15	2	—
3	70	15	12	—
4	80	15	16	—
5	80	24	43	93
6	100	24	13	—

[a] Conditions: See Section A11.6, 0.1 mmol scale. [b] Yields determined by ¹HNMR analysis of the crude reaction mixture using 1,3,5-trimethoxybenzene as a standard. [c] Determined by chiral SFC analysis of the isolated product. PMP = *p*-methoxyphenyl. dm-dba = 3,5,3',5'-dimethoxydibenzylideneacetone.

amount of product was observed at all temperatures up to 80 °C after 15 h (Table A11.3.1, entries 1-4). However, if the reaction time is extended to 24 h, the product is obtained in 43% yield and 93% ee at 80 °C (entry 5). The higher temperature required could be due either to a slower transmetalation to the more sterically hindered Pd(II)-vinyl complex, or a slower O- to C-bound

Table A11.3.2. Effect of the N-Protecting Group^a



[a] Conditions: See Section A11.6, 0.1 mmol scale. Yields determined by ^1H NMR analysis of the crude reaction mixture using 1,3,5-trimethoxybenzene as a standard. PMP = *p*-methoxyphenyl. pm-dba = 4,4'-dimethoxydibenzylideneacetone.

enolate isomerization (see Figure 2.2.1 for plausible mechanism). Nevertheless, we were pleased to see product formation using isocrotyl chloride under slightly modified conditions, and chose to continue the optimization with this electrophile.

The importance of the lactam protecting group on the reaction outcome was also examined (Table A11.3.2), and it was noted that the *p*-methoxyphenyl N-protecting group (**30a**, Table A11.3.1, entry 5) was optimal; switching to a bulkier aryl group (**101bb**), or altering the electronics (**101db** and **101eb**) resulted in significant drops in reactivity.

We next turned our attention to the Pd source. We noted that $\text{Pd}(\text{dba})_2$ (entry 1, Table A11.3.3), performed very similarly to $\text{Pd}_2(\text{dba})_3$, however, all other Pd(0) precatalysts led to

significant drops in reactivity (entries 3–6). Increasing the catalyst loading also led to a significant decrease in yield (entry 2).

Table A11.3.3. Examination of Different Pd(0) Sources^a

entry	Pd source	yield (%) ^b	% ee ^c
1	Pd(dba) ₂	40	94
2 ^d	Pd(dba) ₂	24	–
3	Pd(dm-dba) ₂	8	–
4	(TMEDA)PdMe ₂	11	58
5	(η^3 -allyl)PdCp	12	73
6	(η^3 -cinnamyl)PdCp	27	–

[a] Conditions: 0.1 mmol scale. See A11.6. [b] Yields determined by ¹HNMR analysis of the crude reaction mixture using 1,3,5-trimethoxybenzene as a standard. [c] Determined by chiral SFC analysis of the isolated product. PMP = *p*-methoxyphenyl. dba = dibenzylideneacetone, dm-dba = 3,5,3',5'-dimethoxydibenzylideneacetone. [d] with 10 mol% Pd(dba)₂, and 15 mol% **L10**.

Having examined a number of parameters without observing any significant changes in reactivity, we chose to go back and examine additional ligands in order to ensure that we had identified the optimal ligand for this transformation. Similar to what we found in the arylation, the ferrocene ligands led to the most reactive complexes, and ferrocenes continued to stand out as the optimal class. We also noted that Me-ferrocene (**L10**) seemed to be optimal, and although Et-ferrocene did lead to a slight boost in ee, this was accompanied by a drop in reactivity. It should be noted that in all these reactions, an excess of LiHMDS (1.5 equiv) was used, as in concurrent experiments we had noted that this led to a modest increase in reactivity.

Table A11.3.4 Additional Ligand Screen

30a
1.0 equiv

100b
1.5 equiv

Pd(dba)₂ (5 mol%)
Ligand (7.5 mol%)
LiHMDS (1.5 eq.)
dioxane (0.1 M), 80 °C, 24 h
0.2 mmol scale, 1 dram vial

101ab

Ligands Tested:

(S,S)-Ferrocene
 R = Me: 53% yield, 89% ee
 R = Et: 45% yield, 92% ee
 R = *i*Pr: < 5%, -%ee

(S,S)-Et-FerrotANE
 4% yield, -%ee

SL-J001-1 (JosiPhos)
 47% yield, -47% ee

SL-M001-2 (MandyPhos)
 11% yield, -%ee

(R)-BINAP
 4% yield, -%ee

(R)-MOP
 <1% yield, -%ee

(R)-MonoPhos
 5% yield, -%ee

(S)-tBu-PHOX
 4% yield, -%ee

(R,R)-ChiraPhos
 4% yield, -%ee

(S,S,R,R)-TangPhos
 10% yield, -%ee

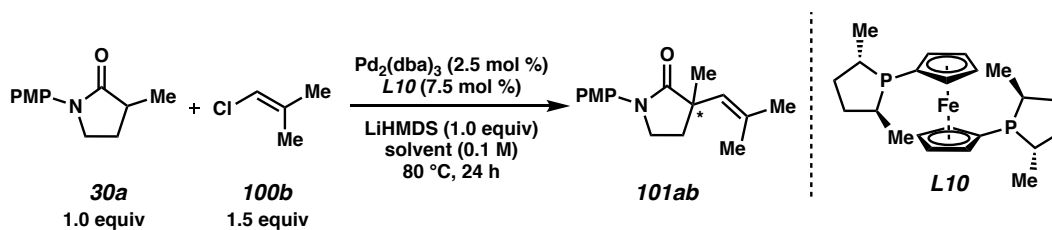
(S,S)-Me-BPE
 5% yield, -%ee

(R,R)-Me-DuPhos
 5% yield, -%ee

[a] 0.1 mmol scale, See A11.6. Yields determined by ^1H NMR analysis of the crude reaction mixture using 1,3,5-trimethoxybenzene as a standard. Enantiomeric excess (ee) was determined by chiral SFC analysis of the isolated product. PMP = *p*-methoxyphenyl. dba = dibenzylideneacetone,

We next decided to take a deeper look at the reaction in order to see if we could understand why we never observed yields above 50%. When 1 equivalent of LiCl is added at the start of the reaction, only a negligible amount of product is observed (Table A11.3.5, entry 1). This result suggests that in the presence of excess Cl anions, Pd may remain in an anionic state which could result in a significantly less viable catalyst for this reaction.¹³ This prompted the investigation into different solvents, as we envisioned that a less polar solvent might encourage the LiCl to precipitate from the solution. However, with less polar solvents (entries 3-5), a significant drop in both reactivity and ee is observed. In addition, the use of electrophiles other than vinyl chlorides, such as vinyl triflates and bromides also led to negligible amounts of product.

Table A11.3.5. Effect of LiCl on the Reaction Outcome and Solvent Screen^a

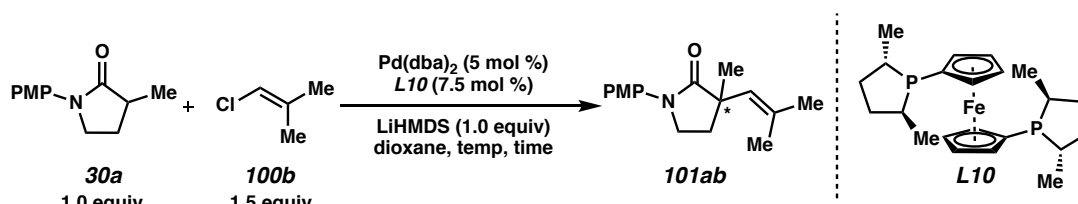
				
entry	equiv LiCl	solvent	yield (%) ^b	% ee ^c
1	0	dioxane	42	93
2	1	dioxane	< 5	–
3	0	1:1 dioxane/toluene	23	83
4	0	toluene	30	84
5	0	DME	26	–

[a] Conditions: See Section A11.6, 0.1 mmol scale. [b] Yields determined by ¹H NMR analysis of the crude reaction mixture using 1,3,5-trimethoxybenzene as a standard. [c] Determined by chiral SFC analysis of the isolated product. PMP = *p*-methoxyphenyl. dba = dibenzylideneacetone.

By reverting the stoichiometry back to excess lactam and base, we were able to slightly improve the yield (entry 1, Table A11.3.6). However, we found that the isolated yield was significantly lower than that determined using ¹H NMR and an internal standard. By extending the

reaction time to 48 h, we were able to improve the outcome of the reaction slightly, and with these conditions, the product is obtained in 56% isolated yield and 88% ee (entry 2). Increasing the reaction concentration to [0.2 M] did lead to a 10% drop in yield (entry 4), and decreasing the concentration did not lead to any significant improvements (entry 3). Gratifyingly, the temperature can be lowered by 10 °C without significantly altering the reaction outcome (entry 5).

Table A11.3.6. Concentration, Temperature, and Reaction Time



entry	concentration (M)	time (h)	temp (°C)	yield (%) ^a	% ee ^b
1	0.1	20	80	45 (58) ^c	88 (89) ^c
2	0.09	48	80	56	88
3	0.077	48	80	53	89
4	0.2	48	80	44	88
5	0.09	48	70	55	87

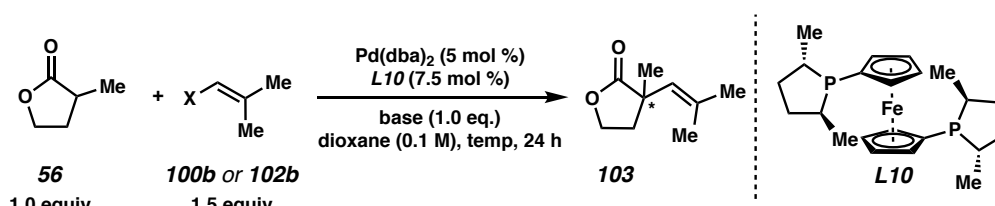
[a] Isolated yields on 0.2 mmol scale, See Section A11.6 for set-up. [b] ee was determined by supercritical fluid chromatography [c] Results from a separate run in parentheses, yield determined by ¹H NMR using trimethoxybenzene as an internal standard.

A11.4 PRELIMINARY RESULTS WITH γ -BUTYROLACTONES AND VINYL BROMIDES

Our initial success in the Pd-catalyzed α -vinylation of γ -lactams prompted the examination of γ -butyrolactones substrates in this reaction. Interestingly, we found that the γ -butyrolactones, in combination with LiHMDS and isocrotyl chloride, led to very little product

formation (entries 1 and 2, Table A11.4.1). When isocrotyl bromide and NaHMDS are used, the desired α -vinyl γ -butyrolactone is obtained in moderate yield and excellent ee at 50 °C (entry 4). We found that the reaction yield can be improved by increasing the temperature to 80 °C, however this is accompanied by a slight decrease in ee (entry 5).

Table A11.4.1. Preliminary Results With α -Methyl γ -Butyrolactone



entry	X	base	temp (°C)	yield (%) ^b	% ee ^c
1 ^d	Cl	LiHMDS	50	< 5	—
2 ^d	Cl	LiHMDS	80	13	—
3	Br	NaHMDS	23	5	89
4	Br	NaHMDS	50	39	93
5	Br	NaHMDS	80	50	84

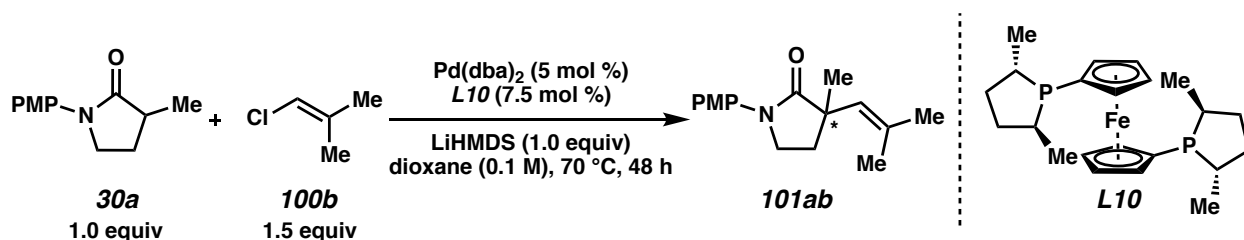
[a] Conditions: See Section 5.6, 0.1 mmol scale. [b] Yields determined by ¹HNMR analysis of the crude reaction mixture using 1,3,5-trimethoxybenzene as a standard. [c] Determined by chiral SFC analysis of the isolated product. [d] with Pd₂dba₃ (2.5 mol %) instead. PMP = *p*-methoxyphenyl. dba = dibenzylideneacetone.

A11.5 CONCLUSION

We have initiated the development of a protocol for the enantioselective α -vinylation of γ -lactams and γ -lactones. Starting from the conditions developed for the enantioselective α -arylation, we examined the effect of the electrophile, protecting group, Pd source, ligand, and reactant stoichiometry on the reaction outcome. We found that the yields could not be improved beyond 50%, and control experiments indicate that the reason for this may be that LiCl is poisoning the Pd catalyst. Future work will focus on examining different strategies for sequestering the Cl

anions in solution as well as determining the origin of enantioselectivity (enantioselective transmetalation vs. equilibration of diastereomeric L*-Pd-enolates). In addition, we have also obtained some promising preliminary results using γ -butyrolactones as nucleophiles. Interestingly, we noted that the reaction conditions that result in the highest yield and ee are highly dependent on the nucleophile; with the γ -lactams, we found that the conditions developed for vinyl chlorides worked best, and with γ -butyrolactones, we found that the conditions developed for vinyl bromides gave the optimal results.

A11.6 REPRESENTATIVE PROCEDURE FOR PALLADIUM-CATALYZED α -VINYLATION OF γ -LACTAMS AND γ -BUTYROLACTONES



In a nitrogen-filled glovebox, to an oven-dried 4 mL vial equipped with a stir bar was added 1,1'-Bis[(2*S*,5*S*)-2,5-dimethylphospholano]ferrocene **L10** (6.2 mg, 15 μmol , 0.075 equiv) and $\text{Pd}(\text{dba})_2$ (5.8 mg, 10 μmol , 0.05 equiv), and dioxane (0.4 mL). The vial was capped with a PTFE-lined septum cap and stirred at 40 °C. After 20 minutes, the mixture was cooled to ambient temperature and the corresponding vinyl chloride (0.2 mmol, 1.0 equiv) was added. A solution of protected lactam **30a** (61.6 mg, 0.3 mmol, 1.5 equiv) and LiHMDS (50 mg, 0.3 mmol, 1.5 equiv) was then added to the resulting mixture, and the reaction sealed with electrical tape and stirred at

70 °C for 48 h, unless otherwise noted. The solution was cooled to ambient temperature, quenched with saturated NH₄Cl solution, and extracted with EtOAc five times. The combined organic layers were dried over Na₂SO₄ and concentrated. The crude reaction mixture was purified by silica gel flash chromatography (33% EtOAc in hexanes) to furnish product **101ab** (28.7 mg, 0.17 mmol, 55% yield); 87% *ee*; ¹H NMR (500 MHz, CDCl₃) δ 7.59 – 7.50 (m, 2H), 6.96 – 6.85 (m, 2H), 5.55 – 5.40 (m, 1H), 3.80 (s, 3H), 3.79 – 3.68 (m, 2H), 2.28 (dt, *J* = 12.5, 8.2 Hz, 1H), 2.17 (ddd, *J* = 12.4, 7.4, 3.7 Hz, 1H), 1.75 (d, *J* = 1.4 Hz, 3H), 1.69 (d, *J* = 1.2 Hz, 3H), 1.36 (s, 3H); δ ¹³C NMR (126 MHz, CDCl₃) δ 177.76, 156.50, 134.54, 133.78, 129.86, 122.32, 114.10, 55.19, 48.75, 45.71, 33.21, 29.82, 27.04, 25.47, 20.33; SFC Conditions: 10% IPA, 2.5 mL/min, Chiralcel OD-H column, λ = 254 nm, *t_R* (min): minor = 9.96, major = 10.52.

A11.7 REFERENCES AND NOTES

1. For pyrrolidine-containing alkaloids, see: (a) Donohoe, T. J.; Bataille, C. J. R.; Churchill, G. W. *Annu. Rep. Prog. Chem., Sect. B* **2006**, *102*, 98–122. (b) Felpin, F. –X.; Lebreton, J. *Eur. J. Org. Chem.* **2003**, *19*, 3693–3712.
2. For recent reviews on the synthesis of pyrrolidinone containing alkaloids, see (a) Long-Wu, Y.; Shu, C.; Gagosz, F. *Org. Biomol. Chem.* **2014**, *12*, 1833–1845. (b) Rivas, F.; Ling, T. *Org. Prep. Proced. Int.* **2016**, *48*, 254–295.
3. For some examples of biologically active pyrrolidines, see: (a) Guzikowski, A. P.; Tamiz, A. P.; Acosta-Burrue, M.; Hong–Bae S.; Cai, S. –X.; Hawkinson, J. E.; Keana, J. F. W.; Kesten, S. R.; Shipp, C. T.; Tran, M.; Whittemore, E. R.; Woodward, R. M.; Wright, J. L.; Zhou, Z. – L. *J. Med. Chem.* **2000**, *43*, 984–994. (b) Lynch, C. L.; Hale, J. J.; Budhu, R. J.; Gentry, A.

- L.; Mills, S. G.; Chapman, K.T.; MacCoss, M.; Malkowitz, L.; Springer, M. S.; Gould, S. L.; DeMartino, J. A.; Siciliano, S. J.; Cascieri, M. A.; Carella, A.; Carver, G.; Holmes, K.; Schleif, W. A.; Danzeisen, R.; Hazuda, D.; Kessler, J.; Lineberger, J.; Miller, M.; Emini, E. A. *Bioorg. Med. Chem. Lett.* **2002**, *12*, 3001–3004. (c) Hensler, M. E.; Bernstein, G.; Nizet, V.; Nefzi, A. *Bioorg. Med. Chem. Lett.* **2006**, *16*, 5073–5079. (d) Li, X.; Li, J. *Mini-Rev. Med. Chem.* **2010**, *10*, 794–805. (e) Lexa, K. W.; Carlson, H. A. *Proteins* **2011**, *79*, 2282–2290. (f) Whitby, L. R.; Ando, Y.; Setola, V.; Vogt, P. K.; Roth, B. L.; Boger, D. L. *J. Am. Chem. Soc.* **2011**, *133*, 10184–10194. (g) Raghuraman, A.; Ko, E.; Perez, L. M. Ioerger, T. R.; Burgess, K. *J. Am. Chem. Soc.* **2011**, *133*, 12350–12353. For select examples of biologically active pyrrolidinones, see: (a) Caruano, J.; Muccioli, G.G.; Robiette, R. *Org. Biomol. Chem.*, **2016**, *14*, 10134–10156. (b) Duan, J. J. –W.; Chen, L.; Wasserman, Z. R.; Lu, Z.; Liu, R. –Q.; Covington, M. B.; Qian, M.; Hardman, K. D.; Magolda, R. L.; Newton, R. C.; Christ, D. D.; Wexler, R. R.; Decicco, C. P. *J. Med. Chem.* **2002**, *45*, 4954–4957.
4. Teodorescu, M.; Bercea, M. *Polym Plast Technol Eng.* **2015**, *54*, 923–943.
5. (a) Dalko, P. I.; Moisan, L.; *Angew. Chem.* **2001**, *113*, 3840–3864. *Angew. Chem. Int. Ed.* **2001**, *40*, 3726–3748. b) Dalko, P. I.; Moisan, L.; *Angew. Chem.* **2004**, *116*, 5248–5286. *Angew. Chem. Int. Ed.* **2004**, *43*, 5138–5175. c) List, B. *Synlett* **2001**, *11*, 1675–1686. d) List, B.; *Tetrahedron* **2002**, *58*, 5573–5590. e) List, B. *Acc. Chem. Res.* **2004**, *37*, 548–557. f) Notz, W.; Tanaka, F.; Barbas III, C. F.; *Acc. Chem. Res.* **2004**, *37*, 580–591. (g) Zhang, S.; Wang, W.; Zhou, Q.–L. *Privileged Chiral Ligands and Catalysts*; Ed.; Wiley-VCH: Weinheim, Germany, 2011; pp 409–439. (h) Watson, A. J. B.; MacMillan, D. W. C.; Ojima, I. *Enantioselective Organocatalysis Involving Iminium, Enamine SOMO and Photoredox*

- Activation. In *Catalytic Asymmetric Synthesis*, 3rd ed.; Ed.; Wiley & Sons: Hoboken, NJ, 2010; pp 39–57. (i) C. A. Caputo, N. D. Jones, *Dalton Trans.* **2007**, 4627.
6. Behenna, D. C.; Liu, Y.; Yurino, T.; Kim, J.; White, D. E.; Virgil, S. C.; Stoltz, B. M.; *Nat. Chem.* **2012**, *4*, 130–133.
7. Hayashi, M.; Bachman, S.; Hashimoto, S.; Eichman, C. C.; Stoltz, B. M. *J. Am. Chem. Soc.* **2016**, *138*, 8997–9000.
8. Jette, C. I.; Geibel, I.; Bachman, S.; Hayashi, M.; Sakurai, S.; Shimizu, H.; Morgan, J. B.; Stoltz, B. M. *Angew. Chem. Int. Ed.* **2019**, *58*, 4297–4301.
9. Radin, N. S.; *Drug. Dev. Res.* **2008**, *69*, 15–25.
10. Anker, T.; Cosner, C. C.; Helquist, P. *Chem. Eur. J.*; **2013**, *19*, 1858–1871.
11. Takashi, B.; Shuji, T.; Keigo, F.; Zen-ichi, Y.; Yoshinao, T. *Bull. Chem. Soc. Jpn.* **1992**, *65*, 97–110.
12. Huang, J.; Bunel, E.; Faul, M. M. *Org. Lett.* **2007**, *9*, 4343–4346.
13. Fagnou, K.; Lautens, M. *Angew. Chem. Int. Ed.* **2002**, *41*, 26–47.

APPENDIX 12

Nickel-Catalyzed Enantioselective Allylic Alkylation of Lactones and Lactams with Unactivated Allylic Alcohols[†]

A12.1 INTRODUCTION, BACKGROUND, AND SYNTHETIC UTILITY

Since the seminal report in 1965 by Tsuji,¹ transition metal-catalyzed allylic alkylation has emerged as one of the most powerful methods for the construction of stereocenters.² In particular, with the use of prochiral nucleophiles that proceed through tetrasubstituted enolates, the transition metal-catalyzed enantioselective allylic alkylation has proven to be a formidable strategy for accessing chiral quaternary stereocenters in catalytic enantioselective fashion.³ Although this transformation has been studied for more than 50 years,⁴ the use of α -substituted lactones or lactams as prochiral nucleophiles remains significantly under-developed.^{5,6}

As part of our ongoing research program directed at the development of new strategies for constructing quaternary stereocenters,⁷ we were drawn to the α -acyl lactones and lactams, as we envisioned that the α -acyl substituent would provide an additional functional handle for further synthetic manipulations. In addition, lactone products could also provide access to acyclic

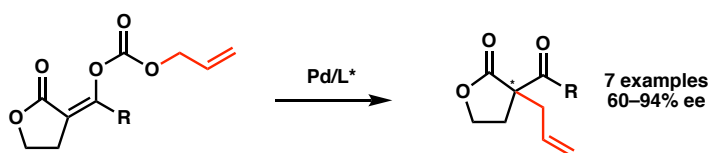
[†] This research was performed with Aurapat Ngamnithiporn and Shoshana Bachman, both alumni in the Stoltz group, as well as Dr. Scott Virgil, director of the Caltech Center for Catalysis and Chemical Synthesis. This research has been published and adapted with permission from Ngaminithiporn, A.; Jette, C. I.; Virgil S. C.; Stoltz, B. M. *Chem. Sci.* **2018**, 9, 2547. Published by The Royal Society of Chemistry.

quaternary stereocenters via ring-opening reactions,⁸ and reduction of the lactam products would enable direct access to functionalized piperidine rings, the most prevalent nitrogenous heterocycle in drug molecules.⁹ However, to the best of our knowledge, there has been only one report of a transition metal-catalyzed enantioselective allylic alkylation of monocyclic α -acyl lactone or lactam prochiral nucleophiles to furnish products bearing a quaternary stereocenter.^{Error! Bookmark not defined.d}

Recently, Cossy disclosed a palladium-catalyzed decarboxylative enantioselective allylic alkylation of enol carbonates derived from γ -butyrolactones (Scheme A12.1.1.A). Various enol carbonates can be used to obtain diverse α -acyl quaternary butyrolactones in moderate to high levels of enantioselectivity. Nonetheless, the limited electrophile scope and challenging nucleophile synthesis limits the practicality of this transformation.

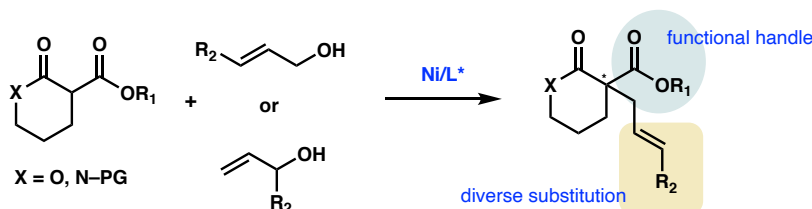
Scheme A12.1.1. Metal-Catalyzed Enantioselective Allylic Alkylations (AA) of α -Acyl Lactone and Lactam Prochiral Nucleophiles

a) Previous Work (1 report):



- Limited to γ -butyrolactone substrates and an allyl group
- Substrates require low yielding, multistep synthesis

b) This Research:



- Inexpensive catalyst and commercially available ligand
- Easily accessible substrates

To address this limitation, we chose to investigate the enantioselective allylic alkylation of α -acyl lactones and lactams by using an inexpensive transition metal catalyst and easily accessible prochiral nucleophiles. Mashima's recent report on nickel-catalyzed enantioselective allylic alkylation of β -keto esters with allyl alcohol prompted us to probe nickel in our system.^{10,11} Furthermore, we anticipated that an intermolecular allylic alkylation would simplify the substrate synthesis and provide a more convergent approach to these α -quaternary products.¹² Herein, we report the first example of nickel-catalyzed intermolecular enantioselective allylic alkylation using easily accessible α -acyl lactones and lactams as prochiral nucleophiles in conjunction with allylic alcohols as electrophilic coupling partners (Scheme A12.1.1.B).

A12.2 REACTION OPTIMIZATION

Our studies commenced with an investigation of the enantioselective allylic alkylation between α -ethoxycarbonyl lactone **120a** and allyl alcohol (**121a**) using Ni(COD)₂ and (R)-BINAP in diethyl ether at 0 °C. Although the α -quaternary lactone product **122aa** was obtained in good yield, only moderate enantioselectivity was achieved.¹³ Seeking to improve the enantioselectivity, we elected to survey a wide variety of commercially available ligand scaffolds. Chiral bisphosphine ligands were discovered to exhibit superior enantioselectivity to other classes of ligands, including those commonly used in asymmetric allylic alkylations such as phosphinooxazolines (PHOX) or C2-asymmetric ligands pioneered by the Trost group.¹⁴ In the presence of Ni(COD)₂ (10 mol %) and chiral bisphosphine ligands **L90–L93** (12 mol %), the reaction proceeds with moderate levels of enantioselectivity (Table A12.2.1, entries **1–4**). The highest enantiomeric excess (ee) was achieved with (R)-P-phos (**L93**), which delivers α -quaternary lactone **122aa** in 82% yield and 82% ee (entry 4). Decreasing the catalyst loading to 5 mol %

requires an exceedingly long reaction time (entry 5). An examination of different temperatures revealed that decreasing the temperature improves ee (entries 6–7), albeit with slightly diminished yields. Prolonged reaction time (48 h) at -10°C affords product **122aa** in 80% yield and 85% ee (entry 8). Importantly, a control experiment performed in the absence of the chiral ligand shows no background reaction (entry 9).

Table A12.2.1. Optimization of Reaction Parameters^a

120a + **121a** $\xrightarrow[\text{Et}_2\text{O (0.1 M), Temp, 19 h}]{\text{Ni(COD)}_2 \text{ (10 mol \%), ligand (12 mol \%)} }$ **122aa**

entry	ligand	temp ($^{\circ}\text{C}$)	% yield ^b	% ee ^c
1	L90	0	53	75
2	L91	0	76	78
3	L92	0	93	79
4	L93	0	82	82
5 ^d	L93	0	62	81
6	L93	23	86	74
7	L93	-10	69	84
8 ^e	L93	-10	80	85
9	—	0	0	—

L90: (R)-BINAP

L91: (R)-H₈-BINAP

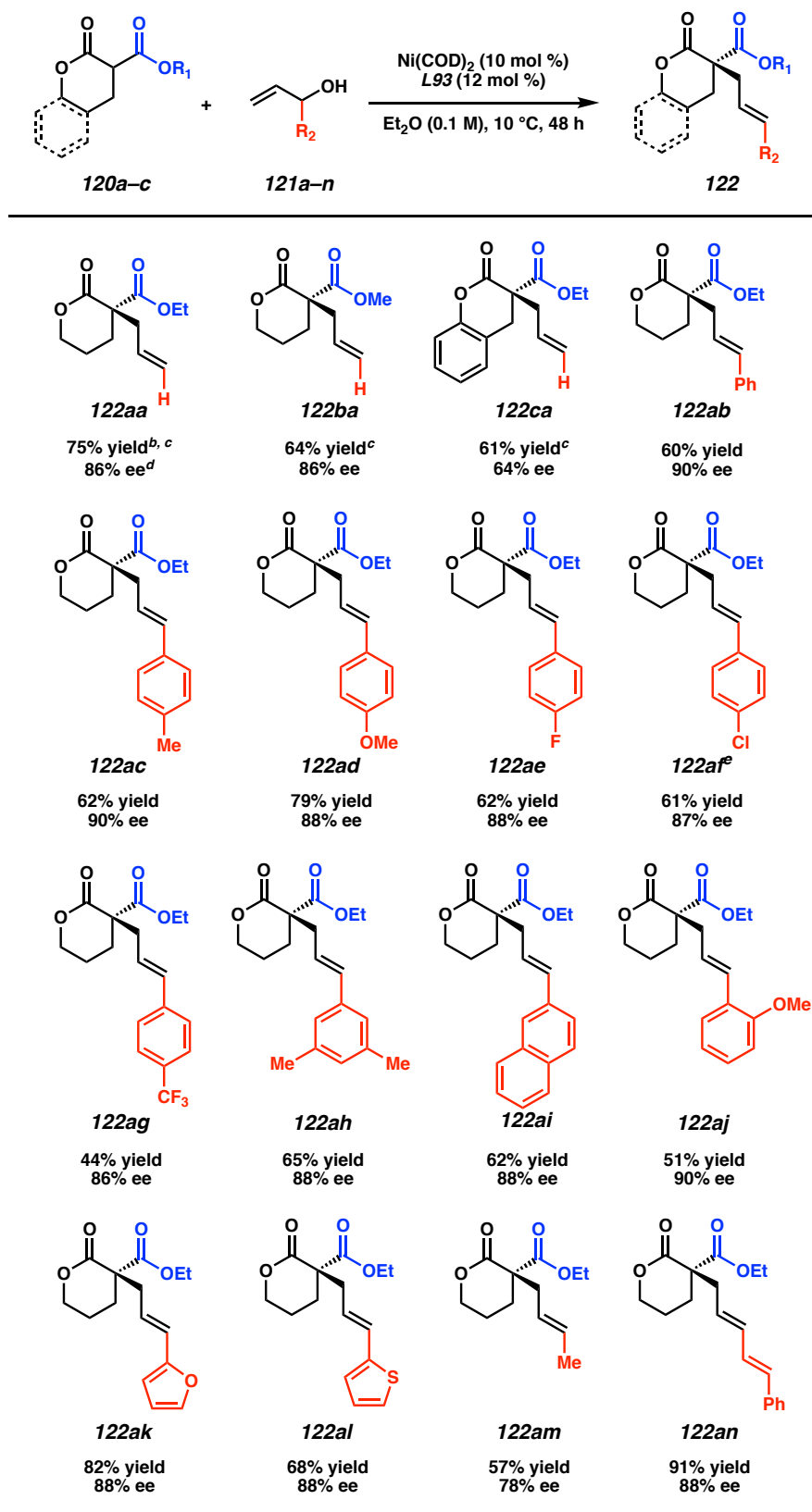
L92: (R)-Segphos

L93: (R)-P-phos

[a] Conditions: **120a** (0.1 mmol), **121a** (0.1 mmol), Ni(COD)_2 (10 mol %), ligand (12 mol %) in Et_2O (1.0 mL). [b] Yields determined by ^1H NMR of crude reaction mixture using 1,3,5-trimethoxybenzene as a standard. [c] Determined by chiral SFC analysis of the isolated product. [d] Ni(COD)_2 (5 mol %) and **L93** (6 mol %) were used. [e] Reaction time = 48 h.

A12.3 SCOPE OF THE NUCLEOPHILE AND ELECTROPHILE

Table A12.3.1. Nucleophile and Electrophile Scope^a

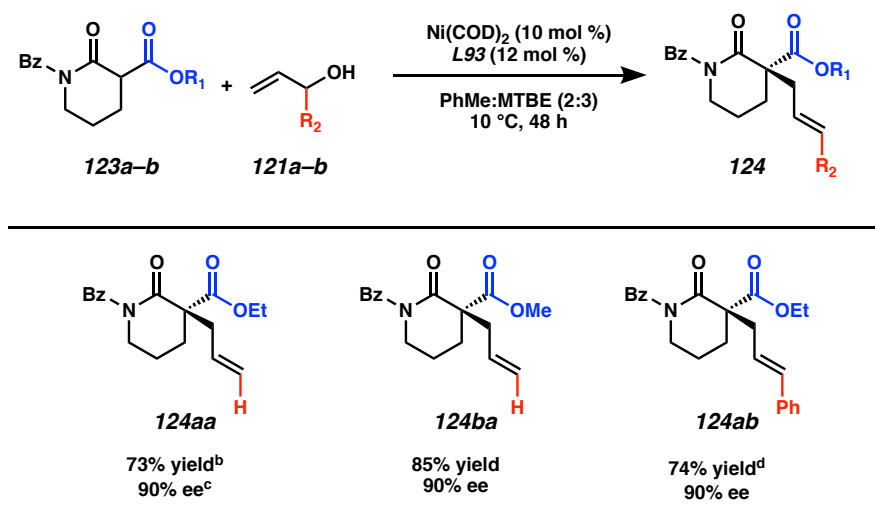


[a] Reactions performed on 0.2 mmol. [b] Yield of isolated product. [c] Reaction performed at –10 °C. [d] Determined by chiral SFC analysis. [e] Absolute configuration determined via single crystal x-ray analysis.

With the optimized reaction conditions in hand, we examined the scope of this asymmetric transformation (Table A12.3.1). The reaction of α -methoxycarbonyl lactone **120b**, possessing a smaller alkyl group at the ester fragment, with allyl alcohol (**121a**) provides α -quaternary lactone **122ba** in comparable yield and ee to the allylated product **122aa**. Bicyclic lactone **120c** could also be used to furnish product **122ca** in slightly diminished yield and enantioselectivity. With respect to the electrophile scope, reactions between lactone **120a** with various substituted allyl alcohols proceed with good ee (78–90% ee) at increased temperature (10 °C). Although a trend in enantioselectivity was not observed, we found that the electronic nature of the aryl substituent does affect the reactivity.

Electrophiles containing electron rich aryl substituents provide the corresponding products in greater yields than their electron-deficient counterparts (**122ac–122ag**). Furthermore, we found that *para*- and *meta*-substituted aryl rings exhibit higher reactivity as compared to the ortho-substituted aryl ring (**122ac**, **122ah–ai** vs. **122aj**). Apart from the aryl-substituted electrophiles,

Table A12.3.2. α -Acyl Lactam Prochiral Nucleophiles^a



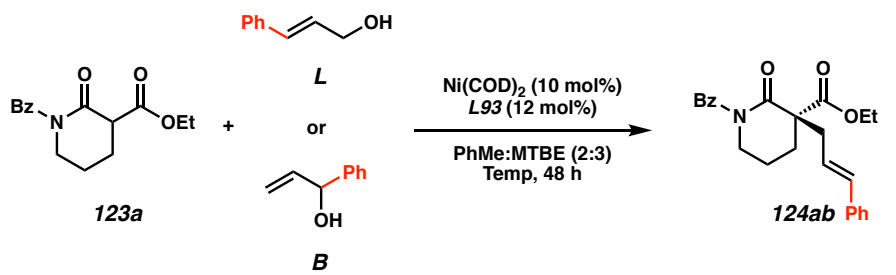
[a] Reactions performed on 0.2 mmol. [b] Yield of isolated product. [c] Determined by chiral SFC analysis. [d] Reaction performed at 30 °C.

we were pleased to find that heteroaryl substitution is also well-tolerated (**122ak–122al**). The reaction with an aliphatic electrophile affords product **122am** in slightly diminished yield and ee. In addition, an alkenyl-substituted electrophile fares well under our reaction conditions, delivering product **122an** in an excellent 91% yield and 88% ee.

At this stage, we questioned whether we could leverage this transformation to include nitrogen-containing lactam nucleophiles. To our delight, under slightly modified reaction conditions using the same chiral bisphosphine ligand **L93**, α -ester lactams **123a–123b** furnish products **124aa–124ba** in good yields and with even higher enantioselectivity as compared to their lactone counterparts (Table A12.3.2). Examination of different protecting groups revealed that the benzoyl-protecting group is optimal.^{15,16} Reaction of α -ethoxycarbonyl benzoyl-protected lactam **123a** with branched cinnamyl alcohol affords linear product **124ab** in 74% yield and 90% ee.

In order to gain mechanistic insights into this transformation, we compared the results from reactions using linear and branched cinnamyl alcohols (Table A12.3.3). Only the linear product

Table A12.3.3. Linear versus Branched Cinnamyl Alcohol^a



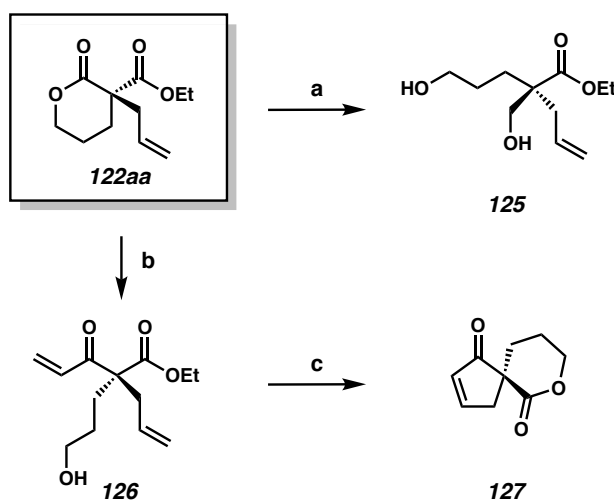
entry	elec	temp (°C)	% conversion ^b	% yield ^b	% ee ^c
1	L	10	60	59	92
2	B	10	58	55	92
<hr/>					
3	L	30	>95	86	91
4	B	30	90	83	91

[a] Reactions performed on 0.1 mmol scale [b] Yields determined by ¹H NMR of crude reaction mixture using benzyl ether as a standard. [c] Determined by chiral SFC analysis of the isolated product.

was detected, indicating that a nickel π -allyl is likely an intermediate in the catalytic cycle.¹⁷ While additional studies are needed to establish the full reaction mechanism and stereocontrolling factors in the process, the ability of this catalyst combination to access a single product from two electrophilic coupling partners highlights its flexibility in potential synthetic applications.

A12.4 PRODUCT TRANSFORMATIONS

Scheme A12.4.1. Product Transformations for **122aa**



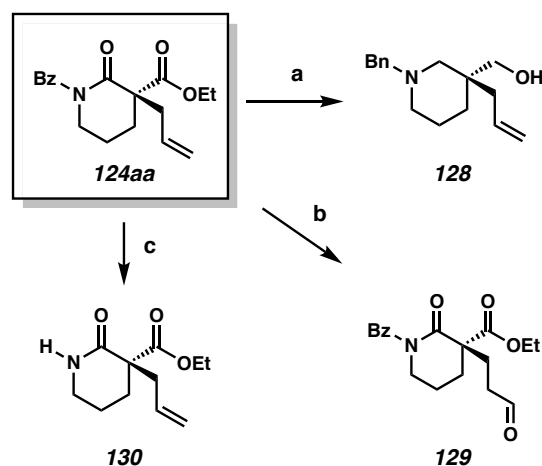
[a] NaBH₄, CeCl₃·7H₂O, THF/MeOH, 0 °C, 88% yield. [b] Vinyl–magnesium bromide, THF, –78 °C, 67% yield, 86% ee; [c] Grubbs' II (5 mol %), Toluene, 40 °C; DBU, MeCN, 23 °C, 53% yield.

To demonstrate the synthetic utility of the α -quaternary products, we performed a number of product transformations on both α -quaternary lactone **122aa** (Scheme A12.4.1) and lactam **124aa** (Scheme A12.4.2). Selective reduction of the lactone functionality in **122aa** provides diol **125** in 88% yield. Additionally, vinyl Grignard addition into lactone **122aa** affords enone **126** in 67% yield with no erosion of enantioselectivity. These enantioenriched acyclic products **125** and **126** bearing a quaternary stereocenter are envisioned to be useful chiral building blocks as they

contain multiple functional handles for further manipulations. For example, enantioenriched spirocycle **127** can be accessed via ring-closing metathesis followed by lactonization of enone **126**.

We also performed experiments to probe the reactivity of our α -quaternary lactam products (Scheme A12.4.2). Reduction of lactam **124aa** with lithium aluminium hydride delivers chiral piperidine derivative **128**, which is of potential value to medicinal chemists.⁹ Use of the aldehyde selective Wacker procedure¹⁸ affords aldehyde **129** in 75% yield. Lastly, cleavage of the benzoyl protecting group under basic conditions provides unprotected lactam **130** in 84% yield.

Scheme A12.4.2. Product Transformations for **124aa**



[a] LAH, Et₂O, 65 °C, 80% yield; [b] CuCl·H₂O (12 mol %), PdCl₂(PhCN)₂ (12 mol %), AgNO₂ (6 mol %), *t*-BuOH, Nitromethane under O₂, 75% yield; [c] NaOEt, EtOH, 23 °C, 84% yield.

A12.5 CONCLUSION

In summary, we have developed the first nickel-catalyzed enantioselective allylic alkylation of α -substituted lactones and lactams with free allylic alcohols. Utilizing a commercially available chiral bisphosphine ligand, α -quaternary lactones and lactams can be constructed in good yield (up to 91% yield) and with high enantiomeric excess (up to 90% ee). A broad range of functional groups are compatible with the reaction conditions. A number of product

derivatizations showed the synthetic utility of this methodology for constructing small chiral building blocks with multiple functional handles. Future work to further elucidate the mechanism of this transformation is underway and will be reported in due course.

A12.6 REFERENCES AND NOTES

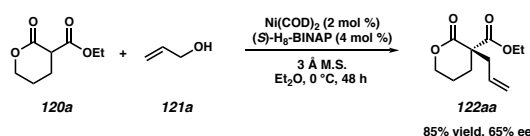
1. Tsuji, J.; Takahashi, H.; Morikawa, M. *Tetrahedron Lett.* **1965**, *6*, 4387–4388.
2. (a) Trost, B. M. *Chem. Rev.* **1996**, *96*, 395–422; (b) Trost, B. M.; Crawley, M. L. *Chem. Rev.* **2003**, *103*, 2921–2943; (c) Trost, B. M.; *J. Org. Chem.* **2004**, *69*, 5813–5837.
3. (a) Liu, Y.; Han, S. J.; Liu, W. B.; Stoltz, B. M. *Acc. Chem. Res.* **2015**, *48*, 740–751; (b) Bhat, V.; Welin, E. R.; Guo, X.; Stoltz, B. M. *Chem. Rev.* **2017**, *117*, 4528–4561; (c) Hethcox, J. C.; Shockley, S. E.; Stoltz, B. M., *ACS Catal.* **2016**, *6*, 6207–6213.
4. For reviews, see (a) Mohr, J. T.; Stoltz, B. M. *Chem. Asian. J.* **2007**, *2*, 1476–1491. (b) Oliver, S.; Evans, P. A. *Synthesis* **2013**, *45*, 3179–3198.
5. For α -quaternary lactones, see; (a) Li, X. H.; Wan, S. L.; Chen, D.; Liu, Q. R.; Ding, C. H.; Fang, P.; Hou, X. L. *Synthesis*, **2016**, *48*, 1568–1572. (b) Akula, R.; Guiry, P. J. *Org. Lett.* **2016**, *18*, 5472–5475. (c) James, J.; Guiry, P. J. *ACS Catal.* **2017**, 1397–1402; (d) Oliveira, M. N.; Fournier, J.; Arseniyadis, S.; Cossy, J. *Org. Lett.* **2017**, *19*, 14–17.
6. For α -quaternary lactams, see (a) Behenna, D. C.; Liu, Y.; Yurino, T.; Kim, J.; White, D. E.; Virgil, S. C.; Stoltz, B. M.; *Nat. Chem.* **2012**, *4*, 130–133. (b) Trost, B. M.; Frederiksen, M. U. *Angew. Chem. Int. Ed.* **2005**, *44*, 308–310 and *Angew. Chem.* **2005**, *117*, 312–314.
7. For selected examples, see (a) Alexy, E. J.; Virgil, S. C.; Bartberger, M. D.; Stoltz, B. M. *Org. Lett.* **2017**, *19*, 5007–5009. (b) Shockley, S. E.; Hethcox, J. C.; Stoltz, B. M. *Angew. Chem. Int. Ed.* **2017**, *56*, 11545–11548 and *Angew. Chem.* **2017**, *129*, 11703–11706. (c)

- Starkov, P.; Moore, J. T.; Duquette, D. C.; Stoltz, B. M.; Marek, I. *J. Am. Chem. Soc.* **2017**, *139*, 9615–9620. (d) Hethcox, J. C.; Shockley, S. E.; Stoltz, B. M. *Angew. Chem. Int. Ed.* **2016**, *55*, 16092–16095 and *Angew. Chem.* **2016**, *128*, 16326–16329. (e) Hayashi, M.; Bachman, S.; Hashimoto, S.; Eichman, C. C.; Stoltz, B. M. *J. Am. Chem. Soc.* **2016**, *138*, 8997–9000. (f) Craig II, R. A.; Loskot, S. A.; Mohr, J. T.; Behenna, D. C.; Harned, A. M.; Stoltz, B. M. *Org. Lett.* **2015**, *17*, 5160–5163. (g) Behenna, D. C.; Mohr, J. T.; Sherden, N. H.; Marinescu, S. C.; Harned, A. M.; Tani, K.; Seto, M.; Ma, S.; Novák, Z.; Krout, M. R.; McFadden, R. M.; Roizen, J. L.; Enquist, J. A.; White, D. E.; Levine, S. R.; Petrova, K. V.; Iwashita, A.; Virgil, S. C.; Stoltz, B. M. *Chem. Eur. J.* **2011**, *17*, 14199–14223.
8. (a) Liu, W.; Xu, D. D.; Repič, O.; Blacklock, T. J. *Tetrahedron Lett.* **2001**, 2439–2441. (b) Delhaye, L.; Merschaert, A.; Diker, K.; Houpis, I. N. *Synthesis*, **2006**, *9*, 1437–1442.
9. Vitaku, E.; Smith, D. T.; Njardarson, J. T.; *J. Med. Chem.* **2014**, *57*, 10257–10274.
10. Kita, Y.; Kavthe, R. D.; Oda, H.; Mashima, K. *Angew. Chem. Int. Ed.* **2016**, *55*, 1098–1101 and *Angew. Chem.* **2016**, *128*, 1110–1113.
11. For success in Ni-catalyzed allylic alkylations from the past 15 years, see (a) Bernhard, Y.; Thomson, B.; Ferey, V.; Sauthier, M., *Angew. Chem. Int. Ed.* **2017**, *56*, 7460–7464 and *Angew. Chem.* **2017**, *129*, 7568–7572. (b) Sha, S. C.; Mao, J.; Bellomo, A.; Jeong, S. A.; Walsh, P. J. *Angew. Chem. Int. Ed.* **2016**, *55*, 1070–1074 and *Angew. Chem.* **2017**, *128*, 1082–1086. (c) Wang, J.; Wang, P.; Wang, L.; Li, D.; Wang, K.; Wang, Y.; Zhu, H.; Yang, D.; Wang, R., *Org. Lett.* **2017**, *19*, 4826–4829. (d) Son, S. Fu, G. C. *J. Am. Chem. Soc.* **2008**, *130*, 2756–2757. (e) Shields, J. D.; Ahneman, D. T.; Graham, T. J. A.; Doyle, A. G. *Org. Lett.* **2014**, *16*, 142–145. (f) Srinivas, H. D.; Zhou, Q.; Watson, M. P. *Org. Lett.* **2014**, *16*, 3596–3599.

12. These α -quaternary products can alternatively be accessed via phase-transfer catalysis: (a)

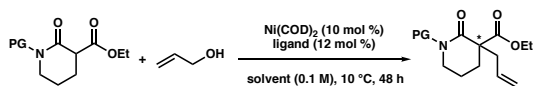
Ha, M. W.; Lee, H.; Yi, H. Y.; Park, Y.; Kim, S.; Hong, S.; Lee, M.; Kim, M.-H.; Kim, T.-S.; Park, H.-G. *Adv. Synth. Catal.* **2013**, 355, 637–642. (b) Park, Y.; Lee, Y. J.; Hong, S.; Kim, M.-H.; Lee, M.; Kim, T.-S.; Lee, J. K.; Jew, S.-S.; Park, H.-G. *Adv. Synth. Catal.* **2011**, 353, 3313–3318.

13. The quaternary lactone product **122aa** was isolated in 85% yield and with 65% ee under Mashima's optimized conditions:



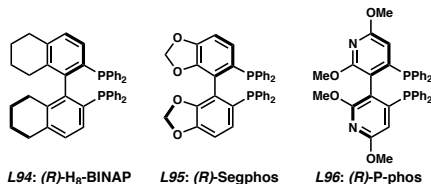
14. A total of 40 ligands were examined.

15. Additional optimization of reaction parameters for lactam nucleophile is required due to the insolubility of substrate in Et₂O. See below for the results from the optimization:

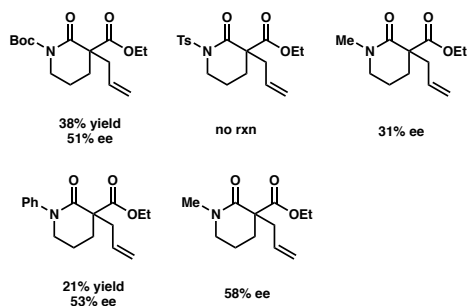


entry	PG	ligand	solvent	yield [%] ^[b]	ee [%] ^[c]
1	Bz	L94	PhMe:MTBE (2:3)	95	77
2	Bz	L95	PhMe:MTBE (2:3)	>95	88
3	Bz	L96	PhMe:MTBE (2:3)	79	90
4 ^[d]	Bz	L96	PhMe:MTBE (2:3)	28	88
5	Bz	L96	PhMe:Et ₂ O (2:3)	70	88
6	Bz	L96	PhMe	51	88
7	Bz	L96	THF	15	76
8 ^[e]	Bz	L96	PhMe:MTBE (2:3)	>95	88

[a] Conditions: lactam (0.1 mmol), alcohol (0.1 mmol), Ni(COD)₂ (10 mol %), ligand (12 mol %) for 48 h.
 [b] Yields determined by ¹H NMR of crude reaction mixture using trimethoxybenzene as a standard.
 [c] Determined by chiral SFC analysis. [d] 5 mol % Ni(COD)₂ and 6 mol % L96 were used. [e] Reaction performed at 23 °C.



16. Results from other protected-acyl lactams under the slightly modified conditions:



17. For previous reports that also proposed a nickel π -allyl intermediate in the catalytic cycle,
see ref 10, 11a and b.

18. Kim, K. E.; Li, J.; Grubbs, R. H.; Stoltz, B. M. *J. Am. Chem. Soc.* **2016**, *138*, 13179–13182.

COMPREHENSIVE BIBLIOGRAPHY

Aikawa, K.; Hioki, Y.; Mikami, K. *Org. Lett.* **2010**, *12*, 5716–5719.

Akiyama, T.; Hara, M.; Fuchibe, K.; Sakamoto, S.; Yamaguchi, K. *Chem. Commun.* **2003**, 1734–1735.

Akula, R.; Guiry, P. J. *Org. Lett.* **2016**, *18*, 5472–5475.

Alexakis, A.; Bäckvall, J. E.; Krause, N.; Pàmies, O.; Diéguez, M. *Chem. Rev.* **2008**, *108*, 2796–2823.

Alexakis, A.; Begouin, J. M.; Crawley, M. L.; Guiry, P. J.; Kammerer-Pentier, C.; Kleimark, J.; Klein, J. E. M. N.; Langlois, J. –B.; Liron, F.; Liu, W. –B.; Milhau, L.; Moberg, C.; Norrby, P. –O.; Plietker, B.; Poli, G.; Prestat, G.; Trost, B. M. Weickmann, D.; Xia, J.–B.; You, S. – L. *Transition Metal Catalyzed Enantioselective Allylic Substitution in Organic Synthesis*; Kazmeier, U., Eds.; Springer, New York, 2012, vol. 38, pp1–341.

Alexy, E. J.; Virgil, S. C.; Bartberger, M. D.; Stoltz, B. M. *Org. Lett.* **2017**, *19*, 5007–5009.

Altman, R. A.; Hyde, A. M.; Huang, X.; Buchwald, S. L. *J. Am. Chem. Soc.* **2008**, *130*, 9613–9620.

Anand, N. K.; Carreira, E. M. *J. Am. Chem. Soc.* **2001**, *123*, 9687–9688.

Anker, T.; Cosner, C. C.; Helquist, P. *Chem. Eur. J.*; **2013**, *19*, 1858–1871.

Asano, Y.; Hara, K.; Ito, H. *Org. Lett.* **2007**, *9*, 3901–3904.

Behenna, D. C.; Liu, Y.; Yurino, T.; Kim, J.; White, D. E.; Virgil, S. C.; Stoltz, B. M.; *Nat. Chem.* **2012**, *4*, 130–133.

Behenna, D. C.; Mohr, J. T.; Sherden, N. H.; Marinescu, S. C.; Harned, A. M.; Tani, K.; Seto, M.; Ma, S.; Novák, Z.; Krout, M. R.; McFadden, R. M.; Roizen, J. L.; Enquist, J. A.; White, D. E.; Levine, S. R.; Petrova, K. V.; Iwashita, A.; Virgil, S. C.; Stoltz, B. M. *Chem. Eur. J.* **2011**, *17*, 14199–14223.

Belda, O.; Kaiser, N. –F.; Bremberg, U.; Larhed, M.; Hallberg, A.; Moberg, C. *J. Org. Chem.* **2000**, *65*, 5868–5870.

Bernhard, Y.; Thomson, B.; Ferey, V.; Sauthier, M. *Angew. Chem. Int. Ed.* **2017**, *56*, 7460–7464 and *Angew. Chem.* **2017**, *129*, 7568–7572.

Bhat, V.; Welin, E. R.; Guo, X.; Stoltz, B. M. *Chem. Rev.* **2017**, *117*, 4528–4561.

Bi, W.-Y.; Lü, X.-Q.; Chai, W.-L.; Song, J.-R.; Wong, W.-Y.; Wong, W.-K.; Jones, R. A. *Journal of Molecular Structure* **2008**, *891*, 450–455.

Bouziane, A.; Hérou, M.; Carboni, B.; Carreaux, F.; Demerseman, B.; Bruneau, C.; Renaud, J.–L. *Chem. Eur. J.* **2008**, *14*, 5630–5637.

Bowmaker, G. A.; Di Nicola, C.; Pettinari, C.; Skelton, B. W.; Somers, N.; White, A. H. *Dalton Trans.*, **2011**, *40*, 5102–5115.

Brak, K.; Jacobsen, E. N. *Angew. Chem. Int. Ed.* **2013**, *52*, 534–561 and *Angew. Chem.* **2013**, *125*, 558–588.

Buswell, M.; Fleming, I.; Ghosh, U.; Mack, S.; Russell, M.; Clark, B.; *Org. Biomol. Chem.* **2004**, *2*, 3006–3017.

Cai, Z.; Xiao, D.; Do, L. H. *J. Am. Chem. Soc.* **2015**, *137*, 15501–15510.

Caputo, C. A.; Jones, N. D. *Dalton Trans.* **2007**, 4627.

Caruano, J.; Muccioli, G.G.; Robiette, R. *Org. Biomol. Chem.*, **2016**, *14*, 10134–10156.

- Chae, J.; Yun, J.; Buchwald, S. L. *Org. Lett.* **2004**, *6*, 4809–4812.
- Chen, C.; Hong, L.; Xu, Z. Q.; Liu, L.; Wang, R. *Org. Lett.* **2006**, *8*, 2277–2280.
- Chen, H. –Y.; Hu, Z. –Y.; Tang, C. –P.; Quinn, T. J.; Feng, Y.; Yao, S.; Ye, Y.; *Tetrahedron Letters*, **2013**, *54*, 4250–4253.
- Chen, S.; Zheng, Y.; Cui, T.; Meggers, E.; Houk, K. N. *J. Am. Chem. Soc.* **2018**, *140*, 5146–5152.
- Chen, Z.; Morimoto, S.; Matsunaga, S.; Shibasaki, M. *J. Am. Chem. Soc.* **2008**, *130*, 2170–2171.
- Cook, A. M.; Wolf, C. *Angew. Chem. Int. Ed.* **2016**, *55*, 2929–2933 and *Angew. Chem.* **2016**, *128*, 2982–2986.
- Corey, E. J.; Posner, G. H. *J. Am. Chem. Soc.* **1967**, *89*, 3911–3912.
- Cormier, M.; Ahmad, M.; Maddaluno, J.; de Paolis, M.; *Organometallics*, **2017**, *36*, 4920–4927.
- Cossy, J.; de Filippis, A.; Pardo, D. G. *Org. Lett.* **2003**, *5*, 3037–3039.
- Cossy, J.; de Filippis, A.; Pardo, D. G. *Synlett*, **2003**, *14*, 2171–2174.
- Cozzi, P.G. *Angew. Chem. Int. Ed.* **2003**, *42*, 2895–2898 and *Angew. Chem.* **2003**, *115*, 3001–3004.
- Craig II, R. A.; Loskot, S. A.; Mohr, J. T.; Behenna, D. C.; Harned, A. M.; Stoltz, B. M. *Org. Lett.* **2015**, *17*, 5160–5163.
- Cram, D. J.; Sogah, G. D. Y. *J. Chem. Soc., Chem. Commun.* **1981**, 625–628.
- Cui, T.; Qin, J.; Harms, K.; Meggers, E. *Eur. J. Inorg. Chem.* **2019**, 195–198.
- Czerwinski, P.; Molga, E.; Cavallo, L.; Poater, A.; Michalak, M. *Chem. Eur. J.* **2016**, *22*, 8089–8094.
- Dalko, P. I.; Moisan, L.; *Angew. Chem.* **2001**, *113*, 3840–3864 and *Angew. Chem. Int. Ed.* **2001**, *40*, 3726–3748.

- Dalko, P. I.; Moisan, L.; *Angew. Chem.* **2004**, *116*, 5248–5286 and *Angew. Chem. Int. Ed.* **2004**, *43*, 5138–5175.
- de Armas, P.; Tejedor, D.; García–Tellado, F. *Angew. Chem. Int. Ed.* **2010**, *49*, 1013–1016 and *Angew. Chem.* **2010**, *122*, 1029–1032.
- de Filippis, A.; Pardo, D. G.; Cossy, J. *Tetrahedron*, **2004**, *60*, 9757–9767 and *Tetrahedron*, **2004**, *60*, 9757–9767.
- Delhaye, L.; Merschaert, A.; Diker, K.; Houpis, I. N. *Synthesis*, **2006**, *9*, 1437–1442.
- Deng, Q.–H.; Wadepohl, H.; Gade, L. H. *J. Am. Chem. Soc.* **2012**, *134*, 2946–2949
- Dhayalan, V.; Murakami, R.; Hayashi, M. *Asian J. Chem.* **2013**, *25*, 7505–7508.
- DiMauro, E. F.; Kozlowski, M. C. *Org. Lett.* **2001**, *3*, 1641–1644.
- DiMucci, M. I.; Lukens, J. T.; Chatterjee, s.; CArsch, K. M.; Titus, C. J.; Lee, S. J.; Nordlund, D.; Betley, T. A.; MacMillan, S. N.; Lancaster, K. M. *J. Am. Chem. Soc.* **2019**, *141*, 18508–18520.
- Donohoe, T. J.; Bataille, C. J. R.; Churchill, G. W. *Annu. Rep. Prog. Chem., Sect. B* **2006**, *102*, 98–122.
- Duan, J. J. –W.; Chen, L.; Wasserman, Z. R.; Lu, Z.; Liu, R. –Q.; Covington, M. B.; Qian, M.; Hardman, K. D.; Magolda, R. L.; Newton, R. C.; Christ, D. D.; Wexler, R. R.; Decicco, C. P. *J. Med. Chem.* **2002**, *45*, 4954–4957.
- Duan, J.; Kwong, F. Y. A. *J. Org. Chem.* **2017**, *82*, 6468–6473.
- Duan, M.; Liu, Y.; Ao, J.; Xue, L.; Luo, S.; Tan, Y.; Qin, W.; Song, C. E.; Yan, H. *Org. Lett.* **2017**, *19*, 2298–2301.
- Durbin, M. J.; Willis, M. C. *Org. Lett.*, **2008**, *10*, 1413–1415.

- Evans, R. W.; Zbieg, J. R.; Zhu, S.; Li, W.; MacMillan, D. W. C. *J. Am. Chem. Soc.* **2013**, *135*, 16074–16077.
- Fagnou, K.; Lautens, M. *Angew. Chem. Int. Ed.* **2002**, *41*, 26–47.
- Falciola, C. A.; Alexakis, A. *Eur. J. Org. Chem.* **2008**, 3765–3780.
- Falciola, C. A.; Tissot-Crosset, K.; Reyneri, H.; Alexakis, A. *Adv. Synth. Catal.* **2008**, *350*, 1090–1100.
- Fan, X.; Zhang, X.; Li, C.; Gu, Z. *ACS Catal.* **2019**, *9*, 2286–2291.
- Felpin, F. –X.; Lebreton, J. *Eur. J. Org. Chem.* **2003**, *19*, 3693–3712.
- Fraser, R. R.; Mansour, T. S. Savard, S. *J. Org. Chem.* **1985**, *50*, 3232–3234.
- Fuchter, M. J.; Levy, J.–N. *Org. Lett.* **2008**, *10*, 4919–4922.
- García-Fortanet, J.; Buchwald, S. L. *Angew. Chem. Int. Ed.* **2008**, *47*, 8108–8111 and *Angew. Chem.* **2008**, *120*, 8228–8231.
- Garnier, T.; Danel, M.; Magné, V.; Pujol, A.; Bénétteau, V.; Pale, P.; Chassaing, S.; *J. Org. Chem.* **2018**, *83*, 6408–6422.
- Genoni, A.; Benaglia, M.; Puglisi, A.; Rossi, S. *Synthesis*, **2011**, *12*, 1926–1929.
- Giri, R.; Brusoe, A. Troshin, K.; Wang, J. Y. Font, M. Hartwig, J. F. *J. Am. Chem. Soc.* **2018**, *140*, 793–806.
- Goodson, F. E.; Wallow, T. I.; Novak, B. M. *J. Am. Chem. Soc.* 1997, *119*, 12441–12453.
- Griffiths, R. J.; Burley, G. A.; Talbot, E. P. A.; *Org. Lett.* **2017**, *19*, 870–873.
- Guangyou, Z.; Yuqing, L.; Zhaohui, W.; Nohira, H.; Hirose, T. *Tetrahedron: Asymmetry* **2003**, *14*, 3297–3300.

- Guzikowski, A. P.; Tamiz, A. P.; Acosta-Burrue, M.; Hong-Bae S.; Cai, S. -X.; Hawkinson, J. E.; Keana, J. F. W.; Kesten, S. R.; Shipp, C. T.; Tran, M.; Whittemore, E. R.; Woodward, R. M.; Wright, J. L.; Zhou, Z. -L. *J. Med. Chem.* **2000**, *43*, 984–994.
- Ha, M. W.; Lee, H.; Yi, H. Y.; Park, Y.; Kim, S.; Hong, S.; Lee, M.; Kim, M.-H.; Kim, T.-S.; Park, H.-G. *Adv. Synth. Catal.* **2013**, *355*, 637–642.
- Hamada, T.; Chieffi, A.; Åhman, J.; Buchwald, S. L. *J. Am. Chem. Soc.* **2002**, *124*, 1261–1268.
- Hamann, B. C. Hartwig, J. F. *J. Am. Chem. Soc.* **1997**, *119*, 12382 – 12383.
- Han, S.-J.; Doi, R.; Stoltz, B. M. *Angew. Chem. Int. Ed.* **2016**, *55*, 7437–7440, *Angew. Chem.* **2016**, *128*, 7563 –7566.
- Handa, V.; Gnanadesikan, S.; Matsunaga, S.; Shibasaki, M. *J. Am. Chem. Soc.* **2007**, *129*, 4900–4901.
- Harada, A.; Makida, Y.; Sato, T.; Ohmiya, H.; Sawamura, M. *J. Am. Chem. Soc.* **2014**, *136*, 13932–13939.
- Hartwig, J. F. *Organotransition Metal Chemistry: From Bonding to Catalysts*; University Science Books: Mill Valley, CA 2010.
- Harutyunyan, S. R.; den Hartog, T.; Geurts, K.; Minnaard, A. J.; Feringa, B. L. *Chem. Rev.* **2008**, *108*, 2824–2852.
- Hayashi, M.; Bachman, S.; Hashimoto, S.; Eichman, C. C.; Stoltz, B. M. *J. Am. Chem. Soc.* **2016**, *138*, 8997–9000
- Hensler, M. E.; Bernstein, G.; Nizet, V.; Nefzi, A. *Bioorg. Med. Chem. Lett.* **2006**, *16*, 5073–5079.
- Hethcox, J. C.; Shockley, S. E.; Stoltz, B. M. *ACS Catal.* **2016**, *6*, 6207–6213.

- Hethcox, J. C.; Shockley, S. E.; Stoltz, B. M. *Angew. Chem. Int. Ed.* **2016**, *55*, 16092–16095 and *Angew. Chem.* **2016**, *128*, 16326–16329.
- Huang, J.; Bunel, E.; Faul, M. M. *Org. Lett.* **2007**, *9*, 4343–4346.
- Huang, Z.; Chen, Z.; Lim, L. H.; Quang, G. C. P.; Hirao, H.; Zhou, J. *Angew. Chem. Int. Ed.* **2013**, *52*, 5807–5812, and *Angew. Chem.* **2013**, *125*, 5919–5924.
- Iqbal, J.; Bhatia, B.; Nayyar, N. K. *Chem. Rev.* **1994**, *94*, 519–564.
- Ito, J.-I.; Asai, R.; Nishiyama, H. *Org. Lett.* **2010**, *12*, 3860–3862.
- Ito, J.-I.; Ubukata, S.; Muraoka, S.; Nishiyama, H. *Chem. Eur. J.* **2016**, *22*, 16801–16804.
- Ito, Y.; Konoike, T.; Saegusa, T. *J. Am. Chem. Soc.* **1975**, *97*, 2912–2914.
- James, J.; Guiry, P. J. *ACS Catal.* **2017**, *7*, 1397–1402.
- Jette, C. I.; Geibel, I.; Bachman, S.; Hayashi, M.; Sakurai, S.; Shimizu, H.; Morgan, J. B.; Stoltz, B. M. *Angew. Chem. Int. Ed.* **2019**, *58*, 4297–4301.
- Jette, C. I.; Tong, Z. J.; Hadt, R. G.; Stoltz, B. M. *Angew. Chem. Int. Ed.* **2020**, *59*, 2033–2038.
- Jiang, X.; Hartwig, J. F. *Angew. Chem. Int. Ed.* **2017**, *56*, 8887–8891 and *Angew. Chem.* **2017**, *129*, 9013–9017.
- Jiang, Y. -J.; Zhang, G. -P.; Huang, J. -Q.; Chen, D.; Ding, C.-H.; Hou, X.-L. *Org. Lett.* **2017**, *19*, 4880–4883.
- Jin, Y.; Chen, M.; Ge, S.; Hartwig, J. F. *Org. Lett.* **2017**, *19*, 1390–1393.
- Johanssen, C. C. C.; Colacot, T. J. *Angew. Chem. Int. Ed.* **2010**, *49*, 676–707.
- Kelly, C.B.; Mercadante, M.A.; Hamlin, T.A.; Fletcher, M.H. *J. Org. Chem.* **2012**, *77*, 8131–814.
- Kim, K. E.; Li, J.; Grubbs, R. H.; Stoltz, B. M. *J. Am. Chem. Soc.* **2016**, *138*, 13179–13182.

- Kim, M. J.; Xue, L.; Liu, Y.; Paladhi, S.; Park, S. J.; Yan, H.; Song, C. E. *Adv. Synth. Catal.* **2017**, *359*, 811–823.
- Kita, Y.; Kavthe, R. D.; Oda, H.; Mashima, K. *Angew. Chem. Int. Ed.* **2016**, *55*, 1098–1101 and *Angew. Chem.* **2016**, *128*, 1110–1113.
- Koch, E.; Takise, R.; Studer, A.; Yamaguchi, J.; Itami, K. *Chem. Commun.* **2015**, *51*, 855–857.
- Kochi, J. K. *J. Am. Chem. Soc.* **1955**, *77*, 5724–5728.
- Kocieński, P.; Jarowicki, K.; Marczak, S.; *Synthesis*, **1991**, 1191–1200.
- Kosower, E. M.; Cole, W. J.; Wu, G. –S, Cardy, D. E.; Meisters, G. *J. Org. Chem.* **1963**, *28*, 630–633.
- Kosower, E. M.; Wu, G. –S. *J. Org. Chem.* **1963**, *28*, 633–638.
- Krska, S. W.; Hughes, D. L.; Reamer, R. A.; Mathre, D. J.; Sun, Y.; Trost, B. M. *J. Am. Chem. Soc.* **2002**, *124*, 43, 12656–12657.
- Lacharity, J. J.; Fournier, J.; Lu, P.; Mailyan, A. K.; Herrmann, A. T. Zakarian, A. *J. Am. Chem. Soc.* **2017**, *139*, 132721–13275.
- Lang, K.; Park, J.; Hong, S. *Angew. Chem. Int. Ed.* **2012**, *51*, 1620–1624 and *Angew. Chem.* **2012**, *124*, 1652–1656.
- Le, H.; Kyne, R. E.; Brozek, L. A.; Morken, J. P. *Org. Lett.* **2013**, *15*, 1432–1435.
- Lexa, K. W.; Carlson, H. A. *Proteins* **2011**, *79*, 2282–2290.
- Li, D.; Ohmiya, H.; Sawamura, M. *J. Am. Chem. Soc.* **2011**, *133*, 5672–5675.
- Li, P.; Buchwald, S. L. *Angew. Chem.* **2011**, *123*, 6520–6524 and *Angew. Chem. Int. Ed.* **2011**, *50*, 6396–6400.

- Li, X. H.; Wan, S. L.; Chen, D.; Liu, Q. R.; Ding, C. H.; Fang, P.; Hou, X. L. *Synthesis*, **2016**, *48*, 1568–1572.
- Li, X.; Li, J. *Mini-Rev. Med. Chem.* **2010**, *10*, 794–805.
- Li, X.; Lu, G.; Kwok, W. H.; Chan, A. S. C. *J. Am. Chem. Soc.* **2002**, *124*, 12636–12637.
- Liao, X.; Weng, Z.; Hartwig, J. F. *J. Am. Chem. Soc.* **2008**, *130*, 195–200.
- List, B.; *Acc. Chem. Res.* **2004**, *37*, 548–557.
- List, B.; *Synlett* **2001**, *11*, 1675–1686.
- List, B.; *Tetrahedron* **2002**, *58*, 5573–5590.
- Liu, L.; Wang, R.; Kang, Y.-F.; Chen, C.; Xu, Z.-Q.; Zhou, Y.-F.; Ni, M.; Cai, H.-Q.; Gong, M.-Z. *J. Org. Chem.* **2005**, *70*, 1084–1086.
- Liu, R.-R.; Zhu, L.; Hu, J.-P.; Lu, C.-J.; Gao, J.-R.; Lan, Y.; Jia, Y.-X. *Chem. Commun.* **2017**, *53*, 5890–5893.
- Liu, W.; Xu, D. D.; Repič, O.; Blacklock, T. J. *Tetrahedron Lett.* **2001**, 2439–2441.
- Liu, Y.; Ao, J.; Paladhi, S.; Song, C. E.; Yan, H. *J. Am. Chem. Soc.* **2016**, *138*, 16486–16492.
- Liu, Y.; Han, S. J.; Liu, W. B.; Stoltz, B. M. *Acc. Chem. Res.* **2015**, *48*, 740–751.
- Liu, Y.; Liu, S.; Li, D.; Zhang, N.; Peng, L.; Ao, J.; Song, C. E.; Lan, Y.; Yan, H. *J. Am. Chem. Soc.* **2019**, *141*, 1150–1159.
- Lölsberg, W.; Ye, S.; Schmalz, H.-G. *Adv. Synth. Catal.* **2010**, *352*, 2023–2031.
- Long-Wu, Y.; Shu, C.; Gagosz, F. *Org. Biomol. Chem.* **2014**, *12*, 1833–1845.
- Lu, G.; Li, X.; Jia, X.; Chan, W. L.; Chan, A. S. C. *Angew. Chem. Int. Ed.* **2003**, *42*, 5057–5058 and *Angew. Chem.* **2003**, *115*, 5211–5212.

- Lu, G.; Li, X.; Li, Y.-M.; Kwong, F. Y.; Chan, A. S. C. *Adv. Synth. Catal.* **2006**, *348*, 1926–1933.
- Lu, G.; Li, Y.-M.; Li, X.-S.; Chan, A. S. C. *Coord. Chem. Rev.* **2005**, *249*, 1736–1744.
- Lynch, C. L.; Hale, J. J.; Budhu, R. J.; Gentry, A. L.; Mills, S. G.; Chapman, K.T.; MacCoss, M.; Malkowitz, L.; Springer, M. S.; Gould, S. L.; DeMartino, J. A.; Siciliano, S. J.; Cascieri, M. A.; Carella, A.; Carver, G.; Holmes, K.; Schleif, W. A.; Danzeisen, R.; Hazuda, D.; Kessler, J.; Lineberger, J.; Miller, M.; Emini, E. A. *Bioorg. Med. Chem. Lett.* **2002**, *12*, 3001–3004.
- Madelaine, C.; Valerio, V.; Maulide, N. *Angew. Chem. Int. Ed.* **2010**, *49*, 1583–1586, *Angew. Chem.* **2010**, *122*, 1628–1631. Huang, Z.; Chen, Z.; Lim, L. H.; Quang, G. C. P.; Hirao, H.; Zhou, J. *Angew. Chem. Int. Ed.* **2013**, *52*, 5807–5812, *Angew. Chem.* **2013**, *125*, 5919–5924.
- Mai, C.-K.; Sammons, M. F.; Sammakia, T. *Org. Lett.* **2010**, *12*, 2306–2309.
- Mao, B.; Fañanás-Mastral, M.; Feringa, B. L. *Chem. Rev.* **2017**, *117*, 10502–10566.
- Marcone, J. E.; Moloy, K. G. *J. Am. Chem. Soc.* **1998**, *120*, 8527–8528.
- Matsunaga, S.; Shibasaki, M. *Chem. Commun.*, **2014**, *50*, 1044–1057.
- Matsunaga, S.; Shibasaki, M. *Synlett*, **2009**, *10*, 1635–1638.
- Mechler, M.; Latendorf, K.; Frey, W.; Peters, R. *Organometallics* **2013**, *32*, 112–130.
- Meletis, P.; Patil, M.; Thiel, W.; Frank, W.; Braun, M. *Chem. Eur. J.* **2011**, *17*, 11243–11249.
- Meyers, A. I.; Yamamoto, Y.; Mihelich, E. D.; Bell, R. A. *J. Org. Chem.* **1980**, *45*, 2792–2796.
- Mitsunuma, H.; Matsunga, S. *Chem. Commun.* **2011**, *47*, 469–471.
- Mohr, J. T.; Stoltz, B. M. *Chem. Asian. J.* **2007**, *2*, 1476–1491.
- Moreno, M.; Elgaher, W. A.; Herrmann, J.; Schläger, N.; Hamed, M. M.; Baumann, S.; Müller, R.; Hartmann, R. W.; Kirschning, A. *Synlett*, **2015**, *26*, 1175–1178.

- Morisaki, K.; Sawa, M.; Nomaguchi, J.-Y.; Morimoto, H.; Takeuchi, Y.; Mashima, K.; Ohshima, T. *Chem. Eur. J.* **2013**, *19*, 8417–8420.
- Morisaki, K.; Sawa, M.; Yonesaki, R.; Morimoto, H.; Mashima, K.; Ohshima, T. *J. Am. Chem. Soc.* **2016**, *138*, 6194–6203.
- Morita, D. K.; Stille, J. K.; Norton, J. R. *J. Am. Chem. Soc.* **1995**, *117*, 8576–8581.
- Motoki, R.; Kanai, M.; Shibasaki, M. *Org. Lett.* **2007**, *9*, 2997–3000.
- Motoki, R.; Tomita, D.; Kanai, M.; Shibasaki, M. *Tetrahedron Lett.* **2006**, *47*, 8083–8086.
- Mulqi, M.; Stephens, F. S.; Vagg, R. S. *Inorg. Chim. Acta*, **1981**, *51*, 9–14.
- Mulqi, M.; Stephens, F. S.; Vagg, R. S. *Inorg. Chim. Acta*, **1981**, *52*, 177–182.
- Nascimento de Oliveira, M.; Fournier, J.; Arseniyadis, S.; Cossy, J. A. *Org. Lett.* **2017**, *19*, 14–17.
- Neese, F. The ORCA program system. *WIREs. Comput. Mol. Sc.* **2012**, *2*, 73–78 (b) Neese, F. Software update: the ORCA program system, version 4.0. *WIREs. Comput. Mol. Sc.* **2017**, *8*, e1327.
- Nenajdenko, V. G.; Krasovsky, A. L.; Lebedev, M. V.; Balenkova, E. S. *Synlett*, **1997**, *12*, 1349–1350.
- Ngamnithiporn, A.; Jette, C.; Bachman, S.; Virgil, S.; Stoltz, B. M. *Chem. Sci.* **2018**, *9*, 2547–2551.
- Nie, J.; Guo, H.-C.; Cahard, D.; Ma, J. -A. *Chem. Rev.* **2011**, 455–529.
- Noda, H.; Kumagai, N.; Shibasaki, M. *Asian J. Org. Chem.* **2018**, *7*, 599–612.
- Notz, W.; Tanaka, F.; Barbas III, C. F.; *Acc. Chem. Res.* **2004**, *37*, 580–591.

- Ohshima, T.; Kawabata, T.; Takeuchi, Y.; Kakinuma, T.; Iwasaki, T.; Yonezawa, T.; Murakami, H.; Nishiyama, H.; Mashima, K. *Angew. Chem., Int. Ed.* **2011**, *50*, 6296–6300.
- Oisaki, K.; Suto, Y.; Kanai, M.; Shibasaki, M.; *J. Am. Chem. Soc.* **2003**, *125*, 5644–5645.
- Okuniewski, A.; Rosiak, D.; Chojnacki, J.; Becker, B. *Polyhedron*. **2015**, *90*, 47–57
- Oliveira, M. N.; Fournier, J.; Arseniyadis, S.; Cossy, J. *Org. Lett.* **2017**, *19*, 14–17.
- Oliveira, M. T.; Lee, J.-W. *Chem. Cat. Chem.* **2017**, *9*, 377–384.
- Oliver, S.; Evans, P. A. *Synthesis* **2013**, *45*, 3179–3198.
- Ortega, A.; Manzano, R.; Uria, U.; Carrillo, L.; Reyes, E.; Tejero, T.; Merino, P.; Vicario, J. L. *Angew. Chem. Int. Ed.* **2018**, *57*, 8225–8229.
- Ouali, A.; Taillefer, M.; Spindler, J. –F. Jutand, A. *Organomet.* **2007**, *26*, 65–74.
- Ouali, A.; Taillefer, M.; Spindler, J. –F.; Jutand, A. *Organometallics*, **2007**, *26*, 65–74.
- Paladhi, S.; Hwang, I.-S.; Yoo, E. J.; Ryu, D. H.; Song, C. E. *Org. Lett.* **2018**, *20*, 2003–2006.
- Paladhi, S.; Liu, Y.; Kumar, B. S.; Jung, M.-J.; Park, S. Y.; Yan, H.; Song, C. E. *Org. Lett.* **2017**, *19*, 3279–3282.
- Paladhi, S.; Park, S. Y.; Yang, J. W.; Song, C. E. *Org. Lett.* **2017**, *19*, 5336–5339.
- Palucki, M.; Buchwald, S. L. *J. Am. Chem. Soc.* **1997**, *119*, 11108 – 11109.
- Panyam, P. K. R.; Ugale, B.; Gandhi, T. *J. Org. Chem.* **2018**, *83*, 7622–7632.
- Park, D. ‡; Jette, C. I. ‡; Kim, J. ‡; Jung, W.-O.; Lee, Y.; Park, J.; Kang, S.; Han, M. S.; Stoltz, B. M.; Hong, S. *Angew. Chem. Int. Ed.* **2020**, *59*, 775–779.
- Park, J.; Hong, S. *Chem. Soc. Rev.* **2012**, *41*, 6931–6943.
- Park, J.; Lang, K.; Abboud, K. A.; Hong, S. *Chem.–Eur. J.* **2011**, *17*, 2236–2245.

- Park, J.; Lang, K.; Abboud, K. A.; Hong, S. *J. Am. Chem. Soc.* **2008**, *130*, 16484–16485.
- Park, S. Y.; Hwang, I.-S.; Lee, H.-J.; Song, C. E. *Nat. Commun.* **2017**, *8*, 14877.
- Park, S. Y.; Lee, J.-W.; Song, C. E. *Nat. Commun.* **2015**, *6*, 7512. (h) Li, L.; Liu, Y.; Peng, Y.; Yu, L.; Wu, X.; Yan, H. *Angew. Chem. Int. Ed.* **2016**, *55*, 331–335 and *Angew. Chem.* **2016**, *128*, 339–343.
- Park, Y.; Lee, Y. J.; Hong, S.; Kim, M.-H.; Lee, M.; Kim, T.-S.; Lee, J. K.; Jew, S.-S.; Park, H.-G. *Adv. Synth. Catal.* **2011**, *353*, 3313–3318.
- Pärssinen, A.; Luhtanen, T.; Pakkanen, T.; Leskelä, M.; Repo, T. *European Journal of Inorganic Chemistry* **2010**, *2010*, 266–274.
- Radin, N. S.; *Drug. Dev. Res.* **2008**, *69*, 15–25.
- Raghuraman, A.; Ko, E.; Perez, L. M. Ioerger, T. R.; Burgess, K. *J. Am. Chem. Soc.* **2011**, *133*, 12350–12353.
- Rathke, M.; Lindert, A. *J. Am. Chem. Soc.* **1971**, *93*, 4605–4606.
- Rexiti, R.; Lu, J.; Wang, G.; Sha, F.; Wu, X. –Y. *Tetrahedron: Asymmetry* **2016**, *27*, 923–929.
- Rivas, F.; Ling, T. *Org. Prep. Proced. Int.* **2016**, *48*, 254–295.
- Sambiagio, Carlo. Investigations on the use of Amidic Ligands in Copper-Catalyzed Arylation Reactions, Ph.D. Dissertation, University of Leeds, Leeds, West Yorkshire, England, 2015.
- Sanz-Marco, A.; Blay, G.; Muñoz, M. C.; Pedro, J. R. *Chem. Commun.* **2015**, *51*, 8958–8961.
- Sasaki, S.; Yamauchi, T.; Higashiyama, K. *Tetrahedron Lett.* **2010**, *51*, 2326–2328.
- Satoh, T.; Inoh, J.; Kawamura, Y.; Miura, M.; Nomura, M.; *Bull. Chem. Soc. Jpn.* **1998**, *71*, 2239 – 2246.
- Satoh, T.; Kawamura, Y.; Miura, M.; Nomura, M.; *Angew. Chem.* **1997**, *109*, 1820–1822; *Angew.*

Chem. Int. Ed. **1997**, *36*, 1740–1742.

Sawamura, M.; Nagata, H.; Sakamoto, H.; Ito, Y. *J. Am. Chem. Soc.* **1992**, *114*, 2586–2592.

Seitz, M.; Reiser, O. *Curr. Opin. Chem. Biol.* **2005**, *9*, 285–292.

Semmelhack, M. F.; Chong, B. P.; Stauffer, R. D.; Rogerson, T. D.; Chong, A.; Jones, L. D. *J. Am. Chem. Soc.* **1975**, *97*, 2507–2516.

Semmelhack, M. F.; Stauffer, R. D.; Rogerson, T. D. *Tetrahedron Lett.* **1973**, *14*, 4519–4522.

Sha, S. C.; Mao, J.; Bellomo, A.; Jeong, S. A.; Walsh, P. J. *Angew. Chem. Int. Ed.* **2016**, *55*, 1070–1074 and *Angew. Chem.* **2017**, *128*, 1082–1086.

Shaughnessy, K. H.; Hamann, B. C.; Hartwig, J. F. *J. Org. Chem.* **1998**, *63*, 6546–6553.

Shepherd, N. E.; Tanabe, H.; Xu, Y.; Matsunaga, S.; Shibasaki, M. *J. Am. Chem. Soc.* **2010**, *132*, 3666–3667.

Shi, Y.; Jung, B.; Torker, S.; Hoveyda, A. H. *J. Am. Chem. Soc.* **2015**, *137*, 8948–8964.

Shibasaki, M.; Sasai, H.; Arai, T. *Angew. Chem. Int. Ed.* **1997**, *36*, 1236–1256.

Shields, J. D.; Ahneman, D. T.; Graham, T. J. A.; Doyle, A. G. *Org. Lett.* **2014**, *16*, 142–145.

Shockley, S. E.; Hethcox, J. C.; Stoltz, B. M. *Angew. Chem. Int. Ed.* **2017**, *56*, 11545–11548 and *Angew. Chem.* **2017**, *129*, 11703–11706.

Son, S. Fu, G. C. *J. Am. Chem. Soc.* **2008**, *130*, 2756–2757.

Song, T.; Zheng, L-S.; Ye, F.; Deng, W.-H.; Wei, Y.-L.; Jiang, K-Z.; Xu, L-W. *Adv. Synth. Catal.* **2014**, *356*, 1708–1718.

Sprague, D. J.; Nugent, B. M.; Yoder, R. A.; Vara, B. A.; Johnston, J. N. *Org. Lett.* **2015**, *17*, 880–883.

- Srinivas, H. D.; Zhou, Q.; Watson, M. P. *Org. Lett.* **2014**, *16*, 3596–3599.
- Starkov, P.; Moore, J. T.; Duquette, D. C.; Stoltz, B. M.; Marek, I. *J. Am. Chem. Soc.* **2017**, *139*, 9615–9620.
- Stewart, J. D.; Fields, S. C.; Kochhar, K. S.; Pinnick, H. W. *J. Org. Chem.* **1987**, *52*, 2110–2113.
- Takashi, B.; Shuji, T.; Keigo, F.; Zen-ichi, Y.; Yoshinao, T. *Bull. Chem. Soc. Jpn.* **1992**, *65*, 97–110.
- Takita, R.; Yakura, K.; Ohshima, T.; Shibasaki, M. *J. Am. Chem. Soc.* **2005**, *127*, 13760–13761.
- Tan, B. Y.; Teo, Y. *Synlett* **2015**, *26*, 1697–1701.
- Tan, Y.; Luo, S.; Li, D.; Zhang, N.; Jia, S.; Liu, Y.; Qin, W.; Song, C. E.; Yan, H. *J. Am. Chem. Soc.* **2017**, *139*, 6431–6436.
- Taylor, A. M.; Altman, R. A.; Buchwald, S. L. *J. Am. Chem. Soc.* **2009**, *131*, 9900–9901.
- Teodorescu, M.; Bercea, M.; *Polym Plast Technol Eng.* **2015**, *54*, 923–943.
- Terao, Y.; Satoh, T.; Miura, M.; Nomura, M.; *Bull. Chem. Soc. Jpn.* **1999**, *72*, 2345 – 2350.
- Tredwell, M.; Gouverneur, V. Fluorine in Medicinal Chemistry: Importance of Chirality. In *Comprehensive Chirality*, Yamamoto, H.; Carreira, E., Eds.; Elsevier Ltd. 2012; Vol. 1, pp 70–85.
- Trillo, P.; Baeza, A. *Adv. Synth. Catal.* **2017**, *359*, 1735–1741
- Trost, B. M. *J. Org. Chem.* **2004**, *69*, 5813–5837.
- Trost, B. M.; Bartlett, M. J.; Weiss, A. H.; von Wangelin, A. J.; Chan, V. S. *Chem.–Eur. J.* **2012**, *18*, 16498–16509.

Trost, B. M.; Burns, A. C.; Bartlett, M. J.; Tautz, T.; Weiss, A. H. *J. Am. Chem. Soc.* **2012**, *134*, 1474–1477.

Trost, B. M.; *Chem. Rev.* **1996**, *96*, 395–422.

Trost, B. M.; Crawley, M. L.; *Chem. Rev.* **2003**, *103*, 2921–2943.

Trost, B. M.; Dogra, K.; Hachiya, I.; Emura, T.; Hughes, D. L.; Krska, S.; Reamer, R. A.; Palucki, M.; Yasuda, N.; Reider, P. *Angew. Chem. Int. Ed.* **2002**, *41*, 1929–1932 and *Angew. Chem.* **2002**, *114*, 2009–2012

Trost, B. M.; Frederiksen, M. U. *Angew. Chem. Int. Ed.* **2005**, *44*, 308–310 and *Angew. Chem.* **2005**, *117*, 312–314.

Trost, B. M.; Hachiya, I. *J. Am. Chem. Soc.* **1998**, *120*, 1104–1105. (b) Krska, S.; Hughes, D. L.; Reamer, R. A.; Mathre, D. J.; Sun, Y.; Trost, B. M. *J. Am. Chem. Soc.* **2002**, *124*, 12656–12657.

Trost, B. M.; Quintard, A. *Angew. Chem. Int. Ed.* **2012**, *51*, 6704–6708, and *Angew. Chem.* **2012**, *124*, 6808–6812.

Trost, B. M.; Radinov, R. *J. Am. Chem. Soc.* **1997**, *119*, 5962–5963.

Trost, B. M.; Rao, M.; Dieskau, A. P. *J. Am. Chem. Soc.* **2013**, *135*, 18697–18704.

Trost, B. M.; Van Vranken, D. L. *Chem. Rev.* **1996**, *96*, 395–422.

Trost, B. M.; Weiss, A. H. *J. Am. Chem. Soc.* **2006**, *128*, 8–9.

Trost, B. M.; Yong, Z.; *Chem. Eur. J.* **2011**, *17*, 2916–2922.

Tsuji, J.; Takahashi, H.; Morikawa, M. *Tetrahedron Lett.* **1965**, *6*, 4387–4388.

Vaithyanathan, V.; Kim, M. J.; Liu, Y.; Yan, H.; Song, C. E. *Chem. –Eur. J.* **2017**, *23*, 1268–1272.

Van Hoomissen, D. J.; Vyas, S. *J. Org. Chem.* **2017**, *82*, 5731–5742.

- Vazquez-Molina, D.; Pope, G. M.; Ezazi, A. A.; Mendoza-Cortes, J. L.; Harper, J. H.; Uribe-Romo, F. J. *Chem. Commun.* **2018**, 54, 6947–6950.
- Vignesh, A.; Kaminsky, W.; Dharmaraj, N. *Chem. Cat. Chem.* **2017**, 9, 910–914.
- Vitaku, E.; Smith, D. T.; Njardarson, J. T. *J. Med. Chem.* **2014**, 57, 10257–10274.
- Vrouenraets, S. M. E.; Wit, F. W. N. M.; Tongeren, J. V.; Lange, J. M. A. **2007**, 8, 851–871.
- Wang, J.; Wang, P.; Wang, L.; Li, D.; Wang, K.; Wang, Y.; Zhu, H.; Yang, D.; Wang, R. *Org. Lett.* **2017**, 19, 4826–4829.
- Wang, L.-N.; Cui, Q.; Yu, Z.-X. *J. Org. Chem.* **2016**, 81, 10165–10171.
- Wang, T.; Niu, J.-L.; Liu, S.L.; Huang, J.-J.; Gong, J.-F.; Song, M.-P. *Adv. Synth. Catal.* **2013**, 355, 927–937.
- Wang, Y.; Han, J.; Chen, J.; Weiguo, C. *Tetrahedron*, **2015**, 71, 8256–8262.
- Watson, A. J. B.; MacMillan, D. W. C.; Ojima, I. Enantioselective Organocatalysis Involving Iminium, Enamine SOMO and Photoredox Activation. In *Catalytic Asymmetric Synthesis*, 3rd ed.; Ed.; Wiley & Sons: Hoboken, NJ, 2010; pp 39–57.
- Whitby, L. R.; Ando, Y.; Setola, V.; Vogt, P. K.; Roth, B. L.; Boger, D. L. *J. Am. Chem. Soc.* **2011**, 133, 10184–10194.
- Wolf, C.; Liu, S. *J. Am. Chem. Soc.* **2006**, 128, 10996–10997.
- Xu, Y.; Lin, L.; Kanai, M.; Matsunaga, S.; Shibasaki, M. *J. Am. Chem. Soc.* **2011**, 133, 5791–5793.
- Yamanaka, M.; Kato, S.; Nakamura, E. *J. Am. Chem. Soc.* **2004**, 126, 6287–6293.

- Yan, H.; Jang, H. B.; Lee, J.-W.; Kim, H. K.; Lee, S. W.; Yang, J. W.; Song, C. E. *Angew. Chem., Int. Ed.* **2010**, *49*, 8915–8917 and *Angew. Chem.* **2010**, *122*, 9099–9101.
- Yan, H.; Oh, J. S.; Lee, J.-W.; Song, C. E. *Nat. Commun.* **2012**, *3*, 1212.
- Yang, D.; Wang, L.; Han, F.; Zhao, D.; Zhang, B.; Wang, R. *Angew. Chem. Int. Ed.* **2013**, *52*, 6739–6742 and *Angew. Chem.* **2013**, *125*, 6871–6874.
- Yingjie, X.; Matsunaga, S.; Shibasaki, M. *Org. Lett.* **2010**, *12*, 3246–3249.
- Yoshikai, N.; Nakamura, E. *Chem. Rev.* **2012**, *112*, 2339–2372.
- Yoshikai, N.; Zhang, S.-L.; Nakamura, E. *J. Am. Chem. Soc.* **2008**, *130*, 12862–12863.
- Yu, L.; Wu, X.; Kim, M. J.; Vaithiyanathan, V.; Liu, Y.; Tan, Y.; Qin, W.; Song, C. E.; Yan, H. *Adv. Synth. Catal.* **2017**, *359*, 1879–1891.
- Zhang, G.-W.; Meng, W.; Ma, H.; Nie, J.; Zhang, W.-Q.; Ma, J.-A. *Angew. Chem. Int. Ed.* **2011**, *50*, 3538–3542 and *Angew. Chem.* **2011**, *123*, 3600–3604.
- Zhang, H.-C.; Huang, W.-S.; Pu, L. *J. Org. Chem.* **2001**, *66*, 481–487.
- Zhang, S.; Wang, W.; Zhou, Q.-L. *Privileged Chiral Ligands and Catalysts*; Ed.; Wiley-VCH: Weinheim, Germany, 2011; pp 409–439.
- Zhang, Y. -Z.; Zhu, S. -F.; Wang, L.-X. Zhou, Q. -L. *Angew. Chem. Int. Ed.* **2008**, *47*, 8496–8498.
- Zheng, C.; Li, Y.; Yang, Y.; Wang, H.; Cui, H.; Zhang, J.; Zhao, G. *Adv. Synth. and Catal.* **2009**, *351*, 1685–1691.
- Zheng, Y.; Harms, K.; Zhang, L.; Meggers, E. *Chem. Eur. J.* **2016**, *22*, 11977–11981.
- Zheng, Y.; Zhang, L.; Meggers, E. *Org. Process Res. Dev.* **2018**, *22*, 103–107.
- Zhou, X.; Zhang, G.; Gao, B.; Huang, H.; *Org. Lett.* **2018**, *20*, 2208–2212

Zhou, Y.; Wang, J.; Gu, Z.; Wang, S.; Zhu, W.; Aceña, J. L.; Soloshonok, V. A.; Izawa, K.; Liu,

H. *Chem. Rev.* **2016**, *116*, 422–518.

Zhou, Y.; Wang, R.; Xu, Z.; Yan, W.; Liu, L.; Kang, Y.; Han, Z. *Org. Lett.* **2004**, *23*, 4147–4149.

INDEX

A

Acyclic Silyl Ketene Acetals.....	397
Allylic Alcohol	640
Allylic Alkylation.....	296, 366
α -Allyl γ -Butyrolactones	298
Allylic Chloride	325, 356, 388
Amino Nitrile	123
ANDEN	317-320, 349
α -Arylation.....	109
Aryl Bromide.....	118, 165
Aryl Chloride.....	112, 165

B

Benzamide	315-317
Benzyl Chloride.....	537
Bicyclo[2.2.2]octane	397
Bifunctional Catalysts	3-5
Bis-Picolinamide Ligand	304, 310
2-Bromopropane	626
γ -Butyrolactone	109, 296, 632, 639

C

Ceric Ammonium Nitrate (CAN).....	123
2-Chloropropene	625

Cinnamyl Alcohol	644
Cinnamyl Bromide	394, 550
Cinnamyl Chloride	304
Cross Metathesis	327

D

Dbal	114
DFT Calculations	541
Diamine	22–27, 342–344
DIBAL-H	326, 362
Diol	326, 645
Dioxane	115
DMAP	125, 329
Dmdba	114

E

ESI-MS	540
α -Ethoxycarbonyl Lactone	640

F

Ferrocene Ligand	116, 630
Ferrocene Ligand	114, 630
FTIR	540, 547

G

Grubbs II	645
-----------------	-----

H

Heteroaryl	325
High-Resolution Mass Spectra (HRMS)	18, 28

I

Iodobenzene	118
Isocrotyl Bromide	633
Isocrotyl Chloride	627

K

β -Ketoesters	311, 535, 640
KHMDS	117, 324

L

γ -Lactam	109
Lactol	326, 383
LDA	129
LiAlH_4	123, 327, 646
LiCl	631
LiHMDS	114, 318, 632
Lithium Triethyl Borohydride	123

M

Malonate	1–6
Methyl Acrylate	327
α -Methyl γ -Butyrolactone	327
2-MeTHF	539
Mol Sieves	13
Mono-picolinyl Ligands	314

N

NaHMDS	119, 163, 324, 633
<i>n</i> -BuLi	129, 311
Nickel	4, 6, 296, 638

O

Olefin Geometry	552-555
-----------------------	---------

P

<i>p</i> -Methoxy Phenyl	125
Palladium	6, 535
Phenethylbenzylamine	109
Phenylacetylene	8
Picolinamide Ligands	335
Pmdba	115, 125
Potassium Cyanide	123
Potassium <i>t</i> -Butoxide	6,
Pyrrolidine.....	109, 158, 635
Pyrrolidinone.....	109, 158, 635

R

Rochelle's Salt	362
-----------------------	-----

S

Salen	6,19
Schiff Base Ligands	314
Silyl Enol Ether	393, 399-403
Silyl Ketene Acetal.....	296, 367

Silyl Ketene Acetal.....	296, 367
Silyl Ketene Aminoal 393	
SIMES-leucinol	404

T

TBAT	403, 550
TEMPO.....	536
Tetrahydrofuran.....	327, 330
Thiolactone	393
Thionyl Chloride	356
TMEDA	367
Triethylphosphonacetate	326
Trifluoromethyl.....	1–3, 6–17, 29, 326
Trifluoromethylcarbinol.....	2

V

δ -Valerolactam	163, 393
α -Vinylation	624
Vinylmagnesium Bromide	364, 645

W

Wacker.....	646
-------------	-----

ABOUT THE AUTHOR

Carina Jette was born in Pasadena, California on May 26th, 1991 to Paul and Claudia Jette, and grew up in the Pasadena area with her two younger sisters, Claudia, and Daniela. Growing up, Carina spent a large part of her time focusing on music, and in the fall of 2009, started attending the University of California, Santa Barbara as a music major. Curious about other subjects, she began to take classes other than music classes, and discovered an interest in research and science. It was not until she took organic chemistry with Bruce Lipshutz, however, that she discovered her passion for chemistry. During her time at UCSB, Carina conducted research in the Lipshutz laboratory, focusing on transition metal-catalysis and surfactant chemistry.

Upon completion of her undergraduate studies in 2015, she moved back to Pasadena, California to pursue graduate studies at the California Institute of Technology under the direction of Professor Brian Stoltz. Her interests focused on the development of asymmetric transition-metal catalysis. Following the completion of her graduate studies in November 2020, Carina will pursue postdoctoral research in the lab of Professor Jenny Yang at the University of California, Irvine.